

THE ROLE OF ncRNAs (NON-CODING RNAs) IN REGULATING TUMOR IMMUNE MICROENVIRONMENT

EDITED BY: Yanyan Tang, Shiv K. Gupta and Zong Sheng Guo
PUBLISHED IN: Frontiers in Cell and Developmental Biology and
Frontiers in Oncology



frontiers

Frontiers eBook Copyright Statement

The copyright in the text of individual articles in this eBook is the property of their respective authors or their respective institutions or funders. The copyright in graphics and images within each article may be subject to copyright of other parties. In both cases this is subject to a license granted to Frontiers.

The compilation of articles constituting this eBook is the property of Frontiers.

Each article within this eBook, and the eBook itself, are published under the most recent version of the Creative Commons CC-BY licence.

The version current at the date of publication of this eBook is CC-BY 4.0. If the CC-BY licence is updated, the licence granted by Frontiers is automatically updated to the new version.

When exercising any right under the CC-BY licence, Frontiers must be attributed as the original publisher of the article or eBook, as applicable.

Authors have the responsibility of ensuring that any graphics or other materials which are the property of others may be included in the CC-BY licence, but this should be checked before relying on the CC-BY licence to reproduce those materials. Any copyright notices relating to those materials must be complied with.

Copyright and source acknowledgement notices may not be removed and must be displayed in any copy, derivative work or partial copy which includes the elements in question.

All copyright, and all rights therein, are protected by national and international copyright laws. The above represents a summary only. For further information please read Frontiers' Conditions for Website Use and Copyright Statement, and the applicable CC-BY licence.

ISSN 1664-8714

ISBN 978-2-88976-957-5

DOI 10.3389/978-2-88976-957-5

About Frontiers

Frontiers is more than just an open-access publisher of scholarly articles: it is a pioneering approach to the world of academia, radically improving the way scholarly research is managed. The grand vision of Frontiers is a world where all people have an equal opportunity to seek, share and generate knowledge. Frontiers provides immediate and permanent online open access to all its publications, but this alone is not enough to realize our grand goals.

Frontiers Journal Series

The Frontiers Journal Series is a multi-tier and interdisciplinary set of open-access, online journals, promising a paradigm shift from the current review, selection and dissemination processes in academic publishing. All Frontiers journals are driven by researchers for researchers; therefore, they constitute a service to the scholarly community. At the same time, the Frontiers Journal Series operates on a revolutionary invention, the tiered publishing system, initially addressing specific communities of scholars, and gradually climbing up to broader public understanding, thus serving the interests of the lay society, too.

Dedication to Quality

Each Frontiers article is a landmark of the highest quality, thanks to genuinely collaborative interactions between authors and review editors, who include some of the world's best academicians. Research must be certified by peers before entering a stream of knowledge that may eventually reach the public - and shape society; therefore, Frontiers only applies the most rigorous and unbiased reviews.

Frontiers revolutionizes research publishing by freely delivering the most outstanding research, evaluated with no bias from both the academic and social point of view. By applying the most advanced information technologies, Frontiers is catapulting scholarly publishing into a new generation.

What are Frontiers Research Topics?

Frontiers Research Topics are very popular trademarks of the Frontiers Journals Series: they are collections of at least ten articles, all centered on a particular subject. With their unique mix of varied contributions from Original Research to Review Articles, Frontiers Research Topics unify the most influential researchers, the latest key findings and historical advances in a hot research area! Find out more on how to host your own Frontiers Research Topic or contribute to one as an author by contacting the Frontiers Editorial Office: frontiersin.org/about/contact

THE ROLE OF ncRNAs (NON-CODING RNAs) IN REGULATING TUMOR IMMUNE MICROENVIRONMENT

Topic Editors:

Yanyan Tang, Central South University, China

Shiv K. Gupta, Mayo Clinic, United States

Zong Sheng Guo, University at Buffalo, United States

Citation: Tang, Y., Gupta, S. K., Guo, Z. S., eds. (2022). The Role of ncRNAs (non-coding RNAs) in Regulating Tumor Immune Microenvironment. Lausanne: Frontiers Media SA. doi: 10.3389/978-2-88976-957-5

Table of Contents

- 06 Comprehensive Analysis of Autophagy-Associated lncRNAs Reveal Potential Prognostic Prediction in Pancreatic Cancer**
Guangyu Chen, Gang Yang, Junyu Long, Jinshou Yang, Cheng Qin, Wenhao Luo, Jiangdong Qiu, Fangyu Zhao, Lei You, Taiping Zhang and Yupei Zhao
- 18 Immune Subtypes Based on Immune-Related lncRNA: Differential Prognostic Mechanism of Pancreatic Cancer**
Qiyao Zhang, Zhihui Wang, Xiao Yu, Menggang Zhang, Qingyuan Zheng, Yuting He and Wenzhi Guo
- 31 Immune Microenvironment Change and Involvement of Circular RNAs in TIL Cells of Recurrent Nasopharyngeal Carcinoma**
Yumin Wang, Zhouying Peng, Yaxuan Wang, Yi Yang, Ruohao Fan, Kelei Gao, Hua Zhang, Zhihai Xie and Weihong Jiang
- 39 A Novel Pyroptosis-Associated Long Non-coding RNA Signature Predicts Prognosis and Tumor Immune Microenvironment of Patients With Breast Cancer**
Liqin Ping, Kaiming Zhang, Xueqi Ou, Xingsheng Qiu and Xiangsheng Xiao
- 57 Effect, Mechanism, and Applications of Coding/Non-coding RNA m6A Modification in Tumor Microenvironment**
Chaohua Si, Chen Chen, Yaxin Guo, Qiaozhen Kang and Zhenqiang Sun
- 73 A Review on the Role of Small Nucleolar RNA Host Gene 6 Long Non-coding RNAs in the Carcinogenic Processes**
Soudeh Ghafouri-Fard, Tayyebbeh Khoshbakht, Mohammad Taheri and Seyedpouzha Shojaei
- 86 MiR-873-5p: A Potential Molecular Marker for Cancer Diagnosis and Prognosis**
Yuhao Zou, Chenming Zhong, Zekai Hu and Shiwei Duan
- 103 SNHG10 Is a Prognostic Biomarker Correlated With Immune Infiltrates in Prostate Cancer**
Qiang Chen, Xiaorong Yang, Binbin Gong, Wenjie Xie, Ming Ma, Shengqiang Fu, Siyuan Wang, Yutang Liu, Zhicheng Zhang, Ting Sun and Zhilong Li
- 116 Immune-Related lncRNAs Affect the Prognosis of Osteosarcoma, Which Are Related to the Tumor Immune Microenvironment**
Qingshan Huang, Yilin Lin, Chenglong Chen, Jingbing Lou, Tingting Ren, Yi Huang, Hongliang Zhang, Yiyang Yu, Yu Guo, Wei Wang, Boyang Wang, Jianfang Niu, Jiuhui Xu, Lei Guo and Wei Guo
- 131 CDKN2B-AS1 Promotes Malignancy as a Novel Prognosis-Related Molecular Marker in the Endometrial Cancer Immune Microenvironment**
Di Yang, Jian Ma and Xiao-Xin Ma
- 146 Identification of an Immune-Related lncRNA Signature in Gastric Cancer to Predict Survival and Response to Immune Checkpoint Inhibitors**
Zuoyou Ding, Ran Li, Jun Han, Diya Sun, Lei Shen and Guohao Wu

- 161 ***LncRNA GAPLINC Promotes Renal Cell Cancer Tumorigenesis by Targeting the miR-135b-5p/CSF1 Axis***
Siyuan Wang, Xiaorong Yang, Wenjie Xie, Shengqiang Fu, Qiang Chen, Zhilong Li, Zhicheng Zhang, Ting Sun, Binbin Gong and Ming Ma
- 176 ***Promising Advances in LINC01116 Related to Cancer***
Yating Xu, Xiao Yu, Menggang Zhang, Qingyuan Zheng, Zongzong Sun, Yuting He and Wenzhi Guo
- 186 ***A miR-129-5P/ARID3A Negative Feedback Loop Modulates Diffuse Large B Cell Lymphoma Progression and Immune Evasion Through Regulating the PD-1/PD-L1 Checkpoint***
Weili Zheng, Guilan Lai, Qiaochu Lin, Mohammed Awal Issah, Haiying Fu and Jianzhen Shen
- 200 ***Construction of a Ferroptosis-Related Long Non-coding RNA Prognostic Signature and Competing Endogenous RNA Network in Lung Adenocarcinoma***
Xiang Fei, Congli Hu, Xinyu Wang, Chaojing Lu, Hezhong Chen, Bin Sun and Chunguang Li
- 213 ***Emerging Roles of Long Noncoding RNAs in Immuno-Oncology***
Xin Wang, Xu Wang, Midie Xu and Weiqi Sheng
- 223 ***A Review on the Role of AFAP1-AS1 in the Pathoetiology of Cancer***
Soudeh Ghafouri-Fard, Tayybeh Khoshbakht, Bashdar Mahmud Hussien, Mohammad Taheri and Majid Mokhtari
- 243 ***Exosomal miRNAs and lncRNAs: The Modulator Keys of Cancer-Associated Fibroblasts in the Genesis and Progression of Malignant Neoplasms***
Julio César Villegas-Pineda, Mélida del Rosario Lizarazo-Taborda, Adrián Ramírez-de-Arellano and Ana Laura Pereira-Suárez
- 252 ***circRNAs: Insight Into Their Role in Tumor-Associated Macrophages***
Saili Duan, Shan Wang, Tao Huang, Junpu Wang and Xiaoqing Yuan
- 264 ***Development and Validation of a Novel Hypoxia-Related Long Noncoding RNA Model With Regard to Prognosis and Immune Features in Breast Cancer***
Peng Gu, Lei Zhang, Ruitao Wang, Wentao Ding, Wei Wang, Yuan Liu, Wenhao Wang, Zuyin Li, Bin Yan and Xing Sun
- 283 ***Long Non-Coding RNAs in Lung Cancer: The Role in Tumor Microenvironment***
Shuang Dai, Ting Liu, Yan-Yang Liu, Yingying He, Tao Liu, Zihan Xu, Zhi-Wu Wang and Feng Luo
- 293 ***Oncogenic Roles of Small Nucleolar RNA Host Gene 7 (SNHG7) Long Noncoding RNA in Human Cancers and Potentials***
Sajad Najafi, Soudeh Ghafouri-Fard, Bashdar Mahmud Hussien, Hazha Hadayat Jamal, Mohammad Taheri and Mohammad Hallajnejad
- 307 ***Identification of Circular RNA-Based Immunomodulatory Networks in Colorectal Cancer***
Zongfeng Feng, Leyan Li, Yi Tu, Xufeng Shu, Yang Zhang, Qingwen Zeng, Lianghua Luo, Ahao Wu, Wenzheng Chen, Yi Cao and Zhengrong Li
- 324 ***A Novel Ferroptosis-Related lncRNA Prognostic Model and Immune Infiltration Features in Skin Cutaneous Melanoma***
Shuya Sun, Guanran Zhang and Litao Zhang

- 338** *Clinical Significance and Immune Landscape of a Pyroptosis-Derived LncRNA Signature for Glioblastoma*
Zhe Xing, Zaoqu Liu, Xudong Fu, Shaolong Zhou, Long Liu, Qin Dang, Chunguang Guo, Xiaoyong Ge, Taoyuan Lu, Youyang Zheng, Lirui Dai, Xinwei Han and Xinjun Wang
- 353** *DLX6-AS1: A Long Non-coding RNA With Oncogenic Features*
Soudeh Ghafouri-Fard, Sajad Najafi, Bashdar Mahmud Hussen, Aryan R. Ganjo, Mohammad Taheri and Mohammad Samadian
- 364** *Immune Infiltration and Clinical Outcome of Super-Enhancer-Associated lncRNAs in Stomach Adenocarcinoma*
Li Peng, Jiang-Yun Peng, Dian-Kui Cai, Yun-Tan Qiu, Qiu-Sheng Lan, Jie Luo, Bing Yang, Hai-Tao Xie, Ze-Peng Du, Xiao-Qing Yuan, Yue Liu and Dong Yin
- 379** *MicroRNAs/LncRNAs Modulate MDSCs in Tumor Microenvironment*
Xiaocui Liu, Shang Zhao, Hongshu Sui, Hui Liu, Minhua Yao, Yanping Su and Peng Qu
- 392** *Comprehensive Analysis of the Prognostic Signature of Mutation-Derived Genome Instability-Related lncRNAs for Patients With Endometrial Cancer*
Jinhui Liu, Guoliang Cui, Jun Ye, Yutong Wang, Can Wang and Jianling Bai
- 410** *miR-874: An Important Regulator in Human Diseases*
Qiudan Zhang, Chenming Zhong, Qianqian Yan, Ling-hui Zeng, Wei Gao and Shiwei Duan
- 422** *Construction of an Immune-Related lncRNA Signature That Predicts Prognosis and Immune Microenvironment in Osteosarcoma Patients*
Yi He, Haiting Zhou, Haoran Xu, Hongbo You and Hao Cheng
- 438** *The Emerging Roles of Circ-ABCB10 in Cancer*
Zhenjun Huang, Renfeng Shan, Wu Wen, Jianfeng Li, Xiaohong Zeng and Renhua Wan



Comprehensive Analysis of Autophagy-Associated lncRNAs Reveal Potential Prognostic Prediction in Pancreatic Cancer

OPEN ACCESS

Edited by:

Yi Zhang,
First Affiliated Hospital of Zhengzhou
University, China

Reviewed by:

Maria Francesca Baietti,
KU Leuven, Belgium
Eswari Dodagatta-Marri,
University of California, San Francisco,
United States

*Correspondence:

Taiping Zhang
tpingzhang@yahoo.com
Yupei Zhao
zhao8028@263.net

Specialty section:

This article was submitted to
Molecular and Cellular Oncology,
a section of the journal
Frontiers in Oncology

Received: 19 August 2020

Accepted: 19 April 2021

Published: 26 May 2021

Citation:

Chen G, Yang G, Long J, Yang J,
Qin C, Luo W, Qiu J, Zhao F, You L,
Zhang T and Zhao Y (2021)
Comprehensive Analysis of
Autophagy-Associated lncRNAs
Reveal Potential Prognostic Prediction
in Pancreatic Cancer.
Front. Oncol. 11:596573.
doi: 10.3389/fonc.2021.596573

Guangyu Chen¹, Gang Yang¹, Junyu Long², Jinshou Yang¹, Cheng Qin¹, Wenhao Luo¹,
Jiangdong Qiu¹, Fangyu Zhao¹, Lei You¹, Taiping Zhang^{1,3*} and Yupei Zhao^{1*}

¹ Department of General Surgery, Peking Union Medical College Hospital, Chinese Academy of Medical Sciences and Peking Union Medical College, Beijing, China, ² Department of Liver Surgery, Peking Union Medical College Hospital, Chinese Academy of Medical Sciences and Peking Union Medical College, Beijing, China, ³ Clinical Immunology Center, Chinese Academy of Medical Sciences and Peking Union Medical College, Beijing, China

Pancreatic cancer (PC) is a highly malignant tumor in the digestive system. Both long noncoding RNAs (lncRNAs) and autophagy play vital roles in the development and progress of PC. Here, we constructed a prognostic risk score system based on the expression profile of autophagy-associated lncRNAs for prognostic prediction in PC patients. Firstly, we extracted the expression profile of lncRNA and clinical information from The Cancer Genome Atlas (TCGA) and International Cancer Genome Consortium (ICGC) databases. The autophagy-associated genes were from The Human Autophagy Database. Through Cox regression and survival analysis, we screened out seven autophagy-associated lncRNAs and built the risk score system in which the patients with PC were distinguished into high- and low-risk groups in both training and validation datasets. PCA plot displayed distinct discrimination, and risk score system displayed independently predictive value for PC patient survival time by multivariate Cox regression. Then, we built a lncRNA and mRNA co-expression network *via* Cytoscape and Sankey diagram. Finally, we analyzed the function of lncRNAs in high- and low-risk groups by gene set enrichment analysis (GSEA). The results showed that autophagy and metabolism might make significant effects on PC patients of low-risk groups. Taken together, our study provides a new insight to understand the role of autophagy-associated lncRNAs and finds novel therapeutic and prognostic targets in PC.

Keywords: pancreatic cancer, long noncoding RNA, autophagy, prognosis, TCGA, ICGC

INTRODUCTION

Pancreatic cancer (PC) is a poorly prognostic malignant tumor. Its incidence and mortality rank second and fifth in digestive system tumors in the United States and China separately, of which the five-year survival rate is about 9% (1, 2). Current treatments cannot significantly improve the prognosis of PC patients; meanwhile, the development of pancreatic cancer treatment is relatively slow compared to other tumors, so surgery still represents the most effective treatment to cure resectable pancreatic cancer. Due to the lack of diagnosis at the early stage and the highly malignant characteristics of PC, PC patients frequently exhibit lymph node metastasis and local invasion when the diagnosis is made, leading to approximately 80% of patients losing surgical chances (3). Therefore, the exploration of more effective innovative targets for pancreatic cancer is urgent and necessary.

Autophagy is the homeostatic mechanism through a membrane-mediated process that delivers cytoplasmic organelles and proteins to lysosomes for degradation. There is growing evidence that the level of autophagy can be responded by intracellular and extracellular stresses, such as ER stress, oxidative stress, hypoxia, nutrient shortage, etc., thereby involving tumor progression (4). In pancreatic cancer, autophagy plays a significant tumorigenic role in keeping cancer cell survival and promoting metabolism (5). Hydroxychloroquine (HCQ), which can inhibit autophagy combined with Gemcitabine, is currently being tested in many clinical trials. Consequently, researching new biomarkers related to autophagy to improve early diagnosis and assess prognosis is a promising avenue for PC patients.

Long noncoding RNAs (lncRNAs) mostly have no protein-coding potential of which transcripts are longer than 200 nucleotides. lncRNA can affect different functions at an epigenetic, transcriptional, and post-transcriptional level, and play a vital role in regulating cancer cell behaviors and autophagy (6). There is a recent study indicated that downregulated lncRNA LINC00160 suppressed autophagy and drug resistance in hepatocellular carcinoma by regulating miR-132-targeted PIK3R3 (7). Zhang et al. elaborated lncRNA PVT1 induced cytoprotective autophagy and promoted growth *via* sponging to miR-20a-5p and regulating ULK1 both *in vitro* and *in vivo* in pancreatic ductal adenocarcinoma (8). Another study also demonstrated that silencing lncRNA LINC00160 facilitated autophagy and apoptosis of pancreatic cancer cells (9). Considering that several lncRNAs may influence cancer behaviors through mediating autophagy, it is crucial to explore autophagy-associated lncRNAs to predict the prognosis of PC patients.

In our current study, we analyze the relationship between autophagy-associated lncRNA profiles and clinical information in 178 PC patients from The Cancer Genome Atlas (TCGA) database. The survival analysis showed that seven lncRNAs (AC245041.2, LINC02257, AC006504.8, AC012306.2, AC125494.2, FLVCR1-DT, and AC005332.6) were prognostic biomarkers for patients with PC. Then, the seven lncRNAs were used to develop a risk score system after Cox regression analysis.

Finally, we constructed a prognostic signature that can be applied to independently predict the prognostic of PC patients. These candidate autophagy-associated lncRNAs may become the potential prognostic prediction for PC.

MATERIALS AND METHODS

Sample Datasets

The RNA-seq data and clinical information of PC patients were downloaded from the TCGA data portal (<https://portal.gdc.cancer.gov/>) and ICGC (<https://icgc.org>) databases, respectively. Then, we transformed the RNA sequence data to the lncRNAs and mRNA (protein coding) based on the annotated gene IDs in the Ensembl project. Because the data were extracted from the public database, there was no requirement for ethics committee approval.

Identification of Autophagy-Related lncRNAs

The autophagy gene list was obtained from The Human Autophagy Database (<http://www.autophagy.lu/index.html>), employing Pearson correlation analysis to screen the relationship between the lncRNAs and autophagy-related genes. An absolute value of correlation coefficient > 0.4 ($|R| > 0.4$) and $P < 0.05$ were considered statistically significant. Based on the above standard, the autophagy-related lncRNAs were filtrated for subsequent analysis.

Survival Analysis

Kaplan–Meier (K-M) survival analyses of the autophagy-associated lncRNA were performed using the survival package in R. The patients were classified into high expression and low expression groups using optimal cut-off values determined by the survminer R package (Version:0.4.3). Log-rank $P < 0.05$ was considered statistical significant.

Construction of Co-Expression Network and Function Analysis

To better understand the relation between lncRNAs and mRNAs, the lncRNA-mRNA co-expression network was visualized by Cytoscape software (<http://www.cytoscape.org/>). To investigate the functions of these lncRNAs, the co-expression of mRNAs was analyzed by gene ontology (GO) terms enrichment including biological process, molecular function, and cellular component. A P value of < 0.05 was statistically significant.

Construction of the Risk Score System

Firstly, we used the univariate Cox regression analysis to confirm prognostic autophagy-associated lncRNAs. These lncRNAs were significantly associated ($P < 0.001$) with overall survival (OS). Then, multivariate Cox regression analysis was employed to screen ultimate autophagy-associated lncRNAs and predict the regression coefficients (β) of the model. Finally, a prognosis risk score system based on seven genes was established. Risk score = ($\beta_1 \times$ expression level of AC006504.8) + ($\beta_2 \times$ expression level of

FLVCR1-DT) + ($\beta_3 \times$ expression level of AC012306.2) + ($\beta_4 \times$ expression level of AC125494.2) + ($\beta_5 \times$ expression level of AC005332.6) + ($\beta_6 \times$ expression level of AC245041.2) + ($\beta_7 \times$ expression level of LINC02257). Based on an optimal cutoff value, all PC patients were divided into low- and high-risk groups. To estimate the predictive capacities of the risk score system by constructing Kaplan–Meier survival curves and receiver operating characteristic (ROC) curves.

Gene Set Enrichment Analysis (GSEA)

We use GSEA software (<http://www.broadinstitute.org/gsea>) to identify the underlying different functions between the high- and low-risk groups. The annotated gene sets c5.all.v7.1.symbols.gmt was chosen for the reference gene sets. Enriched gene sets were considered to be statistically significant by a nominal P value < 0.05 that was set as the cut-off criteria.

Cell Culture

The human pancreatic ductal epithelium cell line HPNE and PC cell line PANC-1 were purchased from the ATCC. The cells were cultured at 37°C in a humidified atmosphere containing 5% CO₂ with high glucose DMEM supplemented with 10% fetal serum. The culture medium and supplements were purchased from HyClone (Northbrook, IL, USA).

RNA Extraction and qRT-PCR

Total RNA was extracted by Trizol reagent (Invitrogen, 15596018). RNAs were reverse transcribed utilizing PrimeScript™ RT Master Mix (TaKaRa, RR036A). qRT-PCR was performed using the TB Green Fast qPCR Mix (TaKaRa, RR430S). The primer sequences were used as follows: AC245041.2: Forward 5'-TCCAGACAAGCAGGATGTGG-3', Reverse 5'-AGAGGTTTATAGAGGGAGATGGGA-3'; LINC02257: Forward 5'-GAGACCTTTCACCGGGCTTT-3', Reverse 5'-GCTTCTTGCTGTGTGTTTCCC-3'; AC006504.8: Forward 5'-GAACACAAGCCCGTTAGCA-3', Reverse 5'-AGTGGGGTATGGGTAATAGGATAG-3'; AC012306.2: Forward 5'-TGCTCCCTTACCCTTATGGC-3', Reverse 5'-GAGCATGGGCGGTATTTTA-3'; AC125494.2: Forward 5'-ATCTCCAACCGTGACATTCGG-3', Reverse 5'-CAGGGAAGAACAGAAGCCGAT-3'; FLVCR1-DT: Forward 5'-TAACGCCAGAAAGTGTTCCAGT-3', Reverse 5'-CTGCTCCATCATAGCCCGTC-3'; AC005332.6: Forward 5'-CTCATGTGCTTCTTCTGGGCTT-3', Reverse 5'-TGGCACTCTAATGTTTGCTGACT-3'; GAPDH: Forward 5'-GTATCGTGGAAGGACTCATGAC-3', Reverse 5'-ACCACCTTCTTGATGTCATCAT-3'.

RESULTS

Identification of Seven Prognostic Autophagy-Associated lncRNAs in PC Patients

We extracted a total of 14,142 lncRNAs expression data of tumors from PC tissues in the TCGA database. Two hundred thirty-two

autophagy-associated genes were selected from The Human Autophagy Database. We then utilized Pearson correlation analysis to screen the co-expression relationship between the lncRNAs and autophagy-associated genes with the criteria of $|R| > 0.4$ and $P < 0.05$. Conclusively, 1,234 autophagy-associated lncRNAs were screened. To identify autophagy-associated lncRNAs related to prognosis, we selected the above filtered autophagy-associated lncRNAs by univariate Cox regression analysis and found that 29 lncRNAs were significantly related to the PC patients' overall survival (OS) (Table 1). Then, we performed multivariate Cox regression analysis to screen the optimal prognostic lncRNAs. Finally, a total of seven lncRNAs were identified (Table 2). Among these lncRNAs, AC245041.2 and LINC02257 were risk factors ($HR > 1$), and AC006504.8, AC012306.2, AC125494.2, FLVCR1-DT, and AC005332.6 were protective factors ($HR < 1$).

Survival Analysis of Autophagy-Associated lncRNAs

Kaplan–Meier survival analyses and log-rank tests for each autophagy-associated lncRNA were performed to evaluate the prognostic characteristics of patients with PC. K-M survival curves of the seven autophagy-associated lncRNAs are shown that the high expression of AC005332.6, AC006504.8, AC012306.2, AC125494.2, and FLVCR1-DT were positively correlated with the longer overall survival of patients with PC ($p < 0.01$), indicating protective impacts of these lncRNAs in PC development (Figure 1A). Furthermore, the high expression of AC245041.2 and LINC02257 was correlated with a short survival time ($p < 0.01$), which meant that these lncRNAs could play a carcinogenic role in PC (Figure 1B).

Construction and Validation of the Risk Score Evaluation System of the Autophagy-Associated lncRNAs

Based on seven lncRNAs that were significantly correlated with overall survival, the autophagy-associated lncRNA signature was constructed to predict the outcome of PC patients. The final risk score formula was as follows: Risk score = ($-0.3765 \times$ expression level of AC006504.8) + ($-0.5525 \times$ expression level of FLVCR1-DT) + ($-0.4120 \times$ expression level of AC012306.2) + ($-0.5192 \times$ expression level of AC125494.2) + ($-0.1040 \times$ expression level of AC005332.6) + ($0.2476 \times$ expression level of AC245041.2) + ($0.2490 \times$ expression level of LINC02257). With the above formula, the risk scores of more than 0.1199 were classified into the high-risk group (88 patients); meanwhile, those with less than the cutoff point belonged to the low-risk group (89 patients). The principal components analysis (PCA) showed that the high-risk and low-risk groups were divided into two obvious distribution patterns, which implied that autophagy made distinctly different effects in two groups (Figure 2A). Based on K-M survival analyses, the patients with low-risk scores had longer survival time than those with high-risk scores; OS had statistical significance between the two subgroups (Figure 2B). We used scatter diagrams to show the risk scores, survival status, and survival time of each PC patient (Figure 2D). The results demonstrated that the PC patient's survival time and rate gradually deteriorated with increasing risk scores. Moreover, lncRNAs' expression

TABLE 1 | Univariate cox regression analysis of prognostic autophagy-associated lncRNAs.

Gene	P value	HR	Lower 95% CI	Upper 95% CI
LINC01004	0.00013	0.669899	0.545603	0.822512
AC005696.1	5.49E-05	0.350479	0.210584	0.58331
AC006504.8	3.04E-05	0.442255	0.301411	0.648913
FLVCR1-DT	0.000122	0.350297	0.205107	0.598264
AC036176.1	0.000401	0.508103	0.349241	0.739229
AC012306.2	1.67E-05	0.513715	0.37932	0.695727
U62317.1	0.000738	1.118986	1.048265	1.194478
AC127024.5	2.28E-05	0.516408	0.380336	0.701163
AL022328.4	8.62E-05	0.316545	0.178267	0.562082
AL513165.1	0.000402	0.793017	0.697425	0.901711
AC090114.2	5.71E-05	0.421068	0.276314	0.641655
AC125494.2	7.25E-05	0.272869	0.143661	0.518286
AC064836.3	0.000284	0.599275	0.454493	0.790178
AC006449.6	0.000149	0.445464	0.293297	0.676579
AC142472.1	0.00021	0.374297	0.222604	0.629361
AC005332.6	0.000205	0.850786	0.781215	0.926553
LINC01089	0.000315	0.763742	0.659587	0.884345
AL022328.1	0.000578	0.573619	0.417996	0.787182
ST20-AS1	7.66E-05	0.19611	0.087474	0.439665
AL122010.1	3.35E-05	0.538231	0.401665	0.72123
AC245041.2	7.99E-05	1.222149	1.106203	1.350247
AC005332.5	0.000223	0.571746	0.424898	0.769345
AC005332.3	7.90E-06	0.735942	0.643327	0.841889
AL358472.2	3.22E-05	0.28793	0.160095	0.517842
AC020765.2	0.000811	0.397367	0.231539	0.681963
PTOV1-AS2	0.000333	0.822028	0.738571	0.914916
AC145207.5	8.70E-05	0.347442	0.204919	0.58909
LINC01705	8.72E-05	1.108166	1.052746	1.166504
LINC02257	6.07E-06	1.525904	1.270616	1.832484

HR, hazard ratio; CI, confidence interval.

TABLE 2 | Multivariate cox regression analysis of prognostic autophagy-associated gene.

Gene	Coef	HR	Lower 95% CI	Upper 95% CI
AC006504.8	-0.3765	0.6862	0.4339	1.0853
FLVCR1-DT	-0.5525	0.5755	0.3283	1.0090
AC012306.2	-0.4120	0.6623	0.4618	0.9500
AC005332.6	-0.1040	0.9012	0.8152	0.9964
AC125494.2	-0.5192	0.5950	0.3221	1.0991
AC245041.2	0.2093	1.2328	1.0870	1.3982
LINC02257	0.2490	1.2828	1.0257	1.6043

Coef, coefficient; HR, hazard ratio; CI, confidence interval.

profiles were shown by a heatmap plot (**Figure 2F**). We extracted the PACA-CA cohort from the ICGC database to further validated the prognostic stability of the risk evaluation system. Then, we utilized the same formula and cutoff value above to classify the PC patients into low-risk and high-risk groups according to the TCGA dataset. Similarly, the patients from the high-risk group (66 patients) had a lower survival time than the low-risk group (76 patients) (**Figure 2C**). Moreover, the scatter diagrams and a heatmap plot of lncRNAs expression profiles were also shown (**Figures 2E, G**).

The Autophagy-Related lncRNA Signature Was an Independent Prognostic Factor

Subsequently, univariate and multivariate Cox regression analyses were conducted to screen potential biomarkers

correlated with OS and total clinical information (**Figures 3A, B**). The results showed that only the prognostic value of the risk score was statistically significant. Finally, the receiver operating characteristic (ROC) curve analysis and the AUC value were utilized to assess the prediction accuracy of the above results. The AUC value of risk score based on expression profiles of autophagy-associated lncRNAs was equal to 0.719, which was much higher than age curve (AUC = 0.534), gender curve (AUC= 0.597), grade curve (AUC= 0.607), stage curve (AUC=0.450), T stage curve (AUC=0.504), and N stage curve (AUC= 0.518) (**Figure 3C**), suggesting that the risk score was superior to traditional clinical indicators. Thus, the risk score evaluation system derived from the expression levels of the seven lncRNAs was the unique independent prognostic indicator of survival time for PC patients.

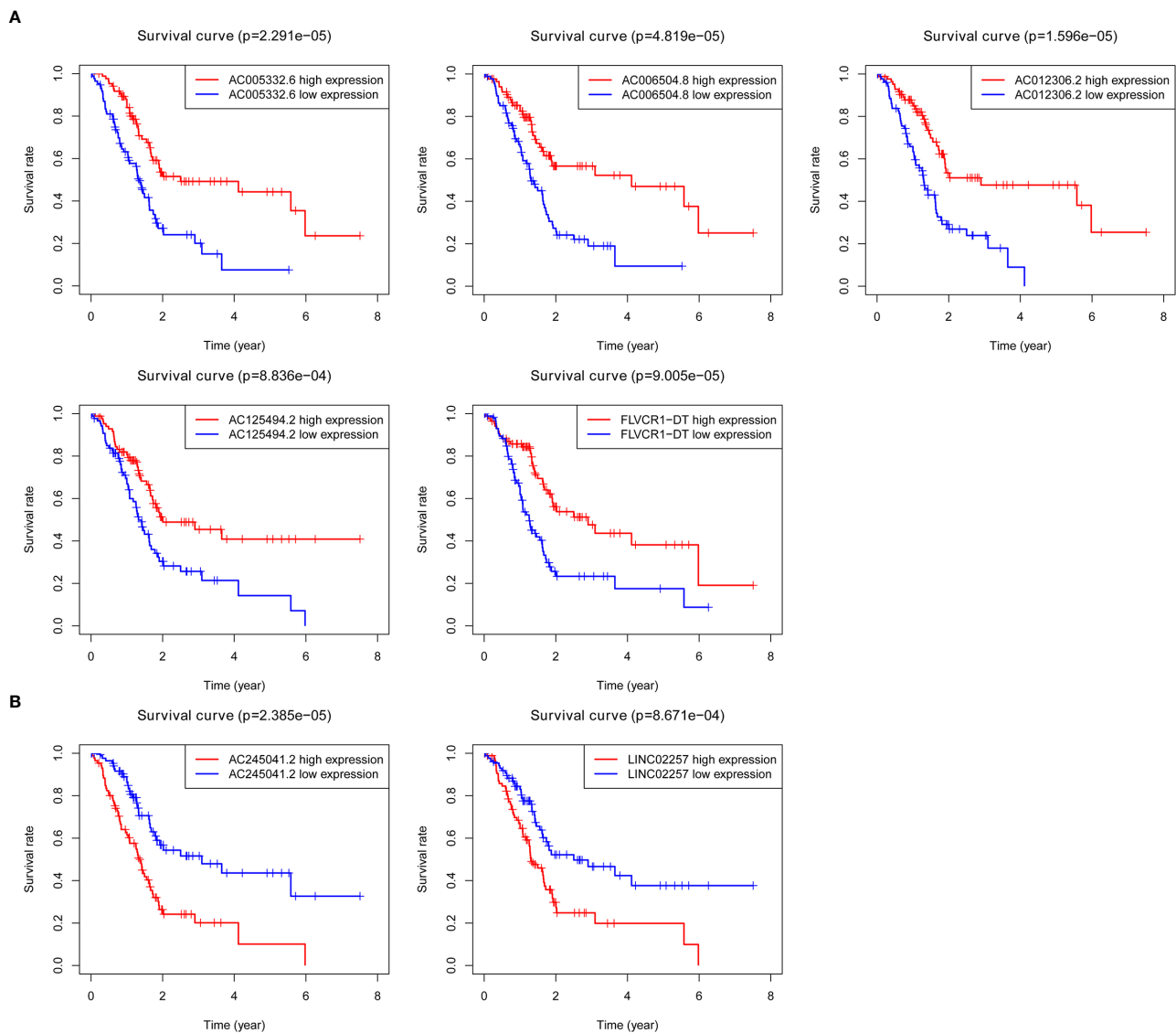


FIGURE 1 | Survival analysis for autophagy-associated lncRNAs. Kaplan–Meier survival curves for autophagy-associated lncRNAs that were positively **(A)** or negatively **(B)** related to OS in PC patients.

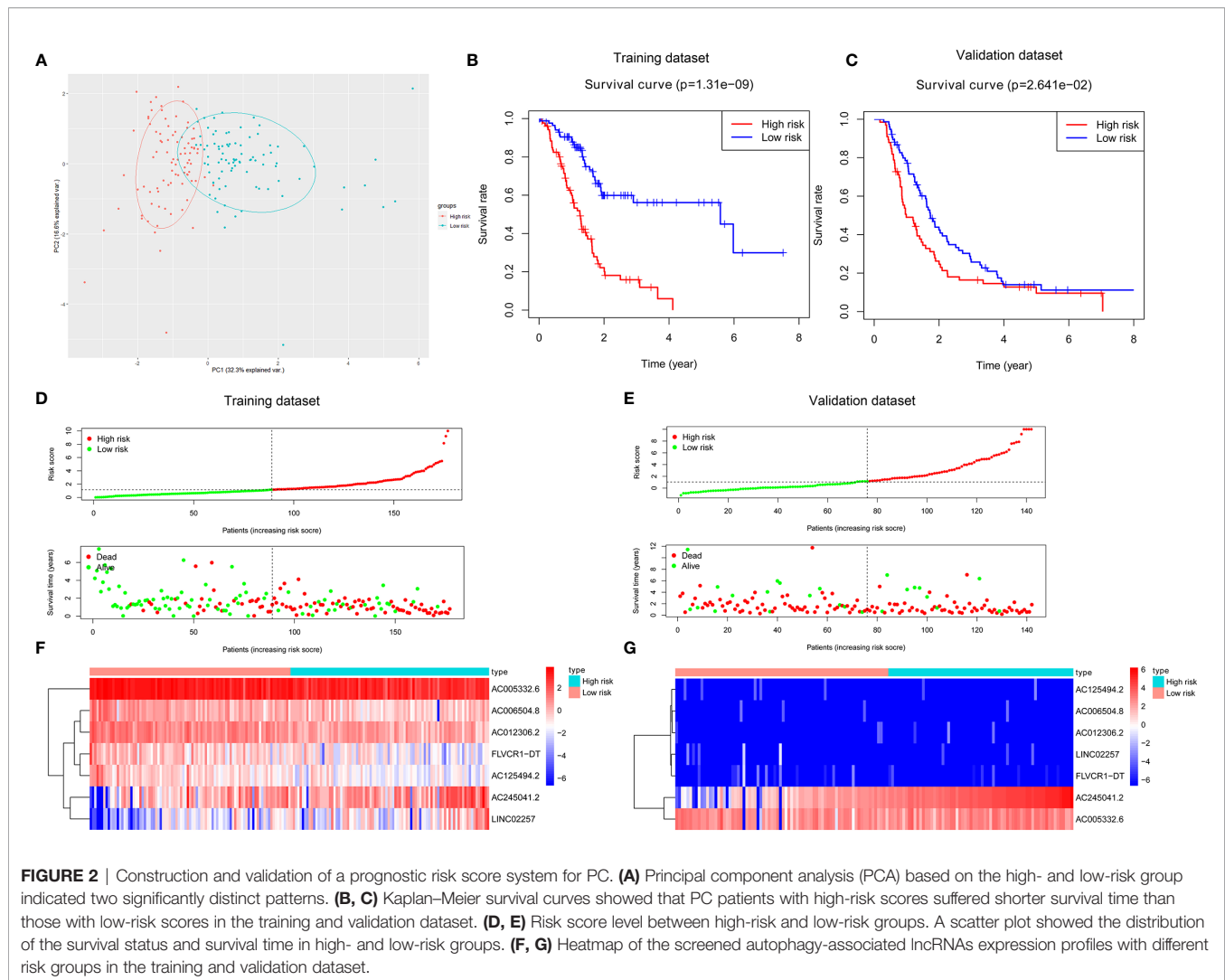
Construction of lncRNA–mRNA Network and Enrichment Analysis of GO and KEGG

Based on the abovementioned analysis, to better understand the potential effect of lncRNAs on mRNAs in PC, we built the lncRNA–mRNA network and used Cytoscape and Sankey diagram to visualize the network. We constructed the lncRNA–mRNA co-expression network using the screened seven autophagy-associated lncRNAs with Pearson correlation analysis ($|R| > 0.4$ and $P < 0.05$). A total of 61 lncRNA–mRNA pairs were filtrated and the correlation between lncRNAs, mRNAs, and risk score groups by the Sankey diagram (Figures 4A, B). Furthermore, GO enrichment analysis was performed to clarify the biological processes, cellular components, and molecular function of mRNAs, which were identified from the lncRNA–mRNA co-expression network. As shown in bubble plot

revealing top 10 GO terms, We found that the foremost biological processes were “autophagy”, “process utilizing autophagic mechanism”, and “macroautophagy”; the top three cellular components were “autophagosome”, “vacuolar membrane”, and “phagophore assembly site”; the top three molecular functions were “ubiquitin protein ligase binding”, “ubiquitin-like protein ligase binding”, and “protein serine/threonine kinase activity” (Figure 4C). KEGG enrichment analysis was shown that autophagy, shigellosis, PI3K–Akt signaling pathway, and FoxO signaling pathway were the top four significantly enriched pathways (Figure 4D).

Gene Set Enrichment Analysis (GSEA)

We carried out the GSEA of the PC samples based on the TCGA to identify the biological pathways associated with the high-risk



group and low-risk group. We did not discover a significantly enriched pathway in the high-risk group; moreover, the low-risk group was most significantly enriched for “neuroactive ligand receptor interaction”, “tryptophan metabolism”, “lysine degradation”, “glycosphingolipid biosynthesis ganglio series”, “regulation of autophagy”, “inositol phosphate metabolism”, “glycerophospholipid metabolism”, “fatty acid metabolism”, etc (**Figure 5**). In summary, the GSEA analysis results elaborated that the low-risk score group was closely correlated with autophagy and metabolism. These KEGG data may provide valuable targets to treat for PC.

Expression of Seven Autophagy-Associated lncRNAs in HPNE and PANC-1 Cells

As is evident from **Figures 1A, B**, AC005332.6, AC006504.8, AC012306.2, AC125494.2, and FLVCR1-DT may protective factors; moreover, AC245041.2 and LINC02257 were carcinogenic factors in PC. Therefore, we analyzed the

expression of these lncRNAs in the PC cell line PANC-1 and normal human pancreatic ductal epithelium cell line HPNE. Our results indicated that AC245041.2 and LINC02257 were high-expressed in PANC-1. The expression of FLVCR1-DT and AC006504.8 was not statistically different between PANC-1 and HPNE, while the low expression of AC005332.6, AC012306.2, and AC125494.2 were in PANC-1 (**Figure 6**).

DISCUSSION

PC is a highly malignant digestive cancer with the lowest five-year survival rate in various types of cancer and is predicted to be the second leading cause of cancer-related death in the U.S. by 2030 (10). Most patients with PC cannot be diagnosed early; meanwhile, carbohydrate antigen (CA19-9) as a conventional diagnostic biomarker is not applied to specifically and sensitively diagnose the PC patients (11, 12). Only a small part of PC patients can be treated by traditional surgery, and a large number

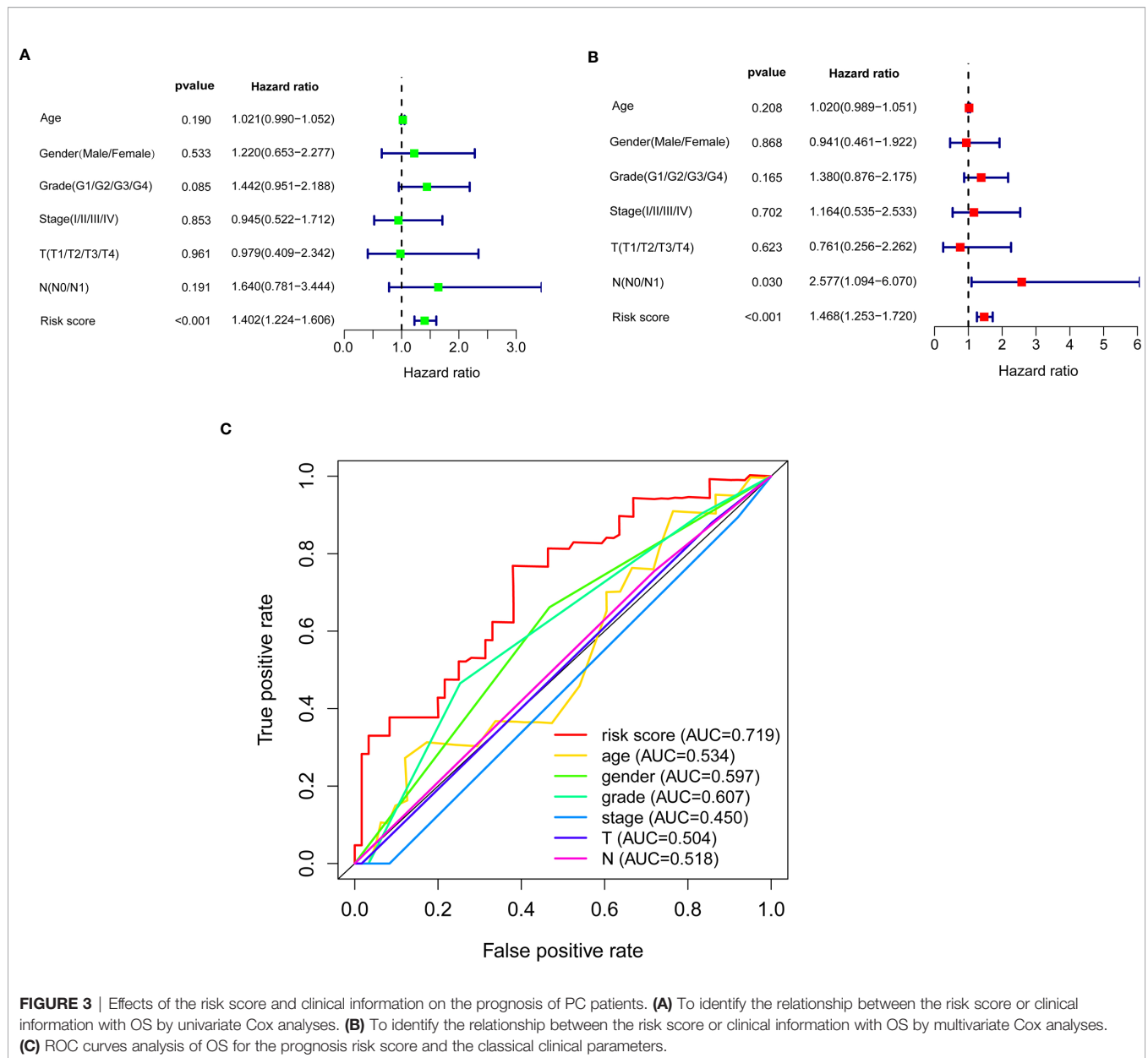
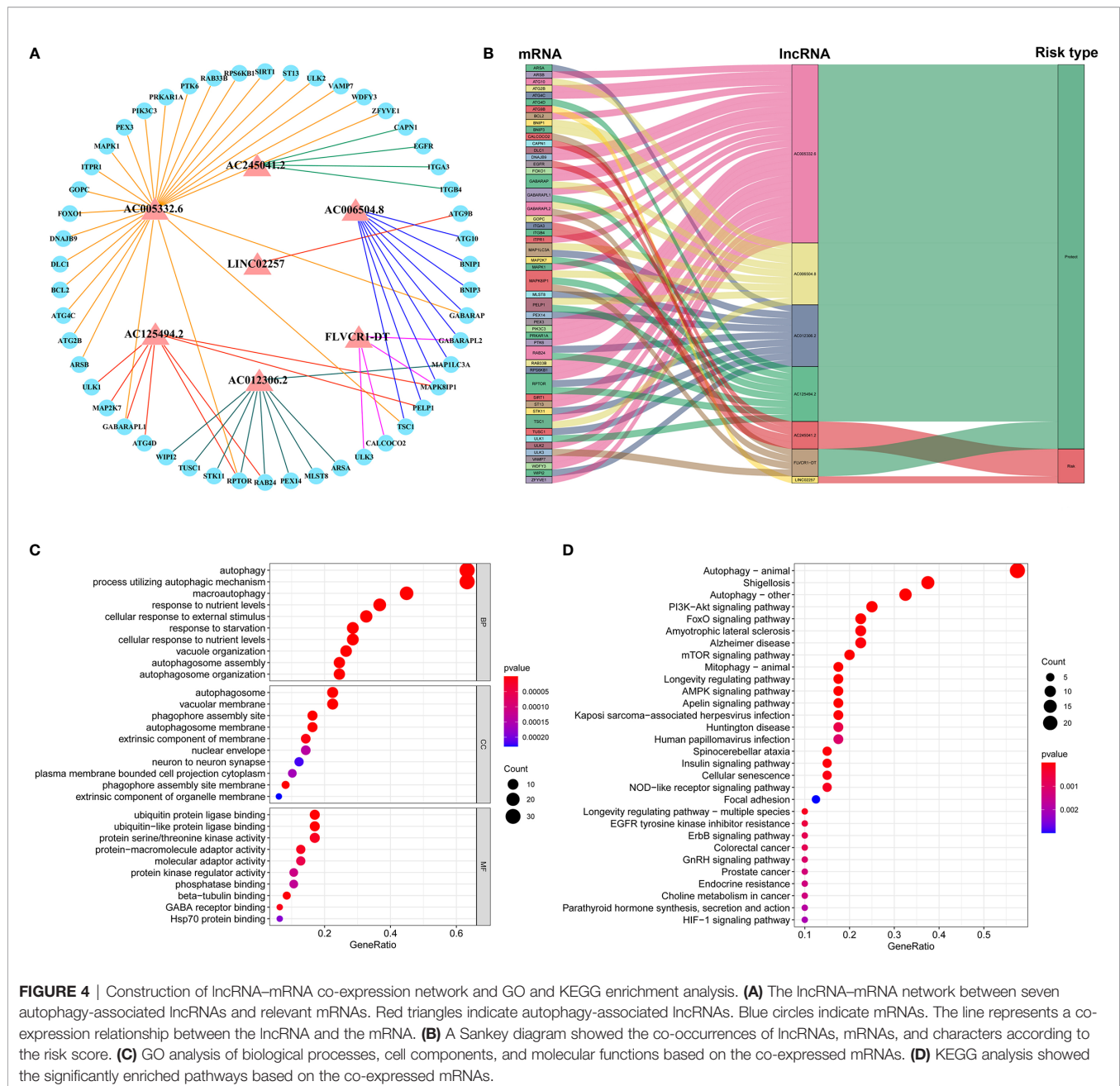


FIGURE 3 | Effects of the risk score and clinical information on the prognosis of PC patients. **(A)** To identify the relationship between the risk score or clinical information with OS by univariate Cox analyses. **(B)** To identify the relationship between the risk score or clinical information with OS by multivariate Cox analyses. **(C)** ROC curves analysis of OS for the prognosis risk score and the classical clinical parameters.

of patients suffer from tumor recurrence and progression. Consequently, the identification of PC regulatory factors has become the focus of recent clinical and basic research. To detect PC early and provide new therapeutic options are of great importance. Currently, lncRNAs have been found to play vital roles in PC and are indispensable for carcinogenetic function, especially autophagy (13, 14). An increasing amount of evidence has shown that autophagy-associated lncRNAs make great effects on the occurrence, development, and prognosis of cancer (15).

To better understand the roles of lncRNAs involved with autophagy in the occurrence of PC. Firstly, we analyzed the expression profiles of lncRNAs in PC patients from the TCGA database. We used Pearson analysis to identify the co-expression relationship between lncRNAs and autophagy-related genes in

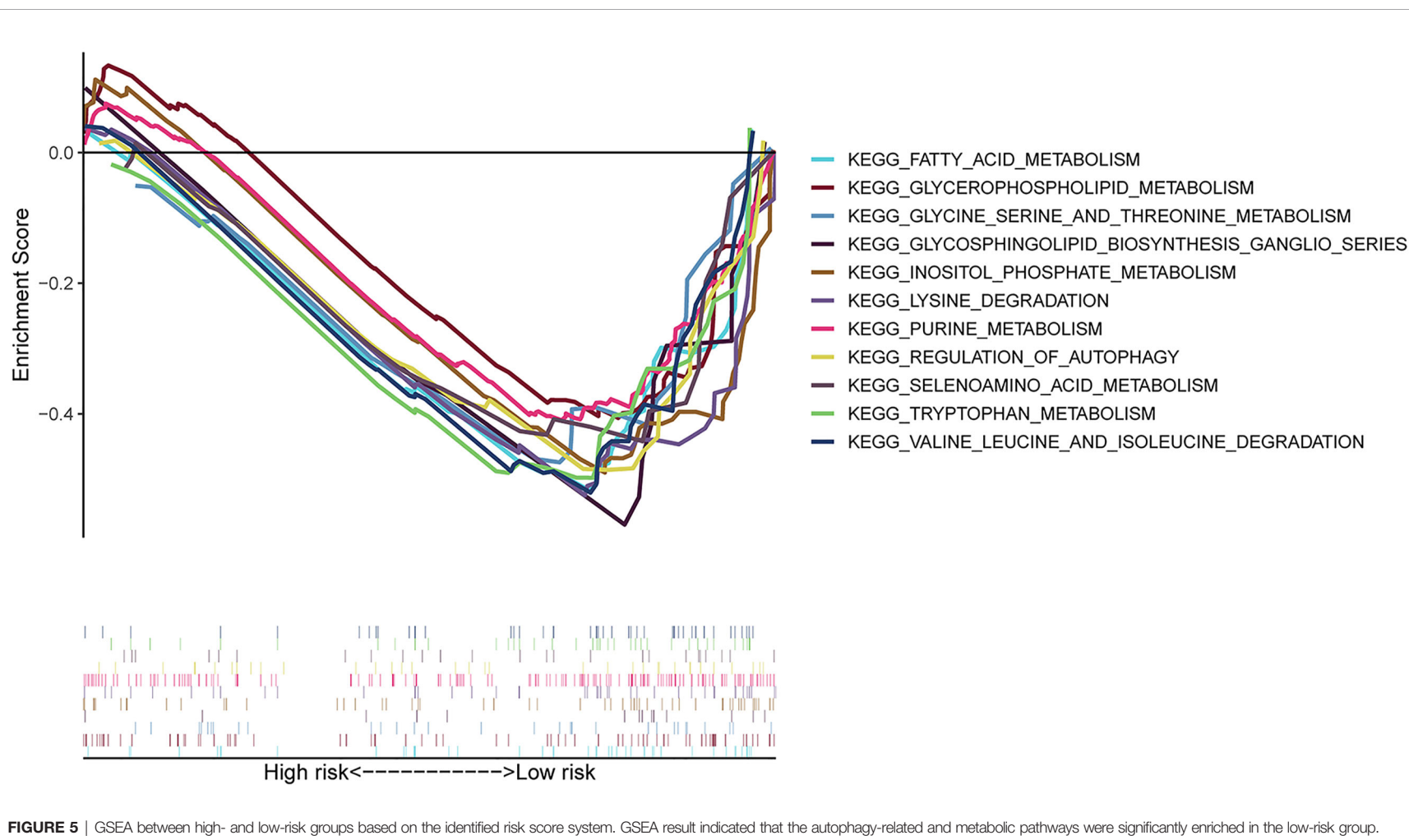
The Human Autophagy Database. Seven autophagy-associated lncRNAs significantly correlated with survival were selected to build the risk score system *via* the multivariate Cox regression analysis. The high- and low-risk patients can be distinguished according to the median risk score, and PCA analysis displayed a significantly distinct distribution between these two groups. Notably, low-risk patients had a better prognosis than patients in the high-risk group. To assess the potency of the risk score model, we utilized the data from the ICGC database as a validation dataset and got the same result. The AUC value that was calculated from the ROC curves indicated that the risk score had considerable prognostic accuracy for PC patients. Furthermore, the risk score was considered as an independent prognostic factor by univariate and multivariate Cox regression analysis.



lncRNAs play an important role in affecting mRNA expression through regulating histone modifications, DNA methylation, and acting as miRNA sponges or precursors of miRNAs, involving the process of transcriptional regulation, post-transcriptional regulation, and epigenetic regulation (16). To elucidate the probable roles of the seven autophagy-associated lncRNAs in PC, the lncRNA-mRNA co-expression network was constructed. The GO and KEGG enrichment analysis was subsequently performed on these mRNAs related to screened lncRNAs, and the results showed that the top enriched GO and KEGG terms were significantly correlated with autophagy. Subsequently, as shown in the GSEA result, we observed that

the low-risk group enriched many pathways about lipid, amino acid metabolism, and autophagy, suggesting that metabolism and autophagy were greatly associated with the PC patients of the low-risk score. The above results have shown that the specific autophagy mechanisms were closely related to PC progression.

Besides, there are some limitations that exist in our study. We built the co-expression network between the lncRNAs and mRNA, but how the lncRNAs make specific effects on mRNA was unknown. Furthermore, the autophagy-associated lncRNAs were only detected in PANC-1 and HPNE. The specific molecular mechanisms have not been verified in the experiments. Furthermore, in the existing studies, there are



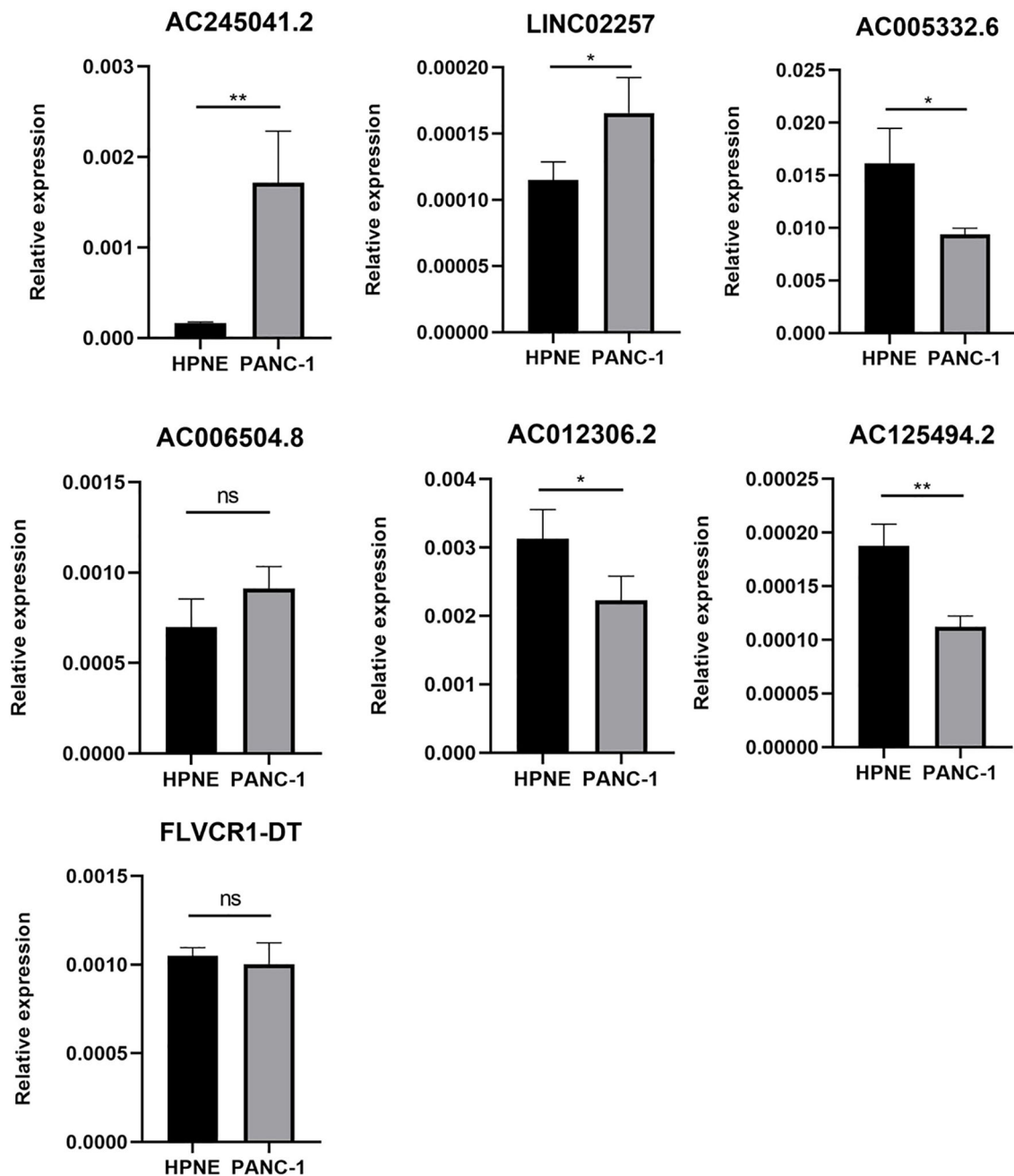


FIGURE 6 | Expression of 7 lncRNAs in HPNE and PANC-1 cells. The qRT-PCR result showed that AC245041.2 and LINC02257 were high-expressed in PANC-1. AC005332.6, AC012306.2, AC125494.2 were low-expressed in PANC-1. The expression of FLVCR1-DT and AC006504.8 was not statistically different between PANC-1 and HPNE. * $P < 0.05$, ** $P < 0.01$, NS, no statistically significant.

only a few bioinformatic analyses about some lncRNAs in our risk score system. Chen J et al. found that AC245041.2 was a risk factor in clear cell renal cell carcinoma (ccRCC) and high expression of AC245041.2 was associated with a poor outcome for patients with ccRCC (17). LINC02257 was found to correlate with the prognosis of patients with colorectal cancer and was a risk factor (18). Besides, AC006504.8 was a risk factor in

cholangiocarcinoma (19). Concerning the filtered lncRNAs, we need exploratory experiments to prove the functions deeply.

In conclusion, we successfully established the risk score system based on the seven autophagy-associated lncRNAs; meanwhile, it was an independent prognostic factor in PC patients. This approach enhances the prediction accuracy for target lncRNAs, and these autophagy-associated lncRNAs might

be of great significance for the prediction of prognosis and therapeutic markers for PC patients.

DATA AVAILABILITY STATEMENT

Publicly available datasets were analyzed in this study. This data can be found here: The Human Autophagy Database (<http://www.autophagy.lu/>), The Cancer Genome Atlas (<https://portal.gdc.cancer.gov/>) and International Cancer Genome Consortium (<https://icgc.org>).

ETHICS STATEMENT

The studies involving human participants were reviewed and approved by The Ethics Committee of Peking Union Medical College Hospital. The patients/participants provided their written informed consent to participate in this study.

AUTHOR CONTRIBUTIONS

GC analyzed the data and wrote the manuscript. TZ and YZ conceived the study and obtained financial support. LY and JL

applied guiding suggestion, GY, JY, CQ, WL, JQ, and FZ prepared the dataset. All authors contributed to the article and approved the submitted version.

FUNDING

This study was supported by grants from the National Natural Science Foundation of China (No. 81772639, No.81802475, No.81972258, No.81974376); Natural Science Foundation of Beijing (No. 7192157); CAMS Innovation Fund for Medical Sciences (CIFMS) (No.2016-I2M-1-001); National Key R&D Program of China (2018YFE0118600); Non-profit Central Research Institute Fund of Chinese Academy of Medical Sciences (2019XK320001). The funder bodies were not involved in the study design, collection, analysis, interpretation of data, the writing of this article or the decision to submit it for publication.

ACKNOWLEDGMENTS

Thanks to all who have contributed to the process of writing this article. Especially, I appreciate that SWT and CTX offered me sufficient information and pointed out correct directions on time. Lastly, I'd like to thank those leaders, teachers, and my families who have encouraged me.

REFERENCES

- Siegel RL, Miller KD, Jemal A. Cancer Statistics, 2020. *CA: Cancer J Clin* (2020) 70(1):7–30. doi: 10.3322/caac.21590
- Chen W, Zheng R, Baade PD, Zhang S, Zeng H, Bray F, et al. Cancer Statistics in China, 2015. *CA: Cancer J Clin* (2016) 66(2):115–32. doi: 10.3322/caac.21338
- Stathis A, Moore MJ. Advanced Pancreatic Carcinoma: Current Treatment and Future Challenges. *Nat Rev Clin Oncol* (2010) 7(3):163–72. doi: 10.1038/nrclinonc.2009.236
- Kenific CM, Debnath J. Cellular and Metabolic Functions for Autophagy in Cancer Cells. *Trends Cell Biol* (2015) 25(1):37–45. doi: 10.1016/j.tcb.2014.09.001
- New M, Van Acker T, Long JS, Sakamaki JL, Ryan KM, Tooze SA. Molecular Pathways Controlling Autophagy in Pancreatic Cancer. *Front Oncol* (2017) 7:28. doi: 10.3389/fonc.2017.00028
- Peng WX, Koirala P, Mo YY. LncRNA-mediated Regulation of Cell Signaling in Cancer. *Oncogene* (2017) 36(41):5661–7. doi: 10.1038/ncr.2017.184
- Zhang W, Liu Y, Fu Y, Han W, Xu H, Wen L, et al. Long Non-Coding RNA LINC00160 Functions as a Decoy of microRNA-132 to Mediate Autophagy and Drug Resistance in Hepatocellular Carcinoma Via Inhibition of PIK3R3. *Cancer Lett* (2020) 478:22–33. doi: 10.1016/j.canlet.2020.02.014
- Huang F, Chen W, Peng J, Li Y, Zhuang Y, Zhu Z, et al. Lncrna PVT1 Triggers Cyto-protective Autophagy and Promotes Pancreatic Ductal Adenocarcinoma Development Via the miR-20a-5p/ULK1 Axis. *Mol Cancer* (2018) 17(1):98. doi: 10.1186/s12943-018-0845-6
- Liu C, Wang JO, Zhou WY, Chang XY, Zhang MM, Zhang Y, et al. Long non-Coding RNA LINC01207 Silencing Suppresses AGR2 Expression to Facilitate Autophagy and Apoptosis of Pancreatic Cancer Cells by Sponging Mir-143-5p. *Mol Cell Endocrinol* (2019) 493:110424. doi: 10.1016/j.mce.2019.04.004
- Rahib L, Smith BD, Aizenberg R, Rosenzweig AB, Fleshman JM, Matrisian LM. Projecting Cancer Incidence and Deaths to 2030: The Unexpected Burden of Thyroid, Liver, and Pancreas Cancers in the United States. *Cancer Res* (2014) 74(11):2913–21. doi: 10.1158/0008-5472.Can-14-0155
- O'Brien DP, Sandanayake NS, Jenkinson C, Gentry-Maharaj A, Apostolidou S, Fourkala EO, et al. Serum CA19-9 is Significantly Upregulated Up to 2 Years Before Diagnosis With Pancreatic Cancer: Implications for Early Disease Detection. *Clin Cancer Res An Off J Am Assoc Cancer Res* (2015) 21(3):622–31. doi: 10.1158/1078-0432.Ccr-14-0365
- Duffy MJ, Sturgeon C, Lamerz R, Haglund C, Holubec VL, Klapdor R, et al. Tumor Markers in Pancreatic Cancer: A European Group on Tumor Markers (EGTM) Status Report. *Ann Oncol Off J Eur Soc Med Oncol* (2010) 21(3):441–7. doi: 10.1093/annonc/ndp332
- Zhou C, Yi C, Yi Y, Qin W, Yan Y, Dong X, et al. Lncrna PVT1 Promotes Gemcitabine Resistance of Pancreatic Cancer Via Activating Wnt/ β -Catenin and Autophagy Pathway Through Modulating the miR-619-5p/Pygo2 and miR-619-5p/ATG14 Axes. *Mol Cancer* (2020) 19(1):118. doi: 10.1186/s12943-020-01237-y
- Wei DM, Jiang MT, Lin P, Yang H, Dang YW, Yu Q, et al. Potential ceRNA Networks Involved in Autophagy Suppression of Pancreatic Cancer Caused by Chloroquine Diphosphate: A Study Based on Differentially-Expressed circRNAs, lncRNAs, miRNAs and Mrnas. *Int J Oncol* (2019) 54(2):600–26. doi: 10.3892/ijo.2018.4660
- Sun T. Long Noncoding RNAs Act as Regulators of Autophagy in Cancer. *Pharmacol Res* (2018) 129:151–5. doi: 10.1016/j.phrs.2017.11.009
- Zhang X, Wang W, Zhu W, Dong J, Cheng Y, Yin Z, et al. Mechanisms and Functions of Long Non-Coding RNAs At Multiple Regulatory Levels. *Int J Mol Sci* (2019) 20(22):5573. doi: 10.3390/ijms20225573
- Wang S, Chai K, Chen J. A Novel Prognostic Nomogram Based on 5 Long non-Coding RNAs in Clear Cell Renal Cell Carcinoma. *Oncol Lett* (2019) 18(6):6605–13. doi: 10.3892/ol.2019.11009
- Wang X, Zhou J, Xu M, Yan Y, Huang L, Kuang Y, et al. A 15-lncRNA Signature Predicts Survival and Functions as a ceRNA in Patients With Colorectal Cancer. *Cancer Manage Res* (2018) 10:5799–806. doi: 10.2147/cmar.S178732

19. Xie X, Wang Y, Zhang S, Li J, Yu Z, Ding X, et al. A Novel Five-lncRNA Signature Panel Improves High-Risk Survival Prediction in Patients With Cholangiocarcinoma. *Aging* (2021) 13(2):2959–81. doi: 10.18632/aging.202446

Conflict of Interest: The authors declare that the research was conducted in the absence of any commercial or financial relationships that could be construed as a potential conflict of interest.

Copyright © 2021 Chen, Yang, Long, Yang, Qin, Luo, Qiu, Zhao, You, Zhang and Zhao. This is an open-access article distributed under the terms of the Creative Commons Attribution License (CC BY). The use, distribution or reproduction in other forums is permitted, provided the original author(s) and the copyright owner(s) are credited and that the original publication in this journal is cited, in accordance with accepted academic practice. No use, distribution or reproduction is permitted which does not comply with these terms.



Immune Subtypes Based on Immune-Related lncRNA: Differential Prognostic Mechanism of Pancreatic Cancer

Qiyao Zhang^{1,2,3,4†}, Zhihui Wang^{1,2,3,4†}, Xiao Yu^{1,2,3,4†}, Menggang Zhang^{1,2,3,4}, Qingyuan Zheng^{1,2,3,4}, Yuting He^{1,2,3,4*} and Wenzhi Guo^{1,2,3,4*}

¹ Department of Hepatobiliary and Pancreatic Surgery, The First Affiliated Hospital of Zhengzhou University, Zhengzhou, China, ² Key Laboratory of Hepatobiliary and Pancreatic Surgery and Digestive Organ Transplantation of Henan Province, The First Affiliated Hospital of Zhengzhou University, Zhengzhou, China, ³ Open and Key Laboratory of Hepatobiliary and Pancreatic Surgery and Digestive Organ Transplantation at Henan Universities, Zhengzhou, China, ⁴ Henan Key Laboratory of Digestive Organ Transplantation, Zhengzhou, China

OPEN ACCESS

Edited by:

Zong Sheng Guo,
University of Pittsburgh, United States

Reviewed by:

Qiuyan Guo,
First Affiliated Hospital of Harbin
Medical University, China
Xiaomin Ying,
Beijing Institute of Basic Medical
Sciences, China

*Correspondence:

Yuting He
fcchey11@zzu.edu.cn
Wenzhi Guo
fccguowz@zzu.edu.cn

[†] These authors have contributed
equally to this work

Specialty section:

This article was submitted to
Molecular and Cellular Oncology,
a section of the journal
Frontiers in Cell and Developmental
Biology

Received: 21 April 2021

Accepted: 17 June 2021

Published: 07 July 2021

Citation:

Zhang Q, Wang Z, Yu X, Zhang M,
Zheng Q, He Y and Guo W (2021)
Immune Subtypes Based on
Immune-Related lncRNA: Differential
Prognostic Mechanism of Pancreatic
Cancer.
Front. Cell Dev. Biol. 9:698296.
doi: 10.3389/fcell.2021.698296

Pancreatic cancer consists one of tumors with the highest degree of malignancy and the worst prognosis. To date, immunotherapy has become an effective means to improve the prognosis of patients with pancreatic cancer. Long non-coding RNAs (lncRNAs) have also been associated with the immune response. However, the role of immune-related lncRNAs in the immune response of pancreatic cancer remains unclear. In this study, we identified immune-related lncRNA pairs through a new combinatorial algorithm, and then clustered and deeply analyzed the immune characteristics and functional differences between subtypes. Subsequently, the prognostic model of 3 candidate lncRNA pairs was determined by multivariate COX analysis. The results showed significant prognostic differences between the C1 and C2 subtypes, which may be due to the differential infiltration of CTL and NK cells and the activation of tumor-related pathways. The prognostic model of the 3 lncRNA pairs (AC244035.1_vs._AC063926.1, AC066612.1_vs._AC090124.1, and AC244035.1_vs._LINC01885) was established, which exhibits stable and effective prognostic prediction performance. These 3 lncRNA pairs may regulate the anti-tumor effect of immune cells through ion channel pathways. In conclusion, our research demonstrated the panoramic differences in immune characteristics between subtypes and stable prognostic models, and identified new potential targets for immunotherapy.

Keywords: pancreatic cancer, immunotherapy, NMF, prognosis, lncRNA pairs

INTRODUCTION

As one of the most malignant tumors, pancreatic adenocarcinoma (PAAD) is the seventh leading cause of cancer-related deaths, which is responsible more than 430,000 deaths each year worldwide (Bray et al., 2018; Ferlay et al., 2019; Khalaf et al., 2020). Although surgical treatment, radiotherapy, chemotherapy and targeted therapy for PAAD have made significant progress in the past decades, due to the rapid progress of the condition and the limitations of treatment methods, the 5-year

survival rate of PAAD patients still does not exceed 5% (David et al., 2009; Von Hoff et al., 2013; Miller et al., 2019). Most PAAD patients still need to rely on chemotherapy and palliative care. However, chemotherapies such as FOLFIRINOX can increase the patients' median survival time only by 2–4 months and have obvious side effects (Vaccaro et al., 2011). Therefore, there is an urgent need to further explore the mechanism of occurrence and development of pancreatic cancer, as well as to find novel therapeutic targets to improve the prognosis of PAAD patients.

In recent years, immunotherapy has made tremendous breakthroughs and seems to have become a new hot topic in cancer treatment (Mellman et al., 2011; Chen et al., 2017). Immune checkpoint inhibitors (ICIs) have been used in a variety of cancers including pancreatic cancer (Long et al., 2017; Wu et al., 2019). ICIs can restore the anti-tumor response of the immune system and prevent tumors from evading immune surveillance through immune checkpoint signaling pathways (Kythreotou et al., 2018; Yi et al., 2018). However, immunotherapy improves only some PAAD patients' condition (Glatzer et al., 2020). Therefore, exploring the immune characteristics of pancreatic cancer and finding new immunotherapy targets are of great significance for improved immunotherapy effects for patients.

Long non-coding RNAs (lncRNAs) are RNAs with a length longer than 200 nucleotides, which are generally considered not translated directly into proteins. Instead, as indicated by a large number of studies in recent years, lncRNAs regulate translation efficiency by binding to mRNAs and exert their biological functions in this manner (Mercer et al., 2009; Castellanos-Rubio and Ghosh, 2019). Evidence shows that lncRNAs are potential immune regulators, deeply involved in cellular immune and inflammatory processes (Geng and Tan, 2016; Chen J. et al., 2019). For example, as a pseudogene of Rps15a-ps4, lncRNA Lethe can block NF- κ B-DNA binding, thereby promoting the anti-inflammatory effect of dexamethasone (Rapicavoli et al., 2013). However, the mechanism of how immune-related lncRNAs affect the prognosis of PAAD patients is still not fully understood.

In this study, we identified immune-related lncRNA pairs by combining the lncRNA expression profile data of PAAD patients with the immune gene library, and clustered two molecular subtypes based on this pairing. We then comprehensively analyzed the differences in prognosis, immune characteristics, gene mutations and potential functions between subtypes. Finally, univariate and multivariate cox analyses were performed to construct a prognostic model based on 3 selected lncRNA pairs. After a variety of verifications, the model was proven to have stable and independent prognostic prediction performance.

MATERIALS AND METHODS

Data Source and Preprocessing

The most up-to-date expression profile data and clinical follow-up information of PAAD patients were downloaded from

the TCGA database¹ on March 17, 2021. Subsequently, we processed the RNA-Seq data of TCGA-PAAD according to the following steps: (1) Remove samples without clinical follow-up information; (2) Remove samples without survival time; (3) Exclude samples without survival status; (4) Convert ensemble to gene symbol; (5) Take genes with multiple Gene Symbols as the median value of their expression. The TCGA-PAAD cohort after data preprocessing contained a total of 176 samples. The expression profile data and follow-up information of the ICGA-PACA-CA cohort (167 samples in total) were downloaded from the ICGC database².

Identification and Pairing of IRGs and lncRNAs

The immune-related gene (IRG) set was downloaded from the ImmPort database³, which contains the comprehensive location information and functional attributes of immune-related genes.

The expression profile of TCGA-PAAD was divided into mRNAs and lncRNAs based on the latest version expression profile annotation file downloaded from the GENCODE website⁴. We calculated the co-expression Pearson correlation coefficient and *p*-value among each IRG and lncRNA. According to the threshold of $Cor > 0.8$ and $P < 0.01$, a total of 1,289 lncRNA-IRG pairs were identified, including 466 lncRNAs and 228 IRGs (Supplementary File 1). Next, 466 immune-related lncRNAs were paired in a cycle. In order to eliminate the huge difference among the expression of lncRNAs, we processed the data as follows: we defined C as the expression of the lncRNA pair (lncRNA A and lncRNA B). If the expression level of lncRNA A was higher than lncRNA B, then C was defined as 1; otherwise, C was defined as 0. Based on this technique, we constructed a matrix containing values of 0 and 1. Next, lncRNA pairs with C = 1 accounting for 30~70% of all lncRNA pairs were retained (Hong et al., 2020).

Identification of Immune-Related Molecular Classes Based on NMF

For the lncRNA pairs obtained by the above processing method, we used the *coxph* function in R to perform univariate cox analysis, and thus obtained 217 lncRNA pairs related to the prognosis of PAAD ($P < 0.001$). Subsequently, the non-negative matrix factorization (NMF) algorithm was used to cluster the PAAD samples. The method was set as the standard called "brunet" that performs 100 iterations. The number of clusters *k* was set from 2 to 10, the average contour width of the shared member matrix was determined by the R package NMF, and the minimum member of each sub-category was set to 10.

Immune Characteristics and Tumor Mutation Burden (TMB) Analysis

The characteristics of the 22 immune cells in each sample between subtypes were determined based on the R package

¹<https://portal.gdc.cancer.gov/>

²<https://dacoi.icgc.org/>

³<http://www.immport.org>

⁴<https://www.genecodegenes.org>

CIBERSORT (Chen et al., 2018). The mutation dataset of the TCGA-PAAD cohort was downloaded from the TCGA database and processed by Mutect2 software to analyze the tumor mutation burden (TMB) of each sample.

Construction of Prognostic Risk Model Based on Immune-Related lncRNA Pairs

We used the Fisher's exact test to calculate the differences between the subtypes of each lncRNA pair, and then obtained the adjusted FDR values by the BH method. With $FDR < 0.0001$ as the threshold, we identified a total of 390 differential lncRNA pairs (**Supplementary File 2**). Subsequently, we divided the 176 samples of the TCGA-PAAD queue into a training set and a validation set. In order to ensure the stability of subsequent modeling, all samples were randomly grouped at 1:1 for 100 times with replacement. We chose the best grouping based on the criteria of no significant difference in age distribution, gender, follow-up time, and the proportion of deaths between the two groups. A total of 88 samples were included the training set and 88 samples in the validation set. As shown in **Table 1**, there was no significant difference between the groups ($P > 0.05$).

The multivariate Cox proportional hazard regression model was carried out for the different lncRNA pairs between subtypes using the R survival package, coxph function based on training set. The significance level of $P < 0.05$ was set as the threshold for filtering. Finally, we performed a multivariate COX analysis on the significantly different lncRNAs to obtain the risk coefficients of lncRNA pairs.

Functional Enrichment Analysis

Gene Ontology (GO) is a structured method of gene product annotation, which consists of three parts: biological process (BP), cell component (CC), and molecular function (MF). The Kyoto Encyclopedia of Genes and Genomes (KEGG) is an open gene set pathway enrichment database. In this study, GO and KEGG were performed to further understand the functional differences between subtypes using the R package WebGestaltR (v0.4.2) (Wang et al., 2017). The GO terms and KEGG pathways with $P < 0.05$ were considered to be significantly different. All analytical processes are described in **Figure 1**.

RESULTS

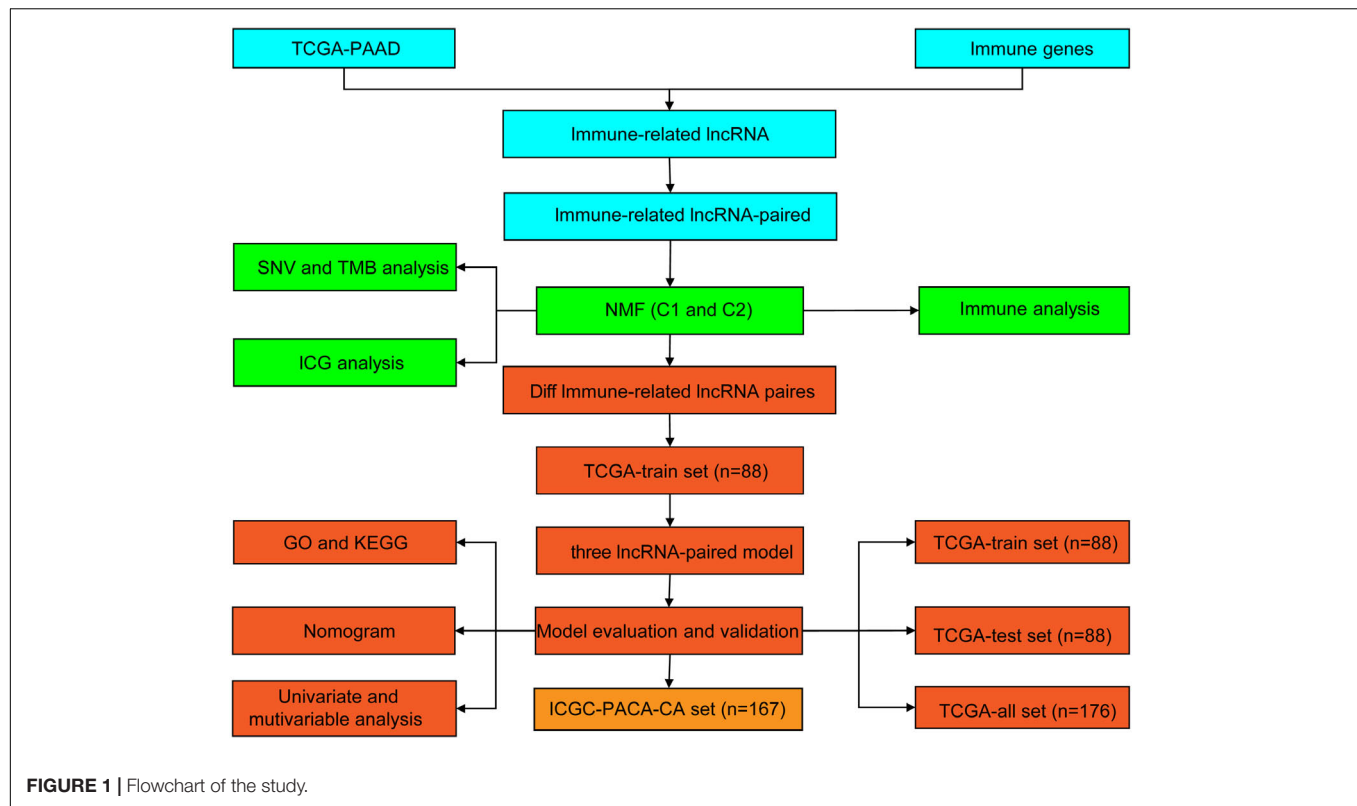
Molecular Typing of PAAD Based on Immune-Related lncRNA Pairs

The immune-related lncRNA pairs were identified through the cyclic pairing of immune lncRNAs. Subsequently, we performed univariate COX analysis of these lncRNA pairs using the coxph function in R. A total of 217 prognostic-related ($P < 0.001$) lncRNA pairs for PAAD were obtained (**Supplementary File 3**). Next, we clustered PAAD samples by non-negative matrix clustering algorithm (NMF) based on the prognostic-related lncRNA pairs (**Supplementary Figure 1**). According to the indicators, such as cophenetic, dispersion and silhouette, we determined the optimal number of clusters as 2 (**Figures 2A,B**).

Accordingly, we divided the samples of the TCGA-PAAD cohort into C1 and C2 subtypes. The further survival analysis between subtypes showed that there were significant differences between them either in terms of overall survival time or progression-free survival (PFS) time. The prognosis of the C1 subtype was much worse than that of the C2 subtype (**Figures 2C,D**).

TABLE 1 | Differences in clinical characteristics between training set and validation set.

Clinical Features	TCGA-train	TCGA-test	P
Event			
Alive	42	42	1
Dead	46	46	
Stage			
I	12	9	0.2715
II	74	71	
III	1	2	
IV	0	4	
X	1	2	
Grade			
G1	16	14	0.3309
G2	50	44	
G3	19	29	
G4	2	0	
GX	1	1	
Age			
≤65	46	47	1
>65	42	41	
T Stage			
T1	6	1	0.3342
T2	10	14	
T3	70	70	
T4	1	2	
TX	1	1	
N Stage			
N0	26	23	0.3709
N1	61	61	
NX	1	4	
M Stage			
M0	40	39	0.1281
M1	0	4	
MX	48	45	
Gender			
Female	39	41	0.8797
Male	49	47	
Alcohol			
NO	32	32	0.4739
YES	48	52	
Unknown	8	4	
Radiation_therapy			
NO	53	48	0.6802
YES	14	18	
Unknown	21	22	
Chemotherapy			
NO	30	30	1
YES	58	58	



Differences of TMB and Common Gene Mutations Between Immune Subtypes

The gene mutation dataset of TCGA-PAAD was downloaded to understand the differences in TMB and gene mutations between subtypes. Results showed that the TMB of the C1 subtype was slightly higher than that of the C2 subtype, although no significant statistical difference was detected (**Figure 3A**). Meanwhile, we also assessed the differences in the number of mutant genes between the samples (**Figure 3B**). There was no difference in the number of mutant genes between the C1 and C2 subtypes. In addition, we showed the mutation characteristics of the top 10 genes with the most frequent mutations in each subtype (**Figure 3C**). Consistently with previous reports, most of the mutations detected in the two subtypes were missense mutations (Zhang et al., 2020). Specifically, only the mutation rate of TP53 in the C1 subtype was significantly higher than that of the C2 subtype ($P = 0.036$).

Differences in Immune Characteristics and Pathway Characteristics Between Subtypes

In order to explore the immune characteristics of the C1 and C2 subtypes, we evaluated the immune cell score of each sample with CIBERSORT (**Figure 4A**). The immune cell scores obtained were different both within and between groups. After statistical testing, we established that the T cell CD8 and Mast cell resting scores in C1 subtype were significantly lower, while the NK cell resting and macrophage M2 cell scores were significantly higher

than those in C2 subtypes (**Figure 4B**). Meanwhile, activated NK cells had a higher score in the C2 subtype, although the difference was not statistically significant. The above results suggest that the poor prognosis of the C1 subtype may be partly due to the inactivation of CTLs and NK cells in the C1 subtype, which causes the immune escape of the tumor. The score of non-polarized M0 macrophages in the C1 subtype was significantly higher than that in C2, which leads to the assumption that the activation of macrophages in C1 subtype was inhibited. Paradoxically, there was no significant difference between M1 and M2, which finding requires further exploration.

Comparison Between TCGA Molecular Subtypes and Existing Immune Subtypes

Thorsson et al. (2018) conducted an extensive tumor immunophenotyping test using more than 10,000 samples of 33 cancers in TCGA. A total of 6 subtypes were identified: wound healing (C1), IFN-gamma dominant (C2), inflammatory (C3), lymphocyte depleted (C4), immunologically quiet (C5), and TGF-beta dominant (C6). Among them, C1 and C2 subtypes correspond to poor prognosis, while C3, C4, and C6 have tumor suppressor effects (Thorsson et al., 2018). By comparing Thorsson and colleague's immune subtypes with those established in our study, results showed that our C1 subtype mostly corresponded to Thorsson's C1 and C2 subtypes, while our C2 subtype had a higher ratio of Thorsson's C3, C4, and C6 (**Figure 4C**). This also illustrates the stability of the subtypes identified herein.

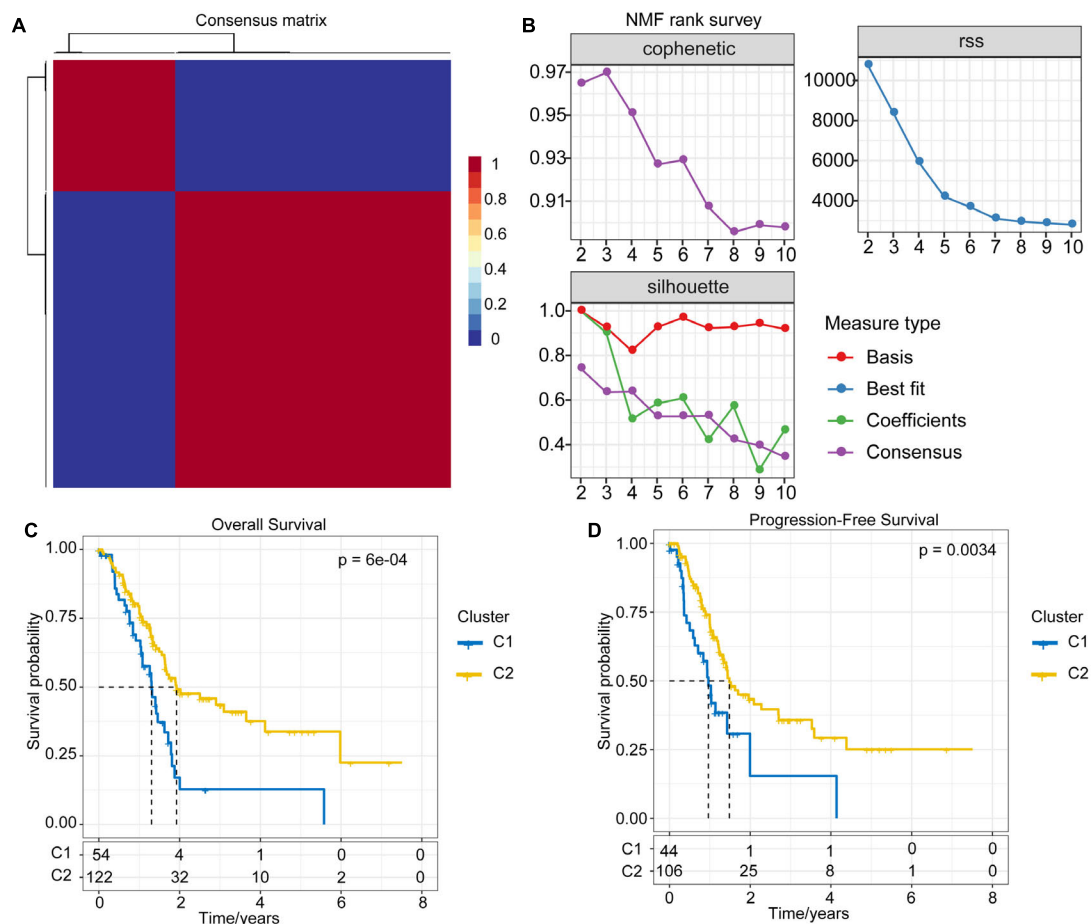


FIGURE 2 | NMF algorithm clustering and prognostic differences between subtypes. **(A)** Consensus map of NMF clustering. **(B)** The cophenetic, RSS and dispersion distributions with rank = 2–10; combining these indicators results in the optimal number of clusters of 2. **(C)** OS time prognostic survival curve of the PAAD molecular subtype. **(D)** PFS time prognostic survival curve of the PAAD molecular subtype.

Gene Set Enrichment Analysis (GSEA) Among Subtypes

The process of GSEA was performed to explore the significantly enriched pathways in each subtype. $P < 0.05$ and $FDR < 0.25$ were set as thresholds to select the enrichment pathways. The results showed that multiple tumor-related pathways, including P53 signaling pathway, DNA replication, Cell cycle, and Base excision repair were enriched in the C1 subtype, while the metabolism-related pathways such as Fatty acid metabolism, Primary bile acid biosynthesis, Renin angiotensin system and Tyrosine metabolism were enriched in C2 (Figures 4D,E). This implies that the poor prognosis of C1 may be due to the further activation of tumor-related pathways and the inhibition of normal metabolism.

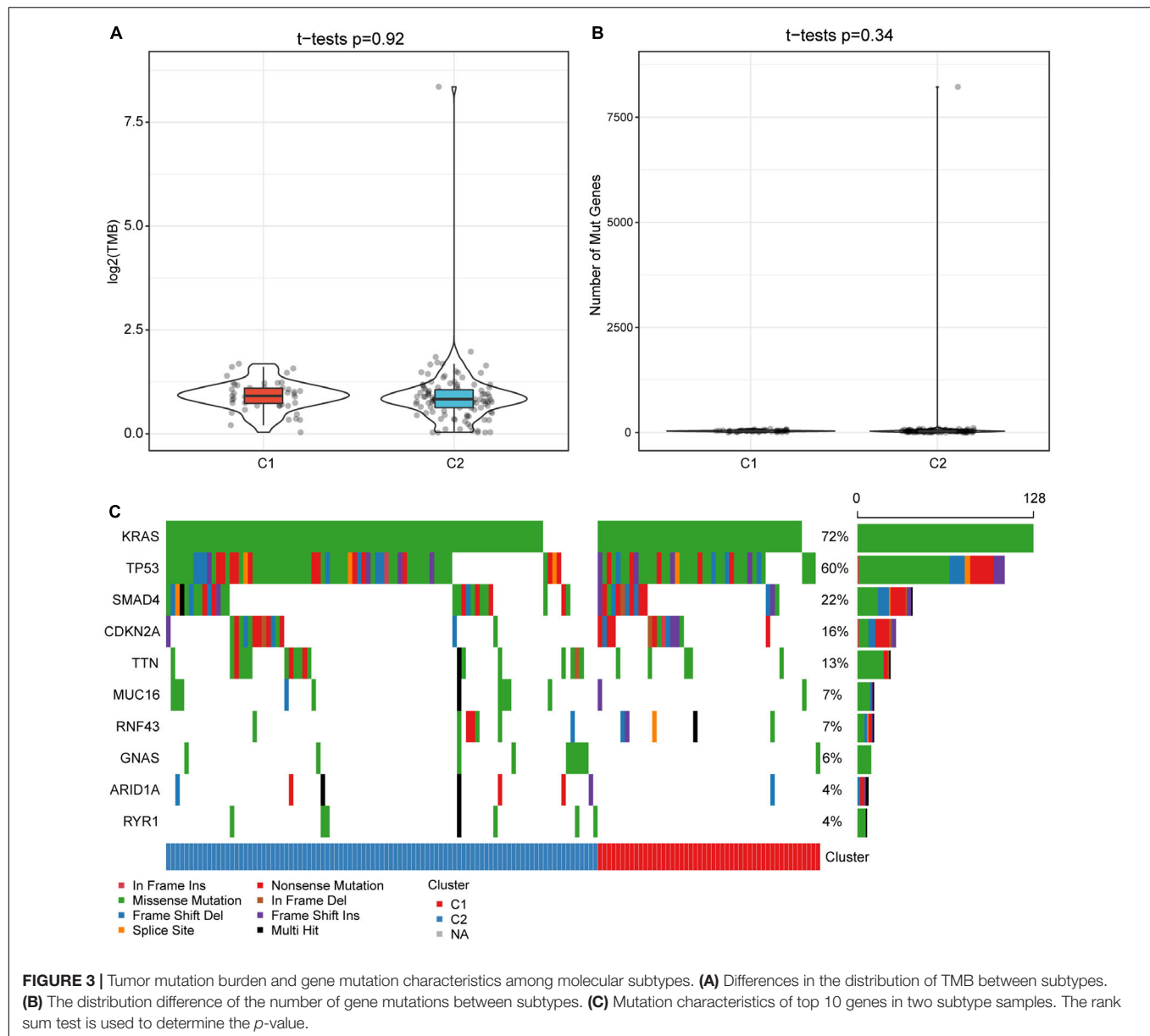
Differences in Intrinsic Immune Escape Characteristics Between Subtypes

The intrinsic immune escape of tumors suggests that tumor cells directly mediate their own immune escape, which leads to tumor progression. The study of Schreiber et al. (2011) proved

that tumor immunogenicity and the expression of immune checkpoint molecules were two aspects of intrinsic immune escape. Herein, to explore the differences in the intrinsic immune escape characteristics between the subtypes, we compared the potential factors that affect tumor immunogenicity, including mutation load, homologous recombination deficient (HRD), neoantigen load and chromosomal instability levels, as well as other factors (Figure 5). The results showed that most of the factors affecting tumor immunogenicity did not differ between the subtypes, while the SCN1 gene proportion in the C1 subtype was significantly higher than that in C2.

Prognostic Risk Model Based on Immune-Related lncRNA Pairs

In order to further explore the key differential lncRNA pairs affecting the prognosis between subtypes and their prognostic prediction ability for PAAD patients, we performed univariate COX proportional hazard regression on differentially expressed lncRNA pairs in the training set, where $P < 0.05$ was considered as a significant difference. A total of three



prognostic-related differential lncRNA pairs were identified: AC244035.1_vs._AC063926.1, AC066612.1_vs._AC090124.1, and AC244035.1_vs._LINC01885. Subsequently, multivariate COX analysis was performed for these 3 prognostic-related lncRNA pairs to obtain the risk coefficient of each lncRNA pair. Based on these coefficients, the RiskScore formula was acquired as follows:

$$\begin{aligned} \text{RiskScore} = & (-0.193 * \text{AC244035.1_vs_AC063926.1}) \\ & + (-0.445 * \text{AC066612.1_vs_AC090124.1}) + (-0.504 * \\ & \text{AC244035.1_vs_LINC01885}) \end{aligned}$$

All of these 3 lncRNA pairs were established as protective factors of PAAD.

The RiskScore of each sample in the training set was calculated, and the Z-score was normalized. Samples with a RiskScore > 0 were classified as high-risk groups, otherwise they were categorized as low-risk groups. Among them, 40 samples were associated with high-risk groups, and 48 samples were classified as low-risk groups. The survival analysis showed that, as expected, the prognosis for the high-risk group was significantly worse than that for the low-risk group ($P = 0.01$, **Figure 6A**). We further performed receiver operating curve analysis using the R software package timeROC. The prognostic prediction power (AUC) of this prognostic model was 0.63 (1 year), 0.72 (2 years), and 0.77 (3 years), respectively (**Figure 6B**). Therefore, our model showed a relatively good long-term survival prediction performance.

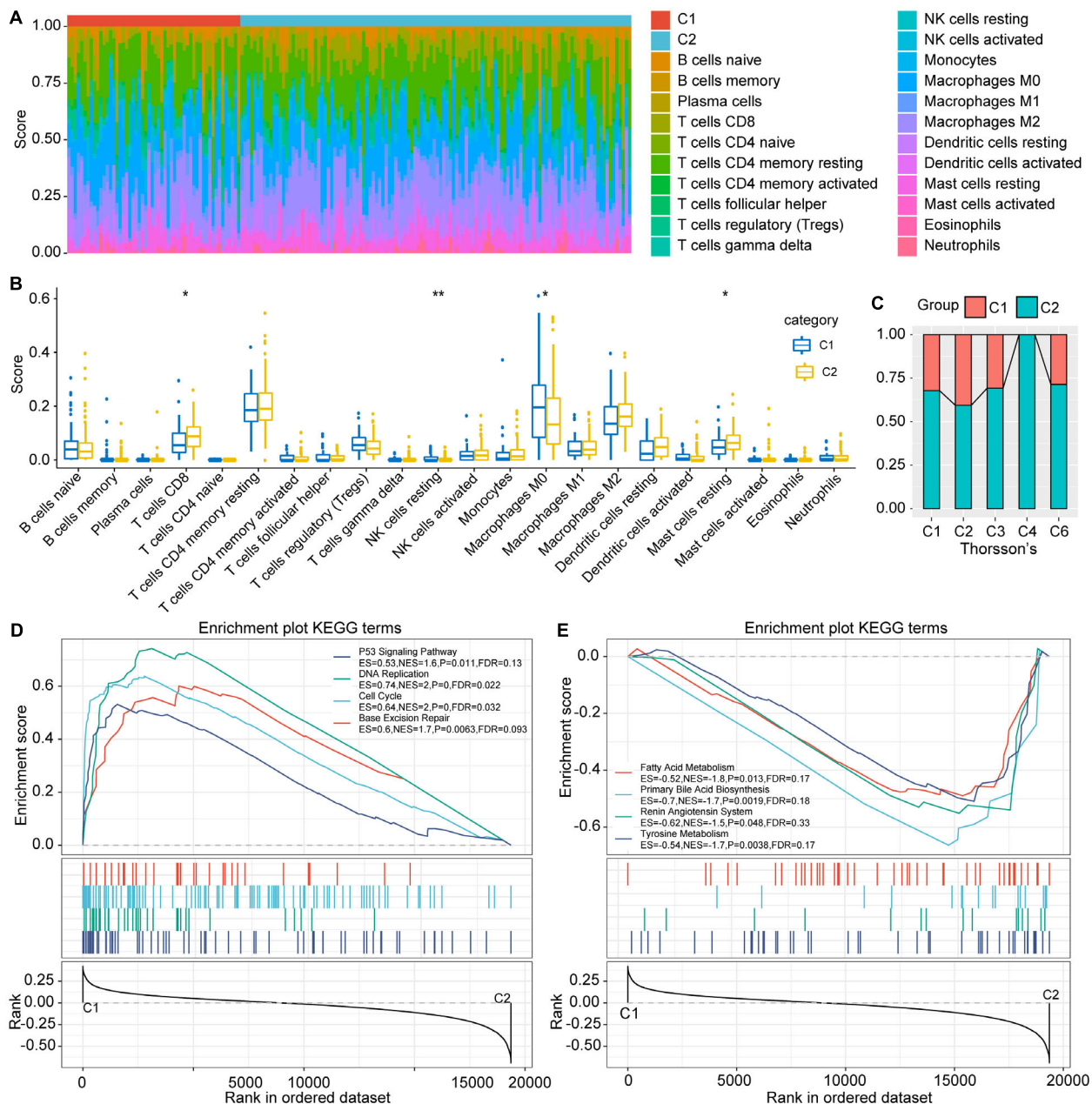
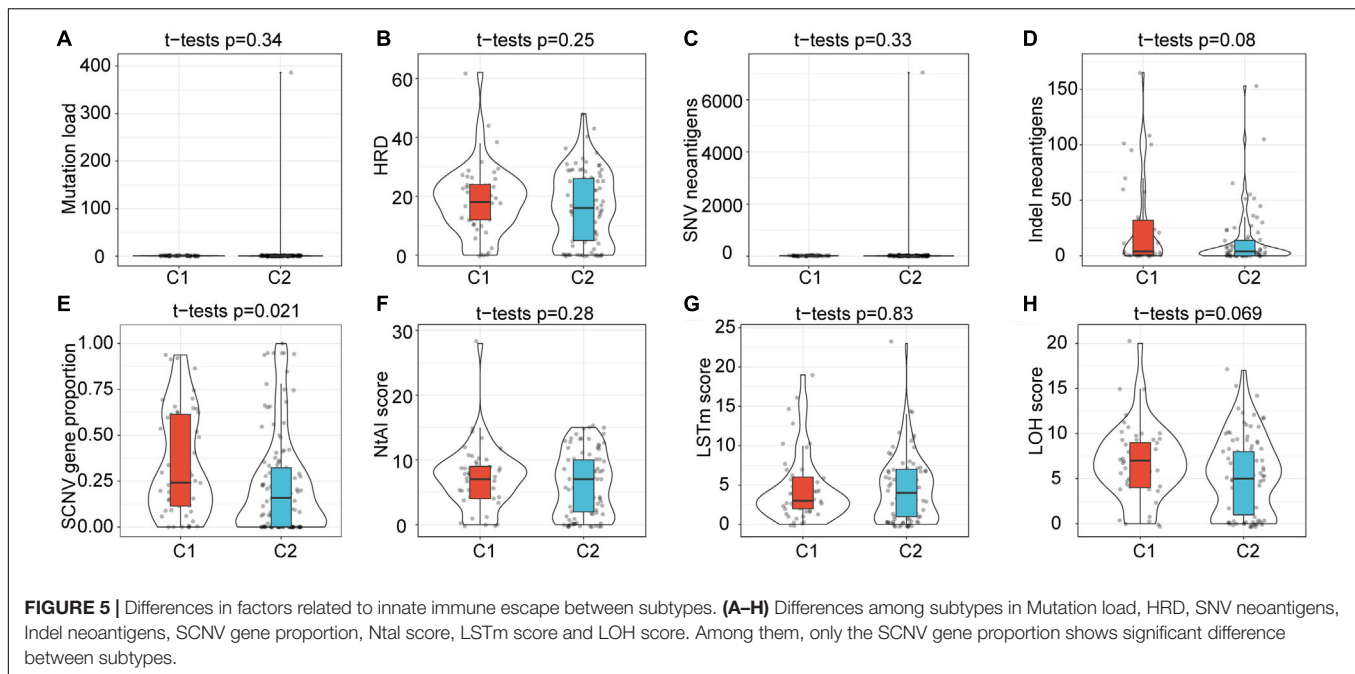


FIGURE 4 | Differences in immune cell characteristics between subtypes and GSEA. **(A)** Ratio of 22 immune cell components of the 2 subtype samples. **(B)** Differences in scores of 22 immune cells in samples between subtypes. **(C)** Intersection of C1 and C2 with the previous pan-cancer immune molecular subtypes. **(D)** The KEGG pathways enriched in C1 subtypes are mainly tumor-related pathways. **(E)** The KEGG pathways enriched in the C2 subtype are mainly metabolic related pathways, *indicates less than 0.05; **indicates less than 0.01.

Validation of Robustness of the Risk Model in the Internal and External Validation Sets

With the aim to verify the robustness of the model, we calculated the RiskScore of each sample in the validation set and all TCGA-PAAD samples with the same model and coefficients as in the training set. In the validation set, the prognosis for the high-risk group proved much worse than that for the

low-risk group ($p = 0.023$, **Figure 6C**). The results of ROC analysis also showed that the AUC of this prognostic model were 0.66 (1 year), 0.69 (2 years), and 0.73 (3 years), respectively (**Figure 6D**). In the TCGA-PAAD cohort, consistently with our expectations, the prognosis of different risk groups showed extremely significant difference ($P = 0.00029$, **Figure 6E**). Its 1-, 2-, and 3-year AUC values were established as 0.65, 0.7, and 0.74, respectively (**Figure 6F**).



In addition, we plotted the distribution of RiskScore and the survival status of all samples (Figure 6G). The results showed that the RiskScore was significantly correlated with the patient survival status. It could be seen that, as the RiskScore increased, the number of alive patients and the survival time significantly reduced. The above results imply that the prognostic model based on the identified 3 lncRNA pairs has a high and stable predictive power for the long-term survival rate of PAAD patients. Furthermore, we adopted the ICGC-PACA-CA cohort to verify the effectiveness of the model. The results showed that the prognosis of the high-risk group was significantly worse than that of the low-risk group ($p = 0.0024$, Figure 6H). The 1-, 2-, and 3-year AUC of the prediction model were 0.66, 0.68, and 0.7 (Figure 6I), respectively, showing the cross-platform effectiveness of the model.

Differences in the RiskScores of Various Clinical Characteristics

Furthermore, we compared the differences in risk scores of clinical features, including TNM stage, grade, molecular subtype, etc. Results indicated that different clusters and M stages have significant differences in their risk scores ($P < 0.05$). The risk score of C1 was much higher than that of C2, which corresponds to the poorer prognosis of C1 (Figure 7A). Meanwhile, a trend was observed that the risk score increases with the advancement of T stage and N stage, although the difference was not statistically significant (Figures 7B,C). Unexpectedly, however, the risk score of MX stage was lower than that of M1 and M0 (Figure 7D). This means that the invasion ability of samples with high RiskScore was decreased. Moreover, we compared the differences in risk scores for age, gender, and treatment, and none of them were statistically significant (Supplementary Figure 2).

Identification and Functional Analysis Genes Related to the 3 lncRNA Pairs

Considering the fact that lncRNAs usually binds with mRNA and proteins to perform biological functions, we calculated the Spearman correlation coefficient and their significance between the 3 prognostic-related lncRNA pairs and mRNA. After filtering with a threshold of $\text{Corr} > 0.4$ and $P < 0.05$, a total of 553 genes were identified. Subsequently, GO and KEGG analyses were performed to explore the potential functions of these genes. For biological functions (BP), 216 items were identified with significant differences ($\text{FDR} < 0.05$), which are mainly related to ion transport and the regulation of transmembrane signals (Figure 7E); for molecular functions (MF), there were 62 items with significant differences ($\text{FDR} < 0.05$), mainly concentrated on the cation channel complex and transmembrane transport complex (Figure 7F); for cell components (CC), 93 entries showed significant differences ($\text{FDR} < 0.05$), and these functions were mainly associated with ion and protein transport channels (Figure 7G). For KEGG, pathways such as Maturity onset diabetes of the young, Type II diabetes mellitus, Insulin secretion, Morphine addiction, GABAergic synapse, and Circadian entrainment were enriched (Figure 7H).

Univariate and Multivariate Analysis of RiskScore

Aiming to verify the stability and independence of the RiskScore determined in clinical applications, we performed a univariate COX regression analysis on the TCGA-PAAD samples. The results showed that T Stage, N Stage, and RiskScore were negatively correlated with patient prognosis ($\text{HR} > 1$, $P < 0.05$), while radiation therapy and chemotherapy were positively correlated with patient prognosis ($\text{HR} < 1$, $P < 0.05$, Figure 8A).

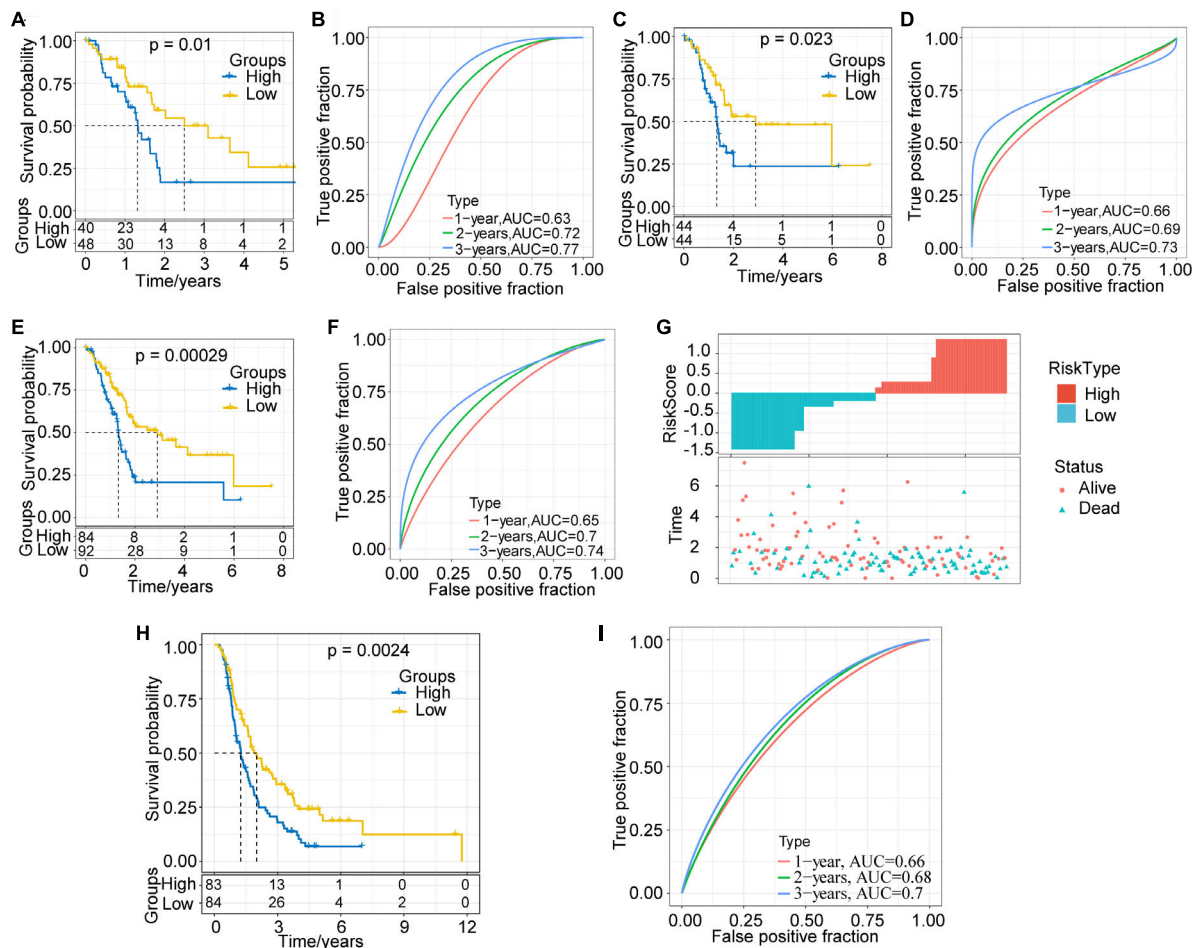


FIGURE 6 | Evaluation and validation of prognostic models. (A) KM survival curve distribution of the high-risk group and the low-risk group in the training set. (B) ROC curve of the prognostic model in the training set. (C) KM survival curve distribution of the high-risk group and the low-risk group in the validation set. (D) ROC curve of the prognostic model in the validation set. (E) KM survival curve distribution of the high-risk group and the low-risk group in all samples of the TCGA-PAAD cohort. (F) ROC curve of the prognostic model of all samples. (G) Correlations among RiskScore, survival time and survival status of the TCGA-PAAD cohort; RiskScore is arranged from low to high. (H) KM survival curve distribution of the high-risk group and the low-risk group in the ICGC-PACA-CA cohort. (I) ROC curve of the prognostic model in the ICGC-PACA-CA cohort.

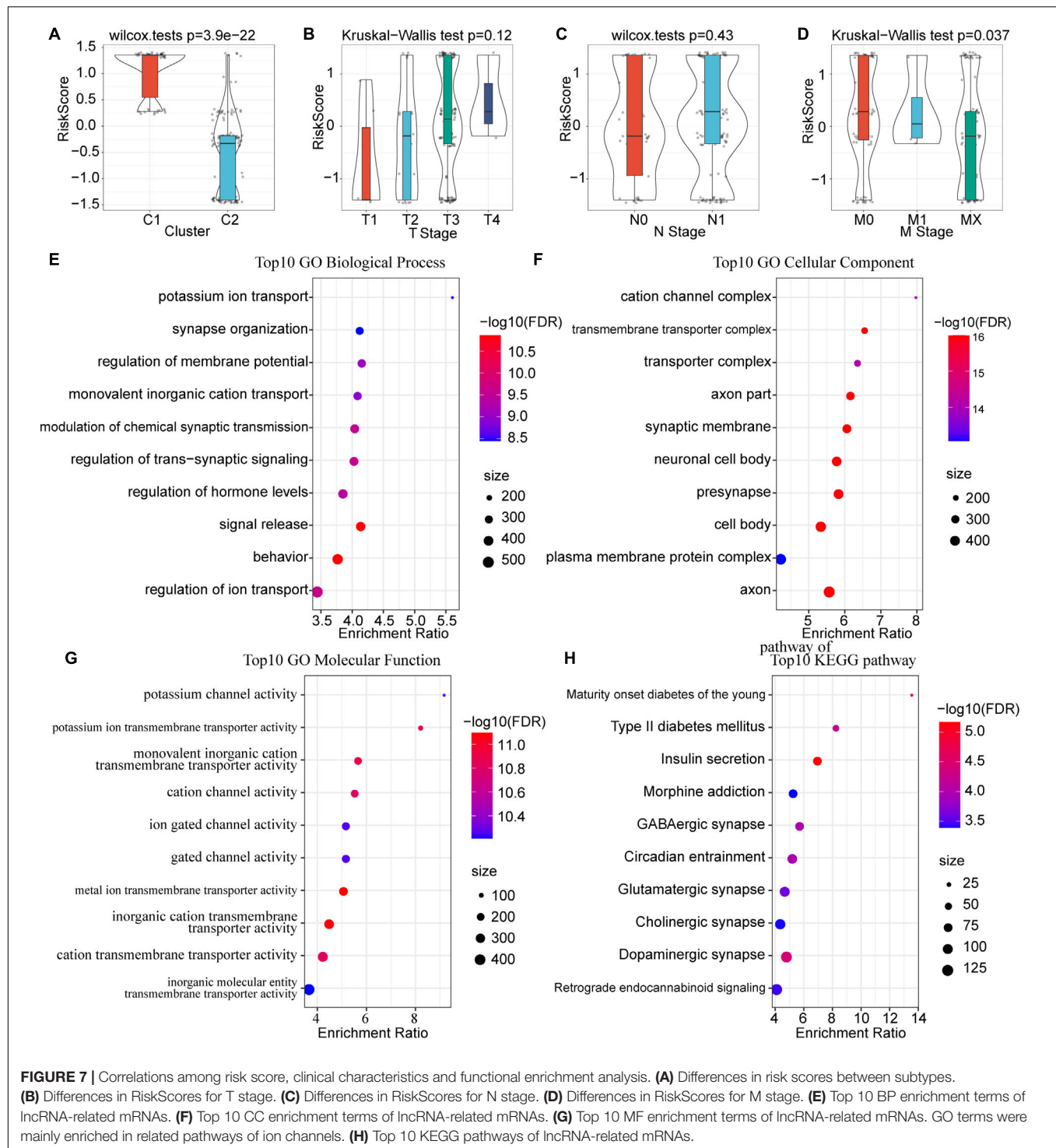
Among them, the RiskScore had the highest Hazard Ratio (HR = 2.14), which also proved that it was highly effective in predicting the prognosis of patients. Meanwhile, the results of multivariate analysis showed that the HR of RiskScore we determined was 2.02 ($P = 0.011$), which still had a strong power in predicting the prognosis of PAAD patients (Figure 8B). The above results prove that our prognostic model based on the selected 3 lncRNA pairs has strong independent predictive power.

Construction of Nomogram of Clinical Characteristics and DCA Curve

A nomogram is a figure that visually and effectively displays the results of a risk model. It uses the length of the straight line to indicate the degree of influence of different variables and the different values of these variables on the outcome. We constructed the nomogram based on the clinical features with significant statistical significance in the multivariate COX

regression analysis. The results of the nomogram showed that the RiskScore had the greatest impact on the prognostic outcome of patients and was relatively stable (Figure 8C), indicating that the risk model based on our lncRNA pairs can stably predict the prognosis of patients. Furthermore, we verified the performance of nomogram data for predicting patient prognosis. We observed that the nomogram-predicted OS data fit the observed OS well with respect to 1-, 2-, and 3-year survival rates, which proves that this method presents excellent performance (Figure 8D).

Moreover, decision curve analysis (DCA) was performed to evaluate the net benefits of different characteristics for patients (Figure 8E). Subsequent results showed that decisions based on nomogram data have the highest net benefits. Meanwhile, the decision based on the RiskScore had a good impact on the patients' net benefits, and its net income was higher than the N stage in most cases.



DISCUSSION

It has been established that PAAD can mediate a unique immune microenvironment and cause immune escape through a variety of mechanisms, such as through tumor “hijacking” immune checkpoints to suppress the immune system’s anti-tumor response (Collisson et al., 2019; Liu et al., 2020). ICIs

effectively prevent this process (Ribas and Wolchok, 2018). Notwithstanding, there are still patients who do not respond to ICIs, and even present negative outcomes (Macherla et al., 2018). However, lncRNAs, which are closely related to immunity, seem to be seldom subject to research in this field. Therefore, exploring the mechanism of immune-related lncRNA in PAAD patients may bring unexpected gains.

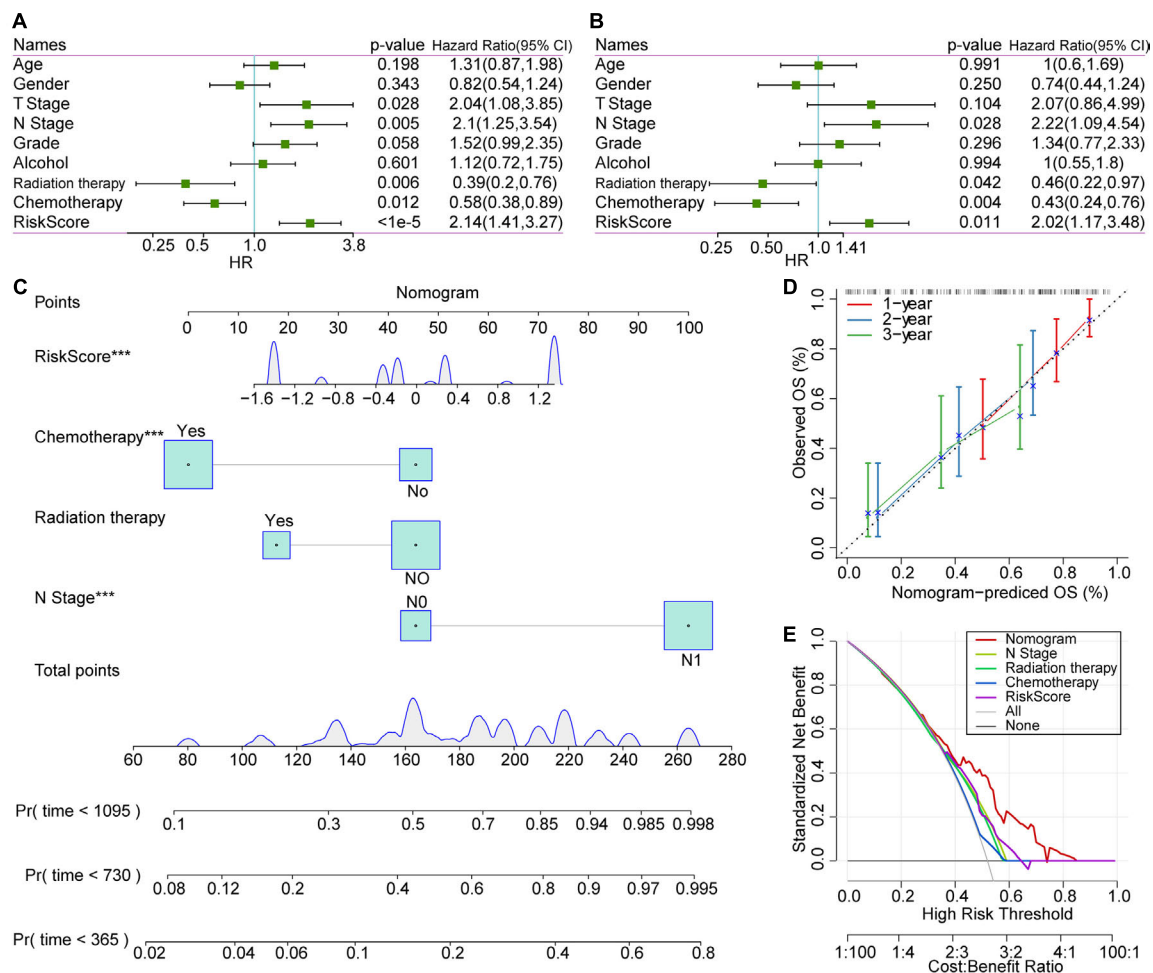


FIGURE 8 | COX analysis of RiskScores, clinical characteristics and nomogram. **(A)** Univariate analysis results of clinical features and RiskScore. **(B)** Multivariate analysis results of clinical features and RiskScore. **(C)** Nomogram based on clinical characteristics and RiskScore. **(D)** Nomogram survival rate correction chart. **(E)** Decision curve analysis (DCA) diagrams of N stage, radiation therapy, chemotherapy, RiskScore, and nomogram.

In this study, we used the lncRNA expression profile of the TCGA-PAAD cohort to identify immune-related lncRNAs combined with the immune dataset. In terms of the accuracy of the cancer diagnosis model, the combination of two biomarkers is better than a single gene, therefore we screened immune-related lncRNA pairs through iteration and pairing, and constructed a new expression matrix based on the relative differences in the expression levels within the combination to eliminate huge differences in expression (Hong et al., 2020; Lv et al., 2020). Based on the expression matrix of the immune-related lncRNA pairs, we determined 2 molecular subtypes using the NMF algorithm. It was found that C1 and C2 had significant differences in overall survival and PFS. Subsequently, the molecular level differences between subtypes were further explored. The TMB proved to have no significant difference between the groups, and the mutation rate of TP53 in the C1 subtype was significantly higher than that in the C2 subtype. TP53 is a thoroughly studied tumor suppressor gene, whose translation product P53 can activate target genes to resist cell stress and mediate cell growth arrest and

apoptosis (Levy et al., 1993; Kanda et al., 2013; Ormanns et al., 2014). Elevated TP53 mutations may cause the loss of P53 protein function and lead to further uncontrollable tumor proliferation, which may be partly the reason for the poor prognosis of C1.

It was further established by the analysis of the immune characteristics between subtypes that the infiltration of CTLs in the C1 subtype was reduced, while the proportion of resting NK cells increased, suggesting that activated NK cells were reduced and the anti-tumor effect of non-specific immunity was suppressed. Zhang et al. (2017) reported that the immunosuppressive state of a tumor microenvironment can cause NK cell dysfunction, which corresponds to poor prognostic outcomes. Previous evidence has indicated that M1 phase macrophages have anti-tumor effects, whereas M2 phase macrophages have tumor-promoting effects (Chen Y. et al., 2019; Vitale et al., 2019). Interestingly, our results showed that there were more non-polarized M0-phase macrophages in C1 subtypes than in C2 subtypes. Meanwhile, there was no significant difference in M1 and M2 phase macrophages between

subtypes. Based on this finding, it can be inferred that the C1 subtype may inhibit the polarization of M0 macrophages through a certain mechanism to exert an effect, which speculation requires more rigorous experiments to validate. In addition, GSEA results suggest that some tumor-related pathways, such as P53 signaling pathway, DNA replication, cell cycle, and base excision repair, are enriched in the C1 subtype, while fatty acid metabolism, primary bile acid biosynthesis, renin, angiotensin, methionine and tyrosine metabolism are enriched in the C2 subtype, indicating that the poor prognosis of C1 subtype is related to the activation of tumor-related pathways and the inhibition of normal metabolism.

Subsequently, based on univariate and multivariate COX analysis, we constructed a prognostic model of the selected 3 immune-related lncRNA pairs (AC244035.1_vs._AC063926.1, AC066612.1_vs._AC090124.1, and AC244035.1_vs._LINC01885). After rigorous verification, the model proved to have a stable and independent prognostic prediction performance, and its long-term prognosis AUC reached 0.77. The RiskScore was found to be significantly related to molecular subtype and M stage. The functional enrichment analysis of mRNAs related to these 3 lncRNA pairs revealed that they are mainly involved in ion transport pathways. There is evidence that K⁺ channels (Kv1.3 channels) accumulate specifically in the immune synapse between CTL and tumor cells to regulate the cell killing effect of CTL and NK cells (Panyi et al., 2004; Hu et al., 2013). Blocking this channel can enhance the tumor killing effect. The Ca²⁺-activated K⁺ channels play a key role in the development and metastasis of tumors (Khaitan et al., 2009; Hanahan and Weinberg, 2011; Schwab et al., 2012). We have reason to believe that the proposed three immune-related lncRNA pairs may regulate the anti-tumor effect of immune cells and the process of tumor invasion through ion channel-related pathways, therefore may become new targets for tumor treatment.

CONCLUSION

In this study, we identified new PAAD molecular subtypes with significant prognostic differences based on immune-related lncRNA pairs. The detected prognostic differences between subtypes may be due to the differential infiltration of CTL and NK cells, and the activation of tumor-related pathways. In addition, the prognostic model based on the 3 identified immune-related lncRNA pair signatures was proved to have an effective and stable

prognostic predictive effect on PAAD. The proposed 3 lncRNA pairs may participate in the anti-tumor effect of immune cells and tumor migration through ion channel pathways, and are expected to become new tumor treatment targets.

DATA AVAILABILITY STATEMENT

The datasets presented in this study can be found in online repositories. The names of the repository/repositories and accession number(s) can be found in the article/Supplementary Material.

AUTHOR CONTRIBUTIONS

YH and WG designed the study. QZa and QZe drafted the manuscript. QZa and ZW analyzed the data. XY and MZ revised the manuscript. All authors read and approved the final manuscript.

FUNDING

This work was supported by the National Natural Science Foundation of China (819028328), the Youth Talent Lifting Project of Henan Province (2021HYTP059), and Key Scientific Research Project of Henan Higher Education Institutions of China (21A320026).

ACKNOWLEDGMENTS

We thank the patients and investigators who participated in TCGA for providing data.

SUPPLEMENTARY MATERIAL

The Supplementary Material for this article can be found online at: <https://www.frontiersin.org/articles/10.3389/fcell.2021.698296/full#supplementary-material>

Supplementary Figure 1 | Consensus map of NMF clustering when $K = 2-10$.

Supplementary Figure 2 | Correlation between risk score and clinical characteristics.

REFERENCES

- Bray, F., Ferlay, J., Soerjomataram, I., Siegel, R. L., Torre, L. A., and Jemal, A. (2018). Global cancer statistics 2018: GLOBOCAN estimates of incidence and mortality worldwide for 36 cancers in 185 countries. *CA Cancer J. Clin.* 68, 394–424. doi: 10.3322/caac.21492
- Castellanos-Rubio, A., and Ghosh, S. (2019). Disease-associated SNPs in inflammation-related lncRNAs. *Front. Immunol.* 10:420. doi: 10.3389/fimmu.2019.00420
- Chen, B., Khodadoust, M. S., Liu, C. L., Newman, A. M., and Alizadeh, A. A. (2018). Profiling tumor infiltrating immune cells with CIBERSORT. *Methods Mol. Biol.* 1711, 243–259. doi: 10.1007/978-1-4939-7493-1_12
- Chen, J., Ao, L., and Yang, J. (2019). Long non-coding RNAs in diseases related to inflammation and immunity. *Ann. Transl. Med.* 7:494. doi: 10.21037/atm.2019.08.37
- Chen, Y., Song, Y., Du, W., Gong, L., Chang, H., and Zou, Z. (2019). Tumor-associated macrophages: an accomplice in solid tumor progression. *J. Biomed. Sci.* 26:78. doi: 10.1186/s12929-019-0568-z
- Chen, J., Xiao-Zhong, G., and Qi, X. S. (2017). Clinical outcomes of specific immunotherapy in advanced pancreatic cancer: a systematic review and meta-analysis. *J. Immunol. Res.* 2017:8282391. doi: 10.1155/2017/8282391
- Collisson, E. A., Bailey, P., Chang, D. K., and Biankin, A. V. (2019). Molecular subtypes of pancreatic cancer. *Nat. Rev. Gastroenterol. Hepatol.* 16, 207–220. doi: 10.1038/s41575-019-0109-y

- David, M., Lepage, C., Jouve, J. L., Jooste, V., Chauvenet, M., Faivre, J., et al. (2009). Management and prognosis of pancreatic cancer over a 30-year period. *Br. J. Cancer* 101, 215–218. doi: 10.1038/sj.bjc.6605150
- Ferlay, J., Colombet, M., Soerjomataram, I., Mathers, C., Parkin, D. M., Pineros, M., et al. (2019). Estimating the global cancer incidence and mortality in 2018: GLOBOCAN sources and methods. *Int. J. Cancer* 144, 1941–1953. doi: 10.1002/ijc.31937
- Geng, H., and Tan, X. D. (2016). Functional diversity of long non-coding RNAs in immune regulation. *Genes Dis.* 3, 72–81. doi: 10.1016/j.gendis.2016.01.004
- Glatzer, M., Horber, D., Montemurro, M., Winterhalder, R., Inauen, R., Berger, M. D., et al. (2020). Choice of first line systemic treatment in pancreatic cancer among national experts. *Pancreatol.* 20, 686–690. doi: 10.1016/j.pan.2020.03.012
- Hanahan, D., and Weinberg, R. A. (2011). Hallmarks of cancer: the next generation. *Cell* 144, 646–674. doi: 10.1016/j.cell.2011.02.013
- Hong, W., Liang, L., Gu, Y., Qi, Z., Qiu, H., Yang, X., et al. (2020). Immune-related lncRNA to construct novel signature and predict the immune landscape of human hepatocellular carcinoma. *Mol. Ther. Nucleic Acids* 22, 937–947. doi: 10.1016/j.omtn.2020.10.002
- Hu, L., Wang, T., Gocke, A. R., Nath, A., Zhang, H., Margolick, J. B., et al. (2013). Blockade of Kv1.3 potassium channels inhibits differentiation and granzyme B secretion of human CD8+ T effector memory lymphocytes. *PLoS One* 8:e54267. doi: 10.1371/journal.pone.0054267
- Kanda, M., Sadakari, Y., Borges, M., Topazian, M., Farrell, J., Syngal, S., et al. (2013). Mutant TP53 in duodenal samples of pancreatic juice from patients with pancreatic cancer or high-grade dysplasia. *Clin. Gastroenterol. Hepatol.* 11, 719.e5–730.5. doi: 10.1016/j.cgh.2012.11.016
- Khaitan, D., Sankpal, U. T., Weksler, B., Meister, E. A., Romero, I. A., Couraud, P. O., et al. (2009). Role of KCNMA1 gene in breast cancer invasion and metastasis to brain. *BMC Cancer* 9:258. doi: 10.1186/1471-2407-9-258
- Khalaf, N., El-Serag, H. B., Abrams, H. R., and Thrift, A. P. (2020). Burden of pancreatic cancer: from epidemiology to practice. *Clin. Gastroenterol. Hepatol.* 19, 876–884. doi: 10.1016/j.cgh.2020.02.054
- Kythreotou, A., Siddique, A., Mauri, F. A., Bower, M., and Pinato, D. J. (2018). Pd-L1. *J. Clin. Pathol.* 71, 189–194. doi: 10.1136/jclinpath-2017-204853
- Levy, N., Yonish-Rouach, E., Oren, M., and Kimchi, A. (1993). Complementation by wild-type p53 of interleukin-6 effects on M1 cells: induction of cell cycle exit and cooperativity with c-myc suppression. *Mol. Cell Biol.* 13, 7942–7952. doi: 10.1128/mcb.13.12.7942
- Liu, Q., Wu, H., Li, Y., Zhang, R., Kleeff, J., Zhang, X., et al. (2020). Combined blockade of TGF-beta1 and GM-CSF improves chemotherapeutic effects for pancreatic cancer by modulating tumor microenvironment. *Cancer Immunol. Immunother.* 69, 1477–1492. doi: 10.1007/s00262-020-02542-7
- Long, J., Lin, J., Wang, A., Wu, L., Zheng, Y., Yang, X., et al. (2017). PD-1/PD-L blockade in gastrointestinal cancers: lessons learned and the road toward precision immunotherapy. *J. Hematol. Oncol.* 10:146. doi: 10.1186/s13045-017-0511-2
- Lv, Y., Lin, S. Y., Hu, F. F., Ye, Z., Zhang, Q., Wang, Y., et al. (2020). Landscape of cancer diagnostic biomarkers from specifically expressed genes. *Brief. Bioinform.* 21, 2175–2184. doi: 10.1093/bib/bbz131
- Macherla, S., Laks, S., Naqash, A. R., Bulumulle, A., Zervos, E., and Muzaffar, M. (2018). Emerging role of immune checkpoint blockade in pancreatic cancer. *Int. J. Mol. Sci.* 19:3505. doi: 10.3390/ijms19113505
- Mellman, I., Coukos, G., and Dranoff, G. (2011). Cancer immunotherapy comes of age. *Nature* 480, 480–489. doi: 10.1038/nature10673
- Mercer, T. R., Dinger, M. E., and Mattick, J. S. (2009). Long non-coding RNAs: insights into functions. *Nat. Rev. Genet.* 10, 155–159. doi: 10.1038/nrg2521
- Miller, K. D., Nogueira, L., Mariotto, A. B., Rowland, J. H., Yabroff, K. R., Alfano, C. M., et al. (2019). Cancer treatment and survivorship statistics, 2019. *CA Cancer J. Clin.* 69, 363–385. doi: 10.3322/caac.21565
- Ormanns, S., Siveke, J. T., Heinemann, V., Haas, M., Sipos, B., Schlitter, A. M., et al. (2014). pERK, pAKT and p53 as tissue biomarkers in erlotinib-treated patients with advanced pancreatic cancer: a translational subgroup analysis from AIO-PK0104. *BMC Cancer* 14:624. doi: 10.1186/1471-2407-14-624
- Panyi, G., Vamosi, G., Bacso, Z., Bagdany, M., Bodnar, A., Varga, Z., et al. (2004). Kv1.3 potassium channels are localized in the immunological synapse formed between cytotoxic and target cells. *Proc. Natl. Acad. Sci. U.S.A.* 101, 1285–1290. doi: 10.1073/pnas.0307421100
- Rapicavoli, N. A., Qu, K., Zhang, J., Mikhail, M., Laberge, R. M., and Chang, H. Y. (2013). A mammalian pseudogene lncRNA at the interface of inflammation and anti-inflammatory therapeutics. *eLife* 2:e00762. doi: 10.7554/eLife.00762
- Ribas, A., and Wolchok, J. D. (2018). Cancer immunotherapy using checkpoint blockade. *Science* 359, 1350–1355. doi: 10.1126/science.aar4060
- Schreiber, R. D., Old, L. J., and Smyth, M. J. (2011). Cancer immunoediting: integrating immunity's roles in cancer suppression and promotion. *Science* 331, 1565–1570. doi: 10.1126/science.1203486
- Schwab, A., Fabian, A., Hanley, P. J., and Stock, C. (2012). Role of ion channels and transporters in cell migration. *Physiol. Rev.* 92, 1865–1913. doi: 10.1152/physrev.00018.2011
- Thorsson, V., Gibbs, D. L., Brown, S. D., Wolf, D., Bortone, D. S., Ou Yang, T. H., et al. (2018). The immune landscape of cancer. *Immunity* 48, 812.e14–830.e14. doi: 10.1016/j.immuni.2018.03.023
- Vaccaro, V., Sperduti, I., and Milella, M. (2011). FOLFIRINOX versus gemcitabine for metastatic pancreatic cancer. *N. Engl. J. Med.* 365, 768–769. doi: 10.1056/NEJMc1107627
- Vitale, I., Manic, G., Coussens, L. M., Kroemer, G., and Galluzzi, L. (2019). Macrophages and Metabolism in the Tumor Microenvironment. *Cell Metab.* 30, 36–50. doi: 10.1016/j.cmet.2019.06.001
- Von Hoff, D. D., Ervin, T., Arena, F. P., Chiorean, E. G., Infante, J., Moore, M., et al. (2013). Increased survival in pancreatic cancer with nab-paclitaxel plus gemcitabine. *N. Engl. J. Med.* 369, 1691–1703. doi: 10.1056/NEJMoa1304369
- Wang, J., Vasaikar, S., Shi, Z., Greer, M., and Zhang, B. (2017). WebGestalt 2017: a more comprehensive, powerful, flexible and interactive gene set enrichment analysis toolkit. *Nucleic Acids Res.* 45, W130–W137. doi: 10.1093/nar/gkx356
- Wu, A. A., Jaffee, E., and Lee, V. (2019). Current status of immunotherapies for treating pancreatic cancer. *Curr. Oncol. Rep.* 21:60. doi: 10.1007/s11912-019-0811-5
- Yi, M., Qin, S., Zhao, W., Yu, S., Chu, Q., and Wu, K. (2018). The role of neoantigen in immune checkpoint blockade therapy. *Exp. Hematol. Oncol.* 7:28. doi: 10.1186/s40164-018-0120-y
- Zhang, Q., Yu, X., Zheng, Q., He, Y., and Guo, W. (2020). A molecular subtype model for liver HBV-Related hepatocellular carcinoma patients based on immune-related genes. *Front. Oncol.* 10:560229. doi: 10.3389/fonc.2020.560229
- Zhang, Q. F., Yin, W. W., Xia, Y., Yi, Y. Y., He, Q. F., Wang, X., et al. (2017). Liver-infiltrating CD11b(-)CD27(-) NK subsets account for NK-cell dysfunction in patients with hepatocellular carcinoma and are associated with tumor progression. *Cell Mol. Immunol.* 14, 819–829. doi: 10.1038/cmi.2016.28

Conflict of Interest: The authors declare that the research was conducted in the absence of any commercial or financial relationships that could be construed as a potential conflict of interest.

Copyright © 2021 Zhang, Wang, Yu, Zhang, Zheng, He and Guo. This is an open-access article distributed under the terms of the Creative Commons Attribution License (CC BY). The use, distribution or reproduction in other forums is permitted, provided the original author(s) and the copyright owner(s) are credited and that the original publication in this journal is cited, in accordance with accepted academic practice. No use, distribution or reproduction is permitted which does not comply with these terms.



Immune Microenvironment Change and Involvement of Circular RNAs in TIL Cells of Recurrent Nasopharyngeal Carcinoma

Yumin Wang^{1†}, Zhouying Peng^{1†}, Yaxuan Wang¹, Yi Yang², Ruohao Fan¹, Kelei Gao¹, Hua Zhang¹, Zhihai Xie¹ and Weihong Jiang^{1*}

¹ Department of Otolaryngology Head and Neck Surgery, Xiangya Hospital, Central South University, Changsha, China,

² Department of Nuclear Medicine, Xiangya Hospital, Central South University, Changsha, China

OPEN ACCESS

Edited by:

Yanyan Tang,
Central South University, China

Reviewed by:

Yuefeng Li,
Jiangsu University, China
Mei Huang,
Anhui Provincial Hospital, China

*Correspondence:

Weihong Jiang
weihongjiang@csu.edu.cn

[†]These authors have contributed
equally to this work

Specialty section:

This article was submitted to
Molecular and Cellular Oncology,
a section of the journal
Frontiers in Cell and Developmental
Biology

Received: 08 June 2021

Accepted: 16 July 2021

Published: 06 August 2021

Citation:

Wang Y, Peng Z, Wang Y, Yang Y,
Fan R, Gao K, Zhang H, Xie Z and
Jiang W (2021) Immune
Microenvironment Change
and Involvement of Circular RNAs
in TIL Cells of Recurrent
Nasopharyngeal Carcinoma.
Front. Cell Dev. Biol. 9:722224.
doi: 10.3389/fcell.2021.722224

Nasopharyngeal carcinoma is a malignant tumor that is highly prevalent in southern China and the Southeast Asian belt. Recent studies have shown that the T cells play important regulatory roles in tumorigenesis and progression. We test TIL cell of recurrent nasopharyngeal carcinoma and primary nasopharyngeal carcinoma cell. We found that T cell change in recurrent nasopharyngeal carcinoma and primary nasopharyngeal carcinoma cell. Based on GEO database, we selected differently expressed circRNAs in nasopharyngeal carcinoma tissues. qRT-PCR show that some circRNAs also highly expressed in TIL cells. In conclusion, immune microenvironment changed in recurrent nasopharyngeal carcinoma. There is involvement of circular RNAs in this progress, with should be researched further.

Keywords: recurrent nasopharyngeal carcinoma, TIL, immune microenvironment, circRNA, non-coding RNA

INTRODUCTION

Nasopharyngeal carcinoma is a malignant tumor that is highly prevalent in southern China and Southeast Asian (Hanahan and Weinberg, 2011; Chen et al., 2019; Jiang et al., 2020). The preferred treatment for nasopharyngeal carcinoma is radiation therapy. However clinical studies have found that recurrence has become the main cause of treatment failure in nasopharyngeal carcinoma (Liu et al., 2021; Wu et al., 2021). Recent studies have shown that the process of nasopharyngeal carcinogenesis and progression is influenced by the immune microenvironment. In which T cells, as the main component of specific immunity, especially cellular immunity, play an important role in the development of tumor (Xia et al., 2021). Among the T cells, Treg, CD4 + T, CD8 + T, and other major T cell taxa play important regulatory roles in tumorigenesis and progression.

Circular RNA (circRNA) is a hot spot for cancer research in recent years. circRNA is now found to be widely involved in tumorigenesis and development (Wang et al., 2017; Zhong et al., 2018; Chen, 2020). circRNA's modes of action include three modes of action, including ceRNA, binding to RBP proteins, and encoding small peptides. In the development of nasopharyngeal carcinoma, numerous circRNAs have been reported to be involved in a series of biological processes related to invasion and metastasis, proliferation, and resistance to radiotherapy (Zheng et al., 2016; Jin et al., 2020; Tessier et al., 2020). However, the circRNAs involved in the regulation of immune microenvironment of recurrent nasopharyngeal carcinoma, especially T-cell regulation, have not been reported yet.

In this study, we will investigate the changes in the distribution of T cells in recurrent nasopharyngeal carcinoma compared with primary nasopharyngeal carcinoma and the changes in the composition of different types of T cells. We will further investigate the expression of circRNAs in recurrent nasopharyngeal carcinoma T cells and the network of their roles in T cells. This study will be the first to reveal the alteration of T cells in nasopharyngeal carcinoma tissues and will explore the potential effect of circRNA on T cells. This study will provide new research ideas to reveal the alteration of immune microenvironment during nasopharyngeal cancer recurrence.

MATERIALS AND METHODS

Patients and Sample

Seven nasopharyngeal carcinoma samples were obtained from patients. All samples were collected with the consent of patients and the experiments were approved by the ethics committee of Xiangya Hospital, Central South University. All fresh tissues were immersed in RNALater (Ambion, Austin, TX, United States). The tissue samples were stored in a -80°C laboratory freezer.

Flow Cytometry to Detect T Cell

The following monoclonal antibodies and reagents were purchased from BD Biosciences and added to 100 μl of cells. The panel of antibodies in were anti-CD25, anti-CD3, anti-CD4, anti-CD8, and anti-CD127. The phenotype of T reg cells were detected using anti-CD25 anti-CD127. Isotype controls with irrelevant specificities were included as negative controls. All of these cell suspensions were incubated for 20 min at room temperature. After incubating, the cells were washed and re-suspended in 200 μl of PBS. The cells were then analyzed with FACSCanto flow cytometer (BD LSRFortessaTM X-20).

RNA Extraction and Quantitative Real-Time PCR Analyses (qRT-PCR)

Tissue RNA isolation and amplification were performed as our laboratory described previously (He et al., 2016; Mo et al., 2019a). Cell RNA was extracted using TRIzol reagent (Invitrogen, Carlsbad, CA, United States). For qRT-PCR, RNA was reverse transcribed to cDNA by using a PrimeScript RT reagent Kit (Takara, Dalian, China). qRT-PCR was performed using a SYBR_Premix ExTaqII kit (Takara, Dalian, China) in the CFX96 Real-Time PCR Detection System (Bio-Rad, Hercules, CA, United States) to determine the relative expression levels of target genes. The sequences of qRT-PCR primers: circ hsa_circ_0006935 forward primer 5'-CCCTGAGTTGGTGCTGAAAAC-3' and reverse primer 5'-AACCACGAAAGCCACCTCTG-3'; hsa_circ_0001730 forward primer 5'-CCCAATATCATCCGCCTGGA-3' and reverse primer 5'-GCAAATTCCTCACAGCCTCA-3'; hsa_circ_0000831 forward primer 5'-CCTCTGGTACTTGGGGAAC-3' and reverse primer 5'-TCCAAAATCCCACTGTTACCAA-3'; hsa_circ_0031584 forward primer 5'-TGGTTACAGCTGAGAAGCC-3' and reverse primer 5'-TTTGTATTTCCCTCATTTCTGTGC-3'; hsa_circ_0005019 forward primer 5'-GTACAC

CACCCATGAGGACG-3' and reverse primer 5'-ACAGATGTGTCAGAACCTCAC-3'; GAPDH: forward primer 5'-TCACCAACTGGGACGACATG-3' and reverse primer 5'-GTCACCGGAGTCCATCAGAT-3'; GAPDH was used as reference and normalization control.

Public Database Profiles Download and Analysis

Nasopharyngeal carcinoma circular RNA expression data sets and the corresponding clinical data were downloaded from publicly available GEO databases. This database included 4 patients with NPC and 4 non-NPC nasopharyngeal epithelial tissues from GSE134797 (Yang et al., 2020). To find functional circRNAs in nasopharyngeal carcinoma, after downloading Nasopharyngeal carcinoma circRNA expression data from GEO database: GSE134797 (Illumina HiSeq 4000). We used Significant Analysis of Microarray (SAM) software to analyze the expression of circRNAs between the non-tumor NPE biopsies and nasopharyngeal carcinoma tissue samples in the dataset. The cut off value for differentially expressed lncRNA was set at ≥ 2 -fold change and the false discovery ratio (FDR) was < 0.05 (Mo et al., 2019a). To analyze tumor infiltration in nasopharyngeal carcinoma, after downloading Nasopharyngeal carcinoma mRNA expression data from GEO database: GSE118719 (Illumina HiSeq 4000). There are seven NPC biopsy specimens and four normal nasopharyngeal mucosal specimens in this dataset. We used Immuneconv software to analyze the expression of circRNAs between the non-tumor NPE biopsies and nasopharyngeal carcinoma tissue samples in the dataset (Sturm et al., 2019).

RESULTS

Characteristics of Nasopharyngeal Carcinoma Tissue Samples

We selected a total of seven nasopharyngeal carcinoma tissues, including six patients with recurrent nasopharyngeal carcinoma, whose PET/CT and MRI are shown in **Figures 1A,B**. From PET/CT and MRI, it can be found that tumor had a recurrence after the treatment. **Figure 1C** shows the imaging data of #N17 patients' illness and the whole process of treatment. The specimen and clinical data of the initial patient are shown in **Figure 1D**, which shows that the patient had an occupying lesion in the nasopharyngeal area. In addition, we collected surgical tissues from patients who developed osteonecrosis after radiotherapy. The PET/CT results and relevant clinical information of the patients before and after treatment can be seen in the figure. Sanky figure show treatment procedure and clinical characteristics of selected nasopharyngeal carcinoma patients (**Figure 1D**).

Screening of T Cells in Nasopharyngeal Carcinoma Tissues

By flow sorting of nasopharyngeal carcinoma tissues, we screened to obtain the percentage of T cells in TIL in several nasopharyngeal carcinoma tissues. The results by using flow

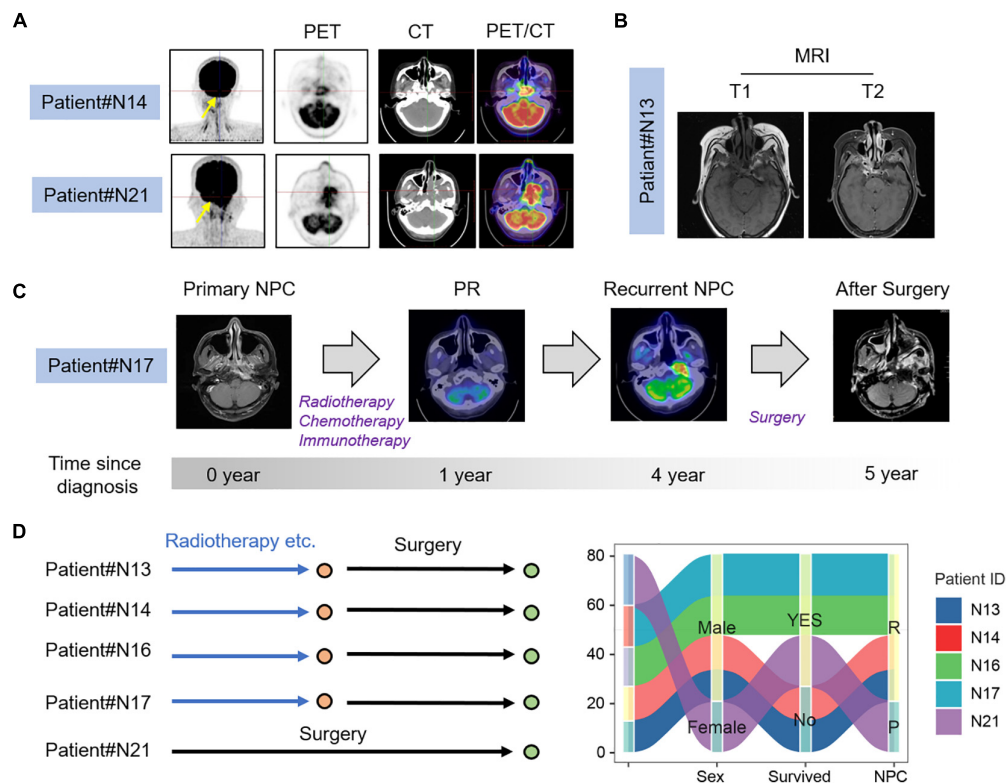


FIGURE 1 | Clinical characteristics of NPC patients. **(A)** PET-CT image of recurrent and primary NPC patients; **(B)** MRI images of recurrent NPC patients; **(C)** Process of treatment for recurrent nasopharyngeal carcinoma patient. **(D)** Clinical characters and treatment history sanky map of selected NPC patients.

cytometry showed that the percentage of T cells in TIL was significantly lower in the recurrent nasopharyngeal carcinoma group compared to the initial nasopharyngeal carcinoma group by comparing the percentage of T cells in the initial nasopharyngeal carcinoma (Figure 2).

T-Cell Distribution in Nasopharyngeal Carcinoma Tissues

To further investigate the distribution of T cells in recurrent nasopharyngeal carcinoma tissues, we further performed flow analysis of T cell subsets in the tissues. Detection of cell surface CD molecules using flow cytometry revealed that CD4 and CD8 were used to classify the CD3-positive cell population, and the proportion of T cells accounted for by CD4 and CD8-positive cells could be obtained, respectively, and it could be found that the ratio of CD4/CD8 accounted for by CD4/CD8 was greater than 1, and some of them could even be twice as high as CD8. This is consistent with the lower value of CD4/CD8 reported in some tumor literature implying a better prognosis. Then this result, the local tumor microenvironment of recurrent nasopharyngeal carcinoma after radiotherapy is altered in the case of certain chemokines and cytokines that contribute to the accumulation of CD4 expression positive cells toward the tumor (Figure 3A).

By comparing the proportion of T cells in TILs in primary nasopharyngeal carcinoma and recurrent nasopharyngeal carcinoma, it was observed that the proportion of T cells in

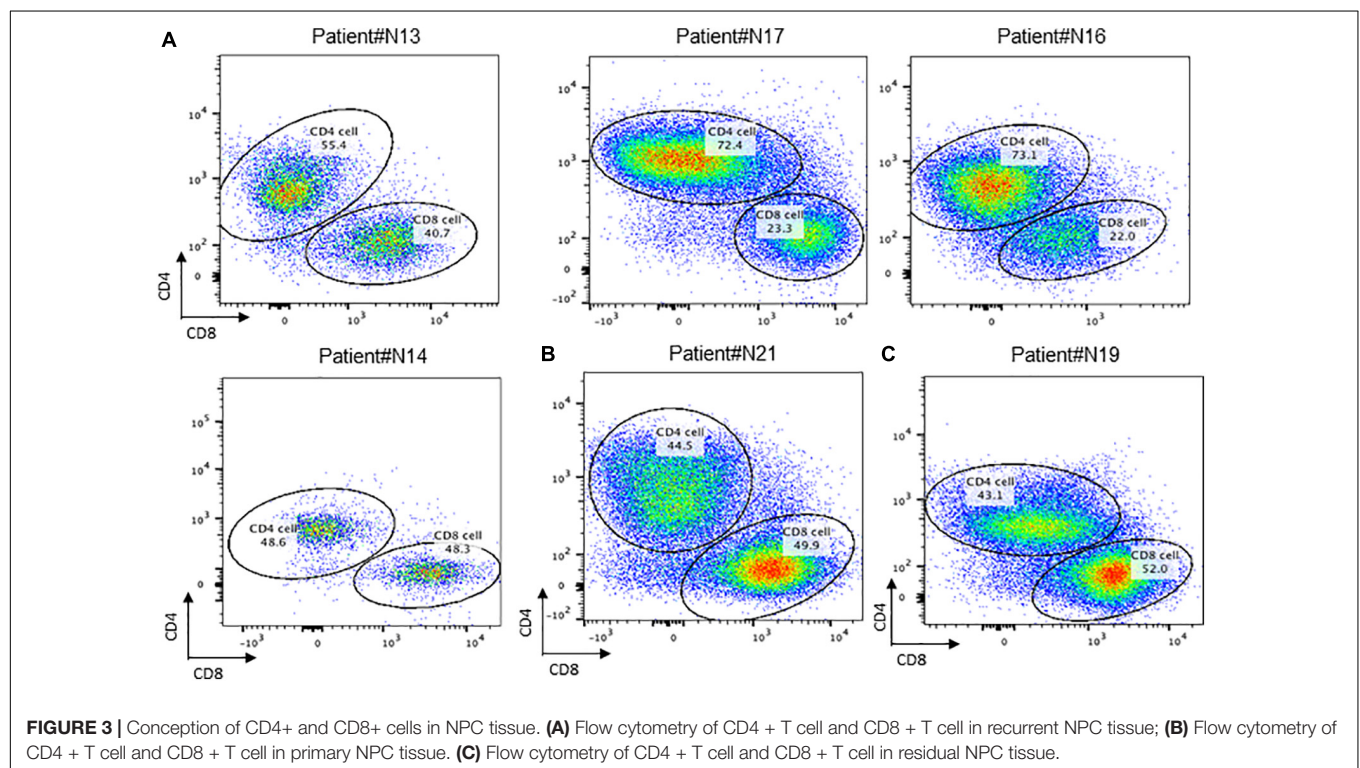
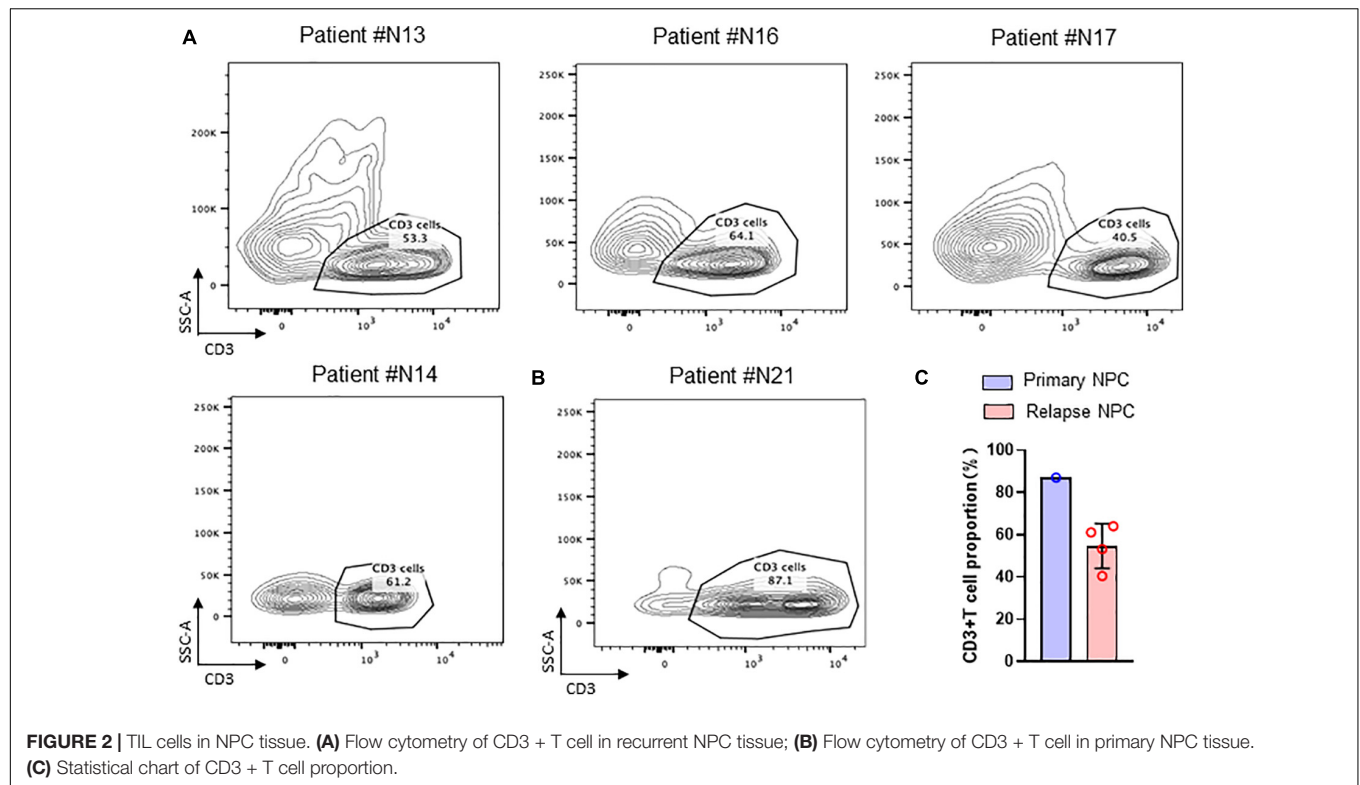
the recurrent nasopharyngeal carcinoma group was generally lower than that in N21, a primary nasopharyngeal carcinoma, which is consistent with the view that radiotherapy may reduce the proportion of T cells, and it has also been reported in the literature that a higher proportion of TILs in primary tumors predicts a better prognosis. However, due to the small number of patients enrolled in primary nasopharyngeal carcinoma, data are not available at this time (Figure 3B).

The ratio of CD4 and CD8 positive cells to T cells can be obtained by using CD4 and CD8 on the CD3 positive cell population circle gate. This result indicated that the local tumor microenvironment of recurrent nasopharyngeal carcinoma after radiotherapy is altered in the presence of certain chemokines and cytokines, which contribute to the accumulation of CD4 expression-positive cells toward the tumor.

It can be found in Figure 4 that the percentage of T reg cells in T cells is generally lower in patients who have undergone radiotherapy than in primary nasopharyngeal carcinoma, which is contrary to what has been reported in some of the literature and needs to be investigated more thoroughly.

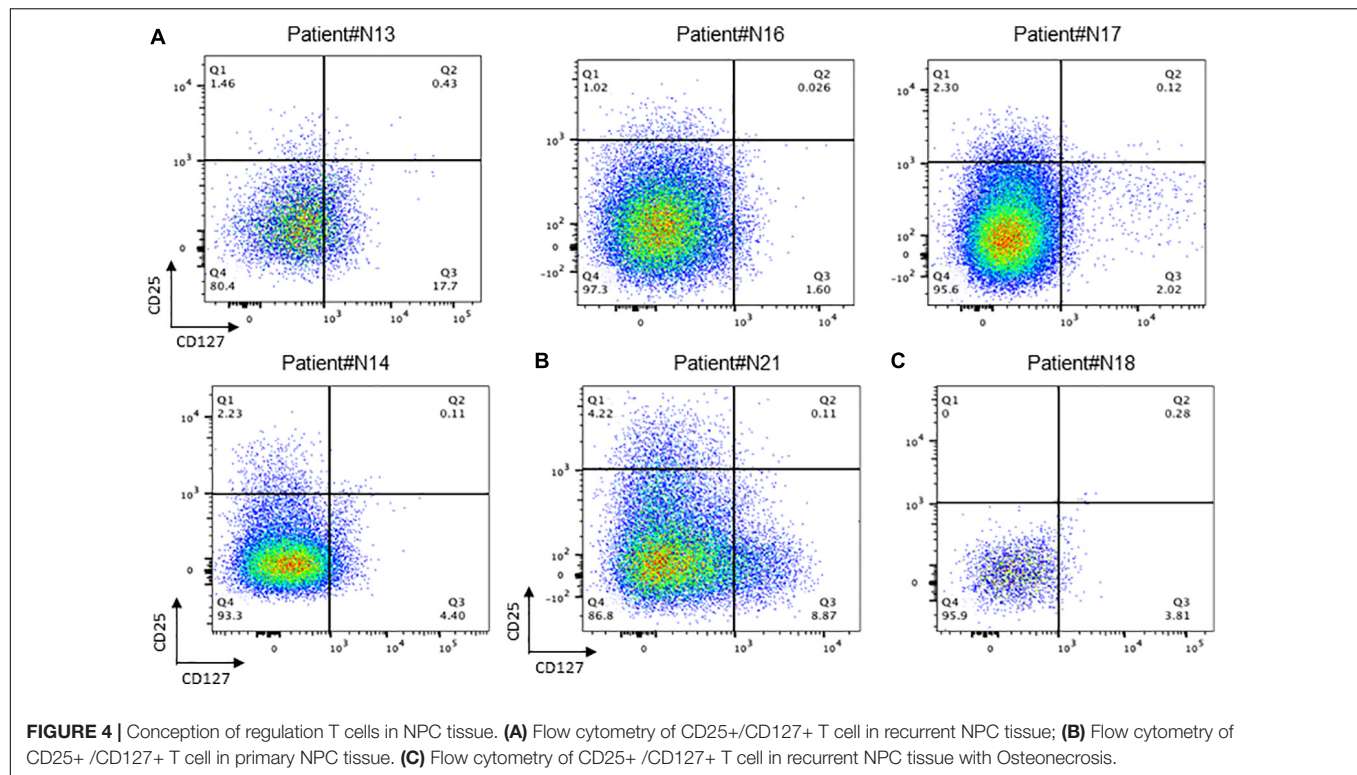
Involvement of Circular RNAs in Immune Microenvironment

As a hot topic in recent years, the expression of circRNA in T cells of nasopharyngeal carcinoma has not been reported yet. We obtained nasopharyngeal carcinoma circRNA sequencing



data (GSE134797). Five differently expressed circRNAs with high expression in nasopharyngeal carcinoma tissues were obtained by differential analysis of RNAseq data (Figure 5A).

CircRNA expression based tSNE map also showed that there are difference between nasopharyngeal carcinoma tissue and non-NPC nasopharyngeal epithelial tissues (Figure 5B).



Further gene immune infiltration analysis of differently expressed gene molecules, we constructed an immune infiltration cell model in both NPC and normal NPE. The results suggested that compared with primary non-NPC nasopharyngeal epithelial tissues, there is much difference in nasopharyngeal carcinoma, especially immune cell and their function (**Figure 5C**).

We then isolated CD4 positive and CD4 negative cells in surgically obtained samples of recurrent nasopharyngeal carcinoma. After extracting RNA from these CD4-positive and negative cells and reverse transcribing to obtain cDNA, qRT-PCR was used to test the expression of selected five circRNAs in CD4-positive and negative cells obtained by screening. Results showed that these five circRNA molecules were all highly expressed in T cells (Ct value < 26) and NPC tissues (**Figure 5C**).

DISCUSSION

Nasopharyngeal carcinoma is a malignant tumor of nasopharyngeal epithelial origin, and the treatment of primary nasopharyngeal carcinoma is mainly based on radiation therapy (Wang et al., 2019; Peng et al., 2021). Although most nasopharyngeal carcinomas are initially sensitive to radiation therapy, more and more clinical applications have found that most nasopharyngeal carcinomas will develop radiation therapy resistance and recurrence. The mechanism of radiation resistance and recurrence has become a major cause of treatment failure in nasopharyngeal carcinoma. However, the mechanisms involved are still very unclear (Suarez et al., 2010; Zhang et al., 2020). Immunity is an important influencing factor in the

development of nasopharyngeal carcinoma. In recent years, the concept of tumor immune microenvironment has also led to a more in-depth study of immune alterations in tumors. Tumor infiltrating cell TIL is a very popular research area in recent years, as a special cell type of T cells, there is an interaction between TIL and tumor cells.

As the main component of cellular immunity, T cells play an important function in tumor immunity. With the intensive study of immunity, T cells have been found to exist in numerous subpopulations (Li et al., 2021). As the main cell type that regulates cellular immunity, Treg plays an important function in immunity. Regulatory T cells (Treg) are a subset of T cells with significant immunosuppressive effects, characterized by a cellular phenotype expressing Foxp3, CD25, and CD4. People have found that Treg plays an important function in the development and progression of diseases such as tumors (Chen et al., 2020). It can suppress the immune response of other cells and is the primary controller of self-tolerance. Often, its absence or abnormal function leads to the development of several autoimmune-related diseases, including tumors. After immune cells, such as T cells, B cells, and NK cells, generate immune responses to recognize and remove harmful substances and thus protect the body from attack, Treg cells suppress these immune cells, including by secreting cytokines, to regulate the body's immune homeostasis and prevent autoimmune diseases (Mo et al., 2019b; Selck and Dominguez-Villar, 2021). Our study shows that the composition of tumor T cells changes significantly during the recurrence of nasopharyngeal carcinoma, both in the number of CD4+ cells and in the CD4+/CD8+ ratio. This also suggests that T-cell subsets are significantly altered during nasopharyngeal carcinoma recurrence. As the main target

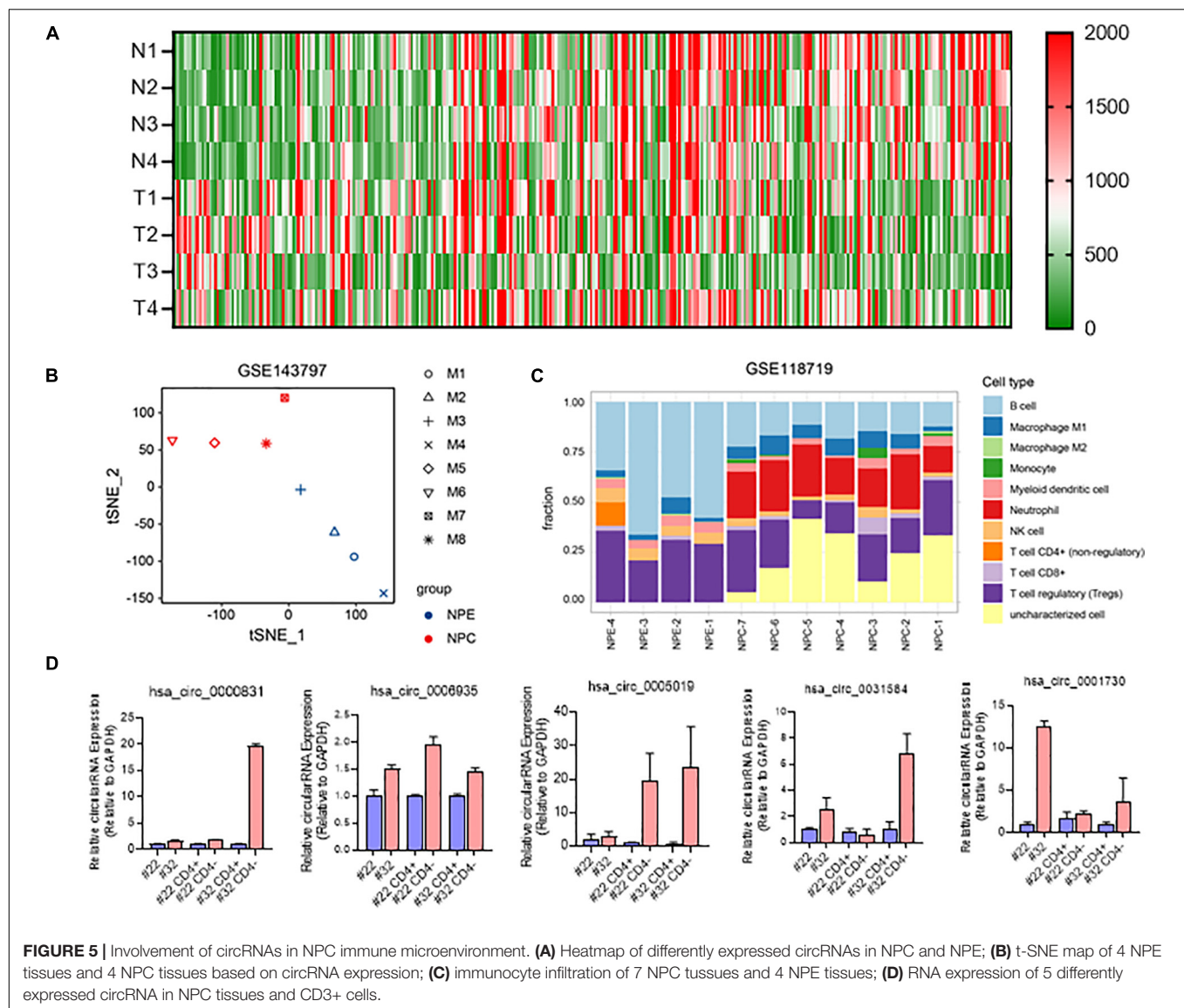


FIGURE 5 | Involvement of circRNAs in NPC immune microenvironment. **(A)** Heatmap of differentially expressed circRNAs in NPC and NPE; **(B)** t-SNE map of 4 NPE tissues and 4 NPC tissues based on circRNA expression; **(C)** immunocyte infiltration of 7 NPC tissues and 4 NPE tissues; **(D)** RNA expression of 5 differently expressed circRNA in NPC tissues and CD3+ cells.

cells for tumor immunotherapy, the altered composition and number of T cells suggest that the immunotherapy regimen for recurrent nasopharyngeal carcinoma may be different from that for primary nasopharyngeal carcinoma.

Circular RNA molecules play an important function in immunity. As a hot topic of non-coding RNA research in recent years, circRNAs have been found to play important functions in numerous life activities (Anczukow et al., 2015; He et al., 2016; Wang et al., 2021). The current modes of action of circRNAs include ceRNA regulation, encoding small peptides, and binding proteins to exert functions (Li et al., 2018; Wang et al., 2019; Chi et al., 2020). Although the latter two modes of action are currently uncommon, a growing number of studies suggest that circRNAs function in a variety of ways. Several studies have been reported on the function of circRNAs in T cells. Reports showing EBV coding circRNA have function in nasopharyngeal carcinoma by regulating PDL1, pathway to function. But the function of circRNA in immune cells is still very unclear. In addition circRNA

has great advantages and potential as a molecular marker of tumor due to its stability brought by its special structure. Whether circRNA can be used as a marker for predicting the effect of immunotherapy is still unclear. It is a direction that deserves further exploration.

As a well-defined factor associated with nasopharyngeal carcinogenesis, EBV infection causing uncontrolled inflammation and nasopharyngeal carcinogenesis are significantly correlated. EBVs, their encoded proteins and microRNAs, and even encoded circRNAs have been shown to be important contributors to the development and progression of nasopharyngeal carcinoma. However, the involvement of circRNAs in the immune microenvironment is still very unclear. Our study, on the other hand, found that has-circ-0006935 and other circRNAs are not only highly expressed in nasopharyngeal carcinoma tissues, but also in immune cells of recurrent nasopharyngeal carcinoma tissues, even compared to CD3- cells, some circRNAs' expression was higher in CD3+ cells. These

results suggest that circRNA plays an important function in the tumor microenvironment caused by tumor recurrence, and further studies are needed to explore.

In recent years, surgery has gradually become one of the main modalities for the treatment of recurrent nasopharyngeal carcinoma (Liu et al., 2019, 2020). In turn, surgery can also have an impact on the immune status of the patient as well as the tumor microenvironment (Jiang et al., 2020; Tseng et al., 2020). Therefore the effect of surgery as a variable on the immune microenvironment of nasopharyngeal carcinoma and whether circRNA plays an important function in this process. This is a question that deserves to be explored in depth.

In conclusion, we found that the ratio of T cells in the tumor microenvironment may be altered in recurrent nasopharyngeal carcinoma compared to primary nasopharyngeal carcinoma. Alterations in Treg and CD4⁺/CD8⁺ ratios may also be found. circRNA is highly expressed in tumor-associated T cells and may play an important function.

DATA AVAILABILITY STATEMENT

The raw data supporting the conclusions of this article will be made available by the authors, without undue reservation.

ETHICS STATEMENT

The studies involving human participants were reviewed and approved by Xiangya Hospital, Central South University. The

patients/participants provided their written informed consent to participate in this study. Written informed consent was obtained from the individual(s) for the publication of any potentially identifiable images or data included in this article.

AUTHOR CONTRIBUTIONS

YuW and ZP contributed to all of the literature review in this work. YaW, YY, and RF collected and analyzed the data of this article. WJ participated in the process of finalizing the final manuscript. All authors have read and approved the manuscript.

FUNDING

This Research was funded by the National Natural Science Foundation of China (81770985), Xiangya Hospital Funds for Young Scholar (2020Q13), the Hunan Province Graduate Education Innovation Project (CX20200386), and China Postdoctoral Science Foundation funded project (2021M693567 and 2021TQ0374). The funders had no role in study design, data collection and analysis, decision to publish, or preparation of the manuscript.

ACKNOWLEDGMENTS

We would like to thank Yongzhen Mo for the discussion.

REFERENCES

- Anczukow, O., Akerman, M., Clery, A., Wu, J., Shen, C., Shirole, N., et al. (2015). SRSF1-regulated alternative splicing in breast cancer. *Mol. Cell* 60, 105–117. doi: 10.1016/j.molcel.2015.09.005
- Chen, H., Chen, H., Zhang, J., Wang, Y., Simoneau, A., Yang, H., et al. (2020). cGAS suppresses genomic instability as a decelerator of replication forks. *Sci. Adv.* 6:eabb8941. doi: 10.1126/sciadv.abb8941
- Chen, L. L. (2020). The expanding regulatory mechanisms and cellular functions of circular RNAs. *Nat. Rev. Mol. Cell Biol.* 21, 475–490. doi: 10.1038/s41580-020-0243-y
- Chen, Y., Chan, A. T. C., Le, Q., Blanchard, P., Sun, Y., Ma, J., et al. (2019). Nasopharyngeal carcinoma. *Lancet* 394, 64–80.
- Chi, G., Yang, F., Xu, D., and Liu, W. (2020). Silencing hsa_circ_PVT1 (circPVT1) suppresses the growth and metastasis of glioblastoma multiforme cells by up-regulation of miR-199a-5p. *Artif. Cells Nanomed. Biotechnol.* 48, 188–196. doi: 10.1080/21691401.2019.1699825
- Hanahan, D., and Weinberg, R. A. (2011). Hallmarks of cancer: the next generation. *Cell* 144, 646–674. doi: 10.1016/j.cell.2011.02.013
- He, B., Li, W., Wu, Y., Wei, F., Gong, Z., Bo, H., et al. (2016). Epstein-Barr virus-encoded miR-BART6-3p inhibits cancer cell metastasis and invasion by targeting long non-coding RNA LOC553103. *Cell Death Dis.* 7:e2353.
- Jiang, W., Xie, S., Wu, X., Gao, K., Feng, Y., Mei, L., et al. (2020). Clinical characteristics and prognosis of sudden sensorineural hearing loss in post-irradiated nasopharyngeal carcinoma survivors. *Otol. Neurotol.* 41, e790–e794. doi: 10.1097/MAO.0000000000002701
- Jin, S., Li, R., Chen, M., Yu, C., Tang, L., Liu, Y., et al. (2020). Single-cell transcriptomic analysis defines the interplay between tumor cells, viral infection, and the microenvironment in nasopharyngeal carcinoma. *Cell Res.* 30, 950–965. doi: 10.1038/s41422-020-00402-8
- Li, L., Xiong, F., Wang, Y., Zhang, S., Gong, Z., Li, X., et al. (2021). What are the applications of single-cell RNA sequencing in cancer research: a systematic review. *J. Exp. Clin. Cancer Res.* 40:163. doi: 10.1186/s13046-021-01955-1
- Li, X., Zhang, Z., Jiang, H., Li, Q., Wang, R., Pan, H., et al. (2018). Circular RNA circPVT1 promotes proliferation and invasion through sponging miR-125b and activating E2F2 signaling in non-small cell lung cancer. *Cell Physiol. Biochem.* 51, 2324–2340. doi: 10.1159/000495876
- Liu, Q., Sun, X., Li, H., Zhou, J., Gu, Y., Zhao, W., et al. (2020). Types of transnasal endoscopic nasopharyngectomy for recurrent nasopharyngeal carcinoma: Shanghai EENT hospital experience. *Front. Oncol.* 10:555862. doi: 10.3389/fonc.2020.555862
- Liu, Y., Lv, X., Zou, X., Hua, Y., You, R., Yang, Q., et al. (2019). Minimally invasive surgery alone compared with intensity-modulated radiotherapy for primary stage I nasopharyngeal carcinoma. *Cancer Commun.* 39:75. doi: 10.1186/s40880-019-0415-3
- Liu, Y., Wen, Y., Tang, J., Wei, Y., You, R., Zhu, X., et al. (2021). Endoscopic surgery compared with intensity-modulated radiotherapy in resectable locally recurrent nasopharyngeal carcinoma: a multicentre, open-label, randomised, controlled, phase 3 trial. *Lancet Oncol.* 22, 381–390. doi: 10.1016/S1470-2045(20)30673-2
- Mo, Y., Wang, Y., Xiong, F., Ge, X., Li, Z., Li, X., et al. (2019a). Proteomic analysis of the molecular mechanism of lovastatin inhibiting the growth of nasopharyngeal carcinoma cells. *J. Cancer* 10, 2342–2349. doi: 10.7150/jca.30454
- Mo, Y., Wang, Y., Zhang, L., Yang, L., Zhou, M., Li, X., et al. (2019b). The role of Wnt signaling pathway in tumor metabolic reprogramming. *J. Cancer* 10, 3789–3797. doi: 10.7150/jca.31166
- Peng, Z., Wang, Y., Wang, Y., Jiang, S., Fan, R., Zhang, H., et al. (2021). Application of radiomics and machine learning in head and neck cancers. *Int. J. Biol. Sci.* 17, 475–486. doi: 10.7150/ijbs.55716
- Selck, C., and Dominguez-Villar, M. (2021). Antigen-specific regulatory T cell therapy in autoimmune diseases and transplantation. *Front. Immunol.* 12:661875. doi: 10.3389/fimmu.2021.661875

- Sturm, G., Finotello, F., Petitprez, F., Zhang, J., Baumbach, J., Fridman, W., et al. (2019). Comprehensive evaluation of transcriptome-based cell-type quantification methods for immuno-oncology. *Bioinformatics* 35, i436–i445. doi: 10.1093/bioinformatics/btz363
- Suarez, C., Rodrigo, J., Rinaldo, A., Langendijk, J., Shaha, A., Ferlito, A., et al. (2010). Current treatment options for recurrent nasopharyngeal cancer. *Eur. Arch. Otorhinolaryngol.* 267, 1811–1824.
- Tessier, S., Doolittle, A., Sao, K., Rotty, J., Bear, J., Ulici, V., et al. (2020). Arp2/3 inactivation causes intervertebral disc and cartilage degeneration with dysregulated TonEBP-mediated osmoadaptation. *JCI Insight* 5:e131382. doi: 10.1172/jci.insight.131382
- Tseng, M., Ho, F., Leong, Y., Wong, L., Tham, I., Cheo, T., et al. (2020). Emerging radiotherapy technologies and trends in nasopharyngeal cancer. *Cancer Commun.* 40, 395–405. doi: 10.1002/cac2.12082
- Wang, W., Zhou, R., Wu, Y., Liu, Y., Su, W., Xiong, W., et al. (2019). PVT1 promotes cancer progression via MicroRNAs. *Front Oncol.* 9:609. doi: 10.3389/fonc.2019.00609
- Wang, Y., Mo, Y., Gong, Z., Yang, X., Yang, M., Zhang, S., et al. (2017). Circular RNAs in human cancer. *Mol. Cancer* 16:25.
- Wang, Y., Zhang, L., Yang, Y., Lu, S., and Chen, H. (2021). Progress of gastric cancer surgery in the era of precision medicine. *Int. J. Biol. Sci.* 17, 1041–1049. doi: 10.7150/ijbs.56735
- Wu, C., Lv, J., Lin, L., Mao, Y., Deng, B., Zheng, W., et al. (2021). Development and validation of a web-based calculator to predict individualized conditional risk of site-specific recurrence in nasopharyngeal carcinoma: analysis of 10,058 endemic cases. *Cancer Commun.* 41, 37–50. doi: 10.1002/cac2.12113
- Xia, L., Oyang, L., Lin, J., Tan, S., Han, Y., Wu, N., et al. (2021). The cancer metabolic reprogramming and immune response. *Mol. Cancer* 20:28.
- Yang, J., Gong, Y., Jiang, Q., Liu, L., Li, S., Zhou, Q., et al. (2020). Circular RNA expression profiles in nasopharyngeal carcinoma by sequence analysis. *Front. Oncol.* 10:601. doi: 10.3389/fonc.2020.00601
- Zhang, L., Giuste, F., Vizcarra, J., Li, X., and Gutman, D. (2020). Radiomics features predict CIC mutation status in lower grade glioma. *Front. Oncol.* 10:937. doi: 10.3389/fonc.2020.00937
- Zheng, Q., Bao, C., Guo, W., Li, S., Chen, J., Chen, B., et al. (2016). Circular RNA profiling reveals an abundant circHIPK3 that regulates cell growth by sponging multiple miRNAs. *Nat. Commun.* 7:11215. doi: 10.1038/ncomms11215
- Zhong, Y., Du, Y., Yang, X., Mo, Y., Fan, C., Xiong, F., et al. (2018). Circular RNAs function as ceRNAs to regulate and control human cancer progression. *Mol. Cancer* 17:79.

Conflict of Interest: The authors declare that the research was conducted in the absence of any commercial or financial relationships that could be construed as a potential conflict of interest.

The handling editor declared a shared affiliation, though no other collaboration, with the authors at the time of the review.

Publisher's Note: All claims expressed in this article are solely those of the authors and do not necessarily represent those of their affiliated organizations, or those of the publisher, the editors and the reviewers. Any product that may be evaluated in this article, or claim that may be made by its manufacturer, is not guaranteed or endorsed by the publisher.

Copyright © 2021 Wang, Peng, Wang, Yang, Fan, Gao, Zhang, Xie and Jiang. This is an open-access article distributed under the terms of the Creative Commons Attribution License (CC BY). The use, distribution or reproduction in other forums is permitted, provided the original author(s) and the copyright owner(s) are credited and that the original publication in this journal is cited, in accordance with accepted academic practice. No use, distribution or reproduction is permitted which does not comply with these terms.



A Novel Pyroptosis-Associated Long Non-coding RNA Signature Predicts Prognosis and Tumor Immune Microenvironment of Patients With Breast Cancer

Liqin Ping^{1†}, Kaiming Zhang^{2†}, Xueqi Ou², Xingsheng Qiu^{3*} and Xiangsheng Xiao^{2*}

¹ State Key Laboratory of Oncology in South China, Department of Medical Oncology, Sun Yat-sen University Cancer Center, Collaborative Innovation Center for Cancer Medicine, Guangzhou, China, ² State Key Laboratory of Oncology in South China, Department of Breast Oncology, Sun Yat-sen University Cancer Center, Collaborative Innovation Center for Cancer Medicine, Guangzhou, China, ³ Department of Radiation Oncology, Sun Yat-sen Memorial Hospital, Sun Yat-sen University, Guangzhou, China

OPEN ACCESS

Edited by:

Zong Sheng Guo,
University of Pittsburgh, United States

Reviewed by:

Xiaoyun Zeng,
Guangxi Medical University, China
Ke-Da Yu,
Fudan University, China

*Correspondence:

Xingsheng Qiu
qxshs@126.com
Xiangsheng Xiao
xiaoxsh@sysucc.org.cn

[†] These authors have contributed
equally to this work and share first
authorship

Specialty section:

This article was submitted to
Molecular and Cellular Oncology,
a section of the journal
Frontiers in Cell and Developmental
Biology

Received: 18 June 2021

Accepted: 23 August 2021

Published: 20 September 2021

Citation:

Ping L, Zhang K, Ou X, Qiu X and
Xiao X (2021) A Novel
Pyroptosis-Associated Long
Non-coding RNA Signature Predicts
Prognosis and Tumor Immune
Microenvironment of Patients With
Breast Cancer.
Front. Cell Dev. Biol. 9:727183.
doi: 10.3389/fcell.2021.727183

Background: Pyroptosis, a kind of programmed cell death characterized by the rupture of cell membranes and the release of inflammatory substances, plays an important role in the occurrence and development of cancer. However, few studies focus on the pyroptosis-associated long non-coding RNAs (lncRNAs) in breast cancer (BC). The prognostic value of pyroptosis-associated lncRNAs and their relationship with tumor microenvironment (TME) in BC remain unclear. The purpose of this study was to explore the prognostic role of pyroptosis-associated lncRNAs and their relationship with TME in BC.

Methods: The transcriptome data and clinical data of female BC patients were downloaded from The Cancer Genome Atlas (TCGA) database. A total of 937 patients were randomly assigned to either training set or validation set. A pyroptosis-associated lncRNA signature was constructed in the training set and verified in the validation set. Functional analysis and immune microenvironment analysis related to pyroptosis-associated lncRNAs were performed. A nomogram based on the risk score and clinical characteristics was established.

Results: A 9-pyroptosis-associated lncRNA signature was constructed to separate BC patients into two risk groups. High-risk patients had poorer prognosis than low-risk patients. The risk score was proven to be an independent prognostic factor by multivariate Cox regression analysis. Function analysis and immune microenvironment analysis showed that low-risk BC tended to be an immunologically “hot” tumor. A nomogram was constructed with risk score and clinical characteristics. Receiver operating characteristic curve (ROC) analysis demonstrated credible predictive power of the nomogram. The area under time-dependent ROC curve (AUC) reached 0.880 at 1 year, 0.804 at 3 years, and 0.769 at 5 years in the training set, and 0.799 at 1 year, 0.794 at 3 years, and 0.728 at 5 years in the validation set.

Conclusion: We identified a novel pyroptosis-associated lncRNA signature that was an independent prognostic indicator for BC patients. Pyroptosis-associated lncRNAs had potential relationship with the immune microenvironment and might be therapeutic targets for BC patients.

Keywords: breast cancer, pyroptosis, lncRNAs, prognosis, tumor infiltrating lymphocytes, immune checkpoints

INTRODUCTION

Breast cancer (BC) is the most common malignant tumor in the world (Sung et al., 2021), and it is a tumor with quite strong heterogeneity (Faria et al., 2021). According to PAM50, BC was classified into five subtypes (i.e., luminal A, luminal B, Her2-enriched, normal-like, and basal-like) (Pu et al., 2020). Even so, patients with the same molecular types and clinical characteristics have different prognosis and different responses to chemotherapy or immunotherapy (Tekpli et al., 2019), suggesting that there are still subtle factors influencing its prognosis and response to treatment.

Pyroptosis is an inflammatory form of programmed cell death mediated by gasdermins (GSDMs; Xia et al., 2019). Inflammasomes activate caspase-1/4/5/11 to cleave GSDMs, and the cleaved GSDMs are transported to the cell membrane to form cellular pores leading to cell swelling and death (Fang et al., 2020). Pyroptosis plays an important role in killing cancer cells. The mechanism of some chemotherapy drugs to kill cancer cells is partly dependent on pyroptosis. It has been proven that etoposide (Wang Y. et al., 2017), paclitaxel, and cisplatin (Zhang et al., 2019) can induce pyroptosis in cancer cells with high expression of gasdermin E (GSDME). In the process of pyroptosis in cancer cells, chemokines and tumor-associated antigens (TAAs) are released to stimulate an antitumor immune response and inhibit the progression of cancer (Garg and Agostinis, 2017). On the other hand, part of the mechanism by which immune cells kill cancer cells depends on inducing pyroptosis. It has been reported that natural killer (NK) cells and cytotoxic T lymphocytes could kill cancer cells by releasing granzyme A (GZMA) to cleave GSDMB (Zhou et al., 2020) and granzyme B (GZMB) to directly cleave GSDME to activate pyroptosis in cancer cells (Zhang et al., 2020). It is suggested that there is a close relationship between pyroptosis and antitumor immunity. Immune checkpoint blockade (ICB) therapy is an effective therapeutic strategy that relies on antitumor immunity in various cancers. However, its efficacy in BC is limited (Nanda et al., 2016; Adams et al., 2019). It has been proven that the tumor-infiltrating lymphocytes (TILs) in the BC are often poor, which makes most BC known as “cold” tumor (Thorsson et al., 2018; Tekpli et al., 2019). How to increase the TILs of the tumor microenvironment (TME) and transform it into “hot” tumor is of great significance for improving the efficacy of ICB therapy in BC. Because there is a close relationship between pyroptosis and antitumor immunity, exploring the role of pyroptosis in BC and pyroptosis-related molecules will help us investigate strategies to transform “cold” BC into “hot” BC.

Long non-coding RNAs (lncRNAs) are RNAs that do not participate in protein coding but are involved in important

regulatory processes, such as genomic imprinting, chromatin modification, transcriptional activation, transcriptional interference, and intranuclear transport, which are involved in the development and metastasis of BC (Liang et al., 2020). At the same time, lncRNAs can also play an important role in mediating pyroptosis. For example, it has been reported that lncRNA MEG3 could increase the expression of NLRP3 and enhance pyroptosis of endothelial cells (Zhang et al., 2018). Wang et al. (2021) revealed that lncRNA XIST promoted pyroptosis through the XIST/miR-150-5p/c-Fos axis, and Wan et al. (2020) discovered that lncRNA-H19 significantly promoted NLRP3/6 inflammasome imbalance and induced pyroptosis of microglia. Furthermore, Tan et al. (2021) found that lncRNA HOTTIP could inhibit pyroptosis of ovarian cancer cells by targeting the miR-148a-3p/AKT2 axis. However, there are limited studies focusing on pyroptosis-associated lncRNAs in BC. The prognostic value of pyroptosis-associated lncRNAs and their relationship with TME in BC remain unclear.

Therefore, this study aims to identify the lncRNAs related to pyroptosis in BC and clarify the role of pyroptosis-associated lncRNAs in the TME and prognosis of BC, which not only provides important insights into the molecular and signaling pathways of pyroptosis in BC but also has important significance in transforming immunologically “cold” BC into “hot” tumor.

MATERIALS AND METHODS

Data Acquisition and Identification of Pyroptosis-Associated lncRNAs

The transcriptome data and clinical data of 1,035 female BC patients were downloaded from The Cancer Genome Atlas (TCGA) database¹. The Ensembl human genome browser GRCh38.p13 was used to distinguish the protein-coding genes and lncRNAs. Patients with incomplete clinical data were excluded from this study, and the details of these excluded patients are shown in **Figure 1**. The data of this study were publicly available from TCGA database, and this study was in accordance with TCGA's publication guidelines. Pyroptosis-associated genes were downloaded from the Molecular Signatures Database version 7.4². The correlation between pyroptosis-associated lncRNAs and pyroptosis-associated genes was evaluated by Pearson correlation analysis, and the pyroptosis-associated lncRNAs were identified according to the standard that the absolute value of Pearson correlation coefficient

¹<https://portal.gdc.cancer.gov/repository>

²<https://www.gsea-msigdb.org/gsea/msigdb/index.jsp>

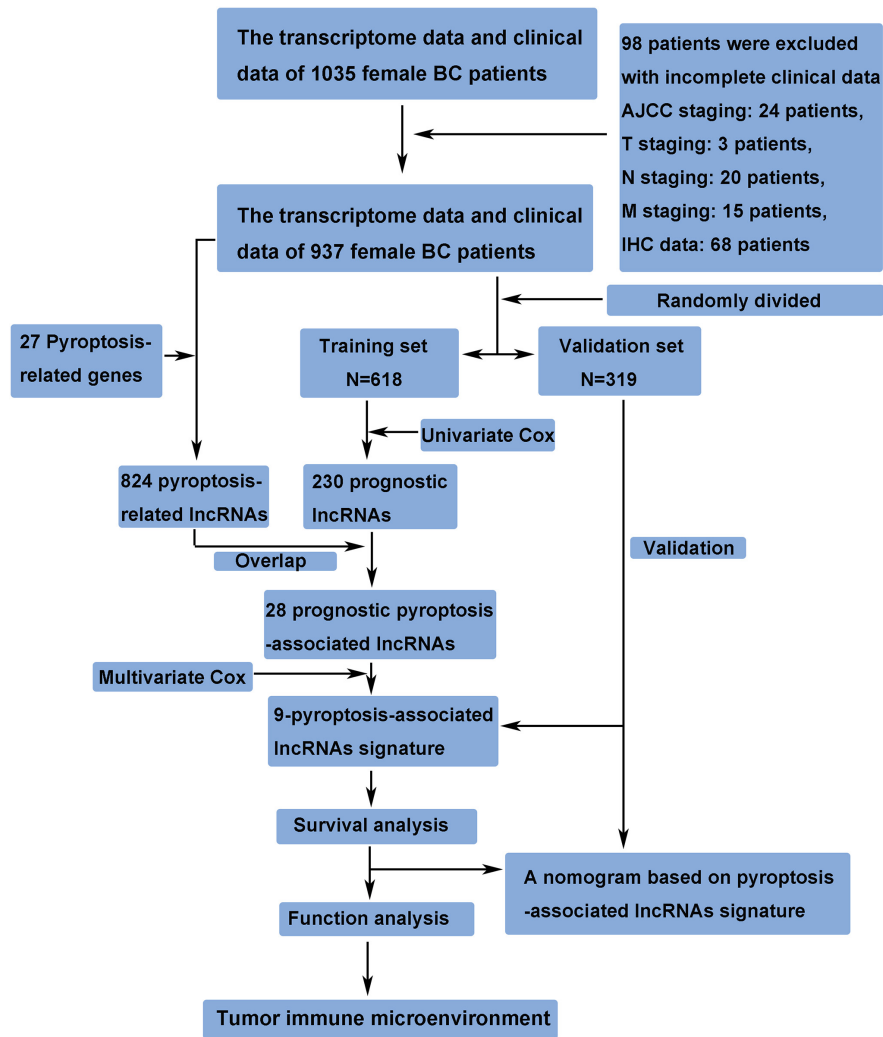


FIGURE 1 | Study design and flowchart of this study.

was more than 0.3 ($|R| > 0.3$) and the p -value was less than 0.05 ($p < 0.05$).

Construction of a Prognostic Pyroptosis-Associated lncRNA Signature

A total of 937 female BC patients were randomly assigned to either training set or validation set. The prognostic lncRNAs were identified based on univariate Cox regression analysis in the training set. The overlapping lncRNAs of prognostic lncRNAs and pyroptosis-associated lncRNAs were identified as the candidate lncRNAs for the pyroptosis-associated lncRNA signature. Then, the pyroptosis-associated lncRNA signature was constructed based on multivariate Cox regression analysis and lowest Akaike information criterion (AIC) value (Vrieze, 2012). Finally, the risk score of each patient was calculated based on this prognostic signature. The formula of risk score was as follows: Risk Score = e^{sum} (normalized expression level of each pyroptosis-associated lncRNA \times corresponding regression

coefficient). Patients in the training set were separated into the high-risk group and low-risk group based on the median value of the risk score. The overall survival (OS) between the high-risk and low-risk groups was compared by Kaplan–Meier analysis.

Validation of the Pyroptosis-Associated lncRNA Signature

The risk score of patients in the validation set was calculated according to the same formula as the training set, and patients in the validation set were separated into the high-risk group and low-risk group based on the same cutoff value as the training set. Then, Kaplan–Meier analysis was performed to compare the OS between the high-risk and low-risk groups in the validation set.

Single Sample Gene Set Enrichment Analysis

The transcriptome data and clinical data of the Molecular Taxonomy of Breast Cancer International Consortium

(METABRIC) database and GSE20685 were downloaded. The single sample gene set enrichment analysis (ssGSEA) was conducted to explore the activation level of pyroptosis pathway in BC expression profile of the METABRIC and GSE20685 database using the R package “GSVA.” Patients in the METABRIC or GSE20685 database were separated into the pyroptosis-upregulated group and pyroptosis-downregulated group based on the median value of the pyroptosis pathway score. Then, Kaplan–Meier analysis was performed to compare the prognosis between the pyroptosis-upregulated group and pyroptosis-downregulated group in the METABRIC or GSE20685 database.

The mRNA-lncRNA Coexpression Network

The Cytoscape software version 3.7.2 was used to construct the mRNA-lncRNA coexpression network between the candidate lncRNAs and their corresponding pyroptosis-associated genes. Subsequently, the Sankey diagram was constructed to demonstrate the relationship between pyroptosis-associated lncRNAs and their corresponding genes.

Gene Set and Function Enrichment Analysis

The differentially expressed genes between the high-risk group and low-risk group were screened with the $|\log_2FC| \geq 1$ and the false discovery rate (FDR) < 0.05 using the “edgeR” R package. The GSEA³ was performed to investigate the differences between the patients in high-risk group and low-risk group. The Gene Ontology (GO) analysis was performed to explore the biological processes related to the pyroptosis-associated lncRNAs, and the Kyoto Encyclopedia of Genes and Genomes (KEGG) pathway analysis was performed to identify the signaling pathways associated with the pyroptosis-associated lncRNAs.

Analysis of Tumor-Infiltrating Immune Cells

The CIBERSORT algorithm (Newman et al., 2015) was used to calculate the proportion of each kind of tumor-infiltrating immune cells in BC samples. The results obtained by the CIBERSORT algorithm were filtered based on p -value < 0.05 . Then, the differences in each type of immune cell between the high-risk and low-risk groups were compared to assess the differences in the tumor immune microenvironment between two groups.

Statistical Analysis

SPSS (Version 23.0) and R software (Version 3.5.3) were used to conduct statistical analyses in this study. The differences in each type of immune cell and the expression of immune checkpoint molecules between the high-risk and low-risk groups were compared by Wilcoxon test. Chi-square test was performed to compare the differences in clinical features. Univariate and multivariate Cox regression analyses were conducted to identify

prognostic indicators of OS. The “rms” package of the R software was used to construct a nomogram including clinical features and risk score. The predictive accuracy of the nomogram was evaluated by time-dependent receiver operating characteristic curve (ROC) curve analysis. Statistical significance was defined as p -value < 0.05 , and all p -values were two-tailed.

RESULTS

Clinical Features of Patients in Training Set and Validation Set

A total of 937 female BC patients were randomly assigned to either training set ($n = 618$) or validation set ($n = 319$) in nearly 2:1 ratio. The clinical features of all patients are shown in detail in **Table 1**. There were no statistically significant differences in clinical features between patients in the training set and validation set.

Construction of a Prognostic Pyroptosis-Associated lncRNA Signature

First, 230 prognostic lncRNAs were identified based on univariate Cox regression analysis in the training set, and 824 lncRNAs were identified as pyroptosis-associated lncRNAs according to the coexpression relationship between lncRNAs and

TABLE 1 | Patients' clinical features of training set and validation set.

Variables	Training set (<i>n</i> = 618)		Validation set (<i>n</i> = 319)		<i>p</i> -Value
	NO.	%	NO.	%	
Age					0.640
— ≤60	347	56.1	174	54.5	
— >60	271	43.9	145	45.5	
Stage					0.352
— I	103	16.7	56	17.6	
— II	356	57.6	190	59.6	
— III	146	23.6	71	22.3	
— IV	13	2.1	2	0.6	
T stage					0.682
— T1	154	24.9	87	27.3	
— T2	368	59.5	184	57.7	
— T3	78	12.6	42	13.2	
— T4	18	2.9	6	1.9	
N stage					0.263
— N0	288	46.6	156	48.9	
— N1	209	33.8	108	33.9	
— N2	79	12.8	28	8.8	
— N3	42	6.8	27	8.5	
M stage					0.088
— M0	605	97.9	317	99.4	
— M1	13	2.1	2	0.6	
Subtype					0.488
— Non-triple negative	526	85.1	266	83.4	
— Triple negative	92	14.9	53	16.6	

³<http://www.broadinstitute.org/gsea>

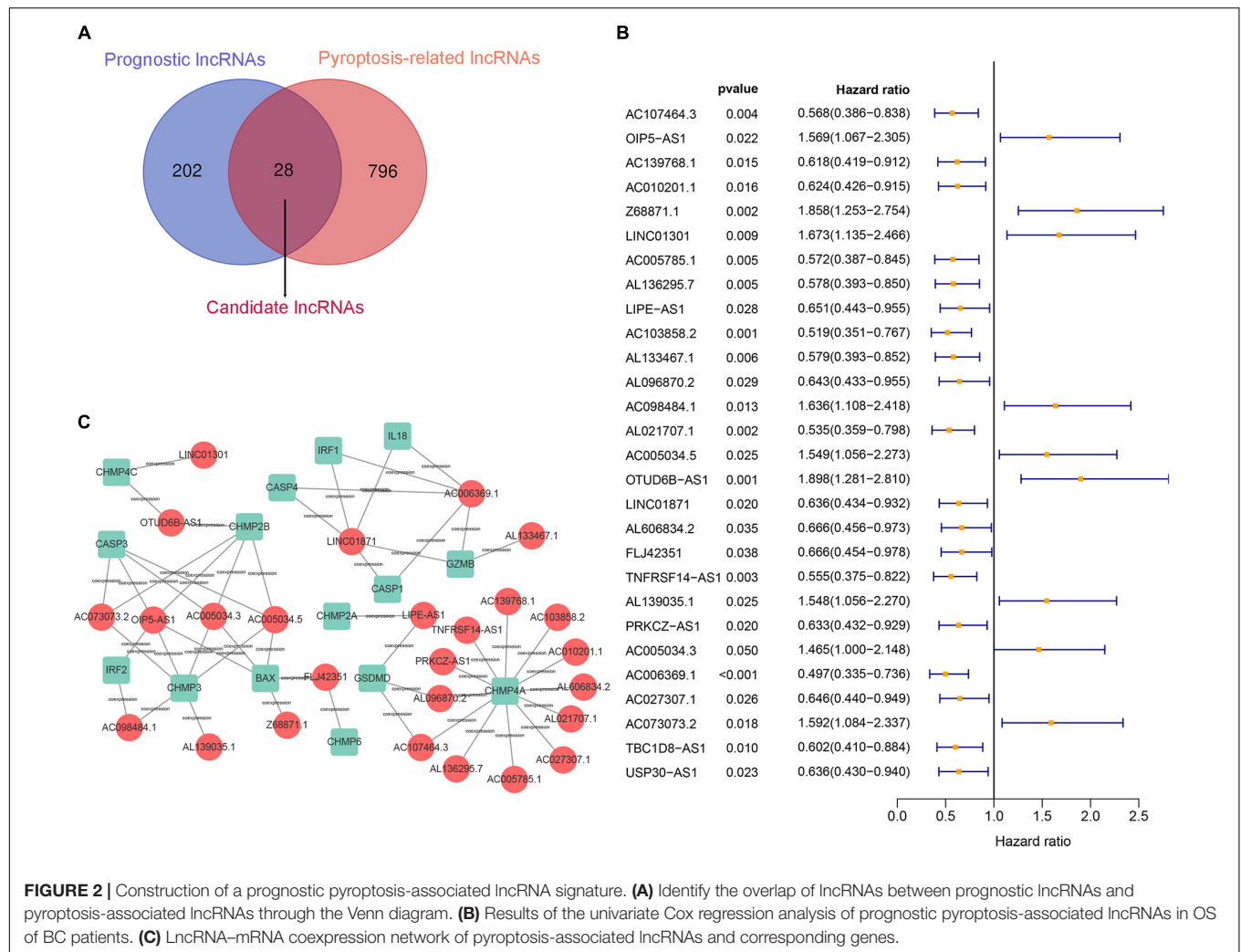


FIGURE 2 | Construction of a prognostic pyroptosis-associated lncRNA signature. **(A)** Identify the overlap of lncRNAs between prognostic lncRNAs and pyroptosis-associated lncRNAs through the Venn diagram. **(B)** Results of the univariate Cox regression analysis of prognostic pyroptosis-associated lncRNAs in OS of BC patients. **(C)** LncRNA-mRNA coexpression network of pyroptosis-associated lncRNAs and corresponding genes.

pyroptosis-associated genes. As shown in **Figure 2A**, 28 lncRNAs were overlapping lncRNAs of pyroptosis-associated lncRNAs and prognostic lncRNAs. These lncRNAs were significantly associated not only with prognosis of BC patients, but also with pyroptosis (**Figures 2B,C**). Finally, nine optimal lncRNAs (OIP5-AS1, Z68871.1, LINC01301, AC103858.2, AC005034.5, LINC01871, AL606834.2, TNFRSF14-AS1, and TBC1D8-AS1) were identified for the pyroptosis-associated lncRNA signature based on the lowest AIC. The risk score based on the signature was calculated according to the following formula:

$$\text{risk score} = e^{(0.016 \times \text{expression level of OIP5-AS1} + 0.090 \times \text{expression level of Z68871.1} + 0.239 \times \text{expression level of LINC01301} - 0.300 \times \text{expression level of AC103858.2} + 0.054 \times \text{expression level of AC005034.5} - 0.057 \times \text{expression level of LINC01871} - 0.084 \times \text{expression level of AL606834.2} - 0.123 \times \text{expression level of TNFRSF14-AS1} - 0.323 \times \text{expression level of TBC1D8-AS1})}$$

Each patient in the training set obtained a risk score based on the formula described above. Then, patients were separated into the high-risk group ($n = 309$) and low-risk group ($n = 309$) based

on the median value of risk score (**Figure 3A**). The risk score was significantly related to T staging and immunohistochemical (IHC) subtype of patients with BC (**Table 2**). As shown in **Figure 3C**, BC patients with high risk score in the training set tended to die earlier. The result of the Kaplan-Meier analysis suggested that BC patients in the high-risk group had shorter OS (**Figure 3E**). We also analyzed disease-specific survival (DSS) and disease-free survival (DFS) of patients in these two groups, the results showed that BC patients in the high-risk group had shorter DSS and DFS than patients in low-risk group (**Figures 4A,C**). The 5-year DFS rate of the low-risk group was higher than that of high-risk group (91.5 vs. 83.8%). The 5-year DSS rate of the low-risk group was also higher (95.2 vs. 84.1%).

Validation of the Pyroptosis-Associated lncRNA Signature

To verify the accuracy of the pyroptosis-associated lncRNA signature, each patient in the validation set obtained a risk score according to the same formula as the training set. Then, these patients were separated into the low-risk group ($n = 174$) and high-risk group ($n = 145$) according to the

same cutoff value as the training set (Figure 3B). Consistent with the training set, BC patients with high risk score tended to die earlier in the validation set (Figure 3D). The result of the Kaplan–Meier analysis showed that BC patients in the high-risk group had poorer prognosis (Figures 3E, 4B,D).

The Activation Level of Pyroptosis Pathway Is Associated With Prognosis of BC Patients

To further confirm the relationship between pyroptosis and prognosis of BC patients, the ssGSEA was conducted to evaluate the activation level of pyroptosis pathway in BC patients of the METABRIC and GSE20685 database. Each patient in the METABRIC and GSE20685 database obtained a pyroptosis pathway score based on ssGSEA. Patients in the METABRIC or GSE20685 database were separated into the pyroptosis-upregulated group and pyroptosis-downregulated group based on the median value of pyroptosis pathway score. Then, the OS and DSS were analyzed in the METABRIC database, and the DFS was analyzed in the GSE20685 database. The result of the Kaplan–Meier analysis showed that BC patients in the

pyroptosis-upregulated group had longer OS, DSS, and DFS (Figures 4E–G).

Independent Prognostic Value of the Pyroptosis-Associated lncRNA Signature

Univariate Cox regression analysis and multivariate Cox regression analysis were conducted to investigate the independent prognostic value of the pyroptosis-associated lncRNA signature for BC patients. As shown in Figures 5A,B, the risk score was a prognostic indicator for OS in both the training set and validation set (training set: hazard ratio (HR) = 2.379, 95% confidence interval (CI) = 1.423–3.975, $p < 0.001$; validation set: HR = 7.578, 95% CI = 3.249–17.676, $p < 0.001$). After including other confounders in the multivariate Cox regression analysis, the risk score was still an independent prognostic indicator for OS (training set: HR = 2.288, 95% CI = 1.367–3.831, $p = 0.002$; validation set: HR = 6.383, 95% CI = 2.764–14.737, $p < 0.001$; Figures 5C,D).

The Relationship of lncRNA–mRNA Coexpression

The pyroptosis-associated lncRNA signature contained nine lncRNAs. In order to clearly demonstrate the prognostic value of these lncRNAs and their relationship with pyroptosis-associated genes, a Sankey diagram was constructed. As shown in Figure 5E, lncRNA AC005034.5 was coexpressed with four pyroptosis-related genes (BAX, CASP3, CHMP2B, and CHMP3), lncRNA LINC01871 had coexpressive relationship with five pyroptosis-related genes (CASP1, CASP4, GZMB, IL18, and IRF1), and lncRNA OIP5-AS1 had coexpressive relationship with five pyroptosis-related genes (BAX, CASP3, CHMP2B, CHMP3, and IRF2). Among the nine pyroptosis-associated lncRNAs, five lncRNAs were protective factors (AC103858.2, AL606834.2, LINC01871, TBC1D8-AS1, and TNFRSF14-AS1), and four lncRNAs were risk factors (AC005034.5, LINC01301, OIP5-AS1, and Z68871.1).

Gene Set and Function Enrichment Analysis

Gene set and function enrichment analysis (GSEA) was conducted to investigate the signal pathways related to the pyroptosis-associated lncRNA signature. The results of the GSEA demonstrated that antipyroptosis pathways, antioxidant pathways, and cell growth pathways, such as transforming growth factor- β (TGF- β) signaling pathways, terpenoid backbone biosynthesis (González-Burgos and Gómez-Serranillos, 2012), pyruvate metabolism, cell cycle, and ERBB signaling pathway, were enriched in the high-risk group (Figure 6A). On the other hand, the pathways promoting pyroptosis were downregulated in the high-risk group, such as tumor necrosis factors (TNFs) bind their physiological receptor, TNF receptor superfamily TNFSF members mediating non-canonical NF- κ B pathway (Wang Y. et al., 2020), and pyroptosis pathway (Figure 6B). Interestingly, the antitumor immune signaling pathways were significantly enriched in the low-risk group, including NK cell-mediated cytotoxicity

TABLE 2 | The association between risk score and patients' clinical features in the training set.

Variables	Low-risk group (n = 309)		High-risk group (n = 309)		p-Value
	NO.	%	NO.	%	
Age					0.808
– ≤60	175	56.6	172	55.7	
– >60	134	43.4	137	44.3	
Stage					0.081
– I	41	13.3	62	20.1	
– II	179	57.9	177	57.3	
– III	81	26.2	65	21.0	
– IV	8	2.6	5	1.6	
T stage					0.045
– T1	68	22.0	86	27.8	
– T2	194	62.8	174	56.3	
– T3	34	11.0	44	14.2	
– T4	13	4.2	5	1.6	
N stage					0.089
– N0	131	42.4	157	50.8	
– N1	107	34.6	102	33.0	
– N2	48	15.5	31	10.0	
– N3	23	7.4	19	6.1	
M stage					0.400
– M0	301	97.4	304	98.4	
– M1	8	2.6	5	1.6	
Subtype					0.042
– Non-triple negative	272	88.0	254	72.2	
– Triple negative	37	12.0	55	17.8	

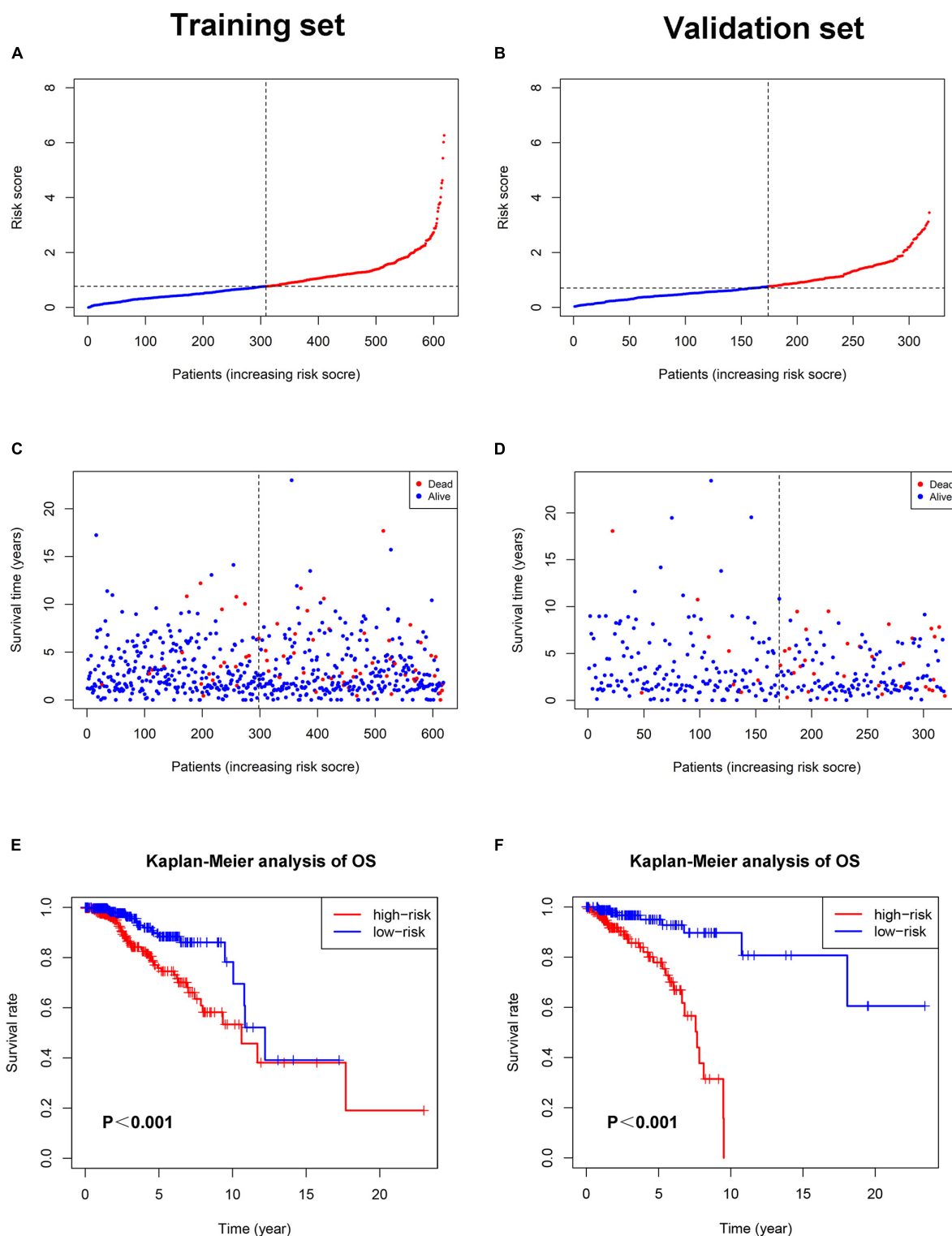


FIGURE 3 | The relationship between pyroptosis-associated lncRNA signature and prognosis in the training set and validation set. The distribution of the risk scores in the training set (A) and validation set (B). The distributions of survival status, OS, and risk score in the training set (C) and validation set (D). (E) Kaplan-Meier curves show the difference in OS between the high-risk and low-risk groups in the training set. (F) Kaplan-Meier curves show the difference in OS between the high-risk and low-risk groups in the validation set.

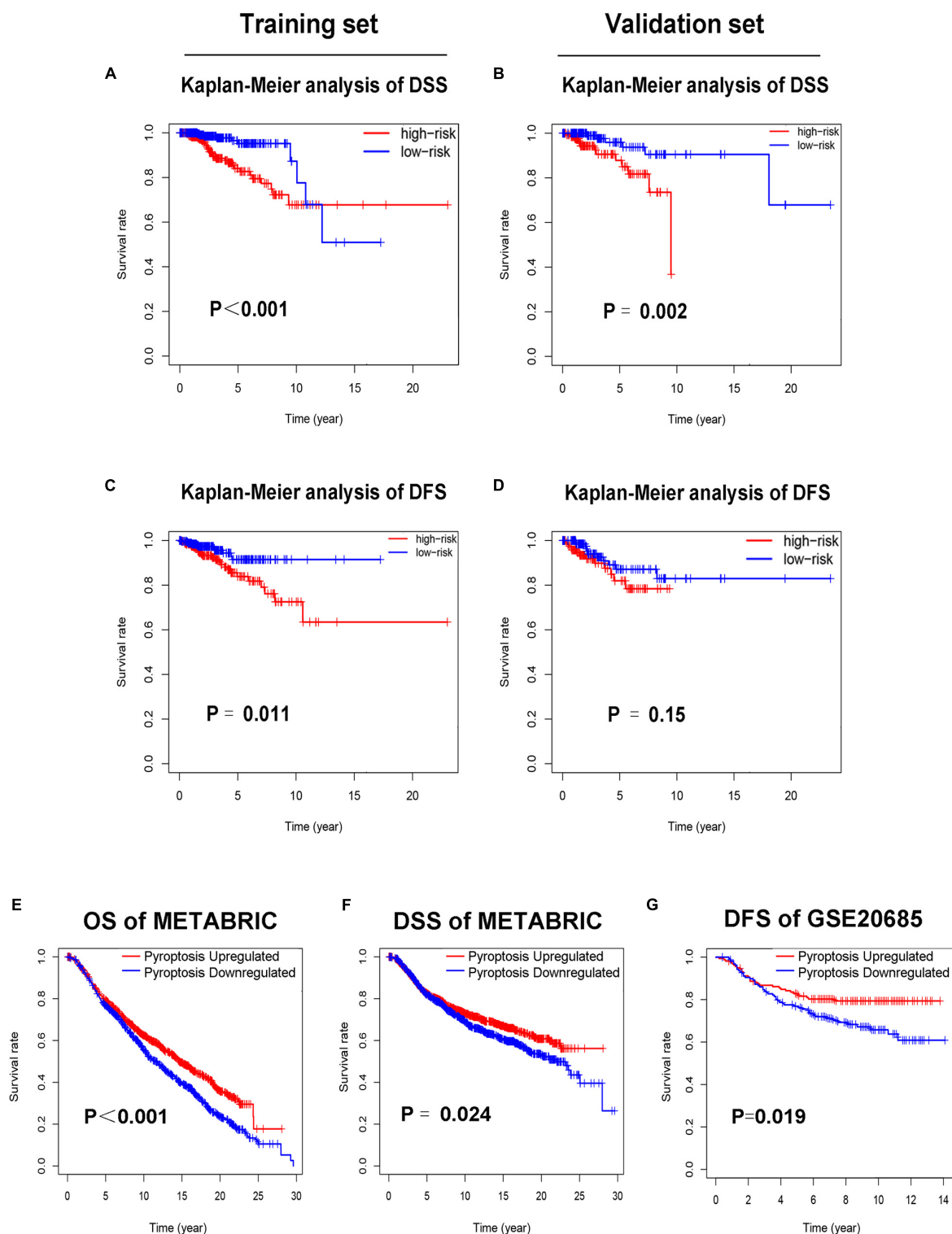


FIGURE 4 | Low-risk patients had better prognosis, and pyroptosis-upregulated group had better prognosis. **(A)** Kaplan-Meier curves of DSS between the high-risk and low-risk groups in the training set. **(B)** Kaplan-Meier curves of DSS between the high-risk and low-risk groups in the validation set. **(C)** Kaplan-Meier curves of DFS between the high-risk and low-risk groups in the training set. **(D)** Kaplan-Meier curves of DFS between the high-risk and low-risk groups in the validation set. **(E)** Kaplan-Meier curves of OS between the pyroptosis-upregulated and pyroptosis-downregulated groups in the METABRIC database. **(F)** Kaplan-Meier curves of DSS between the pyroptosis-upregulated and pyroptosis-downregulated groups in the METABRIC database. **(G)** Kaplan-Meier curves of DFS between the pyroptosis-upregulated and pyroptosis-downregulated groups in the GSE20685 database.

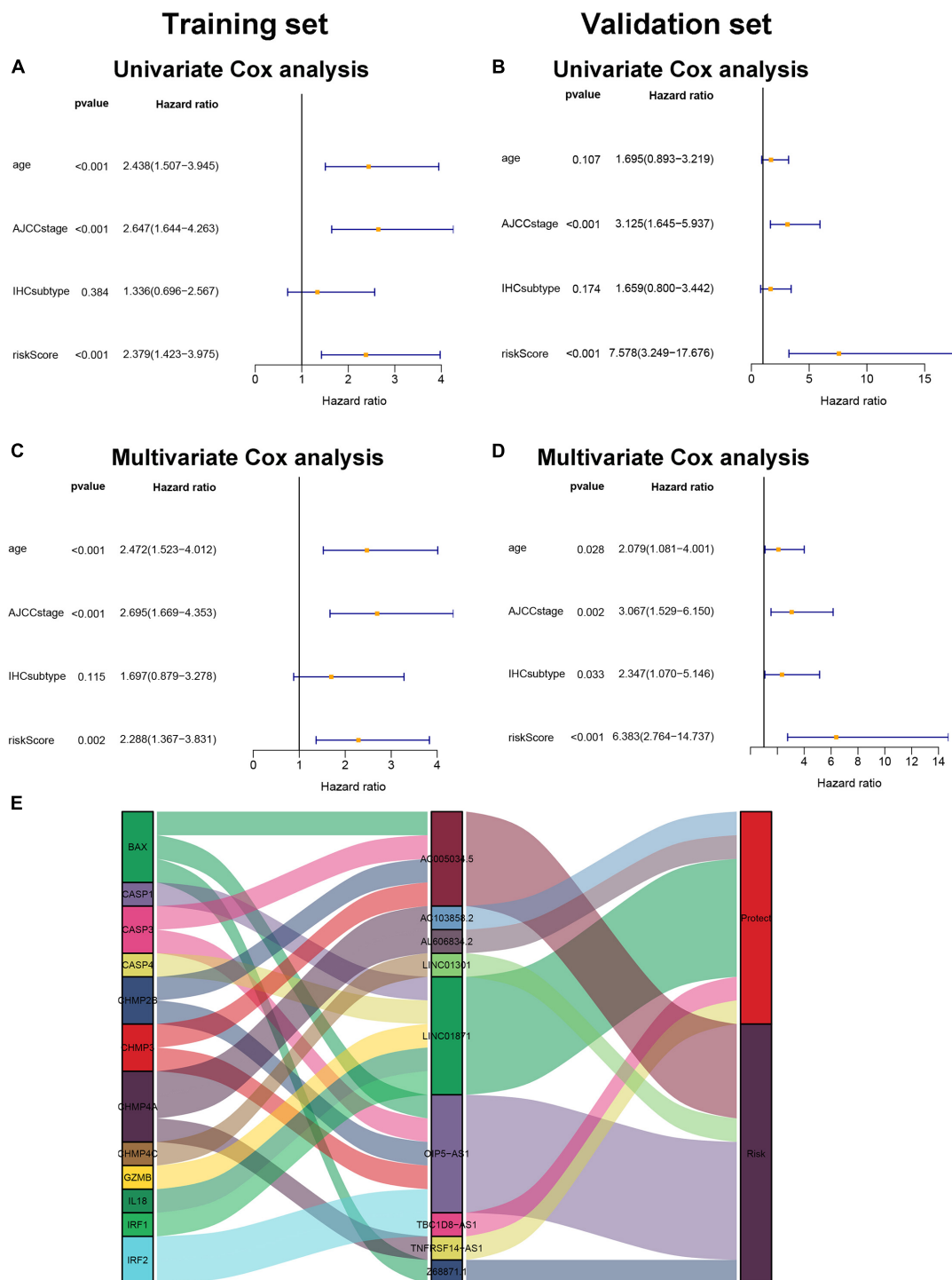


FIGURE 5 | Pyroptosis-associated lncRNA signature is an independent prognostic factor. Univariate Cox regression analysis and multivariate Cox regression analysis of OS are performed in the training set (A,C) and the validation set (B,D). (E). lncRNA-mRNA coexpression relationship between the pyroptosis-associated lncRNAs and corresponding genes shown by Sankey diagram.

pathway, chemokine receptors bind chemokine pathway, and antigen processing and presentation pathway (Figure 6B). To further investigate the biological processes associated with the

pyroptosis-associated lncRNAs, GO enrichment analysis and KEGG pathway analysis were performed. The result of the GO enrichment analysis suggested that the differentially expressed

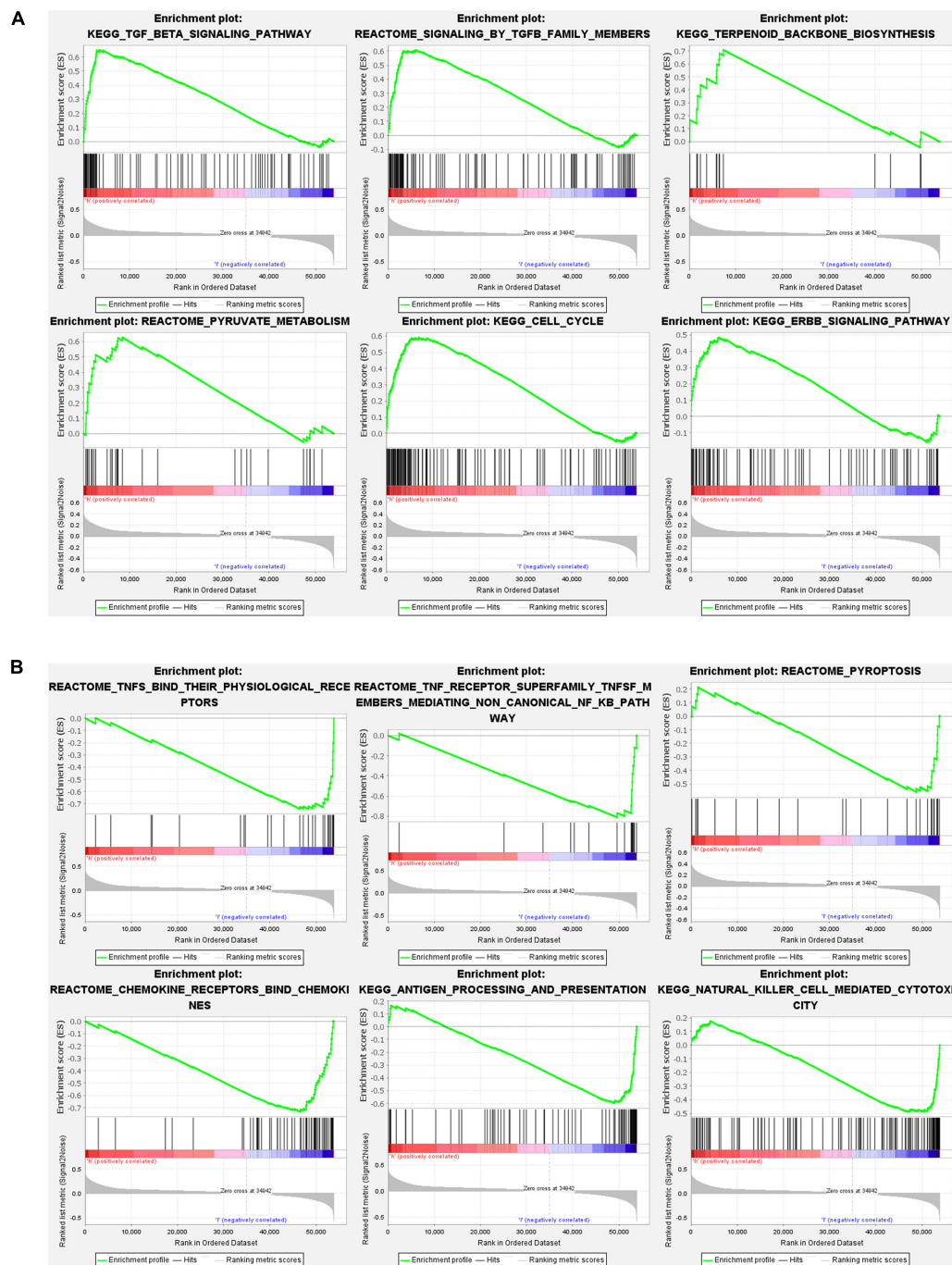


FIGURE 6 | Gene set and function enrichment analysis of differentially expressed genes between the high-risk group and low-risk group. **(A)** TGF- β signaling pathway, terpenoid backbone biosynthesis, pyruvate metabolism, cell cycle, and ERBB signaling pathway are enriched in the high-risk group. **(B)** TNFs bind their physiological receptors, TNF receptor superfamily TNFSF members mediating non-canonical NF- κ B pathway, pyroptosis pathway, chemokine receptors bind chemokines pathway, antigen processing and presentation pathway, and NK cell-mediated cytotoxicity pathway are enriched in the low-risk group.

genes between the low-risk and high-risk groups were mainly enriched in immune-associated biological processes, such as humoral immune response, lymphocyte-mediated immunity, and adaptive immune response (Figure 7A). The result of the KEGG pathway analysis suggested that the differentially

expressed genes between the low-risk and high-risk groups were mainly enriched in immune-associated pathways, such as NK cell-mediated cytotoxicity pathway, cytokine-cytokine receptor interaction pathway, and primary immunodeficiency pathway (Figure 7B).

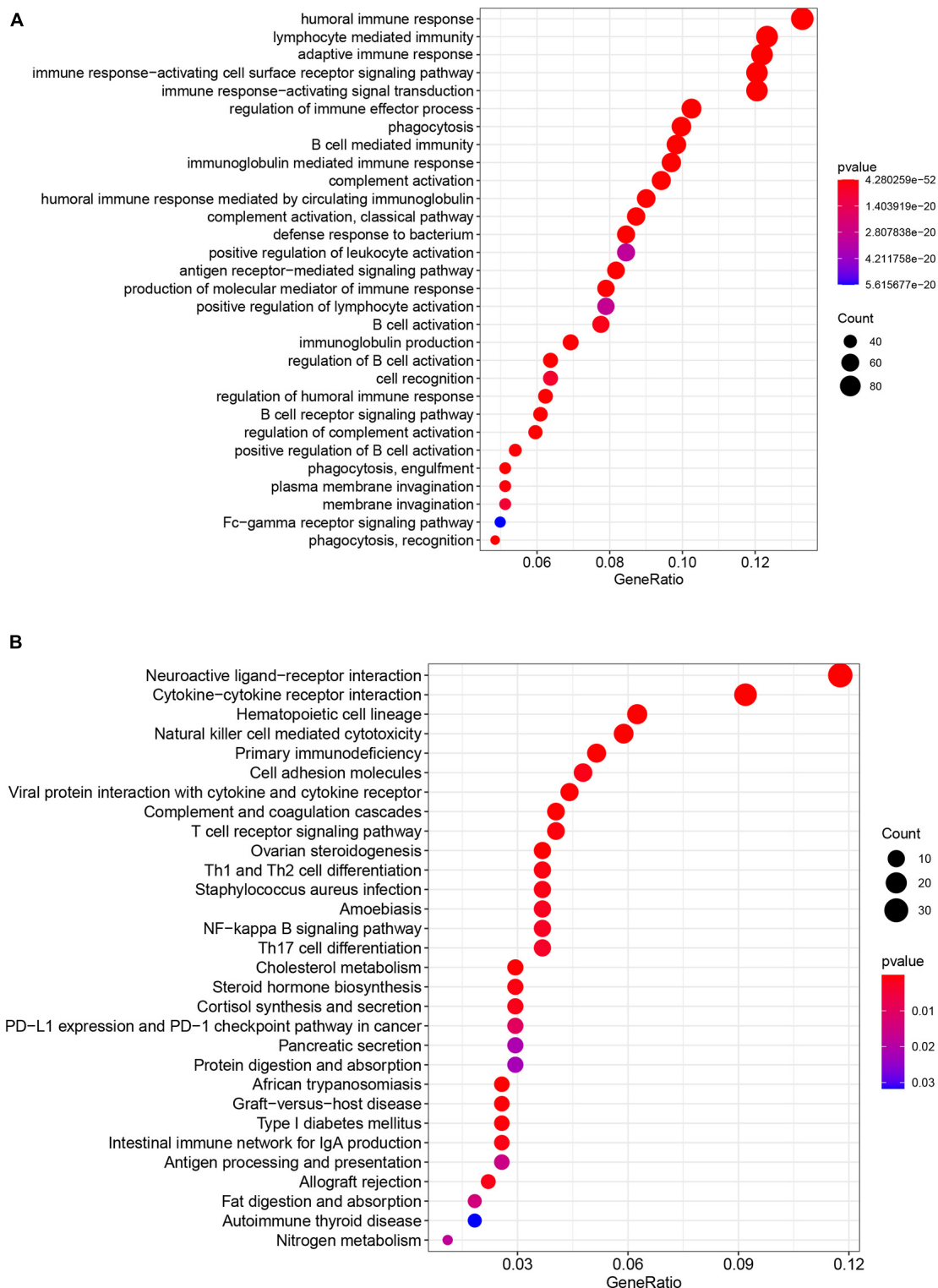


FIGURE 7 | Results of GO enrichment analysis and KEGG pathway analyses. **(A)** GO enrichment analysis suggests that the differentially expressed genes between the low-risk and high-risk groups are mainly enriched in immune-associated biological processes. **(B)** KEGG pathway analysis suggests that the differentially expressed genes between the low-risk and high-risk groups were mainly enriched in immune-associated pathways.

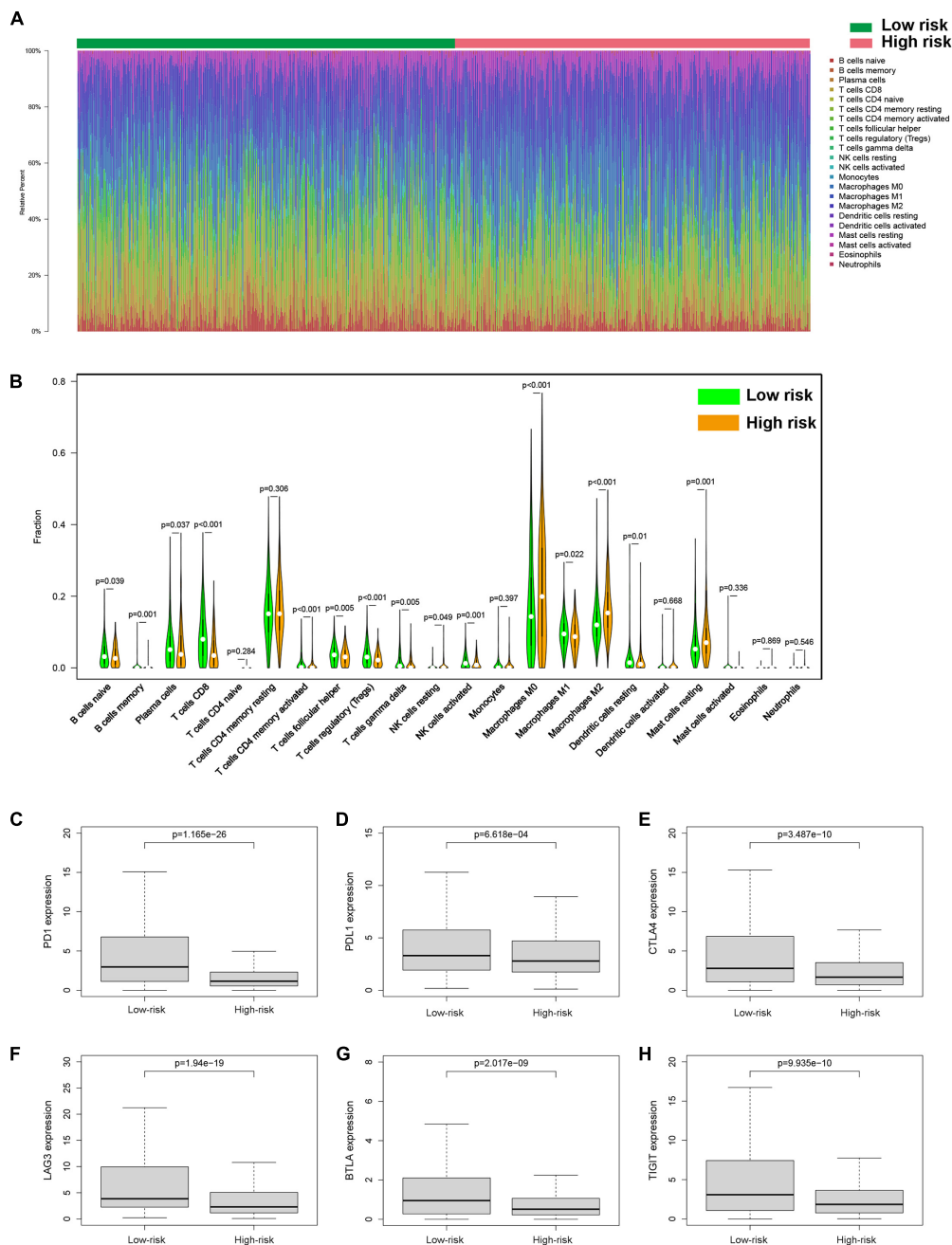


FIGURE 8 | Tumor-infiltrating immune cells of BC patients. **(A)** The proportions of different tumor-infiltrating immune cells in the low-risk and high-risk groups. **(B)** Violin plot showed the different proportions of tumor-infiltrating cells between the high-risk group and low-risk group. The expression levels of PD1 **(C)**, PDL1 **(D)**, CTLA4 **(E)**, LAG3 **(F)**, BTLA **(G)**, and TIGIT **(H)** in the high-risk group and low-risk group.

Tumor Immune Microenvironment of BC

To investigate the relationship between pyroptosis-associated lncRNAs and tumor immune microenvironment (TME), the CIBERSORT algorithm was used to calculate the proportion of each kind of tumor-infiltrating immune cells in BC patients. The result showed that the proportions of different tumor-infiltrating immune cells between the low-risk and high-risk groups had a significant difference (Figure 8A). As shown in Figure 8B,

the proportions of tumor-infiltrating B cell, CD8 + T cell, plasma cell, and activated NK cell were significantly lower in high-risk patients. However, the proportion of tumor-infiltrating M2 macrophages and mast cells was significantly higher in high-risk patients. Then, the difference in immune checkpoint molecules between the two groups was compared. As shown in Figures 8C–H, the expression levels of PD1, PDL1, CTLA4, LAG3, BTLA, and TIGIT were much higher in the low-risk

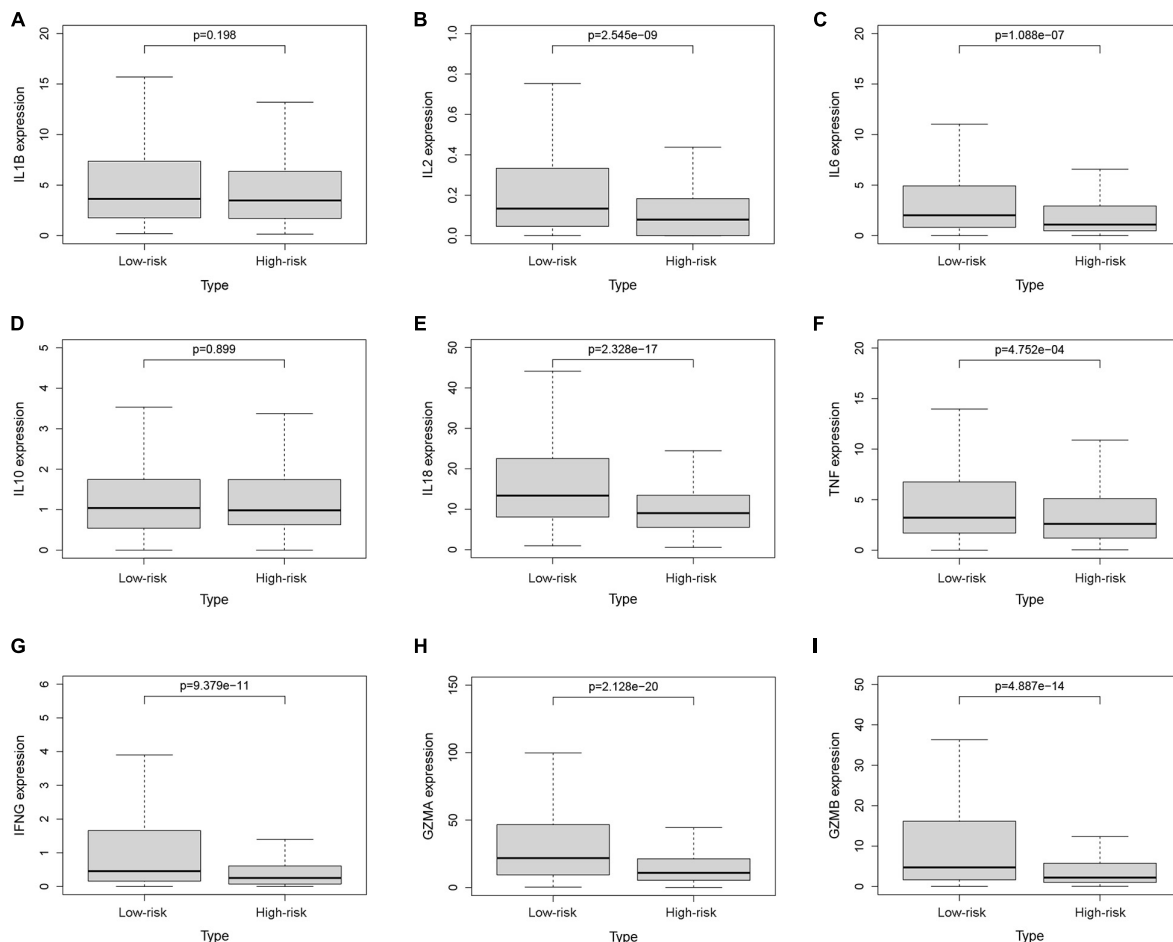


FIGURE 9 | The expression levels of cytokines. The expression levels of IL-1 β (A), IL-2 (B), IL-6 (C), IL-10 (D), IL-18 (E), TNF (F), IFN- γ (G), GZMA (H), and GZMB (I) between the low-risk and high-risk groups.

group. The difference in expression level of cytokines between the high-risk and low-risk groups was also compared. The results showed that the expression levels of interleukin-2 (IL-2), IL-6, IL-18, TNF, interferon- γ (IFN- γ), GZMA, and GZMB were significantly higher in the low-risk group (Figures 9B,C,E-I), while there was no significant difference in the expression level of IL-1 β and IL-10 (Figures 9A,D).

The Pyroptosis-Associated lncRNA Signature in BC Patients Receiving Different Treatments

Then, we explored the prognostic value of the pyroptosis-associated lncRNA signature in BC patients receiving different treatment regimens. Among BC patients receiving chemotherapy, the patients in high-risk group based on pyroptosis-associated lncRNA signature had significantly poorer prognosis (Figure 10A). Among BC patients receiving endocrinotherapy, the patients in the high-risk group had poorer prognosis too (Figure 10C). The prognostic value of pyroptosis-associated lncRNA signature in patients undergoing anti-HER2

therapy was also analyzed, but there was no significant difference in prognosis of low-risk and high-risk patients (Figure 10E). To further investigate the value of pyroptosis-associated lncRNA signature in patients undergoing different chemotherapy regimens, the prognosis of patients treated with anthracycline, cyclophosphamide, or paclitaxel was analyzed, respectively. The results showed that patients in the high-risk group had poorer outcomes among patients treated with anthracycline, cyclophosphamide, or paclitaxel (Figures 10B,D,F).

Construction and Validation of a Nomogram Based on the Pyroptosis-Associated lncRNA Signature

To provide a stable and accurate prediction model for BC patients, clinical features and risk score were included to construct a nomogram (Figure 11A). The predictive accuracy of the nomogram was evaluated by time-dependent ROC curve analysis; the result showed that area under the curve (AUC) of the nomogram in the training set was 0.880, 0.804, and 0.796 to predict 1-, 3-, and 5-year survival rates,

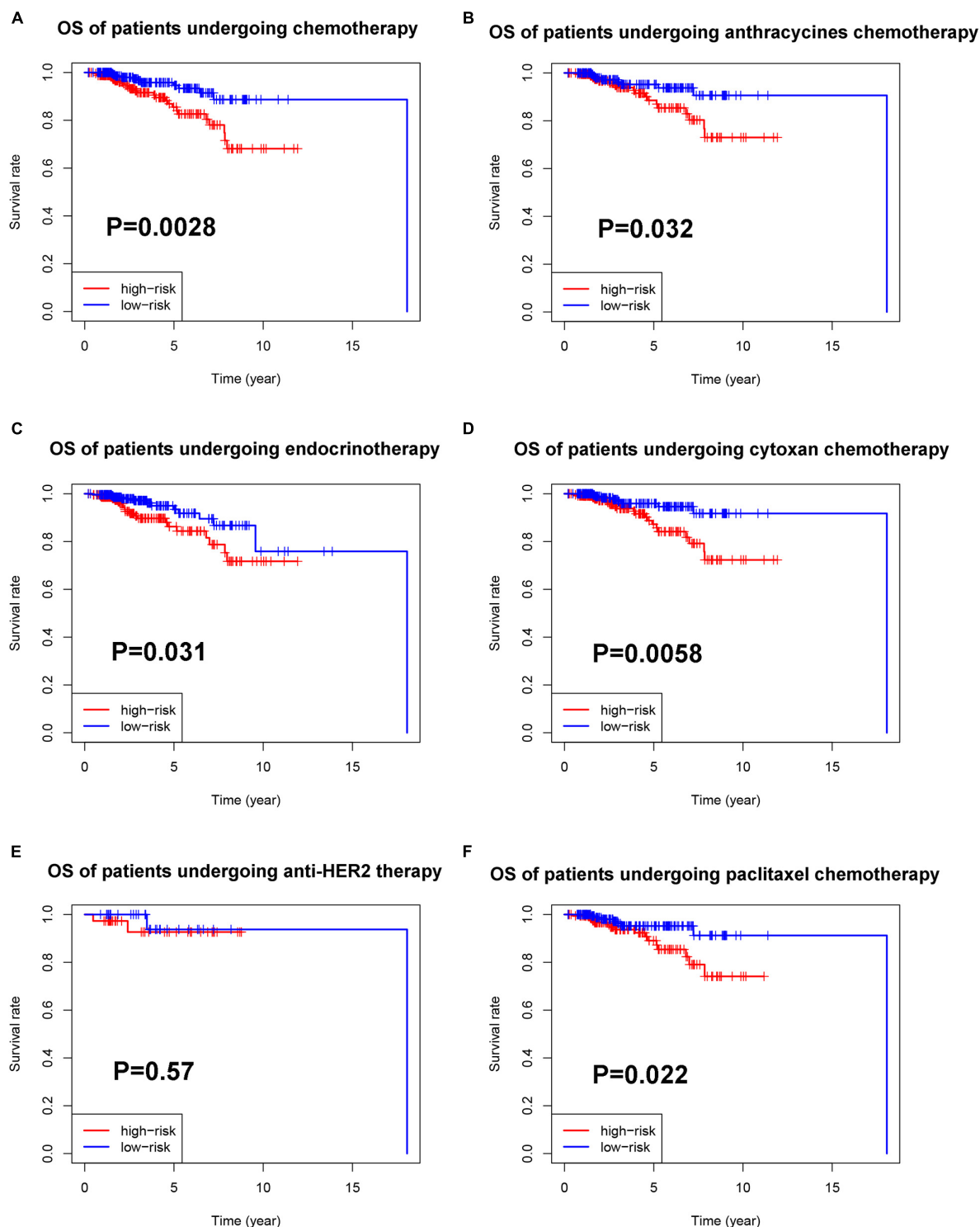


FIGURE 10 | Prognostic value of the pyroptosis-associated lncRNA signature in patients receiving different treatments. **(A)** Kaplan–Meier curves for the OS of patients receiving chemotherapy between the high-risk and low-risk groups. Kaplan–Meier curves for the OS of patients receiving anthracycline **(B)**, cyclophosphamide **(D)**, and paclitaxel **(F)** between the high-risk and low-risk groups. **(C)** Kaplan–Meier curves for the OS of patients receiving endocrinotherapy between the high-risk and low-risk groups. **(E)** Kaplan–Meier curves for the OS of patients receiving anti-HER2 therapy between the high-risk and low-risk groups.

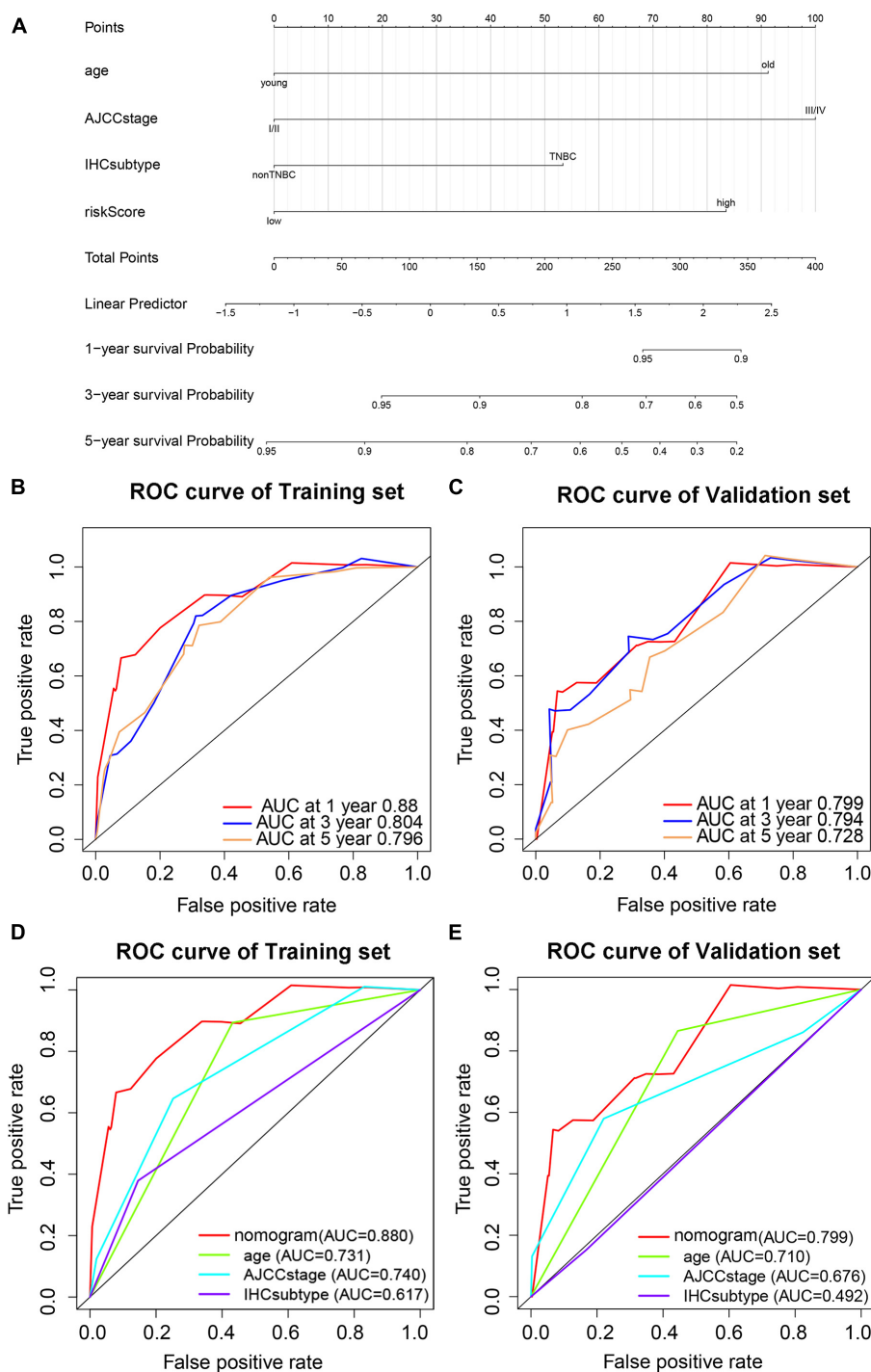


FIGURE 11 | Prediction model based on pyroptosis-associated lncRNA signature for OS of BC patients. **(A)** Nomogram prediction model for OS of BC patients. Time-dependent ROC curves predict 1-year, 3-year, and 5-year OS in the training set **(B)** and validation set **(C)**. Predictive value of the nomogram and traditional prognostic indicators are compared by ROC curve analysis in the training set **(D)** and validation set **(E)**.

respectively. In the validation set, it was 0.799, 0.794, and 0.728, respectively (**Figures 11B,C**). Then, the predictive values of the nomogram and traditional prognostic indicators, such as age, AJCC stage, and IHC subtype, were compared by ROC

curve analysis. As shown in **Figures 11D,E**, the AUC of the nomogram was significantly higher than that of traditional prognostic indicators both in the training set and the validation set (**Table 3**).

TABLE 3 | The AUC of nomogram, age, AJCC stage, and IHC subtype for prediction of OS in the training set and validation set.

Factors	Training set		Validation set	
	AUC (95% CI)	p-Value	AUC (95% CI)	p-Value
Nomogram	0.880 (0.850–0.907)		0.799(0.751–0.842)	
Age	0.731 (0.694–0.766)		0.710(0.656–0.759)	
AJCC stage	0.740 (0.703–0.774)		0.676(0.622–0.727)	
IHC subtype	0.617 (0.577–0.655)		0.492(0.472–0.536)	
Nomogram vs. age		0.019		0.4
Nomogram vs. AJCC stage		0.022		0.034
Nomogram vs. IHC subtype		0.002		0.02

DISCUSSION

Pyroptosis is a new type of programmed cell death characterized by the rupture of cell membranes and the release of inflammatory substances (Fang et al., 2020). In the development of cancer, the expression level of GSDMs in cancer cells is usually lower than that in normal tissues due to the high methylation of the promoters of pyroptosis-related genes, resulting in the growth and metastasis of tumors (Kim et al., 2008; Croes et al., 2017). Chemotherapy drugs and tamoxifen can inhibit the progression of tumors by inducing pyroptosis of tumor cells (Hu et al., 2020; Hwang and Chung, 2020). It has been proven that the expression level of GSDMs was closely related to the prognosis of BC (de Bree et al., 2012). However, only a few lncRNAs related to pyroptosis have been reported at present, and a comprehensive analysis is needed.

In this study, nine optimal lncRNAs were identified for the pyroptosis-associated lncRNA signature. The genes coexpressed with these nine pyroptosis-associated lncRNAs were BAX, CASP1/3/4, CHMP2B/3, IRF1/2, GZMB, and IL-18. Among them, BAX is an important promoter of apoptosis and can also participate in pyroptosis. For example, navitoclax (a Bcl-2 inhibitor) can induce pyroptosis through the BAK/Bax-caspase3-GSDME signaling pathway (Hu et al., 2020). IRF2 is a transcription factor that directly regulates the expression levels of caspase-1 and caspase-4. When IRF2 is deficient, IRF1 can maintain the stable expression of caspase-4 with the presence of IFN- γ (Benaoudia et al., 2019). The nine-pyroptosis-associated lncRNA signature was proven to be an independent prognostic factor of BC patients. Then, a prediction model based on the pyroptosis-associated lncRNA signature was established. The AUC of the model for predicting OS could reach 0.880 in the training set and 0.799 in the validation set.

In order to further explore the relationship between pyroptosis and BC, functional enrichment analysis showed antipyrroptosis, tumor metabolism, and cell cycle-related signaling pathways were enriched in the high-risk group, while the pyroptosis, antigen presentation, and NK cell-mediated cytotoxicity-related

pathways were significantly activated in the low-risk group. TGF- β signaling is an important pathway in cancers and has both tumor-promoting and tumor inhibiting functions. It has been reported that TGF- β can suppress pyroptosis (Tamura et al., 2021). In this study, enrichment of TGF- β signaling pathway and TGF- β family members were observed in the high-risk group.

Moreover, more CD8 + T cells, activated NK cells, and activated CD4 + T memory cells were infiltrated in the TME of the low-risk group, suggesting a correlation between pyroptosis and TILs. In addition, patients in the low-risk group had a higher expression level of cytokines in the tumor tissues, such as IL-2, IL-6, and IL-18, which was consistent with more infiltrating immune cells in the low-risk group. The expression of TNF, IFN- γ , GZMA, and GZMB was higher in the low-risk group, suggesting a stronger cytotoxicity to tumor cells. At the same time, immunosuppressor molecules such as PD1, PDL1, CTLA4, LAG3, BTLA, and TIGIT in the low-risk group were significantly higher than those in the high-risk group. The increased infiltration of TILs and upregulated expression of immune checkpoint molecules suggested that patients in the low-risk group tended to be immunologically “hot” tumor, which was more likely to benefit from ICB therapy (Zhang and Chen, 2016).

Local inflammation caused by pyroptosis can lead to the formation of local immune escape (Kaplanov et al., 2019) and may be related to carcinogenesis (Wu et al., 2018). However, current studies have shown that the expression of GSDMs is positively correlated with the prognosis of cancer patients, and the efficacy of chemotherapy drugs and cytotoxic lymphocyte is partly dependent on pyroptosis (Wang Y. et al., 2017; Zhou et al., 2020). Pyroptosis is different from apoptosis. Theoretically, the former causes the death of cancer cells accompanied by the release of cytoplasmic contents, resulting in the exposure of TAAs, thus recruiting immune cells, such as NK cells, and CD8 + T lymphocytes to inhibit the growth of tumor. The conclusion drawn in this study is consistent with the theory and previous studies.

In this study, our pyroptosis-associated lncRNA signature could accurately predict the prognosis and tumor immune microenvironment of breast cancer patients. Low-risk patients not only had a better prognosis but also tended to be immunologically “hot” tumor, which was more likely to benefit from immune checkpoint inhibitors. Therefore, our signature could not only help clinicians accurately predict patients’ outcomes but also identify patients who were more suitable for immune checkpoint inhibitors. At the same time, we also found that high-risk patients had a poor prognosis and tended to be immunologically “cold” tumors, which was difficult to benefit from immune checkpoint inhibitors. How do we improve the prognosis of patients in the high-risk group? In mice models, bioorthogonal system to gasdermin (a technique that is able to control the release of active gasdermin in mice and selectively enter mouse tumor cells) could increase CD4+ and CD8+ cells in the TME of BC, while the percentage of CD4+ Foxp3+ regulatory T cells decreased, which showed a strong antitumor effect. At the same time, it could play a synergistic role with checkpoint blockade (Wang Q. et al., 2020), suggesting that

pyroptosis could improve the effect of immunotherapy. Thus, we propose a combined regimen of immune checkpoint inhibitors and pyroptosis inducers for high-risk patients because pyroptosis inducers had the potential to recruit immune cells by inducing pyroptosis of cancer cells, and the immunologically “cold” tumor could turn into “hot” tumor, then the immune checkpoint inhibitor could be effective for high-risk patients.

However, our study had some limitations. This research data came from the TCGA public database, and basic experiments *in vivo* or *in vitro* will be conducted to confirm the efficacy of combined regimen of immune checkpoint inhibitors and pyroptosis inducers in the future. In addition, clinical trials are urgently needed to confirm whether inducing pyroptosis could improve the efficacy of immunotherapy in human BC patients.

In conclusion, we are the first to identify the pyroptosis-related lncRNAs associated with the prognosis of BC and establish a prognostic prediction model. At the same time, this study found that the pyroptosis risk score was related to TILs and the expression of immune checkpoint molecules. Thus, inducing pyroptosis may be a potential therapy to improve the efficacy of immunotherapy in BC.

REFERENCES

- Adams, S., Schmid, P., Rugo, H. S., Winer, E. P., Loirat, D., Awada, A., et al. (2019). Pembrolizumab monotherapy for previously treated metastatic triple-negative breast cancer: cohort A of the phase II KEYNOTE-086 study. *Ann. Oncol.* 30, 397–404. doi: 10.1093/annonc/mdy517
- Benaoudia, S., Martin, A., Puig Gamez, M., Gay, G., Lagrange, B., Cornut, M., et al. (2019). A genome-wide screen identifies IRF2 as a key regulator of caspase-4 in human cells. *EMBO Rep.* 20:e48235. doi: 10.15252/embr.201948235
- Croes, L., de Beeck, K. O., Pauwels, P., Vanden Berghe, W., Peeters, M., Fransen, E., et al. (2017). DFNA5 promoter methylation a marker for breast tumorigenesis. *Oncotarget* 8, 31948–31958. doi: 10.18632/oncotarget.16654
- de Beeck, K. O., Van Laer, L., and Van Camp, G. (2012). DFNA5, a gene involved in hearing loss and cancer: a review. *Ann. Otol. Rhinol. Laryngol.* 121, 197–207. doi: 10.1177/000348941212100310
- Fang, Y., Tian, S., Pan, Y., Li, W., Wang, Q., Tang, Y., et al. (2020). Pyroptosis: a new frontier in cancer. *Biomed. Pharmacother.* 121:109595. doi: 10.1016/j.biopha.2019.109595
- Faria, S. S., Costantini, S., de Lima, V. C. C., de Andrade, V. P., Rialland, M., Cedric, R., et al. (2021). NLRP3 inflammasome-mediated cytokine production and pyroptosis cell death in breast cancer. *J. Biomed. Sci.* 28:26. doi: 10.1186/s12929-021-00724-8
- Garg, A. D., and Agostinis, P. (2017). Cell death and immunity in cancer: from danger signals to mimicry of pathogen defense responses. *Immunol. Rev.* 280, 126–148. doi: 10.1111/imr.12574
- González-Burgos, E., and Gómez-Serranillos, M. P. (2012). Terpene compounds in nature: a review of their potential antioxidant activity. *Curr. Med. Chem.* 19, 5319–5341. doi: 10.2174/092986712803833335
- Hu, L., Chen, M., Chen, X., Zhao, C., Fang, Z., Wang, H., et al. (2020). Chemotherapy-induced pyroptosis is mediated by BAK/BAX-caspase-3-GSDME pathway and inhibited by 2-bromopalmitate. *Cell Death Dis.* 11:281. doi: 10.1038/s41419-020-2476-2
- Hwang, N., and Chung, S. W. (2020). Sulfasalazine attenuates tamoxifen-induced toxicity in human retinal pigment epithelial cells. *BMB Rep.* 53, 284–289. doi: 10.5483/BMBRep.2020.53.5.041
- Kaplanov, I., Carmi, Y., Kornetsky, R., Shemesh, A., Shurin, G. V., Shurin, M. R., et al. (2019). Blocking IL-1 β reverses the immunosuppression in mouse breast cancer and synergizes with anti-PD-1 for tumor abrogation. *Proc. Natl. Acad. Sci. U. S. A.* 116, 1361–1369. doi: 10.1073/pnas.1812266115
- Kim, M. S., Lebron, C., Nagpal, J. K., Chae, Y. K., Chang, X., Huang, Y., et al. (2008). Methylation of the DFNA5 increases risk of lymph node metastasis

DATA AVAILABILITY STATEMENT

Publicly available datasets were analyzed in this study. This data can be found here: The data of this study were downloaded from TCGA (<https://portal.gdc.cancer.gov/repository>).

AUTHOR CONTRIBUTIONS

XX, XQ, LP, and KZ participated in this research, including conception and design, drafting, and critical revision of the manuscript. KZ and XO acquired the data. LP and KZ analyzed the data and interpreted the data. LP and XO supported for material. XX and XQ supervised the study. All authors ensured and approved the final version.

ACKNOWLEDGMENTS

Thanks to all the staff involved in setting up the TCGA database.

- in human breast cancer. *Biochem. Biophys. Res. Commun.* 370, 38–43. doi: 10.1016/j.bbrc.2008.03.026
- Liang, Y., Song, X., Li, Y., Chen, B., Zhao, W., Wang, L., et al. (2020). lncRNA BCRT1 promotes breast cancer progression by targeting miR-1303/PTBP3 axis. *Mol. Cancer* 19:85. doi: 10.1186/s12943-020-01206-5
- Nanda, R., Chow, L. Q., Dees, E. C., Berger, R., Gupta, S., Geva, R., et al. (2016). Pembrolizumab in patients with advanced triple-negative breast cancer: phase Ib KEYNOTE-012 study. *J. Clin. Oncol.* 34, 2460–2467. doi: 10.1200/jco.2015.64.8931
- Newman, A. M., Liu, C. L., Green, M. R., Gentles, A. J., Feng, W., Xu, Y., et al. (2015). Robust enumeration of cell subsets from tissue expression profiles. *Nat. Methods* 12, 453–457. doi: 10.1038/nmeth.3337
- Pu, M., Messer, K., Davies, S. R., Vickery, T. L., Pittman, E., Parker, B. A., et al. (2020). Research-based PAM50 signature and long-term breast cancer survival. *Breast Cancer Res. Treat.* 179, 197–206. doi: 10.1007/s10549-019-05446-y
- Sung, H., Ferlay, J., Siegel, R. L., Laversanne, M., Soerjomataram, I., Jemal, A., et al. (2021). Global cancer statistics 2020: GLOBOCAN estimates of incidence and mortality worldwide for 36 cancers in 185 countries. *CA Cancer J. Clin.* 71, 209–249. doi: 10.3322/caac.21660
- Tamura, Y., Morikawa, M., Tanabe, R., Miyazono, K., and Koinuma, D. (2021). Anti-pyroptotic function of TGF- β is suppressed by a synthetic dsRNA analogue in triple negative breast cancer cells. *Mol. Oncol.* 15, 1289–1307. doi: 10.1002/1878-0261.12890
- Tan, C., Liu, W., Zheng, Z. H., and Wan, X. G. (2021). lncRNA HOTTIP inhibits cell pyroptosis by targeting miR-148a-3p/AKT2 axis in ovarian cancer. *Cell Biol. Int.* 45, 1487–1497. doi: 10.1002/cbin.11588
- Tekpli, X., Lien, T., Rossevoel, A. H., Nebdal, D., Borgen, E., Ohnstad, H. O., et al. (2019). An independent poor-prognosis subtype of breast cancer defined by a distinct tumor immune microenvironment. *Nat. Commun.* 10:5499. doi: 10.1038/s41467-019-13329-5
- Thorsson, V., Gibbs, D. L., Brown, S. D., Wolf, D., Bortone, D. S., Ou Yang, T. H., et al. (2018). The immune landscape of cancer. *Immunity* 48, 812–830.e14. doi: 10.1016/j.immuni.2018.03.023
- Vrieze, S. I. (2012). Model selection and psychological theory: a discussion of the differences between the Akaike information criterion (AIC) and the Bayesian information criterion (BIC). *Psychol. Methods* 17, 228–243. doi: 10.1037/a0027127
- Wan, P., Su, W., Zhang, Y., Li, Z., Deng, C., Li, J., et al. (2020). lncRNA H19 initiates microglial pyroptosis and neuronal death in retinal ischemia/reperfusion injury. *Cell Death Differ.* 27, 176–191. doi: 10.1038/s41418-019-0351-4

- Wang, Q., Wang, Y., Ding, J., Wang, C., Zhou, X., Gao, W., et al. (2020). A bioorthogonal system reveals antitumour immune function of pyroptosis. *Nature* 579, 421–426. doi: 10.1038/s41586-020-2079-1
- Wang, X., Li, X. L., and Qin, L. J. (2021). The lncRNA XIST/miR-150-5p/c-Fos axis regulates sepsis-induced myocardial injury via TXNIP-modulated pyroptosis. *Lab. Invest.* 101, 1118–1129. doi: 10.1038/s41374-021-00607-4
- Wang, Y., Gao, W., Shi, X., Ding, J., Liu, W., He, H., et al. (2017). Chemotherapy drugs induce pyroptosis through caspase-3 cleavage of a gasdermin. *Nature* 547, 99–103. doi: 10.1038/nature22393
- Wang, Y., Zhang, H., Chen, Q., Jiao, F., Shi, C., Pei, M., et al. (2020). TNF- α /HMGB1 inflammation signalling pathway regulates pyroptosis during liver failure and acute kidney injury. *Cell Prolif.* 53:e12829. doi: 10.1111/cpr.12829
- Wu, T. C., Xu, K., Martinek, J., Young, R. R., Banchereau, R., George, J., et al. (2018). IL1 receptor antagonist controls transcriptional signature of inflammation in patients with metastatic breast cancer. *Cancer Res.* 78, 5243–5258. doi: 10.1158/0008-5472.Can-18-0413
- Xia, X., Wang, X., Cheng, Z., Qin, W., Lei, L., Jiang, J., et al. (2019). The role of pyroptosis in cancer: pro-cancer or pro-“host”? *Cell Death Dis.* 10:650. doi: 10.1038/s41419-019-1883-8
- Zhang, C. C., Li, C. G., Wang, Y. F., Xu, L. H., He, X. H., Zeng, Q. Z., et al. (2019). Chemotherapeutic paclitaxel and cisplatin differentially induce pyroptosis in A549 lung cancer cells via caspase-3/GSDME activation. *Apoptosis* 24, 312–325. doi: 10.1007/s10495-019-01515-1
- Zhang, Y., and Chen, L. (2016). Classification of advanced human cancers based on Tumor Immunity in the MicroEnvironment (TIME) for cancer immunotherapy. *JAMA Oncol.* 2, 1403–1404. doi: 10.1001/jamaoncol.2016.2450
- Zhang, Y., Liu, X., Bai, X., Lin, Y., Li, Z., Fu, J., et al. (2018). Melatonin prevents endothelial cell pyroptosis via regulation of long noncoding RNA MEG3/miR-223/NLRP3 axis. *J. Pineal. Res.* 64:e12449. doi: 10.1111/jpi.12449
- Zhang, Z., Zhang, Y., Xia, S., Kong, Q., Li, S., Liu, X., et al. (2020). Gasdermin E suppresses tumour growth by activating anti-tumour immunity. *Nature* 579, 415–420. doi: 10.1038/s41586-020-2071-9
- Zhou, Z., He, H., Wang, K., Shi, X., Wang, Y., Su, Y., et al. (2020). Granzyme A from cytotoxic lymphocytes cleaves GSDMB to trigger pyroptosis in target cells. *Science* 368:eaz7548. doi: 10.1126/science.aaz7548

Conflict of Interest: The authors declare that the research was conducted in the absence of any commercial or financial relationships that could be construed as a potential conflict of interest.

Publisher's Note: All claims expressed in this article are solely those of the authors and do not necessarily represent those of their affiliated organizations, or those of the publisher, the editors and the reviewers. Any product that may be evaluated in this article, or claim that may be made by its manufacturer, is not guaranteed or endorsed by the publisher.

Copyright © 2021 Ping, Zhang, Ou, Qiu and Xiao. This is an open-access article distributed under the terms of the Creative Commons Attribution License (CC BY). The use, distribution or reproduction in other forums is permitted, provided the original author(s) and the copyright owner(s) are credited and that the original publication in this journal is cited, in accordance with accepted academic practice. No use, distribution or reproduction is permitted which does not comply with these terms.



Effect, Mechanism, and Applications of Coding/Non-coding RNA m6A Modification in Tumor Microenvironment

Chaohua Si^{1,2}, Chen Chen², Yaxin Guo^{3,4}, Qiaozhen Kang^{2*} and Zhenqiang Sun^{1*}

¹ Department of Colorectal Surgery, The First Affiliated Hospital of Zhengzhou University, Zhengzhou, China, ² School of Life Sciences, Zhengzhou University, Zhengzhou, China, ³ Henan Academy of Medical and Pharmaceutical Sciences, Zhengzhou University, Zhengzhou, China, ⁴ School of Basic Medical Sciences, Zhengzhou University, Zhengzhou, China

OPEN ACCESS

Edited by:

Zong Sheng Guo,
Roswell Park Comprehensive Cancer
Center, United States

Reviewed by:

Mohammad Imran Khan,
King Abdulaziz University,
Saudi Arabia
John Morton,
University of Colorado,
United States

*Correspondence:

Zhenqiang Sun
fcsunzq@zzu.edu.cn
Qiaozhen Kang
qzkang@zzu.edu.cn

Specialty section:

This article was submitted to
Molecular and Cellular Oncology,
a section of the journal
Frontiers in Cell and Developmental
Biology

Received: 19 May 2021

Accepted: 30 August 2021

Published: 30 September 2021

Citation:

Si C, Chen C, Guo Y, Kang Q and
Sun Z (2021) Effect, Mechanism, and
Applications of Coding/Non-coding
RNA m6A Modification in Tumor
Microenvironment.
Front. Cell Dev. Biol. 9:711815.
doi: 10.3389/fcell.2021.711815

The tumor microenvironment (TME), which includes immune cells, fibroblasts, and other components, is the site of tumor cell growth and metastasis and significantly impacts tumor development. Among them, N6-methyladenosine RNA modifications (m6A RNA modifications) are the most abundant internal modifications in coding and non-coding RNAs, which can significantly influence the cancer process and have potential as biomarkers and potential therapeutic targets for tumor therapy. This manuscript reviews the role of m6A RNA modifications in TME and their application in tumor therapy. To some extent, an in-depth understanding of the relationship between TME and m6A RNA modifications will provide new approaches and ideas for future cancer therapy.

Keywords: tumor microenvironment, m6A RNA modification, coding RNA, non-coding RNA, cancer

INTRODUCTION

In recent years, cancer is still one of the most important diseases affecting human life and health. As cancer research has progressed, we found that the tumor microenvironment (TME) also profoundly influences the course of tumor development in addition to the tumor cell (Hinshaw and Shevde, 2019). TME is a dynamic, complex system of multiple components, including immune cells, fibroblasts, and lymphocytes, that play a crucial role in cancer development and progression, and its interaction with tumor cells is a critical factor in the success of tumor cell-tolerant immune escape (Ocana et al., 2019). Meanwhile, we have known that hundreds of chemical modifications occur in TME, which play different roles in TME at different stages of cancer development. In addition, N6-methyladenosine RNA modifications (m6A RNA modifications) are the most abundant modification in TME, and the existing studies have shown that m6A RNA modifications occurring in TME are a vital factor mediating tumor progression and influencing tumor treatment outcome (Chen X. Y. et al., 2019; Cheng H. S. et al., 2019; Wang J. et al., 2020). Therefore,

Abbreviations: TME, tumor microenvironment; m6A RNA modification, the N6-methyladenosine RNA modification; FTO, obesity-associated protein; METTL3/14, methyltransferase-like 3/14; IGF2BP protein, insulin-like growth factor 2 mRNA-binding protein; HDGF, hepatoma-derived growth factor; FOXO3, forkhead box O3; HCC, hepatocellular carcinoma; NSCLC, non-small cell lung cancer; eIF3b, eukaryotic translation initiation factor 3B; SLE, systemic lupus erythematosus; YTHDF, YTH domain-containing family; FTO, obesity-associated protein; YTHDC1, YTH domain-containing protein 1; ALKBH5, alkB homolog 5; CDCP1, CUB-domain containing protein 1; AML, acute myeloid leukemia; HBXIP, hepatitis B X-interacting protein; WTAP, WT1-associated protein; HNRNPG, heterogeneous nuclear ribonucleoprotein G.

enhanced knowledge and understanding of TME may lead to new ideas and approaches for treating cancer patients.

Starting with Crick's central principle 60 years ago, plenty of previous studies have focused on coding RNA, which make up about 2% of the human genome sequence but are vital to humans (Crick, 1970; Poller et al., 2018). However, non-coding RNA, which accounts for 98% of the human genome, has been ignored as "junk sequences" (Fabbri et al., 2019). Furthermore, with technology development, such as high-throughput sequencing technology, non-coding RNA has entered people's field of vision with a new role. As the research goes further, we classified non-coding into microRNA, lncRNA, circRNA, and so on (Matsui and Corey, 2017; Momen-Heravi and Bala, 2018). Non-coding RNA lacks the potential to encode proteins or peptides but has a high degree of transcriptional activity, which plays an essential role in gene regulation, structure and performs biological functions at the RNA level (Wong et al., 2018). Recent studies have shown that aberrant expression of non-coding RNA is ubiquitous in different types of cancers, revealing that it may play an essential role in human cancers.

As the most abundant modification in TME, m6A RNA modification is one of the critical factors affecting the biological function of RNA (Ma et al., 2019; Yang G. et al., 2020). In general, m6A RNA modification requires the involvement of three factors: m6A methylase (writer), m6A demethylase (eraser), and m6A binding protein (reader) (Shi et al., 2019). It usually influences cancer progression by regulating biological functions associated with cancer, including proliferation, metastasis, stem cell differentiation, and stabilization (Roskoski, 2019). Currently, m6A RNA modifications are also increasingly used to detect and diagnose cancer (Niu et al., 2019).

This review mainly outlines the links between coding/non-coding RNA and m6A RNA modification in the TME. Meanwhile, we describe the implications of the interactions between the three for the biological functions that influence the cancer process and discuss their possible future role in clinical applications.

TUMOR MICROENVIRONMENT

Tumor microenvironment consists mainly of an immune microenvironment dominated by immune cells and a non-immune microenvironment dominated by fibroblasts, formed by the combined action of malignant tumor cells and non-transformed cells (Balkwill et al., 2012; Chen and Hambarzumyan, 2018; Costa et al., 2018; Baghban et al., 2020). To date, most of our research has focused on the immune microenvironment, and the results have shown that alterations in TME profoundly influence tumorigenesis and progression, not only by causing tumor heterogeneity but also by influencing patient resistance (Pottier et al., 2015; Wang J. J. et al., 2018). For example, in breast cancer, one of the mechanisms of action of TME is the removal or alteration of tumor components, thereby impeding anti-tumor immunity (Jung et al., 2016). In liver cancer, we predict tumor progression based on the dynamics of

TME. At the same time, the stromal cells in TME can influence the invasion and migration of tumor cells (Yang et al., 2011). Thus, TME can be used as a therapeutic target for cancer and as a signal to detect cancer progression (Jarosz-Biej et al., 2019).

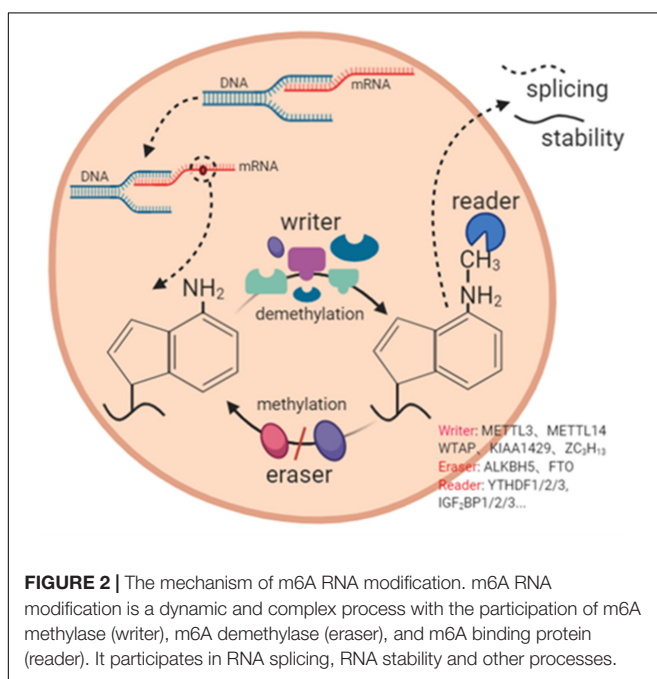
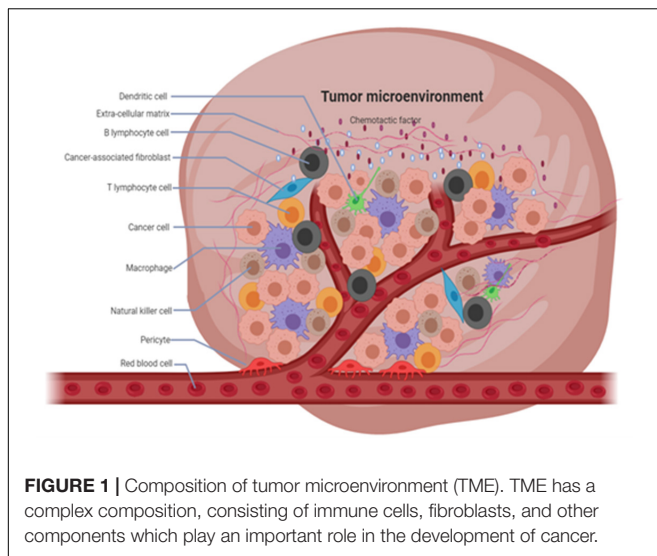
At the same time, TME, as a metabolic site for the growth of numerous cells, is rich in metabolites such as succinic acid, D-2HG, and fumaric acid, which are essential for the normal development of the cells and the organism. These metabolites can act as cofactors or antagonists of epigenetic modification enzymes, affecting numerous epigenetic processes such as m6A RNA modification (Zhao Y. et al., 2020). METTL3 and METTL14 are important components of the m6A modifying enzyme complex, and they can form a stable dimer involved in the methylation process, which is dynamically regulated by substrates and metabolites. S-adenosylmethionine (SAM/AdoMet) acts as a universal intracellular methyl donor. However, because METTL14 does not have a SAM binding site, only METTL3 is active, but METTL14 makes an important contribution in binding substrates, where SAM is produced by a carbon metabolic pathway consisting of the folate and methionine cycles (Sledz and Jinek, 2016; Wang et al., 2016). Similarly, metabolites within TME can influence the demethylation of m6A RNA represented by FTO and ALKBH5, such as 2-oxoglutarate, a key metabolite of the citric acid cycle. If this product is mutated, the demethylation of FTO and ALKBH5 is drastically reduced or even completely lost. In addition, 2-oxoglutarate can also undergo a series of biological reactions to convert to fumaric acid, and due to their structural similarity, these metabolites can often bind to competing products of 2-oxoglutarate become m6A demethylase inhibitors (Feng et al., 2014; Zhang et al., 2019; Figure 1).

M6A RNA MODIFICATION

To date, hundreds of chemical modifications have been reported, among which m6A RNA modification is the most prevalent in coding and non-coding RNA (Ding et al., 2018; Wang et al., 2019a). m6A RNA modification is a dynamic and reversible process (Wang Q. et al., 2020), it requires the involvement of an m6A modifies enzyme complexes (Lin et al., 2016). In recent years, m6A RNA modification has made great progress in regulating RNA transcription (Wang J. et al., 2020), splicing (Ma et al., 2019), translation (Liu et al., 2018c), and stability (Panneerdoss et al., 2018). Below we summarize the relationship between m6A RNA modification and the above biological processes (Figure 2).

M6A RNA MODIFICATION AND RNA SPLICING

The DNA template strand contains introns, and RNA splicing removes introns and joins exons to form a continuous RNA molecule. mRNA splicing produces mRNAs that encode information required for growth and development



(Zhao et al., 2014). FTO, a component of the m6A modifying enzyme complex, is responsible for the regulation of exon splicing in the 3' and 5' exon regions. Zhao et al. showed that the expression level of FTO was negatively correlated with the level of m6A RNA modification during adipogenesis and that the two could interact to influence the development and treatment process of cancer patients.

M6A RNA MODIFICATION AND RNA TRANSCRIPTION

RNA transcription is the process of RNA polymerase catalyzing RNA synthesis from a template strand of DNA and four

nucleotides, i.e., the transfer of biological information from DNA to RNA, guided by the principle of complementary base pairing (Zhao W. et al., 2020). The m6A RNA modification takes part in and affects the transcriptional process of RNA. KIAA1429 is one of the important components of the m6A modifying enzyme complex and participated in the composition of the m6A writer. Lan et al. showed that in the absence of interference by KIAA1429, the interaction between HuR and GATA3 pre-mRNA put them in dynamic equilibrium in hepatocellular carcinoma again. In contrast, the addition of KIAA1429 affected the progression of tumor development by preferentially inducing m6A methylation on the 3' UTR of GATA3 pre-mRNA in hepatocellular carcinoma cells, followed by the isolation of HuR and degradation of GATA3 pre-mRNA, and finally, the down-regulation of GATA3 expression (Lan T. et al., 2019).

M6A RNA MODIFICATION AND RNA TRANSLATION

Proteins are the leading performers of biological functions, and RNA translation belongs to the second part of protein biosynthesis, the first part being RNA transcription. According to the central law, RNA translation is deciphering the base sequences of mature messenger RNA molecules to produce specific amino acids. METTL3, which selectively enhances or inhibits mRNA translation, is one of the significant components of m6A methyltransferase (Choe et al., 2018). Meanwhile, insulin-like growth factor 2 mRNA-binding proteins (IGF2BPs) are important components of the m6A-modifying enzyme complex and act as "readers." Huang et al. (2018) showed that IGF2BP protein recognizes m6A RNA modifications and enhances mRNA stability and translation.

M6A RNA MODIFICATION AND RNA STABILITY

The m6A RNA modification has the function of regulating the stability of RNA, which refers to the ability of RNA to maintain its original structure or resist degradation when external conditions or other factors change (Yang L. et al., 2020). The YTH domain family, which includes YTH domain family proteins 1-3 (YTHDF1-3) and YTH domain-containing proteins 1-2 (YTHDC1-2), i.e., the DF family and DC family, is one of the 'reader' components of the m6A modifying enzyme complex and plays an important function in RNA stability. For example, YTHDF2, as one of the readers of m6A modification, can promote mRNA degradation by recruiting the CCR4-NOT deadenylase complex, thereby reducing the stability of the targeted transcript (Wang et al., 2014; Du et al., 2016). Moreover, Huang et al. (2018) showed that binding of m6A-modified RNA to corresponding binding proteins also could affect RNA stability.

M6A RNA MODIFICATIONS CAN REGULATE BIOLOGICAL FUNCTIONS

m6A RNA modification's ability to affect cancer is proven in various cancers, and it is likely to be a marker for the molecular diagnosis of tumors. Meanwhile, deepening the understanding of the effects of m6A RNA modification on cancer may provide new targets and ideas for researching and developing clinical molecular targeted therapies (Dai et al., 2018; He et al., 2019; Lan Q. et al., 2019; Zhou et al., 2020). In the following, taking gastric cancer as an example, METTL3 can promote the development and progression of gastric cancer by mediating m6A RNA modification of HDGF mRNA (Wang Q. et al., 2020). In contrast, in hepatocellular carcinoma, Chen and Wong (2020) showed that m6A RNA modification regulates the expression of different downstream targets by regulating mRNA stability and translation efficiency (Figure 3).

M6A RNA MODIFICATION AFFECT TUMOR DRUG RESISTANCE

We usually use several approaches in cancer treatment, among which targeted therapies have received more and more attention

because of their more significant effectiveness (Li B. et al., 2020). Although targeted therapies are advancing rapidly, they still face tumor resistance that severely affects the efficacy of cancer treatment (Lin et al., 2020). m6A RNA modifications are the most common RNA modifications that can affect RNA splicing, degradation, and translation by regulating cell proliferation, metabolism, metastasis, and ultimately tumor drug resistance (Huang et al., 2018). For example, Liu et al. showed that RNA m6A modification specifically regulates sorafenib resistance in hepatocellular carcinoma through FOXO3-mediated autophagy. The mechanism is that METTL3 depletion under hypoxic conditions promotes sorafenib resistance and angiogenic genes in HCC cells cultured *in vitro* and subsequently activates the autophagic pathway (Liu et al., 2020b). METTL3 is significantly downregulated in human sorafenib-resistant hepatocellular carcinoma, whereas METTL3 depletion markedly enhances FOXO3 mRNA stability and eliminates METTL3 mediated sensitivity to sorafenib m6A dependence, which could restore resistance to HCC if FOXO3 overexpression was present.

Furthermore, Jin et al. showed that m6A RNA methylation promotes YAP translation and increases YAP activity, thereby inducing drug resistance and metastasis in NSCLC. The mechanism is that m6A methylation causes YTHDF1/3 and eIF3b to join the translation initiation complex, thereby

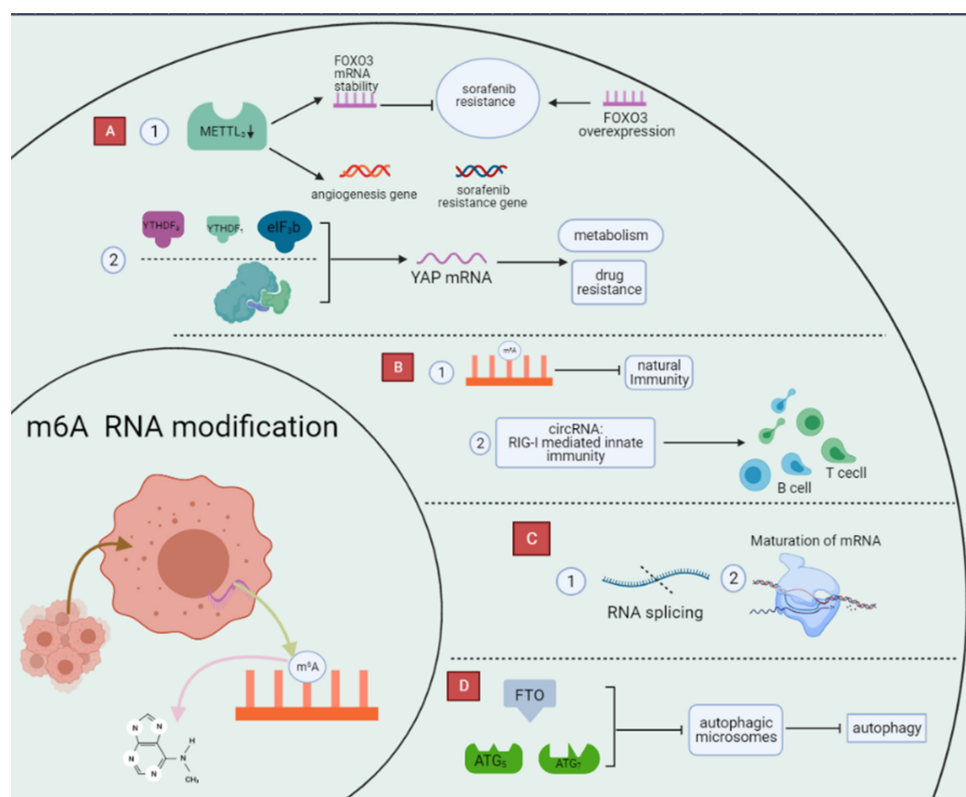


FIGURE 3 | Regulation of biological function of m6A RNA modification. m6A modifications are the most abundant modifications within RNA and can profoundly influence the process of cancer development by regulating biological functions such as drug resistance, immune metabolism, and autophagy through a variety of pathways. **(A)** m6A RNA modification affect tumor drug resistance. **(B)** m6A RNA modification affect immunity. **(C)** m6A RNA modification affect metabolism. **(D)** m6A RNA modification affect autophagy.

promoting the translation of YAP mRNA. Also, m6A RNA methylation improves YAP mRNA stability through the MALAT1-miR-1914-3p-YAP axis (Jin et al., 2019).

M6A RNA MODIFICATION AFFECT IMMUNITY

The immune system is vital to the body and helps us to defend ourselves against many harmful microorganisms. Recent studies have shown that m6A RNA modification affects the immune system and the function of immune cells to a certain extent, the more obvious of which is that deletion of METTL3 will lead to impaired maturation of these cells in response to lipopolysaccharides and decreased expression of CD40 and CD80, thus inducing a decrease in T cell responsiveness. Also, m6A RNA modification can affect the development of the immune system. In a mouse model, high expression of METTL3 is required for the differentiation of blood-derived endothelial cells into hematopoietic stem cells (Shulman and Stern-Ginossar, 2020). What is more, immune dysregulation is an important cause of several immune diseases, including systemic lupus erythematosus (SLE) and rheumatoid arthritis. It has been reported that m6A RNA modifications can regulate RNA and other gene expressions in immune cells, affecting SLE immune cell pathogenesis (Ma et al., 2019; Sekar and Lakshmanan, 2020). Meanwhile, m6A RNA modifications in circRNA play an essential role in tumor development and anti-tumor immunity (Chen Y. G. et al., 2019). Exogenous circRNA can effectively stimulate immune signaling, and m6A RNA modifications are the main contributors to the immune effects of circRNA. For example, exogenous circRNA activates RIG-I-mediated innate immunity, induces activation of antigen-specific B and T cells, and anti-tumor activity *in vivo* (Poller et al., 2018). In addition, m6A-modified RNAs are degraded by YTHDF2, suppressing natural immunity. These results indicate that m6A RNA modification plays an essential regulatory role in the tumor immune process (Paramasivam and Vijayashree Priyadharsini, 2020). Therefore, a deeper understanding of the relationship between m6A RNA modifications and immunity may open new doors to treat immune diseases.

M6A RNA MODIFICATION AFFECT METABOLISM

Epigenetic regulation of organisms is a complex process. m6A RNA modification is the most prevalent modification in eukaryotic cells and represents a new trajectory of epigenetic modifications. It plays a vital role in regulating RNA metabolisms, such as regulating splicing and translation. One way of RNA editing is converting A to I with the involvement of RNA adenosine deaminase (ADAR). Reports suggest that A-to-I is a crucial factor affecting RNA metabolism and that m6A RNA modification is inversely correlated with A-to-I. A possible reason for this is that m6A RNA modification affects RNA structure (Torsin et al., 2021).

Meanwhile, *in vivo* immunofluorescence analysis revealed that METTL3, a component of the m6A methyltransferase complex, is located on the mRNA splicing factor, revealing that m6A RNA modifications may play a regulatory role in RNA metabolism and have an impact on cellular reprogramming (Yang et al., 2018). As the study progressed, Liu Y. et al. (2019) found that m6A methylation affected multiple aspects of mRNA metabolism, from expression in the nucleus to processing of pre-mRNA to attenuation of the translational machinery of mRNA in the cytoplasm. The transition from pre-mRNA to mature mRNA requires a splicing process, and there is evidence that m6A RNA modification is a vital splicing regulator (Liu et al., 2014; Ping et al., 2014). First, based on PAR-CLIP analysis, it was observed that mRNAs with selective splicing have more METTL3 binding and methylation sites. A recent study also showed that METTL3 could play a role in spermatogenesis by initiating selective splicing of related mRNAs to regulate sperm differentiation and meiosis (Dominissini et al., 2012). Secondly, m6A erasers and readers also differentially affect RNA splicing, with FTO binding to pre-mRNAs in the nucleus to initiate selective spliced exons and YTHDF1 binding directly to m6A-modified variable splice exons to facilitate their incorporation into mRNAs (Meyer et al., 2012; Bartosovic et al., 2017).

M6A RNA MODIFICATION AFFECT AUTOPHAGY

Autophagy is a complex biological process that involves the engulfment of organelles and proteins by autophagosomes (Doria et al., 2013; Galluzzi et al., 2017; Russo and Russo, 2018), followed by digestion by lysosomes, and finally, entry and recycling of cellular processes (Kimura et al., 2007; Yuan et al., 2020). It can influence multiple aspects of cancer, such as regulating resistance to sorafenib in hepatocellular carcinoma. The mechanism is the downregulation of the m6A demethylase component FTO, which affects the expression of ATG5 and ATG7, ultimately reducing the ability of autophagic microsome and inhibiting autophagy. That is, after FTO Silencing, YTHDF2, modified with high levels of m6A RNA, binds to ATG5 and ATG7 transcripts, and mRNA degradation increases, leading to reduced protein expression and affecting the autophagic process (Jin et al., 2018; Wang C. Y. et al., 2020; Wang X. et al., 2020).

M6A RNA MODIFICATION AFFECTS THE INFILTRATION CHARACTERISTICS OF CANCER CELLS IN TUMOR MICROENVIRONMENT

m6A RNA Modification Can Activate Oncogenes Within Tumor Microenvironment

m6A RNA modifications can influence cancer development by activating tumor-associated genes (He L. et al., 2018; Zheng W. et al., 2019). Depending on the outcome, we can classify

m6A RNA modification into promoter and suppressor effects. Next, we will specifically summarize the dual role of m6A RNA modification in cancer.

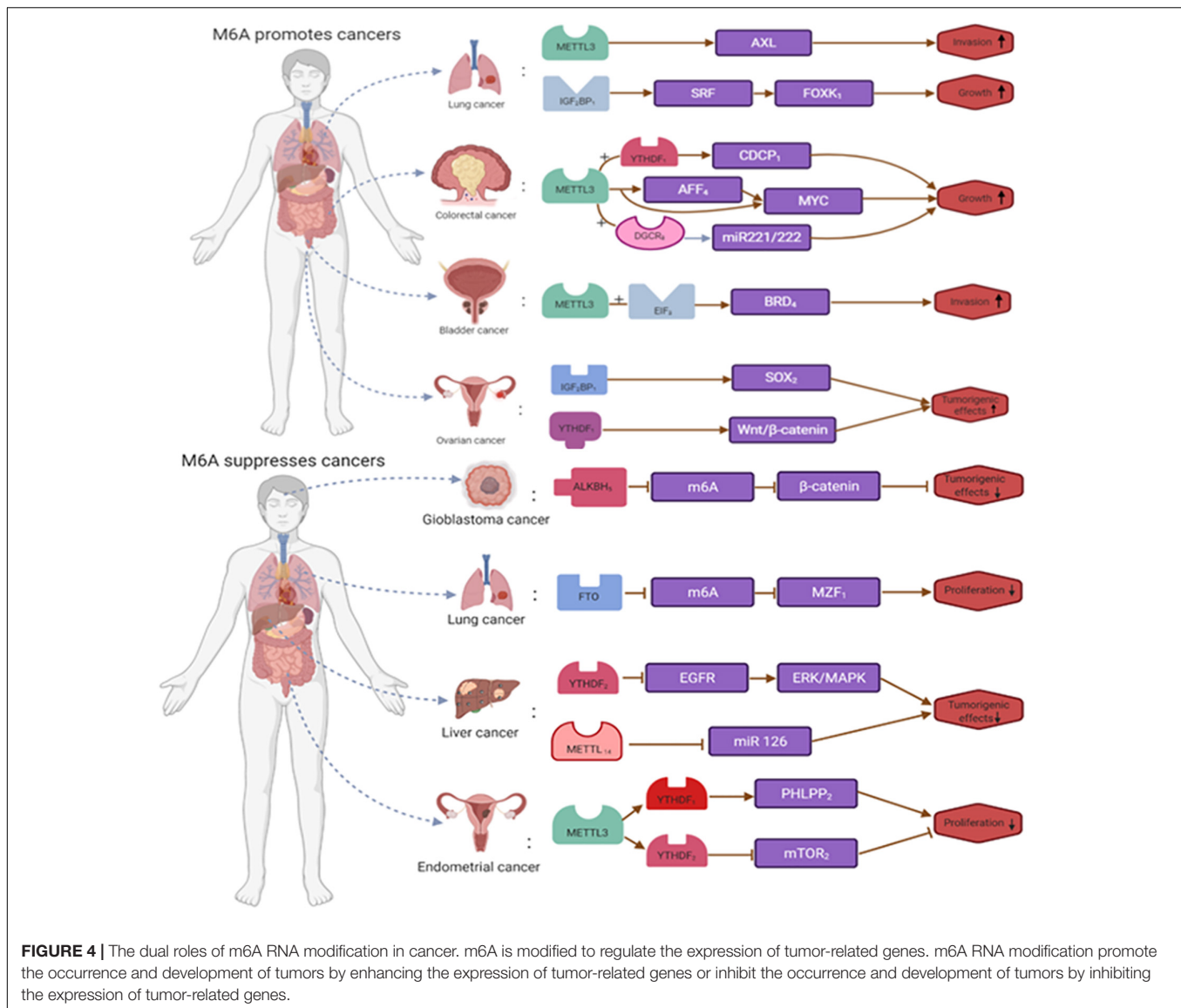
On the one hand, m6A RNA modification can promote tumorigenesis and development. Take bladder cancer, lung cancer, acute myeloid leukemia, ovarian cancer, breast cancer, pancreatic cancer, colorectal cancer, and nasopharyngeal cancer. Gu et al. showed that in bladder cancer, the expression of METTL3, METTL14, and the oncogene CDCP1 influenced the progression of tumor development. In bladder cancer, m6A expression showed upregulation, and inhibition of METTL3 inhibited proliferation, invasion, and migration of bladder cancer tumor cells. In addition, METTL14 expression is downregulated in bladder cancer, and some studies have shown that eliminating METTL14 promotes capsule proliferation (Gu et al., 2019). In lung cancer, METTL3 expression increases. In a mouse model, deletion of METTL3 promoted apoptosis in transplanted tumor cells. Related experiments showed that METTL3 expression levels in A549 cells responded to the induction of simvastatin. Chen et al. (2020) showed that METTL3 positively regulates the level of EZH2 and modifies its mRNA via m6A, thereby affecting tumor progression (Choe et al., 2018). In acute myeloid leukemia, increased expression of METTL3 promotes the translation of SP1, which regulates the expression of the oncogene C-MYC, and METTL14 enhances the translation of MYB and MYC by maintaining its high expression (Barbieri et al., 2017; You et al., 2017). In ovarian cancer, increased expression levels of IGF2BP1 enhanced the expression of SRF and inhibited its degradation, thereby increasing the expression levels of SRF, FOXK1, and PDLIM7 (Ro, 2016; Muller et al., 2018, 2019). Meanwhile, METTL3 promotes growth, invasion, and migration in ovarian cancer by stimulating peripheral mRNA transfer and epithelial-mesenchymal transition. In breast cancer, increased expression levels of METTL3 would promote HBXIP expression and thus affect breast cancer phenotype. In addition, upregulation of ALKBH5 expression promotes mRNA stability and expression of the pluripotent stem cell marker NANOG gene, affecting breast cancer development (Deng et al., 2018). In pancreatic cancer, METTL3 regulates tumor progression and drug resistance through MAPK cascade, RNA splicing, and cellular regulation, and therefore further studies METTL3's interaction with these processes is essential to understand the functional mechanisms of METTL3 (Taketo et al., 2018). The results of Song et al. (2020) showed increased expression of the YTHDF1 gene in colorectal cancer, where activation of the WNT/ β -catenin signaling pathway may initiate transcription-dependent oncogenic effects, promote gross cell cycle progression, and regulate resistance. Knockdown of the YTHDF1 gene would affect the activity of the WNT/ β -catenin signaling pathway and inhibit the tumorigenicity of colorectal cancer cells (Nishizawa et al., 2018; Bai et al., 2019). Multiple research teams have found that Nasopharyngeal carcinoma m6A RNA modification affects the overall tumorigenicity of FAM225A and ultimately affects the proliferation of nasopharyngeal carcinoma tumor cells. In addition, METTL3 promotes the expression of EZH2 protein by mediating m6A modification of EZH2 mRNA, which increases the malignancy of nasopharyngeal carcinoma cells by silencing CDKN1C, thereby affecting the

development and progression of nasopharyngeal carcinoma (Lai et al., 2018; Wang et al., 2019b; Zheng Z. Q. et al., 2019; Meng et al., 2020).

On the other hand, m6A RNA modification inhibits tumorigenesis and progression. We take endometrial cancer, hepatocellular carcinoma, breast cancer, lung squamous cell carcinoma, and glioblastoma. In endometrial tumors, METTL3 expression decreased, and METTL14 mutated to some extent. m6A methylation reduction promoted cell proliferation, clone formation, migration, and invasion, affecting endometrial tumorigenesis and progression. In addition, FTO catalyzes the demethylation of HOXB13 mRNA in the 3'UTR region, thereby eliminating the recognition of YTHDF2 protein-modified m6A that affects tumor metastasis (Zhang L. et al., 2020). In hepatocellular carcinoma, Hou et al. (2019) showed a unique m6A-mRNA editing process in the hypoxic state. m6A RNA modification through YTHDF2-mediated EGFR degradation plays a role in tumor suppression. In addition, YTHDF2 inhibits ERK/MAPK signaling by destabilizing EGFR mRNA and affecting hepatocellular carcinoma progression (Ma et al., 2017). In breast cancer, Zhang et al. (2016a,b) showed that ALKBH5 expression increases, that NANOG can maintain and regulate tumor stem cells, and that increased ALKBH5 expression correlates with decreased NANOG mRNA m6A levels increased mRNA stability. In lung squamous cell carcinoma, the expression level of FTO is lower. By inhibiting m6A methylation, FTO enhances mRNA stability, promotes the expression of the oncogene MZF1, and affects the progression of lung squamous carcinoma. In addition to FTO, METTL3 expression was also abnormal in lung squamous cell carcinoma (Liu et al., 2018b; Cayir et al., 2019). Wang M. et al. (2020)) showed that ALKBH5 expression increases in glioblastoma and that reduced m6A methylation promoted the expression of the oncogene FOX1, enhancing the self-renewal ability and tumorigenicity of glioblastoma stem cells (Zhang et al., 2017; Figure 4).

m6A RNA Modification Can Activate Immune Cells

m6A RNA modifications can influence cancer development by activating immune cells. For example, immune checkpoint blockade therapy is a revolutionary change in cancer treatment, but many patients do not respond to or are resistant to immune checkpoint blockade therapy (Zhang et al., 2017). ALKBH5 is an important component of the m6A modifying enzyme complex, and it has been reported that deletion of the m6A demethylase ALKBH5 can make patients more sensitive to cancer immunotherapy (Fang et al., 2020). The mechanism is that ALKBH5 affects the efficacy of immunotherapy during immune checkpoint blockade by regulating the expression and lactate content of MCT4/Slc16a3 in TME and the composition of tumor-infiltrating T cells and myeloid suppressor cells. Among these, growth factor- α is a target gene for ALKBH5, MCT4/Slc16a3 and is involved in regulating extracellular lactate concentration, regulatory T cells, and MDSC aggregation in TME (Li N. et al., 2020).



m6A RNA Modification Can Suppress Immune Cells

In addition to activating immune cells, m6A RNA modifications can also affect the cancer process by suppressing the expression of immune cells. CD4 regulatory T cells are involved in and resolve immune suppression in TME. The transcription factor Foxp3, a marker molecule of Treg cells, is regulated by the Suppressor of cytokine signaling (SOCS) family and activates STAT5 (Tong et al., 2018). It has been reported that in a mouse model that has been constructed with METTL3 deletion, elevated expression of the SOCS gene compared to controls inhibited IL2-STAT5 signaling pathway and maintained the inhibitory function of Treg (Lou et al., 2021). Secondly, in hepatocellular carcinoma, METTL3 overexpression then inhibited the expression of suppressor of cytokine signaling factor 2 (SOCS2) through an m6A-YTHDF2-dependent mechanism, which ultimately promoted tumor growth (Tuncel and Kalkan, 2019).

THE ROLES OF M6A RNA MODIFICATION IN TME OF VARIOUS CANCERS

m6A RNA modifications found in TMEs of different cancers influence the onset and progression of cancer. In this review, we have selected several cancers and summarized the role of m6A RNA modifications in TME (Figure 5 and Table 1).

Colorectal Cancer

Colorectal cancer is the third most deadly cancer in the world (Bray et al., 2018). Currently, we have made some progress in the diagnosis and treatment of this disease, but the prognosis of patients with advanced cancer remains poor (Nishihara et al., 2013). As research into cancer has intensified, TME has gradually attracted attention and attempted to use it in cancer treatment, in addition to malignant tumor cells. TME is the site

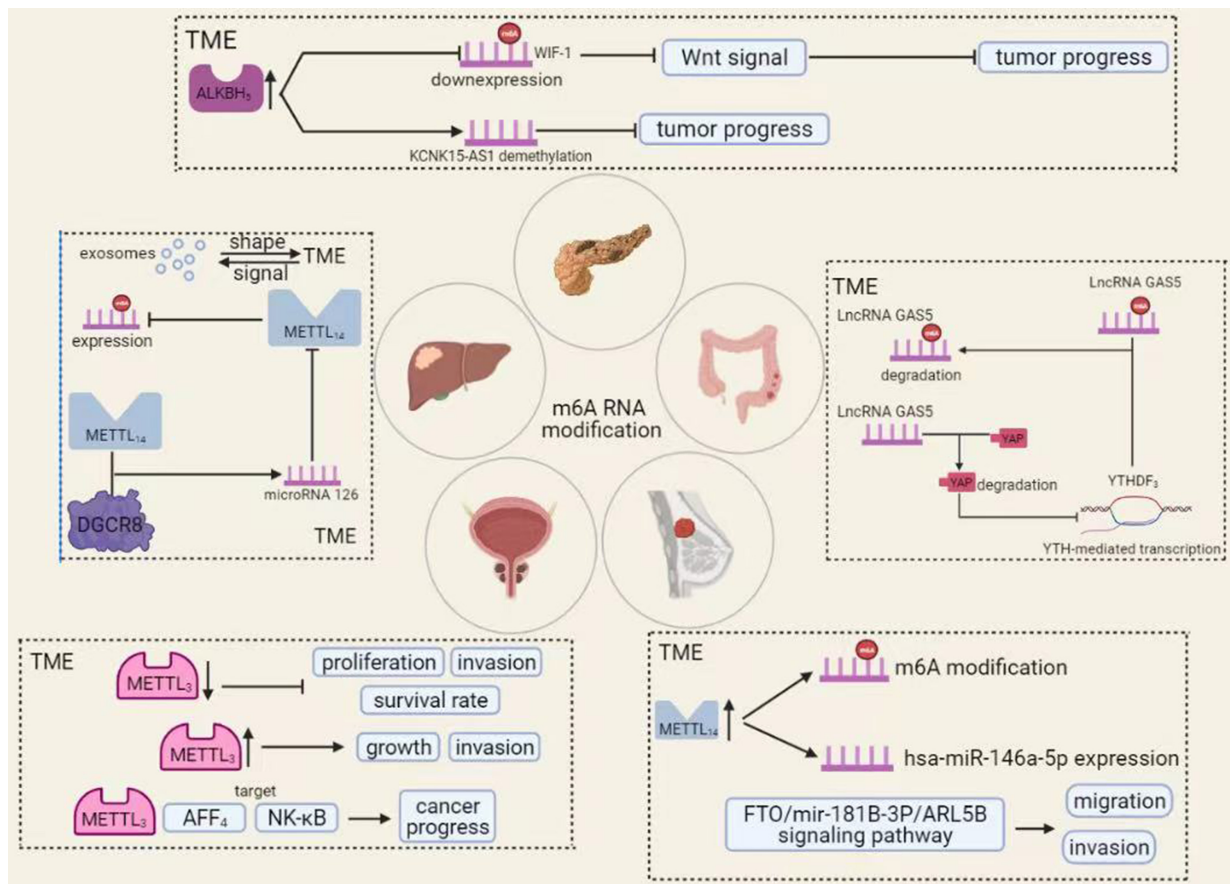


FIGURE 5 | The roles of m6A RNA modification in TME of various cancers. A variety of chemical modifications occur within the tumor microenvironment that is important for tumorigenesis and progression. Among these, m6A RNA modification is the most abundant. In different tumors, m6A RNA modifications can affect cancer progression in various ways.

of growth and transformation of malignant tumor cells, in which it produces and secretes various chemokines and growth factors that promote tumor development and progression (Bahrami et al., 2018). TME contains numerous immune components that can influence tumor development. It is part of the TME and is a very promising therapeutic target. The resulting tumor immune microenvironment has a dynamic character during tumor progression, in which many kinds of cells are involved (Zhang Y. et al., 2020). Ni et al. showed that disruption of the YAP signaling pathway significantly promotes the development and progression of colorectal cancer. The mechanism is that long-stranded non-coding RNA Gas5 is negatively regulated by the m6A reader YTHDF3, forming an adverse regulatory pathway through phosphorylation and degradation of YAP, thereby inhibiting the colorectal carcinogenesis process (Kino et al., 2010; Ni et al., 2019).

Meanwhile, a study by Xu et al. showed that the expression level of long-stranded non-coding RNA SATB2-AS1 was significantly increased in colorectal cancer. This study found that SATB2-AS1 interacted with chromatin regulatory proteins WDR5 and GADD45A in colorectal cancer cell species, with WDR5 catalyzing Lys4 trimethylation and affecting transcription

when bound to methylated H3K4. SATB2-AS1 suppressed tumor metastasis in colorectal cancer by regulating STAB2, i.e., regulating cancer progression by affecting the tumor immune microenvironment (Xu et al., 2019).

Hepatocellular Carcinoma

Hepatocellular carcinoma (HCC) is a common malignancy with high morbidity and mortality worldwide (Zhang et al., 2018). Patients with advanced hepatocellular carcinoma prognosis are poor under existing conditions, and new approaches are urgently needed. In recent years, immunotherapy has gained prominence in cancer treatment. Because TME is more variable at different stages of tumor development, it shows more significant variation in other individuals or distant locations of the same individual (Quail and Joyce, 2013). Immune cells can inhibit tumor development, but when they interact with specific cells of TME, the tendency for tumor development to spread will be more pronounced (Zamarron and Chen, 2011). Secondly, HCC can classify into multiple types that share a similar TME, both of which promote immune tolerance and immune escape through various mechanisms (Fu et al., 2019). TME is an essential partner of tumor cells, providing the necessary conditions

for the development and progression of tumor cells, such as angiogenesis and tumor formation. Exosomes are information carriers for TME and are the molecular entities involved in building TME (Wu et al., 2019). In hepatocellular carcinoma, exosomes shape TME, provide energy, promote tumor growth, and induce angiogenesis. TME contains exosomes regulating cell line survival and development by giving stimulatory or inhibitory signals. The role of m6A RNA modifications, which occur mainly in TME in HCC, has attracted increasing attention (Bissell and Hines, 2011). For example, microRNA 126 is an essential component of the methyltransferase complex and decreased expression *in vitro* and *in vivo* (Ma et al., 2017). MicroRNA 126 is a significant component of METTL14 in HCC. METTL14 can influence the progression of tumor development by m6A-dependent regulation of PRI-microRNA 126 progression, leading to reduced expression of microRNA 126 (Hu et al., 2019).

Bladder Cancer

Bladder cancer is one of the three significant urinary system tumors and is the most common malignancy of the urinary system, with the highest incidence among malignancies (Han et al., 2019). Bladder cancer develops as a result of aberrant genetic alterations and epigenetic abnormalities (Cheng M. et al., 2019). With increased research into bladder cancer and improvements in immunotherapy, methods including intravenous BCG and immune checkpoint inhibitors can influence the development of bladder cancer. At the same time, bladder cancer cells can promote the formation of a tumor immune-suppressive microenvironment. If we can modify or modify TME, it is likely to improve the treatment of bladder cancer. Currently, m6A RNA modification, a very abundant modification in TME, largely influences and alters TME and bladder cancer (Crispen and Kusmartsev, 2020). The level of m6A modification increased significantly in bladder cancer tumor tissues.

Moreover, METTL3 expression levels were similarly upregulated compared to paracancerous tissues. METTL3 can affect the AFF4/NF- κ B/myc signaling network in an m6A-dependent manner, promoting bladder cancer progression (Alarcon et al., 2015). Briefly, low METTL3 expression inhibits the *in vivo* proliferation of bladder cancer and, conversely, METTL3 overexpression promotes its proliferation *in vivo*. Briefly, common METTL3 expression inhibits the *in vivo* proliferation of bladder cancer and, conversely, METTL3 overexpression promotes its proliferation *in vivo* (Cheng M. et al., 2019). The mechanism is that METTL3 interacts with the microprocessor protein Dgcr8 to complete miR221/222 processing, which rescues METTL3-induced proliferation of bladder cancer cells, and its processing exerts an oncogenic effect by positively regulating the pri-miR221/222 process in an m6A-dependent manner (Gu et al., 2016).

Breast Cancer

Breast cancer is the most common malignancy in women and has the second-highest mortality rate in the world (Ahn et al., 2016). Although we have made significant

progress in the diagnosis, surgery, and drug development of breast cancer, drug resistance in metastatic cancers remains an insurmountable problem. As research has progressed, we have focused not only on the anti-cancer treatment of tumor cells but also on the TME where the tumor cells reside (Houthuijzen and Jonkers, 2018). Some studies have shown that breast cancer is associated with molecular heterogeneity (Schnitt, 2010). ROS levels in breast cancer cells are associated with the expression and activity of the transcription factor AHR, which controls tumor growth and chemokine production in the TME, and regulating the TME can influence tumor progression (Kubli et al., 2019). The m6A RNA modification in breast cancer TME has a profound impact on the development of breast cancer. In breast cancer, increased expression of METTL14 enhances m6A RNA modifications and has-miR-146a-5p expression, ultimately enhancing breast cancer cell invasion and migration (Yi et al., 2020).

Meanwhile, as an eraser, FTO also plays a vital role in m6A RNA modification. For example, FTO can regulate the migration and invasion of breast cancer cells by regulating the FTO/Mir-181B-3P/ARL5B signaling pathway, which ultimately affects the development of breast cancer. In conclusion, a good grasp of the relationship between m6A RNA modification, TME, and breast cancer will open a new door for breast cancer treatment (Xu et al., 2020).

Pancreatic Cancer

Pancreatic cancer is cancer with a high mortality rate in the world today. Its late onset makes early diagnosis difficult, and it is often diagnosed late in the patient's life (Cheng et al., 2017). Although we have made significant advances in the genetics and biology of pancreatic cancer, the results in prolonging the survival time of pancreatic cancer are still not substantial (Ren et al., 2018). In pancreatic cancer, the stability of TME refers to a complex balance between pro- and anti-tumor components (Melstrom et al., 2017). We are combined with clinical trials showing that TME in pancreatic cancer results from the interaction between pancreatic epithelial and mesenchymal cells, which influences the efficacy of radiotherapy, chemotherapy, and immunotherapy. Two distinguishing features of TME in pancreatic cancer are extensive immunosuppression and intensive adhesion formation, accelerating the proliferation of tumor cells (Neesse et al., 2015). m6A RNA modifications also play an essential role in pancreatic cancer, with METTL3 promoting chemo- and radiation resistance in pancreatic cancer cells (Taketo et al., 2018). In TME, ALKBH5 overexpression can inhibit pancreatic cancer by decreasing the level of m6A RNA modification of WIF-1, blocking the activation of Wnt signaling, and increasing the sensitivity of pancreatic cancer cells to drugs (Tang et al., 2020). Meanwhile, ALKBH5 could demethylate the long non-coding RNA KCNK15-AS1 and inhibit pancreatic carcinogenesis. In addition, aberrant activation of the Wnt signaling pathway is also a critical factor in the development and progression of pancreatic cancer, directly or indirectly affecting tumor cells' proliferation and drug resistance (Morris et al., 2010; Bailey et al., 2016).

TABLE 1 | The role of m6A methylation in a variety of cancers.

Type	Molecular	Cancer	Role in cancer	Mechanism	Related targets	Function	References
m6A writer	METTL3	Leukemia	Oncogene	Promoting the translation	c-MYC, BCL2, and PTEN	Inhibit and induce differentiation, promote cell growth, and thus delay the occurrence of Leukemia	Visvanathan et al., 2018
			Oncogene	Enhancing the mRNA stability	SOX2	Reduced sensitivity to γ radiation	Chen et al., 2018
		Glioblastoma	Anti-oncogene	Regulating oncogenes	ADAM19, EPHA3, and KLF4	Inhibit the formation, growth, and development of glioblastoma	Cui et al., 2017
				Promote the translation	EGFR, TAZ, MAPK2(MK ₂), DNMT3A	Promotes growth, invasion, and survival	Choe et al., 2018
		Lung cancer	Oncogene	Enhancing the translation	BRD4	Promote tumor growth	Choe et al., 2018
m6A writer	METTL3	Liver cancer	Oncogene	Regulating target	SOCS2	Promotes cell proliferation and migration	Liu et al., 2018a
		Bladder cancer	Oncogene	Promoting the translation	CPCP1	Promote malignant transformation of cells	Vu et al., 2017
		Ovarian carcinoma	Oncogene	Promoting the translation	AXL	Promote cell proliferation Inhibition of cell	Liu et al., 2014
		Endometrial cancer	Anti-oncogene	Stimulating AKT activation	PHLPP2	Inhibition of cell proliferation, invasion and migration	Weng et al., 2018
		Breast cancer	Oncogene	Promoting the expression	HBXIP	Promote cell proliferation	Wang et al., 2017
m6A writer	METTL14	Acute myeloid leukemia	Oncogene	m6A RNA modification and gene expression	SOCS2	Promote tumor growth	Vu et al., 2017
		Leukemia	Oncogene	Regulating mRNA stability and translation	SPI1	Inhibit the differentiation of leukemia cells and promote the self-renewal of stem	Wang et al., 2016
		Glioblastoma	Oncogene	Regulating oncogenes	ADAM19, EPHA3, KLF4	Promote tumor cell growth and self-renewal	Cui et al., 2017
		Endometrial cancer	Anti-oncogene	Stimulating AKT activation	PHLPP2	Inhibition of cell, proliferation, invasion, and migration	Weng et al., 2018
			Anti-oncogene	Regulating the miRNA processing	DGCR8	<i>In vivo</i> inhibits cell invasion and migration, and inhibits tumor growth	Bansal et al., 2014
m6A eraser	Alkbh5	Hepatoma	Oncogene	Regulating its target	SOCS2	Promote cell proliferation	Tang et al., 2018
		Acute myeloid leukemia	Oncogene	Promoting tumorigenesis	MYC and MYB	Promote tumor growth	Weng et al., 2018
		Glioblastoma	Oncogene	Promoting expression	FOXM1	Promote cell proliferation	Bansal et al., 2014
		Breast cancer	Oncogene	Strengthening mRNA stability	NANOG	Increase the number of tumor stem cells	Zheng et al., 2013
		Glioblastoma	Oncogene	Promoting expression	FOXM1	Promote cell proliferation	Zhang et al., 2017
m6A eraser	FTO	Acute myeloid leukemia	Anti-oncogene	Los of ALKBH5 copy number	ALKBH5	Decrease the copy number of ALKBH5	Kwok et al., 2017
		Pancreatic cancer	Anti-oncogene	Reducing methylation	KCNK15-AS1	Reduces methylation and inhibits tumor cell metastasis	He et al., 2018
		Glioblastoma	Anti-oncogene	Regulating oncogenes	ADAM19, EPHA3, and KLF4	Inhibit growth and tumor formation	Cui et al., 2017
		Leukemia	Oncogene	Regulating expression	ASB2 and RARA	It promotes the transformation of AML cells and inhibits cell differentiation	Li et al., 2017
		Lung cancer	Oncogene	Promoting the stability	MZF1	Promote the growth of tumor cells	Mauer et al., 2017
m6A eraser	IGF2BPs	Cervical squamous cell carcinoma	Oncogene	Regulating expression	β -catenin	Promote resistance to radiation therapy	Zhou et al., 2018
				Promoting tumorigenesis	ASB2 and RARA	Reduced m6A levels in transcripts	Li et al., 2017
		Acute myeloid leukemia	Oncogene	Promoting proliferation	MYC and CEBPA	Inhibit tumor cell proliferation and survival	Su et al., 2018
		Ovarian and Liver cancer	Oncogene	Enhancing mRNA stability	SRF	Promote tumor cell growth and cell invasion	Su et al., 2018

(Continued)

TABLE 1 | (Continued)

Type	Molecular	Cancer	Role in cancer	Mechanism	Related targets	Function	References
m6A reader	YTHDF1	Melanoma and colon cancer	Oncogene	Promoting the expression	lysosomal proteases	Promote tumor growth	Zheng et al., 2013
		Liver cancer	Oncogene	Regulating its target	SODS2	Promotes cell proliferation and migration	Liu et al., 2018a
	YTHDF2	Pancreatic cancer	Anti-oncogene	Promoting growth and migration	m6A-containing mRNA	Promote tumor cell growth and cell invasion	Su et al., 2018

THE APPLICATION OF M6A RNA MODIFICATION IN CANCER

m6A RNA modifications are among the most abundant chemical modifications within RNA, and we can now exploit their range of properties in RNA, such as abundance, to explore their potential function in cancer therapy (Liu X. et al., 2019). Below we summarize the present and future applications of m6A RNA modifications and the difficulties we have encountered.

CURRENT CLINICAL APPLICATIONS OF M6A RNA MODIFICATIONS

m6A RNA Modification Might a Biomarker in Cancer

A growing number of studies have shown that m6A RNA modification has excellent cancer diagnosis and prognosis potential (Wu et al., 2020). It relies mainly on the m6A modifying enzyme complex and plays a vital role in the biological processes of cancer cell proliferation, invasion, and migration (Wang Q. et al., 2018). Many experimental and clinical results show that m6A RNA modifications are closely related to the clinical characteristics of patients and show great potential in the diagnosis of tumors as diagnostic biomarkers for human cancers (Meng et al., 2017). For example, the expression level of m6A is significantly higher in circulating tumor cells than in whole blood cells. Suppose the expression level of m6A changed in circulating tumor cells. In that case, the significance of tumorigenesis and progression can be known and used to predict the diagnosis and prognosis of patients (Liu et al., 2020a).

In patients with hepatocellular carcinoma, upregulation of METTL3 and YTHDF expression decreases patient survival (Ma et al., 2017). Patients in the low METTL3/YTHDF1 group have a better prognosis, so the combination of METTL3 and YTHDF1 serves as a biomarker reflecting the malignancy and prognostic outcome of hepatocellular carcinoma. In gastric cancer, abnormal expression of FTO correlates with the progression and metastasis of gastric cancer. The presentation of FTO plays a vital role in promoting the development of gastric cancer. Hence, FTO is an important molecular marker for the diagnosis and prognosis of gastric cancer. In pancreatic cancer, ALKBH also has an important prognostic molecular marker (Yue et al., 2019).

m6A RNA Modification Might Be a Therapeutic Target in Cancer

In addition to being a biomarker for cancer, m6A RNA modifications have great potential in cancer therapy. Radiotherapy and chemotherapy remain the main treatments for cancer patients, but in recent studies, m6A RNA modifications have shown great potential in cancer therapy (Poller et al., 2018). Analyzing the relevant TCGA dataset, we found that aberrant expression of m6A associated with TP53 gene mutations in AML patients and that m6A mutations reduced survival in AML patients. YTHDF1 is an essential component of the m6A modifying enzyme complex. Its deletion significantly improves

the therapeutic effect of PD-L1 checkpoint blockade, revealing that it may be a molecular target for anti-cancer immunotherapy. In addition, m6A RNA modification may also serve as an essential indicator of patients' sensitivity to radiotherapy. For example, METTL3 promoted resistance to radiotherapy and reduced survival in pancreatic cancer patients, while FTO was expressed at significantly higher levels in CSCC tissues than in pre-cancerous tissues (Liu et al., 2020b). Also, FTO promoted resistance to radiotherapy *in vivo* and *in vitro* by reducing the levels of its target m6A RNA modifications. In summary, m6A RNA modification has the potential to be an effective potential therapeutic target for cancer therapy (Wouters and Delwel, 2016; Yang et al., 2017).

Future Clinical Applications of m6A RNA Modifications

In recent years, a growing number of studies have demonstrated the ability of m6A RNA modifications to act as diagnostic biomarkers and therapeutic targets. Based on these studies, we should aim to understand and apply them to clinical treatment more fully. For example, the main clinical treatments for cancer are still chemotherapy and radiotherapy, so drug resistance is an inevitable problem. Since m6A RNA modifications are associated with drug resistance, we can link radiotherapy and m6A RNA modifications to explore a promising therapeutic approach. Secondly, RNA and protein are inextricably linked, and the importance of protein as the main performer of biological functions cannot be overstated. If we affect the relevant biological functions of protein through m6A RNA modification, it may bring us unexpected gains in clinical treatment. At the same time, there are still few readers, writers and erasers identified, and we need more research to deepen our understanding of the biological properties of m6A RNA modifications for human health and disease.

Challenges in Clinical Application

Although m6A RNA modifications are abundantly present in the TME of RNA, the vast majority have no detectable specific biological function, which makes it difficult to further explore their application in clinical aspects. Secondly, the RNA status varies considerably between individuals or different tissues of the same individual, making it difficult to target specific RNA modifications to cells alone and without guaranteeing therapeutic efficacy. Thirdly, little is known about m6A RNA modification,

and further understanding of its regulatory mechanisms or possible biological functions in different cancers is necessary. Similarly, the limited number of readers, writers, and erasers involved in m6A RNA modification has also posed a certain obstacle to our research. Finally, most studies on m6A RNA modification have remained *in vitro* analyses, and translational application of the results remains a great challenge due to the dynamic and complex nature of m6A RNA modification and the organism.

CONCLUSION

Tumor microenvironment is a complex dynamic system consisting of immune cells, fibroblasts, and lymphocytes, whose interaction with malignant cells influences the development and progression of the cancer process. At the same time, there are hundreds of chemical modifications in TME, and different chemical modifications affect the cancer development process to different degrees. As the most abundant modifications in TME, m6A RNA modifications, in addition to regulating various biological functions such as metabolism, are also clinically meaningful and have the potential to become biomarkers or targets for intervention in tumor therapy. In conclusion, an in-depth understanding of the relationship between TME and m6A RNA modifications is essential for exploring the expression and regulation of oncogenes.

AUTHOR CONTRIBUTIONS

All authors conceptualized, wrote, edited, read, and approved the final manuscript.

FUNDING

This study was supported by The National Natural Science Foundation of China (81972663 and U2004112); Key Scientific Research Projects of Institutions of Higher Education in Henan Province (19A310024); The National Natural Science Foundation of Henan Province (182300410342); and The Health Commission Technology Talents Overseas Training Project of Henan Province (2018140).

REFERENCES

- Ahn, S. G., Kim, S. J., Kim, C., and Jeong, J. (2016). Molecular classification of triple-negative breast cancer. *J. Breast Cancer* 19, 223–230. doi: 10.4048/jbc.2016.19.3.223
- Alarcon, C. R., Lee, H., Goodarzi, H., Halberg, N., and Tavazoie, S. F. (2015). N6-methyladenosine marks primary microRNAs for processing. *Nature* 519, 482–485. doi: 10.1038/nature14281
- Baghban, R., Roshangar, L., Jahanban-Esfahlan, R., Seidi, K., Ebrahimi-Kalan, A., Jaymand, M., et al. (2020). Tumor microenvironment complexity and therapeutic implications at a glance. *Cell Commun. Signal.* 18:59. doi: 10.1186/s12964-020-0530-4
- Bahrami, A., Khazaei, M., Hassanian, S. M., ShahidSales, S., Joudi-Mashhad, M., Maftouh, M., et al. (2018). Targeting the tumor microenvironment as a potential therapeutic approach in colorectal cancer: rational and progress. *J. Cell Physiol.* 233, 2928–2936. doi: 10.1002/jcp.26041
- Bai, Y., Yang, C., Wu, R., Huang, L., Song, S., Li, W., et al. (2019). YTHDF1 regulates tumorigenicity and cancer stem cell-like activity in human colorectal carcinoma. *Front. Oncol.* 9:332. doi: 10.3389/fonc.2019.00332
- Bailey, P., Chang, D. K., Nones, K., Johns, A. L., Patch, A. M., Gingras, M. C., et al. (2016). Genomic analyses identify molecular subtypes of pancreatic cancer. *Nature* 531, 47–52. doi: 10.1038/nature16965
- Balkwill, F. R., Capasso, M., and Hagemann, T. (2012). The tumor microenvironment at a glance. *J. Cell Sci.* 125(Pt 23), 5591–5596. doi: 10.1242/jcs.116392

- Bansal, H., Yihua, Q., Iyer, S. P., Ganapathy, S., Proia, D. A., Penalva, L. O., et al. (2014). WTAP is a novel oncogenic protein in acute myeloid leukemia. *Leukemia* 28, 1171–1174. doi: 10.1038/leu.2014.16
- Barbieri, I., Tzelepis, K., Pandolfini, L., Shi, J., Millan-Zambrano, G., Robson, S. C., et al. (2017). Promoter-bound METTL3 maintains myeloid leukaemia by m(6)A-dependent translation control. *Nature* 552, 126–131. doi: 10.1038/nature24678
- Bartosovic, M., Molaes, H. C., Gregorova, P., Hrossova, D., Kudla, G., and Vanacova, S. (2017). N6-methyladenosine demethylase FTO targets pre-mRNAs and regulates alternative splicing and 3'-end processing. *Nucleic Acids Res.* 45, 11356–11370. doi: 10.1093/nar/gkx778
- Bissell, M. J., and Hines, W. C. (2011). Why don't we get more cancer? A proposed role of the microenvironment in restraining cancer progression. *Nat. Med.* 17, 320–329. doi: 10.1038/nm.2328
- Bray, F., Ferlay, J., Soerjomataram, I., Siegel, R. L., Torre, L. A., and Jemal, A. (2018). Global cancer statistics 2018: GLOBOCAN estimates of incidence and mortality worldwide for 36 cancers in 185 countries. *CA Cancer J. Clin.* 68, 394–424. doi: 10.3322/caac.21492
- Cayir, A., Barrow, T. M., Guo, L., and Byun, H. M. (2019). Exposure to environmental toxicants reduces global N6-methyladenosine RNA methylation and alters expression of RNA methylation modulator genes. *Environ. Res.* 175, 228–234. doi: 10.1016/j.envres.2019.05.011
- Chen, M., Wei, L., Law, C. T., Tsang, F. H., Shen, J., Cheng, C. L., et al. (2018). RNA N6-methyladenosine methyltransferase-like 3 promotes liver cancer progression through YTHDF2-dependent posttranscriptional silencing of SOCS2. *Hepatology* 67, 2254–2270. doi: 10.1002/hep.29683
- Chen, M., and Wong, C. M. (2020). The emerging roles of N6-methyladenosine (m6A) deregulation in liver carcinogenesis. *Mol. Cancer* 19:44. doi: 10.1186/s12943-020-01172-y
- Chen, W. W., Qi, J. W., Hang, Y., Wu, J. X., Zhou, X. X., Chen, J. Z., et al. (2020). Simvastatin is beneficial to lung cancer progression by inducing METTL3-induced m6A modification on EZH2 mRNA. *Eur. Rev. Med. Pharmacol. Sci.* 24, 4263–4270.
- Chen, X. Y., Zhang, J., and Zhu, J. S. (2019). The role of m(6)A RNA methylation in human cancer. *Mol. Cancer* 18:103. doi: 10.1186/s12943-019-1033-z
- Chen, Y. G., Chen, R., Ahmad, S., Verma, R., Kasturi, S. P., Amaya, L., et al. (2019). N6-methyladenosine modification controls circular RNA immunity. *Mol. Cell* 76, 96–109. doi: 10.1016/j.molcel.2019.07.016
- Chen, Z., and Hambardzumyan, D. (2018). Immune microenvironment in glioblastoma subtypes. *Front. Immunol.* 9:1004. doi: 10.3389/fimmu.2018.01004
- Cheng, H., Liu, C., Jiang, J., Luo, G., Lu, Y., Jin, K., et al. (2017). Analysis of ctDNA to predict prognosis and monitor treatment responses in metastatic pancreatic cancer patients. *Int. J. Cancer* 140, 2344–2350. doi: 10.1002/ijc.30650
- Cheng, H. S., Lee, J. X. T., Wahli, W., and Tan, N. S. (2019). Exploiting vulnerabilities of cancer by targeting nuclear receptors of stromal cells in tumor microenvironment. *Mol. Cancer* 18:51. doi: 10.1186/s12943-019-0971-9
- Cheng, M., Sheng, L., Gao, Q., Xiong, Q., Zhang, H., Wu, M., et al. (2019). The m(6)A methyltransferase METTL3 promotes bladder cancer progression via AFF4/NF-kappaB/MYC signaling network. *Oncogene* 38, 3667–3680. doi: 10.1038/s41388-019-0683-z
- Choe, J., Lin, S., Zhang, W., Liu, Q., Wang, L., Ramirez-Moya, J., et al. (2018). mRNA circularization by METTL3-eIF3h enhances translation and promotes oncogenesis. *Nature* 561, 556–560. doi: 10.1038/s41586-018-0538-8
- Costa, A., Kieffer, Y., Scholer-Dahirel, A., Pelon, F., Bourachot, B., Cardon, M., et al. (2018). Fibroblast heterogeneity and immunosuppressive environment in human breast cancer. *Cancer Cell* 33, 463–479. doi: 10.1016/j.ccell.2018.01.011
- Crick, F. (1970). Central dogma of molecular biology. *Nature* 227, 561–563. doi: 10.1038/227561a0
- Crispen, P. L., and Kusmartsev, S. (2020). Mechanisms of immune evasion in bladder cancer. *Cancer Immunol. Immunother.* 69, 3–14. doi: 10.1007/s00262-019-02443-4
- Cui, Q., Shi, H., Ye, P., Li, L., Qu, Q., Sun, G., et al. (2017). m(6)A RNA methylation regulates the self-renewal and tumorigenesis of glioblastoma stem cells. *Cell Rep.* 18, 2622–2634. doi: 10.1016/j.celrep.2017.02.059
- Dai, D., Wang, H., Zhu, L., Jin, H., and Wang, X. (2018). N6-methyladenosine links RNA metabolism to cancer progression. *Cell Death Dis.* 9:124. doi: 10.1038/s41419-017-0129-x
- Deng, X., Su, R., Feng, X., Wei, M., and Chen, J. (2018). Role of N(6)-methyladenosine modification in cancer. *Curr. Opin. Genet. Dev.* 48, 1–7. doi: 10.1016/j.gde.2017.10.005
- Ding, C., Zou, Q., Ding, J., Ling, M., Wang, W., Li, H., et al. (2018). Increased N6-methyladenosine causes infertility is associated with FTO expression. *J. Cell Physiol.* 233, 7055–7066. doi: 10.1002/jcp.26507
- Dominissini, D., Moshitch-Moshkovitz, S., Schwartz, S., Salmon-Divon, M., Ungar, L., Osenberg, S., et al. (2012). Topology of the human and mouse m6A RNA methylomes revealed by m6A-seq. *Nature* 485, 201–206. doi: 10.1038/nature11112
- Doria, A., Gatto, M., and Punzi, L. (2013). Autophagy in human health and disease. *N. Engl. J. Med.* 368, 1845. doi: 10.1056/NEJMc1303158
- Du, H., Zhao, Y., He, J., Zhang, Y., Xi, H., Liu, M., et al. (2016). YTHDF2 destabilizes m(6)A-containing RNA through direct recruitment of the CCR4-NOT deadenylase complex. *Nat. Commun.* 7:12626. doi: 10.1038/ncomms12626
- Fabbri, M., Girmata, L., Varani, G., and Calin, G. A. (2019). Decrypting noncoding RNA interactions, structures, and functional networks. *Genome Res.* 29, 1377–1388. doi: 10.1101/gr.247239.118
- Fang, J., Hu, M., Sun, Y., Zhou, S., and Li, H. (2020). Expression profile analysis of m6a RNA methylation regulators indicates they are immune signature associated and can predict survival in kidney renal cell carcinoma. *DNA Cell Biol.* 39, 1–8. doi: 10.1089/dna.2020.5767
- Feng, C., Liu, Y., Wang, G., Deng, Z., Zhang, Q., Wu, W., et al. (2014). Crystal structures of the human RNA demethylase Alkbh5 reveal basis for substrate recognition. *J. Biol. Chem.* 289, 11571–11583. doi: 10.1074/jbc.M113.546168
- Fu, Y., Liu, S., Zeng, S., and Shen, H. (2019). From bench to bed: the tumor immune microenvironment and current immunotherapeutic strategies for hepatocellular carcinoma. *J. Exp. Clin. Cancer Res.* 38:396. doi: 10.1186/s13046-019-1396-4
- Galluzzi, L., Baehrecke, E. H., Ballabio, A., Boya, P., Bravo-San Pedro, J. M., Cecconi, F., et al. (2017). Molecular definitions of autophagy and related processes. *EMBO J.* 36, 1811–1836. doi: 10.15252/embj.201796697
- Gu, C., Wang, Z., Zhou, N., Li, G., Kou, Y., Luo, Y., et al. (2019). Mettl14 inhibits bladder TIC self-renewal and bladder tumorigenesis through N(6)-methyladenosine of Notch1. *Mol. Cancer* 18:168. doi: 10.1186/s12943-019-1084-1
- Gu, J., Wang, D., Zhang, J., Zhu, Y., Li, Y., Chen, H., et al. (2016). GFRalpha2 prompts cell growth and chemoresistance through down-regulating tumor suppressor gene PTEN via Mir-17-5p in pancreatic cancer. *Cancer Lett.* 380, 434–441. doi: 10.1016/j.canlet.2016.06.016
- Han, J., Wang, J. Z., Yang, X., Yu, H., Zhou, R., Lu, H. C., et al. (2019). METTL3 promote tumor proliferation of bladder cancer by accelerating pri-miR221/222 maturation in m6A-dependent manner. *Mol. Cancer* 18:110. doi: 10.1186/s12943-019-1036-9
- He, L., Li, H., Wu, A., Peng, Y., Shu, G., and Yin, G. (2019). Functions of N6-methyladenosine and its role in cancer. *Mol. Cancer* 18:176. doi: 10.1186/s12943-019-1109-9
- He, L., Li, J., Wang, X., Ying, Y., Xie, H., Yan, H., et al. (2018). The dual role of N6-methyladenosine modification of RNAs is involved in human cancers. *J. Cell Mol. Med.* 22, 4630–4639. doi: 10.1111/jcmm.13804
- He, Y., Hu, H., Wang, Y., Yuan, H., Lu, Z., Wu, P., et al. (2018). ALKBH5 inhibits pancreatic cancer motility by decreasing long non-coding RNA KCNK15-AS1 methylation. *Cell Physiol. Biochem.* 48, 838–846. doi: 10.1159/000491915
- Hinshaw, D. C., and Shevde, L. A. (2019). The tumor microenvironment innately modulates cancer progression. *Cancer Res.* 79, 4557–4566. doi: 10.1158/0008-5472.CAN-18-3962
- Hou, J., Zhang, H., Liu, J., Zhao, Z., Wang, J., Lu, Z., et al. (2019). YTHDF2 reduction fuels inflammation and vascular abnormalization in hepatocellular carcinoma. *Mol. Cancer* 18:163. doi: 10.1186/s12943-019-1082-3
- Houthuijzen, J. M., and Jonkers, J. (2018). Cancer-associated fibroblasts as key regulators of the breast cancer tumor microenvironment. *Cancer Metastasis Rev.* 37, 577–597. doi: 10.1007/s10555-018-9768-3
- Hu, B. B., Wang, X. Y., Gu, X. Y., Zou, C., Gao, Z. J., Zhang, H., et al. (2019). N(6)-methyladenosine (m6A) RNA modification in gastrointestinal tract cancers: roles, mechanisms, and applications. *Mol. Cancer* 18:178. doi: 10.1186/s12943-019-1099-7

- Huang, H., Weng, H., Sun, W., Qin, X., Shi, H., Wu, H., et al. (2018). Recognition of RNA N(6)-methyladenosine by IGF2BP proteins enhances mRNA stability and translation. *Nat. Cell Biol.* 20, 285–295. doi: 10.1038/s41556-018-0045-z
- Jarosz-Biej, M., Smolarczyk, R., Cichon, T., and Kulach, N. (2019). Tumor microenvironment as a “game changer” in cancer radiotherapy. *Int. J. Mol. Sci.* 20:3212. doi: 10.3390/ijms20133212
- Jin, D., Guo, J., Wu, Y., Du, J., Yang, L., Wang, X., et al. (2019). m(6)A mRNA methylation initiated by METTL3 directly promotes YAP translation and increases YAP activity by regulating the MALAT1-miR-1914-3p-YAP axis to induce NSCLC drug resistance and metastasis. *J. Hematol. Oncol.* 12:135. doi: 10.1186/s13045-019-0830-6
- Jin, S., Zhang, X., Miao, Y., Liang, P., Zhu, K., She, Y., et al. (2018). m(6)A RNA modification controls autophagy through upregulating ULK1 protein abundance. *Cell Res.* 28, 955–957. doi: 10.1038/s41422-018-0069-8
- Jung, Y. Y., Kim, H. M., and Koo, J. S. (2016). The role of cancer-associated fibroblasts in breast cancer pathobiology. *Histol. Histopathol.* 31, 371–378.
- Kimura, S., Noda, T., and Yoshimori, T. (2007). Dissection of the autophagosome maturation process by a novel reporter protein, tandem fluorescent-tagged LC3. *Autophagy* 3, 452–460. doi: 10.4161/auto.4451
- Kino, T., Hurt, D. E., Ichijo, T., Nader, N., and Chrousos, G. P. (2010). Noncoding RNA gas5 is a growth arrest- and starvation-associated repressor of the glucocorticoid receptor. *Sci. Signal.* 3:ra8. doi: 10.1126/scisignal.2000568
- Kubli, S. P., Bassi, C., Roux, C., Wakeham, A., Gobl, C., Zhou, W., et al. (2019). AHR controls redox homeostasis and shapes the tumor microenvironment in BRCA1-associated breast cancer. *Proc. Natl. Acad. Sci. U.S.A.* 116, 3604–3613. doi: 10.1073/pnas.1815126116
- Kwok, C. T., Marshall, A. D., Rasko, J. E., and Wong, J. J. (2017). Genetic alterations of m(6)A regulators predict poorer survival in acute myeloid leukemia. *J. Hematol. Oncol.* 10:39. doi: 10.1186/s13045-017-0410-6
- Lai, W., Jia, J., Yan, B., Jiang, Y., Shi, Y., Chen, L., et al. (2018). Baicalin hydrate inhibits cancer progression in nasopharyngeal carcinoma by affecting genome instability and splicing. *Oncotarget* 9, 901–914. doi: 10.18632/oncotarget.22868
- Lan, Q., Liu, P. Y., Haase, J., Bell, J. L., Huttelmaier, S., and Liu, T. (2019). The critical role of RNA m(6)A methylation in cancer. *Cancer Res.* 79, 1285–1292. doi: 10.1158/0008-5472.CAN-18-2965
- Lan, T., Li, H., Zhang, D., Xu, L., Liu, H., Hao, X., et al. (2019). KIAA1429 contributes to liver cancer progression through N6-methyladenosine-dependent post-transcriptional modification of GATA3. *Mol. Cancer* 18:186. doi: 10.1186/s12943-019-1106-z
- Li, B., Jiang, J., Assaraf, Y. G., Xiao, H., Chen, Z. S., and Huang, C. (2020). Surmounting cancer drug resistance: new insights from the perspective of N(6)-methyladenosine RNA modification. *Drug Resist. Updat.* 53:100720. doi: 10.1016/j.drug.2020.100720
- Li, N., Kang, Y., Wang, L., Huff, S., Tang, R., Hui, H., et al. (2020). ALKBH5 regulates anti-PD-1 therapy response by modulating lactate and suppressive immune cell accumulation in tumor microenvironment. *Proc. Natl. Acad. Sci. U.S.A.* 117, 20159–20170. doi: 10.1073/pnas.1918986117
- Li, Z., Weng, H., Su, R., Weng, X., Zuo, Z., Li, C., et al. (2017). FTO plays an oncogenic role in acute myeloid leukemia as a N(6)-methyladenosine RNA demethylase. *Cancer Cell.* 31, 127–141. doi: 10.1016/j.ccell.2016.11.017
- Lin, S., Choe, J., Du, P., Triboulet, R., and Gregory, R. I. (2016). The m(6)A methyltransferase METTL3 promotes translation in human cancer cells. *Mol. Cell* 62, 335–345. doi: 10.1016/j.molcel.2016.03.021
- Lin, Z., Niu, Y., Wan, A., Chen, D., Liang, H., Chen, X., et al. (2020). RNA m(6)A methylation regulates sorafenib resistance in liver cancer through FOXO3-mediated autophagy. *EMBO J.* 39:e103181. doi: 10.15252/embj.2019103181
- Liu, Z. X., Li, L. M., Sun, H. L., and Liu, S. M. (2018c). Link between m6A modification and cancers. *Front. Bioeng. Biotechnol.* 6:89. doi: 10.3389/fbioe.2018.00089
- Liu, J., Eckert, M. A., Harada, B. T., Liu, S. M., Lu, Z., Yu, K., et al. (2018a). m(6)A mRNA methylation regulates AKT activity to promote the proliferation and tumorigenicity of endometrial cancer. *Nat. Cell Biol.* 20, 1074–1083. doi: 10.1038/s41556-018-0174-4
- Liu, J., Ren, D., Du, Z., Wang, H., Zhang, H., and Jin, Y. (2018b). m(6)A demethylase FTO facilitates tumor progression in lung squamous cell carcinoma by regulating MZF1 expression. *Biochem. Biophys. Res. Commun.* 502, 456–464. doi: 10.1016/j.bbrc.2018.05.175
- Liu, J., Yue, Y., Han, D., Wang, X., Fu, Y., Zhang, L., et al. (2014). A METTL3-METTL14 complex mediates mammalian nuclear RNA N6-adenosine methylation. *Nat. Chem. Biol.* 10, 93–95. doi: 10.1038/nchembio.1432
- Liu, S., Li, Q., Li, G., Zhang, Q., Zhuo, L., Han, X., et al. (2020b). The mechanism of m(6)A methyltransferase METTL3-mediated autophagy in reversing gefitinib resistance in NSCLC cells by beta-elemene. *Cell Death Dis.* 11:969. doi: 10.1038/s41419-020-03148-8
- Liu, S., Li, Q., Chen, K., Zhang, Q., Li, G., Zhuo, L., et al. (2020a). The emerging molecular mechanism of m(6)A modulators in tumorigenesis and cancer progression. *Biomed. Pharmacother.* 127:110098. doi: 10.1016/j.biopha.2020.110098
- Liu, X., Liu, L., Dong, Z., Li, J., Yu, Y., Chen, X., et al. (2019). Expression patterns and prognostic value of m(6)A-related genes in colorectal cancer. *Am. J. Transl. Res.* 11, 3972–3991.
- Liu, Y., You, Y., Lu, Z., Yang, J., Li, P., Liu, L., et al. (2019). N (6)-methyladenosine RNA modification-mediated cellular metabolism rewiring inhibits viral replication. *Science* 365, 1171–1176. doi: 10.1126/science.aax4468
- Lou, X., Wang, J. J., Wei, Y. Q., and Sun, J. J. (2021). Emerging role of RNA modification N6-methyladenosine in immune evasion. *Cell Death Dis.* 12:300. doi: 10.1038/s41419-021-03585-z
- Ma, J. Z., Yang, F., Zhou, C. C., Liu, F., Yuan, J. H., Wang, F., et al. (2017). METTL14 suppresses the metastatic potential of hepatocellular carcinoma by modulating N(6)-methyladenosine-dependent primary MicroRNA processing. *Hepatology* 65, 529–543. doi: 10.1002/hep.28885
- Ma, S., Chen, C., Ji, X., Liu, J., Zhou, Q., Wang, G., et al. (2019). The interplay between m6A RNA methylation and noncoding RNA in cancer. *J. Hematol. Oncol.* 12:121. doi: 10.1186/s13045-019-0805-7
- Matsui, M., and Corey, D. R. (2017). Non-coding RNAs as drug targets. *Nat. Rev. Drug Discov.* 16, 167–179. doi: 10.1038/nrd.2016.117
- Mauer, J., Luo, X., Blanjoie, A., Jiao, X., Grozhik, A. V., Patil, D. P., et al. (2017). Reversible methylation of m(6)Am in the 5' cap controls mRNA stability. *Nature* 541, 371–375. doi: 10.1038/nature21022
- Melstrom, L. G., Salazar, M. D., and Diamond, D. J. (2017). The pancreatic cancer microenvironment: a true double agent. *J. Surg. Oncol.* 116, 7–15. doi: 10.1002/jso.24643
- Meng, Q. Z., Cong, C. H., Li, X. J., Zhu, F., Zhao, X., and Chen, F. W. (2020). METTL3 promotes the progression of nasopharyngeal carcinoma through mediating M6A modification of EZH2. *Eur. Rev. Med. Pharmacol. Sci.* 24, 4328–4336.
- Meng, S., Zhou, H., Feng, Z., Xu, Z., Tang, Y., Li, P., et al. (2017). CircRNA: functions and properties of a novel potential biomarker for cancer. *Mol. Cancer* 16:94. doi: 10.1186/s12943-017-0663-2
- Meyer, K. D., Saletore, Y., Zumbo, P., Elemento, O., Mason, C. E., and Jaffrey, S. R. (2012). Comprehensive analysis of mRNA methylation reveals enrichment in 3' UTRs and near stop codons. *Cell* 149, 1635–1646. doi: 10.1016/j.cell.2012.05.003
- Momen-Heravi, F., and Bala, S. (2018). Emerging role of non-coding RNA in oral cancer. *Cell Signal.* 42, 134–143. doi: 10.1016/j.cellsig.2017.10.009
- Morris, J. P. T., Wang, S. C., and Hebrok, M. (2010). KRAS, hedgehog, Wnt and the twisted developmental biology of pancreatic ductal adenocarcinoma. *Nat. Rev. Cancer* 10, 683–695. doi: 10.1038/nrc2899
- Muller, S., Bley, N., Glass, M., Busch, B., Rousseau, V., Misiak, D., et al. (2018). IGF2BP1 enhances an aggressive tumor cell phenotype by impairing miRNA-directed downregulation of oncogenic factors. *Nucleic Acids Res.* 46, 6285–6303. doi: 10.1093/nar/gky229
- Muller, S., Glass, M., Singh, A. K., Haase, J., Bley, N., Fuchs, T., et al. (2019). IGF2BP1 promotes SRF-dependent transcription in cancer in a m6A- and miRNA-dependent manner. *Nucleic Acids Res.* 47, 375–390. doi: 10.1093/nar/gky1012
- Neesse, A., Algul, H., Tuveson, D. A., and Gress, T. M. (2015). Stromal biology and therapy in pancreatic cancer: a changing paradigm. *Gut* 64, 1476–1484. doi: 10.1136/gutjnl-2015-309304
- Ni, W., Yao, S., Zhou, Y., Liu, Y., Huang, P., Zhou, A., et al. (2019). Long noncoding RNA GAS5 inhibits progression of colorectal cancer by interacting with and triggering YAP phosphorylation and degradation and is negatively regulated by the m(6)A reader YTHDF3. *Mol. Cancer* 18:143. doi: 10.1186/s12943-019-1079-y

- Nishihara, R., Wu, K., Lochhead, P., Morikawa, T., Liao, X., Qian, Z. R., et al. (2013). Long-term colorectal-cancer incidence and mortality after lower endoscopy. *N. Engl. J. Med.* 369, 1095–1105. doi: 10.1056/NEJMoa1301969
- Nishizawa, Y., Konno, M., Asai, A., Koseki, J., Kawamoto, K., Miyoshi, N., et al. (2018). Oncogene c-Myc promotes epitranscriptome m(6)A reader YTHDF1 expression in colorectal cancer. *Oncotarget* 9, 7476–7486. doi: 10.18632/oncotarget.23554
- Niu, Y., Lin, Z., Wan, A., Chen, H., Liang, H., Sun, L., et al. (2019). RNA N6-methyladenosine demethylase FTO promotes breast tumor progression through inhibiting BNIP3. *Mol. Cancer* 18:46. doi: 10.1186/s12943-019-1004-4
- Ocana, M. C., Martinez-Poveda, B., Quesada, A. R., and Medina, M. A. (2019). Metabolism within the tumor microenvironment and its implication on cancer progression: an ongoing therapeutic target. *Med. Res. Rev.* 39, 70–113. doi: 10.1002/med.21511
- Panneerdoss, S., Eedunuri, V. K., Yadav, P., Timilsina, S., Rajamanickam, S., Viswanadhapalli, S., et al. (2018). Cross-talk among writers, readers, and erasers of m(6)A regulates cancer growth and progression. *Sci. Adv.* 4:eaar8263. doi: 10.1126/sciadv.aar8263
- Paramasivam, A., and Vijayashree Priyadharsini, J. (2020). Novel insights into m6A modification in circular RNA and implications for immunity. *Cell Mol. Immunol.* 17, 668–669. doi: 10.1038/s41423-020-0387-x
- Ping, X. L., Sun, B. F., Wang, L., Xiao, W., Yang, X., Wang, W. J., et al. (2014). Mammalian WTAP is a regulatory subunit of the RNA N6-methyladenosine methyltransferase. *Cell Res.* 24, 177–189. doi: 10.1038/cr.2014.3
- Poller, W., Dimmeler, S., Heymans, S., Zeller, T., Haas, J., Karakas, M., et al. (2018). Non-coding RNAs in cardiovascular diseases: diagnostic and therapeutic perspectives. *Eur. Heart J.* 39, 2704–2716. doi: 10.1093/eurheartj/ehx165
- Pottier, C., Wheatherspoon, A., Roncarati, P., Longuespee, R., Herfs, M., Duray, A., et al. (2015). The importance of the tumor microenvironment in the therapeutic management of cancer. *Expert. Rev. Anticancer Ther.* 15, 943–954. doi: 10.1586/14737140.2015.1059279
- Quail, D. F., and Joyce, J. A. (2013). Microenvironmental regulation of tumor progression and metastasis. *Nat. Med.* 19, 1423–1437. doi: 10.1038/nm.3394
- Ren, B., Cui, M., Yang, G., Wang, H., Feng, M., You, L., et al. (2018). Tumor microenvironment participates in metastasis of pancreatic cancer. *Mol. Cancer* 17:108. doi: 10.1186/s12943-018-0858-1
- Ro, S. (2016). Multi-phenotypic role of serum response factor in the gastrointestinal system. *J. Neurogastroenterol. Motil.* 22, 193–200. doi: 10.5056/jnm15183
- Roskoski, R. Jr. (2019). Small molecule inhibitors targeting the EGFR/ErbB family of protein-tyrosine kinases in human cancers. *Pharmacol. Res.* 139, 395–411. doi: 10.1016/j.phrs.2018.11.014
- Russo, M., and Russo, G. L. (2018). Autophagy inducers in cancer. *Biochem. Pharmacol.* 153, 51–61. doi: 10.1016/j.bcp.2018.02.007
- Schnitt, S. J. (2010). Classification and prognosis of invasive breast cancer: from morphology to molecular taxonomy. *Mod. Pathol.* 23(Suppl. 2), S60–S64. doi: 10.1038/modpathol.2010.33
- Sekar, D., and Lakshmanan, G. (2020). Methylation of N6-adenosine (m6A) modification in miRNAs and its implications in immunity. *Epigenomics* 12, 1083–1085. doi: 10.2217/epi-2020-0131
- Shi, H., Wei, J., and He, C. (2019). Where, when, and how: context-dependent functions of RNA methylation writers, readers, and erasers. *Mol. Cell* 74, 640–650. doi: 10.1016/j.molcel.2019.04.025
- Shulman, Z., and Stern-Ginossar, N. (2020). The RNA modification N(6)-methyladenosine as a novel regulator of the immune system. *Nat. Immunol.* 21, 501–512. doi: 10.1038/s41590-020-0650-4
- Sledz, P., and Jinek, M. (2016). Structural insights into the molecular mechanism of the m(6)A writer complex. *Elife* 5:e18434. doi: 10.7554/eLife.18434
- Song, P., Feng, L., Li, J., Dai, D., Zhu, L., Wang, C., et al. (2020). beta-catenin represses miR455-3p to stimulate m6A modification of HSF1 mRNA and promote its translation in colorectal cancer. *Mol. Cancer* 19:129. doi: 10.1186/s12943-020-01244-z
- Su, R., Dong, L., Li, C., Nachtergaele, S., Wunderlich, M., Qing, Y., et al. (2018). R-2HG exhibits anti-tumor activity by targeting FTO/m(6)A/MYC/CEBPA signaling. *Cell* 172, 90–105. doi: 10.1016/j.cell.2017.11.031
- Taketo, K., Konno, M., Asai, A., Koseki, J., Toratani, M., Satoh, T., et al. (2018). The epitranscriptome m6A writer METTL3 promotes chemo- and radioresistance in pancreatic cancer cells. *Int. J. Oncol.* 52, 621–629. doi: 10.3892/ijo.2017.4219
- Tang, B., Yang, Y., Kang, M., Wang, Y., Wang, Y., Bi, Y., et al. (2020). m(6)A demethylase ALKBH5 inhibits pancreatic cancer tumorigenesis by decreasing WIF-1 RNA methylation and mediating Wnt signaling. *Mol. Cancer* 19:3. doi: 10.1186/s12943-019-1128-6
- Tang, J., Wang, F., Cheng, G., Si, S., Sun, X., Han, J., et al. (2018). Wilms' tumor 1-associating protein promotes renal cell carcinoma proliferation by regulating CDK2 mRNA stability. *J. Exp. Clin. Cancer Res.* 37:40. doi: 10.1186/s13046-018-0706-6
- Tong, J., Cao, G., Zhang, T., Sefik, E., Amezcua Vesely, M. C., Broughton, J. P., et al. (2018). m(6)A mRNA methylation sustains Treg suppressive functions. *Cell Res.* 28, 253–256. doi: 10.1038/cr.2018.7
- Torsin, L. I., Petrescu, G. E. D., Sabo, A. A., Chen, B., Brehar, F. M., Dragomir, M. P., et al. (2021). Editing and chemical modifications on non-coding RNAs in cancer: a new tale with clinical significance. *Int. J. Mol. Sci.* 22:581. doi: 10.3390/ijms22020581
- Tuncel, G., and Kalkan, R. (2019). Importance of m N(6)-methyladenosine (m(6)A) RNA modification in cancer. *Med. Oncol.* 36:36. doi: 10.1007/s12032-019-1260-6
- Visvanathan, A., Patil, V., Arora, A., Hegde, A. S., Arivazhagan, A., Santosh, V., et al. (2018). Essential role of METTL3-mediated m(6)A modification in glioma stem-like cells maintenance and radioresistance. *Oncogene* 37, 522–533. doi: 10.1038/onc.2017.351
- Vu, L. P., Pickering, B. F., Cheng, Y., Zaccara, S., Nguyen, D., Minuesa, G., et al. (2017). The N(6)-methyladenosine (m(6)A)-forming enzyme METTL3 controls myeloid differentiation of normal hematopoietic and leukemia cells. *Nat. Med.* 23, 1369–1376. doi: 10.1038/nm.4416
- Wang, C. Y., Lin, T. A., Ho, M. Y., Yeh, J. K., Tsai, M. L., Hung, K. C., et al. (2020). Regulation of autophagy in leukocytes through RNA N(6)-adenosine methylation in chronic kidney disease patients. *Biochem. Biophys. Res. Commun.* 527, 953–959. doi: 10.1016/j.bbrc.2020.04.138
- Wang, H., Hu, X., Huang, M., Liu, J., Gu, Y., Ma, L., et al. (2019a). Mettl3-mediated mRNA m(6)A methylation promotes dendritic cell activation. *Nat. Commun.* 10:1898. doi: 10.1038/s41467-019-09903-6
- Wang, H., Zhou, Y., Oyang, L., Han, Y., Xia, L., Lin, J., et al. (2019b). LPLUNC1 stabilizes PHB1 by counteracting TRIM21-mediated ubiquitination to inhibit NF-kappaB activity in nasopharyngeal carcinoma. *Oncogene* 38, 5062–5075. doi: 10.1038/s41388-019-0778-6
- Wang, J., Wang, J., Gu, Q., Ma, Y., Yang, Y., Zhu, J., et al. (2020). The biological function of m6A demethylase ALKBH5 and its role in human disease. *Cancer Cell. Int.* 20:347. doi: 10.1186/s12935-020-01450-1
- Wang, J. J., Lei, K. F., and Han, F. (2018). Tumor microenvironment: recent advances in various cancer treatments. *Eur. Rev. Med. Pharmacol. Sci.* 22, 3855–3864.
- Wang, M., Mao, C., Ouyang, L., Liu, Y., Lai, W., Liu, N., et al. (2020). Correction to: long noncoding RNA LINC00336 inhibits ferroptosis in lung cancer by functioning as a competing endogenous RNA. *Cell Death Differ.* 27:1447. doi: 10.1038/s41418-019-0394-6
- Wang, P., Dostader, K. A., and Nam, Y. (2016). Structural basis for cooperative function of mettl3 and mettl14 methyltransferases. *Mol. Cell* 63, 306–317. doi: 10.1016/j.molcel.2016.05.041
- Wang, Q., Chen, C., Ding, Q., Zhao, Y., Wang, Z., Chen, J., et al. (2020). METTL3-mediated m(6)A modification of HDGF mRNA promotes gastric cancer progression and has prognostic significance. *Gut* 69, 1193–1205. doi: 10.1136/gutjnl-2019-319639
- Wang, Q., Chen, J., Wang, A., Sun, L., Qian, L., Zhou, X., et al. (2018). Differentially expressed circRNAs in melanocytes and melanoma cells and their effect on cell proliferation and invasion. *Oncol. Rep.* 39, 1813–1824. doi: 10.3892/or.2018.6263
- Wang, X., Feng, J., Xue, Y., Guan, Z., Zhang, D., Liu, Z., et al. (2017). Corrigendum: structural basis of N(6)-adenosine methylation by the METTL3-METTL14 complex. *Nature* 542:260. doi: 10.1038/nature21073
- Wang, X., Lu, Z., Gomez, A., Hon, G. C., Yue, Y., Han, D., et al. (2014). N6-methyladenosine-dependent regulation of messenger RNA stability. *Nature* 505, 117–120. doi: 10.1038/nature12730
- Wang, X., Wu, R., Liu, Y., Zhao, Y., Bi, Z., Yao, Y., et al. (2020). m(6)A mRNA methylation controls autophagy and adipogenesis by targeting Atg5 and Atg7. *Autophagy* 16, 1221–1235. doi: 10.1080/15548627.2019.1659617

- Weng, H., Huang, H., Wu, H., Qin, X., Zhao, B. S., Dong, L., et al. (2018). METTL14 inhibits hematopoietic stem/progenitor differentiation and promotes leukemogenesis via mRNA m(6)A modification. *Cell Stem Cell* 22, 191–205. doi: 10.1016/j.stem.2017.11.016
- Wong, C. M., Tsang, C. H., and Ng, I. O. (2018). Non-coding RNAs in hepatocellular carcinoma: molecular functions and pathological implications. *Nat. Rev. Gastroenterol. Hepatol.* 15, 137–151. doi: 10.1038/nrgastro.2017.169
- Wouters, B. J., and Delwel, R. (2016). Epigenetics and approaches to targeted epigenetic therapy in acute myeloid leukemia. *Blood* 127, 42–52. doi: 10.1182/blood-2015-07-604512
- Wu, Q., Zhou, L., Lv, D., Zhu, X., and Tang, H. (2019). Exosome-mediated communication in the tumor microenvironment contributes to hepatocellular carcinoma development and progression. *J. Hematol. Oncol.* 12:53. doi: 10.1186/s13045-019-0739-0
- Wu, X., Xiao, Y., Ma, J., and Wang, A. (2020). Circular RNA: a novel potential biomarker for skin diseases. *Pharmacol. Res.* 158:104841. doi: 10.1016/j.phrs.2020.104841
- Xu, M., Xu, X., Pan, B., Chen, X., Lin, K., Zeng, K., et al. (2019). LncRNA SATB2-AS1 inhibits tumor metastasis and affects the tumor immune cell microenvironment in colorectal cancer by regulating SATB2. *Mol. Cancer* 18:135. doi: 10.1186/s12943-019-1063-6
- Xu, Y., Ye, S., Zhang, N., Zheng, S., Liu, H., Zhou, K., et al. (2020). The FTO/miR-181b-3p/ARL5B signaling pathway regulates cell migration and invasion in breast cancer. *Cancer Commun.* 40, 484–500. doi: 10.1002/cac2.12075
- Yang, G., Sun, Z., and Zhang, N. (2020). Reshaping the role of m6A modification in cancer transcriptome: a review. *Cancer Cell Int.* 20:353. doi: 10.1186/s12935-020-01445-y
- Yang, J. D., Nakamura, I., and Roberts, L. R. (2011). The tumor microenvironment in hepatocellular carcinoma: current status and therapeutic targets. *Semin. Cancer Biol.* 21, 35–43. doi: 10.1016/j.semcancer.2010.10.007
- Yang, L., Liu, X., Song, L., Su, G., Di, A., Bai, C., et al. (2020). Melatonin restores the pluripotency of long-term-cultured embryonic stem cells through melatonin receptor-dependent m6A RNA regulation. *J. Pineal. Res.* 69:e12669. doi: 10.1111/jpi.12669
- Yang, Y., Hsu, P. J., Chen, Y. S., and Yang, Y. G. (2018). Dynamic transcriptomic m(6)A decoration: writers, erasers, readers and functions in RNA metabolism. *Cell Res.* 28, 616–624. doi: 10.1038/s41422-018-0040-8
- Yang, Z., Li, J., Feng, G., Gao, S., Wang, Y., Zhang, S., et al. (2017). MicroRNA-145 Modulates N(6)-methyladenosine levels by targeting the 3'-untranslated mRNA region of the N(6)-methyladenosine binding yth domain family 2 protein. *J. Biol. Chem.* 292, 3614–3623. doi: 10.1074/jbc.M116.749689
- Yi, D., Wang, R., Shi, X., Xu, L., Yilihamu, Y., and Sang, J. (2020). METTL14 promotes the migration and invasion of breast cancer cells by modulating N6methyladenosine and hsa-miR146a5p expression. *Oncol. Rep.* 43, 1375–1386. doi: 10.3892/or.2020.7515
- You, C., Dai, X., and Wang, Y. (2017). Position-dependent effects of regioisomeric methylated adenine and guanine ribonucleosides on translation. *Nucleic Acids Res.* 45, 9059–9067. doi: 10.1093/nar/gkx515
- Yuan, Y., Du, Y., Wang, L., and Liu, X. (2020). The M6A methyltransferase METTL3 promotes the development and progression of prostate carcinoma via mediating MYC methylation. *J. Cancer* 11, 3588–3595. doi: 10.7150/jca.42338
- Yue, B., Song, C., Yang, L., Cui, R., Cheng, X., Zhang, Z., et al. (2019). METTL3-mediated N6-methyladenosine modification is critical for epithelial-mesenchymal transition and metastasis of gastric cancer. *Mol. Cancer* 18:142. doi: 10.1186/s12943-019-1065-4
- Zamarron, B. F., and Chen, W. (2011). Dual roles of immune cells and their factors in cancer development and progression. *Int. J. Biol. Sci.* 7, 651–658. doi: 10.7150/ijbs.7.651
- Zhang, C., Samanta, D., Lu, H., Bullen, J. W., Zhang, H., Chen, I., et al. (2016a). Hypoxia induces the breast cancer stem cell phenotype by HIF-dependent and ALKBH5-mediated m(6)A-demethylation of NANOG mRNA. *Proc. Natl. Acad. Sci. U.S.A.* 113, E2047–E2056. doi: 10.1073/pnas.1602883113
- Zhang, C., Zhi, W. I., Lu, H., Samanta, D., Chen, I., Gabrielson, E., et al. (2016b). Hypoxia-inducible factors regulate pluripotency factor expression by ZNF217- and ALKBH5-mediated modulation of RNA methylation in breast cancer cells. *Oncotarget* 7, 64527–64542. doi: 10.18632/oncotarget.11743
- Zhang, L., Wan, Y., Zhang, Z., Jiang, Y., Lang, J., Cheng, W., et al. (2020). FTO demethylates m6A modifications in HOXB13 mRNA and promotes endometrial cancer metastasis by activating the WNT signalling pathway. *RNA Biol.* 18, 1265–1278. doi: 10.1080/15476286.2020.1841458
- Zhang, Q., Lou, Y., Bai, X. L., and Liang, T. B. (2018). Immunometabolism: a novel perspective of liver cancer microenvironment and its influence on tumor progression. *World J. Gastroenterol.* 24, 3500–3512. doi: 10.3748/wjg.v24.i31.3500
- Zhang, S., Zhao, B. S., Zhou, A., Lin, K., Zheng, S., Lu, Z., et al. (2017). m(6)A demethylase ALKBH5 maintains tumorigenicity of glioblastoma stem-like cells by sustaining FOXM1 expression and cell proliferation program. *Cancer Cell* 31, 591–606. doi: 10.1016/j.ccell.2017.02.013
- Zhang, X., Wei, L. H., Wang, Y., Xiao, Y., Liu, J., Zhang, W., et al. (2019). Structural insights into FTO's catalytic mechanism for the demethylation of multiple RNA substrates. *Proc. Natl. Acad. Sci. U.S.A.* 116, 2919–2924. doi: 10.1073/pnas.1820574116
- Zhang, Y., Song, J., Zhao, Z., Yang, M., Chen, M., Liu, C., et al. (2020). Single-cell transcriptome analysis reveals tumor immune microenvironment heterogeneity and granulocytes enrichment in colorectal cancer liver metastases. *Cancer Lett.* 470, 84–94. doi: 10.1016/j.canlet.2019.10.016
- Zhao, W., Qi, X., Liu, L., Ma, S., Liu, J., and Wu, J. (2020). Epigenetic regulation of m(6)A modifications in human cancer. *Mol. Ther. Nucleic Acids.* 19, 405–412. doi: 10.1016/j.omtn.2019.11.022
- Zhao, X., Yang, Y., Sun, B. F., Shi, Y., Yang, X., Xiao, W., et al. (2014). FTO-dependent demethylation of N6-methyladenosine regulates mRNA splicing and is required for adipogenesis. *Cell Res.* 24, 1403–1419. doi: 10.1038/cr.2014.151
- Zhao, Y., Feng, F., Guo, Q. H., Wang, Y. P., and Zhao, R. (2020). Role of succinate dehydrogenase deficiency and oncometabolites in gastrointestinal stromal tumors. *World J. Gastroenterol.* 26, 5074–5089. doi: 10.3748/wjg.v26.i34.5074
- Zheng, G., Dahl, J. A., Niu, Y., Fedorcsak, P., Huang, C. M., Li, C. J., et al. (2013). ALKBH5 is a mammalian RNA demethylase that impacts RNA metabolism and mouse fertility. *Mol. Cell* 49, 18–29. doi: 10.1016/j.molcel.2012.10.015
- Zheng, W., Dong, X., Zhao, Y., Wang, S., Jiang, H., Zhang, M., et al. (2019). Multiple functions and mechanisms underlying the role of METTL3 in human cancers. *Front Oncol* 9:1403. doi: 10.3389/fonc.2019.01403
- Zheng, Z. Q., Li, Z. X., Zhou, G. Q., Lin, L., Zhang, L. L., Lv, J. W., et al. (2019). Long noncoding RNA FAM225A promotes nasopharyngeal carcinoma tumorigenesis and metastasis by acting as ceRNA to sponge miR-590-3p/miR-1275 and upregulate ITGB3. *Cancer Res.* 79, 4612–4626. doi: 10.1158/0008-5472.CAN-19-0799
- Zhou, S., Bai, Z. L., Xia, D., Zhao, Z. J., Zhao, R., Wang, Y. Y., et al. (2018). FTO regulates the chemo-radiotherapy resistance of cervical squamous cell carcinoma (CSCC) by targeting beta-catenin through mRNA demethylation. *Mol. Carcinog.* 57, 590–597. doi: 10.1002/mc.22782
- Zhou, Z., Lv, J., Yu, H., Han, J., Yang, X., Feng, D., et al. (2020). Mechanism of RNA modification N6-methyladenosine in human cancer. *Mol. Cancer* 19:104. doi: 10.1186/s12943-020-01216-3

Conflict of Interest: The authors declare that the research was conducted in the absence of any commercial or financial relationships that could be construed as a potential conflict of interest.

Publisher's Note: All claims expressed in this article are solely those of the authors and do not necessarily represent those of their affiliated organizations, or those of the publisher, the editors and the reviewers. Any product that may be evaluated in this article, or claim that may be made by its manufacturer, is not guaranteed or endorsed by the publisher.

Copyright © 2021 Si, Chen, Guo, Kang and Sun. This is an open-access article distributed under the terms of the Creative Commons Attribution License (CC BY). The use, distribution or reproduction in other forums is permitted, provided the original author(s) and the copyright owner(s) are credited and that the original publication in this journal is cited, in accordance with accepted academic practice. No use, distribution or reproduction is permitted which does not comply with these terms.



A Review on the Role of Small Nucleolar RNA Host Gene 6 Long Non-coding RNAs in the Carcinogenic Processes

Soudeh Ghafouri-Fard¹, Tayyebah Khoshbakht², Mohammad Taheri^{3*} and Seyedpouzhia Shojaei^{4*}

¹ Department of Medical Genetics, School of Medicine, Shahid Beheshti University of Medical Sciences, Tehran, Iran, ² Men's Health and Reproductive Health Research Center, Shahid Beheshti University of Medical Sciences, Tehran, Iran, ³ Skull Base Research Center, Loghman Hakim Hospital, Shahid Beheshti University of Medical Sciences, Tehran, Iran, ⁴ Department of Critical Care Medicine, Imam Hossein Medical and Educational Center, Shahid Beheshti University of Medical Sciences, Tehran, Iran

OPEN ACCESS

Edited by:

Shiv K. Gupta,
Mayo Clinic, United States

Reviewed by:

Rezvan Noroozi,
Jagiellonian University, Poland
Amin Safa,
Complutense University of Madrid,
Spain

*Correspondence:

Mohammad Taheri
mohammad_823@yahoo.com
Seyedpouzhia Shojaei
psh1182002@yahoo.com

Specialty section:

This article was submitted to
Molecular and Cellular Oncology,
a section of the journal
Frontiers in Cell and Developmental
Biology

Received: 15 July 2021

Accepted: 09 September 2021

Published: 04 October 2021

Citation:

Ghafouri-Fard S, Khoshbakht T,
Taheri M and Shojaei S (2021) A
Review on the Role of Small Nucleolar
RNA Host Gene 6 Long Non-coding
RNAs in the Carcinogenic Processes.
Front. Cell Dev. Biol. 9:741684.
doi: 10.3389/fcell.2021.741684

Being located on 17q25.1, small nucleolar RNA host gene 6 (SNHG16) is a member of SNHG family of long non-coding RNAs (lncRNA) with 4 exons and 13 splice variants. This lncRNA serves as a sponge for a variety of miRNAs, namely miR-520a-3p, miR-4500, miR-146a miR-16-5p, miR-98, let-7a-5p, hsa-miR-93, miR-17-5p, miR-186, miR-302a-3p, miR-605-3p, miR-140-5p, miR-195, let-7b-5p, miR-16, miR-340, miR-1301, miR-205, miR-488, miR-1285-3p, miR-146a-5p, and miR-124-3p. This lncRNA can affect activity of TGF- β 1/SMAD5, mTOR, NF- κ B, Wnt, RAS/RAF/MEK/ERK and PI3K/AKT pathways. Almost all studies have reported oncogenic effect of SNHG16 in diverse cell types. Here, we explain the results of studies about the oncogenic role of SNHG16 according to three distinct sets of evidence, i.e., *in vitro*, animal, and clinical evidence.

Keywords: SNHG6, lncRNA, cancer, biomarker, expression

INTRODUCTION

Small nucleolar RNA host gene 6 (SNHG16) is a member of SNHG family of non-coding RNAs. Long non-coding RNAs (lncRNAs) are a class of transcripts that have sizes longer than 200 nt. These transcripts serve as scaffolds for establishment of different complexes of biomolecules. Moreover, they can serve as enhancers, modulators of chromatin structure and decoys for several molecules, particularly miRNAs (Zhang, 2019 #481). Bioinformatics tools have facilitated identification of several classes of lncRNAs among them is SNHG group of lncRNAs (Li, 2020 #482).

Being annotated as NC_000017.11, SNHG16 gene is located on 17q25.1 and has 4 exons. Based on the Ensembl database¹, 13 splice variants have been identified for this SNHG16 with one of them having a retained intron (ENST00000587743.1) and the rest being categorized as long non-coding RNAs (lncRNAs). These transcripts have sizes ranging from 556 nt (SNHG16-208) to 3607 nt (SNHG16-201). No protein has been recognized for any of these variants. It has been shown to be ubiquitously expressed in ovary, skin and several other tissues. This lncRNA has fundamental roles in the carcinogenesis in numerous types of tissues. Here, we summarize the results of these studies based on three distinct categories of evidence, i.e., *in vitro*, animal and clinical evidence.

¹ <http://asia.ensembl.org/>

CELL LINE STUDIES

Small nucleolar RNA host gene 6 has been demonstrated to be up-regulated in lung cancer cell lines, where it acts as a sponge for miR-520a-3p. Through decreasing the availability of this miRNA, SNHG16 increases expression of EphA2. SNHG16 silencing has suppressed proliferation, migratory potential and invasiveness of these cells, while stimulating cell apoptosis. Further experiments have shown the prominence of SNHG16/miR-520a-3p/EphA2 axis in the regulation of oncogenicity in lung cancer (Yu et al., 2020). Being transcriptionally regulated by YY1, SNHG16 also sequesters miR-4500 to modulate expression of the deubiquitinase USP21. USP21 can further increase expression of SNHG16 (Xu P. et al., 2020). Another experiment in lung cancer cells has identified miR-146a as the target of SNHG16, through its sequestering SNHG16 enhances proliferation, migration and invasiveness of lung cancer cells. The sponging effect of SNHG16 on this miRNA leads to over-expression of MUC5AC, a protein which accelerates metastasis and recurrence of lung cancer cells (Han et al., 2019). **Figure 1** depicts the roles of SNHG16 in lung cancer which are exerted via sponging miR-520a-3p, miR-4500 and miR-146a.

Small nucleolar RNA host gene 6 has also important impacts on the modulation of tumor microenvironment through influencing function of $\gamma\delta$ immunosuppressive T cells. Mechanistically, SNHG16 works as a sponge for miR-16-5p, thus augmenting expression of SMAD5 and potentiating the TGF- β 1/SMAD5 pathway to increase expression of CD73 in V δ 1 T cells (Ni et al., 2020). In addition, SNHG16 can enhance migratory potential of breast cancer cells via sequestering miR-98

and releasing E2F5 from its inhibitory effects (Cai et al., 2017). In prostate cancer cells, siRNA-mediated silencing of SNHG16 results in down-regulation of GLUT-1, reduction of glucose uptake and inhibition of proliferation of cancerous cells without affecting normal prostate cells (Shao et al., 2020). **Figure 2** shows the oncogenic roles of SNHG6 in breast and prostate cancers.

In hepatocellular carcinoma (HCC), SNHG16 has diverse oncogenic as well as tumor suppressor roles (**Figures 3, 4**). SNHG16 has been shown to accelerate proliferation, migratory aptitude and invasiveness of HCC cells through sequestering miR-186 and enhancing expression of ROCK1 (Chen et al., 2019). Moreover, miR-4500 is another sponged miRNA by SNHG16 through which this lncRNA promotes development of HCC (Lin et al., 2019). In this type of cancer, SNHG16 also interacts with miR-302a-3p to increase expression of FGF19 and enhance cell proliferation (Li W. et al., 2019). Metastatic ability of HCC cells can be regulated by SNHG16 through sequestering miR-605-3p. This miRNA can suppress epithelial-mesenchymal transition (EMT) and metastatic ability of HCC via directly suppressing TRAF6 expression and further modulating NF- κ B signaling. Being up-regulated by SNHG16, TRAF6 can in turn increase activity of SNHG16 promoter through activation of NF- κ B, thus constructing an positive feedback loop in favor of HCC progression (Hu et al., 2020).

Contrary to the mentioned studies which reported the oncogenic effects of SNHG16 in the development of HCC, a single study has revealed down-regulation of SNHG16 in HCC cell lines. Ectopic virus-mediated over-expression of SNHG16 has repressed proliferation of HCC cells and

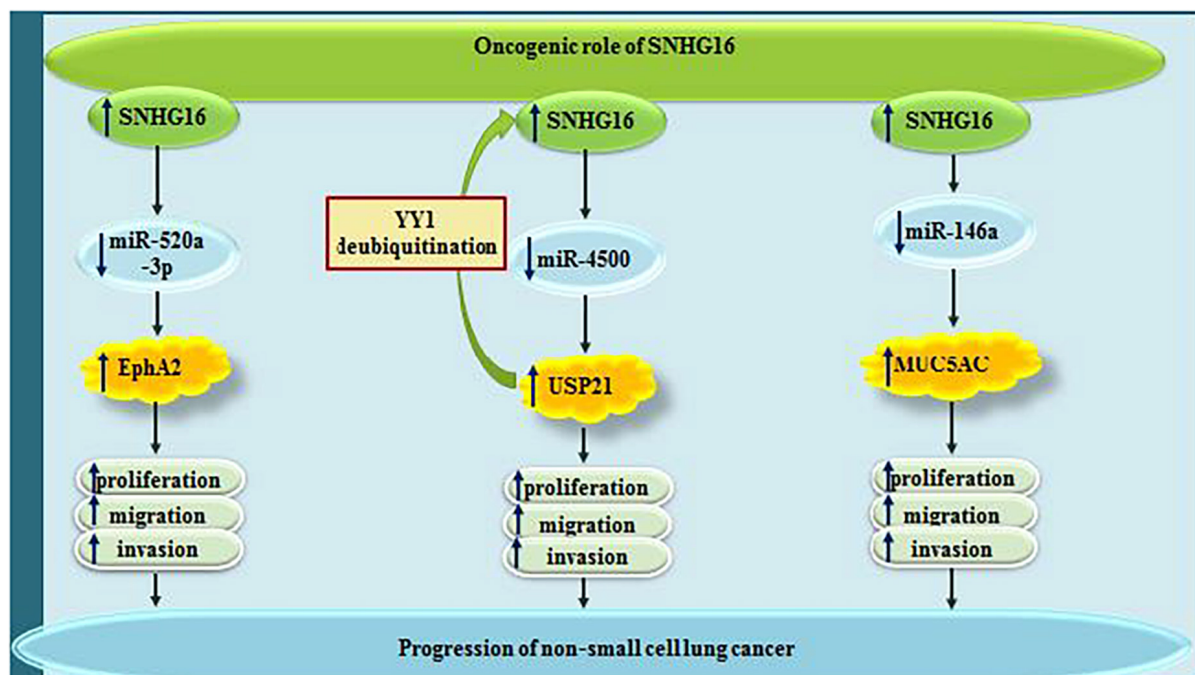


FIGURE 1 | The oncogenic roles of SNHG16 in lung cancer are mainly mediated through sponging miR-520a-3p, miR-4500, and miR-146a.

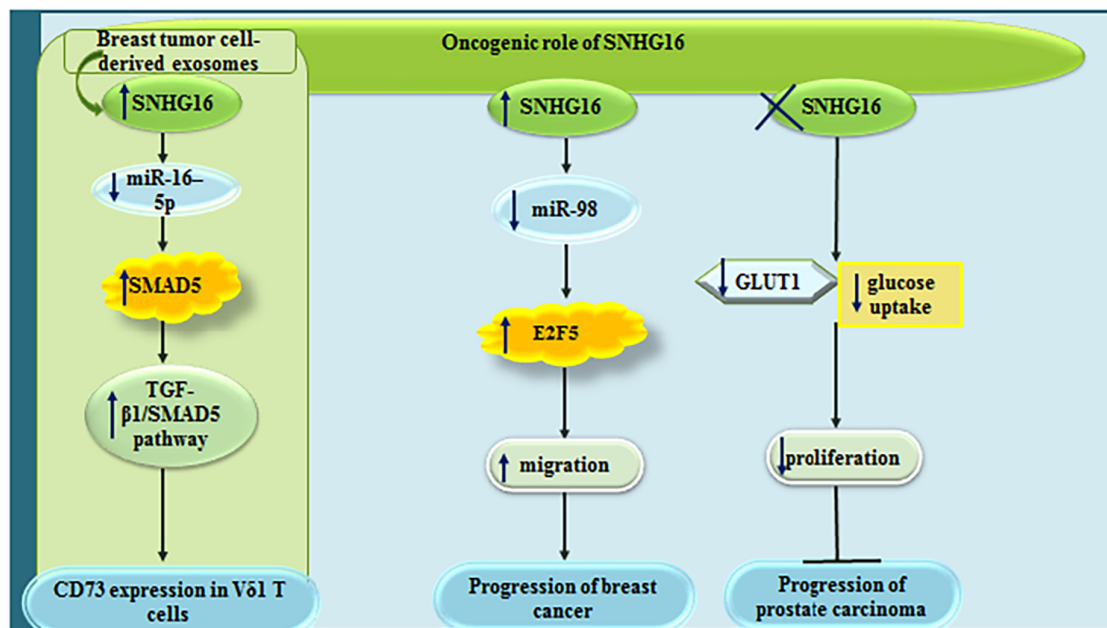


FIGURE 2 | Oncogenic roles of SNHG6 in breast and prostate cancers.

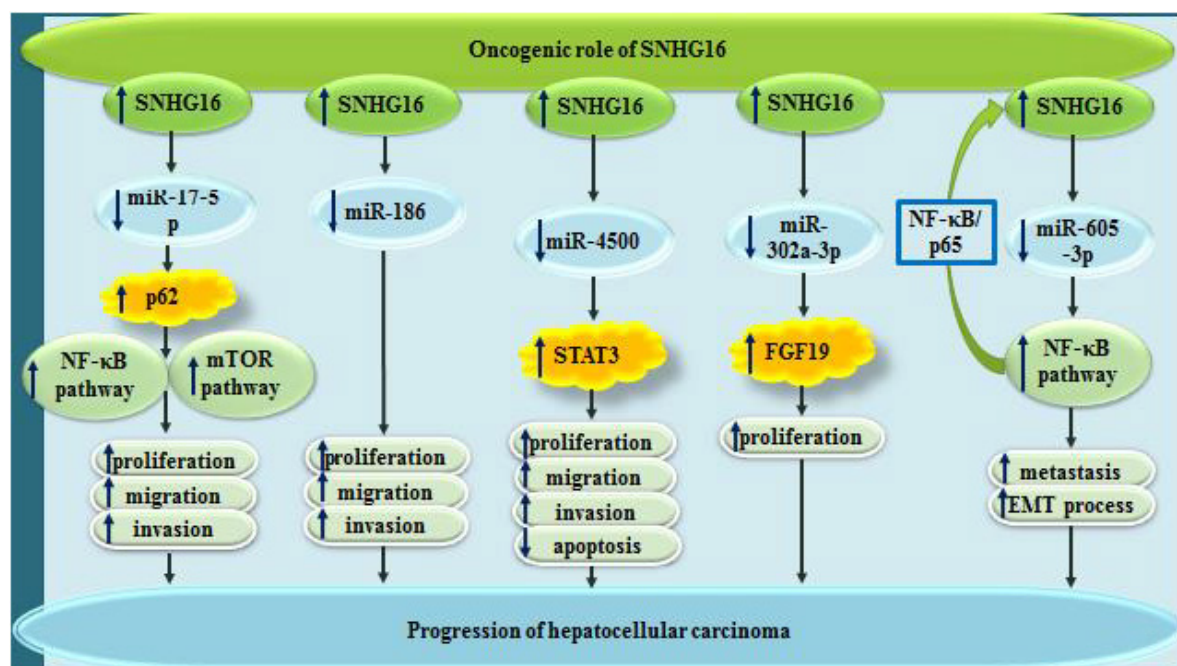


FIGURE 3 | Oncogenic roles of SNHG16 in hepatocellular carcinoma via sponging miR-17-5p, miR-186, miR-4500, miR-302a-3p, and miR-605-3p.

attenuated their resistance to 5-FU through sponging hsa-miR-93 (Xu et al., 2018).

In osteosarcoma, sponging impact of SNHG16 on miR-98-5p has an essential impact on proliferation, migration and invasive aptitude of cancer cell. Simultaneously, it can enhance cell cycle progression and decrease cell apoptosis (Liao et al., 2019).

Meanwhile, through sponging miR-16 and up-regulating ATG4B levels, SNHG16 can induce resistance to cisplatin in these cells (Liu Y. et al., 2019). SNHG16 can also promote proliferation of osteosarcoma cells through sponging miR-205 and enhancing expression of ZEB1 (Zhu C. et al., 2018). Finally, SNHG16 can facilitate EMT of osteosarcoma cells through miR-488/ITGA6

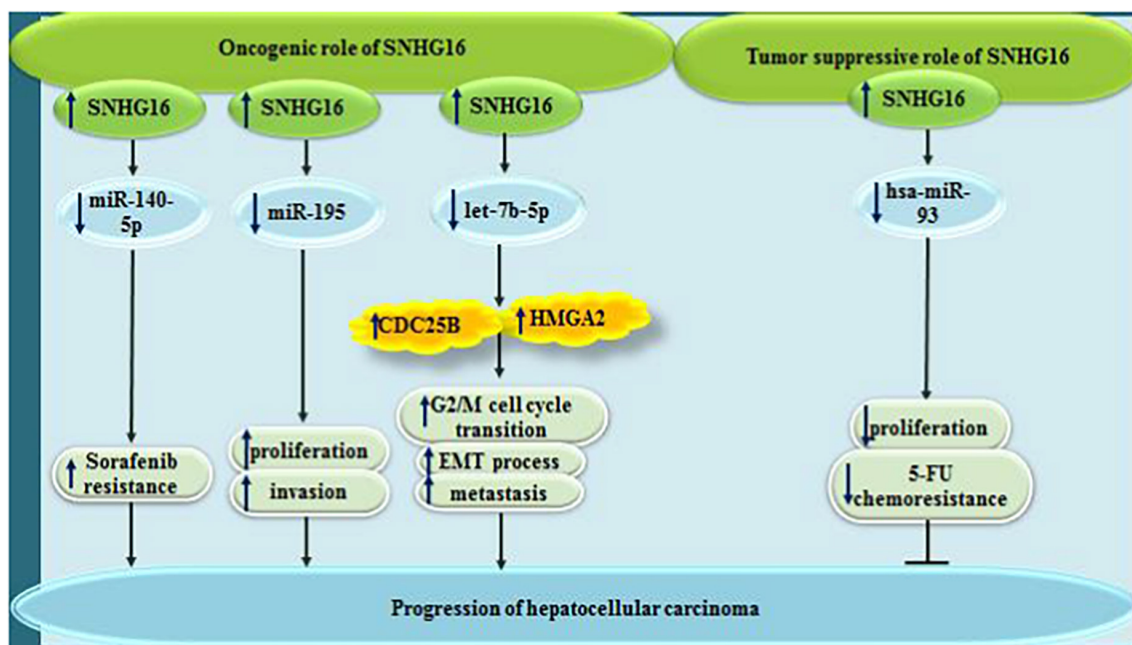


FIGURE 4 | In hepatocellular carcinoma, while SNHG16 exerts oncogenic effect via sponging miR-140-5p, miR-195, and let7b-5p, it can have tumor suppressor effect via sponging has-miR-93.

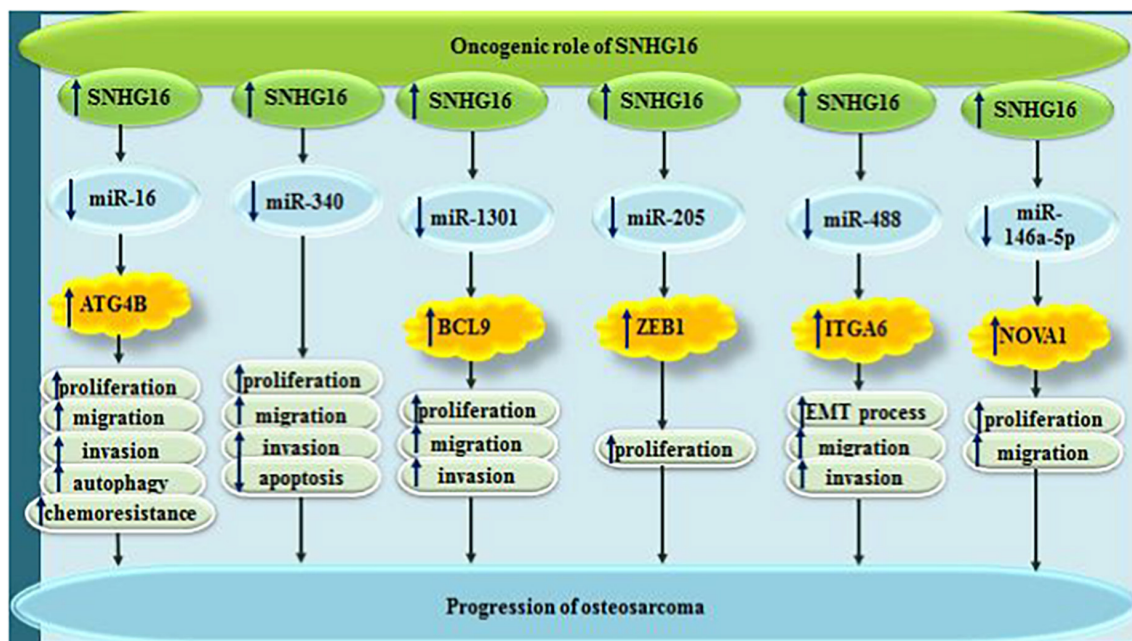


FIGURE 5 | Oncogenic roles of SNHG16 in osteosarcoma.

axis (Bu et al., 2021). **Figure 5** depicts the oncogenic roles of SNHG16 in osteosarcoma.

Small nucleolar RNA host gene 6/miR-124-3p/MCP-1 has an important role in induction of cell proliferation and EMT in colorectal cancer (Chen et al., 2020). The sponging effect of

SNHG16 on miR-200a-3p (Li Y. et al., 2019), miR-132-3p (He et al., 2020), and miR-302a-3p (Ke et al., 2019), also promotes tumorigenicity of colorectal cancer.

In cervical cancer cells, SNHG16 has been found to recruit transcriptional factor SPI1 to increase expression of PARP9,

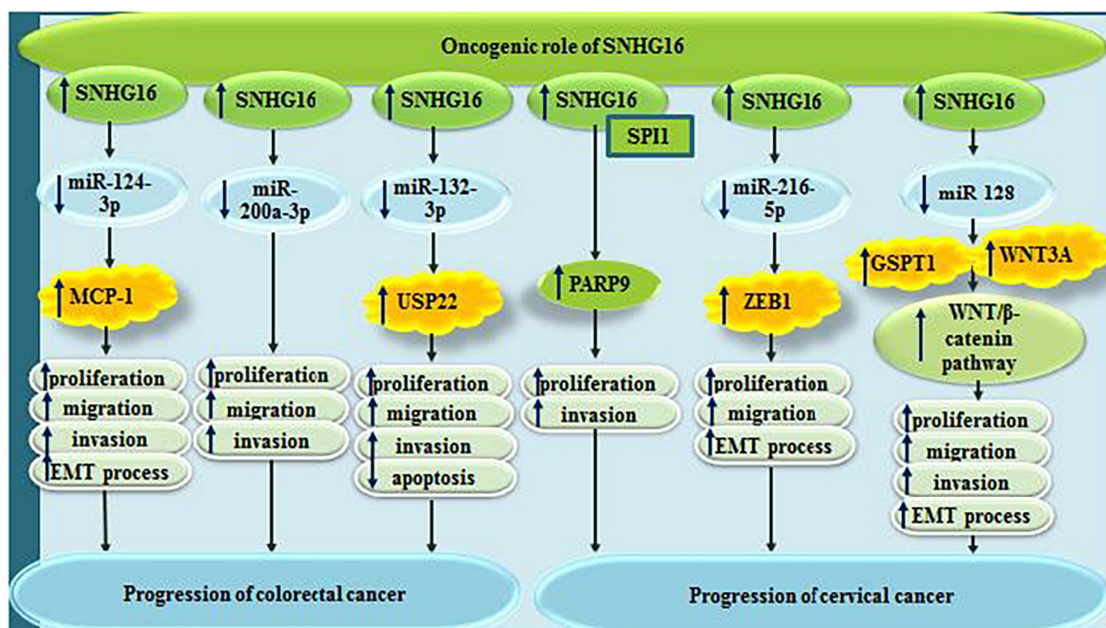


FIGURE 6 | Oncogenic roles of SNHG16 in colorectal and cervical cancers.

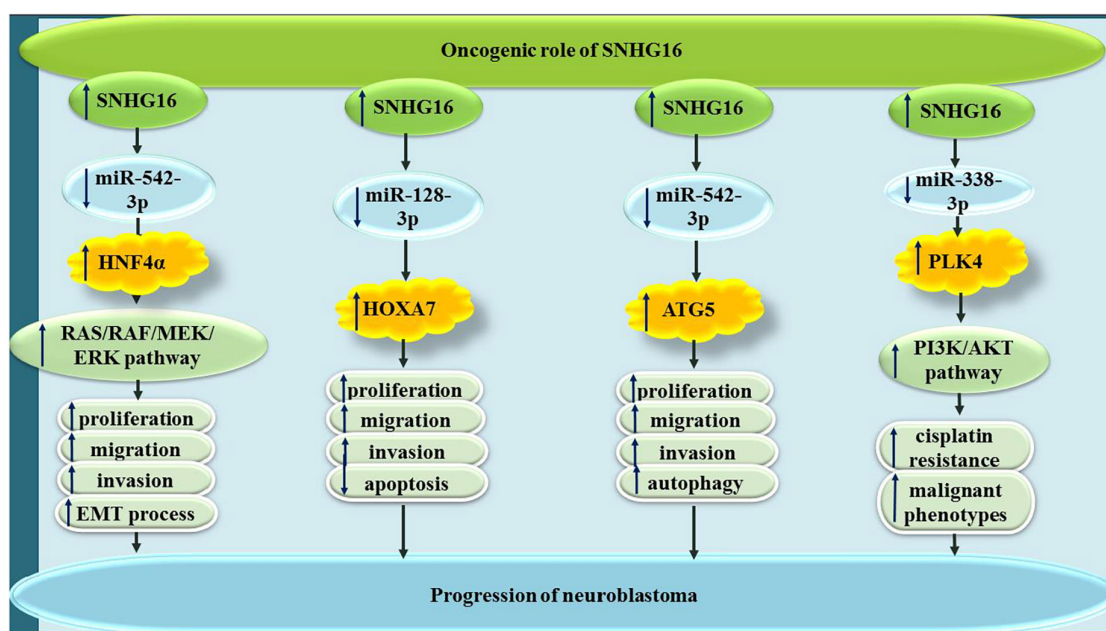


FIGURE 7 | In neuroblastoma, SNHG16 has been revealed to sponge miR-542-3p, miR-128-3p, and miR-338-3p.

thus promoting malignant behaviors of cells (Tao et al., 2020). Moreover, through sponging miR-216-5p, SNHG16 can increase expression of ZEB1, therefore increasing both cell proliferation and EMT process (Zhu H. et al., 2018). Finally, through sponging miR-128, it affects activity Wnt/β-catenin pathway (Wu et al., 2020). **Figure 6** summarizes the role of SNHG16 in colorectal and cervical cancers.

In neuroblastoma cells, SNHG16 has been revealed to sequester miR-542-3p (Deng et al., 2020), miR-128-3p (Bao et al., 2020) and miR-338-3p (Xu Z. et al., 2020), thus increasing expressions of HNF4α, HOXA7, and PLK4, respectively (**Figure 7**).

In other types of cancers, including retinoblastoma, oral squamous cell carcinoma, nasopharyngeal carcinoma, SNHG16

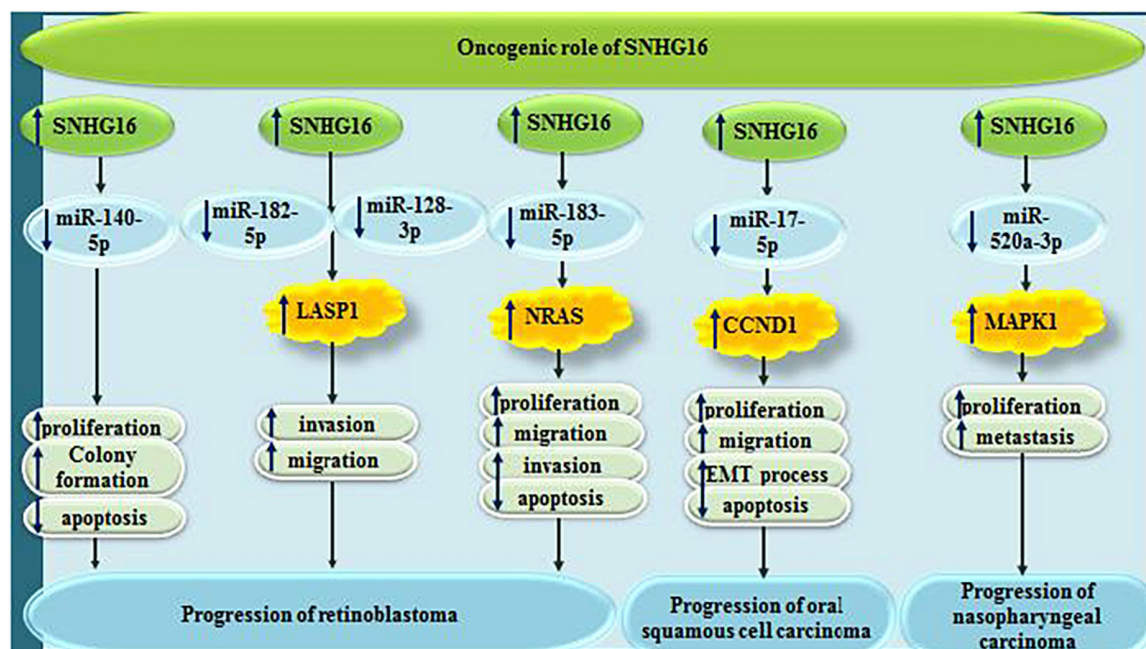


FIGURE 8 | Oncogenic roles of SNHG16 in retinoblastoma, oral squamous cell carcinoma and nasopharyngeal carcinoma.

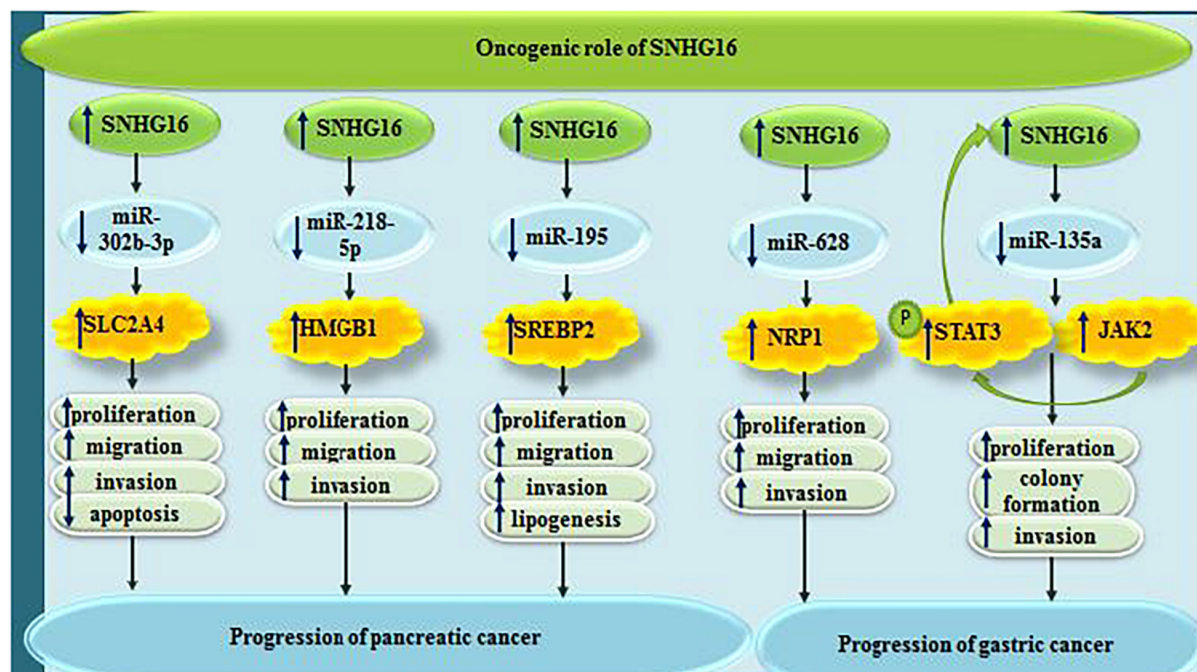


FIGURE 9 | Oncogenic roles of SNHG16 in pancreatic and gastric cancers.

sequesters a number of miRNAs, namely miR-140-5p, miR-182-5p, miR-128-3p, miR-183-5p, miR-17-5p, and miR-520a-3p (Figure 8).

In pancreatic cancer, SNHG16 acts in favor of tumor progression through sponging miR-302b-3p and subsequently

increasing expression of SLC2A4 (Xu et al., 2021). Moreover, it can contribute in this process through sponging miR-218-5p (Liu S. et al., 2019). Finally, SNHG16-mediated enhancement of lipogenesis through affecting expression of SREBP2 facilitates progression of pancreatic cancer (Yu et al., 2019b).

TABLE 1 | Outline of researches which measured expression of SNHG16 in cell lines (Δ , knock-down or deletion; 5-FU, 5-fluorouracil; VM, vasculogenic mimicry).

Tumor type	Interactions	Cell line	Function	References
Non-small cell lung cancer (NSCLC)	miR-520a-3p, EphA2	16HBE, A549, NCI-H292, NCI-H460, NCI-H1703	Δ SNHG16: \downarrow proliferation, \downarrow migration, \downarrow invasion, \uparrow apoptosis	Yu et al., 2020
	miR-4500, USP21, YY1	A549, H1299, NCI-H460, and NCI-H520	Δ USP21: \downarrow proliferation, \downarrow migration, \downarrow invasion	Xu P. et al., 2020
	miR-146a, MUC5AC	A549, NCI-H292, NCI-H460, NCI-H1703, 16HBE	Δ SNHG16: \downarrow proliferation, \downarrow migration, \downarrow invasion \uparrow SNHG16: \uparrow proliferation, \uparrow migration, \uparrow invasion	Han et al., 2019
Breast cancer	miR-16-5p, SMAD5, TGF- β 1/SMAD5 pathway, CD73	MCF-10A, MCF-7, T-47D, MDA-MB-231, HEK293T	–	Ni et al., 2020
	miR-98, E2F5	MDA-MB-231, MCF-7, MDA-MB468 and HEK293T	Δ SNHG16: \downarrow migration, did not affect proliferation \uparrow SNHG16: \uparrow migration, did not affect proliferation	Cai et al., 2017
Prostate carcinoma	let-7a-5p, RRM2	MCF-7	Δ SNHG16: \downarrow proliferation	Zhong et al., 2019
	GLUT1	22Rv1, HPrEC	Δ SNHG16: \downarrow proliferation, \downarrow glucose uptake	Shao et al., 2020
Hepatocellular carcinoma (HCC)	hsa-miR-93	Hep3B, HuH7, SNU398, SNU423, SNU429, Hep3G2, SK-HEP-1, and PLC/PRF/5	\uparrow SNHG16: \downarrow proliferation, \downarrow 5-FU chemoresistance	Xu et al., 2018
	miR-17-5p, p62, mTOR pathway, NF- κ B pathway	Huh-7 and HepG2	Δ SNHG16: \downarrow proliferation, \downarrow migration, \downarrow invasion \uparrow SNHG16: \uparrow proliferation, \uparrow migration, \uparrow invasion, \uparrow cell cycle progression, \downarrow apoptosis	Zhong et al., 2020
Hepatocellular carcinoma (HCC)	miR-186	Hep-3B, Huh7, Sk-hep-1, SMMC-7721, PLC, HL-7702	Δ SNHG16: \downarrow proliferation, \downarrow migration, \downarrow invasion	Chen et al., 2019
	miR-4500, STAT3	SMMC-7721, LO2, MHCC-97H, HepG2	Δ SNHG16: \downarrow proliferation, \downarrow migration, \downarrow invasion, \uparrow apoptosis	Lin et al., 2019
	miR-302a-3p, FGF19	Huh7, HepG2, SMMC7721, SK-Hep1 and Hep 3B, LO2	Δ SNHG16: \downarrow proliferation	Li W. et al., 2019
	miR-605-3p, NF- κ B pathway	HCCLM3, MHCC97L, MHCC-97H, LO2, Hep3B and HepG2	Δ SNHG16: \downarrow metastasis, \downarrow EMT process	Hu et al., 2020
	miR-140-5p	HepG2, SK-hep1, Huh7, and HCCLM3, LO2, HepG2/SOR	Δ SNHG16: \downarrow sorafenib resistance	Ye et al., 2019
	miR-195	HepG2, SMMC7721, Hep3B, Bel7402, Huh7, LO2	Δ SNHG16: \downarrow proliferation, \downarrow invasion	Xie et al., 2019
	–	HL-7702, SK-Hep-1, Huh7, Hep3B, HepG2	Δ SNHG16: \downarrow proliferation, \downarrow migration, \downarrow invasion, \downarrow sorafenib resistance	Guo et al., 2019
	let-7b-5p, CDC25B, HMGA2	MHCC97H, HuH7, SMMC7721, Hep3B, HepG2, LO2, HEK293	Δ SNHG16: \uparrow G2/M cell cycle arrest, \downarrow cisplatin resistance, \downarrow metastasis, \downarrow EMT process	Li S. et al., 2020
	miR-98-5p	U2OS, Saos-2, HOS, MG-63, hFOB 1.19	Δ SNHG16: \downarrow proliferation, \downarrow migration, \downarrow invasion, \uparrow cell cycle arrest, \uparrow apoptosis	Liao et al., 2019
	miR-16, ATG4B	SAOS2, U2OS, OB3, 293T	Δ SNHG16: \downarrow proliferation, \downarrow migration, \downarrow invasion, \downarrow autophagy, \downarrow chemoresistance	Liu Y. et al., 2019
Osteosarcoma	miR-340	hFOB1.19, U2OS, SaOS2	Δ SNHG16: \downarrow viability, \downarrow invasion, \uparrow apoptosis, \uparrow caspase 3/7 activity	Su et al., 2019
	miR-1301, BCL9	U2OS, MG-63	Δ SNHG16: \downarrow proliferation, \downarrow migration, \downarrow invasion	Wang et al., 2019a
	miR-205, ZEB1	MG-63, U2OS, SAOS2, HOS, OB3	Δ SNHG16: \downarrow proliferation	Zhu C. et al., 2018
	miR-488, ITGA6	U2OS, HOS	Δ SNHG16: \downarrow migration, \downarrow invasion, \downarrow EMT process	Bu et al., 2021
	miR-1285-3p, cleaved-caspase-3, Bax, pro-caspase-3, Bcl-2	U2OS, MNNG/HOS, 143b, SJSA, MG63, 293, hFOB 1.19	Δ SNHG16: \downarrow proliferation, \downarrow migration, \downarrow invasion, \uparrow cell cycle arrest, \uparrow apoptosis	Xiao et al., 2021
	miR-146a-5p, NOVA1	hFOB1.19, MG63, U2OS, 143B, MNNG/HOS	\uparrow SNHG16: \uparrow proliferation, \uparrow migration	Zheng et al., 2019
	miR-124-3p, MCP-1	HEK293T, FHC, SW480, HCT116, DLD-1, LOVO	Δ SNHG16: \downarrow proliferation, \downarrow migration, \downarrow invasion, \downarrow EMT process	Chen et al., 2020

(Continued)

TABLE 1 | (Continued)

Tumor type	Interactions	Cell line	Function	References
Cervical cancer	miR-200a-3p	CaCO-2, SW480, HCT116, LoVo, CCC-HIE-2	Δ SNHG16: ↓ proliferation, ↓ migration, ↓ invasion	Li Y. et al., 2019
	Wnt pathway, c-Myc, AGO, HuR, genes involved in lipid metabolism	HCT116, SW480, DLD1, 293T, K562, GM12878	Δ SNHG16: ↓ migration, ↑ apoptosis	Christensen et al., 2016
	miR-132-3p, USP22	SW480, SW620, CD841 CON	Δ SNHG16: ↓ proliferation, ↓ migration, ↓ invasion, ↑ apoptosis	He et al., 2020
	miR-302a-3p, AKT	HCT116, CaCO-2	Δ SNHG16: ↓ proliferation, ↑ SNHG16: ↑ proliferation	Ke et al., 2019
	PARP9, SPI1	SiHa, CaSki, C33A, ME180, HeLa, HcerEpic	Δ SNHG16: ↓ proliferation, ↓ invasion	Tao et al., 2020
	miR-216-5p, ZEB1	HeLa, CaSki, SiHa, C33A, H8	Δ SNHG16: ↓ proliferation, ↓ migration	Zhu H. et al., 2018
Neuroblastoma (NB)	miR-128, GSPT1, WNT3A, WNT pathway	Endl/E6E7, HeLa, C33A	Δ SNHG16: ↓ proliferation, ↓ EMT process	
	–	SH-SY5Y	Δ SNHG16: ↓ proliferation, ↓ migration, ↑ G0/G1 phase arrest, ↑ apoptosis	Yu et al., 2019a
	miR-542-3p, HNF4α, RAS/RAF/MEK/ERK signaling pathway	SKNBE-2, SK-N-SH, HEK293, LAN-5	Δ SNHG16: ↓ proliferation, ↓ migration, ↓ invasion, ↓ EMT process	Deng et al., 2020
Retinoblastoma (RB)	miR-128-3p, HOXA7	SK-N-SH, IMR-32, SK-N-AS, SK-NDZ, HUVEC	Δ SNHG16: ↓ proliferation, ↓ migration, ↓ invasion, ↑ apoptosis	Bao et al., 2020
	miR-542-3p, ATG5	LAN1, SK-N-SH and IMR-32, HUVEC	Δ SNHG16: ↓ proliferation, ↓ migration, ↓ invasion, ↓ autophagy	Wen et al., 2020
	miR-338-3p, PLK4, PI3K/AKT pathway	SK-N-AS, SK-N-SH, SK-N-AS-R and SK-N-SH-R	Δ SNHG16: ↓ cisplatin resistance, ↓ malignant phenotypes	Xu Z. et al., 2020
	miR-140-5p	ARPE-19, WERI Rb1, SO-RB-50, Y79, SO-Rb50	Δ SNHG16: ↓ proliferation, ↓ colony formation, ↑ apoptosis	Xu et al., 2019
	miR-182-5p, miR-128-3p, LASP1	WERI-RB1, SO-RB50, Y79, ARPE-19	Δ SNHG16: ↓ migration, ↓ invasion	Yang L. et al., 2019
	miR-183-5p, NRAS	ARPE-19 and human RB cell lines Y-79, WERI-Rb-1, 67BR and SO-Rb50	Δ SNHG16: ↓ proliferation, ↓ migration, ↓ invasion, ↑ apoptosis	Sun et al., 2019
Oral squamous cell carcinoma (OSCC)	c-Myc, E-cadherin, N-cadherin, Snail, MMP-2, MMP-9, PCNA	SCC-25, CAL-27, NHOK, Tca8113, TSCCA	Δ SNHG16: ↓ proliferation, ↓ migration, ↓ invasion, ↓ EMT process, ↑ apoptosis	Li S. et al., 2019
Pancreatic cancer (PC)	miR-17-5p, CCND1, N-cadherin, Vimentin	NOK, CAL27, TCA8113, OEC-M1, TW2.6	Δ SNHG16: ↓ proliferation, ↑ apoptosis ↑ SNHG16: ↑ proliferation, ↑ migration, ↑ EMT process	Wang et al., 2021
	miR-302b-3p, SLC2A4	HPY-Y5, BxPC3, Panc-1, MIA Paca-2, SW1990	Δ SNHG16: ↓ proliferation, ↓ migration, ↓ invasion, ↑ apoptosis	Xu et al., 2021
	miR-218-5p, HMGB1	BxPC-3, SW1990, PANC-1, AsPC1, HPDE6-C7	Δ SNHG16: ↓ proliferation, ↓ colony formation, ↓ migration, ↓ invasion	Liu S. et al., 2019
Nasopharyngeal carcinoma (NPC)	miR-195, SREBP2	HPDE6-C7, PANC-1, AsPC-1, BxPC-3, SW1990, HEK-293	Δ SNHG16: ↓ proliferation, ↓ migration, ↓ invasion, ↓ lipogenesis	Yu et al., 2019b
	miR-520a-3p, MAPK1	SUNE1, 5–8F, C666-1, NP69	Δ SNHG16: ↓ proliferation, ↓ metastasis	Wu et al., 2021
Gastric cancer	miR-628, NRP1	BGC-823, SGC-7901, MKN-45, AGS, GES-1	Δ SNHG16: ↓ proliferation, ↓ migration, ↓ invasion	Pang et al., 2019
Papillary thyroid cancer (PTC)	miR-135a, JAK2/STAT3 pathway	BGC823, MGC803, MKN45, SGC7901, GES-1	Δ SNHG16: ↓ proliferation, ↓ colony formation, ↓ invasion	Wang et al., 2019b
	miR-497, BDNF, YAP1	IHH-4, TPC-1, HTH83, Nthy-ori 3-1	Δ SNHG16: ↓ proliferation, ↓ migration, ↓ invasion, ↑ apoptosis	Wen et al., 2019
Bladder cancer (BC)	p21	T-24, BIU87, 5637, SV-HUC-1	Δ SNHG16: ↓ proliferation, ↓ colony formation, ↑, G1 phase arrest, ↑ apoptosis	Cao et al., 2018
Ovarian cancer	miR-17-5p, TIMP3	5637, J82, RT4, T24	Δ SNHG16: ↓ proliferation, ↓ viability, ↓ EMT process, ↑ apoptosis	Peng and Li, 2019
	P-AKT, MMP9	SKOV-3, ES2, HO8910, OMC685, OSE-29	Δ SNHG16: ↓ proliferation, ↓ migration, ↓ invasion	Yang et al., 2018

(Continued)

TABLE 1 | (Continued)

Tumor type	Interactions	Cell line	Function	References
Acute myeloid leukemia (AML)	miR183-5p, FOXO1	THP1, HL60, Kasumi 3, AML139, PBMCs	Δ SNHG16: ↓ proliferation, ↑ G0/G1-phase arrest, ↑ apoptosis	Yang R. et al., 2020
	CELF2, PTEN, PI3K/AKT signaling	HS-5, HL60, BDCM, AML-193, Kasumi-6	Δ SNHG16: ↓ proliferation, ↓ migration ↑ SNHG16: ↑ proliferation, ↑ migration	Shi et al., 2021
Leukemia	miR-193a-5p, CDK8	Kasumi-1, KG-1, MV-4-11, THP-1, K-562, HL-60, RPMI-1788	Δ SNHG16: ↓ proliferation, ↓ viability, ↑ apoptosis	Piao and Zhang, 2020
Acute lymphoblastic leukemia	miR-124-3p,	MOLT3, MOLT4, SUP-B15, CCRF-CEM, RS4;11, TALL104, CEM/C1, CEM/C2, Loucy, BMMC, PBMC	↑ SNHG16: ↑ proliferation, ↑ migration	Yang T. et al., 2019
Large B-cell lymphoma	miR-497-5p, PIM1	OCI-LY7, OCI-LY3	Δ SNHG16: ↓ proliferation, ↑ G0/G1 phase arrest, ↑ apoptosis	Zhu et al., 2019
Multiple myeloma	miR-342-3p	RPMI-8226, NCI-H929	Δ SNHG16: ↓ proliferation	Yang X. et al., 2020
Glioma	miR-373, EGFR, PI3K/AKT pathway	NHAs, U251, LN229, U87	Δ SNHG16: ↓ proliferation, ↓ migration, ↓ invasion	Zhou et al., 2020
Glioma	miR-490, PCBP2	T98G, U251, NHA	Δ SNHG16: ↓ proliferation, ↓ migration, ↓ invasion	Kong et al., 2020
	miR-4518, PRMT5, Bcl-2, PI3K/Akt pathway,	NHAs, U251, H4, SW1783, LN229	Δ SNHG16: ↓ proliferation, ↑ apoptosis	Lu et al., 2018
	miR-212-3p, USF1, ALDH1A1	HA, U87, U251, HEK293T	Δ SNHG16: ↓ proliferation, ↓ migration, ↓ invasion, ↓ VM	Wang et al., 2019c
	miR-424-5p,	T98G, LN229	↑ SNHG16: ↓ effect of Ropivacaine, ↑ proliferation, ↑ migration, ↑ invasion, ↓ apoptosis	Liu et al., 2020
	TLR7, NFκB/c-Myc signaling, MyD88	SHG44, U251	Δ SNHG16: ↓ proliferation, ↓ migration, ↓ invasion ↑ SNHG16: ↑ proliferation, ↑ migration, ↑ invasion	Zhang et al., 2021
Endometrial carcinoma	miR-490-3p, TFAP2A, HK2	HEC-1B, HEC-1A, RL95-2, AN3CA, EMC	Δ SNHG16: ↓ proliferation, ↓ glycolysis	Zhang G. et al., 2019
Laryngeal squamous cell carcinoma	miR-877-5p, FOXP4	16HBE, AMC-HN-8	Δ SNHG16: ↓ proliferation, ↓ migration, ↓ invasion	Wang et al., 2020
Esophageal cancer	Wnt/β-catenin pathway	TE-13, TE-1, EC-1, Eca-109, HEEC	Δ SNHG16: ↓ proliferation, ↓ invasion, ↑ apoptosis	Han et al., 2018
	miR-140-5p, ZEB1	eca109, EC9706, TE1, Kyse-30, Kyse-70, HEEC	Δ SNHG16: ↓ proliferation, ↓ migration, ↓ EMT process, ↑ apoptosis	Zhang et al., 2018
Hemangioma (HA)	miR-520d-3p, STAT3	HemECs	Δ SNHG16: ↓ proliferation, ↓ migration, ↓ invasion, ↓ vasoformation, ↑ apoptosis	Zhao et al., 2018

Small nucleolar RNA host gene 6 participates in the progression of gastric cancer via sequestering miR-628-3p and consequently decreasing expression of NRP1 (Pang et al., 2019). In this type of cancer, SNHG16 also sponges miR-135a and activates JAK2/STAT3 signaling (Wang et al., 2019b; **Figure 9**).

Table 1 summarizes the results of *in vitro* studies regarding the role of SNHG16 in carcinogenesis.

ANIMAL STUDIES

Animal studies have consistently shown that SNHG16 silencing decreases malignant feature of the grafted cancer cells (**Table 2**). The only exception has been reported in HCC where SNHG16 over-expression has significantly suppressed the *in vivo* expansion of grafted HuH7 cells (Xu et al., 2018). Another study in HCC xenograft model has shown that SNHG16 silencing enhances response of HepG2/SOR cells to cytotoxic effect of sorafenib and attenuates tumor growth (Ye et al., 2019). In

xenograft models of retinoblastoma, up-regulation SNHG16 (Xu et al., 2019) or its downstream target NRAS (Sun et al., 2019) can increase tumor growth. Finally, in gastric cancer where SNHG16 sponges miR-628, *in vivo* studies have shown that up-regulation of miR-628 can decrease tumor expansion (Pang et al., 2019).

CLINICAL STUDIES

Except for a single study which demonstrated down-regulation of SNHG16 in HCC samples versus nearby non-malignant hepatic tissues (Xu et al., 2018), other studies have indicated up-regulation of SNHG16 in malignant tissues of different origins compared with non-neoplastic samples (**Supplementary Table 1**). Consistent with these findings, up-regulation of SNHG16 has been revealed to predict poor survival of patients. Moreover, its expression has been related with greater chance of

TABLE 2 | Outline of studies which judged function of SNHG16 in animal models (Δ , knock-down or deletion; VM, vasculogenic mimicry).

Tumor Type	Animal models	Results	References
Non-small cell lung cancer (NSCLC)	male Athymic BALB/c mice	Δ SNHG16: \downarrow tumor volume, \downarrow tumor weight, \downarrow tumor growth	Yu et al., 2020
	male Athymic BALB/c mice	Δ SNHG16: \downarrow tumor volume, \downarrow tumor weight	Han et al., 2019
Hepatocellular carcinoma (HCC)	athymic nude mice	\uparrow SNHG16: \downarrow tumorigenicity	Xu et al., 2018
	male athymic nude mice	Δ SNHG16: \downarrow tumor size, \downarrow tumor weight \uparrow SNHG16: \uparrow tumor size, \uparrow tumor weight	Zhong et al., 2020
	female BALB/c nude mice	Δ SNHG16: \downarrow tumor volume, \downarrow tumor weight, \downarrow tumor growth \uparrow SNHG16: \uparrow tumor volume, \downarrow tumor growth	Chen et al., 2019
	nude mice	Δ SNHG16: \downarrow number and size of metastatic colonies, \downarrow tumor weight, \downarrow tumor growth	Hu et al., 2020
	Male Athymic nu/nu nude mice	Δ SNHG16: \downarrow tumor size, \downarrow tumor weight, \downarrow tumor growth, \downarrow sorafenib resistance	Ye et al., 2019
	male BALB/c nude mice	Δ SNHG16: \downarrow tumor weight, \downarrow tumor growth	Xie et al., 2019
	BALB/c nude mice	Δ SNHG16: \downarrow tumor volume, \downarrow tumor weight, \downarrow metastatic	Li S. et al., 2020
	male BALB/c mice	Δ SNHG16: \downarrow tumor volume, \downarrow EMT process, \downarrow tumor growth, \downarrow metastasis	Bu et al., 2021
Osteosarcoma	male BALB/c nude mice	Δ SNHG16: \downarrow tumor volume, \downarrow tumor weight	Xiao et al., 2021
	nude mice	Δ SNHG16: \downarrow tumor size, \downarrow tumor weight, \downarrow metastasis	Chen et al., 2020
Colorectal cancer (CRC)	male BALB/c nude mice	\uparrow SNHG16: \uparrow tumor size	Li Y. et al., 2019
	male BALB/c-nude mice	Δ SNHG16: \downarrow tumor weight, \downarrow metastasis, \downarrow tumor growth	He et al., 2020
Cervical cancer	specific-pathogen-free BALB/c-nu/nu nude mice	Δ SNHG16: \downarrow tumor growth	Tao et al., 2020
Neuroblastoma (NB)	BALB/c nude mice	Δ SNHG16: \downarrow tumor volume, \downarrow tumor weight	Deng et al., 2020; Bao et al., 2020, Wen et al., 2020
Retinoblastoma (RB)	athymic BALB/c mice	Δ SNHG16: \downarrow tumor volume, \downarrow tumor weight	Xu Z. et al., 2020
	male BALB/c nude mice	Δ SNHG16: \downarrow tumor volume, \downarrow tumor weight	Xu et al., 2019
	female BALB/c nude mice	Δ NRAS: \downarrow tumor volume, \downarrow tumor weight	Sun et al., 2019
Oral squamous cell carcinoma	BALB/c-nude mice	Δ SNHG16: \downarrow tumor volume, \downarrow tumor weight	Li S. et al., 2019
	male athymic BALB/c nude mice	Δ SNHG16: \downarrow tumor growth \uparrow SNHG16: \uparrow tumor growth	Wang et al., 2021
Pancreatic cancer	male BALB/c nude mice	Δ SNHG16: \downarrow tumor volume, \downarrow tumor growth	Liu S. et al., 2019
Nasopharyngeal carcinoma (NPC)	male BALB/C nude mice	Δ SNHG16: \downarrow tumor volume, \downarrow tumor weight	Wu et al., 2021
Gastric cancer	female BALB/c nude mice	\uparrow miR-628: \downarrow tumor volume, \downarrow tumor weight	Pang et al., 2019
Acute lymphoblastic leukemia (ALL)	null mice	Δ SNHG16: \downarrow tumor volume, \downarrow ALL tumor transplants	Yang T. et al., 2019
Large B-cell lymphoma (DLBCL)	male NOD/SCID mice	Δ SNHG16: \downarrow tumor growth	Zhu et al., 2019
Glioma	athymic BALB/c nude mice	Δ SNHG16: \downarrow tumor volume, \downarrow number of VMs, \uparrow survival period	Wang et al., 2019c
Endometrial carcinoma	male nude BALB/c mice	Δ SNHG16: \downarrow tumor volume, \downarrow tumor growth	Zhang G. et al., 2019
Laryngeal squamous cell carcinoma (LSCC)	female nude mice	Δ SNHG16: \downarrow tumor volume, \downarrow tumor weight	Wang et al., 2020
Esophageal cancer	female BALB/c athymic nude mice	Δ SNHG16: \downarrow tumor growth	Han et al., 2018

distant metastasis, lymph node involvement and low differentiation of tumor cells.

DISCUSSION

Small nucleolar RNA host gene 6 has been regarded as an oncogenic lncRNA in almost all tissues. This lncRNA affect carcinogenesis through multifaceted mechanisms including mechanisms related to both tumor cells and their niche. In fact, it can both affect cellular functions and processes, particularly those related with proliferation, survival and apoptosis as well as microenvironmental aspects of cancer progression.

More than 20 miRNAs have been found to interact with SNHG16. The sponging effects of SNHG16 on miRNAs have been well studied. miR-520a-3p, miR-4500, miR-146a miR-16-5p, miR-98, let-7a-5p, hsa-miR-93, miR-17-5p, miR-186, miR-302a-3p, miR-605-3p, miR-140-5p, miR-195, let-7b-5p, miR-16, miR-340, miR-1301, miR-205, miR-488, miR-1285-3p, miR-146a-5p, and miR-124-3p are examples of miRNAs sponged by this lncRNA in different types of cancers. Verification of interaction between this lncRNA and a number of miRNAs such as miR-98 in different tissues raises the possibility of independence of such interactions from the tissue type. TGF- β 1/SMAD5, mTOR, NF- κ B, RAS/RAF/MEK/ERK, PI3K/AKT, and Wnt/ β -catenin pathways are among cancer-related pathways

being affected by this lncRNA. Moreover, SNHG16 has been shown to affect expression of a number of EMT-associated transcription factors and enhance this process. SNHG16 has also been found to affect response of cancer cells to 5-FU and sorafenib.

Based on the results of functional studies that confirmed the ability of siRNA-mediated SNHG16 silencing in reduction of cancer cell proliferation and invasiveness, this strategy can be proposed as a therapeutic strategy for cancer. *In vivo* studies have also confirmed applicability of these methods; however no clinical study has applied these methods yet. Antisense oligonucleotides as a promising strategy for suppression of expression of SNHG16 should be appraised in clinical settings considering the bioavailability and safety issues.

Although over-expression of SNHG16 has been verified in tissue samples of different types of tumors, application of this lncRNA as a circulatory marker for early detection of cancer has not been assessed. Since clinical studies have revealed correlation

between expression amounts of SNHG16 and malignant features, one can suppose that SNHG16 can be used as both diagnostic and prognostic marker. However, this speculation should be verified in future.

AUTHOR CONTRIBUTIONS

MT and SG-F wrote the draft and revised it. TK and SS collected the data and designed the tables and figures. All authors read and approved submitted version.

SUPPLEMENTARY MATERIAL

The Supplementary Material for this article can be found online at: <https://www.frontiersin.org/articles/10.3389/fcell.2021.741684/full#supplementary-material>

REFERENCES

- Bao, J., Zhang, S., Meng, Q., and Qin, T. (2020). SNHG16 silencing inhibits neuroblastoma progression by downregulating HOXA7 via sponging miR-128-3p. *Neurochem. Res.* 45, 825–836. doi: 10.1007/s11064-020-02955-x
- Bu, J., Guo, R., Xu, X.-Z., Luo, Y., and Liu, J.-F. (2021). LncRNA SNHG16 promotes epithelial-mesenchymal transition by upregulating ITGA6 through miR-488 inhibition in osteosarcoma. *J. Bone Oncol.* 27:100348. doi: 10.1016/j.jbo.2021.100348
- Cai, C., Huo, Q., Wang, X., Chen, B., and Yang, Q. (2017). SNHG16 contributes to breast cancer cell migration by competitively binding miR-98 with E2F5. *Biochem. Biophys. Res. Commun.* 485, 272–278. doi: 10.1016/j.bbrc.2017.02.094
- Cao, X., Xu, J., and Yue, D. (2018). LncRNA-SNHG16 predicts poor prognosis and promotes tumor proliferation through epigenetically silencing p21 in bladder cancer. *Cancer Gene Ther.* 25, 10–17. doi: 10.1038/s41417-017-0006-x
- Chen, H., Li, M., and Huang, P. (2019). LncRNA SNHG16 promotes hepatocellular carcinoma proliferation, migration and invasion by regulating miR-186 expression. *J. Cancer* 10:3571. doi: 10.7150/jca.28428
- Chen, Z.-Y., Wang, X.-Y., Yang, Y.-M., Wu, M.-H., Yang, L., Jiang, D.-T., et al. (2020). LncRNA SNHG16 promotes colorectal cancer cell proliferation, migration, and epithelial-mesenchymal transition through miR-124-3p/MCP-1. *Gene Ther.* 1–13. doi: 10.1038/s41434-020-0176-2 [Epub ahead of print].
- Christensen, L. L., True, K., Hamilton, M. P., Nielsen, M. M., Damas, N. D., Damgaard, C. K., et al. (2016). SNHG16 is regulated by the Wnt pathway in colorectal cancer and affects genes involved in lipid metabolism. *Mol. Oncol.* 10, 1266–1282. doi: 10.1016/j.molonc.2016.06.003
- Deng, D., Yang, S., and Wang, X. (2020). Long non-coding RNA SNHG16 regulates cell behaviors through miR-542-3p/HNF4α axis via RAS/RAF/MEK/ERK signaling pathway in pediatric neuroblastoma cells. *Biosci. Rep.* 40:BSR20200723.
- Guo, Z., Zhang, J., Fan, L., Liu, J., Yu, H., Li, X., et al. (2019). Long noncoding RNA (lncRNA) small nucleolar RNA host gene 16 (SNHG16) predicts poor prognosis and sorafenib resistance in hepatocellular carcinoma. *Med. Sci. Monit.* 25:2079. doi: 10.12659/msm.915541
- Han, G., Lu, K., Wang, P., Ye, J., Ye, Y., and Huang, J. (2018). LncRNA SNHG16 predicts poor prognosis in ESCC and promotes cell proliferation and invasion by regulating Wnt/beta-catenin signaling pathway. *Eur. Rev. Med. Pharmacol. Sci.* 22, 3795–3803.
- Han, W., Du, X., Liu, M., Wang, J., Sun, L., and Li, Y. (2019). Increased expression of long non-coding RNA SNHG16 correlates with tumor progression and poor prognosis in non-small cell lung cancer. *Int. J. Biol. Macromol.* 121, 270–278. doi: 10.1016/j.ijbiomac.2018.10.004
- He, X., Ma, J., Zhang, M., Cui, J., and Yang, H. (2020). Long non-coding RNA SNHG16 activates USP22 expression to promote colorectal cancer progression by sponging miR-132-3p. *Onco Targets Ther.* 13:4283. doi: 10.2147/ott.s244778
- Hu, Y. L., Feng, Y., Chen, Y. Y., Liu, J. Z., Su, Y., Li, P., et al. (2020). SNHG16/miR-605-3p/TRAF6/NF-κB feedback loop regulates hepatocellular carcinoma metastasis. *J. Cell. Mol. Med.* 24, 7637–7651. doi: 10.1111/jcmm.15399
- Ke, D., Wang, Q., Ke, S., Zou, L., and Wang, Q. (2019). Long-non coding RNA SNHG16 supports colon cancer cell growth by modulating miR-302a-3p/AKT axis. *Pathol. Oncol. Res.* 26, 1605–1613. doi: 10.1007/s12253-019-00743-9
- Kong, F., Yan, Y., Deng, J., Zhu, Y., Li, Y., Li, H., et al. (2020). LncRNA SNHG16 promotes proliferation, migration, and invasion of glioma cells through regulating the miR-490/PCBP2 Axis. *Cancer Biother. Radiopharm.* doi: 10.1089/cbr.2019.3535 [Epub ahead of print].
- Li, S., Peng, F., Ning, Y., Jiang, P., Peng, J., Ding, X., et al. (2020). SNHG16 as the miRNA let-7b-5p sponge facilitates the G2/M and epithelial-mesenchymal transition by regulating CDC25B and HMGA2 expression in hepatocellular carcinoma. *J. Cell. Biochem.* 121, 2543–2558. doi: 10.1002/jcb.29477
- Li, S., Zhang, S., and Chen, J. (2019). c-Myc induced upregulation of long non-coding RNA SNHG16 enhances progression and carcinogenesis in oral squamous cell carcinoma. *Cancer Gene Ther.* 26, 400–410. doi: 10.1038/s41417-018-0072-8
- Li, W., Xu, W., Song, J. S., Wu, T., and Wang, W. X. (2019). LncRNA SNHG16 promotes cell proliferation through miR-302a-3p/FGF19 axis in hepatocellular carcinoma. *Neoplasia* 66, 397–404. doi: 10.4149/neo_2018_180720n504
- Li, Y., Lu, Y., and Chen, Y. (2019). Long non-coding RNA SNHG16 affects cell proliferation and predicts a poor prognosis in patients with colorectal cancer via sponging miR-200a-3p. *Biosci. Rep.* 39:BSR20182498.
- Liao, S., Xing, S., and Ma, Y. (2019). LncRNA SNHG16 sponges miR-98-5p to regulate cellular processes in osteosarcoma. *Cancer Chemother. Pharmacol.* 83, 1065–1074. doi: 10.1007/s00280-019-03822-5
- Lin, Q., Zheng, H., Xu, J., Zhang, F., and Pan, H. (2019). LncRNA SNHG16 aggravates tumorigenesis and development of hepatocellular carcinoma by sponging miR-4500 and targeting STAT3. *J. Cell. Biochem.* 120, 11604–11615. doi: 10.1002/jcb.28440
- Liu, R., Wu, M., Xu, G., Ju, L., Xiao, J., Zhong, W., et al. (2020). Ropivacaine inhibits proliferation, migration, and invasion while inducing apoptosis of glioma cells by regulating the SNHG16/miR-424-5p axis. *Open Life Sci.* 15, 988–999. doi: 10.1515/biol-2020-0108
- Liu, S., Zhang, W., Liu, K., and Liu, Y. (2019). LncRNA SNHG16 promotes tumor growth of pancreatic cancer by targeting miR-218-5p. *Biomed. Pharmacother.* 114:108862. doi: 10.1016/j.biopha.2019.108862

- Liu, Y., Gu, S., Li, H., Wang, J., Wei, C., and Liu, Q. (2019). SNHG16 promotes osteosarcoma progression and enhances cisplatin resistance by sponging miR-16 to upregulate ATG4B expression. *Biochem. Biophys. Res. Commun.* 518, 127–133. doi: 10.1016/j.bbrc.2019.08.019
- Lu, Y.-F., Cai, X.-L., Li, Z.-Z., Lv, J., Xiang, Y.-A., Chen, J.-J., et al. (2018). LncRNA SNHG16 functions as an oncogene by sponging MiR-4518 and up-regulating PRMT5 expression in glioma. *Cell. Physiol. Biochem.* 45, 1975–1985. doi: 10.1159/000487974
- Ni, C., Fang, Q.-Q., Chen, W.-Z., Jiang, J.-X., Jiang, Z., Ye, J., et al. (2020). Breast cancer-derived exosomes transmit LncRNA SNHG16 to induce CD73+ $\gamma\delta$ 1 Treg cells. *Signal Transduct. Target. Ther.* 5:41.
- Pang, W., Zhai, M., Wang, Y., and Li, Z. (2019). Long noncoding RNA SNHG16 silencing inhibits the aggressiveness of gastric cancer via upregulation of microRNA-628-3p and consequent decrease of NRP1. *Cancer Manag. Res.* 11:7263. doi: 10.2147/cmar.s211856
- Peng, H., and Li, H. (2019). The encouraging role of long noncoding RNA small nuclear RNA host gene 16 in epithelial-mesenchymal transition of bladder cancer via directly acting on miR-17-5p/metalloproteinases 3 axis. *Mol. Carcinog.* 58, 1465–1480. doi: 10.1002/mc.23028
- Piao, M., and Zhang, L. (2020). Knockdown of SNHG16 suppresses the proliferation and induces the apoptosis of leukemia cells via miR-193a-5p/CDK8. *Int. J. Mol. Med.* 46, 1175–1185. doi: 10.3892/ijmm.2020.4671
- Shao, M., Yu, Z., and Zou, J. (2020). LncRNA-SNHG16 silencing inhibits prostate carcinoma cell growth, downregulate glut1 expression and reduce glucose uptake. *Cancer Manag. Res.* 12:1751. doi: 10.2147/cmar.s231370
- Shi, M., Yang, R., Lin, J., Wei, Q., Chen, L., Gong, W., et al. (2021). LncRNA-SNHG16 promotes proliferation and migration of acute myeloid leukemia cells via PTEN/PI3K/AKT axis through suppressing CELF2 protein. *J. Biosci.* 46:4.
- Su, P., Mu, S., and Wang, Z. (2019). Long noncoding RNA SNHG16 promotes osteosarcoma cells migration and invasion via sponging miRNA-340. *DNA Cell Biol.* 38, 170–175. doi: 10.1089/dna.2018.4424
- Sun, G., Su, G., Liu, F., and Han, W. N. R. A. S. (2019). Contributes to retinoblastoma progression through SNHG16/miR-183-5p/NRAS regulatory network. *OncoTargets Ther.* 12:10703. doi: 10.2147/ott.s232470
- Tao, L., Wang, X., and Zhou, Q. (2020). Long noncoding RNA SNHG16 promotes the tumorigenicity of cervical cancer cells by recruiting transcriptional factor SPI1 to upregulate PARP9. *Cell Biol. Int.* 44, 773–784. doi: 10.1002/cbin.11272
- Wang, Q., Han, J., Xu, P., Jian, X., Huang, X., and Liu, D. (2021). Silencing of LncRNA SNHG16 downregulates cyclin D1 (CCND1) to abrogate malignant phenotypes in oral squamous cell carcinoma (OSCC) through upregulating miR-17-5p. *Cancer Manag. Res.* 13:1831. doi: 10.2147/cmar.s298236
- Wang, X., Kan, J., Han, J., Zhang, W., Bai, L., and Wu, H. (2019b). LncRNA SNHG16 functions as an oncogene by sponging MiR-135a and promotes JAK2/STAT3 signal pathway in gastric cancer. *J. Cancer* 10:1013. doi: 10.7150/jca.29527
- Wang, X., Hu, K., Chao, Y., and Wang, L. (2019a). LncRNA SNHG16 promotes proliferation, migration and invasion of osteosarcoma cells by targeting miR-1301/BCL9 axis. *Biomed. Pharmacother.* 114:108798. doi: 10.1016/j.biopha.2019.108798
- Wang, D., Zheng, J., Liu, X., Xue, Y., Liu, L., Ma, J., et al. (2019c). Knockdown of USF1 inhibits the vasculogenic mimicry of glioma cells via stimulating SNHG16/miR-212-3p and linc00667/miR-429 axis. *Mol. Ther. Nucleic Acids* 14, 465–482. doi: 10.1016/j.omtn.2018.12.017
- Wang, X., Liu, L., Zhao, W., Li, Q., Wang, G., and Li, H. (2020). LncRNA SNHG16 promotes the progression of laryngeal squamous cell carcinoma by mediating miR-877-5p/FOXP4 Axis. *Onco Targets Ther.* 13:4569. doi: 10.2147/ott.s250752
- Wen, Q., Zhao, L., Wang, T., Lv, N., Cheng, X., Zhang, G., et al. (2019). LncRNA SNHG16 drives proliferation and invasion of papillary thyroid cancer through modulation of miR-497. *Onco Targets Ther.* 12, 699–708. doi: 10.2147/ott.s186923
- Wen, Y., Gong, X., Dong, Y., and Tang, C. (2020). Long non coding RNA SNHG16 facilitates proliferation, migration, invasion and autophagy of neuroblastoma cells via sponging miR-542-3p and upregulating ATG5 expression. *Onco Targets Ther.* 13:263. doi: 10.2147/ott.s226915
- Wu, Q., Zhao, Y., Shi, R., and Wang, T. (2021). LncRNA SNHG16 facilitates nasopharyngeal carcinoma progression by acting as ceRNA to sponge miR-520a-3p and upregulate MAPK1 expression. *Cancer Manag. Res.* 13:4103. doi: 10.2147/cmar.s305544
- Wu, W., Guo, L., Liang, Z., Liu, Y., and Yao, Z. (2020). Lnc-SNHG16/miR-128 axis modulates malignant phenotype through WNT/ β -catenin pathway in cervical cancer cells. *J. Cancer* 11:2201. doi: 10.7150/jca.40319
- Xiao, X., Jiang, G., Zhang, S., Hu, S., Fan, Y., Li, G., et al. (2021). LncRNA SNHG16 contributes to osteosarcoma progression by acting as a ceRNA of miR-1285-3p. *BMC Cancer* 21:355.
- Xie, X., Xu, X., Sun, C., and Yu, Z. (2019). Long intergenic noncoding RNA SNHG16 interacts with miR-195 to promote proliferation, invasion and tumorigenesis in hepatocellular carcinoma. *Exp. Cell Res.* 383:111501. doi: 10.1016/j.yexcr.2019.111501
- Xu, C., Hu, C., Wang, Y., and Liu, S. (2019). Long noncoding RNA SNHG16 promotes human retinoblastoma progression via sponging miR-140-5p. *Biomed. Pharmacother.* 117:109153. doi: 10.1016/j.biopha.2019.109153
- Xu, F., Zha, G., Wu, Y., Cai, W., and Ao, J. (2018). Overexpressing lncRNA SNHG16 inhibited HCC proliferation and chemoresistance by functionally sponging hsa-miR-93. *Onco Targets Ther.* 11:8855. doi: 10.2147/ott.s182005
- Xu, H., Miao, X., Li, X., Chen, H., Zhang, B., and Zhou, W. (2021). LncRNA SNHG16 contributes to tumor progression via the miR-302b-3p/SLC2A4 axis in pancreatic adenocarcinoma. *Cancer Cell Int.* 21:51.
- Xu, P., Xiao, H., Yang, Q., Hu, R., Jiang, L., Bi, R., et al. (2020). The USP21/YY1/SNHG16 axis contributes to tumor proliferation, migration, and invasion of non-small-cell lung cancer. *Exp. Mol. Med.* 52, 41–55. doi: 10.1038/s12276-019-0356-6
- Xu, Z., Sun, Y., Wang, D., Sun, H., and Liu, X. (2020). SNHG16 promotes tumorigenesis and cisplatin resistance by regulating miR-338-3p/PLK4 pathway in neuroblastoma cells. *Cancer Cell Int.* 20:236.
- Yang, L., Zhang, L., Lu, L., and Wang, Y. (2019). Long noncoding RNA SNHG16 sponges miR-182-5p and miR-128-3p to promote retinoblastoma cell migration and invasion by targeting LASP1. *Onco Targets Ther.* 12:8653. doi: 10.2147/ott.s212352
- Yang, R., Ma, D., Wu, Y., Zhang, Y., and Zhang, L. (2020). LncRNA SNHG16 regulates the progress of acute myeloid leukemia through miR183-5p–FOXO1 Axis. *Onco Targets Ther.* 13:12943. doi: 10.2147/ott.s258684
- Yang, T., Jin, X., Lan, J., and Wang, W. (2019). Long non-coding RNA SNHG16 has tumor suppressing effect in acute lymphoblastic leukemia by inverse interaction on hsa-miR-124-3p. *IUBMB Life* 71, 134–142. doi: 10.1002/iub.1947
- Yang, X., Huang, H., Wang, X., Liu, H., Liu, H., and Lin, Z. (2020). Knockdown of lncRNA SNHG16 suppresses multiple myeloma cell proliferation by sponging miR-342-3p. *Cancer Cell Int.* 20:38.
- Yang, X., Wang, G., and Luo, L. (2018). Long non-coding RNA SNHG16 promotes cell growth and metastasis in ovarian cancer. *Eur. Rev. Med. Pharmacol. Sci.* 22, 616–622.
- Ye, J., Zhang, R., Du, X., Chai, W., and Zhou, Q. (2019). Long noncoding RNA SNHG16 induces sorafenib resistance in hepatocellular carcinoma cells through sponging miR-140-5p. *Onco Targets Ther.* 12:415. doi: 10.2147/ott.s175176
- Yu, L., Chen, D., and Song, J. (2020). LncRNA SNHG16 promotes non-small cell lung cancer development through regulating EphA2 expression by sponging miR-520a-3p. *Thorac. Cancer* 11, 603–611. doi: 10.1111/1759-7714.13304
- Yu, Y., Dong, J.-T., He, B., Zou, Y.-F., Li, X.-S., Xi, C.-H., et al. (2019b). LncRNA SNHG16 induces the SREBP2 to promote lipogenesis and enhance the progression of pancreatic cancer. *Future Oncol.* 15, 3831–3844. doi: 10.2217/fon-2019-0321
- Yu, Y., Chen, F., Yang, Y., Jin, Y., Shi, J., Han, S., et al. (2019a). LncRNA SNHG16 is associated with proliferation and poor prognosis of pediatric neuroblastoma. *Int. J. Oncol.* 55, 93–102.
- Zhang, G., Ma, A., Jin, Y., Pan, G., and Wang, C. (2019). LncRNA SNHG16 induced by TFAP2A modulates glycolysis and proliferation of endometrial carcinoma through miR-490-3p/HK2 axis. *Am. J. Transl. Res.* 11:7137.
- Zhang, K., Chen, J., Song, H., and Chen, L. B. (2018). SNHG16/miR-140-5p axis promotes esophagus cancer cell proliferation, migration and EMT formation through regulating ZEB1. *Oncotarget* 9, 1028–1040. doi: 10.18632/oncotarget.23178
- Zhang, R., Li, P., Lv, H., Li, N., Ren, S., and Xu, W. (2021). Exosomal SNHG16 secreted by CSCs promotes glioma development via TLR7. *Stem Cell Res. Ther.* 12:349.
- Zhang, S., Du, L., Wang, L., Jiang, X., Zhan, Y., Li, J., et al. (2019). Evaluation of serum exosomal Lnc RNA-based biomarker panel for diagnosis and recurrence

- prediction of bladder cancer. *J. Cell. Mol. Med.* 23, 1396–1405. doi: 10.1111/jcmm.14042
- Zhao, W., Fu, H., Zhang, S., Sun, S., and Liu, Y. (2018). LncRNA SNHG16 drives proliferation, migration, and invasion of hemangioma endothelial cell through modulation of miR-520d-3p/STAT3 axis. *Cancer Med.* 7, 3311–3320. doi: 10.1002/cam4.1562
- Zheng, S., Ge, D., Tang, J., Yan, J., Qiu, J., Yin, Z., et al. (2019). LncSNHG16 promotes proliferation and migration of osteosarcoma cells by targeting microRNA-146a-5p. *Eur. Rev. Med. Pharmacol. Sci.* 23, 96–104.
- Zhong, G., Lou, W., Yao, M., Du, C., Wei, H., and Fu, P. (2019). Identification of novel mRNA-miRNA-lncRNA competing endogenous RNA network associated with prognosis of breast cancer. *Epigenomics* 11, 1501–1518. doi: 10.2217/epi-2019-0209
- Zhong, J. H., Xiang, X., Wang, Y. Y., Liu, X., Qi, L. N., Luo, C. P., et al. (2020). The lncRNA SNHG16 affects prognosis in hepatocellular carcinoma by regulating p62 expression. *J. Cell. Physiol.* 235, 1090–1102. doi: 10.1002/jcp.29023
- Zhou, X.-Y., Liu, H., Ding, Z.-B., Xi, H.-P., and Wang, G.-W. (2020). lncRNA SNHG16 promotes glioma tumorigenicity through miR-373/EGFR axis by activating PI3K/AKT pathway. *Genomics* 112, 1021–1029. doi: 10.1016/j.ygeno.2019.06.017
- Zhu, C., Cheng, D., Qiu, X., Zhuang, M., and Liu, Z. (2018). Long noncoding RNA SNHG16 promotes cell proliferation by sponging microRNA-205 and upregulating ZEB1 expression in osteosarcoma. *Cell. Physiol. Biochem.* 51, 429–440. doi: 10.1159/000495239
- Zhu, H., Zeng, Y., Zhou, C.-C., and Ye, W. (2018). SNHG16/miR-216-5p/ZEB1 signal pathway contributes to the tumorigenesis of cervical cancer cells. *Arch. Biochem. Biophys.* 637, 1–8.
- Zhu, Q., Li, Y., Guo, Y., Hu, L., Xiao, Z., Liu, X., et al. (2019). Long non-coding RNA SNHG16 promotes proliferation and inhibits apoptosis of diffuse large B-cell lymphoma cells by targeting miR-497-5p/PIM1 axis. *J. Cell. Mol. Med.* 23, 7395–7405.

Conflict of Interest: The authors declare that the research was conducted in the absence of any commercial or financial relationships that could be construed as a potential conflict of interest.

Publisher's Note: All claims expressed in this article are solely those of the authors and do not necessarily represent those of their affiliated organizations, or those of the publisher, the editors and the reviewers. Any product that may be evaluated in this article, or claim that may be made by its manufacturer, is not guaranteed or endorsed by the publisher.

Copyright © 2021 Ghafouri-Fard, Khoshbakht, Taheri and Shojaei. This is an open-access article distributed under the terms of the Creative Commons Attribution License (CC BY). The use, distribution or reproduction in other forums is permitted, provided the original author(s) and the copyright owner(s) are credited and that the original publication in this journal is cited, in accordance with accepted academic practice. No use, distribution or reproduction is permitted which does not comply with these terms.



MiR-873-5p: A Potential Molecular Marker for Cancer Diagnosis and Prognosis

Yuhao Zou^{1,2}, Chenming Zhong², Zekai Hu² and Shiwei Duan^{1,2,3*}

¹ Institute of Translational Medicine, Zhejiang University City College, Hangzhou, China, ² Medical Genetics Center, Ningbo University School of Medicine, Ningbo, China, ³ Department of Clinical Medicine, Zhejiang University City College School of Medicine, Hangzhou, China

OPEN ACCESS

Edited by:

Zong Sheng Guo,
Roswell Park Comprehensive Cancer
Center, United States

Reviewed by:

Sara Sergio,
University of Salento, Italy
Wei Zhang,
Northwestern University,
United States

*Correspondence:

Shiwei Duan
duansw@zucc.edu.cn

Specialty section:

This article was submitted to
Molecular and Cellular Oncology,
a section of the journal
Frontiers in Oncology

Received: 19 July 2021

Accepted: 20 September 2021

Published: 05 October 2021

Citation:

Zou Y, Zhong C, Hu Z and Duan S
(2021) MiR-873-5p: A Potential
Molecular Marker for Cancer
Diagnosis and Prognosis.
Front. Oncol. 11:743701.
doi: 10.3389/fonc.2021.743701

miR-873 is a microRNA located on chromosome 9p21.1. miR-873-5p and miR-873-3p are the two main members of the miR-873 family. Most studies focus on miR-873-5p, and there are a few studies on miR-873-3p. The expression level of miR-873-5p was down-regulated in 14 cancers and up-regulated in 4 cancers. miR-873-5p has many targeted genes, which have unique molecular functions such as catalytic activity, transcription regulation, and binding. miR-873-5p affects cancer development through the PIK3/AKT/mTOR, Wnt/ β -Catenin, NF- κ B, and MEK/ERK signaling pathways. In addition, the target genes of miR-873-5p are closely related to the proliferation, apoptosis, migration, invasion, cell cycle, cell stemness, and glycolysis of cancer cells. The target genes of miR-873-5p are also related to the efficacy of several anti-cancer drugs. Currently, in cancer, the expression of miR-873-5p is regulated by a variety of epigenetic factors. This review summarizes the role and mechanism of miR-873-5p in human tumors shows the potential value of miR-873-5p as a molecular marker for cancer diagnosis and prognosis.

Keywords: miR-873-5p, cancer, cell, prognosis, signaling pathway

INTRODUCTION

With the increasing incidence and mortality of cancer worldwide in recent decades, it has become the second leading cause of human death (1). MicroRNA (miRNA) is a set of non-coding RNA (2) less than 25 nucleotides in length. miRNAs can bind to the 3'-untranslated region (3'-UTR) of target mRNA molecules and regulate the expression of target genes, thus playing an important role in cancer (3). The miR-873 family is located on chromosome 9 (chr9:28888878-28888954). Its family includes two main members of the human genome, including hsa-miR-873-5p (miR-873-5p) and hsa-miR-873-3p (miR-873-3p). Their mature sequences are 21 and 22 nucleotides in length, respectively, and are highly conserved (**Figure 1**). At present, most researches focus on miR-873-5p.

Studies have found that the expression of miR-873-5p is dysregulated in a variety of cancers and plays different roles in different cancers. On the one hand, miR-873-5p is upregulated and carcinogenic in non-small cell lung cancer (NSCLC) (4), and hepatocellular carcinoma (HCC) (5); on the other hand, miR-873-5p is involved in colorectal cancer (CRC) (6) and gastric cancer (GC) (7) are down-regulated and exert a tumor suppressor effect. miR-873-5p can affect cell proliferation (5), apoptosis (6), migration (8), invasion (9), cell stemness (10), and other biological processes by regulating the expression of its target genes. In addition, miR-873-5p also has important

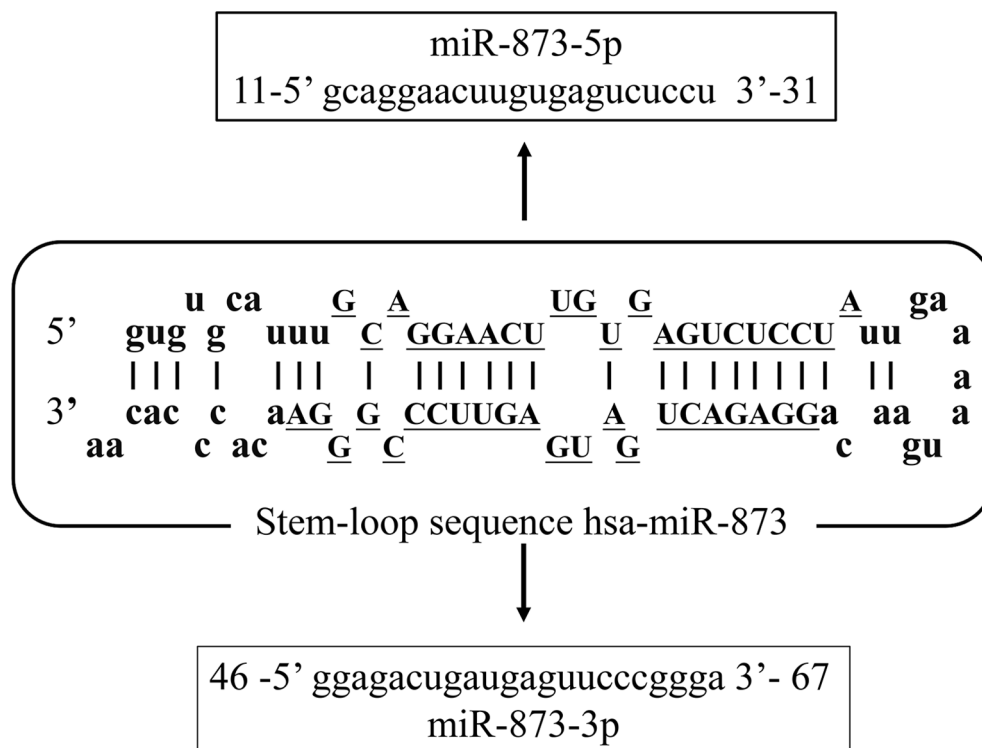


FIGURE 1 | The sequence structure of the miR-873 family. Hsa-miR-873 is located on chromosome 9 (chr9:28888878-28888954). It has two mature sequences, hsa-miR-873-5p (MIMAT0004953, miR-873-5p) and hsa-miR-873-3p (MIMAT0022717, miR-873-3p).

clinical significance in drug sensitivity and prognosis of cancer patients (4, 6). miR-873-5p can also be regulated by a variety of epigenetic factors. Among them, the interaction between non-coding RNA (lncRNA or circRNA) and miR-873-5p is mainly researched. This review focuses on studying the biological role of miR-873-5p in tumors, exploring the molecular functional network of its targeted genes, and predicting the potential role of miR-873-5p in the diagnosis and prognosis of human cancer.

THE BIOLOGICAL FUNCTION OF MIR-873-5P TARGET GENES

miR-873-5p can directly bind to the 3'-UTR of target gene mRNA and regulate gene expression after transcription. The target gene of miR-873-5p has unique molecular functions, including catalytic activity, transcription regulation, binding, etc. (**Figure 2**).

Among the miR-873-5p target genes, CDK3 is a catalytically active gene. CDK3 is a cyclin-dependent kinase, which can phosphorylate the estrogen receptor (ER) and enhance ER activity, thereby promoting the occurrence and development of breast cancer (BC) (11).

Among the miR-873-5p target genes, genes with transcriptional regulatory activity are ELK1, DEC2, ZEB1, and ZIC2. ELK1 is a key transcriptional regulator that mediates the MEK-ERK signal

transduction, and it can activate early oncogene expression (12, 13). DEC2 is the basic helix-loop-helix transcription factor of the clock gene. It plays an important role in the circadian rhythm, cell proliferation, and apoptosis, and thus participates in tumor progression (14). ZEB1 is a member of the zinc finger E-box binding protein (ZEB) transcription factor family (15). ZEB1 can bind to the promoter of the liver cancer-derived growth factor (HDGF) and increase the level of HDGF transcription, leading to the pathogenesis of endometrial cancer (EC) (16). ZIC (Cerebellar Zinc Finger Protein) protein has five highly conserved Cys2His2 motifs, which can bind to DNA and thus function as a transcription factor (17). As a member of the ZIC family, ZIC2 can promote tumor growth and metastasis of hepatocellular carcinoma through transcriptional regulation of p21-activated kinase 4 (18). In addition, ZIC2 can bind to the DNA-binding high mobility base box of TCF4, thereby inhibiting the transcriptional activity of β -catenin (19).

The miR-873-5p target genes with binding activity include DEC2, NDFIP1, STRN4, TNNT1, and CXCL16. DEC2 can inhibit its downstream molecules by binding to the E-box (20). NDFIP1 is a membrane protein with small endosomes containing PY motifs, which can transport E3 ligase and its substrate to endosomes (21). STRN4 is a member of the striatin family. It can combine with MINK1 of the germinal center kinase family to form a large complex, which is essential for the process of cytokinesis (22, 23). Troponin T1 (TNNT1) is a subunit of troponin T, which can

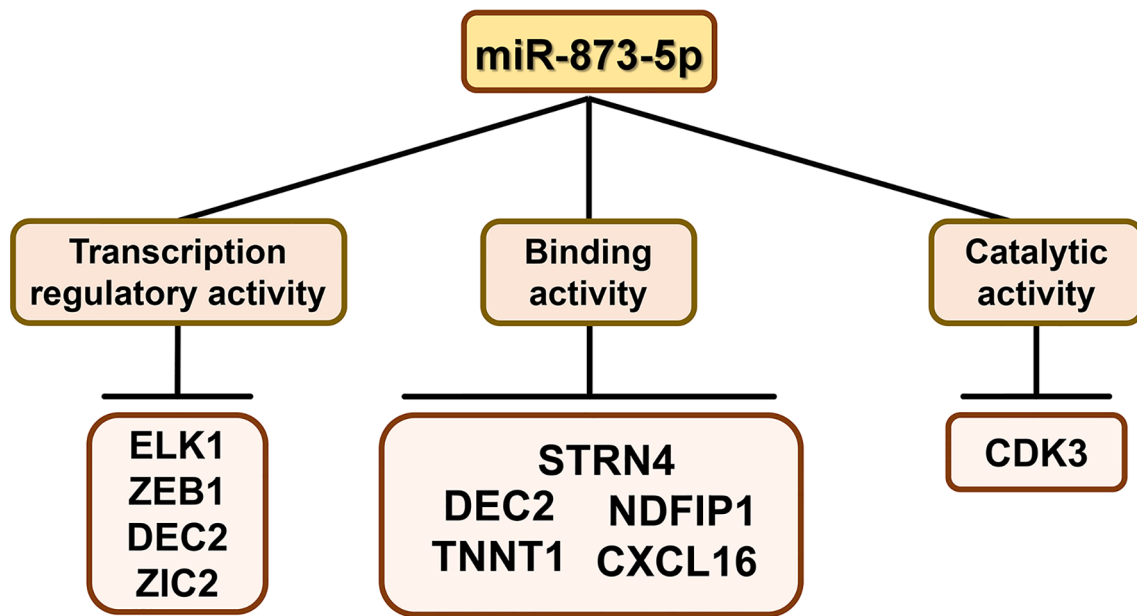


FIGURE 2 | The molecular functions of miR-873-5p target genes. The target genes of miR-873-5p have the molecular functions of binding, catalytic, and transcription regulator activity.

bind to tropomyosin and anchor the troponin complex at a specific location on striated muscle filaments (24). CXCL16-CXCR6 are chemokines and chemokine receptors, respectively, which can bind to each other (25). The mutual binding of CXCL16 and CXCR6 involves a variety of biological activities, including cell adhesion (26) and anti-tumor immunity (27).

MIR-873-5P DYSREGULATION IN VARIOUS CANCERS

As shown in **Table 1**, miR-873-5p is abnormally expressed in 18 types of cancers. Among them, miR-873-5p is up-regulated in 4 types of cancers, including NSCLC (4), lung adenocarcinoma (LUAD) (28, 29), lung cancer (LCA) (5, 8, 30), and Merkel cell carcinoma (MCC) (24627810). miR-873-5p is down-regulated in 14 types of cancers, including nasopharyngeal carcinoma (NPC) (32), lung cancer (LCA) (33), cervical cancer (CC) (34, 35), EC (36), BC (10, 11, 37, 38), pancreatic ductal adenocarcinoma (PDAC) (39), glioblastoma (GM) (9, 40–42), osteosarcoma (OS) (43), papillary thyroid carcinoma (PTC) (44), CRC (6, 45–49), esophageal cancer (ESCA) (50), GC (7, 51, 52), tongue squamous cell carcinoma (TSCC) (53), and pancreatic cancer (PC) (54).

Highly expressed miR-873-5p can inhibit cell proliferation, induce cell apoptosis, inhibit EMT, metastasis, and invasion process, thereby promoting the occurrence and development of cancer. Among the four types of cancers (NSCLC, LUAD, HCC, and MCC), miR-873-5p can promote their progression, indicating that miR-873-5p has tumor suppressor and cancer-promoting effects.

THE BIOLOGICAL ROLE OF MIR-873-5P IN HUMAN CANCER

MiR-873-5p and Different Signaling Pathways

miR-873-5p can affect the occurrence and development of cancer by participating in the PIK3/AKT/mTOR, Wnt/ β -Catenin, NF- κ B, MEK/ERK, and other signaling pathways (**Figure 3**).

The PIK3/AKT signaling pathway is often overactivated in malignant tumors. The PIK3/AKT signaling pathway can participate in cell cycle regulation, promote cell proliferation and metastasis, and inhibit cell apoptosis (55). In HCC, miR-873-5p promotes the development of HCC through the NDFIP1/AKT/mTOR axis (5). miR-873-5p can directly activate PIK3/AKT to promote HCC progression (30). miR-873-5p can down-regulate TUSC3 expression, inhibit the AKT signaling pathway, and thus hinder CRC development (49). In PC, miR-873-5p targets PLEK2 and inhibits the AKT signaling pathway, thereby inhibiting the development of cancer (54).

The Wnt/ β -Catenin signaling pathway is important for tumor development, and the dysregulation of the Wnt/ β -Catenin signaling pathway may lead to cell proliferation and malignancy (56). miR-873-5p inhibits the expression of HOXA9 and STRA6, and blocks the Wnt/ β -Catenin signaling pathway, thereby inhibiting the development of OS and GC (43, 52).

The NF- κ B signaling pathway can inhibit cell apoptosis, and it is closely related to tumor occurrence, growth, and metastasis (57). By inhibiting the expression of JMJD8, TNF receptor-related factor 5 (TRAF5) and TGF- β activated kinase 1 (MAP3K7) binding protein 1 (TAB1), miR-873-5p can inhibit

TABLE 1 | miR-873-5p dysregulation and its target genes in cancer.

Cancer type	Clinical Samples	Cell lines (Cancer cells and Normal cells)	<i>In vitro</i>	<i>In vivo</i>	Expression	Target gene	Reference
NSCLC	30 LUAD tissues and 30 matched non-tumor tissues	PC9 and BEAS-2B, HEK293T	Proliferation↑		Upregulation	GLI1	(4)
LUAD	481 LUAD tissues and 47 normal tissues	H23, H1299, A549, SPC-A1	Proliferation↑; migration and invasion↑		Upregulation	SRCIN1	(28)
					Upregulation	—	(29)
HCC	86 HCC tissues and 86 matched non-tumor tissues	SMMC-7721, HepG2, Hep3B, SK-HEP-1, MHCC97H and L02, 7701, 7702	Proliferation↑; glycolytic metabolism↑		Upregulation	NDFIP1	(5)
	25 HCC tissues and 25 adjacent non-tumor tissues	HuH6, THLE-2 and ATCC, Manassas, VA, USA	Proliferation↑; migration and invasion↑		Upregulation	TRIM25	(8)
	70 HCC tissues and 70 adjacent non-tumor tissues	Hep3B, HepG2, SMMC-7721, Huh-7 and L02	Proliferation↑; migration and invasion↑		Upregulation	TSLC1	(30)
MCC	3 MCC tissues, 1 SCC tissue, 1 BCC tissue, 1 normal skin				Upregulation	—	(31)
NPC	134 NPC tissues and 40 non-NPC tissues	5-8 F, 6-10B, HNE-3, C666-1 and NP69SV40T	Cell stemness↓		Downregulation	ZIC2	(32)
LCA	31 NSCLC tissues and 31 matched normal tissues		Cell stemness↓		Downregulation	CDK3	(33)
CC	306 CC tissues and 3 normal tissues	Caski, HeLa, C33a, SiHa	Proliferation↓		Downregulation	ULBP2	(34)
	20 CC tissues and 20 matched normal tissues	C33A, HeLa, SiHa and Ect1/E6E7	Proliferation↓; migration and invasion↓; EMT↓		Downregulation	GLI1	(35)
EC	47 EC tissues and 47 adjacent non-tumor tissues	AN3CA, HEC-59, HEC-1B, KLE and HUM-CELL-0111	Proliferation↓		Downregulation	HDGF	(36)
BC	4 BC tissues and 4 adjacent mammary gland epithelial tissues		Cell stemness↓	Cell stemness↓	Downregulation	PD-L1	(10)
	43 BC tissues and 10 adjacent non-tumor tissues	MCF-7, ZR75-1, T47D, SKBR3, MDA-MB-231 and HEK293T	Proliferation↓	Tumor growth↓	Downregulation	CDK3	(11)
		MDA-MB-231, BT549 and 293	— —		Downregulation	ZEB1	(37)
	30 TNBC tissues and 30 adjacent normal tissues	MDA-MB-453, BT-549, MDA-MB-231, HCC1937 and HBL-100	Proliferation↓; migration and invasion↓; EMT↓		Downregulation	DCST1-AS1	(38)
PDAC/ TNBC		MDA-MB-436, MDA-MB-231, MDA-MB-453, BT-20, HCC1937, SKBR3, T47D, HEK293 and HPDE	Proliferation↓; migration and invasion↓	Proliferation↓; tumor growth↓	Downregulation	KRAS	(39)
GM	6 GM tissues and 3 non-tumor brain tissue		— —		Downregulation	—	(40)
	12 high-grade GM tissues and 7 normal brain tissues	U87, U251	— —		Downregulation	Bcl-2	(9)
	50 GM tissues and 50 normal tissues		— —		Downregulation		(41)
	6 GBM tissues and 6 adjacent normal tissues	A172, T98G, U87, U373, U251, U138	Proliferation↓; migration and invasion↓; apoptosis↑	apoptosis↑	Downregulation	IGF2BP1	(42)
OS	49 OS tissues and 49 adjacent normal bone tissues	MG-63, SAOS-2, HOS, U2OS and hFOB1.19	Proliferation↓; migration and invasion↓	Tumor growth↓	Downregulation	HOXA9	(43)
PTC	30 PTC tissues and 30 adjacent normal tissues	KTC-1, TPC-1, BCPAP, K1, BHP10-3 and Nthy-ori3-1	Proliferation↓; migration and invasion↓		Downregulation	CXCL16	(44)
CRC	50 CRC tissues and 50 adjacent normal tissues	HCT116, H29, SW620, LOVO, SW480 and NCM460	Proliferation↓; migration and invasion↓; EMT↓; apoptosis↑; cell cycle↑		Downregulation	JMJD8	(6)
	10 CRC tissues and 10 adjacent non-tumor tissues	SW620, SW480, DLD1, HCT116, LoVo, HT-29 and NCM460	Proliferation↓		Downregulation	TRAF5/TAB1	(45)
		DLD-1, HCT-116, SW-480, HT-29, SW-620 and HIEC	Migration and invasion↓; EMT↓		Downregulation	ZEB1	(46)
	55 CRC tissues and 55 adjacent normal tissues	SW620, HCT116, HCT8, SW480, LS174T, HT29, RKO	Proliferation↓; migration and invasion↓; EMT↓	Cell growth↓; liver metastasis↓	Downregulation	ELK1/STRN4	(47)
	45 CRC tissues and 45 adjacent normal tissues	HT29, SW480, HCT116 and CRL1790	Proliferation↓; migration and invasion↓		Downregulation	TNNT1	(48)
					Downregulation	TUSC3	(49)

(Continued)

TABLE 1 | Continued

Cancer type	Clinical Samples	Cell lines (Cancer cells and Normal cells)	<i>In vitro</i>	<i>In vivo</i>	Expression	Target gene	Reference
ESCA	96 CC tissues and 96 adjacent normal tissues	HCT116, SW620, RKO, HCT8, HT29 and NCM460	Proliferation↓; migration and invasion↓; EMT↓	Proliferation↓; metastasis↓	Downregulation	DEC2	(50)
GC	36 EC tissues and 36 adjacent normal tissues	EC-109, EC-1, TE-1, TE-10, KYSE-150 and HEEC	Proliferation↓; migration and invasion↓; EMT↓		Downregulation	GLI1	(51)
	80 GC tissues and 80 adjacent non-tumor tissues	SGC-7901	Proliferation↓; apoptosis↑; cell cycle↑		Downregulation	—	(7)
	15 GC tissues and 15 adjacent non-tumor tissues and 15 normal tissues						
	80 GC tissues and 80 adjacent normal tissues	BGC823, SGC7901, MKN45, MGC803 and GES-1	Proliferation↓; migration and invasion↓; EMT↓; cell cycle↑	Proliferation↓; metastasis↓	Downregulation	STRA6	(52)
TSCC	35 TSCC tissues and 35 adjacent normal tissues	SCC9, SCC15, SCC25, UM1, CAL-27 and HOEC	Apoptosis↑		Downregulation	SEC11A	(53)
PC	30 PC tissues and 45 normal tissues	PANC-1, SW1990, MIA PaCa-2 and hTERT-HPNE	Cell stemness↓		Downregulation	PLEK2	(54)

NSCLC, non-small cell lung cancer; LUAD, lung adenocarcinoma; HCC, hepatocellular carcinoma; MCC, Merkel cell carcinoma; LCA, lung cancer; CC, cervical cancer; EC, endometrial cancer; BC, breast cancer; GM, glioblastoma; TNBC, triple-negative breast cancer; PDAC, pancreatic ductal adenocarcinoma; PTC, papillary thyroid cancer; CRC, carcinoma of colon and rectum; GC, gastric cancer; ESCA, esophageal cancer; OS, osteosarcoma; NPC, nasopharyngeal carcinoma; PC, pancreatic cancer.

↑: promotion; ↓: inhibition.

the NF- κ B signaling pathway, thereby hindering the progression of CRC (6, 45). In PTC, miR-873-5p can down-regulate the expression of CXCL16, and can also inhibit the development of PTC through down-regulating the NF- κ B signaling pathway (44).

The MEK/ERK signaling pathway can promote cell proliferation and migration and is involved in the occurrence and development of a variety of cancers (12). In CRC, miR-873-5p targets ELK1 and STRN4, and exerts a tumor suppressor effect through the ERK signaling pathway (47). By down-regulating KRAS expression, miR-873-5p can also inhibit the ERK signaling pathway to suppress the development of PDAC and TNBC (39). In addition, miR-873-5p can also deactivate the PI3K/AKT and ERK signaling pathways to inhibit the development of BC (58).

MiR-873-5p and Cell Cycle

The regulation of the cell cycle is of great significance to the proliferation and apoptosis of cancer cells (Figure 4). Increased expression of miR-873-5p can inhibit the expression of GLI1 and cyclin B, thereby inducing GC cells to arrest the G2/M cell cycle (51). After miR-873-5p targets to inhibit JMJD8, it blocks CRC HCT116 and SW480 cells in the G1-S cell cycle (6). miRNA-873-5p can accelerate the S phase process of HCC cells, thereby promoting cancer cell proliferation (30). Other studies have shown that miR-873-5p can down-regulate STRA6, thereby inducing GC cells to arrest in the G0/G1 cell cycle and increasing cell mortality (30). After miR-873-5p targeted IGF2BP1, GM cells showed significant G0/G1 block and S phase reduction (42).

MiR-873-5p and Cell Proliferation and Apoptosis

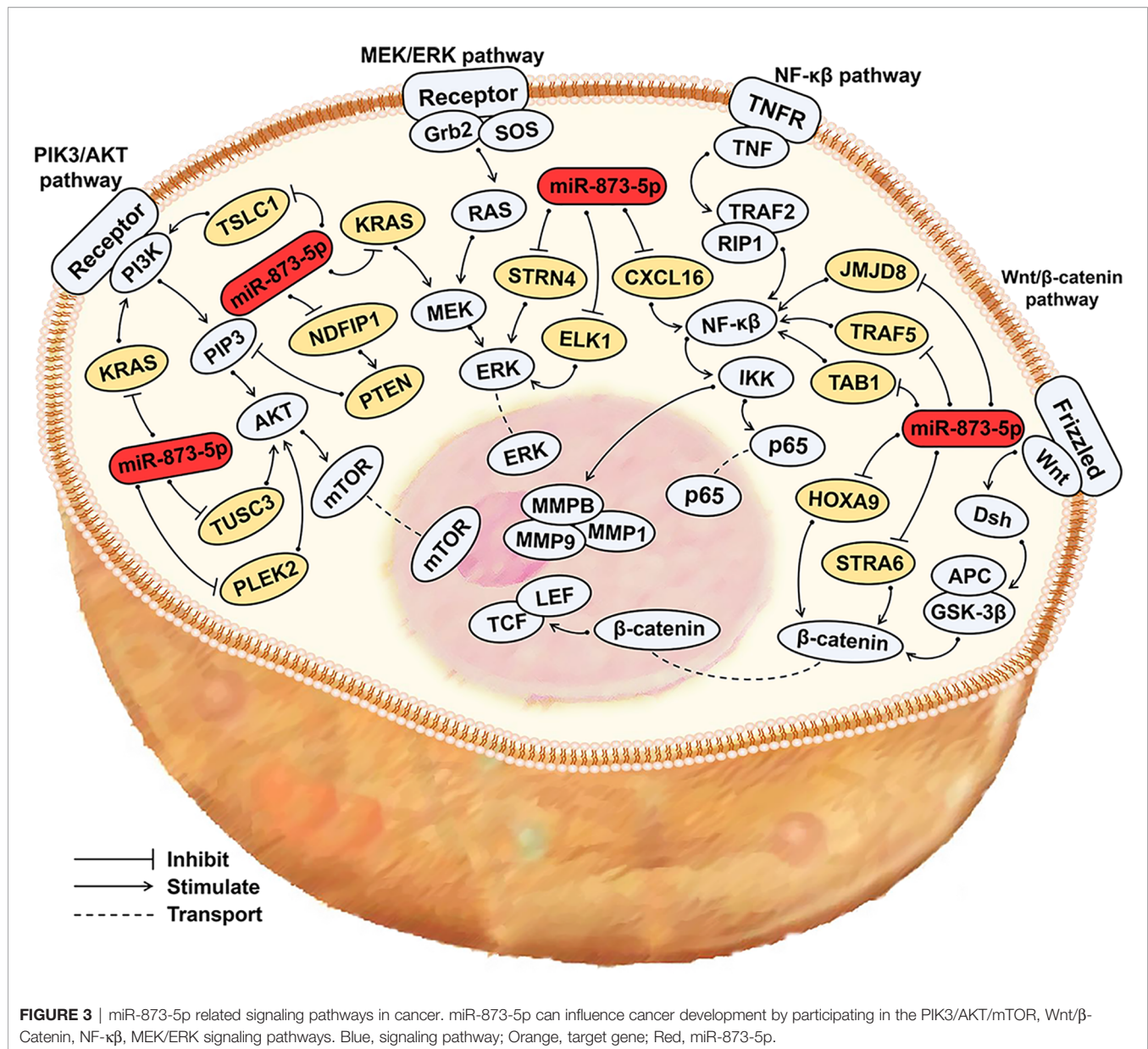
The targeted genes of miR-873-5p are closely related to the process of tumor cell proliferation and apoptosis (Figure 4).

STRN4 directly acts on protein kinases such as MINK1, TNK1, and MAP4K4. The knockdown of STRN4 inhibits the proliferation of PDAC and CRC cancer cells (59). miR-873-5p can target ELK1 and STRN4 and inhibit the proliferation of CRC LoVo and HCT116 cells through the regulation of the ERK-CyclinD1 signaling pathway (47).

Human cytomegalovirus glycoprotein UL16 binding protein 2 (ULBP2) is an important activation receptor on the surface of natural killer cells. In normal tissues, low levels of ULBP2 can lead to the activation of immune cells (60, 61). In CC C33a cells, miR-873-5p activates immune cells by inhibiting ULBP2 expression, thereby attenuating cell proliferation (34).

Jumonji domain-containing protein 8 (JMJD8) contains a JmjC domain (62) at 74-269 amino acid residues. miR-873-5p can inhibit the NF- κ B signaling pathway by down-regulating the expression of JMJD8 in CRC cells, thereby inhibiting cell proliferation, blocking the G1-S transition, and enhancing the apoptosis of CRC HCT116 and SW480 cells (6). miR-873-5p directly targets the 3'-UTR of TUSC3 to down-regulate its expression and inhibit AKT signaling pathway and CRC cell proliferation (49). TNNT1 expression is closely related to the clinical stage of tumor tissues and can promote the proliferation of cancer cells through metastatic G1/S transition (63). miR-873-5p down-regulates TNNT1 and may inhibit the proliferation of CRC cells (48). Besides, TRAF5 and TAB1 are both key components of the NF- κ B signaling pathway (45). miR-873-5p directly targets TRAF5 and TAB1 to inhibit the NF- κ B signaling pathway, thereby inhibiting the cell proliferation of CRC (45).

KRAS can enhance the AKT and ERK signaling pathways that are related to cell proliferation (64). miR-873-5p inhibits the cell proliferation of PDAC and TNBC tissues (38) by targeting KRAS, thereby inhibiting the ERK and PI3K/AKT signaling pathways (39). miR-873-5p can induce apoptosis of PDAC and TNBC by regulating the Caspase-dependent apoptotic pathway



(39). DCST1-AS1 is an oncogenic lncRNA (38). DCST1-AS1 can sponge miR-873-5p and thus reduce the inhibition of miR-873-5p on the expression of IGF2BP1, thereby up-regulating the expression of MYC and promoting the proliferation of TNBC cells (38).

Tripartite motif-containing protein 25 (TRIM25) is a member of TRIM protein, which can target the degradation of MTA-1 (65). MTA-1 is a member of the metastasis-related gene (MTA) family and plays an important role in the proliferation of cancer cells (66). miR-873-5p can inhibit TRIM25 expression, which can promote the proliferation of HCC cells (8). TSLC1 is a new type of tumor suppressor gene, which is related to proliferation, apoptosis, cell cycle, and tumorigenicity of cancer cell (67). The inhibition of TSLC1 by miRNA-873-5p can lead to

hyperphosphorylation of PI3K/AKT/mTOR and other signaling pathways to promote HCC cell proliferation (30).

Src is a tyrosine kinase that is frequently up-regulated in cancer and is very important for cancer cell proliferation (68, 69). Src Kinase Signaling Inhibitor 1 (SRCIN1) is a tumor suppressor gene that suppresses cancer by inactivating Src in cancer (70). miR-873-5p activates the Src signaling pathway by down-regulating of SRCIN1 expression and promotes the proliferation of LUAD cells (28).

Insulin-like growth factor 2 mRNA binding protein 1 (IGF2BP1) is a carcinoembryonic protein that is expressed in various cancers including leukemia (71). IGF2BP1 can stabilize and enhance the expression of c-MYC and MKI67, which are both effective regulators of cell proliferation and apoptosis (72).

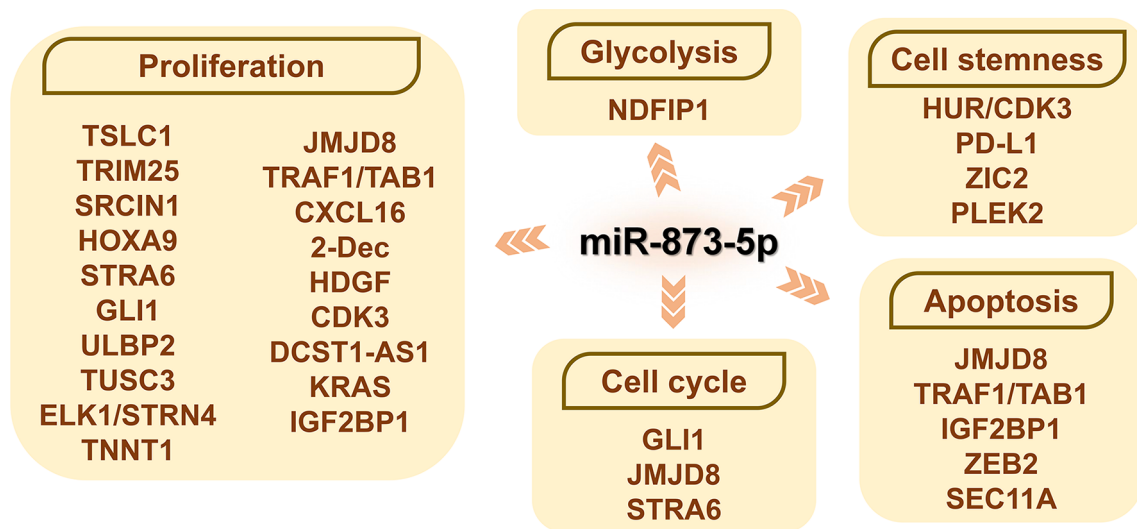


FIGURE 4 | The role of miR-873-5p and its target genes on the cell biology of cancer cells. By promoting or inhibiting cell proliferation and apoptosis, miR-873-5p has both oncogenic or pro-cancer effects in different cancers. miR-873-5p inhibits the aerobic glycolysis of cancer cells by targeting NDFIP1. In addition, miR-873-5p can reduce the stemness of cancer cells by targeting PD-L1 and HUR/CDK3. By targeting GLI1, JMJD8, IGF2BP1, and STRA6, miR-873-5p can inhibit the progression of the cancer cell cycle.

Overexpression of miR-873-5p in GM cells can significantly down-regulate the expression of IGF2BP1, MKI67, and c-MYC, and lead to cell proliferation inhibition and apoptosis (42). ZEB2 is a transcription factor containing zinc fingers, which is essential in early embryonic development (73). ZEB2 can increase the expression of cyclin A1, cyclin D1, and Bcl-2 in GM cells, thereby promoting the growth of GM cells (74). miR-873-5p down-regulates ZEB2 expression, which can promote GM cell apoptosis (74).

HOXA9 is a member of the mammalian HOX family (75), which is abnormally activated in a variety of cancers such as CRC (76) and GC (77). miR-873-5p directly targets HOXA9 and reduces the expression levels of β -catenin and cyclin D1 through the inactivation of the Wnt/ β -catenin signaling pathway, thereby inhibiting OS cell proliferation (43).

Hedgehog (Hh) signaling pathway can participate in the cancer process through mechanisms such as promotion of tumor invasion and metastasis (78, 79). GLI1 is a transcription factor of the Hh signaling pathway and downstream target genes and is usually used as a marker to activate the Hh signaling pathway (80). Studies have found that increased expression of miR-873-5p can inhibit the expression of GLI1 and inhibit the cell proliferation of NSCLC (4), GC (51), and CC (35) through the Hh signaling pathway. STRA6, as a transmembrane protein of RA, is overexpressed in many cancer types (81). Overexpression of STRA6 can upregulate Wnt pathway-related genes, such as β -catenin, MMP-7, and c-myc. miR-873-5p down-regulates the expression of STRA6 in GC and can inhibit GC cell proliferation (52).

The estrogen receptor (ER) is a member of the nuclear receptor superfamily of ligand-activated transcription factors and plays an important role in BC (82). miR-873-5p inhibits

ER activity by targeting CDK3, thereby inhibiting the growth of BC cells (11).

As a chemokine, the binding of CXCL16 to its sole receptor CXCR6 can involve biological activities such as cell adhesion (26) and anti-tumor immunity (27). Silencing CXCL16 can inhibit the proliferation and invasion of cancer cells by regulating the NF- κ B signaling pathway (83). Overexpression of miR-873-5p targets CXCL16 and suppresses the NF- κ B signaling pathway in PTC cells, thereby inhibiting PTC cell proliferation (44).

HDGF is a secreted growth factor (84), which can interact with the β -catenin pathway and promote cancer cell proliferation (85). Therefore, miR-873-5p targeted down-regulation of HDGF may inhibit EC cell proliferation through the β -catenin signaling pathway (36). DEC2 plays an important role in circadian rhythm, cell proliferation, and apoptosis, and is also closely related to tumor progression (14). In ESCA, miR-873-5p can inhibit ESCA cell proliferation by targeting the DEC2 gene, thereby affecting the circadian rhythm (14, 50).

miR-873-5p and Cell Migration, Invasion, and EMT

The migration and invasion of cancer cells are important for the progression of cancer. Epithelial cell-mesenchymal transition (EMT) is a process of epithelial cell changes, which is characterized by weak cell adhesion and enhanced migration ability (86). EMT is an important marker of cancer progression and metastasis of malignant tumors (87) (Figure 5).

In CRC HCT8 cells, the down-regulation of miR-873-5p corresponds to the up-regulation of ELK1 and STRN4, which leads to the down-regulation of E-cadherin and α -E-catenin and enhances EMT, and ultimately promotes the migration of CRC

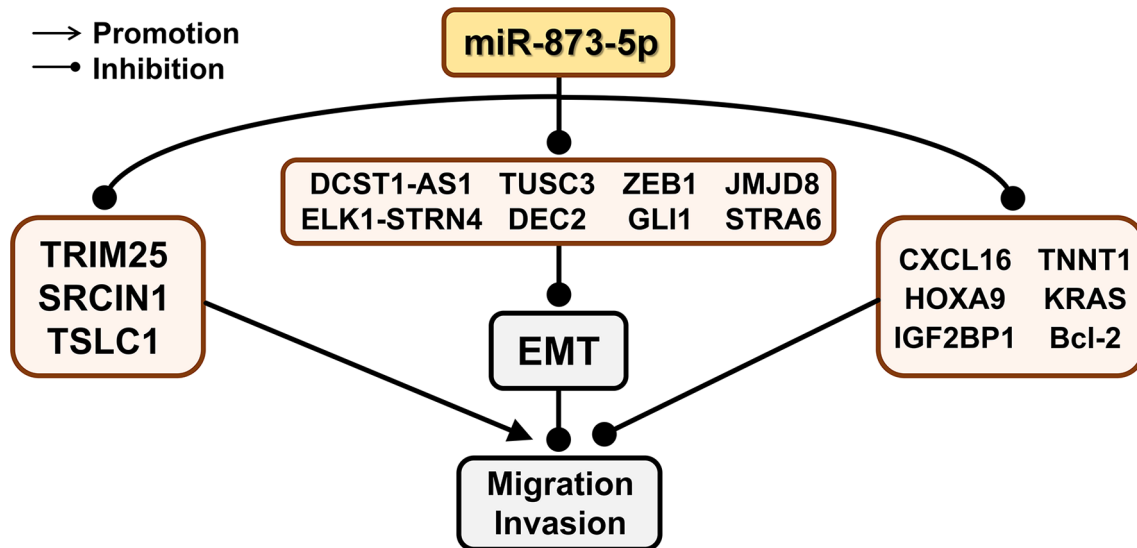


FIGURE 5 | The effect of miR-873-5p target genes on EMT, migration, and invasion of cancer cells. miR-873-5p inhibits the EMT process by inhibiting the expression of ZEB1, TUSC3, DCST1-AS1, JMJD8, ELK1-STRN4, GLI1, STRA6, and DEC2. MiR-873-5p targets TRIM25, SRCIN1, and TSLC1, and promotes cell migration and invasion. In addition, miR-873-5p inhibits the migration and invasion of cancer cells by targeting CXCL16, TNNT1, IGF2BP1, Bcl-2, TNNT1, and HOXA9.

cells (47). ZEB1 is closely related to migration and EMT (88). In CRC, the up-regulation of miR-873-5p also corresponds to the down-regulation of ZEB1 expression, thereby significantly increasing the levels of E-cadherin, β -catenin, and ZO-1. This leads to a decrease in the levels of N-cadherin and vimentin, which changes the cell phenotype from EMT to MET, thereby inhibiting the EMT process of CRC cells (46). When miR-873-5p targets JMJD8, the expression of E-cadherin and cytokeratin is significantly increased, thereby weakening the EMT effect and inhibiting the migration and invasion of CRC cells (6). TUSC3 may change the EMT of CRC by regulating PI3K/Akt and Wnt/ β -catenin signaling pathways, thereby changing its metastasis and invasiveness (89). miR-873-5p can negatively regulate the expression of TUSC3, thereby inhibiting the EMT ability of CRC cells (49). TNNT1 is negatively correlated with the expression of E-cadherin in colon adenocarcinoma (90). miR-873-5p can regulate E-cadherin expression by targeting TNNT1, thereby inhibiting CRC cell migration and invasion (48).

When miR-873-5p targets to inhibit GLI1, the expression level of E-cadherin is significantly increased, while the levels of N-cadherin and vimentin are significantly reduced, thereby inhibiting the EMT process of CC cells (35). miR-873-5p can negatively regulate ULBP2 and activate immune cells, thereby reducing the invasion and metastasis of CC cells (34).

In GC cells, miR-873-5p can lead to the downregulation of N-cadherin and vimentin by inhibiting STRA6, thereby inhibiting the EMT process of GC cells, and cell metastasis and invasion (52).

LEF1 is an important transcription factor involved in the activation of the Wnt signaling pathway, which can promote the synthesis of mesenchymal fibronectin and EMT (91). When miR-873-5p binds to DCST1-AS1, the expression of LEF1 is

up-regulated, and the EMT of TNBC cells is enhanced to promote cancer cell migration and invasion (38).

In ESCA, miR-873-5p can down-regulate the expression of DEC2, thereby inhibiting the effect of EMT and reducing the migration and invasion of ESCA cells (50, 92).

In PDAC and TNBC, miR-873-5p can target KRAS, thereby inhibiting cell migration and invasion through the ERK/AKT signaling pathway (39). The Wnt/ β -catenin signaling pathway is a key mechanism for cell maintenance and development, including cell differentiation, migration, and invasion (93).

miR-873-5p can target HOXA9 and inhibit the migration and invasion of OS cells through suppressing the Wnt/ β -catenin signaling pathway (43).

MTA-1 can promote cell metastasis through histone deacetylation and nucleosome remodeling (66). After miR-873-5p inhibits the expression of TRIM25, the function of MTA-1 is enhanced to promote the metastasis and invasion of HCC cells (8). TSLC1 is a specific tumor suppressor involved in cell adhesion and invasion (94). Therefore, in HCC, miR-873-5p can target TSLC1 to increase HCC cell adhesion, thereby promoting HCC cell migration (30).

SRCIN1 is the main regulator of E-cadherin (95), which can regulate the growth and movement of cell (96). miR-873-5p down-regulates the expression of SRCIN1, which can reduce cell adhesion and promote the migration of LUAD cell A549 (28).

IGF2BP1 can enhance the directionality of cell migration in a PTEN-dependent manner. miR-873-5p can down-regulate the expression of PTEN by targeting IGF2BP1, thereby inhibiting the migration ability of GM cells (42). Matrix metalloproteinases (MMP) have been shown to activate and regulate GM cell migration (97). Bcl-2 is an oncogene and it can promote the

migration and invasiveness of GM cells by enhancing the activity of MMP (98). miR-873-5p can target Bcl-2 to enhance the activity of MMP and inhibit the migration and invasion of GM cells (9). MMPs are related to the development of cancer, which can promote the degradation of extracellular matrix and cell invasion and metastasis (99, 100). Overexpression of miR-873-5p can inhibit the expression of MMP1, MMP9, and MMP13 by down-regulating CXCL16, thereby inhibiting the migration and invasion of PTC cells (44).

MiR-873-5p and Cell Stemness

Although cancer stem cells (CSCs) only account for a small part of cancer cells, they have the ability to self-renew (101). At present, CSC is considered to be the main factor leading to tumor recurrence and drug resistance (102).

Programmed cell death ligand 1 (PD-L1) is an immune checkpoint molecule and a ligand for PD-1 (103). The expression of PD-L1 is highly correlated with stemness-related genes in BC tissues and is overexpressed in basal BC. Therefore, PD-L1 may promote the stemness of BC cells (104, 105). PD-L1 can activate the PI3K/AKT and ERK signaling pathways in BC (106). And miR-873-5p can target PD-L1 and down-regulate its expression, and then inhibit the stemness of BC cells through the PI3K/Akt and ERK1/2 signaling pathways (10).

HuR is an RNA binding protein that can promote the progression of various tumors (107). HuR can directly bind and up-regulate CDK3 to promote the stemness of LCA (33). miR-873-5p can competitively bind to CDK3 with HuR and reduce CDK3 expression, thereby reducing the stemness of LCA cells (33).

Studies have found that ZIC2 may affect the occurrence and development of tumors through the AKT signaling pathway (108). Up-regulation of miR-873-5p can inhibit the expression of ZIC2 and disrupt the AKT signaling pathway, thereby inhibiting the stemness and tumorigenicity of NPC cells (109).

Overexpression of miR-873-5p can silence PLEK2 and inhibit the self-renewal of PC stem cells through the PIK3/AKT signaling pathway, thereby inhibiting the development of PC (54).

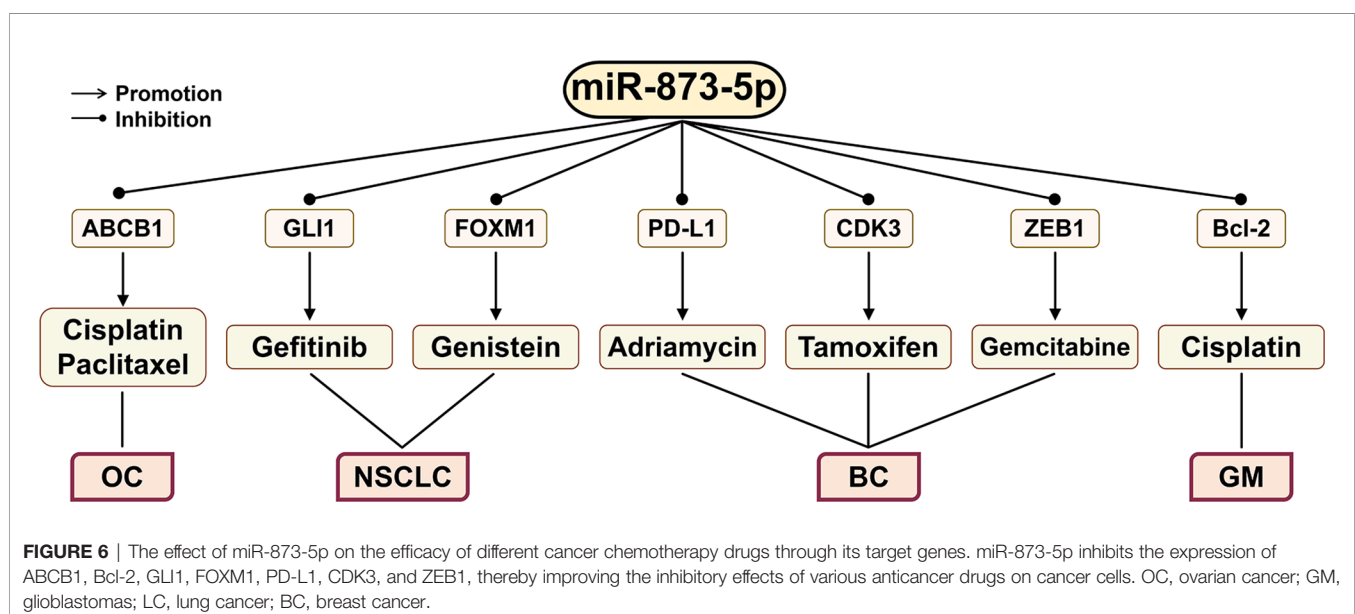
MiR-873-5p and Glycolysis

Tumor cells can change their metabolism to adapt to the challenging hypoxic environment (110). Intermediates in glycolysis can be used to meet the biosynthetic needs of rapidly growing tumors (111). AKT/rapamycin (mTOR) activation enables the continued growth and survival of tumor cells that rely on aerobic glycolysis, while the expression of NDFIP1 reduces the AKT/mTOR signaling pathway in cancer cells (5). In HCC, miR-873-5p inhibits the Warburg effect through the NDFIP1/AKT/mTOR axis, thereby inhibiting the aerobic glycolysis of HCC cells (5).

THE ROLE OF MIR-873-5P IN CANCER TREATMENT

Gefitinib (EGFR-TKI) can reduce viability and proliferation of cancer cells and angiogenesis in NSCLC (Figure 6). However, the resistance of cancer cells to gefitinib has greatly limited its clinical application (4, 112, 113). The enhancement of the GLI1 expression can increase the radiation resistance of NSCLC cells. When GLI1 is silenced, gefitinib can significantly reduce the growth of NSCLC cells (114, 115). The down-regulation of GLI1 by miR-873-5p can reduce the resistance of NSCLC cells to gefitinib, thereby causing NSCLC PC9 cell apoptosis (4).

The main treatments for BC include surgery, targeted therapy, radiotherapy, and chemotherapy. For TNBC, chemotherapy is the only treatment (10). CSCs may contribute to the chemoresistance of cancer (116). By activating the PI3K/Akt and ERK1/2 signaling pathways, the PD-1/PD-L1 axis can



promote the stemness and drug resistance of BC cells. miR-873-5p targeted inhibition of PD-L1 expression can attenuate the resistance of BC cells to Adriamycin (10). In addition, miR-873-5p may also inhibit ERα phosphorylation by targeting CDK3, thereby restoring the sensitivity of BC drug-resistant cells to tamoxifen (11).

Norbiliin (NCTD) is a dimethyl analog of phthalazine, which can inhibit the biological functions of cell proliferation and angiogenesis in a variety of cancers (117–119). NCTD can overcome tamoxifen resistance by targeting the miR-873-5p/CDK3 axis in BC cells (120).

Gemcitabine is a chemotherapy drug that is derived from deoxycytidine and is commonly used to treat BC patients (121). ZEB1 plays a key role in promoting the development of CSCs, and its overexpression is related to cancer chemoresistance (15). miR-873-5p can bind to the 3'-UTR of ZEB1 to directly inhibit its expression, thereby enhancing the cell growth inhibition induced by gemcitabine treatment (37).

Ovarian cancer (OC) is mostly treated with cisplatin and paclitaxel, but OC cancer cells often develop resistance to these drugs (122). The ABC superfamily transporter and P-glycoprotein (MDR1) play a key role in the multidrug resistance (MDR) of cancer. They can mediate the outflow of various chemical drugs, such as anticancer drugs (123–125). Overexpression of miR-873-5p increases the sensitivity of OC cells to cisplatin and paclitaxel by targeting ABCB1 to down-regulate the expression of MDR1 (126).

GM is the most common primary brain tumor in adults, and cisplatin is currently a chemical drug widely used to treat GM (127, 128). A study has found that inhibiting the expression of Bcl-2 can enhance the sensitivity of GM to cisplatin (129). miR-873-5p can enhance the sensitivity of GM cells to cisplatin by targeting Bcl-2 (9).

In addition, genistein is a soy-derived isoflavone that can play a beneficial role in cancer treatment (130). Genistein can inhibit the progression of NSCLC by regulating the circ_0031250/miR-873-5p/FOXO1 axis (131).

THE REGULATION OF MIR-873-5P IN HUMAN CANCER

Current studies have found that methyltransferase, circRNA, and lncRNA are involved in the regulation of miR-873-5p in human cancer (Figure 7).

CircRNA is a new type of non-coding RNA that can bind miRNAs to stop their regulation of target genes (132). Hsa_circ_0000069 can sponge miR-873-5p, which can promote the expression of TUSC3, thereby promoting the proliferation, migration, and invasion of CC cells (133). In Neuroblastoma, circDGKB can sponge miR-873-5p to increase the expression of ZEB1 and GLI1, and promote the occurrence and development of cancer (134). circ-UMAD1 can sponge miR-873-5p, thereby up-regulating the expression of Galectin-3 and inducing lymphatic metastasis of PTC (135). circFAT1(e2) can promote

the proliferation, metastasis, and invasion of PTC cells by inhibiting the miR-873-5p/ZEB1 axis, thereby exerting a carcinogenic effect (136). Knockout of circ_0004507 can up-regulate the expression of miR-873-5p and inhibit the progression of laryngeal cancer (137). circ_0031250 can promote the proliferation, migration, and invasion of NSCLC cells by inhibiting the miR-873-5p/FOXO1 axis (131). circZKSCAN1 can inhibit the progression, proliferation, migration, and invasion of HCC by down-regulating the miR-873-5p/DLC1 axis, thereby hindering the occurrence and development of HCC (138). Infant hemangioma (IH) is one of the most benign endothelial tumors in infants and young children. circATP5SL can eliminate the inhibition of IGF1R by sponging miR-873-5p, thereby promoting IH cell invasion, proliferation, and migration (139). circVPS33B accelerates tumor cells' proliferation, migration, and growth by down-regulating the miR-873-5p/HNRNP axis in invasive GC (140).

LncRNA MCF2L-AS1 can promote CSC-like characteristics of NSCLC cells by down-regulating the expression level of miR-873-5p, thereby exerting carcinogenic effects (141). YY1 is a member of the YY family. It is a zinc finger protein and is overexpressed in a variety of cancers (142). YY1 can down-regulate the level of miR-873-5p, thereby activating the PI3K/AKT and ERK signaling pathways, thereby promoting the stemness of cancer cells (58). LncRNA CYTOR can regulate the expression of genes in the nucleus, thereby participating in the occurrence and development of cancers such as CRC (143). By up-regulating lncRNA CYTOR, TRIM29 inhibits pre-miR-873-5p to produce miR-873-5p, thereby up-regulating FN1 and promoting the migration and invasion of PTC cells (144).

The expression of lncRNA DGCR5 is significantly reduced in LC. DGCR5 shares the same binding site of miR-873-5p with TUSC3 (145). Ki-67 and MMP-3, MMP-9 are the markers of cell proliferation, cell migration, and invasion (100, 146). The binding of DGCR5 to miR-873-5p reduces the expression of TUSC3, Ki-67, MMP-3, and MMP-9, and thus decreases the proliferation and migration ability of LC cells (145). LncRNA TDRG1 is a proto-oncogene for CC (147) and endometrial cancer (148). The expression of lncRNA TDRG1 is up-regulated in human GC tissues and is related to the clinical prognosis of GC patients (149). As an important regulator of cancer, HDGF can be down-regulated through the EMT signaling pathway and the MMP-2 and MMP-9 signaling pathways (150). TDRG1 can target the miR-873-5p/HDGF axis, thereby promoting the tumor phenotype of GC cells (149). In addition, TDRG1 up-regulates the expression of ZEB1 by targeting miR-873-5p, thereby promoting tumorigenesis and the development of NSCLC cell lines (151). LncRNA HOTAIRM1 inhibits the miR-873-5p expression and promotes the expression of ZEB2 in GM, thereby inhibiting tumor cell apoptosis (74).

Competitive endogenous RNA (ceRNA) is considered to be a mechanism in post-transcriptional regulation and is related to tumor progression (152, 153). In OS, miR-873-5p targets to inhibit the expression of DDX11, and thus reduces the expression of MMP2, MMP9, N-cadherin, but increases the expression of E-cadherin, thereby inhibiting the migration and EMT process of OS cell lines (154). LncRNA DDX11-AS1 is

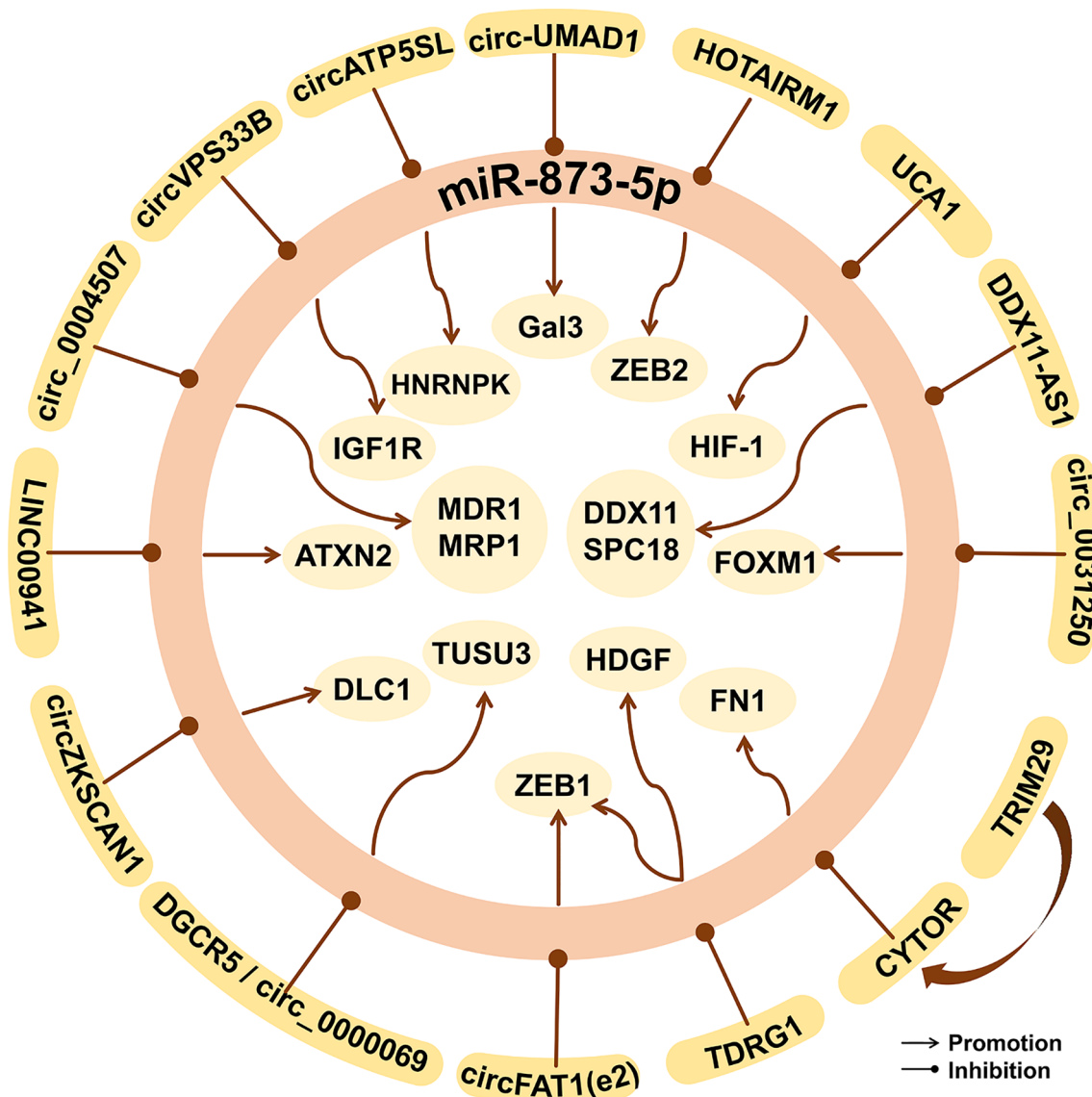


FIGURE 7 | The epigenetic factors of miR-873-5p in human cancer. miR-873-5p can be targeted and regulated by lncRNAs, circRNAs, and other proteins, thus affecting downstream gene expression and playing an important role in cancer.

up-regulated in GC tissues and cell lines, and its expression increases with the development of TNM stages and lymph node metastasis (155). LncRNA DDX11-AS1 as a ceRNA can bind to miR-873-5p and up-regulate the expression of DDX11 in OS and SPC18 in GC, thereby promoting the occurrence and development of OS (154) and GC (155).

Single nucleotide polymorphisms (SNPs) can change the secondary structure of lncRNA, thereby affecting the interaction between lncRNA and its interacting miRNA, and ultimately increasing the risk of cancer (156). The rs12982687 site of lncRNA UCA1 can affect the binding of miR-873-5p, thereby increasing the function of HIF-1 signal transduction, promoting the proliferation and migration of CRC cells (157).

MIR-873-5P AND THE PROGNOSIS OF CANCER PATIENTS

At present, many studies have found that miR-873-5p is significantly related to the prognosis of cancer patients (Table 2). Compared with normal tissues, the expression level of miR-873-5p is increased not only in HCC tissues but also in advanced HCC. Increased expression of miR-873-5p in HCC is positively correlated with lymph node metastasis and metastasis stage, but negatively correlated with tumor differentiation, indicating that miR-873-5p may be related to the aggressiveness and poor prognosis of HCC (5). In addition, low expression of miR-873-5p is associated with poor prognosis of LUAD (29).

TABLE 2 | The prognostic value of miR-873-5p in different cancers.

Cancer	Materials	Results	Reference
HCC	86 HCC tissues and 86 matched non-tumor tissues	The level of miR-873-5p in advanced liver cancer is higher than that in peripheral liver cancer. The overall survival and recurrence time of HCC patients with low miR-873-5p expression levels are much longer than those of HCC patients with high miR-873-5p expression, which indicates that higher miR-873-5p expression is related to the poor prognosis of HCC.	(5)
CRC	50 CRC tissues and 50 adjacent normal tissues; 96 CRC tissues and 96 adjacent normal tissues	The level of miR-873-5p is negatively correlated with the degree of malignancy of CRC. Patients with high miR-873-5p levels have a longer overall survival rate than patients with low miR-873-5p levels, which indicates that lower miR-873-5p expression is related to a poor prognosis of CRC.	(6, 49)
LUAD	481 LUAD tissues and 47 normal tissues	miR-873-5p is an independent prognostic factor of LUAD. The high expression of miR-873-5p indicates that the survival rate of LUAD patients is lower.	(29)
GC	80 GC tissues and 80 adjacent normal tissues	Low miR-873-5p is associated with tumor enlargement in GC patients, advanced T-grade, and poor histological type, and predicts poor OS and DFS.	(52)

LUAD, lung adenocarcinoma; HCC, hepatocellular carcinoma; CRC, carcinoma of colon and rectum; GC, gastric cancer; DFS, disease-free survival; OS, overall survival.

Decreased expression of miR-873-5p is an indicator of poor prognosis in CRC patients (49). In addition, the level of miR-873-5p is negatively correlated with the degree of malignancy of CRC, and high levels of miR-873-5p are significantly correlated with a longer overall survival rate of patients (6). In GC, low expression of miR-873-5p is associated with large tumors, advanced T grade, poor histological type, poor overall survival, and short recurrence-free survival (52). In CC, the overall survival rate of patients with low miR-873-5p expression is lower than that of patients with high miR-873-5p expression (34).

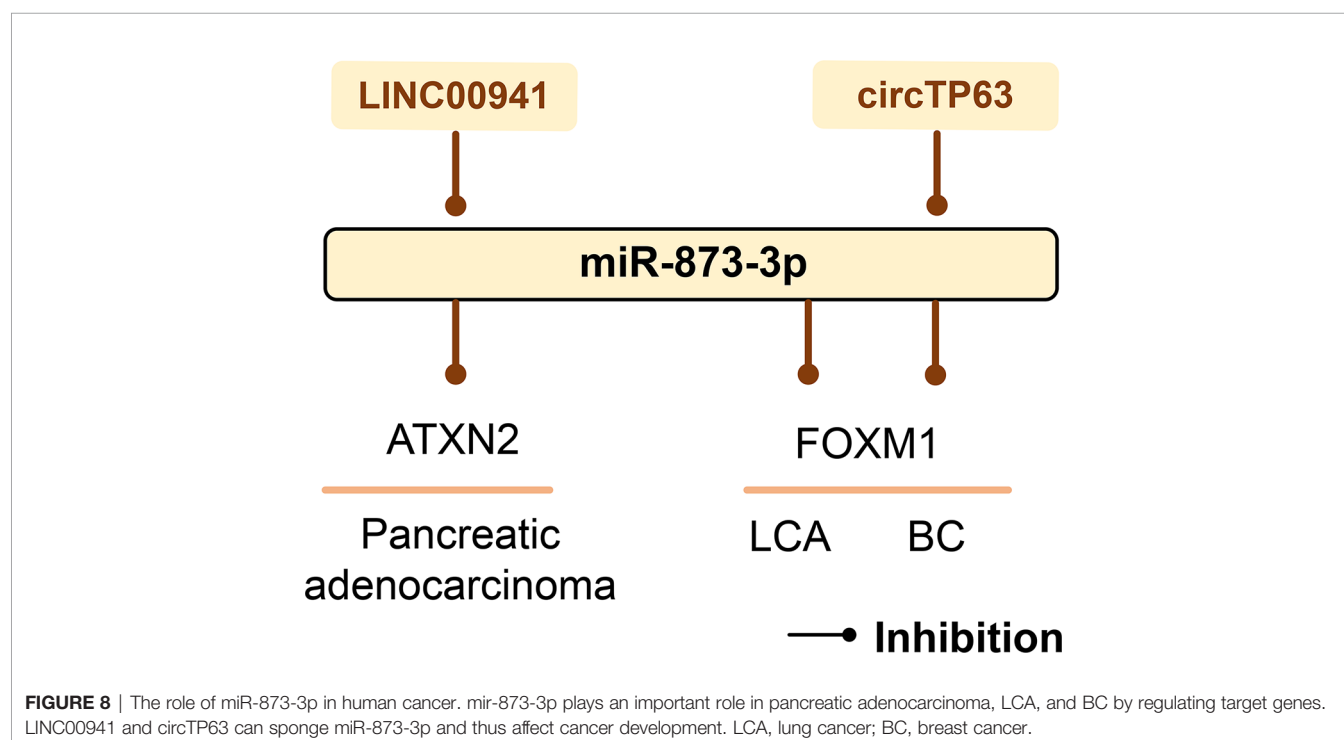
phase (158). miR-873-3p can significantly reduce the mRNA and protein levels of FOXM1. Therefore, miR-873-3p targets FOXM1 to inhibit LCA cell proliferation through its cell cycle regulation function (159). In BC, circTP63 binds to miR-873-3p and prevents its targeted inhibition of FOXM1, thereby inducing the progression and growth of estrogen receptor-positive BC (160). LINC00941 up-regulates the expression of ATXN2 by competitively binding miR-873-3p, stimulates the proliferation and metastasis of pancreatic adenocarcinoma, and promotes its occurrence and development (161) (**Figure 8**).

THE ROLE OF MIR-873-3P IN CANCER

Proliferation-specific fork head box m1 (FOXM1) has been identified as an important cell cycle regulator, which can control the transition of cells from G1 to S phase and cell progression to M

CONCLUSIONS AND PERSPECTIVES

miR-873-5p is widely involved in the progression of cancer, its expression is dysregulated in most cancer tissues and cell lines.



Besides, the target gene of miR-873-5p has a series of molecular regulation functions, such as catalytic activity, transcription regulation, and binding. In cancer, miR-873-5p affects cancer development through the PIK3/AKT/mTOR, Wnt/ β -Catenin, NF- κ B, MEK/ERK signaling pathways. miR-873-5p involves a variety of biological processes through the regulation of target genes, such as cell proliferation and apoptosis, EMT, cell migration and invasion, cell cycle, and cell stemness. miR-873-5p can also inhibit or promote the effects of cancer drugs by regulating its target genes. miR-873-5p can also be used as a specific diagnostic and prognostic indicator for various cancers. Finally, this review also summarizes epigenetic regulatory factors of miR-873-5p, including lncRNA, circRNA, methyltransferase, etc., which are also involved in the occurrence and development of various cancers.

However, there are still many deficiencies in the research on miR-873-5p. First of all, current studies have shown that miR-873-5p is dysregulated in 18 kinds of cancers, and it can cause cancer or suppress cancer. However, existing studies have not proven that miR-873-5p is cancer-specific. This will limit the application of miR-873-5p for cancer diagnosis, and it needs to

be further explored. Second, the specific mechanism of miR-873-5p in some cancers has not been studied. Besides, more preclinical studies and clinical trials are needed to explore the effects of miR-873-5p on the efficacy of anticancer drugs. Finally, most studies are involved with miR-873-5p, and the research on miR-873-3p is very lacking.

Here we show that miR-873-5p plays a significant role in the initiation and progression of key biological and pathological processes in human cancers. Therefore, miR-873-5p can be the main research focus in the fight against human cancers. This review mainly summarizes the research progress of miR-873-5p in human cancers, which will expand our understanding of the molecular and cellular biological mechanisms of miR-873-5p.

AUTHOR CONTRIBUTIONS

SD, ZH, and YZ conceived the review. CZ and YZ collated and analyzed the literature. SD and YZ helped complete diagrams and writing papers. All authors contributed to the article and approved the submitted version.

REFERENCES

- Kumari S, Sharma N, Sahi SV. Advances in Cancer Therapeutics: Conventional Thermal Therapy to Nanotechnology-Based Photothermal Therapy. *Pharmaceutics* (2021) 13(8). doi: 10.3390/pharmaceutics13081174
- Wahid F, Shehzad A, Khan T, Kim YY. MicroRNAs: Synthesis, Mechanism, Function, and Recent Clinical Trials. *Biochim Biophys Acta* (2010) 1803(11):1231–43. doi: 10.1016/j.bbamcr.2010.06.013
- Bartel DP. MicroRNAs: Target Recognition and Regulatory Functions. *Cell* (2009) 136(2):215–33. doi: 10.1016/j.cell.2009.01.002
- Jin S, He J, Li J, Guo R, Shu Y, Liu P. MiR-873 Inhibition Enhances Gefitinib Resistance in non-Small Cell Lung Cancer Cells by Targeting Glioma-Associated Oncogene Homolog 1. *Thorac Cancer* (2018) 9(10):1262–70. doi: 10.1111/1759-7714.12830
- Zhang Y, Zhang C, Zhao Q, Wei W, Dong Z, Shao L, et al. The miR-873/NDP1 Axis Promotes Hepatocellular Carcinoma Growth and Metastasis Through the AKT/mTOR-Mediated Warburg Effect. *Am J Cancer Res* (2019) 9(5):927–44.
- Wang L, Jiang F, Ma F, Zhang B. MiR-873-5p Suppresses Cell Proliferation and Epithelial-Mesenchymal Transition via Directly Targeting Jumonji Domain-Containing Protein 8 Through the NF- κ B Pathway in Colorectal Cancer. *J Cell Commun Signaling* (2019) 13(4):549–60. doi: 10.1007/s12079-019-00522-w
- Pereira A, Moreira F, Vinasco-Sandoval T, Cunha A, Vidal A, Ribeiro-Dos-Santos AM, et al. Mirnome Reveals New Insights Into the Molecular Biology of Field Cancerization in Gastric Cancer. *Front Genet* (2019) 10:592. doi: 10.3389/fgenet.2019.00592
- Li YH, Zhong M, Zang HL, Tian XF. The E3 Ligase for Metastasis Associated 1 Protein, TRIM25, Is Targeted by microRNA-873 in Hepatocellular Carcinoma. *Exp Cell Res* (2018) 368(1):37–41. doi: 10.1016/j.yexcr.2018.04.010
- Chen X, Zhang Y, Shi Y, Lian H, Tu H, Han S, et al. MiR-873 Acts as a Novel Sensitizer of Glioma Cells to Cisplatin by Targeting Bcl-2. *Int J Oncol* (2015) 47(4):1603–11. doi: 10.3892/ijo.2015.3143
- Gao L, Guo Q, Li X, Yang X, Ni H, Wang T, et al. MiR-873/PD-L1 Axis Regulates the Stemness of Breast Cancer Cells. *EBioMedicine* (2019) 41:395–407. doi: 10.1016/j.ebiom.2019.02.034
- Cui J, Yang Y, Li H, Leng Y, Qian K, Huang Q, et al. MiR-873 Regulates ER α Transcriptional Activity and Tamoxifen Resistance via Targeting CDK3 in Breast Cancer Cells. *Oncogene* (2015) 34(30):3895–907. doi: 10.1038/onc.2014.430
- Cohen-Armon M, Visochek L, Rozensal D, Kalal A, Geistrikh I, Klein R, et al. DNA-Independent PARP-1 Activation by Phosphorylated ERK2 Increases Elk1 Activity: A Link to Histone Acetylation. *Mol Cell* (2007) 25(2):297–308. doi: 10.1016/j.molcel.2006.12.012
- Chai Y, Chipitsyna G, Cui J, Liao B, Liu S, Aysola K, et al. C-Fos Oncogene Regulator Elk-1 Interacts With BRCA1 Splice Variants BRCA1a/1b and Enhances BRCA1a/1b-Mediated Growth Suppression in Breast Cancer Cells. *Oncogene* (2001) 20(11):1357–67. doi: 10.1038/sj.onc.1204256
- Sato F, Bhawal UK, Yoshimura T, Muragaki Y. DEC1 and DEC2 Crosstalk Between Circadian Rhythm and Tumor Progression. *J Cancer* (2016) 7(2):153–9. doi: 10.7150/jca.13748
- Zhang P, Sun Y, Ma L. ZEB1: At the Crossroads of Epithelial-Mesenchymal Transition, Metastasis and Therapy Resistance. *Cell Cycle* (2015) 14(4):481–7. doi: 10.1080/15384101.2015.1006048
- Xiao YY, Lin L, Li YH, Jiang HP, Zhu LT, Deng YR, et al. ZEB1 Promotes Invasion and Metastasis of Endometrial Cancer by Interacting With HDGF and Inducing Its Transcription. *Am J Cancer Res* (2019) 9(11):2314–30.
- Houtmeyers R, Souopgui J, Tejpar S, Arkell R. The ZIC Gene Family Encodes Multi-Functional Proteins Essential for Patterning and Morphogenesis. *Cell Mol Life Sci: CMLS* (2013) 70(20):3791–811. doi: 10.1007/s00018-013-1285-5
- Lu SX, Zhang CZ, Luo RZ, Wang CH, Liu LL, Fu J, et al. Zic2 Promotes Tumor Growth and Metastasis via PAK4 in Hepatocellular Carcinoma. *Cancer Lett* (2017) 402:71–80. doi: 10.1016/j.canlet.2017.05.018
- Pourebahram R, Houtmeyers R, Ghogomu S, Janssens S, Thelie A, Tran HT, et al. Transcription Factor Zic2 Inhibits Wnt/ β -Catenin Protein Signaling. *J Biol Chem* (2011) 286(43):37732–40. doi: 10.1074/jbc.M111.242826
- Azmi S, Ozog A, Taneja R. Sharp-1/DEC2 Inhibits Skeletal Muscle Differentiation Through Repression of Myogenic Transcription Factors. *J Biol Chem* (2004) 279(50):52643–52. doi: 10.1074/jbc.M409188200
- Mund T, Pelham HR. Regulation of PTEN/Akt and MAP Kinase Signaling Pathways by the Ubiquitin Ligase Activators Ndfip1 and Ndfip2. *Proc Natl Acad Sci USA* (2010) 107(25):11429–34. doi: 10.1073/pnas.0911714107
- Hyodo T, Ito S, Hasegawa H, Asano E, Maeda M, Urano T, et al. Misshapen-Like Kinase 1 (MINK1) Is a Novel Component of Striatin-Interacting Phosphatase and Kinase (STRIPAK) and is Required for the Completion

- of Cytokinesis. *J Biol Chem* (2012) 287(30):25019–29. doi: 10.1074/jbc.M112.372342
23. Laine A, Martin B, Luka M, Mir L, Auffray C, Lucas B, et al. Foxo1 Is a T Cell-Intrinsic Inhibitor of the RORgammat-Th17 Program. *J Immunol* (2015) 195(4):1791–803. doi: 10.4049/jimmunol.1500849
 24. Kuroda T, Yasuda S, Nakashima H, Takada N, Matsuyama S, Kusakawa S, et al. Identification of a Gene Encoding Slow Skeletal Muscle Troponin T as a Novel Marker for Immortalization of Retinal Pigment Epithelial Cells. *Sci Rep* (2017) 7(1):8163. doi: 10.1038/s41598-017-08014-w
 25. Hu W, Liu Y, Zhou W, Si L, Ren L. CXCL16 and CXCR6 are Coexpressed in Human Lung Cancer *In Vivo* and Mediate the Invasion of Lung Cancer Cell Lines *In Vitro*. *PLoS One* (2014) 9(6):e99056. doi: 10.1371/journal.pone.0099056
 26. Hara T, Katakai T, Lee JH, Nambu Y, Nakajima-Nagata N, Gonda H, et al. A Transmembrane Chemokine, CXC Chemokine Ligand 16, Expressed by Lymph Node Fibroblastic Reticular Cells has the Potential to Regulate T Cell Migration and Adhesion. *Int Immunol* (2006) 18(2):301–11. doi: 10.1093/intimm/dxh369
 27. Hojo S, Koizumi K, Tsuneyama K, Arita Y, Cui Z, Shinohara K, et al. High-Level Expression of Chemokine CXCL16 by Tumor Cells Correlates With a Good Prognosis and Increased Tumor-Infiltrating Lymphocytes in Colorectal Cancer. *Cancer Res* (2007) 67(10):4725–31. doi: 10.1158/0008-5472.CAN-06-3424
 28. Gao Y, Xue Q, Wang D, Du M, Zhang Y, Gao S. miR-873 Induces Lung Adenocarcinoma Cell Proliferation and Migration by Targeting SRCIN1. *Am J Trans Res* (2015) 7(11):2519–26.
 29. Zheng R, Mao W, Du Z, Zhang J, Wang M, Hu M. Three Differential Expression Profiles of miRNAs as Potential Biomarkers for Lung Adenocarcinoma. *Biochem Biophys Res Commun* (2018) 507(1-4):377–82. doi: 10.1016/j.bbrc.2018.11.046
 30. Han G, Zhang L, Ni X, Chen Z, Pan X, Zhu Q, et al. MicroRNA-873 Promotes Cell Proliferation, Migration, and Invasion by Directly Targeting TSLC1 in Hepatocellular Carcinoma. *Cell Physiol Biochem: Int J Exp Cell Physiol Biochem Pharmacol* (2018) 46(6):2261–70. doi: 10.1159/000489594
 31. Ning MS, Kim AS, Prasad N, Levy SE, Zhang H, Andl T. Characterization of the Merkel Cell Carcinoma Mirnome. *J Skin Cancer* (2014) 2014:289548. doi: 10.1155/2014/289548
 32. Lv B, Li F, Liu X, Lin L. The Tumor-Suppressive Role of microRNA-873 in Nasopharyngeal Carcinoma Correlates With Downregulation of ZIC2 and Inhibition of AKT Signaling Pathway. *Cancer Gene Ther* (2021) 28(1-2):74–88. doi: 10.1038/s41417-020-0185-8
 33. Zhang Y, Yang L, Ling C, Heng W. HuR Facilitates Cancer Stemness of Lung Cancer Cells via Regulating miR-873/CDK3 and miR-125a-3p/CDK3 Axis. *Biotechnol Lett* (2018) 40(4):623–31. doi: 10.1007/s10529-018-2512-9
 34. Liang HX, Li YH. MiR-873, as a Suppressor in Cervical Cancer, Inhibits Cells Proliferation, Invasion and Migration via Negatively Regulating ULBP2. *Genes Genomics* (2020) 42(4):371–82. doi: 10.1007/s13258-019-00905-8
 35. Feng J, Wang T. MicroRNA-873 Serves a Critical Role in Human Cervical Cancer Proliferation and Metastasis via Regulating Glioma-Associated Oncogene Homolog 1. *Exp Ther Med* (2020) 19(2):1243–50. doi: 10.3892/etm.2019.8348
 36. Wang Q, Zhu W. MicroRNA-873 Inhibits the Proliferation and Invasion of Endometrial Cancer Cells by Directly Targeting Hepatoma-Derived Growth Factor. *Exp Ther Med* (2019) 18(2):1291–8. doi: 10.3892/etm.2019.7713
 37. Wang G, Dong Y, Liu H, Ji N, Cao J, Liu A, et al. Loss of miR-873 Contributes to Gemcitabine Resistance in Triple-Negative Breast Cancer via Targeting ZEB1. *Oncol Lett* (2019) 18(4):3837–44. doi: 10.3892/ol.2019.10697
 38. Tang L, Chen Y, Tang X, Wei D, Xu X, Yan F. Long Noncoding RNA DCST1-AS1 Promotes Cell Proliferation and Metastasis in Triple-Negative Breast Cancer by Forming a Positive Regulatory Loop With miR-873-5p and MYC. *J Cancer* (2020) 11(2):311–23. doi: 10.7150/jca.33982
 39. Mokhlis HA, Bayraktar R, Kabil NN, Caner A, Kahraman N, Rodriguez-Aguayo C, et al. The Modulatory Role of MicroRNA-873 in the Progression of KRAS-Driven Cancers. *Mol Ther Nucleic Acids* (2019) 14:301–17. doi: 10.1016/j.omtn.2018.11.019
 40. Skalsky RL, Cullen BR. Reduced Expression of Brain-Enriched microRNAs in Glioblastomas Permits Targeted Regulation of a Cell Death Gene. *PLoS One* (2011) 6(9):e24248. doi: 10.1371/journal.pone.0024248
 41. Li K, Zhang Q, Niu D, Xing H. Mining Mirnas' Expressions in Glioma Based on GEO Database and Their Effects on Biological Functions. *BioMed Res Int* (2020) 2020:5637864. doi: 10.1155/2020/5637864
 42. Wang RJ, Li JW, Bao BH, Wu HC, Du ZH, Su JL, et al. MicroRNA-873 (miRNA-873) Inhibits Glioblastoma Tumorigenesis and Metastasis by Suppressing the Expression of IGF2BP1. *J Biol Chem* (2015) 290(14):8938–48. doi: 10.1074/jbc.M114.624700
 43. Liu Y, Wang Y, Yang H, Zhao L, Song R, Tan H, et al. MicroRNA873 Targets HOXA9 to Inhibit the Aggressive Phenotype of Osteosarcoma by Deactivating the Wnt/betacatenin Pathway. *Int J Oncol* (2019) 54(5):1809–20. doi: 10.3892/ijo.2019.4735
 44. Wang Z, Liu W, Wang C, Ai Z. miR-873-5p Inhibits Cell Migration and Invasion of Papillary Thyroid Cancer via Regulation of CXCL16. *Oncotargets Ther* (2020) 13:1037–46. doi: 10.2147/OTT.S213168
 45. Gong H, Fang L, Li Y, Du J, Zhou B, Wang X, et al. Mir873 Inhibits Colorectal Cancer Cell Proliferation by Targeting TRAF5 and TAB1. *Oncol Rep* (2018) 39(3):1090–8. doi: 10.3892/or.2018.6199
 46. Li G, Xu Y, Wang S, Yan W, Zhao Q, Guo J. MiR-873-5p Inhibits Cell Migration, Invasion and Epithelial-Mesenchymal Transition in Colorectal Cancer via Targeting ZEB1. *Pathol Res Pract* (2019) 215(1):34–9. doi: 10.1016/j.prp.2018.10.008
 47. Fan C, Lin B, Huang Z, Cui D, Zhu M, Ma Z, et al. MicroRNA-873 Inhibits Colorectal Cancer Metastasis by Targeting ELK1 and STRN4. *Oncotarget* (2019) 10(41):4192–204. doi: 10.18632/oncotarget.24115
 48. Chen Y, Wang J, Wang D, Kang T, Du J, Yan Z, et al. TNNT1, Negatively Regulated by miR-873, Promotes the Progression of Colorectal Cancer. *J Gene Med* (2020) 22(2):e3152. doi: 10.1002/jgm.3152
 49. Zhu Y, Zhang X, Qi M, Zhang Y, Ding F. miR-873-5p Inhibits the Progression of Colon Cancer via Repression of Tumor Suppressor Candidate 3/AKT Signaling. *J Gastroenterol Hepatol* (2019) 34(12):2126–34. doi: 10.1111/jgh.14697
 50. Liang Y, Zhang P, Li S, Li H, Song S, Lu B. MicroRNA-873 Acts as a Tumor Suppressor in Esophageal Cancer by Inhibiting Differentiated Embryonic Chondrocyte Expressed Gene 2. *Biomed Pharmacother Biomed Pharmacother* (2018) 105:582–9. doi: 10.1016/j.biopha.2018.05.152
 51. Cao D, Yu T, Ou X. MiR-873-5P Controls Gastric Cancer Progression by Targeting Hedgehog-Gli Signaling. *Die Pharmazie* (2016) 71(10):603–6. doi: 10.1691/ph.2016.6618
 52. Lin L, Xiao J, Shi L, Chen W, Ge Y, Jiang M, et al. STRA6 Exerts Oncogenic Role in Gastric Tumorigenesis by Acting as a Crucial Target of miR-873. *J Exp Clin Cancer Res: CR* (2019) 38(1):452. doi: 10.1186/s13046-019-1450-2
 53. Yao Y, Liu XQ, Yang FY, Mu JW. MiR-873-5p Modulates Progression of Tongue Squamous Cell Carcinoma via Targeting SEC11A. *Oral Dis* (2021). doi: 10.1111/odi.13830
 54. Yang XL, Ma YS, Liu YS, Jiang XH, Ding H, Shi Y, et al. microRNA-873 Inhibits Self-Renewal and Proliferation of Pancreatic Cancer Stem Cells Through Pleckstrin-2-Dependent PI3K/AKT Pathway. *Cell Signalling* (2021) 84:110025. doi: 10.1016/j.cellsig.2021.110025
 55. Xu J, Gong L, Qian Z, Song G, Liu J. ERBB4 Promotes the Proliferation of Gastric Cancer Cells via the PI3K/Akt Signaling Pathway. *Oncol Rep* (2018) 39(6):2892–8. doi: 10.3892/or.2018.6343
 56. Chen J, Rajasekaran M, Hui KM. Atypical Regulators of Wnt/beta-Catenin Signaling as Potential Therapeutic Targets in Hepatocellular Carcinoma. *Exp Biol Med* (2017) 242(11):1142–9. doi: 10.1177/1535370217705865
 57. Pahl HL. Activators and Target Genes of Rel/NF-kappaB Transcription Factors. *Oncogene* (1999) 18(49):6853–66. doi: 10.1038/sj.onc.1203239
 58. Guo Q, Wang T, Yang Y, Gao L, Zhao Q, Zhang W, et al. Transcriptional Factor Yin Yang 1 Promotes the Stemness of Breast Cancer Cells by Suppressing miR-873-5p Transcriptional Activity. *Mol Ther Nucleic Acids* (2020) 21:527–41. doi: 10.1016/j.omtn.2020.06.018
 59. Wong M, Hyodo T, Asano E, Funasaka K, Miyahara R, Hirooka Y, et al. Silencing of STRN4 Suppresses the Malignant Characteristics of Cancer Cells. *Cancer Sci* (2014) 105(12):1526–32. doi: 10.1111/cas.12541
 60. Champsaur M, Lanier LL. Effect of NKG2D Ligand Expression on Host Immune Responses. *Immunol Rev* (2010) 235(1):267–85. doi: 10.1111/j.0105-2896.2010.00893.x
 61. Cosman D, Mullberg J, Sutherland CL, Chin W, Armitage R, Fanslow W, et al. ULBPs, Novel MHC Class I-Related Molecules, Bind to CMV

- Glycoprotein UL16 and Stimulate NK Cytotoxicity Through the NKG2D Receptor. *Immunity* (2001) 14(2):123–33. doi: 10.1016/S1074-7613(01)00095-4
62. Yeo KS, Tan MC, Wong WY, Loh SW, Lam YL, Tan CL, et al. JMJD8 is a Positive Regulator of TNF-Induced NF- κ B Signaling. *Sci Rep* (2016) 6:34125. doi: 10.1038/srep34125
 63. Shi Y, Zhao Y, Zhang Y, AiErken N, Shao N, Ye R, et al. TNNT1 Facilitates Proliferation of Breast Cancer Cells by Promoting G1/S Phase Transition. *Life Sci* (2018) 208:161–6. doi: 10.1016/j.lfs.2018.07.034
 64. Hubbard PA, Moody CL, Murali R. Allosteric Modulation of Ras and the PI3K/AKT/mTOR Pathway: Emerging Therapeutic Opportunities. *Front Physiol* (2014) 5:478. doi: 10.3389/fphys.2014.00478
 65. Zang HL, Ren SN, Cao H, Tian XF. The Ubiquitin Ligase TRIM25 Inhibits Hepatocellular Carcinoma Progression by Targeting Metastasis Associated 1 Protein. *IUBMB Life* (2017) 69(10):795–801. doi: 10.1002/iub.1661
 66. Nicolson GL, Nawa A, Toh Y, Taniguchi S, Nishimori K, Moustafa A. Tumor Metastasis-Associated Human MTA1 Gene and its MTA1 Protein Product: Role in Epithelial Cancer Cell Invasion, Proliferation and Nuclear Regulation. *Clin Exp Metastasis* (2003) 20(1):19–24. doi: 10.1023/A:1022534217769
 67. Liu D, Feng X, Wu X, Li Z, Wang W, Tao Y, et al. Tumor Suppressor in Lung Cancer 1 (TSLC1), a Novel Tumor Suppressor Gene, is Implicated in the Regulation of Proliferation, Invasion, Cell Cycle, Apoptosis, and Tumorigenicity in Cutaneous Squamous Cell Carcinoma. *Tumour Biol: J Int Soc Oncodevelopmental Biol Med* (2013) 34(6):3773–83. doi: 10.1007/s13277-013-0961-2
 68. Liu W, Yue F, Zheng M, Merlot A, Bae DH, Huang M, et al. The Proto-Oncogene C-Src and its Downstream Signaling Pathways Are Inhibited by the Metastasis Suppressor, NDRG1. *Oncotarget* (2015) 6(11):8851–74. doi: 10.18632/oncotarget.3316
 69. Le XF, Bast RC Jr. Src Family Kinases and Paclitaxel Sensitivity. *Cancer Biol Ther* (2011) 12(4):260–9. doi: 10.4161/cbt.12.4.16430
 70. Kennedy S, Clynes M, Doolan P, Mehta JP, Rani S, Crown J, et al. SNIP/p140Cap mRNA Expression is an Unfavourable Prognostic Factor in Breast Cancer and is Not Expressed in Normal Breast Tissue. *Br J Cancer* (2008) 98(10):1641–5. doi: 10.1038/sj.bjc.6604365
 71. Elcheva IA, Wood T, Chiarolanzio K, Chim B, Wong M, Singh V, et al. RNA-Binding Protein IGF2BP1 Maintains Leukemia Stem Cell Properties by Regulating HOXB4, MYB, and ALDH1A1. *Leukemia* (2020) 34(5):1354–63. doi: 10.1038/s41375-019-0656-9
 72. Gutschner T, Hammerle M, Pazaitis N, Bley N, Fiskin E, Uckelmann H, et al. Insulin-Like Growth Factor 2 mRNA-Binding Protein 1 (IGF2BP1) is an Important Protumorigenic Factor in Hepatocellular Carcinoma. *Hepatology* (2014) 59(5):1900–11. doi: 10.1002/hep.26997
 73. Goossens S, Janzen V, Bartunkova S, Yokomizo T, Drogat B, Crisan M, et al. The EMT Regulator Zeb2/Sip1 is Essential for Murine Embryonic Hematopoietic Stem/Progenitor Cell Differentiation and Mobilization. *Blood* (2011) 117(21):5620–30. doi: 10.1182/blood-2010-08-300236
 74. Lin YH, Guo L, Yan F, Dou ZQ, Yu Q, Chen G. Long non-Coding RNA HOTAIRM1 Promotes Proliferation and Inhibits Apoptosis of Glioma Cells by Regulating the miR-873-5p/ZEB2 Axis. *Chin Med J* (2020) 133(2):174–82. doi: 10.1097/CM9.0000000000000615
 75. Lawrence HJ, Christensen J, Fong S, Hu YL, Weissman I, Sauvageau G, et al. Loss of Expression of the Hoxa-9 Homeobox Gene Impairs the Proliferation and Repopulating Ability of Hematopoietic Stem Cells. *Blood* (2005) 106(12):3988–94. doi: 10.1182/blood-2005-05-2003
 76. Wang X, Bu J, Liu X, Wang W, Mai W, Lv B, et al. miR-133b Suppresses Metastasis by Targeting HOXA9 in Human Colorectal Cancer. *Oncotarget* (2017) 8(38):63935–48. doi: 10.18632/oncotarget.19212
 77. Ma YY, Zhang Y, Mou XZ, Liu ZC, Ru GQ, Li E. High Level of Homeobox A9 and PBX Homeobox 3 Expression in Gastric Cancer Correlates With Poor Prognosis. *Oncol Lett* (2017) 14(5):5883–9. doi: 10.3892/ol.2017.6937
 78. Armas-Lopez L, Zuniga J, Arrieta O, Avila-Moreno F. The Hedgehog-GLI Pathway in Embryonic Development and Cancer: Implications for Pulmonary Oncology Therapy. *Oncotarget* (2017) 8(36):60684–703. doi: 10.18632/oncotarget.19527
 79. Lemjabbar-Alaoui H, Dasari V, Sidhu SS, Mengistab A, Finkbeiner W, Gallup M, et al. Wnt and Hedgehog are Critical Mediators of Cigarette Smoke-Induced Lung Cancer. *PLoS One* (2006) 1:e93. doi: 10.1371/journal.pone.0000093
 80. Pietrobono S, Santini R, Gagliardi S, Dapporto F, Colecchia D, Chiariello M, et al. Targeted Inhibition of Hedgehog-GLI Signaling by Novel Acylguanidine Derivatives Inhibits Melanoma Cell Growth by Inducing Replication Stress and Mitotic Catastrophe. *Cell Death Dis* (2018) 9(2):142. doi: 10.1038/s41419-017-0142-0
 81. Karunanithi S, Levi L, DeVecchio J, Karagkounis G, Reizes O, Lathia JD, et al. RBP4-STRA6 Pathway Drives Cancer Stem Cell Maintenance and Mediates High-Fat Diet-Induced Colon Carcinogenesis. *Stem Cell Rep* (2017) 9(2):438–50. doi: 10.1016/j.stemcr.2017.06.002
 82. Yager JD, Davidson NE. Estrogen Carcinogenesis in Breast Cancer. *New Engl J Med* (2006) 354(3):270–82. doi: 10.1056/NEJMra050776
 83. Liang K, Liu Y, Eer D, Liu J, Yang F, Hu K. High CXCL16 Expression Promotes Proliferation and Metastasis of Lung Cancer via Regulating the NF- κ B Pathway. *Med Sci Monitor: Int Med J Exp Clin Res* (2018) 24:405–11. doi: 10.12659/MSM.906230
 84. Kishima Y, Yoshida K, Enomoto H, Yamamoto M, Kuroda T, Okuda Y, et al. Antisense Oligonucleotides of Hepatoma-Derived Growth Factor (HDGF) Suppress the Proliferation of Hepatoma Cells. *Hepato-Gastroenterology* (2002) 49(48):1639–44.
 85. Tang J, Shi H, Li H, Zhen T, Dong Y, Zhang F, et al. The Interaction of Hepatoma-Derived Growth Factor and Beta-Catenin Promotes Tumorigenesis of Synovial Sarcoma. *Tumour Biol: J Int Soc Oncodevelopmental Biol Med* (2016) 37(8):10287–301. doi: 10.1007/s13277-016-4905-5
 86. De Craene B, Berx G. Regulatory Networks Defining EMT During Cancer Initiation and Progression. *Nat Rev Cancer* (2013) 13(2):97–110. doi: 10.1038/nrc3447
 87. Spaderna S, Schmalhofer O, Hlubek F, Berx G, Eger A, Merkel S, et al. A Transient, EMT-Linked Loss of Basement Membranes Indicates Metastasis and Poor Survival in Colorectal Cancer. *Gastroenterology* (2006) 131(3):830–40. doi: 10.1053/j.gastro.2006.06.016
 88. Yao X, Wang Y, Duan Y, Zhang Q, Li P, Jin R, et al. IGFBP2 Promotes Salivary Adenoid Cystic Carcinoma Metastasis by Activating the NF- κ B/ZEB1 Signaling Pathway. *Cancer Lett* (2018) 432:38–46. doi: 10.1016/j.canlet.2018.06.008
 89. Gu Y, Wang Q, Guo K, Qin W, Liao W, Wang S, et al. TUSC3 Promotes Colorectal Cancer Progression and Epithelial-Mesenchymal Transition (EMT) Through WNT/beta-Catenin and MAPK Signalling. *J Pathol* (2016) 239(1):60–71. doi: 10.1002/path.4697
 90. Hao YH, Yu SY, Tu RS, Cai YQ. TNNT1, a Prognostic Indicator in Colon Adenocarcinoma, Regulates Cell Behaviors and Mediates EMT Process. *Biosci Biotechnol Biochem* (2020) 84(1):111–7. doi: 10.1080/09168451.2019.1664891
 91. Ye X, Brabletz T, Kang Y, Longmore GD, Nieto MA, Stanger BZ, et al. Upholding a Role for EMT in Breast Cancer Metastasis. *Nature* (2017) 547(7661):E1–3. doi: 10.1038/nature22816
 92. Liu Q, Wu Y, Seino H, Haga T, Yoshizawa T, Morohashi S, et al. Correlation Between DEC1/DEC2 and Epithelial-mesenchymal Transition in Human Prostate Cancer PC3 Cells. *Mol Med Rep* (2018) 18(4):3859–65. doi: 10.3892/mmr.2018.9367
 93. Serman L, Nikuseva Martic T, Serman A, Vranic S. Epigenetic Alterations of the Wnt Signaling Pathway in Cancer: A Mini Review. *Bosnian J Basic Med Sci* (2014) 14(4):191–4. doi: 10.17305/bjbm.2014.4.205
 94. Chen K, Wang G, Peng L, Liu S, Fu X, Zhou Y, et al. CADM1/TSLC1 Inactivation by Promoter Hypermethylation Is a Frequent Event in Colorectal Carcinogenesis and Correlates With Late Stages of the Disease. *Int J Cancer* (2011) 128(2):266–73. doi: 10.1002/ijc.25356
 95. Di Stefano P, Leal MP, Tornillo G, Bisaro B, Repetto D, Pincini A, et al. The Adaptor Proteins P140cap and P130cas as Molecular Hubs in Cell Migration and Invasion of Cancer Cells. *Am J Cancer Res* (2011) 1(5):663–73.
 96. Cabodi S, del Pilar Camacho-Leal M, Di Stefano P, Defilippi P. Integrin Signalling Adaptors: Not Only Figurants in the Cancer Story. *Nat Rev Cancer* (2010) 10(12):858–70. doi: 10.1038/nrc2967
 97. Deryugina EI, Bourdon MA, Luo GX, Reisfeld RA, Strongin A. Matrix Metalloproteinase-2 Activation Modulates Glioma Cell Migration. *J Cell Sci* (1997) 110(Pt 19):2473–82. doi: 10.1242/jcs.110.19.2473

98. Wick W, Wagner S, Kerkau S, Dichgans J, Tonn JC, Weller M. BCL-2 Promotes Migration and Invasiveness of Human Glioma Cells. *FEBS Lett* (1998) 440(3):419–24. doi: 10.1016/S0014-5793(98)01494-X
99. Kessenbrock K, Wang CY, Werb Z. Matrix Metalloproteinases in Stem Cell Regulation and Cancer. *Matrix Biol: J Int Soc Matrix Biol* (2015) 44–46:184–90. doi: 10.1016/j.matbio.2015.01.022
100. Shay G, Lynch CC, Fingleton B. Moving Targets: Emerging Roles for MMPs in Cancer Progression and Metastasis. *Matrix Biol: J Int Soc Matrix Biol* (2015) 44–46:200–6. doi: 10.1016/j.matbio.2015.01.019
101. Won HY, Lee JY, Shin DH, Park JH, Nam JS, Kim HC, et al. Loss of Mel-18 Enhances Breast Cancer Stem Cell Activity and Tumorigenicity Through Activating Notch Signaling Mediated by the Wnt/TCF Pathway. *FASEB J: Off Publ Fed Am Societies Exp Biol* (2012) 26(12):5002–13. doi: 10.1096/fj.12-209247
102. Butler SJ, Richardson L, Farias N, Morrison J, Coomber BL. Characterization of Cancer Stem Cell Drug Resistance in the Human Colorectal Cancer Cell Lines HCT116 and SW480. *Biochem Biophys Res Commun* (2017) 490(1):29–35. doi: 10.1016/j.bbrc.2017.05.176
103. Ishibashi M, Tamura H, Sunakawa M, Kondo-Onodera A, Okuyama N, Hamada Y, et al. Myeloma Drug Resistance Induced by Binding of Myeloma B7-H1 (PD-L1) to PD-1. *Cancer Immunol Res* (2016) 4(9):779–88. doi: 10.1158/2326-6066.CIR-15-0296
104. Almozayn S, Colak D, Mansour F, Alaiya A, Al-Harazi O, Qattan A, et al. PD-L1 Promotes OCT4 and Nanog Expression in Breast Cancer Stem Cells by Sustaining PI3K/AKT Pathway Activation. *Int J Cancer* (2017) 141(7):1402–12. doi: 10.1002/ijc.30834
105. Soliman H, Khalil F, Antonia S. PD-L1 Expression Is Increased in a Subset of Basal Type Breast Cancer Cells. *PLoS One* (2014) 9(2):e88557. doi: 10.1371/journal.pone.0088557
106. Liu S, Chen S, Yuan W, Wang H, Chen K, Li D, et al. PD-1/PD-L1 Interaction Up-Regulates MDR1/P-Gp Expression in Breast Cancer Cells via PI3K/AKT and MAPK/ERK Pathways. *Oncotarget* (2017) 8(59):99901–12. doi: 10.18632/oncotarget.21914
107. Zhang W, Vreeland AC, Noy N. RNA-Binding Protein HuR Regulates Nuclear Import of Protein. *J Cell Sci* (2016) 129(21):4025–33. doi: 10.1242/jcs.192096
108. Wang J, Ma W, Liu Y. Long non-Coding RNA HULC Promotes Bladder Cancer Cells Proliferation But Inhibits Apoptosis via Regulation of ZIC2 and PI3K/AKT Signaling Pathway. *Cancer Biomarkers: Section A Dis Markers* (2017) 20(4):425–34. doi: 10.3233/CBM-170188
109. Lv B, Li F, Liu X, Lin L. The Tumor-Suppressive Role of microRNA-873 in Nasopharyngeal Carcinoma Correlates With Downregulation of ZIC2 and Inhibition of AKT Signaling Pathway. *Cancer Gene Ther* (2020). doi: 10.1038/s41417-020-0185-8
110. Qu C, He, Lu X, Dong L, Zhu Y, Zhao Q, et al. Salt-Inducible Kinase (SIK1) Regulates HCC Progression and WNT/beta-Catenin Activation. *J Hepatol* (2016) 64(5):1076–89. doi: 10.1016/j.jhep.2016.01.005
111. Song H, Pu J, Wang L, Wu L, Xiao J, Liu Q, et al. ATG16L1 Phosphorylation is Oppositely Regulated by CSNK2/casein Kinase 2 and PPP1/protein Phosphatase 1 Which Determines the Fate of Cardiomyocytes During Hypoxia/Reoxygenation. *Autophagy* (2015) 11(8):1308–25. doi: 10.1080/15548627.2015.1060386
112. Lee DH. Treatments for EGFR-Mutant Non-Small Cell Lung Cancer (NSCLC): The Road to a Success, Paved With Failures. *Pharmacol Ther* (2017) 174:1–21. doi: 10.1016/j.pharmthera.2017.02.001
113. Duan X, Shi J. Advance in microRNAs and EGFR-TKIs Secondary Resistance Research in non-Small Cell Lung Cancer. *Zhongguo Fei Ai Za Zhi Chin J Lung Cancer* (2014) 17(12):860–4. doi: 10.3779/j.issn.1009-3419.2014.12.07
114. Xie SY, Li G, Han C, Yu YY, Li N. RKIP Reduction Enhances Radioresistance by Activating the Shh Signaling Pathway in Non-Small-Cell Lung Cancer. *OncoTargets Ther* (2017) 10:5605–19. doi: 10.2147/OTT.S149200
115. Bora-Singhal N, Perumal D, Nguyen J, Chellappan S. Gli1-Mediated Regulation of Sox2 Facilitates Self-Renewal of Stem-Like Cells and Confers Resistance to EGFR Inhibitors in Non-Small Cell Lung Cancer. *Neoplasia* (2015) 17(7):538–51. doi: 10.1016/j.neo.2015.07.001
116. Yu F, Yao H, Zhu P, Zhang X, Pan Q, Gong C, et al. Let-7 Regulates Self Renewal and Tumorigenicity of Breast Cancer Cells. *Cell* (2007) 131(6):1109–23. doi: 10.1016/j.cell.2007.10.054
117. Jin D, Wu Y, Shao C, Gao Y, Wang D, Guo J. Norcantharidin Reverses Cisplatin Resistance and Inhibits the Epithelial Mesenchymal Transition of Human Non-small Lung Cancer Cells by Regulating the YAP Pathway. *Oncol Rep* (2018) 40(2):609–20. doi: 10.3892/or.2020.7830
118. Mo L, Zhang X, Shi X, Wei L, Zheng D, Li H, et al. Norcantharidin Enhances Antitumor Immunity of GM-CSF Prostate Cancer Cells Vaccine by Inducing Apoptosis of Regulatory T Cells. *Cancer Sci* (2018) 109(7):2109–18. doi: 10.1111/cas.13639
119. Zhang JT, Sun W, Zhang WZ, Ge CY, Liu ZY, Zhao ZM, et al. Norcantharidin Inhibits Tumor Growth and Vasculogenic Mimicry of Human Gallbladder Carcinomas by Suppression of the PI3-K/MMPs/Ln-5gamma2 Signaling Pathway. *BMC Cancer* (2014) 14:193. doi: 10.1186/1471-2407-14-193
120. Zhang X, Zhang B, Zhang P, Lian L, Li L, Qiu Z, et al. Norcantharidin Regulates ERalpha Signaling and Tamoxifen Resistance via Targeting miR-873/CDK3 in Breast Cancer Cells. *PLoS One* (2019) 14(5):e0217181. doi: 10.1371/journal.pone.0217181
121. Papa AL, Sidiqui A, Balasubramanian SU, Sarangi S, Luchette M, Sengupta S, et al. PEGylated Liposomal Gemcitabine: Insights Into a Potential Breast Cancer Therapeutic. *Cell Oncol* (2013) 36(6):449–57. doi: 10.1007/s13402-013-0146-4
122. Kumar S, Kumar A, Shah PP, Rai SN, Panguluri SK, Kakar SS. MicroRNA Signature of Cis-Platin Resistant vs. Cis-Platin Sensitive Ovarian Cancer Cell Lines. *J Ovarian Res* (2011) 4(1):17. doi: 10.1186/1757-2215-4-17
123. Qiu JG, Zhang YJ, Li Y, Zhao JM, Zhang WJ, Jiang QW, et al. Trametinib Modulates Cancer Multidrug Resistance by Targeting ABCB1 Transporter. *Oncotarget* (2015) 6(17):15494–509. doi: 10.18632/oncotarget.3820
124. Hung TH, Hsu SC, Cheng CY, Choo KB, Tseng CP, Chen TC, et al. Wnt5A Regulates ABCB1 Expression in Multidrug-Resistant Cancer Cells Through Activation of the Non-Canonical PKA/beta-Catenin Pathway. *Oncotarget* (2014) 5(23):12273–90. doi: 10.18632/oncotarget.2631
125. Gisel A, Valvano M, El Idrissi IG, Nardulli P, Azzariti A, Carrieri A, et al. miRNAs for the Detection of Multidrug Resistance: Overview and Perspectives. *Molecules* (2014) 19(5):5611–23. doi: 10.3390/molecules19055611
126. Wu DD, Li XS, Meng XN, Yan J, Zong ZH. MicroRNA-873 Mediates Multidrug Resistance in Ovarian Cancer Cells by Targeting ABCB1. *Tumour Biol: J Int Soc Oncodevelopmental Biol Med* (2016) 37(8):10499–506. doi: 10.1007/s13277-016-4944-y
127. Rocha CR, Garcia CC, Vieira DB, Quinet A, de Andrade-Lima LC, Munford V, et al. Glutathione Depletion Sensitizes Cisplatin- and Temozolomide-Resistant Glioma Cells *In Vitro* and *In Vivo*. *Cell Death Dis* (2015) 6:e1727. doi: 10.1038/cddis.2015.101
128. Baraniskin A, Kuhnhen U, Schlegel U, Maghnouj A, Zollner H, Schmiegel W, et al. Identification of microRNAs in the Cerebrospinal Fluid as Biomarker for the Diagnosis of Glioma. *Neuro-Oncology* (2012) 14(1):29–33. doi: 10.1093/neuonc/nor169
129. Zhu CJ, Li YB, Wong MC. Expression of Antisense Bcl-2 cDNA Abolishes Tumorigenicity and Enhances Chemosensitivity of Human Malignant Glioma Cells. *J Neurosci Res* (2003) 74(1):60–6. doi: 10.1002/jnr.10722
130. Komeil IA, El-Refaie WM, Gawayed MA, El-Ganainy SO, El Achy SN, Huttunen KM, et al. Oral Genistein-Loaded Phytosomes With Enhanced Hepatic Uptake, Residence and Improved Therapeutic Efficacy Against Hepatocellular Carcinoma. *Int J Pharmaceut* (2021) 601:120564. doi: 10.1016/j.ijpharm.2021.120564
131. Yu Y, Xing Y, Zhang Q, Zhang Q, Huang S, Li X, et al. Soy Isoflavone Genistein Inhibits Hsa_Circ_0031250/miR-873-5p/FOXO1 Axis to Suppress Non-Small-Cell Lung Cancer Progression. *IUBMB Life* (2021) 73(1):92–107. doi: 10.1002/iub.2404
132. Hansen TB, Jensen TI, Clausen BH, Bramsen JB, Finsen B, Damgaard CK, et al. Natural RNA Circles Function as Efficient microRNA Sponges. *Nature* (2013) 495(7441):384–8. doi: 10.1038/nature11993
133. Zhang S, Chen Z, Sun J, An N, Xi Q. CircRNA Hsa_circRNA_0000069 Promotes the Proliferation, Migration and Invasion of Cervical Cancer Through miR-873-5p/TUSC3 Axis. *Cancer Cell Int* (2020) 20:287. doi: 10.1186/s12935-020-01387-5
134. Yang J, Yu L, Yan J, Xiao Y, Li W, Xiao J, et al. Circular RNA DGKB Promotes the Progression of Neuroblastoma by Targeting miR-873/GLI1 Axis. *Front Oncol* (2020) 10:1104. doi: 10.3389/fonc.2020.01104

135. Yu W, Ma B, Zhao W, Liu J, Yu H, Tian Z, et al. The Combination of circRNA-UMAD1 and Galectin-3 in Peripheral Circulation Is a Co-Biomarker for Predicting Lymph Node Metastasis of Thyroid Carcinoma. *Am J Trans Res* (2020) 12(9):5399–415.
136. Liu J, Li H, Wei C, Ding J, Lu J, Pan G, et al. Circfat1(E2) Promotes Papillary Thyroid Cancer Proliferation, Migration, and Invasion via the miRNA-873/ZEB1 Axis. *Comput Math Methods Med* (2020) 2020:1459368. doi: 10.1155/2020/1459368
137. Yi X, Chen W, Li C, Chen X, Lin Q, Lin S, et al. Circular RNA Circ_0004507 Contributes to Laryngeal Cancer Progression and Cisplatin Resistance by Sponging miR-873 to Upregulate Multidrug Resistance 1 and Multidrug Resistance Protein 1. *Head Neck* (2021) 43(3):928–41. doi: 10.1002/hed.26549
138. Li J, Bao S, Wang L, Wang R. CircZKSCAN1 Suppresses Hepatocellular Carcinoma Tumorigenesis by Regulating miR-873-5p/Downregulation of Deleted in Liver Cancer 1. *Digestive Dis Sci* (2021). doi: 10.1007/s10620-020-06789-z
139. Wei Z, Yuan X, Ding Q, Xu Y, Hong L, Wang J. CircATP5SL Promotes Infantile Haemangiomas Progression via IGF1R Regulation by Targeting miR-873-5p. *Am J Trans Res* (2021) 13(3):1322–36.
140. Lu Y, Cheng J, Cai W, Zhuo H, Wu G, Cai J. Inhibition of circRNA Circvps33b Reduces Warburg Effect and Tumor Growth Through Regulating the miR-873-5p/HNRNP K Axis in Infiltrative Gastric Cancer. *Oncotargets Ther* (2021) 14:3095–108. doi: 10.2147/OTT.S292575
141. Li S, Lin L. Long Noncoding RNA MCF2L-AS1 Promotes the Cancer Stem Cell-Like Traits in Non-Small Cell Lung Cancer Cells Through Regulating miR-873-5p Level. *Environ Toxicol* (2021) 36(7):1457–65. doi: 10.1002/tox.23142
142. Shi Y, Seto E, Chang LS, Shenk T. Transcriptional Repression by YY1, a Human GLI-Kruppel-Related Protein, and Relief of Repression by Adenovirus E1A Protein. *Cell* (1991) 67(2):377–88. doi: 10.1016/0092-8674(91)90189-6
143. Yue B, Cai D, Liu C, Fang C, Yan D. Linc00152 Functions as a Competing Endogenous RNA to Confer Oxaliplatin Resistance and Holds Prognostic Values in Colon Cancer. *Mol Ther: J Am Soc Gene Ther* (2016) 24(12):2064–77. doi: 10.1038/mt.2016.180
144. Wu T, Zhang DL, Wang JM, Jiang JY, Du X, Zeng XY, et al. TRIM29 Inhibits miR-873-5P Biogenesis via CYTOR to Upregulate Fibronectin 1 and Promotes Invasion of Papillary Thyroid Cancer Cells. *Cell Death Dis* (2020) 11(9):813. doi: 10.1038/s41419-020-03018-3
145. Luo J, Zhu H, Jiang H, Cui Y, Wang M, Ni X, et al. The Effects of Aberrant Expression of LncRNA DGCR5/miR-873-5p/TUSC3 in Lung Cancer Cell Progression. *Cancer Med* (2018). doi: 10.1002/cam4.1566
146. Scholzen T, Gerdes J. The Ki-67 Protein: From the Known and the Unknown. *J Cell Physiol* (2000) 182(3):311–22. doi: 10.1002/(SICI)1097-4652(200003)182:3<311::AID-JCP1>3.0.CO;2-9
147. Jiang H, Liang M, Jiang Y, Zhang T, Mo K, Su S, et al. The LncRNA TDRG1 Promotes Cell Proliferation, Migration and Invasion by Targeting miR-326 to Regulate MAPK1 Expression in Cervical Cancer. *Cancer Cell Int* (2019) 19:152. doi: 10.1186/s12935-019-0872-4
148. Chen S, Wang LL, Sun KX, Liu Y, Guan X, Zong ZH, et al. LncRNA TDRG1 Enhances Tumorigenicity in Endometrial Carcinoma by Binding and Targeting VEGF-A Protein. *Biochim Biophys Acta Mol Basis Dis* (2018) 1864(9 Pt B):3013–21. doi: 10.1016/j.bbdis.2018.06.013
149. Ma Y, Xu XL, Huang HG, Li YF, Li ZG. LncRNA TDRG1 Promotes the Aggressiveness of Gastric Carcinoma Through Regulating miR-873-5p/HDGF Axis. *Biomed Pharmacother Biomed Pharmacother* (2020) 121:109425. doi: 10.1016/j.biopha.2019.109425
150. Li M, Shen J, Wu X, Zhang B, Zhang R, Weng H, et al. Downregulated Expression of Hepatoma-Derived Growth Factor (HDGF) Reduces Gallbladder Cancer Cell Proliferation and Invasion. *Med Oncol* (2013) 30(2):587. doi: 10.1007/s12032-013-0587-7
151. Hu X, Mu Y, Wang J, Zhao Y. LncRNA TDRG1 Promotes the Metastasis of NSCLC Cell Through Regulating miR-873-5p/ZEB1 Axis. *J Cell Biochem* (2019). doi: 10.1002/jcb.29559
152. Lian Y, Xiong F, Yang L, Bo H, Gong Z, Wang Y, et al. Long Noncoding RNA AFAP1-AS1 Acts as a Competing Endogenous RNA of miR-423-5p to Facilitate Nasopharyngeal Carcinoma Metastasis Through Regulating the Rho/Rac Pathway. *J Exp Clin Cancer Res: CR* (2018) 37(1):253. doi: 10.1186/s13046-018-0918-9
153. Feng K, Liu Y, Xu LJ, Zhao LF, Jia CW, Xu MY. Long Noncoding RNA PVT1 Enhances the Viability and Invasion of Papillary Thyroid Carcinoma Cells by Functioning as ceRNA of microRNA-30a Through Mediating Expression of Insulin Like Growth Factor 1 Receptor. *Biomed Pharmacother Biomed Pharmacother* (2018) 104:686–98. doi: 10.1016/j.biopha.2018.05.078
154. Zhang H, Lin J, Chen J, Gu W, Mao Y, Wang H, et al. DDX11-AS1 Contributes to Osteosarcoma Progression via Stabilizing DDX11. *Life Sci* (2020) 254:117392. doi: 10.1016/j.lfs.2020.117392
155. Ren Z, Liu X, Si Y, Yang D. Long non-Coding RNA DDX11-AS1 Facilitates Gastric Cancer Progression by Regulating miR-873-5p/SPC18 Axis. *Artif Cells Nanomed Biotechnol* (2020) 48(1):572–83. doi: 10.1080/21691401.2020.1726937
156. Gong J, Liu W, Zhang J, Miao X, Guo AY. lncRNASNP: A Database of SNPs in lncRNAs and Their Potential Functions in Human and Mouse. *Nucleic Acids Res* (2015) 43(Database issue):D181–6. doi: 10.1093/nar/gku1000
157. Fu Y, Zhang Y, Cui J, Yang G, Peng S, Mi W, et al. SNP Rs12982687 Affects Binding Capacity of lncRNA UCA1 With miR-873-5p: Involvement in Smoking-Triggered Colorectal Cancer Progression. *Cell Commun Signaling: CCS* (2020) 18(1):37. doi: 10.1186/s12964-020-0518-0
158. Kim IM, Ackerson T, Ramakrishna S, Tretiakova M, Wang IC, Kalin TV, et al. The Forkhead Box M1 Transcription Factor Stimulates the Proliferation of Tumor Cells During Development of Lung Cancer. *Cancer Res* (2006) 66(4):2153–61. doi: 10.1158/0008-5472.CAN-05-3003
159. Cheng Z, Yu C, Cui S, Wang H, Jin H, Wang C, et al. Circp63 Functions as a ceRNA to Promote Lung Squamous Cell Carcinoma Progression by Upregulating FOXM1. *Nat Commun* (2019) 10(1):3200. doi: 10.1038/s41467-019-11162-4
160. Deng Y, Xia J, Xu YE. Circular RNA Circp63 Enhances Estrogen Receptor-Positive Breast Cancer Progression and Malignant Behaviors Through the miR-873-3p/FOXM1 Axis. *Anti-Cancer Drugs* (2021) 32(1):44–52. doi: 10.1097/CAD.0000000000001010
161. Fang L, Wang SH, Cui YG, Huang L. LINC00941 Promotes Proliferation and Metastasis of Pancreatic Adenocarcinoma by Competitively Binding miR-873-3p and Thus Upregulates ATXN2. *Eur Rev Med Pharmacol Sci* (2021) 25(4):1861–8. doi: 10.26355/eurev.202102_25081

Conflict of Interest: The authors declare that the research was conducted in the absence of any commercial or financial relationships that could be construed as a potential conflict of interest.

Publisher's Note: All claims expressed in this article are solely those of the authors and do not necessarily represent those of their affiliated organizations, or those of the publisher, the editors and the reviewers. Any product that may be evaluated in this article, or claim that may be made by its manufacturer, is not guaranteed or endorsed by the publisher.

Copyright © 2021 Zou, Zhong, Hu and Duan. This is an open-access article distributed under the terms of the Creative Commons Attribution License (CC BY). The use, distribution or reproduction in other forums is permitted, provided the original author(s) and the copyright owner(s) are credited and that the original publication in this journal is cited, in accordance with accepted academic practice. No use, distribution or reproduction is permitted which does not comply with these terms.



SNHG10 Is a Prognostic Biomarker Correlated With Immune Infiltrates in Prostate Cancer

Qiang Chen, Xiaorong Yang, Binbin Gong, Wenjie Xie, Ming Ma, Shengqiang Fu, Siyuan Wang, Yutang Liu, Zhicheng Zhang, Ting Sun and Zhilong Li*

Department of Urology, The First Affiliated Hospital of Nanchang University, Nanchang, China

OPEN ACCESS

Edited by:

Shiv K. Gupta,
Mayo Clinic, United States

Reviewed by:

Jiao Hu,
Central South University, China
Michaela B. Kirschner,
University of Zurich, Switzerland

*Correspondence:

Zhilong Li
18770426026@163.com

Specialty section:

This article was submitted to
Molecular and Cellular Oncology,
a section of the journal
Frontiers in Cell and Developmental
Biology

Received: 26 June 2021

Accepted: 09 September 2021

Published: 05 October 2021

Citation:

Chen Q, Yang X, Gong B, Xie W,
Ma M, Fu S, Wang S, Liu Y, Zhang Z,
Sun T and Li Z (2021) SNHG10 Is
a Prognostic Biomarker Correlated
With Immune Infiltrates in Prostate
Cancer.
Front. Cell Dev. Biol. 9:731042.
doi: 10.3389/fcell.2021.731042

SNHG10 is a long non-coding RNA (lncRNA) found to be overexpressed in multiple human cancers including prostate cancer (PC). However, the underlying mechanisms of SNHG10 driving the progression of PC remains unclear. In this study, we investigated the role of SNHG10 in PC and found that SNHG10 expression was significantly increased in datasets extracted from The Cancer Genome Atlas. Increased expression of SNHG10 was related to advanced clinical parameters. Receiver operating curve analysis revealed the significant diagnostic ability of SNHG10 (AUC = 0.805). In addition, immune infiltration analysis, and GSEA showed that SNHG10 expression was correlated with oxidative phosphorylation and immune infiltrated cells. Finally, we determined that SNHG10 regulated cell proliferation, migration, and invasion of PC *in vitro*. In conclusion, our data demonstrated that SNHG10 was correlated with progression and immune infiltration, and could serve as a prognostic biomarker for PC.

Keywords: SNHG10, prostate cancer, prognosis, biomarker, proliferation

INTRODUCTION

Prostate cancer (PC) is the most frequently diagnosed malignancy among men worldwide accounting for approximately 21% of new cancer cases in 2020 (Siegel et al., 2020). With the development of magnetic resonance imaging (MRI) and prostate specific antigen (PSA) screening, detection of PC has increased (Hayes and Barry, 2014; Rastinehad et al., 2014). Although androgen deprivation therapy (ADT) has improved the prognosis of patients with localized PC, progression to castration-resistant PC is inevitable. Therefore, it is critical to identify significant biomarkers for diagnosing the occurrence and progression of PC.

Long noncoding RNAs (lncRNAs) belong to a subset of non-coding RNA transcripts of over 200 nucleotides in length (Shi et al., 2013; Hua et al., 2019; Goodall and Wickramasinghe, 2021). Recent studies have indicated that lncRNAs might play a crucial role in the progression of different cancers (De Troyer et al., 2020; Luo et al., 2020; Statello et al., 2021). For example, the lncRNA NEAT1 promotes PC metastasis to the bone (Wen et al., 2020). lncRNA PVT1 plays a pivotal role in PC progression by inhibiting KIF23 expression via enriched miR-15a-5p levels (Wu et al., 2020). Small nucleolar RNA host gene 10 (SNHG10) has been reported to be a cancer-promoting gene in various human cancers. For instance, SNHG10 promotes cell proliferation and invasion in osteosarcoma (Zhu et al., 2020). Recently, SNHG10 has been identified as having a tumor facilitator role in hepatocellular carcinoma and gastric carcinoma (Lan et al., 2019; Zhang et al., 2020). However,

the clinical value of SNHG10 in PC has not been explored. Hence, this study aimed to investigate the role of SNHG10 in the progression of PC.

In this study, we compared the expression of SNHG10 between PC tissues and normal samples, and investigated the correlation between SNHG10 expression and clinical parameters of PC. In addition, we explored the prognostic value and clinical significance of SNHG10 in PC. Meanwhile, the correlation between SNHG10 expression and immune infiltration was analyzed to explore the potential mechanisms involved in SNHG10 modulation in the carcinogenesis of PC. Finally, the biological role of SNHG10 was identified in PC. In summary,

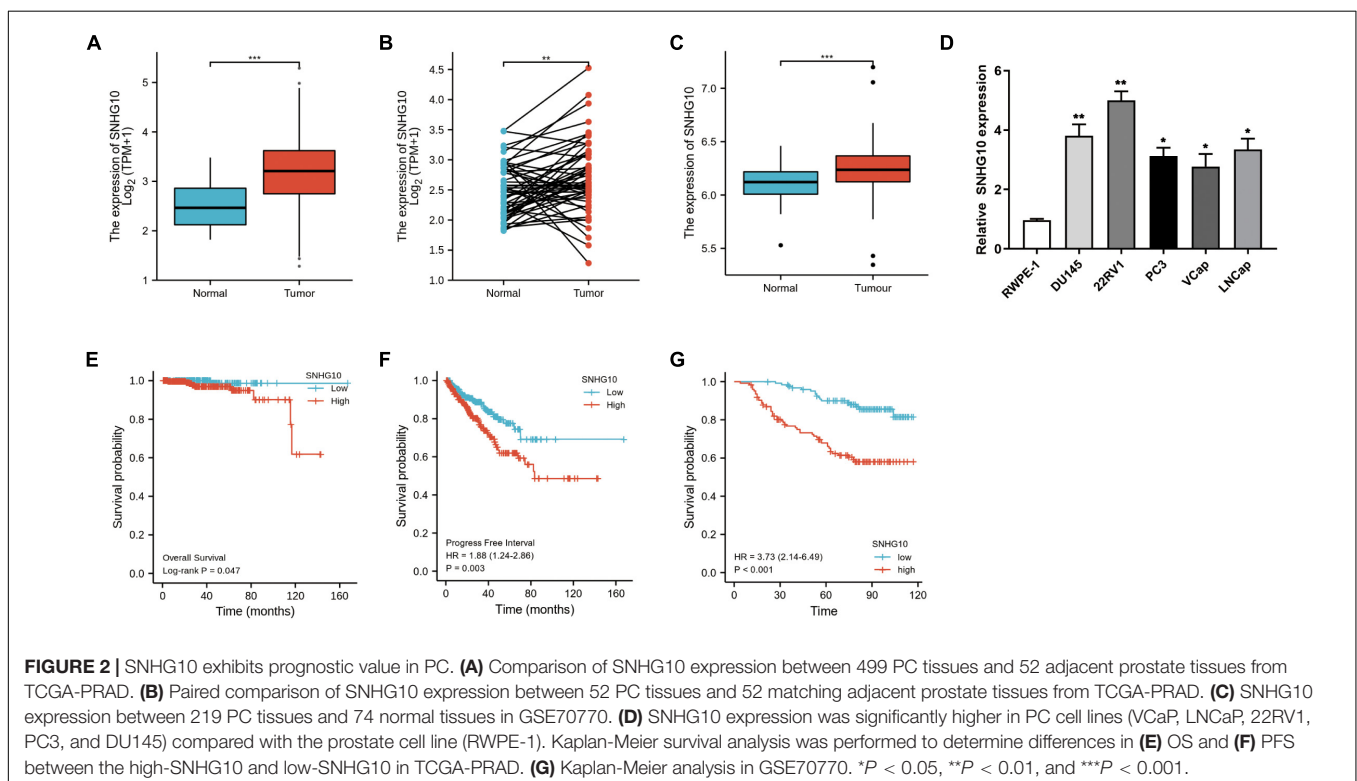
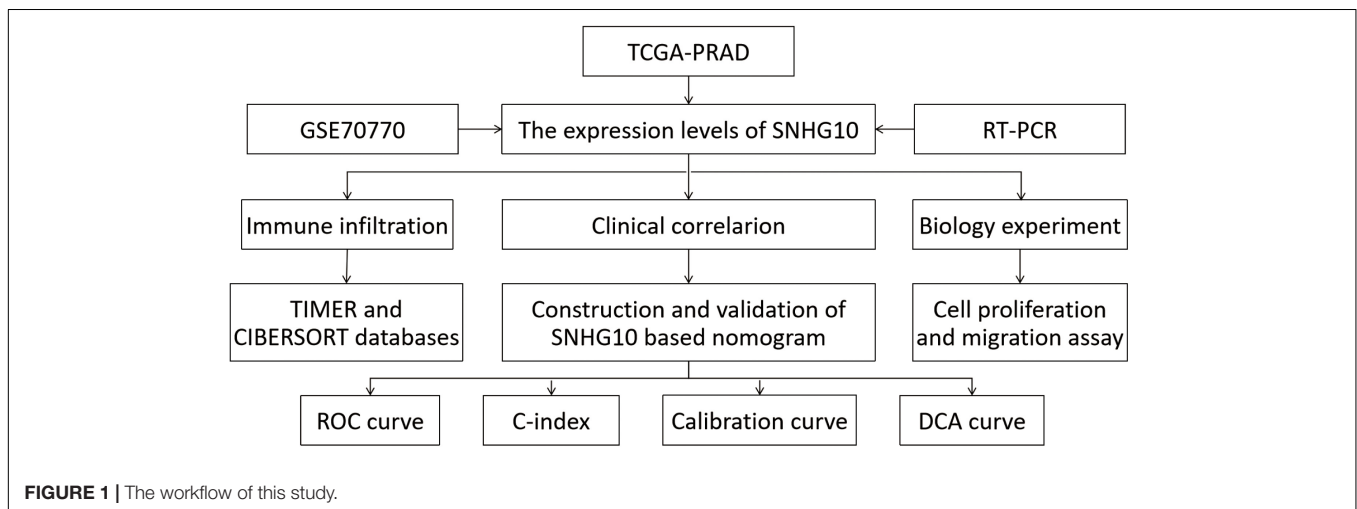
we demonstrated that the potential role of SNHG10 in regulating tumor progression and its potential application in the diagnosis and prognostic evaluation in PC.

MATERIALS AND METHODS

Data Source

The gene expression profiles of PC patients were downloaded from The Cancer Genome Atlas (TCGA) database¹, as well as

¹<https://portal.gdc.cancer.gov>



the corresponding clinical and DNA methylation information. This included 499 PC samples and 52 adjacent normal tissues which were retrospectively studied. For validation, additional PRAD cohorts of 293 and 248 patients were obtained with the accession number GSE70770 and GSE116918 from the GEO database². Gene expression data and clinical data were downloaded.

Construction and Validation of the Nomogram

Firstly, patients that lack information of T stage, N stage, PSA, Gleason score, residual tumor, SNHG10 expression, and survival status were excluded from following analysis. Then, 288 prostate cancer samples were screened from the TCGA data. These samples were randomly classified into the training cohort ($n = 144$) and the test cohort

($n = 144$). Subsequently, we developed the nomogram in the training cohort using cox regression analysis, and validated in the test cohort. R package “rms” was used to establish the nomogram for predict the probability of 3-year and 5-year survival. The ROC curve for nomogram was performed via “timeROC” R package. The calibration curve was conducted via “calibrate” function of “rms” R package. We performed the DCA analysis of survival outcome by “ggDCA” R package.

Gene Set Enrichment Analysis

The Gene set enrichment analysis (GSEA) was downloaded from the GSEA website³. A customized Perl script⁴ was used to perform GSEA between high-SNHG10 and low-SNHG10

²<https://www.ncbi.nlm.nih.gov/gds>

³<http://www.gsea-msigdb.org/gsea/index.jsp>

⁴<https://www.perl.org>

TABLE 1 | Correlation between SNHG10 expression and clinical parameters in PC.

Clinical parameters	Levels	Low expression of SNHG10	High expression of SNHG10	P-value
n		249	250	
T stage, n (%)	T2	101 (20.5%)	88 (17.9%)	0.013
	T3/T4	144 (29.3%)	159 (32.3%)	
N stage, n (%)	N0	173 (40.6%)	174 (40.8%)	0.005
	N1	30 (7%)	49 (11.5%)	
M stage, n (%)	M0	226 (49.3%)	229 (50%)	1.000
	M1	1 (0.2%)	2 (0.4%)	
Gleason score, n (%)	6	26 (5.2%)	20 (4%)	<0.001
	7	147 (29.5%)	100 (20%)	
	8	21 (4.2%)	43 (8.6%)	
	9	52 (10.4%)	86 (17.2%)	
	10	3 (0.6%)	1 (0.2%)	
Primary therapy outcome, n (%)	PD	17 (3.9%)	11 (2.5%)	<0.001
	SD	8 (1.8%)	21 (4.8%)	
	PR	12 (2.7%)	28 (6.4%)	
	CR	188 (42.9%)	153 (34.9%)	
Residual tumor, n (%)	R0	168 (35.9%)	147 (31.4%)	0.112
	R1	66 (14.1%)	82 (17.5%)	
	R2	4 (0.9%)	1 (0.2%)	
Zone of origin, n (%)	Central Zone	2 (0.7%)	2 (0.7%)	0.541
	Overlapping/Multiple Zones	48 (17.5%)	78 (28.4%)	
	Peripheral Zone	43 (15.6%)	94 (34.2%)	
	Transition Zone	2 (0.7%)	6 (2.2%)	
PSA (ng/ml), n (%)	<4	211 (47.7%)	204 (46.2%)	0.942
	≥4	13 (2.9%)	14 (3.2%)	
Age, n (%)	≤60	120 (24%)	104 (20.8%)	0.164
	> 60	129 (25.9%)	146 (29.3%)	
Race, n (%)	Asian	4 (0.8%)	8 (1.7%)	0.008
	Black or African American	19 (3.9%)	38 (7.9%)	
	White	222 (45.9%)	193 (39.9%)	
Age, median (IQR)		61 (56, 66)	62 (56, 66)	0.430
PSA (ng/ml), median		0.1 (0.03, 0.1)	0.1 (0.02, 0.2)	0.916

SD, stable disease; PD, progressive disease; PR, partial response; CR, complete response; PSA, prostate specific antigen. Bold values represent the statistically significant p-values ($P < 0.05$).

groups. According to the default statistical methods, an adjusted P -value < 0.05 was considered significant.

Immune Infiltration Analysis by Single Sample Gene Set Enrichment Analysis

Single sample GSEA (ssGSEA) using the R package “GSVA” was applied to perform the immune infiltration analysis of PC. The infiltration levels of 24 immune cell types were determined based on gene expression profiles in the literature (Bindea et al., 2013; Hänzelmann et al., 2013). The correlation between SNHG10 and the infiltration levels of 24 immune cells was evaluated by Spearman’s test and the Wilcoxon rank sum test. In addition, TIMER website⁵ was used to further investigate the association between immune infiltration and the expression of SNHG10, which is a comprehensive resource for systematical analysis of immune infiltrates across diverse cancer types.

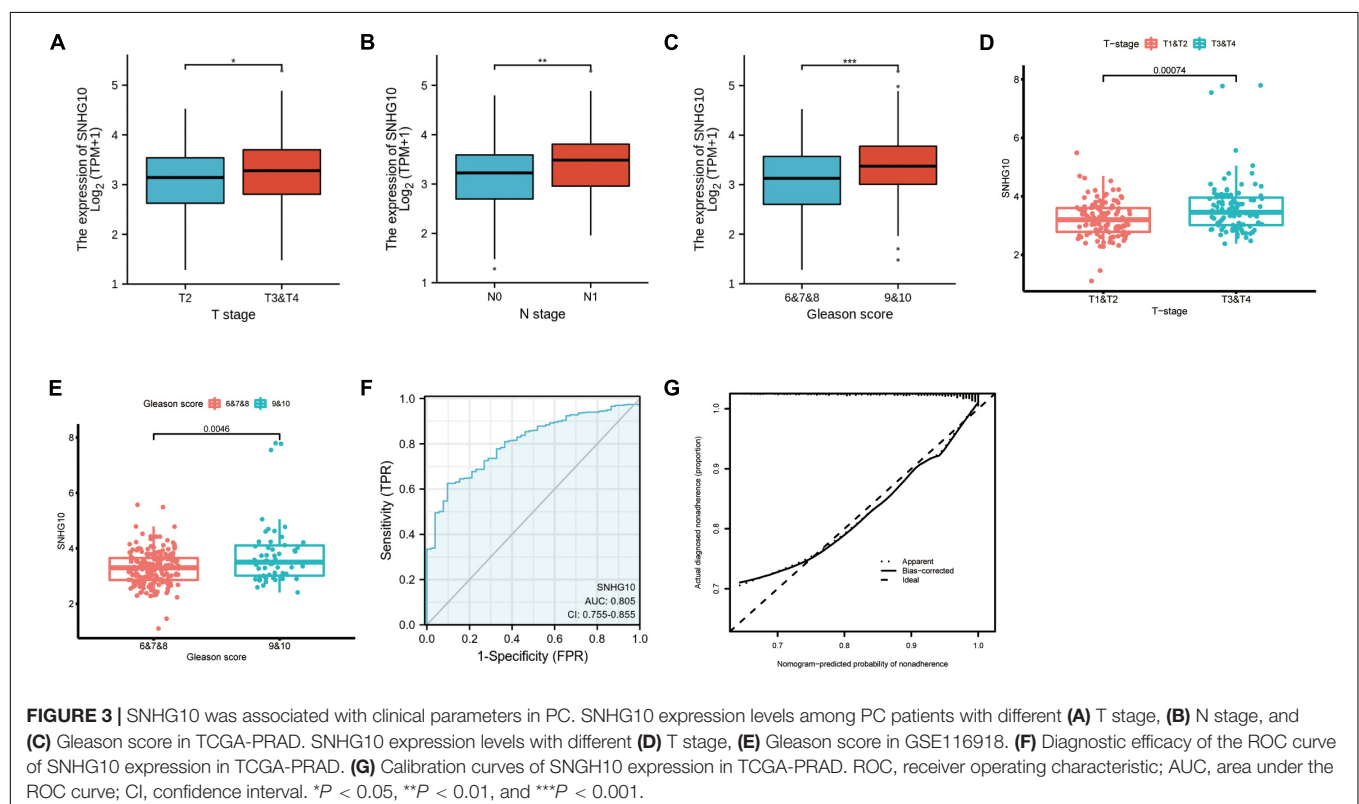
Cell Culture and siRNA Transfection

Human PC cell lines (VCaP, LNCaP, 22RV1, PC3, and DU145) and the human normal human prostate epithelial cell line (RWPE-1) were purchased from the American Type Culture Collection (ATCC⁶, United States). LNCaP, 22RV1, and DU145 cells were cultured in RPMI-1640 (Gibco, United States). PC3 cells were cultured in F12K medium (Gibco, Australia). VCaP and RWPE-1 cells were cultured in DMEM (Gibco, United States). All cells were cultured with 10% fetal bovine

serum (Gibco, Australia) at 37°C in a 5% CO₂ atmosphere. SNHG10 siRNAs were synthesized by Hanbio (Shanghai, China). The sequences of the siRNAs were as follows: si-SNHG10: 5′-CAACCGCUUUGUUAGUUAATT-3′; si-NC: 5′-UUCUCCGAACGUGUCACGUTT-3′. For the silencing of SNHG10 in the DU145 and 22RV1 cells, the cells were transfected with 50 nM small interfering RNA targeting si-SNHG10 or negative control si-NC according to the manufacturer’s instructions of Lipofectamine 2000 (Invitrogen). Scrambled siRNAs were used as negative control.

RNA Extraction and Quantitative Real-Time PCR

Total RNA was isolated and reversely transcribed into cDNA using Trizol reagent (Thermo Fisher Scientific, Inc.) and TaKaRa Prime Script RT Reagent Kit (TaKaRa, China) based on the manufacturer’s protocols. RT-qPCR was performed using SYBR Premix Ex Taq (TaKaRa, China) according to standard methodology. The relative expression levels were calculated using the $2^{-\Delta\Delta C_t}$ method relative to GAPDH. The PCR primers used were as follows: GAPDH: 5′-AAAAGCATCACCCGAGGAGAA-3′ (forward) and 5′-AAGGAAATGAATGGCAGCCG-3′ (reverse); SNHG10: 5′-GTTGGTCTCTTGGGAGGTAG-3′ (forward) and 5′-CGCCACGACGAAGTGCATGC-3′ (reverse). All experiments were performed in triplicate.



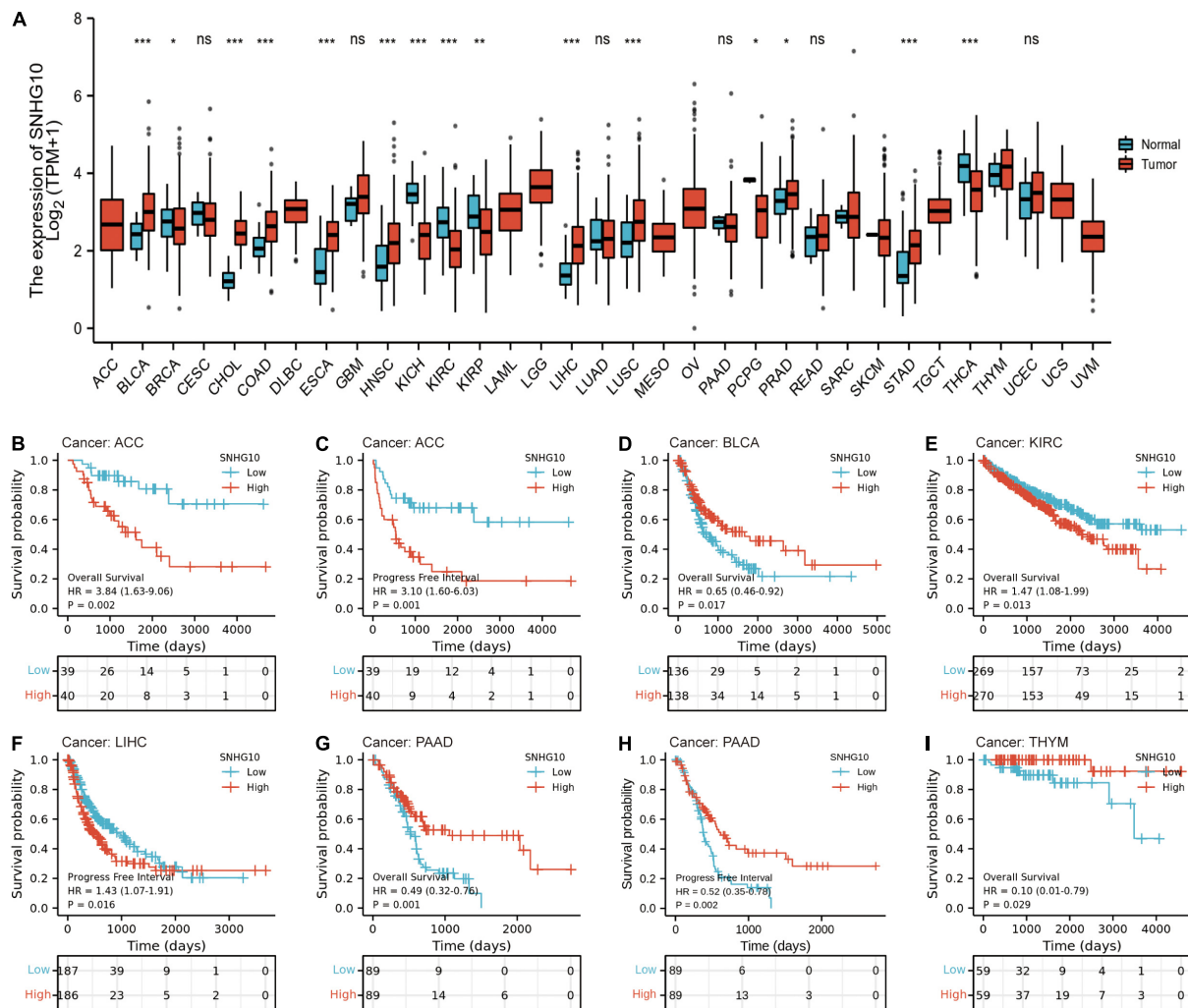


FIGURE 4 | SNHG10 expression and prognosis in patients with other cancer types. **(A)** Differences in expression of SNHG10 in normal and tumor tissues of TCGA. **(B–I)** Kaplan-Meier curves were drawn to evaluate the prognostic value of SNHG10 in OS or PFS of other cancers. * $P < 0.05$, ** $P < 0.01$, and *** $P < 0.001$.

Cell Proliferation

Cell Counting Kit 8 (CCK-8) and colony formation assays were used to measure cell proliferation. For CCK-8 assays, PC cells were seeded into a 96-well plate (6000 cells per well). CCK-8 reagent (Hanbio, China) was added into wells at 24, 48, and 72 h. After the cells were incubated at 37°C for 2 h, the optical density (OD) was measured at 450 nm using a microplate reader. For colony formation, 2000 cells per well were seeded in 6-well plates in 3 mL medium per well. After approximately 2 weeks, cell colonies were fixed with 4% paraformaldehyde for 15 min. Then, the colonies were stained with 0.2% crystal violet (Solarbio, China) and counted using ImageJ software. Each experiment was repeated three times.

Transwell Assay

Cell migration assays were performed using 8- μ m pore size chambers coated without Matrigel gel. A total of 5×10^4

transfected cells were seeded into the upper chamber with serum-free medium and 20% FBS medium was added into the lower well. After incubation for 1 day, the cells were stained and observed under an optical microscope. Three random fields were analyzed for each sample. Cell invasion assays were performed using chambers with Matrigel gel. Other procedures were the same as above. All the assays were conducted three times independently.

Statistical Analysis

For the datasets from TCGA database, statistical analyses were performed using R (v.3.6.3). The Wilcoxon rank sum test, Chi-square test, and Fisher exact test were used to estimate the association between SNHG10 and clinical pathologic characteristics. The Kaplan-Meier method was used to calculate PC patient survival rates. Univariate and multivariate cox analysis were performed to assess the relationship between clinical features and progression-free survival (PFS). For the data regarding the function of SNHG10, GraphPad Prism 7.01 was

TABLE 2 | Univariate and multivariate regression analyses of PC.

Variables	Total (N)	Univariate analysis		Multivariate analysis	
		Hazard ratio (95% CI)	P value	Hazard ratio (95% CI)	P value
T stage (T3&T4 vs. T2)	492	3.785 (2.140-6.693)	<0.001	1.512 (0.722-3.165)	0.273
N stage (N1 vs. N0)	426	1.946 (1.202-3.150)	0.007	0.803 (0.455-1.417)	0.449
M stage (M1 vs. M0)	458	3.566 (0.494-25.753)	0.208		
Gleason score (9&10 vs. 6&7&8)	499	4.590 (3.038-6.934)	<0.001	2.385 (1.374-4.140)	0.002
Primary therapy outcome (CR vs. PD&SD&PR)	438	0.151 (0.099-0.231)	<0.001	0.283 (0.159-0.502)	<0.001
Residual tumor (R1&R2 vs. R0)	468	2.365 (1.566-3.570)	<0.001	0.961 (0.566-1.632)	0.883
PSA (ng/ml) (≥ 4 vs. <4)	442	4.196 (2.095-8.405)	<0.001	1.711 (0.764-3.829)	0.191
Age (>60 vs. ≤ 60)	499	1.302 (0.863-1.963)	0.208		
Race (Black or African American vs. White&Asian)	484	0.579 (0.290-1.154)	0.120		
Zone of origin (Peripheral Zone vs. Overlapping/Multiple Zones)	263	0.799 (0.492-1.296)	0.363		
SNHG10 (High vs. Low)	499	1.874 (1.232-2.849)	0.003	1.651 (1.012-2.694)	0.045

SD, stable disease; PD, progressive disease; PR, partial response; CR, complete response; PSA, prostate specific antigen. Bold values represent the statistically significant p-values ($P < 0.05$).

used for statistical analyses. The Student's t-test evaluated the statistical significance between groups. The data was shown as mean \pm SD from at least three independent experiments and $P < 0.05$ was considered statistically significant.

RESULTS

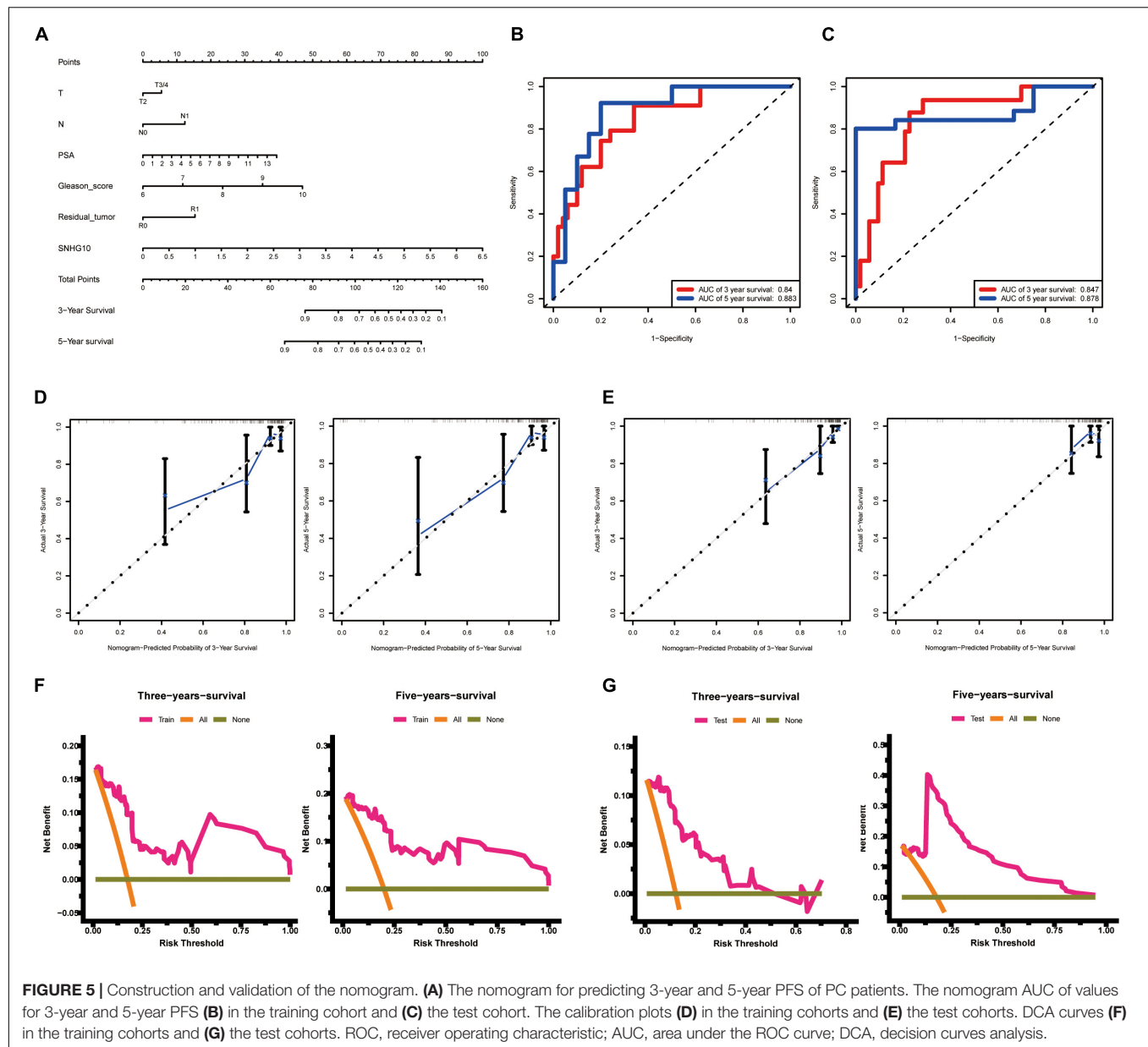
SNHG10 Was Over-Expressed in Prostate Cancer

The workflow of this study is presented in **Figure 1**. To compare the expression of SNHG10 in PC and normal samples, we analyzed the expression of SNHG10 in 499 tumor tissues and 52 normal prostate tissues of TCGA data, and found that SNHG10 was over-expressed in PC tissues ($P < 0.001$) (**Figure 2A**). There were 52 pairs of cancer samples and matched adjacent normal samples in TCGA data. The expression of SNHG10 was also higher in cancer samples than matched adjacent normal samples ($P < 0.01$) (**Figure 2B**). In addition, we compared the expression of SNHG10 between normal and prostate cancer in GSE70770, and found that SNHG10 was over-expressed in cancer tissues ($P < 0.001$) (**Figure 2C**). Meanwhile, SNHG10 expression was significantly higher in PC cell lines (DU145, 22RV1, PC3, VCaP, and LNCaP) than the prostate cell line (RWPE-1) (**Figure 2D**). Additionally, Kaplan-Meier survival analysis was used to investigate the relationship of SNHG10 expression and overall survival (OS) or progression-free survival (PFS) in the PC patients of TCGA data. SNHG10 expression has great significance in predicting OS ($P < 0.05$) (**Figure 2E**). As shown in **Figure 2F**, SNHG10 expression was significantly associated with poor PFS of PC patients ($P = 0.003$).

Additionally, the concordance-index (C-index) was calculated to evaluate SNHG10 expression in predicting the OS and PFS. The C-index for SNHG10 in predicting the OS was 0.619. The performance of SNHG10 for predicting the PFS showed a better prognostic power with a C-index of 0.727. Then, patients with high SNHG10 expression had a worse PFS compared with low expression group in GSE70770 ($P < 0.001$) (**Figure 2G**).

Overexpression of SNHG10 Was Associated With Poor Clinical Parameters in Prostate Cancer

Overall, 499 PC patients with clinical parameters were classified into two subgroups according to the mean value of relative SNHG10 expression. We then analyzed the relationships between SNHG10 and clinical parameters, including T stage, N stage, M stage, Gleason score, primary therapy outcome, residual tumor, zone of origin, prostate specific antigen (PSA), age, and race. SNHG10 expression was significantly associated with T stage ($P = 0.013$), N stage ($P = 0.005$), Gleason score ($P < 0.001$), primary therapy outcome ($P < 0.001$), and race ($P = 0.008$), while patients of different ages, M stage, residual tumor, zone of origin, and PSA shown no significant difference (**Table 1**). To visualize and clarify these relationships, we divided patients into subgroups (T2 vs. T3+T4, N0 vs. N1, Gleason score 6+7+8 vs. Gleason score 9+10). As shown in **Figures 3A-C**, advanced T stage, lymph node, and Gleason score patients exhibited higher SNHG10 expression levels. Moreover, in the GSE116918, SNHG10 expression was significantly correlated with advanced T stage and Gleason score (**Figures 3D,E**). Then, ROC analysis showed that the SNHG10 could be used



to differentiate PC patients from normal control with a cut-off of 2.31 which resulted in 59.9% for sensitivity and 90.2% for specificity (AUC = 0.805, C-index = 0.806, Youden index = 0.501) (Figure 3F). Besides, calibration curve of SNHG10 were coincident with the reference line, which indicated a high degree of credibility (Figure 3G).

Overexpression of SNHG10 Expression Was Correlated With Poor Prognosis in Numerous Cancers

TCGA database was used to identify the aberrant expression of SNHG10 across multiple cancers. As shown in the Figure 4A, SNHG10 expression was higher in multiple cancer types compared to the normal samples.

In addition, SNHG10 expression and patient survival was further investigated in various cancer types to expand our analysis to a pan-cancer level. There are significant associations between SNHG10 expression and OS or PFS in adrenocortical carcinoma (ACC), bladder urothelial carcinoma (BLCA), kidney renal clear cell carcinoma (KIRC), liver hepatocellular carcinoma (LIHC), pancreatic adenocarcinoma (PAAD), and thymoma (THYM) (Figures 4B–I).

Cox Univariate and Multivariate Analysis of Prognostic Factors in Prostate Cancer

As shown in the Table 2, patients having complete clinical data were included in further Cox regression analysis. In

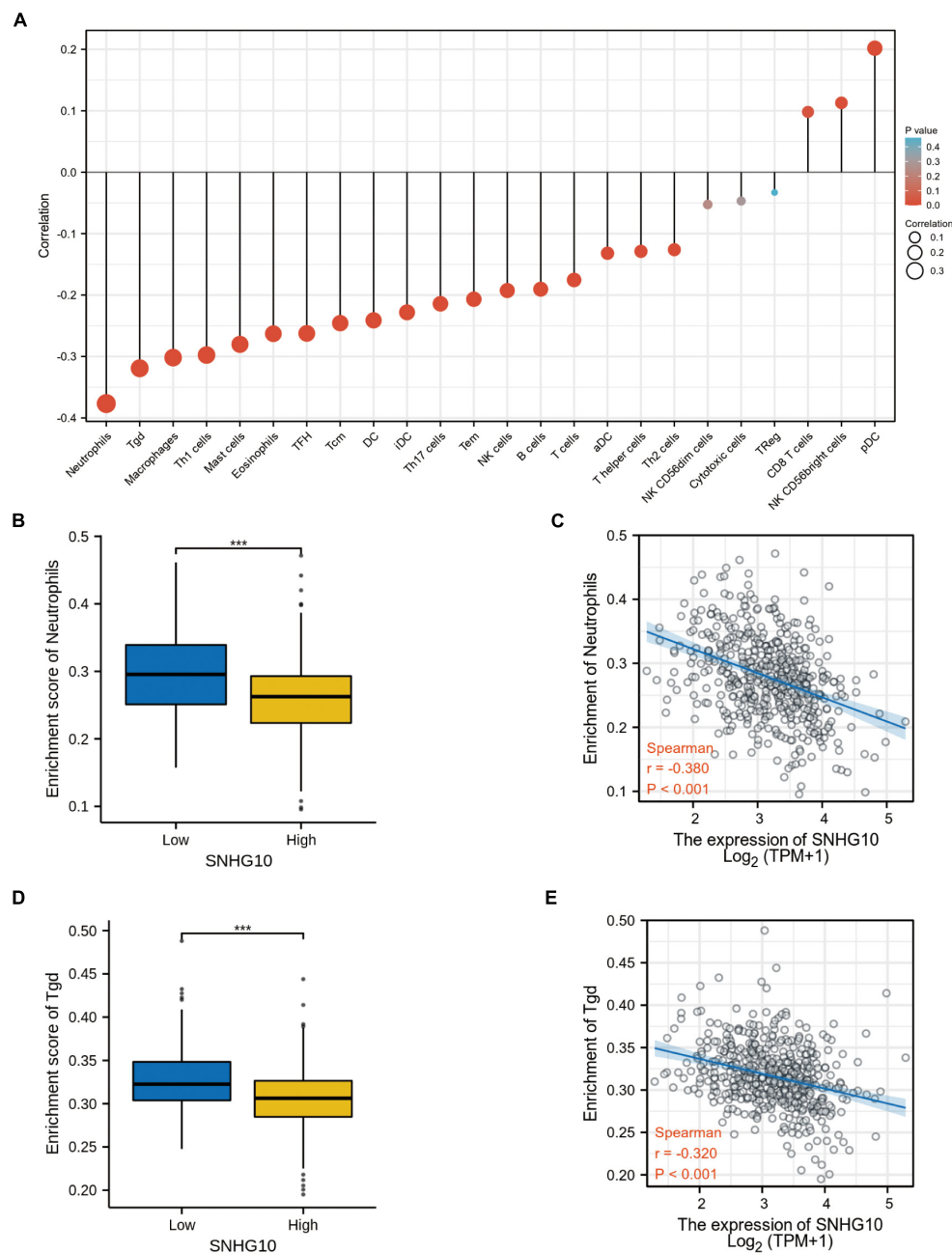


FIGURE 6 | SNHG10 expression associates with immune infiltration in the tumor microenvironment. **(A)** The forest plot shows the correlation between SNHG10 expression and 24 immune cell types. **(B)** Differences in neutrophils cell infiltration between SNHG10 low and high expression groups. **(C)** The correlation between SNHG10 expression and proportion of neutrophils. **(D)** Differences in T $\gamma\delta$ infiltration between SNHG10 low and high expression groups. **(E)** Correlation between SNHG10 expression and T $\gamma\delta$. T $\gamma\delta$, T gamma delta. *** $P < 0.001$.

the Cox univariate regression analysis, high expression of SNHG10, T stage, N stage, Gleason score, primary therapy outcome, residual tumor, and PSA were associated with PFS in PC patients. Multivariate Cox analysis further indicated that SNHG10 ($P < 0.05$) was an independent prognostic factor for PFS in PC patients, along with Gleason score and primary therapy outcome.

Construction and Validation of SNHG10 Based Nomogram

To allow clinical application of our findings, we construct the nomogram by TCGA data. The nomogram for predicting 3-year and 5-year PFS of PC was showed in **Figure 5A**. ROC curve, calibration, and discrimination were employed to evaluate the performance of the model. The C-index of the nomogram were

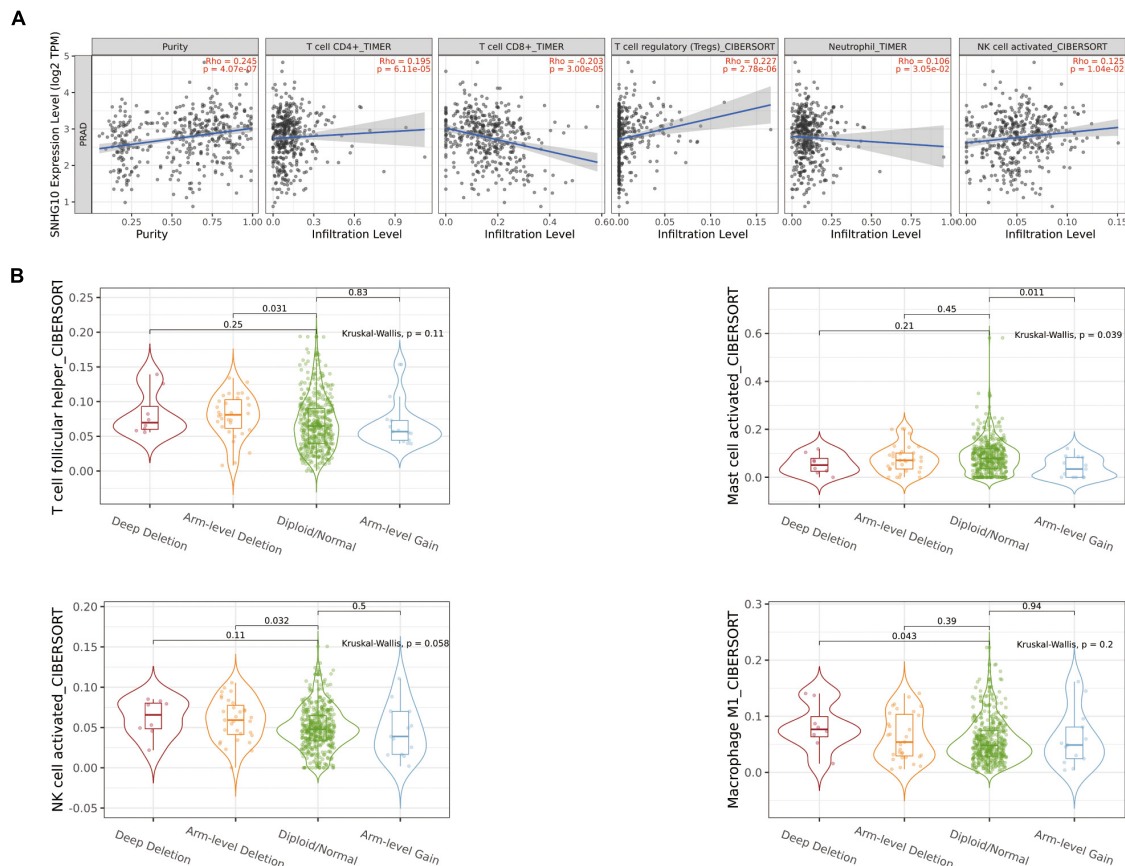


FIGURE 7 | The relationship between SNHG10 expression and tumor-infiltrated immune cells. **(A)** Significant correlation between SNHG10 expression and different type of immune cells. **(B)** Different mutational forms of SNHG10 were associated with immune infiltrates of four leukocytes.

0.848 for the training cohort and 0.825 for the test cohort. The discriminative ability of the nomogram was measured using the 3-year and 5-year survival AUC values from time-dependent ROC curve. In the training cohort, the nomogram AUC values for 3-year and 5-year PFS were 0.84 and 0.883, respectively (**Figure 5B**). In addition, in the test cohort, the nomogram AUC values for 3-year and 5-year PFS were 0.847 and 0.878, respectively (**Figure 5C**). Moreover, the calibration plots in the training cohorts and test cohorts demonstrated that the nomogram-based predictive results were mostly consistent with the actual prognosis results (**Figures 5D,E**). DCA plots showed that our nomogram had great net benefits for predicting 3-year and 5-year PFS of patients both in the training cohorts and test cohorts (**Figures 5F,G**), demonstrating its application in guiding clinical decision for PC patients.

Correlation Between SNHG10 Expression and Immune Infiltration

Using the ssGSEA method, we analyzed the relationship between SNHG10 expression and immune infiltration. These results suggested that SNHG10 expression was negatively associated with infiltration levels of neutrophils and T gamma delta ($\gamma\delta$ T)

($P < 0.001$) (**Figure 6**), and was positively correlated with that of natural killer (NK) CD56bright cells and plasmacytoid dendritic cells (pDC) ($P < 0.001$) (**Supplementary Figure 1**). In addition, the tool of TIMER was also used to identify the relationship between SNHG10 expression and tumor-infiltrated immune cells. There was a significant correlation between SNHG10 expression and different type of immune cells, including CD4+ T cells ($P = 6.11 \times 10^{-5}$, $\text{cor} = 0.195$), CD8+ T cells ($P = 3 \times 10^{-5}$, $\text{cor} = -0.203$), T cells regulatory ($P = 2.78 \times 10^{-6}$, $\text{cor} = 0.227$), Neutrophils ($P = 3.05 \times 10^{-2}$, $\text{cor} = 0.106$), and NK cells activated ($P = 1.04 \times 10^{-2}$, $\text{cor} = 0.125$) (**Figure 7A**). Besides, different mutational forms of SNHG10 were associated with immune infiltrates of four leukocytes, which also revealed its influence on immune microenvironment (**Figure 7B**).

SNHG10-Related Signaling Pathways Based on Gene Set Enrichment Analysis

Gene set enrichment analysis was used to identify signaling pathways that were differentially activated between low and high SNHG10 expression groups. As shown in **Figures 8A–F**, there were six significant Kyoto Encyclopedia of Genes

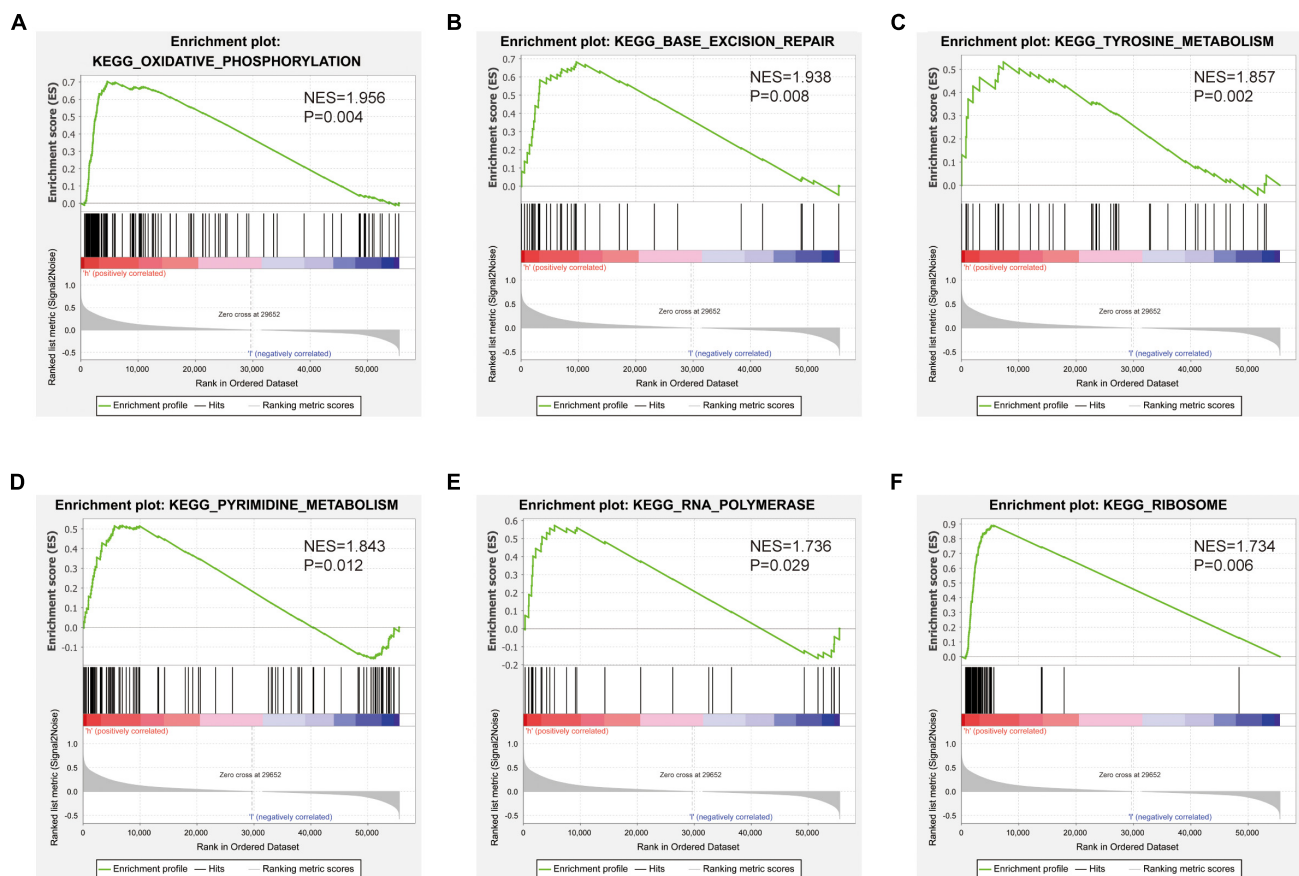


FIGURE 8 | Pathways involved in the pathogenesis of SNHG10 from the GSEA. Enrichment plots comparing SNHG10 expression in terms of (A) oxidative phosphorylation, (B) base excision repair, (C) tyrosine metabolism, (D) pyrimidine metabolism, (E) RNA polymerase, and (F) ribosome.

and Genomes pathways related with the high SNHG10 expression phenotype: oxidative phosphorylation, base excision repair, tyrosine metabolism, pyrimidine metabolism, RNA polymerase, and ribosome.

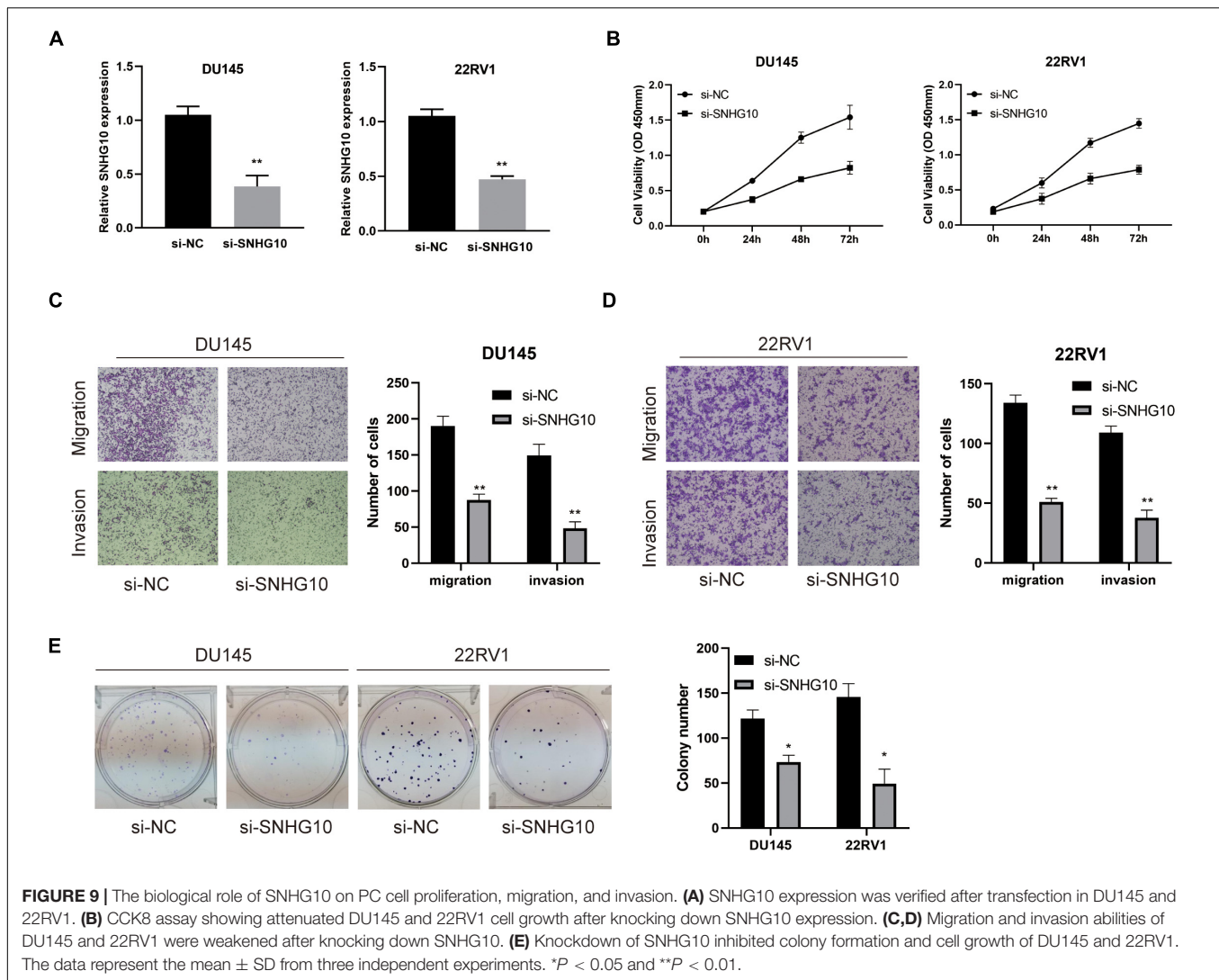
SNHG10 Promoted Cell Proliferation, Migration, and Invasion in Prostate Cancer

The above studies indicated that SNHG10 expression was distinctly up-regulated in PC tissues, and SNHG10 might influence the progression in PC. To further investigate the biological role of SNHG10 in PC, specific siRNA was used to construct DU145 and 22RV1 cells with stable knockdown of SNHG10 expression (Figure 9A). Our results demonstrated that, in DU145 and 22RV1 cells, cell growth was dramatically inhibited in SNHG10 knockdown cells compared with the control groups (Figure 9B). Next, Transwell assays showed that SNHG10 knockdown suppressed the migratory and invasive abilities of DU145 and 22RV1 cells (Figures 9C,D). SNHG10 inhibition also decreased tumor cell colony formation (Figure 9E). These results demonstrated that SNHG10 was

involved in PC progression by inhibiting cell growth, migration, and invasion.

DISCUSSION

Long non-coding RNAs exert diverse regulatory roles in physiological and pathological processes, including interaction with mRNAs, proteins and miRNAs, to regulate gene expression and induce chromatin remodeling (Kopp and Mendell, 2018; Chi et al., 2019). Previous studies have revealed that lncRNAs were related to various malignant biological behaviors of cancer, such as cell proliferation, apoptosis, migration, and invasion (Sanchez Calle et al., 2018; Yang et al., 2020). It has also been reported that lncAMPC serves as prognostic biomarker in PC (Zhang et al., 2020). Combining bioinformatics analyses and biological function validation, our study provides evidence that SNHG10 was overexpressed in PC, which was also associated with poor prognosis. Aberrant expression of SNHG10 has been elucidated in various human cancers. For example, SNHG10 exerted oncogenic functions in glioma by sponging miR-532-3p and enhancing FBXL19 expression (Jin et al., 2020). In addition, SNHG10 has reported to promote cell proliferation



in osteosarcoma via increasing glucose uptake and miR-218 gene methylation (He et al., 2020). SNHG10 facilitates gastric cancer cell proliferation and migration by targeting the miR-495/CTNNB1 axis and activating the WNT pathway (Yuan et al., 2020). All these studies indicated that SNHG10 might exert a pivotal function in human cancers. In our study, we observed increased SNHG10 in PC, which was also associated with poor prognosis. Similarly, high expression of SNHG10 was related to overall survival in hepatocellular carcinoma and non-small cell lung cancer (Lan et al., 2019; Liang et al., 2020).

In this study, we investigated the underlying mechanisms through which SNHG10 influenced the progression of PC. GSEA demonstrated that SNHG10 was significantly associated with oxidative phosphorylation, tyrosine metabolism, and pyrimidine metabolism, which indicated that SNHG10 might have a crucial role in cell metabolism. In addition to the above, we also explored the relationship between the expression of SNHG10 and diverse immune infiltration levels in PC. In our study, we found a moderate correlation between SNHG10

expression and the infiltration of neutrophils, $\gamma\delta$ T cells, and macrophages in PC. These results could indicate that SNHG10 may inhibit the function of neutrophils and macrophages, and may promote the function of plasmacytoid dendritic cells and NK CD56 bright cells, and thus exert a pro-carcinogenic role in PC. *In vitro*, knockdown of SNHG10 in 22RV1 and DU145 cells impaired cell proliferation, migration, and invasion. Based on these findings, we proposed that SNHG10 exerts an essential function in regulating pathologic progression of PC.

To the best of our knowledge, this is the first study to explore the relationship between SNHG10 and PC. However, there are some limitations in our research. First, our study was based on expression data extracted from TCGA, but may be more convincing if supported by validation studies using other public datasets. Second, the our study was based on a retrospective analysis, and our conclusions should be investigated by a prospective clinical study. Finally, the biological functions of SNHG10 need to be further explored.

CONCLUSION

Our study found that SNHG10 expression was increased in PC, which was also associated with poor prognosis. Furthermore, SNHG10 might be involved in the progression of PC by regulating the function of immune infiltrating cells and oxidative phosphorylation. Herein, we revealed the biological functions of SNHG10 in PC and offered a potential strategy for the diagnosis and treatment of PC.

DATA AVAILABILITY STATEMENT

The datasets presented in this study can be found in online repositories. The names of the repository/repositories and accession number(s) can be found in the article/**Supplementary Material**.

AUTHOR CONTRIBUTIONS

QC, XY, and WX collected, validated, and visualized TCGA data. QC, BG, and ZL designed and drafted the manuscript. MM, SF, and SW performed the experiments and data analysis. TS, YL,

and ZZ helped to revise the manuscript. All authors reviewed and approved the published version of the manuscript.

FUNDING

This work was supported by the National Natural Science Foundation of China (82060144), the Natural Science Foundation of Jiangxi Province (20202BABL206023), and Special Fund for Postgraduate Innovation of Nanchang University (CX2018183).

SUPPLEMENTARY MATERIAL

The Supplementary Material for this article can be found online at: <https://www.frontiersin.org/articles/10.3389/fcell.2021.731042/full#supplementary-material>

Supplementary Figure 1 | The correlation between SNHG10 expression and the immune infiltration in the tumor microenvironment. (A) Differences in pDC infiltration between SNHG10 low and high expression groups. (B) Correlation between SNHG10 expression and pDC. (C) Differences in NK CD56bright infiltration levels in SNHG10 low and high expression groups. (D) Correlation between SNHG10 expression and NK CD56bright. NK, natural killer; pDC, plasmacytoid dendritic cell. * $P < 0.05$ and *** $P < 0.001$.

REFERENCES

- Bindea, G., Mlecnik, B., Tosolini, M., Kirilovsky, A., Waldner, M., Obenauf, A., et al. (2013). Spatiotemporal dynamics of intratumoral immune cells reveal the immune landscape in human cancer. *Immunity* 39, 782–795. doi: 10.1016/j.immuni.2013.10.003
- Chi, Y., Wang, D., Wang, J., Yu, W., and Yang, J. (2019). Long non-coding RNA in the pathogenesis of cancers. *Cells* 8:1015. doi: 10.3390/cells8091015
- De Troyer, L., Zhao, P., Pastor, T., Baietti, M., Barra, J., Vendramin, R., et al. (2020). Stress-induced lncRNA LSTR fosters cancer cell fitness by regulating the activity of the U4/U6 recycling factor SART3. *Nucleic Acids Res.* 48, 2502–2517. doi: 10.1093/nar/gkz1237
- Goodall, G., and Wickramasinghe, V. (2021). RNA in cancer. *Nat. Rev. Cancer* 21, 22–36. doi: 10.1038/s41568-020-00306-0
- Hänzelmann, S., Castelo, R., and Guinney, J. (2013). GSEA: gene set variation analysis for microarray and RNA-seq data. *BMC Bioinformatics* 14:7. doi: 10.1186/1471-2105-14-7
- Hayes, J., and Barry, M. (2014). Screening for prostate cancer with the prostate-specific antigen test: a review of current evidence. *JAMA* 311, 1143–1149. doi: 10.1001/jama.2014.2085
- He, P., Xu, Y., and Wang, Z. (2020). LncRNA SNHG10 increases the methylation of miR-218 gene to promote glucose uptake and cell proliferation in osteosarcoma. *J. Orthop. Surg. Res.* 15:353. doi: 10.1186/s13018-020-01865-6
- Hua, J. T., Chen, S., and He, H. H. (2019). Landscape of noncoding RNA in prostate cancer. *Trends Genet.* 35, 840–851. doi: 10.1016/j.tig.2019.08.004
- Jin, L., Huang, S., Guan, C., and Chang, S. (2020). ETS1-activated SNHG10 exerts oncogenic functions in glioma via targeting miR-532-3p/FBXL19 axis. *Cancer Cell Int.* 20:589. doi: 10.1186/s12935-020-01649-2
- Kopp, F., and Mendell, J. (2018). Functional classification and experimental dissection of long noncoding RNAs. *Cell* 172, 393–407. doi: 10.1016/j.cell.2018.01.011
- Lan, T., Yuan, K., Yan, X., Xu, L., Liao, H., Hao, X., et al. (2019). LncRNA SNHG10 facilitates hepatocarcinogenesis and metastasis by modulating its homolog SCARNA13 via a positive feedback loop. *Cancer Res.* 79, 3220–3234. doi: 10.1158/0008-5472.can-18-4044
- Liang, M., Wang, L., Cao, C., Song, S., and Wu, F. (2020). LncRNA SNHG10 is downregulated in non-small cell lung cancer and predicts poor survival. *BMC Pulm. Med.* 20:273. doi: 10.1186/s12890-020-01281-w
- Luo, M., Li, J., Shen, L., Chu, J., Guo, Q., Liang, G., et al. (2020). The role of APAL/ST8SIA6-AS1 lncRNA in PLK1 activation and mitotic catastrophe of tumor cells. *J. Natl. Cancer Inst.* 112, 356–368. doi: 10.1093/jnci/djz134
- Rastinehad, A., Turkbey, B., Salami, S., Yaskiv, O., George, A., Fakhoury, M., et al. (2014). Improving detection of clinically significant prostate cancer: magnetic resonance imaging/transrectal ultrasound fusion guided prostate biopsy. *J. Urol.* 191, 1749–1754. doi: 10.1016/j.juro.2013.12.007
- Sanchez Calle, A., Kawamura, Y., Yamamoto, Y., Takeshita, F., and Ochiya, T. (2018). Emerging roles of long non-coding RNA in cancer. *Cancer Sci.* 109, 2093–2100. doi: 10.1111/cas.13642
- Shi, X., Sun, M., Liu, H., Yao, Y., and Song, Y. (2013). Long non-coding RNAs: a new frontier in the study of human diseases. *Cancer Lett.* 339, 159–166. doi: 10.1016/j.canlet.2013.06.013
- Siegel, R., Miller, K., and Jemal, A. (2020). Cancer statistics, 2020. *CA Cancer J. Clin.* 70, 7–30. doi: 10.3322/caac.21590
- Statello, L., Guo, C., Chen, L., and Huarte, M. (2021). Gene regulation by long non-coding RNAs and its biological functions. *Nat. Rev. Mol. Cell Biol.* 22, 96–118. doi: 10.1038/s41580-020-00315-9
- Wen, S., Wei, Y., Zen, C., Xiong, W., Niu, Y., and Zhao, Y. (2020). Long non-coding RNA NEAT1 promotes bone metastasis of prostate cancer through N6-methyladenosine. *Mol. Cancer* 19:171. doi: 10.1186/s12943-020-01293-4
- Wu, H., Tian, X., and Zhu, C. (2020). Knockdown of lncRNA PVT1 inhibits prostate cancer progression in vitro and in vivo by the suppression of KIF23 through stimulating miR-15a-5p. *Cancer Cell Int.* 20:283. doi: 10.1186/s12935-020-01363-z
- Yang, X., Liu, M., Li, M., Zhang, S., Hiju, H., Sun, J., et al. (2020). Epigenetic modulations of noncoding RNA: a novel dimension

- of cancer biology. *Mol. Cancer* 19:64. doi: 10.1186/s12943-020-01159-9
- Yuan, X., Yang, T., Xu, Y., Ou, S., Shi, P., Cao, M., et al. (2020). SNHG10 promotes cell proliferation and migration in gastric cancer by targeting miR-495-3p/CTNNB1 axis. *Dig. Dis. Sci.* 66, 2627–2636. doi: 10.1007/s10620-020-06576-w
- Zhang, W., Shi, X., Chen, R., Zhu, Y., Peng, S., Chang, Y., et al. (2020). Novel long non-coding RNA lncAMPC promotes metastasis and immunosuppression in prostate cancer by stimulating LIF/LIFR expression. *Mol. Ther. J. Am. Soc. Gene Ther.* 28, 2473–2487. doi: 10.1016/j.ymthe.2020.06.013
- Zhang, Y., Guo, H., and Zhang, H. (2020). SNHG10/DDX54/PBX3 feedback loop contributes to gastric cancer cell growth. *Dig. Dis. Sci.* 66, 1875–1884. doi: 10.1007/s10620-020-06488-9
- Zhu, S., Liu, Y., Wang, X., Wang, J., and Xi, G. (2020). lncRNA SNHG10 promotes the proliferation and invasion of osteosarcoma via Wnt/ β -catenin signaling. *Mol. Ther. Nucleic Acids* 22, 957–970. doi: 10.1016/j.omtn.2020.10.010

Conflict of Interest: The authors declare that the research was conducted in the absence of any commercial or financial relationships that could be construed as a potential conflict of interest.

Publisher's Note: All claims expressed in this article are solely those of the authors and do not necessarily represent those of their affiliated organizations, or those of the publisher, the editors and the reviewers. Any product that may be evaluated in this article, or claim that may be made by its manufacturer, is not guaranteed or endorsed by the publisher.

Copyright © 2021 Chen, Yang, Gong, Xie, Ma, Fu, Wang, Liu, Zhang, Sun and Li. This is an open-access article distributed under the terms of the Creative Commons Attribution License (CC BY). The use, distribution or reproduction in other forums is permitted, provided the original author(s) and the copyright owner(s) are credited and that the original publication in this journal is cited, in accordance with accepted academic practice. No use, distribution or reproduction is permitted which does not comply with these terms.



Immune-Related LncRNAs Affect the Prognosis of Osteosarcoma, Which Are Related to the Tumor Immune Microenvironment

Qingshan Huang^{1,2}, Yilin Lin³, Chenglong Chen^{1,2}, Jingbing Lou^{1,2}, Tingting Ren^{1,2}, Yi Huang^{1,2}, Hongliang Zhang^{1,2}, Yiyang Yu^{1,2}, Yu Guo^{1,2}, Wei Wang^{1,2}, Boyang Wang^{1,2}, Jianfang Niu^{1,2}, Jiuhui Xu^{1,2}, Lei Guo^{1,2} and Wei Guo^{1,2*}

OPEN ACCESS

Edited by:

Zong Sheng Guo,
Roswell Park Comprehensive Cancer
Center, United States

Reviewed by:

Juliano Andreoli Miyake,
Federal University of Santa Catarina,
Brazil
Jaira Ferreira de Vasconcellos,
James Madison University,
United States

*Correspondence:

Wei Guo
bonettumor@163.com

Specialty section:

This article was submitted to
Molecular and Cellular Oncology,
a section of the journal
Frontiers in Cell and Developmental
Biology

Received: 26 June 2021

Accepted: 20 September 2021

Published: 07 October 2021

Citation:

Huang Q, Lin Y, Chen C, Lou J,
Ren T, Huang Y, Zhang H, Yu Y,
Guo Y, Wang W, Wang B, Niu J, Xu J,
Guo L and Guo W (2021)
Immune-Related LncRNAs Affect the
Prognosis of Osteosarcoma, Which
Are Related to the Tumor Immune
Microenvironment.
Front. Cell Dev. Biol. 9:731311.
doi: 10.3389/fcell.2021.731311

¹ Musculoskeletal Tumor Center, Peking University People's Hospital, Beijing, China, ² Beijing Key Laboratory of Musculoskeletal Tumor, Peking University People's Hospital, Beijing, China, ³ Laboratory of Surgical Oncology, Peking University People's Hospital, Beijing, China

Background: Abnormal expression of lncRNA is closely related to the occurrence and metastasis of osteosarcoma. The tumor immune microenvironment (TIM) is considered to be an important factor affecting the prognosis and treatment of osteosarcoma. This study aims to explore the effect of immune-related lncRNAs (IRLs) on the prognosis of osteosarcoma and its relationship with the TIM.

Methods: Ninety-five osteosarcoma samples from the TARGET database were included. Iterative LASSO regression and multivariate Cox regression analysis were used to screen the IRLs signature with the optimal AUC. The predict function was used to calculate the risk score and divide osteosarcoma into a high-risk group and low-risk group based on the optimal cut-off value of the risk score. The lncRNAs in IRLs signature that affect metastasis were screened for *in vitro* validation. Single sample gene set enrichment analysis (ssGSEA) and ESTIMATE algorithms were used to evaluate the role of TIM in the influence of IRLs on osteosarcoma prognosis.

Results: Ten IRLs constituted the IRLs signature, with an AUC of 0.96. The recurrence and metastasis rates of osteosarcoma in the high-risk group were higher than those in the low-risk group. *In vitro* experiments showed that knockdown of lncRNA (AC006033.2) could increase the proliferation, migration, and invasion of osteosarcoma. ssGSEA and ESTIMATE results showed that the immune cell content and immune score in the low-risk group were generally higher than those in the high-risk group. In addition, the expression levels of immune escape-related genes were higher in the high-risk group.

Conclusion: The IRLs signature is a reliable biomarker for the prognosis of osteosarcoma, and they alter the prognosis of osteosarcoma. In addition, IRLs signature

and patient prognosis may be related to TIM in osteosarcoma. The higher the content of immune cells in the TIM of osteosarcoma, the lower the risk score of patients and the better the prognosis. The higher the expression of immune escape-related genes, the lower the risk score of patients and the better the prognosis.

Keywords: osteosarcoma, lncRNA, tumor immune microenvironment, immune escape, metastasis

INTRODUCTION

Osteosarcoma is the most common primary malignant bone tumor, most commonly occurring in adolescents and children (Huang et al., 2021). Its incidence is about 4.4 per million, accounting for 5% of all childhood malignancies (Han et al., 2021). Nearly 60% of osteosarcomas occur in the femur, tibia, and pelvis (Zhou and Mu, 2021). Osteosarcoma has the characteristics of high malignancy, rapid growth, and easy metastasis. Pulmonary metastasis is one of the major factors leading to the poor prognosis of osteosarcoma, and more than 20% of patients with osteosarcoma have had pulmonary metastasis at the time of diagnosis (Anderson, 2016). Therefore, it is important to clarify the causes and mechanisms affecting the prognosis of osteosarcoma to prolong the survival time of osteosarcoma.

lncRNA regulates gene transcription, translation, editing, and other biological processes (Qian et al., 2019). Its abnormal expression is closely related to the occurrence and metastasis of tumors (Kornfeld and Bruning, 2014; Bartonicek et al., 2016). It has been confirmed that multiple lncRNAs can promote the occurrence and metastasis of osteosarcoma through competitive inhibition of miRNA expression (Pan et al., 2021; Zhou and Mu, 2021). Notably, lncRNAs can regulate the development and activation of a variety of immune cells (Atianand et al., 2017). The tumor microenvironment is composed of extracellular matrix, mesenchymal cells, immune cells, and other components, and plays an important role in the occurrence of tumors (Pitt et al., 2016; De Nola et al., 2019). The immune cells in the tumor microenvironment are closely related to the treatment and prognosis of tumors. Studies have shown that lncRNA can promote tumor-associated macrophage polarization to regulate the proliferation and migration of tumor cells (Zhao et al., 2021). lncRNA NKILA can also act on T cells to promote the immune escape of tumor cells (Huang et al., 2018). lncRNA THRIL has also been shown to regulate TNF- α expression and participate in immune response in osteosarcoma (Xu et al., 2020). Therefore, these lncRNAs mediated tumor immune microenvironment (TIM) regulation may play an important role in the metastasis and prognosis of osteosarcoma.

In this study, immune-related lncRNAs (IRLs) signature was constructed from the publicly available RNA-Seq dataset to evaluate the prognosis of osteosarcoma. In particular, the role of IRLs signature in osteosarcoma metastasis was

evaluated and validated *in vitro*. Because the metastasis of osteosarcoma is an important factor affecting its poor prognosis. In addition, this study further explored the role of TIM in the influence of IRLs on the progression of osteosarcoma.

MATERIALS AND METHODS

Data Collection and Processing

Osteosarcoma expression spectrum and clinical information from the TARGET database.¹ Samples were selected and data were processed by the following steps: (1) samples with both expression profiles and prognostic information were selected; (2) delete the samples with a survival time of 0 months; (3) according to the human gene annotation file (version GRCH38.p13), the ID of the gene of the osteosarcoma samples was converted into the gene symbol; and (4) there were multiple expression levels of the same gene in the expression profile, and the mean expression level was taken.

Co-expression Analyses of Immune-Related lncRNAs

A gene set named “IMMUNE RESPONSE TO TUMOR CELL” was download from Molecular Signatures Database.²

Correlation analysis was conducted between all lncRNAs and the gene set, and IRLs with a correlation coefficient greater than 0.6 were obtained.

Construction Immune-Related lncRNAs Prognostic Signature

lncRNAs with expression variance greater than 0.2 in IRLs were screened. Univariate Cox regression analysis was performed on these lncRNAs and those with *P*-value less than 0.5 were screened (Sveen et al., 2012). Iterative LASSO regression was used to identify high-frequency lncRNA (Zhang et al., 2021). Through 1000 iterations, a total of 11 lncRNAs with a frequency greater than 300 were screened out. These lncRNAs were incorporated into the Cox regression analysis one by one until the AUC value of IRLs signature reached the maximum. The risk score of each osteosarcoma sample was calculated using the predict function. The patients were divided into a high-risk group and low-risk group using the optimal risk score cut-off value and the Survminer R package was used for survival analysis.

Abbreviations: EdU, 5-ethynyl-2'-deoxyuridine; FBS, fetal bovine serum; GSEA, gene set enrichment analysis; GSVA, Gene Set Variation Analysis; IRLs, immune-related lncRNAs; PCA, principal component analysis; ssGSEA, single sample gene set enrichment analysis; TIM, tumor immune microenvironment.

¹<https://ocg.cancer.gov/programs/target>

²<http://www.gsea-msigdb.org/gsea/msigdb/index.jsp>

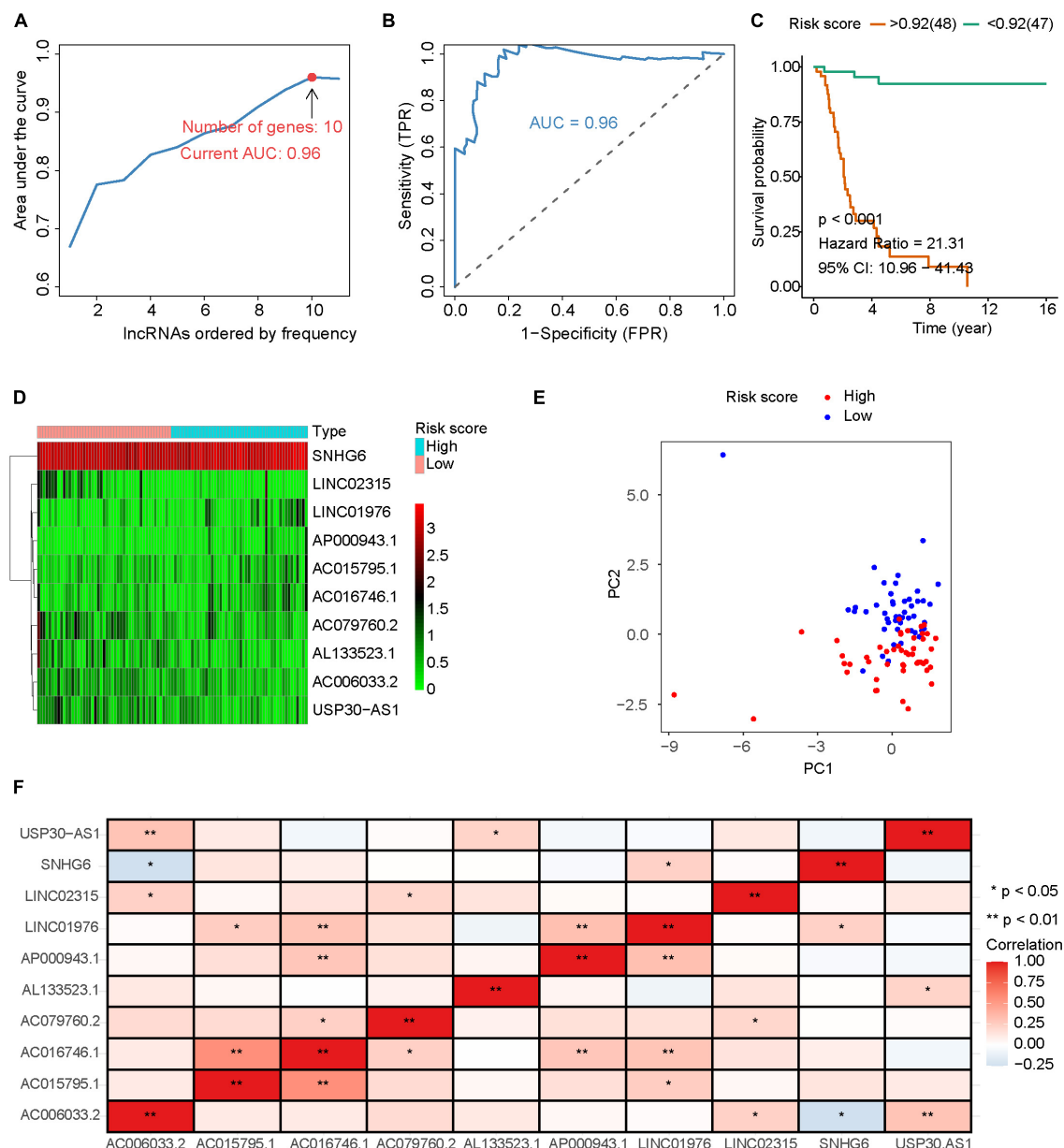


FIGURE 1 | Construction of IRLs prognostic signature. (A) Iterative LASSO and Cox regression analysis are used to screen IRLs signature with the best AUC. **(B)** The ROC curve with the best AUC. **(C)** Osteosarcomas were grouped according to the optimal cut-off value of risk score, and survival analysis was performed. **(D)** Expression levels of 10 lncRNA in IRLs signature. **(E)** PCA analysis was performed with IRLs signature. **(F)** Correlation analysis among 10 IRLs in IRLs signature.

Single Sample Gene Set Enrichment Analysis and Gene Set Enrichment Analysis

Fifty immune cell gene sets (Bindea et al., 2013; Cheng et al., 2013; Newman et al., 2015; Senbabaoglu et al., 2016), stromal cell gene set, and total immune cell gene set included in this study (Yoshihara et al., 2013) came from previous studies. Single sample gene set enrichment analysis (ssGSEA) of these gene sets were performed using Gene Set Variation Analysis (GSVA) R package (Wang et al., 2021), and the results

of ssGSEA were normalized. KEGG pathway enrichment and GO function enrichment analysis were performed using GSEA software (version 4.0.1). Gene sets of KEGG and GO (C2.Cp.KEGG.v7.1 and C5.All.V7.1.Symbols) download from Molecular Signatures Database (see text footnote 2).

Construction of the Nomogram

The risk score and osteosarcoma features such as age, gender, recurrence, metastasis, and tumor site were used to construct a

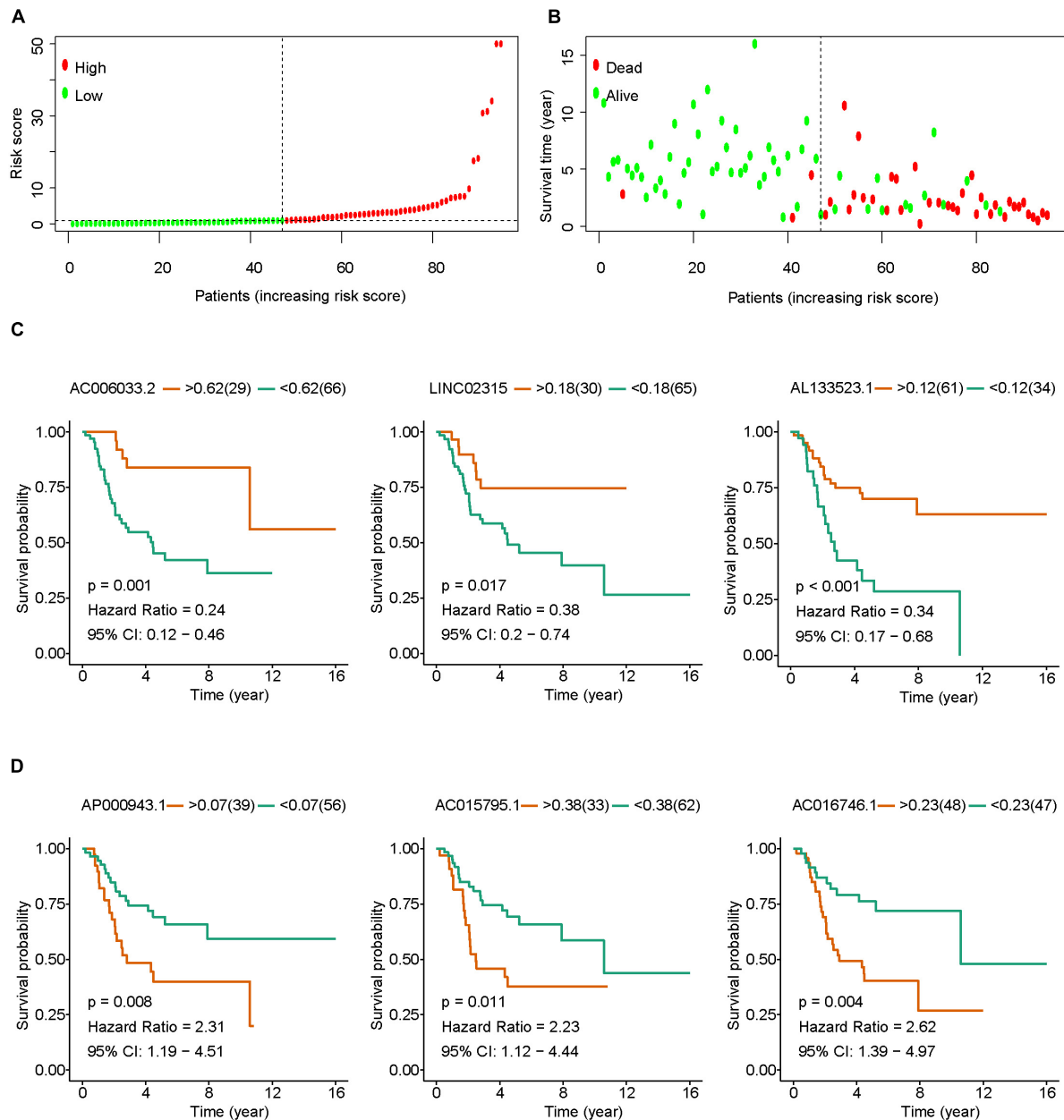


FIGURE 2 | The role of IRLs signature in the prognosis of osteosarcoma. **(A)** Osteosarcoma was divided into high-risk group and low-risk group according to the optimal cut-off value of risk score. **(B)** Relationship between risk score and survival states in patients with osteosarcoma. **(C,D)** Osteosarcomas were grouped according to the optimal cut-off value of lncRNAs expression in IRLs signature, and survival analysis was performed.

nomogram (Iasonos et al., 2008; Wang et al., 2013) to intuitively evaluate the prognosis of patients with osteosarcoma. The decision curve was used to verify the accuracy of the nomogram.

Estimation of Tumor Microenvironment Score

ESTIMATE algorithm was used to evaluate stromal score, immune score, and tumor cell purity of osteosarcoma (Hu et al., 2021). Kruskal–Wallis was used to analyze the differences in the

stromal score, immune score, Estimate score, and tumor cell purity of different risk score osteosarcomas.

Cell Culture and Transfection

Human osteosarcoma cell lines KHOS and 143B were derived from American Type Culture Collection (ATCC, VA, United States). 143B cells were cultured in DMEM medium (HyClone, UT, United States) containing 10% fetal bovine serum (FBS, Gibco, NY, United States), and KHOS

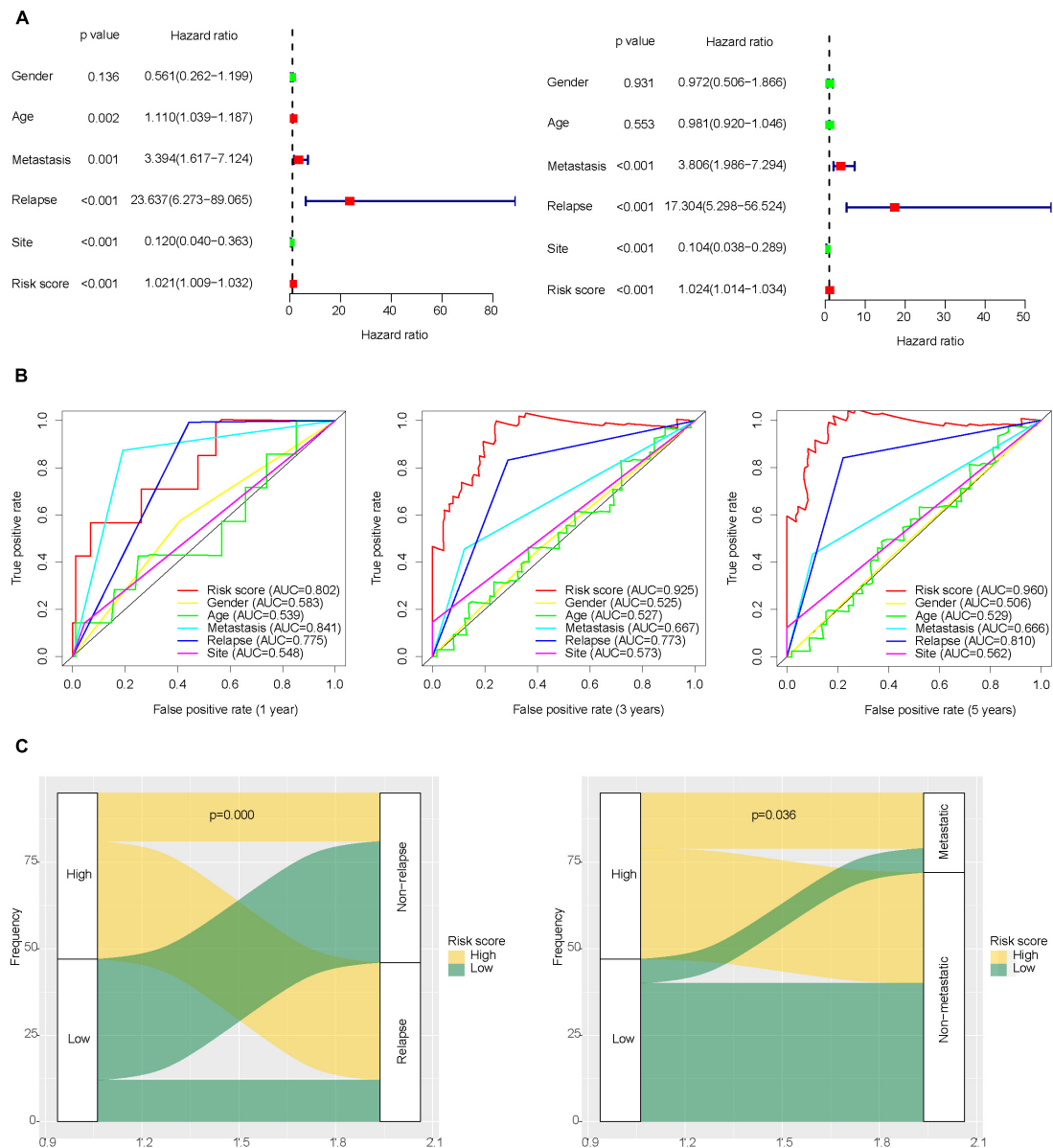


FIGURE 3 | Role of clinical features in the prognosis of osteosarcoma. **(A)** Univariate and multivariate Cox regression analysis of clinical features of osteosarcoma. **(B)** ROC curve for predicting the prognosis of osteosarcoma based on risk score and clinical features of osteosarcoma. **(C)** Differences in metastasis and recurrence rates between the high-risk group and low-risk group.

cells were cultured in RPMI-1640 medium (HyClone, UT, United States) containing 10% FBS. Si-AC006033.2 was obtained from Gemma Gene (Suzhou, China) (sequences: 5'-GCAGCUGCUUUGACAGUUUTT-3'). Lipofectamine 3000 (Invitrogen, CA, United States) was used for transfection. The transfection process was carried out according to the instructions.

Reverse Transcription-Quantitative Polymerase Chain Reaction

RNA extraction from osteosarcoma cell lines was performed using TRIzol (Invitrogen, CA, United States). GAPDH was

selected as an endogenous control. The primers of AC006033.2 and GAPDH are shown in **Supplementary Table 1**.

Cell Proliferation Assay (Cell Counting Kit-8 and 5-Ethynyl-2'-Deoxyuridine)

Osteosarcoma cells were cultured in 96-well plates with a cell density of 3000 cells per well. A total of 10 μ L Cell Counting Kit-8 (CCK-8) solution (Beyotime, Shanghai, China) was added at 0, 24, 48, and 72 h, respectively. OD values were measured at 450 nm wavelength.

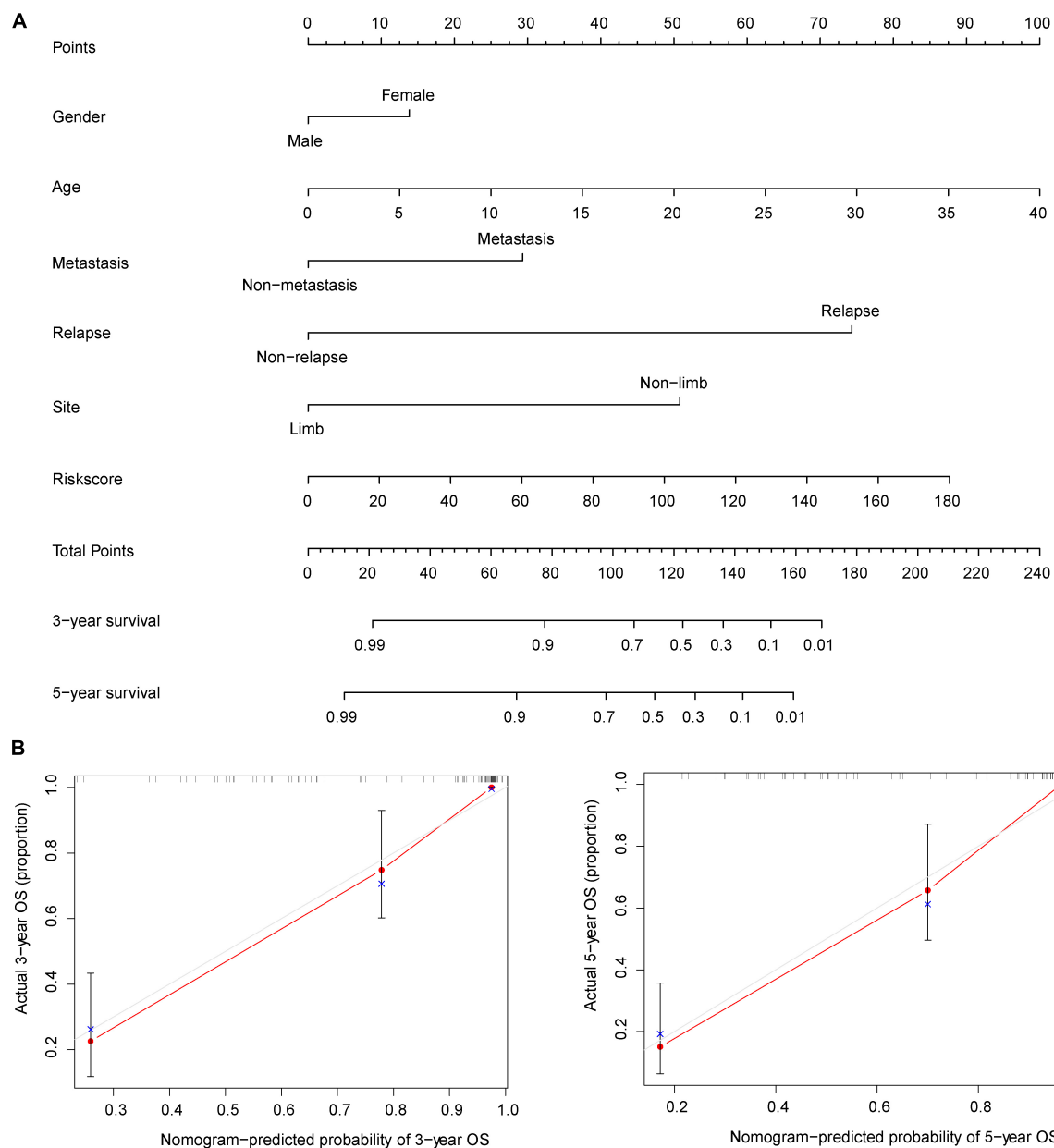


FIGURE 4 | Nomogram for evaluating the prognosis of osteosarcoma at 3 and 5 years. **(A)** The risk score and clinical characteristics of osteosarcoma were used to construct the nomogram. **(B)** Calibration curves were used to verify the accuracy of the nomogram.

Osteosarcoma cells were inoculated in six-well plates and cultured for 12 h, 5-ethynyl-2'-deoxyuridine (EdU, Beyotime, Shanghai, China), was added. The final concentration of EdU was 10 μ M. It was incubated in an incubator at 37°C for 2 h and fixed with 4% paraformaldehyde. A total of 1 mL of osmotic solution was added to each well and incubate at room temperature for 15 min. A total of 0.5 mL click reaction solution was added to each well and incubate at room temperature in dark for 30 min. Finally, the nuclei were stained with DAPI (Beyotime, Shanghai, China).

Wound Healing Assay and Transwell Invasion Assay

The wound-healing assay was performed in a six-well plate. Scratches were made with the tip of a sterile pipette. The changes of scratches at 24 h were observed under a microscope. Image-Pro Plus 6.0 software (Media Cybernetics, United States) was used to calculate the area change of the scratches. Invasion experiments were performed in transwell chambers (Corning, NY, United States) with an 8 μ m pore diameter membrane. The upper layer of the chamber was added with

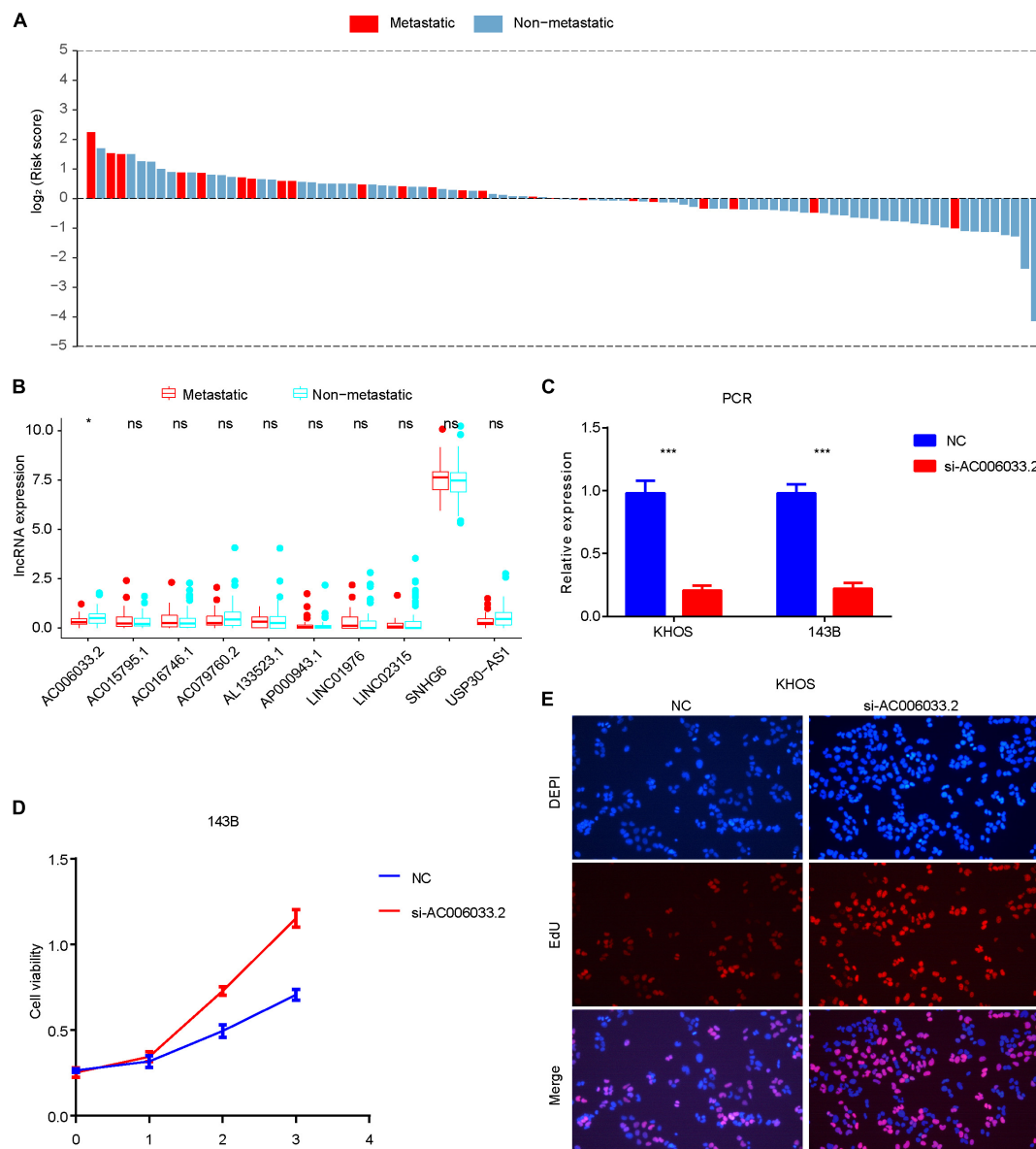


FIGURE 5 | Role of IRLs signature in metastasis and proliferation of osteosarcoma. **(A)** The probability of metastasis of osteosarcoma gradually decreases with the decrease of risk score. **(B)** Differential expression of 10 IRLs in metastatic and non-metastatic osteosarcomas. Only the expression level of AC006033.2 was different. **(C)** Knockdown results of AC006033.2 in osteosarcoma cell lines. **(D,E)** Effects of AC006033.2 knockdown on proliferation of osteosarcoma cells. * $P < 0.05$ and *** $P < 0.001$. EdU, 5-ethynyl-2'-deoxyuridine.

matrigel (BD, NJ, United States). The number of osteosarcoma cells inoculated was 1×10^5 pre well. The upper chamber was cultured with serum-free medium, and the lower chamber was cultured with a 700 μ L complete medium. After 48 h, the cells in the upper part of the basement membrane were erased, and the cells in the lower part of the basement membrane were fixed and stained.

Statistical Analysis

The statistical software R (version 3.6.1) was used for data analysis and image production. The Chi-square test was used

to compare differences in recurrence rates or metastasis rates of osteosarcoma. Spearman correlation analysis was used to evaluate the correlation between the expression level of lncRNAs, the correlation between risk score and lncRNA expression level, or the correlation between lncRNA expression level and immune cell content. The Kruskal–Wallis test was used to analyze the differences in immune cell content, tumor microenvironment score, or gene expression level. Kaplan–Meier survival analysis was used to evaluate prognostic differences between different risk scores or between different lncRNAs expression levels in osteosarcoma. Univariate Cox regression

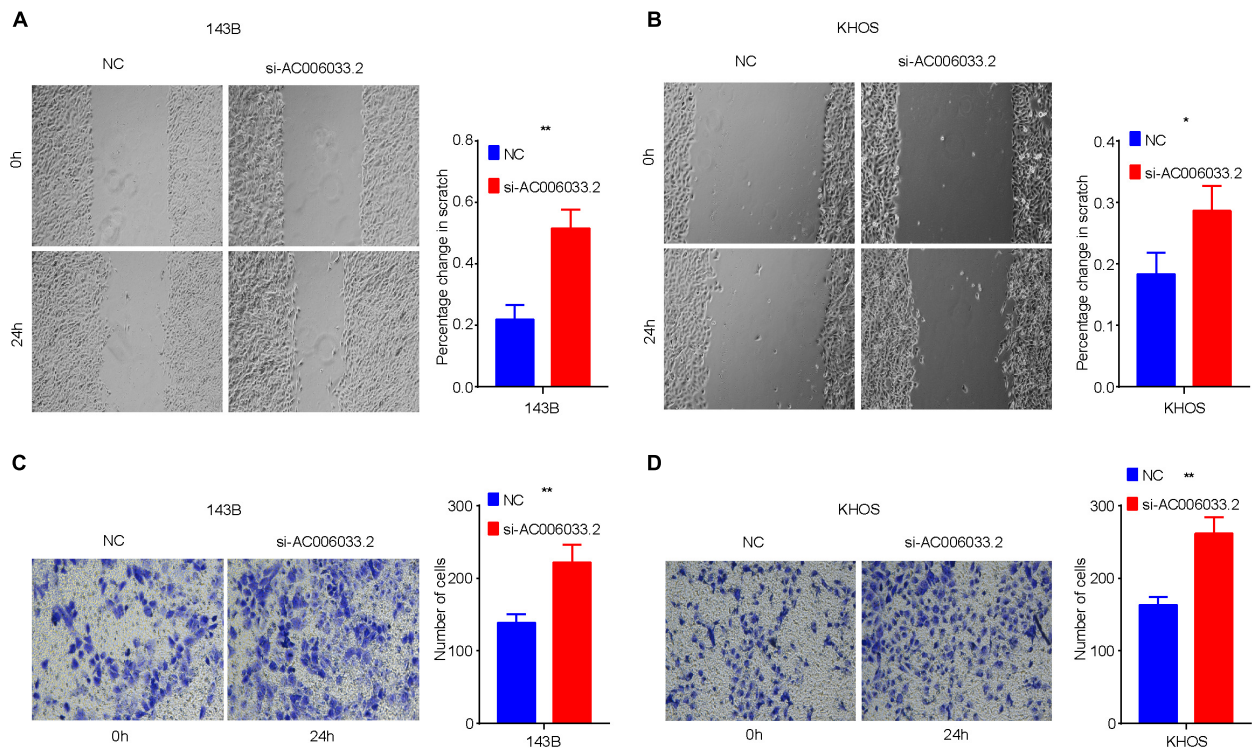


FIGURE 6 | Influence of AC006033.2 on migration and invasion ability of osteosarcoma. **(A,B)** Effects of AC006033.2 knockdown on the migration ability of osteosarcoma cells. **(C,D)** Effects of AC006033.2 knockdown on the invasion ability of osteosarcoma cells. * $P < 0.05$ and ** $P < 0.01$.

analysis and multivariate Cox regression analysis were used to evaluating the effects of lncRNA, clinical characteristics, or risk score on the prognosis of osteosarcoma. Two-tailed P -values were used, and the statistical significance was set at $P < 0.05$.

RESULTS

Data Processing and Co-expression Analyses of Immune-Related lncRNAs

Sequencing data and clinical data were downloaded from the TARGET database and expression levels of all samples were combined into an expression profile. The names of samples with both clinical and sequencing data are shown in **Supplementary Table 2**. Follow the above method, 95 osteosarcoma samples were included in the study. The expression levels of all lncRNA were shown in **Supplementary Table 3**. Correlation analysis was conducted between all lncRNAs and the gene set (IMMUNE RESPONSE TO TUMOR CELL), and 4986 IRLs were obtained (**Supplementary Table 4**).

Construction of Immune-Related lncRNAs Prognostic Signature

There were 4986 lncRNAs with variances greater than 0.2 expressed in IRLs. Univariate Cox regression analysis was performed on these IRLs, among which 1743 IRLs with P -value less than 0.5 were identified. Iterative LASSO regression was used

to identify high-frequency lncRNAs. One thousand iterations were executed, and 11 lncRNAs with a frequency greater than 300 were screened out. These lncRNAs were incorporated into the Cox regression analysis one by one until the AUC of ROC reached the maximum. At this point, the number of lncRNAs was 10 and the AUC was 0.96 (**Figures 1A,B**). The predict function was used to calculate the risk score of each osteosarcoma sample, and the osteosarcoma patients are divided into the high-risk group ($n = 48$) and low-risk group ($n = 47$) according to the optimal cut-off value (0.92) of risk score. Kaplan–Meier survival analysis showed that the lower risk score was associated with a better prognosis for osteosarcoma (**Figure 1C**). The distribution of 10 IRLs expression levels with the change of risk score was shown in **Figure 1D**. The results of principal component analysis (PCA) showed that IRLs signature can achieve better dimension reduction (**Figure 1E**). Correlation analysis results showed that the expression levels of these lncRNAs were not highly correlated (**Figure 1F**), which further demonstrated the rationality of IRLs signature.

The Role of Immune-Related lncRNAs Signature in the Prognosis of Osteosarcoma

Osteosarcoma patients were divided into high-risk group and low-risk group according to the optimal cut-off value of risk score (**Figure 2A**). With the increase of

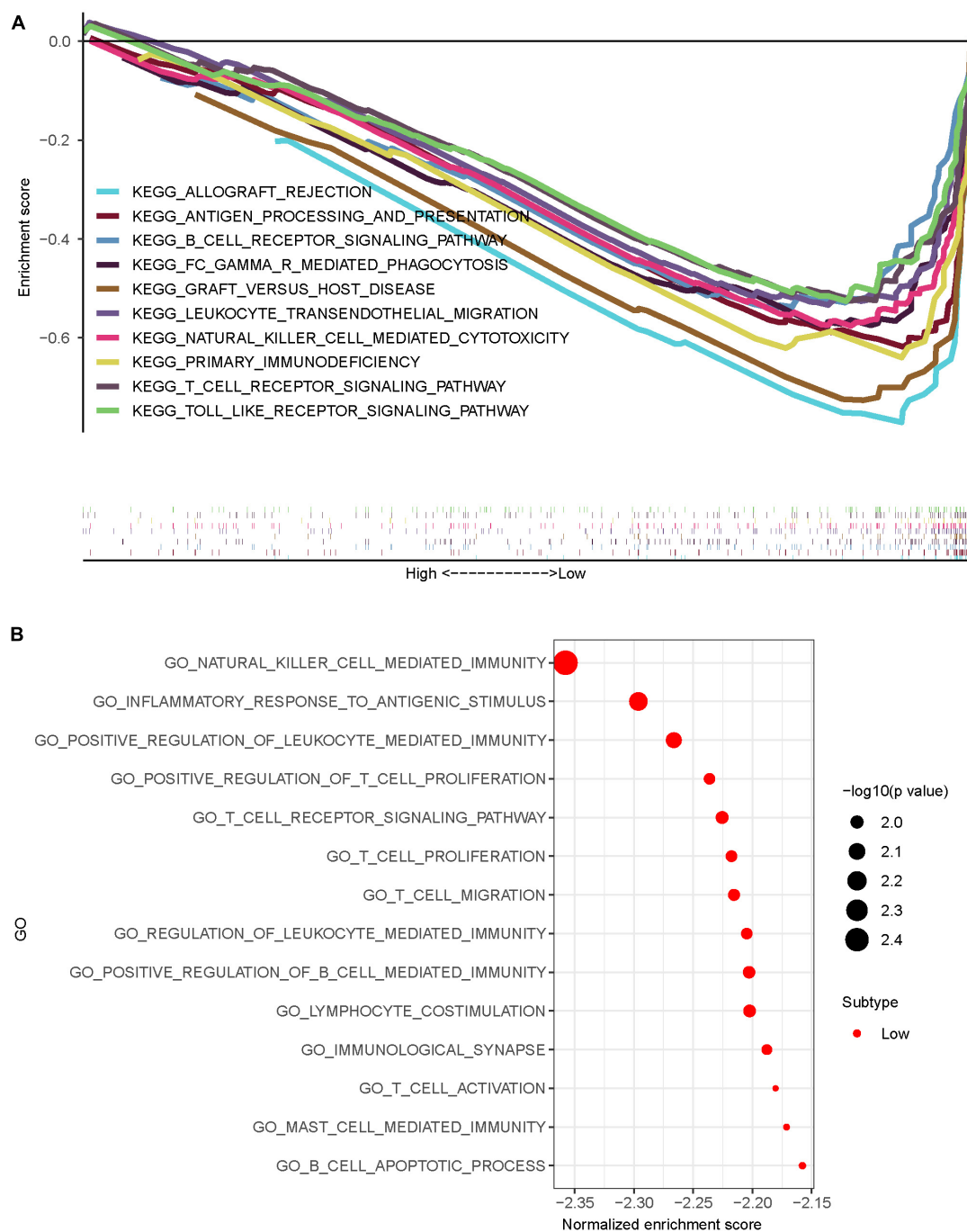


FIGURE 7 | Pathway and functional enrichment analysis of osteosarcoma in the high-risk and low-risk group osteosarcomas. **(A)** KEGG enrichment analysis of osteosarcomas showed that osteosarcomas in the low-risk group were mostly enriched in immune-related pathways. **(B)** GO enrichment analysis of osteosarcomas showed that osteosarcomas in the low-risk group were mostly enriched in immune-related functions.

risk score, the mortality rate of osteosarcoma increased significantly (**Figure 2B**). Results of survival analysis showed that osteosarcoma with high expression of AC006033.2, LINC02315, AL133523.1, USP30-AS1, or AC079760.2 had a better prognosis (**Figure 2C** and **Supplementary Figure 1A**). High expression of AP000943.1, AC015795.1,

AC016746.1, LINC01976, and SNHG6 was not conducive to the prognosis of osteosarcoma (**Figure 2D** and **Supplementary Figure 1B**). Cox regression analysis showed that AL133523.1, AC079760.2, and LINC01976 were independent prognostic factors for osteosarcoma (**Supplementary Tables 5, 6** and **Supplementary Figure 2**).

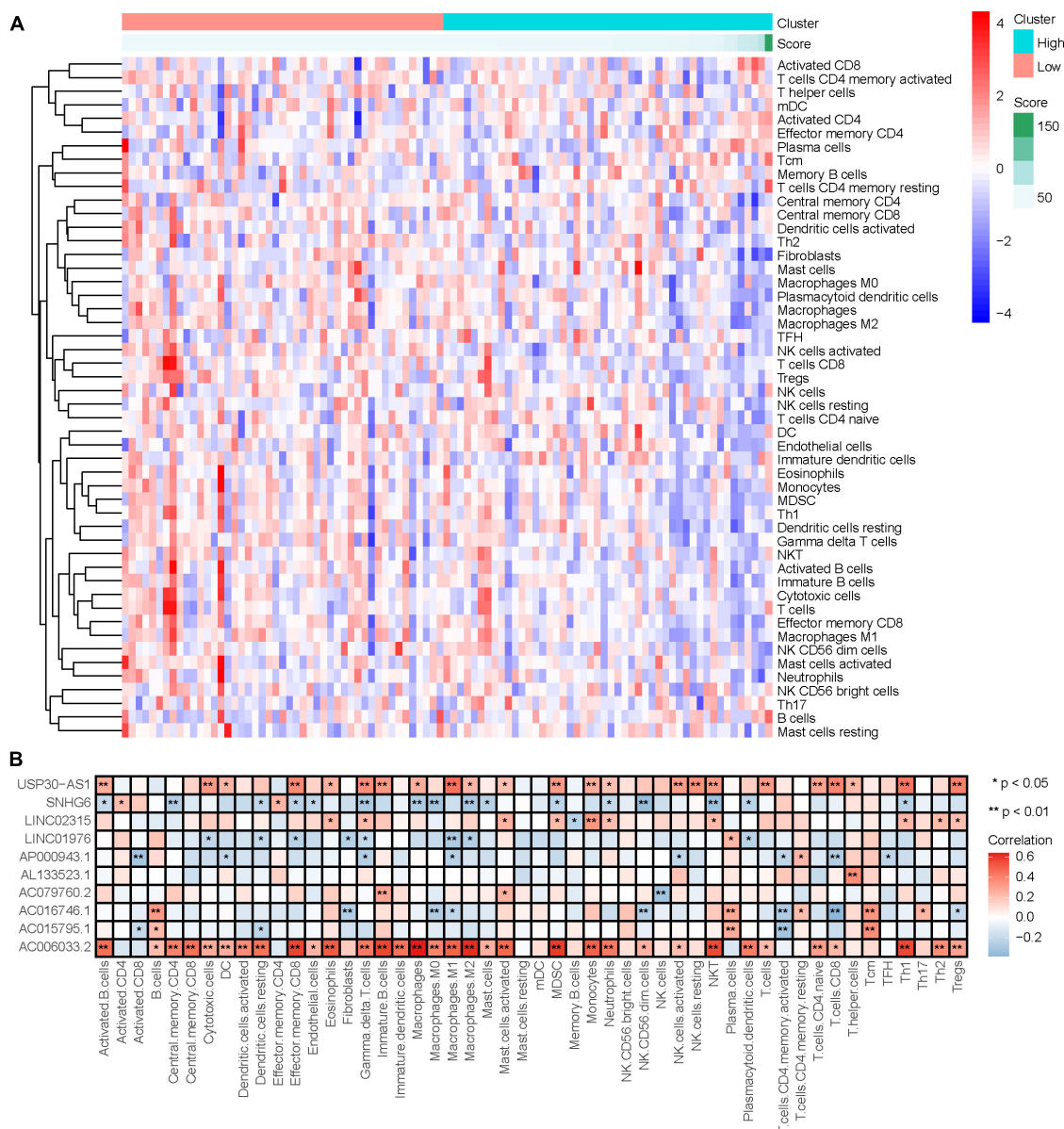


FIGURE 8 | Relationship between IRLs signature and the degree of immune cell infiltration. **(A)** Changes of the degree of immune cell infiltration in osteosarcoma with the change of risk score. **(B)** Correlation analysis between 10 IRLs and the degree of immune cell infiltration.

The Role of Clinical Features in the Prognosis of Osteosarcoma

Univariate and multivariate Cox regression analysis results showed that IRLs signature and the clinical features of osteosarcoma including recurrence, metastasis, and tumor location could all be independent prognostic factors for osteosarcoma (Figure 3A and Supplementary Tables 7, 8). In the prognostic evaluation of osteosarcoma, the predictive performance of IRLs signature was the highest among these features. In the ROC curve, the 1-, 3-, and 5-year AUC values were 0.802, 0.925, and 0.96, respectively (Figure 3B). In addition, the Chi-square test confirmed that the recurrence rates and

metastasis rates were higher in the high-risk group than in the low-risk group (Figure 3C). Survival analysis showed a poor prognosis for recurrent, metastatic, and non-limb osteosarcomas (Supplementary Figure 3A), and no significant difference in prognosis between sex and age (Supplementary Figure 3B).

The Construction and Verification of the Nomogram

The nomogram is widely used to evaluate the prognosis of tumors. It can reduce the statistical prediction model to a probability value. In this study, risk score, gender, age, recurrence, metastasis, and tumor location were integrated to

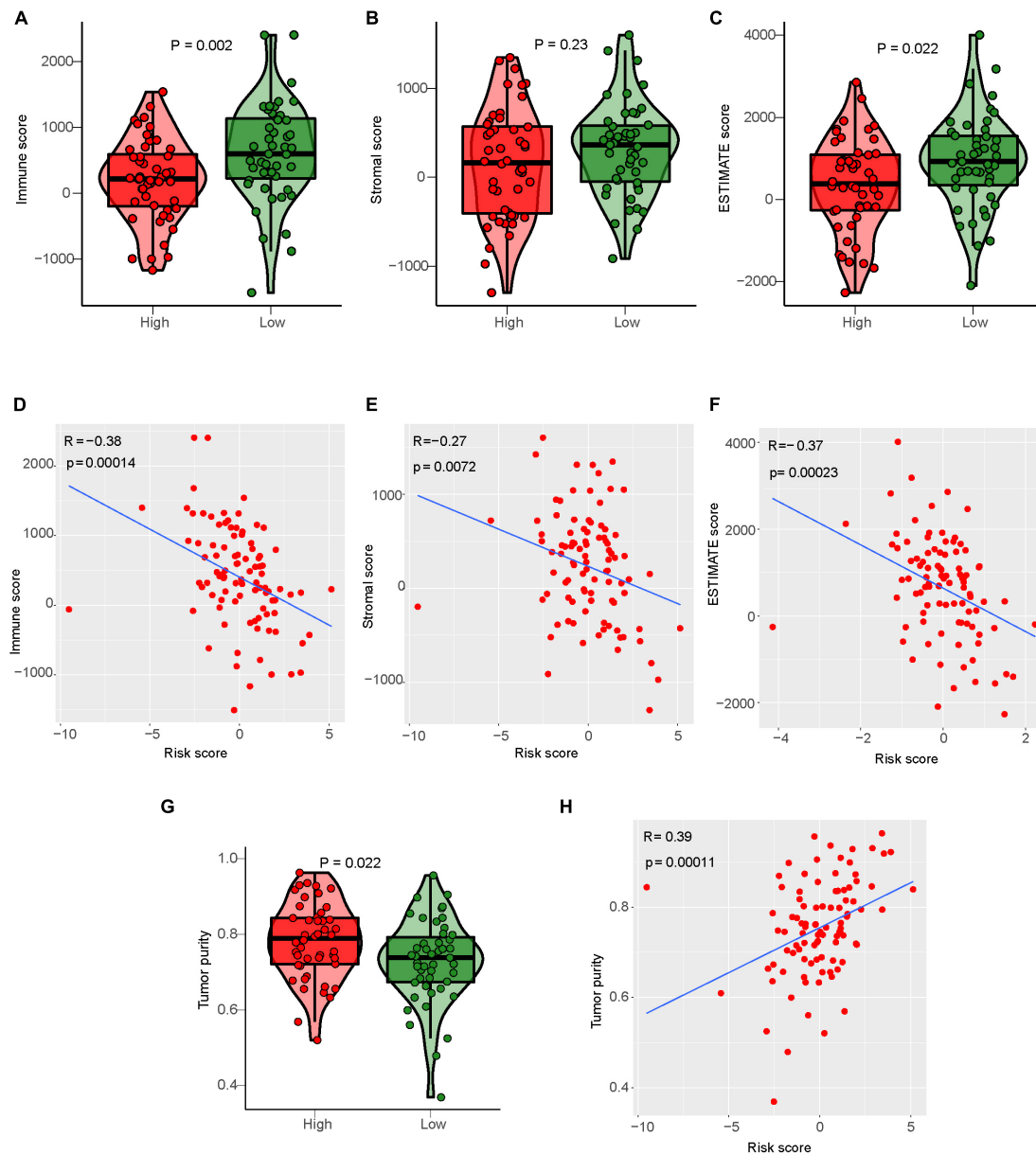


FIGURE 9 | Relationship between IRLs signature and tumor microenvironment score. **(A–C)** Analysis of differences in the immune score, stromal score, and Estimate score between high-risk and low-risk osteosarcoma. **(D–F)** Correlation analysis between risk score and osteosarcoma immune score, matrix score, and Estimate score. **(G)** Analysis of difference in tumor cell purity between high-risk and low-risk osteosarcoma. **(H)** Correlation analysis between risk score and tumor cell purity of osteosarcoma.

construct a nomogram to evaluate the prognosis of osteosarcoma (Figure 4A). The nomogram showed the predicted survival rates for 3 and 5 years, respectively. Calibration curves showed that the nomogram was able to accurately evaluate the prognosis of osteosarcoma (Figure 4B).

The Role of Immune-Related LncRNAs Signature in Osteosarcoma Metastasis

The metastasis of osteosarcoma is one of the most important factors affecting its prognosis. Therefore, this study focused on

the role of the IRLs signature in the metastasis of osteosarcoma. The Chi-square test confirmed that the metastatic rate of osteosarcoma was higher in the high-risk group than in the low-risk group (Figure 3C). The waterfall chart also shows that the probability of metastasis gradually decreases with the decrease of risk score (Figure 5A). Therefore, IRLs signature may play an important role in the metastasis of osteosarcoma. The results of the differential analysis showed that only AC006033.2 of the 10 lncRNAs of IRLs signature was different between the metastatic and non-metastatic osteosarcomas, and the expression

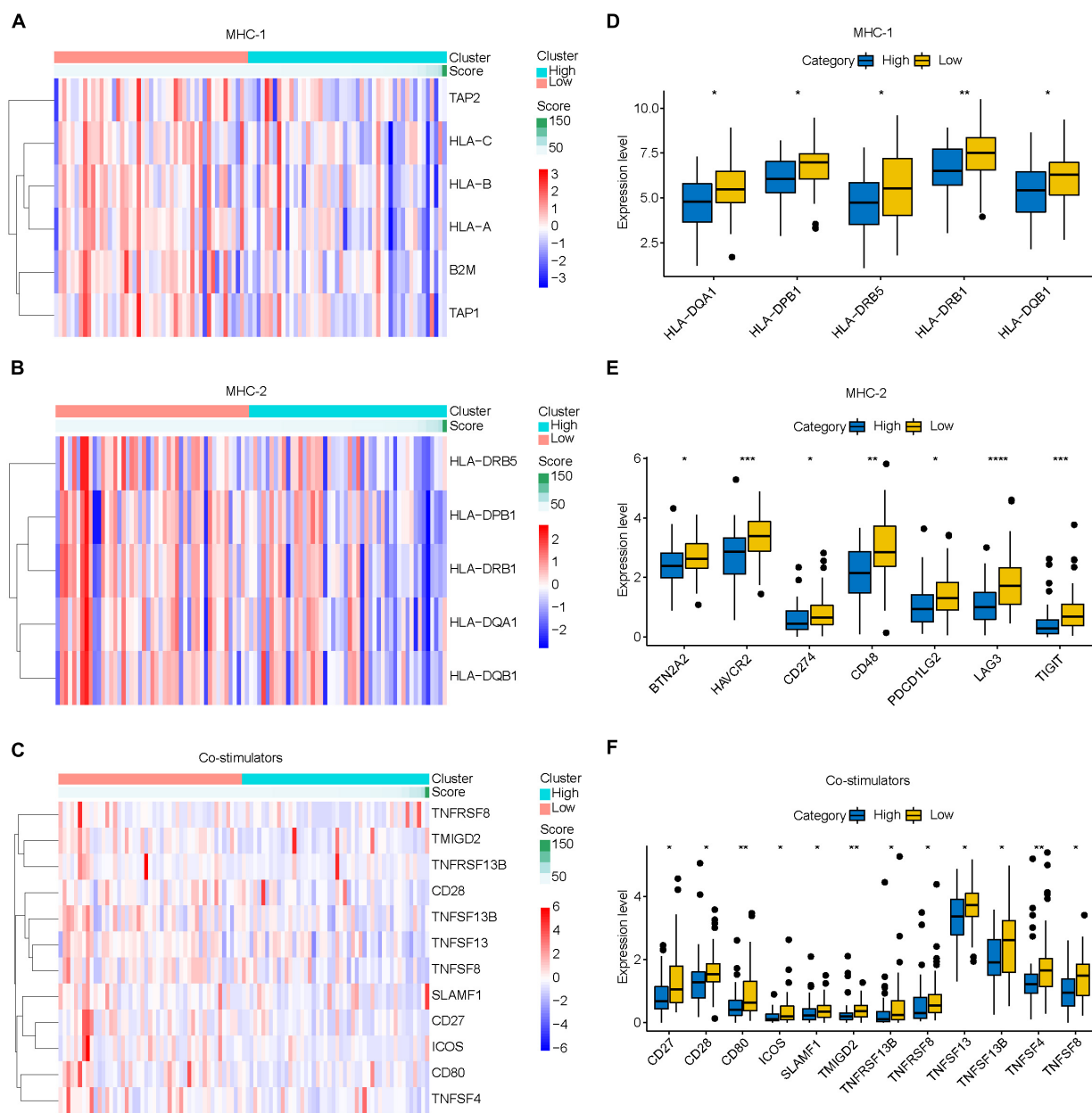


FIGURE 10 | Relationship between IRLs signature and endogenous immune escape in osteosarcoma. **(A–C)** The expression of MHC-I molecule, MHC-II molecule, and costimulatory molecule changed with the increase of risk score. **(D–F)** Differential analysis of the expression of MHC-I, MHC-II, and costimulatory molecules in high-risk and low-risk osteosarcoma. * $P < 0.05$; ** $P < 0.01$; *** $P < 0.001$; **** $P < 0.0001$.

level of AC006033.2 was low in the metastatic osteosarcomas (**Figure 5B**). For this reason, AC006033.2 was knocked down and validated in osteosarcoma cell lines. Knockdown efficacy was confirmed by PCR in osteosarcoma cell line 143B and KHOS (**Figure 5C**). We first conducted a cell proliferation experiment, and the results showed that knocking down AC006033.2 could increase the proliferation ability of osteosarcoma cells (**Figures 5D,E**). The wound-healing assay results further showed that knocking down AC006033.2 increased the migration ability of osteosarcoma cells (**Figures 6A,B**). Transwell invasion assay

showed increased invasiveness of osteosarcoma cells after AC006033.2 knockdown (**Figures 6C,D**).

KEGG Pathway Enrichment and GO Function Enrichment

Gene set enrichment analysis (GSEA) software was used to assess KEGG pathway enrichment in high-risk and low-risk osteosarcomas. The pathways that enriched in low-risk osteosarcomas were mainly immune-related (**Figure 7A**), while

no associated pathways enriched in high-risk osteosarcomas. The better prognosis of osteosarcoma in the low-risk group may be related to the local immune microenvironment.

To further explore the possible role of IRLs signature in osteosarcoma, GO enrichment analysis was performed using GSEA software. The results showed that osteosarcomas in the low-risk group were mainly enriched in immune-related functions (Figure 7B), while the high-risk group osteosarcomas were also not enriched in any meaningfully related functions.

The Role of Tumor Immune Microenvironment in the Influence of Immune-Related LncRNAs on Osteosarcoma Prognosis

Relationship Between Immune-Related LncRNAs Signature and Immune Cell Infiltration

LncRNA can regulate the development and activation of various immune cells (Atianand et al., 2017). Therefore, our study investigated the relationship between the degree of immune cell infiltration and IRLs signature in the immune microenvironment of osteosarcoma. The results of ssGSEA are shown in Supplementary Table 9, and the content of immune cells in osteosarcoma decreased with the increase of risk score (Figure 8A), and the correlation analysis results showed that risk score was negatively correlated with the content of most immune cells (Supplementary Figure 4), which suggested that the low degree of immune cell infiltration might be an important reason for recurrence and metastasis in the high-risk osteosarcoma. In addition, AC006033.2 was also positively correlated with the content of most immune cells (Figure 8B). Osteosarcoma with low AC006033.2 expression had a low level of immune cell infiltration, which was not conducive to the prognosis of osteosarcoma. This was consistent with the conclusion that AC006033.2 knockdown *in vitro* enhanced the invasiveness of osteosarcoma cells (Figures 6C,D).

Relationship Between Immune-Related LncRNAs Signature and Tumor Microenvironment Score

ESTIMATE algorithm can be used to evaluate the tumor microenvironment score of osteosarcoma to evaluate tumor stroma content, immune cell content, and tumor cell purity (Supplementary Table 10; Hu et al., 2021). Our study calculated the tumor microenvironment score of osteosarcoma by the ESTIMATE algorithm, and analyzed the relationship between them and risk score or the degree of immune cell infiltration (Supplementary Figure 5). Differential analysis results showed that the immunoscore, stromal score, and Estimate score of the low-risk group were higher than those of the high-risk group (Figures 9A–C). Correlation analysis results showed that risk score was negatively correlated with immune score, stromal score, and Estimate score. With the increase of risk score, the immune score, stromal score, and Estimate score of osteosarcoma gradually decreased (Figures 9D–F). Conversely, the purity of tumor cells in the low-risk osteosarcoma group was lower than that in the high-risk group, and the purity of tumor cells was negatively correlated with the risk score (Figures 9G,H).

Relationship Between Immune-Related LncRNAs Signature and Immune Escape in Osteosarcoma

Immune escape is an important reason for the rapid growth of tumor cells in the human body. In this study, we found that the prognosis of osteosarcoma may be related to the mechanism of endogenous immune escape. The molecules involved in endogenous immune escape include MHC-I molecules, MHC-II molecules, costimulatory molecules. Our results showed that the expression levels of MHC-I molecules, MHC-II molecules, and costimulatory molecules decreased with the increase of risk score (Figures 10A–C), and the different analysis results showed that the expression levels of these molecules in the high-risk group were lower than those in the low-risk group (Figures 10D–F). This suggests that immune escape is more likely to occur in the high-risk group osteosarcoma.

DISCUSSION

Compared with previous amputations alone, the survival rate for osteosarcoma has improved from 20% to more than 60% (Koster et al., 2018; Wang et al., 2018) but has not improved further in recent years. The high incidence of pulmonary metastasis is one of the important reasons. Therefore, searching for effective prognostic markers is an important method for early diagnosis of the prognosis of osteosarcoma and early intervention. In recent years, the role of TIM in the treatment of osteosarcoma has become increasingly evident. A growing number of immunotherapy agents are entering clinical trials (NCT04668300, NCT04544995, and NCT02500797). Therefore, we hope to find immune-related biomarkers that can not only better predict patient survival, but also provide potential therapeutic targets for future immunotherapy. LncRNA has been proved to be involved in the immune response of osteosarcoma by regulating the expression of TNF- α (Xu et al., 2020). To this end, we constructed a prognostic signature using IRLs to explore its role in the prognosis of osteosarcoma. Further, we explored the relationship between the IRLs signature and the TIM of osteosarcoma.

In this study, 10 IRLs with good predictive ability were selected as a prognostic marker for osteosarcoma by iterative LSSSO regression and multivariate Cox regression analysis. Compared with the simple univariate and multivariate Cox regression analysis, the IRLs signature has better predictive performance, with an AUC of 0.96. The results of PCA showed that IRLs signature could classify osteosarcoma into two groups. With the increase of risk score, the mortality of patients with osteosarcoma showed a significant upward trend. Recurrence and metastasis are important clinical features for the prognosis of osteosarcoma. Compared with the common clinical features of osteosarcoma, IRLs signature has higher predictive power for the prognosis of osteosarcoma, even higher than the two clinical features of osteosarcoma recurrence and metastasis.

Our study showed that the metastatic rate of osteosarcoma in the high-risk group was significantly higher than that in

the low-risk group, and the probability of metastasis tended to increase with the increase of risk score. It is worth noting that the differential expression analysis of lncRNA in IRLs signature between the metastatic group and the non-metastatic group showed that only the expression level of AC006033.2 was different. Therefore, our study further verified the role of AC006033.2 in the biological behavior of osteosarcoma through an *in vitro* experiment. By interfering with AC006033.2, we found that the proliferation, migration, and invasion of osteosarcoma cell lines were enhanced. Studies have shown that AC006033.2 is also an effective biomarker for anti-tumor immunity in gastric cancer (He and Wang, 2020), which is similar to the results of our study. We found that IRLs signature is closely related to the TIM of osteosarcoma. In addition, the expression level of AC006033.2 was significantly positively correlated with the content of various immune cells. Therefore, AC006033.2 may be an important molecule affecting the prognosis of osteosarcoma.

LncRNA THRIL has been shown to regulate TNF- α expression and participate in immune response in osteosarcoma (Xu et al., 2020). KEGG and GO enrichment analysis results also showed that osteosarcoma in the low-risk group was highly correlated with immune pathways and functions. Therefore, we further explored the relationship between IRLs signature and TIM of osteosarcoma. Firstly, the ssGSEA was used in the study to evaluate the level of immune cell infiltration in the microenvironment of osteosarcoma, and the level of immune cell infiltration was higher in the low-risk group. Results of the ESTIMATE algorithm also indicated a higher immune score in osteosarcoma in the low-risk group. These suggest that IRLs may be associated with the immune cell infiltration in the microenvironment of osteosarcoma.

Studies have shown that lncRNA can also act on T cells to promote the immune escape of tumor cells (Huang et al., 2018). Therefore, we further explored the relationship between the IRLs signature and the TIM of osteosarcoma. The decrease of MHC-I molecular presentation function is considered to be an important reason for the immune escape of tumor cells (Lee et al., 2005). Low expression of MHC-II molecules can also lead to the occurrence of immune escape due to the inability to effectively activate T cells (Zhi et al., 2021). In addition, the activation of T cells also requires the participation of costimulatory molecules (Angulo et al., 2021). We found that MHC-I molecules, MHC-II molecules, and costimulatory molecules, which are associated with endogenous immune escape, were all low expressed in the high-risk group. These results suggest that immune escape may

be prevalent in high-risk group osteosarcoma, and IRLs may be associated with the immune escape of osteosarcoma cells.

CONCLUSION

The IRLs signature is a reliable biomarker for the prognosis of osteosarcoma, and they alter the prognosis of osteosarcoma. In addition, IRLs signature and patient prognosis may be related to TIM in osteosarcoma. The higher the content of immune cells in the TIM of osteosarcoma, the lower the risk score of patients and the better the prognosis. The higher the expression of immune escape-related genes, the lower the risk score of patients and the better the prognosis.

DATA AVAILABILITY STATEMENT

The datasets presented in this study can be found in online repositories. The names of the repositories and accession numbers can be found in the article material.

AUTHOR CONTRIBUTIONS

WG conceived the project. QH, YL, CC, JL, TR, YH, HZ, YY, YG, WW, BW, JN, JX, and LG performed the literature search and data analysis. QH and WG drafted and critically revised the work. All authors contributed to manuscript revision, read, and approved the submitted version.

FUNDING

This work was supported by the Beijing Science and Technology Planning Project (No. Z16110000116100) and the National Natural Science Foundation of China (Nos. 81572633 and 82072970).

SUPPLEMENTARY MATERIAL

The Supplementary Material for this article can be found online at: <https://www.frontiersin.org/articles/10.3389/fcell.2021.731311/full#supplementary-material>

REFERENCES

- Anderson, M. E. (2016). Update on Survival in Osteosarcoma. *Orthop. Clin. North Am.* 47, 283–292. doi: 10.1016/j.ocln.2015.08.022
- Angulo, G., Zeleznjak, J., Martinez-Vicente, P., Punet-Ortiz, J., Hengel, H., Messerle, M., et al. (2021). Cytomegalovirus restricts ICOSL expression on antigen-presenting cells disabling T cell co-stimulation and contributing to immune evasion. *Elife* 10:e59350. doi: 10.7554/eLife.59350
- Atianand, M. K., Caffrey, D. R., and Fitzgerald, K. A. (2017). Immunobiology of long noncoding RNAs. *Annu. Rev. Immunol.* 35, 177–198. doi: 10.1146/annurev-immunol-041015-055459
- Bartonicek, N., Maag, J. L., and Dinger, M. E. (2016). Long noncoding RNAs in cancer: mechanisms of action and technological advancements. *Mol. Cancer* 15:43. doi: 10.1186/s12943-016-0530-6
- Bindea, G., Mlecnik, B., Tosolini, M., Kirilovsky, A., Waldner, M., Obenaus, A. C., et al. (2013). Spatiotemporal dynamics of intratumoral immune cells reveal the immune landscape in human cancer. *Immunity* 39, 782–795. doi: 10.1016/j.immuni.2013.10.003
- Cheng, W. Y., Ou Yang, T. H., and Anastassiou, D. (2013). Biomolecular events in cancer revealed by attractor metagenes. *PLoS Comput. Biol.* 9:e1002920. doi: 10.1371/journal.pcbi.1002920
- De Nola, R., Menga, A., Castegna, A., Loizzi, V., Ranieri, G., Cicinelli, E., et al. (2019). The crowded crosstalk between cancer cells and stromal

- microenvironment in gynecological malignancies: biological pathways and therapeutic implication. *Int. J. Mol. Sci.* 20:2401. doi: 10.3390/ijms20102401
- Han, G., Guo, Q., Ma, N., Bi, W., Xu, M., Jia, J., et al. (2021). lncRNA BCRT1 facilitates osteosarcoma progression via regulating miR-1303/FGF7 axis. *Aging (Albany N. Y.)* 13, 15501–15510. doi: 10.18632/aging.203106
- He, Y., and Wang, X. (2020). Identification of molecular features correlating with tumor immunity in gastric cancer by multi-omics data analysis. *Ann. Transl. Med.* 8:1050. doi: 10.21037/atm-20-922
- Hu, X., Wu, L., Liu, B., and Chen, K. (2021). Immune infiltration subtypes characterization and identification of prognosis-related lncRNAs in adenocarcinoma of the esophagogastric junction. *Front. Immunol.* 12:651056. doi: 10.3389/fimmu.2021.651056
- Huang, D., Chen, J., Yang, L., Ouyang, Q., Li, J., Lao, L., et al. (2018). NKILA lncRNA promotes tumor immune evasion by sensitizing T cells to activation-induced cell death. *Nat. Immunol.* 19, 1112–1125. doi: 10.1038/s41590-018-0207-y
- Huang, Q., Liang, X., Ren, T., Huang, Y., Zhang, H., Yu, Y., et al. (2021). The role of tumor-associated macrophages in osteosarcoma progression-therapeutic implications. *Cell. Oncol. (Dordr.)* 44, 525–539. doi: 10.1007/s13402-021-00598-w
- Iasonos, A., Schrag, D., Raj, G. V., and Panageas, K. S. (2008). How to build and interpret a nomogram for cancer prognosis. *J. Clin. Oncol.* 26, 1364–1370. doi: 10.1200/JCO.2007.12.9791
- Kornfeld, J. W., and Bruning, J. C. (2014). Regulation of metabolism by long, non-coding RNAs. *Front. Genet.* 5:57. doi: 10.3389/fgene.2014.00057
- Koster, R., Panagiotou, O. A., Wheeler, W. A., Karlins, E., and Gastier-Foster, J. M. (2018). Caminada de Toledo SR, et al. Genome-wide association study identifies the GLDC/IL33 locus associated with survival of osteosarcoma patients. *Int. J. Cancer* 142, 1594–1601. doi: 10.1002/ijc.31195
- Lee, F. T., Mountain, A. J., Kelly, M. P., Hall, C., Rigopoulos, A., Johns, T. G., et al. (2005). Enhanced efficacy of radioimmunotherapy with 90Y-CHX-A⁺-DTPA-hu3S193 by inhibition of epidermal growth factor receptor (EGFR) signaling with EGFR tyrosine kinase inhibitor AG1478. *Clin. Cancer Res.* 11(19 Pt 2), 7080s–7086s. doi: 10.1158/1078-0432.CCR-1004-0019
- Newman, A. M., Liu, C. L., Green, M. R., Gentles, A. J., Feng, W., Xu, Y., et al. (2015). Robust enumeration of cell subsets from tissue expression profiles. *Nat. Methods* 12, 453–457. doi: 10.1038/nmeth.3337
- Pan, X., Tan, J., Tao, T., Zhang, X., Weng, Y., Weng, X., et al. (2021). LINC01123 enhances osteosarcoma cell growth by activating the Hedgehog pathway via the miR-516b-5p/Gli1 axis. *Cancer Sci.* 112, 2260–2271. doi: 10.1111/cas.14913
- Pitt, J. M., Marabelle, A., Eggermont, A., Soria, J. C., Kroemer, G., and Zitvogel, L. (2016). Targeting the tumor microenvironment: removing obstruction to anticancer immune responses and immunotherapy. *Ann. Oncol.* 27, 1482–1492. doi: 10.1093/annonc/mdw168
- Qian, X., Zhao, J., Yeung, P. Y., Zhang, Q. C., and Kwok, C. K. (2019). Revealing lncRNA structures and interactions by sequencing-based approaches. *Trends Biochem. Sci.* 44, 33–52. doi: 10.1016/j.tibs.2018.09.012
- Senbabaoglu, Y., Gejman, R. S., Winer, A. G., Liu, M., Van Allen, E. M., de Velasco, G., et al. (2016). Tumor immune microenvironment characterization in clear cell renal cell carcinoma identifies prognostic and immunotherapeutically relevant messenger RNA signatures. *Genome Biol.* 17:231. doi: 10.1186/s13059-016-1092-z
- Sveen, A., Agesen, T. H., Nesbakken, A., Meling, G. I., Rognum, T. O., Liestol, K., et al. (2012). ColoGuidePro: a prognostic 7-gene expression signature for stage III colorectal cancer patients. *Clin. Cancer Res.* 18, 6001–6010. doi: 10.1158/1078-0432.CCR-11-3302
- Wang, H., Sun, W., Sun, M., Fu, Z., Zhou, C., Wang, C., et al. (2018). HER4 promotes cell survival and chemoresistance in osteosarcoma via interaction with NDRG1. *Biochim. Biophys. Acta Mol. Basis Dis.* 1864(5 Pt A), 1839–1849. doi: 10.1016/j.bbdis.2018.03.008
- Wang, S., Zhang, Q., Yu, C., Cao, Y., Zuo, Y., and Yang, L. (2021). Immune cell infiltration-based signature for prognosis and immunogenomic analysis in breast cancer. *Brief. Bioinform.* 22, 2020–2031. doi: 10.1093/bib/bbaa026
- Wang, Y., Li, J., Xia, Y., Gong, R., Wang, K., Yan, Z., et al. (2013). Prognostic nomogram for intrahepatic cholangiocarcinoma after partial hepatectomy. *J. Clin. Oncol.* 31, 1188–1195. doi: 10.1200/JCO.2012.41.5984
- Xu, B., Jin, X., Yang, T., Zhang, Y., Liu, S., Wu, L., et al. (2020). Upregulated lncRNA THRIL/TNF- α signals promote cell growth and predict poor clinical outcomes of osteosarcoma. *Onco Targets Ther.* 13, 119–129. doi: 10.2147/OTT.S235798
- Yoshihara, K., Shahmoradgol, M., Martinez, E., Vegesna, R., Kim, H., Torres-Garcia, W., et al. (2013). Inferring tumour purity and stromal and immune cell admixture from expression data. *Nat. Commun.* 4:2612. doi: 10.1038/ncomms3612
- Zhang, G. Z., Wu, Z. L., Li, C. Y., Ren, E. H., Yuan, W. H., Deng, Y. J., et al. (2021). Development of a machine learning-based autophagy-related lncRNA signature to improve prognosis prediction in osteosarcoma patients. *Front. Mol. Biosci.* 8:615084. doi: 10.3389/fmolb.2021.615084
- Zhao, Y., Yu, Z., Ma, R., Zhang, Y., Zhao, L., Yan, Y., et al. (2021). lncRNA-Xist/miR-101-3p/KLF6/C/EBP α axis promotes TAM polarization to regulate cancer cell proliferation and migration. *Mol. Ther. Nucleic Acids* 23, 536–551. doi: 10.1016/j.omtn.2020.12.005
- Zhi, J., Zhang, P., Zhang, W., Ruan, X., Tian, M., Guo, S., et al. (2021). Inhibition of BRAF sensitizes thyroid carcinoma to immunotherapy by enhancing tsMHCII-mediated immune recognition. *J. Clin. Endocrinol. Metab.* 106, 91–107. doi: 10.1210/clinem/dgaa656
- Zhou, Y., and Mu, T. (2021). lncRNA LINC00958 promotes tumor progression through miR-4306/CEMIP axis in osteosarcoma. *Eur. Rev. Med. Pharmacol. Sci.* 25, 3182–3199. doi: 10.26355/eurrev_202104_25727

Conflict of Interest: The authors declare that the research was conducted in the absence of any commercial or financial relationships that could be construed as a potential conflict of interest.

Publisher's Note: All claims expressed in this article are solely those of the authors and do not necessarily represent those of their affiliated organizations, or those of the publisher, the editors and the reviewers. Any product that may be evaluated in this article, or claim that may be made by its manufacturer, is not guaranteed or endorsed by the publisher.

Copyright © 2021 Huang, Lin, Chen, Lou, Ren, Huang, Zhang, Yu, Guo, Wang, Wang, Niu, Xu, Guo and Guo. This is an open-access article distributed under the terms of the Creative Commons Attribution License (CC BY). The use, distribution or reproduction in other forums is permitted, provided the original author(s) and the copyright owner(s) are credited and that the original publication in this journal is cited, in accordance with accepted academic practice. No use, distribution or reproduction is permitted which does not comply with these terms.



CDKN2B-AS1 Promotes Malignancy as a Novel Prognosis-Related Molecular Marker in the Endometrial Cancer Immune Microenvironment

Di Yang¹, Jian Ma² and Xiao-Xin Ma^{2*}

¹ Department of Gynecology, Cancer Hospital of China Medical University, Liaoning Cancer Hospital and Institute, Shenyang, China, ² Department of Obstetrics and Gynecology, Shengjing Hospital of China Medical University, Shenyang, China

OPEN ACCESS

Edited by:

Zong Sheng Guo,
Roswell Park Comprehensive Cancer
Center, United States

Reviewed by:

Pranshu Sahgal,
Dana-Farber Cancer Institute,
United States
Muhammad Mosaraf Hossain,
University of Chittagong, Bangladesh

*Correspondence:

Xiao-Xin Ma
maxiaoxin666@aliyun.com

Specialty section:

This article was submitted to
Molecular and Cellular Oncology,
a section of the journal
Frontiers in Cell and Developmental
Biology

Received: 07 June 2021

Accepted: 17 September 2021

Published: 12 October 2021

Citation:

Yang D, Ma J and Ma X-X (2021)
CDKN2B-AS1 Promotes Malignancy
as a Novel Prognosis-Related
Molecular Marker in the Endometrial
Cancer Immune Microenvironment.
Front. Cell Dev. Biol. 9:721676.
doi: 10.3389/fcell.2021.721676

The prognosis of patients with endometrial cancer (EC) is closely associated with immune cell infiltration. Although abnormal long non-coding RNA (lncRNA) expression is also linked to poor prognosis in patients with EC, the function and action mechanism of immune infiltration-related lncRNAs underlying the occurrence and development of EC remains unclear. In this study, we analyzed lncRNA expression using The Cancer Genome Atlas and clinical data and identified six lncRNAs as prognostic markers for EC, all of which are associated with the infiltration of immune cell subtypes, as illustrated by ImmLnc database and ssGSEA analysis. Real-time quantitative polymerase chain reaction showed that CDKN2B-AS1 was significantly overexpressed in EC, whereas its knockdown inhibited the proliferation and invasion of EC cells and the *in vivo* growth of transplanted tumors in nude mice. Finally, we constructed a competing endogenous RNA regulatory network and conducted Gene Ontology enrichment analysis to elucidate the potential molecular mechanism underlying CDKN2B-AS1 function. Overall, we identified molecular targets associated with immune infiltration and prognosis and provide new insights into the development of molecular therapies and treatment strategies against EC.

Keywords: endometrial cancer, lncRNA, prognostic signature, immune infiltration, CDKN2B-AS1

INTRODUCTION

Endometrial cancer (EC) is one of the most common malignant tumors of the female reproductive system, and its incidence has increased in recent years, particularly in younger females (Smrz et al., 2020). In 2020, approximately 65,620 new cases of EC in the United States and 12,590 related deaths have been reported, with a mortality rate second only to ovarian cancer (Siegel et al., 2020). The efficacy of the currently available treatments for patients with recurrent or advanced EC remains poor (Leslie et al., 2021); however, novel immunotherapies have attracted significant attention as potential treatment strategies for patients with EC (Meng et al., 2021). It is therefore important to explore and develop reliable immune-related targets and prognostic markers for EC for individualized treatment of EC.

In 2013, The Cancer Genome Atlas (TCGA) had proposed a molecular typing system that divided EC into four subtypes, namely, DNA polymerase epsilon (POLE), microsatellite instability (MSI), copy number abnormalities low (CNL), and copy number abnormalities high (CNH) (Du et al., 2019). These subtypes can help to more accurately classify post-operative

treatments (including immunotherapy) and prognosis of patients with EC than the traditional pathomorphology (Zhou et al., 2021). In POLE hypermutant and MSI EC, PD-1, and PD-L1 expression are correlated with the degree of T lymphocyte infiltration, with a higher number of infiltrating T lymphocytes eliciting a stronger local immune response associated with better prognosis (Liu et al., 2021). The diagnosis and treatment of EC has influenced its molecular classification (Kahn et al., 2019), and this has prompted the use of immunotherapies based on the tumor microenvironment (TME), genotype, and epigenetic alterations. Although some patients with EC have shown encouraging results following immunotherapy, some have failed to respond (Meng et al., 2021). However, the therapeutic efficacy of immune checkpoint inhibitors can be predicted based on PD-L1 expression, mutational load, lymphocyte infiltration, and mutation-related neoantigens (Post et al., 2020).

Less than 2% of the human genome encodes transcribable protein-coding genes, whereas 85% encodes non-coding RNAs. Long non-coding RNAs (lncRNAs) are RNAs over 200 nucleotides in length that do not encode proteins but play key roles in regulating transcription and post-transcriptional events affecting cell function (Zheng et al., 2019). lncRNA are being actively explored as biomarkers, supporting their prevalent link with diseases. For example, through experiments in humans and mice showed that there is an lncRNA locus *maenli* on human chromosome 2 (Allou et al., 2021), and its deletion result in human Mendelian disease. Transcription of the lncRNA *upperhand* controls *Hand2* expression and heart development (Anderson et al., 2016). Such promising developments suggest that the entrance of lncRNA-based therapeutics into clinical testing is imminent. Recent findings have demonstrated that lncRNAs can shape the TME by changing the internal characteristics of tumor cells, thereby promoting and maintaining tumor occurrence and development (Dong et al., 2019). In breast and ovarian cancer cells, the lncRNA *Xist* mediates macrophage polarization by competing with microRNA (miR)-101 to regulate *KLF6* expression, thereby affecting proliferation and migration (Zhao et al., 2021). Similarly, the lncRNA *HEIH* can improve the immunogenicity of triple-negative breast cancer (TNBC) cells and regulate TNBC progression by inducing *MICA/B* and suppressing the immune checkpoint inhibitor, PD-L1 (Nafea et al., 2021). lncRNAs can induce tumor occurrence and metastasis by activating the immune system and responses, including antigen release, antigen presentation, immune cell differentiation, immune cell migration, and T cell infiltration (Huang et al., 2018). However, the roles of immune-related lncRNAs in EC remain to be investigated.

In this study, we analyzed results for EC samples in TCGA and identified six lncRNAs, namely, *PRRT3-AS1*, *LINC01503*, *CDKN2B-AS1*, *LINC01629*, *LINC01833*, and *LINC01936*, associated with the immune microenvironment whose high expression may be correlated with poor patient prognosis. We also analyzed the correlation between the expression of these lncRNAs and immune cell infiltration, common immune checkpoints, MHC molecules, chemokines, and chemokine receptors. In addition, their expression was verified using

real-time polymerase chain reaction (PCR) in EC tissues and normal tissues while *in vitro* and *in vivo* experiments confirmed that *CDKN2B-AS1* knockdown inhibited EC cell proliferation and invasion, as well as their ability to form tumors. Together, the findings of this study provide new insights and theoretical basis for future immunotherapies to treat EC.

MATERIALS AND METHODS

Identification of Immune-Related Long Non-coding RNAs in Endometrial Cancer

The transcriptome profiles and corresponding clinical data of 575 patients with EC were downloaded from TCGA, including 552 patients with UCEC and 23 normal samples. First, we screened differentially expressed genes (DEGs) using the “limma” program package with the following criteria: $|\log_2FC| > 1$ and $FsDR < 0.05$. A heat map and volcano map were produced from the resulting DEGs. Immune-related lncRNA genes were obtained using the official ImmLnc website. Differentially expressed immune-related lncRNAs were screened using $|\log_2FC| > 1$ and $p < 0.05$ and then analyzed using the Edger software package.

Identification of Immune-Related Long Non-coding RNA Prognostic Indicators for Endometrial Cancer

To screen immune-related lncRNAs associated with survival from the clinical EC data from TCGA, we performed univariate Cox proportional hazard regression (PHR) analysis with $p < 0.001$. Multivariate Cox PHR analysis was used to identify prognostic markers, while the risk score of each patient was calculated based on lncRNA expression levels. According to the median risk score, patients with EC were divided into high- and low-risk groups. Univariate and multivariate Cox regression analyses were then used to evaluate the relationships between risk score and age, tumor grade, tumor differentiation, and depth of invasion. Survival differences between the two groups were determined using Kaplan–Meier (KM) survival analysis.

Correlation Analysis of Immune Cell Infiltration

Immune infiltration analysis was performed based on the ssGSEA scores of activated dendritic cells (aDCs), B cells, CD8 T cells, cytotoxic cells, DCs, eosinophils, immature DCs (iDCs), macrophages, mast cells, neutrophils, natural killer (NK) CD56bright cells, NK CD56dim cells, NK cells, plasmacytoid DCs (pDCs), T cells, T helper cells, T central memory cells (Tcm), T effector memory cells (Tem), T follicular helper (Tfh), T gamma delta (Tgd), Th1 cells, Th17 cells, Th2 cells, and Treg cells to determine whether immune infiltration correlated with lncRNA expression. The online analysis website, ImmLnc,¹ was used to determine the immune-related functions of lncRNAs in cancer,

¹<http://bio-bigdata.hrbmu.edu.cn/ImmLnc>

as well as lncRNA pathways, correlations between lncRNAs and immune cell types, and cancer-related lncRNAs.

Construction of the ceRNA Regulatory Network

Differentially expressed lncRNAs and miRNAs were paired using the miRcode database. Based on the miRDB, miRTarBase, and TargetScan databases, starBase online software was used to predict the target genes of the screened differentially expressed miRNAs to obtain a ceRNA regulatory network diagram of lncRNA–miRNA–mRNAs using the visual analysis software, Cytoscape V3.5.2.

Functional Enrichment Analysis

We used Metascape² to analyze the pathways enriched by the 100 molecules most relevant to CDKN2B-AS1.

Patients and Samples

This study enrolled patients (aged 23–69-years-old) who had undergone surgical uterus removal at the Department of Obstetrics and Gynecology, Shengjing Hospital Affiliated to China Medical University, from 2017 to 2018. We collected 20 EC tissue samples and 20 normal endometrial tissue samples. No patients had received anti-cancer treatments, such as radiotherapy, chemotherapy, or immunotherapy, prior to surgery. Histopathological analysis was performed by two pathologists. The study was approved by the Ethics Committee of Shengjing Hospital Affiliated to China Medical University (Ethics number: 2018PS251K). All study participants provided informed consent.

Cell Culture

Ishikawa cells were cultured in RPMI 1640 medium (Gibco, Carlsbad, CA, United States), while HEC-1A cells were cultured in McCoy's 5A medium (Gibco). Both cell lines were obtained from the Institute of Biochemistry and Cell Biology at the Chinese Academy of Sciences (Shanghai, China).

Fluorescence *in situ* Hybridization

To determine the localization of lncRNAs in EC cells, fluorescence *in situ* hybridization (FISH) probes (RiboBio, Guangzhou, China) were constructed. Both Ishikawa and HEC-1A cells were treated with 1% paraformaldehyde at 37°C for 1 h and then incubated with the hybridization probe at 37°C for 16 h. On the second day, the cells were washed with hybridization solutions I, II, and III, and images were taken and analyzed using a fluorescent inverted microscope (20× magnification).

Cell Transfection

CDKN2B-AS1 interference lentiviral vectors and a corresponding negative control (NC) were purchased from GenePharma (Shanghai, China) and transfected at a multiplicity of infection (MOI) of 50. Cells were transfected using Lipofectamine 3000 (Invitrogen) according to the manufacturer's

instructions, and stably transfected cells were selected using puromycin. The primers used for cloning and the shRNA sequences are listed in **Supplementary Table 1**.

Cell Proliferation Assay

During their logarithmic growth phase, Ishikawa and HEC-1A cells were transferred into 96-well plates that included a blank control and three parallel wells per group. Cell proliferation was detected using an EdU cell proliferation detection kit (RiboBio, Guangzhou, China) according to the manufacturer's instructions. Briefly, cells were incubated with 50 μM of pre-prepared EdU mixed reagent for 2 h, fixed, and subjected to DNA staining. The cells were then washed with phosphate-buffered saline (PBS) and images were acquired and analyzed using a fluorescence microscope (Nikon, Japan) at 20× magnification.

Cell Invasion Assay

Sterilized Transwell chambers were coated with Matrigel (pore size 8 μM; Corning, NY, United States) and incubated at 37°C overnight to solidify. Logarithmic phase cells were harvested, centrifuged, and resuspended in serum-free medium after the supernatant had been discarded. Next, 800 μL of culture medium (containing 10% fetal bovine serum) was added to a 24-well plate and the Transwell chamber was added. The cell suspension (5×10^4 cells) was then added to the upper chamber and incubated for 24 h at 5% CO₂ and 37°C. After the Transwell chamber had been removed, the cells in each well were absorbed and the liquid in the upper chamber was discarded. The wells were then air-dried, fixed with 4% paraformaldehyde, stained with crystal violet dye, and rinsed with PBS. Images were acquired under a microscope (Nikon, Japan) and the cells were counted.

RNA Extraction and Quantitative Real-Time-Polymerase Chain Reaction

Total RNA was extracted from cultured cells or tissues using TRIzol reagent (Takara, Shiga, Japan) and reverse-transcribed into cDNA using a PrimeScriptTM RT-PCR Kit (Takara) with SYBR[®] TB GreenTM Premix Ex Taq II (Takara). PCR-specific primers were designed by Sangon Biotech (Shanghai, China). Fold changes in expression were calculated using the $2^{-\Delta\Delta C_t}$ method, with *GAPDH* as an internal control. The primer sequences used are listed in **Supplementary Table 1**.

Tumor Xenografts in Nude Mice

All animal experiments were approved by the Ethics Committee of Shengjing Hospital Affiliated to China Medical University and were conducted in strict accordance with ethical standards. Athymic BALB/c nude mice (4–6 weeks old) were purchased from HFK Bioscience (Beijing, China). For the *in vivo* study, CDKN2B-AS1 shRNA and control shRNA stably transfected Ishikawa cells were harvested, the underarm tumor of each mouse was injected with transfected cells suspended in $10^6/100$ μL PBS, tumor sizes were measured by caliper and recorded every 4 days. The mice were sacrificed after 28 days. Tumors were excised, placed in 4% paraformaldehyde, and embedded in paraffin.

²<http://metascape.org>

Statistical Analysis

Statistical analyses were performed using R software (Version 3.5.1) and GraphPad Prism 8 software (GraphPad, La Jolla, CA, United States). Differences between count data were calculated using the χ^2 test, with the data expressed as the mean \pm SEM. Data between two groups were compared using unpaired *t*-tests. *p*-Values of <0.05 were considered statistically significant.

RESULTS

Analysis of Differentially Expressed Immune-Related Long Non-coding RNAs in Endometrial Cancer Tissues

We analyzed the data of EC samples ($n = 552$) and normal endometrium samples ($n = 23$) in the TCGA database, with criteria of $|\log_2\text{FC}| > 1$ and $\text{FDR} < 0.05$, and identified a total of 6,266 DEGs, of which 3,860 were upregulated and 2,406 were downregulated (Figure 1A). Immune-related lncRNA gene information was obtained using the ImmLnc website and 340 differentially expressed immune-related lncRNAs were screened according to the nature of the gene, of which 228 were upregulated and 112 were downregulated (Figure 1B).

Identification and Prognostic Characteristics of Six Immune-Related Long Non-coding RNAs

To predict the prognosis of EC patients, we constructed a risk scoring model based on the survival data for the EC samples. Univariate Cox PHR analysis on the expression profiles of 340 lncRNAs identified seven immune-related lncRNAs with $p < 0.001$ whose expression was related to prognosis (Figure 2A). Subsequent stepwise multiple Cox regression analysis determined that the expression of six immune-related lncRNAs was related to prognosis: PRRT3-AS1, LINC01503, LINC01936, CDKN2B-AS1, LINC01629, and LINC01833 (Figure 2B). The coefficient of each molecule factors were calculated with multivariate Cox proportional risk regression analysis. The risk score was then calculated for each sample based on the expression levels of these six lncRNAs using the following equation (Table 1):

$$\begin{aligned} \text{Risk score} = & (0.06 \times \text{PRRT3}) - \text{AS1} + (0.02 \times \text{LINC01503}) + \\ & (0.32 + \text{LINC01936}) + (1.03 + \text{CDKN2B}) - \text{AS1} \\ & + (0.20 + \text{LINC01629}) + (0.05 \times \text{LINC01833}). \end{aligned}$$

Correlation Between the Immune-Related Long Non-coding RNA Signature and the Overall Survival and Prognosis of Patients With Endometrial Cancer

According to the median risk score, EC samples were divided into high- and low-risk groups and a KM curve was created to calculate overall survival (OS) rates. The high-risk group

displayed poor OS, indicating that the risk score effectively evaluated prognosis [$p = 3.505e^{-07}$, area under the curve (AUC) = 0.687; Figures 3A,B]. The risk curve and scatter plot were generated to show the risk score and survival status of each endometrial cancer sample. The risk coefficient and mortality of samples in the high-risk group were higher than those in the low-risk group (Figure 3C). A heat map of the expression profiles of the six lncRNAs in EC samples showed that all six were highly expressed in the high-risk group (Figure 3D). Together, these findings suggest that the six immune-related lncRNAs can be used as prognostic markers for EC.

To verify the applicability of this prognostic signature based on the complete TCGA data set, we randomly divided 541 patients with EC in TCGA into two test sets (1, $n = 271$, Supplementary Figure 1, 2, $n = 270$, Supplementary Figure 2) to build a verification model. Consistent with the results observed in the entire data set, the OS rate of patients in the high-risk group was lower than that of patients in the low-risk group in both test sets 1 and 2 (Supplementary Figure 1A, $p = 4.059e^{-06}$ and Supplementary Figure 2A, $p = 4.034e^{-03}$, respectively). In addition, the receiver operating characteristic (ROC) curve showed good performance, with AUCs for 5-year OS of 0.711 (Supplementary Figure 1B) and 0.675 (Supplementary Figure 2B).

Relationship Between the Immune-Related Long Non-coding RNA Signature and Clinicopathological Parameters of Endometrial Cancer

Next, we investigated whether the prognosis of the six immune-related lncRNAs was related to clinicopathological factors, such as age, clinical stage, tumor differentiation, and depth of invasion. Univariate Cox regression analysis showed that age, depth of tumor invasion, and risk score correlated significantly with OS in patients with EC (Figure 4A), while multivariate Cox regression analysis showed that the risk score significantly correlated with OS (Figure 4B), suggesting that these six lncRNAs act as independent prognostic factors in patients with EC. To determine the sensitivity and specificity of the risk score for evaluating the prognosis of patients with EC, we performed time-dependent ROC analysis. The AUC of the risk score was 0.712 (Figure 4C), indicating that the six lncRNAs are highly reliable prognostic markers for EC. In addition, we produced a box plot showing the relationship between the expression levels of the lncRNAs and age, clinical stage, tumor differentiation, and depth of invasion (Figure 4D), while the KM-Plotter showed that PRRT3-AS1, LINC01503, CDKN2B-AS1, LINC01629, LINC01833, and LINC01936 significantly correlated with shorter OS in UCEC (Figure 4E). Together, these results indicate that the expression of the six immune-related lncRNAs is an independent prognostic factor for patients with EC.

Correlation Between Long Non-coding RNA Expression and the Immune Microenvironment

To evaluate the association between the expression of the six lncRNAs and immune cell infiltration, we used the ImmLnc

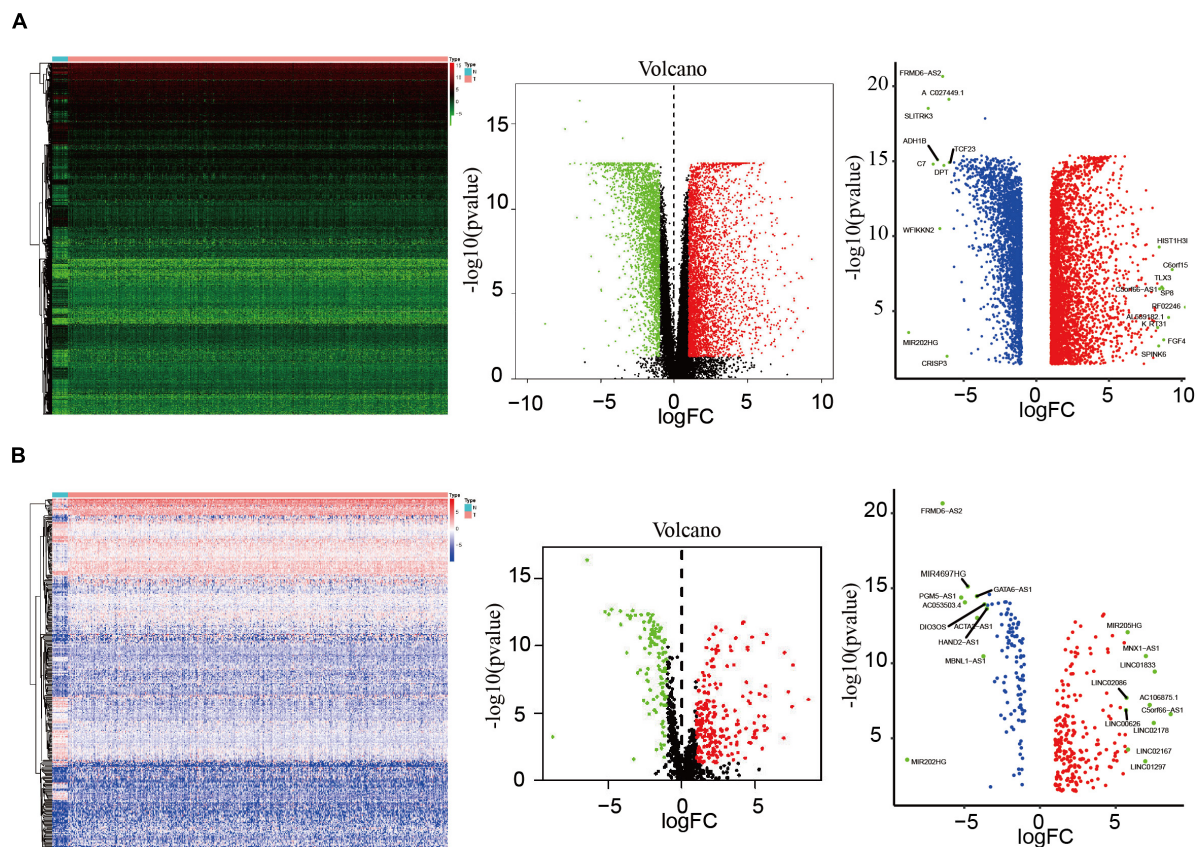


FIGURE 1 | Analysis of differentially expressed lncRNAs. **(A)** Heatmap and volcano map of 552 EC samples and 23 normal endometrium samples showing 3,860 upregulated molecules and 2,406 downregulated molecules (fold change > 4, $p = 0.001$), and showed the most differentially expressed molecules. **(B)** Heatmap and volcano plots of 340 differentially expressed lncRNAs showing 228 upregulated and 112 downregulated, and showed the most differentially expressed molecules.

database to detect their correlation with immune cell types, including CD8+ T cells, DCs, neutrophils, B cells, macrophages, and CD4+ T cells. We found that CDKN2B-AS1 expression correlated negatively with CD8+ T cells and positively with B cells, macrophages, and CD4+ T cells. Conversely, LINC01503 expression correlated negatively with CD8+ T cells and macrophages but positively with neutrophils and CD4+ T cells. LINC01936 expression correlated negatively with CD8+ T cells and DCs, whereas PRRT3-AS1 expression correlated negatively with CD8+ T cells, DCs, and neutrophils. Furthermore, LINC01629 expression correlated negatively with macrophage and positively with neutrophils, while LINC01833 expression correlated negatively with CD8+ T cells and macrophages but positively with CD4+ T cells and neutrophils (**Supplementary Table 2**). We then used ssGSEA to analyze the correlation between immune cell infiltration and the expression of PRRT3-AS1, LINC01503, CDKN2B-AS1, LINC01629, LINC01833, and LINC01936, respectively. The results revealed that all six lncRNAs were associated with immune cell infiltration, and that the infiltration of various immune cells was related (**Figure 5A** and **Supplementary Table 3**).

Tumor mutational burden (TMB) has attracted considerable attention in immunotherapy; PD-L1 is a biomarker for predicting the response of two important PD-1 antibody treatments.

Therefore, we investigated the association between TMB and the expression of PRRT3-AS1, LINC01503, CDKN2B-AS1, LINC01629, and LINC01833 using the online database assistant for clinical bioinformatics.³ The relationships between satellite instability and LINC01936 data were unavailable. Notably, we found a significant negative correlation between PRRT3-AS1, LINC01503, and CDKN2B-AS1 expression and TMB (**Figure 5B**).

In addition, we used Spearman's correlation analysis to evaluate the relationship between PRRT3-AS1, LINC01503, CDKN2B-AS1, LINC01629, and LINC01833 and common immune checkpoints, MHC molecules, chemokines, and chemokine receptors *via* the online database assistant for clinical bioinformatics (see text footnote 3), this website was not predicted the information of LINC01936 (**Figures 6A,B**). All these lncRNAs displayed significant correlations with multiple immune checkpoints and immune-related genes.

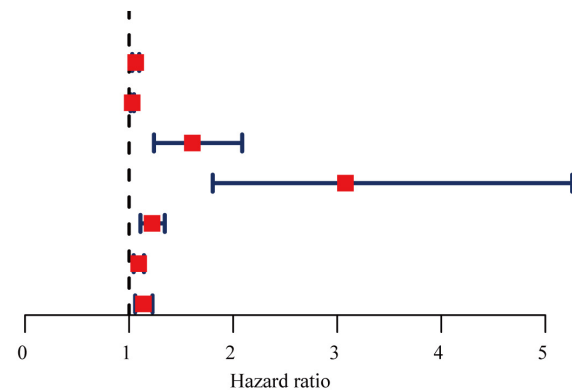
Specimen Verification

Fluorescent RT-qPCR was used to detect the mRNA expression of PRRT3-AS1, LINC01503, LINC01936, CDKN2B-AS1,

³<https://www.aclbi.com/static/index.html/>

A

	pvalue	Hazard ratio
PRRT3-AS1	<0.001	1.063(1.030–1.097)
LINC01503	<0.001	1.030(1.014–1.047)
LINC01936	<0.001	1.608(1.239–2.086)
CDKN2B-AS1	<0.001	3.079(1.803–5.258)
LINC01629	<0.001	1.220(1.109–1.343)
LINC01833	<0.001	1.092(1.044–1.143)
LINC01224	<0.001	1.138(1.058–1.225)



B

	pvalue	Hazard ratio
PRRT3-AS1	0.001	1.060(1.023–1.099)
LINC01629	<0.001	1.220(1.094–1.354)
CDKN2B-AS1	<0.001	2.793(1.546–5.047)
LINC01936	0.044	1.378(1.008–1.886)
LINC01503	0.033	1.019(1.001–1.038)
LINC01833	0.044	1.051(0.999–1.106)

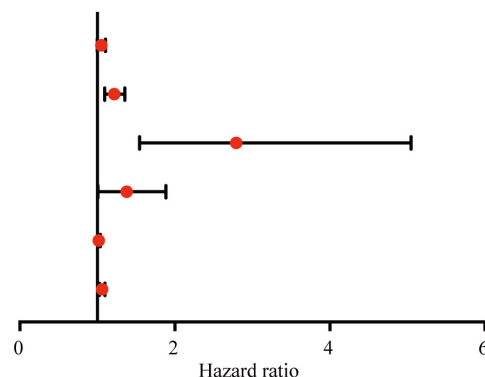


FIGURE 2 | Identification and assessment of the immune-related lncRNA prognostic signature for EC. HR and p -values from univariate Cox (A) and multivariate Cox (B) HR regression of selected genes and immune terms (criteria: p -value < 0.001).

TABLE 1 | The expression levels of these six lncRNAs.

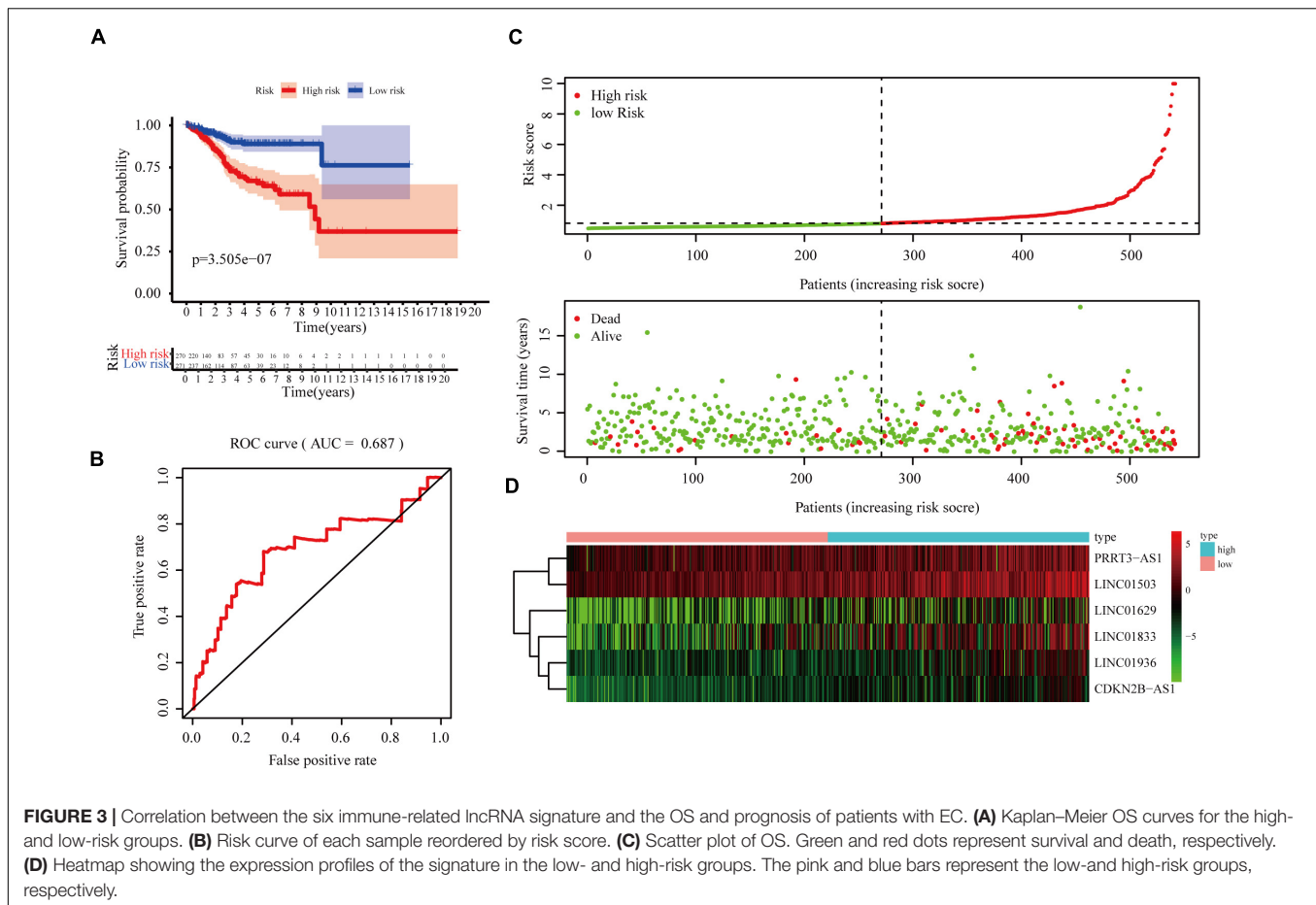
ID	PRRT3-AS1	LINC01503	LINC01936	CDKN2B-AS1	LINC01629	LINC01833
Lower limit	1.023583	1.00155	1.008181	1.545618	1.09442	0.999163
Relative risk	1.060732	1.019693	1.378964	2.793029	1.217429	1.05138
Upper limit	1.09923	1.038164	1.886111	5.04718	1.354264	1.106327
p -Value	0.001189	0.033254	0.04433	0.000668	0.000294	0.043889
Coefficient	0.058959	0.019501	0.321332	1.027127	0.196742	0.050104

LINC01629, and LINC01833 in 30 EC tissues and 19 normal endometrial tissues. These analyses confirmed that CDKN2B-AS1 expression is higher in EC tissues than in normal endometrial tissues (Figures 7A–F).

CDKN2B-AS1 Knockdown Inhibits Endometrial Cancer Progression *in vitro* and *in vivo*

Endometrial cancer is divided into two types, of which type I is estrogen-dependent, while type II is non-estrogen-dependent. The Ishikawa cell line is derived from type I tumors, and HEC-1A cells derived from type II tumors (Albitar et al., 2007). Next,

we evaluated the effect of knockdown CDKN2B-AS1 on the malignant biological behavior of EC cell lines by transfecting Ishikawa and HEC-1A cells with sh-CDKN2B-AS1 chronic virus vector and a corresponding NC. We found that two constructs, LV-CDKN2B-AS1 -1, LV-CDKN2B-AS1 -2 decreased the CDKN2B-AS1 expression. After the transfection efficiency had been confirmed using quantitative real-time-polymerase chain reaction (qRT-PCR; Figure 8A), EdU assays revealed that knockdown of CDKN2B-AS1 inhibited the proliferation of Ishikawa and HEC-1A cells (Figure 8B), while Transwell assays demonstrated that knockdown of CDKN2B-AS1 also inhibited their invasion ability (Figure 8C). Next, we investigated the function of CDKN2B-AS1 in an *in vivo* tumor model using



nude mice ($n = 2$ per group) and found that the tumor volume was smaller in the sh-CDKN2B-AS1 than in the control groups (Figure 8D).

CDKN2B-AS1 Cellular Localization and Functional Enrichment Analysis

Since cellular localization significantly influences lncRNAs function and molecular mechanism in tumors, we investigated the subcellular localization of CDKN2B-AS1 using FISH assays. CDKN2B-AS1 was located in both the nucleus and cytoplasm of Ishikawa and HEC-1A cells (Figure 9A), suggesting that CDKN2B-AS1 exerts its biological functions *via* a ceRNA mechanism. Therefore, we analyzed the lncRNA-miRNA-mRNA network using STARBASE and miRTarBase and found that CDKN2B-AS1 was related to 10 miRNAs and 100 target genes (Figure 9B).

Considering the important role of CDKN2B-AS1 in regulating the malignant phenotype of EC cells along with our findings, we investigated the role of CDKN2B-AS1 dysregulation in the pathogenesis of EC by examining the enriched gene sets in samples with different CDKN2B-AS1 mRNA expression levels. First, we used Metascape to perform Gene Ontology (GO) enrichment analysis on the function of CDKN2B-AS1 and its top 100 related molecules (Supplementary Table 4), which were primarily involved

in bicarbonate transport, chloride transport, the regulation of guanylate cyclase activity, the phase II-conjugation of compounds, immune response-regulating cell surface receptor signaling pathway, excretion plasma lipoprotein assembly, remodeling and clearance, organic acid transport, post-translational modification, synthesis of GPI-anchored proteins, glycosylation, and small molecule catabolic processes (Figures 9C,D and Supplementary Table 5). Together, these findings provide important clues regarding the mechanism underlying the pathogenesis of EC. Based on the TCGA dataset, the relationship between CDKN2B-AS1 expression and risk coefficient HR and confidence interval of clinical characteristics was analyzed by univariate Cox, and spearman correlation analysis heat map of immune score and CDKN2B-AS1 expression in multiple tumor tissues. The results suggest that CDKN2B-AS1 is an independent prognostic factor in a variety of tumors (Supplementary Figure 3A). Immune score evaluation analysis showed that the expression of CDKN2B-AS1 was related to a variety of immune cell infiltration (Supplementary Figure 3B).

DISCUSSION

The incidence of EC, the most common and deadly cancer among females worldwide, has been increasing worldwide.

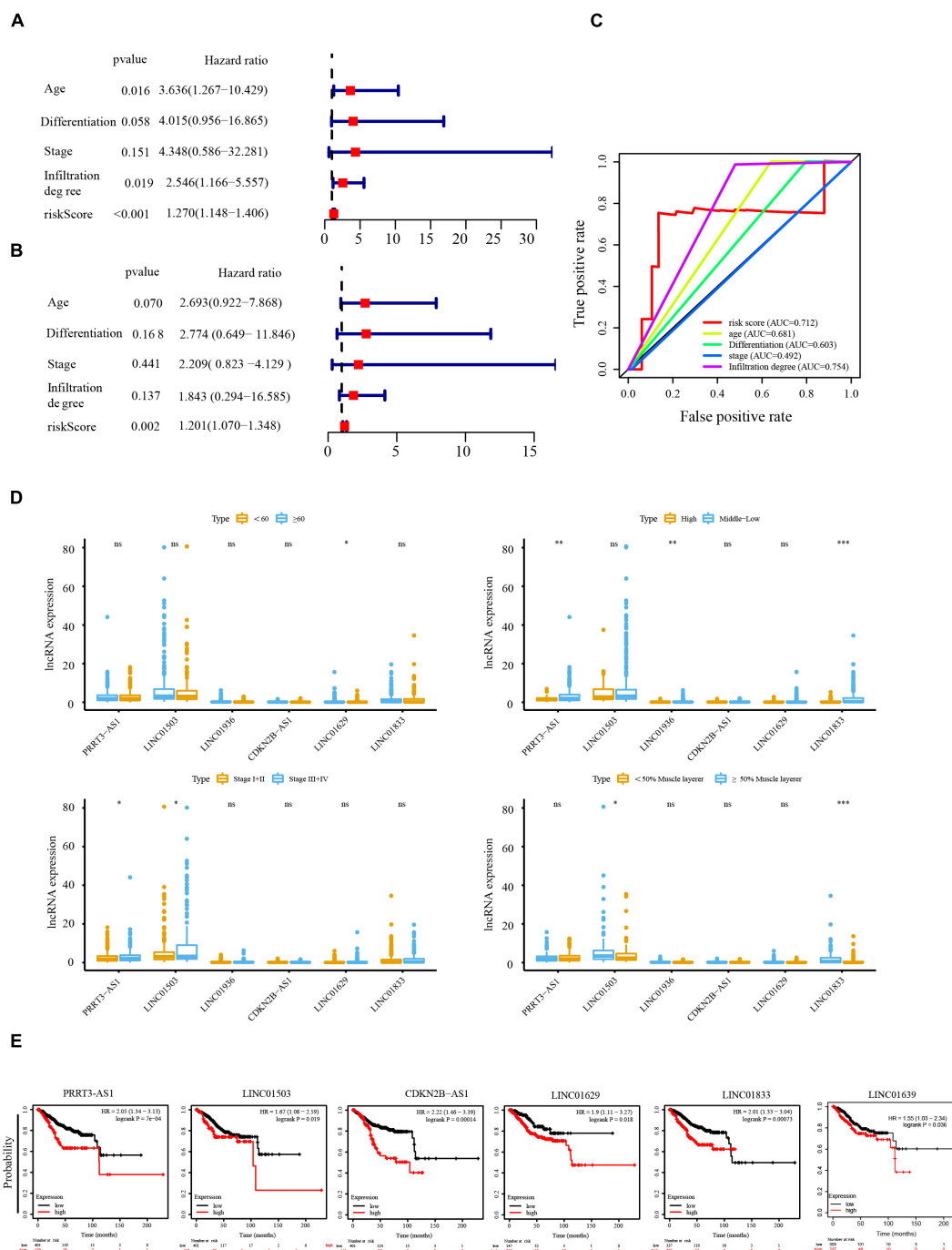


FIGURE 4 | Cox regression analysis of the independent prognostic value of the risk score. Univariate **(A)** and multivariate **(B)** Cox regression analysis of risk score, age, clinical stage, tumor differentiation, and depth of invasion. **(C)** The AUC of risk score, age, clinical stage, tumor differentiation, and depth of invasion was calculated from the total survival risk score according to the ROC curve. **(D)** Relationship between lncRNA expression and age, clinical stage, tumor differentiation, and depth of invasion. **(E)** Prognostic value of PRRT3-AS1, LINC01503, CDKN2B-AS1, LINC01629, LINC01833, and LINC01936 in UCEC analyzed using Kaplan–Meier (KM) Plotter. * $P < 0.05$, ** $P < 0.01$, *** $P < 0.001$.

EC has a high degree of heterogeneity not only in the genes and phenotypes of EC cells, but also in the TME (Engerud et al., 2020), which contains various immune cells. Tumor and immune cells interact and form complexes. LncRNAs

influence the occurrence, development, invasion, and metastasis of EC *via* immune pathways (Gao et al., 2021). Therefore, we explored immune-related lncRNAs in EC to improve our understanding of the mechanisms underlying EC occurrence

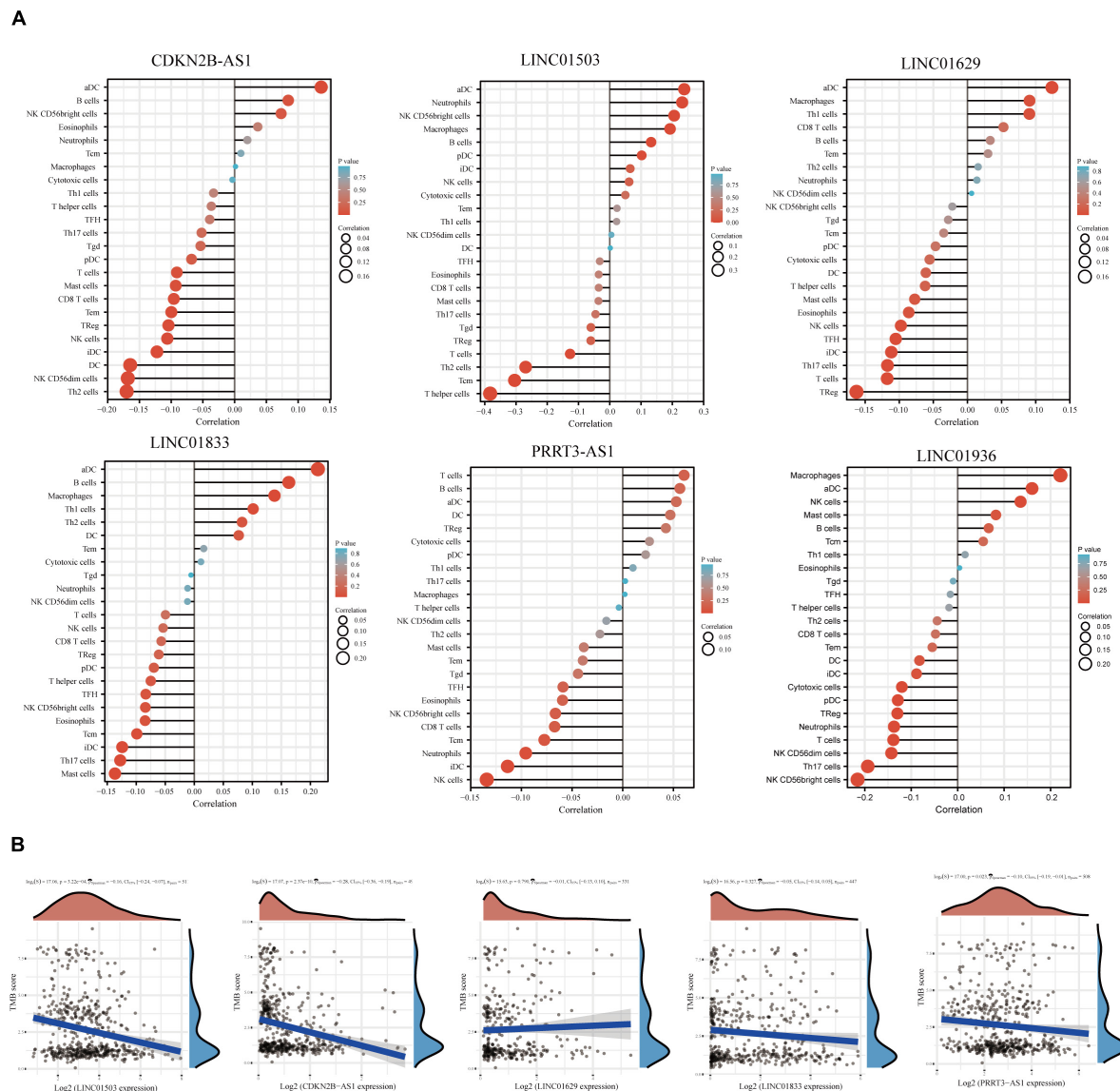


FIGURE 5 | Correlation between lncRNA expression and immune infiltration. **(A)** Correlation analysis of immune-related lncRNA expression and the infiltration of aDCs, B cells, CD8+ T cells, cytotoxic cells, DCs, eosinophils, iDCs, macrophages, mast cells, neutrophils, NK CD56bright cells, NK CD56dim cells, NK cells, pDCs, T cells, T helper cells, Tcm, Tem, Tfh, Tgd, Th1 cells, Th17 cells, Th2 cells, and Tregs. **(B)** Spearman correlation analysis of TMB/MSI and immune-related lncRNA expression. Horizontal axis represents gene expression distribution. Ordinate represents TMB/MSI score distribution. The density curve on the right represents the TMB/MSI score distribution trend. The upper density curve represents the gene expression distribution trend. The uppermost value represents the correlation p -value, correlation coefficient, and correlation calculation method. p -Values of <0.05 were considered significant. The correlation coefficient range was $(-1, 1)$, with a negative number representing a negative correlation between the expression of two genes and a positive value representing a positive correlation. The closer to 1 or -1 , the stronger the correlation. The closer to 0, the weaker the correlation.

and development, and to develop new diagnosis and therapeutic strategies, for better treatment outcomes.

To this end, we screened differentially expressed immune-related lncRNAs using TCGA database and the ImmLnc website, identifying six immune-related lncRNAs as prognostic markers: PRRT3-AS1, LINC01503, LINC01936, CDKN2B-AS1, LINC01629, and LINC01833. Importantly, the risk scores calculated using the coefficients of these six lncRNAs showed that the OS of high-risk patients with EC was

significantly shorter than that of patients in the low-risk group in both the training and test data sets. Multi-factor Cox regression analysis of age, clinical stage, tumor differentiation, and depth of invasion confirmed that the six immune-related lncRNAs are an independent prognostic factor in EC. It has been shown that PRRT3-AS1 silencing in PC cells can inhibit their proliferation by activating the PPAR γ gene, thereby blocking the mTOR signaling pathway (Fan et al., 2020). mTOR is an important eukaryotic cell signal whose stability affects the expression of cytokines in T cells

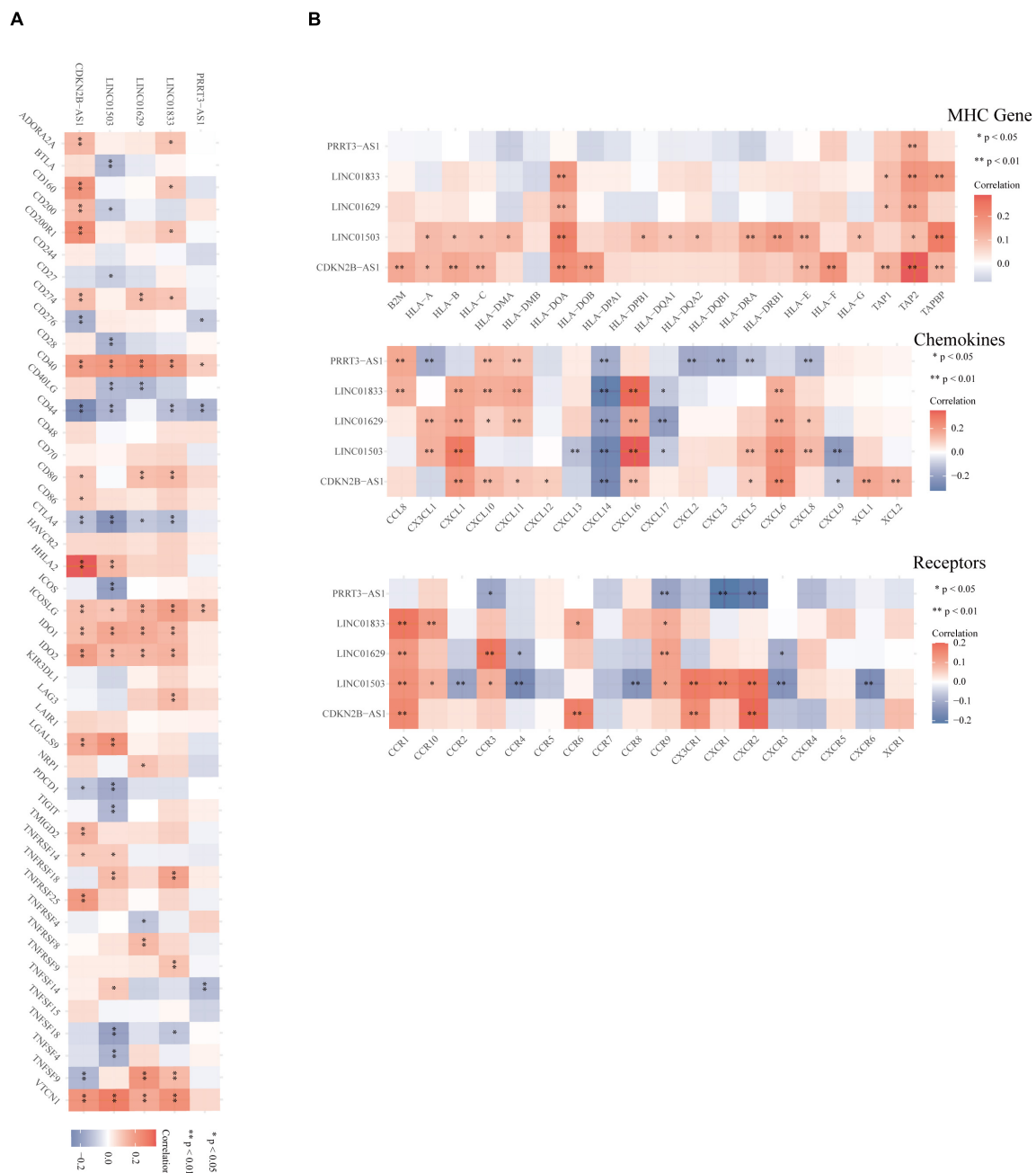
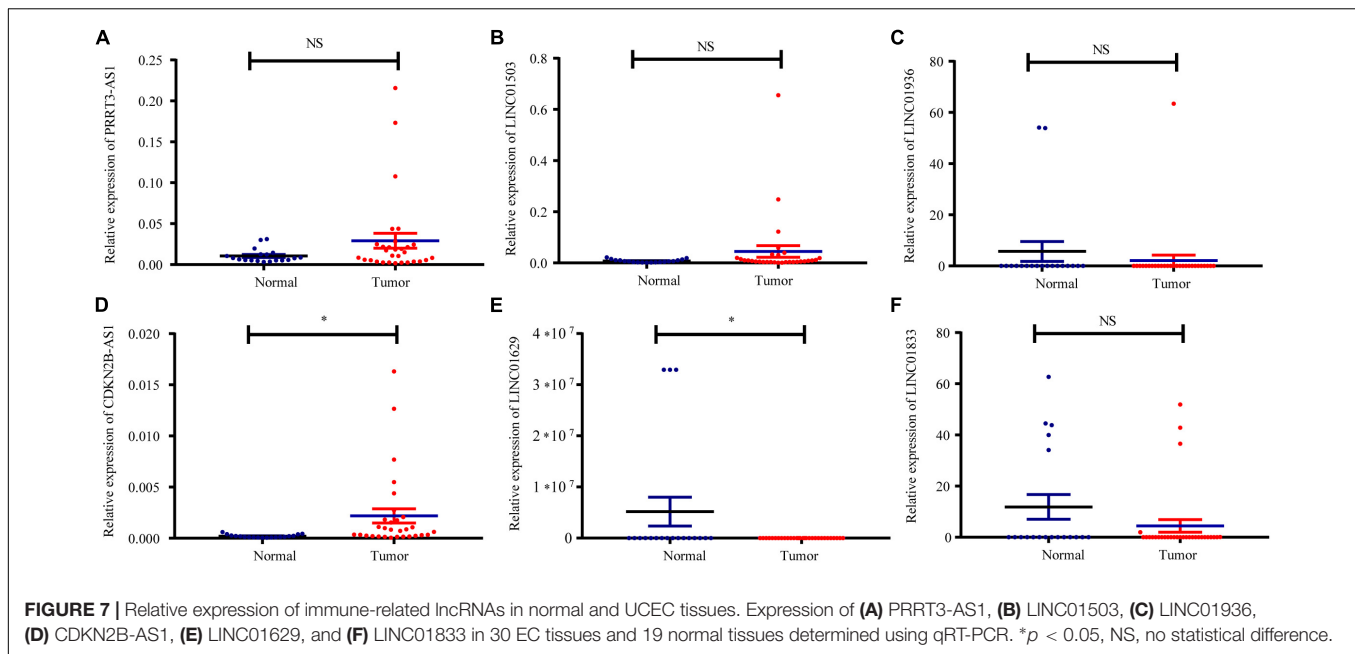


FIGURE 6 | Correlation between the immune-related lncRNA expression and immune factors. **(A,B)** Spearman's correlation analysis between immune-related lncRNAs and immune checkpoints, MHC molecules, chemokines, and chemokine receptors. Different colors represent the correlation coefficient (red, positive; blue, negative). A darker color indicates a stronger correlation, * $p < 0.05$, ** $p < 0.01$.

and immunosuppression (Dumas et al., 2020). Recent research has also identified PRRT3-AS1 as an immune-related prognostic lncRNA in patients with HCC (Kong et al., 2020). Together, these studies suggest that PRRT3-AS1 may be a potential therapeutic target for immunotherapy in EC.

CDKN2B-AS1 is a multifunctional lncRNA that exerts carcinogenic effects in various tumors. In renal clear cell carcinoma, CDKN2B-AS1 exerts its carcinogenic activity

by recruiting CREB-binding protein and three epigenetic modification complexes containing SET and MYND domains to the promoter region of the Ndc80 mitochondrial complex (NUF2) (Xie et al., 2021). In lung cancer, CDKN2B-AS1 acts as a cavernous body by adsorbing miR-378b and regulating miR-378b/NR2C2 to promote cancer development (Wang et al., 2020). However, the expression and role of CDKN2B-AS1 in EC remains unclear. LINC01503 acts as a carcinogen in



cancers such as lung cancer (Zhang et al., 2020), bowel cancer (Wei et al., 2020), and gastric cancer (Ma et al., 2021), and promotes tumor progression. Previous analyses of TCGA database have shown that the lncRNA LINC01833 is associated with glycolysis and that its high expression is correlated to poor prognosis in patients with EC (Jiang et al., 2021); however, its expression and role in EC warrant further study.

To investigate the association between these immune-related lncRNAs and immune cell infiltration, we used the ImmLnc database to analyze the correlation between PRRT3-AS1, LINC01503, CDKN2B-AS1, LINC01629, and LINC01833 and CD8⁺ T cells, DCs, neutrophils, B cells, macrophages, and CD4⁺ T cells. We found that all six lncRNAs were associated with the infiltration of various interrelated immune cells. Considerable evidence suggests that CD8⁺ T cell subsets play important roles in tumor control, as reflected by the relationship between the number of CD8⁺ T cells in the tumor before treatment and the response to PD-1 therapy (Kim et al., 2021). After circulating CD8⁺ T cells infiltrate tumor tissues, they are activated by tumor antigens to transform into effector CD8⁺ T cells which kill tumor cells. In addition, CD4⁺ T helper cells help DCs to prepare and activate CD8⁺ T cells (Yang et al., 2020). Meanwhile, CD4⁺ Treg cell-mediated anti-tumor immunosuppression is the main mechanism of tumor immune evasion and immunotherapy resistance (Polanczyk et al., 2019). Effector CD8⁺ T cells gradually degenerate due to continuous tumor antigen stimulation, immunosuppressive cell suppression (e.g., Treg cells and immunosuppressive B cells), and imbalance between physical and chemical status, thereby reducing their proliferation and secretion of effector cytokines (IL-6, TNF- α , and IFN- γ), known as “T cell exhaustion” (Chen et al., 2021). Thus, the repair of CD8⁺ T cell anti-cancer immune activity has become the greatest limitation in tumor immunotherapy. T cell dysfunction in human tumors is characterized by an

increase in the expression of inhibitory receptors (e.g., PD-1, LAG3, TIM3, 2B4, CD200, and CTLA4) on the cell surface; therefore, immune checkpoint inhibitors can partially reverse T cell depletion (Li et al., 2021).

We also analyzed the correlation between the lncRNAs and common immune checkpoints using Spearman's correlation analysis. Notably, LINC01629, LINC01833, and CDKN2B-AS1 correlated positively with the immune checkpoint CD274, while LINC01503, CDKN2B-AS1, LINC01629, and LINC01833 correlated positively with IDO1 and IDO2. IDO1 and PD-L1 have become important targets for tumor immunotherapy and multiple inhibitors have entered clinical trials and achieved certain efficacy (Takada et al., 2020). Therefore, our findings provide new theoretical targets for EC immunotherapy.

Tumor cells display altered MHC antigen expression on their surface. The weakening of MHC antigen expression reduces the functional presentation of antigens to immune cells and thus the activation of helper T cells (Algarra et al., 2021). However, some tumors can also escape the lysis caused by cytotoxic T lymphocytes and NK cells by overexpressing non-classical MHC-I molecules, thereby escaping immune system surveillance (Catalán et al., 2015). When we analyzed the correlation between PRRT3-AS1, LINC01503, LINC01936, CDKN2B-AS1, LINC01629, and LINC01833 and MHC molecules, we found that all six immune-related lncRNAs correlated positively with multiple MHC-related molecules.

In the TME, various chemokines can be secreted by tumor, immune, and stromal cells, which ultimately activate multiple signal pathways *via* cell surface receptors and recruit immune cell subgroups to the TME, thereby spatiotemporally regulating the tumor immune response. The chemokine network can either promote or inhibit tumor cell growth, invasion, and metastasis by influencing tumor cells or tumor-related immune cells (Valeta-Magara et al., 2019). Thus, targeting chemokines

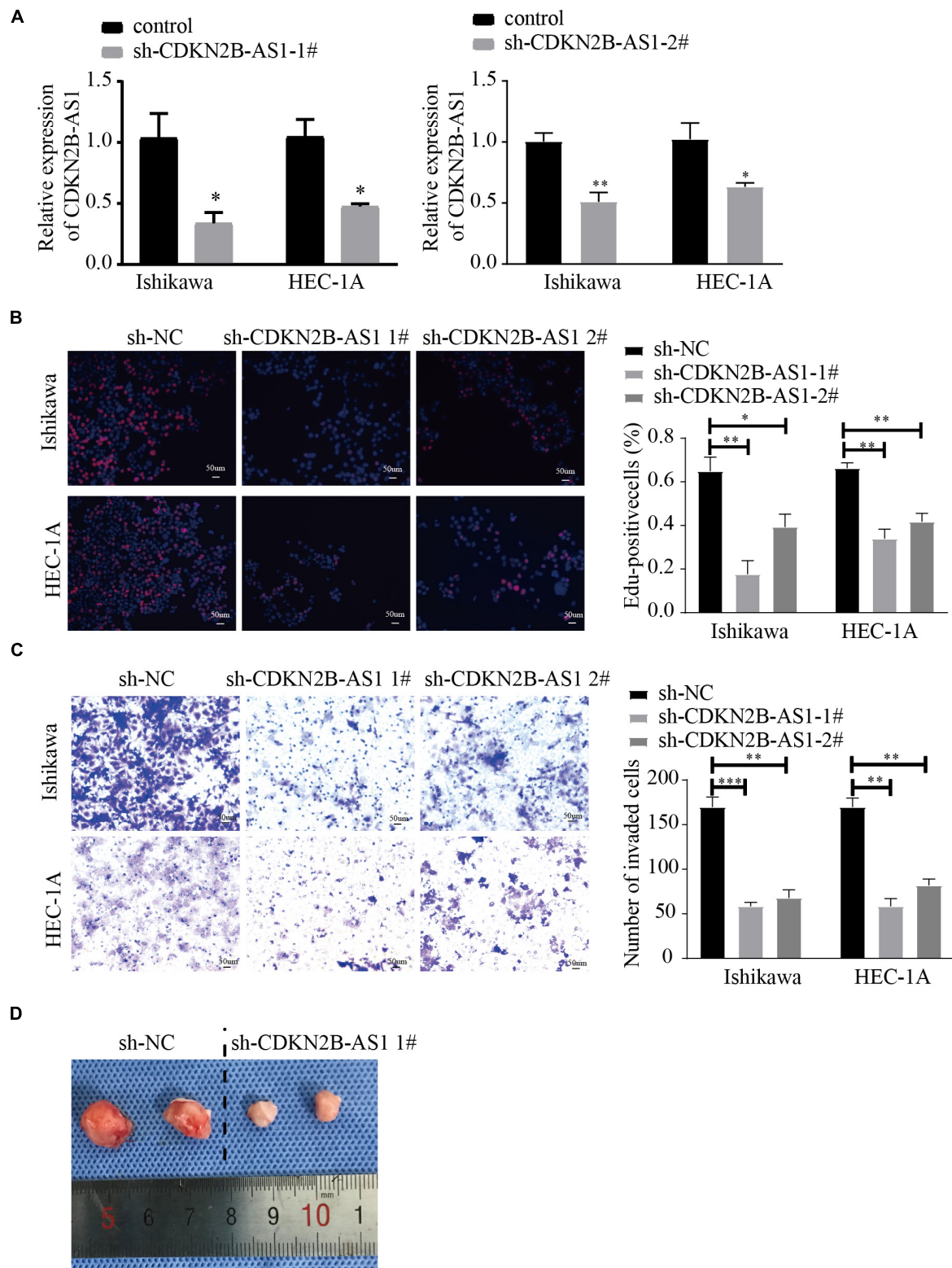


FIGURE 8 | CDKN2B-AS1 knockdown inhibits malignant biological behavior in EC cells. **(A)** CDKN2B-AS1 expression in Ishikawa and HEC-1A cell lines measured using RT-qPCR. **(B)** Effect of CDKN2B-AS1 expression on proliferation determined using EdU assays in Ishikawa and HEC-1A cells. **(C)** Transwell assays to determine the number of invading cells. **(D)** Nude mice bearing tumors. A specimen from each respective group is shown ($n = 2$ per group), $*p < 0.05$, $**p < 0.01$, $***p < 0.001$ vs. the NC group.

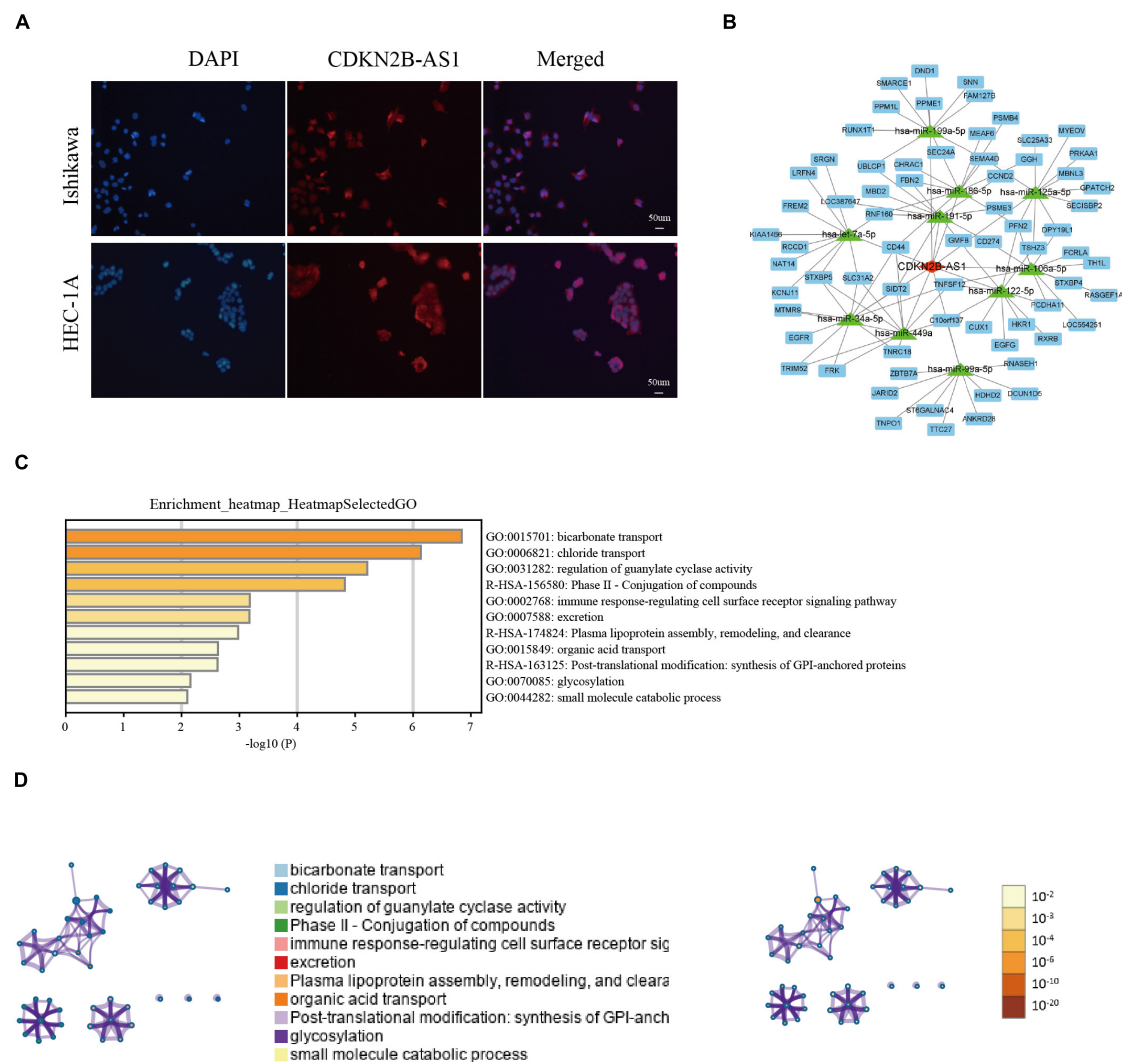


FIGURE 9 | CDKN2B-AS1 cellular location, lncRNA-miRNA-mRNA regulatory network, and GSEA results. **(A)** FISH assay of CDKN2B-AS1 localization in Ishikawa and HEC-1A cells. **(B)** CDKN2B-AS1-binding miRNAs were predicted using STARBASE and their targets were retrieved from miRTarBase. The regulatory network of lncRNA-miRNA-mRNAs was visualized using Cytoscape 3.7.1. **(C,D)** Biological processes related to CDKN2B-AS1.

and their receptors is an effective treatment strategy against malignant tumors. The findings of our Spearman's analysis of the correlation between the immune-related lncRNAs and chemokines and their receptors will therefore help to discover new approaches for efficient and specific EC treatments based on targeted multi-chemokines.

Unfortunately, the efficacy of PD-1/PD-L1 blockade therapy in most tumors is approximately 40%; therefore, it is important to accurately screen patients who can benefit from the treatment to avoid treatment-related adverse reactions (Yin et al., 2021). One biomarker for screening patients who may benefit from PD-1/PD-L1 blockade therapy is TMB, which represents the number of mutations per megabase in the coding region of gene exons in a tumor sample. A higher TMB elicits stronger antigenicity, enabling more immune T cells to recognize and kill tumor cells in the TME (Li et al., 2020). EC is divided

into four molecular types namely POLE (7%), MSI (28%), CNL (39%), and CNH (26%). EC has the highest known POLE mutation rate, meaning that POLE mutant EC has a very high mutational load. Indeed, POLE and MSI hypermutation type EC have by far the highest TMBs of all four molecular types (232×106 and $18 \times 106/\text{Mb}$ vs. 2.6×106 and $2.9 \times 106/\text{Mb}$), suggesting that patients with POLE and MSI hypermutation EC are most likely to benefit from PD-1/PD-L1 blockade therapy (Gargiulo et al., 2016). In this study, we analyzed the correlation between PRRT3-AS1, LINC01503, CDKN2B-AS1, LINC01629, LINC01833, and TMB, finding that the expression of PRRT3-AS1, LINC01503, CDKN2B-AS1, and LINC01833 correlated significantly and negatively with the distribution of TMB.

To verify the findings of our bioinformatics analyses, we detected the expression of PRRT3-AS1, LINC01503, LINC01936,

CDKN2B-AS1, LINC01629, and LINC01833 in EC and normal endometrial tissues using RT-qPCR. Interestingly, CDKN2B-AS1 was significantly overexpressed in EC tissues; however, its expression and function in EC remain poorly understood. We also found that CDKN2B-AS1 knockdown in Ishikawa and HEC-1A cells inhibited their proliferation and invasion. Moreover, interference with CDKN2B-AS1 *in vivo* inhibited the growth of EC cell-transplanted tumors in nude mice. FISH assays further revealed that CDKN2B-AS1 is located in the nucleus and cytoplasm of Ishikawa and HEC-1A cells. Since the subcellular location of lncRNAs influences their potential functions and underlying mechanisms in tumors, these results suggest that CDKN2B-AS1 achieves its biological function *via* a ceRNA mechanism; therefore, we constructed a ceRNA regulatory network. The microenvironment of EC is very complicated compared with that of other malignant tumors, and hence its microstructure and correlation with prognosis warrant further investigation. Therefore, future studies, with a larger sample size and *in vitro* experiments, must examine the immune regulation mechanism of EC in greater depth. In addition, RNA-Seq of EC cell lines treated with sh-CDKN2B-AS1 will help us to further study the important mechanism that CDKN2B-AS1 plays in the immune regulation and malignant progression of EC.

CONCLUSION

In conclusion, this study identified six lncRNAs as a prognostic signature for EC associated with the infiltration of immune cell subtypes. Together, our results provide a new strategy for prognostic evaluation of EC, as well as possible therapeutic targets and a theoretical basis for individualized EC immunotherapy.

DATA AVAILABILITY STATEMENT

The datasets presented in this study can be found in online repositories. The names of the repository/repositories and accession number(s) can be found in the article/**Supplementary Material**.

REFERENCES

- Albitar, L., Pickett, G., Morgan, M., Davies, S., and Leslie, K. (2007). Models representing type I and type II human endometrial cancers: ishikawa H and Hec50co cells. *Gynecol. Oncol.* 106, 52–64. doi: 10.1016/j.ygyno.2007.02.033
- Algarra, I., Garrido, F., and Garcia-Lora, A. (2021). MHC heterogeneity and response of metastases to immunotherapy. *Cancer Metastasis Rev.* 40, 501–517. doi: 10.1007/s10555-021-09964-4
- Allou, L., Balzano, S., Magg, A., Quinodoz, M., Royer-Bertrand, B., Schöpflin, R., et al. (2021). Non-coding deletions identify Maenli lncRNA as a limb-specific En1 regulator. *Nature* 592, 93–98. doi: 10.1038/s41586-021-03208-9
- Anderson, K., Anderson, D., McAnally, J., Shelton, J., Bassel-Duby, R., and Olson, E. (2016). Transcription of the non-coding RNA upperhand controls Hand2 expression and heart development. *Nature* 539, 433–436. doi: 10.1038/nature20128
- Catalán, E., Charni, S., Jaime, P., Aguiló, J., Enríquez, J., Naval, J., et al. (2015). MHC-I modulation due to changes in tumor cell metabolism regulates tumor

ETHICS STATEMENT

The studies involving human participants were reviewed and approved by the Ethics Committee of Shengjing Hospital Affiliated to China Medical University (Ethics number: 2018PS251K). Written informed consent for participation was not required for this study in accordance with the national legislation and the institutional requirements. The animal study was reviewed and approved by the Scientific Research and New Technology Ethical Committee of the Shengjing Hospital of China Medical University (Ethics number: 2018PS251K).

AUTHOR CONTRIBUTIONS

DY performed most of the experiments and contributed toward writing the manuscript. DY and X-XM conceived the study, participated in its design and coordination, and helped draft the manuscript. DY and JM performed qRT-PCR and cell culture experiments. All authors read and approved the final manuscript.

FUNDING

This work was supported by the National Natural Science Foundation of China (grant number 81872123). Leading Talents of Innovation in Liaoning Province (grant number XLYC1902003).

ACKNOWLEDGMENTS

The authors thank the members of their laboratory and collaborators for supporting this research.

SUPPLEMENTARY MATERIAL

The Supplementary Material for this article can be found online at: <https://www.frontiersin.org/articles/10.3389/fcell.2021.721676/full#supplementary-material>

sensitivity to CTL and NK cells. *Oncoimmunology* 4:e985924. doi: 10.4161/2162402X.2014.985924

Chen, C., Gu, Y., Zhang, F., Zhang, Z., Zhang, Y., He, Y., et al. (2021). Construction of PD1/CD28 chimeric-switch receptor enhances anti-tumor ability of c-Met CAR-T in gastric cancer. *Oncoimmunology* 10:1901434. doi: 10.1080/2162402X.2021.1901434

Dong, P., Xiong, Y., Yue, J., Xu, D., Ihira, K., Konno, Y., et al. (2019). Long noncoding RNA NEAT1 drives aggressive endometrial cancer progression via miR-361-regulated networks involving STAT3 and tumor microenvironment-related genes. *J. Exp. Clin. Cancer Res.* 38:295. doi: 10.1186/s13046-019-1306-9

Du, N., Liu, Y., Ren, C., Wang, Y., Du, J., Yang, J., et al. (2019). Clinical application of TCGA molecular classification in endometrial endometrioid carcinoma. *Zhonghua Bing Li Xue Za Zhi* 48, 596–603. doi: 10.3760/cma.j.issn.0529-5807.2019.08.003

Dumas, A., Pomella, N., Rosser, G., Guglielmi, L., Vinel, C., Millner, T., et al. (2020). Microglia promote glioblastoma via mTOR-mediated immunosuppression of

- the tumour microenvironment. *EMBO. J.* 39:e103790. doi: 10.15252/embj.2019103790
- Engerud, H., Berg, H., Myrvold, M., Halle, M., Bjorge, L., Haldorsen, I., et al. (2020). High degree of heterogeneity of PD-L1 and PD-1 from primary to metastatic endometrial cancer. *Gynecol. Oncol.* 157, 260–267. doi: 10.1016/j.ygyno.2020.01.020
- Fan, L., Li, H., and Wang, W. (2020). Long non-coding RNA PRRT3-AS1 silencing inhibits prostate cancer cell proliferation and promotes apoptosis and autophagy. *Exp. Physiol.* 105, 793–808. doi: 10.1113/EP088011
- Gao, Q., Huang, Q., Li, F., and Luo, F. (2021). LncRNA MCTP1-AS1 regulates EMT process in endometrial cancer by targeting the miR-650/SMAD7 axis. *OncoTargets Ther.* 14, 751–761. doi: 10.2147/OTT.S240010
- Gargiulo, P., Della, P. C., Berardi, S., Califano, D., Scala, S., Buonaguro, L., et al. (2016). Tumor genotype and immune microenvironment in POLE-ultramutated and MSI-hypermutated endometrial cancers: new candidates for checkpoint blockade immunotherapy? *Cancer Treat. Rev.* 48, 61–68. doi: 10.1016/j.ctrv.2016.06.008
- Huang, D., Chen, J., Yang, L., Ouyang, Q., Li, J., Lao, L., et al. (2018). NKILA lncRNA promotes tumor immune evasion by sensitizing T cells to activation-induced cell death. *Nat. Immunol.* 19, 1112–1115. doi: 10.1038/s41590-018-0207-y
- Jiang, Y., Chen, J., Ling, J., Zhu, X., Jiang, P., Tang, X., et al. (2021). Construction of a glycolysis-related long noncoding RNA signature for predicting survival in endometrial cancer. *J. Cancer* 12, 1431–1444. doi: 10.7150/jca.50413
- Kahn, R., Gordhandas, S., Maddy, B., Baltich, N. B., Askin, G., Christos, P., et al. (2019). Universal endometrial cancer tumor typing: how much has immunohistochemistry, microsatellite instability, and MLH1 methylation improved the diagnosis of Lynch syndrome across the population? *Cancer* 125, 3172–3183. doi: 10.1002/cncr.32203
- Kim, C., Hong, M., Kim, K., Seo, I., Ahn, B., Pyo, K., et al. (2021). Dynamic changes in circulating PD-1CD8 T lymphocytes for predicting treatment response to PD-1 blockade in patients with non-small-cell lung cancer. *Eur. J. Cancer* 143, 113–126. doi: 10.1016/j.ejca.2020.10.028
- Kong, W., Wang, X., Zuo, X., Mao, Z., Cheng, Y., and Chen, W. (2020). Development and validation of an immune-related lncRNA signature for predicting the prognosis of hepatocellular carcinoma. *Front. Gene.* 11:1037. doi: 10.3389/fgene.2020.01037
- Leslie, K., Filiaci, V., Mallen, A., Thiel, K., Devor, E., Moxley, K., et al. (2021). Mutated p53 portends improvement in outcomes when bevacizumab is combined with chemotherapy in advanced/recurrent endometrial cancer: an NRG Oncology study. *Gynecol. Oncol.* 161, 113–121. doi: 10.1016/j.ygyno.2021.01.025
- Li, H., Li, J., Zhang, C., Zhang, C., and Wang, H. (2020). TERT mutations correlate with higher TMB value and unique tumor microenvironment and may be a potential biomarker for anti-CTLA4 treatment. *Cancer Med.* 9, 7151–7160. doi: 10.1002/cam4.3376
- Li, R., Salehi-Rad, R., Crosson, W., Momcilovic, M., Lim, R., Ong, S., et al. (2021). Inhibition of granulocytic myeloid-derived suppressor cells overcomes resistance to immune checkpoint inhibition in LKB1-deficient non-small cell lung cancer. *Cancer Res.* 81, 3295–3308. doi: 10.1158/0008-5472.CAN-20-3564
- Liu, W., Sun, L., Zhang, J., Song, W., Li, M., and Wang, H. (2021). The landscape and prognostic value of immune characteristics in uterine corpus endometrial cancer. *Biosci. Rep.* 41:BSR20202321. doi: 10.1042/BSR20202321
- Ma, Z., Gao, X., Shuai, Y., Wu, X., Yan, Y., Xing, X., et al. (2021). EGR1-mediated linc01503 promotes cell cycle progression and tumorigenesis in gastric cancer. *Cell Prolif.* 54:e12922. doi: 10.1111/cpr.12922
- Meng, Y., Yang, Y., Zhang, Y., Yang, X., Li, X., and Hu, C. (2021). The role of an immune signature for prognosis and immunotherapy response in endometrial cancer. *Am. J. Transl. Res.* 13, 532–548.
- Nafea, H., Youness, R., Abou-Aisha, K., and Gad, M. (2021). LncRNA HEIH/miR-939-5p interplay modulates triple-negative breast cancer progression through NOS2-induced nitric oxide production. *J. Cell Physiol.* 236, 5362–5372. doi: 10.1002/jcp.30234
- Polanczyk, M., Walker, E., Haley, D., Guerrouahen, B., and Akporiaye, E. (2019). Blockade of TGF- β signaling to enhance the antitumor response is accompanied by dysregulation of the functional activity of CD4CD25Foxp3 and CD4CD25Foxp3 T cells. *J. Transl. Med.* 17:219. doi: 10.1186/s12967-019-1967-3
- Post, C., Westermann, A., Bosse, T., Creutzberg, C., and Kroep, J. (2020). PARP and PD-1/PD-L1 checkpoint inhibition in recurrent or metastatic endometrial cancer. *Crit. Rev. Oncol. Hematol.* 152:102973. doi: 10.1016/j.critrevonc.2020.102973
- Siegel, R., Miller, K., and Jemal, A. (2020). Cancer statistics, 2020. *CA Cancer J. Clin.* 70, 7–30. doi: 10.3322/caac.21590
- Smrz, S., Calo, C., Fisher, J., and Salani, R. (2020). An ecological evaluation of the increasing incidence of endometrial cancer and the obesity epidemic. *Am. J. Obstet. Gynecol.* 224, 506.e1–506.e8.
- Takada, K., Toyokawa, G., Kinoshita, F., Jogo, T., Kohashi, K., Wakasu, S., et al. (2020). Expression of PD-L1, PD-L2, and IDO1 on tumor cells and density of CD8-positive tumor-infiltrating lymphocytes in early-stage lung adenocarcinoma according to histological subtype. *J. Cancer Res. Clin. Oncol.* 146, 2639–2650. doi: 10.1007/s00432-020-03250-6
- Valeta-Magara, A., Gadi, A., Volta, V., Walters, B., Arju, R., Giashuddin, S., et al. (2019). Inflammatory breast cancer promotes development of M2 tumor-associated macrophages and cancer mesenchymal cells through a complex chemokine network. *Cancer Res.* 79, 3360–3371. doi: 10.1158/0008-5472
- Wang, G., Xu, G., and Wang, W. (2020). Long noncoding RNA CDKN2B-AS1 facilitates lung cancer development through regulating miR-378b/NR2C2. *OncoTargets Ther.* 13, 10641–10649. doi: 10.2147/OTT.S261973
- Wei, J., Ge, X., Tang, Y., Qian, Y., Lu, W., Jiang, K., et al. (2020). An autophagy-related long noncoding RNA signature contributes to poor prognosis in colorectal cancer. *J. Oncol.* 2020:4728947. doi: 10.1155/2020/4728947
- Xie, X., Lin, J., Fan, X., Zhong, Y., Chen, Y., Liu, K., et al. (2021). LncRNA CDKN2B-AS1 stabilized by IGF2BP3 drives the malignancy of renal clear cell carcinoma through epigenetically activating NUF2 transcription. *Cell Death Dis.* 12:201. doi: 10.1038/s41419-021-03489-y
- Yang, X., Wu, W., Pan, Y., Zhou, Q., Xu, J., and Han, S. (2020). Immune-related genes in tumor-specific CD4 and CD8 T cells in colon cancer. *BMC Cancer* 20:585. doi: 10.1186/s12885-020-07075-x
- Yin, Z., Yu, M., Ma, T., Zhang, C., Huang, S., Karimzadeh, M., et al. (2021). Mechanisms underlying low-clinical responses to PD-1/PD-L1 blocking antibodies in immunotherapy of cancer: a key role of exosomal PD-L1. *J. Immunother. Cancer* 9:e001698. doi: 10.1136/jitc-2020-001698
- Zhang, M., Zhao, T., Du, W., Yang, Z., Peng, W., and Cui, Z. (2020). C-MYC-induced upregulation of LINC01503 promotes progression of non-small cell lung cancer. *Eur. Rev. Med. Pharmacol. Sci.* 24, 11120–11127. doi: 10.26355/eurrev_202011_23599
- Zhao, Y., Yu, Z., Ma, R., Zhang, Y., Zhao, L., Yan, Y., et al. (2021). LncRNA-Xist/miR-101-3p/KLF6/C/EBP α axis promotes TAM polarization to regulate cancer cell proliferation and migration. *Mol. Ther. Nucleic Acids* 23, 536–551. doi: 10.1016/j.omtn.2020.12.005
- Zheng, X., Liu, M., Song, Y., and Feng, C. (2019). Long noncoding RNA-ATB impairs the function of tumor suppressor miR-126-mediated signals in endometrial cancer for tumor growth and metastasis. *Cancer Biother. Radiopharm.* 34, 47–55. doi: 10.1089/cbr.2018.2565
- Zhou, H., Chen, L., Lei, Y., Li, T., Li, H., and Cheng, X. (2021). Integrated analysis of tumor mutation burden and immune infiltrates in endometrial cancer. *Curr. Probl. Cancer* 45:100660. doi: 10.1016/j.cupr.2020.100660

Conflict of Interest: The authors declare that the research was conducted in the absence of any commercial or financial relationships that could be construed as a potential conflict of interest.

Publisher's Note: All claims expressed in this article are solely those of the authors and do not necessarily represent those of their affiliated organizations, or those of the publisher, the editors and the reviewers. Any product that may be evaluated in this article, or claim that may be made by its manufacturer, is not guaranteed or endorsed by the publisher.

Copyright © 2021 Yang, Ma and Ma. This is an open-access article distributed under the terms of the Creative Commons Attribution License (CC BY). The use, distribution or reproduction in other forums is permitted, provided the original author(s) and the copyright owner(s) are credited and that the original publication in this journal is cited, in accordance with accepted academic practice. No use, distribution or reproduction is permitted which does not comply with these terms.



Identification of an Immune-Related LncRNA Signature in Gastric Cancer to Predict Survival and Response to Immune Checkpoint Inhibitors

Zuoyou Ding^{1†}, Ran Li^{2†}, Jun Han^{1*†}, Diya Sun¹, Lei Shen¹ and Guohao Wu^{1*}

¹ Department of General Surgery, Zhongshan Hospital of Fudan University, Shanghai, China, ² State Key Laboratory of Medical Genomics, National Research Center for Translational Medicine at Shanghai, Shanghai Institute of Hematology, Ruijin Hospital Affiliated to Shanghai Jiao Tong University School of Medicine, Shanghai, China

OPEN ACCESS

Edited by:

Zong Sheng Guo,
Roswell Park Comprehensive Cancer
Center, United States

Reviewed by:

Jinhui Liu,
Nanjing Medical University, China
Chuan Liu,
China Medical University, China

*Correspondence:

Jun Han
hanjun198626@163.com
Guohao Wu
profwugh@163.com

[†] These authors have contributed
equally to this work

Specialty section:

This article was submitted to
Molecular and Cellular Oncology,
a section of the journal
Frontiers in Cell and Developmental
Biology

Received: 11 July 2021

Accepted: 10 September 2021

Published: 13 October 2021

Citation:

Ding Z, Li R, Han J, Sun D,
Shen L and Wu G (2021) Identification
of an Immune-Related LncRNA
Signature in Gastric Cancer to Predict
Survival and Response to Immune
Checkpoint Inhibitors.
Front. Cell Dev. Biol. 9:739583.
doi: 10.3389/fcell.2021.739583

Immune microenvironment in gastric cancer is closely associated with patient's prognosis. Long non-coding RNAs (lncRNAs) are emerging as key regulators of immune responses. In this study, we aimed to construct a prognostic model based on immune-related lncRNAs (IRLs) to predict the overall survival and response to immune checkpoint inhibitors (ICIs) of gastric cancer (GC) patients. The IRL signature was constructed through a bioinformatics method, and its predictive capability was validated. A stratification analysis indicates that the IRL signature can distinguish different risk patients. A nomogram based on the IRL and other clinical variables efficiently predicted the overall survival of GC patients. The landscape of tumor microenvironment and mutation status partially explain this signature's predictive capability. We found the level of cancer-associated fibroblasts, endothelial cells, M2 macrophages, and stroma cells was high in the high-risk group, while the number of CD8⁺ T cells and T follicular helper cells was high in the low-risk group. Immunophenoscore (IPS) is validated for ICI response, and the IRL signature low-risk group received higher IPS, representing a more immunogenic phenotype that was more inclined to respond to ICIs. In addition, we found RNF144A-AS1 was highly expressed in GC patients and promoted the proliferation, migration, and invasive capacity of GC cells. We concluded that the IRL signature represents a novel useful model for evaluating GC survival outcomes and could be implemented to optimize the selection of patients to receive ICI treatment.

Keywords: gastric cancer, tumor mutational burden, immune-related lncRNAs, immune checkpoint inhibitors, immunophenoscore

INTRODUCTION

Gastric cancer (GC) is the fifth most common malignant tumor and the fourth leading cause of cancer-related deaths worldwide. According to recent statistics, GC patients usually have a poor prognosis, with a 5-year survival rate of less than 25% and an average overall survival (OS) of 7–10 months after diagnosis (Bray et al., 2018). The early asymptomatic nature of the disease contributes to the poor prognosis of GC, leading to the late diagnosis of GC and a high risk of distant metastasis. Currently, radical surgical resection is still the most effective method to significantly prolong the survival time of GC patients (Yu et al., 2019). Despite the development of postoperative

adjuvant chemotherapy and targeted drugs in the last decade, the prognosis remains extremely poor for advanced GC patients (Coutzac et al., 2019).

Recent breakthrough in immunotherapy, most prominently using immune checkpoint inhibitors (ICIs), has yielded impressive results in several solid tumors and emerged as a novel optional treatment strategy for advanced GC (Kono et al., 2020). Inhibition of programmed death-1 (PD-1)/programmed death-ligand 1 (PD-L1) with ICIs, such as nivolumab and pembrolizumab, has entered clinical trials for GC patients (Kang et al., 2017; Janjigian et al., 2018). A meta-analysis for clinical trials with ICI for advanced GC or esophago-gastric junction tumors indicated that ICI treatment could provide modest survival benefit for advanced GC patients (Chen et al., 2019). Although ICI treatment is a promising treatment strategy, only a subset of GC patients can receive a survival benefit. Hence, a practical assessment model is urgently needed to assess the prognosis of patients with GC and response to ICI treatment.

Previously, long non-coding RNAs (lncRNAs) were believed to have no coding function and were considered as transcriptional noise. In fact, lncRNAs play an essential role in gene regulation (Statello et al., 2021). Recent studies have identified that many lncRNAs are aberrantly expressed in multiple cancers and involved in immune-related gene expression and function, thus affecting the tumor immune microenvironment (Mathy and Chen, 2017; Botti et al., 2019; Pang et al., 2020). lncRNAs should be increasingly considered as novel prognostic markers and therapeutic targets for human cancer.

In this study, we aimed to develop a novel immune-related lncRNA signature to predict the OS and response to ICI of GC patients. We investigated the relationship of the immune-related lncRNA (IRL) signature to clinicopathological characteristics and prognosis in The Cancer Genome Atlas Stomach Adenocarcinoma (TCGA-STAD) cohort. In addition, immune cell infiltration, mutation status, and immunophenoscore (IPS) associated with this signature in GC were also thoroughly explored. This signature may be implemented to predict the OS of GC patients and contribute to more precise ICI treatment for GC in the next future.

MATERIALS AND METHODS

Data Acquisition

The RNA sequencing data (FPKM value), clinical information, and mutation data of GC patients were downloaded from TCGA. Patients lacking survival information were excluded from further evaluation. IRLs were obtained from the ImmLnc database¹ (Li et al., 2020). The clinical information of GC samples is detailed in **Supplementary Table 1**. The IPSs of patients with GC were obtained from The Cancer Immunome Atlas (TCIA).²

¹<http://bio-bigdata.hrbmu.edu.cn/ImmLnc/>

²<https://tcia.at/home>

Establishment of an Immune-Related lncRNA Prognosis Model

The “limma” R package was used to identify differentially expressed genes (DEGs) between GC tissues and matched adjacent non-cancerous tissues. The significance criteria was set as $|\log FC| > 1$ and $P\text{-value} < 0.05$. After integrating IRLs from the ImmLnc database, DELs were identified. From the perspective of clinical features of patients, we used the R package “caret” to randomly divide the TCGA-STAD cohort into training and test groups to make sure the consistency of the patient composition between training and test groups. In the training cohort, identified DELs were subjected to univariate Cox regression analysis using the “survival” R package to pinpoint potential IRLs of prognostic value. LASSO regression analysis was used to minimize the risk of overfitting, and multiple stepwise Cox regression method was applied to identify hub IRLs for constructing the prognostic model. The risk score was calculated using the following equation: $\beta_1 \times \text{gene1 expression} + \beta_2 \times \text{gene2 expression} + \dots + \beta_n \times \text{gene } n \text{ expression}$, where β was the correlation coefficient generated by the multiple Cox regression analysis.

Evaluation of the Established Immune-Related lncRNA Signature

According to the median risk score, GC patients were divided into high-risk and low-risk groups. The Kaplan–Meier analysis was conducted using “survminer” and “survival” R packages to evaluate the prognostic value of the IRL signature. The sensitivity and specificity of the IRL signature were evaluated in terms of the area under the curve (AUC) of receiver operating characteristic (ROC) using “survivalROC” R package. Risk score curve, survival scatter diagram, and heatmap were carried out using the “pheatmap” package. Univariate and multivariate Cox analyses using “survival” R package were conducted to demonstrate that the signature establishes an independent prognostic model. A prognostic nomogram was then constructed using “rms” R package to predict 1-, 2-, and 3-year OS of GC patients, and a concordance index (C-index) was calculated to determine the discrimination of the nomogram via a bootstrap method with 1,000 resamples. Calibration curves were performed to assess the accuracy of this nomogram. In addition, a decision curve analysis (DCA) was performed to evaluate the clinical usefulness. Gene set enrichment analysis (GSEA) performed by GSEA software (version 4.1.0, downloaded from <http://www.gsea-msigdb.org/gsea/index.jsp>) was applied to evaluate all genes based on their \log_2 fold changes and assess functions associated with different risk groups.

Estimation of Tumor-Infiltrating Immune Cells in Different Risk Groups

To explore the association between tumor-infiltrating immune cells and the risk score, we used TIMER, CIBERSORT, CIBERSORT-ABS, QUANTISEQ, XCELL, MCP-counter, and EPIC algorithms to examine the status of immune infiltration among GC patients from TCGA database. Wilcoxon signed-rank test was applied to analyze the differences of tumor-infiltrating

immune cell level between high-risk and low-risk groups. The relationship of risk score values and immune infiltrating cells was determined by Spearman correlation analysis. Boxplots for immune infiltrating cells in high-risk and low-risk groups were conducted using “ggpubr” R package. ESTIMATE algorithm was applied to explore the status of immune cell infiltration among two subgroups, in which R script was downloaded from <https://sourceforge.net/projects/estimateproject/to> calculate immune scores, stromal scores, and estimate scores.

Mutation Analysis

Mutation data in the form of Mutation Annotation Format (MAF) was applied, and we used the “maftools” R package to analyze the mutation data.

Immunophenoscore Analysis

The calculation process of immunophenoscore was detailed in a previous article (Charoentong et al., 2017). Briefly, according to a panel of immune-related genes yielded from random forest

results, a sample-wise Z score was calculated. The IPS was calculated on an arbitrary 0–10 scale based on the sum of the weighted averaged Z score to predict the response of ICIs, where higher scores are associated with the increased response to ICIs. The IPS results of 20 solid cancers can be acquired in the site of <https://tcia.at/home>.

Patients and Gastric Cancer Samples

GC tissue samples and matched adjacent normal gastric tissues were acquired from patients with gastric cancer who had undergone radical gastrectomy at the Department of Surgery, Zhongshan Hospital, Fudan University, from 2013 to 2014. This study was approved by the Ethics Committee of Zhongshan Hospital, Fudan University (Approval No. B2019-193R). Written informed consents were collected from all patients. No patient received preoperative chemotherapy. Clinicopathological variables were collected from all patients before surgery. All patients were followed up until December 2019. The eight lncRNA expressions were evaluated in eight pairs of GC tissues

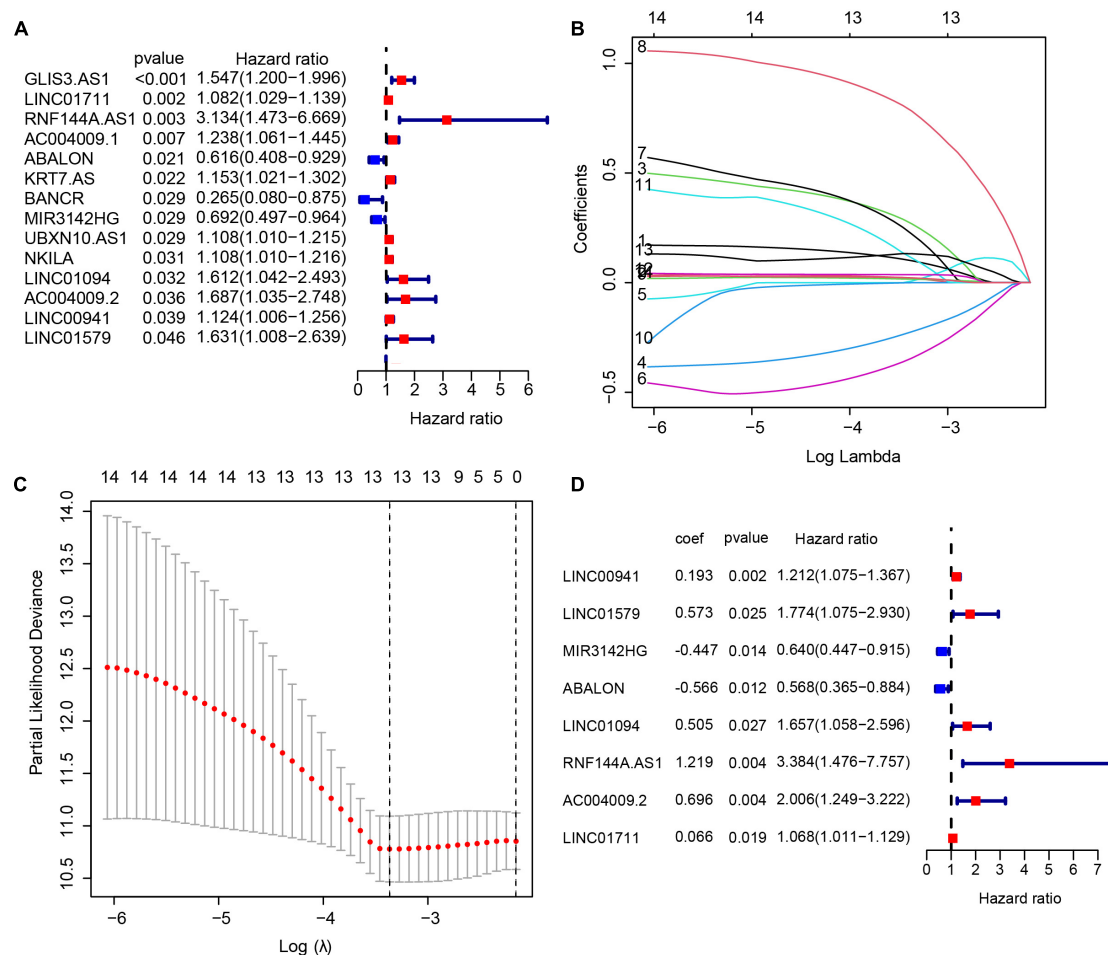


FIGURE 1 | Construction of an immune-related long non-coding RNA (lncRNA) signature to predict the prognosis of patients with gastric cancer. **(A)** 14 immune-related lncRNAs associated with OS identified by the univariate Cox regression model. **(B,C)** LASSO regression was performed to identify the minimum criteria. **(D)** Coefficients of eight genes calculated by multivariate Cox regression.

and matched adjacent non-cancerous tissues. The expression of RNF144A-AS1 was detected in 47 pairs of GC tissues and matched adjacent non-cancerous tissues. OS was calculated from the date of gastrectomy to the date of death or last follow-up. The clinical information of GC samples is detailed in **Supplementary Table 2**.

Cell Culture

The human GC cell lines (HGC27, AGS, NCIN87, and SUN1) and human normal gastric epithelial cells (GES1) were obtained from the American Type Culture Collection (ATCC, United States) and cultured in RPMI 1640 medium (Gibco, United States) with 10% fetal bovine serum (Gibco,

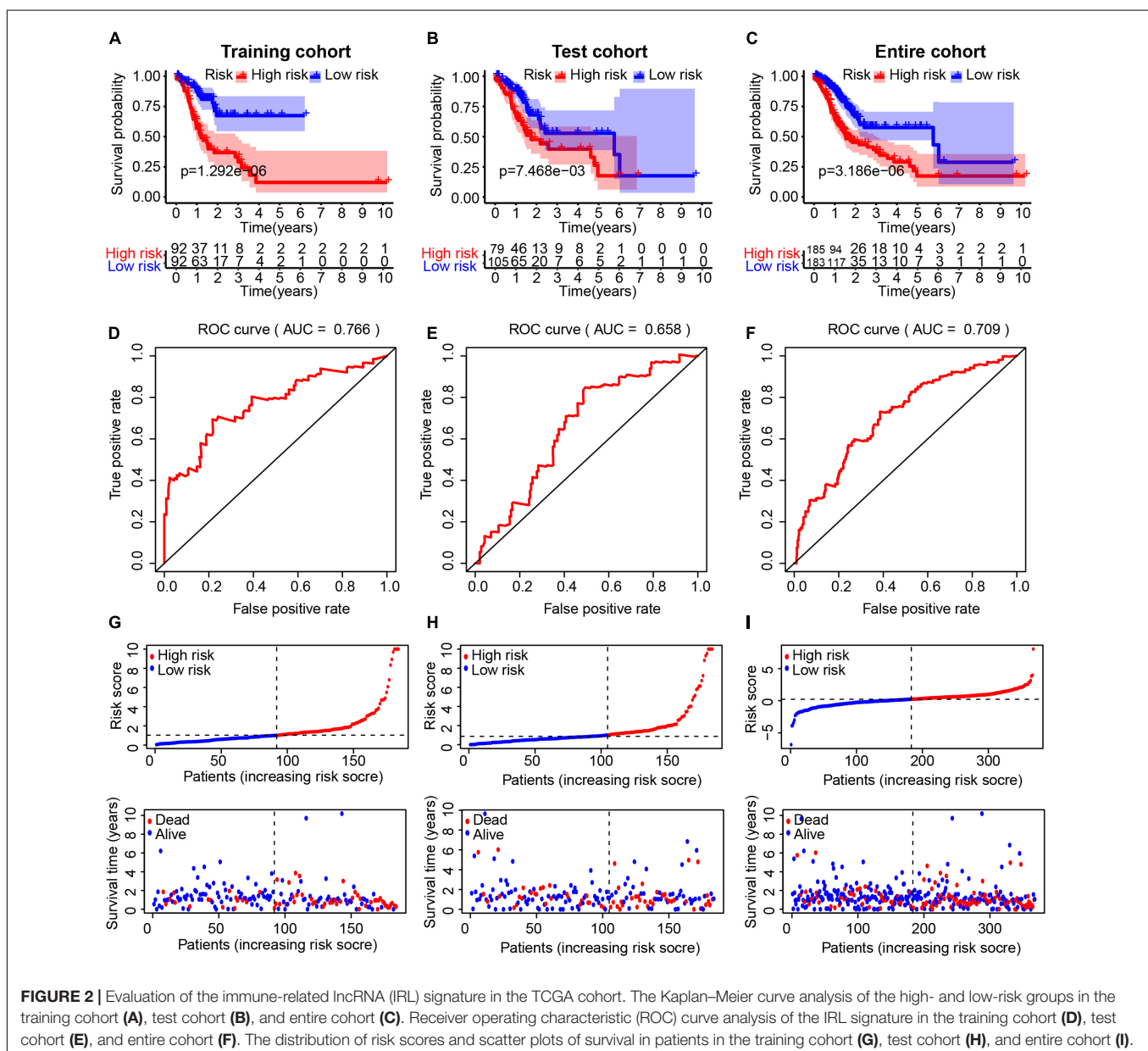
United States) supplemented with 1% penicillin and streptomycin (Invitrogen, United States) at 5% CO₂ and 37°C.

Quantitative Real-Time PCR

Total RNA from GC tissues and cell lines was extracted using TRIzol reagent (Invitrogen, United States). Quantitative real-time PCR (qRT-PCR) was performed as previously described (Li et al., 2019). The primers used for qRT-PCR are detailed in **Supplementary Table 3**.

Western Blot

Western blot was performed as previously described (Li et al., 2019). The primary antibodies (N-cadherin, E-cadherin, vimentin, and β -actin) were purchased from



Abcam, United States. The anti-mouse and anti-rabbit secondary antibodies were obtained from Cell Signaling Technology, United States.

Transfection

Lentivirus packaging cells were transfected with LV3-pGLV-h1-GFP-puro vector (GenePharma, China) containing RNF144A-AS1 knockdown (sh-RNF144A-AS1-1 and sh-RNF144A-AS1-2) and a negative control sequence (NC), respectively. Lentiviral transduction was performed in HGC27 and AGS cells. Pools of

stable transductants were generated by selection using puromycin (4 $\mu\text{g/ml}$) for 2 weeks.

Colony-Forming Assay

The cells at the density of 5×10^2 cells/well were seeded into a six-well plate and cultured for 2 weeks. The colonies were washed with PBS, fixed for 20 min with 100% methanol, and stained for 15 min with 1% crystal violet in 20% methanol. After washing three times with PBS, the number of colonies was calculated.

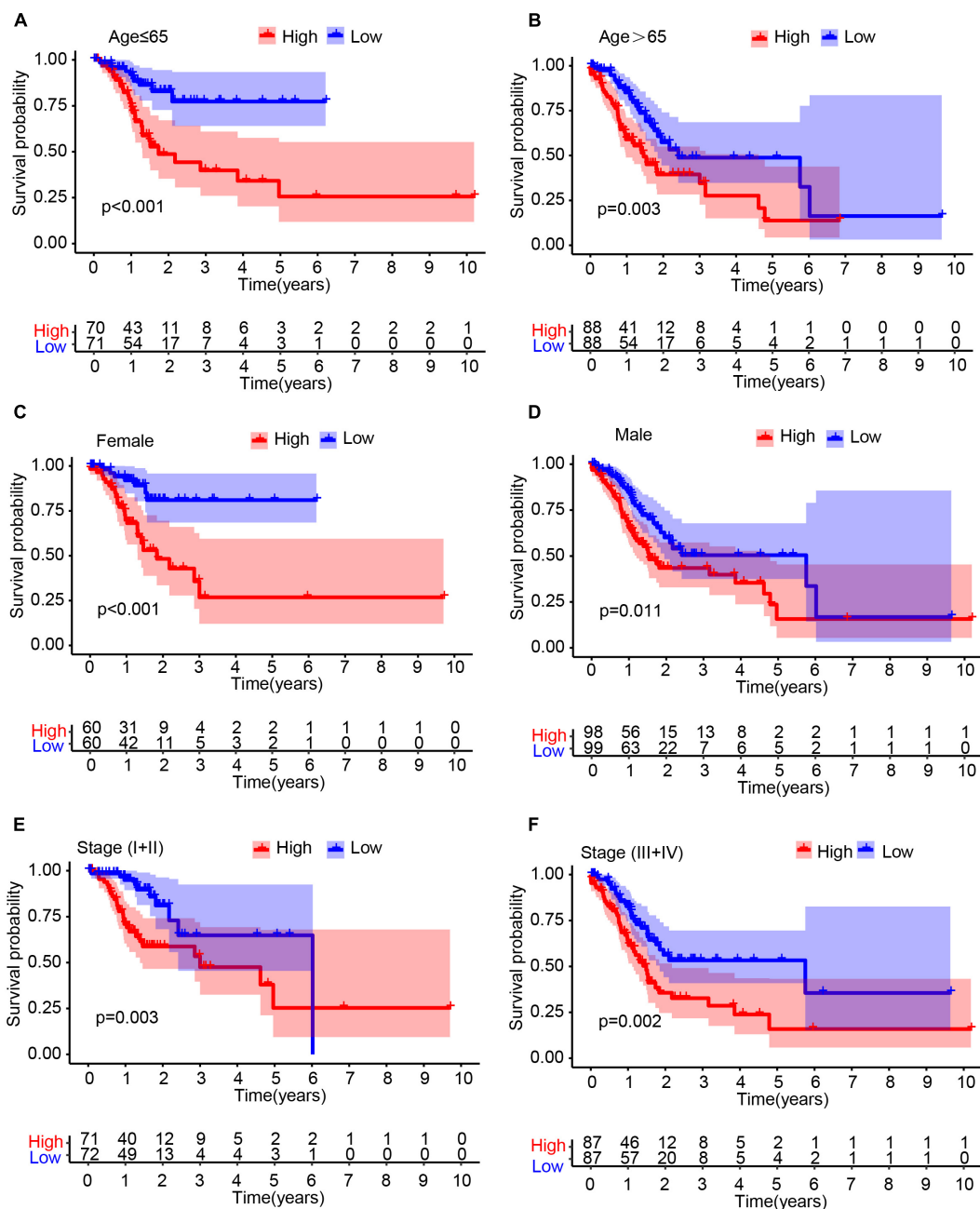


FIGURE 3 | Stratification analysis. The Kaplan-Meier survival analysis of gastric cancer (GC) patients stratified by age (A,B), male (C,D), and stage (E,F).

Cell Counting Kit-8 Proliferation Assay

Cell Counting Kit-8 (CCK-8) proliferation assay (Dojindo, Japan) was used to detect cell viability. Cells were seeded in 96-well plates at a density of 3×10^3 cells/well. After 10 μ l CCK-8 reagent was added, cells were incubated at standard conditions for 1 h. Then, the absorbance at 450 nm was measured using a microplate reader (Bio-Rad Laboratories, United States).

Wound-Healing Assay

The GC cells were seeded onto a coverslip at the density of 3×10^5 cells/well in six-well plates. The monolayer was scratched with a sterile 20- μ l pipette tip. The wound area was photographed under a light microscope (Leica, Wetzlar, Germany) at 0, 24, and 48 h.

Transwell Cell Invasion Assay

Cell migration and invasion were measured using Transwell assay as described elsewhere (Lin et al., 2019).

Statistical Analysis

The R software (version 4.0.2)³ was used to perform all statistical analyses. All data are represented in the format of mean \pm SD from three independent experiments. Student *t*-test or one-way ANOVA was applied to evaluate differences between groups. *P* < 0.05 was considered as statistically significant.

RESULTS

Construction of an Immune-Related lncRNA Signature Associated With the Prognosis of Gastric Cancer Patients

In the TCGA-STAD cohort, 6,739 DEGs were identified between 375 GC samples and 32 adjacent normal samples. After integrating 3044 IRLs, we obtained 164 differentially expressed IRLs (Supplementary Table 4) including 30 down-regulated genes and 134 up-regulated lncRNAs. A univariate Cox regression analysis was performed among DELs to identify lncRNAs related significantly to OS, which produced 14 lncRNAs likely to carry a prognostic value (Figure 1A). LASSO regression was conducted to remove IRLs highly correlated with one another (Figures 1B,C). To further select key IRLs with greater prognostic value, multiple stepwise Cox regression was performed to obtain eight hub IRLs constructing an immune prognostic signature (Figure 1D).

Evaluation of the Immune-Related lncRNA Signature in the TCGA Cohort

We divided GC patients into high- and low-risk groups according to the median risk score in the training, test, and entire cohort. A Kaplan–Meier analysis indicated that there was a significantly shorter OS in patients in the high-risk group (Figures 2A–C). The prognostic AUC value of this model achieved 0.766, 0.658, and 0.709 in the training, test, and entire cohort, respectively

(Figures 2D–F). A higher risk score was associated with a higher likelihood that a patient would experience poor survival (Figures 2G–I).

Stratification Analysis in the Cancer Genome Atlas Cohort

To determine whether the IRL signature was able to predict the prognosis of GC patient subgroups, we performed the Kaplan–Meier survival analysis in patients stratified by age (Figures 3A,B), gender (Figures 3C,D), and stage (Figures 3E,F), respectively. The results demonstrated that the IRL signature was able to distinguish low-risk from high-risk patients in different stratified groups.

Construction of a Nomogram Model Integrated With the Immune-Related lncRNA Signature

Univariate (Figure 4A) and multivariate (Figure 4B) Cox regression analyses indicated that IRL signature was able to independently predict the prognosis of GC patients. Multivariable ROC analysis demonstrated that the IRL signature possessed the highest prognostic accuracy (AUC = 0.713) compared to other factors, including age, gender, grade, T, M, and N (Figure 4C). Compared with the existing model, including the HanSignature (Han et al., 2021), WangSignature (Wang et al., 2021), and ZhouSignature (Zhou et al., 2021), our model showed a better prediction accuracy (Figure 4D). Subsequently, we constructed a nomogram-integrated IRL signature with other conventional prognosis factors and calculated its C-index (Figure 4E). The results of calibration curves demonstrated that the nomogram was able to accurately predict the OS of GC patients (Supplementary Figure 1). DCA of the nomogram was performed and revealed that the nomogram model had an excellent net benefit for GC patients' OS (Figure 4F). In order to figure out which factors drive the different OS between high- and low-risk patients, we performed GSEA. The results indicated the epithelial–mesenchymal transition plays an important role in GC progression (Figures 4G,H).

Investigation of Tumor-Infiltrating Immune Cells

A Spearman correlation analysis showed that the immune infiltrating status was significantly associated with risk score (Figure 5A). Specifically, the level of cancer-associated fibroblasts (Figure 5B), endothelial cells (Figure 5C), M2 macrophages (Figure 5D), and stroma score (Figure 5E) was higher in the high-risk group, while the expression of CD8⁺ T cells (Figure 5F) and T follicular helper (Tfh) cells (Figure 5G) was higher in the low-risk group. The results of ESTIMATE algorithm showed the immune score had no significant difference between the high- and the low-risk groups (Supplementary Figure 2A), while the stromal score was higher in the high-risk group (Supplementary Figure 2B). The results of correlation analyses between immune cell infiltration and risk score indicated that the terms of macrophages M2, monocytes, and mast cell resting were positively related to the risk score, while the

³<https://www.r-project.org/>

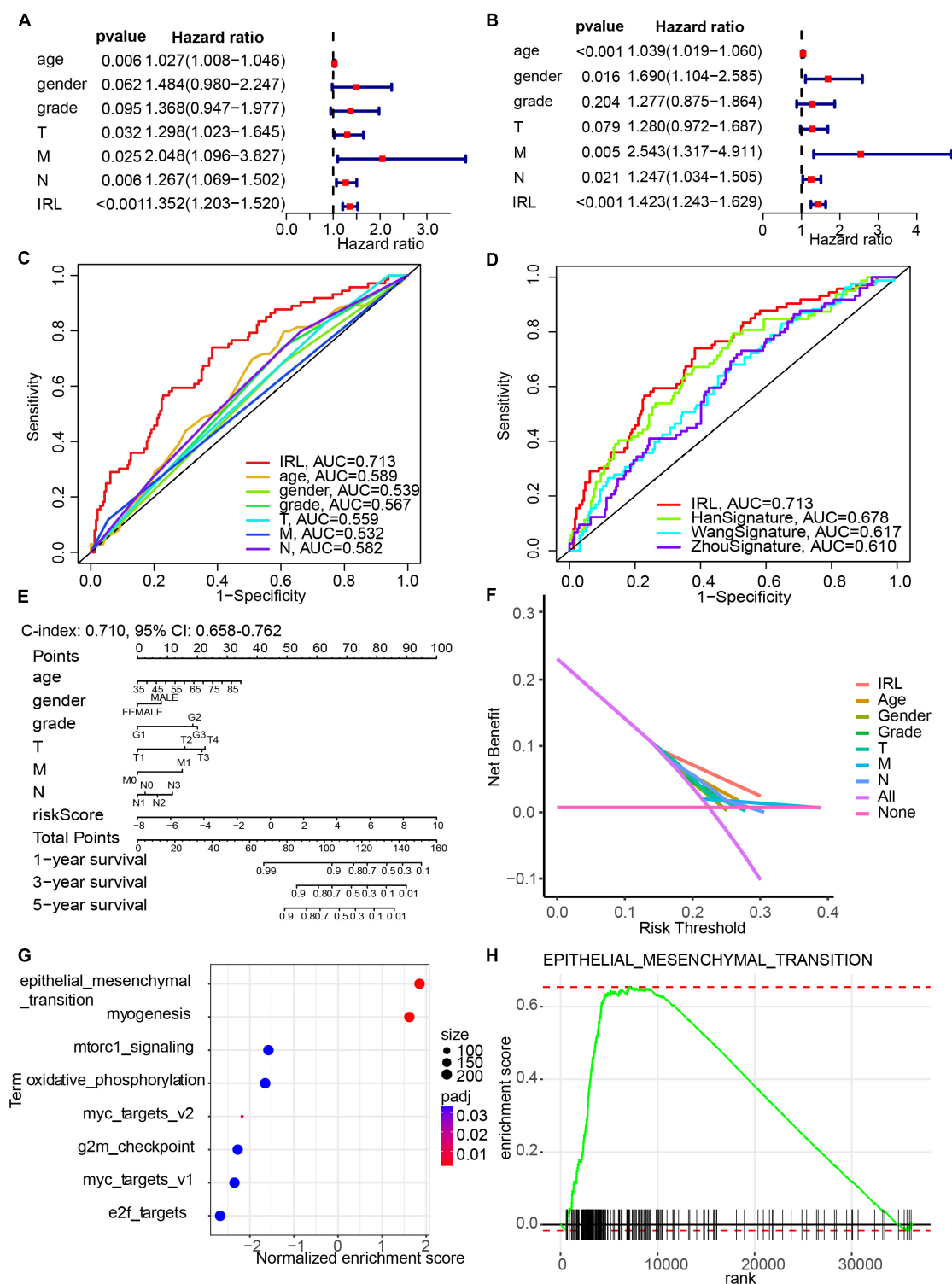


FIGURE 4 | Construction of a nomogram model integrated with the IRL signature. **(A,B)** Univariate and multivariate Cox analyses included different clinicopathologic features. **(C,D)** Multivariable ROC curves for overall survival (OS). **(E)** Nomogram model for predicting the 1-, 3-, and 5-year OS of GC patients. **(F)** Decision curve analysis of the OS-related nomogram. "None" indicates that all samples were negative without intervention and the net benefit was 0. "All" indicates that all samples were positive with intervention. **(G)** The bubble plot of gene set enrichment analysis (GSEA) results. **(H)** The enrichment plot of epithelial-mesenchymal transition.

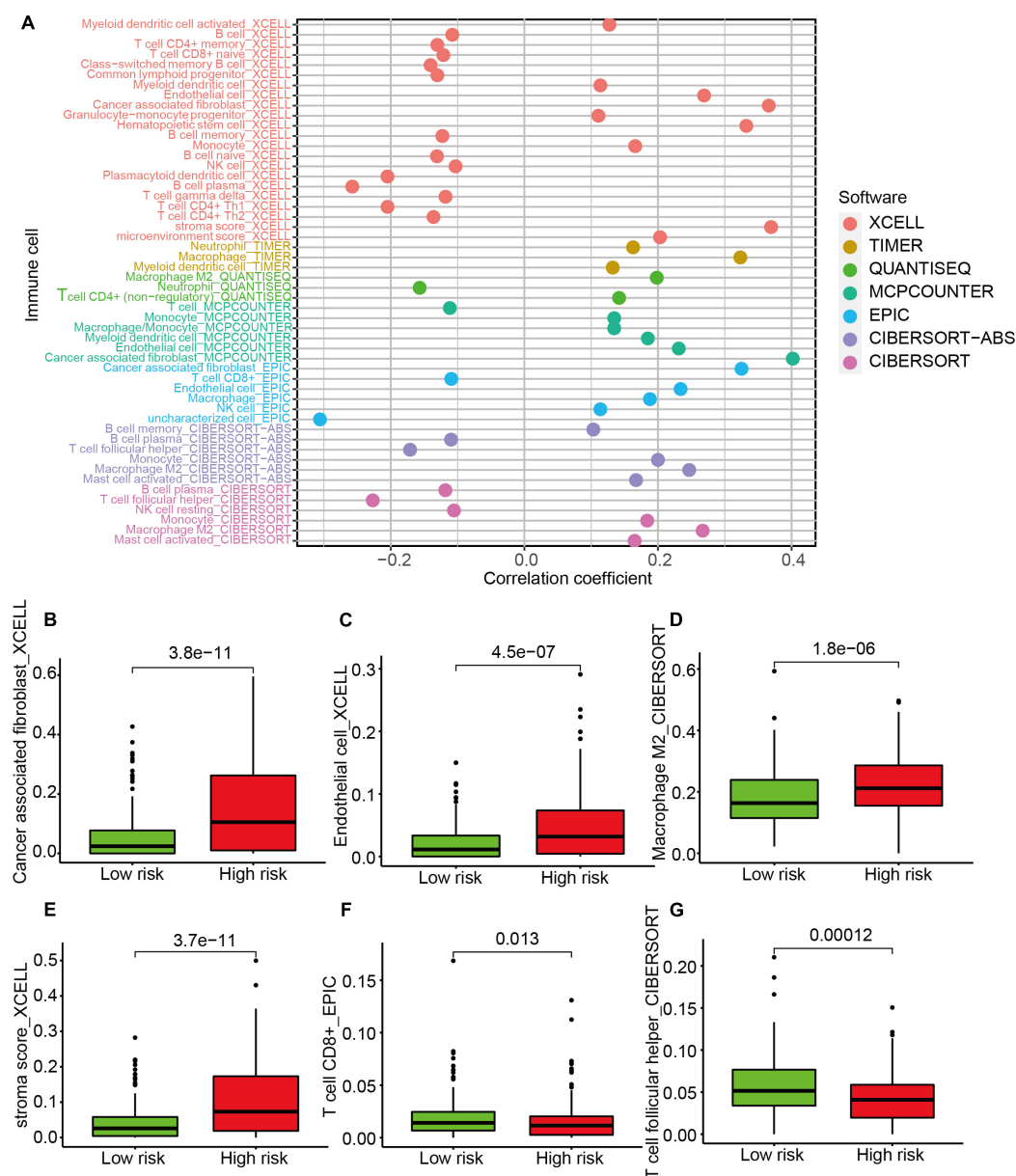


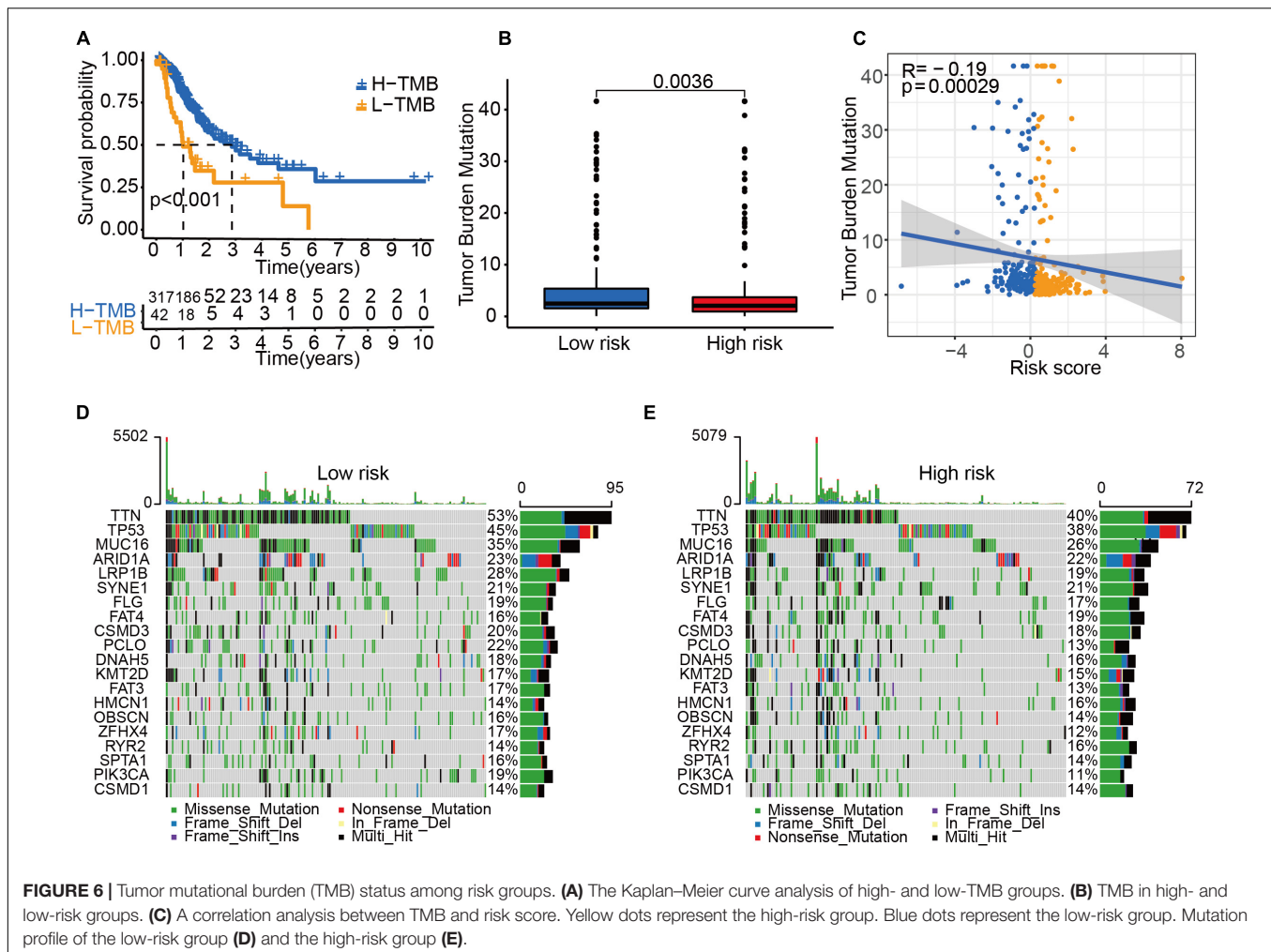
FIGURE 5 | The analysis of tumor-infiltrating immune cells between the high-risk and low-risk groups. **(A)** Spearman correlation analysis. The type terms represent different algorithms. The abscissa indicates the correlation between risk score and immune cell infiltration. If the correlation > 0, the specific immune cell infiltration is positively associated with the risk score. If the correlation < 0, the specific immune cell infiltration is negatively associated with the risk score. The distribution levels of cancer-associated fibroblast **(B)**, endothelial cell **(C)**, macrophage M2 **(D)**, stroma score **(E)**, CD8⁺ T cell **(F)**, and T cell follicular helper **(G)** between the high-risk and low-risk groups.

terms of memory CD4 T cell activation, plasma cells, and T follicular helper cells were negatively related to the risk score (Supplementary Figure 2C).

Tumor Mutational Burden Status Among Risk Groups

Next, we explored the role of tumor mutational burden (TMB) in the prognosis of GC patients. GC patients with higher TMB

had a better OS (Figure 6A), and patients allocated to the low-risk group had a higher TMB than those allocated to the high-risk group (Figure 6B). The TMB was negatively associated with the risk score (Figure 6C). The mutation profile is illustrated in Figures 6D,E. We found that the mutation rate of most genes was high in the low-risk group except for SYNE1, FAT4, HMCN1, RYR2, and CSMD1. These genes with a high mutation rate could be potential biomarkers for predicting GC patients' OS or responses to ICIs.



The Association Between Risk Groups and Response to Immune Checkpoint Inhibitor

According to the transcriptional data, we found immune checkpoint-related genes were differently expressed between the high-risk and low-risk groups (Figure 7A). IPS has been confirmed to have a predictive value in melanoma patients treated with the CTLA-4 and PD-1 blockers (Van Allen et al., 2015; Charoentong et al., 2017). We used the immunophenoscore to evaluate whether the risk score could predict the response to ICIs in GC patients. The IPS was significantly higher in the low-risk group, which indicated the low-risk group patients had a better opportunity for ICI application (Figure 7B).

RNF144A-AS1 Is Highly Expressed in Gastric Cancer and Promotes Cell Proliferation, Migratory, and Invasive Potential

To identify the key lncRNA involved in GC progression, we determined the expression of eight lncRNAs in the IRL

signature. From the TCGA-STAD cohort, the eight lncRNAs were highly expressed in GC tissues except for LINC01579 (Supplementary Figure 3). We found that the difference in RNF144A-AS1 expression is the most significant between normal and tumor tissues (Figure 8A). We also found that RNF144A-AS1 was highly expressed in GC tissues from TCGA database (Figure 8B). Next, we analyzed RNF144A-AS1 expression in 47 pairs of GC tissues and matched adjacent non-cancerous tissues. The results indicated RNF144A-AS1 expression was upregulated in GC tissues (Figure 8C). Meanwhile, a higher expression of RNF144A-AS1 was observed in GC cells compared with human normal gastric epithelial cells (Figure 8D). Patients with a high expression of RNF144A-AS1 predicted poor overall survival (Figure 8E).

RNF144A-AS1 expression was knocked down in HGC27 and AGS cells so that the biological role of RNF144A-AS1 in GC can be elucidated (Figure 9A). Colony-forming assay showed RNF144A-AS1 knockdown decreased the colony-forming ability in both HGC27 and AGS cells (Figure 9B). In CCK-8 proliferation assay, RNF144A-AS1 knockdown led to a significant proliferation reduction (Figures 9C,D). As shown in Figure 9E, RNF144A-AS1 knockdown decreased migration

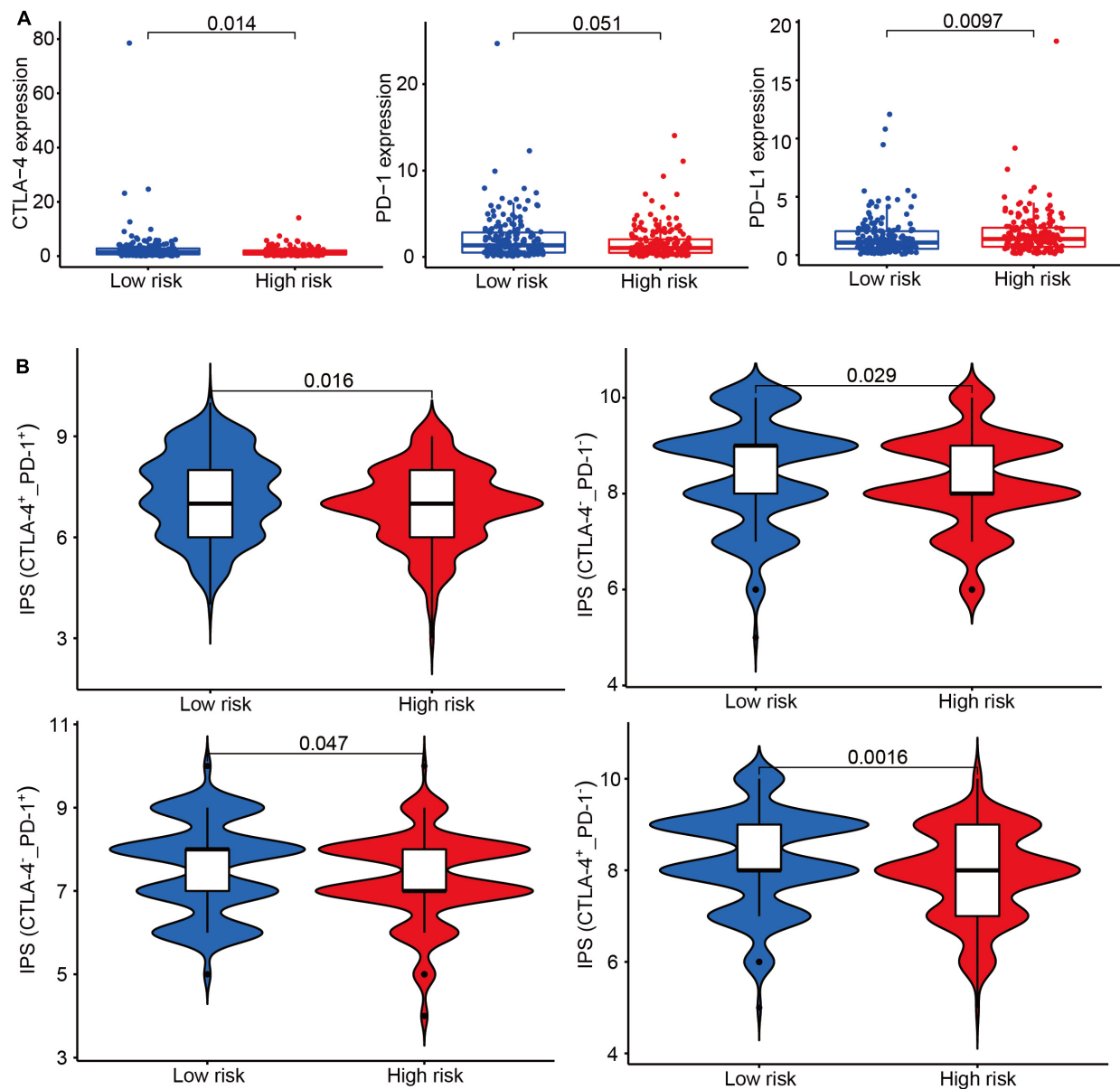


FIGURE 7 | The association between risk groups and response to immune checkpoint inhibitors (ICI). **(A)** The gene expression of CTLA-4, PD-1, and PD-L1 in the high-risk and low-risk groups. **(B)** The association between IPS and the IRL signature of GC patients. Patients were divided into four groups: CTLA-4⁺PD1⁺, CTLA-4⁻PD1⁻, CTLA-4⁺PD1⁻, and CTLA-4⁻PD1⁺.

potential in both HGC27 and AGS cells. In Transwell invasion assay, a reduced number of invasive cells was observed in the RNF144A-AS1 knockdown group (Figure 9F). Combined with the GSEA results, we evaluated the expression of N-cadherin, E-cadherin, and vimentin to further explore the mechanisms of how RNF144A-AS1 affects GC cell phenotypes in HGC27 cells. The results revealed that RNF144A-AS1 knockdown decreased the expression of N-cadherin and vimentin, while increased E-cadherin expression (Figure 9G). Hence, the change of GC cell phenotypes induced by RNF144A-AS1 expression may be mediated by the activation of EMT signaling pathways.

DISCUSSION

Recent striking results from ICI treatment have provided a promising therapy option for GC patients. However, only a subset of patients could respond to the ICI therapy. It is urgent to identify predictive biomarkers for the response of ICI. It is unlikely to develop a single predictive biomarker because of the complexity of the tumor biology and immune response. The integration of multiple tumor and immune response parameters may contribute to accurate predictions (Masucci et al., 2016). Emerging evidence indicates that lncRNAs play a critical role in

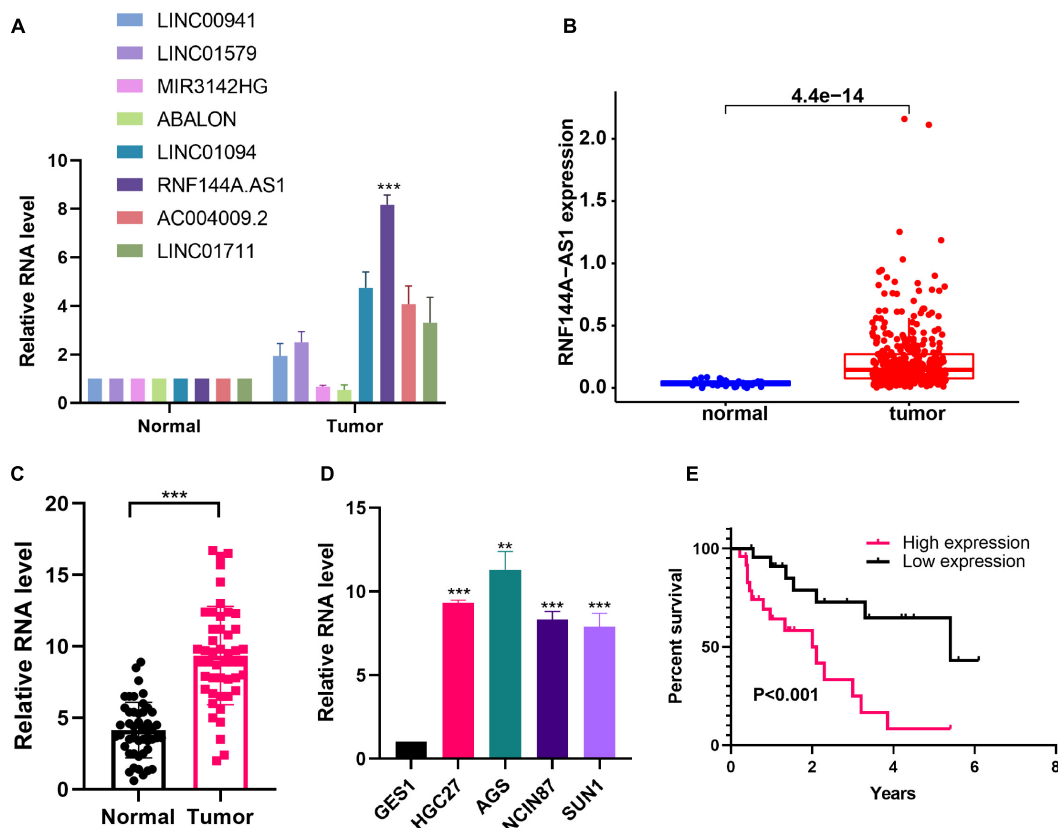


FIGURE 8 | RNF144A-AS1 is highly expressed in GC tissues and cells. **(A)** The RNA expression of eight lncRNAs included in the IRL in normal and tumor tissues. **(B)** RNF144A-AS1 expression in The Cancer Genome Atlas Stomach Adenocarcinoma (TCGA-STAD) cohort. **(C)** RNF144A-AS1 expression in 47 pairs of GC tissues and matched adjacent non-cancerous tissues. **(D)** The expression of RNF144A-AS1 in human normal gastric epithelial cells and GC cell lines. **(E)** The Kaplan-Meier curve analysis of 47 GC patients. The patients were divided into high-risk and low-risk groups according to the median expression of RNF144A-AS1. All measurements are shown as the means \pm SD from three independent experiments, ** $p < 0.01$; *** $p < 0.001$.

the immune system and the development of cancer by interacting with DNA, RNA, or proteins to regulate the expression of protein-coding genes (Atianand et al., 2017). It is of great significance to develop an IRL model to predict the OS and ICI response of GC patients.

Wang et al. (2021) developed an IRL prognostic signature according to the differentially expressed lncRNAs between high and low immune-infiltrating cell groups based on a single-sample gene-set enrichment analysis (ssGSEA) algorithm. We take another method to discover the potential DELs. Based on the hypothesis that if a lncRNA plays a critical role in the immune system, their correlated genes are supposed to be enriched in immune-related pathways, multiple lncRNA regulators that are associated with immune-related pathways were identified (Li et al., 2020). We acquired the IRLs of gastric cancer from this study and constructed a prognostic IRL signature. In addition, the published article only had a training set and lacked a validation set. We also explored the association between the IRL signature and tumor microenvironment (TME), mutation status, and IPS in gastric cancer. Moreover, we found RNF144A-AS1 deriving from our signature promotes GC through activating the EMT signaling pathway.

Eight IRLs are involved in the established signature. LINC00941 has been confirmed to exhibit pro-tumorigenic and pro-metastatic abilities during tumorigenesis. RNF144A-AS1 was found to be an oncogene in bladder cancer, which promotes proliferation, migration, and invasion in tumor progression by regulating SOX11 via sponging miR-455-5p (Bi et al., 2020). However, its role and function in gastric cancer has not been elucidated. LINC00941 is highly expressed in GC samples and promotes GC progression by affecting tumor depth and distant metastasis (Liu et al., 2019). LINC01579 was found to promote glioblastoma cell proliferation in a ceRNA manner of absorbing miR-139-5p to increase EIF4G2 expression (Chai and Xie, 2019). MIR3142HG is a critical regulator of the inflammatory response, and the attenuated expression of MIR3142HG/miR-146a contributes to the reduced inflammatory response in IPF fibroblast (Hadjicharalambous et al., 2018). As for LINC01094, several studies reported that it is a pro-tumorigenic lncRNA, and microRNA-184 (Xu H. et al., 2020), miR-126-5p (Li and Yu, 2020), miR-577 (Xu J. et al., 2020), miR-330-3p (Zhu et al., 2020), and miR-224-5p (Jiang et al., 2020) were identified as its targets. The role of ABALON, AC004009-2, and LINC01711 has not been explored by biological assays, providing directions

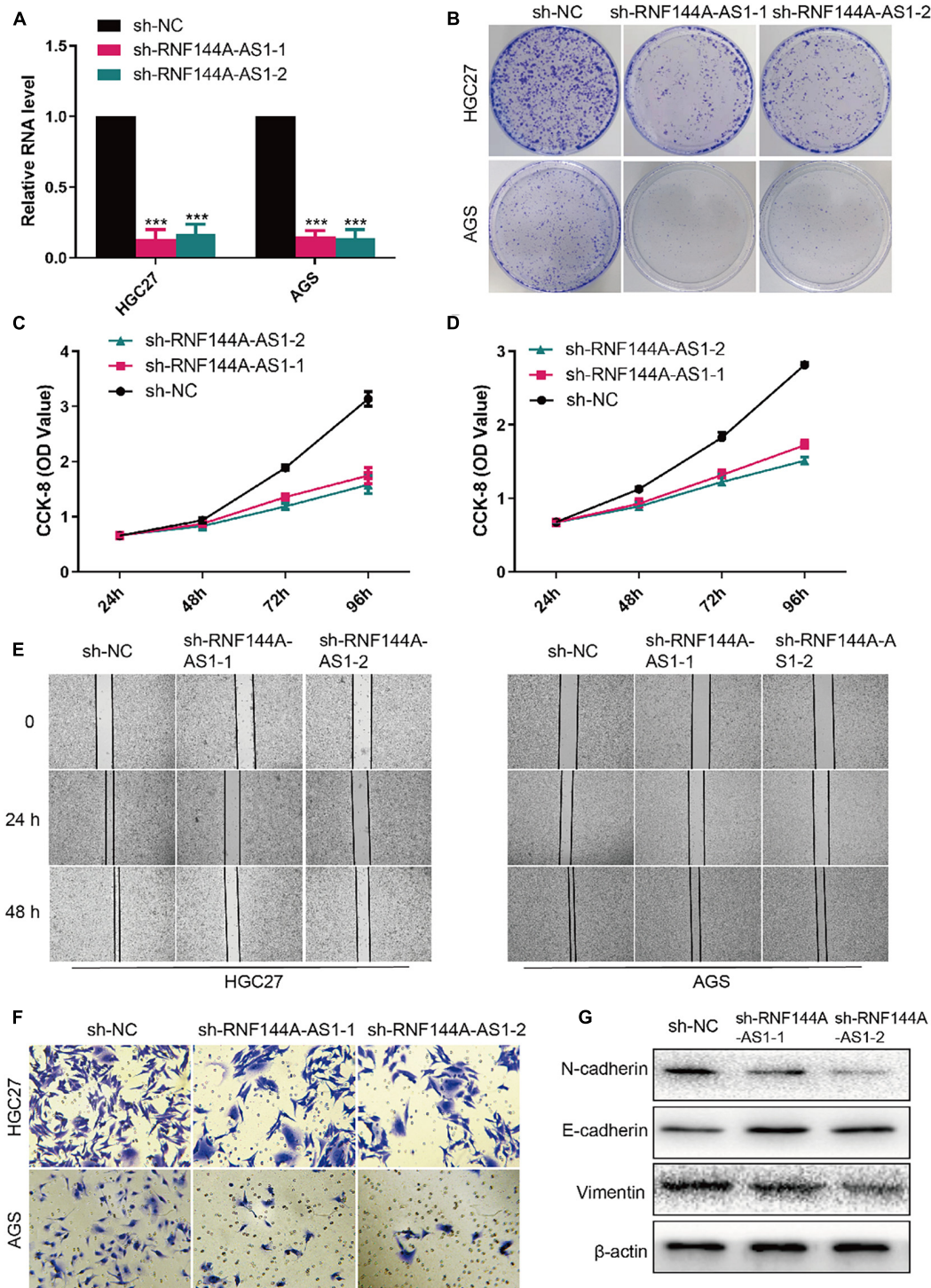


FIGURE 9 | RNF144A-AS1 promotes cell proliferation, migratory, and invasive potential. **(A)** The efficiency of RNF144A-AS1 knockdown was detected by quantitative real-time PCR (qRT-PCR). **(B)** Representative pictures of colony-forming assay. A growth curve analysis showing the cell growth of HGC27 **(C)** and AGS **(D)** cells with RNF144A-AS1 knockdown. **(E)** The migration distance was measured to analyze the migration ability of GC cells that were treated with sh-NC or sh-RNF144A-AS1-1 or sh-RNF144A-AS1-2. **(F)** Transwell Matrigel invasion assay in GC cells with RNF144A-AS1 knockdown. **(G)** Representative WB images showing the protein level of N-cadherin, E-cadherin, and vimentin in GC cells with RNF144A-AS1 knockdown. All measurements are shown as the means \pm SD from three independent experiments, *** p < 0.001.

and clues for future research. Moreover, all the published studies mentioned above focused on the role of IRLs in the proliferation, invasion, and migration of cancer cells but largely ignored its role in the immune system.

The TME is complex and constantly evolving. It consists of stromal cells, fibroblasts, endothelial cells, and innate and adaptive immune cells (Hinshaw and Shevde, 2019). The cross-talk of these cells determines the fate of tumor cells. A greater understanding of the TME will contribute to improving the prognosis of cancer patients. We applied seven different algorithms to examine the immune infiltration status between the high-risk and low-risk groups. High infiltration of M2 macrophages in cancerous tissues is considered as a negative prognosis in gastric cancer, breast cancer, lung cancer, hepatoma, and other malignancies (Cardoso et al., 2014; Wang et al., 2018). Other components of the TME, such as cancer-associated fibroblasts (CAFs), endothelial cells, and stromal cells, also play a role in the development of cancer (Hinshaw and Shevde, 2019). CAFs possess wound-healing ability and are found to promote tumor proliferation, invasion, and metastasis. Also, CAFs could secrete immune-suppressive cytokines that polarize macrophages to the M2 phenotype and lead to the exhaustion and depletion of CD8⁺ T cells (Lakins et al., 2018). Hence, it is not surprising that the level of CAFs, endothelial cells, M2 macrophages, and stroma cells was high in the high-risk group. The presence of Tfh cells has been positively associated with long-term survival of patients with breast cancer or colorectal cancer (Bindea et al., 2013). Tfh cells are found to produce CXCL13 that plays an immune-protective role in anti-tumor immunity (Crotty, 2019). Our results indicated the numbers of CD8⁺ T cells and Tfh cells are higher in the low-risk group. In addition, the term of NK cell from the EPIC algorithm is contrary to the term of NK cell resting from the CIBERSORT algorithm. The term of NK cell consists of NK cell resting and NK cell activation. Hence, the explanation of this contrast may be that the NK cell resting is negatively associated with a risk score, and when considering the whole level of NK cells, the relationship changes into a positive association. Taken together, our findings show that tumor-immune cross-talk and tumor-stromal cross-talk might play a role in the prognosis of patients with GC.

We demonstrate that the IRL signature low-risk group has higher TMB, which means higher TMB was related to a better prognosis in this study. This finding may partially explain the predictive value of this model. Also, the TMB-high group exhibited a better OS in the TCGA-STAD cohort, which was consistent with previous studies (Wang et al., 2019; Zhang et al., 2020). Recently, the question of whether TMB status could be considered as a general prognostic biomarker to predict patients' OS has been proposed, and several studies indicated that high tumor mutation burden failed to predict immune checkpoint blockade response across all cancer types (Passaro et al., 2020; McGrail et al., 2021). In the future, more study should be performed to determine the predictive value of TMB in GC patients.

The association between IPS and our IRL signature in GC was explored. We found that the IRL signature low-risk group had

a better chance to receive ICI treatment and may stand for an immunogenic tumor microenvironment. These results indicate that the IRL signature was a potential model to determine which GC patients are more inclined to respond to ICI.

In conclusion, we constructed an IRL-based prognostic model, which is a reliable and accurate model to predict the OS and ICI response of GC patients. This signature may be implemented to improve GC prognosis and, in the future, to inform treatment with novel immunotherapies.

DATA AVAILABILITY STATEMENT

The original contributions presented in the study are included in the article/**Supplementary Material**, further inquiries can be directed to the corresponding author/s.

ETHICS STATEMENT

The studies involving human participants were reviewed and approved by the Ethics Committee of Zhongshan Hospital, Fudan University (Approval No. B2019-193R). The patients/participants provided their written informed consent to participate in this study.

AUTHOR CONTRIBUTIONS

ZD, RL, JH, and GW conceived, revised the manuscript, and designed the study. ZD, DS, and LS performed the experiments. ZD, RL, and JH conducted the statistical analysis. ZD wrote the manuscript. All authors contributed to the article and approved the submitted version.

FUNDING

This work was supported by the Shanghai Natural Science Foundation Project (19ZR1409100).

ACKNOWLEDGMENTS

We thank Prof. Ying Feng from the CAS Key Laboratory of Nutrition, Metabolism and Food Safety, Shanghai Institute of Nutrition and Health, University of Chinese Academy of Sciences, Chinese Academy of Sciences. She provided the experiment equipment and offered some helpful advice during the experiments.

SUPPLEMENTARY MATERIAL

The Supplementary Material for this article can be found online at: <https://www.frontiersin.org/articles/10.3389/fcell.2021.739583/full#supplementary-material>

Supplementary Figure 1 | Calibration plots of the nomogram-predicted probability of 1-, 2-, and 3-year OS.

Supplementary Figure 2 (A,B) The results of the ESTIMATE algorithm in the high-risk and the low-risk groups. **(C)** The correlation analyses between CIBERSORT-Results and risk score.

Supplementary Figure 3 | The expression of eight genes between tumor and normal tissues in the TCGA-STAD cohort.

Supplementary Table 1 | Baseline characteristics of the patients in the TCGA cohorts.

Supplementary Table 2 | Association of RNF144A-AS1 expression with clinicopathologic characteristics of gastric cancer patients.

Supplementary Table 3 | The primers used for qRT-PCR.

Supplementary Table 4 | One hundred sixty-four differentially expressed IRGs between GC patients and healthy individuals.

REFERENCES

- Atianand, M. K., Caffrey, D. R., and Fitzgerald, K. A. (2017). Immunobiology of long noncoding RNAs. *Annu. Rev. Immunol.* 35, 177–198.
- Bi, H., Shang, Z., Jia, C., Wu, J., Cui, B., Wang, Q., et al. (2020). lncRNA RNF144A-AS1 promotes bladder cancer progression via RNF144A-AS1/miR-455-5p/SOX11 Axis. *Oncotargets Ther.* 13, 11277–11288. doi: 10.2147/ott.s266067
- Bindea, G., Mlecnik, B., Tosolini, M., Kirilovsky, A., Waldner, M., Obenaus, A. C., et al. (2013). Spatiotemporal dynamics of intratumoral immune cells reveal the immune landscape in human cancer. *Immunity* 39, 782–795. doi: 10.1016/j.immuni.2013.10.003
- Botti, G., Scognamiglio, G., Aquino, G., Liguori, G., and Cantile, M. (2019). lncRNA HOTAIR in tumor microenvironment: what role? *Int. J. Mol. Sci.* 20:2279. doi: 10.3390/ijms20092279
- Bray, F., Ferlay, J., Soerjomataram, I., Siegel, R. L., Torre, L. A., and Jemal, A. (2018). Global cancer statistics 2018: GLOBOCAN estimates of incidence and mortality worldwide for 36 cancers in 185 countries. *CA Cancer J. Clin.* 68, 394–424. doi: 10.3322/caac.21492
- Cardoso, A. P., Pinto, M. L., Pinto, A. T., Oliveira, M. I., Pinto, M. T., Gonçalves, R., et al. (2014). Macrophages stimulate gastric and colorectal cancer invasion through EGFR Y(1086), c-Src, Erk1/2 and Akt phosphorylation and smallGTPase activity. *Oncogene* 33, 2123–2133. doi: 10.1038/onc.2013.154
- Chai, Y., and Xie, M. (2019). LINC01579 promotes cell proliferation by acting as a ceRNA of miR-139-5p to upregulate EIF4G2 expression in glioblastoma. *J. Cell. Physiol.* 234, 23658–23666. doi: 10.1002/jcp.28933
- Charoentong, P., Finotello, F., Angelova, M., Mayer, C., Efremova, M., Rieder, D., et al. (2017). Pan-cancer immunogenomic analyses reveal genotype-immunophenotype relationships and predictors of response to checkpoint blockade. *Cell Rep.* 18, 248–262. doi: 10.1016/j.celrep.2016.12.019
- Chen, C., Zhang, F., Zhou, N., Gu, Y. M., Zhang, Y. T., He, Y. D., et al. (2019). Efficacy and safety of immune checkpoint inhibitors in advanced gastric or gastroesophageal junction cancer: a systematic review and meta-analysis. *Oncoimmunology* 8:e1581547. doi: 10.1080/2162402x.2019.1581547
- Coutzac, C., Pernot, S., Chaput, N., and Zaanan, A. (2019). Immunotherapy in advanced gastric cancer, is it the future? *Crit. Rev. Oncol. Hematol.* 133, 25–32. doi: 10.1016/j.critrevonc.2018.10.007
- Crotty, S. (2019). T follicular helper cell biology: a decade of discovery and diseases. *Immunity* 50, 1132–1148. doi: 10.1016/j.immuni.2019.04.011
- Hadjicharalambous, M. R., Roux, B. T., Feghali-Bostwick, C. A., Murray, L. A., Clarke, D. L., and Lindsay, M. A. (2018). Long non-coding RNAs are central regulators of the IL-1 β -induced inflammatory response in normal and idiopathic pulmonary lung fibroblasts. *Front. Immunol.* 9:2906. doi: 10.3389/fimmu.2018.02906
- Han, T., Xu, D., Zhu, J., Li, J., Liu, L., and Deng, Y. (2021). Identification of a robust signature for clinical outcomes and immunotherapy response in gastric cancer: based on N6-methyladenosine related long noncoding RNAs. *Cancer Cell Int.* 21:432.
- Hinshaw, D. C., and Shevde, L. A. (2019). The tumor microenvironment innately modulates cancer progression. *Cancer Res.* 79, 4557–4566. doi: 10.1158/0008-5472.can-18-3962
- Janjigian, Y. Y., Bendell, J., Calvo, E., Kim, J. W., Ascierto, P. A., Sharma, P., et al. (2018). CheckMate-032 study: efficacy and safety of nivolumab and nivolumab plus ipilimumab in patients with metastatic esophagogastric cancer. *J. Clin. Oncol.* 36, 2836–2844. doi: 10.1200/jco.2017.76.6212
- Jiang, Y., Zhang, H., Li, W., Yan, Y., Yao, X., and Gu, W. (2020). FOXM1-activated LINC01094 promotes clear cell renal cell carcinoma development via MicroRNA 224-5p/CHSY1. *Mol. Cell. Biol.* 40:e00357-19.
- Kang, Y. K., Boku, N., Satoh, T., Ryu, M. H., Chao, Y., Kato, K., et al. (2017). Nivolumab in patients with advanced gastric or gastro-oesophageal junction cancer refractory to, or intolerant of, at least two previous chemotherapy regimens (ONO-4538-12, ATTRACTION-2): a randomised, double-blind, placebo-controlled, phase 3 trial. *Lancet* 390, 2461–2471. doi: 10.1016/s0140-6736(17)31827-5
- Kono, K., Nakajima, S., and Mimura, K. (2020). Current status of immune checkpoint inhibitors for gastric cancer. *Gastric Cancer* 23, 565–578. doi: 10.1007/s10120-020-01090-4
- Lakins, M. A., Ghorani, E., Munir, H., Martins, C. P., and Shields, J. D. (2018). Cancer-associated fibroblasts induce antigen-specific deletion of CD8 (+) T Cells to protect tumour cells. *Nat. Commun.* 9:948.
- Li, R., Zhang, L., Qin, Z., Wei, Y., Deng, Z., Zhu, C., et al. (2019). High LINC00536 expression promotes tumor progression and poor prognosis in bladder cancer. *Exp. Cell Res.* 378, 32–40. doi: 10.1016/j.yexcr.2019.03.009
- Li, X. X., and Yu, Q. (2020). LINC01094 accelerates the growth and metastatic-related traits of glioblastoma by sponging miR-126-5p. *Oncotargets Ther.* 13, 9917–9928. doi: 10.2147/ott.s263091
- Li, Y., Jiang, T., Zhou, W., Li, J., Li, X., Wang, Q., et al. (2020). Pan-cancer characterization of immune-related lncRNAs identifies potential oncogenic biomarkers. *Nat. Commun.* 11:1000.
- Lin, X., Wang, S., Sun, M., Zhang, C., Wei, C., Yang, C., et al. (2019). miR-195-5p/NOTCH2-mediated EMT modulates IL-4 secretion in colorectal cancer to affect M2-like TAM polarization. *J. Hematol. Oncol.* 12:20.
- Liu, H., Wu, N., Zhang, Z., Zhong, X., Zhang, H., Guo, H., et al. (2019). Long non-coding RNA LINC00941 as a potential biomarker promotes the proliferation and metastasis of gastric cancer. *Front. Genet.* 10:5. doi: 10.3389/fgene.2019.00005
- Masucci, G. V., Cesano, A., Hawtin, R., Janetzki, S., Zhang, J., Kirsch, I., et al. (2016). Validation of biomarkers to predict response to immunotherapy in cancer: volume I – pre-analytical and analytical validation. *J. Immunother. Cancer* 4:76.
- Mathy, N. W., and Chen, X. M. (2017). Long non-coding RNAs (lncRNAs) and their transcriptional control of inflammatory responses. *J. Biol. Chem.* 292, 12375–12382. doi: 10.1074/jbc.r116.760884
- McGrail, D. J., Pilié, P. G., Rashid, N. U., Voorwerk, L., Slagter, M., Kok, M., et al. (2021). High tumor mutation burden fails to predict immune checkpoint blockade response across all cancer types. *Ann. Oncol.* 32, 661–672. doi: 10.1016/j.annonc.2021.02.006
- Pang, Z., Chen, X., Wang, Y., Wang, Y., Yan, T., Wan, J., et al. (2020). Long non-coding RNA C5orf64 is a potential indicator for tumor microenvironment and mutation pattern remodeling in lung adenocarcinoma. *Genomics* 113(1 Pt 1), 291–304. doi: 10.1016/j.ygeno.2020.12.010
- Passaro, A., Stenzinger, A., and Peters, S. (2020). Tumor mutational burden as a pan-cancer biomarker for immunotherapy: the limits and potential for convergence. *Cancer Cell* 38, 624–625. doi: 10.1016/j.ccell.2020.10.019
- Statello, L., Guo, C. J., Chen, L. L., and Huarte, M. (2021). Gene regulation by long non-coding RNAs and its biological functions. *Nat. Rev. Mol. Cell Biol.* 22, 96–118.
- Van Allen, E. M., Miao, D., Schilling, B., Shukla, S. A., Blank, C., Zimmer, L., et al. (2015). Genomic correlates of response to CTLA-4 blockade in metastatic melanoma. *Science* 350, 207–211. doi: 10.1126/science.aad0095
- Wang, F., Wei, X. L., Wang, F. H., Xu, N., Shen, L., Dai, G. H., et al. (2019). Safety, efficacy and tumor mutational burden as a biomarker of overall survival

- benefit in chemo-refractory gastric cancer treated with toripalimab, a PD-1 antibody in phase Ib/II clinical trial NCT02915432. *Ann. Oncol.* 30, 1479–1486. doi: 10.1093/annonc/mdz197
- Wang, N., Liu, W., Zheng, Y., Wang, S., Yang, B., Li, M., et al. (2018). CXCL1 derived from tumor-associated macrophages promotes breast cancer metastasis via activating NF- κ B/SOX4 signaling. *Cell Death Dis.* 9:880.
- Wang, Y., Zou, Y., Zhang, Y., and Li, C. (2021). Developing a risk scoring system based on immune-related lncRNAs for patients with gastric cancer. *Biosci. Rep.* 41:BSR20202203.
- Xu, H., Wang, X., Wu, J., Ji, H., Chen, Z., Guo, H., et al. (2020). Long non-coding RNA LINC01094 promotes the development of clear cell renal cell carcinoma by upregulating SLC2A3 via microRNA-184. *Front. Genet.* 11:562967. doi: 10.3389/fgene.2020.562967
- Xu, J., Zhang, P., Sun, H., and Liu, Y. (2020). LINC01094/miR-577 axis regulates the progression of ovarian cancer. *J. Ovarian Res.* 13:122.
- Yu, J., Huang, C., Sun, Y., Su, X., Cao, H., Hu, J., et al. (2019). Effect of laparoscopic vs open distal gastrectomy on 3-year disease-free survival in patients with locally advanced gastric cancer: the CLASS-01 randomized clinical trial. *JAMA* 321, 1983–1992. doi: 10.1001/jama.2019.5359
- Zhang, B., Wu, Q., Li, B., Wang, D., Wang, L., and Zhou, Y. L. (2020). m(6)A regulator-mediated methylation modification patterns and tumor microenvironment infiltration characterization in gastric cancer. *Mol. Cancer* 19:53.
- Zhou, L., Chen, Z., Wu, Y., Lu, H., and Xin, L. (2021). Prognostic signature composed of transcription factors accurately predicts the prognosis of gastric cancer patients. *Cancer Cell Int.* 21:357.
- Zhu, B., Liu, W., Liu, H., Xu, Q., and Xu, W. (2020). LINC01094 down-regulates miR-330-3p and enhances the expression of MSI1 to promote the progression of glioma. *Cancer Manag. Res.* 12, 6511–6521. doi: 10.2147/cmar.s254630
- Conflict of Interest:** The authors declare that the research was conducted in the absence of any commercial or financial relationships that could be construed as a potential conflict of interest.
- Publisher's Note:** All claims expressed in this article are solely those of the authors and do not necessarily represent those of their affiliated organizations, or those of the publisher, the editors and the reviewers. Any product that may be evaluated in this article, or claim that may be made by its manufacturer, is not guaranteed or endorsed by the publisher.
- Copyright © 2021 Ding, Li, Han, Sun, Shen and Wu. This is an open-access article distributed under the terms of the Creative Commons Attribution License (CC BY). The use, distribution or reproduction in other forums is permitted, provided the original author(s) and the copyright owner(s) are credited and that the original publication in this journal is cited, in accordance with accepted academic practice. No use, distribution or reproduction is permitted which does not comply with these terms.



LncRNA GAPLINC Promotes Renal Cell Cancer Tumorigenesis by Targeting the miR-135b-5p/CSF1 Axis

Siyuan Wang, Xiaorong Yang, Wenjie Xie, Shengqiang Fu, Qiang Chen, Zhilong Li, Zhicheng Zhang, Ting Sun*, Binbin Gong* and Ming Ma*

Department of Urology, The First Affiliated Hospital of Nanchang University, Nanchang, China

OPEN ACCESS

Edited by:

Shiv K. Gupta,
Mayo Clinic, United States

Reviewed by:

Macrina Beatriz Silva Cázares,
Autonomous University of San Luis
Potosí, Mexico
Massimiliano Cadamuro,
University of Padua, Italy

*Correspondence:

Ting Sun
journal_123@163.com
Binbin Gong
15270993912@163.com
Ming Ma
303216740@qq.com

Specialty section:

This article was submitted to
Molecular and Cellular Oncology,
a section of the journal
Frontiers in Oncology

Received: 01 June 2021

Accepted: 27 September 2021

Published: 14 October 2021

Citation:

Wang S, Yang X, Xie W, Fu S,
Chen Q, Li Z, Zhang Z, Sun T,
Gong B and Ma M (2021) LncRNA
GAPLINC Promotes Renal Cell
Cancer Tumorigenesis by Targeting
the miR-135b-5p/CSF1 Axis.
Front. Oncol. 11:718532.
doi: 10.3389/fonc.2021.718532

Background: Long noncoding RNAs (lncRNAs) are closely related to the occurrence and development of cancer. Gastric adenocarcinoma-associated, positive CD44 regulator, long intergenic noncoding RNA (GAPLINC) is a recently identified lncRNA that can actively participate in the tumorigenesis of various cancers. Here, we investigated the functional roles and mechanism of GAPLINC in renal cell carcinoma (RCC) development.

Methods: Differentially expressed lncRNAs between RCC tissues and normal kidney tissues were detected by using a microarray technique. RNA sequencing was applied to explore the mRNA expression profile changes after GAPLINC silencing. After gain- and loss-of-function approaches were implemented, the effect of GAPLINC on RCC *in vitro* and *in vivo* was assessed by cell proliferation and migration assays. Moreover, rescue experiments and luciferase reporter assays were used to study the interactions between GAPLINC, miR-135b-5p and CSF1.

Results: GAPLINC was significantly upregulated in RCC tissues and cell lines and was associated with a poor prognosis in RCC patients. Knockdown of GAPLINC repressed RCC growth *in vitro* and *in vivo*, while overexpression of GAPLINC exhibited the opposite effect. Mechanistically, we found that GAPLINC upregulates oncogene CSF1 expression by acting as a sponge of miR-135b-5p.

Conclusion: Taken together, our results suggest that GAPLINC is a novel prognostic marker and molecular therapeutic target for RCC.

Keywords: long noncoding RNA, GAPLINC, miR-135b-5p, CSF1, renal cell carcinomas

BACKGROUND

With the expansion of routine imaging examinations of many diseases, an increasing number of patients with renal cell carcinoma (RCC) have been identified (1). Worldwide, RCC ranks sixth in terms of cancer incidence among men and tenth among women, accounting for 5% and 3% of all cancers, respectively (2). Approximately 17% of patients present with metastatic disease at diagnosis (3). Despite the development and wide application of drugs with different mechanisms of action,

metastatic renal cell carcinoma (mRCC) is still a highly lethal malignant tumor that presents great challenges (4). Therefore, it is of important clinical value to further explore the possible molecular mechanisms related to the occurrence and development of RCC.

Long noncoding RNAs (lncRNAs) have been identified as RNA molecules with a length of more than 200 bp that lack coding potential (5). In the past few years, the number of tumor-related lncRNAs has increased significantly, and lncRNAs may play a key role at the transcriptional, posttranscriptional or epigenetic level (6). MicroRNAs (miRNAs) are small noncoding regulatory RNAs with sizes of 17–25 nucleotides. After transcription, miRNAs suppress gene expression by identifying complementary target sites in the 3′ untranslated region (UTR) of the target mRNAs (7). MiRNAs are post-transcriptional regulators of gene expression and promising candidates for biomarker development. They play pivotal roles in a wide variety of biological processes, including cell proliferation, survival, differentiation, and tumorigenesis (8). Certain miRNA mimics and miRNA inhibitors have shown promise as novel therapeutic agents (9). Some lncRNAs have a common function; that is, they can act as miRNA decoys to regulate gene expression, which is called the competing endogenous RNA (ceRNA) hypothesis (10). CeRNA hypothesis proposes that the miRNAs can bind to mRNAs, resulting in inactivation for translation, unstable structure and rapid degradation of binded mRNAs. This network links the function of non-coding RNAs to the function of protein-encoding mRNAs (11). The role of ceRNAs in regulating tumor cell proliferation, migration, apoptosis, cell cycle, metastasis, angiogenesis and metabolism has been reported by many laboratories (12).

Gastric adenocarcinoma-associated, positive CD44 regulator, long intergenic noncoding RNA (GAPLINC), a new lncRNA, is abnormally highly expressed in many human tumors and participates in the regulation of malignant biological behavior of tumors (13). MiR-135b-5p can promote or inhibit tumor cell proliferation, migration, invasion and angiogenesis through a variety of biological pathways and can affect the survival and prognosis of tumor patients (14–16). However, the mechanisms of GAPLINC and miR-135b-5p in the occurrence and development of RCC have not been reported. CSF1 is a protein coding gene. The protein it encodes is a cytokine that controls the production, differentiation and function of macrophages (17). Studies have confirmed *in vitro* and *in vivo* that CSF-1 interacts with CSF-1R to promote the survival and proliferation of RCC and reduce apoptosis. Blocking CSF-1R with a CSF-1R tyrosine kinase inhibitor can reduce RCC proliferation and macrophage infiltration, which corresponds to a significant reduction in tumor volume (18–20).

In this study, we found that GAPLINC was highly expressed in RCC tissues and was associated with a poor prognosis. Mechanistic analysis showed that through competitive binding with miR-135b-5p, GAPLINC acts as a ceRNA and regulates the expression of CSF1, thus promoting the proliferation and migration of RCC cells. Overall, our research shows that GAPLINC is a carcinogenic regulatory factor in the occurrence

and development of RCC and has potential diagnostic and clinical application value as a therapeutic target.

MATERIALS AND METHODS

RNA Extraction and Transcriptome Data Analysis

Total RNA was extracted from three RCC tissues and three corresponding normal kidney tissues and from three GAPLINC-silenced A498 (renal cancer) cell lines and the corresponding negative control cells using TRIzol reagent (Transgen biotech, China), following the manufacturer's instructions and then sent to Biotechnology Co., Ltd. (Shanghai, China) and Novogene Co., Ltd. (Beijing, China) for Agilent microarray analysis and sequencing on an Illumina HiSeq 4000 platform. The expression of GAPLINC and CSF1 and patient survival were evaluated in 539 RCC patients and 72 normal controls from the TCGA database (<http://tcga-data.nci.nih.gov>) using the R programming language.

Cell Lines and Cell Culture

Human clear cell renal cell carcinoma (ccRCC) cell lines (A498, OSRC-2, ACHN, 786-O and Caki-1) and human renal tubular epithelial cells (HK-2) were purchased from the Chinese Academy of Sciences. OSRC-2 and 786-O cell lines were cultured in RPMI-1640 medium (Gibco, USA), while A498 and ACHN cells were cultured in MEM (Boster, China). The Caki-1 cell line was cultured in McCoy's 5A medium, and the HK-2 cell line was cultured in DMEM/F12 medium. The medium was supplemented with 10% fetal bovine serum (FBS), penicillin (100 U/mL) and streptomycin (100 µg/mL).

Real-Time Quantitative PCR

Total RNA was extracted with TRIzol. EasyScript cDNA Synthesis SuperMix (Transgen, China) was used to prepare cDNA. Real-time PCR was conducted in triplicate with TransStart Top Green qPCR SuperMix (+Dye II) (TransGen). **Supplementary Table 1** lists the primers used in this study. β -Actin and U6 were detected as internal controls. The relative amount of RNA was calculated by the $2^{-\Delta\Delta Ct}$ method.

Subcellular Fractionation

Cytoplasmic and nuclear extracts were prepared in accordance with the manufacturer's instructions using a cytoplasmic and nuclear RNA purification kit (Norgen, Canada).

Cell Transfection

SiRNAs and miRNA mimics and inhibitors were synthesized by RiboBio (Guangzhou, China). Cells were transfected with siRNA and miRNA mimics and inhibitors using Lipofectamine 2000 (Invitrogen) following the manufacturer's protocol. Lentiviruses expressing GAPLINC, sh-GAPLINC and negative control were purchased from HanBio (Shanghai, China). All stably transfected cells were selected with 2 µg/ml puromycin for 48 h.

Cell Proliferation Assay

The cells were harvested by trypsinization to obtain single-cell suspensions. Then, the cells were quantified by electronic counting (BioRad) and plated in 96-well plates at a density of $3-4 \times 10^3$ cells per well. After 24 h, 48 h, 72 h and 96 h of treatment, 10 μ l of Cell Counting Kit-8 (CCK-8) solution was added to each well, and the cells were further incubated for 2-4 h. The absorbance values of each sample were measured at 450 nm.

Wound Healing Assay

When cells in 6-well plates reached confluence, a 200 μ l pathogen-free tip was used to scratch the cells. Following washes with PBS, the cells were incubated in medium for 0 h and 24 h at 37°C. Photographs were taken 0 h and 24 h after the scratch, and ImageJ software was used to measure the wound healing capacity.

Transwell Assay

A total of $3-4 \times 10^4$ cells suspended in 200 μ l serum-free medium were seeded into the upper chamber of the Transwell (Corning). Medium containing 15-20% fetal bovine serum (600 μ l) was added to the lower chamber. After incubation for 24 h, cells on the lower side were fixed with 4% paraformaldehyde for 15 minutes and stained with crystal violet for 15 minutes. The numbers of stained cells in five random visual fields were counted under a microscope.

Western Blotting

Proteins were loaded onto 10% SDS-PAGE gels, separated electrophoretically and transferred to PVDF membranes. After blocking in 5% nonfat milk for 1-2 h at room temperature, the membranes were incubated with primary antibody (**Supplementary Table 2**) overnight at 4°C and subsequently incubated with horseradish peroxidase-conjugated secondary antibody. The Western blotting results were visualized using an enhance chemiluminescence (ECL) detection system and quantified by ImageJ software.

Luciferase Reporter Assay

Wild-type or mutant 3'-UTR segments of the GAPLINC and CSF1, which are related to the miR-135b-5p binding sites, were cloned downstream of the luciferase gene in pmiR-RB-REPORTTM (RiboBio, China) vector. HEK293T cells of logarithmic growth phase were inoculated in 96-well plates (1.0×10^4 cells/well), and incubated in incubator for 24 h. Then, cells were cotransfected with GAPLINC-WT/CSF1-WT or GAPLINC-MUT/CSF1-MUT and mimic NC and miR-135b-5p mimic using Lipofectamine 2000 (Invitrogen) according to the manufacturer's protocols. The transfection medium was replaced 6 h after transfection with fresh complete medium, and cells were collected 48 h later. Luciferase activity for each group was detected using a dual-luciferase reporter assay system (Promega, USA).

Tumor Xenograft Model

Four-week-old male BALB/c nude mice were purchased from Slake Jingda Laboratory Animal Company (Hunan, China). A498

cells (5×10^6) that had been lentivirally transduced with LV-sh-NC or LV-sh-GAPLINC were suspended in a 100- μ l mixture of equal volumes of PBS and Matrigel and injected into the flanks of mice. Tumor volume was measured every 7 days when the tumors were obvious and was calculated using the formula: volume = (length \times width²)/2 (mm³). Studies on animals were conducted with approval from the ethics committee of the First Affiliated Hospital of Nanchang University.

Immunohistochemistry (IHC)

The tissue samples were fixed in 10% formalin, dehydrated in ethanol, embedded in paraffin and sectioned. The slides were dewaxed, rehydrated, placed in sodium citrate, and microwaved for antigen retrieval. Blocking was performed with 1% BSA, and the sections were then incubated with primary antibodies (anti-Ki-67, anti-MMP-9 or anti-CSF1) at 4°C overnight. Each section was incubated with secondary antibody at 37°C for 1 h, stained with diaminobenzidine, and counterstained with hematoxylin. Images were captured using a Zeiss microscope and analyzed using ImageJ software.

Statistical Analyses

Data are presented as the mean \pm SD and were analyzed with GraphPad Prism 6 software. Comparisons between groups were performed using unpaired, two-tailed Student's t tests or the Mann-Whitney U test. Correlations between variables were assessed by the Spearman correlation test. A $p < 0.05$ indicated statistical significance.

RESULTS

GAPLINC Expression Is Upregulated in RCC and Associated With a Poor Prognosis

To explore the expression profiles of lncRNAs in RCC, high-throughput ceRNA microarray assays of 3 RCC tissues and matched normal kidney tissues were performed. Gene ontology (GO) and Kyoto Encyclopedia of Genes and Genomes (KEGG) analyses demonstrated that the differentially expressed lncRNAs were mainly involved in the immune response and cancer-related biological processes (**Figures 1A, B**). The variation in lncRNA expression was revealed in the volcano plot (**Figure 1C**). We used the more stringent criteria ($p < 0.02$, fold change > 5) to capture the top 20 upregulated potential candidate genes (**Figure 1D**). Then, GAPLINC, which has not been studied in RCC and is highly expressed in RCC tissues and cell lines, was selected as our study object. The lncRNA expression of GAPLINC in 539 RCC tumor tissues and 72 nontumor tissues was analyzed based on the TCGA database (**Figure 1E**). RT-qPCR was used to detect the GAPLINC expression levels in the cells, and the results showed that the expression of GAPLINC was higher in tumor cells than in normal cells (**Figure 1F**). Kaplan-Meier survival analysis was used to assess the relationship between GAPLINC expression and patient survival (disease-specific survival: DSS, progression-free interval: PFI,

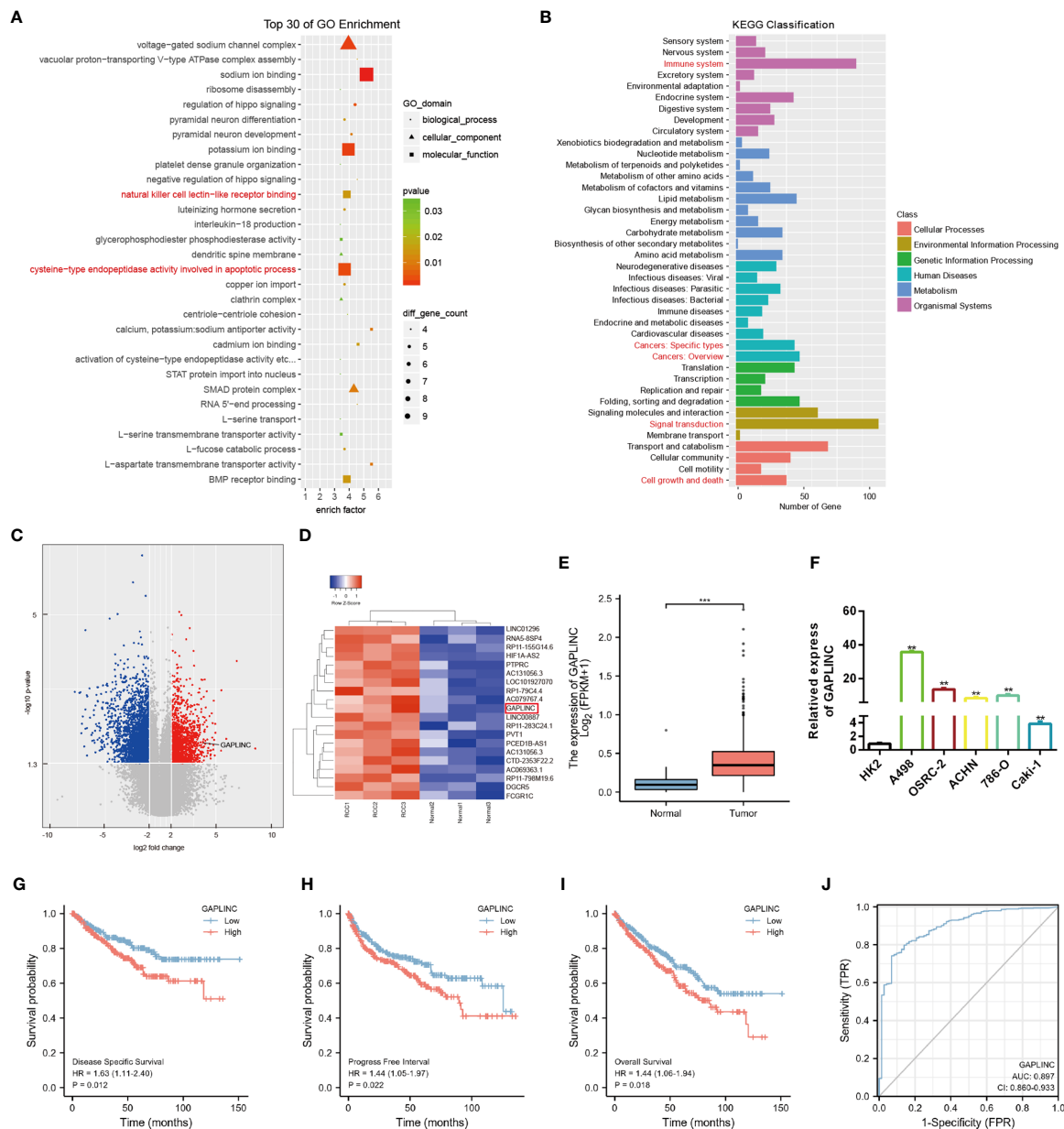


FIGURE 1 | GAPLINC expression is upregulated in RCC and associated with a poor prognosis. **(A)** Top 30 enriched GO terms of the differentially expressed lncRNAs. **(B)** KEGG pathway enrichment analysis of differentially expressed genes. **(C)** The volcano plot shows the expression profiles of lncRNAs. **(D)** Heatmap of the top 20 lncRNAs by expression that are differentially expressed. Red represents high expression, and green represents low expression. **(E)** GAPLINC expression levels in whole tumor tissues and normal tissues in TCGA cohorts. **(F)** RT-qPCR analysis of GAPLINC expression in a human normal renal epithelial cell line (HK-2) and four human RCC cell lines (A498, OSRC-2, ACHN, 786-O, Caki-1). Kaplan-Meier survival analysis according to GAPLINC expression showing the DSS **(G)**, PFI **(H)** and OS **(I)** of RCC patients from the TCGA database. **(J)** ROC curve analysis of the sensitivity and specificity of GAPLINC. ** $p < 0.01$; *** $p < 0.001$.

and overall survival: OS). Survival analysis showed that high expression of GAPLINC predicted poor DSS, a short PFI and poor OS (**Figures 1G–I**). Receiver operating characteristic (ROC) analysis demonstrated that GAPLINC exhibited satisfactory value in RCC diagnosis (AUC = 0.897, 95% CI: 0.860–0.933) (**Figure 1J**). Taken together, these results indicate that GAPLINC is upregulated in RCC and associated with a poor prognosis.

GAPLINC Promotes RCC Cell Proliferation and Migration *In Vitro*

RCC cell lines (A498 and OSRC-2) displayed markedly higher GAPLINC expression levels than the kidney normal cell line (HK-2) (**Figure 1D**). Thus, these two cell lines were selected for subsequent functional analyses. To further investigate the effect of GAPLINC on cell proliferation, GAPLINC knockdown or

overexpression was carried out. We downregulated the expression of GAPLINC in A498 and OSRC-2 cells using small interfering RNA (siRNA). Stable overexpression of GAPLINC was achieved by lentivirus transduction. GAPLINC knockdown and overexpression were confirmed by RT-PCR. As shown in **Figures 2A, B**, the expression levels of GAPLINC were significantly downregulated after transfection with GAPLINC siRNAs (si-1, si-2, and si-3) compared with negative control siRNA (si-NC). In contrast, compared with control vector (OE-NC) transfection, transfection of the GAPLINC overexpression vector (OE) significantly upregulated GAPLINC levels in A498 and OSRC-2 cells (**Figures 2C, D**).

We assessed the effects of GAPLINC on cell proliferation using the CCK-8 assay. The results revealed that GAPLINC knockdown remarkably inhibited cell proliferation at 72 h and 96 h compared with that in the si-NC transfection group (**Figures 2E, F**). Cell proliferation was increased in the GAPLINC OE group compared to the OE-NC group at 72 h and 96 h ($p < 0.05$) (**Figures 2G, H**). Cell migration was assessed *via* scratch wound healing and Transwell assays. The results indicated that knockdown of GAPLINC inhibited cell migration and that overexpression of GAPLINC promoted the migration of RCC cells (**Figures 2I–N**).

GAPLINC Facilitates RCC Progression by Enhancing CSF1 Expression

To elucidate the potential molecular mechanisms through which GAPLINC contributes to the progression of RCC, we explored the gene expression profiles under GAPLINC silencing conditions. The top 20 genes with the greatest differential expression in GAPLINC-silenced versus control A498 cells were clustered in a heat map plot, and we found that there were many more downregulated genes than upregulated genes (**Figure 3A**). DO and KEGG enrichment analyses of downregulated genes was performed to identify the main biological processes (**Figures 3B, C**). The results suggested the significant involvement of these genes in the development of RCC. According to ChIPBase v2.0 (<http://rna.sysu.edu.cn/chipbase/>) coexpression analysis and Pearson's correlation coefficient analysis, there was a positive correlation between CSF1 expression and GAPLINC expression in 603 RCC samples ($r=0.3171$, $P<0.001$) (**Figure 3D**). We also confirmed that the expression of CSF1 was higher in RCC cells than in HK-2 cells, and with GAPLINC knockdown and overexpression, CSF1 expression also changed at the transcriptional and protein levels (**Figures 3E–K**). Additionally, TCGA database analysis showed that the expression of CSF1 was upregulated in RCC and that CSF1 expression was higher in more advanced RCC tumor stages (**Figures 3L, M**). In addition, OS analysis revealed that high CSF1 expression was associated with a poor prognosis, and the area under the curve (AUC) value was suggestive of modest diagnostic value in RCC (**Figures 3N, O**). Previous studies showed that CSF1 could act as a promoting regulator in variety of cancers, including RCC (18, 21, 22). Moreover, blocking CSF1 signaling with a CSF1 receptor inhibitor (PLX-3397) has also been shown to suppress tumor progression (23). Our Scratch wound healing experiments and Transwell migration assays indicated that PLX-3397 attenuated the

stimulative effects of GAPLINC on RCC cell migration (**Figures 3P–S**). CCK-8 assays showed that PLX-3397 attenuated the promoting effect of GAPLINC on RCC cell proliferation (**Figures 3T, U**). These results demonstrate that CSF1 is a major candidate target of GAPLINC and that CSF1 plays a major role in mediating the effect of GAPLINC on RCC.

MiR-135b-5p Inhibits RCC Cell Proliferation and Migration *In Vitro* via CSF1

The lncRNA-miRNA-mRNA regulatory network, which involves many ceRNAs, has been shown to play a key role in a variety of cancers. Luo et al. predicted the top ten miRNA target sites around the GAPLINC region (24). We also used the TargetScan platform to predict the top ten miRNAs that may target CSF1. Finally, we took the intersection of the results obtained from the two databases and identified miR-135b-5p as a common result (**Figure 4A**). Many studies have shown that only lncRNAs located in the cytoplasm can act as molecular sponges to adsorb miRNAs. As shown in **Figures 4B, C**, the subcellular fractionation assays clarified that GAPLINC was mainly located in the cytoplasm. We then detected miR-135b-5p expression in A498 and OSRC-2 cells by RT-qPCR, and the results showed that the expression of miR-135b-5p was downregulated in these cells versus HK-2 cells (**Figure 4D**). Moreover, TCGA database analysis showed that miR-135b-5p expression was decreased in non-paired RCC samples (**Figure 4E**) and paired RCC samples (**Figure 4F**) compared with normal tissue samples. To explore the function of miR-135b-5p in RCC, we separately transfected A498 and OSRC-2 cells with miR-135b-5p inhibitor or inhibitor NC and miR-135b-5p mimic or mimic NC. The transfection efficiency of the miR-135b-5p inhibitor and mimic was determined by RT-qPCR (**Figures 4G, H**). Scratch and Transwell chamber assay results showed that the miR-135b-5p inhibitor promoted the migration of RCC cells, while the miR-135b-5p mimic suppressed their migration (**Figures 4I–N**). Additionally, the CCK-8 assay demonstrated that the miR-135b-5p inhibitor increased the proliferation of RCC cells, whereas the miR-135b-5p mimic exhibited the opposite effects (**Figures 4O–R**). Moreover, as shown in **Figure 4S**, the miR-135b-5p inhibitor increased the level of CSF1 mRNA, whereas the miR-135b-5p mimic decreased the level of CSF1 mRNA. These results were also verified by Western blotting at the protein level, as shown in **Figure 4T**. Subsequently, scratch wound healing experiments (**Figure 4U**) and Transwell migration assays (**Figure 4V**) demonstrated that PLX-3397 attenuated the effect of miR-135b-5p inhibitors on the migration of RCC cells. Similarly, the CCK-8 assay (**Figures 4W, X**) detected that PLX-3397 could partially reverse the effect of miR-135b-5p on the proliferation of RCC cells. Overall, these results indicate that miR-135b-5p inhibits the migration and proliferation of RCC cells *in vitro* via CSF1.

GAPLINC Promotes Tumor Progression in RCC *via* the miR-135b-5p/CSF1 Axis

Numerous studies have shown that cytoplasmic lncRNAs can act as effective miRNA sponges, as they contain conserved miRNA target sites, competitively inhibiting miRNAs to regulate

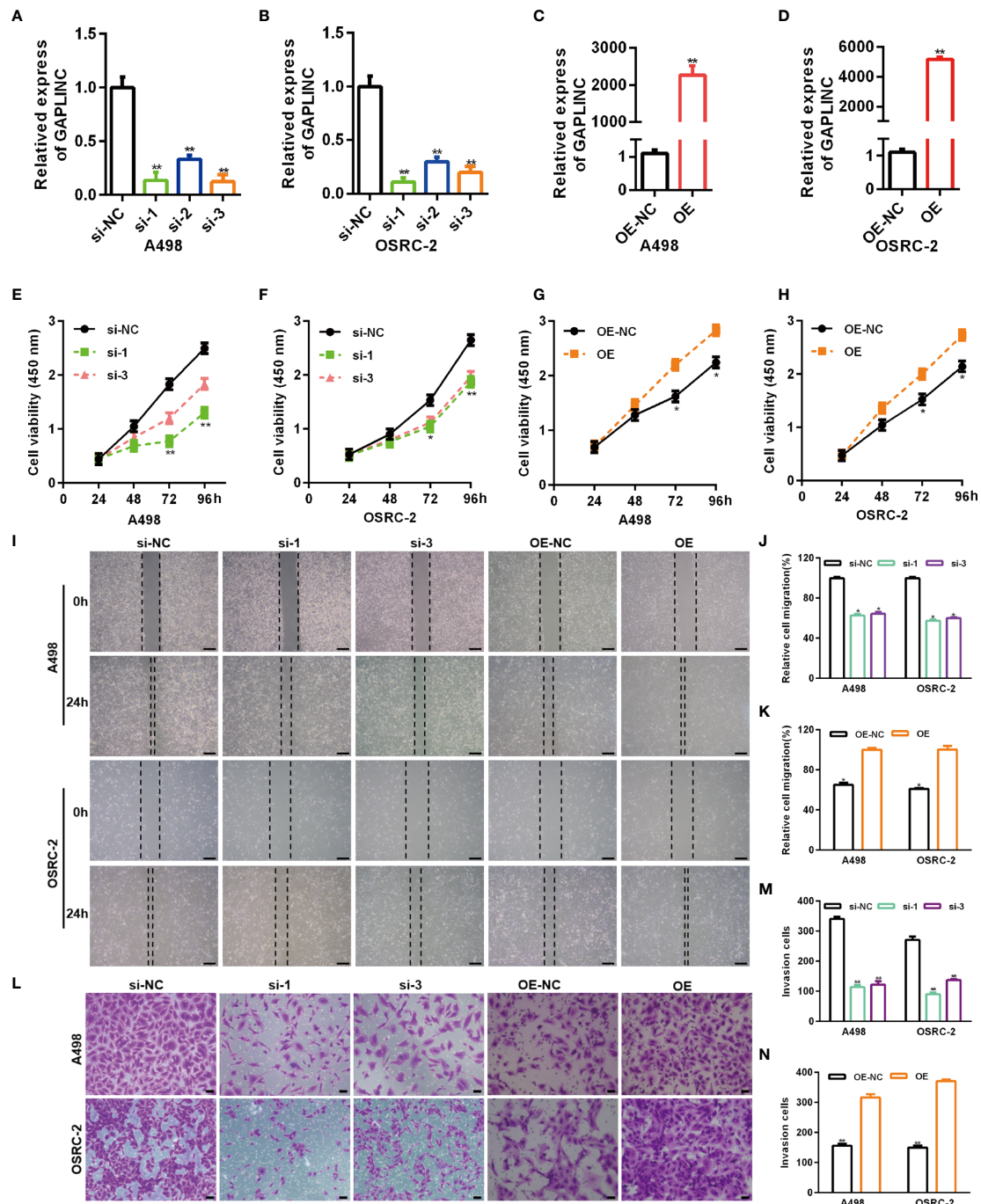


FIGURE 2 | GAPLINC promotes RCC cell proliferation and migration *in vitro*. Validation of the GAPLINC knockdown (A, B) and overexpression (C, D) efficacy in RCC cell lines by RT-qPCR. (E–H) CCK-8 assays in A498 and OSRC-2 cells with silenced or overexpressed GAPLINC. (I–K) Wound healing assay of cells after silencing or overexpressing GAPLINC expression. Scale bars, 200 μ m. (L–N) Transwell migration assays were performed to detect the migration ability when GAPLINC was knocked down or overexpressed. Scale bars, 50 μ m. * $p < 0.05$; ** $p < 0.01$.

downstream target gene expression at the posttranscriptional level. The online miRNA databases RNAhybrid and TargetScan were used to reveal potential binding sites between miR-135b-5p and GAPLINC and between miR-135b-5p and CSF1, respectively. Then, we performed a dual-luciferase reporter

assay to verify their paired binding. Then, to verify this, the sequences of GAPLINC-Wt, GAPLINC-Mut, CSF1-Wt or CSF1-Mut were inserted into the luciferase reporter plasmid (Figures 5A, C). Then, Wt and Mut reporter constructs were cotransfected into HEK 293 cells with miR-135b-5p mimic or

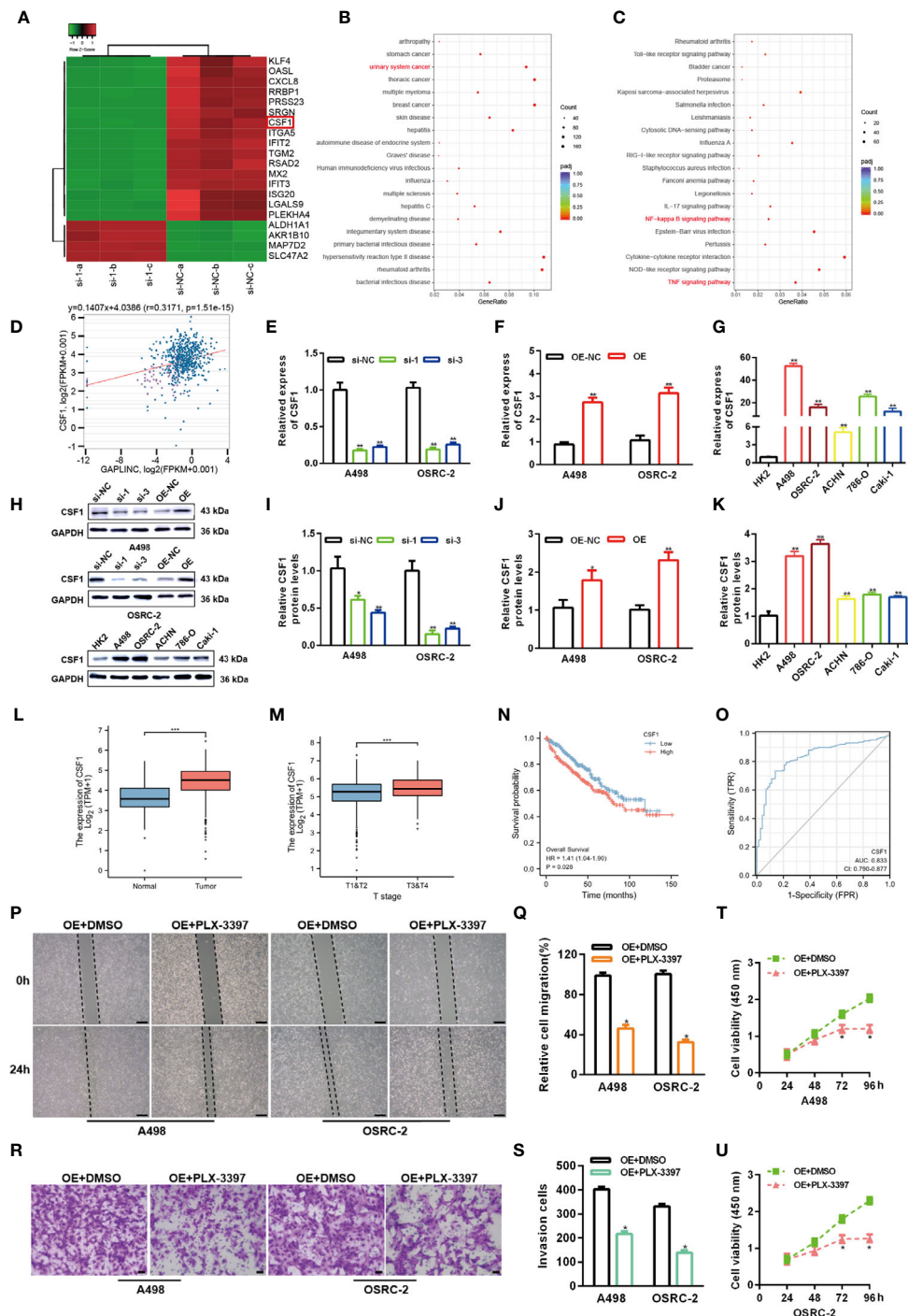


FIGURE 3 | GAPLINC facilitates RCC progression by enhancing CSF1 expression. **(A)** Heat map showing the top 20 transcripts that are altered in A498 cells following GAPLINC silencing. **(B)** DO and **(C)** KEGG enrichment analysis of the differentially expressed genes upon GAPLINC knockdown. **(D)** Pearson correlation analysis between GAPLINC levels and CSF1 levels in RCC tissues according to an online database (<http://ma.sysu.edu.cn/chipbase/>). CSF1 expression by RT-qPCR after silencing **(E)** or overexpressing **(F)** GAPLINC in A498 and OSRC-2 cells. **(G)** Expression level of CSF1 mRNA in HK-2 and RCC cells measured by RT-qPCR. **(H-K)** Western blotting analysis of the expression of CSF1 protein after silencing or overexpression of GAPLINC and the expression of CSF1 protein in HK-2 and RCC cells. **(L)** TCGA cohort analysis of CSF1 expression levels in RCC samples and adjacent normal tissues. **(M)** CSF1 expression levels in patients with different tumor stages of RCC (TCGA). **(N)** Kaplan-Meier OS curves according to CSF1 expression level. **(O)** The sensitivity and specificity of CSF1 were assessed using ROC curve analysis. Effects of the CSF1 inhibitor PLC-3397 on the migration and proliferation of GAPLINC-overexpressing RCC cells according to wound closure **(P, Q)** (scale bars = 200 μ m), Transwell **(R, S)** (scale bars = 50 μ m) and CCK-8 assays **(T, U)**. * $p < 0.05$; ** $p < 0.01$; *** $p < 0.001$.

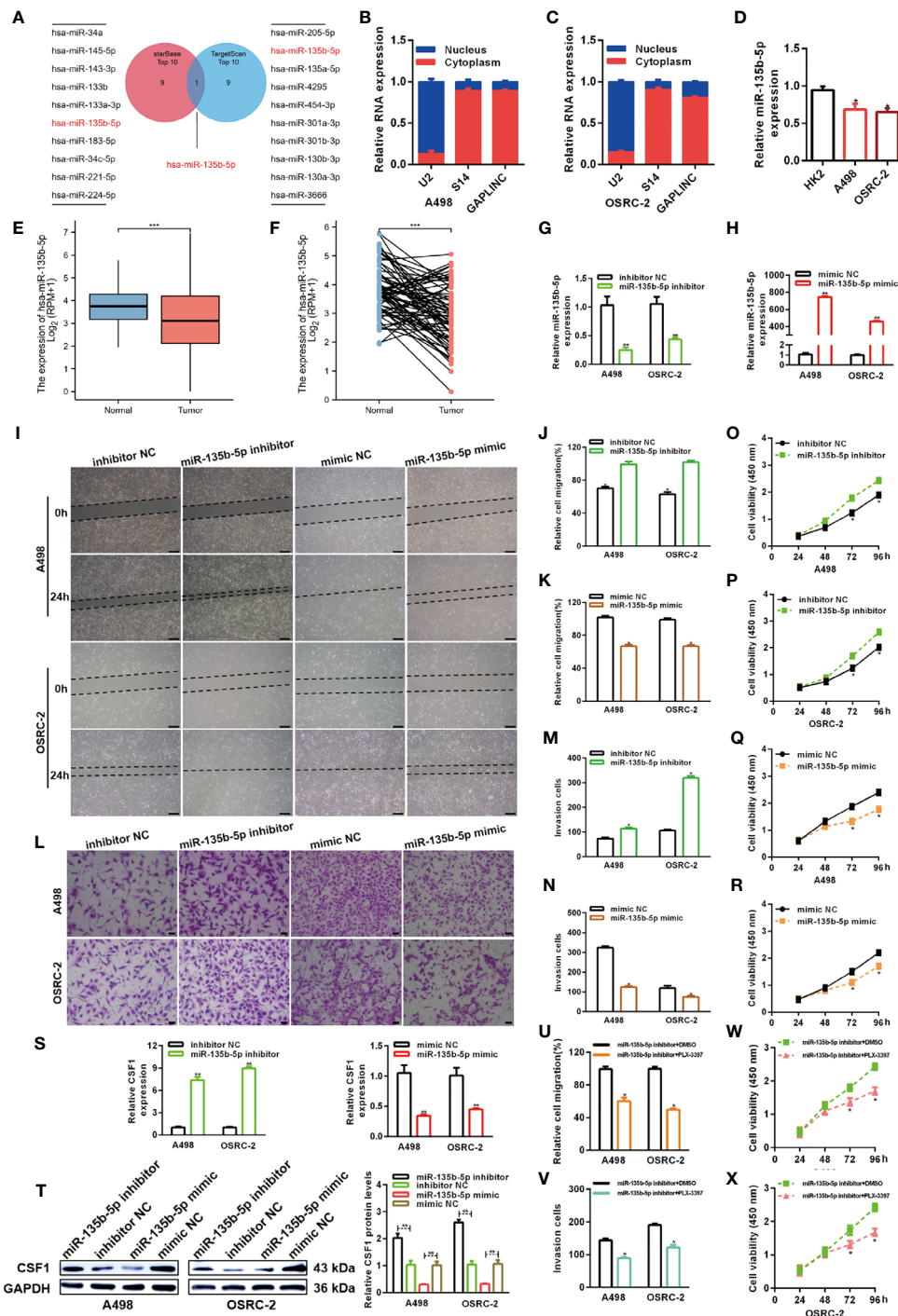


FIGURE 4 | MiR-135b-5p inhibits RCC cell proliferation and migration *in vitro*. **(A)** Schematic showing overlapping miRNAs predicted by the starBase and TargetScan databases to target GAPLINC and CSF1. **(B, C)** Relative level of GAPLINC in the nuclear and cytoplasmic fractions of A498 and OSRC-2 cells. **(D)** Relative expression of miR-135b-5p in A498 and OSRC-2 cells detected using RT-qPCR. TCGA analysis of the expression levels of GAPLINC in paired **(E)** and unpaired **(F)** RCC tissues. MiR-135b-5p expression levels following transfection of A498 and OSRC-2 cells with miRNA inhibitors **(G)** or miRNA mimics **(H)**. The migration capacities were measured by wound closure **(I–K)** (scale bars = 200 μ m) and transwell **(L–N)** (scale bars = 50 μ m) assays after the cells were transfected with miR-135b-5p inhibitors or mimics. The effect of miR-135b-5p inhibitors **(O, P)** or mimics **(Q, R)** on A498 and OSRC-2 cell proliferation was detected by CCK-8 assay. **(S)** RT-qPCR was performed to detect CSF1 expression after transfection with miR-135b-5p inhibitors and mimics. **(T)** The protein expression level of CSF1 was detected using Western blotting following RCC cell transfection with miR-135b-5p inhibitors or mimics. The effect of PLX-3379 on the migration and proliferation of RCC cells transfected with miR-135b-5p inhibitor was detected by wound closure **(U)**, Transwell **(V)** and CCK-8 **(W, X)** assays. * $p < 0.05$; ** $p < 0.01$; *** $p < 0.001$.

mimic NC as indicated. The results showed that only the miR-135b-5p mimic effectively inhibited the luciferase activity of the Wt group compared with the other groups (**Figures 5B, D**). In addition, RT-qPCR experiments revealed that knockdown of GAPLINC promoted the expression of miR-135b-5p, whereas GAPLINC overexpression decreased miR-135b-5p expression (**Figures 5E, F**). These results show that GAPLINC can bind to miR-135b-5p and that there is a direct relationship between miR-135b-5p and CSF1. Next, we performed miR-135b-5p inhibitor or inhibitor NC and GAPLINC si-1 cotransfection and miR-135b-5p mimic or mimic NC cotransfection with the GAPLINC OE vector, to study whether the effect of GAPLINC on CSF1 expression is dependent on miR-135b-5p. Cotransfection of miR-135b-5p inhibitor and si-1 led to a decrease in miR-135b-5p expression compared with that in the inhibitor NC + si-1 group. In addition, the expression of miR-135b-3p was increased in the OE vector + miR-135b-5p mimic group compared with the OE + mimic NC group (**Figures 5G, H**). We quantitatively detected the effect of cotransfection on the expression of CSF1 at the protein expression and transcriptional levels. The results showed that cotransfection with the miR-135b-5p inhibitor reversed the downregulation of CSF1 mRNA and protein expression mediated by si-1. However, cotransfection with the miR-135b-5p mimic reversed the upregulation of CSF1 mRNA and protein expression mediated by the OE vector (**Figures 5I–L**). To further explore the functional significance of the miR-135b-5p/CSF1 axis in the protumor role of GAPLINC in RCC, we conducted rescue experiments. We observed that the miR-135b-5p inhibitor attenuated the decreases in the migration and proliferation of cells induced by GAPLINC knockdown. In contrast, the miR-135b-5p mimic weakened the promoting effect of GAPLINC overexpression on the migration and proliferation of A498 and OSRC-2 cells (**Figures 5M–V**). All these data demonstrate that GAPLINC promotes the proliferation and migration of RCC cells *in vitro*, partly by sponging miR-135b-5p, thereby regulating CSF1 levels.

Knockdown of GAPLINC Inhibits the Tumorigenicity of RCC *In Vivo*

To further evaluate the functional role of GAPLINC in the growth of RCC tumors *in vivo*, A498 cells stably transduced with LV-sh-NC or LV-sh-GAPLINC were subcutaneously inoculated into nude mice. The scheme of the experimental procedure is outlined in **Figure 6A**. As shown in **Figures 6B, C**, we examined orthotopic tumors under the skin and tumors resected from nude mice. According to the analysis of tumor volume over time, we observed that from the second week, the tumor volume was effectively lower in the LV-sh-GAPLINC group than in the LV-sh-NC group (**Figure 6D**). At 10 weeks after tumor implantation, GAPLINC knockdown had dramatically reduced the tumor volume and the tumor weight compared with that in the control group (**Figures 6E, F**). Then, RT-qPCR was performed to measure the expression levels of GAPLINC, miR-135b-5p and CSF1 in tumor tissue specimens from engrafted nude mice. The results showed that GAPLINC

and CSF1 mRNA levels in the LV-sh-GAPLINC group were lower than those in the LV-sh-NC group (**Figures 6G, I**). However, the miRNA level displayed the opposite trend (**Figure 6H**). Hematoxylin and eosin (H&E) staining and immunohistochemistry staining analysis of CSF1, Ki-67 and MMP-9 expression in tumors from xenograft mice of the two groups. The results confirmed that the expression of Ki-67, MMP-9 and CSF1 was decreased in tumors upon GAPLINC downregulation (**Figures 6J, K**). The above results indicate that GAPLINC can also promote the proliferation and migration of RCC *in vivo*, which is consistent with our *in vitro* results.

DISCUSSION

Renal cell tumors are a group of histopathologically and molecularly heterogeneous tumors with different genetic and epigenetic abnormalities (25, 26). With the development of sequencing technology, it is possible to detect hundreds of molecular biomarkers in clinical samples. Therefore, further research on molecular biomarkers in RCC is needed to facilitate diagnose and prognostic risk stratification and to identify potential treatment targets for patients with advanced disease (27). The study of the molecular pathogenesis of RCC is used to determine the target of treatment intervention to guide the choice of treatment for each patient in a personalized approach. This has led to the development of a variety of drugs that play an important role in the management of mRCC. Drugs targeting the vascular endothelial growth factor (VEGF) pathway and drugs inhibiting the mammalian target of rapamycin (mTOR) protein have been used in the treatment of mRCC. In addition, the recent emergence of immune checkpoint inhibitors has led to significant changes in mRCC treatment. The PD-1 inhibitor nivolumab has been shown to improve the OS of mRCC patients after VEGF inhibitor treatment (28). As these types of sequencing-based assays are incorporated into routine clinical care, they have the potential to fundamentally change the way we manage renal cell carcinoma (29).

From the perspective of genome and transcriptome expansion, our catalog of genetic elements is now full of lncRNAs. It is estimated that the number of human lncRNAs exceeds the number of protein-coding genes (30). The functions of most lncRNAs are not clear, and many lncRNAs may not have obvious functions, but the functions and mechanisms of some classically defined lncRNAs, such as XIST and HOTAIR, are already clear (31). LncRNAs have been discovered to function as scaffolds, decoys or signals that can function through genomic targeting, cis or trans regulation and antisense interference (32). Like proteins, lncRNAs must be located in a specific subcellular compartment to perform their functions. For example, the lncRNA NKILA, a cytoplasmic lncRNA, can interfere with protein posttranslational modification, resulting in abnormal signal transduction (33). In addition, cytoplasmic lncRNAs such as linc-MD1 (34) and lncRNA NORAD (35) can affect gene regulation by acting as decoys for miRNAs and proteins. Quantitative analysis of the abundance of miRNAs and target

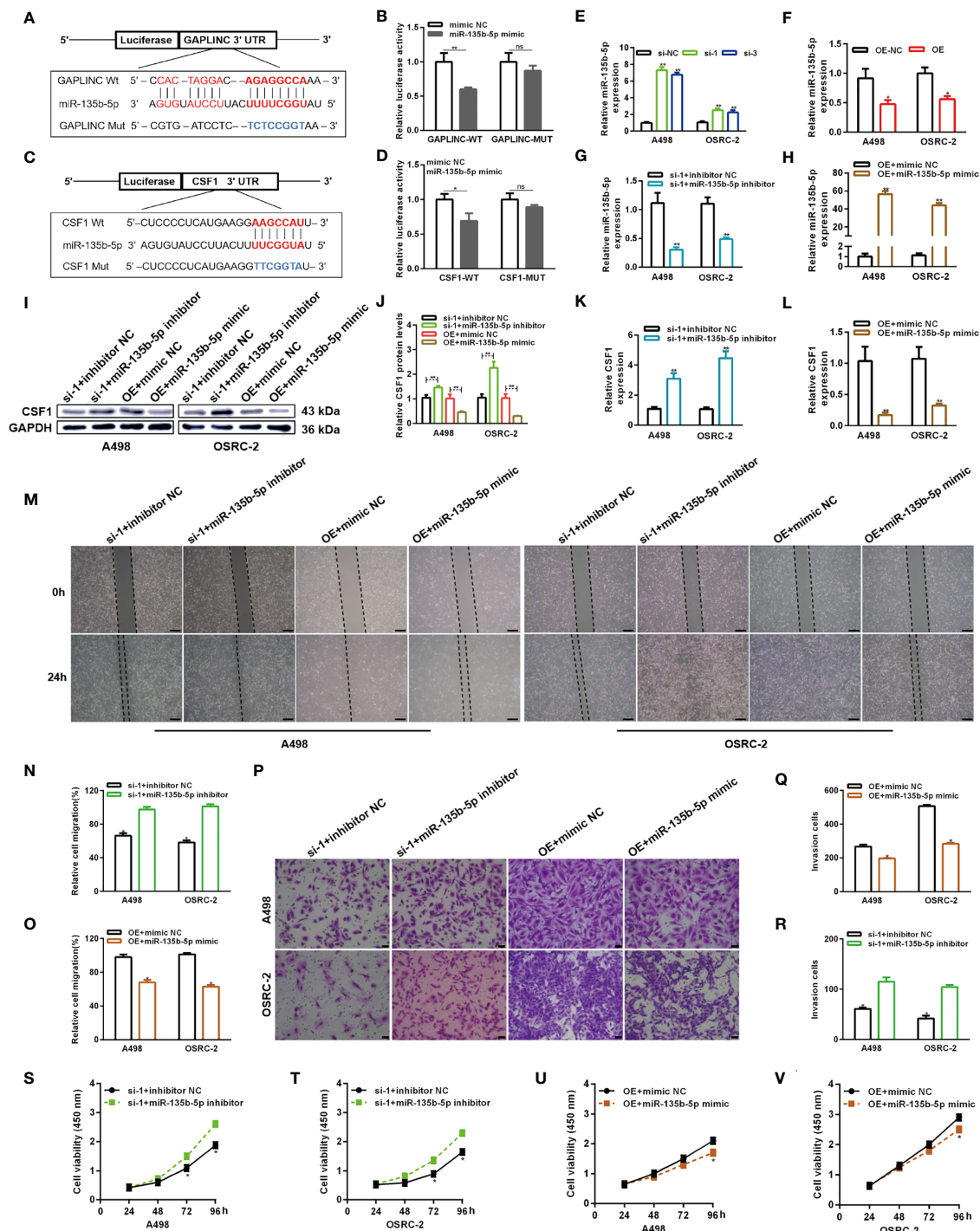


FIGURE 5 | GAPLINC promotes RCC tumor progression via the miR-135b-5p/CSF1 axis. (A–D) Luciferase reporter assay of A498 cells cotransfected with miR-135b-5p mimics and luciferase reporters containing the wild-type or mutant 3' UTRs of GAPLINC or CSF1. (E, F) MiR-135b-5p expression after silencing or overexpressing GAPLINC in A498 and OSRC-2 cells by RT-qPCR. (G, H) The relative expression of miR-135b-5p in RCC cells transfected with si-1/OE vector alone or cotransfected with miR-135b-5p inhibitors/mimics. Western blot (I, J) and RT-qPCR (K, L) analysis of CSF1 protein and mRNA expression levels after cotransfection with si-1+miR-135b-5p inhibitor or OE vector+135b-5p mimic. Wound healing (M–O) (scale bars = 200 μ m) and Transwell (P–R) (scale bars = 50 μ m) assays were employed to investigate the migratory capacity of si-1+miR-135b-5p inhibitor- or OE vector+135b-5p mimic-cotransfected RCC cells. The proliferation ability of RCC cells cotransfected with si-1+miR-135b-5p inhibitor (S, T) or OE vector+135b-5p mimic (U, V) was determined by CCK-8 assays. * $p < 0.05$; ** $p < 0.01$; ns, no significance.

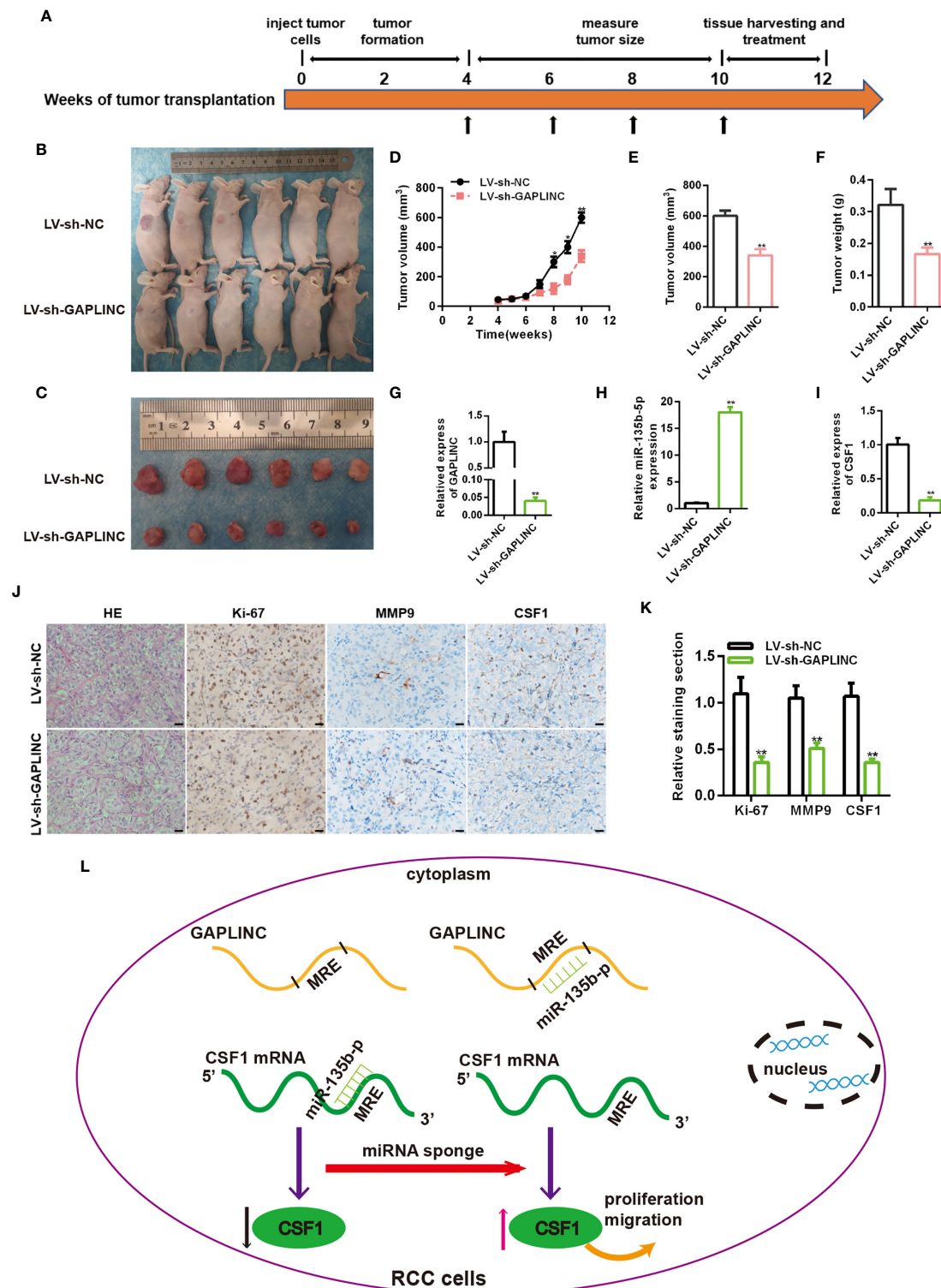


FIGURE 6 | Knockdown of GAPLINC inhibits the tumorigenicity of RCC *in vivo*. **(A)** Schematic representation of the nude mouse xenograft tumor experimental protocol. **(B, C)** Photographs of tumors obtained from the LV-sh-NC and LV-sh-GAPLINC groups of nude mice. The tumor volumes were measured once a week after tumor formation **(D)**, and the tumor nodules were removed 10 weeks after transplantation, after which the final volumes **(E)** and weights **(F)** were measured. Xenograft tissues were subjected to RT-qPCR to assess GAPLINC **(G)**, miR-135b-5p **(H)** and CSF1 **(I)** expression. **(J, K)** Representative images showing H&E, Ki-67, MMP-9 and CSF1 staining of xenograft tumor tissues; the histogram shows the statistical analysis of their expression levels. Scale bars, 20 μ m. **(L)** Schematic representation of the mechanism of GAPLINC in RCC cells. * $p < 0.05$; ** $p < 0.01$.

mRNAs shows that the ceRNA mechanism of cytoplasmic lncRNAs can work only when there is proper stoichiometry between lncRNAs and miRNAs. Therefore, in addition to matching miRNA seed sequences, experimental analysis and knockout studies are needed to verify the ceRNA mechanism (36).

Evidence suggests that lncRNAs may be involved in almost all human cancers and may play a role in stem cell maintenance, cell proliferation, apoptosis, cell invasion and metastasis (37, 38). The latest progress in the study of the molecular mechanism of lncRNAs provides a tool for the functional annotation of these cancer-related transcripts, making these molecules an attractive target for cancer therapy and intervention (39). As many as 35000 different lncRNAs have been found in RCC. However, only hundreds to thousands of these lncRNAs exhibit differential expressions in RCC tissues and normal renal tissues (40). Malouf et al. identified 1934 abnormally expressed lncRNAs in RCC and established the first genome-wide classification of RCC-related lncRNAs, revealing their correlation with clinicopathology and genomic characteristics (41). Because lncRNAs have tissue-specific expression compared with mRNAs, the interaction between lncRNAs and their binding proteins or miRNAs can be blocked by antisense oligodeoxynucleotides and small molecular compounds, and abnormally expressed lncRNAs can be targeted to treat RCC (42).

Hu et al. reported in 2014 that a new lncRNA located on human chromosome 18p11.31 was found in gastric cancer and affects the proliferation and migration of gastric cancer cells by sponging miR-211-3p to regulate the expression of CD44; this lncRNA was named GAPLINC (43). Subsequently, GAPLINC was found to be highly expressed in hepatocellular carcinoma (44) and non-small-cell lung cancer (45) and was found to promote cancer through different mechanisms. Vollmers et al. found that GAPLINC knockout mice showed resistance to endotoxic shock induced by lipopolysaccharide (46). At the same time, Mo and other studies have shown that GAPLINC can promote the tumor-like biological behavior of fibroblast-like synoviocytes in patients with rheumatoid arthritis through a ceRNA mechanism (47). As a member of the miRNA family, miR-135b-5p plays a role in a variety of cancers. Studies have shown that miR-135b-5p is upregulated or downregulated in cancer tissues and plays a role in promoting or inhibiting cancer through a variety of mechanisms (14, 48–50). Similarly, miR-135b-5p can also lead to neuronal damage after stroke (51) and contributes to rheumatoid arthritis (52) by participating in the inflammatory response. The present study reported for the first time that GAPLINC was upregulated in RCC tissues and was associated with a poor prognosis. The relationship between the expression levels of GAPLINC and miR-135b-5p was proven by RT-qPCR. GAPLINC silencing led to increased miR-135b-5p expression in RCC cells. However, overexpression of GAPLINC gave the opposite result. Cell experiments *in vitro* confirmed that GAPLINC promotes the proliferation and migration of RCC cells, while miR-135b-5p does the opposite. Animal experiments also show that GAPLINC promotes the proliferation of RCC and makes Ki-67 highly expressed. We further discovered that the protein levels of MMP9 were decreased after GAPLINC knockdown in the tumor tissues of

nude mice. It indicates that GAPLINC promotes cell migration in animal models, which may be related to the high expression of MMP9, which plays an important role in extracellular matrix remodeling and membrane protein cleavage.

The tumor microenvironment (TME) is made up of noncancer cells in the tumor, including fibroblasts, immune cells, cells that make up blood vessels and proteins produced by cells that support the growth of cancer cells (53). Cancers develop in complex tissue environments in which they can continue to grow, invade and metastasize. Unlike tumor cells, the stromal cells in the TME are genetically stable, so they provide attractive therapeutic targets for reducing drug resistance and the risk of tumor recurrence (54). Macrophages are the most abundant cells in the tumor stroma and have obvious plasticity, so they can play a variety of roles in the TME. Tumor-associated macrophages (TAMs) usually refer to M2 macrophages, which have anti-inflammatory and protumor effects. M2 macrophages can also neutralize inflammation-promoting effects and the antitumor M1 phenotype. The shift of macrophages to the anti-inflammatory M1 phenotype can be used as an adjuvant approach with other methods including radiotherapy and immune checkpoint blockade, such as anti-PD-L1/PD-1 strategies (55).

Evidence suggests that noncoding RNAs (ncRNAs) can guide the development of a variety of immune cells and control dynamic transcriptional procedures (56). Linear ncRNAs, such as lncRNAs and miRNAs, have been found to play an important role in the regulation of tumor immunity and immunotherapy (57). As the core of a wide range of regulatory elements that control the inflammatory response circuit, lncRNA-Cox2 mediates the activation and inhibition of different kinds of immune genes (58). Li et al. showed that miR-146a can promote the growth of subcutaneous breast tumors in mice by promoting M2 polarization or regulating the recruitment of TAMs (59). RCC is an effective immunotherapy disease, and it is worthwhile to study whether lncRNAs can regulate the immune pathway of RCC (60). Because linear ncRNA has its own function in regulating the response to different immunotherapies, the use of ncRNA as an adjuvant for immunotherapy has great potential (61).

Macrophage colony stimulating factor (CSF-1) is a hematopoietic growth factor that is related to the survival, proliferation and differentiation of macrophages, monocytes and bone marrow progenitor cells. After CSF-1 treatment, macrophages polarize to the M2 phenotype (62). Pyonteck et al. used CSF-1R inhibitors to target TAMs in mouse glioma models. The results showed that the inhibitor slowed down the intracranial growth of patient-derived glioma xenografts and significantly increased the survival time (63). CSF-1 has been shown to interact with CSF-1R to promote the survival and proliferation of RCC cells and reduce apoptosis. *In vivo*, the use of a CSF-1R tyrosine kinase inhibitor to block CSF-1R reduced RCC proliferation and macrophage infiltration, which was related to a significant reduction in tumor volume (18). PLX-3397 (pexidartinib) is an oral, effective, CSF-1R inhibitor that has entered the stage of clinical development. The clinical efficacy of it as a single treatment or adjuvant therapy is being evaluated (23). In this study, we observed that CSF1 is a target protein of the GAPLINC/miR-135b-5p axis. Through dual-

luciferase reporter gene analysis, it was proven that CSF1 is a direct target gene of miR-135b-5p. In addition, we showed that overexpression of GAPLINC led to increased expression of CSF1, which was partially reversed by the overexpression of miR-135b-5p.

In brief, we identified the high expression of GAPLINC in RCC and confirmed that it was associated with a poor clinical prognosis. *In vitro* proliferation, scratch, Transwell assays and *in vivo* experiments proved that GAPLINC promoted the proliferation and migration of RCC cells. Low expression of CSF1 protein was found after GAPLINC knockdown. Phenotypic experiments proved that GAPLINC plays a role in promoting cancer through CSF1. Subsequently, the ceRNA mechanism by which GAPLINC upregulates CSF1 by sponging miR-135b-5p was identified by luciferase assays and phenotypic rescue experiments. Overall, we elucidated the significance of the GAPLINC/miR-135b-5p axis in RCC (Figure 6L). This may provide a new perspective for the molecular targeted treatment of RCC.

CONCLUSION

Our study revealed that the high expression of GAPLINC in RCC is associated with a poor prognosis. GAPLINC increases the expression of CSF1 by sponging miR-135b-5p, thus promoting the proliferation and migration of RCC cells. Our study further deepens the understanding of the pathogenic roles of lncRNAs in RCC and provides a potential new therapeutic target for patients with RCC.

DATA AVAILABILITY STATEMENT

The original contributions presented in the study are included in the article/Supplementary Material. Further inquiries can be directed to the corresponding authors.

REFERENCES

- Capitani U, Bensalah K, Bex A, Boorjian SA, Bray F, Coleman J, et al. Epidemiology of Renal Cell Carcinoma. *Eur Urol* (2019) 75(1):74–84. doi: 10.1016/j.eururo.2018.08.036
- Siegel RL, Miller KD, Jemal A. Cancer Statistics, 2018. *CA Cancer J Clin* (2018) 68(1):7–30. doi: 10.3322/caac.21442
- Capitani U, Montorsi F. Renal Cancer. *Lancet* (2016) 387(10021):894–906. doi: 10.1016/s0140-6736(15)00046-x
- Longo N, Capece M, Celentano G, La Rocca R, Califano G, Collà Ruvolo C, et al. Clinical and Pathological Characteristics of Metastatic Renal Cell Carcinoma Patients Needing a Second-Line Therapy: A Systematic Review. *Cancers (Basel)* (2020) 12(12):3634. doi: 10.3390/cancers12123634
- Nelson BR, Makarewicz CA, Anderson DM, Winders BR, Troupes CD, Wu F, et al. A Peptide Encoded by a Transcript Annotated as Long Noncoding RNA Enhances SERCA Activity in Muscle. *Science* (2016) 351(6270):271–5. doi: 10.1126/science.aad4076
- Quinn JJ, Chang HY. Unique Features of Long Non-Coding RNA Biogenesis and Function. *Nat Rev Genet* (2016) 17(1):47–62. doi: 10.1038/nrg.2015.10
- Lee YS, Dutta A. MicroRNAs in Cancer. *Annu Rev Pathol* (2009) 4:199–227. doi: 10.1146/annurev.pathol.4.110807.092222
- Mohr AM, Mott JL. Overview of MicroRNA Biology. *Semin Liver Dis* (2015) 35(1):3–11. doi: 10.1055/s-0034-1397344

ETHICS STATEMENT

The studies involving human participants were reviewed and approved by Institutional Review Board of the First Affiliated Hospital of Nanchang University. The patients/participants provided their written informed consent to participate in this study. The animal study was reviewed and approved by Animal Care and Use Committee of the First Affiliated Hospital of Nanchang University, China.

AUTHOR CONTRIBUTIONS

TS, BG, and MM designed the experiments. SW performed the experiments. XY and WX analyzed the data. SF, QC, ZL, and ZZ interpreted the results. SW, BG, and MM wrote the paper. All authors contributed to the article and approved the submitted version.

FUNDING

This work was supported by the National Natural Science Foundation of China (91200212), the Provincial Natural Science Foundation of Jiangxi (20202BABL206023), China and Graduate Student Innovation Special Fund Project of Jiangxi Province (YC2020-B042).

SUPPLEMENTARY MATERIAL

The Supplementary Material for this article can be found online at: <https://www.frontiersin.org/articles/10.3389/fonc.2021.718532/full#supplementary-material>

- Lu TX, Rothenberg ME. MicroRNA. *J Allergy Clin Immunol* (2018) 141(4):1202–7. doi: 10.1016/j.jaci.2017.08.034
- Tay Y, Rinn J, Pandolfi PP. The Multilayered Complexity of Cerna Crosstalk and Competition. *Nature* (2014) 505(7483):344–52. doi: 10.1038/nature12986
- Karret FA, Pandolfi PP. CeRNA Cross-Talk in Cancer: When Ce-Bling Rivalries Go Awry. *Cancer Discovery* (2013) 3(10):1113–21. doi: 10.1158/2159-8290.Cd-13-0202
- Qi X, Zhang DH, Wu N, Xiao JH, Wang X, Ma W. CeRNA in Cancer: Possible Functions and Clinical Implications. *J Med Genet* (2015) 52(10):710–8. doi: 10.1136/jmedgenet-2015-103334
- Zhou YS, Xu SW, Guan CH, Hu ZT, Jiang XM. The Regulatory Effect of GAPLINC in Malignant Tumors and its Relationship With the Prognosis of Patients. *Zhonghua Bing Li Xue Za Zhi* (2019) 48(11):902–5. doi: 10.3760/cma.j.issn.0529-5807.2019.11.017
- Ren R, Wu J, Zhou MY. MiR-135b-5p Affected Malignant Behaviors of Ovarian Cancer Cells by Targeting KDM5B. *Eur Rev Med Pharmacol Sci* (2020) 24(7):3548–54. doi: 10.26355/eurrev_202004_20815
- Zhang Y, Xia F, Zhang F, Cui Y, Wang Q, Liu H, et al. MiR-135b-5p Enhances Doxorubicin-Sensitivity of Breast Cancer Cells Through Targeting Anterior Gradient 2. *J Exp Clin Cancer Res* (2019) 38(1):26. doi: 10.1186/s13046-019-1024-3
- Chen Z, Gao Y, Gao S, Song D, Feng Y. MiR-135b-5p Promotes Viability, Proliferation, Migration and Invasion of Gastric Cancer Cells by Targeting

- Krüppel-Like Factor 4 (KLF4). *Arch Med Sci* (2020) 16(1):167–76. doi: 10.5114/aoms.2019.87761
17. Saltman DL, Dolganov GM, Hinton LM, Lovett M. Reassignment of the Human Macrophage Colony Stimulating Factor Gene to Chromosome 1p13–21. *Biochem Biophys Res Commun* (1992) 182(3):1139–43. doi: 10.1016/0006-291x(92)91850-p
 18. Menke J, Kriegsmann J, Schimanski CC, Schwartz MM, Schwarting A, Kelley VR. Autocrine CSF-1 and CSF-1 Receptor Coexpression Promotes Renal Cell Carcinoma Growth. *Cancer Res* (2012) 72(1):187–200. doi: 10.1158/0008-5472.Can-11-1232
 19. Yang L, Wu Q, Xu L, Zhang W, Zhu Y, Liu H, et al. Increased Expression of Colony Stimulating Factor-1 Is a Predictor of Poor Prognosis in Patients With Clear-Cell Renal Cell Carcinoma. *BMC Cancer* (2015) 15:67. doi: 10.1186/s12885-015-1076-5
 20. Gerharz CD, Reinecke P, Schneider EM, Schmitz M, Gabbert HE. Secretion of GM-CSF and M-CSF by Human Renal Cell Carcinomas of Different Histologic Types. *Urology* (2001) 58(5):821–7. doi: 10.1016/s0090-4295(01)01371-1
 21. Lin W, Xu D, Austin CD, Caplazi P, Senger K, Sun Y, et al. Function of CSF1 and IL34 in Macrophage Homeostasis, Inflammation, and Cancer. *Front Immunol* (2019) 10: (2019):. doi: 10.3389/fimmu.2019.02019
 22. Batool A, Wang YQ, Hao XX, Chen SR, Liu YX. A MiR-125b/CSF1-CX3CL1/Tumor-Associated Macrophage Recruitment Axis Controls Testicular Germ Cell Tumor Growth. *Cell Death Dis* (2018) 9(10):962. doi: 10.1038/s41419-018-1021-z
 23. Peyraud F, Cousin S, Italiano A. Csf-1r Inhibitor Development: Current Clinical Status. *Curr Oncol Rep* (2017) 19(11):70. doi: 10.1007/s11912-017-0634-1
 24. Luo Y, Ouyang J, Zhou D, Zhong S, Wen M, Ou W, et al. Long Noncoding RNA GAPLINC Promotes Cells Migration and Invasion in Colorectal Cancer Cell by Regulating MiR-34a/C-MET Signal Pathway. *Dig Dis Sci* (2018) 63(4):890–9. doi: 10.1007/s10620-018-4915-9
 25. Linehan WM, Spellman PT, Ricketts CJ, Creighton CJ, Fei SS, Davis C, et al. Comprehensive Molecular Characterization of Papillary Renal-Cell Carcinoma. *N Engl J Med* (2016) 374(2):135–45. doi: 10.1056/NEJMoa1505917
 26. Davis CF, Ricketts CJ, Wang M, Yang L, Cherniack AD, Shen H, et al. The Somatic Genomic Landscape of Chromophobe Renal Cell Carcinoma. *Cancer Cell* (2014) 26(3):319–30. doi: 10.1016/j.ccr.2014.07.014
 27. Hovelson DH, McDaniel AS, Cani AK, Johnson B, Rhodes K, Williams PD, et al. Development and Validation of a Scalable Next-Generation Sequencing System for Assessing Relevant Somatic Variants in Solid Tumors. *Neoplasia (New York NY)* (2015) 17(4):385–99. doi: 10.1016/j.neo.2015.03.004
 28. Osawa T, Takeuchi A, Kojima T, Shinohara N, Eto M, Nishiyama H. Overview of Current and Future Systemic Therapy for Metastatic Renal Cell Carcinoma. *Jpn J Clin Oncol* (2019) 49(5):395–403. doi: 10.1093/jjco/hyz013
 29. Salami SS, George AK, Udager AM. The Genomics of Renal Cell Carcinoma and Its Role in Renal Mass Biopsy. *Curr Opin Urol* (2018) 28(4):383–91. doi: 10.1097/mou.0000000000000516
 30. Derrier T, Johnson R, Bussotti G, Tanzer A, Djebali S, Tilgner H, et al. The GENCODE V7 Catalog of Human Long Noncoding Rnas: Analysis of Their Gene Structure, Evolution, and Expression. *Genome Res* (2012) 22(9):1775–89. doi: 10.1101/gr.132159.111
 31. Ulitsky I, Bartel DP. Lincrnas: Genomics, Evolution, and Mechanisms. *Cell* (2013) 154(1):26–46. doi: 10.1016/j.cell.2013.06.020
 32. Kornienko AE, Guenzl PM, Barlow DP, Pauler FM. Gene Regulation by the Act of Long non-Coding RNA Transcription. *BMC Biol* (2013) 11:59. doi: 10.1186/1741-7007-11-59
 33. Liu B, Sun L, Liu Q, Gong C, Yao Y, Lv X, et al. A Cytoplasmic NF- κ B Interacting Long Noncoding RNA Blocks I κ B Phosphorylation and Suppresses Breast Cancer Metastasis. *Cancer Cell* (2015) 27(3):370–81. doi: 10.1016/j.ccr.2015.02.004
 34. Cesana M, Cacchiarelli D, Legnini I, Santini T, Sthandier O, Chinappi M, et al. A Long Noncoding RNA Controls Muscle Differentiation by Functioning as a Competing Endogenous RNA. *Cell* (2011) 147(2):358–69. doi: 10.1016/j.cell.2011.09.028
 35. Lee S, Kopp F, Chang TC, Sataluri A, Chen B, Sivakumar S, et al. Noncoding RNA NORAD Regulates Genomic Stability by Sequestering PUMILIO Proteins. *Cell* (2016) 164(1–2):69–80. doi: 10.1016/j.cell.2015.12.017
 36. Denzler R, Agarwal V, Stefano J, Bartel DP, Stoffel M. Assessing the Cerna Hypothesis With Quantitative Measurements of miRNA and Target Abundance. *Mol Cell* (2014) 54(5):766–76. doi: 10.1016/j.molcel.2014.03.045
 37. Loewer S, Cabili MN, Guttman M, Loh YH, Thomas K, Park IH, et al. Large Intergenic non-Coding RNA-Ror Modulates Reprogramming of Human Induced Pluripotent Stem Cells. *Nat Genet* (2010) 42(12):1113–7. doi: 10.1038/ng.710
 38. Li J, Meng H, Bai Y, Wang K. Regulation of Lncrna and its Role in Cancer Metastasis. *Oncol Res* (2016) 23(5):205–17. doi: 10.3727/096504016x14549667334007
 39. Schmitt AM, Chang HY. Long Noncoding RNAs in Cancer Pathways. *Cancer Cell* (2016) 29(4):452–63. doi: 10.1016/j.ccell.2016.03.010
 40. Blondeau JJ, Deng M, Syring I, Schrödter S, Schmidt D, Perner S, et al. Identification of Novel Long non-Coding Rnas in Clear Cell Renal Cell Carcinoma. *Clin Epigenet* (2015) 7(1):10. doi: 10.1186/s13148-015-0047-7
 41. Malouf GG, Zhang J, Yuan Y, Compérat E, Roupriet M, Cussenot O, et al. Characterization of Long non-Coding RNA Transcriptome in Clear-Cell Renal Cell Carcinoma by Next-Generation Deep Sequencing. *Mol Oncol* (2015) 9(1):32–43. doi: 10.1016/j.molonc.2014.07.007
 42. Shen H, Luo G, Chen Q. Long Noncoding Rnas as Tumorigenic Factors and Therapeutic Targets for Renal Cell Carcinoma. *Cancer Cell Int* (2021) 21(1):110. doi: 10.1186/s12935-021-01805-2
 43. Hu Y, Wang J, Qian J, Kong X, Tang J, Wang Y, et al. Long Noncoding RNA GAPLINC Regulates CD44-Dependent Cell Invasiveness and Associates With Poor Prognosis of Gastric Cancer. *Cancer Res* (2014) 74(23):6890–902. doi: 10.1158/0008-5472.Can-14-0686
 44. Zhang W, Yao H, Wu Y. Poor Expression of Long-Chain Noncoding RNA GAPLINC Inhibits Epithelial-Mesenchymal Transition, and Invasion and Migration of Hepatocellular Carcinoma Cells. *Anticancer Drugs* (2019) 30(8):784–94. doi: 10.1097/cad.0000000000000752
 45. Zhao J, Wang C, Liu S, Su X, Ouyang A. Tgf- β 1 Mediates Lncrna GAPLINC Expression to Promote the Migration and Invasion of non-Small Cell Lung Cancer. *Oncotargets Ther* (2019) 12:6175–80. doi: 10.2147/ott.S207079
 46. Vollmers AC, Covarrubias S, Kuang D, Shulkin A, Iwuagwu J, Katzman S, et al. A Conserved Long Noncoding RNA, GAPLINC, Modulates the Immune Response During Endotoxic Shock. *Proc Natl Acad Sci USA* (2021) 118(7): e2016648118. doi: 10.1073/pnas.2016648118
 47. Mo BY, Guo XH, Yang MR, Liu F, Bi X, Liu Y, et al. Long non-Coding RNA GAPLINC Promotes Tumor-Like Biologic Behaviors of Fibroblast-Like Synoviocytes as MicroRNA Sponging in Rheumatoid Arthritis Patients. *Front Immunol* (2018) 9:702. doi: 10.3389/fimmu.2018.00702
 48. Zhang Y, Zhang Z, Yi Y, Wang Y, Fu J. Circno10 Acts as a Sponge of MiR-135a/B-5p in Suppressing Colorectal Cancer Progression via Regulating KLF9. *Oncotargets Ther* (2020) 13:5165–76. doi: 10.2147/ott.S242001
 49. Chen N, Yin D, Lun B, Guo X. LncRNA GAS8-AS1 Suppresses Papillary Thyroid Carcinoma Cell Growth Through the Mir-135b-5p/CCND2 Axis. *Biosci Rep* (2019) 39(1):BSR20181440. doi: 10.1042/bsr.20181440
 50. Pu T, Shen M, Li S, Yang L, Gao H, Xiao L, et al. Bsr of MiR-135b-5p Promotes Metastasis of Early-Stage Breast Cancer by Regulating Downstream Target SDCBP. *Lab Invest* (2019) 99(9):1296–308. doi: 10.1038/s41374-019-0258-1
 51. Huang Y, Wang Y, Ouyang Y. Elevated MicroRNA-135b-5p Relieves Neuronal Injury and Inflammation in Post-Stroke Cognitive Impairment by Targeting NR3C2. *Int J Neurosci* (2020) 4:1–9. doi: 10.1080/00207454.2020.1802265
 52. Liu C, Pan A, Chen X, Tu J, Xia X, Sun L. MiR-5571-3p and MiR-135b-5p, Derived From Analyses of Microna Profile Sequencing, Correlate With Increased Disease Risk and Activity of Rheumatoid Arthritis. *Clin Rheumatol* (2019) 38(6):1753–65. doi: 10.1007/s10067-018-04417-w
 53. Wang JJ, Lei KF, Han F. Tumor Microenvironment: Recent Advances in Various Cancer Treatments. *Eur Rev Med Pharmacol Sci* (2018) 22(12):3855–64. doi: 10.26355/eurrev_201806_15270
 54. Quail DF, Joyce JA. Microenvironmental Regulation of Tumor Progression and Metastasis. *Nat Med* (2013) 19(11):1423–37. doi: 10.1038/nm.3394
 55. Najafi M, Hashemi Goradel N, Farhood B, Salehi E, Nashtaei MS, Khanlarkhani N, et al. Macrophage Polarity in Cancer: A Review. *J Cell Biochem* (2019) 120(3):2756–65. doi: 10.1002/jcb.27646

56. Atianand MK, Caffrey DR, Fitzgerald KA. Immunobiology of Long Noncoding RNAs. *Annu Rev Immunol* (2017) 35:177–98. doi: 10.1146/annurev-immunol-041015-055459
57. Xu Z, Li P, Fan L, Wu M. The Potential Role of Circrna in Tumor Immunity Regulation and Immunotherapy. *Front Immunol* (2018) 9:9. doi: 10.3389/fimmu.2018.00009
58. Carpenter S, Aiello D, Atianand MK, Ricci EP, Gandhi P, Hall LL, et al. A Long Noncoding RNA Mediates Both Activation and Repression of Immune Response Genes. *Science* (2013) 341(6147):789–92. doi: 10.1126/science.1240925
59. Li Y, Zhao L, Shi B, Ma S, Xu Z, Ge Y, et al. Functions of MiR-146a and Mir-222 in Tumor-Associated Macrophages in Breast Cancer. *Sci Rep* (2015) 5:18648. doi: 10.1038/srep18648
60. Hah YS, Koo KC. Immunology and Immunotherapeutic Approaches for Advanced Renal Cell Carcinoma: A Comprehensive Review. *Int J Mol Sci* (2021) 22(9):4452. doi: 10.3390/ijms22094452
61. Nallasamy P, Chava S, Verma SS, Mishra S, Gorantla S, Coulter DW, et al. PD-L1, Inflammation, Non-Coding RNAs, and Neuroblastoma: Immuno-Oncology Perspective. *Semin Cancer Biol* (2018) 52(Pt 2):53–65. doi: 10.1016/j.semcancer.2017.11.009
62. Röszer T. Understanding the Mysterious M2 Macrophage Through Activation Markers and Effector Mechanisms. *Mediators Inflammation* (2015) 2015:816460. doi: 10.1155/2015/816460
63. Pyonteck SM, Akkari L, Schuhmacher AJ, Bowman RL, Sevenich L, Quail DF, et al. CSF-1R Inhibition Alters Macrophage Polarization and Blocks Glioma Progression. *Nat Med* (2013) 19(10):1264–72. doi: 10.1038/nm.3337

Conflict of Interest: The authors declare that the research was conducted in the absence of any commercial or financial relationships that could be construed as a potential conflict of interest.

Publisher's Note: All claims expressed in this article are solely those of the authors and do not necessarily represent those of their affiliated organizations, or those of the publisher, the editors and the reviewers. Any product that may be evaluated in this article, or claim that may be made by its manufacturer, is not guaranteed or endorsed by the publisher.

Copyright © 2021 Wang, Yang, Xie, Fu, Chen, Li, Zhang, Sun, Gong and Ma. This is an open-access article distributed under the terms of the Creative Commons Attribution License (CC BY). The use, distribution or reproduction in other forums is permitted, provided the original author(s) and the copyright owner(s) are credited and that the original publication in this journal is cited, in accordance with accepted academic practice. No use, distribution or reproduction is permitted which does not comply with these terms.



Promising Advances in LINC01116 Related to Cancer

Yating Xu^{1,2,3,4†}, Xiao Yu^{1,2,3,4†}, Menggang Zhang^{1,2,3,4†}, Qingyuan Zheng^{1,2,3,4}, Zongzong Sun⁵, Yuting He^{1,2,3,4*} and Wenzhi Guo^{1,2,3,4*}

¹ Department of Hepatobiliary and Pancreatic Surgery, The First Affiliated Hospital of Zhengzhou University, Zhengzhou, China, ² Key Laboratory of Hepatobiliary and Pancreatic Surgery and Digestive Organ Transplantation of Henan Province, The First Affiliated Hospital of Zhengzhou University, Zhengzhou, China, ³ Open and Key Laboratory of Hepatobiliary and Pancreatic Surgery and Digestive Organ Transplantation at Henan Universities, Zhengzhou, China, ⁴ Henan Key Laboratory of Digestive Organ Transplantation, Zhengzhou, China, ⁵ Department of Obstetrics and Gynecology, The Third Affiliated Hospital of Zhengzhou University, Zhengzhou, China

OPEN ACCESS

Edited by:

Shiv K. Gupta,
Mayo Clinic, United States

Reviewed by:

Luciana N. S. Andrade,
Universidade de São Paulo, Brazil
Juliano Andreoli Miyake,
Federal University of Santa Catarina,
Brazil

*Correspondence:

Yuting He
fcchey11@zzu.edu.cn
Wenzhi Guo
fccguowz@zzu.edu.cn

[†]These authors have contributed
equally to this work

Specialty section:

This article was submitted to
Molecular and Cellular Oncology,
a section of the journal
Frontiers in Cell and Developmental
Biology

Received: 06 July 2021

Accepted: 24 September 2021

Published: 14 October 2021

Citation:

Xu Y, Yu X, Zhang M, Zheng Q,
Sun Z, He Y and Guo W (2021)
Promising Advances in LINC01116
Related to Cancer.
Front. Cell Dev. Biol. 9:736927.
doi: 10.3389/fcell.2021.736927

Long non-coding RNAs (lncRNAs) are RNAs with a length of no less than 200 nucleotides that are not translated into proteins. Accumulating evidence indicates that lncRNAs are pivotal regulators of biological processes in several diseases, particularly in several malignant tumors. Long intergenic non-protein coding RNA 1116 (LINC01116) is a lncRNA, whose aberrant expression is correlated with a variety of cancers, including lung cancer, gastric cancer, colorectal cancer, glioma, and osteosarcoma. LINC01116 plays a crucial role in facilitating cell proliferation, invasion, migration, and apoptosis. In addition, numerous studies have recently suggested that LINC01116 has emerged as a novel biomarker for prognosis and therapy in malignant tumors. Consequently, we summarize the clinical significance of LINC01116 associated with biological processes in various tumors and provide a hopeful orientation to guide clinical treatment of various cancers in future studies.

Keywords: long non-coding RNA, LINC01116, human cancers, prognosis, chemoresistance

INTRODUCTION

Cancer is one of the leading causes of death (Seow et al., 2020; Wang et al., 2020d; Buneviciene et al., 2021; Eloranta et al., 2021) worldwide and threatens human health and social happiness. Despite the advancements (Blessin et al., 2020) in clinical diagnosis and treatment of malignancies (Jung et al., 2020; Grady et al., 2021; Hussain et al., 2021), most patients still have a poor prognosis, and the overall survival (OS) rate remains low. Due to the lack of early diagnostic biomarkers, most cancers progress to the terminal stage. Therefore, it is urgent to understand the underlying molecular mechanisms in cancer, which is crucial for finding effective early diagnostic biomarkers and therapeutic methods.

Owing to the development of multiple RNA detection techniques (Shu et al., 2021; Toden et al., 2021; Wang et al., 2021; Zhong et al., 2021a), most RNAs have been found to lack the capacity to encode proteins. Although these RNAs do not directly translate into proteins (Gupta et al., 2020), driving evidence clarifies that they play an essential role in biological functions (Chen et al., 2020b; Jantrapirom et al., 2021; Jin et al., 2021; Lai et al., 2021; Zhang et al., 2021b). Such is the case of long non-coding RNAs (lncRNAs), which are no less than 200 nucleotides and participate in the initiation and progression of various diseases, especially cancers (Chen et al., 2020a; Huang et al., 2021; Kotani et al., 2021; Luo et al., 2021; Teng et al., 2021). Abnormal expression of these

lncRNAs is involved in a variety of biological processes in tumors *via* regulation of gene expression that affects tumor size, metastasis, pathological stage, and prognosis in patients (Yin et al., 2018; Shuai et al., 2020; Li et al., 2021a; Zheng et al., 2021; Zhong et al., 2021b). Moreover, studies have confirmed that lncRNAs serve as competitive endogenous RNAs (ceRNAs) and could sponge microRNAs to regulate the expression of messenger RNA, which provides a promising direction for exploring the complicated molecular mechanisms of malignancies.

Long intergenic non-protein coding RNA 1116 (LINC01116), located in the 2q31.1 region, is currently reported to be an extraordinary regulator of proliferation, migration, and invasion of cancer cells (Meng et al., 2020; Cui et al., 2021; Lou et al., 2021; Ren et al., 2021; Zhang et al., 2021a). High expression of LINC01116 was identified in malignant tumors; LINC01116 might participate in tumorigenesis. For instance, previous studies have demonstrated that hepatocellular carcinoma (HCC) patients with LINC01116 overexpression generally have a dismal survival time (Jiang et al., 2019). Further studies verified that LINC01116 promoted oral squamous cell carcinoma (OSCC) proliferation, migration, and invasion (Chen et al., 2019). In contrast, knockdown of LINC01116 positively inhibited the proliferation of prostate cancer cells. Additionally, numerous reports have shown that LINC01116 functions as a major regulator of lung cancer (LC), gastric cancer (GC), colorectal cancer (CRC), glioma, osteosarcoma, glioma, head and neck squamous cell carcinoma (HNSC), epithelial ovarian cancer (EOC), and breast cancer (BC).

In this review, we highlight the latest studies concerning LINC01116, its abnormal expression related to clinical characteristics, and its influence on multiple biological functions of cancers. The present review could guide the further discovery of prospective and creative therapeutic targets.

EXPRESSION AND CLINICAL CHARACTERISTICS OF LINC01116 IN VARIOUS CANCER TYPES

Numerous studies have elucidated the significance of LINC01116 in malignancy. Therefore, we review the specific process in **Table 1**, which shows how LINC01116 expression exerts its impact on a variety of cancers.

Lung Cancer

Lung cancer is predominant worldwide and its incidence rate is the highest in men and the second in women (Bade and Dela Cruz, 2020; Chen et al., 2021; Ma et al., 2021; Yuan et al., 2021). Zeng et al. (2020) showed that LINC01116 was overexpressed in LC tumor tissues compared to normal adjacent tissues. LINC01116 expression is high in LC patients, and they generally have more unsatisfactory outcomes than the others. Thus, previous reports have suggested that LINC01116 is an independent prognostic factor in LC. Furthermore, the expression of LINC01116 was shown to be high in patients with advanced tumor stages. For instance, recent studies showed that a considerable number of patients with low expression

of LINC01116 were generally diagnosed with TNM I rather than TNM I/III. These results indicate that LINC01116 can be considered as a latent regulator that participates in the progression of metastasis and invasiveness in LC (Shang et al., 2021). Additionally, silencing of LINC01116 reverses this effect. Eventually, LINC01116 plays crucial roles in tumor processes and could provide an orientation for being diagnostic and prognostic markers of LC, but its actual situation of clinical application still requires massive clinical and basic research.

Gastric Cancer

Gastric cancer is the 4th most prevalent malignant tumor. Due to the lack of early diagnostic markers, patients are commonly diagnosed at terminal stages, with tumors that have metastasized to proximal or even remote regions in the body (Lin et al., 2019; Arnold et al., 2020; Ascherman et al., 2021; Puliga et al., 2021). Su et al. (2019) discovered that LINC01116 and CASC11 were upregulated in GC tissues, compared with cancer-adjacent tissues, and were positively correlated with clinical stages. In addition, the overexpression of LINC01116 and CASC11 was found to collectively increase the migration and invasion of GC cells. In contrast, low expression of LINC01116 was found to be associated with suppressed metastasis and invasiveness in GC patients. Moreover,

TABLE 1 | Expression and effect on clinical characters of LINC01116 in different cancer types.

Cancer type	Sample	Expression	Clinical characters	Prognosis	PMID
Lung cancer	594 cases	High	Advanced tumor stage	Poor	32913506
	84 cases	High	Prognosis	Poor	32913506
	62 cases	High	Advanced tumor stage	Poor	33535997
Osteosarcoma	318 cases	High	Prognosis	Poor	33987935
	104 cases	High	Higher clinical stage	Poor	31486480
Glioma	135 cases	High	Early tumor metastasis	Poor	31933922
	37 cases	High	Prognosis	Poor	32358484
Gastric cancer	73 cases	High	Prognosis	Poor	32141549
	76 cases	High	Prognosis	Poor	31632064
Colorectal cancer	62 cases	High	Lower clinical stage	Poor	33116633
	80 cases	High	Prognosis	Poor	33499872
Oral squamous cell carcinoma	58 cases	High	Prognosis	Poor	31308744
Neck squamous cell carcinoma	44 cases	High	/	/	31452270
Prostate adenocarcinoma cell	15 cases	High	/	/	28131897
Epithelial ovarian cancer	90 cases	High	Prognosis	Poor	30178832
Breast cancer	94 cases	High	Advanced tumor stage	Poor	29687853

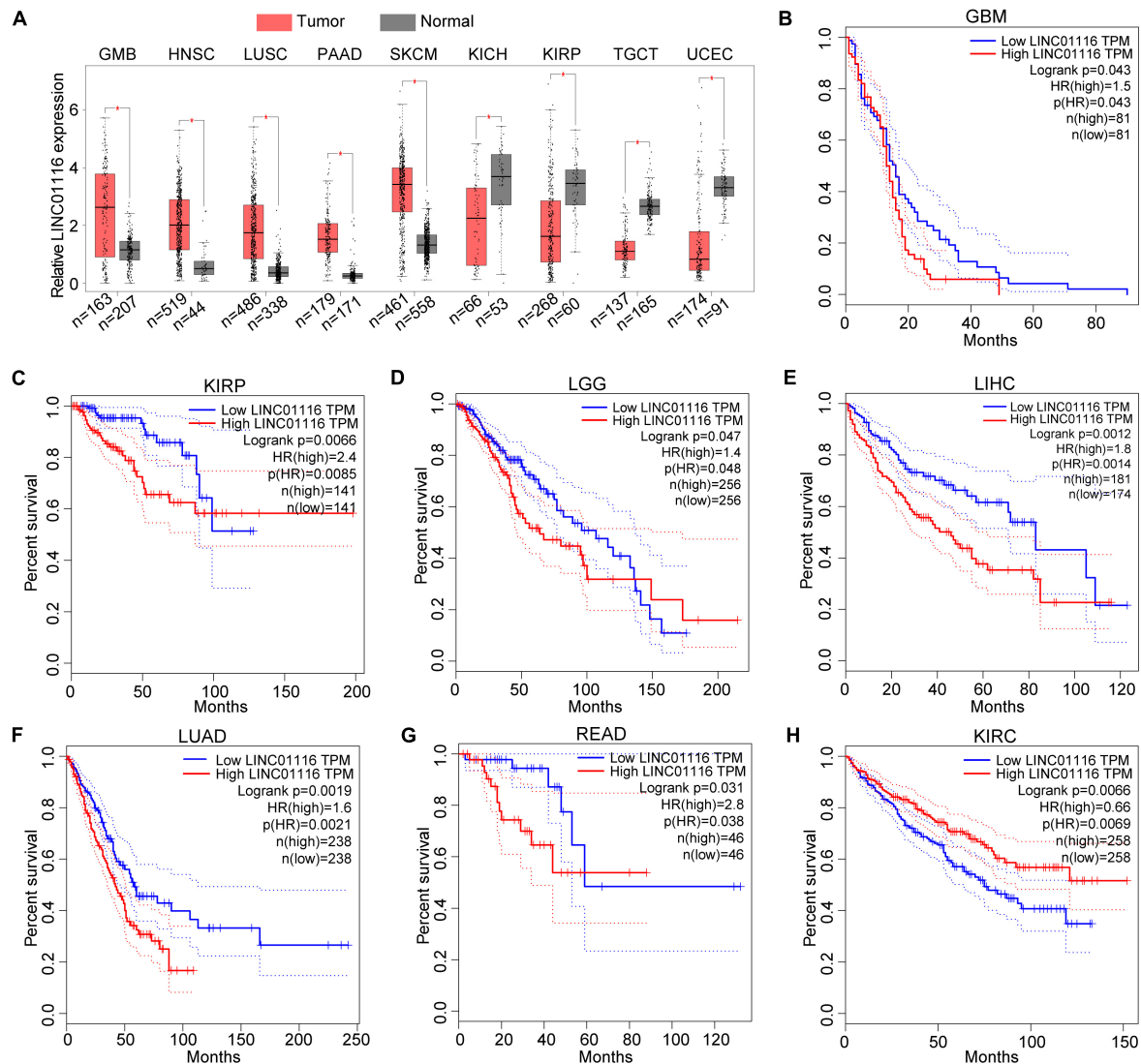


FIGURE 1 | Expression and prognostic roles of LINC01116 in different cancer types. **(A)** Dysregulated expression of LINC01116 in GMB, HNSC, LUSC, PAAD, SKCM, KICH, KIRP, TGCT, and UCEC. **(B–G)** Patients with highly expressed LINC01116 had poor overall survival (OS) rate compared those with lowly expressed LINC01116 in GBM, KIRP, LGG, LIHC, LUAD, and READ. **(H)** Patients with decreased LINC01116 expression had poor overall survival (OS) rate compared those with increased LINC01116 expressed in KIRC.

CASC11 silencing alleviated the overexpression of LINC01116. Additionally, Chen et al. (2020c) demonstrated that patients with abundant expression of LINC01116 in GC cells generally have shorter survival time than those with low expression levels, and that the inhibition of LINC01116 expression could impede the proliferation of GC cells. These findings provide a novel direction for the diagnosis and treatment of GC.

Colorectal Cancer

Colorectal cancer is the frequent cancer globally and has high mortality and incidence rates (Wieszczy et al., 2020; Świerczyński et al., 2021; Zaborowski et al., 2021; Zhao et al., 2021). Bi et al. (2020) revealed that LINC01116 was highly expressed in CRC tissues compared to normal tissues, and patients with

high expression of LINC01116 had a very poor prognosis. LINC01116 knockdown substantially prevented the migration, proliferation, and invasion of CRC cells and activated cell apoptosis. Emerging evidence showed that a large number of patients were commonly diagnosed at terminal stages with high expression of LINC01116. Liang et al. (2021) identified that LINC01116 facilitated the growth of CRC cells and tumorigenicity through the downregulation of TPM1 expression. Specifically, LINC01116 can bind with EZH2 to accelerate the methylation of TPM1, which blocks the transcription of TPM1. Additionally, low expression of LINC01116 considerably impeded the tumorigenicity and angiogenesis of CRC cells in nude mice. Despite LINC01116 could serve as a diagnostic biomarker for in CRC, the deficiency of clinical application needs

to be further investigated. For instance, researches of LINC01116 participated in CRC are only tested in tissues, and diverse effects between LINC01116 and molecular target markers are supposed to be probed in blood and other body fluids.

Glioma

Brain gliomas are the most common primary malignant tumors in the central nervous system, presenting with an increasing mortality rate. Several patients present with an OS time of less than 2 years (Mondal and Kulshreshtha, 2021; Petridis et al., 2021; Tanabe et al., 2021; Tu et al., 2021). Wang et al. (2020c) found that the upregulation of LINC01116 in glioma cells is related to poor prognosis. When LINC01116 is knocked, G1-G0 phase arrest in Ln229 and U87 cells might be induced. Therefore, the apoptosis of glioma could be significantly inhibited. Moreover, LINC01116 has been shown to stimulate IL-1 β transcription to generate an army of cytokines, which are associated with tumorigenicity *via* DDX5. Wang et al. (2020c) showed that LINC01116 positively regulates MDM2 to repress the p53 pathway, which activates the development of glioma cells. Current research shows that LINC01116 can substantially promote the proliferation and invasion abilities of glioma cells (Cole et al., 1986). Ye et al. revealed that LINC01116 expression is higher in glioma tissues than in normal tissues, and it could elevate the capacity of the cell cycle and cell proliferation by regulating the expression of VEGFA. In summary, these findings further clarify the biological functions of LINC01116 in glioma tumorigenesis and provide a promising treatment target for glioma patients.

Osteosarcoma

Osteosarcoma is a leading cause of cancer-related death among young adolescents. Osteosarcoma patients retain high levels of metastasis and recurrence, accounting for approximately 30%–40% of cases (Lu et al., 2020; Zheng et al., 2020; Li et al., 2021c; Liu et al., 2021b). Zhang et al. (2019) reported that LINC01116 might remarkably accelerate the proliferation, migration, and invasion of osteosarcoma cells, but substantially precludes cell apoptosis. These results corroborated that LINC01116 directly interacted with EZH2 to mediate PTEN and p53. Thus, EZH2 knockdown reverses the LINC01116 functional effect on osteosarcoma cells (Zhang et al., 2019). Zhang et al. (2018) silenced LINC01116, inhibiting the viability of osteosarcoma cells and promoting cell apoptosis. Moreover, high expression of LINC01116 in patients generally results in a poorer prognosis. These results revealed a crucial role for LINC01116 in osteosarcoma. However, further investigation is required before clinical application.

Other Cancers

Wu et al. (2020) shed new light on the silencing of LINC01116, which was shown to inhibit the tumorigenicity of OSCC through the upregulation of miRNA-136. Likewise, LINC01116 knockdown was shown to decrease the migration and invasion of HNSC cells, probably *via* the epithelial-mesenchymal transition pathway (Xing et al., 2020). Yu et al. (2021) suggested that LINC01116 was an oncogene that accelerates the development of prostate adenocarcinoma (PRAD) cells. Fang et al. (2018) reported that the proliferation and migration of EOC cells was

TABLE 2 | The roles and functions of LINC01116 in cancers.

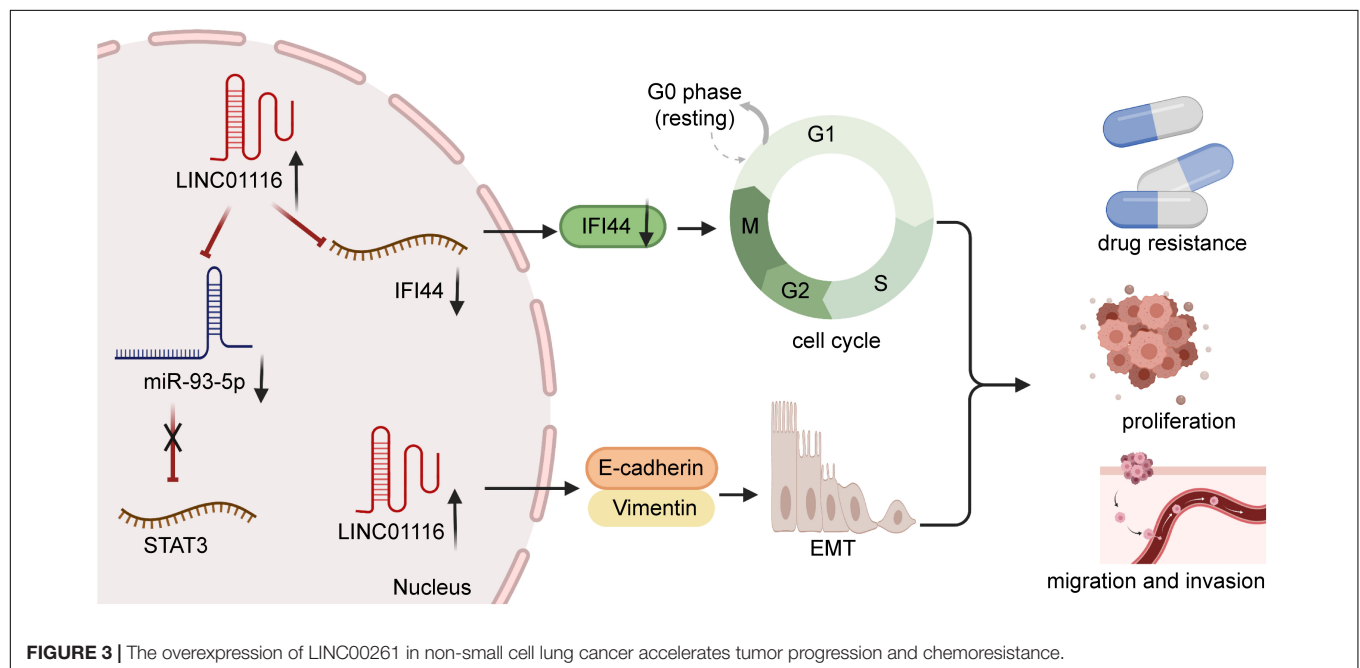
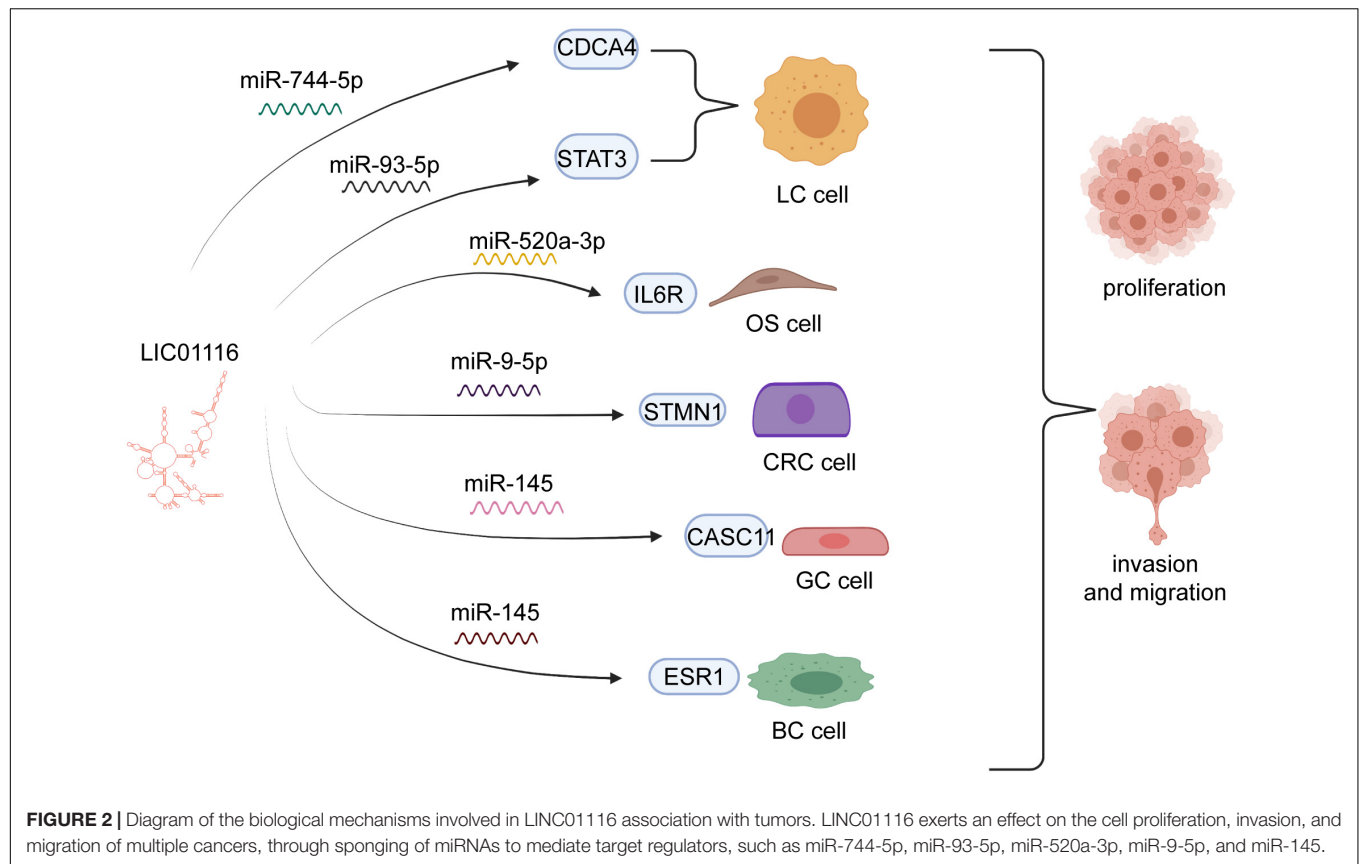
Cancer type	Role	Related genes	Functions	PMID
Lung cancer	Oncogene	miR-744-5P/CDC44	Proliferation	34090440
		miR-93-5P/STAT3	Proliferation	33535997
		IFI44	Chemoresistance	31841994
Gastric cancer	Oncogene	miR-145/CASC11	Invasion and migration	31632064
Glioma	Oncogene	IL-1 β	Proliferation and migration	32358484
		VEGFA	Proliferation, invasion, and migration	33760190
Osteosarcoma	Oncogene	miR-744-5P/MDM2	Proliferation	33760190
		miR-520a-3P/IL6R	Cell viability and migration	30098545
Colorectal cancer	Oncogene	TPM1	Proliferation and angiogenesis	33499872
		miR-9-5P/STMN1	Proliferation, invasion and migration	33116633
Oral squamous cell carcinoma	Oncogene	miRNA-136	Tumorigenicity	31452270
Neck squamous cell carcinoma	Oncogene	MYC	Migration and invasion	31703161
Prostate adenocarcinoma cell	Oncogene	/	Proliferation	33311496
Epithelial ovarian cancer	Oncogene	/	Proliferation and migration	30178832
Breast cancer	Oncogene	miR-145/ESR1	Proliferation	29687853

increased with the overexpression of LINC01116. Knockdown of LINC01116 could function as an essential suppressor to block the viability and cloning ability of BC cells (Hu et al., 2018). Consequently, LINC01116 is a promising prognostic and therapeutic target for OSCC, HNSC, PRAD, EOC, and BC.

EXPRESSION AND PROGNOSTIC VALUE OF LINC01116 IN CANCERS

To further assess the expression pattern of LINC01116 across pan-cancer, we used the GEPIA¹ website to explore the expression level based on The Cancer Genome Atlas database (Tang et al., 2019). The results demonstrated that LINC01116 expression is upregulated in glioblastoma multiforme (GBM), head and neck squamous cell carcinoma (HNSC), lung squamous cell carcinoma (LUSC), pancreatic adenocarcinoma (PAAD), and skin cutaneous melanoma (SKCM). However, decreased expression of LINC01116 has been observed in kidney chromophobe (KICH), kidney renal papillary cell carcinoma

¹<http://gepia.cancer-pku.cn/>



(KIRP), testicular germ cell tumor (TGCT), and uterine corpus endometrial carcinoma (UCEC) (**Figure 1A**).

Likewise, we evaluated the effect of LINC01116 expression on the survival time of cancer patients. As shown in **Figure 1B**, when

LINC01116 is highly expressed, patients with GBM generally have a shorter OS time than when the expression of LINC01116 is low. Similar results have been observed in KIRP, lower grade glioma (LGG), liver hepatocellular carcinoma (LIHC),

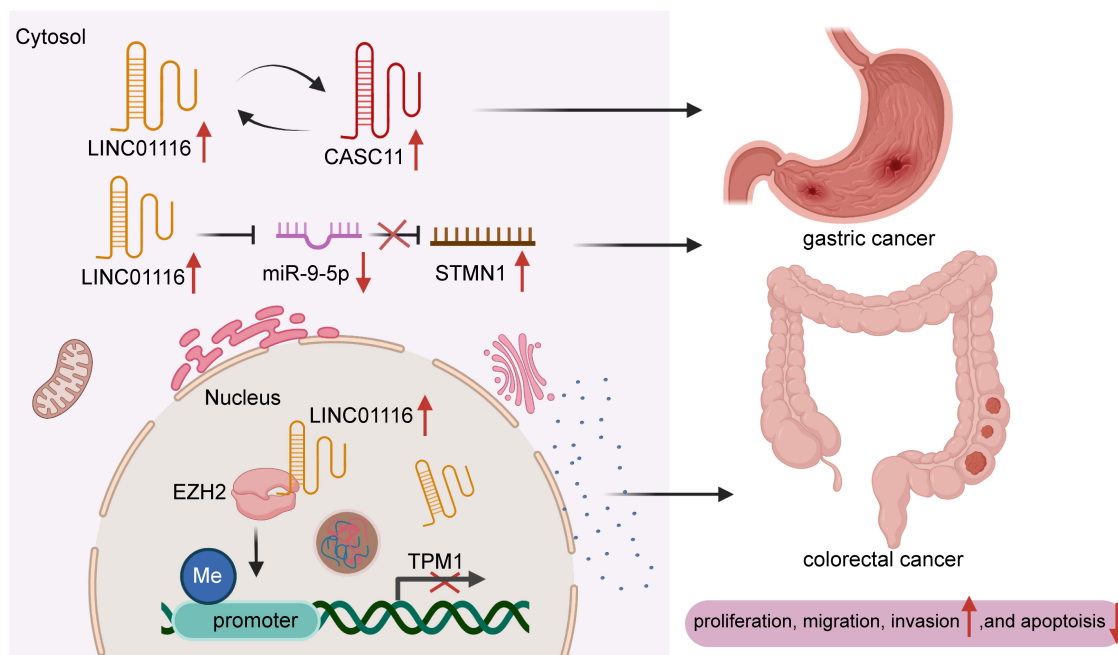


FIGURE 4 | The molecular mechanism map of LINC00261 in gastric cancer and colorectal cancer.

lung adenocarcinoma (LUAD), and rectum adenocarcinoma (READ) (**Figures 1C–G**). Conversely, patients with decreased LINC01116 expression had a lower OS rate in kidney renal clear cell carcinoma (KIRC) (**Figure 1H**). Collectively, LINC01116 could be a novel biomarker for the diagnosis and prognostic determination of different cancer types.

LINC01116 INFLUENCES DIVERSE BIOLOGICAL FUNCTIONS IN CANCERS

LINC01116 has effects on multiple functions of tumors *via* complicated molecular mechanisms. To further explore these underlying processes, we summarize the complex molecular mechanisms in **Table 2** and elucidate the association between LINC01116 and the biological functions of various cancers (**Figure 2**).

Cell Proliferation, Invasion, and Migration

Proliferation of cancer cells generally occurs rapidly, which markedly affects the prognosis of patients (Liu et al., 2019; Zhang et al., 2020). A recent study validated that miR-744-5p might be a novel target of LINC01116 in lung (LAD). miR-744-5p was known as the suppressor to involving in malignant tumors and negatively through regulating CDCA4. Knockdown of miR-744-5p could promote tumor cell proliferation and migration in LAD. LINC01116 could mediate the expression of CDCA4 by competitively binding the sites of CDCA4 with miR-744-5p, which markedly increased cell growth in LAD (Ren et al., 2021). Numerous experiments have shown that LINC01116 is overexpressed in small cell lung carcinoma (SCLC) and that

it could upregulate STAT3 to boost SCLC cell invasion and migration. However, high expression of miR-93-5p suppresses the effect of LINC01116 overexpression. Thus, LINC01116 is likely to modulate miR-93-5p, which contributes to the expression levels of STAT3 (**Figure 3**). However, high expression of miR-93-5p and LINC01116 did not exert an influence on mutual expression, implying that miR-93-5p might have other targets (Xiang et al., 2017). In osteosarcoma cells, LINC01116 was shown to accelerate cell proliferation by targeting miR-520a-3p and upregulating IL6R (Zhang et al., 2018). Similarly, Liu et al. showed that LINC01116 interacts with CASC11, which regulates the invasion and migration of GC cells (**Figure 4**). Accumulating evidence suggests that miR-145 might bridge the interaction between LINC01116 and CASC11 (Su et al., 2019).

In nasopharyngeal carcinoma (NPC) cells, LINC01116 was shown to induce the translation of MYC and enhance the expression of MYC protein, which plays an essential role in proliferation. Likewise, when MYC remains highly expressed, the effect of LINC01116 deletion can be recovered to some degree (Tran et al., 2016). In CRC cells, LINC01116 negatively correlates with miR-9-5p regulation, promoting the proliferation, invasion, and migration of cancer cells. In contrast, miR-9-5p rescues the function of LINC01116. miR-9-5p tends to bind STMN1 to preclude its expression. LINC01116 partly regulates STMN1 to target miR-9-5p (Bi et al., 2020; **Figure 4**). Liang et al. reported that LINC01116 enhanced the CRC cell proliferation, invasion and migration through interacting with EZH2 to potentiate methylation in the TPM1 promoter region to suppress the transcription of TPM1 (**Figure 4**). In addition, a previous study confirmed that LINC01116 was a regulator of ESR1 related to the proliferation of BC cells by sponging miR-145.

In brief, LINC01116 actively stimulates the development of cell proliferation in many cancers by prompting miRNAs to mediate the expression of several proteins.

Chemoresistance

Chemotherapy is one of the primary treatment methods for several malignant tumors. However, the phenomenon of chemoresistance has increased, which has led to a serious dilemma in clinical treatment (Fatma et al., 2020; Jiang et al., 2020). Thus, there has been a great deal of research focusing on the molecular mechanisms of chemoresistance. Previous evidence has indicated that LINC01116 contributes to chemoresistance in some cancers (Li et al., 2021b), namely gefitinib and cisplatin resistance. Wang et al. (2020a) corroborated that LINC01116 contributed positively to the development of cisplatin resistance in LUAD, which depends on the EMT process (Figure 3). In contrast, LINC01116 silencing increases cisplatin sensitivity by mediating apoptosis and cell cycle distribution. Recent experiments have shed new light on the LINC01116-increasing effect of gefitinib resistance by regulating cell cycle through mediating IFI44 expression (Wang et al., 2020a; Figure 3). Furthermore, when LINC01116 is upregulated, the sensitivity of A549 cells to cisplatin is low. Conversely, silencing of LINC01116 generally leads to the inhibition of cisplatin resistance in A549 cells, *via* the stimulation of apoptosis and cell cycle arrest at the G0/G1 phase (Wang et al., 2020b). In summary, an abundance of chemoresistance mechanisms remain unclear. Thus, further studies are necessary.

CONCLUSION

The improvement of research technology generates numerous possibilities for the study of lncRNAs. Substantial research has shown that lncRNAs are relevant to the biological process of tumor advancement as essential regulators of gene expression (Ramnarine et al., 2019; Olivero et al., 2020; Katsushima et al., 2021), and the dysregulation of LINC01116 has been identified as the promoter of the occurrence and progression of a variety of tumors. Plentiful expression of LINC01116 can be found in various cancers, such as lung cancer (Liu et al., 2021a; Mu et al., 2021; Zeng et al., 2021), gastric cancer, colorectal cancer, glioma, and osteosarcoma. When LINC01116 is highly expressed in multiple cancers, the survival time of these patients

tends to be shorter. In several experiments, LINC01116 was found to be an independent prognostic factor in malignant tumors. Furthermore, accumulating evidence has revealed that LINC01116 can be regarded as a ceRNA that mediates gene expression by sponging miRNA, which plays an indispensable role in the proliferation, invasion, metastasis, chemoresistance, and apoptosis of tumors. For instance, LINC01116 functions as a regulator to positively promote the expression of STMN1 by interacting with miR-9-5p. In conclusion, we demonstrated that LINC01116 expression is linked to cancer, and LINC01116 has the potential of being a promising target in clinical tumor treatments. However, there are several dilemmas of LINC0116 applying to clinical treatment still need to be solved. Firstly, the molecular structure and functional information on LINC0116 remain uncharted. Without detailed understanding on the structure and functions of LINC0116, boosting LINC0116-based therapy exists difficulty. Additionally, lncRNAs are considered to be weakly conserved across different species, the conversion from animal models to human clinical application might emerge block. Thus, it is necessary to further research to explore numerous mechanisms of LINC01116 associated with tumor biological processes.

AUTHOR CONTRIBUTIONS

YX, MZ, and XY drafted the manuscript. QZ and ZS drew the mechanism diagrams. YH and WG conceived of the study and guided the analysis. YH and YX edited and reviewed the manuscript. All authors read and approved the final manuscript.

FUNDING

This work was supported by the Youth Talent Lifting Project of Henan Province (2021HYTP059), Key Scientific Research Project of Henan Higher Education Institutions of China (21A320026), the Leading Talents of Zhongyuan Science and Technology Innovation (214200510027), the Henan Provincial Medical Science and Technology Research Plan (SBGJ2018002), the Science and Technology Innovation Talents in Henan Universities (19HASTIT003), and the Outstanding Foreign Scientist Studio in Henan Province (GZS2020004).

REFERENCES

- Arnold, M., Park, J. Y., Camargo, M. C., Lunet, N., Forman, D., and Soerjomataram, I. (2020). Is gastric cancer becoming a rare disease? a global assessment of predicted incidence trends to 2035. *Gut* 69, 823–829. doi: 10.1136/gutjnl-2019-320234
- Ascherman, B., Oh, A., and Hur, C. (2021). International cost-effectiveness analysis evaluating endoscopic screening for gastric cancer for populations with low and high risk. *Gastric Cancer* 24, 878–887. doi: 10.1007/s10120-021-01162-z
- Bade, B. C., and Dela Cruz, C. S. (2020). Lung cancer 2020: epidemiology, etiology, and prevention. *Clin. Chest. Med.* 41, 1–24. doi: 10.1016/j.ccm.2019.10.001
- Bi, C., Cui, H., Fan, H., and Li, L. (2020). LncRNA LINC01116 promotes the development of colorectal cancer by targeting miR-9-5p/STMN1. *Onco Targets Ther.* 13, 10547–10558. doi: 10.2147/ott.S253532
- Blessin, N. C., Priestestersbach, P., Li, W., Mandelkow, T., Dum, D., Simon, R., et al. (2020). Prevalence of CD8(+) cytotoxic lymphocytes in human neoplasms. *Cell Oncol. (Dordr)* 43, 421–430. doi: 10.1007/s13402-020-0049-6-497
- Buneviciene, I., Mekary, R. A., Smith, T. R., Onnela, J. P., and Bunevicius, A. (2021). Can mHealth interventions improve quality of life of cancer patients? a systematic review and meta-analysis. *Crit. Rev. Oncol. Hematol.* 157:103123. doi: 10.1016/j.critrevonc.2020.103123

- Chen, J., Sun, Y., Ou, Z., Yeh, S., Huang, C. P., You, B., et al. (2020b). Androgen receptor-regulated circFNTA activates KRAS signaling to promote bladder cancer invasion. *EMBO Rep.* 21:e48467. doi: 10.15252/embr.201948467
- Chen, C., Luo, Y., He, W., Zhao, Y., Kong, Y., Liu, H., et al. (2020a). Exosomal long noncoding RNA LNMAT2 promotes lymphatic metastasis in bladder cancer. *J. Clin. Invest.* 130, 404–421. doi: 10.1172/jci130892
- Chen, J., Yuan, Z. H., Hou, X. H., Shi, M. H., and Jiang, R. (2020c). LINC01116 promotes the proliferation and inhibits the apoptosis of gastric cancer cells. *Eur. Rev. Med. Pharmacol. Sci.* 24, 1807–1814. doi: 10.26355/eurrev_202002_20358
- Chen, X., Hao, B., Li, D., Reiter, R. J., Bai, Y., Abay, B., et al. (2021). Melatonin inhibits lung cancer development by reversing the Warburg effect via stimulating the SIRT3/PDH axis. *J. Pineal. Res.* doi: 10.1111/jpi.12755 Online ahead of print.
- Chen, Z., Tao, Q., Qiao, B., and Zhang, L. (2019). Silencing of LINC01116 suppresses the development of oral squamous cell carcinoma by up-regulating microRNA-136 to inhibit FN1. *Cancer Manag. Res.* 11, 6043–6059. doi: 10.2147/cmar.S197583
- Cole, E. H., Sweet, J., and Levy, G. A. (1986). Expression of macrophage procoagulant activity in murine systemic lupus erythematosus. *J. Clin. Invest.* 78, 887–893. doi: 10.1172/jci112676
- Cui, L., Chen, S., Wang, D., and Yang, Q. (2021). LINC01116 promotes proliferation and migration of endometrial stromal cells by targeting FOXF1 via sponging miR-9-5p in endometriosis. *J. Cell Mol. Med.* 25, 2000–2012. doi: 10.1111/jcmm.16039
- Eloranta, S., Smedby, K. E., Dickman, P. W., and Andersson, T. M. (2021). Cancer survival statistics for patients and healthcare professionals - a tutorial of real-world data analysis. *J. Intern. Med.* 289, 12–28. doi: 10.1111/joim.13139
- Fang, Y. N., Huang, Z. L., Li, H., Tan, W. B., Zhang, Q. G., Wang, L., et al. (2018). LINC01116 promotes the progression of epithelial ovarian cancer via regulating cell apoptosis. *Eur. Rev. Med. Pharmacol. Sci.* 22, 5127–5133. doi: 10.26355/eurrev_201808_15707
- Fatma, H., Maurya, S. K., and Siddique, H. R. (2020). Epigenetic modifications of c-MYC: role in cancer cell reprogramming, progression and chemoresistance. *Semin. Cancer Biol.* doi: 10.1016/j.semcancer.2020.11.008 Online ahead of print.
- Grady, W. M., Yu, M., and Markowitz, S. D. (2021). Epigenetic alterations in the gastrointestinal tract: current and emerging use for biomarkers of cancer. *Gastroenterology* 160, 690–709. doi: 10.1053/j.gastro.2020.09.058
- Gupta, S. C., Awasthee, N., Rai, V., Chava, S., Gunda, V., and Challagundla, K. B. (2020). Long non-coding RNAs and nuclear factor- κ B crosstalk in cancer and other human diseases. *Biochim. Biophys. Acta Rev. Cancer* 1873:188316. doi: 10.1016/j.bbcan.2019.188316
- Hu, H. B., Chen, Q., and Ding, S. Q. (2018). LncRNA LINC01116 competes with miR-145 for the regulation of ESR1 expression in breast cancer. *Eur. Rev. Med. Pharmacol. Sci.* 22, 1987–1993. doi: 10.26355/eurrev_201804_14726
- Huang, X., Pan, L., Zuo, Z., Li, M., Zeng, L., Li, R., et al. (2021). LINC00842 inactivates transcription co-regulator PGC-1 α to promote pancreatic cancer malignancy through metabolic remodelling. *Nat. Commun.* 12:3830. doi: 10.1038/s41467-021-23904-23904
- Hussain, S., Tulsyan, S., Dar, S. A., Sisodiya, S., Abiha, U., Kumar, R., et al. (2021). Role of epigenetics in carcinogenesis: recent advancements in anticancer therapy. *Semin. Cancer Biol.* doi: 10.1016/j.semcancer.2021.06.023 Online ahead of print.
- Jantrapirom, S., Koonrunsesomboon, N., Yoshida, H., Candeias, M. M., Pruksakorn, D., and Lo Piccolo, L. (2021). Long noncoding RNA-dependent methylation of nonhistone proteins. *Wiley Interdiscip. Rev. RNA*. doi: 10.1002/wrna.1661 Online ahead of print.
- Jiang, H., Shi, X., Ye, G., Xu, Y., Xu, J., Lu, J., et al. (2019). Up-regulated long non-coding RNA DUXAP8 promotes cell growth through repressing Krüppel-like factor 2 expression in human hepatocellular carcinoma. *Onco. Targets Ther.* 12, 7429–7436. doi: 10.2147/ott.S214336
- Jiang, W., Xia, J., Xie, S., Zou, R., Pan, S., Wang, Z. W., et al. (2020). Long non-coding RNAs as a determinant of cancer drug resistance: towards the overcoming of chemoresistance via modulation of lncRNAs. *Drug Resist. Update* 50:100683. doi: 10.1016/j.drug.2020.100683
- Jin, F., Li, J., Zhang, Y. B., Liu, X., Cai, M., Liu, M., et al. (2021). A functional motif of long noncoding RNA Nron against osteoporosis. *Nat. Commun.* 12:3319. doi: 10.1038/s41467-021-23642-23647
- Jung, G., Hernández-Illán, E., Moreira, L., Balaguer, F., and Goel, A. (2020). Epigenetics of colorectal cancer: biomarker and therapeutic potential. *Nat. Rev. Gastroenterol. Hepatol.* 17, 111–130. doi: 10.1038/s41575-019-0230-y
- Katsushima, K., Lee, B., Kunhiraman, H., Zhong, C., Murad, R., Yin, J., et al. (2021). The long noncoding RNA lnc-HLX-2-7 is oncogenic in Group 3 medulloblastomas. *Neuro. Oncol.* 23, 572–585. doi: 10.1093/neuonc/noaa235
- Kotani, A., Ito, M., and Kudo, K. (2021). Non-coding RNAs and lipids mediate the function of extracellular vesicles in cancer cross-talk. *Semin. Cancer Biol.* 74, 121–133. doi: 10.1016/j.semcancer.2021.04.017
- Lai, C., Liu, L., Liu, Q., Wang, K., Cheng, S., Zhao, L., et al. (2021). Long noncoding RNA AVAN promotes antiviral innate immunity by interacting with TRIM25 and enhancing the transcription of FOXO3a. *Cell Death Differ.* doi: 10.1038/s41418-021-00791-792 Online ahead of print.
- Li, M., Yu, X., Zheng, Q., Zhang, Q., He, Y., and Guo, W. (2021a). Promising role of long non-coding RNA PCAT6 in malignancies. *Biomed. Pharmacother.* 137:111402. doi: 10.1016/j.biopha.2021.111402
- Li, Z., Li, X., Xu, D., Chen, X., Li, S., Zhang, L., et al. (2021c). An update on the roles of circular RNAs in osteosarcoma. *Cell Prolif.* 54:e12936. doi: 10.1111/cpr.12936
- Li, R., Ruan, Q., Zheng, J., Zhang, B., and Yang, H. (2021b). LINC01116 promotes doxorubicin resistance in osteosarcoma by epigenetically silencing miR-424-5p and inducing epithelial-mesenchymal transition. *Front. Pharmacol.* 12:632206. doi: 10.3389/fphar.2021.632206
- Liang, W., Wu, J., and Qiu, X. (2021). LINC01116 facilitates colorectal cancer cell proliferation and angiogenesis through targeting EZH2-regulated TPM1. *J. Transl. Med.* 19:45. doi: 10.1186/s12967-021-02707-2707
- Lin, C., He, H., Liu, H., Li, R., Chen, Y., Qi, Y., et al. (2019). Tumour-associated macrophages-derived CXCL8 determines immune evasion through autonomous PD-L1 expression in gastric cancer. *Gut* 68, 1764–1773. doi: 10.1136/gutjnl-2018-316324
- Liu, Y., Qiao, Z., Gao, J., Wu, F., Sun, B., Lian, M., et al. (2021b). Hydroxyapatite-Bovine serum albumin-paclitaxel nanoparticles for locoregional treatment of osteosarcoma. *Adv. Healthc. Mater.* 10:e2000573. doi: 10.1002/adhm.202000573
- Liu, W., Liang, F., Yang, G., and Xian, L. (2021a). LncRNA LINC01116 sponges miR-93-5p to promote cell invasion and migration in small cell lung cancer. *BMC Pulm. Med.* 21:50. doi: 10.1186/s12890-020-01369-1363
- Liu, X., Chen, Y., Li, Y., Petersen, R. B., and Huang, K. (2019). Targeting mitosis exit: a brake for cancer cell proliferation. *Biochim. Biophys. Acta Rev. Cancer* 1871, 179–191. doi: 10.1016/j.bbcan.2018.12.007
- Lou, J., Wang, P., Chang, K., Wang, G., Geng, X., Wu, Y., et al. (2021). Knocking down LINC01116 can inhibit the regulation of TGF- β through miR-774-5p axis and inhibit the occurrence and development of glioma. *Am. J. Transl. Res.* 13, 5702–5719.
- Lu, K. H., Lu, E. W., Lin, C. W., Yang, J. S., and Yang, S. F. (2020). New insights into molecular and cellular mechanisms of zoledronate in human osteosarcoma. *Pharmacol. Ther.* 214:107611. doi: 10.1016/j.pharmthera.2020.107611
- Luo, Y., Zheng, S., Wu, Q., Wu, J., Zhou, R., Wang, C., et al. (2021). Long noncoding RNA (lncRNA) EIF3J-DT induces chemoresistance of gastric cancer via autophagy activation. *Autophagy* doi: 10.1080/15548627.2021.1901204 Online ahead of print.
- Ma, Y., Liu, Y., Teng, L., Luo, E., Liu, D., Zhou, F., et al. (2021). Zi shen decoction inhibits growth and metastasis of lung cancer via regulating the AKT/GSK-3 β /Catenin pathway. *Oxid. Med. Cell Longev.* 2021:6685282. doi: 10.1155/2021/6685282
- Meng, L., Xing, Z., Guo, Z., and Liu, Z. (2020). LINC01106 post-transcriptionally regulates ELK3 and HOXD8 to promote bladder cancer progression. *Cell Death Dis.* 11:1063. doi: 10.1038/s41419-020-03236-3239
- Mondal, I., and Kulshreshtha, R. (2021). Potential of microRNA based diagnostics and therapeutics in glioma: a patent review. *Expert Opin. Ther. Pat.* 31, 91–106. doi: 10.1080/13543776.2021.1837775
- Mu, L., Ding, K., Tu, R., and Yang, W. (2021). Identification of 4 immune cells and a 5-lncRNA risk signature with prognosis for early-stage lung adenocarcinoma. *J. Transl. Med.* 19:127. doi: 10.1186/s12967-021-02800-x
- Olivero, C. E., Martínez-Terroba, E., Zimmer, J., Liao, C., Tesfaye, E., Hooshdar, N., et al. (2020). p53 activates the long noncoding RNA Pvt1b to inhibit Myc and suppress tumorigenesis. *Mol. Cell* 77, 761–774.e8. doi: 10.1016/j.molcel.2019.12.014

- Petridis, P. D., Horenstein, C., Pereira, B., Wu, P., Samanamud, J., Marie, T., et al. (2021). BOLD asynchrony elucidates tumor burden in IDH-Mutated gliomas. *Neuro Oncol.* doi: 10.1093/neuonc/noab154 Online ahead of print.
- Puliga, E., Corso, S., Pietrantonio, F., and Giordano, S. (2021). Microsatellite instability in Gastric cancer: between lights and shadows. *Cancer Treat. Rev.* 95:102175. doi: 10.1016/j.ctrv.2021.102175
- Ramnarine, V. R., Kobelev, M., Gibb, E. A., Nouri, M., Lin, D., Wang, Y., et al. (2019). The evolution of long noncoding RNA acceptance in prostate cancer initiation, progression, and its clinical utility in disease management. *Eur. Urol.* 76, 546–559. doi: 10.1016/j.eururo.2019.07.040
- Ren, P., Chang, L., Hong, X., Xing, L., and Zhang, H. (2021). Long non-coding RNA LINC01116 is activated by EGR1 and facilitates lung adenocarcinoma oncogenicity via targeting miR-744-5p/CDCA4 axis. *Cancer Cell Int.* 21:292. doi: 10.1186/s12935-021-01994-w
- Seow, H., Tanuseputro, P., Barbera, L., Earle, C., Guthrie, D., Isenberg, S., et al. (2020). Development and validation of a prognostic survival model with patient-reported outcomes for patients with cancer. *JAMA Netw. Open* 3:e201768. doi: 10.1001/jamanetworkopen.2020.1768
- Shang, B., Li, Z., Li, M., Jiang, S., Feng, Z., Cao, Z., et al. (2021). Silencing LINC01116 suppresses the development of lung adenocarcinoma via the AKT signaling pathway. *Thorac. Cancer* 12, 2093–2103. doi: 10.1111/1759-7714.14042
- Shu, B., Lin, L., Wu, B., Huang, E., Wang, Y., Li, Z., et al. (2021). A pocket-sized device automates multiplexed point-of-care RNA testing for rapid screening of infectious pathogens. *Biosens. Bioelectron.* 181:113145. doi: 10.1016/j.bios.2021.113145
- Shuai, Y., Ma, Z., Liu, W., Yu, T., Yan, C., Jiang, H., et al. (2020). TEAD4 modulated LncRNA MNX1-AS1 contributes to gastric cancer progression partly through suppressing BTG2 and activating BCL2. *Mol. Cancer* 19:6. doi: 10.1186/s12943-019-1104-1101
- Su, X., Zhang, J., Luo, X., Yang, W., Liu, Y., Liu, Y., et al. (2019). LncRNA LINC01116 promotes cancer cell proliferation, migration and invasion in gastric cancer by positively interacting with lncRNA CASC11. *Onco Targets Ther.* 12, 8117–8123. doi: 10.2147/ott.S208133
- Świerczyński, M., Szymaszkiewicz, A., Fichna, J., and Zielińska, M. (2021). New insights into molecular pathways in colorectal cancer: adiponectin, interleukin-6 and opioid signaling. *Biochim. Biophys. Acta Rev. Cancer* 1875:188460. doi: 10.1016/j.bbcan.2020.188460
- Tanabe, R., Miyazono, K., Todo, T., Saito, N., Iwata, C., Komuro, A., et al. (2021). PRRX1 induced by BMP signaling decreases tumorigenesis by epigenetically regulating glioma-initiating cell properties via DNA methyltransferase 3A. *Mol. Oncol.* doi: 10.1002/1878-0261.13051 Online ahead of print.
- Tang, Z., Kang, B., Li, C., Chen, T., and Zhang, Z. (2019). GEPIA2: an enhanced web server for large-scale expression profiling and interactive analysis. *Nucleic Acids Res.* 47, W556–W560. doi: 10.1093/nar/gkz430
- Teng, L., Feng, Y. C., Guo, S. T., Wang, P. L., Qi, T. F., Yue, Y. M., et al. (2021). The pan-cancer lncRNA PLANE regulates an alternative splicing program to promote cancer pathogenesis. *Nat. Commun.* 12:3734. doi: 10.1038/s41467-021-24099-24094
- Toden, S., Zumwalt, T. J., and Goel, A. (2021). Non-coding RNAs and potential therapeutic targeting in cancer. *Biochim. Biophys. Acta Rev. Cancer* 1875:188491. doi: 10.1016/j.bbcan.2020.188491
- Tran, N. T., Su, H., Khodadadi-Jamayran, A., Lin, S., Zhang, L., Zhou, D., et al. (2016). The AS-RBM15 lncRNA enhances RBM15 protein translation during megakaryocyte differentiation. *EMBO Rep.* 17, 887–900. doi: 10.15252/embr.201541970
- Tu, J., Fang, Y., Han, D., Tan, X., Jiang, H., Gong, X., et al. (2021). Activation of nuclear factor- κ B in the angiogenesis of glioma: insights into the associated molecular mechanisms and targeted therapies. *Cell Prolif.* 54:e12929. doi: 10.1111/cpr.12929
- Wang, W., Hu, S., Gu, Y., Yan, Y., Stovall, D. B., Li, D., et al. (2020d). Human MYC G-quadruplex: from discovery to a cancer therapeutic target. *Biochim. Biophys. Acta Rev. Cancer* 1874:188410. doi: 10.1016/j.bbcan.2020.188410
- Wang, T., Cao, L., Dong, X., Wu, F., De, W., Huang, L., et al. (2020c). LINC01116 promotes tumor proliferation and neutrophil recruitment via DDX5-mediated regulation of IL-1 β in glioma cell. *Cell Death Dis.* 11:302. doi: 10.1038/s41419-020-2506-2500
- Wang, H., Lu, B., Ren, S., Wu, F., Wang, X., Yan, C., et al. (2020a). Long noncoding RNA LINC01116 contributes to gefitinib resistance in non-small cell lung cancer through regulating IFI44. *Mol. Ther. Nucleic Acids* 19, 218–227. doi: 10.1016/j.omtn.2019.10.039
- Wang, J., Gao, J., Chen, Q., Zou, W., Yang, F., Wei, C., et al. (2020b). LncRNA LINC01116 contributes to cisplatin resistance in lung adenocarcinoma. *Onco Targets Ther.* 13, 9333–9348. doi: 10.2147/ott.S244879
- Wang, J., Yang, J., Li, D., and Li, J. (2021). Technologies for targeting DNA methylation modifications: basic mechanism and potential application in cancer. *Biochim. Biophys. Acta Rev. Cancer* 1875:188454. doi: 10.1016/j.bbcan.2020.188454
- Wieszczy, P., Kaminski, M. F., Franczyk, R., Loberg, M., Kobiela, J., Rupinska, M., et al. (2020). Colorectal cancer incidence and mortality after removal of adenomas during screening colonoscopies. *Gastroenterology* 158, 875–883.e5. doi: 10.1053/j.gastro.2019.09.011
- Wu, J., Chen, Z., Zhang, L., Cao, J., Li, X., Gong, Z., et al. (2020). Knockdown of LINC01116 inhibits cell migration and invasion in head and neck squamous cell carcinoma through epithelial-mesenchymal transition pathway. *J. Cell. Biochem.* 121, 867–875. doi: 10.1002/jcb.29331
- Xiang, Y., Liao, X. H., Yu, C. X., Yao, A., Qin, H., Li, J. P., et al. (2017). MiR-93-5p inhibits the EMT of breast cancer cells via targeting MKL-1 and STAT3. *Exp. Cell Res.* 357, 135–144. doi: 10.1016/j.yexcr.2017.05.007
- Xing, H., Sun, H., and Du, W. (2020). LINC01116 accelerates nasopharyngeal carcinoma progression based on its enhancement on MYC transcription activity. *Cancer Med.* 9, 269–277. doi: 10.1002/cam4.2624
- Yin, D., Lu, X., Su, J., He, X., De, W., Yang, J., et al. (2018). Long noncoding RNA AFAP1-AS1 predicts a poor prognosis and regulates non-small cell lung cancer cell proliferation by epigenetically repressing p21 expression. *Mol. Cancer* 17:92. doi: 10.1186/s12943-018-0836-837
- Yu, S., Yu, H., Zhang, Y., Liu, C., Zhang, W., and Zhang, Y. (2021). Long non-coding RNA LINC01116 acts as an oncogene in prostate cancer cells through regulation of miR-744-5p/UBE2L3 axis. *Cancer Cell Int.* 21:168. doi: 10.1186/s12935-021-01843-w
- Yuan, J., Xing, H., Li, Y., Song, Y., Zhang, N., Xie, M., et al. (2021). EPB41 suppresses the Wnt/ β -catenin signaling in non-small cell lung cancer by sponging ALDOC. *Cancer Lett.* 499, 255–264. doi: 10.1016/j.canlet.2020.11.024
- Zaborowski, A. M., Abdile, A., Adamina, M., Aigner, F., D'allens, L., Allmer, C., et al. (2021). Characteristics of early-onset vs late-onset colorectal cancer: a review. *JAMA Surg.* 156, 865–874. doi: 10.1001/jamasurg.2021.2380
- Zeng, L., Lyu, X., Yuan, J., Wang, W., Zhao, N., Liu, B., et al. (2020). Long non-coding RNA LINC01116 is overexpressed in lung adenocarcinoma and promotes tumor proliferation and metastasis. *Am. J. Transl. Res.* 12, 4302–4313.
- Zeng, L., Lyu, X., Yuan, J., Wang, W., Zhao, N., Liu, B., et al. (2021). Erratum: long non-coding RNA LINC01116 is overexpressed in lung adenocarcinoma and promotes tumor proliferation and metastasis. *Am. J. Transl. Res.* 13, 3919–3920.
- Zhang, B., Yu, L., Han, N., Hu, Z., Wang, S., Ding, L., et al. (2018). LINC01116 targets miR-520a-3p and affects IL6R to promote the proliferation and migration of osteosarcoma cells through the Jak-stat signaling pathway. *Biomed. Pharmacother.* 107, 270–282. doi: 10.1016/j.biopha.2018.07.119
- Zhang, B., Yu, L., Han, N., Hu, Z., Wang, S., Ding, L., et al. (2021a). Corrigendum to “LINC01116 targets miR-520a-3p and affects IL6R to promote the proliferation and migration of osteosarcoma cells through the Jak-stat signaling pathway” [Biomed. Pharmacother. 107 (2018) 270–282]. *Biomed. Pharmacother.* 133:110893. doi: 10.1016/j.biopha.2020.110893
- Zhang, F., Yang, Y., Chen, X., et al. (2021b). The long non-coding RNA β Faar regulates islet β -cell function and survival during obesity in mice. *Nat. Commun.* 12:3997. doi: 10.1038/s41467-021-24302-24306
- Zhang, K., Zhang, M., Luo, Z., Wen, Z., and Yan, X. (2020). The dichotomous role of TGF- β in controlling liver cancer cell survival and proliferation. *J. Genet. Genomics* 47, 497–512. doi: 10.1016/j.jgg.2020.09.005
- Zhang, Z. F., Xu, H. H., Hu, W. H., Hu, T. Y., and Wang, X. B. (2019). LINC01116 promotes proliferation, invasion and migration of osteosarcoma cells by silencing p53 and EZH2. *Eur. Rev. Med. Pharmacol. Sci.* 23, 6813–6823. doi: 10.26355/eurrev_201908_18720
- Zhao, Y., Wang, C., and Goel, A. (2021). Role of gut microbiota in epigenetic regulation of colorectal Cancer. *Biochim. Biophys. Acta Rev. Cancer* 1875:188490. doi: 10.1016/j.bbcan.2020.188490

- Zheng, C., Tang, F., Min, L., Hornicek, F., Duan, Z., and Tu, C. (2020). PTEN in osteosarcoma: recent advances and the therapeutic potential. *Biochim. Biophys. Acta Rev. Cancer* 1874:188405. doi: 10.1016/j.bbcan.2020.188405
- Zheng, Q., Zhang, Q., Yu, X., He, Y., and Guo, W. (2021). FENDRR: a pivotal, cancer-related, long non-coding RNA. *Biomed. Pharmacother.* 137:111390. doi: 10.1016/j.biopha.2021.111390
- Zhong, G. X., Ye, C. L., Wei, H. X., Yang, L. Y., Wei, Q. X., Liu, Z. J., et al. (2021a). Ultrasensitive detection of RNA with single-base resolution by coupling electrochemical sensing strategy with chimeric DNA probe-aided ligase chain reaction. *Anal. Chem.* 93, 911–919. doi: 10.1021/acs.analchem.0c03563
- Zhong, Y., Yang, L., Xiong, F., He, Y., Tang, Y., Shi, L., et al. (2021b). Long non-coding RNA AFAP1-AS1 accelerates lung cancer cells migration and invasion by interacting with SNIP1 to upregulate c-Myc. *Signal Transduct. Target Ther.* 6:240. doi: 10.1038/s41392-021-00562-y

Conflict of Interest: The authors declare that the research was conducted in the absence of any commercial or financial relationships that could be construed as a potential conflict of interest.

Publisher's Note: All claims expressed in this article are solely those of the authors and do not necessarily represent those of their affiliated organizations, or those of the publisher, the editors and the reviewers. Any product that may be evaluated in this article, or claim that may be made by its manufacturer, is not guaranteed or endorsed by the publisher.

Copyright © 2021 Xu, Yu, Zhang, Zheng, Sun, He and Guo. This is an open-access article distributed under the terms of the Creative Commons Attribution License (CC BY). The use, distribution or reproduction in other forums is permitted, provided the original author(s) and the copyright owner(s) are credited and that the original publication in this journal is cited, in accordance with accepted academic practice. No use, distribution or reproduction is permitted which does not comply with these terms.



A miR-129-5P/ARID3A Negative Feedback Loop Modulates Diffuse Large B Cell Lymphoma Progression and Immune Evasion Through Regulating the PD-1/PD-L1 Checkpoint

Weili Zheng[†], Guilan Lai[†], Qiaochu Lin, Mohammed Awal Issah, Haiying Fu and Jianzhen Shen*

OPEN ACCESS

Edited by:

Zong Sheng Guo,
Roswell Park Comprehensive Cancer
Center, United States

Reviewed by:

Nissar Ahmad Wani,
Central University of Kashmir, India
Prasanna Ekambaram,
University of Pittsburgh, United States

*Correspondence:

Jianzhen Shen
shenjzhen@fjmu.edu.cn

[†] These authors have contributed
equally to this work

Specialty section:

This article was submitted to
Molecular and Cellular Oncology,
a section of the journal
Frontiers in Cell and Developmental
Biology

Received: 03 July 2021

Accepted: 05 October 2021

Published: 27 October 2021

Citation:

Zheng W, Lai G, Lin Q, Issah MA,
Fu H and Shen J (2021) A
miR-129-5P/ARID3A Negative
Feedback Loop Modulates Diffuse
Large B Cell Lymphoma Progression
and Immune Evasion Through
Regulating the PD-1/PD-L1
Checkpoint.
Front. Cell Dev. Biol. 9:735855.
doi: 10.3389/fcell.2021.735855

Fujian Provincial Key Laboratory on Hematology, Fujian Medical Center of Hematology, Fujian Institute of Hematology, Clinical
Research Center for Hematological Malignancies of Fujian Province, Fujian Medical University Union Hospital, Fuzhou, China

The activated B cell (ABC) and germinal center B cell (GCB) subtypes of diffuse large B cell lymphoma (DLBCL) have different gene expression profiles and clinical outcomes, and miRNAs have been reported to play important roles in tumorigenesis, progression, and metastasis. This study aimed to explore the differentially expressed miRNAs and target genes in the two main subtypes of DLBCL. Hub miRNAs were identified by constructing a regulatory network, and *in vitro* experiments and peripheral blood samples of DLBCL were used to explore the functions and mechanisms of differential miRNAs and mRNAs. Differentially expressed miRNAs and genes associated with the two DLBCL subtypes were identified using GEO datasets. Weighted gene co-expression network analysis shows that one gene module was associated with a better prognosis of patients with the GCB subtype. Through the construction of a regulatory network and qPCR verification of clinical samples and cell lines, miR-129-5p was identified as an important differential miRNA between the ABC and GCB subtypes. The negative relationship between miR-129-5p and ARID3A in DLBCL was confirmed using luciferase reporter assays. Overexpression of miR-129-5p and knockdown of ARID3A inhibited the proliferation of SU-DHL-2 (ABC-type) cells and promoted their apoptosis through the JAK and STAT6 signaling pathways. In addition, inhibition of miR-129-5p and overexpression of ARID3A promoted the proliferation and reduced apoptosis of DB and SU-DHL-6 (GCB-type) cells. Inhibition of miR-129-5p and overexpression of ARID3A in DB and SU-DHL-6 promoted immune escape by increasing PD-L1 expression, which was transcriptionally activated by ARID3A. In conclusion, we showed for the first time that the miR-129-5P/ARID3A negative feedback loop modulates DLBCL progression and immune evasion by regulating PD-1/PD-L1.

Keywords: miR-129-5p, ARID3a, PD-1/PD-L1, lymphoma, ABC-type

INTRODUCTION

Diffuse large B cell lymphoma (DLBCL) is the most common form of malignant lymphoma, accounting for 25–35% of all non-Hodgkin lymphomas (Miao et al., 2019). R-CHOP chemotherapy has improved outcomes for DLBCL patients; however, approximately 40% of them relapse or fail to respond to treatment (Li M. et al., 2019). With the development of high-throughput technologies, the genomic profile of DLBCL has been widely characterized. DLBCL is classified into two molecular subtypes based on cell of origin (COO), germinal center B cell (GCB)-like, and activated B cell (ABC)-like (Alizadeh et al., 2000), which is also associated with different clinical outcomes. It has been reported that the ABC subtype is related to inferior chemotherapeutic responses and clinical outcomes compared to the GCB subtype (Fu et al., 2008) following R-CHOP therapy. Therefore, various studies have identified miRNA- (Yang et al., 2018) or lncRNA-focused (Zhou et al., 2017) prognostic biomarkers or signatures between different COO subtypes.

MicroRNAs, comprised of 18–25 nucleotides, widely participate in many biological processes to regulate gene expression by specifically combining to mRNAs, promoting their degradation, and eventually reducing translation (Bruch et al., 2019). Dysregulation of miRNAs has been found to play a crucial role in tumorigenesis, tumor progression, and metastasis by negatively regulating tumor-suppressive protein-coding genes (Wong et al., 2018). In addition, several miRNAs modulate the sensitivity of tumor cells to anticancer drugs, which affects treatment response and prognosis. For example, miR145-3p enhances bortezomib sensitivity in multiple myeloma by promoting apoptosis and autophagy (Wu et al., 2019). Additionally, miR-34a is associated with a superior response to doxorubicin in DLBCL (Marques et al., 2016). Hence, miRNAs have been evaluated as novel diagnostic and prognostic biomarkers in various malignancies, including DLBCL (Marchesi et al., 2018). Moreover, some studies have shown that miRNAs can distinguish between GCB and ABC subtypes (Larrabeiti-Etxebarria et al., 2019).

ARID3a/Bright, an AT-rich interacting domain family of DNA-binding proteins, was originally discovered because of its ability to enhance antigen-ABC immunoglobulin gene transcription. ARID3a forms a dimer with DNA through an arid zone or an a/t-rich interaction domain. Overexpression of ARID3a leads to skewing of mature B cell subsets and changes in gene expression patterns of follicular B cells, whereas loss of its function leads to the loss of B1 lineage B cells and defects in hematopoiesis (Nixon et al., 2004). ARID3A expression is tightly regulated, and B cell-restricted and abnormal expression of ARID3A may result in malignancy and proliferative capacity (Puissegur et al., 2012).

Programmed cell death 1 ligand 1 (PD-L1), also known as cluster of differentiation 274 or B7 homolog 1 (Butte et al., 2007), plays an important role in tumor progression and survival by evading immune surveillance when interacting with PD-1 to regulate tumor-specific T cells. PD-L1 overexpression in tumor cells confers protection against CD8⁺ cell damage, leading to immune evasion (Freeman et al., 2002). Blocking the

PD-1/PD-L1 checkpoint by antibodies is therefore considered an effective method for tumor immunotherapy, including lymphoma (Sun et al., 2018).

In this study, we aimed to screen miRNAs and target genes in two main subtypes of DLBCL through bioinformatics and experiments, and to explore their functions and mechanisms.

MATERIALS AND METHODS

Acquisition of Gene Expression Profiles and Identification of Differentially Expressed Genes

MiRNA (GSE15250) and mRNA (GSE56313 and GSE32918) expression data from DLBCL patients were acquired from the GEO database. Data from 23 ABC-type and 29 GCB-type patients were obtained dataset GSE56313, and data from 80 ABC-type and 120 GCB-type patients were obtained from dataset GSE32918. The miRNA dataset GSE15250, which included data from 20 ABC-type and 20 GCB-type patients, was analyzed. Differentially expressed miRNAs and mRNAs between ABC-type and GCB-type patients were identified using the LIMMA package in R software.

Weighted Gene Co-expression Network Analysis

After obtaining differentially expressed genes (DEGs) from the GSE32918 database, the expression of these genes was analyzed using the weighted gene co-expression network analysis (WGCNA) package in R software (Langfelder and Horvath, 2008). WGCNA was used to construct a weighted adjacency matrix that expressed the connection strength of gene pairs by calculating Pearson's correlation. Then, the appropriate soft threshold power β was selected using the scale-free topology criterion and the adjacency matrix was transformed into a topological overlapping matrix. Topological overlapping points were applied to perform hierarchical clustering. Mean linkage hierarchical clustering was applied to generate a clustering tree, and the dendrogram was defined as Module (Langfelder et al., 2008).

Construction of the Regulatory Network

A regulatory network of the differentially expressed miRNAs and mRNAs was constructed using the miRMap (Vejnar and Zdobnov, 2012), miRanda (Betel et al., 2008), miRDB (Wong and Wang, 2015), TargetScan (Agarwal et al., 2015), and miTarBase (Chou et al., 2018) databases. Only the miRNA-mRNA pairs present in at least two databases were considered significant and were preserved for further investigation. Eventually, cytoscape (Shannon et al., 2003) was used for network visualization.

Cell Culture

Human B-lymphoma cell lines (ABC subtype) SU-DHL-2, (GCB subtype) DB were obtained from Procell Life (Wuhan, China), and (GCB subtype) SU-DHL-6 were obtained from American Type Culture Collection (ATCC, Manassas, VA, United States),

and were grown in RPMI-1640 (Invitrogen, Carlsbad, CA, United States) containing 10% fetal bovine serum (FBS; Gibco, Waltham, MA, United States). Human renal epithelial cells (293T) were gifted by the Fujian Institute of Hematology and grown in DMEM (Invitrogen) containing 10% FBS. All cells were cultured in a humidified incubator at 37°C and 5% CO₂.

Cell Transfection

Specific shRNAs and oeRNAs against ARID3A (sh-ARID3A, oe-ARID3A) and sh-NC and oe-NC were obtained using pLVshRNA and pCDH-CMV vector designed by Miaolingbio (P0268, P0684, Wuhan, China). MiR-129-5p mimic/inhibitor and NC mimic/inhibitor were generated by Genechem (Shanghai, China). These plasmids were transfected into DLBCL cells using Lipofectamine 3000.

Quantitative Real-Time Polymerase Chain Reaction

Total RNA from peripheral blood and cells was extracted by Trizol and purified by chloroform and ethanol. Reverse transcription for miRNA and mRNA based on All-in-One™ miRNA qRT-PCR Detection Kit (QP115, GeneCopoeia, United States) and Revert Aid First Strand cDNA Synthesis Kit (K1621, Thermo Fisher Scientific, United States), respectively. Relative expression levels were detected by FastStart Universal SYBR Green Master (Roche) and Biosystems 7500 Real-Time PCR Systems and calculated by 2^{−ΔΔCt} method. miRNA and mRNA were normalized to U6 and GAPDH levels, respectively. The experiment was repeated three times. Primers used for qRT-PCR analysis are listed in **Supplementary Table 1**.

Assessment of Cell Proliferation and Apoptosis

Cell counting assays at different times were used to assess cell proliferation ability. Transfected cells were seeded in 24-well plates. Following incubation for 0, 24, 72, or 96 h, homogenized single cell suspension and trypan blue were mixed 1:1. The cells were counted directly under a light microscope with the inclusion of three counting replicates per well. An APC Annexin V Apoptosis Detection kit (Biolegend, San Diego, CA, United States) was used to analyze cells following the manufacturer's instructions. A BD Accuri C6 flow cytometer was used to analyze the samples.

In vitro Co-culture System and Flow Cytometry

In vitro co-culture was performed using a Transwell cell incubator (Millipore Corporation, Billerica, MA, United States). In the co-culture system, lymphoma cells were placed in the upper cavity and immune cells in the lower cavity, with both cells in direct contact. Immune cells were mononuclear cells (including lymphocytes and monocytes) isolated from peripheral blood of healthy volunteers using Ficoll by density gradient centrifugation. After 48-h incubation, the immune cells were centrifuged at 500 × g, 4°C for 5 min. Then, the cells were first blocked with mouse IgG mAb and then surface-stained

with anti-CD8 (555369, BD) and anti-PD-1 (367404, Biolegend) antibody at 4°C for 20 min in the dark. The cells were washed twice with FACS and were then loaded for data collection. At least 200,000 events were measured using BD Accuri C6 flow cytometer. An isotype control was used for the antibodies. The data were analyzed using the FlowJo software (TriStar Inc., El Segundo, CA, United States). The gating strategy for the ICS assay is shown in **Supplementary Figure 1**. These results are representative from six independent experiments.

Luciferase Report Assay

The pmirGLO dual-luciferase vector (P0198, Miaolingbio, China), including the ARID3A and miR-129-5p mimics, were transfected into 293T cells with Lipofectamine 3000. The PD-L1 promoter WT/Mut was included into the pGL3-basic vector (P0193, Miaolingbio, China) and transfected into 293T cells with oe-ARID3A or oe-NC. Luciferase activity was measured using the Dual-Luciferase Reporter Assay System (E2920, Promega), and a Glomax 96 spectrophotometer was used to detect the fluorescence intensity.

Western Blot Analysis

Briefly, cells were lysed with RIPA buffer (keyGEN, China) containing protease inhibitors. 20 μg of protein per sample was loaded, run on 10% SDS-polyacrylamide gel electrophoresis, and transferred to a PVDF membrane. After being blocked with 5% bovine serum albumin, membranes were incubated with primary antibodies including PD-L1 (66248, Proteintech), JAK1(3344T, Cell signaling technology), STAT6 (51073, Proteintech) GAPDH (ab8245, Abcam) at 4°C overnight, 1 h of incubation with secondary antibodies and detected by FlourChemE system (Protein Simple).

Survival Analysis

DLBCL patients were divided into low-and high-expression groups based on their gene expression profiles. Kaplan-Meier survival curves were drawn to demonstrate the relevance between expression of DEGs and overall survival (OS) of patients, which was tested by the log-rank test.

Statistical Analysis

Student's *t*-test or one-way analysis of variance were implemented. Pearson correlation analysis was used to determine the relationship between miR-129-5p, ARID3A, and CD8⁺ T cells. Statistical significance was set at *P* < 0.05.

RESULTS

Identification of Differentially Expressed Genes Associated With Clinical Molecular Subtypes

We compared the gene expression profiles of GSE56313 and GSE32918 datasets and identified DEGs associated with two major clinical molecular subtypes of DLBCL (ABC and GCB). Of these, 331 genes were downregulated and 422 upregulated

in the GSE56313 dataset, and 176 genes were downregulated and 278 upregulated in the GSE32918 dataset (**Figures 1A,B**). The miRNA dataset GSE15250 was also analyzed, finding 171 downregulated and 129 upregulated miRNAs related to different DLBCL subtypes (**Figure 1C**). By analyzing the intersection of the DEGs, 115 common DEGs were identified, which were named as differentially intersected genes (DIGs) (**Figure 1D** and **Supplementary Table 2**).

Weighted Gene Co-expression Network Analysis Network Construction

We conducted WGCNA based on 454 DEGs and survival data from the GSE32918 dataset. Hierarchical clustering of samples based on Euclidean distance calculated using log10 was converted (**Figure 1E**). By merging modules with high similarity, we identified five different modules of co-expressed genes that were drawn in different colors (**Figure 1F**). Among the five modules, the blue module was significantly correlated with good survival status of GCB subtype patients compared to ABC subtype patients, with Pearson $r = 0.66$ ($p = 2e^{-26}$). There were 124 genes in the blue module, which are likely associated with a better prognosis of patients of the GCB subtype. These 124 significant genes were intersected with DEGs from the GSE56313 dataset to generated modular intersection genes (MIGs, **Supplementary Table 3**), which were selected for subsequent analysis.

Regulatory Networks of Modular Intersection Genes

Construction of regulatory networks of MIGs was performed based on the correlation between differentially expressed miRNAs and target genes using Cytoscape. A total of 21 upregulated miRNAs, 35 downregulated miRNAs, and 39 matched mRNAs were identified in comparison to the GCB and ABC subtypes (**Figure 1G** and **Supplementary Table 4**). Among them, hsa-miR-142-5p possessed the most regulatory target genes ($n = 10$). In addition, hsa-miR-199b-5p and hsa-miR-129-5p had nine target genes. Therefore, these miRNAs were considered to be the key miRNA differences between the ABC and GCB subtypes.

Validation of Differentially Expressed miRNAs for Clinical Subtypes in Diffuse Large B Cell Lymphoma Samples

The expression of the three important miRNAs mentioned above, hsa-miR-142-5p, hsa-miR-199b-5p, and hsa-miR-129-5p, in DLBCL patients with ABC and GCB subtypes was detected using qRT-PCR (**Figures 2A–C**). Except for hsa-miR-199b-5p, the miRNAs were highly expressed in the GCB subtype compared to the ABC subtype. In addition, the expression of the three miRNAs in the DLBCL cell line was investigated (**Figures 2D–F**). The results demonstrate that hsa-miR-129-5p was expressed at significantly higher levels in the DB and SU-DHL-6 (GCB subtype) cell lines than in the SU-DHL-2 (ABC subtype). According to the above results, hsa-miR-129-5p has nine target genes, of which ARID3A has been reported to be involved in progression of a variety of tumors (Ma et al., 2017; Dausinas et al., 2020; Tang et al., 2020). To identify the role of ARID3A in

DLBCL subtypes, we also explored its expression in the peripheral blood of DLBCL patients and in DLBCL cell lines. Conversely, ARID3A was significantly increased in ABC subtype DLBCL patients and in the SU-DHL-2 cell line, in contrast to the GCB subtype (**Figures 2G,H**).

A Negative Regulatory Feedback Loop Between miR-129-5p and ARID3A in Diffuse Large B Cell Lymphoma

To detect the detailed relationship between miR-129-5p and ARID3A, the site of miR-129-5p for ARID3A was predicted, mutated, and evaluated in dual-luciferase reporter gene assays (**Figure 3A**). Overexpression of miR-129-5p weakened the luciferase activity of ARID3A WT (wild-type), but did not influence the luciferase activity of ARID3A Mut (mutation), demonstrating that miR-129-5p affects ARID3A at the predicted binding site (**Figure 3B**). Pearson correlation coefficient analysis shows a negative interaction between miR-129-5p and ARID3A in DLBCL samples, although the difference was not statistically significant (**Figure 3C**). Furthermore, the reciprocal relationship between miR-129-5p and ARID3A was verified in DLBCL cells. After confirming the inhibition and overexpression of miR-129-5p in DLBCL cells via qRT-PCR (**Figure 3D**), ARID3A was found to be downregulated in miR-129-5p-overexpressing SU-DHL-2 cells and upregulated in miR-129-5p-knockdown DB and SU-DHL-6 cells (**Figure 3E**). We conclude that miR-129-5p and ARID3A form a negative regulatory feedback loop in DLBC.

Effect of miR-129-5p and ARID3A on Diffuse Large B Cell Lymphoma Proliferation and Apoptosis

Based on the above results, the high expression of miR-129-5p was considered a better prognostic factor for GCB subtype DLBCL compared to the ABC subtype. To further determine the specific mechanism, the ABC subtype SU-DHL-2 cells were transfected with miR-129-5p mimics and the GCB subtype DB and SU-DHL-6 cells with the miR-129-5p inhibitor. The results show that the proliferation ability of SU-DHL-2 cells was significantly stronger than that of DB and SU-DHL-6 cells. Meanwhile, overexpression of miR-129-5p impaired the proliferation ability of SU-DHL-2 cells. In contrast, inhibition of miR-129-5p promoted the proliferation of DB and SU-DHL-6 cells (**Figure 3F**). Cell apoptosis analysis shows that miR-129-5p overexpression in SU-DHL-2 cells resulted in a significantly increase in the number of apoptotic cells compared to control cells (8.29% vs. 5.38%, $P = 0.0018$), whereas knockdown of miR-129-5p in DB and SU-DHL-6 cells significantly decreased the percentage of apoptotic cells (7.14% vs. 3.03% and $P = 0.0002$, 7.89% vs. 3.22% and $P < 0.0001$, respectively, **Figure 3G**). We subsequently suppressed ARID3A expression levels in SU-DHL-2 cells and enhanced it in DB and SU-DHL-6 cells, which was verified by qRT-PCR (**Figure 4A**). The results show that the proliferation ability of SU-DHL-2 cells decreased and the number of apoptotic cells remarkably increased following ARID3A knockdown (4.34% vs. 39.97% and $P < 0.0001$). In

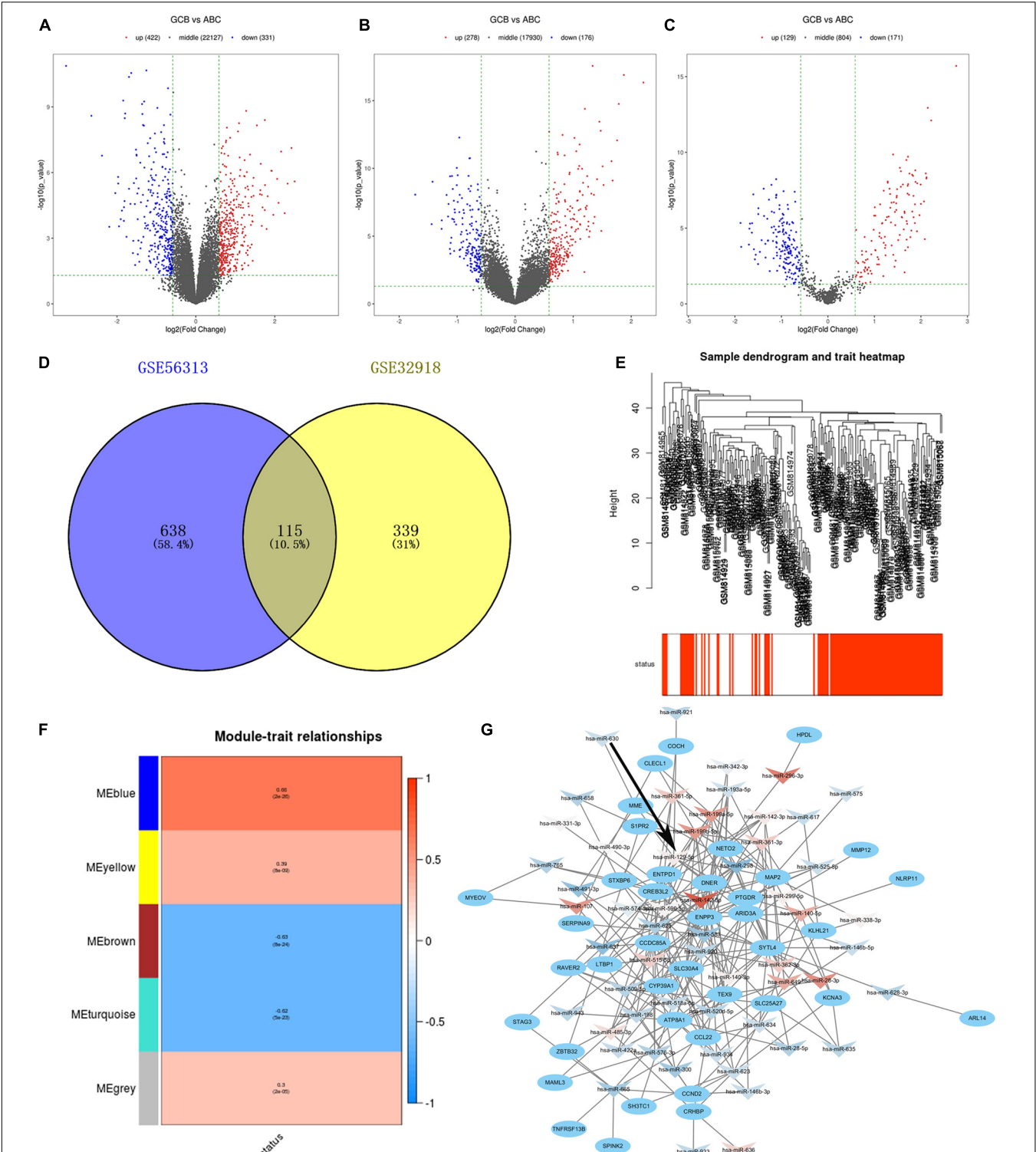


FIGURE 1 | (A–C) Volcano plots show gene expression in the GSE56313, GSE32918, and GSE15250 datasets. Red and blue symbols indicate genes that were significantly up- and downregulated, respectively. **(D)** Venn diagrams showing the number of common DEGs between GSE56313 and GSE32918. **(E)** A hierarchical clustering dendrogram is used to arrange DLBCL samples based on GSE32918, with survival outcomes shown at the bottom. **(F)** A module-trait relationship matrix is shown with rows and columns corresponding to survival status and the module eigengenes, and the correlation and *p*-values are represented in a every box. **(G)** Regulatory network of miRNA-target mRNA pairs in modular intersection genes. The network contained 56 differentially expressed miRNAs (arrow triangle) and 39 target mRNAs (oval). Red and blue arrow triangles indicate genes that were significantly up- and downregulated, respectively, in the GCB subtype.

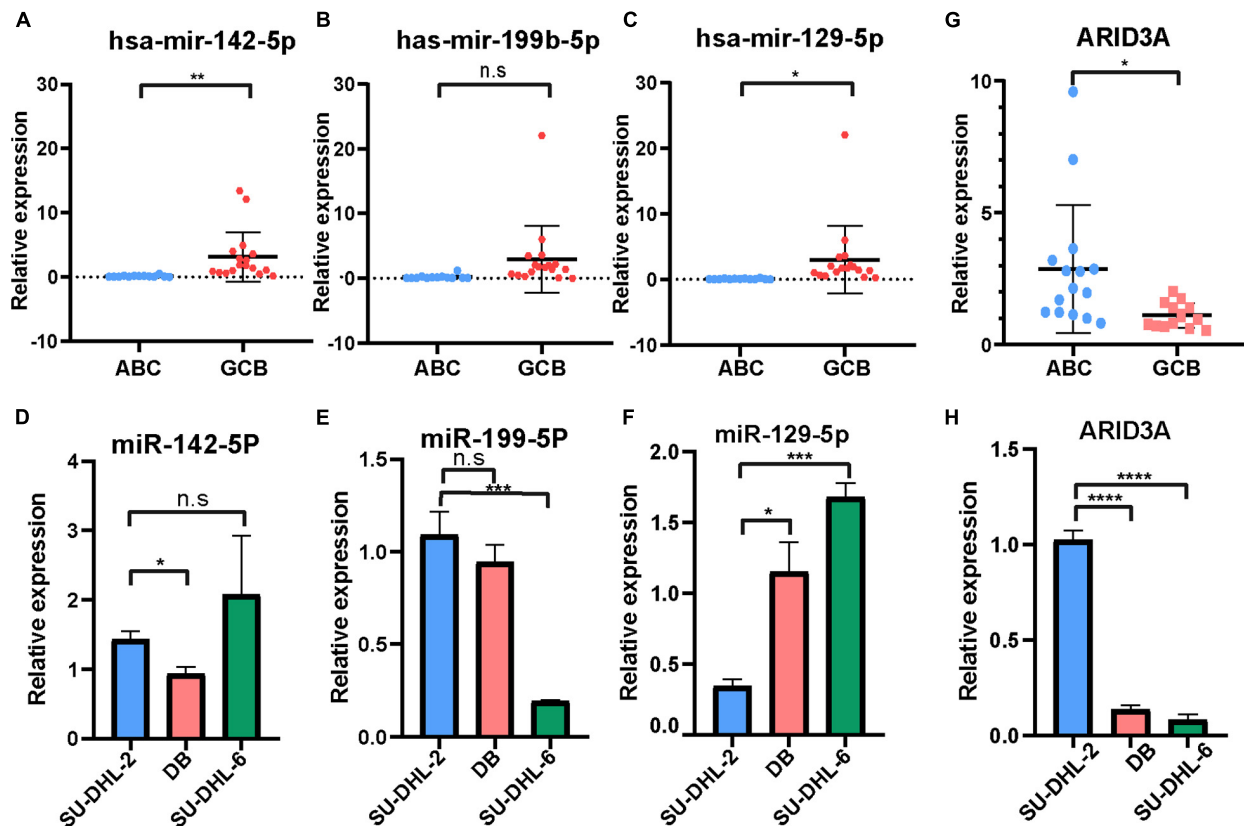


FIGURE 2 | (A–C) RT-qPCR showing the expression of hsa-miR-142-5p, hsa-miR-199b-5p, and hsa-miR-129-5p in the ABC and GCB subtypes DLBCL patients. **(D–F)** RT-qPCR showing the expression of hsa-miR-142-5p, hsa-miR-199b-5p, and hsa-miR-129-5p in the SU-DHL-2 (ABC subtype) and DB and SU-DHL-6 (GCB subtype) cell lines. **(G,H)** QRT-PCR showing the expression of ARID3A in the ABC and GCB subtypes DLBCL patients and cell lines, respectively. All data represented mean \pm SD from three independent experiments. NS: $P > 0.05$; * $P < 0.05$; ** $P < 0.01$; *** $P < 0.001$; **** $P < 0.0001$.

addition, the overexpression of ARID3A in DB and SU-DHL-6 cells enhanced the proliferation ability and inhibited cell apoptosis (7.69% vs. 1.37% and $P < 0.0001$, 6.05% vs. 4.73% and $P = 0.0036$, respectively, **Figures 4B,C**). Together, these data suggest that downregulation of miR-129-5p and upregulation of ARID3A are responsible for the progression of ABC subtype DLBCL by promoting cell proliferation and inhibiting apoptosis.

MiR-129-5p and ARID3A Affect the Interaction Between Diffuse Large B Cell Lymphoma Cells and CD8⁺ T Cells Through the PD-1/PD-L1 Immune Checkpoint

To further explore the downstream mechanisms of miR-129-5p and ARID3A, enrichment analysis of DIGs was conducted based on the Gene Ontology (GO) using DAVID (Huang et al., 2009). As a result (**Figure 4D**), the top GO terms included T-helper 17 cell differentiation and CD4-positive or CD8-positive alpha-beta T cell lineage commitment, among others, which implies that these genes are closely related to the immune response. As reported, PD-L1 on tumor cells interferes with CD8⁺ T cell activity when communicating with PD-1 in the

tumor microenvironment (Zheng et al., 2019). Therefore, we speculated that miR-129-5p and ARID3A could alter CD8⁺ T cells in DLBCL by changing the expression of PD-L1. To simulate the immune environment, DLBCL cells were co-cultured with immune cells. The results demonstrate that the proportion of CD8⁺ T cells co-cultured with SU-DHL-2 cells was significantly lower than that co-cultured with DB and SU-DHL-6 cells. And the expression of PD-1 on CD8⁺ T cells is higher than that co-cultured with GCB-subtype DLBCL cells. Thus, SU-DHL-2 cells have a stronger immune escape ability (**Figure 4E**). Moreover, knockdown of miR-129-5p or ectopic expression of ARID3A in DB and SU-DHL-6 cells reduced the percentage of CD8⁺ T cells and increased the PD-1 expression on the surface of CD8⁺ T cells, however, SU-DHL-6 failed to affect the PD-1 expression (**Figure 5A**). In contrast, the number of CD8⁺ T cells was significantly increased and PD-1 expression reduced after overexpression of miR-129-5p or knockdown of ARID3A in SU-DHL-2 cells. Furthermore, a significant association between CD8⁺ T cells and miR-129-5p or ARID3A expression was observed in patients with DLBCL (**Figure 5B**). A high level of miR-129-5p was associated with a higher number of peripheral blood CD8⁺ T cells ($P = 0.042$, $r = 0.498$). Conversely, low ARID3A expression was significantly correlated with a high

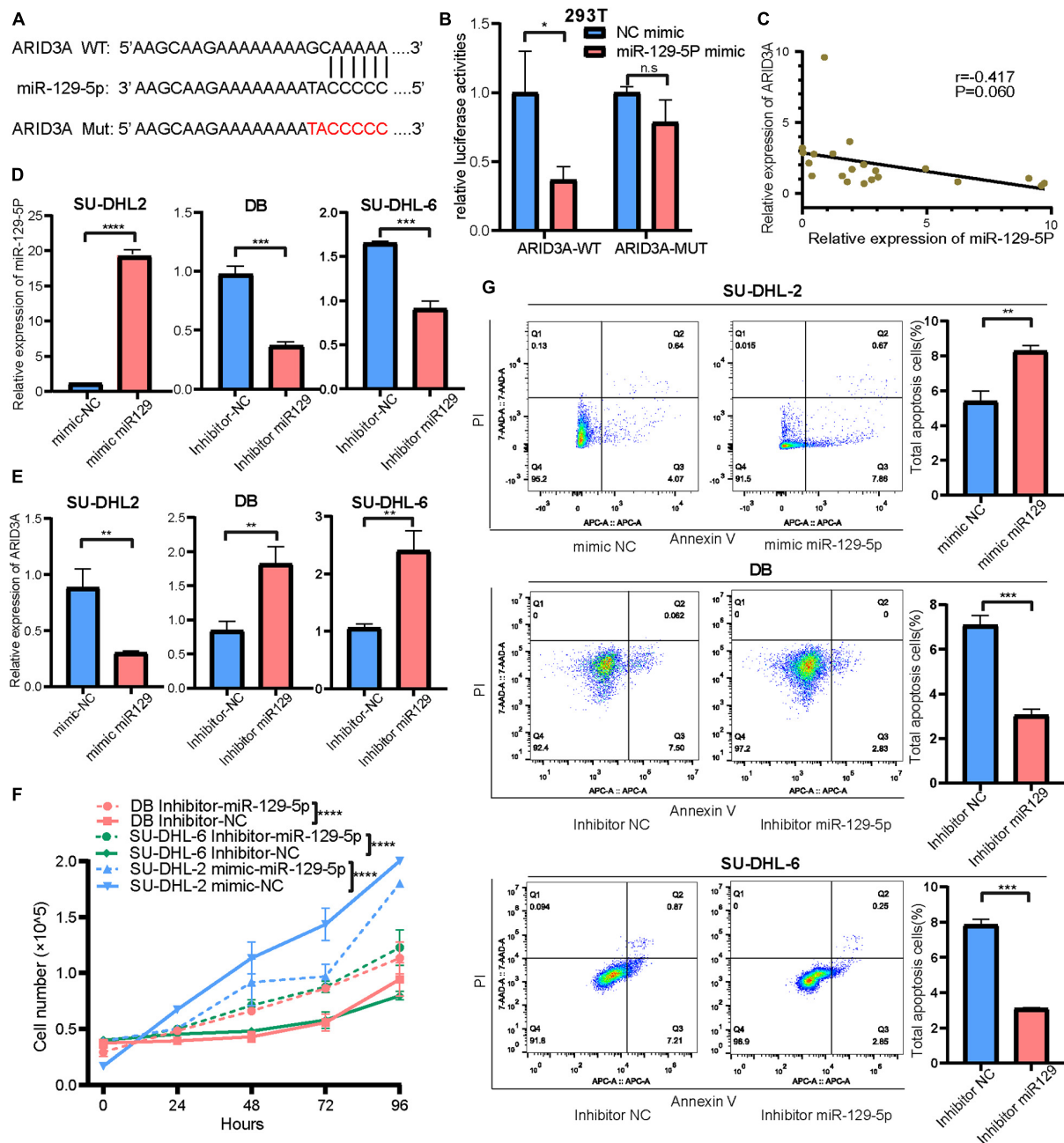


FIGURE 3 | (A) Interaction sequences of ARID3A for miR-129-5p binding were acquired from Starbase v3.0 and mutated by altering them with complementary sequences. **(B)** Dual-luciferase reporter gene assays were performed to detect the interaction between ARID3A and miR-129-5p. **(C)** Pearson's correlation curve showing that ARID3A was negatively correlated with miR-129-5p in DLBCL peripheral blood. **(D)** The inhibition and overexpression of miR-129-5p in DLBCL cells was confirmed with RT-qPCR assays. **(E)** RT-qPCR showing the expression of ARID3A in miR-129-5p-overexpressing SU-DHL-2 cells and miR-129-5p-knockdown DB and SU-DHL-6 cells. **(F)** Cell proliferation ability of transfected cells. Cells were placed in 24-well plates and counted after 0, 24, 72, and 96 h and the cell number were determined with trypan blue exclusion staining. **(G)** Cell apoptosis of SU-DHL-2 with mimic miR-129-5p, DB and SU-DHL-6 with inhibitor miR-129-5p, and negative control cells was measured through flow cytometry analysis. All data represented mean \pm SD from three independent experiments. * $P < 0.05$; ** $P < 0.01$; *** $P < 0.001$; **** $P < 0.0001$.

CD8⁺ T cell ratio ($P = 0.028$, $r = -0.532$). Additionally, overexpression of miR-129-5p or silencing of ARID3A reduced the protein and mRNA levels of PD-L1 in SU-DHL-2 cells (Figures 5C–E). Inhibition of miR-129-5p or overexpression

of ARID3A increased the protein and mRNA levels of PD-L1 in DB and SU-DHL-6. Next, we explored the regulatory mechanism of ARID3A on PD-L1 expression. ARID3A, a member of the ARID3 family, is a well-known transcription

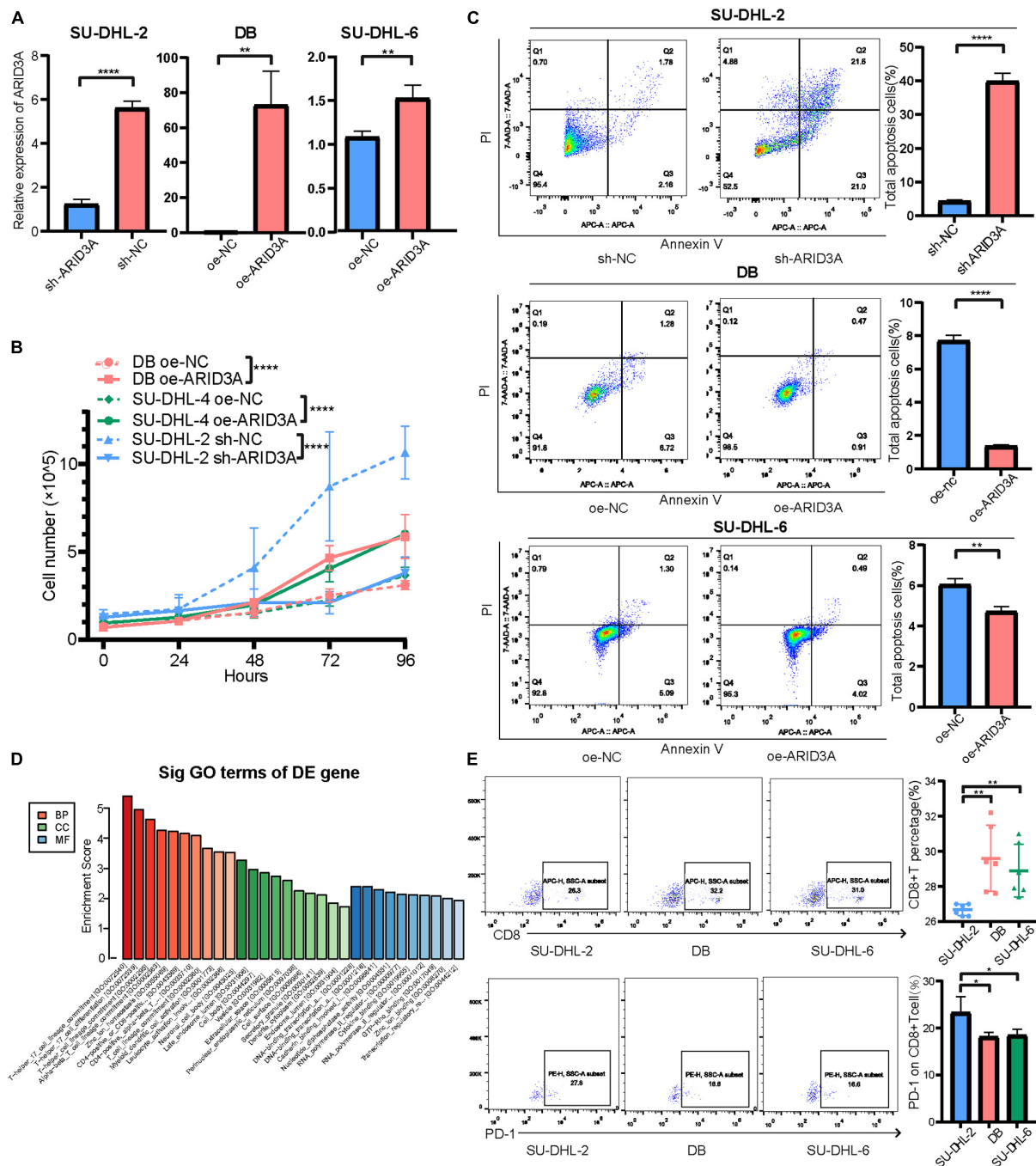


FIGURE 4 | (A) Inhibition and overexpression of ARID3A in DLBCL cells was confirmed with RT-qPCR assays. (B) Cell proliferation ability of ARID3A knockdown SU-DHL-2 cells, ARID3A overexpressing DB and SU-DHL6 cells, and negative control cells was counted using trypan blue exclusion staining. (C) Cell apoptosis assays showing the effect of ARID3A knockdown on SU-DHL-2 cells and ARID3A overexpression on DB and SU-DHL-6 cell apoptosis. (D) Differentially intersected genes were subjected to GO term enrichment analyses. (E) CD8⁺ T cell percentage and the surface PD-1 expression was determined using flow cytometry analysis when co-cultured with DB and SU-DHL-2 cells and transfected cells. All data represented mean \pm SD from three independent experiments. * $P < 0.05$, ** $P < 0.01$; **** $P < 0.0001$.

factor that can transcriptionally regulate gene expression by binding to the corresponding DNA sites (Tang et al., 2020). Therefore, we investigated whether ARID3A regulates PD-L1 expression at the transcriptional level. The ARID3A binding

site of the PD-L1 promoter was obtained using the JASPAR tool (Figure 5F). Dual-luciferase reporter gene assay results show that the PD-L1 promoter transcription was increased after ARID3A overexpression, and this effect was significantly reversed

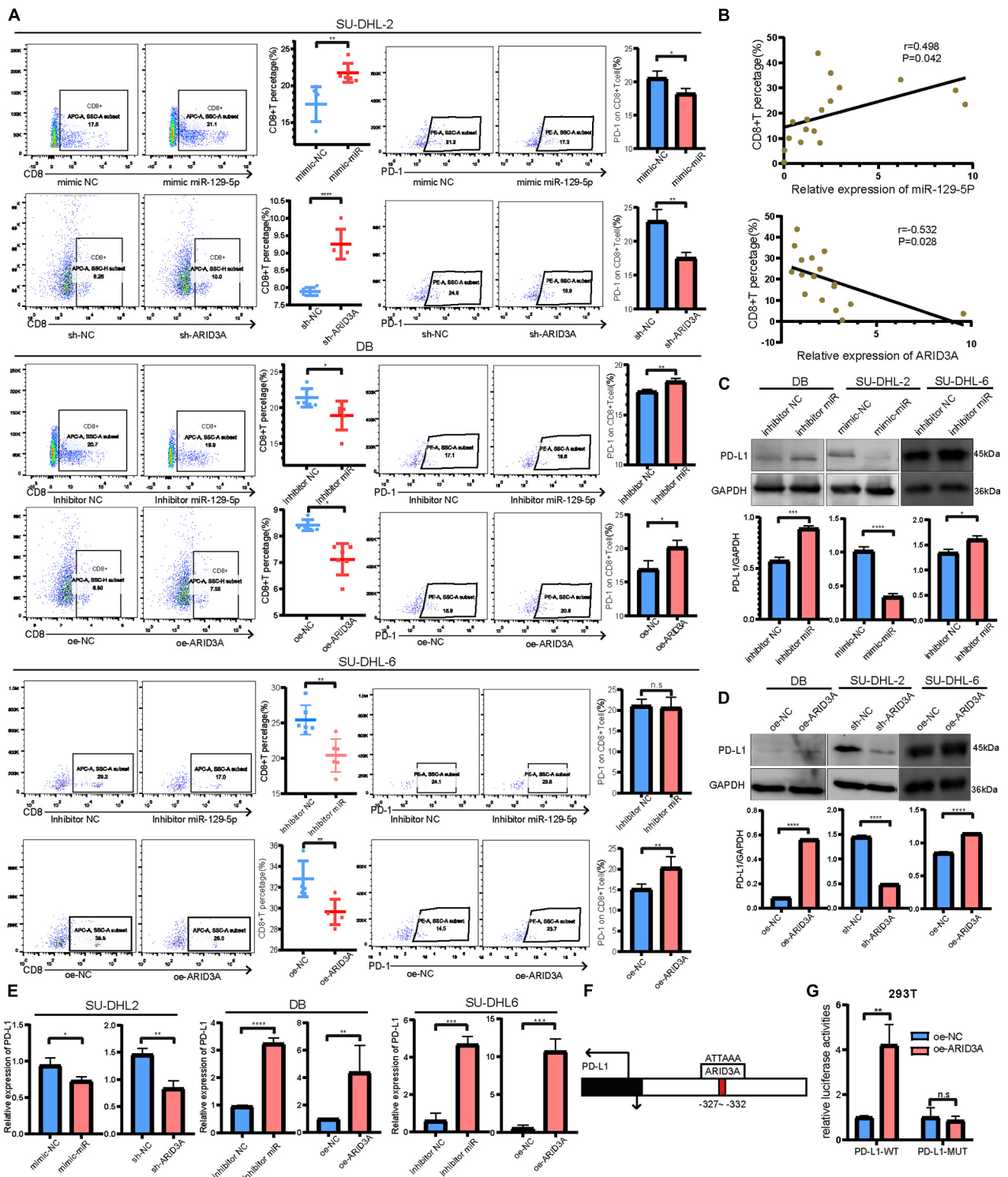
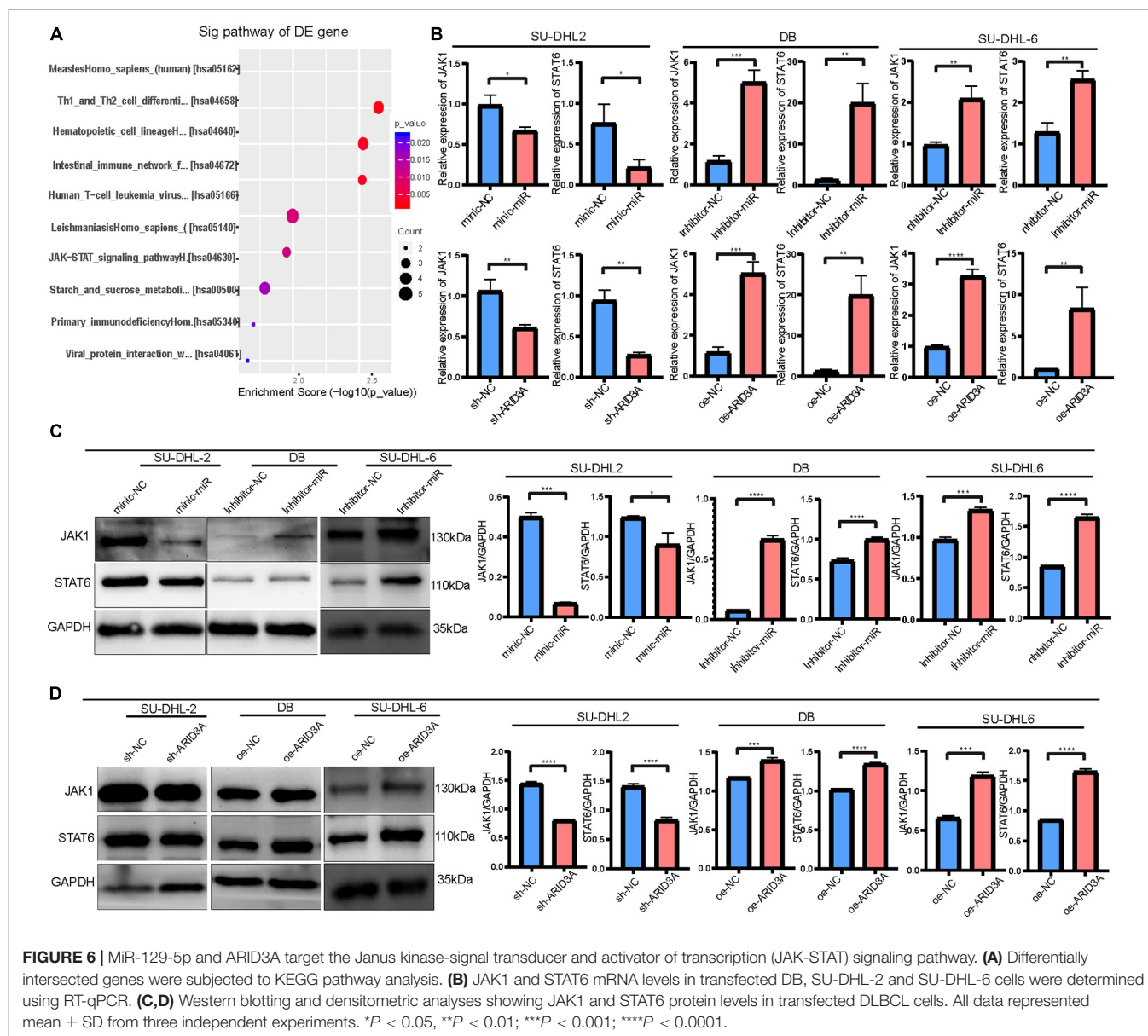


FIGURE 5 | (A) CD8⁺ T cell percentage and the surface PD-1 expression were determined using flow cytometry analysis when co-cultured with SU-DHL-2, DB and SU-DHL-6 cells and transfected cells. Mean \pm SD ($n = 6$). **(B)** Pearson's correlation curve showing the positive relation between CD8⁺ T cells and miR-129-5p and the negative relation between CD8⁺ T cells and ARID3A in DLBCL peripheral blood. **(C,D)** Western blotting and densitometric analyses showing PD-L1 protein levels in transfected and negative control DB, SU-DHL-2 and SU-DHL-6 cells. **(E)** Expression of PD-L1 mRNA in transfected and negative control cells were determined using RT-qPCR. **(F)** Predicted ARID3A binding site in the PD-L1 promoter were acquired using JASPAR. **(G)** Dual-luciferase reporter gene assays were performed to show that ARID3A regulated PD-L1 as a transcription factor. Mean \pm SD ($n = 3$). * $P < 0.05$; ** $P < 0.01$; *** $P < 0.001$; **** $P < 0.0001$.



by mutating the binding site (Figure 5G). In summary, it was validated that ARID3A, which is negatively regulated by miR-129-5p, can upregulate PD-L1 as a transcription factor.

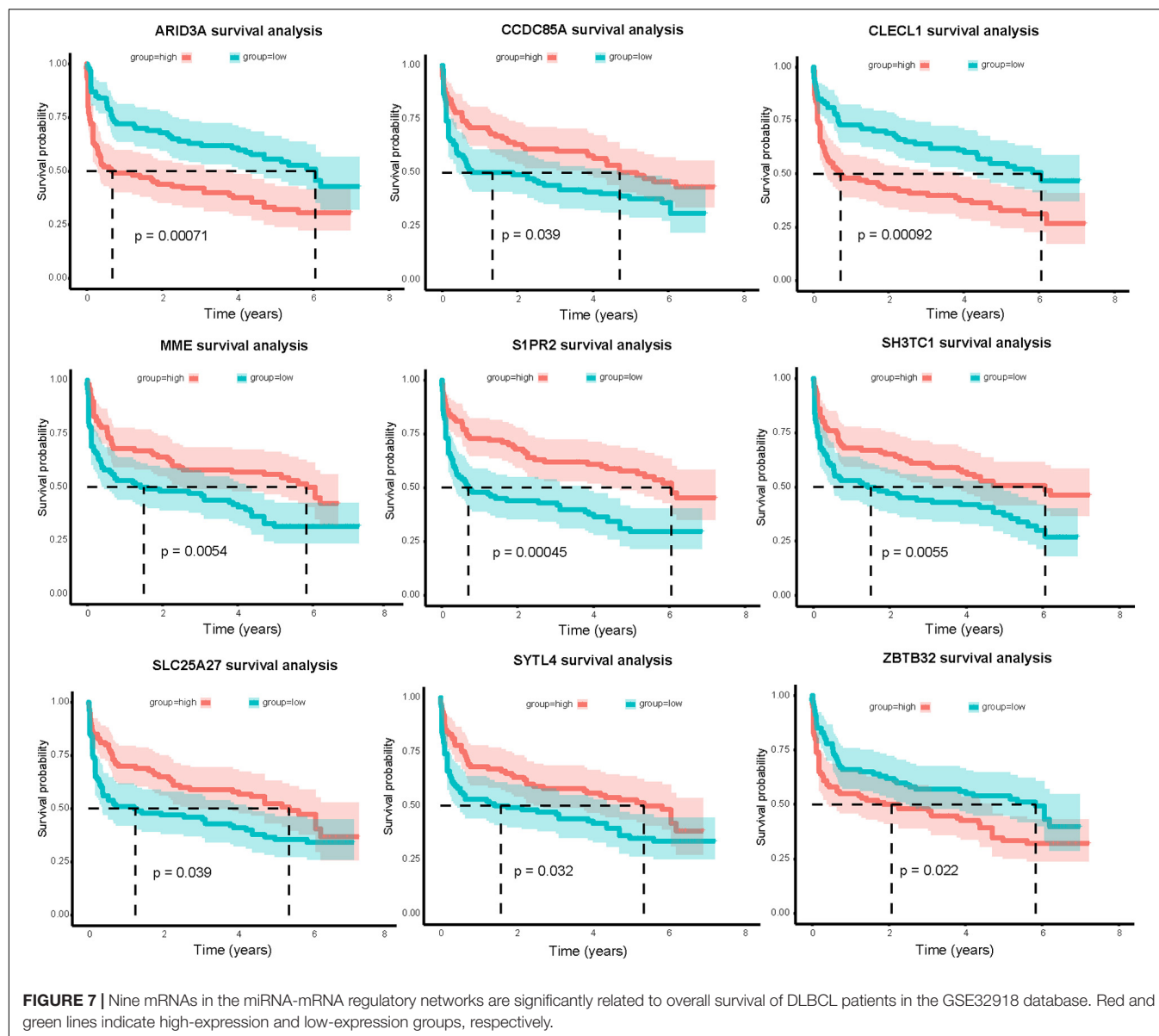
MiR-129-5p and ARID3A Targeted the Janus Kinase-Signal Transducer and Activator of Transcription Pathway

To further explore the differences between the ABC and GCB subtypes, DIGs were subjected to KEGG pathway analysis. Among them, the Janus kinase-signal transducer and activator of transcription (JAK-STAT) signaling pathway, associated with aggressive growth, invasion, and tumor-mediated immunosuppression, attracted our attention (Figure 6A). Therefore, JAK1 and STAT6 mRNA and protein levels were detected in DLBCL cells. As shown in Figure 6B, JAK1 and

STAT6 mRNA levels in DB and SU-DHL-6 cells significantly augmented via inhibition of miR-129-5p and ARID3A overexpression. Meanwhile, Figures 6C,D demonstrate that miR-129-5p inhibitor and ARID3A overexpression significantly increased the protein expression of JAK1 and STAT6 in DB and SU-DHL-6 cells. In addition, both JAK1 and STAT6 were effectively reduced in miR-129-5p mimics or sh-ARID3A SU-DHL-2 cells compared with the negative control group. Our results indicate that miR-129-5p/ARID3A regulates DLBCL cell proliferation, apoptosis, and immune escape through the JAK-STAT signaling pathway.

Relevance of Genes to Overall Survival

Combining clinical information and gene expression information in GSE32918, 39 DEGs in miRNA-mRNA regulatory networks



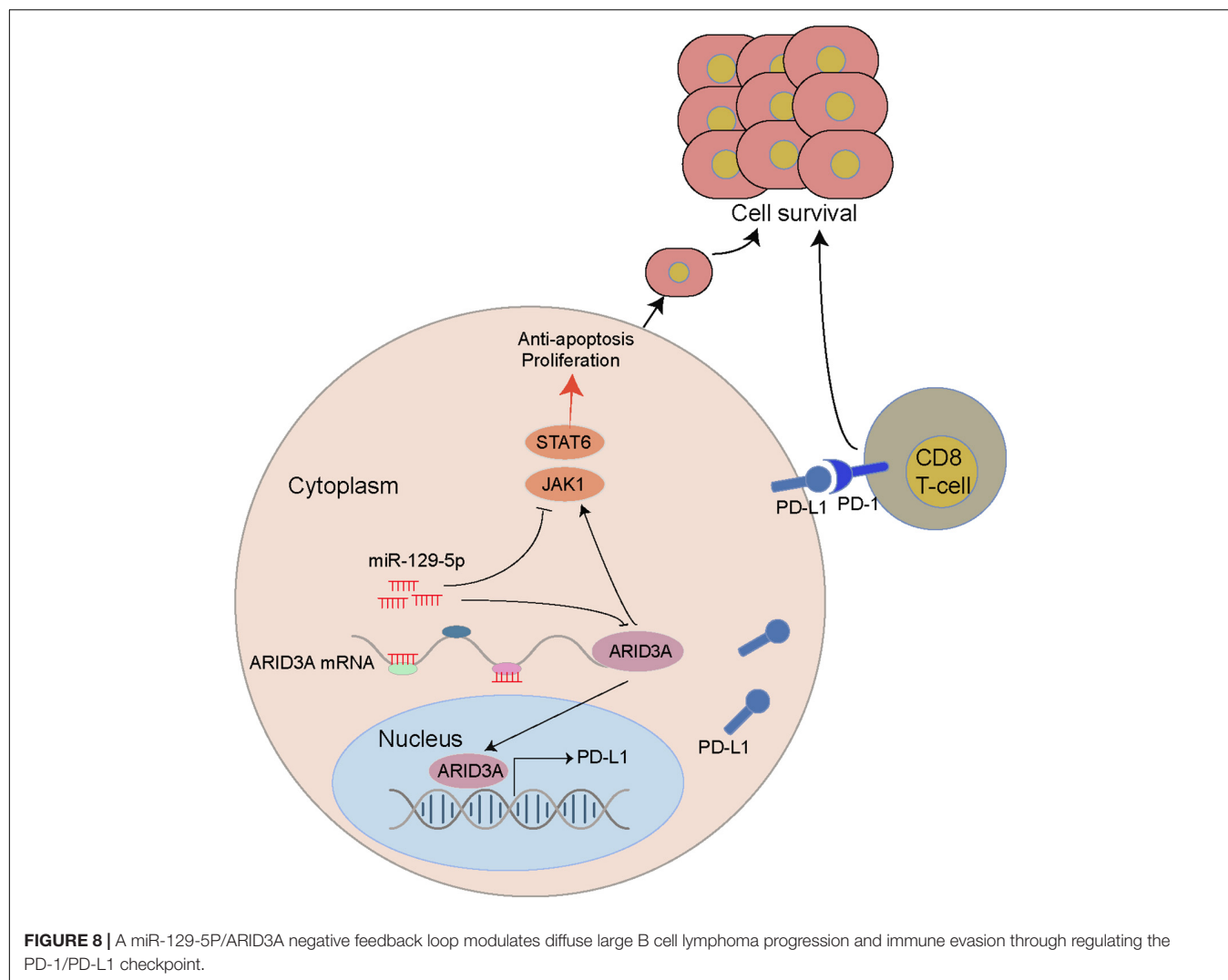
were evaluated using Kaplan-Meier survival analysis. As a result, the expression of nine mRNAs was significantly correlated with OS ($P < 0.05$, **Figure 7**). Surprisingly, we found a significant correlation between high ARID3A expression and poor prognosis in DLBCL patients. Therefore, we believe that ARID3A is an important prognostic and therapeutic target for DLBCL.

DISCUSSION

DLBCL is mainly divided into two COO subtypes, the GCB and ABC subtypes, with obvious differences in gene expression profiles and clinical outcomes. However, R-CHOP is the standard treatment for newly diagnosed DLBCL, regardless of the COO subtype. Although the combination of chemotherapy and rituximab result in a 5-year progression-free survival of 70–75%

and OS of 75–80% (Cunningham et al., 2013), some patients, especially of the ABC subtype, still experience a high rate of relapse or refractoriness. Therefore, targeting strategies that are concentrated on different subtypes should be considered.

In recent years, miRNA expression profiles have been identified in a variety of cancers, including non-small-cell lung cancer (Niemira et al., 2019), breast cancer (Dastmalchi et al., 2020), and gliomas (Zeng et al., 2018), including DLBCL. However, the involvement of miRNAs in the pathogenesis and therapeutic response of different DLBCL subtypes needs to be further clarified. To identify the differential biomarkers of ABC and GCB subtypes, differentially expressed miRNAs and targeted genes between the two subtypes were identified based on one miRNA expression dataset and two gene expression profiles. Through bioinformatics analysis, a module with a strong correlation with a better prognosis of GCB subtypes was



identified. By constructing a regulatory network between the MIGs and differential miRNAs, we identified three important miRNAs with the most targeted genes. Through the validation of DLBCL patient samples and cells, only miR-129-5p was significantly upregulated in the GCB subtype.

Studies have reported that miR-129-5p can inhibit the progression of rectal cancer (Wan et al., 2020), nasopharyngeal cancer (Yu et al., 2020), and liver cancer (Li Z. et al., 2019), but its role in DLBCL has not yet been reported. Our study found that miR-129-5p inhibited the proliferation and promoted apoptosis of DLBCL cells. This may be the reason why ABC-the subtype DLBCL with a low expression of miR-129-5p has a higher degree of malignancy. In addition, through bioinformatics analysis and *in vitro* experiments, miR-129-5p was found to negatively regulate ARID3A, which was confirmed by a luciferase reporter assay. As a transcription factor, ARID3A participates in many cellular processes and is reported to promote the progression of tumors such as ovarian cancer, colorectal cancer, and nasopharyngeal cancer (Dausinas et al., 2020; Tang et al., 2020). Our study demonstrated that ARID3A was highly expressed in ABC subtype DLBCL patients and cell lines, and the

overexpression of ARID3A facilitated the proliferation of GCB DLBCL cells and inhibited cell apoptosis. The results of survival analysis based on the GEO dataset suggested that DLBCL with high ARID3A expression had a shorter survival time. Therefore, we believe that the high expression of ARID3A promotes the progression of DLBCL and leads to poor prognosis of ABC subtype DLBCL. Through KEGG pathway analysis of DEGs and *in vitro* experimental validation, we revealed that knocking down miR-129-5p and overexpression of ARID3A both resulted in increased expression of JAK1 and STAT6. An increasing body of evidence demonstrates that the JAK/STAT signaling pathway is an important target for tumor therapy because of its important role in aggressive growth, invasion, treatment resistance, and tumor-mediated immunosuppression (Ou et al., 2021). In addition, activation of the JAK/STAT signaling pathway is related to a worse prognosis in various cancers (Qureshy et al., 2020). Therefore, we suspected that tumor progression of the ABC subtype DLBCL is promoted through miR-129-5p/ARID3A-mediated activation of the JAK/STAT pathway.

GO function enrichment analysis indicates that genes were highly enriched in immune response-related signaling pathway.

It has been reported that, in the tumor microenvironment, tumor cells can attenuate the activity of T cells and evade the immune response. Previous studies have pointed out that an increase in PD-L1 expression in tumor cells leads to a decrease in the proportion of CD8⁺ T cells that interact with it, thereby promoting tumor cell survival (Zheng et al., 2019). In the current study, miR-129-5p and ARID3A were found to alter the proportion of CD8⁺ T cells in the immune environment through PD-L1 activation, thereby promoting immune escape. We also show that ARID3A activated PD-L1 transcription by binding to its promoter. In this study, we first revealed that ARID3A, which is negatively regulated by miR-129-5p, activates PD-L1, leading to the immune escape of DLBCL, especially the ABC subtype.

However, there are some limitations in our study. First, the clinical sample size is too small, which may be one of the factors affecting our experimental data. Second, our experiments lack validation from animal experiments. Therefore, further studies are needed to elucidate the mechanisms of miR-129-5p and ARID3A.

CONCLUSION

Through bioinformatics analysis and *in vitro* experiments, we revealed that miR-129-5p, a differentially expressed miRNA between the ABC and GCB subtypes of DLBCL, promoted apoptosis and inhibited proliferation and immune escape of DLBCL through targeted regulation of ARID3A. Specifically, we clarified that the miR-129-5P/ARID3A axis constitutes a negative feedback loop, which modulates PD-L1 expression in DLBCL and leads to changes in CD8⁺ T cell activity, ultimately promoting the immune escape of tumor cells (Figure 8).

DATA AVAILABILITY STATEMENT

The original contributions presented in the study are included in the article/Supplementary Material, further inquiries can be directed to the corresponding author/s.

ETHICS STATEMENT

The study was approved by the Medical Ethics Committee of Fujian Medical University Union Hospital. The

patients/participants provided their written informed consent to participate in this study.

AUTHOR CONTRIBUTIONS

WZ: conceptualization, methodology, investigation, original draft, review, and editing. GL: methodology, original draft, review, and editing. QL: original draft, review, and editing. MI: original draft, review, and editing. HF: review, editing, and supervision. JS: funding acquisition and supervision. All authors read and approved the final version of the manuscript.

FUNDING

This study was supported in part by a Grant-in-Aid for the National Natural Science Foundation of China (81300428 and 81800167), the Joints Funds for the Innovation of Science and Technology, Fujian Province (2018Y9010 and 2018Y9205), the Qihang Foundation of Fujian Medical University (2020QH2015), the Clinical Research Center for Hematological Malignancies of Fujian Province, Construction Project of Fujian Medical Center of Hematology (Min201704), and sponsored by the National and Fujian Provincial Key Clinical Specialty Discipline Construction Program, P.R.C.

ACKNOWLEDGMENTS

We would like to express our sincere gratitude to our seniors Huron Zhou, Feng Zhang, and Qian Huang for their instructive advice and useful suggestions on the experiments.

SUPPLEMENTARY MATERIAL

The Supplementary Material for this article can be found online at: <https://www.frontiersin.org/articles/10.3389/fcell.2021.735855/full#supplementary-material>

Supplementary Figure 1 | Gating strategy for the CD8⁺ T cell and PD-1-expressing CD8⁺ T cell. (A) Total lymphocytes were gated based on side-scatter and forward-scatter. (B) Doublets were eliminated from the analysis by FS-area (FS-A) and FS-height (FS-H). (C) Cells were further analyzed by expression of CD8. (D) Within CD8⁺ T cells and PD-1-expressing cells were identified.

REFERENCES

- Agarwal, V., Bell, G. W., Nam, J. W., and Bartel, D. P. (2015). Predicting effective microRNA target sites in mammalian mRNAs. *eLife* 4:e05005. doi: 10.7554/eLife.05005
- Alizadeh, A. A., Eisen, M. B., Davis, R. E., Ma, C., Lossos, I. S., Rosenwald, A., et al. (2000). Distinct types of diffuse large B-cell lymphoma identified by gene expression profiling. *Nature* 403, 503–511. doi: 10.1038/35000501
- Betel, D., Wilson, M., Gabow, A., Marks, D. S., and Sander, C. (2008). The microRNA.org resource: targets and expression. *Nucleic Acids Res.* 36, D149–D153. doi: 10.1093/nar/gkm995
- Bruch, R., Baaske, J., Chatelle, C., Meirich, M., Madlener, S., Weber, W., et al. (2019). CRISPR/Cas13a-Powered electrochemical microfluidic biosensor for nucleic acid amplification-free miRNA diagnostics. *Adv. Mater.* 31:e1905311.
- Butte, M., Keir, M., Phamduy, T., Sharpe, A., and Freeman, G. J. (2007). Programmed death-1 ligand 1 interacts specifically with the B7-1 costimulatory molecule to inhibit T cell responses. *Immunity* 27, 111–122. doi: 10.1016/j.immuni.2007.05.016
- Chou, C. H., Shrestha, S., Yang, C. D., Chang, N. W., Lin, Y. L., Liao, K. W., et al. (2018). miRTarBase update 2018: a resource for experimentally validated microRNA-target interactions. *Nucleic Acids Res.* 46, D296–D302. doi: 10.1093/nar/gkx1067

- Cunningham, D., Hawkes, E. A., Jack, A., Qian, W., Smith, P., Mouncey, P., et al. (2013). Rituximab plus cyclophosphamide, doxorubicin, vincristine, and prednisolone in patients with newly diagnosed diffuse large B-cell non-Hodgkin lymphoma: a phase 3 comparison of dose intensification with 14-day versus 21-day cycles. *Lancet (London, England)* 381, 1817–1826. doi: 10.1016/S0140-6736(13)60313-X
- Dastmalchi, N., Safaralizadeh, R., Baradaran, B., Hosseinpourfeizi, M., and Baghbanzadeh, A. (2020). An update review of deregulated tumor suppressive microRNAs and their contribution in various molecular subtypes of breast cancer. *Gene* 729:144301. doi: 10.1016/j.gene.2019.144301
- Dausinas, P., Pulakanti, K., Rao, S., Cole, J., Dahl, R., and Cowden Dahl, K. J. G. (2020). ARID3A and ARID3B induce stem promoting pathways in ovarian cancer cells. *Gene* 738:144458. doi: 10.1016/j.gene.2020.144458
- Freeman, G., Sharpe, A., and Kuchroo, V. (2002). Protect the killer: CTLs need defenses against the tumor. *Nat. Med.* 8, 787–789. doi: 10.1038/nm0802-787
- Fu, K., Weisenburger, D. D., Choi, W. W., Perry, K. D., Smith, L. M., Shi, X., et al. (2008). Addition of rituximab to standard chemotherapy improves the survival of both the germinal center B-cell-like and non-germinal center B-cell-like subtypes of diffuse large B-cell lymphoma. *J. Clin. Oncol.* 26, 4587–4594. doi: 10.1200/JCO.2007.15.9277
- Huang, da, W., Sherman, B. T., and Lempicki, R. A. (2009). Systematic and integrative analysis of large gene lists using DAVID bioinformatics resources. *Nat. Protoc.* 4, 44–57. doi: 10.1038/nprot.2008.211
- Langfelder, P., and Horvath, S. (2008). WGCNA: an R package for weighted correlation network analysis. *BMC Bioinformatics* 9:559. doi: 10.1186/1471-2105-9-559
- Langfelder, P., Zhang, B., and Horvath, S. (2008). Defining clusters from a hierarchical cluster tree: the dynamic tree cut package for R. *Bioinformatics (Oxford, England)* 24, 719–720. doi: 10.1093/bioinformatics/btm563
- Larrabeiti-Etxebarria, A., Lopez-Santillan, M., Santos-Zorroza, B., Lopez-Lopez, E., and Garcia-Orad, A. (2019). Systematic review of the potential of MicroRNAs in diffuse large B cell lymphoma. *Cancers* 11:44. doi: 10.3390/cancers11020144
- Li, M., Chiang, Y. L., Lyssiotis, C. A., Teater, M. R., Hong, J. Y., Shen, H., et al. (2019). Non-oncogene addiction to SIRT3 plays a critical role in lymphomagenesis. *Cancer Cell* 35, 916–931.e9. doi: 10.1016/j.ccell.2019.05.002
- Li, Z., Lu, J., Zeng, G., Pang, J., Zheng, X., Feng, J., et al. (2019). MiR-129-5p inhibits liver cancer growth by targeting calcium calmodulin-dependent protein kinase IV (CAMK4). *Cell Death Dis.* 10:789. doi: 10.1038/s41419-019-1923-4
- Ma, J., Zhan, Y., Xu, Z., Li, Y., Luo, A., Ding, F., et al. (2017). ZEB1 induced miR-99b/let-7e/miR-125a cluster promotes invasion and metastasis in esophageal squamous cell carcinoma. *Cancer Lett.* 398, 37–45. doi: 10.1016/j.canlet.2017.04.006
- Marchesi, F., Regazzo, G., Palombi, F., Terrenato, I., Sacconi, A., Spagnuolo, M., et al. (2018). Serum miR-22 as potential non-invasive predictor of poor clinical outcome in newly diagnosed, uniformly treated patients with diffuse large B-cell lymphoma: an explorative pilot study. *J. Exp. Clin. Cancer Res.* 37:95. doi: 10.1186/s13046-018-0768-5
- Marques, S. C., Ranjbar, B., Laursen, M. B., Falgreen, S., Bilgrau, A. E., Bødker, J. S., et al. (2016). High miR-34a expression improves response to doxorubicin in diffuse large B-cell lymphoma. *Exp. Hematol.* 44, 238–246.e2. doi: 10.1016/j.exphem.2015.12.007
- Miao, Y., Medeiros, L. J., Li, Y., Li, J., and Young, K. H. (2019). Genetic alterations and their clinical implications in DLBCL. *Nat. Rev. Clin. Oncol.* 16, 634–652. doi: 10.1038/s41571-019-0225-1
- Niemira, M., Collin, F., Szalkowska, A., Bielska, A., Chwialkowska, K., Reszec, J., et al. (2019). Molecular signature of subtypes of non-small-cell lung cancer by large-scale transcriptional profiling: identification of key modules and genes by weighted gene co-expression network analysis (WGCNA). *Cancers* 12:37. doi: 10.3390/cancers12010037
- Nixon, J. C., Rajaiya, J. B., Ayers, N., Evetts, S., and Webb, C. F. (2004). The transcription factor, bright, is not expressed in all human B lymphocyte subpopulations. *Cell Immunol.* 228, 42–53. doi: 10.1016/j.cellimm.2004.03.004
- Ou, A., Ott, M., Fang, D., and Heimberger, A. B. (2021). The role and therapeutic targeting of JAK/STAT signaling in glioblastoma. *Cancers* 13:437. doi: 10.3390/cancers13030437
- Puissegur, M. P., Eichner, R., Quelen, C., Coyaude, E., Mari, B., Lebrigand, K., et al. (2012). B-cell regulator of immunoglobulin heavy-chain transcription (Bright)/ARID3a is a direct target of the oncomir microRNA-125b in progenitor B-cells. *Leukemia* 26, 2224–2232. doi: 10.1038/leu.2012.95
- Qureshy, Z., Johnson, D., and Grandis, J. (2020). Targeting the JAK/STAT pathway in solid tumors. *Cancer Metastasis Treat* 6:27. doi: 10.20517/2394-4722.2020.58
- Shannon, P., Markiel, A., Ozier, O., Baliga, N. S., Wang, J. T., Ramage, D., et al. (2003). Cytoscape: a software environment for integrated models of biomolecular interaction networks. *Genome Res.* 13, 2498–2504. doi: 10.1101/gr.1239303
- Sun, C., Mezzadra, R., and Schumacher, T. (2018). Regulation and function of the PD-L1 checkpoint. *Immunity* 48, 434–452. doi: 10.1016/j.immuni.2018.03.014
- Tang, J., Yang, L., Li, Y., Ning, X., Chaulagain, A., Wang, T., et al. (2020). ARID3A promotes the development of colorectal cancer by upregulating AURKA. *Carcinogenesis* 42, 578–586. doi: 10.1093/carcin/bgaa118
- Vejnar, C. E., and Zdobnov, E. M. (2012). MiRmap: comprehensive prediction of microRNA target repression strength. *Nucleic Acids Res.* 40, 11673–11683. doi: 10.1093/nar/gks901
- Wan, P., Bai, X., Yang, C., He, T., Luo, L., Wang, Y., et al. (2020). miR-129-5p inhibits proliferation, migration, and invasion in rectal adenocarcinoma cells through targeting E2F7. *J. Cell. Physiol.* 235, 5689–5701. doi: 10.1002/jcp.29501
- Wong, C. M., Tsang, F. H., and Ng, I. O. (2018). Non-coding RNAs in hepatocellular carcinoma: molecular functions and pathological implications. *Nat. Rev. Gastroenterol. Hepatol.* 15, 137–151. doi: 10.1038/nrgastro.2017.169
- Wong, N., and Wang, X. (2015). miRDB: an online resource for microRNA target prediction and functional annotations. *Nucleic Acids Res.* 43, D146–D152. doi: 10.1093/nar/gku1104
- Wu, H., Liu, C., Yang, Q., Xin, C., Du, J., Sun, F., et al. (2019). MIR145-3p promotes autophagy and enhances bortezomib sensitivity in multiple myeloma by targeting. *Autophagy* 16, 683–697. doi: 10.1080/15548627.2019.1635380
- Yang, J. M., Jang, J. Y., Jeon, Y. K., and Paik, J. H. (2018). Clinicopathologic implication of microRNA-197 in diffuse large B cell lymphoma. *J. Trans. Med.* 16:162. doi: 10.1186/s12967-018-1537-0
- Yu, D., Han, G. H., Zhao, X., Liu, X., Xue, K., Wang, D., et al. (2020). MicroRNA-129-5p suppresses nasopharyngeal carcinoma lymphangiogenesis and lymph node metastasis by targeting ZIC2. *Cell Oncol. (Dordr)* 43, 249–261. doi: 10.1007/s13402-019-00485-5
- Zeng, A., Yin, J., Wang, Z., Zhang, C., Li, R., Zhang, Z., et al. (2018). miR-17-5p-CXCL14 axis related transcriptome profile and clinical outcome in diffuse gliomas. *Oncoimmunology* 7:e1510277. doi: 10.1080/2162402X.2018.1510277
- Zheng, Z., Sun, R., Zhao, H. J., Fu, D., Zhong, H. J., Weng, X. Q., et al. (2019). MiR155 sensitized B-lymphoma cells to anti-PD-L1 antibody via PD-1/PD-L1-mediated lymphoma cell interaction with CD8+T cells. *Mol. Cancer* 18:54. doi: 10.1186/s12943-019-0977-3
- Zhou, M., Zhao, H., Xu, W., Bao, S., Cheng, L., and Sun, J. (2017). Discovery and validation of immune-associated long non-coding RNA biomarkers associated with clinically molecular subtype and prognosis in diffuse large B cell lymphoma. *Mol. Cancer* 16:16. doi: 10.1186/s12943-017-0580-4

Conflict of Interest: The authors declare that the research was conducted in the absence of any commercial or financial relationships that could be construed as a potential conflict of interest.

Publisher's Note: All claims expressed in this article are solely those of the authors and do not necessarily represent those of their affiliated organizations, or those of the publisher, the editors and the reviewers. Any product that may be evaluated in this article, or claim that may be made by its manufacturer, is not guaranteed or endorsed by the publisher.

Copyright © 2021 Zheng, Lai, Lin, Issah, Fu and Shen. This is an open-access article distributed under the terms of the Creative Commons Attribution License (CC BY). The use, distribution or reproduction in other forums is permitted, provided the original author(s) and the copyright owner(s) are credited and that the original publication in this journal is cited, in accordance with accepted academic practice. No use, distribution or reproduction is permitted which does not comply with these terms.



Construction of a Ferroptosis-Related Long Non-coding RNA Prognostic Signature and Competing Endogenous RNA Network in Lung Adenocarcinoma

Xiang Fei^{††}, Congli Hu^{2†}, Xinyu Wang^{3†}, Chaojing Lu¹, Hezhong Chen¹, Bin Sun^{4*} and Chunguang Li^{1*}

OPEN ACCESS

Edited by:

Shiv K. Gupta,
Mayo Clinic, United States

Reviewed by:

Youliang Wang,
Beijing Institute of Technology, China
Wei Kong,
Shanghai Maritime University, China
Ruyi He,
Wuhan Polytechnic University, China

*Correspondence:

Bin Sun
sunbin05301984@aliyun.com
Chunguang Li
dr_ljichunguang@sina.com

^{††}These authors have contributed
equally to this work

Specialty section:

This article was submitted to
Molecular and Cellular Oncology,
a section of the journal
Frontiers in Cell and Developmental
Biology

Received: 01 August 2021

Accepted: 05 October 2021

Published: 08 November 2021

Citation:

Fei X, Hu C, Wang X, Lu C,
Chen H, Sun B and Li C (2021)
Construction of a Ferroptosis-Related
Long Non-coding RNA Prognostic
Signature and Competing
Endogenous RNA Network in Lung
Adenocarcinoma.
Front. Cell Dev. Biol. 9:751490.
doi: 10.3389/fcell.2021.751490

¹ Department of Thoracic Surgery, Changhai Hospital, Navy Military Medical University, Shanghai, China, ² Department of Medical Oncology, Shanghai Pulmonary Hospital, Thoracic Cancer Institute, Tongji University School of Medicine, Shanghai, China, ³ Department of Thoracic Surgery, Renji Hospital, Shanghai Jiao Tong University School of Medicine, Shanghai, China, ⁴ Department of Molecular Oncology, Eastern Hepatobiliary Surgical Hospital & National Center for Liver Cancer, Navy Military Medical University, Shanghai, China

Ferroptosis-related genes play an important role in the progression of lung adenocarcinoma (LUAD). However, the potential function of ferroptosis-related lncRNAs in LUAD has not been fully elucidated. Thus, to explore the potential role of ferroptosis-related lncRNAs in LUAD, the transcriptome RNA-seq data and corresponding clinical data of LUAD were downloaded from the TCGA dataset. Pearson correlation was used to mine ferroptosis-related lncRNAs. Differential expression and univariate Cox analysis were performed to screen prognosis related lncRNAs. A ferroptosis-related lncRNA prognostic signature (FLPS), which included six ferroptosis-related lncRNAs, was constructed by the least absolute shrinkage and selection operator (LASSO) Cox regression. Patients were divided into a high risk-score group and low risk-score group by the median risk score. Receiver operating characteristic (ROC) curves, principal component analysis (PCA), and univariate and multivariate Cox regression were performed to confirm the validity of FLPS. Enrichment analysis showed that the biological processes, pathways and markers associated with malignant tumors were more common in high-risk subgroups. There were significant differences in immune microenvironment and immune cells between high- and low-risk groups. Then, a nomogram was constructed. We further investigated the relationship between six ferroptosis-related lncRNAs and tumor microenvironment and tumor stemness. A competing endogenous RNA (ceRNA) network was established based on the six ferroptosis-related lncRNAs. Finally, we detected the expression levels of ferroptosis-related lncRNAs in clinical samples through quantitative real-time polymerase chain reaction assay (qRT-PCR). In conclusion, we identified the prognostic ferroptosis-related lncRNAs in LUAD and constructed a prognostic signature which provided a new strategy for the evaluation and prediction of prognosis in LUAD.

Keywords: LUAD, ferroptosis, lncRNAs, prognostic signature, ceRNA network

INTRODUCTION

Lung cancer is the disease with the highest morbidity and mortality, among which lung adenocarcinoma (LUAD) is accounted for 40–50% of all lung cancer cases (Bray et al., 2018). At present, local resection is still the first choice for the treatment of LUAD. In recent years, molecular targeted therapy and immunotherapy have developed rapidly, which has brought success in the clinical treatment of a series of malignant tumors. Although the prognosis of some patients has improved significantly with the application of targeted therapy and immunotherapy, the survival rate is far from satisfaction (Miller et al., 2019). There is evidence showing that identification and application of novel biomarkers could bring benefits for the effective treatment of patients (Xu et al., 2021).

Ferroptosis is a form of regulatory cell death with iron dependence, caused by excessive lipid peroxidation and related to the occurrence of a variety of tumors and therapeutic response (Chen et al., 2021). Ferroptosis also plays an important role in LUAD. CAMP responsive element binding protein 1 (CREB) can directly bind to the promoter region of GPX4 to promote its expression, thereby inhibiting potential ferroptosis and promote the growth of LUAD (Wang Z. et al., 2021). P53 is a well-known tumor suppressor, which mediates apoptosis and cell-cycle arrest. In addition, it also can modulate ferroptosis in an ALOX12-dependent way and inhibit the proliferation of H1299 (Chu et al., 2019).

The abnormal expression of lncRNAs in LUAD is widely involved in the process of tumor proliferation and metastasis (Li and Chen, 2016). PD-L1-lnc was reported to directly bind to c-Myc and enhance its transcriptional activity, ultimately promoting proliferation and invasion of LUAD (Qu et al., 2021). Knockdown of lncRNA MSC-AS1 could inhibit LUAD cell growth and accelerate apoptosis through miR-33b-5p/GPAM axis (Li S. et al., 2021). What's more, accumulating studies demonstrated that lncRNAs also regulated ferroptosis of lung cancer by interacting with ELAVL1 or miR-365a-3p (Wang et al., 2019; Gai et al., 2020). Previous studies have shown that ferroptosis-related lncRNAs could be prognostic risk factors and the signatures constructed with them can be used to distinguish high-risk patients from low-risk patients (Cai et al., 2021; Tang et al., 2021). However, the full role of ferroptosis-related lncRNAs in LUAD needs to be further explored.

Therefore, we retrieved ferroptosis-related genes from previous studies and mined potential dysregulated ferroptosis-related lncRNAs through bioinformatic analysis, based on the LUAD dataset of TCGA. Our study showed 33 lncRNAs were differentially expressed in LUAD and correlated with prognosis. Furthermore, a ferroptosis-related lncRNA prognostic signature (FLPS) was constructed based on LASSO regression. We confirmed the validity of FLPS through ROC, PCA, and Cox regression. Finally, a nomogram was constructed to predict overall survival (OS) of LUAD patients and a ceRNA network was built to further clarify the function of those lncRNAs in LUAD.

MATERIALS AND METHODS

Data Collection

The RNA-seq transcriptome data, including 497 LUAD samples and 54 adjacent normal tissues, and corresponding clinical data were extracted from TCGA database¹ for differential expression analysis. All patients included in the prognostic analysis fit the following criteria: (1) histologically confirmed LUAD and (2) available information on gene expression and survival. Lastly, 468 patients with corresponding clinicopathological information were enrolled for further study. A total of 468 patients with LUAD were randomly classified into a training cohort (235 patients) and a test cohort (233 patients) at a 1:1 ratio by using the “caret” package, according to previous studies (Yang et al., 2019; Geng et al., 2021). Then 283 ferroptosis-related genes were retrieved from the previous study, including 132 drivers and 151 suppressors (Liu et al., 2020). TCGA pan-cancer data, including RNA-seq and clinical data and stemness scores based on mRNA (RNAss) and DNA-methylation (DNAss) of LUAD were extracted from xena browser². TCGA pan-cancer data include 33 cancer types. Among them, 18 cancer types had more than five associated normal tissue samples and were used to be further investigated.

Establishment and Validation of the Ferroptosis-Related Long Non-coding RNA Prognostic Signature

The annotation of lncRNA was performed as a previous study (Tu et al., 2020). Pearson correlation was used to mine ferroptosis-related lncRNAs (with the $| \text{Person R} | > 0.4$ and $p < 0.001$).

Differentially expressed genes (DEGs), miRNAs (DEMs) and lncRNAs between tumor and adjacent normal tissues were identified by using the “limma” or “edgeR” R package ($|\log_2\text{FC}| > 1$, FDR < 0.05). Univariate Cox analysis of overall survival (OS) was performed to screen ferroptosis-related genes and lncRNAs with prognostic value. Then, R package “glmnet” was used to conduct least absolute shrinkage and selection operator (LASSO) Cox regression. A ferroptosis-related lncRNA prognostic signature (FLPS) was constructed for the LUAD patients, which involved six ferroptosis-related lncRNAs. The risk score was calculated as the formula:

$$\text{Risk score} = \sum_{i=1}^n \beta_i \chi_i$$

where β_i means the coefficients, whereas χ_i is the FPKM value of each ferroptosis-related lncRNAs.

Risk scores were calculated for all patients in our study. Kaplan–Meier curve was used to compare the OS between the high-risk and low-risk group through R package “survival” and “survminer.” Time-dependent ROC analyses and the area under the curve (AUC) were performed to assess the model by using “timeROC.” Principal component analysis (PCA) and scatter diagrams were performed by R package “ggplot2.”

¹<https://portal.gdc.cancer.gov/>

²<https://xenabrowser.net/datapages/>

Functional Enrichment and Immune-Related Scores Analysis

Differentially expressed genes between the high-risk subgroup and low-risk group were identified based on the standards of $|\log_2FC| > 1$ and $p < 0.05$ using the R package “limma.” Then the DEGs were inputted into the “Metascape” website for functional and pathway enrichment analysis (Zhou et al., 2019). In addition, GSEA software was used to explore the hallmarks which were highly enriched in the high-risk group. The infiltrating score of 16 immune cells and the activity of 13 immune-related pathways were calculated with single-sample gene set enrichment analysis (ssGSEA) in the “gsva” R package. The immune, stromal and estimate score for each patient was calculated by the R “estimate” package.

Competing Endogenous RNA Network Construction

The online tool LncBase V2.0³ (Paraskevopoulou et al., 2016) was used to predict the downstream target miRNA with a 0.6 threshold (Paraskevopoulou et al., 2016). TargetScan⁴ (Agarwal et al., 2015), miRDB⁵ (Chen and Wang, 2020), and miWalk⁶ (Dweep and Gretz, 2015) were used to predict the target genes. Then, the predicted target genes and miRNAs were intersected with the DEGs and DEMs, respectively. MiRNAs or mRNAs that were not consistent with the expression of lncRNAs or miRNAs were eliminated. Then the network of lncRNAs, miRNAs, and mRNAs was constructed by Cytoscape (version 3.8.2) (Shannon et al., 2003).

Screening of Hub Genes and Survival-Related Genes

The STRING database⁷ (Szklarczyk et al., 2021) was applied to construct PPI network and discover the relationship among the target genes with high confidence (0.7). Then, the gene relationship was imported into Cytoscape and the top 10 hub genes were calculated by cytoHubba. Kaplan–Meier curve and log-rank test were used to mine prognostic genes.

Samples and Quantitative Real-Time Polymerase Chain Reaction

A total of 20 paired LUAD tissues and corresponding adjacent non-tumorous tissues were obtained from patients who underwent radical resection of lung cancer in Changhai Hospital, from June 2020 to September 2020. This study was approved by Ethics Committee of Changhai Hospital (Shanghai, China), and informed consent was signed before the operation for each patient. Total RNA was extracted from samples with TRIzolTM Reagent (Invitrogen). RNA was reverse-transcribed using PrimeScriptTM RT Master Mix (Takara). Real-time PCR was performed with TB GreenTM Premix EX TaqTM II

(Takara). The expression levels of lncRNAs were normalized by GAPDH. The sequences of primers were as follows: AC021016.1 forward 5'-GGGTCAAGCACACTGAGGGT-3', and reverse 5'-ACCAGGTGTGAACCCTTGGG-3'; KTN1-AS1 forward 5'-AGGGAATTTGGGCAGAAAGT-3', and reverse 5'-GTTACCCGTGTGAGCCTGAT-3'; GAPDH forward 5'-GTCTCCTCTGACTTCAACAGCG-3', and reverse 5'-ACCACCCTGTTGCTGTAGCCAA-3'.

Statistical Analysis

All statistical analyses were performed using R language 4.0.4 version and attached packages. Differentially expressed genes (DEGs), miRNAs (DEMs), and lncRNAs between tumor and adjacent normal tissues were identified by Wilcox test. Kaplan–Meier curve and log-rank test were used to compare OS between subgroups. Time-dependent ROC analyses and the area under the curve (AUC) were used to assess the performance of the model. Independent risk factor was screened by univariate and multivariate COX regression analysis. Spearman correlation was used to test the correlation between gene expression and stemness score, stromal score, immune score, and estimate score. Comparison of gene expression between the normal and tumors were performed in 18 cancer types which had more than five associated adjacent normal samples using linear mixed effects models. Mann–Whitney *U* test was used to compare the ssGSEA scores of immune cells or pathways between the high-risk and low-risk group.

RESULTS

Identification of Ferroptosis-Related Long Non-coding RNA in Lung Adenocarcinoma Patients

The workflow for construction of risk model and subsequent analyses is shown in **Supplementary Figure 1**. Firstly, a total of 283 ferroptosis-related gene expression matrices were extracted from the TCGA dataset. Among 283 genes, 18 genes were differentially expressed between tumor and adjacent normal tissues (**Figure 1A**) and consistent with univariate Cox regression analysis results (**Figure 1B**). A lncRNA whose expression value was correlated with one or more of the 18 ferroptosis-related genes was defined as a ferroptosis-related lncRNA. Through Pearson correlation analysis ($|\text{Pearson } R| > 0.4$ and $p < 0.001$), 590 ferroptosis-related lncRNAs were uncovered. Through analysis of differential expression and univariate Cox regression, we finally obtained 33 lncRNAs which were highly expressed in tumor and predicted a worse prognosis or were lowly expressed and predicted a better prognosis (**Figures 1C,D**).

Construction and Validation of the Prognostic Signature for Ferroptosis-Related Long Non-coding RNA

To build the ferroptosis-LPS for predicting the OS of LUAD patients, a total of 468 patients with LUAD were randomly

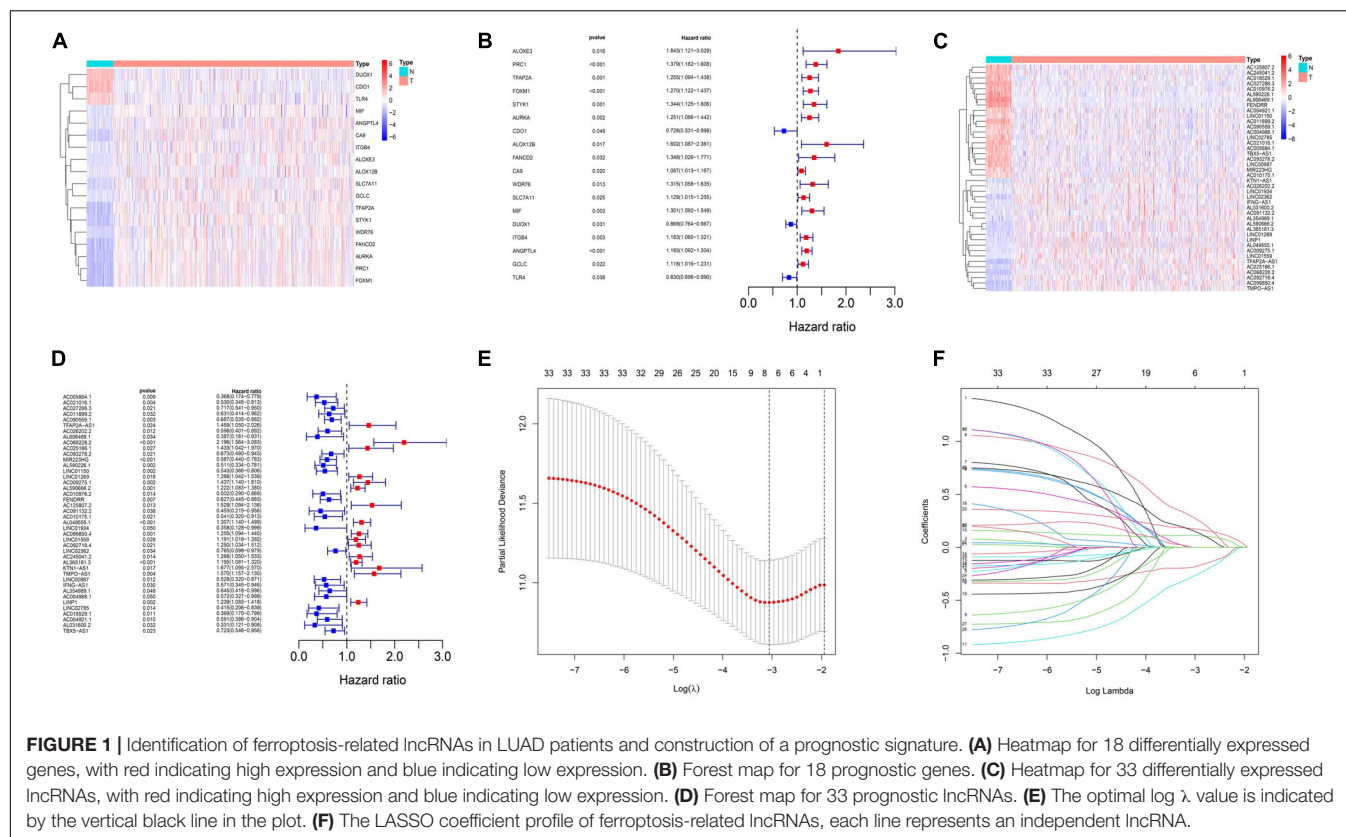
³<http://carolina.imis.athena-innovation.gr>

⁴<http://www.targetscan.org>

⁵<http://www.mirdb.org/mirdb/>

⁶<http://mirwalk.umm.uni-heidelberg.de/>

⁷<https://string-db.org/>



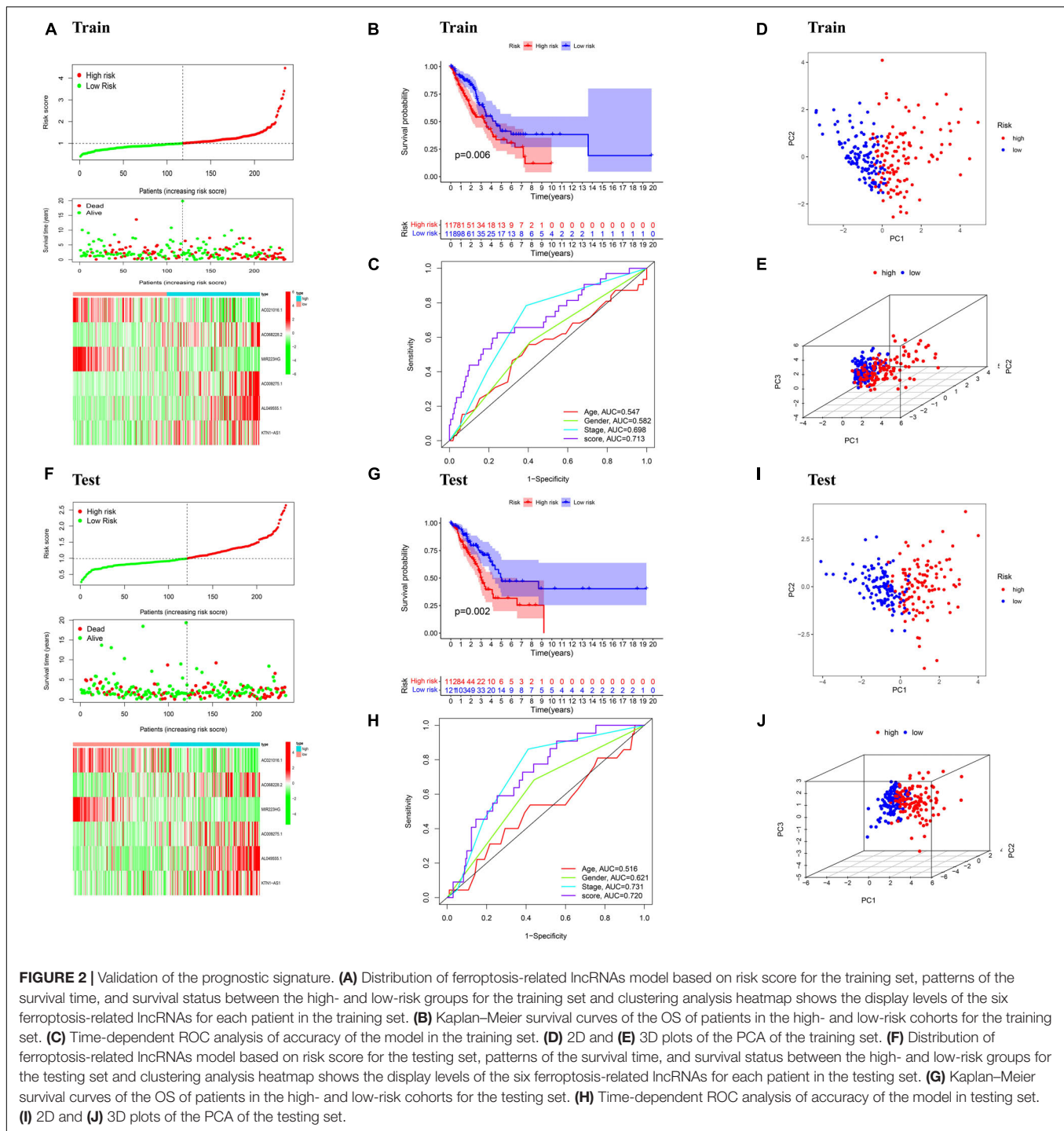
classified into a training cohort (235 patients) and a test cohort (233 patients) at a 1:1 ratio firstly. Then we performed the least absolute shrinkage and selection operator (LASSO) regression analysis based on the expression values of 33 ferroptosis-related lncRNA in the training cohort (Figures 1E,F). Six lncRNAs, namely, AC021016.1, AC068228.2, MIR223HG, AC009275.1, AL049555.1, and KTN1-AS1, were identified. The risk scores of each patient in TCGA training and validation cohorts were calculated based on the coefficient for each lncRNA, and the formula is as follows: risk score = $-0.1889 \times \text{AC021016.1 expression level} + (0.2885 \times \text{AC068228.2 expression level}) - (0.2782 \times \text{MIR223HG expression level}) + (0.1150 \times \text{AC009275.1 expression level}) + (0.1759 \times \text{AL049555.1 expression level}) + (0.1607 \times \text{KTN1-AS1 expression level})$. Patients in the TCGA training and test cohorts were divided into high-risk-score and low-risk-score subgroups based on the median value of risk scores. Risk score and survival status distributions are plotted in Figures 2A,F. The heatmap results suggested that AC021016.1 and MIR223HG were downregulated in the high-risk group, whereas the expression of AC068228.2, AC009275.1, AL049555.1, and KTN1-AS1 were upregulated in the high-risk group. Kaplan–Meier survival curves indicated that LUAD patients with low-risk scores had better clinical outcomes in either training or validation cohort (Figures 2B,G), and the ROC curves showed that ferroptosis-LPS had a promising ability to predict OS in the training and validation cohorts (Figures 2C,H). PCA analysis indicated the patients in two risk groups were distributed in two directions (Figures 2D,E,I,J).

Independence of the Ferroptosis-LPS Considering Other Clinical Factors

Univariate and multivariate Cox regression were performed to assess whether ferroptosis-LPS was an independent prognostic factor for patients with LUAD. In the TCGA training dataset, univariate Cox analysis indicated that ferroptosis-LPS and stage were remarkably associated with OS ($p < 0.001$, Figure 3A) and multivariate Cox analysis further confirmed that ferroptosis-LPS was a prognostic risk factor (Figure 3B). The same result was found in the testing cohort, which confirmed that ferroptosis-LPS was an independent risk factor for LUAD patients (univariate: $p < 0.001$; multivariate: $p < 0.05$; Figures 3C,D). These results suggested that our ferroptosis-LPS might be useful for clinical prognosis evaluation.

Functional Analyses in the TCGA Training and Testing Cohort

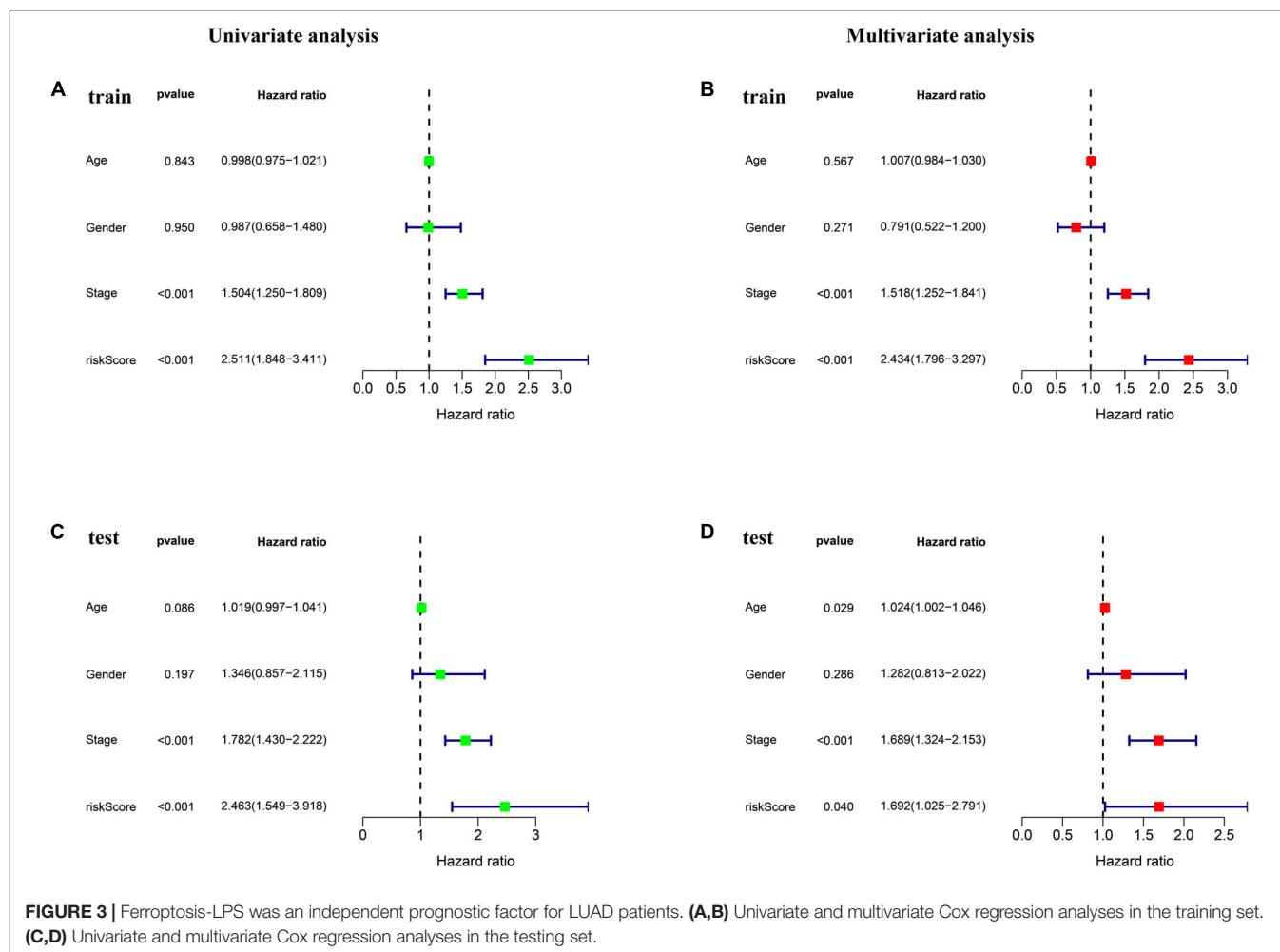
To investigate the biological functions and pathways which were associated with risk score in the training and test cohorts, the DEGs between the low- and high-risk groups were used to performed functional and pathway enrichment analysis. As expected, these DEGs were significantly enriched in cell cycle, retinoblastoma gene in cancer, and meiotic cell cycle ($p < 0.05$, Figures 4A,C). Gene set enrichment analysis showed that the genes in high-risk group of both train and test cohorts were significantly enriched in several hallmarks, such as MTORC1 signaling,



MYC targets, G2M checkpoint, E2F targets, and so on (Figures 4B,D).

To further explore the relationship between the risk score and immune status, ssGSEA was performed to calculate the infiltrating score of immune cells and immune-related pathways. The scores of CCR, Check-point, HLA, T_cell_co-stimulation, and Type_II_IFN_Response were lower in the high-risk group, which were confirmed by the results of

testing cohort. Moreover, the infiltrating scores of aDCs, B cells, DCs, iDCs, pDCs, neutrophils, T helper cells, and TIL were obviously higher in the low-risk groups of training and testing cohorts (Figures 5A,C). We further investigated the relationship between risk score with tumor microenvironment. Interestingly, the immune, stromal, and estimate score were higher in the low risk-score group (Figures 5B,D).



Stratification Analysis of the Ferroptosis-LPS and Construction of the Ferroptosis-LPS-Based Nomogram

The clinicopathological features and risk score of each patient in the TCGA dataset are shown in the heatmap (Figure 6A). For better assessment of the prognostic ability of the FLPS, we performed a stratification analysis to confirm its ability to predict OS in various subgroups. Compared to low-risk groups, high-risk LUAD patients had worse OS in the male and female subgroup. The same results were found in patients with age ≤ 65 or > 65 , T1-2 or T3-4, and stage I-II, N0 and M0 (Figure 6B).

To create a clinically applicable quantitative tool to predict the OS of LUAD patients, we established a nomogram using the risk score, age, and stage in the TCGA dataset (Figure 6C).

Association of Six Ferroptosis-Related Long Non-coding RNAs With Tumor Microenvironment and Tumor Stemness

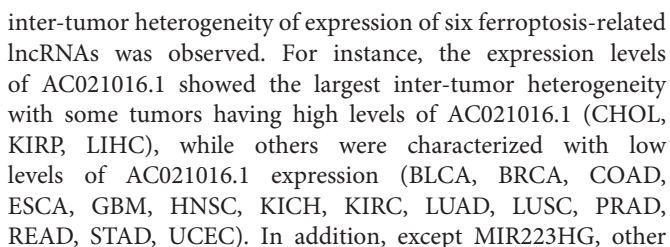
As the risk score was significantly correlated with tumor microenvironment, we investigated the association between the expression levels of the six ferroptosis-related lncRNAs and

the tumor microenvironment. We found that AC021016.1 and MIR223HG had a positive correlation with stromal scores, immune score and estimate score, whereas AC068228.2 had a negative correlation ($p < 0.001$, Figure 7A).

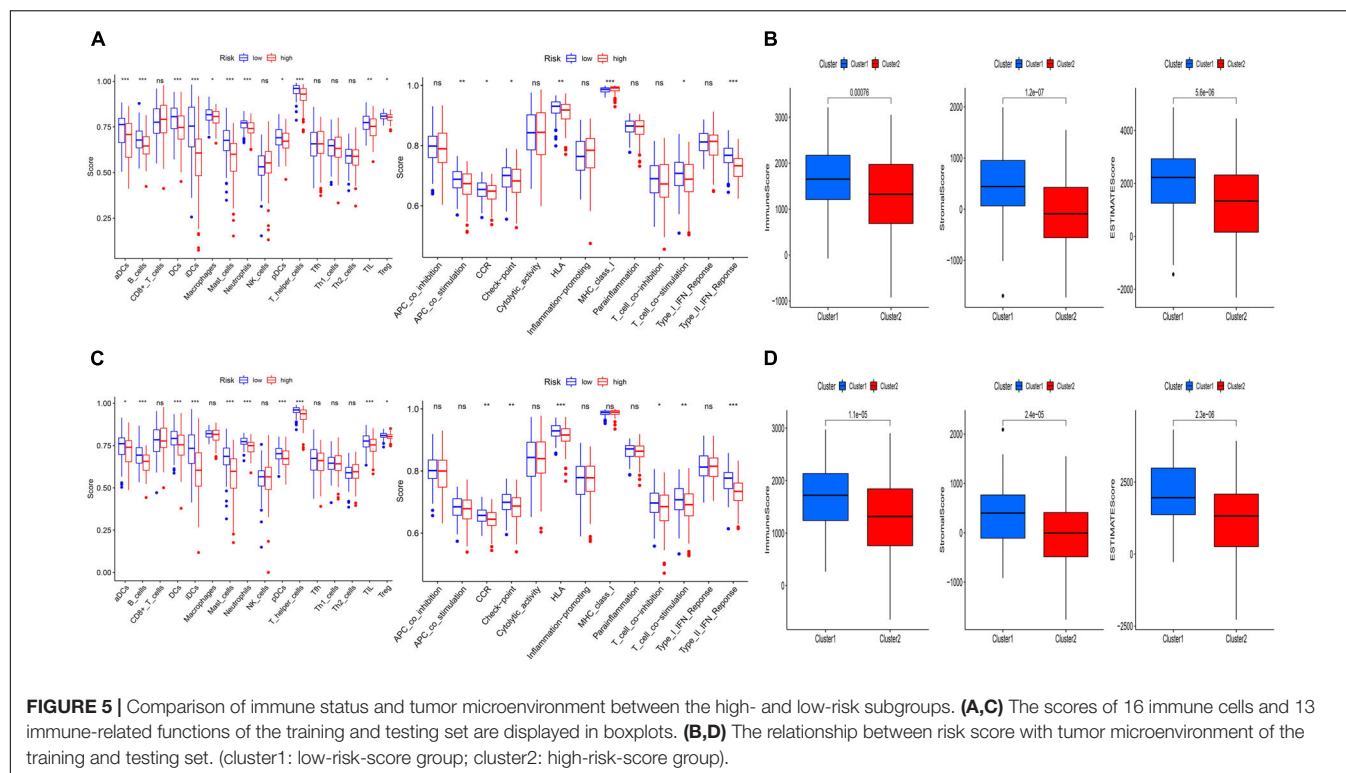
In the process of cancer progression, tumor cells can gradually lose the phenotype of differentiation and acquire the characteristics of progenitor cells and stem cells, which might increase tumor resistance. Since those six lncRNAs were prognostic risk factors, we explored the correlation between them and RNA stemness score (RNAss) and DNA stemness score (DNAss), which were indicators of tumor stemness. The results showed that AC021016.1 and MIR223HG were negatively correlated with tumor stemness in both RNAss and DNAss while AC068228.2 and KTN1-AS1 had the positive correlation ($p < 0.001$, Figure 7A).

Analysis of Six Ferroptosis-Related Long Non-coding RNAs in Pan-Cancer

To further understand the roles of six ferroptosis-related lncRNAs in tumors, we examined their expression levels in 18 cancer types in TCGA pan-cancer data. A striking



Then we further explored the prognostic value of lncRNAs in tumors. Median was used to distinguish between high and low expression groups, whereas KM curves were performed to compare outcomes between the two groups. The results showed that the altered expression of ferroptosis-related lncRNAs were generally associated with patients' overall survival. In most



tumors, high expression of AC009275.1 and AC068228.2 were associated with poor prognosis, while other lncRNAs' prognostic effect depended on the type of tumors (Supplementary Figure 2).

Construction of the Competing Endogenous RNA Network and Functional Enrichment Analysis

Several lncRNAs were found to act as miRNA sponges to participate in the regulation of gene expression. Then we explored the DEMs and DEGs based on the TCGA-LUAD dataset ($|\log_2FC| > 1$, $FDR < 0.05$); 369 DEMs and 1,517 DEGs were identified by the "edgeR" package. Top 20 up- and downregulated DEMs and DEGs are shown in Supplementary Figure 3. Using the LncBase Predicted v.2, we predicted the targeted miRNA of the six ferroptosis-related lncRNAs with a 0.6 threshold. Then the intersection of target miRNAs for downregulated lncRNAs with upregulated miRNAs of TCGA dataset and target miRNAs for upregulated lncRNAs with downregulated miRNAs of LUAD were taken. To further explore the target genes of the miRNAs, we applied TargetScan, miRDB, and miRWalk to predict the target genes. We used the negative correlation criteria [(a) miRNAs should be targeted to the mRNA; (b) the expression level of mRNAs should be opposite to miRNAs; and (c) the mRNAs belong to DEGs] to screen the downstream mRNAs. Ultimately, five ferroptosis-related lncRNAs, 45 miRNAs, and 107 mRNAs were included in our ceRNA network (Figure 8A).

Furthermore, GO and KEGG enrichment analyses were performed to clarify the biological function of 107 downstream genes. Through BP analysis, response to peptide hormone, cell

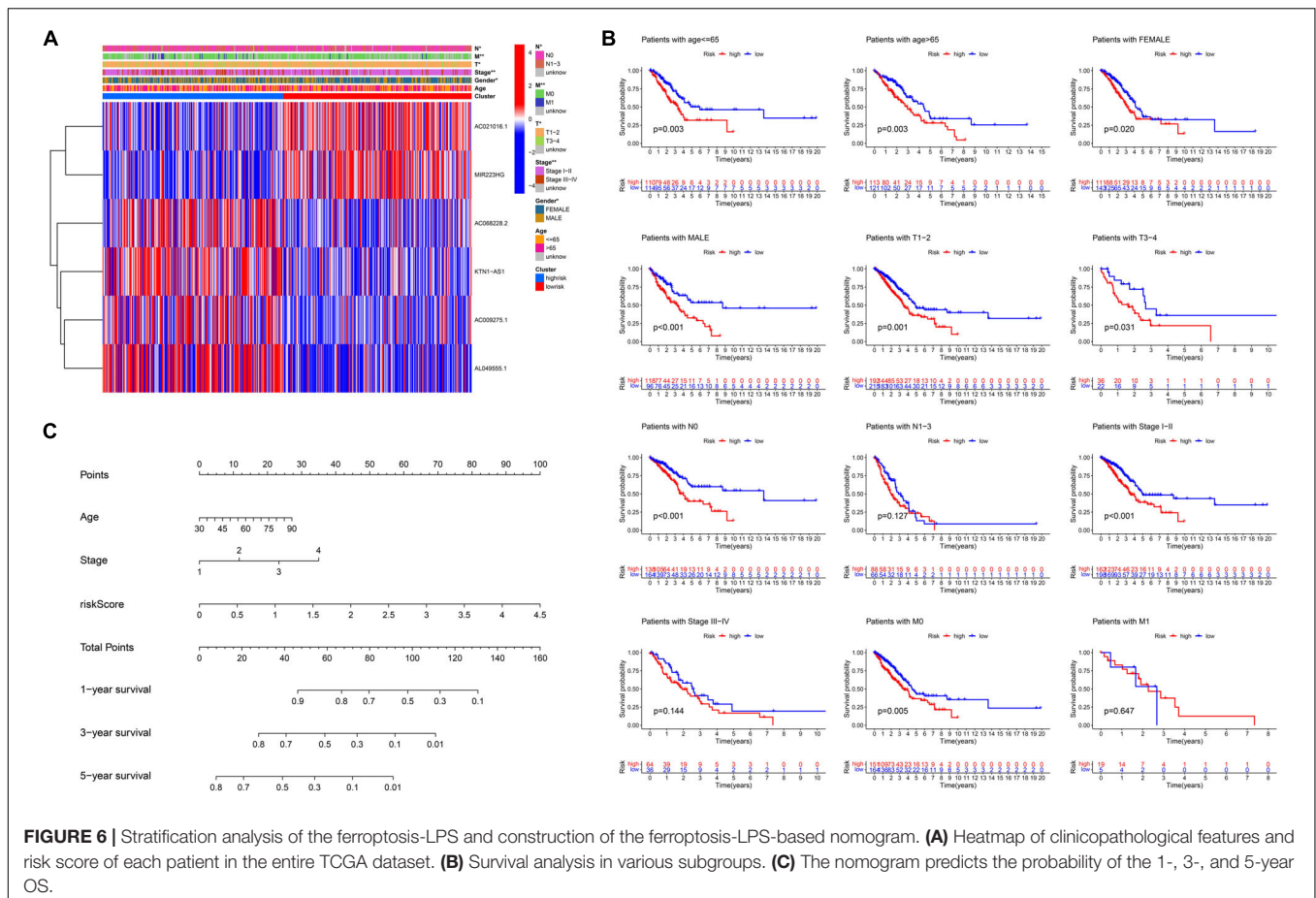
growth, regulation of cell growth, and regulation of cell-cell adhesion were obviously enriched (Figure 8B). The results of CC analysis contained membrane raft, membrane microdomain, membrane region, and focal adhesion (Figure 8C). Moreover, MF analysis revealed that downstream genes were mostly enriched in protein serine/threonine kinase activity (Figure 8D). KEGG analysis demonstrated that axon guidance, hippo signaling pathway, TGF-beta signaling pathway, cellular senescence, and steroid biosynthesis were the top five enriched pathways (Figure 8E).

Screening of Hub Genes and Survival-Related Genes

Through STRING database, a total of 41 genes were screened out of 107 target genes to construct the PPI network, which contained 41 nodes and 42 edges (Figure 8F). The 10 hub genes (CAV1, BIRC5, CKS1B, SMAD7, BMP2, PTPN1, BMP2, EDN1, TGFBR2, and CXCL12) were screened out by the rank of degree which was calculated by cytoHubba in cytoscape (Figure 8G). The KM curve showed that the expression of BIRC5 and CKS1B were negatively correlated with survival prognosis ($p < 0.01$, Figures 8H,I).

Validation of the Expression Level of Ferroptosis-Related Long Non-coding RNAs in Lung Adenocarcinoma Samples

To validate the expression levels of ferroptosis-related lncRNAs, we detected two ferroptosis-related lncRNAs expression levels in 20 LUAD samples and 20 adjacent normal tissues through



qRT-PCR. The results showed that AC021016.1 was significantly downregulated in LUAD while KTN1-AS1 was highly expressed in LUAD (Supplementary Figure 4).

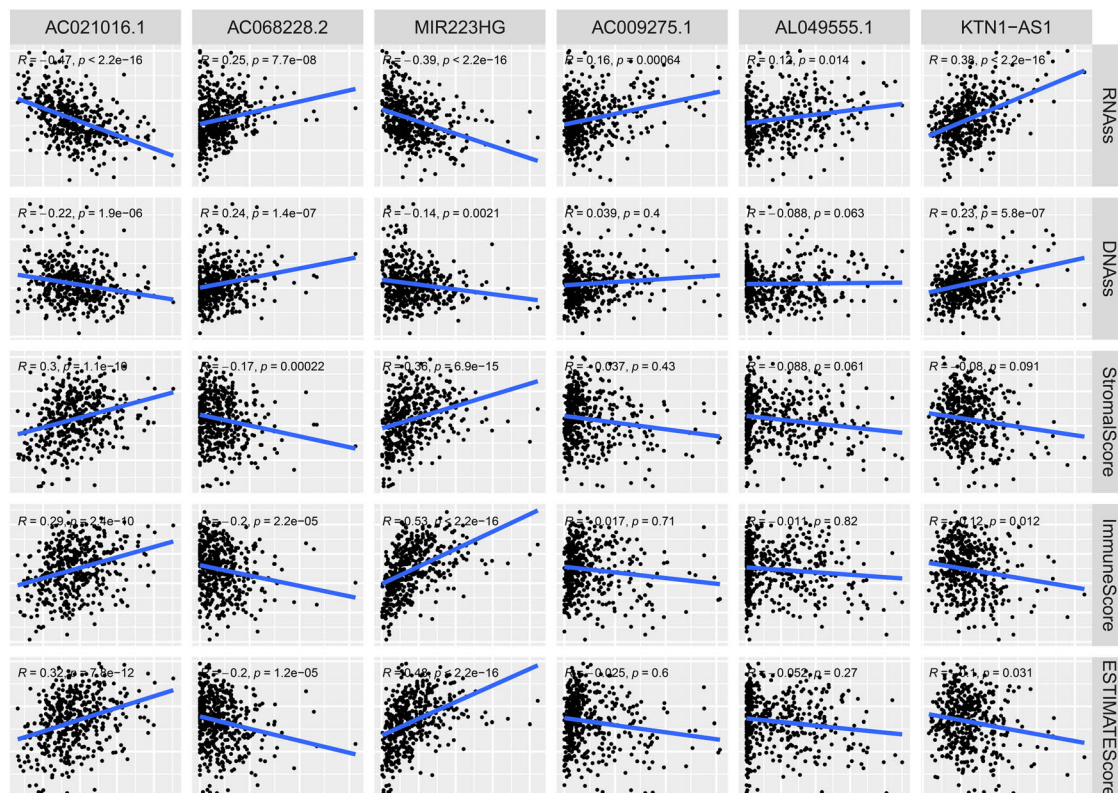
DISCUSSION

Long non-coding RNAs (lncRNAs) are a kind of non-protein coding RNAs with over 200 nucleotides (Wang J. et al., 2021). They are widely expressed in human cells and play vital roles in regulation of pathological and physiological processes in various types of malignant tumors (Zhou et al., 2020). Previous studies have constructed a few of lncRNA prognosis signatures, like m6A-related lncRNA signature (Xu et al., 2021), immune-related lncRNA signature (Wang J. et al., 2021), and autophagy-related lncRNA signature (Zhou et al., 2020), which can be used to identify high-risk patients and judge the prognosis of them. Ferroptosis is a form of regulatory cell death and plays an important role in the occurrence and development of LUAD. Some studies have shown that lncRNAs can participate in the regulation of ferroptosis and growth of LUAD (Sánchez et al., 2014; Johnson et al., 2017; Zhang et al., 2017; Wang et al., 2019; Gai et al., 2020). Thus, ferroptosis-related lncRNAs are potential markers for prognosis and a prognostic model based on them for LUAD is still lacking.

To construct a prognostic model, we firstly uncovered 18 ferroptosis-related genes through gene expression differential analysis and Cox regression. Among them, cysteine dioxygenase 1 (CDO1), toll-like receptor 4 (TLR4), and dual oxidase 1 (DUOX1) were downregulated in tumors and played a protective role, while Fanconi anemia complementation group D2 (FANCD2) and others were with high expression in tumors and were risk factors for prognosis. CDO1 was found to transform cysteine to taurine while cysteine was an indispensable substrate of glutathione peroxidase 4 (GPX4), a lipid repair enzyme of ferroptosis. The suppression of CDO1 increased the expression of GSH and inhibited ferroptosis in gastric cancer (Hao et al., 2017). In another study (Chen et al., 2019), Chen et al. reported that the silence of TLR4 and NOX4 significantly retarded the autophagy and ferroptosis in rats with heart failure. FANCD2, a nuclear protein that responds to DNA damage repair, negatively regulated ferroptosis of bone marrow injury in cancer treatment and could be a potential target of anticancer therapies (Song et al., 2016). In addition, a 10 ferroptosis-related genes signature and a ferroptosis-related gene signature with five genes were constructed to predict the prognosis of patients with LUAD (Wang S. et al., 2021; Zhu et al., 2021). In general, ferroptosis-related genes play important roles in the progression of LUAD.

It has been reported that ferroptosis-related lncRNAs were prognostic risk factors and the signatures constructed with

A Cancer: LUAD



Gene expression

B

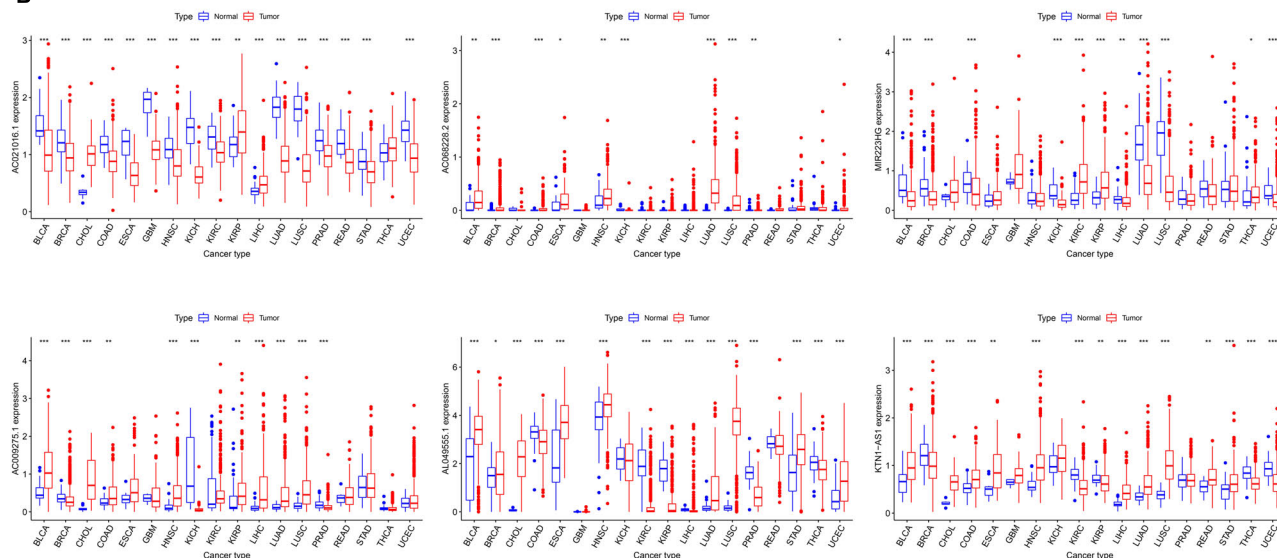
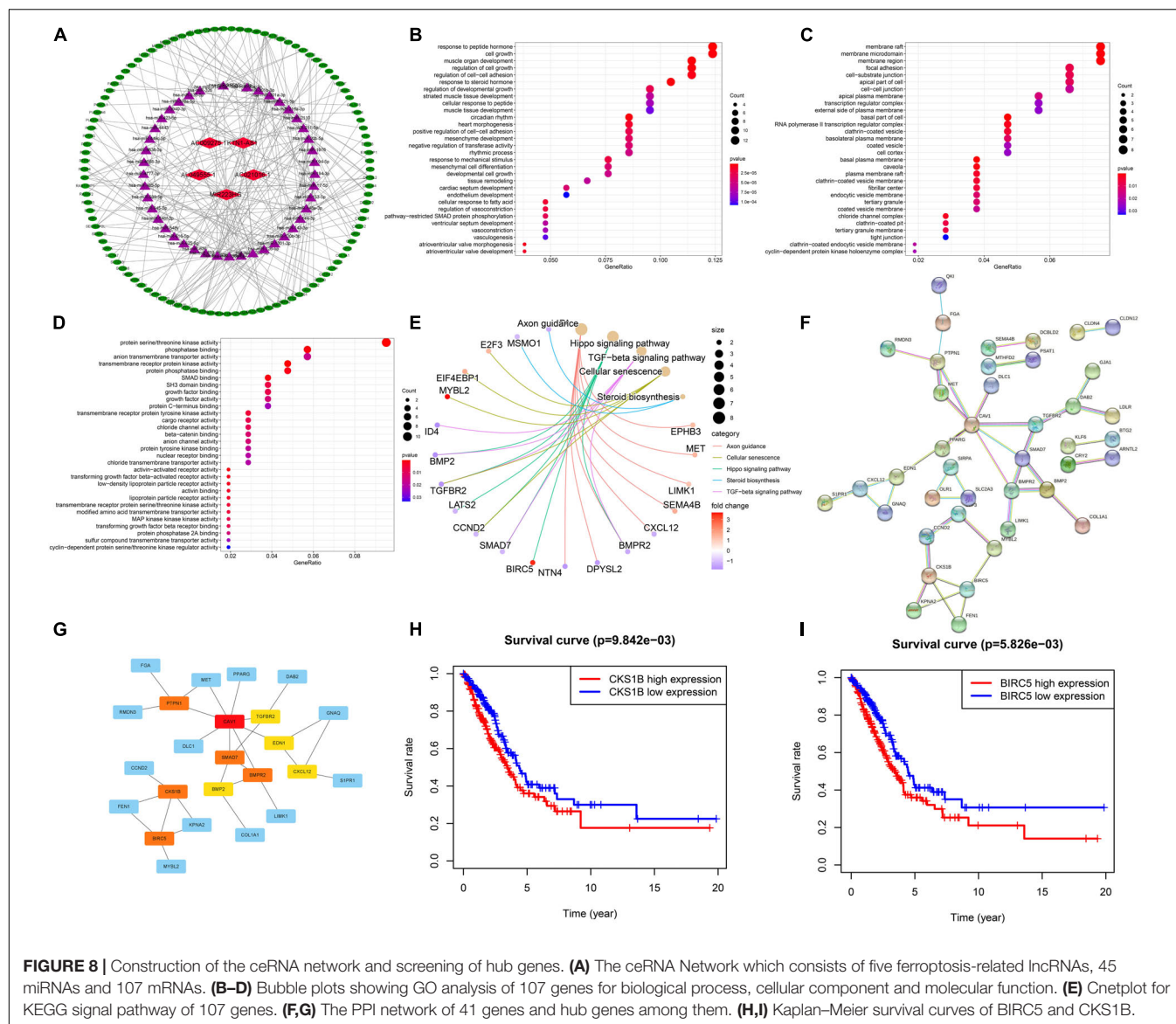


FIGURE 7 | Association of expression of six lncRNAs with tumor microenvironment and tumor stemness and the pan-cancer expression analysis. **(A)** Correlation matrices between six lncRNAs expression and RNAss, DNAss, stromal score, immune score, and estimate score. **(B)** The expression level of six lncRNAs in tumors compared with normal tissue in 18 cancer types which were composed of more than five normal samples.

ferroptosis-related lncRNAs can be used to distinguish high-risk patients from low-risk patients (Cai et al., 2021; Tang et al., 2021). However, the full role of ferroptosis-related lncRNAs

in LUAD remains to be further explored. Here, we mined ferroptosis-related lncRNAs through Pearson correlation and constructed a prognostic Signature with six ferroptosis-related



lncRNAs. Through Kaplan–Meier survival curves, ROC curve, PCA, and univariate and multivariate COX regression, we further confirmed the validity of our signature. Among the six lncRNAs, AC021016.1 and MIR223HG were downregulated in LUAD and were protective factors for prognosis, while KTN1-AS1 and others were upregulated and were risk factors for prognosis. lncRNA KTN1-AS1 was upregulated in several tumors, such as non-small cell lung cancer, bladder cancer, head and neck squamous cell carcinoma, and hepatocellular carcinoma and promoted the progression of tumors (Zhang et al., 2019; Jiang et al., 2020; Hu et al., 2021; Li Y. Y. et al., 2021). In our study, we find that lncRNA KTN1-AS1 was significantly upregulated in LUAD and correlated with tumor stemness and tumor microenvironment. In another study (Geng et al., 2021), MIR223HG was found to be a genome instability-related lncRNA and used to construct a genome instability-related lncRNA signature, which further confirmed the potential function of

MIR223HG in LUAD. AL049555.1 was demonstrated to be highly expressed and associated with high risk of PAAD (Wang et al., 2020). The function of AC021016.1, AC068228.2, and AC009275.1 has not been elucidated and our research uncovered their potential roles in LUAD.

To further elucidate the potential function of six ferroptosis-related lncRNAs, we constructed ceRNA network to find the downstream genes. Through STRING and Cytoscape, we found the 10 hub genes of PPI network. Among them, the high expression of BIRC5 and CKS1B were significantly correlated with poor prognosis. BIRC5 is a well-known therapeutic target of cancers (Li et al., 2019) and plays an important role in cell division and inhibits cell death (Wheatley and Altieri, 2019). Previous research revealed that BIRC5 was elevated and promoted the development of lung cancer (Han et al., 2020). CKS1B, a member of Cks/Suc1 family, is involved in the regulation of cell cycle

and chemotherapeutic resistance in cancers (Wang et al., 2017). In lung cancer, it also promotes cell growth and induces drug resistance (Shi et al., 2020). In addition, although CAV1, SMAD7, BMP2, EDN1, and CXCL12 were not significantly different in the prognostic analysis in our study, they also play important roles in the occurrence and development of lung cancer (Katsura et al., 2018; Yan et al., 2019; Huang et al., 2020; Pulido et al., 2020; Tong et al., 2020). In general, the functions of target genes further confirmed the potential roles of those lncRNAs. Finally, we detected two ferroptosis-related lncRNAs expression levels through qRT-PCR with 20 pairs of samples, which increased the reliability of our results.

Ferroptosis is a new form of cell death that might potentially provide a new strategy in clinical cancer therapy. However, the crosstalk among ferroptosis and other cell death processes, auto-immune microenvironment, and maintenance and transformation of tumor stem cells remain unsolved. In this study, we constructed a ferroptosis-related lncRNA signature and confirmed its validity in predicting survival outcomes of LUAD. We hope that these findings will provide some useful insights for clinical practice. However, several limitations were in our study. Firstly, multicenter LUAD datasets are needed to verify the validity of our model. Secondly, although we confirmed the expression in our own samples through qRT-PCR, the application of this prognostic prediction model in LUAD need to be further explored.

DATA AVAILABILITY STATEMENT

The original contributions presented in the study are included in the article/**Supplementary Material**, further inquiries can be directed to the corresponding author/s.

REFERENCES

- Agarwal, V., Bell, G. W., Nam, J. W., and Bartel, D. P. (2015). Predicting effective microRNA target sites in mammalian mRNAs. *Elife* 4:e05005.
- Bray, F., Ferlay, J., Soerjomataram, I., Siegel, R. L., Torre, L. A., and Jemal, A. (2018). Global cancer statistics 2018: GLOBOCAN estimates of incidence and mortality worldwide for 36 cancers in 185 countries. *CA Cancer J. Clin.* 68, 394–424. doi: 10.3322/caac.21492
- Cai, H. J., Zhuang, Z. C., Wu, Y., Zhang, Y. Y., Liu, X., Zhuang, J. F., et al. (2021). Development and validation of a ferroptosis-related lncRNAs prognosis signature in colon cancer. *Bosn. J. Basic Med. Sci.* 21, 569–576. doi: 10.17305/bjbm.2020.5617
- Chen, X., Kang, R., Kroemer, G., and Tang, D. (2021). Broadening horizons: the role of ferroptosis in cancer. *Nat. Rev. Clin. Oncol.* 18, 280–296. doi: 10.1038/s41571-020-00462-0
- Chen, X., Xu, S., Zhao, C., and Liu, B. (2019). Role of TLR4/NADPH oxidase 4 pathway in promoting cell death through autophagy and ferroptosis during heart failure. *Biochem. Biophys. Res. Commun.* 516, 37–43. doi: 10.1016/j.bbrc.2019.06.015
- Chen, Y., and Wang, X. (2020). miRDB: an online database for prediction of functional microRNA targets. *Nucleic Acids Res.* 48, D127–D131.
- Chu, B., Kon, N., Chen, D., Li, T., Liu, T., Jiang, L., et al. (2019). ALOX12 is required for p53-mediated tumour suppression through a distinct ferroptosis pathway. *Nat. Cell Biol.* 21, 579–591. doi: 10.1038/s41556-019-0305-6

ETHICS STATEMENT

The studies involving human participants were reviewed and approved by the Medical Ethics Committee of Changhai Hospital, Navy Military Medical University. The patients/participants provided their written informed consent to participate in this study.

AUTHOR CONTRIBUTIONS

XF, CH, and XW constructed this study. XF, CH, XW, CJL, and HC collected and analyzed the data. BS and CL wrote and revised the manuscript and were responsible for the critical reading of the manuscript. All authors contributed to the article and approved the submitted version.

FUNDING

This study was sponsored by Natural Science Foundation of Shanghai (19ZR1456400) and National Natural Science Foundation of China (81802288).

ACKNOWLEDGMENTS

We sincerely appreciate the contribution of the TCGA project.

SUPPLEMENTARY MATERIAL

The Supplementary Material for this article can be found online at: <https://www.frontiersin.org/articles/10.3389/fcell.2021.751490/full#supplementary-material>

- Dweep, H., and Gretz, N. (2015). miRWalk2.0: a comprehensive atlas of microRNA-target interactions. *Nat. Methods* 12:697. doi: 10.1038/nmeth.3485
- Gai, C., Liu, C., Wu, X., Yu, M., Zheng, J., Zhang, W., et al. (2020). MT1DP loaded by folate-modified liposomes sensitizes erastin-induced ferroptosis via regulating miR-365a-3p/NRF2 axis in non-small cell lung cancer cells. *Cell Death Dis.* 11:751. doi: 10.1038/s41419-020-02939-3
- Geng, W., Lv, Z., Fan, J., Xu, J., Mao, K., Yin, Z., et al. (2021). Identification of the prognostic significance of somatic mutation-derived lncRNA signatures of genomic instability in lung adenocarcinoma. *Front. Cell Dev. Biol.* 9:657667. doi: 10.3389/fcell.2021.657667
- Han, F., Yang, S., Wang, W., Huang, X., Huang, D., and Chen, S. (2020). Silencing of lncRNA LINC00857 enhances BIRC5-dependent radio-sensitivity of lung adenocarcinoma cells by recruiting NF-κB1. *Mol. Ther. Nucleic Acids* 22, 981–993. doi: 10.1016/j.omtn.2020.09.020
- Hao, S., Yu, J., He, W., Huang, Q., Zhao, Y., Liang, B., et al. (2017). Cysteine dioxygenase 1 mediates erastin-induced ferroptosis in human gastric cancer cells. *Neoplasia* 19, 1022–1032. doi: 10.1016/j.neo.2017.10.005
- Hu, X., Xiang, L., He, D., Zhu, R., Fang, J., Wang, Z., et al. (2021). The long noncoding RNA KTN1-AS1 promotes bladder cancer tumorigenesis via KTN1 cis-activation and the consequent initiation of Rho GTPase-mediated signaling. *Clin. Sci. (Lond.)* 135, 555–574. doi: 10.1042/CS20200908
- Huang, F., Cao, Y., Wu, G., Chen, J., Wang, C., Lin, W., et al. (2020). BMP2 signalling activation enhances bone metastases of non-small cell lung cancer. *J. Cell Mol. Med.* 24, 10768–10784.

- Jiang, Y., Wu, K., Cao, W., Xu, Q., Wang, X., Qin, X., et al. (2020). Long noncoding RNA KTN1-AS1 promotes head and neck squamous cell carcinoma cell epithelial-mesenchymal transition by targeting miR-153-3p. *Epigenomics* 12, 487–505. doi: 10.2217/epi-2019-0173
- Johnson, G. S., Li, J., Beaver, L. M., Dashwood, W. M., Sun, D., Rajendran, P., et al. (2017). A functional pseudogene, NMRAL2P, is regulated by Nrf2 and serves as a coactivator of NQO1 in sulforaphane-treated colon cancer cells. *Mol. Nutr. Food Res.* 61:10. doi: 10.1002/mnfr.201600769
- Katsura, M., Shoji, F., Okamoto, T., Shimamatsu, S., Hirai, F., Toyokawa, G., et al. (2018). Correlation between CXCR4/CXCR7/CXCL12 chemokine axis expression and prognosis in lymph-node-positive lung cancer patients. *Cancer Sci.* 109, 154–165. doi: 10.1111/cas.13422
- Li, C. H., and Chen, Y. (2016). Insight into the role of long noncoding RNA in cancer development and progression. *Int. Rev. Cell Mol. Biol.* 326, 33–65. doi: 10.1016/bs.ircmb.2016.04.001
- Li, F., Aljahdali, I., and Ling, X. (2019). Cancer therapeutics using survivin BIRC5 as a target: what can we do after over two decades of study? *J. Exp. Clin. Cancer Res.* 38:368. doi: 10.1186/s13046-019-1362-1
- Li, S., Yang, S., Qiu, C., and Sun, D. (2021). lncRNA MSC-AS1 facilitates lung adenocarcinoma through sponging miR-33b-5p to up-regulate GPAM. *Biochem. Cell. Biol.* 99, 241–248. doi: 10.1139/bcb-2020-0239
- Li, Y. Y., Li, W., Chang, G. Z., and Li, Y. M. (2021). Long noncoding RNA KTN1 antisense RNA l exerts an oncogenic function in lung adenocarcinoma by regulating DEP domain containing 1 expression via activating epithelial-mesenchymal transition. *Anticancer Drugs* 32, 614–625. doi: 10.1097/CAD.0000000000001035
- Liu, Y., Zhang, X., Zhang, J., Tan, J., Li, J., and Song, Z. (2020). Development and validation of a combined ferroptosis and immune prognostic classifier for hepatocellular carcinoma. *Front. Cell Dev. Biol.* 8:596679. doi: 10.3389/fcell.2020.596679
- Miller, K. D., Nogueira, L., Mariotto, A. B., Rowland, J. H., Yabroff, K. R., Alfano, C. M., et al. (2019). Cancer treatment and survivorship statistics, 2019. *CA Cancer J. Clin.* 69, 363–385.
- Paraskevopoulou, M. D., Vlachos, I. S., Karagkouni, D., Georgakilas, G., Kanellos, I., Vergoulis, T., et al. (2016). DIANA-LncBase v2: indexing microRNA targets on non-coding transcripts. *Nucleic Acids Res.* 44, D231–D238. doi: 10.1093/nar/gkv1270
- Pulido, I., Ollosi, S., Aparisi, S., Becker, J. H., Aliena-Valero, A., Benet, M., et al. (2020). Endothelin-1-mediated drug resistance in EGFR-mutant non-small cell lung carcinoma. *Cancer Res.* 80, 4224–4232. doi: 10.1158/0008-5472.CAN-20-0141
- Qu, S., Jiao, Z., Lu, G., Yao, B., Wang, T., Rong, W., et al. (2021). PD-L1 lncRNA splice isoform promotes lung adenocarcinoma progression via enhancing c-Myc activity. *Genome Biol.* 22:104. doi: 10.1186/s13059-021-02331-0
- Sánchez, Y., Segura, V., Marín-Béjar, O., Athie, A., Marchese, F. P., González, J., et al. (2014). Genome-wide analysis of the human p53 transcriptional network unveils a lncRNA tumour suppressor signature. *Nat. Commun.* 5:5812. doi: 10.1038/ncomms6812
- Shannon, P., Markiel, A., Ozier, O., Baliga, N. S., Wang, J. T., Ramage, D., et al. (2003). Cytoscape: a software environment for integrated models of biomolecular interaction networks. *Genome Res.* 13, 2498–2504. doi: 10.1101/gr.1239303
- Shi, W., Huang, Q., Xie, J., Wang, H., Yu, X., and Zhou, Y. (2020). CKS1B as drug resistance-inducing gene-a potential target to improve cancer therapy. *Front. Oncol.* 10:582451. doi: 10.3389/fonc.2020.582451
- Song, X., Xie, Y., Kang, R., Hou, W., Sun, X., Epperly, M. W., et al. (2016). FANCD2 protects against bone marrow injury from ferroptosis. *Biochem. Biophys. Res. Commun.* 480, 443–449. doi: 10.1016/j.bbrc.2016.10.068
- Szklarczyk, D., Gable, A. L., Nastou, K. C., Lyon, D., Kirsch, R., Pyysalo, S., et al. (2021). The STRING database in 2021: customizable protein-protein networks, and functional characterization of user-uploaded gene/measurement sets. *Nucleic Acids Res.* 49, D605–D612.
- Tang, Y., Li, C., Zhang, Y. J., and Wu, Z. H. (2021). Ferroptosis-related long non-coding RNA signature predicts the prognosis of Head and neck squamous cell carcinoma. *Int. J. Biol. Sci.* 17, 702–711. doi: 10.7150/ijbs.55552
- Tong, L., Shen, S., Huang, Q., Fu, J., Wang, T., Pan, L., et al. (2020). Proteasome-dependent degradation of Smad7 is critical for lung cancer metastasis. *Cell Death Differ.* 27, 1795–1806. doi: 10.1038/s41418-019-0459-6
- Tu, Z., Wu, L., Wang, P., Hu, Q., Tao, C., Li, K., et al. (2020). N6-methyladenosine-related lncRNAs are potential biomarkers for predicting the overall survival of lower-grade glioma patients. *Front. Cell Dev. Biol.* 8:642. doi: 10.3389/fcell.2020.00642
- Wang, H., Sun, M., Guo, J., Ma, L., Jiang, H., Gu, L., et al. (2017). 3-O-(Z)-coumaroyloleanolic acid overcomes Cks1b-induced chemoresistance in lung cancer by inhibiting Hsp90 and MEK pathways. *Biochem. Pharmacol.* 135, 35–49. doi: 10.1016/j.bcp.2017.03.007
- Wang, J., Xiang, J., and Li, X. (2020). Construction of a competitive endogenous RNA network for pancreatic adenocarcinoma based on weighted gene co-expression network analysis and a prognosis model. *Front. Bioeng. Biotechnol.* 8:515. doi: 10.3389/fbioe.2020.00515
- Wang, J., Yin, X., Zhang, Y. Q., and Ji, X. (2021). Identification and validation of a novel immune-related four-lncRNA signature for lung adenocarcinoma. *Front. Genet.* 12:639254. doi: 10.3389/fgene.2021.639254
- Wang, M., Mao, C., Ouyang, L., Liu, Y., Lai, W., Liu, N., et al. (2019). Long noncoding RNA LINC00336 inhibits ferroptosis in lung cancer by functioning as a competing endogenous RNA. *Cell Death Differ.* 26, 2329–2343.
- Wang, S., Wu, C., Ma, D., and Hu, Q. (2021). Identification of a ferroptosis-related gene signature (FRGS) for predicting clinical outcome in lung adenocarcinoma. *PeerJ* 9:e11233. doi: 10.7717/peerj.11233
- Wang, Z., Zhang, X., Tian, X., Yang, Y., Ma, L., Wang, J., et al. (2021). CREB stimulates GPX4 transcription to inhibit ferroptosis in lung adenocarcinoma. *Oncol. Rep.* 45:88. doi: 10.3892/or.2021.8039
- Wheatley, S. P., and Altieri, D. C. (2019). Survivin at a glance. *J. Cell Sci.* 132:jcs.223826. doi: 10.1242/jcs.223826
- Xu, F., Huang, X., Li, Y., Chen, Y., and Lin, L. (2021). m⁶A-related lncRNAs are potential biomarkers for predicting prognoses and immune responses in patients with LUAD. *Mol. Ther. Nucleic Acids* 24, 780–791. doi: 10.1016/j.omtn.2021.04.003
- Yan, Y., Xu, Z., Qian, L., Zeng, S., Zhou, Y., Chen, X., et al. (2019). Identification of CAV1 and DCN as potential predictive biomarkers for lung adenocarcinoma. *Am. J. Physiol. Lung Cell Mol. Physiol.* 316, L630–L643. doi: 10.1152/ajplung.00364.2018
- Yang, G., Zhang, Y., and Yang, J. (2019). A five-microRNA signature as prognostic biomarker in colorectal cancer by bioinformatics analysis. *Front. Oncol.* 9:1207. doi: 10.3389/fonc.2019.01207
- Zhang, D., Zhang, G., Hu, X., Wu, L., Feng, Y., He, S., et al. (2017). Oncogenic RAS regulates long noncoding RNA Orilnc1 in human cancer. *Cancer Res.* 77, 3745–3757. doi: 10.1158/0008-5472.CAN-16-1768
- Zhang, L., Wang, L., Wang, Y., Chen, T., Liu, R., Yang, W., et al. (2019). lncRNA KTN1-AS1 promotes tumor growth of hepatocellular carcinoma by targeting miR-23c/ERBB2IP axis. *Biomed. Pharmacother.* 109, 1140–1147. doi: 10.1016/j.biopha.2018.10.105
- Zhou, M., Shao, W., Dai, H., and Zhu, X. (2020). A robust signature based on autophagy-associated lncRNAs for predicting prognosis in lung adenocarcinoma. *Biomed. Res. Int.* 2020:3858373. doi: 10.1155/2020/3858373
- Zhou, Y., Zhou, B., Pache, L., Chang, M., Khodabakhshi, A. H., Tanaseichuk, O., et al. (2019). Metascape provides a biologist-oriented resource for the analysis of systems-level datasets. *Nat. Commun.* 10:1523. doi: 10.1038/s41467-019-09234-6
- Zhu, G., Huang, H., Xu, S., Shi, R., Gao, Z., Lei, X., et al. (2021). Prognostic value of ferroptosis-related genes in patients with lung adenocarcinoma. *Thorac. Cancer* 12, 1890–1899.

Conflict of Interest: The authors declare that the research was conducted in the absence of any commercial or financial relationships that could be construed as a potential conflict of interest.

Publisher's Note: All claims expressed in this article are solely those of the authors and do not necessarily represent those of their affiliated organizations, or those of the publisher, the editors and the reviewers. Any product that may be evaluated in this article, or claim that may be made by its manufacturer, is not guaranteed or endorsed by the publisher.

Copyright © 2021 Fei, Hu, Wang, Lu, Chen, Sun and Li. This is an open-access article distributed under the terms of the Creative Commons Attribution License (CC BY). The use, distribution or reproduction in other forums is permitted, provided the original author(s) and the copyright owner(s) are credited and that the original publication in this journal is cited, in accordance with accepted academic practice. No use, distribution or reproduction is permitted which does not comply with these terms.



Emerging Roles of Long Noncoding RNAs in Immuno-Oncology

Xin Wang^{1,2}, Xu Wang^{1,2}, Midie Xu^{1,2*} and Weiqi Sheng^{1,2*}

¹Department of Pathology, Fudan University Shanghai Cancer Center, Shanghai, China, ²Department of Medical Oncology, Shanghai Medical College, Fudan University, Shanghai, China, ³Institute of Pathology, Fudan University, Shanghai, China

OPEN ACCESS

Edited by:

Zong Sheng Guo,
Roswell Park Comprehensive Cancer
Center, United States

Reviewed by:

Ma Del Rocio Banos-Lara,
Universidad Popular Autónoma del
Estado de Puebla, Mexico
Guillaume Chemin,
University of Limoges, France

*Correspondence:

Weiqi Sheng
shengweiqi2006@163.com
Midie Xu
xumd27202003@sina.com

Specialty section:

This article was submitted to
Molecular and Cellular Oncology,
a section of the journal
Frontiers in Cell and Developmental
Biology

Received: 09 June 2021

Accepted: 01 November 2021

Published: 25 November 2021

Citation:

Wang X, Wang X, Xu M and Sheng W
(2021) Emerging Roles of Long
Noncoding RNAs in Immuno-
Oncology.
Front. Cell Dev. Biol. 9:722904.
doi: 10.3389/fcell.2021.722904

Long noncoding RNAs (lncRNAs), defined as ncRNAs no longer than 200 nucleotides, play an important role in cancer development. Accumulating research on lncRNAs offers a compelling new aspect of genome modulation, in which they are involved in chromatin remodeling, transcriptional and post-transcriptional regulation, and cross-talk with other nucleic acids. Increasing evidence suggests that lncRNAs reshape the tumor microenvironment (TME), which accounts for tumor development and progression. At the same time, the insightful findings on lncRNAs in immune recognition and evasion in tumor-infiltrating immune cells raise concerns with regard to immuno-oncology. In this review, we describe the essential characteristics of lncRNAs, elucidate functions of immune components engaged in tumor surveillance, and present some instructive examples in this new area.

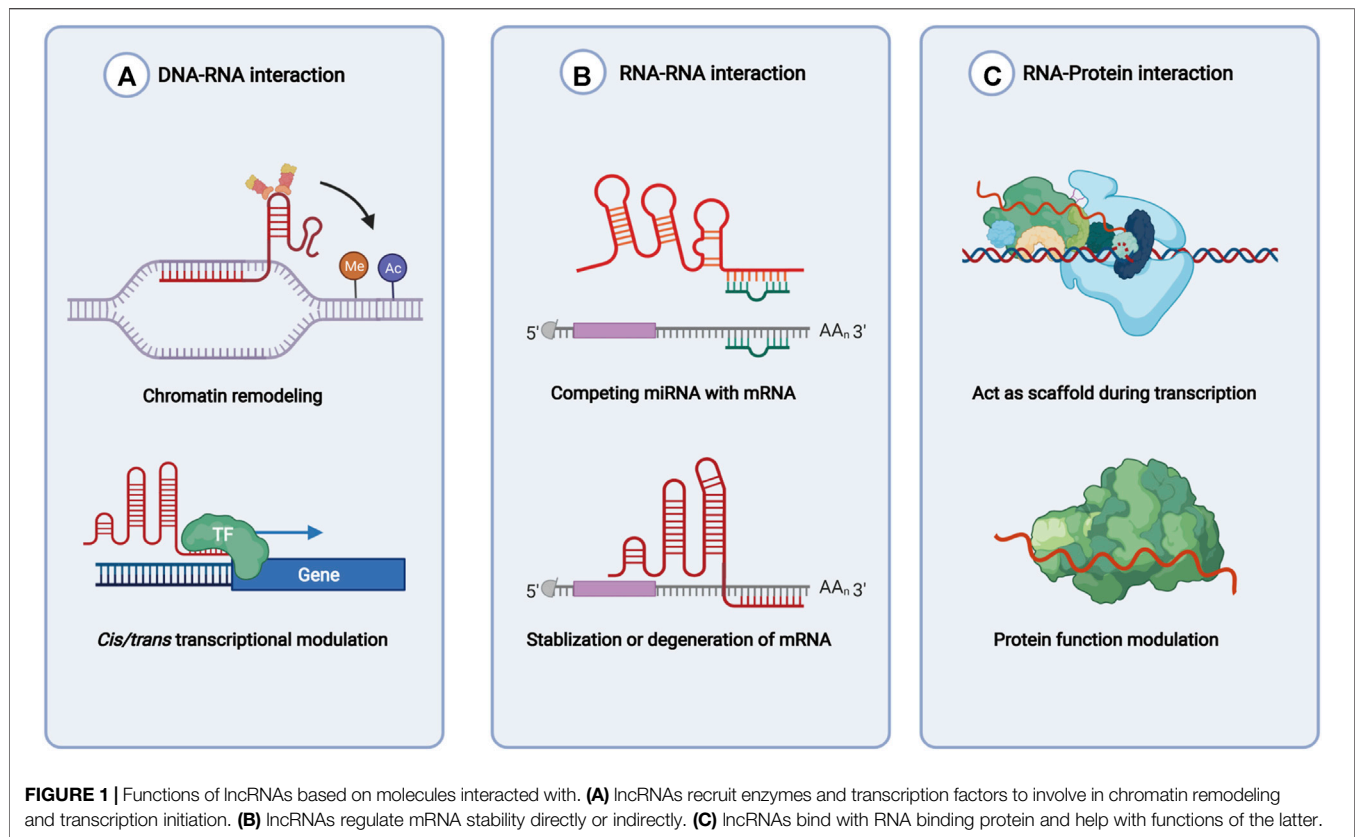
Keywords: lncRNA, cancer, tumor environment, immune surveillance, immuno-oncology

INTRODUCTION

In recent years, in both basic and clinical medical research, a popular and widely appreciated topic is elucidating the role of noncoding RNAs in human physiology and diseases. Decades ago, the major part of the genome, which does not encode proteins, was recognized as the “junk” DNA (Pennisi, 2012; McNally, 2017). Owing to the development of high-throughput sequencing technology, the GENCODE project has helped researchers to understand that ncRNAs cover over 90% of the human genome, and has annotated various kinds of ncRNAs, which promoted a widespread interest in long noncoding RNAs (Harrow et al., 2012; Frankish et al., 2019). The extensive studies of lncRNA have revolutionized our understanding of genetic and cellular molecule regulation in physiological and pathological phenomena.

An increasing number of studies have emphasized the view that lncRNAs are frequently involved in the process of cancer development. Controversy remains regarding the regulatory actions and effects of some lncRNAs in tumorigenesis. While in clinic translation, research on lncRNAs as a genetic screening marker or therapeutic target is ongoing (Do and Kim, 2018; Slack and Chinnaiyan, 2019). Meanwhile, immuno-oncology is becoming one of the most active fields in academic discovery. The abundant signal networks of immune cells, the multi-layered mechanisms of innate and adaptive immunity, and the numerous compositions of the tumor microenvironment (TME) add complexity to the explication of cancer immunity (Mayes et al., 2018; Weiden et al., 2018; Jones et al., 2019). We propose that, for immuno-oncology, besides the recognized protein-coding oncogenes and suppressors, studies on lncRNAs provide an important way to broaden our horizons in cancer immune biology.

In this review, we intend to summarize the definition and classification of lncRNAs considering their functions, to reveal the connections of lncRNAs with cancer immunity, and to highlight the relative translational research.



CHARACTERISTICS AND FUNCTIONS OF LNCRNA

lncRNAs are defined as the noncoding RNAs with a length of at least 200 nucleotides (nt). Compared with conventional protein-coding RNAs, lncRNAs are generally characterized as having lower abundance, more frequent nuclear location, and less evolutionary conservation (Ulitsky and Bartel, 2013; Ulitsky, 2016). For molecular structure, the mature polynucleotide strand is often 5' capped, tailed with poly adenosine (Poly A) and/or spliced (Gruber and Zavolan, 2019). The functions of lncRNAs rely on their interactions with biomolecules, such as DNA (enhancer, promoter), proteins (transcription factor, enzyme) and other types of RNA (mRNA, miRNA) (Figure 1). Given their interactions with DNA, RNA, and proteins, several key technologies and tools are commonly used to identify and annotate their roles, such as ChIP (Chu et al., 2012), RIP (Gagliardi and Matarazzo, 2016), RNA-FISH (Mahadevaiah et al., 2009), and PAR-CLIP (Spitzer et al., 2014). Notably, new evidence has convinced scientists that most transcripts of the annotated lncRNAs do not have direct biological functions (Uszczynska-Ratajczak et al., 2018). The functional activity of some transcripts is not related to their abundance in cells and the specific-sequence, which might be consistent with the above features. Given the discovery of bi-directional transcription initiation in promoters and enhancers, lncRNAs represent the major group of RNAs that are initiated at the DNA elements, which lacks encoding functions. According to

the relative location to the coding-gene and the direction of transcription, lncRNAs are broadly classified as antisense, intronic, intergenic, sense overlapping, and bidirectional lncRNAs (Figure 2) (Harrow et al., 2012).

COMPONENTS AND EVENTS OF CANCER IMMUNE RECOGNITION AND ESCAPE

The recent compelling achievements in cancer immune therapy are attributable to the persistent exploration of immunobiology during all stages of cancer development. It has been gradually appreciated that many, if not most, neoantigens from distinct cancer cells can be presented to T cells and set off a series of effects (Woo et al., 2015; Altorki et al., 2019). However, in observing individuals, the progression of cancer continues, arguing that the neoplasm finally escaped from the hunting of the immune system. This phenomenon involves the close cooperation of cells and molecules in the immune system.

The initial recognition of neoantigens starts with antigen exposure and uptake, which is accomplished by dendritic cells (DCs). The immigrated DCs present antigen peptides and promote the activation of adaptive immune cells, such as CD8⁺ T cells. The cascade activated CD8⁺ T cells flow back to the tumor microenvironment (TME), recognizing and attacking malignant cells. Simultaneously, other innate immune cells, also participate in the TME, including natural killer cells (NK cells), $\gamma\delta$ T cells, plasmacytoid DCs, macrophages, monocytes, and some

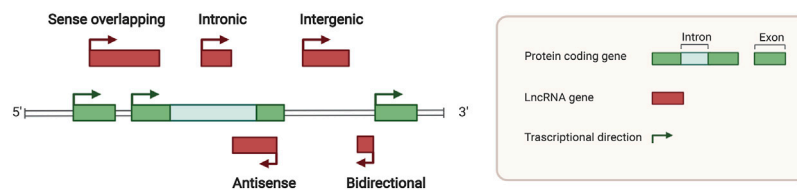


FIGURE 2 | Locations of long noncoding RNAs in the genome. Green squares indicate protein coding genes in the genome, while red squares indicate noncoding RNA transcripts. Sense overlapping, antisense, intronic, intergenic, and bidirectional lncRNA loci was classified by different relative locations with protein coding genes.

myeloid cells (Ribas, 2015; Patel and Minn, 2018). Different kinds of innate immune cells comprise a great network to respond to the emergence of neoantigens.

Some macrophages are described as essential populations of cells in immune-oncology. The conventional recognized macrophages that are involved in the inflammatory response and act as antimicrobial and antitumor components of innate immunity are classified as M1 macrophages. M2 macrophages often have alternative activation, and function as immune modulators in Th2-related mechanisms and cancer development (Allavena et al., 2008; Mantovani and Locati, 2016). The term “tumor-associated macrophages” (TAMs) refers to macrophages existing in TME and share similar surface markers with M2 macrophages. Scientists have proposed that TAMs do not represent a subset of macrophages owing to their instability and dependence on tumors.

Myeloid-derived suppressor cells (MDSCs) comprise a group of myeloid cells generated in pathology, mainly cancer. The most remarkable proposed function of MDSCs is as a suppressor of T cell response. MDSCs are often closely involved in the progression of metastasis in different kinds of malignancies. Tumor cells secrete growth factors and chemokines to expand and recruit MDSCs, which play a role in protecting tumor cells from destruction by host immunity and physical injury, facilitate immune escape and support angiogenesis in neoplasms (Gabrilovich and Nagaraj, 2009; Talmadge and Gabrilovich, 2013; Veglia et al., 2018).

LATEST ACHIEVEMENTS IN LNCRNAs MODULATION IN IMMUNE-ONCOLOGY

Here, we retrieved all relative original studies in PubMed (www.ncbi.nlm.nih.gov/pubmed). The Medical Subject Headings (MeSH) terms used were “RNA, Long Noncoding” AND “Neoplasms” AND cell types, containing “Macrophages” (51 results), “Dendritic Cells” (5 results), “Killer Cells, Natural” (4 results), “Neutrophils” (6 results), “Myeloid-Derived Suppressor Cells” (8 results), “T-Lymphocytes” (49 results), “B-Lymphocytes” (20 results) and “Lymphocytes, Tumor-Infiltrating” (14 results). Ultimately, all results were checked artificially. We only enrolled the lncRNA research referring to the immune effects confirmed by cell and/or animal oncological experiments. Studies on lymphomas caused by immune cell development disorders were eliminated (Table 1; Figure 3).

Macrophages

In all articles retrieved, three classes of mechanisms of macrophages engaging in the immune modulation of tumor behavior were identified. Studies on macrophage polarization reported the most numerous RNA molecules. The epigenetic regulation implemented by lncRNAs influences the expression of CCL2, which is prominent in macrophage recruitment. The interaction of glucometabolism between TAM and cancer cells provides an interesting method for signaling communication via extracellular vesicles (EVs).

LINC00662 is identified as a tumor-promoting marker because of its involvement in patient’s prognosis in hepatocellular carcinoma (HCC). Its endogenous competing mechanism explains its behavior in cytoplasm. During competitive binding with miR-15a, miR-16, and miR-107, LINC00662 activates the expression and secretion of WNT3A. By the way of autocrine and paracrine, both in HCC cells and macrophages upregulate the Wnt/ β -catenin pathway to promote cancer cell migration and macrophage polarization in TME, respectively (Tian et al., 2020a).

The lncRNA, LNMAT1, is highly expressed in tissue from lymph nodes of bladder cancer patients, which is significantly related to their prognosis and tumor metastasis. LNMAT1, as an intergenic gene, can dramatically enhance the transcription of CCL2, by recruiting hnRNPL to its promoter and mediating H3K4 tri-methylation. The silenced cells demonstrate that CCL2 is the essential protein inducing LNMAT1-related lymph node metastasis. CCL2 enrolled macrophages can lead to TAM infiltration and lymph angiogenesis (Chen et al., 2018).

Lnc-BM also affects metastasis by CCL2 function of recruiting macrophages. A study of breast cancer brain metastases showed that the interaction between Lnc-BM and JAK activates the latter and results in phosphorylation of STAT3, of which the downstream proteins contain ICAM1 and CCL2. The consecutive action of Lnc-BM/JAK/STAT3 pathway prompts the vascular co-option and ultimately induces macrophages migration and penetration of the blood-brain barrier. Notably, the critical factors IL-6 and endostatin M, which trigger STAT3 phosphorylation, can in return be secreted by recruited macrophages. The mechanism shows a positive feedback loop in cytokines action (Wang et al., 2017).

HISLA is a myeloid-specific molecule, which is packaged in the EV secreted from TAMs of breast cancer cells. The extracellular vesicle has been reported as an efficient transporter in TME, carrying critical signaling molecules (Luga et al., 2012; Boelens et al., 2014). The transmission of HISLA from TAM to cancer cells restrains the hydroxylation via a reduction of the binding between

TABLE 1 | Research on lncRNAs as regulators in cancer immunity.

LncRNA	Immune component	Mechanism	Function	Reference
HISLA	Macrophage	Stabilize HIF-1 α in cancer cells via extracellular vesicle	Upregulate aerobic glycolysis in breast cancer cells	Chen et al. (2019)
CamK-a	Macrophage	Activate NF- κ B pathway through Ca ²⁺ signaling	Remodel tumor microenvironment and recruit macrophages	Sang et al. (2018)
Lnc-BM	Macrophage	Bind and regulate JAK2/STAT3 pathway, express CCL2	Recruit macrophages and promote brain metastasis in breast cancer	Wang et al. (2017)
LNMT1	Macrophage	Recruit hnRNPL to promoter and upregulate expression of CCL2	Recruit macrophages and promote lymphatic metastasis of bladder cancer	Chen et al. (2018)
LncRNA-MM2P	Macrophage	Reducing phosphorylation of STAT6 and regulate secretion of cytokines	Promote M2 macrophages polarization	Cao et al. (2019)
H19	Macrophage	Upregulate activation of miR-193b/MAPK axis induced by macrophages	Promote cell aggressiveness in hepatocellular carcinoma	Ye et al. (2020)
LINC00662	Macrophage	Activate Wnt/ β -catenin signaling	Promote M2 macrophages polarization and hepatocellular carcinoma progression	Tian et al. (2020a)
RPPH1	Macrophage	Interact with TUBB3 mediated by exosomes	Promote M2 macrophages polarization and colon cancer metastasis	Liang et al. (2019)
MALAT1	Macrophage	Activate STAT3/MALAT1 pathway mediated by M2 macrophages secreted IL-8	Promote tumorigenesis of prostate cancer	Zheng et al. (2018)
JHDM1D-AS1	Macrophage	Increase the formation of CD31 ⁺ blood vessels	Promote infiltration of CD11b ⁺ macrophages and tumor growth	Kondo et al. (2017)
lncRNA cox-2	Macrophage	Decrease the expression of 1L-10, iNOS, and TNF- α in M1 macrophages	Reduce cell proliferation invasion, EMT, and angiogenesis in hepatocellular carcinoma	Ye et al. (2018)
MALAT1	Macrophage	Modulate FGF2 protein secreted by tumor-associated macrophages	Promote angiogenesis of thyroid cancer	Huang et al. (2017)
NIFK-AS1	Macrophage	Act as ceRNA of miR-146a	Inhibit M2 polarization of macrophages	Zhou et al. (2018b)
Xist	Macrophage	Suppress the expression of IL-4, mediated by TCG-4	Promote M2 polarization of macrophages and progression of lung cancer	Sun and Xu, (2019)
ANCR	Macrophage	Regulate expression of FoxO1	Inhibit M1 polarization of macrophages and promote invasion and migration of gastric cancer	Xie et al. (2020)
CCAT1	Macrophage	Act as ceRNA via CCAT1/miR-148a/PKC ζ regulation	Inhibit M2 polarization of macrophages and migration of prostate cancer	Liu et al. (2019)
UCA1	Macrophage	Upregulate protein levels of p-AKT	Promote invasiveness of breast cancer cell	Chen et al. (2015)
LOC100129620	Macrophage	Promote IL-10 expression in osteosarcoma cells	Promote M2 polarization of macrophages, proliferation, angiogenesis of osteosarcoma	Chen et al. (2021b)
LINC01140	Macrophage	Act as ceRNA via LINC01140/miR-140-5p/FGF9 axis	Promote aggressiveness and macrophage M2 polarization of bladder cancer cell	Wu et al. (2020a)
LINC00514	Macrophage	Upregulate Jagged1-mediated notch signaling pathway	Promote M2 polarization and metastasis of breast cancer	Tao et al. (2020)
PCAT6	Macrophage	M2 macrophages secrete VEGF to stimulate the upregulation of PCAT6 in breast cancer cell	Promoting angiogenesis in triple-negative breast cancer	Dong et al. (2020)
LincRNA-p21	Macrophage	MDM2 eliciting proteasome-dependent regulation to p53/NF- κ B/STAT3 pathway	Promote M2 polarization and progression of breast cancer	Zhou et al. (2020)
RP11-361F15.2	Macrophage	Act as ceRNA via RP11-361F15.2/miR-30c-5p/CPEB4 axis	Promote M2 polarization and tumorigenesis of osteosarcoma	Yang et al. (2020)
SNHG15	Macrophage	Act as SNHG15/CDK6/miR-627 circuit by palbociclib	Promote M2 polarization of glioma associated microglia in glioblastoma multiforme	Li et al. (2019)
HOTTIP	Neutrophil	Enhance IL-6 expression	Upregulate the expression of PD-L1 in neutrophils to potentiate immune escape of ovarian cancer cells	Shang et al. (2019)
LINC01116	Neutrophil	Enhance DDX5-mediated IL-1 β expression in glioma cell	Promote tumor proliferation and tumor-associated neutrophils recruitment	Wang et al. (2020a)
MALAT1	Dendritic cell	Upregulate expression of Snail and activate functions of CCL5	Promote colon cancer progression	Kan et al. (2015)
Pvt1	MDSC	Regulate the downstream functions of G-MDSC	Enhance suppressive immunity in tumor microenvironment	Zheng et al. (2019)
Olf29-ps1	MDSC	Regulate the activity of transcripts, such as COX2, NOX2, NOS2, and Arg-1	Suppressive functions of MDSCs	Gao et al. (2018a)
Lnc-C/EBP β	MDSC	Act as ceRNA via miR-133a-3p/RhoA regulation	Promote inflammation-driven colorectal cancer progression	Yu et al. (2019)
Xist	MDSC	Interact with CHOP and the C/EBP β isoform liver-enriched inhibitory protein	Regulate impressive functions MDSCs in TME	Gao et al. (2018b)

(Continued on following page)

TABLE 1 | (Continued) Research on lncRNAs as regulators in cancer immunity.

LncRNA	Immune component	Mechanism	Function	Reference
Lnc-C/EBP β	MDSC	Regulate IL4i1 mediated by C/EBP β LIP and WDR5	Modulate differentiation of MDSCs	Gao et al. (2019)
MALAT1	MDSC	Upregulate of Arg-1 and increase proportions of MDSCs	Inhibit Immunosuppression in lung cancer	Zhou et al. (2018a)
RNUXOR	MDSC	Bind with RUNX1 and increase levels of Arg-1 in MDSC	Immunosuppression in lung cancer	Tian et al. (2018)
AK036396	MDSC	Enhance stability of Ficolin B	Inhibit maturation and accelerate immunosuppression of PMN-MDSCs in lung cancer	Tian et al. (2020b)
NKILA	T cell	Modulate activated-induced cell death via NKILA activity mediated by Ca ²⁺	Sensitizing T cells and promote tumor immune evasion	Huang et al. (2018)
lnc-EGFR	T cell	Protect EGFR from ubiquitination and activate AP-1/NF-AT1 pathway	Stimulate differentiation of Tregs and promote immune evasion in hepatocellular carcinoma	Jiang et al. (2017)
Flicr	T cell	Regulate transcription of Foxp3 mediated by modifying chromatin accessibility in CNS3/AR5 region of Foxp3	Enhance immune escape dominated by Tregs	Zemmour et al. (2017)
Lnc-Tim3	T cell	Bind to Tim-3 and induce nuclear translocation of Bat3	Exacerbate CD8 ⁺ T cell exhaustion	Ji et al. (2018)
SNHG1	T cell	Act as ceRNA via miR-448/IDO regulation	Regulate Tregs differentiation and affect immune escape of breast cancer	Pei et al. (2018)
MALAT1	T cell	Act as ceRNA mediated by miR-195	Promotes tumorigenesis and immune escape of diffuse B cell lymphoma	Wang et al. (2019)
Lnc-sox5	T cell	Upregulate expression of IDO1 and modulate infiltration and cytotoxicity of CD3 ⁺ CD8 ⁺ T cells	Promote progression in colorectal cancer	Wu et al. (2017)
NEAT1	T cell	Act as ceRNA via miR-155/Tim-3	Enhance the antitumor activity of CD8 ⁺ T cell against hepatocellular carcinoma	Yan et al. (2019)
LINC00473	T cell	Act as ceRNA mediated by miR-195-5p/PD-L1 regulation	Modulate the activation of CD8 ⁺ T cells for attacking cancer cells	Zhou et al. (2019)
LIMIT	T cell	Upregulate the LIMIT-GBP-HSP1 axis to boost MHC-I, but not PD-L1	Promote tumor antigen recognition and T cells infiltration	Li et al. (2021)
UCA1	T cell	Upregulate the miR-148a/PD-L1 pathway in tumor cells	Attenuate the killing effect of cytotoxic CD8 ⁺ T cells on anaplastic thyroid carcinoma cells	Wang et al. (2021b)
NNT-AS1	T cell	Upregulate the TGF- β signaling pathway	Decrease tumor CD4 lymphocyte infiltration in hepatocellular carcinoma	Wang et al. (2020b)
LINC00301	T cell	Upregulate the TGF- β signaling pathway via the FOXC1/LINC00301/HIF1 α pathways	Triggers an immune-suppressing microenvironment in non-small cell lung cancer	Sun et al. (2020a)
LINC00473	T cell	Upregulate PD-L1 via LINC00473/miR-195-5p	Suppress the activation of CD8 ⁺ T cell	Zhou et al. (2019)
LINC00240	Natural killer T cell	Induction of miR-124-3p/STAT3/MICA-mediated NKT cell tolerance	Suppress natural killer T cell cytotoxic activity in cervical cancer	Zhang et al. (2020a)

PHD2 and HIF-1 α , and stabilizes the latter (Semenza, 2012; Semenza, 2013). The relatively high level of the oxygen-sensing transcription factor, HIF-1 α , enhances aerobic glycolysis and the capability of apoptosis resistance in breast cancer cells. Correspondingly, the accumulation of lactate up-regulates the abundance in cancer cells, which creates a positive feedback loop between interactions of TAMs and cancer cells, leading to the survival of cancer cells under stress and therapy. Finally, the resistance of chemotherapy was validated in a mouse model experiment (Chen et al., 2019).

Neutrophils

Tumor-associated neutrophils are cells in the TME that have gradually attracted attention, which can be recruited to regulate adaptive immunity through the PD-1/PD-L1 pathway (He et al., 2015). HOTTIP, a long noncoding RNA, promotes the secretion of IL-6 in ovarian cancer cells, maintaining high levels of PD-L1 on the surface of neutrophils. Consequently, the accumulating immune exhaustion inhibits the function of T cells and causing tumor cells to escape immune surveillance (Shang et al., 2019).

Dendritic Cells

MALAT-1 is a well-known lncRNA with a long history in epigenetic research (Ji et al., 2003). The latest studies report that MALAT1 expressed by tumor associated DCs is attributable to the epithelial-to-mesenchymal transition (EMT), invasion, and migration of tumor cells in colon cancer. Upregulation of MALAT-1 stimulates the expression of Snail, and subsequently activates the functions of CCL5. The downstream manner of CCL5 also refers to proliferation, angiogenesis, and chemotherapeutic resistance, as reported in other oncological studies (Kan et al., 2015; Aldinucci and Casagrande, 2018).

MDSCs

Studies have shown that MDSCs modulate immune responses in the TME. Lnc-C/EBP β has been demonstrated as a suppressor in functional regulation of MDSCs. The functioning of Lnc-C/EBP β depends on a series of transcripts, including COX2, NOX2, NOS2, and Arg-1. The downstream targets of these molecules cover the secretion of IFN- γ , the distribution of CD4⁺ and CD8⁺ T cells, and the differentiation of MDSCs. Mechanically, the binding of lncRNA with C/EBP β (located at the LIP isoform) obstructs the activation of the protein (Gao et al., 2018a).

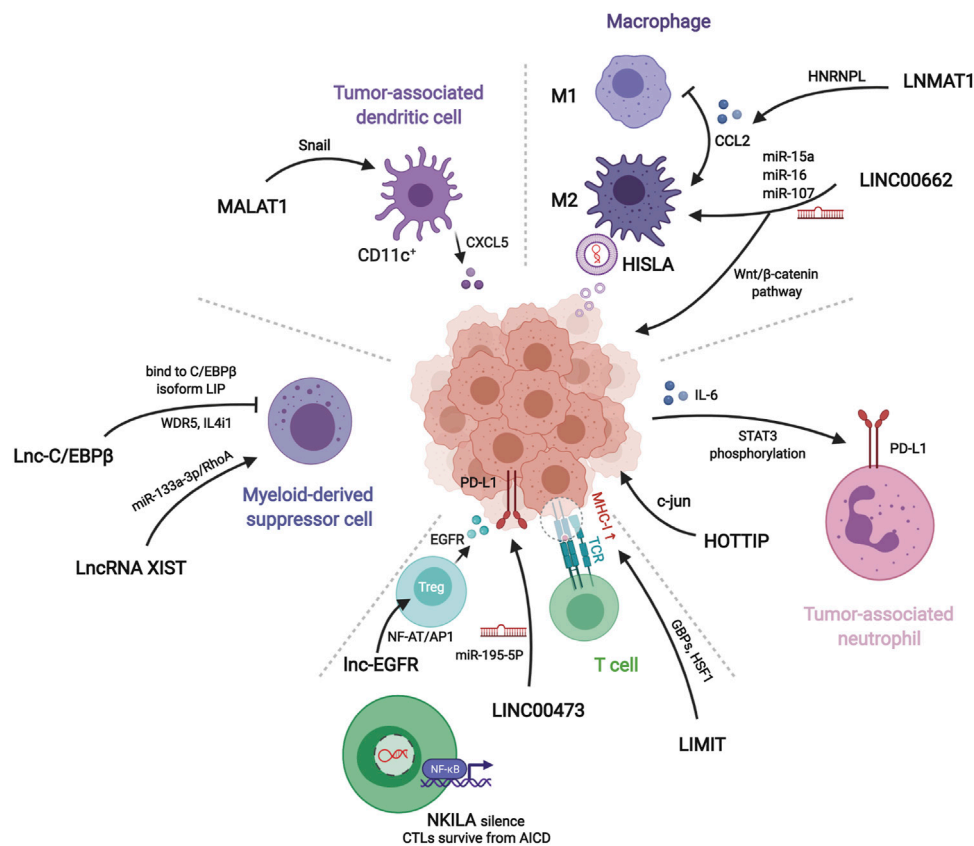


FIGURE 3 | Mechanisms of lncRNAs related to different immune components in tumor microenvironment. LNMAT1, LINC00662, and HISLA regulate macrophages polarization or tumor growth through chemokine, wnt pathway, or extracellular vesicles, respectively. HOTTIP stimulates tumor cells to secrete IL-6 for inducing PD-L1 on the surface of tumor-associated neutrophils. LINC00473, NKILA, and Lnc-EGFR modulate recognition and cytotoxicity of T cells to tumor cells. Myeloid-derived suppressor cells and tumor-associated dendritic cells assist tumor immune evasion by Lnc-C/EBPβ, LncRNA XIST, and MALAT1.

Other researchers describe different effects of Lnc-C/EBPβ on the subset transformation of CD11b⁺Ly6C^{hi}Ly6G[−] monocytic MDSC (Mo-MDSC) and CD11b⁺Ly6C^{low/neg}Ly6G⁺ polymorphonuclear MDSC (PMN-MDSC). *In vitro* and *in vivo* experiments demonstrate that Lnc-C/EBPβ induces bias of PMN-promotion and Mo-suppression during development. This tendency occurs by a two-way method: One is the aforementioned binding to LIP, and the other is interaction with WDR5 to stop the activation of H3K4me3 in the promoter of IL4i1. The distinct functions of the two subsets of MDSC lead to different influences on neighboring tumor cells (Gao et al., 2019).

Transgenic mouse model experiments showed that LncRNA XIST acts as a regulator of the CXCL12/CXCR4 axis. Higher levels of LncRNA XIST bind with miR-133a-3p and functioning as molecule sponge, liberating the block of RhoA by miRNA. These actions promote the EMT, recruitment of MDSCs and macrophages, and accumulation of antigen-presenting cells, contributing to tumorigenesis under a continuous inflammatory environment (Yu et al., 2019).

T Cells

In cancer immunosurveillance, cytotoxic T lymphocytes are dominant in the identification and destruction of cancer cells.

However, for the existence of regulation factors, such as TNF, FasL, and TRAIL, activated T cells in TME often suffer immunological elimination, called activation-induced cell death (AICD) (Schietering and Greenberg, 2014). NKILA, an lncRNA translated in T cells, sets off the activating threshold of AICD. Under the status of T cell activation, the Ca²⁺ related signal removes the deacetylase in area of NKILA promoter and up-regulates the transcription mediated by STAT1. Treatment of patient-derived xenografts (PDXs) of breast cancer with NKILA-CTLs injection has shown compelling efficiency in suppressing tumor growth. This study indicates the stirring potential strategies of immunotherapy of lncRNAs engineering (Huang et al., 2018).

The promotion of differentiation of regulatory T cells (Tregs) is also a subject of T cell studies in cancer immunity. Lnc-EGFR can combine with the target transcript EGFR in a sequence-specific manner and protect it from ubiquitination mediated by c-CBL. Stabilization of EGFR sets up the AP-1/NF-AT1 pathway, which consists of positive feedback enhancing the expression of EGFR. The modulation of Lnc-EGFR was confirmed in both PDX and humans with HCC, and results in Treg differentiation, CTL suppression, and tumor growth (Jiang et al., 2017).

The co-stimulation signals between activated T cells and tumor cells have been proposed as a convincing target of immune therapy. LINC00473 has been identified as a regulator of programmed death-ligand-1 (PD-L1) in pancreatic cancer. The RNA molecule works as a ceRNA, buffering the levels of miR-195-5p and mRNA of PD-L1. The results demonstrated that silencing of LINC00473 contributes to enhanced expression of IFN- γ , Bax, and IL-4, and, simultaneously, decreases the levels of MMP-2, MMP-9, IL-10, and Bcl-2. Thus, LINC00473 induces a reduction of apoptosis and enhanced proliferation, invasion, and migration of cancer cells (Zhou et al., 2019).

Major histocompatibility complex-I (MHC-I) represents a type of molecule that presents antigens to CD8⁺ T cells, involving tumor antigen recognition. The lncRNA, inducing MHC-I and immunogenicity of tumor (LIMIT) acts as an accelerator in MHC-I generation. LIMIT can be stimulated by IFN- γ and cis-activate the guanylate-binding protein (GBP) gene cluster. GBPs can disrupt the interaction between HSP90 and HSF1, followed by transcriptional activation of MHC-I, but not PD-L1. This finding indicates a potential pan-cancer epigenetic target of immune therapy (Li et al., 2021).

Clinical Translational Research

Exploring the mechanisms of lncRNAs provides new insights into applications of the molecules as drugs and biomarkers. As this is still an emerging field, only a handful of lncRNA drugs have been approved, but there is accumulated experience with RNA drugs. Small interfering RNAs (siRNAs), antisense oligonucleotides (ASOs), and the CRISPR/Cas9 system are commonly used in drug design (Matsui and Corey, 2017; Chen et al., 2021a). Malat1, a well-studied lncRNA, was systemically knocked down using ASOs in a mouse mammary carcinoma model, and showed lower tumor burden and significant reduction in metastasis. Given the roles of the drugs acting on cancer immunity have not been well elucidated, and their efficacy and safety determined through lncRNAs primary studies will stimulate confidence for them to be tested in clinical trials (Arun et al., 2016). In the meantime, bioinformatics is used in an attempt to filter out the vital lncRNAs in cancer immunity of different kinds of malignancies (Wang et al., 2018; Sun J. et al., 2020; Wu Y. et al., 2020; Zhang et al., 2020b; Wang J. et al., 2021; Mao et al., 2021; Zhou et al., 2021), and the findings may help with biomarker construction or further mechanism research. In a clinical trial of efficacy biomarkers based on the phase 2 IMvigor210 cohort, the authors reported a novel lncRNA-based immune classification in cancer immunotherapy and recommended immunotherapy for the immune-active class.

CONCLUSION AND PERSPECTIVE

Research on the immunological modulation of lncRNAs in affecting cancer manners is an emerging area enriched by interactive innovation in multiple disciplines. As detailed in the review, lncRNAs engage in many critical events in the immunological balance of elimination or escape in tumor locations. For oncologists, much more attention should be paid to the interactions between cells rather than focusing on single cancer cells and doubling the difficulty. The major challenge to study on lncRNAs is that despite their importance, the current technologies are used to reveal their molecular mechanisms are quite technically difficult. Explaining the mechanism of lncRNA regulation requires the excellent ability to perform epigenetic and molecular biologic experiments. New technologies, for example, new sequencing methods that can directly sequence DNA, RNA, and RNA modifications as well as proteomics will shed light on their role in the transcription processes, immune modulation, and cancer progression. All this technological progress may enhance our understanding of lncRNAs in cancer and will give a better view of disease etiology and will help guide future diagnosis and ultimately therapeutic options. Nevertheless, the possibility of enhancing our understanding of immune surveillance and finding new therapeutic targets for cancer offers continuous motion of relative discovery.

AUTHOR CONTRIBUTIONS

Xi W conceived the idea of the review and wrote the paper. Xu W contributed to revision. MX and WS are responsible for ensuring that the descriptions are accurate and agreed by all authors.

FUNDING

This work was supported by National Natural Science Foundation of China (81972249, 81802367, 81802361), Shanghai Clinical science and technology innovation project of municipal hospital (SHDC12020102), Shanghai Clinical Research Plan of SHDC (SHDC2020CR4068), Shanghai Nova Young Medical Talents Funding Program, Shanghai Health Personnel (2020 No. 087), Fudan University's 2019 "Double First-class" Original Research Personalized Support Project (XM03190634), Shanghai Science and Technology Development Fund (18ZR1408000), Shanghai Science and technology development fund 19MC1911000), Clinical Research Project of Shanghai Municipal Health Committee (20194Y0348), and Shanghai Anticancer Association EYAS project (SACA-CY19B10).

REFERENCES

- Aldinucci, D., and Casagrande, N. (2018). Inhibition of the CCL5/CCR5 Axis against the Progression of Gastric Cancer. *Int. J. Mol. Sci.* 19 (5), 1477. doi:10.3390/ijms19051477
- Allavena, P., Sica, A., Garlanda, C., and Mantovani, A. (2008). The Yin-Yang of Tumor-Associated Macrophages in Neoplastic Progression and Immune Surveillance. *Immunol. Rev.* 222, 155–161. doi:10.1111/j.1600-065X.2008.00607.x
- Altorki, N. K., Markowitz, G. J., Gao, D., Port, J. L., Saxena, A., Stiles, B., et al. (2019). The Lung Microenvironment: an Important Regulator of Tumour Growth and Metastasis. *Nat. Rev. Cancer* 19 (1), 9–31. doi:10.1038/s41568-018-0081-9
- Arun, G., Diermeier, S., Akerman, M., Chang, K.-C., Wilkinson, J. E., Hearn, S., et al. (2016). Differentiation of Mammary Tumors and Reduction in Metastasis upon Malat1 lncRNA Loss. *Genes Dev.* 30 (1), 34–51. doi:10.1101/gad.270959.115
- Boelens, M. C., Wu, T. J., Nabet, B. Y., Xu, B., Qiu, Y., Yoon, T., et al. (2014). Exosome Transfer from Stromal to Breast Cancer Cells Regulates Therapy Resistance Pathways. *Cell* 159 (3), 499–513. doi:10.1016/j.cell.2014.09.051
- Cao, J., Dong, R., Jiang, L., Gong, Y., Yuan, M., You, J., et al. (2019). lncRNA-MM2P Identified as a Modulator of Macrophage M2 Polarization. *Cancer Immunol. Res.* 7 (2), 292–305. doi:10.1158/2326-6066.CIR-18-0145
- Chen, C., He, W., Huang, J., Wang, B., Li, H., Cai, Q., et al. (2018). LNMAT1 Promotes Lymphatic Metastasis of Bladder Cancer via CCL2 Dependent Macrophage Recruitment. *Nat. Commun.* 9 (1), 3826. doi:10.1038/s41467-018-06152-x
- Chen, F., Chen, J., Yang, L., Liu, J., Zhang, X., Zhang, Y., et al. (2019). Extracellular Vesicle-Packaged HIF-1 α -Stabilizing lncRNA from Tumour-Associated Macrophages Regulates Aerobic Glycolysis of Breast Cancer Cells. *Nat. Cell Biol.* 21 (4), 498–510. doi:10.1038/s41556-019-0299-0
- Chen, S., Shao, C., Xu, M., Ji, J., Xie, Y., Lei, Y., et al. (2015). Macrophage Infiltration Promotes Invasiveness of Breast Cancer Cells via Activating Long Non-coding RNA UCA1. *Int. J. Clin. Exp. Pathol.* 8 (8), 9052–9061.
- Chen, Y., Li, Z., Chen, X., and Zhang, S. (2021a). Long Non-coding RNAs: From Disease Code to Drug Role. *Acta Pharmaceutica Sinica B* 11 (2), 340–354. doi:10.1016/j.apsb.2020.10.001
- Chen, Y., Tang, G., Qian, H., Chen, J., Cheng, B., Zhou, C., et al. (2021b). lncRNA LOC100129620 Promotes Osteosarcoma Progression through Regulating CDK6 Expression, Tumor Angiogenesis, and Macrophage Polarization. *Aging* 13 (10), 14258–14276. doi:10.18632/aging.203042
- Chu, C., Quinn, J., and Chang, H. Y. (2012). Chromatin Isolation by RNA Purification (ChIRP). *J. Vis. Exp.* 25 (61), 3912. doi:10.3791/3912
- Do, H., and Kim, W. (2018). Roles of Oncogenic Long Non-coding RNAs in Cancer Development. *Genomics Inform.* 16 (4), e18. doi:10.5808/GI.2018.16.4.e18
- Dong, F., Ruan, S., Wang, J., Xia, Y., Le, K., Xiao, X., et al. (2020). M2 Macrophage-Induced lncRNA PCAT6 Facilitates Tumorigenesis and Angiogenesis of Triple-Negative Breast Cancer through Modulation of VEGFR2. *Cell Death Dis* 11 (9), 728. doi:10.1038/s41419-020-02926-8
- Frankish, A., Diekhans, M., Ferreira, A.-M., Johnson, R., Jungreis, I., Loveland, J., et al. (2019). GENCODE Reference Annotation for the Human and Mouse Genomes. *Nucleic Acids Res.* 47 (D1), D766–D773. doi:10.1093/nar/gky955
- Gabrilovich, D. I., and Nagaraj, S. (2009). Myeloid-derived Suppressor Cells as Regulators of the Immune System. *Nat. Rev. Immunol.* 9 (3), 162–174. doi:10.1038/nri2506
- Gagliardi, M., and Matarazzo, M. R. (2016). RIP: RNA Immunoprecipitation. *Methods Mol. Biol.* 1480, 73–86. doi:10.1007/978-1-4939-6380-5_7
- Gao, Y., Shang, W., Zhang, D., Zhang, S., Zhang, X., Zhang, Y., et al. (2019). Lnc-C/Ebp β Modulates Differentiation of MDSCs through Downregulating IL4i1 with C/EBP β LIP and WDR5. *Front. Immunol.* 10 (1661), 1661. doi:10.3389/fimmu.2019.01661
- Gao, Y., Sun, W., Shang, W., Li, Y., Zhang, D., Wang, T., et al. (2018a). Lnc-C/Ebp β Negatively Regulates the Suppressive Function of Myeloid-Derived Suppressor Cells. *Cancer Immunol. Res.* 6 (11), 1352–1363. doi:10.1158/2326-6066.CIR-18-0108
- Gao, Y., Wang, T., Li, Y., Zhang, Y., and Yang, R. (2018b). Lnc-chop Promotes Immunosuppressive Function of Myeloid-Derived Suppressor Cells in Tumor and Inflammatory Environments. *J. Immunol.* 200 (8), 2603–2614. doi:10.4049/jimmunol.1701721
- Gruber, A. J., and Zavolan, M. (2019). Alternative Cleavage and Polyadenylation in Health and Disease. *Nat. Rev. Genet.* 20 (10), 599–614. doi:10.1038/s41576-019-0145-z
- Harrow, J., Frankish, A., Gonzalez, J. M., Tapanari, E., Diekhans, M., Kokocinski, F., et al. (2012). GENCODE: the Reference Human Genome Annotation for the ENCODE Project. *Genome Res.* 22 (9), 1760–1774. doi:10.1101/gr.135350.111
- He, G., Zhang, H., Zhou, J., Wang, B., Chen, Y., Kong, Y., et al. (2015). Peritumoural Neutrophils Negatively Regulate Adaptive Immunity via the PD-L1/pd-1 Signalling Pathway in Hepatocellular Carcinoma. *J. Exp. Clin. Cancer Res.* 34, 141. doi:10.1186/s13046-015-0256-0
- Huang, D., Chen, J., Yang, L., Ouyang, Q., Li, J., Lao, L., et al. (2018). NKILA lncRNA Promotes Tumor Immune Evasion by Sensitizing T Cells to Activation-Induced Cell Death. *Nat. Immunol.* 19 (10), 1112–1125. doi:10.1038/s41590-018-0207-y
- Huang, J. k., Ma, L., Song, W. h., Lu, B. y., Huang, Y. b., Dong, H. m., et al. (2017). lncRNA-MALAT1 Promotes Angiogenesis of Thyroid Cancer by Modulating Tumor-Associated Macrophage FGF2 Protein Secretion. *J. Cel. Biochem.* 118 (12), 4821–4830. doi:10.1002/jcb.26153
- Ji, J., Yin, Y., Ju, H., Xu, X., Liu, W., Fu, Q., et al. (2018). Long Non-coding RNA Lnc-Tim3 Exacerbates CD8 T Cell Exhaustion via Binding to Tim-3 and Inducing Nuclear Translocation of Bat3 in HCC. *Cel Death Dis* 9 (5), 478. doi:10.1038/s41419-018-0528-7
- Ji, P., Diederichs, S., Wang, W., Böing, S., Metzger, R., Schneider, P. M., et al. (2003). MALAT-1, a Novel Noncoding RNA, and Thymosin β 4 Predict Metastasis and Survival in Early-Stage Non-small Cell Lung Cancer. *Oncogene* 22 (39), 8031–8041. doi:10.1038/sj.onc.1206928
- Jiang, R., Tang, J., Chen, Y., Deng, L., Ji, J., Xie, Y., et al. (2017). The Long Noncoding RNA Lnc-EGFR Stimulates T-Regulatory Cells Differentiation Thus Promoting Hepatocellular Carcinoma Immune Evasion. *Nat. Commun.* 8 (1), 15129. doi:10.1038/ncomms15129
- Jones, P. A., Ohtani, H., Chakravarthy, A., and De Carvalho, D. D. (2019). Epigenetic Therapy in Immune-Oncology. *Nat. Rev. Cancer* 19 (3), 151–161. doi:10.1038/s41568-019-0109-9
- Kan, J.-Y., Wu, D.-C., Yu, F.-J., Wu, C.-Y., Ho, Y.-W., Chiu, Y.-J., et al. (2015). Chemokine (C-C Motif) Ligand 5 Is Involved in Tumor-Associated Dendritic Cell-Mediated Colon Cancer Progression through Non-coding RNA MALAT-1. *J. Cel. Physiol.* 230 (8), 1883–1894. doi:10.1002/jcp.24918
- Kondo, A., Nonaka, A., Shimamura, T., Yamamoto, S., Yoshida, T., Kodama, T., et al. (2017). Long Noncoding RNA JHDM1D-AS1 Promotes Tumor Growth by Regulating Angiogenesis in Response to Nutrient Starvation. *Mol. Cel Biol* 37 (18). doi:10.1128/MCB.00125-17
- Li, G., Kryczek, I., Nam, J., Li, X., Li, S., Li, J., et al. (2021). LIMIT Is an Immunogenic lncRNA in Cancer Immunity and Immunotherapy. *Nat. Cel Biol* 23 (5), 526–537. doi:10.1038/s41556-021-00672-3
- Li, Z., Zhang, J., Zheng, H., Li, C., Xiong, J., Wang, W., et al. (2019). Modulating lncRNA SNHG15/CDK6/miR-627 Circuit by Palbociclib, Overcomes Temozolomide Resistance and Reduces M2-Polarization of Glioma Associated Microglia in Glioblastoma Multiforme. *J. Exp. Clin. Cancer Res.* 38 (1), 380. doi:10.1186/s13046-019-1371-0
- Liang, Z.-x., Liu, H.-s., Wang, F.-w., Xiong, L., Zhou, C., Hu, T., et al. (2019). lncRNA RPPH1 Promotes Colorectal Cancer Metastasis by Interacting with TUBB3 and by Promoting Exosomes-Mediated Macrophage M2 Polarization. *Cel Death Dis* 10 (11), 829. doi:10.1038/s41419-019-2077-0
- Liu, J., Ding, D., Jiang, Z., Du, T., Liu, J., and Kong, Z. (2019). Long Non-coding RNA CCAT1/miR-148a/PKC ζ Prevents Cell Migration of Prostate Cancer by Altering Macrophage Polarization. *Prostate* 79 (1), 105–112. doi:10.1002/pros.23716
- Luga, V., Zhang, L., Vilorio-Petit, A. M., Ogunjimi, A. A., Inanlou, M. R., Chiu, E., et al. (2012). Exosomes Mediate Stromal Mobilization of Autocrine Wnt-PCP Signaling in Breast Cancer Cell Migration. *Cell* 151 (7), 1542–1556. doi:10.1016/j.cell.2012.11.024
- Mahadevaiah, S. K., Costa, Y., and Turner, J. M. A. (2009). Using RNA FISH to Study Gene Expression during Mammalian Meiosis. *Methods Mol. Biol.* 558, 433–444. doi:10.1007/978-1-60761-103-5_25

- Mantovani, A., and Locati, M. (2016). Macrophage Metabolism Shapes Angiogenesis in Tumors. *Cel Metab.* 24 (6), 887–888. doi:10.1016/j.cmet.2016.11.007
- Mao, X., Chen, S., and Li, G. (2021). Identification of a Ten-Long Noncoding RNA Signature for Predicting the Survival and Immune Status of Patients with Bladder Urothelial Carcinoma Based on the GEO Database: a superior Machine Learning Model. *Aging* 13 (5), 6957–6981. doi:10.18632/aging.202553
- Matsui, M., and Corey, D. R. (2017). Non-coding RNAs as Drug Targets. *Nat. Rev. Drug Discov.* 16 (3), 167–179. doi:10.1038/nrd.2016.117
- Mayes, P. A., Hance, K. W., and Hoos, A. (2018). The Promise and Challenges of Immune Agonist Antibody Development in Cancer. *Nat. Rev. Drug Discov.* 17 (7), 509–527. doi:10.1038/nrd.2018.75
- McNally, F. J. (2017). Competing Chromosomes Explain Junk DNA. *Science* 358 (6363), 594–595. doi:10.1126/science.aag0200
- Patel, S. A., and Minn, A. J. (2018). Combination Cancer Therapy with Immune Checkpoint Blockade: Mechanisms and Strategies. *Immunity* 48 (3), 417–433. doi:10.1016/j.immuni.2018.03.007
- Pei, X., Wang, X., and Li, H. (2018). LncRNA SNHG1 Regulates the Differentiation of Treg Cells and Affects the Immune Escape of Breast Cancer via Regulating miR-448/Ido. *Int. J. Biol. Macromolecules* 118 (Pt A), 24–30. doi:10.1016/j.ijbiomac.2018.06.033
- Pennisi, E. (2012). ENCODE Project Writes Eulogy for Junk DNA. *Science* 337 (6099), 1159–1161. doi:10.1126/science.337.6099.1159
- Ribas, A. (2015). Adaptive Immune Resistance: How Cancer Protects from Immune Attack. *Cancer Discov.* 5 (9), 915–919. doi:10.1158/2159-8290.CD-15-0563
- Sang, L.-j., Ju, H.-q., Liu, G.-p., Tian, T., Ma, G.-l., Lu, Y.-x., et al. (2018). LncRNA CamK-A Regulates Ca²⁺-Signaling-Mediated Tumor Microenvironment Remodeling. *Mol. Cel* 72 (1), 71–83. doi:10.1016/j.molcel.2018.08.014
- Schietinger, A., and Greenberg, P. D. (2014). Tolerance and Exhaustion: Defining Mechanisms of T Cell Dysfunction. *Trends Immunol.* 35 (2), 51–60. doi:10.1016/j.it.2013.10.001
- Semenza, G. L. (2013). HIF-1 Mediates Metabolic Responses to Intratumoral Hypoxia and Oncogenic Mutations. *J. Clin. Invest.* 123 (9), 3664–3671. doi:10.1172/JCI67230
- Semenza, G. L. (2012). Hypoxia-inducible Factors: Mediators of Cancer Progression and Targets for Cancer Therapy. *Trends Pharmacol. Sci.* 33 (4), 207–214. doi:10.1016/j.tips.2012.01.005
- Shang, A., Wang, W., Gu, C., Chen, C., Zeng, B., Yang, Y., et al. (2019). Long Non-coding RNA HOTTIP Enhances IL-6 Expression to Potentiate Immune Escape of Ovarian Cancer Cells by Upregulating the Expression of PD-L1 in Neutrophils. *J. Exp. Clin. Cancer Res.* 38 (1), 411. doi:10.1186/s13046-019-1394-6
- Slack, F. J., and Chinnaiyan, A. M. (2019). The Role of Non-coding RNAs in Oncology. *Cell* 179 (5), 1033–1055. doi:10.1016/j.cell.2019.10.017
- Spitzer, J., Hafner, M., Landthaler, M., Ascano, M., Farazi, T., Wardle, G., et al. (2014). PAR-CLIP (Photoactivatable Ribonucleoside-Enhanced Crosslinking and Immunoprecipitation). *Methods Enzymol.* 539, 113–161. doi:10.1016/b978-0-12-420120-0.00008-6
- Sun, C.-C., Zhu, W., Li, S.-J., Hu, W., Zhang, J., Zhuo, Y., et al. (2020a). FOXC1-mediated LINC00301 Facilitates Tumor Progression and Triggers an Immune-Suppressing Microenvironment in Non-small Cell Lung Cancer by Regulating the HIF1 α Pathway. *Genome Med.* 12 (1), 77. doi:10.1186/s13073-020-00773-y
- Sun, J., Zhang, Z., Bao, S., Yan, C., Hou, P., Wu, N., et al. (2020b). Identification of Tumor Immune Infiltration-Associated lncRNAs for Improving Prognosis and Immunotherapy Response of Patients with Non-small Cell Lung Cancer. *J. Immunother. Cancer* 8 (1), e000110. doi:10.1136/jitc-2019-000110
- Sun, Y., and Xu, J. (2019). TCF-4 Regulated lncRNA-XIST Promotes M2 Polarization of Macrophages and Is Associated with Lung Cancer. *OncoTargets Ther.* 2, 8055–8062. doi:10.2147/OTT.S210952
- Talmadge, J. E., and Gabrilovich, D. I. (2013). History of Myeloid-Derived Suppressor Cells. *Nat. Rev. Cancer* 13 (10), 739–752. doi:10.1038/nrc3581
- Tao, S., Chen, Q., Lin, C., and Dong, H. (2020). Linc00514 Promotes Breast Cancer Metastasis and M2 Polarization of Tumor-Associated Macrophages via Jagged1-Mediated Notch Signaling Pathway. *J. Exp. Clin. Cancer Res.* 39 (1), 191. doi:10.1186/s13046-020-01676-x
- Tian, X., Ma, J., Wang, T., Tian, J., Zheng, Y., Peng, R., et al. (2018). Long Non-coding RNA RUNXOR Accelerates MDSC-Mediated Immunosuppression in Lung Cancer. *BMC Cancer* 18 (1), 660. doi:10.1186/s12885-018-4564-6
- Tian, X., Wu, Y., Yang, Y., Wang, J., Niu, M., Gao, S., et al. (2020a). Long Noncoding RNA LINC00662 Promotes M2 Macrophage Polarization and Hepatocellular Carcinoma Progression via Activating Wnt/ β -catenin Signaling. *Mol. Oncol.* 14 (2), 462–483. doi:10.1002/1878-0261.12606
- Tian, X., Zheng, Y., Yin, K., Ma, J., Tian, J., Zhang, Y., et al. (2020b). LncRNAK036396 Inhibits Maturation and Accelerates Immunosuppression of Polymorphonuclear Myeloid-Derived Suppressor Cells by Enhancing the Stability of Ficolin B. *Cancer Immunol. Res.* 8 (4), 565–577. doi:10.1158/2326-6066.CIR-19-0595
- Ulitsky, I., and Bartel, D. P. (2013). lincRNAs: Genomics, Evolution, and Mechanisms. *Cell* 154 (1), 26–46. doi:10.1016/j.cell.2013.06.020
- Ulitsky, I. (2016). Evolution to the rescue: Using Comparative Genomics to Understand Long Non-coding RNAs. *Nat. Rev. Genet.* 17 (10), 601–614. doi:10.1038/nrg.2016.85
- Uszczynska-Ratajczak, B., Lagarde, J., Frankish, A., Guigó, R., and Johnson, R. (2018). Towards a Complete Map of the Human Long Non-coding RNA Transcriptome. *Nat. Rev. Genet.* 19 (9), 535–548. doi:10.1038/s41576-018-0017-y
- Veglia, F., Perego, M., and Gabrilovich, D. (2018). Myeloid-derived Suppressor Cells Coming of Age. *Nat. Immunol.* 19 (2), 108–119. doi:10.1038/s41590-017-0022-x
- Wang, J., Shen, C., Dong, D., Zhong, X., Wang, Y., and Yang, X. (2021a). Identification and Verification of an Immune-Related lncRNA Signature for Predicting the Prognosis of Patients with Bladder Cancer. *Int. Immunopharmacology* 90, 107146. doi:10.1016/j.intimp.2020.107146
- Wang, L., Felts, S. J., Van Keulen, V. P., Scheid, A. D., Block, M. S., Markovic, S. N., et al. (2018). Integrative Genome-wide Analysis of Long Noncoding RNAs in Diverse Immune Cell Types of Melanoma Patients. *Cancer Res.* 78 (15), 4411–4423. doi:10.1158/0008-5472.CAN-18-0529
- Wang, Q.-M., Lian, G.-Y., Song, Y., Huang, Y.-F., and Gong, Y. (2019). LncRNA MALAT1 Promotes Tumorigenesis and Immune Escape of Diffuse Large B Cell Lymphoma by Sponging miR-195. *Life Sci.* 231, 116335. doi:10.1016/j.lfs.2019.03.040
- Wang, S., Liang, K., Hu, Q., Li, P., Song, J., Yang, Y., et al. (2017). JAK2-binding Long Noncoding RNA Promotes Breast Cancer Brain Metastasis. *J. Clin. Invest.* 127 (12), 4498–4515. doi:10.1172/JCI91553
- Wang, T., Cao, L., Dong, X., Wu, F., De, W., Huang, L., et al. (2020a). LINC01116 Promotes Tumor Proliferation and Neutrophil Recruitment via DDX5-Mediated Regulation of IL-1 β in Glioma Cell. *Cel Death Dis* 11 (5), 302. doi:10.1038/s41419-020-2506-0
- Wang, X., Zhang, Y., Zheng, J., Yao, C., and Lu, X. (2021b). LncRNA UCA1 Attenuated the Killing Effect of Cytotoxic CD8⁺ T Cells on Anaplastic Thyroid Carcinoma via miR-148a/PD-L1 Pathway. *Cancer Immunol. Immunother.* 70 (8), 2235–2245. doi:10.1007/s00262-020-02753-y
- Wang, Y., Yang, L., Dong, X., Yang, X., Zhang, X., Liu, Z., et al. (2020b). Overexpression of NNT-AS1 Activates TGF- β Signaling to Decrease Tumor CD4 Lymphocyte Infiltration in Hepatocellular Carcinoma. *Biomed. Res. Int.* 2020, 1–11. doi:10.1155/2020/8216541
- Weiden, J., Tel, J., and Figdor, C. G. (2018). Synthetic Immune Niches for Cancer Immunotherapy. *Nat. Rev. Immunol.* 18 (3), 212–219. doi:10.1038/nri.2017.89
- Woo, S.-R., Corrales, L., and Gajewski, T. F. (2015). Innate Immune Recognition of Cancer. *Annu. Rev. Immunol.* 33 (1), 445–474. doi:10.1146/annurev-immunol-032414-112043
- Wu, K., Zhao, Z., Liu, K., Zhang, J., Li, G., and Wang, L. (2017). Long Noncoding RNA Lnc-Sox5 Modulates CRC Tumorigenesis by Unbalancing Tumor Microenvironment. *Cell Cycle* 16 (13), 1295–1301. doi:10.1080/15384101.2017.1317416
- Wu, S., Xu, R., Zhu, X., He, H., Zhang, J., Zeng, Q., et al. (2020a). The Long Noncoding RNA LINC01140/miR-140-5p/FGF9 axis Modulates Bladder Cancer Cell Aggressiveness and Macrophage M2 Polarization. *Aging* 12 (24), 25845–25864. doi:10.18632/aging.202147
- Wu, Y., Zhang, L., He, S., Guan, B., He, A., Yang, K., et al. (2020b). Identification of Immune-Related lncRNA for Predicting Prognosis and Immunotherapeutic Response in Bladder Cancer. *aging* 12 (22), 23306–23325. doi:10.18632/aging.104115

- Xie, C., Guo, Y., and Lou, S. (2020). LncRNA ANCR Promotes Invasion and Migration of Gastric Cancer by Regulating FoxO1 Expression to Inhibit Macrophage M1 Polarization. *Dig. Dis. Sci.* 65 (10), 2863–2872. doi:10.1007/s10620-019-06019-1
- Yan, K., Fu, Y., Zhu, N., Wang, Z., Hong, J.-L., Li, Y., et al. (2019). Repression of lncRNA NEAT1 Enhances the Antitumor Activity of CD8⁺T Cells against Hepatocellular Carcinoma via Regulating miR-155/Tim-3. *Int. J. Biochem. Cel Biol.* 110, 1–8. doi:10.1016/j.biocel.2019.01.019
- Yang, D., Liu, K., Fan, L., Liang, W., Xu, T., Jiang, W., et al. (2020). LncRNA RP11-361F15.2 Promotes Osteosarcoma Tumorigenesis by Inhibiting M2-like Polarization of Tumor-Associated Macrophages of CPEB4. *Cancer Lett.* 473, 33–49. doi:10.1016/j.canlet.2019.12.041
- Ye, Y., Guo, J., Xiao, P., Ning, J., Zhang, R., Liu, P., et al. (2020). Macrophages-induced Long Noncoding RNA H19 Up-Regulation Triggers and Activates the miR-193b/MAPK1 axis and Promotes Cell Aggressiveness in Hepatocellular Carcinoma. *Cancer Lett.* 469, 310–322. doi:10.1016/j.canlet.2019.11.001
- Ye, Y., Xu, Y., Lai, Y., He, W., Li, Y., Wang, R., et al. (2018). Long Non-coding RNA Cox-2 Prevents Immune Evasion and Metastasis of Hepatocellular Carcinoma by Altering M1/M2 Macrophage Polarization. *J. Cel. Biochem.* 119 (3), 2951–2963. doi:10.1002/jcb.26509
- Yu, X., Wang, D., Wang, X., Sun, S., Zhang, Y., Wang, S., et al. (2019). CXCL12/CXCR4 Promotes Inflammation-Driven Colorectal Cancer Progression through Activation of RhoA Signaling by Sponging miR-133a-3p. *J. Exp. Clin. Cancer Res.* 38 (1), 32. doi:10.1186/s13046-018-1014-x
- Zemmour, D., Pratama, A., Loughhead, S. M., Mathis, D., and Benoist, C. (2017). Flicr, a Long Noncoding RNA, Modulates Foxp3 Expression and Autoimmunity. *Proc. Natl. Acad. Sci. USA* 114 (17), E3472–E3480. doi:10.1073/pnas.1700946114
- Zhang, Y., Li, X., Zhang, J., and Liang, H. (2020a). Natural Killer T Cell Cytotoxic Activity in Cervical Cancer Is Facilitated by the LINC00240/microRNA-124-3p/STAT3/MICA axis. *Cancer Lett.* 474, 63–73. doi:10.1016/j.canlet.2019.12.038
- Zhang, Y., Zhang, L., Xu, Y., Wu, X., Zhou, Y., and Mo, J. (2020b). Immune-related Long Noncoding RNA Signature for Predicting Survival and Immune Checkpoint Blockade in Hepatocellular Carcinoma. *J. Cel Physiol* 235 (12), 9304–9316. doi:10.1002/jcp.29730
- Zheng, T., Ma, G., Tang, M., Li, Z., and Xu, R. (2018). IL-8 Secreted from M2 Macrophages Promoted Prostate Tumorigenesis via STAT3/MALAT1 Pathway. *Int. J. Mol. Sci.* 20 (1), 98. doi:10.3390/ijms20010098
- Zheng, Y., Tian, X., Wang, T., Xia, X., Cao, F., Tian, J., et al. (2019). Long Noncoding RNA Pvt1 Regulates the Immunosuppression Activity of Granulocytic Myeloid-Derived Suppressor Cells in Tumor-Bearing Mice. *Mol. Cancer* 18 (1), 61. doi:10.1186/s12943-019-0978-2
- Zhou, L., Tian, Y., Guo, F., Yu, B., Li, J., Xu, H., et al. (2020). LincRNA-p21 Knockdown Reversed Tumor-Associated Macrophages Function by Promoting MDM2 to Antagonize* P53 Activation and Alleviate Breast Cancer Development. *Cancer Immunol. Immunother.* 69 (5), 835–846. doi:10.1007/s00262-020-02511-0
- Zhou, M., Zhang, Z., Bao, S., Hou, P., Yan, C., Su, J., et al. (2021). Computational Recognition of lncRNA Signature of Tumor-Infiltrating B Lymphocytes with Potential Implications in Prognosis and Immunotherapy of Bladder Cancer. *Brief Bioinform* 22 (3). doi:10.1093/bib/bbaa047
- Zhou, Q., Tang, X., Tian, X., Tian, J., Zhang, Y., Ma, J., et al. (2018a). LncRNA MALAT1 Negatively Regulates MDSCs in Patients with Lung Cancer. *J. Cancer* 9 (14), 2436–2442. doi:10.7150/jca.24796
- Zhou, W. Y., Zhang, M. M., Liu, C., Kang, Y., Wang, J. O., and Yang, X. H. (2019). Long Noncoding RNA LINC00473 Drives the Progression of Pancreatic Cancer via Upregulating Programmed Death-ligand 1 by Sponging microRNA-195-5p. *J. Cel Physiol* 234 (12), 23176–23189. doi:10.1002/jcp.28884
- Zhou, Y.-x., Zhao, W., Mao, L.-w., Wang, Y.-l., Xia, L.-q., Cao, M., et al. (2018b). Long Non-coding RNA NIFK-AS1 Inhibits M2 Polarization of Macrophages in Endometrial Cancer through Targeting miR-146a. *Int. J. Biochem. Cel Biol.* 104, 25–33. doi:10.1016/j.biocel.2018.08.017

Conflict of Interest: The authors declare that the research was conducted in the absence of any commercial or financial relationships that could be construed as a potential conflict of interest.

Publisher's Note: All claims expressed in this article are solely those of the authors and do not necessarily represent those of their affiliated organizations, or those of the publisher, the editors, and the reviewers. Any product that may be evaluated in this article, or claim that may be made by its manufacturer, is not guaranteed or endorsed by the publisher.

Copyright © 2021 Wang, Wang, Xu and Sheng. This is an open-access article distributed under the terms of the Creative Commons Attribution License (CC BY). The use, distribution or reproduction in other forums is permitted, provided the original author(s) and the copyright owner(s) are credited and that the original publication in this journal is cited, in accordance with accepted academic practice. No use, distribution or reproduction is permitted which does not comply with these terms.



A Review on the Role of AFAP1-AS1 in the Pathoetiology of Cancer

Soudeh Ghafouri-Fard¹, Tayybeh Khoshbakht², Bashdar Mahmud Hussen³,
Mohammad Taheri^{4,5*} and Majid Mokhtari^{6*}

¹ Department of Medical Genetics, School of Medicine, Shahid Beheshti University of Medical Sciences, Tehran, Iran,

² Phytochemistry Research Center, Shahid Beheshti University of Medical Sciences, Tehran, Iran, ³ Department of

Pharmacognosy, College of Pharmacy, Hawler Medical University, Erbil, Iraq, ⁴ Urology and Nephrology Research Center,

Shahid Beheshti University of Medical Sciences, Tehran, Iran, ⁵ Institute of Human Genetics, Jena University Hospital, Jena,

Germany, ⁶ Skull Base Research Center, Lohman Hakim Hospital, Shahid Beheshti University of Medical Sciences, Tehran, Iran

OPEN ACCESS

Edited by:

Shiv K. Gupta,
Mayo Clinic, United States

Reviewed by:

Rezvan Noroozi,
Jagiellonian University, Poland
Amin Safa,
Complutense University of Madrid,
Spain

*Correspondence:

Mohammad Taheri
mohammad_823@yahoo.com
Majid Mokhtari
majidmokh@gmail.com

Specialty section:

This article was submitted to
Molecular and Cellular Oncology,
a section of the journal
Frontiers in Oncology

Received: 15 September 2021

Accepted: 09 November 2021

Published: 29 November 2021

Citation:

Ghafouri-Fard S, Khoshbakht T,
Hussen BM, Taheri M and
Mokhtari M (2021) A Review on the
Role of AFAP1-AS1 in the
Pathoetiology of Cancer.
Front. Oncol. 11:777849.
doi: 10.3389/fonc.2021.777849

AFAP1-AS1 is a long non-coding RNA which partakes in the pathoetiology of several cancers. The sense protein coding gene from this locus partakes in the regulation of cytophagy, cell motility, invasive characteristics of cells and metastatic ability. In addition to acting in concert with AFAP1, AFAP1-AS1 can sequester a number of cancer-related miRNAs, thus affecting activity of signaling pathways involved in cancer progression. Most of animal studies have confirmed that AFAP1-AS1 silencing can reduce tumor volume and invasive behavior of tumor cells in the xenograft models. Moreover, statistical analyses in the human subjects have shown strong correlation between expression levels of this lncRNA and clinical outcomes. In the present work, we review the impact of AFAP1-AS1 in the carcinogenesis.

Keywords: AFAP1-AS1, cancer, biomarker, expression, ncRNA

INTRODUCTION

Actin filament-associated protein 1 antisense RNA 1 (AFAP1-AS1, NC_000004.12) is a long non-coding RNA (lncRNA) which contributes in the pathoetiology of several cancers (1). It is transcribed from *AFAP1* gene locus on 4p16.1. It has two alternatively spliced variants. Its second exon overlaps with exons 14–16 of *AFAP1* gene. The motor fiber-associated protein encoded by *AFAP1* has been shown to organize a platform for joining a number of tumor-related proteins such as SRC and protein kinase C (2). This platform can influence the organization and activity of actin filaments, therefore participating in cytophagy, cell motility, invasive characteristics of cells and metastatic ability (3). Both AFAP1 and FAP1-AS1 participate in the carcinogenesis through modulation of related signaling pathways. AFAP1 has acknowledged roles in the pathogenesis of a number of cancers, namely breast (4) and prostate cancer (5), yet its expression has been found to decreased in gastric cancer samples (6). AFAP1-AS1 is mainly regarded as an oncogenic lncRNA (1). However, the oncogenic effect of this lncRNA is not necessarily exerted through AFAP1-dependent routes. A number of deletion type copy-number variants (CNVs) have been identified in *AFAP1-AS1* coding gene through application of whole genome sequencing (7). AFAP1-AS1 has been shown to affect several aspects of carcinogenesis through modulation of expression of cancer-related miRNAs. Since it has been shown to be dysregulated in diverse types of cancer, this lncRNA is a putative marker for a wide variety of cancers. Functional impacts of AFAP1-AS1 in the carcinogenesis have been appraised through knock-down and over-

expression studies in cell lines and animal models. Moreover, the impact of AFAP1-AS1 deregulation has been assessed in human samples. In the present review, we discuss the role of AFAP1-AS1 in the carcinogenesis based on the evidence from these three types of studies.

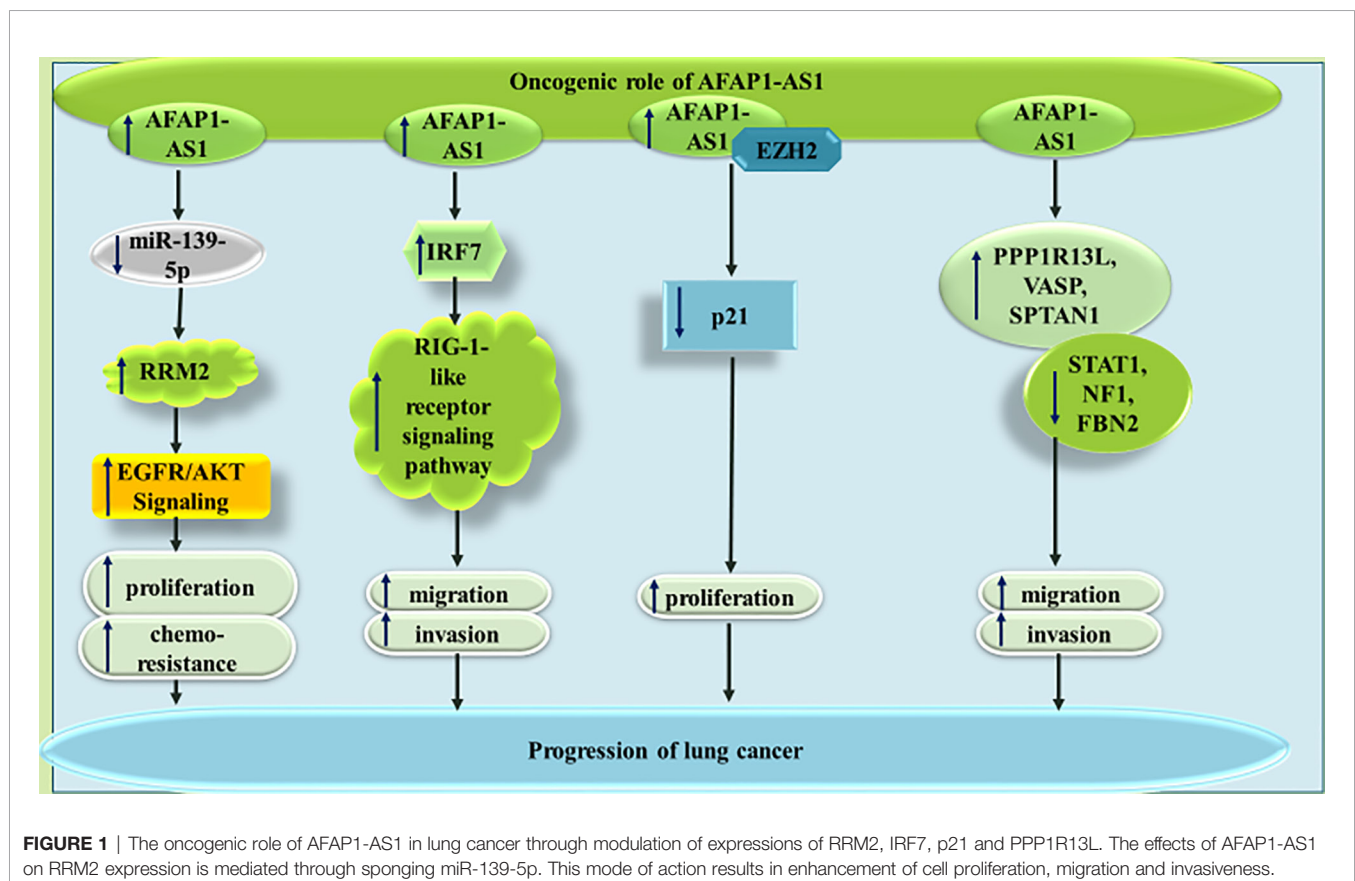
CELL LINE STUDIES

Lung Cancer

AFAP1-AS1 has been found to be over-expressed in non-small cell lung cancer (NSCLC) cells H1975, PC-9, A549, and SPCA-1 compared with the human non-tumorigenic lung epithelial cell line BEAS-2B. Functional studies in these cells have confirmed the ability of this lncRNA in binding with and sequestering miR-139-5p, a down-regulated miRNA in NSCLC samples. AFAP1-AS1 silencing and miR-139-5p up-regulation could similarly inhibit proliferation, colony forming ability and chemoresistance of NSCLC cells, while increasing their apoptosis. The sequestering impact of AFAP1-AS1 on miR-139-5p leads to up-regulation of RRM2, a protein which has been demonstrated to increase chemoresistance of NSCLC cells *via* activation of EGFR/AKT pathway (8). Another study in NSCLC has shown up-regulation of FAP1-AS1 parallel with down-regulation of IL-12 and up-regulation of IL-10 and IFN- γ . Functionally, AFAP1-AS1 has been shown to induce activity of IRF7, RIG-I-like receptor signals

and Bcl-2. Cumulatively, AFAP1-AS1 enhances migration and invasive properties of NSCLC cells through activating IRF7 and the RIG-I-like receptor signaling pathway (9). Moreover, the interaction between AFAP1-AS1 and EZH2 and subsequent recruitment of EZH2 to the promoter of p21 has been shown to repress expression of p21 in this type of cancer (10). AFAP1-AS1 has also been shown to enhance expression of AFAP1 in lung cancer cells. Expression of AFAP1-AS1 in lung cancer cells is regulated through CpG methylation marks in its promoter, since the DNA methyltransferase inhibitor agent decitabine has been demonstrated to activate AFAP1-AS1 expression. AFAP1-AS1 has been reported to increase expression levels of pro-invasive genes PPP1R13L, VASP and SPTAN1, while decreasing expression levels of a number of anti-metastatic genes such as STAT1, NF1, and FBN2 (11). **Figure 1** summarizes the mentioned routes of participation of AFAP1-As1 in the pathogenesis of lung cancer.

AFAP1-AS1 can also affect lung cancer through a variety of other mechanisms being summarized in **Figure 2**. For instance, AFAP1-AS1 has been shown to regulate expression of numerous members of the small GTPase proteins as well as those participating in the actin cytoskeleton signaling. Thus, the promoting effect of AFAP1-AS1 on cancer metastasis is most probably exerted through modulation of actin filament integrity (12). GTPases harmonize several cellular processes, such as cell polarity, migration, and cell cycle transition, thus they can participate in the pathogenesis of cancer (13). Moreover, cytokeratins as members of intermediate



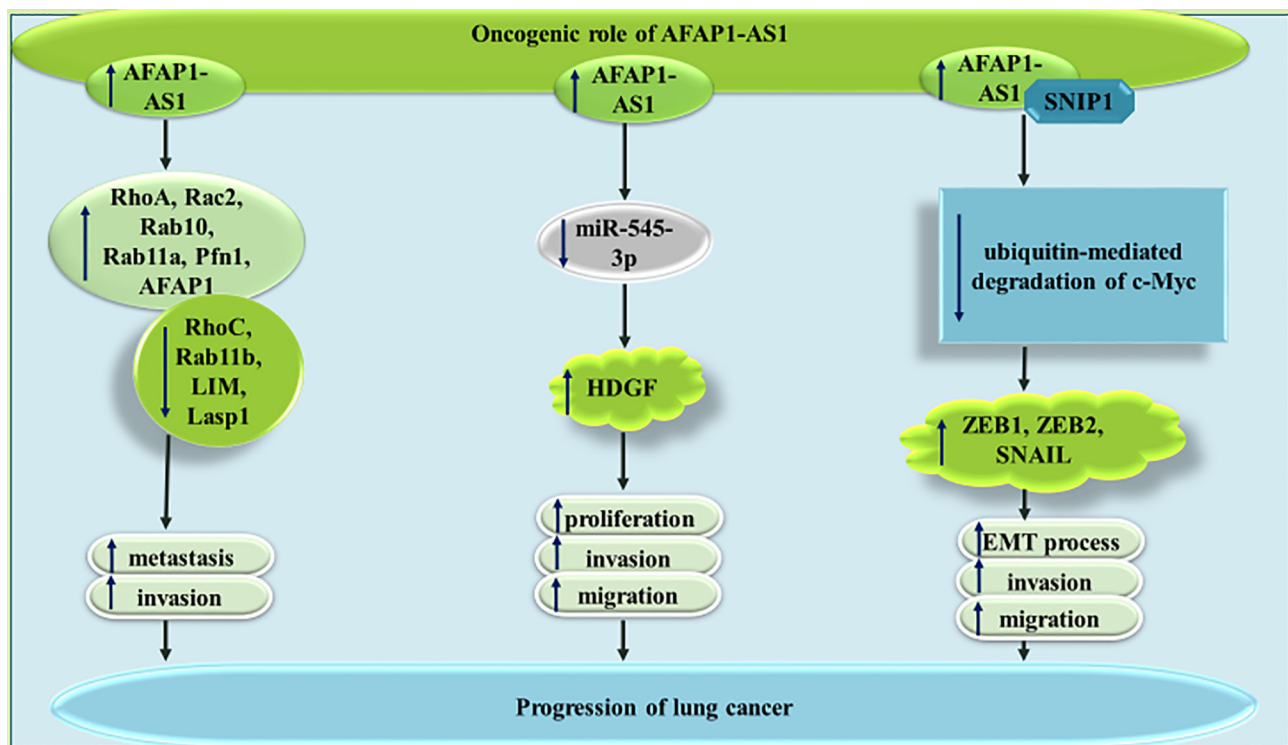


FIGURE 2 | The oncogenic role of AFAP1-AS1 in lung cancer metastasis.

filament protein family have been shown to affect carcinogenesis. They can also be used as cancer biomarkers (14).

AFAP1-AS1 can also enhance expression of HDGF through decreasing miR-545-3p levels in lung cancer cells. Thus, AFAP1-AS1 silencing could inhibit progression of lung cancer through influencing activity of miR-545-3p/HDGF axis (15). Finally, AFAP1-AS1 can interact with Smad nuclear interacting protein 1 (SNIP1), a protein which suppresses ubiquitination and subsequent destruction of c-Myc. This function of AFAP1-AS1 leads to over-expression of c-Myc, increase in ZEB1, ZEB2, and SNAIL levels, and enhancement of epithelial to mesenchymal transition (EMT) (16).

Breast Cancer

In breast cancer cells, AFAP1-AS1 silencing could decrease proliferation and migratory potential, and increase cell apoptosis. miR-497-5p has been recognized as a target of AFAP1-AS1 in breast cancer cells. Since this miRNA targets SEPT2, AFAP1-AS1 up-regulation results in up-regulation of SEPT2 (17). miR-145 is another target of AFAP1-AS1 in triple negative breast cancer cells (TNBC) MDA-MB-231 breast cancer cells. According to the results of luciferase reporter assay, miR-145 can directly target MTH1. Thus, the effects of AFAP1-AS1 in enhancement of proliferation and invasiveness of TNBC are exerted through miR-145/MTH1 axis (18). Moreover, in this type of cancer, AFAP1-AS1 can sequester miR-2110 to enhance expression of Sp1 (19). AFAP1-AS1 has also been shown to enhance EMT of TNBC cells *via* influencing Wnt/ β -catenin signaling (20). Finally,

AFAP1-AS1 has been found to have significant over-expression in trastuzumab-resistant breast cancer cells versus responsive cells. Expression of this lncRNA has been enhanced by H3K27ac at its promoter. Most notably, trastuzumab resistant cells have been shown to secrete AFAP1-AS1 into exosomes, thus disseminating trastuzumab resistance in other cells. The impact of exosomal AFAP1-AS1 in induction of trastuzumab resistance is exerted *via* its interaction with AUF1 and subsequent induction of ERBB2 translation (21). **Figure 3** depicts the impact of AFAP1-AS1 in carcinogenesis and therapy resistance of breast cancer cells.

Osteosarcoma

In MNNG/HOS and U2OS osteosarcoma cells, AFAP1-AS1 has been found to promote tumorigenesis *via* influencing RhoC/ROCK1/p38MAPK/Twist1 cascade (22). The AFAP1-AS1-mediated increase in Twist1 can enhance expression of N-cadherin and Vimentin, while diminishing E-cadherin levels, thus promoting EMT of osteosarcoma cells (22). Moreover, AFAP1-AS1 can sequester miR-497 and miR-4695-5p in these cells, therefore increasing expressions of IGF1R and TCF4, respectively (23, 24). The latter can activate Wnt- β catenin pathway and increase both proliferation and invasive abilities of osteosarcoma cells (24). **Figure 4** depicts the oncogenic role of AFAP1-AS1 in osteosarcoma.

Gastric Cancer

Similarly, AFAP1-AS1 has an oncogenic role in gastric cancer. AFAP1-AS1 silencing has significantly suppressed proliferation

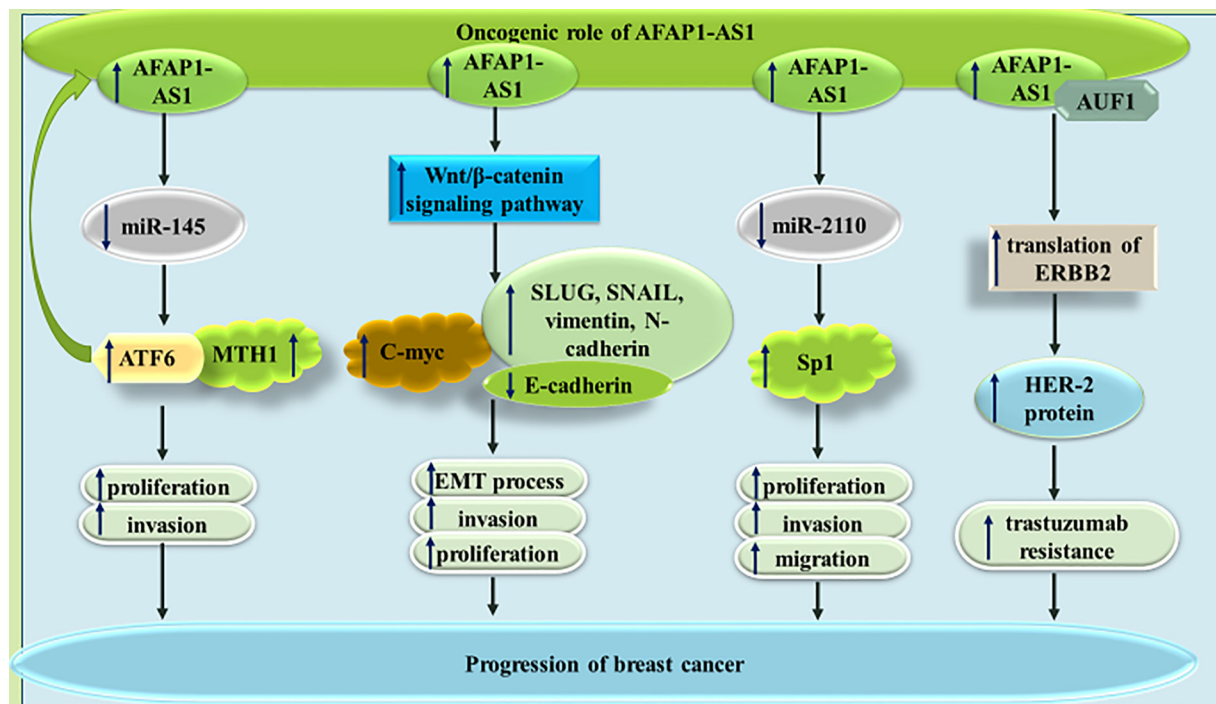


FIGURE 3 | The impact of AFAP1-AS1 in breast cancer progression and resistance to therapy. In addition to increasing cell proliferation and invasion, this lncRNA can increase expression of Her-2 protein, thus increasing resistance to trastuzumab.

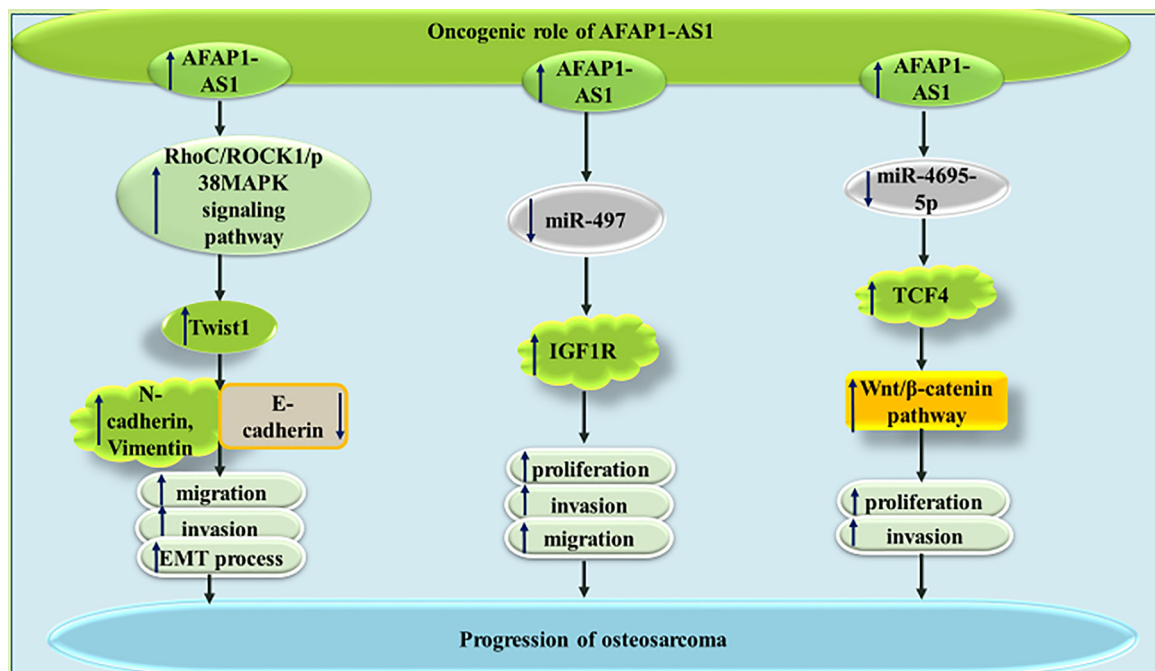


FIGURE 4 | The oncogenic role of AFAP1-AS1 in osteosarcoma is exerted through modulation of RhoC/ROCK1/p38MAPK/Twist1 cascade as well as sponging miR-497 and miR-4695-5p.

and cell cycle transition in this kind of cancer. Besides, reduction in the levels of this lncRNA can inhibit invasive capacity through affecting EMT (25). Down-regulation of KLF2 is another mechanism by which AFAP1-AS1 enhances proliferative and migratory aptitudes of gastric cancer cells (26). AFAP1-AS1 silencing in gastric cancer cells has led to a significant increase in the levels of Bax, cleaved PARP, Caspase 3, and Caspase 9, while decreasing Bcl-2 level. AFAP1-AS1 silencing has also reduced p-AKT levels and enhanced expression of PTEN in gastric cancer cells. Taken together, AFAP1-AS1 regulates proliferation and apoptotic processes in gastric cancer cell through PTEN/p-AKT cascade (27). AFAP1-AS1 can also promote proliferation and metastatic ability of gastric cancer cell through sequestering miR-155-5p and enhancing expression of FGF7 (28). **Figure 5** shows the oncogenic role of AFAP1-AS1 in gastric cancer.

Esophageal Cancer

AFAP1-AS1 have also been shown to bind with miR-26a, therefore influencing expression of its target gene, i.e. ATF2. Exosomes originated from M2 macrophages have higher expression of AFAP1-AS1 and ATF2 and reduced expression of miR-26a, compared with M1 macrophages. These exosomes could transfer AFAP1-AS1 to esophageal cancer cells, thus downregulating miR-26a and enhancing ATF2 levels in the recipient cells. These expression changes affect phenotype of esophageal cancer cells (29). The regulatory role of AFAP1-AS1

on miR-498/VEGFA axis is another mechanism of participation of this lncRNA in the pathetiology of esophageal cancer (30).

Other Types of Cancers

In prostate cancer cells, AFAP1-AS1 has been shown to promote sequester miR-195-5p (31) and miR-512-3p (32), thus affecting malignnat behaviours of these cells.

A number of other miRNAs, namely miR-423-5p (33), miR-320a (34), miR-107 (35) and miR-384 (36) have been found to be sequestered by AFAP1-AS1 in different cancer tissues (**Figure 6**).

Table 1 summarizes the results of studies which appraised oncogenic roles of AFAP1-AS1 in different tissues.

ANIMAL STUDIES

Investigations, particularly those conducted in BALB/c nude mice models have verified the oncogenic roles of AFAP1-AS1 in different types of cancers. AFAP1-AS1 knock-down has consistently led to significant reduction in tumor size/weight, attenuation of tumor growth rate and enhancement of response of cancer cells to therapeutic modalities (**Table 2**). In NSCLC, AFAP1-As1 silencing not only reduces tumorigenicity, but also confers chemosensitivity (8). Moreover, its silencing can affect IRF7 and RIG-I-like receptor signals (9). In breast cancer, AFAP1-AS1 down-regulation can affect trastuzumab resistance (21).

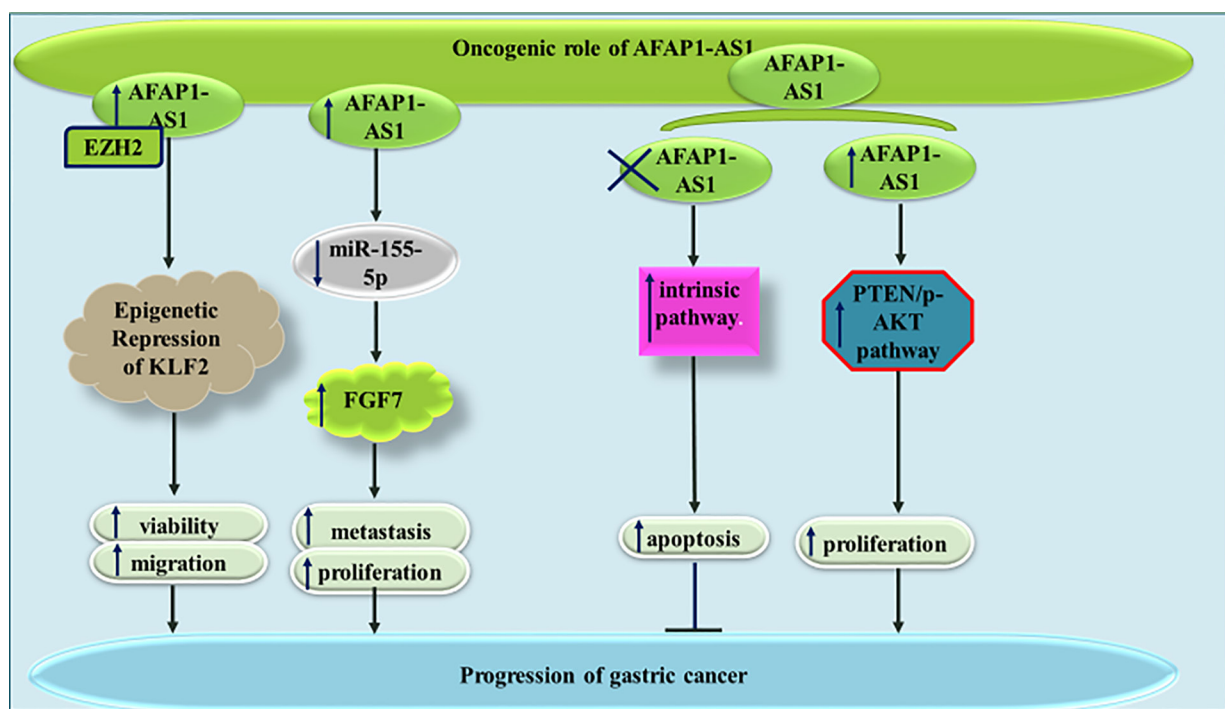


FIGURE 5 | The oncogenic role of AFAP1-AS1 in gastric cancer is exerted through repression of KLF2, sponging miR-155-5p and enhancing activity of PTEN/p-AKT pathway.

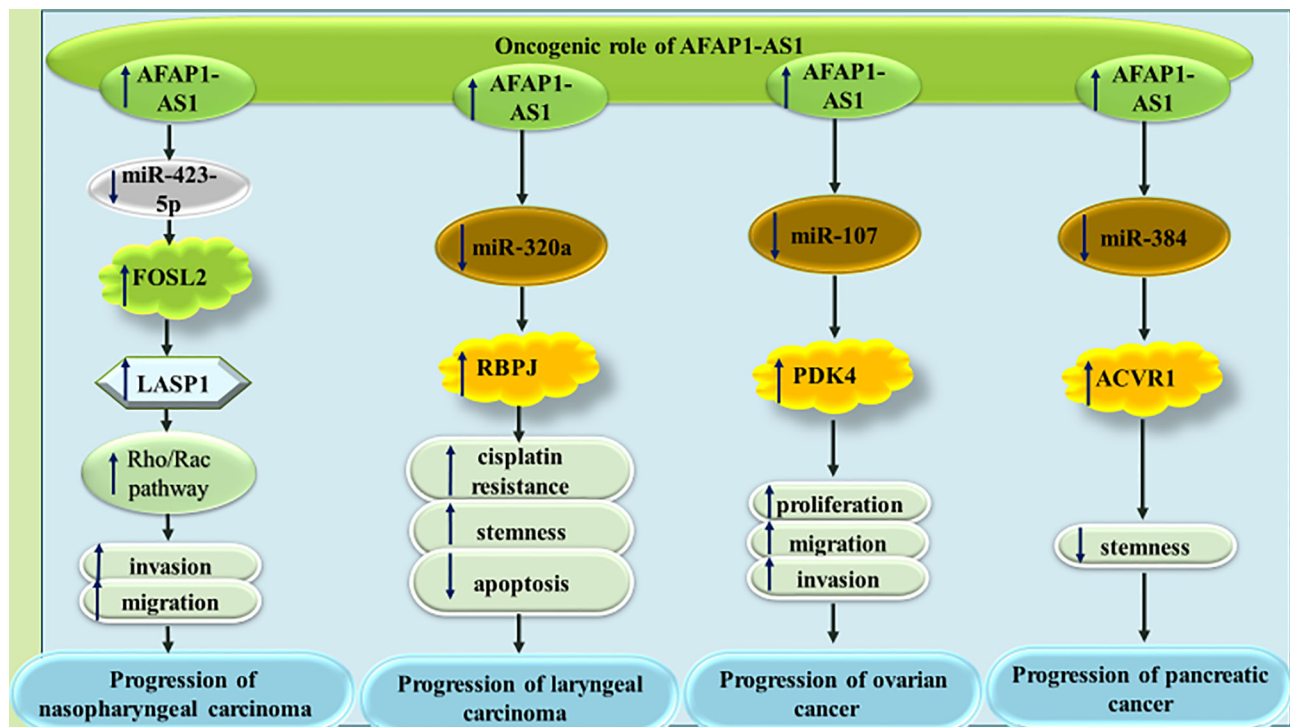


FIGURE 6 | The oncogenic role of AFAP1-AS1 in nasopharyngeal carcinoma, laryngeal carcinoma, ovarian cancer and pancreatic cancer. In all types of mentioned cancers, AFAP1-AS1 can act as molecular sponge for tumor suppressor miRNAs.

CLINICAL STUDIES

Except from a single low-sample size study in gastric cancer which reported down-regulation of AFAP1-AS1 in tumoral tissues versus nearby samples (6), other studies consistently reported over-expression of AFAP1-AS1 in different neoplastic tissues compared with non-neoplastic tissues of the same origin (Table 3). Even in the mentioned study, levels of AFAP1-AS1 were higher in patients who showed lymphatic or vascular invasion in comparison with those without these properties (6). Moreover, different statistical methods have been applied to assess correlations between expression level of AFAP1-AS1 and clinical outcomes, all of them reporting significant impact of up-regulation of this lncRNA on increasing malignant behaviors of tumors and decreasing patients' survival. In pancreatic cancer, up-regulation of AFAP1-AS1 has been associated with lymph node involvement, perineural invasion, and poor clinical outcome. An *in silico* analysis of TCGA data of breast cancer patients has revealed AFAP1-AS1, as a differentially expressed lncRNA in basal tumors whose expression levels are associated with poor survival. Expression of this lncRNA has also been associated with hormone receptors status, HER2 expression, and PAM50 classification (81).

Tissue levels of AFAP1-AS1 could be used as a prognostic biomarker with the areas under ROC curves values of 0.86 and 0.93 for forecasting cancer progression in the periods of 6 and 12 months, respectively (66).

The ability of tissue levels of AFAP1-AS1 or its circulatory levels in differentiation of patients' samples from control samples has been appraised in different types of cancers (Table 4). For instance, Li et al. have shown that over-expression of AFAP1-AS1 in serum samples of patients with NSCLC compared with normal controls can be used to distinguish these two sets of samples with an area under the curve (AUC) of 0.759. Combination of expression levels of this lncRNA with those of cyfra21-1 has increased AUC value to 0.860. Moreover, AFAP1-AS1 over-expression has been more prominent in patients with distant or lymph node metastasis, advanced clinical stage, and greater tumor burden (75). Serum levels of AFAP1-AS1 have also been shown to separate gastric cancer patients from controls with higher AUC value compared with conventional markers, i.e. CEA and CA19-9. Notably, serum levels of AFAP1-AS1 have been shown to be reduced following surgical treatment of patients (45).

DISCUSSION

AFAP1-AS1 has been found to be up-regulated in almost all kinds of malignant tissues. This lncRNA has multiple effects in the carcinogenesis process, most of them being exerted through AFAP1-independent manners. Most notably, AFAP1-AS1 can sequester a number of tumor suppressor miRNAs, thus releasing the targets of these miRNAs from inhibitory effects of miRNAs.

TABLE 1 | Outlines of papers which judged expression of AFAP1-AS1 in cell lines.

Tumor type	Interactions	Cell lines	Effects	Reference
Non-small Cell Lung Cancer	miR-139-5p, RRM2, EGFR/AKT signaling pathway	H1975, PC-9, A549, SPCA-1, BEAS-2B	Δ AFAP1-AS1: ↓ proliferation, ↓ chemo-resistance, ↑ apoptosis	(8)
	–	A549, H1975, H1650, H1395, H12994	Δ AFAP1-AS1: ↓ proliferation ↑ AFAP1-AS1: ↑ invasion, ↑ migration, ↓ apoptosis	(9)
	p21, EZH2	16HBE, A549, SPC-A, H1299	Δ AFAP1-AS1: ↓ proliferation, ↑ cell cycle arrest	(10)
	PPP1R13L, VASP, SPTAN1, STAT1, NF1, FBN2, AFAP1	H1299, PC9, H1975, 293T	Δ AFAP1-AS1: ↓ invasion, ↓ migration ↑ AFAP1-AS1: ↑ invasion, ↑ migration	(11)
	HBP1	16HBE, A549, SPC-A1, PC-9, H1299, H1975	Δ AFAP1-AS1: ↓ proliferation, ↓ migration, ↑ G0/G1 cell cycle arrest, ↑ apoptosis	(37)
Lung cancer	AFAP1, KRT1	A549, H1299 and H460, 95-D, 16HBE	Δ AFAP1-AS1: ↓ proliferation, ↓ migration	(38)
	RhoA, Rac2, Rab10, Rab11a, Rhogdi proteins, Pfn1, RhoC, Rab11b, LIM, Lasp1	A549	Δ AFAP1-AS1: ↓ invasion, ↓ migration, ↓ metastasis	(12)
	miR-545-3p, HDGF	–	Δ AFAP1-AS1: ↓ proliferation ↓ invasion, ↓ migration, ↑ apoptosis	(15)
Breast cancer (BC)	SNIP1, c-Myc, ZEB1, ZEB2, SNAIL	A549, PC9	Δ AFAP1-AS1: ↓ invasion, ↓ migration, ↓ EMT process	(16)
	–	H1915, HCC827	Δ AFAP1-AS1: ↓ invasion, ↓ growth, ↑ apoptosis	(39)
	–	MCF-10A, MCF-7, SK-RB-3, MDA-MB231, MDA-MB-468	Δ AFAP1-AS1: ↓ proliferation, ↓ colony formation, ↓ metastasis ↑ apoptosis, did not affect AFAP1 expression, did not affect actin filament integrity	(40)
	miR-497-5p	HCC70, BT-549, MCF-7, MDA-MB-231, MCF-10A	Δ AFAP1-AS1: ↓ proliferation, ↓ migration, ↑ apoptosis	(17)
	miR-145, MTH1, ATF6	MDA-MB-231, MDA-MB-468, MDA-MB-435S, and HCC1937, MCF-10A	Δ AFAP1-AS1: ↓ viability, ↓ colony formation, ↓ invasion	(18)
Osteosarcoma	Wnt/β-catenin signaling pathway, C-myc, SLUG, SNAIL, vimentin, fibronectin, N-cadherin, E-cadherin	184A1, MCF-10A, BT474, MCF-7, T47D, BT483, BT20, MDA-MB-468, BT549, MDA-MB-231	Δ AFAP1-AS1: ↓ proliferation ↓ invasion, ↓ migration, ↓ EMT process, ↑ apoptosis	(20)
	miR-2110, Sp1	MCF-10A, BT-549, MDA-MB-468	Δ AFAP1-AS1: ↓ proliferation ↓ invasion, ↓ migration	(19)
	ERBB2, AUF1	KBR-3, BT474,	Δ AFAP1-AS1: ↓ trastuzumab resistance	(21)
	Twist1, N-cadherin and Vimentin, E-cadherin, RhoC/ROCK1/p38MAPK signaling pathway	MNNG/HOS, MG63, SaOS-2, hFOB 1.19	Δ AFAP1-AS1: ↓ proliferation, ↓ invasion, ↓ migration, ↓ actin filament integrity, ↓ EMT process, ↓ VM formation capacity, ↑ apoptosis, ↑ G0/G1 cycle arrest	(22)
	miR-497, IGF1R	MG-63, 143B, U2OS, Saos-2, hFOB 1.19	Δ AFAP1-AS1: ↓ proliferation ↓ invasion, ↓ migration, ↑ apoptosis,	(23)
Esophageal cancer (EC)	miR-4695-5p, TCF4, Wnt/β-catenin pathway	hFOB 1.19, Saos-2, U2OS, MG-63, 143B	Δ AFAP1-AS1: ↓ proliferation ↓ invasion	(24)
	miR-26a, ATF2	PBMCs, KYSE410	Δ AFAP1-AS1 in M2 Macrophage-Derived Exosomes: ↓ invasion, ↓ migration, ↓ metastasis	(29)
	miR-498, VEGFA	HET-1A, Eca109, KYSE-30	Δ AFAP1-AS1: ↓ proliferation, ↓ Migration, ↑ apoptosis	(30)
	–	ECA-109, TE-1, HEEC	Δ AFAP1-AS1: ↓ proliferation, ↑ apoptosis	(41)
	–	OE-33, SK-GT-4, FLO-1, HEEpic	Δ AFAP1-AS1: ↓ proliferation, ↓ invasion, ↓ anchorage-dependent growth did not affect the expression level of AFAP1	(42)
Gastric cancer (GC)	KLF2, EZH2	GES-1, AGS and SGC-7901	Δ AFAP1-AS1: ↓ proliferation, ↓ invasion, ↓ viability, ↑ apoptosis	(26)
	intrinsic pathway, PTEN/p-AKT Pathway	AGS, MGC-803, SGC-7901, BGC-823, GES-1	Δ AFAP1-AS1: ↓ proliferation, ↑ apoptosis	(27)
	–	MKN-45, MGC-803 and AGS	Δ AFAP1-AS1: ↓ proliferation, ↓ migration, ↓ invasion, ↑ G0/G1 phase arrest, ↑ apoptosis	(43)
	–	AGS, BGC823, MGC-803, SGC-7901, GES-1	Δ AFAP1-AS1: ↓ proliferation, ↓ invasion, ↓ EMT process, ↓ cell cycle progress	(25)
	miR-155-5p, FGF7	MKN-28, BGC-823, MGC-803, SGC-7901, GES-1	Δ AFAP1-AS1: ↓ proliferation, ↓ migration, ↓ invasion	(28)
Prostate cancer	–	GES-1, HGC-27, MGC-803, BGC-823, SGC-7901	Δ AFAP1-AS1: ↓ proliferation, ↓ migration, ↓ invasion	(44)
	–	GES-1, AGS, BGC-823, MKN-45, SGC-7901	Δ AFAP1-AS1: ↓ proliferation, ↓ migration, ↓ invasion, ↓ EMT process	(45)
	miR-195-5p, FKBP1A	PC3, DU145	Δ AFAP1-AS1: ↑ PTX sensitivity, ↑ apoptosis, ↓ migration, ↓ invasion	(31)
	miR-512-3p	22RV1		(32)

(Continued)

TABLE 1 | Continued

Tumor type	Interactions	Cell lines	Effects	Reference
Nasopharyngeal carcinoma (NPC)	YAP, KAT2B, RBM3	HNE-1, C666-1, SUNE-1, CNE-1, CNE-2, NP69	Δ AFAP1-AS1: ↓ proliferation, ↓ migration, ↓ invasion, ↑ G0/G1 phase arrest	(46)
	miR-423-5p, Rho/Rac signaling, FOSL2, LASP1	5-8F, HNE2	Δ AFAP1-AS1: ↓ proliferation	(33)
	AFAP1, RhoA, Rac2, Rab10, Rab11a, Rhogdi, Pfn1, RhoC, Rab11b, Lasp1	5-8F, HNE2 and HK-1	↑ AFAP1-AS1: ↑ migration, ↑ invasion	(47)
	miR-545-3p, VEGFA	Ishikawa, HEC-1-B, HEC1-A, AN3-CA, hEEC,	Δ AFAP1-AS1: ↓ migration, ↓ invasion, ↓ stress filament integrity	(48)
Endometrial carcinoma (EC)	AFAP1	HuCC-T1, TFK-1, HIBEpC	Δ AFAP1-AS1: ↓ proliferation, ↓ migration, ↓ invasion, ↓ angiogenesis	(49)
Cholangiocarcinoma (CCA)	MMP-2, MMP-9	QBC939, CCLP1, HuCC-T1 and RBE, BEC, 293T	Δ AFAP1-AS1: ↓ proliferation, ↓ migration, ↓ invasion, ↓ stress filament integrity	(50)
Colorectal cancer (CRC)	GAS8-AS1	CR4 (Sigma-Aldrich, USA), RKO (ATCC, USA)	Δ AFAP1-AS1: ↓ proliferation, ↓ migration, ↓ invasion, ↓ G0/G1 phase arrest	(51)
	–	HCT116, SW480	↑ AFAP1-AS1: ↑ proliferation	(52)
	AFAP1	HCT116, SW480	Δ AFAP1-AS1: ↓ proliferation, ↓ migration, ↓ invasion	(53)
	EZH2	LOVO, SW1116, SW480, HCT116, SW620, HT29	Δ AFAP1-AS1: ↓ proliferation, ↑ cell-cycle arrest	(54)
Colon cancer	actin-cytokeratin signaling pathway, E-cadherin, vimentin, MMP9, ZEB1, ZO-1, β-catenin	SW480, SW620, HCT116, HT-29	Δ AFAP1-AS1: ↓ proliferation, ↓ migration, ↓ invasion	(55)
Hepatocellular carcinoma (HCC)	N-cadherin, vimentin, E-cadherin, CRKL, Ras, MEK, c-Jun	Huh7, HepG2, HCCLM3, LO2	Δ AFAP1-AS1: ↓ proliferation, ↓ migration, ↓ invasion, ↓ EMT process	(56)
	RhoA/Rac2 signaling	SMCC7721 and HepG2	Δ AFAP1-AS1: ↓ proliferation, ↓ invasion, ↑ S phase arrest, ↑ apoptosis	(57)
	–	LO2, SMMC-7721, Bel-7402, MHCC-97 L, MHCC-97H	Δ AFAP1-AS1: ↓ proliferation, ↓ migration, ↓ invasion	(58)
	–	ATCC no. CCL-2,	Δ AFAP1-AS1: ↓ proliferation, ↓ migration, ↓ invasion	(59)
Cervical cancer (CC)	RhoA/Rac2 signaling, Vimentin, β-catenin, ZO-1	ATCC no. CCL-2,	Δ AFAP1-AS1: ↓ migration, ↓ invasion, ↓ EMT process	(59)
Laryngeal carcinoma	miR-320a, RBPJ	HEp-2	Δ AFAP1-AS1: ↓ stemness, ↓ cisplatin resistance, ↑ apoptosis	(34)
Thyroid cancer	–	K-1, TPC-1, SW579, FTC133, XTC-1, I Nthy-ori3-1	Δ AFAP1-AS1: ↓ proliferation, ↓ migration, ↓ EMT process, ↑ apoptosis	(60)
Glioma	–	U87MG, U251, SHG-44, A172	Δ AFAP1-AS1: ↓ invasion	(61)
Ovarian cancer (OC)	–	SKOV3, OV90, TOV112D, ES2	Δ AFAP1-AS1: ↓ proliferation, ↑ apoptosis	(62)
	–	–	Δ AFAP1-AS1: ↓ proliferation, ↑ AFAP1-AS1: ↑ proliferation	(62)
	miR-107, PDK4	IOSE80, COV504, OVI5E, OV90 and SKOV3	Δ AFAP1-AS1: ↓ proliferation, ↓ migration, ↓ invasion	(35)
	–	–	Δ AFAP1-AS1: ↓ proliferation, ↓ migration, ↓ invasion	(35)
Pancreatic cancer (PC)	miR-384, ACVR1	SW1990, Capan-1, AsPC-1, MIAPaCa-2, PANC-1, HPC-Y5	Δ AFAP1-AS1: ↓ stemness	(36)
	ZEB1, N-cadherin, E-cadherin, MMP-2, MMP-9, Slug, Snail	BxPC-3, PANC-1	Oridonin-induced Δ AFAP1-AS1: ↓ proliferation, ↓ migration, ↓ EMT process, ↑ apoptosis, ↑ cell cycle arrest	(63)
	miR-133a, IGF1R	AsPC-1, BxPC-3, PANC-1, PaCa-2 and SW1990	Δ AFAP1-AS1: ↓ proliferation, ↓ invasion, ↓ metastasis, ↑ apoptosis	(64)
	EGFR/Akt signaling, miR-146b-5p	ASPC-1, BxPC-3, HPAC, MiaPaCa-2, HPDE6-C7	CUB-induced Δ AFAP1-AS1: ↓ proliferation, ↑ cell cycle arrest	(65)
Pancreatic ductal adenocarcinoma (PDAC)	–	Panc1, MIAPaCa-2, Capan2, SW1990, BXPc-3, HPDE6	Δ AFAP1-AS1: ↓ proliferation, ↓ migration, ↓ invasion	(66)
Renal cell carcinoma (RCC)	PTEN/AKT signaling	HK2, 786-O, Caki-1, ACHN, A498	Δ AFAP1-AS1: ↓ proliferation, ↓ migration, ↓ invasion, ↓ EMT process	(67)
Gallbladder cancer (GBC)	–	NOZ, H69, GBC-SD, SGC-996	Δ AFAP1-AS1: ↓ proliferation, ↓ invasion, ↓ epithelial phenotype to mesenchymal phenotype	(68)
Pituitary adenoma	miR-103a-3p, PI3K/AKT Signaling Pathway	GH3 and MMQ	Δ AFAP1-AS1 + miR-103a-3p inhibitor: ↑ proliferation, ↑ cell cycle progression, ↓ apoptosis	(69)
Melanoma	PTEN/PI3K/AKT signaling pathway	GH3, MMQ	Δ AFAP1-AS1: ↓ proliferation, ↑ cell cycle arrest, ↑ apoptosis	(70)
	–	–	–	–
	miR-653-5p, RAI14, E-cadherin, N-cadherin, Ki67	HEMa-LP, A375, M21, B16F10, SK-MEL-2	Δ AFAP1-AS1: ↓ proliferation, ↓ migration, ↓ invasion	(71)
	–	–	–	–

(Continued)

TABLE 1 | Continued

Tumor type	Interactions	Cell lines	Effects	Reference
Retinoblastoma	–	Weri-Rb1 and Y79, ARPE-19, HRMECs	Δ AFAP1-AS1: ↓ proliferation, ↓ migration, ↓ invasion	(72)
Tongue squamous cell carcinoma (TSCC)	Wnt/β-catenin, SLUG, SNAIL1, VIM, CADN, ZEB1, ZEB2, and TWIST1	SCC-15, Tca8113, SCC-4, SCC-9, CAL-27	Δ AFAP1-AS1: ↓ proliferation, ↓ migration, ↓ invasion, ↑ G0/G1 cell cycle arrest	(73)
Oral squamous cell carcinoma (OSCC)	miR-145, HOXA1	SCC9, SCC15, SCC25, HOKs	Δ AFAP1-AS1: ↓ proliferation, ↓ migration, ↓ invasion	(74)

(Δ: knock-down, CuB: Cucurbitacin B).

miR-139-5p, miR-545-3p, miR-497-5p, miR-145, miR-2110, miR-4695-5p, miR-26a, miR-498, miR-155-5p, miR-195-5p, miR-512-3p, miR-423-5p, miR-545-3p, miR-320a, miR-107, miR-384, miR-133a, miR-146b-5p, miR-103a-3p and

miR-653-5p are among miRNAs which have been found to be sequestered by AFAP1-AS1 through functional studies in different types of cancer cells. Notably, the interaction between AFAP1-AS1 and miR-497 has been verified in breast cancer and

TABLE 2 | Outlines of studies which tested function of AFAP1-AS1 in xenografts.

Tumor Type	Animal models	Results	Reference
Non-small Cell Lung Cancer	male athymic nude BALB/c mice	Δ AFAP1-AS1: ↓ tumorigenicity, ↓ chemo-resistance	(8)
	–	Δ AFAP1-AS1: ↓ mRNA and protein of IRF7 and RIG-I-like receptor signals ↑ AFAP1-AS1: ↑ mRNA and protein of IRF7 and RIG-I-like receptor signals	(9)
	male BALB/c nude mice	Δ AFAP1-AS1: ↓ tumor volume, ↓ tumor weight	(10)
	BALB/c nude mice	Δ AFAP1-AS1: ↓ tumor weight, ↓ tumor size	(37)
Lung cancer	BALB/c nude mice	Δ AFAP1-AS1: ↓ tumor volume, ↓ tumor weight, ↓ tumor growth	(38)
	murine xenograft mice	Δ AFAP1-AS1: ↓ tumor growth	(15)
	female nude mice	Δ AFAP1-AS1: ↓ metastatic nodules	(16)
Breast cancer (BC)	female nude mice	Δ AFAP1-AS1: ↓ tumor growth	(17)
	Female BALB/c nude mice	Δ AFAP1-AS1: ↓ tumor growth	(18)
	female nude mice	Δ AFAP1-AS1: ↓ tumor growth, ↓ tumor weight	(20)
	BALB/C specific-pathogen-free nude mice	Δ AFAP1-AS1: ↓ tumor volume, ↓ tumor weight, ↓ tumor growth	(19)
	male BALB/c nude mice	Δ AFAP1-AS1: ↓ tumor resistance, ↓ metastasis	(21)
Osteosarcoma	female BALB/c nude mice	Δ AFAP1-AS1: ↓ tumor growth, ↓ invasion	(22)
	male athymic BALB/c nude mice	Δ AFAP1-AS1: ↓ tumor volume, ↓ tumor weight, ↓ tumor growth	(23)
	female BALB/c nude mice	Δ AFAP1-AS1: ↓ tumor size, ↓ tumor weight	(24)
Esophageal cancer (EC)	–	Δ AFAP1-AS1: ↓ATF2, ↑ miR-26a	(29)
Gastric cancer (GC)	male BALB/c nude mice	Δ AFAP1-AS1: ↓ tumor volume, ↓ tumor weight, ↓ tumor growth	(44)
Prostate cancer	nude mice	Δ AFAP1-AS1: ↓ tumor volume, ↓ tumor weight, ↑ C-caspase 3	(31)
Nasopharyngeal carcinoma (NPC)	male BALB/C nude mice	↑ AFAP1-AS1: ↑ metastasis	(33)
	nude mice	Δ AFAP1-AS1: ↓ number and size of the metastatic foci	(47)
Endometrial carcinoma (EC)	male BALB/c nude mice	Δ AFAP1-AS1: ↓ tumor volume, ↓ tumor weight	(48)
Cholangiocarcinoma (CCA)	female BALB/c/nu nude mice	Δ AFAP1-AS1: ↓ tumor volume, ↓ tumor weight, ↓ number and size of the metastatic foci	(49)
	female BALB/c athymic nude mice	Δ AFAP1-AS1: ↓ tumor volume, ↓ tumor weight	(50)
Colorectal cancer (CRC)	male C57BL/6 nude mice	Δ AFAP1-AS1: ↓ tumor volume, ↓ tumor weight	(53)
	female BALB/c-nude mice	Δ AFAP1-AS1: ↓ tumor growth	(54)
Hepatocellular carcinoma (HCC)	female immune-deficient BALB/c-nu nude mice	Δ AFAP1-AS1: ↓ tumor weight	(57)
	nude mice	Δ AFAP1-AS1: ↓ tumor weight, ↓ tumor growth, ↓ Ki-67 expression	(58)
Pancreatic cancer (PC)	nude mice	Δ AFAP1-AS1: ↓ tumor volume, ↓ tumor weight	(36)
	male/female BALB/C nude mice	Δ AFAP1-AS1: ↓ tumorigenicity, ↓ EMT process	(63)
	female BALB/c nude mice	CUB-induced Δ AFAP1-AS1: ↓ tumor volume, ↓ tumor weight, ↓ tumor growth	(65)
Pancreatic ductal adenocarcinoma (PDAC)	nude mice	Δ AFAP1-AS1: ↓ tumor volume, ↓ tumor weight	(66)
Renal cell carcinoma (RCC)	female BALB/c athymic nude mice	Δ AFAP1-AS1: ↓ tumor volume, ↓ tumor weight	(67)
Melanoma	male BALB/c nude mice	Δ AFAP1-AS1: ↓ tumor volume, ↓ tumor weight, ↓ tumor size	(71)
Tongue squamous cell carcinoma (TSCC)	female BALB/c athymic nude mice	Δ AFAP1-AS1: ↓ tumor growth, ↓ tumor weight, ↓ tumor size	(73)
Oral squamous cell carcinoma (OSCC)	male BALB/c nude mice	Δ AFAP1-AS1: ↓ tumor volume, ↓ tumor weight	(74)

(Δ: knock down or deletion).

TABLE 3 | Outlines of studies that appraised levels of AFAP1- AS1 in clinical setting.

Tumor type	Numbers of clinical samples	Expression (Tumor vs. Normal)	Kaplan-Meier analysis	Univariate cox regression	Multivariate cox regression	Clinicopathologic characteristics of patients	Reference
Non-small Cell Lung Cancer (NSCLC)	44 NSCLC patient tissues and ANCTs	high	–	–	–	–	(8)
	165 NSCLC patients, 118 benign lung tumor tissues, and 173 healthy samples	high	–	–	–	Paired t test: AFAP1- AS1 was correlated with pathological grade, TNM staging and metastatic ability.	(9)
	GEO analysis	high	–	–	–	–	(10)
	92 pairs of NSCLC tissues and ANCTs	high	Patients with high levels of AFAP1-AS1 had poorer OS.	Histological grade, TNM stage, and AFAP1-AS1 expression were identified as three prognostic factors.	Histological grade, TNM stage, and AFAP1-AS1 expression were independent predictors for OS in NSCLC patients.	Chi-square test: Relative levels of AFAP1-AS1 were associated with tumor burden.	
	7 NSCLC tumor tissues and ANCTs	high	–	–	–	–	(11)
	126 NSCLC patients and 60 healthy controls	high	–	–	–	Mann-Whitney U test: High serum levels of AFAP1-AS1 were strongly associated with DM, LNM, poor clinical stage, and larger tumor size.	(75)
	82 pairs of NSCLC tissue and ANCTs	high	–	–	–	–	(76)
	52 NSCLC patients	high	AFAP1-AS1 down-regulation was correlated with improved survival time.	–	High expression level of ASAP1-S1 was an indicator of poor survival.	–	
	96 pairs of lung cancer tissues and ANCTs	high	AFAP1-AS1 over-expression was related with short OS and PFS.	–	–	–	(37)
	GEO and TCGA analysis: _	high	–	–	–	–	(77)
Non-small Cell Lung Cancer (NSCLC)	121 NSCLC patients and 79 healthy controls	high	AFAP1-AS1 over-expression was related with short OS.	–	AFAP1-AS1 was an independent prognostic indicator for NSCLC patients.	Chi-square test: AFAP1-AS1 expression was influenced by clinical stage, smoking history, infiltration extent, LNM and distant metastasis.	
	36 studies: 6267 NSCLC patients	high	–	–	–	–	(78)
	TCGA analysis: 465 LUAD patients and 49 ANCTs	high	–	–	–	–	(79)
	53 newly diagnosed LUAD tissues and ANCTs	high	–	–	–	–	(80)
	20 pairs of LUAD and LUSC tumor tissues and ANCTs	high	–	–	–	–	

(Continued)

TABLE 3 | Continued

Tumor type	Numbers of clinical samples	Expression (Tumor vs. Normal)	Kaplan-Meier analysis	Univariate cox regression	Multivariate cox regression	Clinicopathologic characteristics of patients	Reference
Lung cancer	TCGA analysis: 57 paired LUAD and normal samples and 16 paired LUSC and normal samples	high	–	–	–	–	
	98 pairs of lung cancer tissues and ANCTs	high	–	–	–	Patients with high levels of AFAP1-AS1 had poor histology type, great tumor size, LNM, distant metastasis, and advanced TNM stage.	(38)
	GSE31210 analysis: 226 primary lung cancer samples and 20 normal lung samples	high	High levels of were associated with poor OS.	–	–	–	(12)
Lung cancer	GSE19804 analysis: 60 pairs of lung cancer tissues and ANCTs	high	–	–	–	–	
	GSE27262 analysis: 25 pairs of tumor tissues and ANCTs	high	–	–	–	–	
	GSE18842 analysis: 46 pairs of tumor tissues and ANCTs	high	–	–	–	–	
	GSE37745 analysis: 106 lung cancer biopsies	high	High levels of were associated with poor OS.	–	–	–	
	187 paraffin-embedded lung cancer tissues and 36 normal lung specimens	high	High AFAP1-AS1 expression was tightly correlated with poorer OS.	–	–	–	(16)
	36 lung adenocarcinoma tissue samples and ANCTs	high	High levels of AFAP1-AS1 were associated with shorter DFS.	–	–	–	(39)
	160 pairs of breast cancer tissues and ANCTs	high	The 3-years OS of patients with high AFAP1-AS1 expression was lower.	AFAP1-AS1 expression, tumor grade, TNM stage, and LNM were Significant factors.	High level of AFAP1-AS1 was correlated with the malignant features.	–	(40)
Breast cancer (BC)	20 pairs of breast cancer tissues and ANCTs	high	–	–	–	–	(17)
	TCGA analysis: _	high	–	–	–	–	(18)
		high	–	–	–	–	(20)

(Continued)

TABLE 3 | Continued

Tumor type	Numbers of clinical samples	Expression (Tumor vs. Normal)	Kaplan-Meier analysis	Univariate cox regression	Multivariate cox regression	Clinicopathologic characteristics of patients	Reference
Osteosarcoma	31 pairs of TNBC tissues and ANCTs		High levels of AFAP1-AS1 were correlated with poorer DFS and OS.		AFAP1-AS1 could be regarded as an independent prognostic factor in TNBC.		
	TCGA analysis: _	high	High expression of AFAP1 was correlated with short survival in patients with Luminal B, HER2 +, and basal tumors and worse OS Luminal A and HER2 + tumor subtypes.	—	—	—	(81)
	8 pairs of TNBC tissues and ANCTs	high	—	—	—	—	(19)
	64 HER-2 positive patients and 40 HER-2 negative patients	Higher in HER-2 positive than HER-2 negative	—	—	—	—	(21)
	51 pairs of tumor tissues and ANCTs	high	—	—	—	Its expression was low in ki-67 negative tumor tissues.	(82)
	8 pairs of Osteosarcoma tissues and ANCTs	high	—	—	—	—	(22)
	45 OS tissues and ANCTs	high	Patients who had high AFAP1-AS1 expression level indicated poor OS rate than those who had low AFAP1-AS1 expression level.	—	—	—	(23)
	49 pairs of OS tissues and ANCTs	high	Patients with higher expression of AFAP1-AS1 showed lower OS and PFS rates.	—	—	—	(24)
	42 ESCC tissues and 35 ANCTs	high	—	—	—	—	(30)
	65 pairs of tissues and ANCTs	high	—	—	—	Chi-squared test: high level of AFAP1-AS1 was correlated with tumor size and advanced TNM stage.	(41)
Gastric cancer (GC)	48 pairs of ESCC tissues and ANCTs	high	—	—	—	—	(83)
	162 pairs of ESCC tissues and ANCTs	high	High levels of AFAP1-AS1 were strongly associated with shorter PFS.	Tumor depth, LNM, TNM stage, dCRT response, and AFAP1-AS1 expression were associated with PFS and OS.	Tumor depth, dCRT response, and AFAP1-AS1 expression were independent prognostic factors for PFS. Moreover, high levels of AFAP1-AS1 indicated unfavorable OS.	Chi-squared test: higher expression of AFAP1-AS1 was strongly correlated with LNM, distant metastasis, advanced clinical stage, and lack of response to dCRT.	
	20 pairs of GC tissues and ANCTs	high	—	—	—	—	(27)
	52 pairs of GC tissues and ANCTs	high	—	—	—	—	(43)

(Continued)

TABLE 3 | Continued

Tumor type	Numbers of clinical samples	Expression (Tumor vs. Normal)	Kaplan-Meier analysis	Univariate cox regression	Multivariate cox regression	Clinicopathologic characteristics of patients	Reference
	91 pairs of primary gastric cancer tissues and their ANCTs	high	Patients with high levels of AFAP1-AS1 showed poor OS than those with low levels.	–	Lymph node metastasis, TNM stage, and AFAP1-AS1 expression levels were independent prognostic factors for OS time.	X2 test: expression of AFAP1-AS1 was associated with LNM and TNM stage.	(25)
	52 pairs of GC tissues and ANCTs	high	Patients with high expression of AFAP1-AS1 had a significantly poorer OS compared to those with low-expression of AFAP1-AS1.	–	–	–	(28)
	30 tumor tissues and ANCTs	down	–	–	–	Levels of AFAP1-AS1 were higher in patients who showed lymphatic or vascular invasion in comparison with those who did not.	(6)
	66 pairs of GC tissues and ANCTs	high	–	–	Expression of AFAP1-AS1, clinical stage, and tumor differentiation could be regarded as the factors that were independently correlated with OS.	Higher expression level of AFAP1-AS1 was correlated with tumor mass, clinical stage, and tumor differentiation.	(44)
	89 GC patients, 55 benign gastric lesion groups, 73 age-matched healthy volunteers	high	–	–	–	Logistic regression analysis: high level of AFAP1-AS1 was significantly correlated with tumor size, TNM stage and LNM.	(45)
	80 pairs of GC tissues and ANCTs	high	Patients with high levels of AFAP1-AS1 had shorter OS than those with low levels of AFAP1-AS1.	–	–	–	(84)
Prostate cancer	30 PCa tissues and corresponding nearby healthy tissues	high	–	–	–	–	(31)
	38 pairs of prostate cancer tissues and ANCTs	high	Patients with high expression of AFAP1-AS1 had lower OS.	–	–	Chi-Square test: AFAP1-AS1 expression was associated with histological grade and distant metastasis.	(32)
Nasopharyngeal carcinoma (NPC)	10 pairs of freshly frozen samples and ANCTs	high	Patients with high expression of AFAP1-AS1 showed lower OS.	–	–	–	(46)
	100 pairs of paraffin-embedded samples and ANCTs	high	Patients with high expression of AFAP1-AS1 had a poor prognosis, with shorter OS.	–	–	Patients with high expression of AFAP1-AS1 were showed distant metastasis when they relapsed.	(85)
	96 paraffin-embedded NPC samples	high	–	–	–	High expression of AFAP1-AS1 was highly correlated with clinical TNM stages, neck LNM, and T stages of the patients.	(33)
	32 nasopharyngeal carcinoma samples and 13 non tumor	high	–	–	–	–	

(Continued)

TABLE 3 | Continued

Tumor type	Numbers of clinical samples	Expression (Tumor vs. Normal)	Kaplan-Meier analysis	Univariate cox regression	Multivariate cox regression	Clinicopathologic characteristics of patients	Reference
Endometrial carcinoma (EC) Cholangiocarcinoma (CCA)	nasopharyngeal epithelium tissues 101 NPC patients and 101 healthy controls	high	–	–	–	–	(86)
	101 NPC patients and 20 chronic nasopharyngitis patients						
	101 NPC patients and 20 asymptomatic EBV carriers						
	23 NPC samples and 7 non-tumor nasopharyngeal epithelium samples	high	–	–	–	–	(47)
	112 paraffin-embedded NPC and 10 NPE tissue samples	high	High expression of AFAP1-AS1 was correlated with poor OS and poor RFS.	–	–	Expression of AFAP1-AS1 was associated with distant tumor metastasis.	
	73 pairs of EC tissues and ANCTs	high	–	–	–	–	(48)
Colorectal cancer (CRC)	20 pairs of CCA tissues and ANCTs	high	–	–	–	–	(49)
	56 pairs of tumor tissues and ANCTs	high	Patients with high expression of AFAP1-AS1 showed shorter OS.	–	–	High expression of AFAP1-AS1 had positive association with tumor size, vascular invasion, and advance TNM stage.	(50)
Colorectal cancer (CRC)	68 CRC patients and 60 healthy volunteers	high	–	–	–	Chi-squared test: plasma levels of AFAP1-AS1 were correlated with clinical stage.	(51)
	52 pairs of CRC tissues and ANCTs	high	Patients with up-regulation of AFAP1-AS1 had a significantly poorer prognosis.	AFAP1-AS1 expression, tumor size, TNM stage, and distant metastasis were significantly correlated with OS and DFS.	AFAP1-AS1 expression, TNM stage, and distant metastasis were strongly correlated with OS and DFS.	High levels of AFAP1-AS1 were associated with tumor size, TNM stage and remote metastasis.	(52)
	15 pairs of CRC tissues and ANCTs TCGA analysis: 50 pairs of clinical colorectal cancer tumors and the peritumoral tissues	high	–	–	–	–	(53)

(Continued)

TABLE 3 | Continued

Tumor type	Numbers of clinical samples	Expression (Tumor vs. Normal)	Kaplan-Meier analysis	Univariate cox regression	Multivariate cox regression	Clinicopathologic characteristics of patients	Reference
Colon Cancer	80 CRC tissues and 10 normal colon tissues	high	Patients who had high AFAP1-AS1 mRNA levels indicated worse prognosis compared with those with low.	–	–	–	(54)
	GEO analysis: _ TCGA-COAD analysis	high high	– Patients with high expression of AFAP1-AS1 indicated shorter OS and DFS.	– –	– –	– –	(55)
Hepatocellular carcinoma	17 pairs of tumor tissues and ANCTs	high	–	–	–	–	(56)
	17 pairs of HCC tissues and ANCTs	high	Patients with high levels of AFAP1-AS1 showed a shorter median survival time.	–	AFAP1-AS1 expression could be regarded as an independent prognostic factor for OS in HCC patients.	High levels of AFAP1-AS1 were correlated with pathological staging and lymph-vascular space invasion.	(57)
Cervical cancer (CC)	156 pairs of HCC tissues and ANCTs	high	Patients with low levels of AFAP1-AS1 showed better OS and DFS.	–	–	High levels of AFAP1-AS1 were correlated with tumor size, vascular invasion, and TNM stage.	(58)
	TCGA analysis: _	high	Patients with high expression of AFAP1-AS1 expression had a short OS.	–	–	High levels of AFAP1-AS1 were correlated with TNM stage.	(59)
Laryngeal carcinoma	24 pairs of tumor tissues and ANCTs	high	–	–	–	–	(34)
Thyroid cancer	36 pairs of tumor tissues and ANCTs	high	Patients with high expression of AFAP1-AS1 expression had a short OS	–	AFAP1-AS1 expression might be a positive, independent prognostic factor.	–	(60)
Glioma	52 glioma cases and 5 non-tumor control cases	high	High expression of AFAP1-AS1 predicted worse prognosis in glioma patients.	–	–	Expression of AFAP1-AS1 was closely correlated with glioma grading and KPS scores.	(61)
Ovarian cancer (OC)	65 pairs of OC tissues and ANCTs	high	–	–	–	Upregulation of AFAP1-AS1 was correlated with high FIGO stage and resistance response.	(62)
	39 pairs of OC tissues and ANCTs	high	Patients with low expression of AFAP1-AS1 showed greater survival probability.	–	–	Chi-square analysis: Upregulation of AFAP1-AS1 was correlated with FIGO stage.	(35)
Pancreatic cancer (PC)	75 pairs of PC tissues and ANCTs	high	–	–	–	Upregulation of AFAP1-AS1 was positively associated with TNM stage, LNM, and tumor size.	(36)
	GEO analysis: _ 63 pairs of PC tissues and ANCTs	high high	– Patients with high AFAP1-AS1 expression showed a shorter 5-year OS rate.	– –	– –	– Upregulation of AFAP1-AS1 was positively associated with advanced TNM stage, tumor size and LNM.	(64)
Pancreatic ductal adenocarcinoma (PDAC)	8 cases of PDAC tissues and 4 cases of CP tissues	high	–	–	–	–	(66)

(Continued)

TABLE 3 | Continued

Tumor type	Numbers of clinical samples	Expression (Tumor vs. Normal)	Kaplan-Meier analysis	Univariate cox regression	Multivariate cox regression	Clinicopathologic characteristics of patients	Reference
	90 pairs of PDAC tissues and ANCTs	high	Patients with high expression of AFAP1-AS1 showed worse OS and PFS.	–	–	Upregulation of AFAP1-AS1 was positively associated with LNM and perineural invasion.	
Renal cell carcinoma (RCC)	60 ccRCC tissues and 20 ANCTs	high	Patients with high expression of AFAP1-AS1 showed worse OS.	–	–	Upregulation of AFAP1-AS1 was positively associated with LNM and TNM stage.	(67)
Gallbladder cancer (GBC)	40 pairs of GBC tissues and ANCTs	high	Upregulation of AFAP1-AS1 indicated a poor prognosis in gallbladder cancer.	–	–	Upregulation of AFAP1-AS1 was positively associated with tumor size.	(68)
Pituitary adenoma	60 pairs of pituitary adenomas tissues and ANCTs	high	–	–	–	–	(70)
Retinoblastoma	58 freshly frozen retinoblastoma tissue samples and 10 non-cancerous retina samples	high	Patients with high expression of AFAP1-AS1 had shorter OS.	High-expression of AFAP1-AS1 was found to be an unfavorable prognostic factor.	High-expression of AFAP1-AS1 was found to be an independent unfavorable prognostic factor.	Upregulation of AFAP1-AS1 was positively associated with tumor bulk as well as choroidal or optic nerve invasion.	(72)
Tongue squamous cell carcinoma	103 pairs of tumor tissues and ANCTs	high	High AFAP1-AS1 expression was related to poor survival.	–	–	Expression level of AFAP1-AS1 was associated with tumor differentiation, T classification, clinical stage, invasion depth, and relapse.	(73)
Oral squamous cell carcinoma (OSCC)	48 pairs of OSCC tissues and ANCTs	high	Patients with high AFAP1-AS1 expression had a poor OS.	–	–	Expression level of AFAP1-AS1 was associated with an advanced clinical stage and LNM.	(74)

(ANCTs, adjacent non-cancerous tissues; OS, Overall survival; DFS, Disease-free survival; PFS, progression free survival; TNM, tumor-node-metastasis; dCRT, definitive chemoradiotherapy; DM, distant metastasis; LNM, lymph node metastasis; TCGA, The Cancer Genome Atlas; GEO, Gene Expression Omnibus; KPS, Karnofsky Performance Status; CP, chronic pancreatitis tissues).

TABLE 4 | Diagnostic value of AFAP1-AS1 in different cancers.

Tumor Type	Numbers of clinical samples	Distinguish between	Area Under Curve	Sensitivity	Specificity	Accuracy	Reference
Non-small Cell Lung Cancer (NSCLC)	126 NSCLC patients and 60 healthy controls	patients with NSCLC vs. healthy controls	0.759	0.693	0.883	0.759	(75)
Breast cancer	160 pairs of breast cancer tissues and ANCTs	Cancer tissues vs. ANCTs	0.736	74%	69%	—	(40)
Esophageal cancer (EC)	162 pairs of ESCC tissues and ANCTs	Cancer tissues vs. ANCTs	0.802	73.3%	79.4%	—	(83)
Gastric cancer (GC)	30 tumor tissues and ANCTs	Cancer tissues vs. ANCTs	0.67	70%	63.3%	—	(6)
	89 GC patients and 73 healthy controls	patients with GC vs. healthy controls	0.820	76.4%	56.2%	67.3%	(45)
	80 pairs of GC tissues and ANCTs	Cancer tissues vs. ANCTs	0.8802	81.25%	83.75%	—	(84)
	101 NPC patients and 101 healthy controls	patients with NPC vs. healthy controls	0.665	0.640	0.838	—	(86)
	101 NPC patients and 20 chronic nasopharyngitis patients	patients with NPC vs. chronic nasopharyngitis patients	0.625	0.590	0.822	—	
Nasopharyngeal carcinoma (NPC)	101 NPC patients and 20 asymptomatic EBV carriers	patients with NPC vs. asymptomatic EBV carriers	0.620	0.592	0.819	—	

ANCTs, adjacent non-cancerous tissues; ESCC, esophageal squamous cell carcinoma.

osteosarcoma. Moreover, similar interaction has been verified between this lncRNA and miR-145 in breast cancer and oral squamous cell carcinoma.

In fact, AFAP1-AS1 has multiple binding sites for miRNAs, thus regulating expression of a wide array of miRNAs. It is not clear whether binding of this lncRNA with a certain miRNA affects its interactions with other miRNAs. The crosstalk between AFAP1-AS1 and miRNAs can regulate activity of signaling pathways, angiogenic processes as well as EMT.

AFAP1-AS1 can indirectly influence activity of some cancer-related pathways such as EGFR/AKT, Wnt/ β -catenin, PTEN/p-AKT, RhoA/Rac2 and PI3K/AKT. The effects of this lncRNA on Wnt/ β -catenin, EGF/AKT and PI3K/AKT are mediated through sponging miR-4695-5p, miR-139-5p and miR-103a-3p, respectively. However, its effects on other pathways might be exerted in an independent manner from miRNAs sponging.

Lung cancer, nasopharyngeal carcinoma, colorectal cancer and cholangiocarcinoma are among cancers in which the interaction between AFAP1-AS1 and AFAP1 has been verified. However, the results of these studies are conflicting. For instance, AFAP1-AS1 silencing has been shown to increase expression of AFAP1 in a single study in lung cancer cells (12), while another study in this type of cancer has shown its effect on enhancement of expression of AFAP1 (11). Moreover, in a single study in MCF-7 breast cancer cells, AFAP1-AS1 silencing has not affected AFAP1 levels or actin filament integrity (40). Therefore, future studies are needed to elaborate the mechanistical impacts of AFAP1/AFAP1-AS1 interactions.

AFAP1-AS1 can affect response of cancer cells to a variety of anti-cancer modalities ranging from conventional

chemotherapeutics to targeted therapeutics such as trastuzumab. Therefore, measurement of expression levels of this lncRNA can guide clinical oncologists to find the most appropriate therapeutic option for each patient. AFAP1-AS1 can also affect EMT and stemness of cancer cells, thus promoting their metastatic ability and increasing the propensity to tumor recurrence.

From a prognostic point of view, AFAP1-AS1 levels have been associated with tumor depth, tumor differentiation, TNM stage and other determinants of patients' survival, thus could be used as markers for prediction of clinical outcomes of patients with a variety of malignant conditions. Diagnostic application of AFAP1-AS1 has been appraised in several types of cancers, with the best results being obtained from studies in gastric and esophageal cancers.

Cumulatively, AFAP1-AS1 is a prototype of cancer-related lncRNAs that regulates carcinogenesis not only through modification of expression of its sense transcript, but also through a variety of other methods such as miRNA sequestering and epigenetically affecting expression of tumor suppressor genes.

AUTHOR CONTRIBUTIONS

SG-F and BH wrote the draft and revised it. MT designed and supervised the study. TK and MM collected the data and designed the figures and tables. All authors contributed to the article and approved the submitted version.

REFERENCES

- Ji D, Zhong X, Jiang X, Leng K, Xu Y, Li Z, et al. The Role of Long Non-Coding RNA AFAP1-AS1 in Human Malignant Tumors. *Pathol Res Pract* (2018) 214(10):1524–31. doi: 10.1016/j.prp.2018.08.014
- Baisden JM, Qian Y, Zot HM, Flynn DC. The Actin Filament-Associated Protein AFAP-110 Is an Adaptor Protein That Modulates Changes in Actin Filament Integrity. *Oncogene* (2001) 20(44):6435–47. doi: 10.1038/sj.onc.1204784
- Liu F-T, Xue Q-Z, Zhu P-Q, Luo H-L, Zhang Y, Hao T. Long Noncoding RNA AFAP1-AS1, a Potential Novel Biomarker to Predict the Clinical

- Outcome of Cancer Patients: A Meta-Analysis. *OncoTargets Ther* (2016) 9:4247. doi: 10.2147/OTT.S107188
4. Dorflautner A, Stehlik C, Zhang J, Gallick GE, Flynn DC. AFAP-110 Is Required for Actin Stress Fiber Formation and Cell Adhesion in MDA-MB-231 Breast Cancer Cells. *J Cell Physiol* (2007) 213(3):740–9. doi: 10.1002/jcp.21143
 5. Zhang J, Park SI, Artime MC, Summy JM, Shah AN, Bomser JA, et al. AFAP-110 Is Overexpressed in Prostate Cancer and Contributes to Tumorigenic Growth by Regulating Focal Contacts. *J Clin Invest* (2007) 117(10):2962–73. doi: 10.1172/JCI30710
 6. Esfandi F, Taheri M, Namvar A, Kholghi Oskoei V, Ghafari-Fard S. AFAP1 and its Naturally Occurring Antisense RNA Are Downregulated in Gastric Cancer Samples. *Biomed Rep* (2019) 10(5):296–302. doi: 10.3892/br.2019.1207
 7. Wong L-P, Ong RT-H, Poh W-T, Liu X, Chen P, Li R, et al. Deep Whole-Genome Sequencing of 100 Southeast Asian Malays. *Am J Hum Genet* (2013) 92(1):52–66. doi: 10.1016/j.ajhg.2012.12.005
 8. Huang N, Guo W, Ren K, Li W, Jiang Y, Sun J, et al. LncRNA AFAP1-AS1 Suppresses miR-139-5p and Promotes Cell Proliferation and Chemotherapy Resistance of Non-Small Cell Lung Cancer by Competitively Upregulating RRM2. *Front Oncol* (2019) 9:1103. doi: 10.3389/fonc.2019.01103
 9. Tang X-D, Zhang D-D, Jia L, Ji W, Zhao Y-S. LncRNA AFAP1-AS1 Promotes Migration and Invasion of Non-Small Cell Lung Cancer via Up-Regulating IRE7 and the RIG-I-Like Receptor Signaling Pathway. *Cell Physiol Biochem* (2018) 50(1):179–95. doi: 10.1159/000493967
 10. Yin D, Lu X, Su J, He X, De W, Yang J, et al. Long Noncoding RNA AFAP1-AS1 Predicts a Poor Prognosis and Regulates Non-Small Cell Lung Cancer Cell Proliferation by Epigenetically Repressing P21 Expression. *Mol Cancer* (2018) 17(1):1–12. doi: 10.1186/s12943-018-0836-7
 11. He J, Wu K, Guo C, Zhou J-K, Pu W, Deng Y, et al. Long Non-Coding RNA AFAP1-AS1 Plays an Oncogenic Role in Promoting Cell Migration in Non-Small Cell Lung Cancer. *Cell Mol Life Sci* (2018) 75(24):4667–81. doi: 10.1007/s00018-018-2923-8
 12. Zeng Z, Bo H, Gong Z, Lian Y, Li X, Li X, et al. AFAP1-AS1, a Long Noncoding RNA Upregulated in Lung Cancer and Promotes Invasion and Metastasis. *Tumor Biol* (2016) 37(1):729–37. doi: 10.1007/s13277-015-3860-x
 13. Clayton NS, Ridley AJ. Targeting Rho GTPase Signaling Networks in Cancer. *Front Cell Dev Biol* (2020) 8:222. doi: 10.3389/fcell.2020.00222
 14. Barak V, Goike H, Panaretakis KW, Einarsson R. Clinical Utility of Cytokeratins as Tumor Markers. *Clin Biochem* (2004) 37(7):529–40. doi: 10.1016/j.clinbiochem.2004.05.009
 15. Sun J, Min H, Yu L, Yu G, Shi Y, Sun J. The Knockdown of LncRNA AFAP1-AS1 Suppressed Cell Proliferation, Migration, and Invasion, and Promoted Apoptosis by Regulating miR-545-3p/Hepatoma-Derived Growth Factor Axis in Lung Cancer. *Anti-Cancer Drugs* (2020) 32(1):11–21. doi: 10.1097/CAD.0000000000001003
 16. Zhong Y, Yang L, Xiong F, He Y, Tang Y, Shi L, et al. Long Non-Coding RNA AFAP1-AS1 Accelerates Lung Cancer Cells Migration and Invasion by Interacting With SNIP1 to Upregulate C-Myc. *Signal Transduction Targeted Ther* (2021) 6(1):1–13. doi: 10.1038/s41392-021-00562-y
 17. Cai B, Wang X, Qa B, Li P, Xue Q, Zhang J, et al. LncRNA AFAP1-AS1 Knockdown Represses Cell Proliferation, Migration, and Induced Apoptosis in Breast Cancer by Downregulating SEPT2 via Sponging miR-497-5p. *Cancer Biother Radiopharmaceut* (2020). doi: 10.1089/cbr.2020.3688
 18. Zhang X, Zhou Y, Mao F, Lin Y, Shen S, Sun Q. LncRNA AFAP1-AS1 Promotes Triple Negative Breast Cancer Cell Proliferation and Invasion via Targeting miR-145 to Regulate MTH1 Expression. *Sci Rep* (2020) 10(1):1–11. doi: 10.1038/s41598-020-64713-x
 19. Zhang X, Li F, Zhou Y, Mao F, Lin Y, Shen S, et al. Long Noncoding RNA AFAP1-AS1 Promotes Tumor Progression and Invasion by Regulating the miR-2110/Sp1 Axis in Triple-Negative Breast Cancer. *Cell Death Dis* (2021) 12(7):1–11. doi: 10.1038/s41419-021-03917-z
 20. Zhang K, Liu P, Tang H, Xie X, Kong Y, Song C, et al. AFAP1-AS1 Promotes Epithelial-Mesenchymal Transition and Tumorigenesis Through Wnt/ β -Catenin Signaling Pathway in Triple-Negative Breast Cancer. *Front Pharmacol* (2018) 9:1248. doi: 10.3389/fphar.2018.01248
 21. Han M, Gu Y, Lu P, Li J, Cao H, Li X, et al. Exosome-Mediated LncRNA AFAP1-AS1 Promotes Trastuzumab Resistance Through Binding With AUF1 and Activating ERBB2 Translation. *Mol Cancer* (2020) 19(1):1–18. doi: 10.1186/s12943-020-1145-5
 22. Shi D, Wu F, Mu S, Hu B, Zhong B, Gao F, et al. LncRNA AFAP1-AS1 Promotes Tumorigenesis and Epithelial-Mesenchymal Transition of Osteosarcoma Through RhoC/ROCK1/p38MAPK/Twist1 Signaling Pathway. *J Exp Clin Cancer Res* (2019) 38(1):1–12. doi: 10.1186/s13046-019-1363-0
 23. Fei D, Zhang X, Lu Y, Tan L, Xu M, Zhang Y. Long Noncoding RNA AFAP1-AS1 Promotes Osteosarcoma Progression by Regulating miR-497/IGF1R Axis. *Am J Trans Res* (2020) 12(5):2155. doi: 10.1038/s41419-021-03917-z
 24. Li R, Liu S, Li Y, Tang Q, Xie Y, Zhai R. Long Noncoding RNA AFAP1-AS1 Enhances Cell Proliferation and Invasion in Osteosarcoma Through Regulating Mir-4695-5p/TCF4- β -Catenin Signaling. *Mol Med Rep* (2018) 18(2):1616–22. doi: 10.3892/mmr.2018.9131
 25. Feng Y, Zhang Q, Wang J, Liu P. Increased LncRNA AFAP1-AS1 Expression Predicts Poor Prognosis and Promotes Malignant Phenotypes in Gastric Cancer. *Eur Rev Med Pharmacol Sci* (2017) 21(17):3842–9.
 26. Yuan X, Li J, Cao Y, Jie Z, Zeng Y. Long Non-Coding RNA AFAP1-AS1 Promotes Proliferation and Migration of Gastric Cancer by Downregulating KLF2. *Eur Rev Med Pharmacol Sci* (2020) 24(2):673–80.
 27. Guo J-Q, Li S-J, Guo G-X. Long Noncoding RNA AFAP1-AS1 Promotes Cell Proliferation and Apoptosis of Gastric Cancer Cells via PTEN/p-AKT Pathway. *Digestive Dis Sci* (2017) 62(8):2004–10. doi: 10.1007/s10620-017-4584-0
 28. Ma H-W, Xi D-Y, Ma J-Z, Guo M, Ma L, Ma D-H, et al. Long Noncoding RNA AFAP1-AS1 Promotes Cell Proliferation and Metastasis via the miR-155-5p/FGF7 Axis and Predicts Poor Prognosis in Gastric Cancer. *Dis Markers* (2020) 2020. doi: 10.1155/2020/8140989
 29. Mi X, Xu R, Hong S, Xu T, Zhang W, Liu M. M2 Macrophage-Derived Exosomal LncRNA AFAP1-AS1 and microRNA-26a Affect Cell Migration and Metastasis in Esophageal Cancer. *Mol Ther-Nucleic Acids* (2020) 22:779–90. doi: 10.1016/j.omtn.2020.09.035
 30. Shen W, Yu L, Cong A, Yang S, Wang P, Han G, et al. Silencing LncRNA AFAP1-AS1 Inhibits the Progression of Esophageal Squamous Cell Carcinoma Cells via Regulating the miR-498/VEGFA Axis. *Cancer Manage Res* (2020) 12:6397. doi: 10.2147/CMAR.S254302
 31. Leng W, Liu Q, Zhang S, Sun D, Guo Y. LncRNA AFAP1-AS1 Modulates the Sensitivity of Paclitaxel-Resistant Prostate Cancer Cells to Paclitaxel via miR-195-5p/FKBP1A Axis. *Cancer Biol Ther* (2020) 21(11):1072–80. doi: 10.1080/15384047.2020.1829266
 32. Wang K, Sun H, Sun T, Qu H, Xie Q, Lv H, et al. Long Non-Coding RNA AFAP1-AS1 Promotes Proliferation and Invasion in Prostate Cancer via Targeting miR-512-3p. *Gene* (2020) 726:144169. doi: 10.1016/j.jgene.2019.144169
 33. Lian Y, Xiong F, Yang L, Bo H, Gong Z, Wang Y, et al. Long Noncoding RNA AFAP1-AS1 Acts as a Competing Endogenous RNA of miR-423-5p to Facilitate Nasopharyngeal Carcinoma Metastasis Through Regulating the Rho/Rac Pathway. *J Exp Clin Cancer Res* (2018) 37(1):1–17. doi: 10.1186/s13046-018-0918-9
 34. Yuan Z, Xiu C, Song K, Pei R, Miao S, Mao X, et al. Long Non-Coding RNA AFAP1-AS1/miR-320a/RBPJ Axis Regulates Laryngeal Carcinoma Cell Stemness and Chemoresistance. *J Cell Mol Med* (2018) 22(9):4253–62. doi: 10.1111/jcmm.13707
 35. Liu B, Yan L, Chi Y, Sun Y, Yang X. Long Non-Coding RNA AFAP1-AS1 Facilitates Ovarian Cancer Progression by Regulating the miR-107/PDK4 Axis. *J Ovarian Res* (2021) 14(1):1–11. doi: 10.1186/s13048-021-00808-x
 36. Wu X-B, Feng X, Chang Q-M, Zhang C-W, Wang Z-F, Liu J, et al. Cross-Talk Among AFAP1-AS1, ACVR1 and microRNA-384 Regulates the Stemness of Pancreatic Cancer Cells and Tumorigenicity in Nude Mice. *J Exp Clin Cancer Res* (2019) 38(1):1–15. doi: 10.1186/s13046-019-1051-0
 37. Yu S, Yang D, Ye Y, Liu P, Chen Z, Lei T, et al. Long Noncoding RNA Actin Filament-Associated Protein 1 Antisense RNA 1 Promotes Malignant Phenotype Through Binding With Lysine-Specific Demethylase 1 and Repressing HMG Box-Containing Protein 1 in Non-Small-Cell Lung Cancer. *Cancer Sci* (2019) 110(7):2211–25. doi: 10.1111/cas.14039
 38. Peng B, Liu A, Yu X, Xu E, Dai J, Li M, et al. Silencing of LncRNA AFAP1-AS1 Suppressed Lung Cancer Development by Regulatory Mechanism in Cis and Trans. *Oncotarget* (2017) 8(55):93608. doi: 10.18632/oncotarget.20549

39. Zhuang Y, Jiang H, Li H, Dai J, Liu Y, Li Y, et al. Down-Regulation of Long Non-Coding RNA AFAP1-AS1 Inhibits Tumor Cell Growth and Invasion in Lung Adenocarcinoma. *Am J Trans Res* (2017) 9(6):2997.
40. Liu Y, Li Q, Hosen MR, Zietzer A, Flender A, Levermann P, et al. Atherosclerotic Conditions Promote the Packaging of Functional microRNA-92a-3p Into Endothelial Microvesicles. *Circ Res* (2019) 124(4):575–87. doi: 10.1161/CIRCRESAHA.118.314010
41. Luo HL, Huang MD, Guo JN, Fan RH, Xia XT, He JD, et al. AFAP1-AS1 Is Upregulated and Promotes Esophageal Squamous Cell Carcinoma Cell Proliferation and Inhibits Cell Apoptosis. *Cancer Med* (2016) 5(10):2879–85. doi: 10.1002/cam4.848
42. Wu W, Bhagat TD, Yang X, Song JH, Cheng Y, Agarwal R, et al. Hypomethylation of Noncoding DNA Regions and Overexpression of the Long Noncoding RNA, AFAP1-AS1, in Barrett's Esophagus and Esophageal Adenocarcinoma. *Gastroenterology* (2013) 144(5):956–66. e4. doi: 10.1053/j.gastro.2013.01.019
43. Li Z, Ding Z, Rong D, Tang W, Cao H. Overexpression of lncRNA AFAP1-AS1 Promotes Cell Proliferation and Invasion in Gastric Cancer. *Oncol Lett* (2019) 18(3):3211–7. doi: 10.3892/ol.2019.10640
44. Lai Z, Lin P, Weng X, Su J, Chen Y, He Y, et al. MicroRNA-574-5p Promotes Cell Growth of Vascular Smooth Muscle Cells in the Progression of Coronary Artery Disease. *Biomed Pharmacother* (2018) 97:162–7. doi: 10.1016/j.biopha.2017.10.062
45. Liu W, Li Y, Zhang Y, Shen X, Su Z, Chen L, et al. Circulating long Non-Coding RNA FEZF1-AS1 and AFAP1-AS1 Serve as Potential Diagnostic Biomarkers for Gastric Cancer. *Pathol-Res Pract* (2020) 216(1):152757. doi: 10.1016/j.prp.2019.152757
46. Fang M, Zhang M, Wang Y, Wei F, Wu J, Mou X, et al. Long Noncoding RNA AFAP1-AS1 Is a Critical Regulator of Nasopharyngeal Carcinoma Tumorigenicity. *Front Oncol* (2020) 10:2510. doi: 10.3389/fonc.2020.601055
47. Bo H, Gong Z, Zhang W, Li X, Zeng Y, Liao Q, et al. Upregulated Long Non-Coding RNA AFAP1-AS1 Expression Is Associated With Progression and Poor Prognosis of Nasopharyngeal Carcinoma. *Oncotarget* (2015) 6(24):20404. doi: 10.18632/oncotarget.4057
48. Zhong Y, Wang Y, Dang H, Wu X. LncRNA AFAP1-AS1 Contributes to the Progression of Endometrial Carcinoma by Regulating miR-545-3p/VEGFA Pathway. *Mol Cell Probes* (2020) 53:101606. doi: 10.1016/j.mcp.2020.101606
49. Shi X, Zhang H, Wang M, Xu X, Zhao Y, He R, et al. LncRNA AFAP1-AS1 Promotes Growth and Metastasis of Cholangiocarcinoma Cells. *Oncotarget* (2017) 8(35):58394. doi: 10.18632/oncotarget.16880
50. Lu X, Zhou C, Li R, Deng Y, Zhao L, Zhai W. Long Noncoding RNA AFAP1-AS1 Promoted Tumor Growth and Invasion in Cholangiocarcinoma. *Cell Physiol Biochem* (2017) 42(1):222–30. doi: 10.1159/000477319
51. Zhao Y, Chu Y, Sun J, Song R, Li Y, Xu F. LncRNA GAS8-AS Inhibits Colorectal Cancer (CRC) Cell Proliferation by Downregulating lncRNA AFAP1-AS1. *Gene* (2019) 710:140–4. doi: 10.1016/j.gene.2019.05.040
52. Wang F, Ni H, Sun F, Li M, Chen L. Overexpression of lncRNA AFAP1-AS1 Correlates With Poor Prognosis and Promotes Tumorigenesis in Colorectal Cancer. *Biomed Pharmacother* (2016) 81:152–9. doi: 10.1016/j.biopha.2016.04.009
53. Han X, Wang L, Ning Y, Li S, Wang Z. Long Non-Coding RNA AFAP1-AS1 Facilitates Tumor Growth and Promotes Metastasis in Colorectal Cancer. *Biol Res* (2016) 49(1):1–7. doi: 10.1186/s40659-016-0094-3
54. Tang J, Zhong G, Wu J, Chen H, Jia Y. Long Noncoding RNA AFAP1-AS1 Facilitates Tumor Growth Through Enhancer of Zeste Homolog 2 in Colorectal Cancer. *Am J Cancer Res* (2018) 8(5):892.
55. Bo H, Fan L, Li J, Liu Z, Zhang S, Shi L, et al. High Expression of lncRNA AFAP1-AS1 Promotes the Progression of Colon Cancer and Predicts Poor Prognosis. *J Cancer* (2018) 9(24):4677. doi: 10.7150/jca.26461
56. Abdul S, Majid A, Wang J, Liu Q, Sun M-Z, Liu S. Bidirectional Interaction of lncRNA AFAP1-AS1 and CRKL Accelerates the Proliferative and Metastatic Abilities of Hepatocarcinoma Cells. *J Advanced Res* (2020) 24:121–30. doi: 10.1016/j.jare.2020.03.010
57. Zhang J-Y, Weng M-Z, Song F-B, Xu Y-G, Liu Q, Wu J-Y, et al. Long Noncoding RNA AFAP1-AS1 Indicates a Poor Prognosis of Hepatocellular Carcinoma and Promotes Cell Proliferation and Invasion via Upregulation of the RhoA/Rac2 Signaling. *Int J Oncol* (2016) 48(4):1590–8. doi: 10.3892/ijo.2016.3385
58. Lu X, Zhou C, Li R, Liang Z, Zhai W, Zhao L, et al. Critical Role for the Long Non-Coding RNA AFAP1-AS1 in the Proliferation and Metastasis of Hepatocellular Carcinoma. *Tumor Biol* (2016) 37(7):9699–707. doi: 10.1007/s13277-016-4858-8
59. Bo H, Fan L, Gong Z, Liu Z, Shi L, Guo C, et al. Upregulation and Hypomethylation of lncRNA AFAP1-AS1 Predicts a Poor Prognosis and Promotes the Migration and Invasion of Cervical Cancer. *Oncol Rep* (2019) 41(4):2431–9. doi: 10.3892/or.2019.7027
60. Dai W, Tian Y, Jiang B, Chen W. Down-Regulation of Long Non-Coding RNA AFAP1-AS1 Inhibits Tumor Growth, Promotes Apoptosis and Decreases Metastasis in Thyroid Cancer. *Biomed Pharmacother* (2018) 99:191–7. doi: 10.1016/j.biopha.2017.12.105
61. Wang Y, Lan Q. Long Non-Coding RNA AFAP1-AS1 Accelerates Invasion and Predicts Poor Prognosis of Glioma. *Eur Rev Med Pharmacol Sci* (2018) 22(16):5223–9.
62. Yang S, Lin R, Si L, Cui M, Zhang X, Fan L. Expression and Functional Role of Long Non-Coding RNA AFAP1-AS1 in Ovarian Cancer. *Eur Rev Med Pharmacol Sci* (2016) 20(24):5107–12.
63. Lou S, Xu J, Wang B, Li S, Ren J, Hu Z, et al. Downregulation of lncRNA AFAP1-AS1 by Oridonin Inhibits the Epithelial-to-Mesenchymal Transition and Proliferation of Pancreatic Cancer Cells. *Acta Biochim Biophys Sin* (2019) 51(8):814–25. doi: 10.1093/abbs/gmz071
64. Chen B, Li Q, Zhou Y, Wang X, Zhang Q, Wang Y, et al. The Long Coding RNA AFAP1-AS1 Promotes Tumor Cell Growth and Invasion in Pancreatic Cancer Through Upregulating the IGF1R Oncogene via Sequestration of miR-133a. *Cell Cycle* (2018) 17(16):1949–66. doi: 10.1080/15384101.2018.1496741
65. Zhou J, Liu M, Chen Y, Xu S, Guo Y, Zhao L. Cucurbitacin B Suppresses Proliferation of Pancreatic Cancer Cells by ceRNA: Effect of miR-146b-5p and lncRNA-AFAP1-As1. *J Cell Physiol* (2019) 234(4):4655–67. doi: 10.1002/jcp.27264
66. Ye Y, Chen J, Zhou Y, Fu Z, Zhou Q, Wang Y, et al. High Expression of AFAP1-AS1 Is Associated With Poor Survival and Short-Term Recurrence in Pancreatic Ductal Adenocarcinoma. *J Trans Med* (2015) 13(1):1–11. doi: 10.1186/s12967-015-0490-4
67. Mu Z, Dong D, Wei N, Sun M, Wang W, Shao Y, et al. Silencing of lncRNA AFAP1-AS1 Inhibits Cell Growth and Metastasis in Clear Cell Renal Cell Carcinoma. *Oncol Res* (2019) 27(6):653. doi: 10.3727/096504018X15420748671075
68. Ma F, Wang S-H, Cai Q, Zhang M-D, Yang Y, Ding J. Overexpression of lncRNA AFAP1-AS1 Predicts Poor Prognosis and Promotes Cells Proliferation and Invasion in Gallbladder Cancer. *Biomed Pharmacother* (2016) 84:1249–55. doi: 10.1016/j.biopha.2016.10.064
69. Tang H, Zhu D, Zhang G, Luo X, Xie W. AFAP1-AS1 Promotes Proliferation of Pituitary Adenoma Cells Through miR-103a-3p to Activate PI3K/AKT Signaling Pathway. *World Neurosurg* (2019) 130:e888–e98. doi: 10.1016/j.wneu.2019.07.032
70. Tang H, Hou B, Ye Z, Ling C, Guo Y. Knockdown of Long Non-Coding RNA AFAP1-AS1 Inhibits Growth and Promotes Apoptosis in Pituitary Adenomas. *Int J Clin Exp Pathol* (2018) 11(3):1238.
71. Liu F, Hu L, Pei Y, Zheng K, Wang W, Li S, et al. Long Non-Coding RNA AFAP1-AS1 Accelerates the Progression of Melanoma by Targeting miR-653-5p/RAI14 Axis. *BMC Cancer* (2020) 20(1):1–11. doi: 10.1186/s12885-020-6665-2
72. Hao F, Mou Y, Zhang L, Wang S, Yang Y. LncRNA AFAP1-AS1 Is a Prognostic Biomarker and Serves as Oncogenic Role in Retinoblastoma. *Biosci Rep* (2018) 38(3):BSR20180384. doi: 10.1042/BSR20180384
73. Wang Z-Y, Hu M, Dai M-H, Xiong J, Zhang S, Wu H-J, et al. Upregulation of the Long Non-Coding RNA AFAP1-AS1 Affects the Proliferation, Invasion and Survival of Tongue Squamous Cell Carcinoma via the Wnt/beta-Catenin Signaling Pathway (Retraction of Vol 17, Art No 3, 2018). 4 CRINAN ST, LONDON N1 9XW, ENGLAND: BMC CAMPUS (2019).
74. Li M, Yu D, Li Z, Zhao C, Su C, Ning J. Long Non-Coding RNA AFAP1-AS1 Facilitates the Growth and Invasiveness of Oral Squamous Cell Carcinoma by Regulating the Mir-145/HOXA1 Axis. *Oncol Rep* (2021) 45(3):1094–104. doi: 10.3892/or.2020.7908
75. Li W, Li N, Kang X, Shi K. Circulating Long Non-Coding RNA AFAP1-AS1 Is a Potential Diagnostic Biomarker for Non-Small Cell Lung Cancer. *Clin Chim Acta* (2017) 475:152–6. doi: 10.1016/j.cca.2017.10.027

76. Leng X, Ding X, Wang S, Fang T, Shen W, Xia W, et al. Long Noncoding RNA AFAP1-AS1 Is Upregulated in NSCLC and Associated With Lymph Node Metastasis and Poor Prognosis. *Oncol Lett* (2018) 16(1):727–32. doi: 10.3892/ol.2018.8784
77. Deng J, Liang Y, Liu C, He S, Wang S. The Up-Regulation of Long Non-Coding RNA AFAP1-AS1 Is Associated With the Poor Prognosis of NSCLC Patients. *Biomed Pharmacother* (2015) 75:8–11. doi: 10.1016/j.biopha.2015.07.003
78. Wang M, Ma X, Zhu C, Guo L, Li Q, Liu M, et al. The Prognostic Value of Long non Coding RNAs in non Small Cell Lung Cancer: A Meta-Analysis. *Oncotarget* (2016) 7(49):81292. doi: 10.18632/oncotarget.13223
79. Sui J, Li Y-H, Zhang Y-Q, Li C-Y, Shen X, Yao W-Z, et al. Integrated Analysis of Long Non-Coding RNA-associated ceRNA Network Reveals Potential lncRNA Biomarkers in Human Lung Adenocarcinoma. *Int J Oncol* (2016) 49(5):2023–36. doi: 10.3892/ijo.2016.3716
80. Wei Y, Zhang X. Transcriptome Analysis of Distinct Long Non-Coding RNA Transcriptional Fingerprints in Lung Adenocarcinoma and Squamous Cell Carcinoma. *Tumor Biol* (2016) 37(12):16275–85. doi: 10.1007/s13277-016-5422-2
81. Rodrigues de Bastos D, Nagai MA. In Silico Analyses Identify lncRNAs: WDFY3-AS2, BDNF-AS and AFAP1-AS1 as Potential Prognostic Factors for Patients With Triple-Negative Breast Tumors. *PloS One* (2020) 15(5): e0232284. doi: 10.1371/journal.pone.0232284
82. Dianatpour A, Faramarzi S, Geranpayeh L, Mirfakhraie R, Motevaseli E, Ghafouri-Fard S. Expression Analysis of AFAP1-AS1 and AFAP1 in Breast Cancer. *Cancer biomark* (2018) 22(1):49–54. doi: 10.3233/CBM-170831
83. Zhou XL, Wang WW, Zhu WG, Yu CH, Tao GZ, Wu QQ, et al. High Expression of Long Non-Coding RNA AFAP1-AS1 Predicts Chemoradioresistance and Poor Prognosis in Patients With Esophageal Squamous Cell Carcinoma Treated With Definitive Chemoradiotherapy. *Mol Carcinogenesis* (2016) 55(12):2095–105. doi: 10.1002/mc.22454
84. Zhao H, Zhang K, Wang T, Cui J, Xi H, Wang Y, et al. Long Non-Coding RNA AFAP1-Antisense RNA 1 Promotes the Proliferation, Migration and Invasion of Gastric Cancer Cells and Is Associated With Poor Patient Survival. *Oncol Lett* (2018) 15(6):8620–6. doi: 10.3892/ol.2018.8389
85. Tang Y, He Y, Shi L, Yang L, Wang J, Lian Y, et al. Co-Expression of AFAP1-AS1 and PD-1 Predicts Poor Prognosis in Nasopharyngeal Carcinoma. *Oncotarget* (2017) 8(24):39001. doi: 10.18632/oncotarget.16545
86. He B, Zeng J, Chao W, Chen X, Huang Y, Deng K, et al. Serum Long Non-Coding RNAs MALAT1, AFAP1-AS1 and AL359062 as Diagnostic and Prognostic Biomarkers for Nasopharyngeal Carcinoma. *Oncotarget* (2017) 8(25):41166. doi: 10.18632/oncotarget.17083

Conflict of Interest: The authors declare that the research was conducted in the absence of any commercial or financial relationships that could be construed as a potential conflict of interest.

Publisher's Note: All claims expressed in this article are solely those of the authors and do not necessarily represent those of their affiliated organizations, or those of the publisher, the editors and the reviewers. Any product that may be evaluated in this article, or claim that may be made by its manufacturer, is not guaranteed or endorsed by the publisher.

Copyright © 2021 Ghafouri-Fard, Khoshbakht, Hussen, Taheri and Mokhtari. This is an open-access article distributed under the terms of the Creative Commons Attribution License (CC BY). The use, distribution or reproduction in other forums is permitted, provided the original author(s) and the copyright owner(s) are credited and that the original publication in this journal is cited, in accordance with accepted academic practice. No use, distribution or reproduction is permitted which does not comply with these terms.



Exosomal miRNAs and lncRNAs: The Modulator Keys of Cancer-Associated Fibroblasts in the Genesis and Progression of Malignant Neoplasms

Julio César Villegas-Pineda^{1,2}, Mélida del Rosario Lizarazo-Taborda³,
Adrián Ramírez-de-Arellano² and Ana Laura Pereira-Suárez^{2,4*}

¹Doctorado en Ciencias Biomédicas, Departamento de Fisiología, Centro Universitario de Ciencias de la Salud, Universidad de Guadalajara, Guadalajara, Mexico, ²Instituto de Investigación en Ciencias Biomédicas, Centro Universitario de Ciencias de la Salud, Universidad de Guadalajara, Guadalajara, Mexico, ³Programa de Bacteriología y Laboratorio Clínico, Facultad de Ciencias de la Salud, Universidad de Santander, Cúcuta, Colombia, ⁴Departamento de Microbiología y Patología, Centro Universitario de Ciencias de la Salud, Universidad de Guadalajara, Guadalajara, Mexico

OPEN ACCESS

Edited by:

Shiv K. Gupta,
Mayo Clinic, United States

Reviewed by:

Sharanjot Saini,
University of California, San Francisco,
United States
Mihnea P. Dragomir,
Charité University Medicine Berlin,
Germany
Dongya Zhang,
Nanjing University of Chinese
Medicine, China

*Correspondence:

Ana Laura Pereira-Suárez
analaurs@hotmial.com

Specialty section:

This article was submitted to
Molecular and Cellular Oncology,
a section of the journal
Frontiers in Cell and Developmental
Biology

Received: 31 May 2021

Accepted: 31 October 2021

Published: 29 November 2021

Citation:

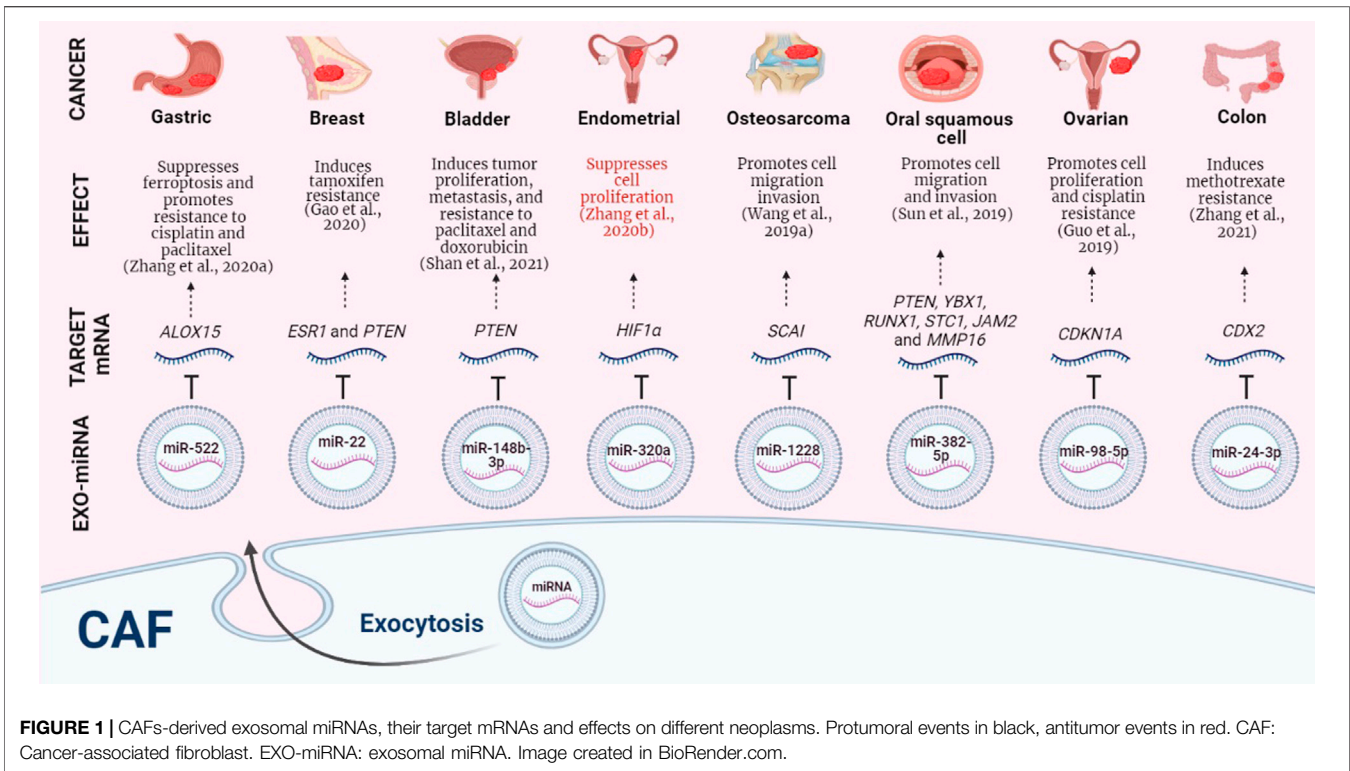
Villegas-Pineda JC,
Lizarazo-Taborda MdR,
Ramírez-de-Arellano A and
Pereira-Suárez AL (2021) Exosomal
miRNAs and lncRNAs: The Modulator
Keys of Cancer-Associated
Fibroblasts in the Genesis and
Progression of Malignant Neoplasms.
Front. Cell Dev. Biol. 9:717478.
doi: 10.3389/fcell.2021.717478

The tumor microenvironment is made up of a universe of molecular and cellular components that promote or inhibit the development of neoplasms. Among the molecular elements are cytokines, metalloproteinases, proteins, mitochondrial DNA, and nucleic acids, within which the ncRNAs: miRNAs and lncRNAs stand out due to their direct modulating effects on the genesis and progression of various cancers. Regarding cellular elements, the solid tumor microenvironment is made up of tumor cells, healthy adjacent epithelial cells, immune system cells, endothelial cells, and stromal cells, such as cancer-associated fibroblasts, which are capable of generating a modulating communication network with the other components of the tumor microenvironment through, among other mechanisms, the secretion of exosomal vesicles loaded with miRNAs and lncRNAs. These ncRNAs are key pieces in developing neoplasms since they have diverse effects on cancer cells and healthy cells, favoring or negatively regulating protumoral cellular events, such as migration, invasion, proliferation, metastasis, epithelial-mesenchymal transition, and resistance to treatment. Due to the growing number of relevant evidence in recent years, this work focused on reviewing, analyzing, highlighting, and showing the current state of research on exosomal ncRNAs derived from cancer-associated fibroblasts and their effects on different neoplasms. A future perspective on using these ncRNAs as real therapeutic tools in the treatment of cancer patients is also proposed.

Keywords: cancer, cancer-associated fibroblast, tumor microenvironment, exosomes, miRNAs, lncRNAs

INTRODUCTION

Malignant tumors consist of cancer cells and tumor-associated host cells (De Wever et al., 2014), the interaction between tumor microenvironment (TME) and tumor cells plays a key role in cancer progression (Dayan et al., 2012; Ali et al., 2015; Shah et al., 2015; Vered et al., 2015; Ringuette Goulet et al., 2018; Zhang Y.-F. et al., 2019; Dou et al., 2020; Wu et al., 2020). Remarkably, the dynamic interplay between cancer-associated fibroblasts (CAFs), cancer cells, and healthy cells has an essential role during tumor initiation and growth (Zhao et al., 2016; Li K. et al., 2020; Lv et al., 2020). In recent years, exosomes have gained relevance due to their regulatory role in the carcinogenesis of different neoplasms (Nilsson



et al., 2009; Ramteke et al., 2015; Donnarumma et al., 2017; Seo et al., 2018; Zhang Y. et al., 2019; Lee et al., 2020). Exosomes are MHC class I- and class II-bearing nanovesicles of endocytic origin; their size is in the range of 30–100 nm (Admyre et al., 2007; Nilsson et al., 2009). Exosomes can participate in intercellular communication between cells that make up the TME by transmitting intracellular cargoes (Achreja et al., 2017; Qin et al., 2019), their content can be miscellaneous and include macromolecules such as cytokines (Mashouri et al., 2019), metalloproteinases (Shimoda et al., 2014), proteins (Mathivanan et al., 2010; Zhang Y.-F. et al., 2019; Zhao et al., 2020), mitochondrial DNA (mtDNA) (Sansone et al., 2017) and can be enriched with different types of RNAs, such as messenger RNAs (mRNAs) (Gener Lahav et al., 2019), microRNAs [miRNAs or miR-, single-stranded non-coding RNAs (ncRNAs) of 20 nucleotides in length that are endogenously expressed (Beermann et al., 2016)] (Théry, 2011; Nouraei et al., 2016; Qin et al., 2019), about this type of ncRNAs, Dragomir et al., in their work entitled “*SnapShot: Unconventional miRNA Functions*,” mention that miRNAs can regulate gene expression at the post-transcriptional level in a conventional way by binding to mRNAs, resulting in the disintegration of target mRNAs and inhibition of translation, additionally, the authors also highlight in an exceptional way that through various mechanisms, such as the activation of Toll-like receptors, the upregulation of protein expression, the targeting of mitochondrial transcripts, the direct activation of transcription, among others, miRNAs can carry out their regulatory functions in an unconventional way (Dragomir et al., 2018), and long non-coding RNAs (lncRNAs, transcripts that are longer than 200 nucleotides and do not harbor protein-coding signatures (Beermann et al., 2016)) (Zhou et al., 2021). Exosomes can be produced by immune system

cells (Elashiry et al., 2021), epithelial cells (Han et al., 2017), tumor cells (Gu et al., 2012; Cheng et al., 2017; Ding et al., 2018; Chen et al., 2019; Hu and Hu, 2019; Amit et al., 2020; Jung et al., 2020; Yang et al., 2020) and CAFs (Herrera et al., 2018; Principe et al., 2018; Liu et al., 2020). CAFs are resident stromal cells of the TME; they have a promoting effect on carcinogenesis and progression of different neoplasms (Luga and Wrana, 2013; Huang et al., 2019; Sun and Fu, 2019) by transferring exosomes carrying ncRNAs to cells of the TME (Richards et al., 2017; Fiori et al., 2019) (Figure 1).

For everything mentioned above, the present work is based on the recent findings on the protumoral and antitumoral effects of CAFs-derived exosomal miRNAs and lncRNAs; it focuses on analyzing and highlighting the importance of these ncRNAs in the genesis and progression of different cancers. At the same time, it shows the current situation of this new growing research area, and a future perspective on the use of these ncRNAs as real therapeutic tools in the treatment of cancer patients is also proposed.

EXOSOMES: INDUCING FACTOR IN THE FORMATION OF CAFs AND TUMOR MICROENVIRONMENT MODULATOR

Exosomes are among the most recognized inducers for generating CAFs (Li K. et al., 2020). CAFs are known as cells capable of secreting exosomes (You et al., 2019), and in turn, exosomes derived from cancer cells containing TGF- β can induce the generation of CAFs from stromal cells (Goulet et al., 2019). It has also been observed that exosomes derived from CAFs containing TGF- β activate the SMAD signaling pathway in cancer cells through a particular type of

epithelial-mesenchymal transition (EMT), which increases their malignant behavior (Li et al., 2017), thus generating a loop between CAFs and exosomes. It has been shown that chronic lymphocytic leukemia cells-derived exosomes can transfer miR-146a to bone marrow-derived mesenchymal stem cells to generate CAFs; this is done by promoting EMT by targeting ubiquitin specific peptidase 16 (*USP16*) (Yang et al., 2020). Another cellular transition process in which exosomes are involved to originate CAFs is the endothelial-mesenchymal transition; this event was demonstrated by observing that melanoma-derived exosomes loaded with TGF- β induced the transition from human umbilical vein endothelial cells (HUVECs) to differentiated CAFs (Yeon et al., 2018). For their part, Baroni et al. demonstrated that triple-negative breast CAFs-derived exosomal miR-9 could generate a cell type with CAF-like properties in human breast fibroblasts, in which this miRNA enhanced the capacity for migration and invasion, as in breast cancer cell lines. Additionally, overexpression of this ncRNA in normal fibroblasts was able to promote tumor growth in a murine orthotopic xenograft model (Baroni et al., 2016).

It has also been observed that the exosomes produced by CAFs can modulate TME. For example, miR-21, which is packed in CAF-derived exosomes, induces the generation of monocytic myeloid-derived suppressor cells by activating STAT3 (Zhao et al., 2021). On a breast cancer model, exosomes produced by CAFs can also interfere with immunologic processes. In breast cancer cells treated with exosomes derived from CAFs, an increase of miR-92 was observed, which was essential for migration and invasion and correlated with the suppression of the immune cell function and the promotion of PD-L1 expression in these cells (Dou et al., 2020). Also, in the metastatic lung niche, a higher capacity to induce the transformation fibroblast into CAFs has been observed due to exosomal transport of miR-1247-3p from high-metastatic hepatocellular carcinoma cells; leading to a pro-inflammatory microenvironment promoted by CAFs, which secrete IL-6 and IL8, among other cytokines (Fang et al., 2018).

Considering this evidence, the important reciprocal relationship between exosomes and CAFs in the latter's self-generation and consequently in neoplasms' development is manifest. This relationship could be explored in greater depth and considered a previous or potentiating stage of carcinogenesis to inhibit the exosomal release and block exosomal molecules essential for the initiation, establishment, and progression of different cancers.

CELLULAR EFFECTS OF CAFs-DERIVED EXOSOMAL MIRNAS AND LNCRNAs ON KEY EVENTS FOR GENESIS AND PROGRESSION OF NEOPLASMS

Migration and Invasion, Processes Upregulated by CAFs-Derived Exosomal ncRNAs

Migration and invasion of cancer cells are essential for the establishment of the malignant neoplasm. Sun et al. isolated CAFs from patients with oral squamous cell carcinoma

(OSCC) and showed that in tongue squamous cell carcinoma CAL-27 cells, CAFs could promote these two events through the transfer of exosomal miR-382-5p, which facilitated the OSCC progression. Despite not having biologically determined the interaction, an analysis *in silico* predicted *PTEN*, *YBX1*, *RUNX1*, *STC1*, *JAM2*, and *MMP16* as candidate target genes for this miRNA (Sun et al., 2019). Another exosomal miRNA that has been shown to promote cell migration and invasion is miR-1228; this small non-coding regulatory RNA was enriched in exosomes secreted by CAFs and could downregulate endogenous *SCAI* mRNA and protein level in osteosarcoma, contributing to carcinogenesis of this neoplasm (Wang J.-W. et al., 2019).

CAFs-derived exosomes can also carry lncRNAs; LINC00659 is an example of this; it was found enriched in CAFs-derived exosomes and was shown to have multiple effects on human colorectal cancer (CRC) cells, it was able to induce cell proliferation, migration, invasion, and EMT *in vitro*. Furthermore, it was determined that these events were promoted by directly interacting with the tumor suppressor miR-342-3p to increase *ANXA2* expression in CRC cells (Zhou et al., 2021).

The protumoral effects exerted by various CAFs-derived exosomal miRNAs and lncRNAs enhance the migration and invasion of cancer cells and convert them into key pieces within the universe of participants in developing neoplasms.

CAFs-Derived Exosomal ncRNAs Promote Proliferation and Metastasis, Essential Malignant Characteristics for Tumor Progression

Among the multiple protumoral effects that CAFs-derived exosomal ncRNAs exert on cancer cells are the promotion of cell proliferation and metastasis. Chen et al. determined that CAFs isolated from samples of patients with invasive ductal carcinoma were capable of transferring exosomal miR-500a-5p to breast cancer cell lines, this miRNA bound to ubiquitin-specific peptidase 28 (*USP28*) promoting cell proliferation and metastasis in a nude mouse xenograft model (Chen et al., 2021). It has also been shown that miR-181d-5p can promote various protumoral cellular events in breast cancer cells, such as proliferation, invasion, and migration. If not enough, it can also induce EMT, antagonize apoptosis *in vitro* of breast cancer cells and promote tumor growth in nude mice xenografted with MCF-7 cells *via* downregulation of the transcription factors *CDX2* and *HOXA5* (Wang et al., 2020).

Another important effect carried out by CAFs exosomal ncRNAs is the reprogramming of metabolic pathways. Although to date, this aspect has not yet been studied in-depth, there is a report where a protumoral role is proposed for lncRNA *SNHG3*, which positively regulated pyruvate kinase isozymes M1/M2 (*PKM*) expression, inhibited mitochondrial oxidative phosphorylation, increased glycolysis, and proliferation of breast tumor cells through a mechanism similar to a molecular sponge for antitumoral miR-330-5p (Li Y. et al., 2020); this highlights the multifunctionality that CAFs-derived exosomal ncRNAs can exert on various processes related to carcinogenesis and tumor progression.

Considering the evidence reported, CAFs-derived exosomal miRNAs and lncRNAs can participate directly in tumor growth and the dissemination of cancer cells to other anatomical sites adjacent or far from the primary site, which could cause functional compromise of multiple organs and consequent serious complications in cancer patients.

Treatment Resistance Generated by CAFs-Derived Exosomal miRNAs and lncRNAs

CAFs are an important factor in generating tumor resistance to treatment (Fiori et al., 2019); this protumoral feature is associated with worsening cancer patients' prognosis (Domvri et al., 2020; Huang et al., 2020). CAFs possess chemoresistance by innate nature and, it has been observed that in the presence of gemcitabine, a cytotoxic anticancer chemotherapy drug, they can transfer this characteristic to cancer cells. CAFs exposed to this antineoplastic drug could increase the release of miR-146a-loaded exosomes; in *in vitro* assays, this miRNA transmitted gemcitabine resistance to pancreatic cancer epithelial cell lines, promoting cell proliferation and survival. In the same work, it was shown that miR-146a is directly regulated by the promoter binding transcription factor, Snail, which acts as a chemoresistance-inducing factor, and that it was also found to be overexpressed in human pancreatic CAFs-derived exosomes (Richards et al., 2017). Recently, Gao et al. identified and characterized a subtype of CAFs which particularly has the presence of the cell surface protein CD63; these CD63⁺ CAFs are capable of secreting exosomes enriched in miR-22, which can bind to their targets, *ERα* and *PTEN*, and deregulate their expression, thus conferring tamoxifen resistance to breast cancer cells (Gao et al., 2020).

Gemcitabine and tamoxifen are not the only drugs for which CAFs-derived exosomal miRNAs generate resistance in cancer cells; in fact, a considerable number of reports show that the cytotoxic effect caused by cisplatin in cancer cells can be diminished or eliminated by the action of CAFs-derived exosomal ncRNAs. It has been shown that, in cisplatin-sensitive ovarian cancer cells, CAFs-derived exosomal miR-98-5p was capable of binding to cyclin-dependent kinase inhibitor 1A (*CDKN1A*) to inhibit its expression, which increased ovarian cancer cell proliferation and cell cycle entry, suppressed cell apoptosis, and promoted cisplatin resistance *in vitro* and in a xenotransplanted nude mouse model (Guo et al., 2019). The intrinsic resistance that CAFs have towards cisplatin also favors the progression of head and neck cancer (HNC). It has been observed that CAFs can transfer exosomal miR-196a to HNC cells, which generated cell survival, proliferation, and inhibition of apoptosis, also conferred cisplatin resistance by targeting *CDKN1B* and *ING5*, cell cycle inhibitor and tumor suppressor molecules, respectively. Additionally, high levels of exosomal miR-196a in plasma were clinically correlated with poor overall survival and chemoresistance in patients with HNC (Qin et al., 2019).

There is a great diversity between the protumoral effects generated by CAFs-derived exosomal miRNAs and lncRNAs; it has been shown that miR-522 is capable of inhibiting ferroptosis, a novel mode of non-apoptotic cell death induced

by a build-up of toxic lipid peroxides (lipid-ROS) in an iron-dependent manner, in gastric cancer cells by targeting *ALOX15* and blocking lipid-ROS accumulation. Additionally, assays performed in an orthotopic implantation model in nude mice to evaluate gastric tumor growth and chemosensitivity led the authors to suggest that CAFs-derived exosomes containing miR-522 promote a new mechanism of acquired chemoresistance to cisplatin through an intercellular pathway, comprising USP7, hnRNP A1, miR-522, and *ALOX15* (Zhang H. et al., 2020).

On the other hand, it has been observed that miR-423-5p-loaded exosomes derived from CAFs can decrease the chemosensitivity of prostate cancer cells and increase the resistance of cells resistant to taxanes; in addition, it was shown that the inhibition of this miRNA enhanced the drug sensitivity of prostate cancer cells in a tumor xenograft model in nude mice. These protumoral events were favored due to the inhibitory effect of miR-423-5p on *GREM2* and the impact exerted on the TGF- β pathway (Shan et al., 2020). In another type of neoplasm, in bladder cancer, it was found that miR-148b-3p can also induce resistance to treatment. Shan et al. validated *PTEN* as a target of miR-148b-3p; the negative dysregulation of *PTEN* promoted metastasis, EMT, and resistance to doxorubicin and paclitaxel both in *in vitro* assays using bladder cancer cells and in *in vivo* assays using a xenograft mouse model. These events were generated due to the tumor-promoting effects of miR-148b-3p via the Wnt/ β -catenin pathway (Shan et al., 2021).

CAFs-derived exosomal miRNAs have also shown an inhibitory effect on the cytotoxic action that methotrexate exerts on the metabolism of colon cancer cells. In an *in vivo* model of colon cancer, it was shown that miR-24-3p induced resistance to this drug, favoring tumor growth under treatment of methotrexate by down-regulating the CDX2/HEPH axis (Zhang et al., 2021).

As mentioned previously, CAFs are also capable of secreting exosomal lncRNAs that promote tumor progression. Such is the case of exosomal lncUCA1, which conferred resistance to cisplatin in vulvar squamous cell carcinoma cells. Mechanistically, lncUCA1 functioned as a sponge for miR-103a, a miRNA with antitumoral function in various human cancers, this sequestration of miR-103a by lncUCA1 promoted the expression of WEE1 G2 checkpoint kinase (*WEE1*), a direct target of miR-103a, enhancing tumor growth and cisplatin resistance in a BALB/c nude xenograft model (Gao et al., 2021). Another CAFs-derived exosomal lncRNA with protumoral effect is H19, highly expressed in tumors generated in an azoxymethane (AOM)/dextran sodium sulfate (DSS) model of colitis-associated cancer, as well as in CRC samples from patients in different tumor-node-metastasis stages. Additionally, this lncRNA promoted the stemness of CRC stem cells, increased the frequency of tumor-initiating cells, and promoted the resistance of CRC cells to oxaliplatin both *in vitro* and *in vivo*. Mechanistically, H19 activated the β -catenin pathway by acting as an endogenous competitor for miR-141, a miRNA with antitumoral effect, in CRC cells (Ren et al., 2018).

These findings propose miRNAs and lncRNAs as important obstacles to achieving a successful chemotherapeutic treatment;

TABLE 1 | Cellular and tumor effects and mechanisms exerted by exosomal miRNAs and lncRNAs derived from CAFs in various cancers.

Exosomal ncRNAs Tumor effect	Cellular effects	Mechanisms	Cancer	References
miR-92 PRO-TUMOR	Promotes apoptosis and impairs proliferation of T cells, increases proliferation and migration of breast cancer cells, and facilitates tumor progression	Targets <i>LATS2</i> and modulates the LATS2-YAP1 axis generating an incremented expression of PD-L1	Breast	Dou et al. (2020)
miR-196a PRO-TUMOR	Promotes cell proliferation and confers cisplatin resistance	Targets and downregulates <i>CDKN1B</i> and <i>ING5</i>	Head and neck	Qin et al. (2019)
lncRNA LINC00659 PRO-TUMOR	Promotes cell proliferation, migration, invasion, and EMT progression	Interacts directly with miR-342-3p to increase ANXA2 expression	Colorectal	Zhou et al. (2021)
lncRNA-CAF PRO-TUMOR	Increases cell proliferation and promotes tumor growth	Stabilizes and up-regulates cytokine IL-33 to reprogram CAFs	Oral squamous cell	Ding et al. (2018)
miR-500a-5p PRO-TUMOR	Enhances cell proliferation and induces metastasis	Binds to tumor suppressor ubiquitin-specific peptidase 28 (<i>USP28</i>)	Breast	Chen et al. (2021)
miR-181d-5p PRO-TUMOR	Induces cell proliferation, invasion, migration, and EMT, antagonizes apoptosis <i>in vitro</i> , and promotes tumor growth <i>in vivo</i>	Downregulates the expression of the transcription factors CDX2 and HOXA5	Breast	Wang et al. (2020)
miR-423-5p PRO-TUMOR	Promotes chemotherapy resistance	Targets <i>GREM2</i> to inhibit its expression and favors the TGF- β pathway	Prostate	Shan et al. (2020)
lncRNA UCA1 PRO-TUMOR	Enhances tumor growth and chemoresistance	Favors the expression of WEE1 through sponging miR-103a	Vulvar squamous cell	Gao et al. (2021)
lncRNA H19 PRO-TUMOR	Promotes stemness and chemoresistance	Activates the β -catenin pathway, acting as a competing endogenous RNA sponge for miR-141	Colorectal	Ren et al. (2018)
lncRNA SNHG3 PRO-TUMOR	Inhibits mitochondrial oxidative phosphorylation, increases glycolysis, and enhances cell proliferation	Functions as a molecular sponge of miR-330-5p to regulate the expression of PKM	Breast	Li et al. (2020b)
miR-148b ANTI-TUMOR	Inhibits EMT and reduces cell invasion and metastasis	Directly binds to <i>DNMT1</i> and decreases MMP-9 activity	Endometrial	Li et al. (2019)
miR-4516 ANTI-TUMOR	Suppresses cell proliferation	Targets <i>FOSL1</i> , proliferation-related gene	Breast	Kim et al. (2020)
miR-320a ANTI-TUMOR	Inhibits EMT, cell proliferation, migration, invasion, tumorigenesis, and metastasis	Binds to <i>PBX3</i> , suppresses the activation of the MAPK pathway, affects the expression of CDK2, and MMP2 proteins due to reduced phosphorylation of ERK1/2	Hepatocellular	Zhang et al. (2017)
miR-3188 ANTI-TUMOR	Reduces cell proliferation, promotes apoptosis, and inhibits tumor growth	Directly targets <i>BCL2</i>	Head and neck	Wang et al. (2019b)
miR-34a-5p ANTI-TUMOR	Inhibits cell proliferation, migration, invasion, EMT, and tumorigenesis	Targets <i>AXL</i> , regulates the AKT/GSK-3 β / β -catenin/ Snail signaling cascade, and inhibits MMP-2/9	Oral	Li et al. (2018)

subject to further studies confirming this evidence, the elimination or reduction of CAFs-derived exosomal ncRNAs that generate chemoresistance should be considered as a new oncological therapeutic strategy.

Exosomal miRNAs With Antitumoral Effects

miRNAs have generally been reported as protumoral molecules; however, some reports suggest that their silencing or elimination could favor tumor development. A feature shared between the antitumoral miRNAs is that they are significantly reduced in CAFs-derived exosomes. *In vitro* and *in vivo* studies carried out by Li et al. revealed that miR-148b could function as a tumor suppressor, the downregulation of this miRNA induced EMT, migration, invasion, and increased MMP-9 activity in endometrial cancer cell lines, as well as metastasis in a nude mouse model, additionally, DNA methyltransferase 1 (*DNMT1*) was determined as the target gene of miR-148b (Li et al., 2019). This enzyme has also been associated with tumorigenesis in breast cancer due to its indispensable role in the maintenance of mammary stem/progenitor cell and cancer stem cell maintenance (Pathania et al., 2015), and chemoresistance to cisplatin in human non-small cell lung cancer cell lines (Sui

et al., 2015). Another study also carried out in endometrial cancer showed that the CAFs-derived exosomal miR-320a inhibited the proliferation of cell lines by direct targeting and downregulation of hypoxia-inducible factor 1- α (*HIF α*) (Zhang N. et al., 2020). This transcription factor has been strongly related to metastasis, angiogenesis, poor patient prognosis, and tumor resistance therapy (Masoud and Li, 2015). In another neoplasm typical of women, the CAFs-derived exosomal miR-4516 was isolated from tumor tissue obtained from a patient with invasive breast ductal carcinoma; this miRNA suppressed the proliferation of breast cancer cell lines by targeting *FOSL1* (Kim et al., 2020).

The antitumoral effects that some miRNAs possess have not only been reported in gynecological cancers. *In vitro* and *in vivo* studies carried out in human hepatocellular carcinoma cell lines and in a nude mouse model, respectively, showed that miR-320a could function as an antitumoral miRNA, whose binding to *PBX3* affected the protein expression of cyclin-dependent kinase 2 (CDK2) and MMP-2 due to the reduction of the phosphorylation of ERK1/2. In this way, the miR-320a/*PBX3* axis suppressed essential events for cancer progression such as EMT, cell proliferation, migration, invasion, tumorigenesis, and metastasis (Zhang et al., 2017). miR-3188 is another miRNA that

has an antitumoral effect; its loss of CAFs-derived exosomes contributed to the malignancy of HNC cells, increasing cell proliferation, migration, and invasion, and inhibited apoptosis by derepressing its target B-cell lymphoma 2 (*BCL2*) mRNA, this miRNA was also able to inhibit tumor growth in a BALB/c nude mice model (Wang X. et al., 2019).

Another of the few reports in which evidence is presented about the antitumoral effect of miRNAs is made by Li et al. It was observed that the overexpression of CAFs-derived exosomal miR-34a-5p suppressed the tumorigenesis of OSCC cells in an immunodeficient BALB/c mice subcutaneous tumor model. Additionally, in OSCC cell lines, it was shown that this miRNA is capable of binding directly to *AXL*, thus modulating the AKT/GSK-3 β / β -catenin signaling pathway; this event reduced proliferation, migration, and invasion, and decreased nuclear translocation of β -catenin, which led to decreased expression of Snail, a transcription factor of MMP-2 and MMP-9, important for EMT (Li et al., 2018).

Considering the reported evidence of some miRNAs' antitumoral effects in gynecological and non-gynecological cancers, these ncRNAs could become valuable tools to inhibit essential points in carcinogenesis and disease progression.

CAFS-DERIVED EXOSOMAL MIRNAS AND LNCRNAs AS CANDIDATES FOR THERAPEUTIC TOOLS AND BIOMARKERS

Given the importance of protumoral and antitumoral miRNAs and lncRNAs in processes such as cell proliferation, migration, invasion, EMT, metastasis, metabolism, resistance to treatment (Table 1), these exosomal ncRNAs derived from CAFs have been suggested as strong candidates that could be used as new targets or therapeutic tools in breast, ovarian, vulvar squamous cell, endometrial, head and neck, pancreas, oral squamous cell, gastric, bladder, colon, liver, prostate cancer, as well as biomarkers of clinical relevance; CAFs-derived exosomal ncRNAs can be considered cornerstones in neoplastic processes.

CONCLUSION AND PERSPECTIVES

Exosomes loaded with miRNAs and lncRNAs are a key communication pathway between CAFs and the different elements of the TME. Its relevance lies mainly in the promoter effect of protumoral and antitumoral events that modulate the genesis and the progression of various neoplasms. In the present work, the conventional effect of two types of exosomal ncRNAs derived from CAFs: miRNAs and lncRNAs, has been reviewed; this effect inhibits the translation by binding to its target mRNAs (Dragomir et al., 2018). Considering that cancer cells need different stimuli to form tumors and that CAFs, through the secretion of exosomal ncRNAs, among other mechanisms, can contribute significantly by favoring protumoral events, this type of extracellular vesicles derived from CAFs

loaded with miRNAs and lncRNAs can be considered as a potential therapeutic target to prevent the development of cancer. Nevertheless, despite the increase in the last 5 years of strong evidence suggesting CAFs-derived exosomal ncRNAs as therapeutic targets, more studies are needed to confirm the protumoral or antitumoral effects exerted by the various miRNAs and lncRNAs. Probably like miRNAs, lncRNAs have unconventional effects on gene expression that are still awaiting to be studied.

Regardless of future studies, the translational way from the laboratory to the clinic has begun. At present, an extensive database of ncRNAs in extracellular vesicles called EVAtlas, a product of enormous work, is available (Liu et al., 2021). In the site <http://bioinfo.life.hust.edu.cn/EVAtlas>, different characteristics such as extracellular vesicle types and isolation methods, expression level, functions, related drugs, and target genes of seven types of ncRNA of human extracellular vesicles can be consulted, as well as the pathological or physiological condition, tissues, cells, and biological fluids from which they have been isolated. This great bioinformatic tool could be part of the foundations to transfer the findings found *in vitro*, *ex vivo* and, *in silico* on the modulating effects of exosomal ncRNAs, derived and not derived from CAFs in the development of neoplasms, towards therapeutic regimens that improve the prognosis of cancer patients.

Although it is true that it will not be an easy task to incorporate miRNAs and lncRNAs as targets or tools in cancer treatment schemes, their relevance should not be underestimated. In the analysis carried out by GLOBOCAN (Ferlay et al., 2019; Ferlay et al., 2020), the global incidence and mortality rates of different cancers show an increase as the years go by, highlighting the need for additional options than those currently available to help in the fight against neoplasms. Designing and performing safe clinical trials, in which miRNAs and lncRNAs are used as therapeutic tools, is a great challenge and it will be essential to consider them a new real therapeutic alternative that benefits oncological patients.

AUTHOR CONTRIBUTIONS

JV-P conceptualized and drafted the manuscript. ML-T designed the table and the figure. AR-d-A and AP-S critically reviewed the manuscript. AP-S led the activities. All authors approved the submitted version of the manuscript.

FUNDING

This work was supported by Sectorial Research Fund for Education, SEP-CONACYT (A1-S-51207), and Jalisco Scientific Development Fund (FODECIJAL) to Attend State Problems 2019 (Project #8168). JV-P received a CONACYT fellowship (#769371, second year of Continuity of Post-Doctoral Stays Linked to Strengthening the Quality of the National Postgraduate 2020(2), CVU: 377666).

REFERENCES

- Achreja, A., Zhao, H., Yang, L., Yun, T. H., Marini, J., and Nagrath, D. (2017). Exo-MFA - A ¹³C Metabolic Flux Analysis Framework to Dissect Tumor Microenvironment-Secreted Exosome Contributions Towards Cancer Cell Metabolism. *Metab. Eng.* 43 (Pt B), 156–172. doi:10.1016/j.ymben.2017.01.001
- Admyre, C., Johansson, S. M., Qazi, K. R., Filén, J.-J., Lahesmaa, R., Norman, M., et al. (2007). Exosomes With Immune Modulatory Features Are Present in Human Breast Milk. *J. Immunol.* 179 (3), 1969–1978. doi:10.4049/jimmunol.179.3.1969
- Ali, S., Suresh, R., Banerjee, S., Bao, B., Xu, Z., Wilson, J., et al. (2015). Contribution of microRNAs in Understanding the Pancreatic Tumor Microenvironment Involving Cancer Associated Stellate and Fibroblast Cells. *Am. J. Cancer Res.* 5 (3), 1251–1264.
- Amit, M., Takahashi, H., Dragomir, M. P., Lindemann, A., Gleber-Netto, F. O., Pickering, C. R., et al. (2020). Loss of P53 Drives Neuron Reprogramming in Head and Neck Cancer. *Nature.* 578 (7795), 449–454. doi:10.1038/s41586-020-1996-3
- Baroni, S., Romero-Cordoba, S., Plantamura, I., Dugo, M., D'Ippolito, E., Cataldo, A., et al. (2016). Exosome-Mediated Delivery of miR-9 Induces Cancer-Associated Fibroblast-Like Properties in Human Breast Fibroblasts. *Cell Death Dis.* 7 (7), e2312. doi:10.1038/cddis.2016.224
- Beermann, J., Piccoli, M.-T., Viereck, J., and Thum, T. (2016). Non-Coding RNAs in Development and Disease: Background, Mechanisms, and Therapeutic Approaches. *Physiol. Rev.* 96 (4), 1297–1325. doi:10.1152/physrev.00041.2015
- Chen, B., Sang, Y., Song, X., Zhang, D., Wang, L., Zhao, W., et al. (2021). Exosomal miR-500a-5p Derived From Cancer-Associated Fibroblasts Promotes Breast Cancer Cell Proliferation and Metastasis through Targeting USP28. *Theranostics.* 11 (8), 3932–3947. doi:10.7150/thno.53412
- Chen, J.-H., Wu, A. T. H., Bamodu, O. A., Yadav, V. K., Chao, T.-Y., Tzeng, Y.-M., et al. (2019). Ovotodiolide Suppresses Oral Cancer Malignancy by Down-Regulating Exosomal Mir-21/stat3/β-Catenin Cargo and Preventing Oncogenic Transformation of Normal Gingival Fibroblasts. *Cancers.* 12, 56. doi:10.3390/cancers12010056
- Cheng, Q., Li, X., Liu, J., Ye, Q., Chen, Y., Tan, S., et al. (2017). Multiple Myeloma-Derived Exosomes Regulate the Functions of Mesenchymal Stem Cells Partially via Modulating miR-21 and miR-146a. *Stem Cell Int.* 2017, 1–9. doi:10.1155/2017/9012152
- Dayan, D., Salo, T., Salo, S., Nyberg, P., Nurmenniemi, S., Costea, D. E., et al. (2012). Molecular Crosstalk Between Cancer Cells and Tumor Microenvironment Components Suggests Potential Targets for New Therapeutic Approaches in Mobile Tongue Cancer. *Cancer Med.* 1 (2), 128–140. doi:10.1002/cam4.24
- De Wever, O., Van Bockstal, M., Mareel, M., Hendrix, A., and Bracke, M. (2014). Cancer-Associated Fibroblasts Provide Operational Flexibility in Metastasis. *Semin. Cancer Biol.* 25, 33–46. doi:10.1016/j.semcancer.2013.12.009
- Ding, L., Ren, J., Zhang, D., Li, Y., Huang, X., Hu, Q., et al. (2018). A Novel Stromal lncRNA Signature Reprograms Fibroblasts to Promote the Growth of Oral Squamous Cell Carcinoma via lncRNA-CAF/Interleukin-33. *Carcinogenesis.* 39 (3), 397–406. doi:10.1093/carcin/bgy006
- Domvri, K., Petanidis, S., Anastakis, D., Porpodis, K., Bai, C., Zarogoulidis, P., et al. (2020). Exosomal lncRNA PCAT-1 Promotes Kras-Associated Chemoresistance via Immunosuppressive miR-182/miR-217 Signaling and p27/CDK6 Regulation. *Oncotarget.* 11 (29), 2847–2862. doi:10.18632/oncotarget.27675
- Donnarumma, E., Fiore, D., Nappa, M., Roscigno, G., Adamo, A., Iaboni, M., et al. (2017). Cancer-associated Fibroblasts Release Exosomal microRNAs That Dictate an Aggressive Phenotype in Breast Cancer. *Oncotarget.* 8 (12), 19592–19608. doi:10.18632/oncotarget.14752
- Dou, D., Ren, X., Han, M., Xu, X., Ge, X., Gu, Y., et al. (2020). Cancer-Associated Fibroblasts-Derived Exosomes Suppress Immune Cell Function in Breast Cancer via the miR-92/pd-L1 Pathway. *Front. Immunol.* 11, 2026. doi:10.3389/fimmu.2020.02026
- Dragomir, M. P., Knutsen, E., and Calin, G. A. (2018). SnapShot: Unconventional miRNA Functions. *Cell.* 174 (4), 1038. doi:10.1016/j.cell.2018.07.040
- Elashiry, M., Elsayed, R., Elashiry, M. M., Rashid, M. H., Ara, R., Arbab, A. S., et al. (2021). Proteomic Characterization, Biodistribution, and Functional Studies of Immune-Therapeutic Exosomes: Implications for Inflammatory Lung Diseases. *Front. Immunol.* 12, 636222. doi:10.3389/fimmu.2021.636222
- Fang, T., Lv, H., Lv, G., Li, T., Wang, C., Han, Q., et al. (2018). Tumor-Derived Exosomal miR-1247-3p Induces Cancer-Associated Fibroblast Activation to foster Lung Metastasis of Liver Cancer. *Nat. Commun.* 9 (1), 191. doi:10.1038/s41467-017-02583-0
- Ferlay, J., Colombet, M., Soerjomataram, I., Mathers, C., Parkin, D. M., Piñeros, M., et al. (2019). Estimating the Global Cancer Incidence and Mortality in 2018: GLOBOCAN Sources and Methods. *Int. J. Cancer.* 144 (8), 1941–1953. doi:10.1002/ijc.31937
- Ferlay, J., Laversanne, M., Ervik, M., Lam, F., Colombet, M., Mery, L., et al. (2020). *Global Cancer Observatory: Cancer Tomorrow*. Lyon, France: International Agency for Research on Cancer. Available at: <https://gco.iarc.fr/tomorrow> (Accessed 20 May, 2021).
- Fiori, M. E., Di Franco, S., Villanova, L., Bianca, P., Stassi, G., and De Maria, R. (2019). Cancer-Associated Fibroblasts as Abettors of Tumor Progression at the Crossroads of EMT and Therapy Resistance. *Mol. Cancer.* 18, 70. doi:10.1186/s12943-019-0994-2
- Gao, Q., Fang, X., Chen, Y., Li, Z., and Wang, M. (2021). Exosomal lncRNA UCA1 From Cancer-Associated Fibroblasts Enhances Chemoresistance in Vulvar Squamous Cell Carcinoma Cells. *J. Obstet. Gynaecol. Res.* 47 (1), 73–87. doi:10.1111/jog.14418
- Gao, Y., Li, X., Zeng, C., Liu, C., Hao, Q., Li, W., et al. (2020). CD63 + Cancer-Associated Fibroblasts Confer Tamoxifen Resistance to Breast Cancer Cells Through Exosomal miR-22. *Adv. Sci.* 7 (21), 2002518. doi:10.1002/advs.200202518
- Gener Lahav, T., Adler, O., Zait, Y., Shani, O., Amer, M., Doron, H., et al. (2019). Melanoma-Derived Extracellular Vesicles Instigate Proinflammatory Signaling in the Metastatic Microenvironment. *Int. J. Cancer.* 145 (9), 2521–2534. doi:10.1002/ijc.32521
- Goulet, C. R., Champagne, A., Bernard, G., Vandal, D., Chabaud, S., Pouliot, F., et al. (2019). Cancer-Associated Fibroblasts Induce Epithelial-Mesenchymal Transition of Bladder Cancer Cells through Paracrine IL-6 Signalling. *BMC Cancer.* 19, 137. doi:10.1186/s12885-019-5353-6
- Gu, J., Qian, H., Shen, L., Zhang, X., Zhu, W., Huang, L., et al. (2012). Gastric Cancer Exosomes Trigger Differentiation of Umbilical Cord Derived Mesenchymal Stem Cells to Carcinoma-Associated Fibroblasts Through TGF-β/Smad Pathway. *PLoS One.* 7 (12), e52465. doi:10.1371/journal.pone.0052465
- Guo, H., Ha, C., Dong, H., Yang, Z., Ma, Y., and Ding, Y. (2019). Cancer-Associated Fibroblast-Derived Exosomal MicroRNA-98-5p Promotes Cisplatin Resistance in Ovarian Cancer by Targeting CDKN1A. *Cancer Cell Int.* 19, 347. doi:10.1186/s12935-019-1051-3
- Han, K.-Y., Tran, J. A., Chang, J.-H., Azar, D. T., and Zieske, J. D. (2017). Potential Role of Corneal Epithelial Cell-Derived Exosomes in Corneal Wound Healing and Neovascularization. *Sci. Rep.* 7, 40548. doi:10.1038/srep40548
- Herrera, M., Llorens, C., Rodríguez, M., Herrera, A., Ramos, R., Gil, B., et al. (2018). Differential Distribution and Enrichment of Non-Coding RNAs in Exosomes From Normal and Cancer-Associated Fibroblasts in Colorectal Cancer. *Mol. Cancer.* 17, 114. doi:10.1186/s12943-018-0863-4
- Hu, T., and Hu, J. (2019). Melanoma-derived Exosomes Induce Reprogramming Fibroblasts Into Cancer-Associated Fibroblasts via Gm26809 Delivery. *Cell Cycle.* 18 (22), 3085–3094. doi:10.1080/15384101.2019.1669380
- Huang, T. X., Guan, X. Y., and Fu, L. (2019). Therapeutic Targeting of the Crosstalk Between Cancer-Associated Fibroblasts and Cancer Stem Cells. *Am. J. Cancer Res.* 9 (9), 1889–1904.
- Huang, Y. J., Huang, T. H., Yadav, V. K., Sumitra, M. R., Tzeng, D. T., Wei, P. L., et al. (2020). Preclinical Investigation of Ovotodiolide as a Potential Inhibitor of colon Cancer Stem Cells via Downregulating Sphere-Derived Exosomal β-Catenin/STAT3/miR-1246 Cargoes. *Am. J. Cancer Res.* 1010 (128), 46402337–46422354.
- Jung, W.-H., Yam, N., Chen, C.-C., Elawad, K., Hu, B., and Chen, Y. (2020). Force-Dependent Extracellular Matrix Remodeling by Early-Stage Cancer Cells Alters Diffusion and Induces Carcinoma-Associated Fibroblasts. *Biomaterials.* 234, 119756. doi:10.1016/j.biomaterials.2020.119756
- Kim, J. E., Kim, B. G., Jang, Y., Kang, S., Lee, J. H., and Cho, N. H. (2020). The Stromal Loss of miR-4516 Promotes the FOSL1-dependent Proliferation and Malignancy of Triple Negative Breast Cancer. *Cancer Lett.* 469, 256–265. doi:10.1016/j.canlet.2019.10.039

- Lee, J.-C., Wu, A. T. H., Chen, J.-H., Huang, W.-Y., Lawal, B., Mokgautsi, N., et al. (2020). HNC0014, a Multi-Targeted Small-Molecule, Inhibits Head and Neck Squamous Cell Carcinoma by Suppressing C-Met/STAT3/CD44/PD-L1 Oncoimmune Signature and Eliciting Antitumor Immune Responses. *Cancers*. 12, 3759. doi:10.3390/cancers12123759
- Li, B. L., Lu, W., Qu, J. J., Ye, L., Du, G. Q., and Wan, X. P. (2019). Loss of Exosomal miR-148b From Cancer-Associated Fibroblasts Promotes Endometrial Cancer Cell Invasion and Cancer Metastasis. *J. Cell Physiol.* 234 (3), 2943–2953. doi:10.1002/jcp.27111
- Li, K., Liu, T., Chen, J., Ni, H., and Li, W. (2020a). Survivin in Breast Cancer-Derived Exosomes Activates Fibroblasts by Up-Regulating SOD1, Whose Feedback Promotes Cancer Proliferation and Metastasis. *J. Biol. Chem.* 295 (40), 13737–13752. doi:10.1074/jbc.RA120.013805
- Li, Y., Zhao, Z., Liu, W., and Li, X. (2020b). SNHG3 Functions as miRNA Sponge to Promote Breast Cancer Cells Growth Through the Metabolic Reprogramming. *Appl. Biochem. Biotechnol.* 191 (3), 1084–1099. doi:10.1007/s12010-020-03244-7
- Li, W., Zhang, X., Wang, J., Li, M., Cao, C., Tan, J., et al. (2017). TGF β 1 in Fibroblasts-Derived Exosomes Promotes Epithelial-Mesenchymal Transition of Ovarian Cancer Cells. *Oncotarget*. 8 (56), 96035–96047. doi:10.18632/oncotarget.21635
- Li, Y.-y., Tao, Y.-w., Gao, S., Li, P., Zheng, J.-m., Zhang, S.-e., et al. (2018). Cancer-Associated Fibroblasts Contribute to Oral Cancer Cells Proliferation and Metastasis via Exosome-Mediated Paracrine miR-34a-5p. *EBioMedicine*. 36, 209–220. doi:10.1016/j.ebiom.2018.09.006
- Liu, C.-J., Xie, G.-Y., Miao, Y.-R., Xia, M., Wang, Y., Lei, Q., et al. (2021). EVAtlas: a Comprehensive Database for ncRNA Expression in Human Extracellular Vesicles. *Nucleic Acids Res.* 1–7. doi:10.1093/nar/gkab668
- Liu, L., Zhang, Z., Zhou, L., Hu, L., Yin, C., Qing, D., et al. (2020). Cancer Associated Fibroblasts-Derived Exosomes Contribute to Radioresistance Through Promoting Colorectal Cancer Stem Cells Phenotype. *Exp. Cell Res.* 391 (2), 111956. doi:10.1016/j.yexcr.2020.111956
- Luga, V., and Wrana, J. L. (2013). Tumor-Stroma Interaction: Revealing Fibroblast-Secreted Exosomes as Potent Regulators of Wnt-Planar Cell Polarity Signaling in Cancer Metastasis. *Cancer Res.* 73 (23), 6843–6847. doi:10.1158/0008-5472.CAN-13-1791
- Lv, B., Zhu, W., and Feng, C. (2020). Coptisine Blocks Secretion of Exosomal Circct3 From Cancer-Associated Fibroblasts to Reprogram Glucose Metabolism in Hepatocellular Carcinoma. *DNA Cell Biol.* 39 (12), 2281–2288. doi:10.1089/dna.2020.6058
- Mashouri, L., Yousefi, H., Aref, A. R., Ahadi, A. m., Molaei, F., and Alahari, S. K. (2019). Exosomes: Composition, Biogenesis, and Mechanisms in Cancer Metastasis and Drug Resistance. *Mol. Cancer*. 18, 75. doi:10.1186/s12943-019-0991-5
- Masoud, G. N., and Li, W. (2015). HIF-1 α Pathway: Role, Regulation and Intervention for Cancer Therapy. *Acta Pharmaceutica Sinica B*. 5 (5), 378–389. doi:10.1016/j.apsb.2015.05.007
- Mathivanan, S., Ji, H., and Simpson, R. J. (2010). Exosomes: Extracellular Organelles Important in Intercellular Communication. *J. Proteomics*. 73 (10), 1907–1920. doi:10.1016/j.jprot.2010.06.006
- Nilsson, J., Skog, J., Nordstrand, A., Baranov, V., Mincheva-Nilsson, L., Breakefield, X. O., et al. (2009). Prostate Cancer-Derived Urine Exosomes: a Novel Approach to Biomarkers for Prostate Cancer. *Br. J. Cancer*. 100 (10), 1603–1607. doi:10.1038/sj.bjc.6605058
- Nouraei, N., Khazaei, S., Vasei, M., Razavipour, S. F., Sadeghizadeh, M., and Mowla, S. J. (2016). MicroRNAs Contribution in Tumor Microenvironment of Esophageal Cancer. *Cbm*. 16 (3), 367–376. doi:10.3233/CBM-160575
- Pathania, R., Ramachandran, S., Elangovan, S., Padia, R., Yang, P., Cinghu, S., et al. (2015). DNMT1 Is Essential for Mammary and Cancer Stem Cell Maintenance and Tumorigenesis. *Nat. Commun.* 6, 6910. doi:10.1038/ncomms7910
- Principe, S., Mejia-Guerrero, S., Ignatchenko, V., Sinha, A., Ignatchenko, A., Shi, W., et al. (2018). Proteomic Analysis of Cancer-Associated Fibroblasts Reveals a Paracrine Role for MFAP5 in Human Oral Tongue Squamous Cell Carcinoma. *J. Proteome Res.* 17 (6), 2045–2059. doi:10.1021/acs.jproteome.7b00925
- Qin, X., Guo, H., Wang, X., Zhu, X., Yan, M., Wang, X., et al. (2019). Exosomal miR-196a Derived from Cancer-Associated Fibroblasts Confers Cisplatin Resistance in Head and Neck Cancer Through Targeting CDKN1B and ING5. *Genome Biol.* 20, 12. doi:10.1186/s13059-018-1604-0
- Ramteke, A., Ting, H., Agarwal, C., Mateen, S., Somasagara, R., Hussain, A., et al. (2015). Exosomes Secreted under Hypoxia Enhance Invasiveness and Stemness of Prostate Cancer Cells by Targeting Adherens Junction Molecules. *Mol. Carcinog.* 54 (7), 554–565. doi:10.1002/mc.22124
- Ren, J., Ding, L., Zhang, D., Shi, G., Xu, Q., Shen, S., et al. (2018). Carcinoma-Associated Fibroblasts Promote the Stemness and Chemoresistance of Colorectal Cancer by Transferring Exosomal lncRNA H19. *Theranostics*. 8 (14), 3932–3948. doi:10.7150/thno.25541
- Richards, K. E., Zeleniak, A. E., Fishel, M. L., Wu, J., Littlepage, L. E., and Hill, R. (2017). Cancer-Associated Fibroblast Exosomes Regulate Survival and Proliferation of Pancreatic Cancer Cells. *Oncogene*. 36 (13), 1770–1778. doi:10.1038/onc.2016.353
- Ringuette Goulet, C., Bernard, G., Tremblay, S., Chabaud, S., Bolduc, S., and Pouliot, F. (2018). Exosomes Induce Fibroblast Differentiation Into Cancer-Associated Fibroblasts Through TGF β Signaling. *Mol. Cancer Res.* 16 (7), 1196–1204. doi:10.1158/1541-7786.MCR-17-0784
- Sansone, P., Savini, C., Kurelac, I., Chang, Q., Amato, L. B., Strillacci, A., et al. (2017). Packaging and Transfer of Mitochondrial DNA via Exosomes Regulate Escape From Dormancy in Hormonal Therapy-Resistant Breast Cancer. *Proc. Natl. Acad. Sci. USA*. 114 (43), E9066–E9075. doi:10.1073/pnas.1704862114
- Seo, N., Akiyoshi, K., and Shiku, H. (2018). Exosome-Mediated Regulation of Tumor Immunology. *Cancer Sci.* 109 (10), 2998–3004. doi:10.1111/cas.13735
- Shah, S. H., Miller, P., Garcia-Conteras, M., Ao, Z., Machlin, L., Issa, E., et al. (2015). Hierarchical Paracrine Interaction of Breast Cancer Associated Fibroblasts With Cancer Cells via hMAPK-microRNAs to Drive ER-Negative Breast Cancer Phenotype. *Cancer Biol. Ther.* 16 (11), 1671–1681. doi:10.1080/15384047.2015.1071742
- Shan, G., Gu, J., Zhou, D., Li, L., Cheng, W., Wang, Y., et al. (2020). Cancer-Associated Fibroblast-Secreted Exosomal miR-423-5p Promotes Chemotherapy Resistance in Prostate Cancer by Targeting GREM2 Through the TGF- β Signaling Pathway. *Exp. Mol. Med.* 52 (11), 1809–1822. doi:10.1038/s12276-020-0431-z
- Shan, G., Zhou, X., Gu, J., Zhou, D., Cheng, W., Wu, H., et al. (2021). Downregulated Exosomal microRNA-148b-3p in Cancer Associated Fibroblasts Enhance Chemosensitivity of Bladder Cancer Cells by Downregulating the Wnt/ β -Catenin Pathway and Upregulating PTEN. *Cell Oncol.* 44, 45–59. doi:10.1007/s13402-020-00500-0
- Shimoda, M., Principe, S., Jackson, H. W., Luga, V., Fang, H., Molyneux, S. D., et al. (2014). Loss of the Timp Gene Family Is Sufficient for the Acquisition of the CAF-Like Cell State. *Nat. Cell Biol.* 16 (9), 889–901. doi:10.1038/ncb3021
- Sui, C., Meng, F., Li, Y., and Jiang, Y. (2015). miR-148b Reverses Cisplatin-Resistance in Non-Small Cell Cancer Cells via Negatively Regulating DNA (Cytosine-5)-Methyltransferase 1(DNMT1) Expression. *J. Transl. Med.* 13, 132. doi:10.1186/s12967-015-0488-y
- Sun, L. P., Xu, K., Cui, J., Yuan, D. Y., Zou, B., Li, J., et al. (2019). Cancer associated Fibroblast derived Exosomal miR3825p Promotes the Migration and Invasion of Oral Squamous Cell Carcinoma. *Oncol. Rep.* 42 (4), 1319–1328. doi:10.3892/or.2019.7255
- Sun, W., and Fu, S. (2019). Role of Cancer-Associated Fibroblasts in Tumor Structure, Composition and the Microenvironment in Ovarian Cancer (Review). *Oncol. Lett.* 18 (3), 2173–2178. doi:10.3892/ol.2019.10587
- Théry, C. (2011). Exosomes: Secreted Vesicles and Intercellular Communications. *Fl1000 Biol. Rep.* 3, 15. doi:10.3410/B3-15
- Vered, M., Lehtonen, M., Hotakainen, L., Pirilä, E., Teppo, S., Nyberg, P., et al. (2015). Caveolin-1 Accumulation in the Tongue Cancer Tumor Microenvironment Is Significantly Associated with Poor Prognosis: an *In-Vivo* and *In-Vitro* Study. *BMC Cancer*. 15, 25. doi:10.1186/s12885-015-1030-6
- Wang, H., Wei, H., Wang, J., Li, L., Chen, A., and Li, Z. (2020). MicroRNA-181d-5p-Containing Exosomes Derived From CAFs Promote EMT by Regulating CDX2/HOXA5 in Breast Cancer. *Mol. Ther. - Nucleic Acids*. 19, 654–667. doi:10.1016/j.omtn.2019.11.024
- Wang, J.-W., Wu, X.-F., Gu, X.-J., and Jiang, X.-H. (2019a). Exosomal miR-1228 From Cancer-Associated Fibroblasts Promotes Cell Migration and Invasion of Osteosarcoma by Directly Targeting SCAI. *Oncol. Res.* 27 (9), 979–986. doi:10.3727/096504018X15336368805108
- Wang, X., Qin, X., Yan, M., Shi, J., Xu, Q., Li, Z., et al. (2019b). Loss of Exosomal miR-3188 in Cancer-Associated Fibroblasts Contributes to HNC Progression. *J. Exp. Clin. Cancer Res.* 38, 151. doi:10.1186/s13046-019-1144-9

- Wu, H.-J., Hao, M., Yeo, S. K., and Guan, J.-L. (2020). FAK Signaling in Cancer-Associated Fibroblasts Promotes Breast Cancer Cell Migration and Metastasis by Exosomal miRNAs-Mediated Intercellular Communication. *Oncogene*. 39 (12), 2539–2549. doi:10.1038/s41388-020-1162-2
- Yang, Y., Li, J., and Geng, Y. (2020). Exosomes Derived from Chronic Lymphocytic Leukemia Cells Transfer miR-146a to Induce the Transition of Mesenchymal Stromal Cells into Cancer-Associated Fibroblasts. *J. Biochem.* 168 (5), 491–498. doi:10.1093/jb/mvaa064
- Yeon, J. H., Jeong, H. E., Seo, H., Cho, S., Kim, K., Na, D., et al. (2018). Cancer-Derived Exosomes Trigger Endothelial to Mesenchymal Transition Followed by the Induction of Cancer-Associated Fibroblasts. *Acta Biomater.* 76, 146–153. doi:10.1016/j.actbio.2018.07.001
- You, J., Li, M., Cao, L. M., Gu, Q. H., Deng, P. B., Tan, Y., et al. (2019). Snail1-Dependent Cancer-Associated Fibroblasts Induce Epithelial-Mesenchymal Transition in Lung Cancer Cells via Exosomes. *QJM.* 112 (8), 581–590. doi:10.1093/qjmed/hcz093
- Zhang, H., Deng, T., Liu, R., Ning, T., Yang, H., Liu, D., et al. (2020a). CAF Secreted miR-522 Suppresses Ferroptosis and Promotes Acquired Chemo-Resistance in Gastric Cancer. *Mol. Cancer.* 19, 43. doi:10.1186/s12943-020-01168-8
- Zhang, N., Wang, Y., Liu, H., and Shen, W. (2020b). Extracellular Vesicle Encapsulated microRNA-320a Inhibits Endometrial Cancer by Suppression of the HIF1 α /VEGFA axis. *Exp. Cel Res.* 394 (2), 112113. doi:10.1016/j.yexcr.2020.112113
- Zhang, H. W., Shi, Y., Liu, J. B., Wang, H. M., Wang, P. Y., Wu, Z. J., et al. (2021). Cancer-associated Fibroblast-Derived Exosomal microRNA-24-3p Enhances Colon Cancer Cell Resistance to MTX by Down-Regulating CDX2/HEPH axis. *J. Cel Mol. Med.* 25 (8), 3699–3713. doi:10.1111/jcmm.15765
- Zhang, Y.-F., Zhou, Y.-Z., Zhang, B., Huang, S.-F., Li, P.-P., He, X.-M., et al. (2019a). Pancreatic Cancer-Derived Exosomes Promoted Pancreatic Stellate Cells Recruitment by Pancreatic Cancer. *J. Cancer.* 10 (18), 4397–4407. doi:10.7150/jca.27590
- Zhang, Y., Cai, H., Chen, S., Sun, D., Zhang, D., and He, Y. (2019b). Exosomal Transfer of miR-124 Inhibits normal Fibroblasts to Cancer-Associated Fibroblasts Transition by Targeting Sphingosine Kinase 1 in Ovarian Cancer. *J. Cel Biochem.* 120 (8), 13187–13201. doi:10.1002/jcb.28593
- Zhang, Z., Li, X., Sun, W., Yue, S., Yang, J., Li, J., et al. (2017). Loss of Exosomal miR-320a From Cancer-Associated Fibroblasts Contributes to HCC Proliferation and Metastasis. *Cancer Lett.* 397, 33–42. doi:10.1016/j.canlet.2017.03.004
- Zhao, G., Li, H., Guo, Q., Zhou, A., Wang, X., Li, P., et al. (2020). Exosomal Sonic Hedgehog Derived From Cancer-Associated Fibroblasts Promotes Proliferation and Migration of Esophageal Squamous Cell Carcinoma. *Cancer Med.* 9 (7), 2500–2513. doi:10.1002/cam4.2873
- Zhao, H., Yang, L., Baddour, J., Achreja, A., Bernard, V., Moss, T., et al. (2016). Tumor Microenvironment Derived Exosomes Pleiotropically Modulate Cancer Cell Metabolism. *Elife*. 5, e10250. doi:10.7554/eLife.10250
- Zhao, Q., Huang, L., Qin, G., Qiao, Y., Ren, F., Shen, C., et al. (2021). Cancer-associated Fibroblasts Induce Monocytic Myeloid-Derived Suppressor Cell Generation via IL-6/Exosomal miR-21-Activated STAT3 Signaling to Promote Cisplatin Resistance in Esophageal Squamous Cell Carcinoma. *Cancer Lett.* 518, 35–48. doi:10.1016/j.canlet.2021.06.009
- Zhou, L., Li, J., Tang, Y., and Yang, M. (2021). Exosomal LncRNA LINC00659 Transferred From Cancer-Associated Fibroblasts Promotes Colorectal Cancer Cell Progression via miR-342-3p/ANXA2 axis. *J. Transl. Med.* 19, 8. doi:10.1186/s12967-020-02648-7

Conflict of Interest: The authors declare that the research was conducted in the absence of any commercial or financial relationships that could be construed as a potential conflict of interest.

Publisher's Note: All claims expressed in this article are solely those of the authors and do not necessarily represent those of their affiliated organizations, or those of the publisher, the editors and the reviewers. Any product that may be evaluated in this article, or claim that may be made by its manufacturer, is not guaranteed or endorsed by the publisher.

Copyright © 2021 Villegas-Pineda, Lizarazo-Taborda, Ramírez-de-Arellano and Pereira-Suárez. This is an open-access article distributed under the terms of the Creative Commons Attribution License (CC BY). The use, distribution or reproduction in other forums is permitted, provided the original author(s) and the copyright owner(s) are credited and that the original publication in this journal is cited, in accordance with accepted academic practice. No use, distribution or reproduction is permitted which does not comply with these terms.



circRNAs: Insight Into Their Role in Tumor-Associated Macrophages

Saili Duan^{1,2,3,4†}, Shan Wang^{1,2,3,4†}, Tao Huang^{1,2,3,4}, Junpu Wang^{1,2,3,4*} and Xiaoqing Yuan^{5,6*}

¹ Department of Pathology, Xiangya Hospital, Central South University, Changsha, China, ² Xiangya School of Medicine, Central South University, Changsha, China, ³ Department of Pathology, School of Basic Medicine, Central South University, Changsha City, China, ⁴ National Clinical Research Center for Geriatric Disorders, Xiangya Hospital, Central South University, Changsha, China, ⁵ Guangdong Provincial Key Laboratory of Malignant Tumor Epigenetics and Gene Regulation, Sun Yat-Sen Memorial Hospital, Sun Yat-Sen University, Guangzhou, China, ⁶ Breast Tumor Center, Sun Yat-Sen Memorial Hospital, Sun Yat-Sen University, Guangzhou, China

OPEN ACCESS

Edited by:

Shiv K. Gupta,
Mayo Clinic, United States

Reviewed by:

Giovanna Lucia Liguori,
Institute of Genetics and Biophysics
(CNR), Italy
Zehuan Liao,
Nanyang Technological University,
Singapore
Peng Wei,
Beijing University of Chinese Medicine,
China

*Correspondence:

Junpu Wang
wang-jp2013@csu.edu.cn
Xiaoqing Yuan
yuanxq7@mail.sysu.edu.cn

[†]These authors have contributed
equally to this work

Specialty section:

This article was submitted to
Molecular and Cellular Oncology,
a section of the journal
Frontiers in Oncology

Received: 21 September 2021

Accepted: 08 November 2021

Published: 01 December 2021

Citation:

Duan S, Wang S, Huang T, Wang J
and Yuan X (2021) circRNAs:
Insight Into Their Role in
Tumor-Associated Macrophages.
Front. Oncol. 11:780744.
doi: 10.3389/fonc.2021.780744

Currently, it is well known that the tumor microenvironment not only provides energy support for tumor growth but also regulates tumor signaling pathways and promotes the proliferation, invasion, metastasis, and drug resistance of tumor cells. The tumor microenvironment, especially the function and mechanism of tumor-associated macrophages (TAMs), has attracted great attention. TAMs are the most common immune cells in the tumor microenvironment and play a vital role in the occurrence and development of tumors. circular RNA (circRNA) is a unique, widespread, and stable form of non-coding RNA (ncRNA), but little is known about the role of circRNAs in TAMs or how TAMs affect circRNAs. In this review, we summarize the specific manifestations of circRNAs that affect the tumor-associated macrophages and play a significant role in tumor progression. This review helps improve our understanding of the association between circRNAs and TAMs, thereby promoting the development and progress of potential clinical targeted therapies.

Keywords: circRNA, TAMs, M2 macrophage, polarization, cancer

INTRODUCTION

With the continuous development of high-throughput sequencing, a class of covalently closed RNA molecules with extensiveness, diversity, stability, and evolutionary conservation has come into view, known as circular RNA (circRNA) (1, 2). circRNA has a unique covalently closed loop structure and a specific tertiary structure and exhibits tissue- and developmental stage-specific expression, which

Abbreviations: APCs, antigen-presenting cells; CAE, cancer-associated endothelial cells; CAFs, cancer-associated fibroblasts; circ-CDR1as, cerebellar degeneration-related 1 antisense; circ-PAIP2, circRNA poly(A) binding protein-interacting protein 2; circRNA, circular RNA; circ-ZNF609CSCs, circRNA zinc-finger protein 609; CSC, cancer stem cells; CRC, colorectal cancer; CTLA4, cytotoxic T-lymphocyte-associated protein 4; ECM, extracellular matrix; EcRNA, exonic circRNA; EGF, epithelial growth factor; EGFR, epidermal growth factor receptor; ElciRNA, exon-intron circRNA; ceRNA, competing endogenous RNA; HCC, hepatocellular carcinoma; HGF, hepatocyte growth factor; IL-10, interleukin 10; IL-17, interleukin 17; IL-23, interleukin 23; IRF, interferon regulatory factor; LPS, lipopolysaccharide stimulation; MBLs, mannose-binding lectins; MHC, major histocompatibility complex; miR, microRNA; ncRNA, non-coding RNA; NGS, next-generation sequencing; PD-L1, programmed death ligand 1; PDGF, platelet-derived growth factor; PGE2, prostaglandin 2; Pol II, polymerase II; RBPs, retinol-binding proteins; STAT, signal transducer and activator of transcription; TAMs, tumor-associated macrophages; TGF- β 1, transforming growth factor- β 1; TLR4, toll-like receptor 4; TME, tumor microenvironment.

plays an essential role in multiple cellular processes (3). Some circRNAs have been reported to be involved in tumor genesis, progression, and metastasis (4, 5), and circRNAs have been identified as important markers of various tumors (6–9). As a critical determinant of all stages of cancer development and progression, the tumor microenvironment (TME) is a complex ecosystem involving the coevolution of cancer cells and the surrounding matrix (10). A variety of cellular components in TME include immune cells [T cells, tumor-associated macrophages (TAMs), dendritic cells, mast cells, *etc.*], cancer-associated endothelial cells (CAE), cancer-associated fibroblasts (CAFs), and cancer stem cells (11, 12). Non-cellular counterparts include growth factors, cytokines, and extracellular matrix (ECM) (13). Other studies have shown that circRNAs play a variety of roles in the TME, promote or inhibit the immune system and angiogenesis, improve the permeability of endothelial cells, promote tumor metastasis, lead to ECM remodeling, and jointly support tumor progression (14, 15)—for example, CAFs can release circEIF3k under hypoxia, upregulate miR-214, and downregulate the programmed death ligand-1 (PD-L1) expression in colorectal cancer, thus inhibiting the progression of colorectal cancer (16). CAF-derived cytokines promote the progression and metastasis of hepatocellular carcinoma (HCC) by activating the circRNA–miRNA–mRNA axis in tumor cells (17). The high expression of cerebellar degeneration-related 1 antisense (circ-CDR1as) can enhance the penetration level of CAEs to promote tumor growth and metastasis (18). circRNAs may become the entry point of the entire ncRNA network, providing broad prospects for the clinical treatment of tumors (19).

Currently, circRNAs participate in the progression of tumorigenesis by acting on the TME and affecting the polarization of TAMs. However, the relationship and interactions of circRNAs and TAMs have not been systematically summarized. In this review, we will outline the specific manifestations of circRNAs affecting the tumor microenvironment as well as the latest findings suggesting that they participate in the metabolic reprogramming of tumor-associated macrophages and play an important role in tumor progression. Our review will improve the understanding of the relationship between circRNA and TAMs to promote the development and progress of potential clinical targeted therapies.

circRNAs

circRNAs are single-stranded RNAs with covalently closed circular structures with tissue/developmental stage-specific expression patterns (20–23), which are highly regulated by cis-acting elements and trans-acting factors (24–27). The covalently closed loops formed by circRNAs are produced by the back-splicing of the exon and/or intron sequences of the primary transcript and endow them with the inherent ability to resist the decay of extranuclear RNA (28). Back-splicing is catalyzed by the standard spliceosome mechanism, but protein factors and cis-complementary sequences, especially Alu repeats, can regulate this process (29). Alu complementary-dependent base-pairing supports the connection of downstream splicing donor pairs with non-splicing upstream splicing receptors, and the contributed RNA is covalently

closed (30). circRNAs exist in a wide range of species, ranging from viruses to mammals, and can function as transcriptional regulators, microRNA (miR) sponges, and protein templates (6, 31–33). Based on the diversity of source sequences, circRNAs can be divided into three categories: exonic circRNAs (EcRNA), exon–intron circRNAs (EiRNAs), and circular intronic RNAs (ciRNAs) (8, 29, 34–36). However, a fourth tricRNA may be isolated, which corresponds to intronic circular tRNA (37). Most circRNAs are derived from pre-mRNA, while a small portion of intron-derived circRNAs are derived from pre-tRNA (36, 38).

Many studies have shown that circRNA has several characteristics, namely (22):

(1) Abundance and diversity: thousands of different circRNAs have been identified in eukaryotes through RNA-seq technology, and the complexity of the circRNA production mechanism leads to its diversity (29, 39). The enrichment of circRNA can also be found in saliva and blood (22).

(2) Stability: a unique ring structure makes circRNA resistant to ribonuclease, without 5′–3′ polarity and a polyadenylated tail, which results in higher stability than linear RNA (22).

(3) Conservation: circRNAs are highly conserved in different species (40).

(4) Specificity: circRNAs are usually specifically expressed in a tissue or developmental stage-specific manner (8, 41). The characteristics of circRNAs give them the following different functions:

(a) They have miRNA sponges, such as circRNA sex-determining region Y (cir-SRY) (42). (b) They interact with proteins and their expression, such as retinol-binding proteins and mannose-binding lectins (43).

(c) They have translation templates, such as circRNA zinc-finger protein 609 (circ-ZNF609) (44).

(d) They have transcription regulators, such as circRNA poly (A) binding protein-interacting protein 2 (circ-PAIP2) (45).

circRNAs are generated in the nucleus, but most of them are found in the cytoplasm—for example, circRNAs formed by exons are generally located in the cytoplasm (22), which suggests specific rules for circRNA transport or localization. Although most circRNAs are located primarily in the cytoplasm, ciRNAs and EiRNAs are limited to the nucleus (23, 35, 46), which means that their role is in nuclear events, such as transcriptional regulation. ciRNAs regulate the transcription of their parental genes by promoting the elongation of polymerase II. The binding of circRNAs to proteins may depend not only on nucleotide sequences but also on the different secondary or tertiary structures of circRNAs (47). Abnormally regulated circRNAs play a suppressive or carcinogenic role in the initiation and progression of cancer, affecting a number of cellular functions, such as the maintenance of proliferation signals, promotion of cell migration and invasion, resistance to apoptosis, and induction of angiogenesis (48, 49). Meanwhile, circRNAs play an important regulatory role in diseases by interacting with disease-related miRNAs (50). Studies have shown that circRNAs are helpful for the treatment of osteoporosis, which is related to the differentiation of osteoclasts (51).

circRNAs, with a closed-loop structure and high stability, are gene expression regulators that play a variety of regulatory roles in

transcription, splicing, and chromatin interactions (52). The differences in the formation process and shape of the four circRNAs as well as the characteristics and functions of circRNAs are shown in **Figure 1** (53). circRNAs exhibit inherent conserved and environmental resistance stability due to their circular structure, presence in blood and peripheral tissues, and coexistence with exosomes and may be considered as potential biomarkers or therapeutic targets for a number of immune diseases (54). Most circRNA translation products have an impact on cancer progression or inhibition (49, 55), which leads to abnormal expression in various types of cancer (28), including colorectal cancer (56), hepatocellular carcinoma (5, 57, 58), gastric cancer (59, 60), acute promyelocytic leukemia (61), and breast cancer (62, 63). Listed in **Table 1** is the relationship between some circRNAs and tumors, suggesting that circRNAs are mainly related to inflammatory responses, including the interaction between cytokines and chemokines, and are a potential disease marker that can be used as promising biomarkers for diagnosis, providing a new therapeutic target for tumor treatment (65, 66).

TAMs

A tumor has a highly heterogeneous structure. Tumor cells interact with a variety of cells and factors, including immune cells and immune factors, to form a complex tumor immune microenvironment (67). The TME is a complex environment where tumor cells coexist with immune cells and other cells, blood vessels, signaling molecules, and the ECM and is the place where the immune system interacts with tumor cells (68). Exosomes are a component of the TME (69); they act as effective signaling molecules between cancer cells and surrounding cells that make up the TME (9, 70). Studies have found that circRNA molecules can be transferred to exosomes and are more abundant in exosomes than in cells, suggesting that they may be promising cancer biomarkers (9). Meanwhile, the TME can actively reprogram macrophage metabolism through the direct exchange of metabolites, cytokines, and other signaling mediators in cancer (71).

Macrophages are composed of many cell types with complex and delicate regulatory networks. The type, density, and location of macrophages, as well as other inflammatory infiltrates, have good

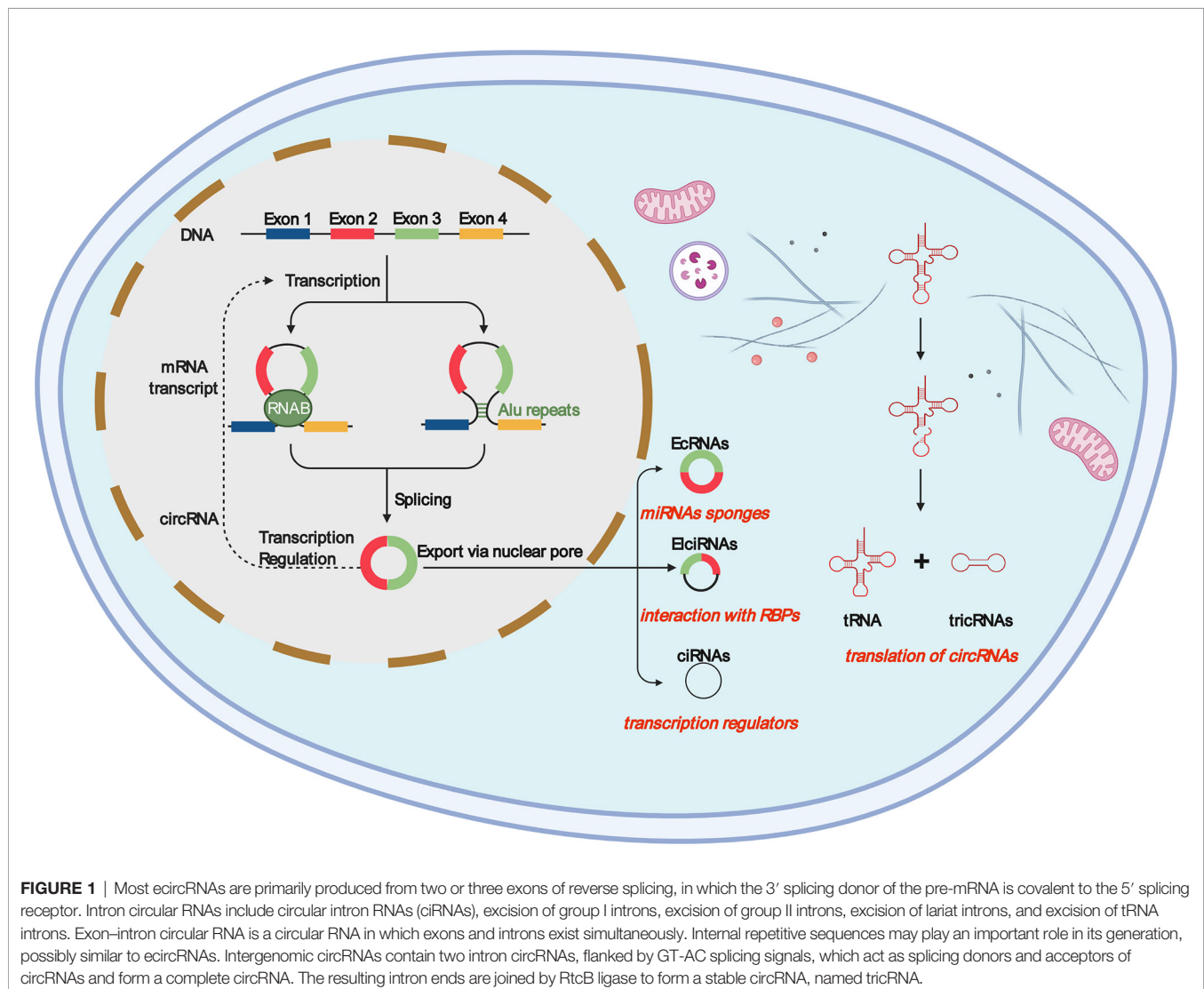


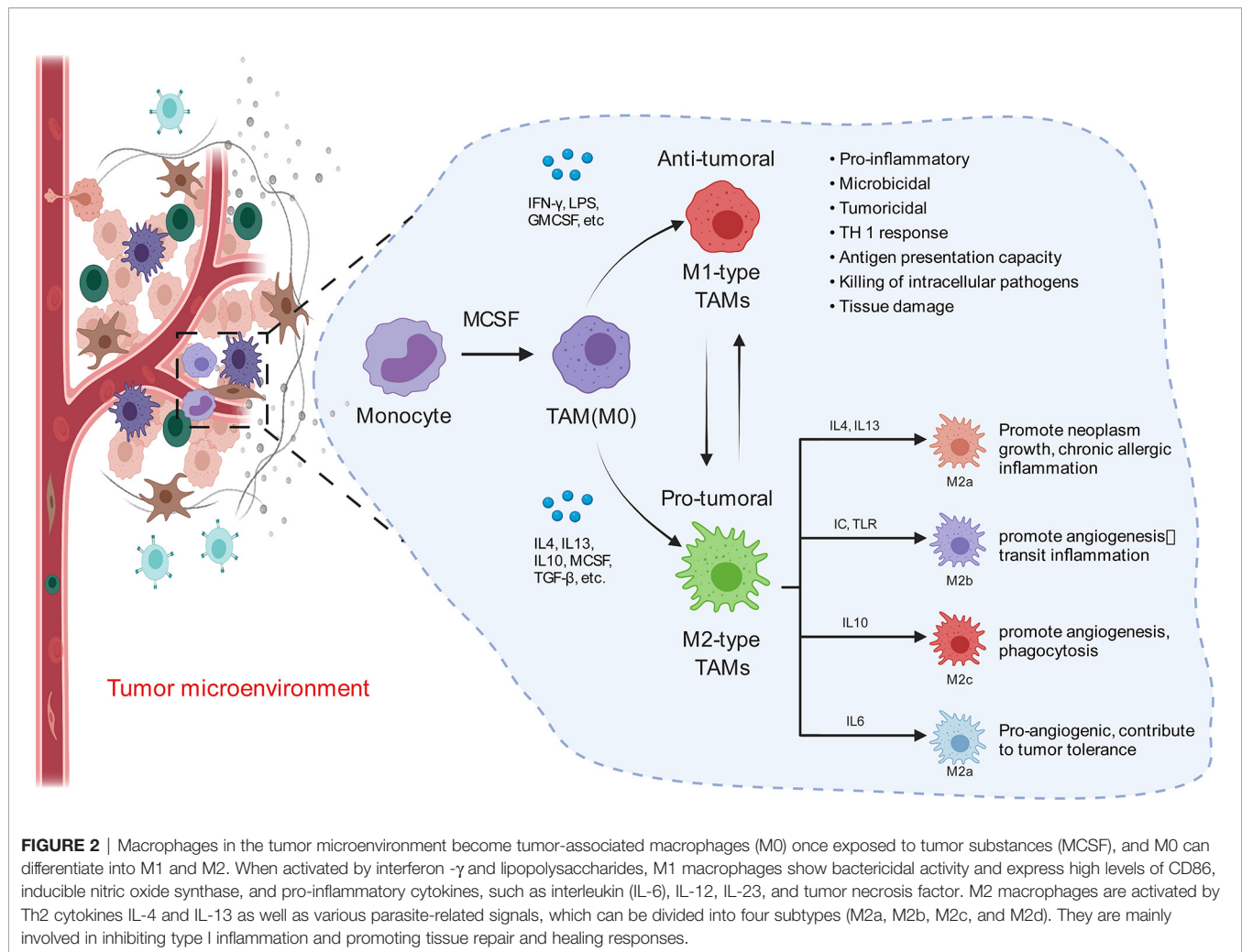
TABLE 1 | Some circRNA types in cancers.

Types	Expression	Cancers	miRNA sponges	Roles	Influence	References
circMTO1	Under-expressed	Hepatocellular carcinoma	miR-9	Tumor suppressor	It affects the expression of downstream P21 protein	(57)
circRNA cSMARCA5	Downregulated	Hepatocellular carcinoma	miR-181b-5p miR-17-3p	Tumor suppressor	It inhibits the proliferation and metastasis of the cancer by regulating TIMP3 expression	(5, 58)
circRNA circ-Ccnb1	Downregulated	Breast cancer	/	Cell death agent	It results in the induction of cell death in cancer	(62)
circGFRA1	Upregulated	Breast cancer	miR-34a ceRNA	Tumor suppressor	It regulates GFRA1 expression	(63)
circRNA f-circM9	Upregulated	Acute promyelocytic leukemia	/	Proto-oncogene	It contributes to cellular transformation in cancer	(61)
circRNA circ0006916	Downregulated	Lung cancer	miR-522-3p	Tumor suppressor	It inhibits cell proliferation by slowing down the cell cycle process	(64)
ciRS-7	Upregulated	Gastric cancer	miR-7	Tumor suppressor	It antagonizes the miR-7-mediated PTEN/PI3K/AKT pathway in gastric cancer	(59)
circ-ITCH	Upregulated	Gastric cancer	miR-199a-5p	Tumor suppressor	It affects the EMT process of gastric cancer	(60)
circCCDC66	Upregulated	Colorectal cancer	miR-33b miR-93 miR-185	Proto-oncogene	It is associated with poor cancer prognosis	(56)

prognostic value in various cancer types (72–74). Macrophages are key mediators of tissue homeostasis, while tumors upset this balance; macrophages can even become drivers of metastasis (72, 75). Macrophages are specialized phagocytes that differentiate from circulating classical monocytes after extravasation into tissues (76, 77) and express both activating and inhibiting receptors in the phagocytosis of opsonic or apoptotic cells (78). Macrophages can engulf a large number of pathogens and kill bacteria in cells (79–81). In addition to directly killing tumor cells, macrophages also serve as specialized antigen-presenting cells, which can present tumor cell-derived antigens on major histocompatibility complex (MHC) class I (82) and class II (83) molecules, thereby activating endogenous antitumor T cell responses, amplifying the therapeutic effect and reducing the risk of tumor cell escape due to antigen loss (84–86). TAMs are derived from bone marrow-derived monocytes and tissue macrophages that are recruited into and fill the TME, promoting the spread and diffusion of cancer cells (87–90). TAMs are key cells that generate immunosuppressive tumor microenvironments by producing cytokines, chemokines, and growth factors and triggering T cells to release inhibitory immune checkpoint proteins. TAMs can directly help tumor cells migrate through the paracrine ring between macrophages and tumor cells, which involves macrophages secreting epithelial growth factor (EGF) family ligands and tumor cells secreting CSF1, to improve the invasive characteristics of tumor cells (91).

Consistent with macrophages, TAMs are also highly plastic (92) and adapt to microenvironmental changes by regulating cell metabolism and reprogramming phenotypes (93, 94). TAMs enhance tumor progression by promoting genetic instability, angiogenesis, fibrosis, immunosuppression, lymphocyte rejection, invasion, and metastasis and promote the inflammatory environment by secreting cytokines, such as interleukin-17 (IL-17) and interleukin-23 (IL-23) (95, 96). Many studies have shown that TAM infiltration is closely related to tumor cell proliferation

and can express a variety of cytokines that stimulate tumor cell proliferation and survival, including EGF, platelet-derived growth factor, transforming growth factor- β 1, hepatocyte growth factor, and epidermal growth factor receptor (97, 98). **Figure 2** shows that, once monocytes from peripheral blood are recruited into the tumor, the tumor environment rapidly promotes their differentiation into TAMs (96). Initially, monocytes and macrophages are recruited to the site of tumorigenesis. Under the guidance of different microenvironmental signals, macrophages can differentiate into two functional phenotypes, namely, classical activated macrophages (M1) and alternately activated macrophages (M2). In contrast to the antitumor effects of M1, M2 has anti-inflammatory and tumorigenic properties. M2 TAMs are predominant in progressive tumors and are important regulatory cells in the TME response (99, 100). The major event in the tumor microenvironment is the polarization of macrophages into the tumor-suppressor M1 or tumor-promoting M2 macrophages. Although there is considerable evidence that TAMs are predominantly M2-like macrophages, the mechanisms by which TAMs polarize into M1 and M2 macrophages remain unclear (101). TAMs exhibit the patterns of M1 and M2 macrophages, but these cells are known to have transcriptional profiles different from those of M1 or M2 macrophages (102). However, it is certain that TAMs are related to the occurrence and development of various tumors, such as breast cancer, prostate cancer, glioma, lymphoma, bladder cancer, lung cancer, cervical cancer, and melanoma (103–105). TAMs, which are abundant in most types of malignancies, can promote tumor angiogenesis, allowing cancer cells to escape from the tumor into the circulation and inhibit anti-tumor immune mechanisms (106, 107). Some studies have shown that CSF1, IL-4, IL-13, and IL-10 can promote the polarization of M1-like TAMs to M2-like TAMs in the TME (102). Under specific conditions, the transformation of M2-like TAMs into M1-like TAMs may lead to tumor regression (108). By releasing pro-inflammatory molecules,



such as $\text{TNF-}\alpha$ and $\text{IFN-}\gamma$, activating TLR, and reducing anti-inflammatory factors (such as ARG1, $\text{TGF-}\beta$, and IL10), M1-like TAMs can promote the inflammatory response and antitumor activity of the TME (109). TAMs can antagonize, enhance, or mediate the antitumor effects of cytotoxic agents, tumor irradiation, antiangiogenic/vascular injury agents, and checkpoint inhibitors (73, 110–113).

THE RELATIONSHIP BETWEEN circRNAs AND MACROPHAGE POLARIZATION

In primary tumors, TAMs have an M1-like phenotype and can eliminate certain immunogenic tumor cells (114). However, the TME can induce the M2-like polarization of TAMs, which is the cause of the formation of primary carcinoma (111, 115). Studies have demonstrated the relationship between circRNAs and macrophages—for example, circASAP1 can act as a competing endogenous RNA (ceRNA) of miR-326 and miR-532-5p to mediate TAM infiltration, and circRNA-CDR1as may be crucial for tumor tissue immunity and cell penetration, such as CD8^+ T cells, activated

natural killer (NK) cells, and M2 macrophages (116). circASAP1 can mediate TAM osmosis by regulating the miR-326/miR-532-5P-CSF-1 pathway (117). There is no specific mechanism elucidated in this respect, which suggests that the next step is to study how circRNAs interact with tumor-associated macrophages. Studies have shown that circRNAs can regulate macrophage differentiation and polarization, while the pathways regulating macrophage polarization are not completely clear. Several molecules are involved in this process (Figure 3), such as interferon regulatory factor (IRF) and signal transducer and activator of transcription (STAT) (118, 119). Lipopolysaccharide stimulation (LPS) stimulates M1 macrophages by inducing $\text{STAT1-}\alpha$ and $\text{STAT1-}\beta$ and interacting with the receptor TLR-4 (120). circPPM1F can play an active role in the LPS-induced activation of M1 macrophages through the circPPM1F-HuR-PPM1F-NF- κ B axis (121), and circCdy can promote M1 polarization by inhibiting the entry of IRF4 into the nucleus (122). CSF-1, IL-4, IL-10, $\text{TGF-}\beta$, and IL-13 are conducive to the polarization of the M2 subgroup (123, 124). The overexpression of has-circ-0005567 inhibits the polarization of M1 macrophages and promotes the polarization of M2 macrophages (125). Compared with M2-type macrophages, circRNA-003780, circRNA-010056, and

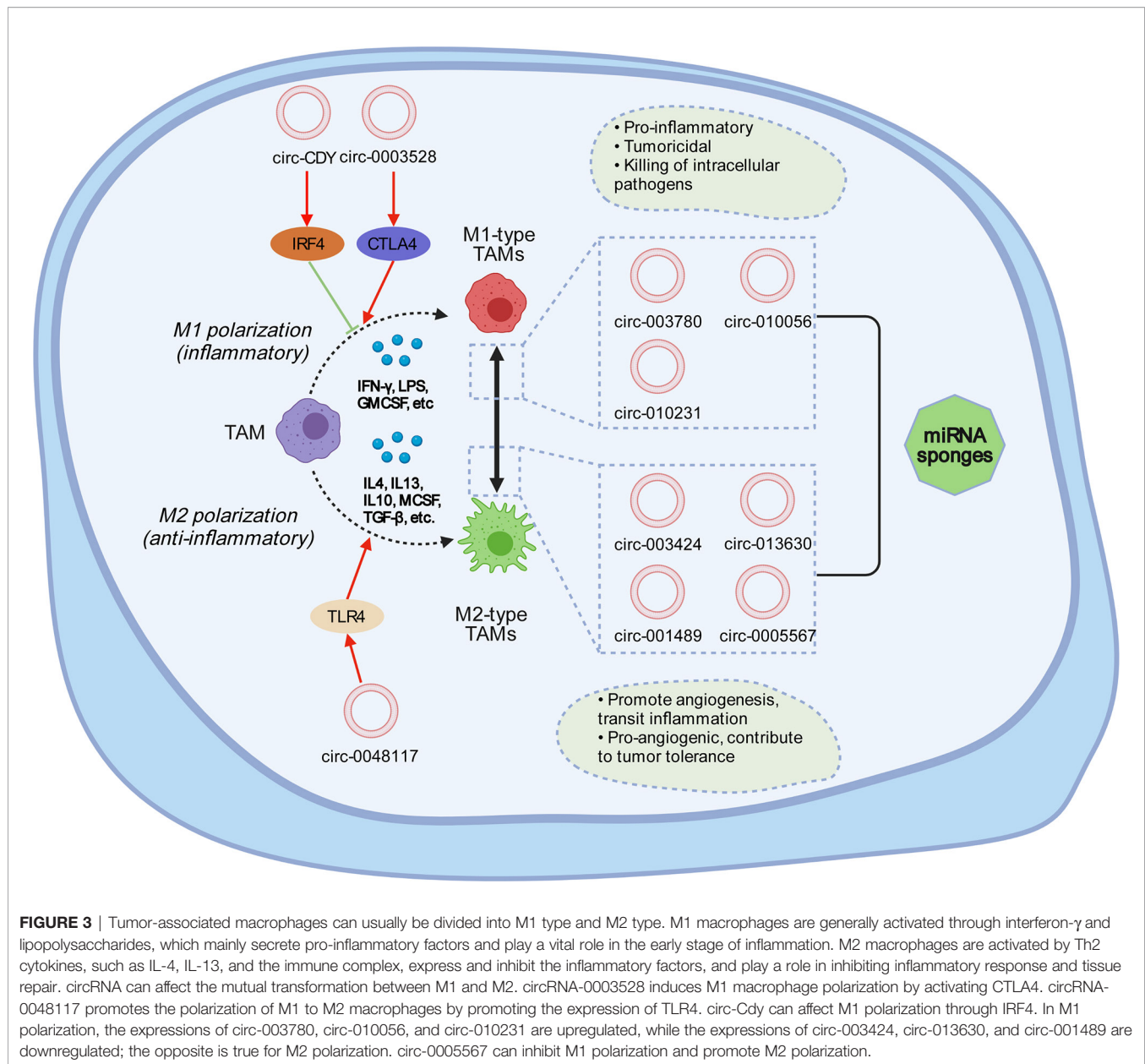


FIGURE 3 | Tumor-associated macrophages can usually be divided into M1 type and M2 type. M1 macrophages are generally activated through interferon- γ and lipopolysaccharides, which mainly secrete pro-inflammatory factors and play a vital role in the early stage of inflammation. M2 macrophages are activated by Th2 cytokines, such as IL-4, IL-13, and the immune complex, express and inhibit the inflammatory factors, and play a role in inhibiting inflammatory response and tissue repair. circRNA can affect the mutual transformation between M1 and M2. circRNA-0003528 induces M1 macrophage polarization by activating CTLA4. circRNA-0048117 promotes the polarization of M1 to M2 macrophages by promoting the expression of TLR4. circ-Cdy can affect M1 polarization through IRF4. In M1 polarization, the expressions of circ-003780, circ-010056, and circ-010231 are upregulated, while the expressions of circ-003424, circ-013630, and circ-001489 are downregulated; the opposite is true for M2 polarization. circ-0005567 can inhibit M1 polarization and promote M2 polarization.

circRNA-010231 are upregulated in M1 macrophages. However, the expression of circRNA-003424, circRNA-013630, circRNA-001489, and circRNA-018127 is downregulated (126). Studies have shown that, in general, M1 is expressed in bones, the brain, and other adult tissues, and M2 is expressed in embryonic development stages, undifferentiated tissues, and tumors (127). circ-0048117 can regulate toll-like receptor 4 (TLR4) by acting as a miR-140 sponge to promote the polarization of M2 macrophages. Studies have confirmed that the activation of TLR4 on the surface of macrophages plays an important role in macrophage differentiation (128). TLR4 is strongly expressed in lung cancer TAMs and promotes the transformation of TAMs to M2-type macrophages by promoting the oxidative phosphorylation process in mitochondrial metabolism and inhibiting the glycolysis pathway

(129). circRNA-0003528 promotes tuberculosis-associated macrophage polarization by upregulating the expression of cytotoxic T-lymphocyte-associated protein 4 (130).

Although most studies have found that circRNAs are more closely related to M2 polarization, the specific mechanism between circRNAs and M2 is not clear. Under the influence of tumor-derived factors, TAMs can secrete a series of cytokines, including IL-10, TGF- β , and prostaglandin 2 (PGE2), to further inhibit T cell-mediated immune responses and establish a self-proliferative immunosuppressive TME (72, 74). These cytokines can also affect circRNA expression. Accordingly, interleukin-10 (IL-10) can also inhibit the function of a variety of immune cells and the expression of anti-inflammatory macrophages; additionally, IL-10 can induce Tregs. Besides these, the abnormally expressed extracellular

circRNA may induce Treg cells and interact directly with immune factors to mediate immune activity and facilitate intercellular communication (131, 132). IL-10 produced by TAMs can inhibit the function of antigen-presenting cells and then block the function of T cell effects, such as cytotoxicity, to inactivate the anti-tumor response, which leads to the downregulation of circRNAs related to the tumor response, thus promoting tumor growth (133). It was found that the transformation from M2-like TAMs to M1-like TAMs can lead to tumor regression under specific conditions (134). The mutual regulation between M1-like and M2-like TAMs is achieved by signal axes, such as STAT1/STAT6 and IRF5/IRF4, which are very important for the occurrence, development, and cessation of tumor inflammation (135). This may be a potential target for the regulation of M1-like and M2-like TAM transformation in clinical cancer immunotherapy. Promoting the conversion of M2 macrophages to the M1 phenotype can become a tumor treatment method (136).

Complex interactions exist between circRNAs and key counterparts in the TME (137), which can affect a variety of physiological and pathological activities, including tumor angiogenesis (138, 139). CAE is arranged on the inner surface of tumor blood vessels and lymphatic vessels, which can support angiogenesis and tumor neovascularization (140), while circ-CDR1as is positively correlated with the CAE infiltration level (18). Endothelial cells are the key to tumor angiogenesis, and the effect of circRNA on endothelial cells can affect tumor progression (141, 142)—for example, circ-IAR can destroy the tight junctions between endothelial cells, increase the permeability of vascular endothelial cells, and promote tumor metastasis (143). Some circRNAs can induce the expression of PD-L1 in the TME and mediate the regulation of tumor immunity—for example, the upregulation of PD-L1 mediated by has-circ-0020397 can lead to the inhibition of apoptosis and the acquisition of tumor immune escape in the TME (144). In short, tumor development is generally related to M2 polarization, and circRNA is also more closely related to M2 polarization and can act with related factors in the TME. The transformation from M2 to M1 can promote tumor regression, which suggests that we can further study key targeted circRNAs to inhibit M2 polarization and promote the transformation from M2 to M1 to treat tumors.

circRNAs ARE ASSOCIATED WITH TAMs IN DIFFERENT CANCERS

TAMs infiltrate most solid tumors in large numbers and contribute to tumor progression by stimulating proliferation, angiogenesis, and metastasis and providing anti-tumor immune barriers. Co-existing with circRNAs in the TME, TAMs may establish and reshape the extracellular matrix structure by allowing tumor cells to invade through the TME. circRNAs enable TAMs to interact with tumor cells or other stromal cells by secreting growth factors, cytokines, and chemokines (72, 76). Signals from tumor cells, lymphocytes, and stromal cells affect TAM function and diversity as well as the corresponding changes in circRNA expression (145, 146). circRNAs play a key role in the development and progression of human

cancers such as lung, liver, breast, and colon cancers. Because of the large number of circRNAs, their functions may be complex and different from each other, so the functions and mechanisms of most circRNAs, such as has-circ-0014235, have not been fully identified, and little is known about the existence or effect of circRNA modification. The specific interactions between circRNAs and TAMs are also unknown. In TAMs, circPTK2 is mainly expressed in the tumor invasion frontier (M1-rich area) and stroma (M2-rich area). In contrast, circHIPK3 is mainly expressed in M2, located in the tumor nest and surrounding tumor invasion, suggesting that circRNA is closely related to tumor pathology and prognosis (147). Meanwhile, circRNAs have been found to be enriched in exosomes (4). circRNAs can specifically bind to tumor-specific miRNAs or mRNAs in exons and can be used as new tumor antigens to regulate the immune response (141). Some circRNAs can be detected in exosomes from the serum, urine, and tumors. Exosome circRNAs may be involved in cell growth, angiogenesis, epithelial-mesenchymal transformation, and targeted therapy (148, 149)—for example, circFBLIM1 carried by serum exosomes can be transferred to HCC cells, thereby promoting disease progression and suggesting that circRNA may be a biomarker of various diseases (150). In colorectal cancer, the exons secreted by M2 macrophages highly express miR-21-5p and miR-155-5p to regulate the migration and invasion of colorectal cancer cells (151). circ-BACH1 (has-circ-0061395) is significantly upregulated in HCC tissues, and p27 inhibition is regulated by HUR, which reduces circ-BACH1 to inhibit the proliferation and increase the apoptosis of HCC cells (152). Studies have shown that circASAP1 promotes the proliferation and invasion of HCC cells by regulating miR-326/miR-532-5p-MAPK1 signaling and regulates the infiltration of tumor-associated macrophages by regulating the miR-326/miR-532-5p-CSF-1 pathway (117).

High TAM infiltration is associated with a low overall survival rate in breast, gastric, oral, ovarian, bladder, and thyroid cancers but is not associated with low overall survival in colorectal cancer (CRC) (153). In bladder cancer, circPTK2 promotes the proliferation and migration of bladder tumor cells through the interaction of M2 tumor-associated macrophages (154), while circHIPK3 has been found in CRC by activating the downstream Bcl/Beclin 1 signaling pathway in the TME, thus promoting the growth and differentiation of TAMs (155). circRNA-002178 can act as a ceRNA and induce T cell depletion in lung adenocarcinoma by promoting PD-L1/PD1 expression in cancer cells with spongy miR-34 (156), which affects the polarization process of tumor-associated macrophages, as shown in **Figure 3**. Mutated p53 cancer cells can be re-transformed from macrophages to TAM through miR-1246 (157), which is beneficial for anti-inflammatory immunosuppression and the increased activities of TGF- β , while it also affects the expression of related circRNAs (158).

In TAMs, circ-0061395 competitively combines with miR-877-5p to improve the expression of PIK3R3 and promote the degree of malignancy of HCC cells. The inhibition of circWHSC1 *in vitro* can inhibit the proliferation and metastasis of HCC cells and inhibit tumorigenesis *in vivo* (159). Other studies have shown that circWHSC1, as a sponge for miR-142-3p, directly targets HOXA1, which inhibits the polarization of TAMs, while inhibiting miR-142-

3p can improve the effects of circWHSC1 gene knockdown on the proliferation and metastasis of HCC cells. The overexpression of miR-142-3p inhibits the growth and motility of HCC cells, and the elevation of HOXA1 reverses this effect (160). The overexpression of circMCTP2 in gastric cancer can restore MTMR3 expression in gastric cancer cells to cisplatin through sponging miR-99a-5p, which also affects the process of macrophage reprogramming TAMs (161). Other studies have also shown that exosomal circRNA can promote cell growth and inhibit DNA damage (162). Experimental results have shown that circPPM1F can accelerate the activation of M1 macrophages and accelerate the apoptosis of islet cells in diabetic mice (121). Therefore, further studies of exosomal circRNAs will provide a new method for the diagnosis and targeted treatment of many diseases.

CONCLUSION AND PROSPECT ON circRNAs AND TAMs

With the development of next-generation sequencing technology, an increasing number of circRNAs have been discovered. circRNAs are a novel class of non-coding endogenous RNAs with closed-loop characteristics. At present, there is no evidence that circRNAs are directly related to the differentiation of tumor-associated macrophages, but some studies have shown that they can be transformed into endogenous RNA to participate in the differentiation process. However, not all circRNAs are positively correlated with tumor-associated macrophages, and the specific correlation between them deserves further study. In general, M1 macrophages promote inflammatory responses against invading pathogens and tumor cells, while M2 macrophages tend to exhibit an immunosuppressive phenotype that is conducive to tissue repair and tumor progression. The abundance of TAMs in tumors is often related to the acquisition of tumor-specific pathological features, such as immunosuppression, neovascularization, invasiveness, metastasis, and poor response to treatment, which indirectly suggests that TAMs may have a tumor-promoting function. TAMs may affect the expression of circRNAs in various cancers, such as lung cancer, liver cancer, colon cancer, and gastric cancer.

Tumor-associated macrophages, especially those that infiltrate tumor tissues, secrete various cytokines according to their polarity and play an important role in the occurrence, invasion, and metastasis of tumors. circRNAs, on the other hand, can specifically adsorb miRNAs to be used as competitive endogenous RNAs. By enhancing exon expression, circRNAs interact with the TME to establish an immunosuppressive environment and promote tumor

cell proliferation, anti-apoptosis, invasion, and migration. Unfortunately, the cause and function of circRNA are not entirely clear; this is also true for the role of the specific mechanism between circRNAs and TAMs. However, previous studies have shown that there is little correlation between the two. Further research will help us delve into the role of circRNA and TAMs in tumor growth. The dynamic balance and interaction between TAMs and tumor cells play an important role in the occurrence and development of tumors. circRNAs can also affect TAM differentiation by influencing the TME, thus further affecting tumor growth and development. It was found that the expression of circRNAs in tumor tissues is not absolutely upregulated or downregulated; it may be upregulated in lung cancer but downregulated in breast cancer. Such contradictions make it difficult to connect the polarization of TAMs with the expression of circRNAs, but they show a correlation. Studies on the relationship between circRNAs and TAMs are still at a superficial stage, and there are not enough studies to prove a clear logical relationship between them. circRNAs have many small molecular subtypes, and the TAM polarization process involves many small molecular substances. Perhaps an algorithm can be developed to study the pairwise collocation or mixed collocation between the two to further reveal the relationship between them; this is a direction for future research. Further studies on the relationship between circRNAs and TAMs can help elucidate the role of circRNAs in the nervous system, cancer development, innate immune response, and other biological environments and diseases. circRNA is expected to become a new tumor marker and potential target, providing a new direction for tumor diagnosis and targeted therapy.

AUTHOR CONTRIBUTIONS

All authors listed have made a substantial, direct, and intellectual contribution to the work and approved it for publication.

FUNDING

This work was partially supported by the National Natural Science Foundation of China (project no. 81602167), the Hunan Provincial Natural Science Foundation of China (project no. 2017JJ3494 and 2021JJ31100), and the Science and Technology Program Foundation of Changsha City (project no. kq2004085). This work was also supported in part by the National Natural Science Foundation of China (project no. 81803636 to XY) and Guangdong Basic and Applied Basic Research Foundation (project no. 2018A0303130329 to XY).

REFERENCES

- Chen LL, Yang L. Regulation of CircRNA Biogenesis. *RNA Biol* (2015) 12:381–8. doi: 10.1080/15476286.2015.1020271
- Zhang L, Hou C, Chen C, Guo Y, Yuan W, Yin D, et al. The Role of N(6)-Methyladenosine (m6a) Modification in the Regulation of CircRNAs. *Mol Cancer* (2020) 19:105. doi: 10.1186/s12943-020-01224-3
- Du WW, Zhang C, Yang W, Yong T, Awan FM, Yang BB. Identifying and Characterizing CircRNA-Protein Interaction. *Theranostics* (2017) 7:4183–91. doi: 10.7150/thno.21299
- Wang Y, Liu J, Ma J, Sun T, Zhou Q, Wang W, et al. Exosomal CircRNAs: Biogenesis, Effect and Application in Human Diseases. *Mol Cancer* (2019) 18:116. doi: 10.1186/s12943-019-1041-z
- Yu J, Xu QG, Wang ZG, Yang Y, Zhang L, Ma JZ, et al. Circular RNA Csmar5 Inhibits Growth and Metastasis in Hepatocellular Carcinoma. *J Hepatol* (2018) 68:1214–27. doi: 10.1016/j.jhep.2018.01.012
- Hansen TB, Kjems J, Damgaard CK. Circular RNA and Mir-7 in Cancer. *Cancer Res* (2013) 73:5609–12. doi: 10.1158/0008-5472.CAN-13-1568
- Wang R, Zhang S, Chen X, Li N, Li J, Jia R, et al. Circnt5e Acts as a Sponge of MiR-422a to Promote Glioblastoma Tumorigenesis.

- Cancer Res* (2018) 78:4812–25. doi: 10.1158/0008-5472.CAN-18-0532
8. Salzman J, Chen RE, Olsen MN, Wang PL, Brown PO. Cell-Type Specific Features of Circular RNA Expression. *PLoS Genet* (2013) 9:e1003777. doi: 10.1371/journal.pgen.1003777
 9. Zhao W, Dong M, Pan J, Wang Y, Zhou J, Ma J, et al. Circular RNAs: A Novel Target Among Non-Coding RNAs With Potential Roles in Malignant Tumors (Review). *Mol Med Rep* (2019) 20:3463–74. doi: 10.3892/mmr.2019.10637
 10. Belli C, Trapani D, Viale G, D'Amico P, Duso BA, Della Vigna P, et al. Targeting the Microenvironment in Solid Tumors. *Cancer Treat Rev* (2018) 65:22–32. doi: 10.1016/j.ctrv.2018.02.004
 11. Quail DF, Joyce JA. Microenvironmental Regulation of Tumor Progression and Metastasis. *Nat Med* (2013) 19:1423–37. doi: 10.1038/nm.3394
 12. Ringuette Goulet C, Bernard G, Tremblay S, Chabaud S, Bolduc S, Pouliot F. Exosomes Induce Fibroblast Differentiation Into Cancer-Associated Fibroblasts Through Tgf β Signaling. *Mol Cancer Res: MCR* (2018) 16:1196–204. doi: 10.1158/1541-7786.MCR-17-0784
 13. Natua S, Dhamdhare SG, Mutnuru SA, Shukla S. Interplay Within Tumor Microenvironment Orchestrates Neoplastic RNA Metabolism and Transcriptome Diversity. *Wiley Interdisciplinary Reviews. RNA* (2021) 2021:e1676. doi: 10.1002/wrna.1676
 14. Zhang Q, Wang W, Zhou Q, Chen C, Yuan W, Liu J, et al. Roles of CircRNAs in the Tumour Microenvironment. *Mol Cancer* (2020) 19:14. doi: 10.1186/s12943-019-1125-9
 15. Chen LL. The Expanding Regulatory Mechanisms and Cellular Functions of Circular RNAs. *Nat Rev Mol Cell Biol* (2020) 21:475–90. doi: 10.1038/s41580-020-0243-y
 16. Yang K, Zhang J, Bao C. Exosomal CircRNA From Cancer-Associated Fibroblast Promotes Colorectal Cancer (CRC) Progression via MiR-214/PD-L1 Axis. *BMC Cancer* (2021) 21:933. doi: 10.1186/s12885-021-08669-9
 17. Liu G, Sun J, Yang ZF, Zhou C, Zhou PY, Guan RY, et al. Cancer-Associated Fibroblast-Derived CXCL11 Modulates Hepatocellular Carcinoma Cell Migration and Tumor Metastasis Through the Circubap2/Mir-4756/IFIT1/3 Axis. *Cell Death Dis* (2021) 12:260. doi: 10.1038/s41419-021-03545-7
 18. Zou Y, Zheng S, Deng X, Yang A, Xie X, Tang H, et al. The Role of Circular RNA CDR1as/Circ-7 in Regulating Tumor Microenvironment: A Pan-Cancer Analysis. *Biomolecules* (2019) 9:429. doi: 10.3390/biom9090429
 19. Yu T, Wang Y, Fan Y, Fang N, Wang T, Xu T, et al. CircRNAs in Cancer Metabolism: A Review. *J Hematol Oncol* (2019) 12:90. doi: 10.1186/s13045-019-0776-8
 20. Greene J, Baird AM, Brady L, Lim M, Gray SG, McDermott R, et al. Circular RNAs: Biogenesis, Function and Role in Human Diseases. *Front Mol Biosci* (2017) 4:38. doi: 10.3389/fmolb.2017.00038
 21. Panni S, Lovering RC, Porras P, Orchard S. Non-Coding RNA Regulatory Networks. *Biochim Biophys Acta Gene Regul Mech* (2020) 1863:194417. doi: 10.1016/j.bbagr.2019.194417
 22. Salzman J, Gawad C, Wang PL, Lacayo N, Brown PO. Circular RNAs Are the Predominant Transcript Isoform From Hundreds of Human Genes in Diverse Cell Types. *PLoS One* (2012) 7:e30733. doi: 10.1371/journal.pone.0030733
 23. Memczak S, Jens M, Elefsinioti A, Torti F, Krueger J, Rybak A, et al. Circular RNAs Are a Large Class of Animal RNAs With Regulatory Potency. *Nature* (2013) 495:333–8. doi: 10.1038/nature11928
 24. Li P, Chen S, Chen H, Mo X, Li T, Shao Y, et al. Using Circular RNA as a Novel Type of Biomarker in the Screening of Gastric Cancer. *Clinica Chimica Acta; Int J Clin Chem* (2015) 444:132–6. doi: 10.1016/j.cca.2015.02.018
 25. Wilusz JE. Circular RNAs: Unexpected Outputs of Many Protein-Coding Genes. *RNA Biol* (2017) 14:1007–17. doi: 10.1080/15476286.2016.1227905
 26. Ebbesen KK, Kjems J, Hansen TB. Circular RNAs: Identification, Biogenesis and Function. *Biochim Biophys Acta* (2016) 1859:163–8. doi: 10.1016/j.bbagr.2015.07.007
 27. Sun J, Li B, Shu C, Ma Q, Wang J. Functions and Clinical Significance of Circular RNAs in Glioma. *Mol Cancer* (2020) 19:34. doi: 10.1186/s12943-019-1121-0
 28. Goodall GJ, Wickramasinghe VO. RNA in Cancer. *Nat Rev Cancer* (2021) 21:22–36. doi: 10.1038/s41568-020-00306-0
 29. Jeck WR, Sorrentino JA, Wang K, Slevin MK, Burd CE, Liu J, et al. Circular RNAs Are Abundant, Conserved, and Associated With ALU Repeats. *RNA (New York NY)* (2013) 19:141–57. doi: 10.1261/rna.035667.112
 30. Zhang XO, Wang HB, Zhang Y, Lu X, Chen LL, Yang L. Complementary Sequence-Mediated Exon Circularization. *Cell* (2014) 159:134–47. doi: 10.1016/j.cell.2014.09.001
 31. Zhou WY, Cai ZR, Liu J, Wang DS, Ju HQ, Xu RH. Circular RNA: Metabolism, Functions and Interactions With Proteins. *Mol Cancer* (2020) 19:172. doi: 10.1186/s12943-020-01286-3
 32. Zhang HD, Jiang LH, Sun DW, Hou JC, Ji ZL. CircRNA: A Novel Type of Biomarker for Cancer. *Breast Cancer* (2018) 25:1–7. doi: 10.1007/s12282-017-0793-9
 33. Nair AA, Niu N, Tang X, Thompson KJ, Wang L, Kocher JP, et al. Circular RNAs and Their Associations With Breast Cancer Subtypes. *Oncotarget* (2016) 7:80967–79. doi: 10.18632/oncotarget.13134
 34. Zang J, Lu D, Xu A. The Interaction of CircRNAs and RNA Binding Proteins: An Important Part of CircRNA Maintenance and Function. *J Neurosci Res* (2020) 98:87–97. doi: 10.1002/jnr.24356
 35. Li Z, Huang C, Bao C, Chen L, Lin M, Wang X, et al. Exon-Intron Circular RNAs Regulate Transcription in the Nucleus. *Nat Struct Mol Biol* (2015) 22:256–64. doi: 10.1038/nsmb.2959
 36. Lu Z, Filonov GS, Noto JJ, Schmidt CA, Hatkevich TL, Wen Y, et al. Metazoan tRNA Introns Generate Stable Circular RNAs *In Vivo*. *RNA (New York NY)* (2015) 21:1554–65. doi: 10.1261/rna.052944.115
 37. Wang F, Nazarali AJ, Ji S. Circular RNAs as Potential Biomarkers for Cancer Diagnosis and Therapy. *Am J Cancer Res* (2016) 6:1167–76.
 38. Schmidt CA, Giusto JD, Bao A, Hopper AK, Matera AG. Molecular Determinants of Metazoan TricrRNA Biogenesis. *Nucleic Acids Res* (2019) 47:6452–65. doi: 10.1093/nar/gkz311
 39. Suzuki H, Tsukahara T. A View of Pre-mRNA Splicing From RNase R Resistant RNAs. *Int J Mol Sci* (2014) 15:9331–42. doi: 10.3390/ijms15069331
 40. Wang PL, Bao Y, Yee MC, Barrett SP, Hogan GJ, Olsen MN, et al. Circular RNA Is Expressed Across the Eukaryotic Tree of Life. *PLoS One* (2014) 9:e90859. doi: 10.1371/journal.pone.0090859
 41. Rybak-Wolf A, Stottmeister C, Glažar P, Jens M, Pino N, Giusti S, et al. Circular RNAs in the Mammalian Brain Are Highly Abundant, Conserved, and Dynamically Expressed. *Mol Cell* (2015) 58:870–85. doi: 10.1016/j.molcel.2015.03.027
 42. Hansen TB, Jensen TI, Clausen BH, Bramsen JB, Finsen B, Damgaard CK, et al. Natural RNA Circles Function as Efficient MicroRNA Sponges. *Nature* (2013) 495:384–8. doi: 10.1038/nature11993
 43. Du WW, Yang W, Liu E, Yang Z, Dhaliwal P, Yang BB. Foxo3 Circular RNA Retards Cell Cycle Progression via Forming Ternary Complexes With P21 and CDK2. *Nucleic Acids Res* (2016) 44:2846–58. doi: 10.1093/nar/gkw027
 44. Legnini I, Di Timoteo G, Rossi F, Morlando M, Briganti F, Standider O, et al. Circ-ZNF609 Is a Circular RNA That can be Translated and Functions in Myogenesis. *Mol Cell* (2017) 66:22–37.e29. doi: 10.1016/j.molcel.2017.02.017
 45. Lu D, Xu AD. Mini Review: Circular RNAs as Potential Clinical Biomarkers for Disorders in the Central Nervous System. *Front Genet* (2016) 7:53. doi: 10.3389/fgene.2016.00053
 46. Zhang Y, Zhang XO, Chen T, Xiang JF, Yin QF, Xing YH, et al. Circular Intronic Long Noncoding RNAs. *Mol Cell* (2013) 51:792–806. doi: 10.1016/j.molcel.2013.08.017
 47. You X, Vlatkovic I, Babic A, Will T, Epstein I, Tushev G, et al. Neural Circular RNAs Are Derived From Synaptic Genes and Regulated by Development and Plasticity. *Nat Neurosci* (2015) 18:603–10. doi: 10.1038/nn.3975
 48. Li J, Sun D, Pu W, Wang J, Peng Y. Circular RNAs in Cancer: Biogenesis, Function, and Clinical Significance. *Trends Cancer* (2020) 6:319–36. doi: 10.1016/j.trecan.2020.01.012
 49. Wu P, Mo Y, Peng M, Tang T, Zhong Y, Deng X, et al. Emerging Role of Tumor-Related Functional Peptides Encoded by LncRNA and CircRNA. *Mol Cancer* (2020) 19:22. doi: 10.1186/s12943-020-1147-3
 50. Jin D, Wu X, Yu H, Jiang L, Zhou P, Yao X, et al. Systematic Analysis of LncRNAs, mRNAs, CircRNAs and MiRNAs in Patients With Postmenopausal Osteoporosis. *Am J Trans Res* (2018) 10:1498–510.
 51. Yang Y, Yujiao W, Fang W, Linhui Y, Ziqi G, Zhichen W, et al. The Roles of MiRNA, LncRNA and CircRNA in the Development of Osteoporosis. *Biol Res* (2020) 53:40. doi: 10.1186/s40659-020-00309-z
 52. Kristensen LS, Andersen MS, Stagsted LWV, Ebbesen KK, Hansen TB, Kjems J. The Biogenesis, Biology and Characterization of Circular RNAs. *Nat Rev Genet* (2019) 20:675–91. doi: 10.1038/s41576-019-0158-7

53. Lei M, Zheng G, Ning Q, Zheng J, Dong D. Translation and Functional Roles of Circular RNAs in Human Cancer. *Mol Cancer* (2020) 19:30. doi: 10.1186/s12943-020-1135-7
54. Chen X, Yang T, Wang W, Xi W, Zhang T, Li Q, et al. Circular RNAs in Immune Responses and Immune Diseases. *Theranostics* (2019) 9:588–607. doi: 10.7150/thno.29678
55. Prats AC, David F, Diallo LH, Roussel E, Tatin F, Garmy-Susini B, et al. Circular RNA, the Key for Translation. *Int J Mol Sci* (2020) 21:8591. doi: 10.3390/ijms21228591
56. Hsiao KY, Lin YC, Gupta SK, Chang N, Yen L, Sun HS, et al. Noncoding Effects of Circular RNA CCDC66 Promote Colon Cancer Growth and Metastasis. *Cancer Res* (2017) 77:2339–50. doi: 10.1158/0008-5472.CAN-16-1883
57. Han D, Li J, Wang H, Su X, Hou J, Gu Y, et al. Circular RNA Circmtol Acts as the Sponge of MicroRNA-9 to Suppress Hepatocellular Carcinoma Progression. *Hepatol (Baltimore Md)* (2017) 66:1151–64. doi: 10.1002/hep.29270
58. Barbagallo D, Caponnetto A, Brex D, Mirabella F, Barbagallo C, Lauretta G, et al. Circsmar5 Regulates VEGFA Mrna Splicing and Angiogenesis in Glioblastoma Multiforme Through the Binding of SRSF1. *Cancers* (2019) 11:194. doi: 10.3390/cancers11020194
59. Pan H, Li T, Jiang Y, Pan C, Ding Y, Huang Z, et al. Overexpression of Circular RNA Cirs-7 Abrogates the Tumor Suppressive Effect of MiR-7 on Gastric Cancer via PTEN/PI3K/AKT Signaling Pathway. *J Cell Biochem* (2018) 119:440–6. doi: 10.1002/jcb.26201
60. Wang Y, Wang H, Zheng R, Wu P, Sun Z, Chen J, et al. Circular RNA ITCH Suppresses Metastasis of Gastric Cancer via Regulating MiR-199a-5p/Klotho Axis. *Cell Cycle (Georgetown Tex)* (2021) 20:522–36. doi: 10.1080/15384101.2021.1878327
61. Shang Q, Yang Z, Jia R, Ge S. The Novel Roles of CircRNAs in Human Cancer. *Mol Cancer* (2019) 18:6. doi: 10.1186/s12943-018-0934-6
62. Fang L, Du WW, Lyu J, Dong J, Zhang C, Yang W, et al. Enhanced Breast Cancer Progression by Mutant P53 Is Inhibited by the Circular RNA Circ-Ccnb1. *Cell Death Differ* (2018) 25:2195–208. doi: 10.1038/s41418-018-0115-6
63. He R, Liu P, Xie X, Zhou Y, Liao Q, Xiong W, et al. Circgfra1 and GFRA1 Act as Cernas in Triple Negative Breast Cancer by Regulating MiR-34a. *J Exp Clin Cancer Res: CR* (2017) 36:145. doi: 10.1186/s13046-017-0614-1
64. Dai X, Zhang N, Cheng Y, Yang T, Chen Y, Liu Z, et al. RNA-Binding Protein Trinucleotide Repeat-Containing 6A Regulates the Formation of Circular RNA Circ0006916, With Important Functions in Lung Cancer Cells. *Carcinogenesis* (2018) 39:981–92. doi: 10.1093/carcin/bgy061
65. Ojha R, Nandani R, Chatterjee N, Prajapati VK. Emerging Role of Circular RNAs as Potential Biomarkers for the Diagnosis of Human Diseases. *Adv Exp Med Biol* (2018) 1087:141–57. doi: 10.1007/978-981-13-1426-1_12
66. Qian Z, Liu H, Li M, Shi J, Li N, Zhang Y, et al. Potential Diagnostic Power of Blood Circular RNA Expression in Active Pulmonary Tuberculosis. *EBioMedicine* (2018) 27:18–26. doi: 10.1016/j.ebiom.2017.12.007
67. Wang M, Zhao J, Zhang L, Wei F, Lian Y, Wu Y, et al. Role of Tumor Microenvironment in Tumorigenesis. *J Cancer* (2017) 8:761–73. doi: 10.7150/jca.17648
68. Whiteside TL. The Tumor Microenvironment and Its Role in Promoting Tumor Growth. *Oncogene* (2008) 27:5904–12. doi: 10.1038/onc.2008.271
69. Wang J, De Veirman K, Faict S, Frassanito MA, Ribatti D, Vacca A, et al. Multiple Myeloma Exosomes Establish a Favourable Bone Marrow Microenvironment With Enhanced Angiogenesis and Immunosuppression. *J Pathol* (2016) 239:162–73. doi: 10.1002/path.4712
70. Li J, Nabet BY. Exosomes in the Tumor Microenvironment as Mediators of Cancer Therapy Resistance. *Mol Cancer* (2019) 18:32. doi: 10.1186/s12943-019-0975-5
71. Mehla K, Singh PK. Metabolic Regulation of Macrophage Polarization in Cancer. *Trends Cancer* (2019) 5:822–34. doi: 10.1016/j.trecan.2019.10.007
72. Noy R, Pollard JW. Tumor-Associated Macrophages: From Mechanisms to Therapy. *Immunity* (2014) 41:49–61. doi: 10.1016/j.immuni.2014.06.010
73. Guerriero JL. Macrophages: The Road Less Traveled, Changing Anticancer Therapy. *Trends Mol Med* (2018) 24:472–89. doi: 10.1016/j.molmed.2018.03.006
74. De Palma M, Lewis CE. Macrophage Regulation of Tumor Responses to Anticancer Therapies. *Cancer Cell* (2013) 23:277–86. doi: 10.1016/j.ccr.2013.02.013
75. Yan S, Wan G. Tumor-Associated Macrophages in Immunotherapy. *FEBS J* (2021) 288:6174–86. doi: 10.1111/febs.15726
76. Gonzalez H, Hagerling C, Werb Z. Roles of the Immune System in Cancer: From Tumor Initiation to Metastatic Progression. *Genes Dev* (2018) 32:1267–84. doi: 10.1101/gad.314617.118
77. Ngambenjawong C, Gustafson HH, Pun SH. Progress in Tumor-Associated Macrophage (TAM)-Targeted Therapeutics. *Adv Drug Deliv Rev* (2017) 114:206–21. doi: 10.1016/j.addr.2017.04.010
78. Nimmerjahn F, Gordon S, Lux A. FcγR Dependent Mechanisms of Cytotoxic, Agonistic, and Neutralizing Antibody Activities. *Trends Immunol* (2015) 36:325–36. doi: 10.1016/j.it.2015.04.005
79. Andrade MR, Amaral EP, Ribeiro SC, Almeida FM, Peres TV, Lanes V, et al. Pathogenic Mycobacterium Bovis Strains Differ in Their Ability to Modulate the Proinflammatory Activation Phenotype of Macrophages. *BMC Microbiol* (2012) 12:166. doi: 10.1186/1471-2180-12-166
80. Nairz M, Schleicher U, Schroll A, Sonnweber T, Theurl I, Ludwiczek S, et al. Nitric Oxide-Mediated Regulation of Ferroptin-1 Controls Macrophage Iron Homeostasis and Immune Function in Salmonella Infection. *J Exp Med* (2013) 210:855–73. doi: 10.1084/jem.20121946
81. Podinovskaia M, Lee W, Caldwell S, Russell DG. Infection of Macrophages With Mycobacterium Tuberculosis Induces Global Modifications to Phagosomal Function. *Cell Microbiol* (2013) 15:843–59. doi: 10.1111/cmi.12092
82. Schliehe C, Redaelli C, Engelhardt S, Fehlings M, Mueller M, van Rooijen N, et al. CD8⁺ Dendritic Cells and Macrophages Cross-Present Poly(D,L-Lactate-Co-Glycolate) Acid Microsphere-Encapsulated Antigen *In Vivo*. *J Immunol (Baltimore Md: 1950)* (2011) 187:2112–21. doi: 10.4049/jimmunol.1002084
83. Abès R, Gélizé E, Fridman WH, Teillaud JL. Long-Lasting Antitumor Protection by Anti-CD20 Antibody Through Cellular Immune Response. *Blood* (2010) 116:926–34. doi: 10.1182/blood-2009-10-248609
84. Gül N, Babes L, Siegmund K, Korthouwer R, Bögel M, Braster R, et al. Macrophages Eliminate Circulating Tumor Cells After Monoclonal Antibody Therapy. *J Clin Invest* (2014) 124:812–23. doi: 10.1172/JCI66776
85. Anderson NR, Minutolo NG, Gill S, Klichinsky M. Macrophage-Based Approaches for Cancer Immunotherapy. *Cancer Res* (2021) 81:1201–8. doi: 10.1158/0008-5472.CAN-20-2990
86. Wynn TA, Chawla A, Pollard JW. Macrophage Biology in Development, Homeostasis and Disease. *Nature* (2013) 496:445–55. doi: 10.1038/nature12034
87. Ostuni R, Kratochvill F, Murray PJ, Natoli G. Macrophages and Cancer: From Mechanisms to Therapeutic Implications. *Trends Immunol* (2015) 36:229–39. doi: 10.1016/j.it.2015.02.004
88. Fu LQ, Du WL, Cai MH, Yao JY, Zhao YY, Mou XZ. The Roles of Tumor-Associated Macrophages in Tumor Angiogenesis and Metastasis. *Cell Immunol* (2020) 353:104119. doi: 10.1016/j.cellimm.2020.104119
89. Movahedi K, Laoui D, Gysemans C, Baeten M, Stangé G, Van den Bossche J, et al. Different Tumor Microenvironments Contain Functionally Distinct Subsets of Macrophages Derived From Ly6C(High) Monocytes. *Cancer Res* (2010) 70:5728–39. doi: 10.1158/0008-5472.CAN-09-4672
90. Kes MMG, Van den Bossche J, Griffioen AW, Huijbers EJM. Oncometabolites Lactate and Succinate Drive Pro-Angiogenic Macrophage Response in Tumors. *Biochim Biophys Acta Rev Cancer* (2020) 1874:188427. doi: 10.1016/j.bbcan.2020.188427
91. Cassetta L, Pollard JW. Targeting Macrophages: Therapeutic Approaches in Cancer. *Nat Rev Drug Discov* (2018) 17:887–904. doi: 10.1038/nrd.2018.169
92. Varol C, Mildner A, Jung S. Macrophages: Development and Tissue Specialization. *Annu Rev Immunol* (2015) 33:643–75. doi: 10.1146/annurev-immunol-032414-112220
93. Mantuano NR, Oliveira-Nunes MC, Alisson-Silva F, Dias WB, Todeschini AR. Emerging Role of Glycosylation in the Polarization of Tumor-Associated Macrophages. *Pharmacol Res* (2019) 146:104285. doi: 10.1016/j.phrs.2019.104285
94. Cortese N, Carriero R, Laghi L, Mantovani A, Marchesi F. Prognostic Significance of Tumor-Associated Macrophages: Past, Present and Future. *Semin Immunol* (2020) 48:101408. doi: 10.1016/j.smim.2020.101408
95. Grivennikov SI, Wang K, Mucida D, Stewart CA, Schnabl B, Jauch D, et al. Adenoma-Linked Barrier Defects and Microbial Products Drive IL-23/IL-

- 17-Mediated Tumour Growth. *Nature* (2012) 491:254–8. doi: 10.1038/nature11465
96. Yang L, Zhang Y. Tumor-Associated Macrophages: From Basic Research to Clinical Application. *J Hematol Oncol* (2017) 10:58. doi: 10.1186/s13045-017-0430-2
97. Yin M, Li X, Tan S, Zhou HJ, Ji W, Bellone S, et al. Tumor-Associated Macrophages Drive Spheroid Formation During Early Transcoelomic Metastasis of Ovarian Cancer. *J Clin Invest* (2016) 126:4157–73. doi: 10.1172/JCI87252
98. Pan Y, Yu Y, Wang X, Zhang T. Tumor-Associated Macrophages in Tumor Immunity. *Front Immunol* (2020) 11:583084. doi: 10.3389/fimmu.2020.583084
99. Yang Q, Guo N, Zhou Y, Chen J, Wei Q, Han M. The Role of Tumor-Associated Macrophages (Tams) in Tumor Progression and Relevant Advance in Targeted Therapy. *Acta Pharm Sin B* (2020) 10:2156–70. doi: 10.1016/j.apsb.2020.04.004
100. Kim J, Bae JS. Tumor-Associated Macrophages and Neutrophils in Tumor Microenvironment. *Mediators Inflamm* (2016) 2016:6058147. doi: 10.1155/2016/6058147
101. Malekghasemi S, Majidi J, Baghbanzadeh A, Abdolalizadeh J, Baradaran B, Aghebati-Maleki L. Tumor-Associated Macrophages: Protumoral Macrophages in Inflammatory Tumor Microenvironment. *Adv Pharm Bull* (2020) 10:556–65. doi: 10.34172/apb.2020.066
102. Chávez-Galán L, Olleros ML, Vesin D, García I. Much More Than M1 and M2 Macrophages, There Are Also CD169(+) and TCR(+) Macrophages. *Front Immunol* (2015) 6:263. doi: 10.3389/fimmu.2015.00263
103. Wang N, Wang S, Wang X, Zheng Y, Yang B, Zhang J, et al. Research Trends in Pharmacological Modulation of Tumor-Associated Macrophages. *Clin Transl Med* (2021) 11:e288. doi: 10.1002/ctm2.288
104. Cheng Y, Song S, Wu P, Lyu B, Qin M, Sun Y, et al. Tumor Associated Macrophages and Tams-Based Anti-Tumor Nanomedicines. *Adv Healthc Mater* (2021) 2021:e2100590. doi: 10.1002/adhm.202100590
105. Mukhtar RA, Nseyo O, Campbell MJ, Esserman LJ. Tumor-Associated Macrophages in Breast Cancer as Potential Biomarkers for New Treatments and Diagnostics. *Expert Rev Mol Diagnostics* (2011) 11:91–100. doi: 10.1586/erm.10.97
106. Pathria P, Louis TL, Varner JA. Targeting Tumor-Associated Macrophages in Cancer. *Trends Immunol* (2019) 40:310–27. doi: 10.1016/j.it.2019.02.003
107. Chen D, Zhang X, Li Z, Zhu B. Metabolic Regulatory Crosstalk Between Tumor Microenvironment and Tumor-Associated Macrophages. *Theranostics* (2021) 11:1016–30. doi: 10.7150/thno.51777
108. Hoves S, Ooi CH, Wolter C, Sade H, Bissinger S, Schmittnaegel M, et al. Rapid Activation of Tumor-Associated Macrophages Boosts Preexisting Tumor Immunity. *J Exp Med* (2018) 215:859–76. doi: 10.1084/jem.20171440
109. Zhou K, Cheng T, Zhan J, Peng X, Zhang Y, Wen J, et al. Targeting Tumor-Associated Macrophages in the Tumor Microenvironment. *Oncol Lett* (2020) 20:234. doi: 10.3892/ol.2020.12097
110. Long KB, Collier AI, Beatty GL. Macrophages: Key Orchestrators of a Tumor Microenvironment Defined by Therapeutic Resistance. *Mol Immunol* (2019) 110:3–12. doi: 10.1016/j.molimm.2017.12.003
111. Mantovani A, Marchesi F, Malesci A, Laghi L, Allavena P. Tumour-Associated Macrophages as Treatment Targets in Oncology. *Nat Rev Clin Oncol* (2017) 14:399–416. doi: 10.1038/nrclinonc.2016.217
112. Yang M, McKay D, Pollard JW, Lewis CE. Diverse Functions of Macrophages in Different Tumor Microenvironments. *Cancer Res* (2018) 78:5492–503. doi: 10.1158/0008-5472.CAN-18-1367
113. Chen C, Liu JM, Luo YP. MicroRNAs in Tumor Immunity: Functional Regulation in Tumor-Associated Macrophages. *J Zhejiang Univ Sci B* (2020) 21:12–28. doi: 10.1631/jzus.B1900452
114. Myers KV, Amend SR, Pienta KJ. Targeting Tyro3, Axl and MerTK (TAM Receptors): Implications for Macrophages in the Tumor Microenvironment. *Mol Cancer* (2019) 18:94. doi: 10.1186/s12943-019-1022-2
115. Vesely MD, Kershaw MH, Schreiber RD, Smyth MJ. Natural Innate and Adaptive Immunity to Cancer. *Annu Rev Immunol* (2011) 29:235–71. doi: 10.1146/annurev-immunol-031210-101324
116. Li X, Yao W, Yuan Y, Chen P, Li B, Li J, et al. Targeting of Tumour-Infiltrating Macrophages via CCL2/CCR2 Signalling as a Therapeutic Strategy Against Hepatocellular Carcinoma. *Gut* (2017) 66:157–67. doi: 10.1136/gutjnl-2015-310514
117. Hu ZQ, Zhou SL, Li J, Zhou ZJ, Wang PC, Xin HY, et al. Circular RNA Sequencing Identifies Circasap1 as a Key Regulator in Hepatocellular Carcinoma Metastasis. *Hepatol (Baltimore Md)* (2020) 72:906–22. doi: 10.1002/hep.31068
118. Shuai K, Stark GR, Kerr IM, Darnell JE Jr. A Single Phosphotyrosine Residue of Stat91 Required for Gene Activation by Interferon-Gamma. *Sci (New York NY)* (1993) 261:1744–6. doi: 10.1126/science.7690989
119. Zhong Z, Wen Z, Darnell JE Jr. Stat3: A STAT Family Member Activated by Tyrosine Phosphorylation in Response to Epidermal Growth Factor and Interleukin-6. *Sci (New York NY)* (1994) 264:95–8. doi: 10.1126/science.8140422
120. Toshchakov V, Jones BW, Perera PY, Thomas K, Cody MJ, Zhang S, et al. TLR4, But Not TLR2, Mediates IFN-Beta-Induced STAT1alpha/Beta-Dependent Gene Expression in Macrophages. *Nat Immunol* (2002) 3:392–8. doi: 10.1038/ni774
121. Zhang C, Han X, Yang L, Fu J, Sun C, Huang S, et al. Circular RNA Circppm1f Modulates M1 Macrophage Activation and Pancreatic Islet Inflammation in Type 1 Diabetes Mellitus. *Theranostics* (2020) 10:10908–24. doi: 10.7150/thno.48264
122. Song H, Yang Y, Sun Y, Wei G, Zheng H, Chen Y, et al. Circular RNA Cdy1 Promotes Abdominal Aortic Aneurysm Formation by Inducing M1 Macrophage Polarization and M1-Type Inflammation. *Mol therapy: J Am Soc Gene Ther* (2021) S1525-0016(21):00472–X. doi: 10.1016/j.ymthe.2021.09.017
123. Jenkins SJ, Ruckerl D, Thomas GD, Hewitson JP, Duncan S, Brombacher F, et al. IL-4 Directly Signals Tissue-Resident Macrophages to Proliferate Beyond Homeostatic Levels Controlled by CSF-1. *J Exp Med* (2013) 210:2477–91. doi: 10.1084/jem.20121999
124. Murray PJ, Allen JE, Biswas SK, Fisher EA, Gilroy DW, Goerdt S, et al. Macrophage Activation and Polarization: Nomenclature and Experimental Guidelines. *Immunity* (2014) 41:14–20. doi: 10.1016/j.immuni.2014.06.008
125. Zhang J, Cheng F, Rong G, Tang Z, Gui B. Circular RNA Hsa_Circ_0005567 Overexpression Promotes M2 Type Macrophage Polarization Through Mir-492/SOCS2 Axis to Inhibit Osteoarthritis Progression. *Bioengineered* (2021) 12(1):8920–30. doi: 10.1080/21655979.2021.1989999
126. Zhang Y, Zhang Y, Li X, Zhang M, Lv K. Microarray Analysis of Circular RNA Expression Patterns in Polarized Macrophages. *Int J Mol Med* (2017) 39:373–9. doi: 10.3892/ijmm.2017.2852
127. Zhu S, Guo Y, Zhang X, Liu H, Yin M, Chen X, et al. Pyruvate Kinase M2 (PKM2) in Cancer and Cancer Therapeutics. *Cancer Lett* (2021) 503:240–8. doi: 10.1016/j.canlet.2020.11.018
128. Lu Q, Wang X, Zhu J, Fei X, Chen H, Li C. Hypoxic Tumor-Derived Exosomal Circ0048117 Facilitates M2 Macrophage Polarization Acting as MiR-140 Sponge in Esophageal Squamous Cell Carcinoma. *Oncotargets Ther* (2020) 13:11883–97. doi: 10.2147/OTT.S284192
129. Liu WT, Jing YY, Yu GF, Han ZP, Yu DD, Fan QM, et al. Toll Like Receptor 4 Facilitates Invasion and Migration as a Cancer Stem Cell Marker in Hepatocellular Carcinoma. *Cancer Lett* (2015) 358:136–43. doi: 10.1016/j.canlet.2014.12.019
130. Huang Z, Yao F, Liu J, Xu J, Guo Y, Su R, et al. Up-Regulation of CircRNA-0003528 Promotes Mycobacterium Tuberculosis Associated Macrophage Polarization via Down-Regulating Mir-224-5p, MiR-324-5p and MiR-488-5p and Up-Regulating CTLA4. *Aging* (2020) 12:25658–72. doi: 10.18632/aging.104175
131. Lasda E, Parker R. Circular RNAs Co-Precipitate With Extracellular Vesicles: A Possible Mechanism for CircRNA Clearance. *PLoS One* (2016) 11: e0148407. doi: 10.1371/journal.pone.0148407
132. Li P, Liu C, Yu Z, Wu M. New Insights Into Regulatory T Cells: Exosome- and Non-Coding RNA-Mediated Regulation of Homeostasis and Resident Treg Cells. *Front Immunol* (2016) 7:574. doi: 10.3389/fimmu.2016.00574
133. Ouyang W, O'Garra A. IL-10 Family Cytokines IL-10 and IL-22: From Basic Science to Clinical Translation. *Immunity* (2019) 50:871–91. doi: 10.1016/j.immuni.2019.03.020
134. Sarode P, Zheng X, Giotopoulou GA, Weigert A, Kuenne C, Günther S, et al. Reprogramming of Tumor-Associated Macrophages by Targeting β -Catenin/FOSL2/ARID5A Signaling: A Potential Treatment of Lung Cancer. *Sci Adv* (2020) 6:eaz6105. doi: 10.1126/sciadv.aaz6105

135. Liu YC, Zou XB, Chai YF, Yao YM. Macrophage Polarization in Inflammatory Diseases. *Int J Biol Sci* (2014) 10:520–9. doi: 10.7150/ijbs.8879
136. Mantovani A, Germano G, Marchesi F, Locatelli M, Biswas SK. Cancer-Promoting Tumor-Associated Macrophages: New Vistas and Open Questions. *Eur J Immunol* (2011) 41:2522–5. doi: 10.1002/eji.201141894
137. Ma Z, Shuai Y, Gao X, Wen X, Ji J. Circular RNAs in the Tumour Microenvironment. *Mol Cancer* (2020) 19:8. doi: 10.1186/s12943-019-1113-0
138. Zhong Z, Huang M, Lv M, He Y, Duan C, Zhang L, et al. Circular RNA MYLK as a Competing Endogenous RNA Promotes Bladder Cancer Progression Through Modulating VEGFA/VEGFR2 Signaling Pathway. *Cancer Lett* (2017) 403:305–17. doi: 10.1016/j.canlet.2017.06.027
139. Li CY, Ma L, Yu B. Circular RNA Hsa_Circ_0003575 Regulates Oxldl Induced Vascular Endothelial Cells Proliferation and Angiogenesis. *Biomed Pharmacother* (2017) 95:1514–9. doi: 10.1016/j.biopha.2017.09.064
140. Kugerafski FG, Atkinson SJ, Neilson LJ, Lilla S, Knight JRP, Serneels J, et al. Hypoxic Cancer-Associated Fibroblasts Increase NCBP2-AS2/HIAR to Promote Endothelial Sprouting Through Enhanced VEGF Signaling. *Sci Signal* (2019) 12:eaa8247. doi: 10.1126/scisignal.aan8247
141. Li X, Liu CX, Xue W, Zhang Y, Jiang S, Yin QF, et al. Coordinated CircRNA Biogenesis and Function With NF90/NF110 in Viral Infection. *Mol Cell* (2017) 67:214–27.e217. doi: 10.1016/j.molcel.2017.05.023
142. Wang M, Yu F, Wu W, Zhang Y, Chang W, Ponnusamy M, et al. Circular RNAs: A Novel Type of Non-Coding RNA and Their Potential Implications in Antiviral Immunity. *Int J Biol Sci* (2017) 13:1497–506. doi: 10.7150/ijbs.22531
143. Li J, Li Z, Jiang P, Peng M, Zhang X, Chen K, et al. Circular RNA IARS (Circ-IARS) Secreted by Pancreatic Cancer Cells and Located Within Exosomes Regulates Endothelial Monolayer Permeability to Promote Tumor Metastasis. *J Exp Clin Cancer Res: CR* (2018) 37:177. doi: 10.1186/s13046-018-0822-3
144. Zhang XL, Xu LL, Wang F. Hsa_Circ_0020397 Regulates Colorectal Cancer Cell Viability, Apoptosis and Invasion by Promoting the Expression of the MiR-138 Targets TERT and PD-L1. *Cell Biol Int* (2017) 41:1056–64. doi: 10.1002/cbin.10826
145. Lankadasari MB, Mukhopadhyay P, Mohammed S, Harikumar KB. Taming Pancreatic Cancer: Combat With a Double Edged Sword. *Mol Cancer* (2019) 18:48. doi: 10.1186/s12943-019-0966-6
146. Lewis CE, Pollard JW. Distinct Role of Macrophages in Different Tumor Microenvironments. *Cancer Res* (2006) 66:605–12. doi: 10.1158/0008-5472.CAN-05-4005
147. Katopodi T, Petanidis S, Domvri K, Zarogoulidis P, Anastakis D, Charalampidis C, et al. Kras-Driven Intratumoral Heterogeneity Triggers Infiltration of M2 Polarized Macrophages via the Circchipk3/PTK2 Immunosuppressive Circuit. *Sci Rep* (2021) 11:15455. doi: 10.1038/s41598-021-94671-x
148. Lobb RJ, Lima LG, Möller A. Exosomes: Key Mediators of Metastasis and Pre-Metastatic Niche Formation. *Semin Cell Dev Biol* (2017) 67:3–10. doi: 10.1016/j.semcdb.2017.01.004
149. Zhang L, Zhang S, Yao J, Lowery FJ, Zhang Q, Huang WC, et al. Microenvironment-Induced PTEN Loss by Exosomal MicroRNA Primes Brain Metastasis Outgrowth. *Nature* (2015) 527:100–4. doi: 10.1038/nature15376
150. Wang X, Sheng W, Xu T, Xu J, Gao R, Zhang Z. CircRNA Hsa_Circ_0110102 Inhibited Macrophage Activation and Hepatocellular Carcinoma Progression via MiR-580-5p/Ppar α /CCL2 Pathway. *Aging* (2021) 13:11969–87. doi: 10.18632/aging.202900
151. Lan J, Sun L, Xu F, Liu L, Hu F, Song D, et al. M2 Macrophage-Derived Exosomes Promote Cell Migration and Invasion in Colon Cancer. *Cancer Res* (2019) 79:146–58. doi: 10.1158/0008-5472.CAN-18-0014
152. Qiu L, Xu H, Ji M, Shang D, Lu Z, Wu Y, et al. Circular RNAs in Hepatocellular Carcinoma: Biomarkers, Functions and Mechanisms. *Life Sci* (2019) 231:116660. doi: 10.1016/j.lfs.2019.116660
153. Zhang QW, Liu L, Gong CY, Shi HS, Zeng YH, Wang XZ, et al. Prognostic Significance of Tumor-Associated Macrophages in Solid Tumor: A Meta-Analysis of the Literature. *PLoS One* (2012) 7:e50946. doi: 10.1371/journal.pone.0050946
154. Xu ZQ, Yang MG, Liu HJ, Su CQ. Circular RNA Hsa_Circ_0003221 (Circptk2) Promotes the Proliferation and Migration of Bladder Cancer Cells. *J Cell Biochem* (2018) 119:3317–25. doi: 10.1002/jcb.26492
155. Zhang Y, Li C, Liu X, Wang Y, Zhao R, Yang Y, et al. Circchipk3 Promotes Oxaliplatin-Resistance in Colorectal Cancer Through Autophagy by Sponging MiR-637. *EBioMedicine* (2019) 48:277–88. doi: 10.1016/j.ebiom.2019.09.051
156. Wang J, Zhao X, Wang Y, Ren F, Sun D, Yan Y, et al. CircRNA-002178 Act as a Cerna to Promote PDL1/PD1 Expression in Lung Adenocarcinoma. *Cell Death Dis* (2020) 11:32. doi: 10.1038/s41419-020-2230-9
157. Cooks T, Pateras IS, Jenkins LM, Patel KM, Robles AI, Morris J, et al. Mutant P53 Cancers Reprogram Macrophages to Tumor Supporting Macrophages via Exosomal MiR-1246. *Nat Commun* (2018) 9:771. doi: 10.1038/s41467-018-03224-w
158. Shang A, Gu C, Wang W, Wang X, Sun J, Zeng B, et al. Exosomal Circpacrgl Promotes Progression of Colorectal Cancer via the MiR-142-3p/MiR-506-3p-TGF- β 1 Axis. *Mol Cancer* (2020) 19:117. doi: 10.1186/s12943-020-01235-0
159. Yu Y, Bian L, Liu R, Wang Y, Xiao X. Circular RNA Hsa_Circ_0061395 Accelerates Hepatocellular Carcinoma Progression via Regulation of the MiR-877-5p/PIK3R3 Axis. *Cancer Cell Int* (2021) 21:10. doi: 10.1186/s12935-020-01695-w
160. Lyu P, Zhai Z, Hao Z, Zhang H, He J. Circwhsc1 Serves as an Oncogene to Promote Hepatocellular Carcinoma Progression. *Eur J Clin Invest* (2021) 51: e13487. doi: 10.1111/eci.13487
161. Sun G, Li Z, He Z, Wang W, Wang S, Zhang X, et al. Circular RNA MCTP2 Inhibits Cisplatin Resistance in Gastric Cancer by Mir-99a-5p-Mediated Induction of MTMR3 Expression. *J Exp Clin Cancer Research: CR* (2020) 39:246. doi: 10.1186/s13046-020-01758-w
162. Zhang H, Deng T, Ge S, Liu Y, Bai M, Zhu K, et al. Exosome Circrna Secreted From Adipocytes Promotes the Growth of Hepatocellular Carcinoma by Targeting Deubiquitination-Related USP7. *Oncogene* (2019) 38:2844–59. doi: 10.1038/s41388-018-0619-z

Conflict of Interest: The authors declare that the research was conducted in the absence of any commercial or financial relationships that could be construed as a potential conflict of interest.

Publisher's Note: All claims expressed in this article are solely those of the authors and do not necessarily represent those of their affiliated organizations, or those of the publisher, the editors and the reviewers. Any product that may be evaluated in this article, or claim that may be made by its manufacturer, is not guaranteed or endorsed by the publisher.

Copyright © 2021 Duan, Wang, Huang, Wang and Yuan. This is an open-access article distributed under the terms of the Creative Commons Attribution License (CC BY). The use, distribution or reproduction in other forums is permitted, provided the original author(s) and the copyright owner(s) are credited and that the original publication in this journal is cited, in accordance with accepted academic practice. No use, distribution or reproduction is permitted which does not comply with these terms.



Development and Validation of a Novel Hypoxia-Related Long Noncoding RNA Model With Regard to Prognosis and Immune Features in Breast Cancer

Peng Gu^{1†}, Lei Zhang^{2†}, Ruitao Wang^{1†}, Wentao Ding¹, Wei Wang¹, Yuan Liu¹, Wenhao Wang³, Zuyin Li⁴, Bin Yan^{1*} and Xing Sun^{1*}

OPEN ACCESS

Edited by:

Zong Sheng Guo,
Roswell Park Comprehensive Cancer
Center, United States

Reviewed by:

Liangyou Gu,
People's Liberation Army General
Hospital, China
Guo-Jiang Zhao,
Capital Medical University, China

*Correspondence:

Bin Yan
yanbin8988@sjtu.edu.cn
Xing Sun
xingsun_sjtu@aliyun.com

[†]These authors have contributed
equally to this work

Specialty section:

This article was submitted to
Molecular and Cellular Oncology,
a section of the journal
Frontiers in Cell and Developmental
Biology

Received: 17 October 2021

Accepted: 30 November 2021

Published: 16 December 2021

Citation:

Gu P, Zhang L, Wang R, Ding W,
Wang W, Liu Y, Wang W, Li Z, Yan B
and Sun X (2021) Development and
Validation of a Novel Hypoxia-Related
Long Noncoding RNA Model With
Regard to Prognosis and Immune
Features in Breast Cancer.
Front. Cell Dev. Biol. 9:796729.
doi: 10.3389/fcell.2021.796729

¹Department of General Surgery, Shanghai General Hospital, School of Medicine, Shanghai Jiao Tong University, Shanghai, China, ²Department of Vascular Surgery, Intervention Center, Shanghai General Hospital, School of Medicine, Shanghai Jiao Tong University, Shanghai, China, ³Department of Urology, Shanghai General Hospital, School of Medicine, Shanghai Jiao Tong University, Shanghai, China, ⁴Department of Hepatobiliary Surgery, Peking University Organ Transplantation Institute, Peking University People's Hospital, Beijing, China

Background: Female breast cancer is currently the most frequently diagnosed cancer in the world. This study aimed to develop and validate a novel hypoxia-related long noncoding RNA (HRL) prognostic model for predicting the overall survival (OS) of patients with breast cancer.

Methods: The gene expression profiles were downloaded from The Cancer Genome Atlas (TCGA) database. A total of 200 hypoxia-related mRNAs were obtained from the Molecular Signatures Database. The co-expression analysis between differentially expressed hypoxia-related mRNAs and lncRNAs based on Spearman's rank correlation was performed to screen out 166 HRLs. Based on univariate Cox regression and least absolute shrinkage and selection operator Cox regression analysis in the training set, we filtered out 12 optimal prognostic hypoxia-related lncRNAs (PHRLs) to develop a prognostic model. Kaplan–Meier survival analysis, receiver operating characteristic curves, area under the curve, and univariate and multivariate Cox regression analyses were used to test the predictive ability of the risk model in the training, testing, and total sets.

Results: A 12-HRL prognostic model was developed to predict the survival outcome of patients with breast cancer. Patients in the high-risk group had significantly shorter median OS, DFS (disease-free survival), and predicted lower chemosensitivity (paclitaxel, docetaxel) compared with those in the low-risk group. Also, the risk score based on

Abbreviations: lncRNA, Long noncoding RNA; TCGA, The Cancer Genome Atlas; GSEA, Gene Set Enrichment Analysis; GO, Gene Ontology; KEGG, Kyoto Encyclopedia of Genes and Genomes; OS, Overall survival; DFS (disease-free survival); ER, Estrogen receptor; PR, Progesterone receptor; HR, Hormone receptor; HER2, Human epidermal growth factor receptor 2; TNBC, Triple-negative breast cancer; LASSO, Least absolute shrinkage and selection operator; ROC, Receiver operating characteristic; AUC, Area under the ROC; HRL, Hypoxia-related lncRNA; PHRLs, Prognostic hypoxia-related lncRNAs; DEHmRNAs, Differentially expressed hypoxia-related mRNAs.

the expression of the 12 HRLs acted as an independent prognostic factor. The immune cell infiltration analysis revealed that the immune scores of patients in the high-risk group were lower than those of the patients in the low-risk group. RT-qPCR assays were conducted to verify the expression of the 12 PHRLs in breast cancer tissues and cell lines.

Conclusion: Our study uncovered dozens of potential prognostic biomarkers and therapeutic targets related to the hypoxia signaling pathway in breast cancer.

Keywords: breast cancer, hypoxia, long noncoding RNA, prognosis, immune infiltration, nomogram

BACKGROUND

Female breast cancer surpassed lung cancer as the most frequently diagnosed cancer (representing 11.7% of total cases and 24.5% of female cancers) worldwide in 2020 (Sung et al., 2021). Despite recent advances in high-quality prevention, early detection, and treatment services, breast cancer is still the leading cause of cancer-related death for female patients (15.5%) (Loibl et al., 2021a). Thus, it is of great importance to identify novel prognosticators and develop a more precise prognostic model to help optimize the individual treatment for patients.

Tumor cells grow in and continuously interact with an incredibly complex and dynamic network called tumor microenvironment (TME). TME consists of noncellular components, such as extracellular matrix, growth factors, cytokines, enzymes, and hormones, as well as diverse types of cells, including endothelial cells, pericytes, immune inflammatory cells, and fibroblasts (Hanahan and Weinberg, 2011). Hypoxia, as one of the most important abnormal microenvironments that tumor cells are continuously exposed to, has a significant impact on tumor biology, leading to a higher phenotypic heterogeneity (Marusyk et al., 2012). The hypoxic tissue areas of many breast cancers are heterogeneously distributed within the tumor mass (Vaupel et al., 2004). Oxygen tension (pO_2) measured in normal breast tissue exhibited a mean (and median) of 65 mm Hg (Vaupel et al., 2007), whereas for breast cancers in T1b–T4 stages, the median pO_2 was 28 mm Hg (Vaupel et al., 1991). The hypoxic response is mainly ascribed to HIF. The HIF is a heterodimer comprising an inducible α subunit (HIF- α) and a constitutively expressed β subunit (HIF- β), which functions as a transcriptional factor that regulates the expression of genes involved in diverse biological characteristics of tumors (Wang et al., 1995). The levels of HIF-1 α have been implicated as an independent prognostic factor for patients with breast cancer (Bos et al., 2003). The hallmarks of cancer, such as angiogenesis (Niu et al., 2020), invasion and metastasis (Bristow and Hill, 2008), evading immune destruction (Hsing et al., 2012) and reprogramming of energy metabolism (Samanta and Semenza, 2018), have been validated to be tumor supportive and associated with the hypoxic tumor environment of breast cancer.

lncRNAs are defined as RNA transcripts longer than 200 nucleotides in length, with no potential to encode proteins (Kopp and Mendell, 2018). Accumulating evidence suggests that lncRNAs play crucial roles in the occurrence and development of a large variety of cancers including breast cancer (Gao et al., 2020; Liu et al., 2021). During tumor hypoxia, hypoxia-inducible factors (HIFs) are upregulated

and either positively or negatively regulate lncRNAs through hypoxia response elements within their promoters. Or vice versa, some lncRNAs can regulate the HIF signaling pathway directly or indirectly (Choudhry et al., 2016). Moreover, increasing evidence reveals the potential of lncRNAs as diagnostic or prognostic biomarkers (Bin et al., 2018; Qian et al., 2020; Chen Y. et al., 2021).

Though there was a similar study proposing a prognostic signature based on HRLs (Zhao et al., 2021), which served to stratify patients with early-stage breast cancer, we aimed to develop and validate a more comprehensive and reliable prognostic model for predicting the survival of all breast cancer patients. By means of both bioinformatic analysis and experimental validation, we were also meant to mine some potential tumor-supportive or tumor-suppressive lncRNAs to indicate the further research direction on their functions in breast cancer.

MATERIALS AND METHODS

Data Acquisition

We downloaded RNA sequencing data (1,109 breast cancer tissues and 113 matched normal tissues) and corresponding clinical and pathological information of patients with breast cancer from The Cancer Genome Atlas (TCGA) (<https://gdc.cancer.gov/>) database in March 2021. The clinical characteristics of the patients are listed in **Table 1**. A total of 200 hypoxia-related mRNAs were obtained from the Molecular Signatures Database V7.3 (Subramanian et al., 2005) (<https://www.gsea-msigdb.org/gsea/msigdb/>, M5891).

Screening of Hypoxia-Related lncRNAs

Differentially expressed hypoxia-related mRNAs (DEHmRNAs) between the breast cancer and normal tissues were identified via the differential expression analysis using the R package “DEseq” with the threshold value set as $|\log_2 \text{fold change (FC)}| > 1$ and adjusted p value of < 0.05 . Heatmap and volcano plots were drawn using the R packages “pheatmap” and “EnhancedVolcano,” respectively. The PPI (protein–protein interaction) network was constructed using the STRING version 11.0 Program (Szklarczyk et al., 2017). Further, we performed Gene Ontology (GO) functional enrichment analysis and Kyoto Encyclopedia of Genes and Genomes (KEGG) pathway enrichment analysis via the R package “clusterProfiler”. Finally, we identified the HRLs by Spearman correlation analysis of DEHmRNAs according to the criteria of |

Correlation Coefficient| > 0.4 and $p < 0.001$. The mRNAs–lncRNAs network were constructed via Cytoscape 3.8.2.

Construction of a Hypoxia-Related lncRNA Prognostic Model

Univariate Cox regression analysis was used to identify prognostic hypoxia-related lncRNAs via the R package “survival” with $p < 0.05$ as the criteria. Heatmap and box plot were drawn using the R packages “pheatmap” and “ggplot2,” respectively. Spearman’s rank correlation was performed to assess the correlation among these genes using the R package “corrplot.” Then, we randomly divided patients into a training set and a testing set in the ratio of 1:1 using the R package “caret.” The R package “glmnet” was used to perform least absolute shrinkage and selection operator (LASSO) Cox regression analysis in the training set to generate a coefficient for each hypoxia survival-related lncRNA. Then, the risk score for each sample was calculated based on the formula: $Risk\ Score\ (RS) = \sum_{i=1}^n (Exp_i * Coef_i)$. Coef means the coefficient of lncRNAs associated with survival, and Exp means the expression of lncRNAs. Hence, breast cancer samples were divided into a high-risk group and a low-risk group according to the median risk score.

Validation of the Model

Kaplan–Meier survival analysis was conducted to investigate the differences in OS and DFS between high- and low-risk groups using the R packages “survival” and “survminer,” no matter whether we classified the patients into different groups based on their clinicopathological characteristics. Receiver operating characteristic (ROC) curves and area under the curve (AUC) were used to evaluate the sensitivity and specificity of this prognostic model via the R package “survivalROC.” Additionally, we used “survival” R package to perform univariate and multivariate Cox regression analyses so as to estimate the prognostic value of the model constructed. Finally, we formulated a nomogram using the R package “rms,” which could assign points for independent prognostic factors to predict 1-, 3-, 5-, and 10-year OS of individual patients with breast cancer (Sui et al., 2020). Meanwhile, we calculated the concordance index (C-index) using “survcomp” and constructed calibration curves to evaluate the predictive power of the nomogram.

Drug Sensitivity Analysis

We used the R package “pRRophetic” to predict the differences in chemosensitivity from tumor gene expression levels for some chemotherapy drugs, which was decided by the half-maximal inhibitory concentration (IC₅₀), between high- and low-risk groups based on our prognostic model (Geeleher et al., 2014).

Gene Set Enrichment Analysis

We performed gene set enrichment analysis (GSEA) (version 4.1.0, <https://www.gsea-msigdb.org/gsea/index.jsp>) to identify the related differential biological function and pathways between high- and low-risk groups as separated by the prognostic model using the following gene sets: Hallmark, GO, KEGG and BioCarta. Each analysis included 1,000 random permutations. The statistical significance level was set to be $p < 0.05$ and the false discovery rate as < 0.25 . The plots were drawn using the R package “ggplot2.”

TABLE 1 | Baseline patients characteristics (n = 1,097).

Characteristic	N (1,097)	%
Age		
≤65 years	776	70.7
>65 years	321	29.3
Unknown	0	0
Sex		
Female	1,085	98.9
Male	12	1.1
Unknown	0	0
Clinical Stage		
I	183	16.7
II	621	56.6
III	249	22.7
IV	20	1.8
Unknown	24	2.2
Pathologic T Stage		
T1	281	25.6
T2	635	57.9
T3	138	12.6
T4	40	3.6
Unknown	3	0.3
Pathologic N Stage		
N0	516	47.0
N1	364	33.2
N2	120	10.9
N3	77	7.0
Unknown	20	1.8
Pathologic M Stage		
M0	912	83.1
M1	22	2.0
Unknown	163	14.9
ER status		
Positive	808	73.7
Negative	238	21.7
Unknown	51	4.6
PR status		
Positive	699	63.7
Negative	344	31.4
Unknown	54	4.9
HER2 status		
Positive	149	13.6
Negative	640	58.3
Unknown	308	28.1
Molecular subtypes		
Luminal A/B	501	45.7
HER2 positive	149	13
TNBC	139	12.7
Unknown	308	28.1

Immune Cell Infiltration Analysis

The CIBERSORT (Floberg et al., 2021), CIBERSORT-ABS (Yuan et al., 2021), TIMER (tumor immune estimation resource) (Jiang et al., 2021), xCELL (Sui et al., 2020), quanTIseq (Subramanian et al., 2005), EPIC (extended polydimensional immunome characterization) (Yeo et al., 2020), MCPcounter (Dienstmann et al., 2019) algorithms were used to further analyze the differences in immune cell infiltration between high- and low-risk groups. The immune score for each single sample was calculated using the R package “estimate.” Additionally, we calculated the correlation between infiltrating immune cells and risk scores using Spearman’s rank correlation with the criteria of $p < 0.05$. Subsequently, 11 immune checkpoints

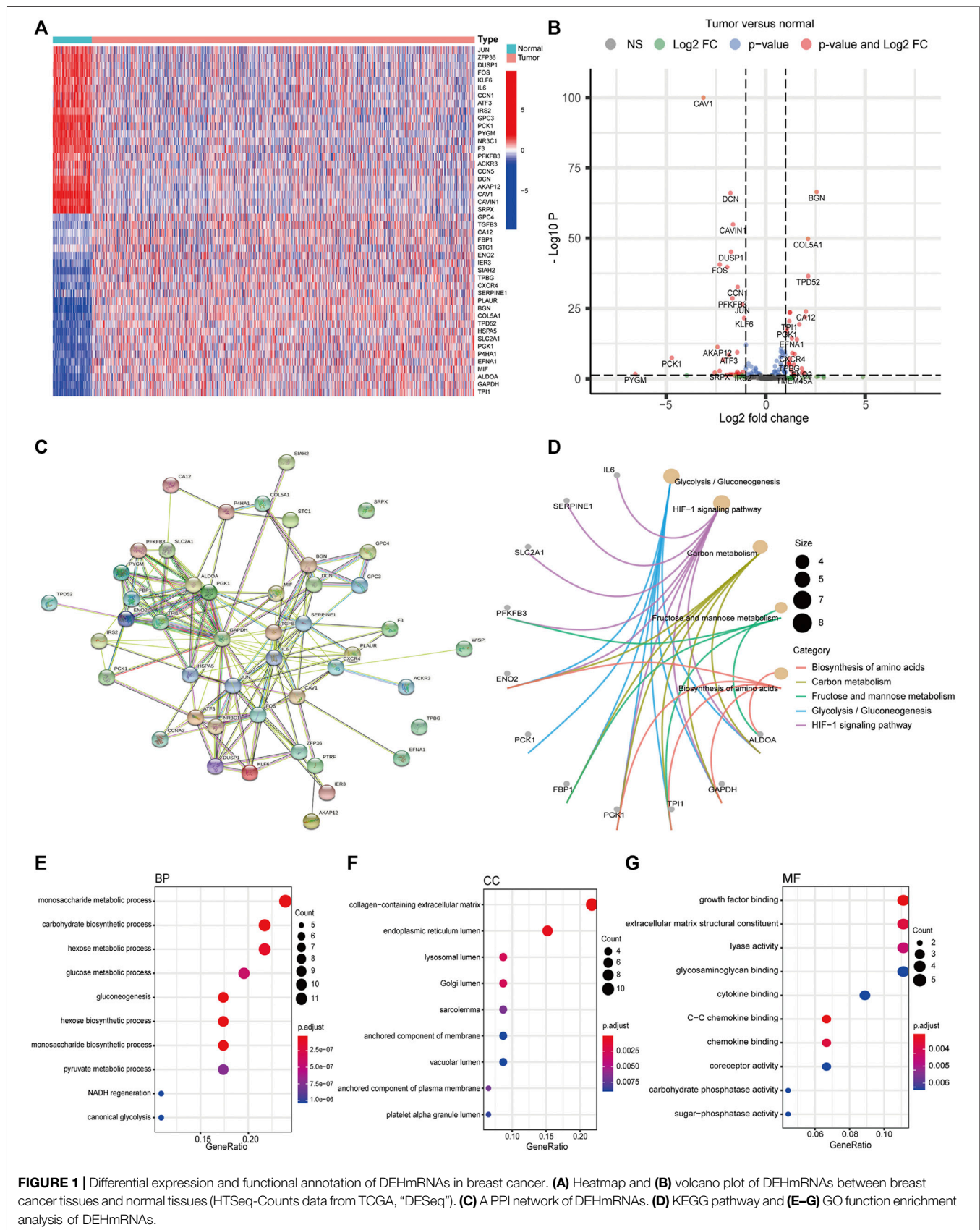


FIGURE 1 | Differential expression and functional annotation of DEHmRNAs in breast cancer. **(A)** Heatmap and **(B)** volcano plot of DEHmRNAs between breast cancer tissues and normal tissues (HTSeq-Counts data from TCGA, “DESeq”). **(C)** A PPI network of DEHmRNAs. **(D)** KEGG pathway and **(E–G)** GO function enrichment analysis of DEHmRNAs.

were selected from the previous literature (Marin-Acevedo et al., 2018).

RNA Extraction and Real-Time Quantitative PCR

Total RNA was extracted from 11 breast cancer tissues, paired adjacent normal tissues, and breast cell lines including MCF10A and MDA-MB-231 (under normoxia or hypoxia conditions) cell lines. RT-qPCR experiments were performed as previously described. The primers used in this study were shown in **Supplementary Table S1**. The mRNA quantification of the 12 PHRLs was based on the $2^{-\Delta\Delta C_t}$ method and the expression levels were plotted by using *ACTB* as the reference gene.

Statistical Analysis

Data were processed using Perl language (version 5.26.1) and analyzed using R software (version 1.3.1073). The Wilcoxon test was applied to compare gene expression, risk scores, drug sensitivity (IC50), and immune cell infiltration scores between two independent groups. Univariate Cox regression and LASSO Cox regression analyses were applied to identify the most useful lncRNAs to build a prognostic model. Survival analysis was conducted using the Kaplan-Meier method and log-rank tests. The chi-square test was used to compare the relationship between risk and immune score level and other categorical clinicopathological factors. Correlation analysis was assessed by Spearman's rank correlation. Statistical significance was set at $p < 0.05$ or 0.001 for diverse analysis.

RESULTS

Identification of Differentially Expressed Hypoxia-Related mRNAs in Breast Cancer

We obtained 200 hypoxia-related mRNAs from the Molecular Signatures Database V7.3 (HALLMARK_HYPOXIA, M5891), which were previously validated to be hypoxia-regulated in multiple kinds of cancer including breast cancer (Wang et al., 2009; Xia and Kung, 2009; Leithner et al., 2014). By comparing their expression levels between 1,109 breast cancer tissues and 113 normal tissues using the R package "DEseq," we identified 46 DEHmRNAs (**Supplementary Table S2**). The heatmap and volcano plot are shown in **Figures 1A,B**. A PPI network showed that almost all proteins encoded by the aforementioned genes interacted with each other except SRPX and TPBG (**Figure 1C**). Further, we performed KEGG (**Figure 1D**) and GO (**Figures 1E–G**) analyses to investigate the biological function of 46 DEHmRNAs. The top 3 most enriched KEGG pathways were "HIF-1 signaling pathway", "Glycolysis/Gluconeogenesis", and "Carbon metabolism".

Screening of Hypoxia-Related lncRNAs and Construction of a Co-Expression Network

Co-expression analysis between DEHmRNAs and lncRNAs based on Spearman's rank correlation was performed to screen out 166 HRLs according to the criteria of $|\text{Correlation Coefficient}| > 0.4$ and

$p < 0.001$ (**Supplementary Table S3**), of which 46 were significantly upregulated and 41 were downregulated (**Supplementary Figure S1** and **Supplementary Table S4**). Based on the mRNA-lncRNA co-expression pattern, we constructed a network to show the relationships among them (**Supplementary Figure S2**).

Development of Hypoxia-Related lncRNA Prognostic Model

By matching the sample IDs in the expression matrix and clinical information profile, we collected 1,090 samples for subsequent analysis after excluding 19 samples. We performed univariate Cox regression analysis to identify 20 PHRLs significantly associated with survival ($p < 0.05$) (**Figure 2A**). The differential expression of these 20 PHRLs is shown in **Figures 2B,C**. Most of them were notably correlated with each other (**Figure 2D**). Then, we randomly divided these 1,090 patients with breast cancer into two groups in the ratio of 1:1: a training set ($n = 546$) and a testing set ($n = 544$). LASSO-penalized Cox regression was performed in the training set, and finally a prognostic model was developed, which consisted of seven risk lncRNAs and five protective lncRNAs on the basis of the coefficient value (**Figures 2E–G**). We calculated the risk scores for all samples using the following formula: Risk score = $(0.309031851 \times \text{Exp of TDRKH-AS1}) + (0.213481355 \times \text{Exp of AC011978.2}) + (0.170772984 \times \text{Exp of AC110995.1}) + (0.051734285 \times \text{Exp of OTUD6B-AS1}) + (0.046646469 \times \text{Exp of YTHDF3-AS1}) + (0.019875191 \times \text{Exp of AL512380.1}) + (0.019087737 \times \text{Exp of MIR4435-2HG}) + (-0.037067764 \times \text{Exp of HSD11B1-AS1}) + (-0.063799579 \times \text{Exp of LINC02084}) + (-0.162152639 \times \text{Exp of TRG-AS1}) + (-0.399031951 \times \text{Exp of AL451085.3}) + (-0.886350422 \times \text{Exp of AL109955.1})$. All the patients were further separated into high- and low-risk groups according to the median risk score in the training set.

Validation of the Prognostic Model

We performed Kaplan-Meier survival analysis to investigate whether there any differences in survival outcomes existed between the high and low-risk groups. The results shown in **Figure 3A** indicated that in the training set, patients in the high-risk group had shorter median OS compared with those in the low-risk group (log-rank test, $p = 4.385e-08$). This significant difference can also be seen in both the testing set and the total set ($p = 0.0026$ in the former, $p = 8.537e-10$ in the latter) (**Figures 3B,C**). Then we built time-dependent ROC curves for the three sets. The AUC for 1-, 3-, 5-, and 10-year OS was 0.734, 0.727, 0.741, and 0.786 in the training set and 0.681, 0.637, 0.612, and 0.749 in the testing set, respectively (**Figure 3D**). In the total set, it was 0.707, 0.691, 0.684, and 0.769 (**Figures 3E,F**). Additionally, we compared the DFS of 984 patients with breast cancer. As expected, the patients in the high-risk group had significantly shorter median DFS than those in the low-risk group when the best cut point of the risk score was set as 1.55 (**Figures 3G–I**).

We next visualized risk score distribution, survival status, and PHRLs expression in all three sets. The plots showed that, whether in the training (**Figures 4A,D**), testing (**Figures 4B,E**), or total (**Figures 4C,F**) set, patients in the high-risk group had poorer survival and higher risk scores compared

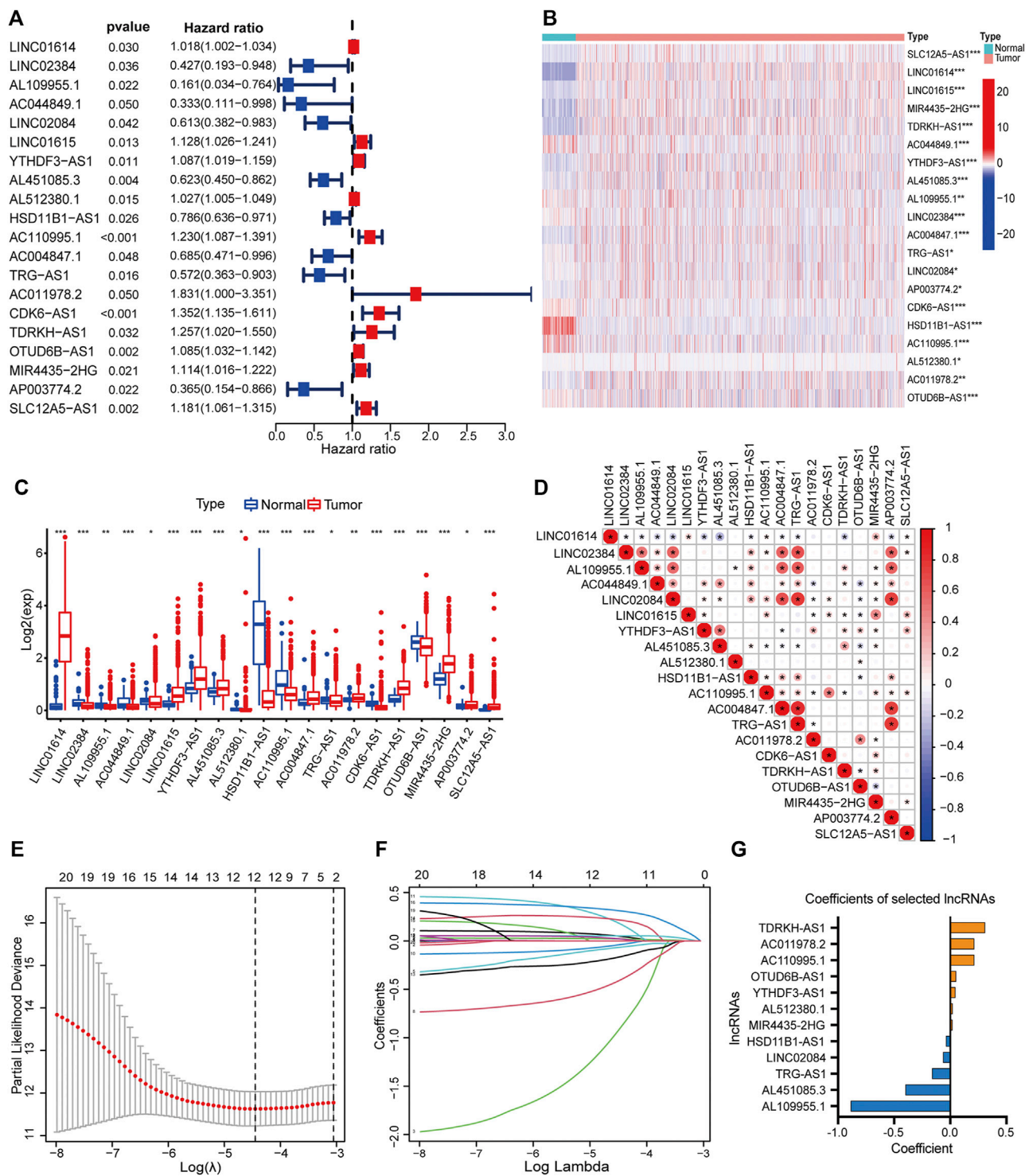
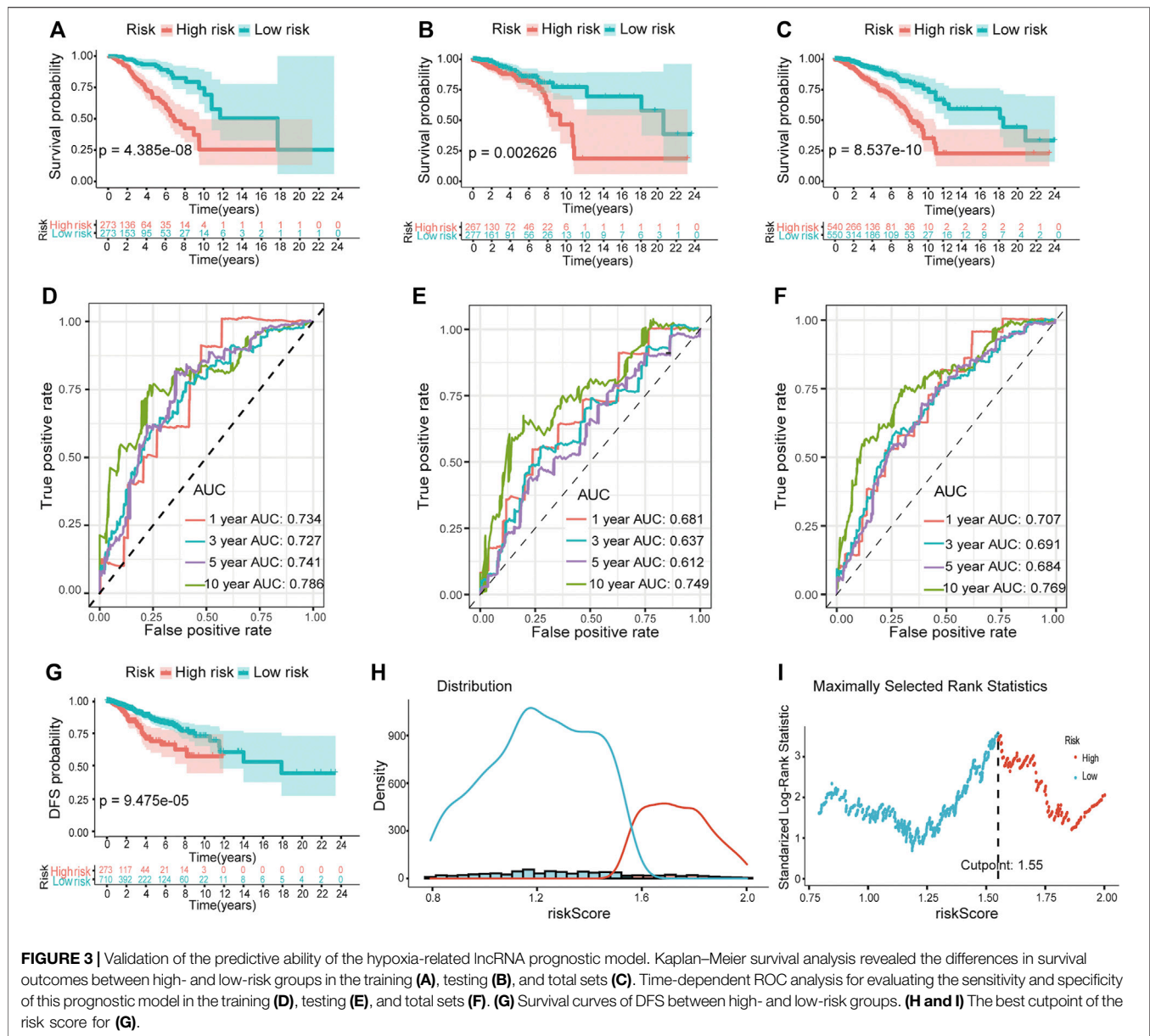


FIGURE 2 | Development of a hypoxia-related lncRNA prognostic model. **(A)** Forest plot showed the hazard ratio (HR, 95% CI) and the p value of 20 PHRLs by univariate Cox regression analysis. Heatmap **(B)** and box plot **(C)** showed the expression level of the 20 PHRLs in breast cancer tissues compared with normal tissues (Wilcoxon test). **(D)** Spearman rank's correlation analysis based on the expression of the 20 PHRLs. **(E and F)** LASSO-penalized Cox regression was performed to filter out 12 optimal PHRLs. **(G)** 12 PHRLs and their coefficients. * $p < 0.05$, ** $p < 0.01$, and *** $p < 0.001$.



with those in the low-risk group. The heatmaps manifested the differential expression pattern of PHRLs between the high- and low-risk groups (Figures 4G–I).

We excluded 305 patients with incomplete clinical and pathological information to further test the independent predictive ability of the risk model. In order to ensure the accuracy of the following analyses, we compared the difference in clinicopathological factors of breast cancer patients between training ($n = 383$) and testing ($n = 402$) sets (Supplementary Table S5). As expected, there was no significant difference between the two sets randomly sampled. Then, we performed univariate and multivariate Cox regression analyses. The results showed that the risk score was significantly associated with OS ($p \leq 0.001$) after adjustment for age, stage, TNM stage, ER/PR status, and

HER2 status in the training (Figures 5A,D), testing (Figures 5B,E), and total sets (Figures 5C,F), suggesting that the risk score could act as an independent prognostic factor.

Moreover, we divided patients in the total set into multiple groups according to their clinicopathological characteristics and then used Kaplan-Meier survival analysis to verify the prognostic value of the risk model for them. The results shown in Figures 6A–M indicated that the prognosis of patients in the high-risk group was significantly worse than that of the patients in the low-risk group. It is worth noting that this model was applicable to patients with breast cancer of three different molecular subtypes [HR-positive/luminal, HER2-positive, or triple-negative breast cancer (TNBC)]. By comparing the risk scores of patients in different groups, we found that patients over 65 years and those

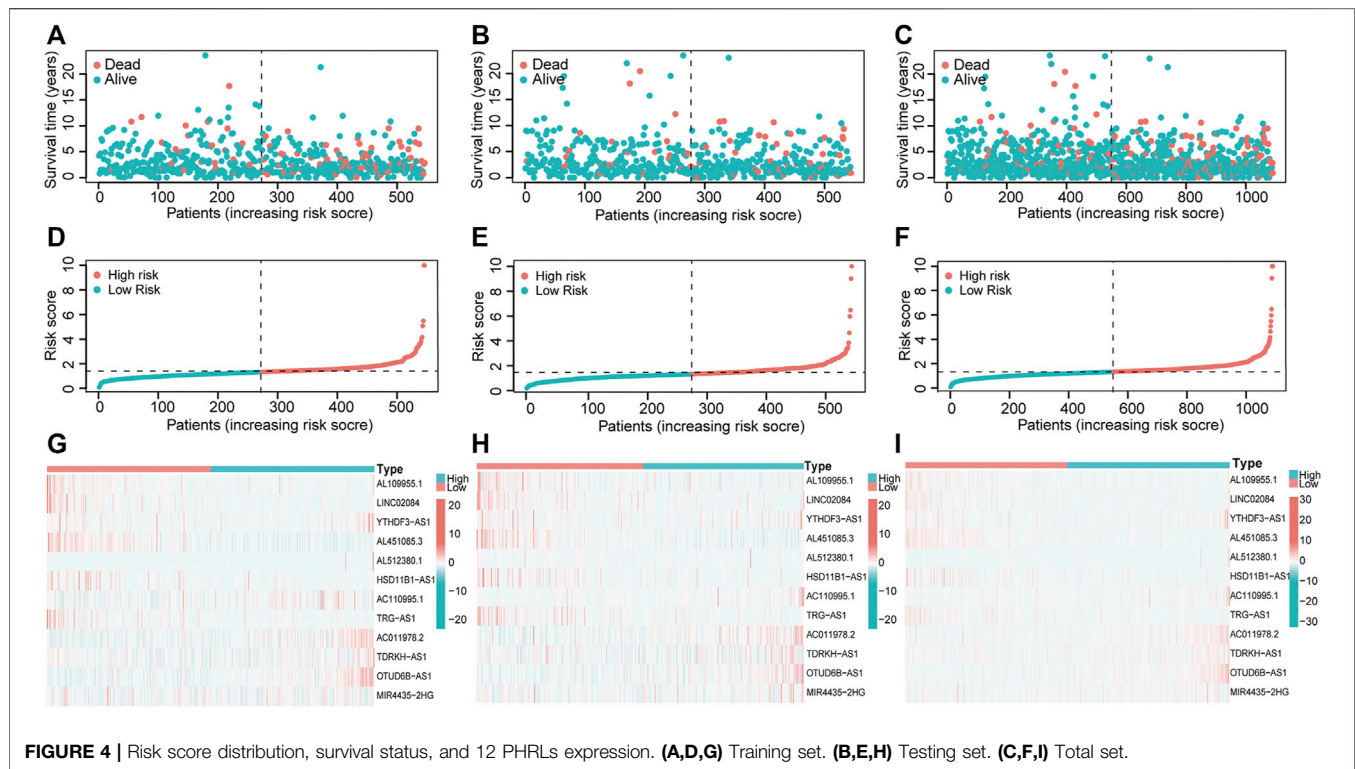


FIGURE 4 | Risk score distribution, survival status, and 12 PHRLs expression. (A,D,G) Training set. (B,E,H) Testing set. (C,F,I) Total set.

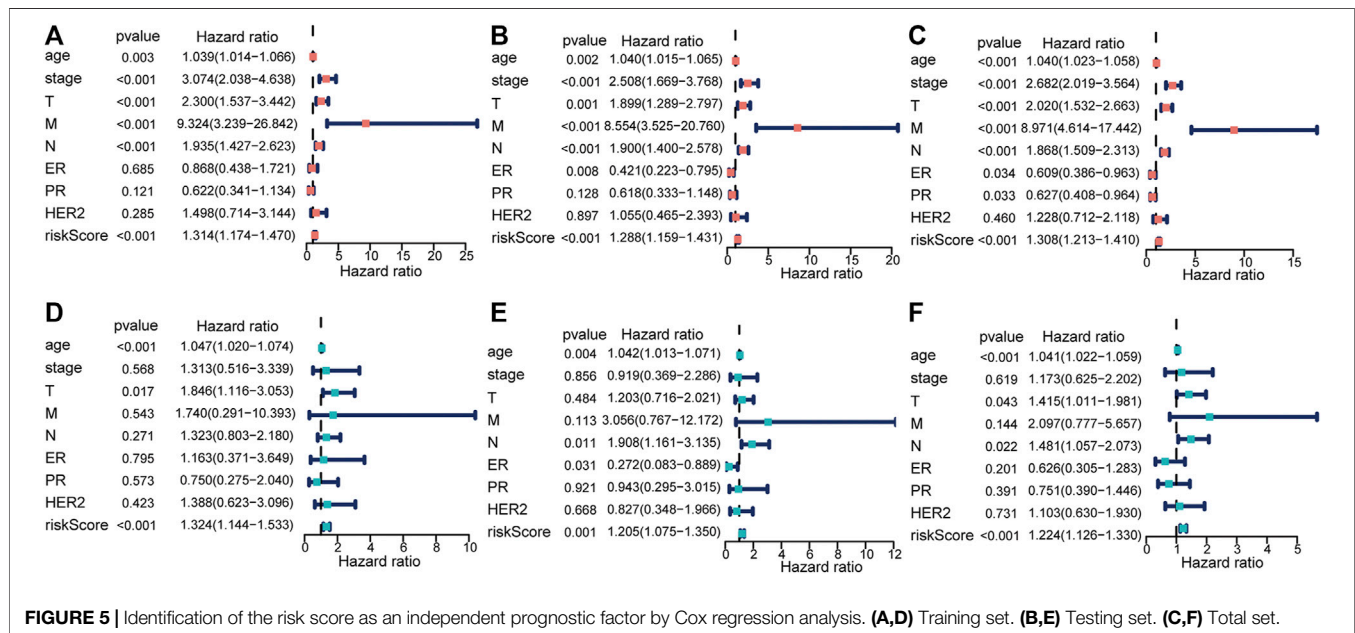


FIGURE 5 | Identification of the risk score as an independent prognostic factor by Cox regression analysis. (A,D) Training set. (B,E) Testing set. (C,F) Total set.

with higher clinical stage had higher risk scores while patients with TNBC had lower risk scores (Supplementary Figure S3).

Establishment and Validation of a Nomogram and Drug Sensitivity Analysis

The independent prognosticators, including age, stage, ER, PR, HER2 status, and risk score, were used to establish a nomogram

for the total set, which could assign a point for each subgroup of these prognosticators. Then, we could calculate the total points to predict the 1-, 3-, 5-, and 10-year OS. As shown in Figure 7A, a 54-year-old patient with clinical stage II, risk score of 10.02, and TNBC had a total point of 236 and predicted 1-, 3-, 5-, and 10-year OS of 93.8, 70.3, 49.7, and 7.2%, respectively. The C-index was 0.816 (95% CI 0.760–0.873) in the training set ($n = 383$), 0.800 (95% CI 0.725–0.874) in the testing set ($n = 402$), and 0.797

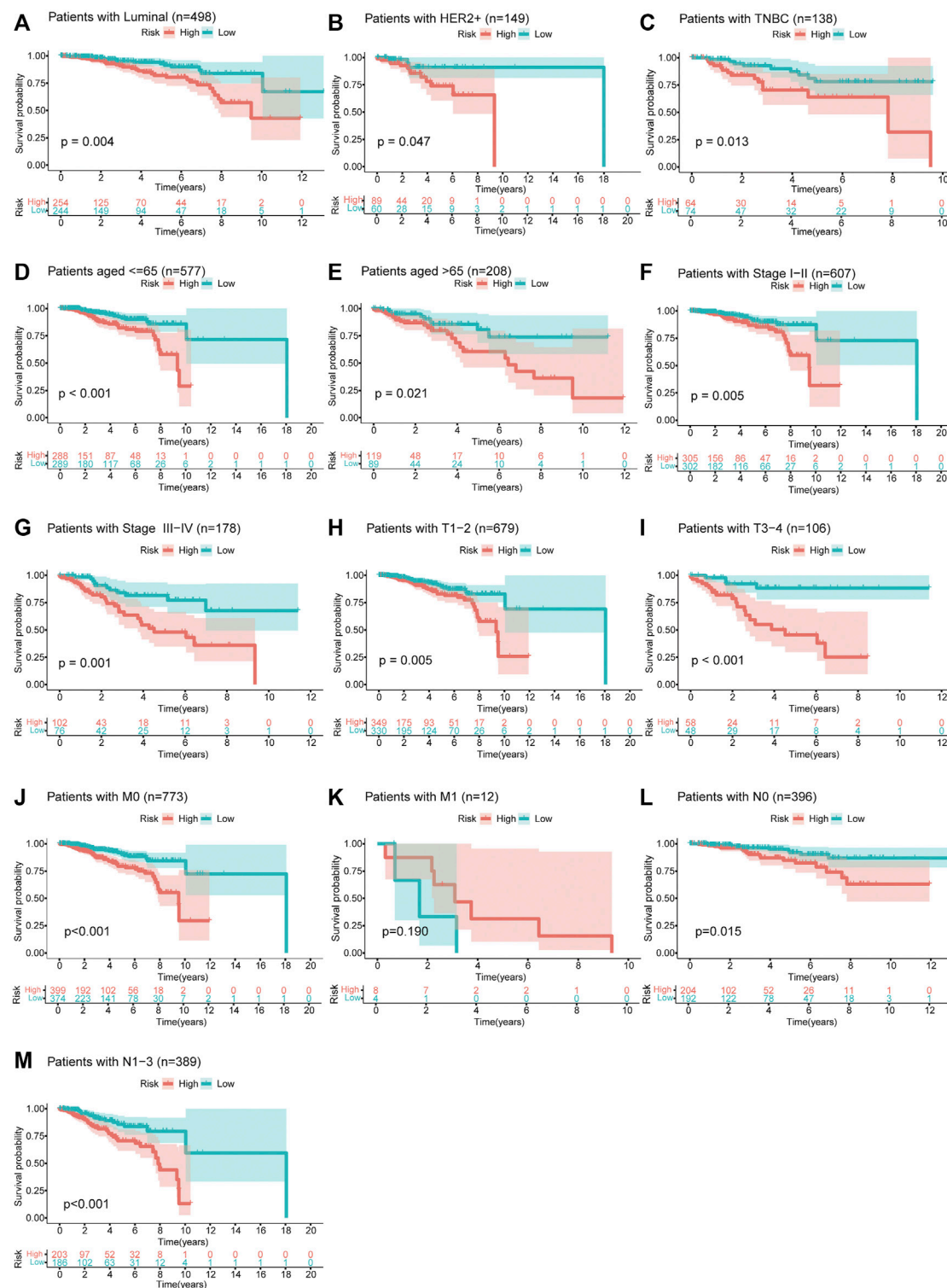


FIGURE 6 | Survival curves of OS between high- and low-risk groups for patients classified in different ways. **(A–C)** Patients with HR-positive/luminal breast cancer, HER2-positive breast cancer, or TNBC. **(D,E)** Patients aged ≤65 or >65 years. **(F,G)** Patients with clinical stage I-II or III-IV. **(H,I)** Patients with T1-2 or T3-4. **(J,K)** Patients with M0 or M1. **(L,M)** Patients with N0 or N1-3.

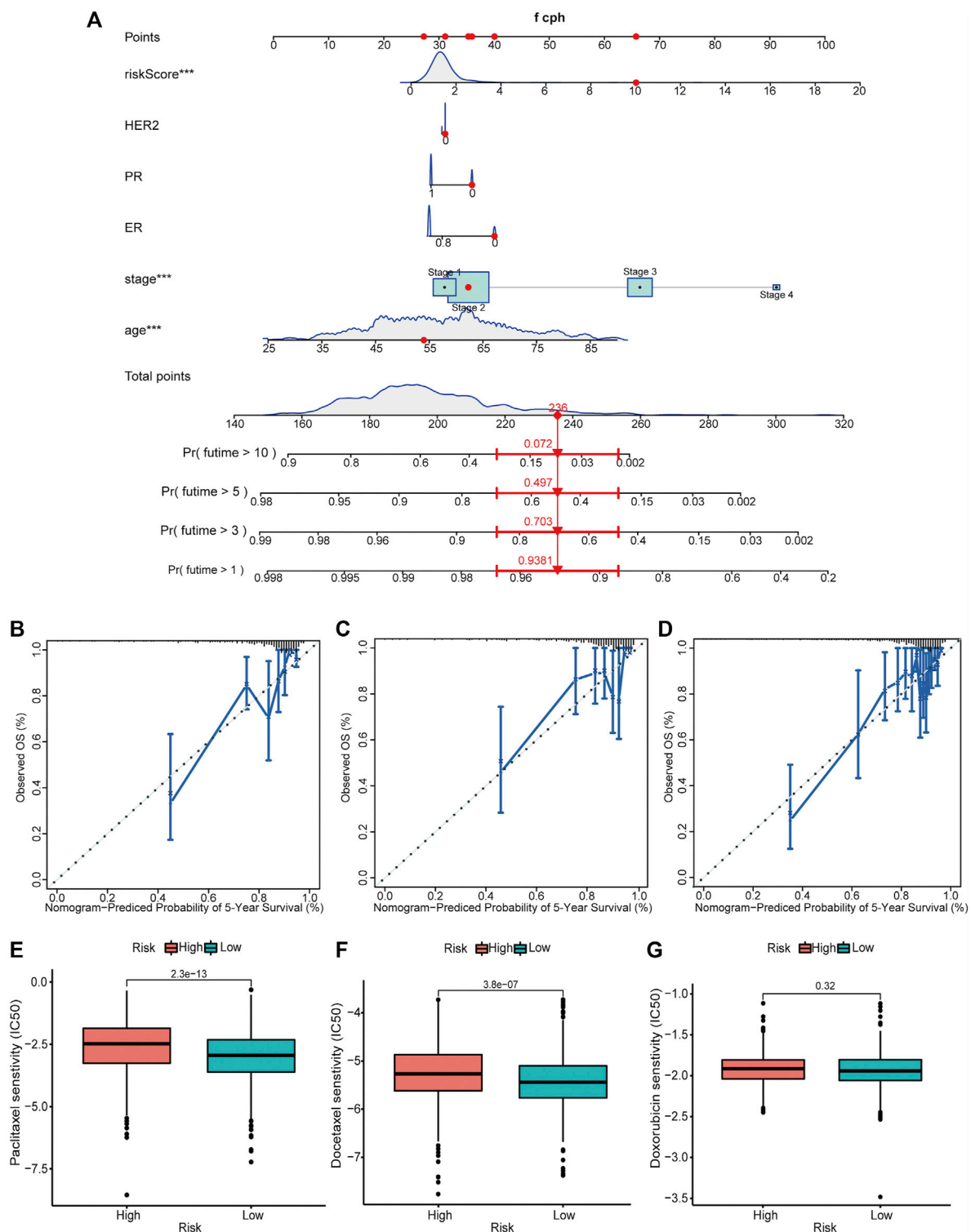


FIGURE 7 | Establishment and validation of a nomogram for predicting the OS of patients with breast cancer along with the drug sensitivity analysis. **(A)** A nomogram considering multiple independent prognosticators, including age, stage, ER, PR, HER2 status, and risk score for predicting the 1-, 3-, 5-, and 10-year OS of patients in the total set. Calibration curves of the nomogram predicting 5-year OS in the training set **(B)**, testing set **(C)**, and total set **(D)**. (We did not show the nomograms of the training set and the testing set.) Drug sensitivity of patients in high- and low-risk groups to paclitaxel **(E)**, docetaxel **(F)**, and doxorubicin **(G)** in the total set. *** $p < 0.001$.

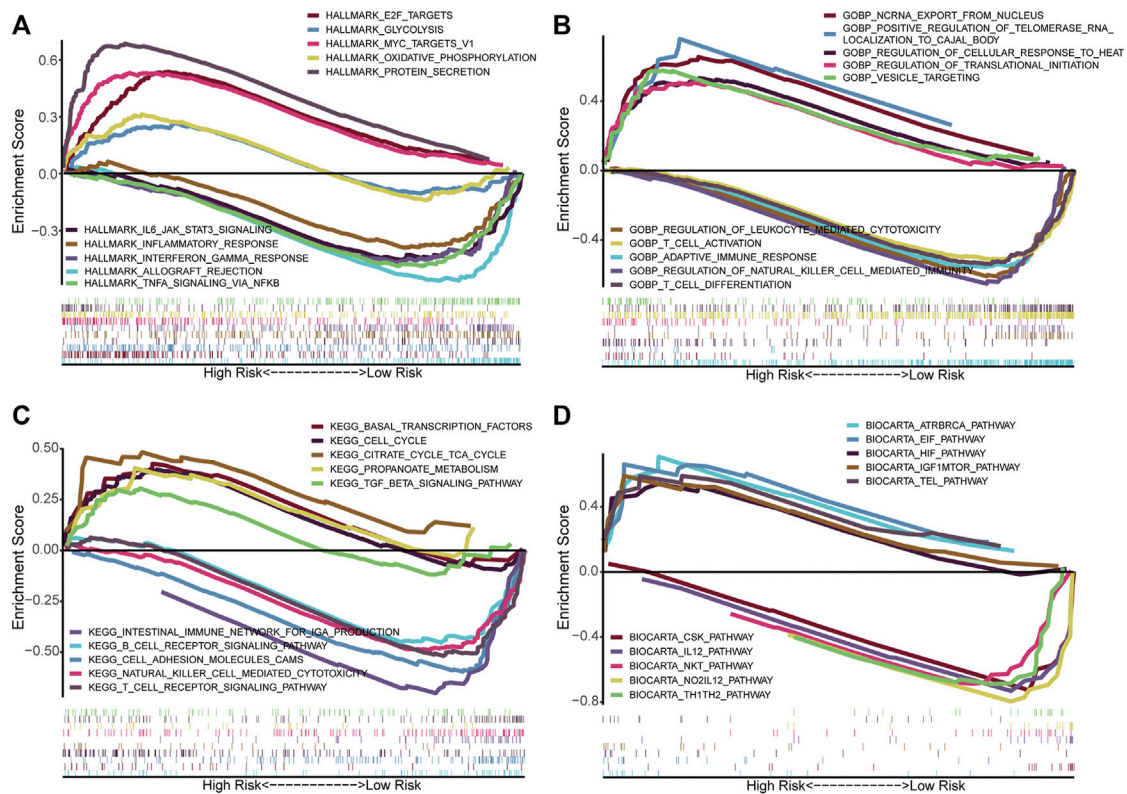


FIGURE 8 | Functional annotation in high- and low-risk groups by GSEA. The GSEA results based on the gene sets, including Hallmark (A), GO_BP (B), KEGG (C), and BioCarta (D). BP, Biological process.

(95% CI 0.746–0.848) in the total set ($n = 785$). Moreover, we constructed calibration curves for three sets to predict 5-year OS, which validated the great repeatability and reliability of the established nomogram (Figures 7B–D). Intrinsic and acquired resistance to chemotherapy remains a major challenge in effective breast cancer treatment. Hence, we calculated the differences in drug sensitivity, which was decided by IC50 between high- and low-risk groups. As predicted, patients in the high-risk group had lower chemosensitivity to paclitaxel ($p = 2.3e-13$), docetaxel ($p = 3.8e-07$), and doxorubicin (not significant) compared with those in the low-risk group (Figures 7E–G).

Functional Annotation in High- and Low-Risk Groups by GSEA

We performed GSEA using the gene sets, including Hallmark (Figure 8A), GO (Figure 8B), KEGG (Figure 8C), and BioCarta (Figure 8D), to identify the related differential biological function and pathways between high- and low-risk groups. Remarkably, multiple immune-related signaling pathways were enriched in the low-risk group, such as inflammatory response, interferon gamma response, TNFA signaling via NFkB, T cell activation, regulation of natural killer cell mediated immunity, T cell differentiation, T cell receptor signaling pathway, B cell receptor signaling pathway, IL12 pathway, Th1Th2 pathway, NKT pathway, and so on. Based on the GSEA results, we

would like to further explore the difference in immune infiltration between the groups.

Immune Cell Infiltration Analysis

With the CIBERSORT algorithm, we compared the differential infiltration levels of 22 kinds of immune cells for each sample between the high- and low-risk groups. As shown in Figure 9A, plasma cells ($p < 0.001$), resting NK cells ($p = 0.049$), M0 macrophages ($p < 0.001$), M2 macrophages ($p < 0.001$), and neutrophils ($p < 0.001$) were significantly enriched in the high-risk group while the proportions of naïve B cells ($p < 0.001$), CD8+T cells ($p < 0.001$), regulatory T cells (Tregs) ($p < 0.001$), and activated NK cells ($p = 0.004$) were significantly higher in the low-risk group. To validate the observed differences, we divided the patients into high- and low-immune score groups according to the median immune score. We then compared the risk scores between them (Wilcoxon test). Obviously, patients with high immune scores had lower risk scores ($p < 0.001$) (Figure 9B). Consistently, the immune scores of patients in the high-risk group were lower than those of patients in the low-risk group ($p < 0.001$) (Figures 9C,D). Additionally, we calculated the correlation between infiltrating immune cells and risk scores and exhibited it in a bubble chart ($p < 0.05$) (Figure 9E). Immune checkpoints are immunomodulators of both stimulatory and inhibitory pathways (Pardoll, 2012). We

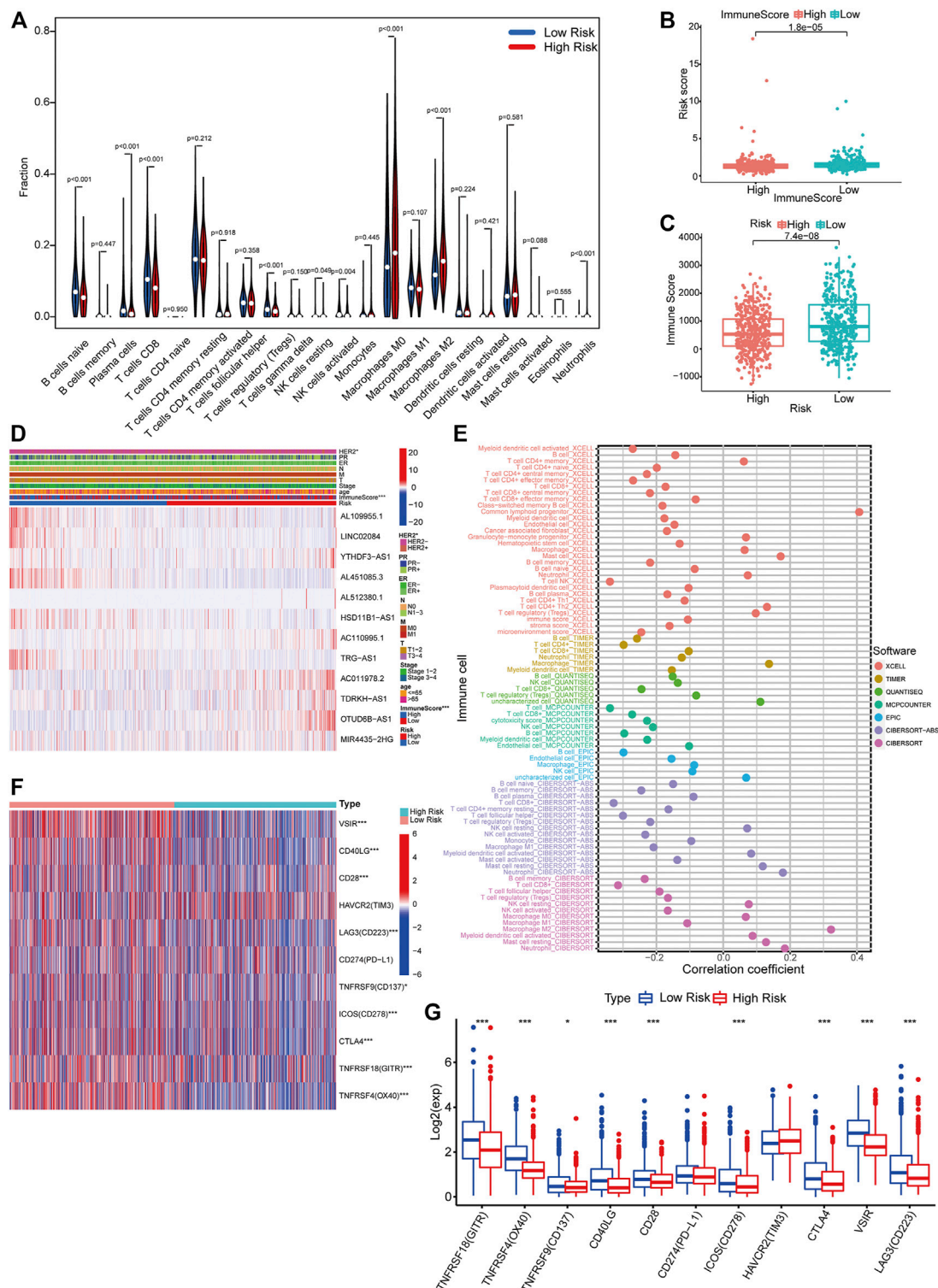
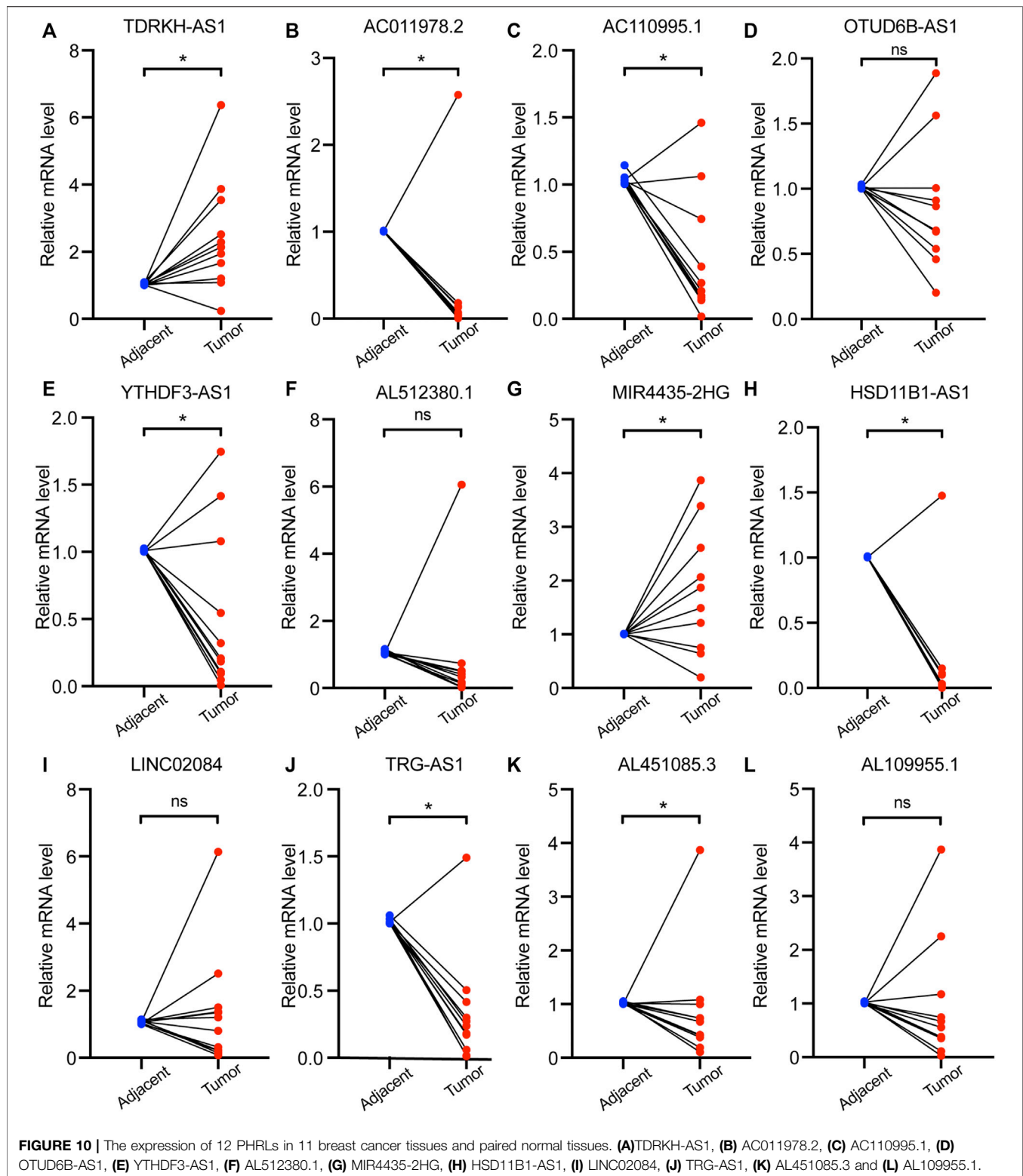
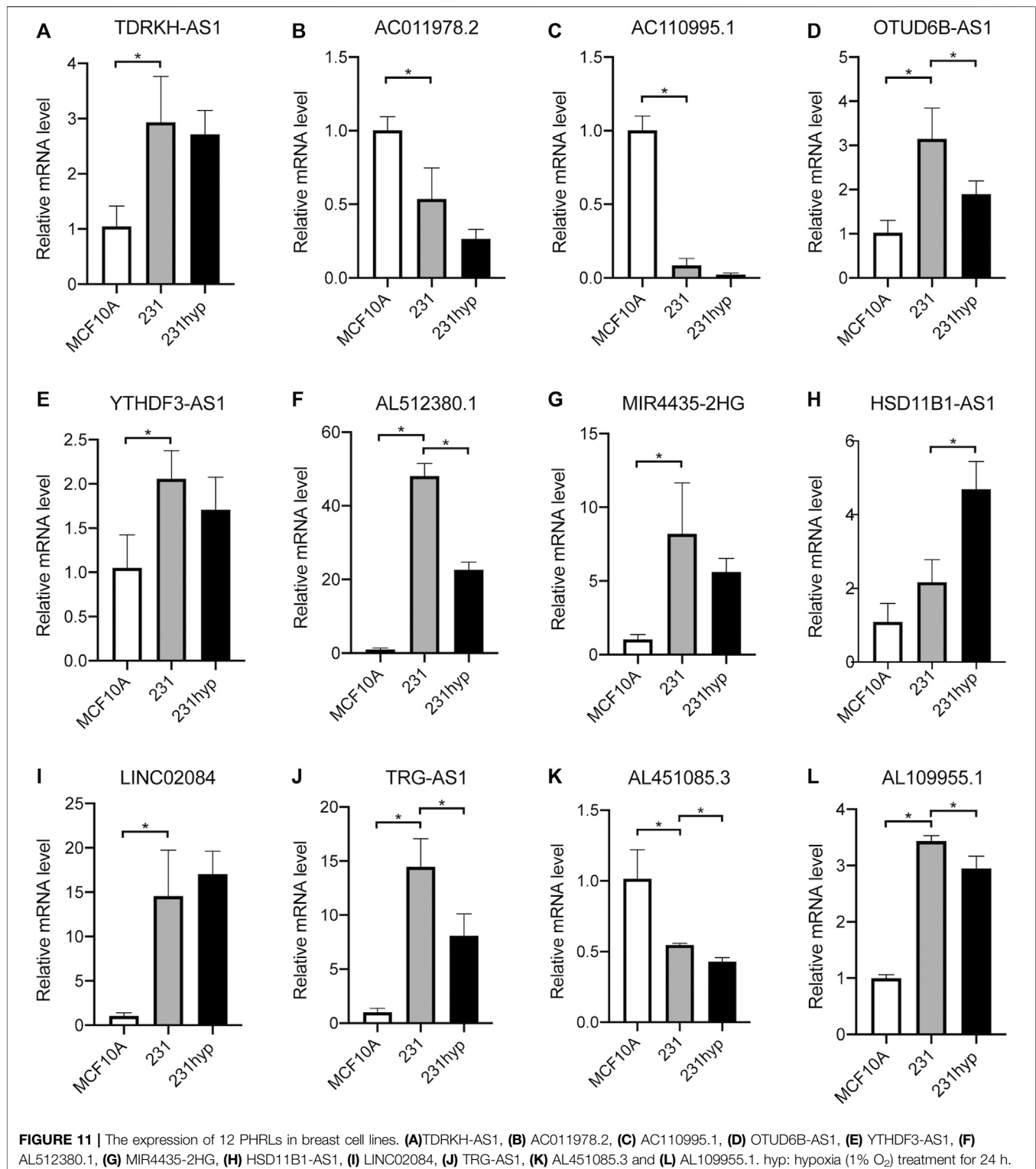


FIGURE 9 | Differential immune features between risk groups. **(A)** CIBERSORT algorithm results demonstrated the differential infiltration levels of 22 kinds of immune cells for each sample in TCGA between the high- and low-risk groups (Wilcoxon test). **(B)** Comparison of immune scores of patients between the high- and low-risk groups (Wilcoxon test). **(C)** Comparison of risk scores of patients between the high- and low-immune score groups (Wilcoxon test). **(D)** A comprehensive heatmap integrating the expression of 12 PHRLs and the distribution of multiple clinicopathological factors (HER2, PR, ER, TNM, stage, age, and immune score) between the high- and low-risk groups (chi-square test). **(E)** A bubble chart exhibited the correlation between infiltrating immune cells and risk scores using CIBERSORT, CIBERSORT-ABS, TIMER, xCELL, quanTiseq, EPIC, and MCPcounter algorithms (Spearman's rank correlation). **(F,G)** Heatmap and box plot showed the expression of 11 immune checkpoints in the high- and low-risk groups (Wilcoxon test). * $p < 0.05$, ** $p < 0.01$, and *** $p < 0.001$.



obtained 11 immune checkpoints from the previous literature (Marin-Acevedo et al., 2018) and then compared their expression level between the high- and low-risk groups.

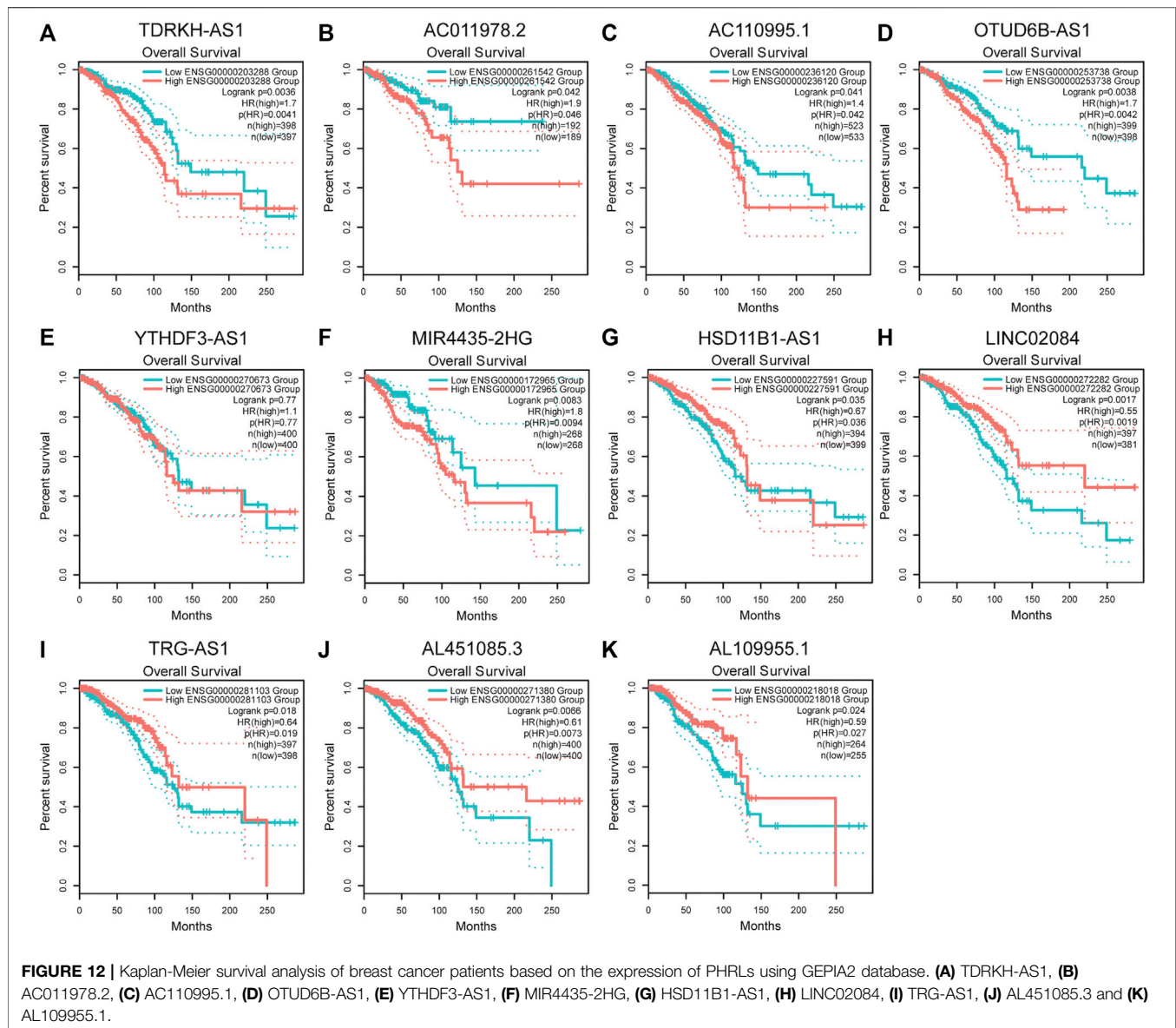
Most of them (GITR, OX40, CD137, CD40LG, CD28, CD278, CTLA4, VSIR, and CD223) were dramatically downregulated in the high-risk group (Figures 9F,G).



Validation of the Expression of the 12 PHRLs in Breast Cancer Tissues and Breast Cell Lines

To verify the differential expression of the 12 PHRLs, 11 breast cancer tissues and the corresponding adjacent normal tissues were collected

for RT-qPCR assay. Two lncRNAs were significantly overexpressed in tumor tissues while six were significantly underexpressed (Figure 10). We further explored the expression of the 12 PHRLs in MCF10A (normoxia, 21% O₂), MDA-MB-231 (normoxia, 21% O₂), and MDA-MB-231 (hypoxia, 1% O₂). The results were shown in Figure 11. We next carried out the Kaplan–Meier survival analysis



for the 12 PHRLs using GEPIA2 database (<http://gepia2.cancer-pku.cn/>) except AL512380.1 for its median expression being zero (Figure 12). Based on the transcriptomic data from TCGA and the Genotype-Tissue Expression (GTEx) database, we analyzed the differential expression of the 12 PHRLs between breast cancer tissues or TNBC tissues and normal breast tissues (Supplementary Figures S4 and S5). Taken together, we could also draw a conclusion that TDRKH-AS1, MIR4435-2HG, HSD11B1-AS1, TRG-AS1, and AL451085.3 were valuable prognostic indicators for patients with breast cancer.

DISCUSSION

Breast cancer remains the most common cancer worldwide, with continuously increasing incidence and various factors affecting its

development (Bray et al., 2015; Loibl et al., 2021b). Hypoxic areas are distributed heterogeneously throughout the tumor mass and surrounding environment. The crosstalk between tumor cells and the local microenvironment contributes to carcinogenesis, metastasis, and chemoresistance and even determines clinical outcomes. Over the past decade, an increasing number of lncRNAs have been verified to play crucial roles under hypoxia TME in breast cancer. For example, lncRNA BCRT1, which is transcriptionally regulated by HIF-1 α under hypoxic conditions, promoted breast cancer cell proliferation and progression (Byrne et al., 2020). Interestingly, another study showed that hypoxia-induced lincRNA-P21 promoted the Warburg effect to increase ATP generation by regulating HIF-1 α transcriptional activity in breast cancer (Yang et al., 2014). Most of these studies focused on the role of lncRNAs in the occurrence and development of breast cancer.

Although several articles concerning prognostic models in breast cancer have been published (Li et al., 2020; Pei et al., 2020; Zhao et al., 2021), in this study, we selected a well-recognized gene set “HALLMARK_HYPOXIA” which consists of 200 canonical hypoxia-related mRNAs to perform a differential expression analysis between breast cancer tissues and normal tissues and obtained 46 DEHmRNAs. The co-expression analysis was performed to screen out 166 HRLs. Using these HRLs, we finally constructed a novel prognostic model for patients with breast cancer, which consisted of 12 PHRLs: TDRKH-AS1, AC011978.2, AC110995.1, OTUD6B-AS1, YTHDF3-AS1, AL512380.1, MIR4435-2HG, HSD11B1-AS1, LINC02084, TRG-AS1, AL451085.3, and AL109955.1 (RBM38-AS1). The PHRLs above were totally different from those four of Zhao et al.’s: AL031316.1, AC004585.1, LINC01235, and ACTA2-AS1. The principle reason for this difference is the different hypoxia-related gene sets we chose, which led to only 13 overlapped DEHmRNAs and 34 overlapped HRLs between our study and theirs in the co-expression network (**Supplementary Table S6**). Nevertheless, the KEGG analysis for the 46 DEHmRNAs we filtered out verified the accurate and strong correlation with hypoxia. Moreover, our prognostic model could divide the patients with breast cancer into high- and low-risk groups more effectively in both training and testing sets and was found to have greater prognostic value by multiple verification methods. The AUCs for 1-, 3-, 5-, and 10-year OS in three sets were calculated to evaluate the predictive accuracy. Beside OS, the difference in DFS between high- and low-risk patients was also significant. It’s also worth noting that our prognostic model was applicable to all breast cancer patients with different clinical stages or molecular subtypes (HR-positive/luminal, HER2-positive, or TNBC) while Zhao et al.’s model applied only to early-stage breast cancer patients. When we compared the risk scores of patients in different groups, we found that patients over 65 years or those with later clinical stage had higher risk scores while patients with TNBC had lower risk scores. There may be two reasons accounting for this result: For one thing, among the 208 patients over 65 years in TCGA breast cancer database, only 21 of them were with TNBC; for another, there were merely 23 TNBC patients among a total of 178 patients with late stage (stage III or stage IV). This seems to indicate that the roles of age and clinical stage as clinicopathological factors outweigh the role of molecular subtypes to predict the survival of patients in the current study, which has also been proved by previous studies (Ferguson et al., 2013; O’Brien et al., 2018). The nomogram established in the present study, which took the clinicopathological factors (HER2, PR, ER, stage, and age) and risk scores into consideration, could precisely predict the OS of patients with breast cancer. The drug sensitivity analysis showed that patients in the high-risk group may be more likely to be resistant to chemotherapy drugs including paclitaxel, docetaxel, and doxorubicin. Though we failed to retrieve ideal GEO datasets including all the 12 PHRLs for independent validation, the validation process above was still sufficient to underscore the utility of our model in predicting the prognosis of breast cancer patients.

Among the 12 PHRLs, AC011978.2, AC110995.1, YTHDF3-AS1, AL512380.1, HSD11B1-AS1, AL451085.3, and AL109955.1 have not been reported to date. TDRKH-AS1 was reported to

promote colorectal cancer (CRC) progression through the Wnt/ β -catenin signaling pathway (Jiao et al., 2020). In addition, its differential expression with copy number alteration was positively associated with longer OS in lung adenocarcinoma (Wang L. et al., 2019). OTUD6B-AS1 was demonstrated to indicate poor prognosis in ovarian cancer, clear cell renal cell carcinoma (ccRCC), and breast cancer (as an immune-related lncRNA) while its overexpression inhibited ccRCC proliferation (Wang G. et al., 2019; Li and Zhan, 2019; Ma et al., 2020). Similarly, OTUD6B-AS1 played a tumor-suppressive role in thyroid carcinoma (Wang Z. et al., 2020), bladder carcinoma (Wang Y. et al., 2020), and CRC (Cai et al., 2021; Wang et al., 2021). In contrast, in hepatocellular carcinoma (HCC), OTUD6B-AS1 could enhance cell proliferation and invasion ability via the GSKIP/Wnt/ β -catenin signaling pathway (Kong et al., 2020). MIR4435-2HG has been verified to be tumor supportive in multiple forms of cancer including breast cancer (Chen D. et al., 2021). Linc02084, as a low-risk immune-related lncRNA in ccRCC (Sun Z. et al., 2020), could also be used to construct a classifier for predicting early recurrence in HCC after curative resection (Lv et al., 2018). TRG-AS1 acted as a molecular sponge to stimulate tongue squamous cell carcinoma (He et al., 2020), HCC (Sun X. et al., 2020), and glioblastoma (Xie et al., 2019) progression. By means of both bioinformatic analysis and experimental validation, our research also indicated that TDRKH-AS1, MIR4435-2HG, HSD11B1-AS1, TRG-AS1, and AL451085.3 were likely to play tumor-supportive or tumor-suppressive roles in the development and progression of breast cancer and may be valuable independent prognostic indicators for patients with breast cancer.

Immune escape has emerged as a key mechanism for breast cancer progression and a crucial step in the preinvasive-to-invasive transition (Gil Del Alcazar et al., 2020). The hypoxic areas in solid tumors are highly infiltrated with immunosuppressive cells, such as tumor-associated macrophages (TAMs), myeloid-derived suppressor cells, and Tregs (Noman et al., 2014). Liang et al. showed that hypoxia-induced exosomal lncRNA BCRT1 contributed to M2 phenotype polarization of TAMs and enhanced its tumor-promoting function (Liang et al., 2020). Ben-Shoshan et al. revealed that hypoxia induced the differentiation of nonspecific CD4⁺ T cells into functionally active Foxp3 + CD4⁺CD25⁺ Treg cells to initiate an anti-inflammatory program via HIF-1 α (Ben-Shoshan et al., 2008). Neutrophils with HIF2A gain of function displayed a reduction of apoptosis both *ex vivo* and *in vivo* (Thompson et al., 2014). The presence of CD8⁺ T cells in breast cancer is a reliable predictor of clinical outcome and treatment response (Ali et al., 2014; Byrne et al., 2020). By univariable analysis, Denkert et al. found that high tumor-infiltrating lymphocytes predicted longer disease-free survival in patients with HER2-positive breast cancer and TNBC treated with neoadjuvant therapy (Denkert et al., 2018). Our GSEA results showed that multiple immune-related signaling pathways were significantly enriched in the low-risk group. To validate these findings, we performed immune cell infiltration analysis. Obviously, patients with high immune scores had lower risk scores, indicating better prognosis, in line with the findings of Bruni et al. (2020), Jiang

et al. (2019), Mlecnik et al. (2016), and Savas et al. (2016). Naïve B cells, CD8+T cells, activated NK cells, and Tregs were significantly enriched in the low-risk group, which was also partially consistent with the aforementioned previous findings. Considering the importance of immune checkpoint inhibitor-based immunotherapies, we further investigated the differences in the expression of 11 immune checkpoints between the high- and low-risk groups. We found that the expression GTR, OX40, CD137, CD40LG, CD28, CD278, CTLA4, VSIR, and CD233 were downregulated in the high-risk group, which corroborated the results of the study of Hu et al. that upregulated immune checkpoint genes were positively associated with high immune infiltration and favorable prognosis in patients with invasive breast carcinoma (Hu et al., 2020). The immune cell infiltration analysis based on our prognostic model suggests that patients in the low-risk group (with high prevalence of tumor-infiltrating cells lymphocytes, elevated immune-related signaling, and high mRNA expression levels of immune checkpoints) may benefit from immune checkpoint inhibitors while patients in the high-risk group (with low prevalence of tumor-infiltrating cells lymphocytes, downregulated immune-related signaling, and low mRNA expression levels of immune checkpoints) may not. Whether and how the PHRLs influence the immune microenvironment of breast cancer still remains to be explored.

CONCLUSION

In conclusion, we developed a novel prognostic model consisting of 12 hypoxia-related lncRNAs and an integrative nomogram that could predict the OS accurately and effectively for patients with breast cancer. Furthermore, we analyzed the immune cell infiltration conditions and drug sensitivity between high- and low-risk breast cancer classified based on the prognostic model. Our study uncovered dozens of potential prognostic biomarkers and therapeutic targets concerning the hypoxia signaling pathway in breast cancer.

REFERENCES

- Ali, H. R., Provenzano, E., Dawson, S.-J., Blows, F. M., Liu, B., Shah, M., et al. (2014). Association between CD8+ T-Cell Infiltration and Breast Cancer Survival in 12 439 Patients. *Ann. Oncol.* 25 (8), 1536–1543. doi:10.1093/annonc/mdu191
- Ben-Shoshan, J., Maysel-Auslender, S., Mor, A., Keren, G., and George, J. (2008). Hypoxia Controls CD4+CD25+ Regulatory T-Cell Homeostasis via Hypoxia-Inducible Factor-1 α . *Eur. J. Immunol.* 38 (9), 2412–2418. doi:10.1002/eji.200838318
- Bin, X., Hongjian, Y., Xiping, Z., Bo, C., Shifeng, Y., and Binbin, T. (2018). Research Progresses in Roles of lncRNA and its Relationships with Breast Cancer. *Cancer Cel Int* 18, 179. doi:10.1186/s12935-018-0674-0
- Bos, R., van der Groep, P., Greijer, A. E., Shvarts, A., Meijer, S., Pinedo, H. M., et al. (2003). Levels of Hypoxia-Inducible Factor-1? Independently Predict Prognosis in Patients with Lymph Node Negative Breast Carcinoma. *Cancer* 97 (6), 1573–1581. doi:10.1002/cncr.11246
- Bray, F., Ferlay, J., Laversanne, M., Brewster, D. H., Gombe Mbalawa, C., Kohler, B., et al. (2015). Cancer Incidence in Five Continents: Inclusion Criteria, Highlights from Volume X and the Global Status of Cancer Registration. *Int. J. Cancer* 137 (9), 2060–2071. doi:10.1002/ijc.29670

DATA AVAILABILITY STATEMENT

The datasets presented in this study can be found in online repositories. The names of the repository/repositories and accession number(s) can be found in the article/Supplementary Material.

AUTHOR CONTRIBUTIONS

PG, BY, and XS conceived and designed the study. PG, WWH, YL, and LZ acquired the data and analyzed the data. PG drafted the manuscript. PG, LZ, and WD prepared the tables and figures. PG, LZ, RW, and WW revised the manuscript. All authors read and approved the final manuscript.

FUNDING

Natural Science Foundation of Shanghai (Grant No.19ZR1441300). National Natural Science Foundation of China (Grant No.81270556). Shanghai Sailing Program (Grant No.20YF1438800).

ACKNOWLEDGMENTS

We sincerely acknowledge TCGA, GTEx, and GEPIA2 databases for providing their platforms and contributors for uploading their meaningful datasets.

SUPPLEMENTARY MATERIAL

The Supplementary Material for this article can be found online at: <https://www.frontiersin.org/articles/10.3389/fcell.2021.796729/full#supplementary-material>

- Bristow, R. G., and Hill, R. P. (2008). Hypoxia, DNA Repair and Genetic Instability. *Nat. Rev. Cancer* 8 (3), 180–192. doi:10.1038/nrc2344
- Bruni, D., Angell, H. K., and Galon, J. (2020). The Immune Contexture and Immunoscore in Cancer Prognosis and Therapeutic Efficacy. *Nat. Rev. Cancer* 20 (11), 662–680. doi:10.1038/s41568-020-0285-7
- Byrne, A., Savas, P., Sant, S., Li, R., Virassamy, B., Luen, S. J., et al. (2020). Tissue-resident Memory T Cells in Breast Cancer Control and Immunotherapy Responses. *Nat. Rev. Clin. Oncol.* 17 (6), 341–348. doi:10.1038/s41571-020-0333-y
- Cai, Y., Li, Y., Shi, C., Zhang, Z., Xu, J., and Sun, B. (2021). lncRNA OTUD6B-AS1 Inhibits many Cellular Processes in Colorectal Cancer by Sponging miR-21-5p and Regulating PNC2. *Hum. Exp. Toxicol.* 40, 1463–1473. doi:10.1177/0960327121997976
- Chen, D., Tang, P., Wang, Y., Wan, F., Long, J., Zhou, J., et al. (2021a). Downregulation of Long Noncoding RNA MR44352HG Suppresses Breast Cancer Progression via the Wnt/ β catenin Signaling Pathway. *Oncol. Lett.* 21 (5), 373. doi:10.3892/ol.2021.12634
- Chen, Y., Zitello, E., Guo, R., and Deng, Y. (2021b). The Function of lncRNAs and Their Role in the Prediction, Diagnosis, and Prognosis of Lung Cancer. *Clin. Translational Med.* 11 (4), e367. doi:10.1002/ctm2.367
- Choudhry, H., Harris, A. L., and McIntyre, A. (2016). The Tumour Hypoxia Induced Non-coding Transcriptome. *Mol. Aspects Med.* 47–48, 35–53. doi:10.1016/j.mam.2016.01.003

- Denkert, C., von Minckwitz, G., Darb-Esfahani, S., Lederer, B., Heppner, B. I., Weber, K. E., et al. (2018). Tumour-infiltrating Lymphocytes and Prognosis in Different Subtypes of Breast Cancer: a Pooled Analysis of 3771 Patients Treated with Neoadjuvant Therapy. *Lancet Oncol.* 19 (1), 40–50. doi:10.1016/s1470-2045(17)30904-x
- Dienstmann, R., Villacampa, G., Sveen, A., Mason, M. J., Niedzwiecki, D., Nesbakken, A., et al. (2019). Relative Contribution of Clinicopathological Variables, Genomic Markers, Transcriptomic Subtyping and Microenvironment Features for Outcome Prediction in Stage II/III Colorectal Cancer. *Ann. Oncol.* 30 (10), 1622–1629. doi:10.1093/annonc/mdz287
- Ferguson, N. L., Bell, J., Heide, R., Lee, S., Vanmeter, S., Duncan, L., et al. (2013). Prognostic Value of Breast Cancer Subtypes, Ki-67 Proliferation index, Age, and Pathologic Tumor Characteristics on Breast Cancer Survival in Caucasian Women. *Breast J.* 19 (1), 22–30. doi:10.1111/tbj.12059
- Floberg, J. M., Zhang, J., Muhammad, N., DeWees, T. A., Inkman, M., Chen, K., et al. (2021). Standardized Uptake Value for 18F-Fluorodeoxyglucose Is a Marker of Inflammatory State and Immune Infiltrate in Cervical Cancer. *Clin. Cancer Res.* 27, 4245–4255. doi:10.1158/1078-0432.Ccr-20-4450
- Gao, N., Li, Y., Li, J., Gao, Z., Yang, Z., Li, Y., et al. (2020). Long Non-coding RNAs: The Regulatory Mechanisms, Research Strategies, and Future Directions in Cancers. *Front. Oncol.* 10, 598817. doi:10.3389/fonc.2020.598817
- Geeleher, P., Cox, N., and Huang, R. S. (2014). pRRophetic: an R Package for Prediction of Clinical Chemotherapeutic Response from Tumor Gene Expression Levels. *PLoS One* 9 (9), e107468. doi:10.1371/journal.pone.0107468
- Gil Del Alcazar, C. R., Alečković, M., and Polyak, K. (2020). Immune Escape during Breast Tumor Progression. *Cancer Immunol. Res.* 8 (4), 422–427. doi:10.1158/2326-6066.Cir-19-0786
- Hanahan, D., and Weinberg, R. A. (2011). Hallmarks of Cancer: the Next Generation. *Cell* 144 (5), 646–674. doi:10.1016/j.cell.2011.02.013
- He, S., Wang, X., Zhang, J., Zhou, F., Li, L., and Han, X. (2020). TRG-AS1 Is a Potent Driver of Oncogenicity of Tongue Squamous Cell Carcinoma through microRNA-543/Yes-Associated Protein 1 axis Regulation. *Cell Cycle* 19 (15), 1969–1982. doi:10.1080/15384101.2020.1786622
- Hsing, C.-H., Cheng, H.-C., Hsu, Y.-H., Chan, C.-H., Yeh, C.-H., Li, C.-F., et al. (2012). Upregulated IL-19 in Breast Cancer Promotes Tumor Progression and Affects Clinical Outcome. *Clin. Cancer Res.* 18 (3), 713–725. doi:10.1158/1078-0432.Ccr-11-1532
- Hu, F.-F., Liu, C.-J., Liu, L.-L., Zhang, Q., and Guo, A.-Y. (2020). Expression Profile of Immune Checkpoint Genes and Their Roles in Predicting Immunotherapy Response. *Brief Bioinform.* 21, bbaa176. doi:10.1093/bib/bbaa176
- Jiang, Y.-Z., Ma, D., Suo, C., Shi, J., Xue, M., Hu, X., et al. (2019). Genomic and Transcriptomic Landscape of Triple-Negative Breast Cancers: Subtypes and Treatment Strategies. *Cancer Cell* 35 (3), 428–440. doi:10.1016/j.ccell.2019.02.001
- Jiang, Y., Chen, S., Li, Q., Liang, J., Lin, W., Li, J., et al. (2021). TANK-binding Kinase 1 (TBK1) Serves as a Potential Target for Hepatocellular Carcinoma by Enhancing Tumor Immune Infiltration. *Front. Immunol.* 12, 612139. doi:10.3389/fimmu.2021.612139
- Jiao, Y., Zhou, J., Jin, Y., Yang, Y., Song, M., Zhang, L., et al. (2020). Long Non-coding RNA TDRKH-AS1 Promotes Colorectal Cancer Cell Proliferation and Invasion through the β -Catenin Activated Wnt Signaling Pathway. *Front. Oncol.* 10, 639. doi:10.3389/fonc.2020.00639
- Kong, S., Xue, H., Li, Y., Li, P., Ma, F., Liu, M., et al. (2020). The Long Noncoding RNA OTUD6B-AS1 Enhances Cell Proliferation and the Invasion of Hepatocellular Carcinoma Cells through Modulating GSKIP/Wnt/ β -catenin Signalling via the Sequestration of miR-664b-3p. *Exp. Cell Res.* 395 (1), 112180. doi:10.1016/j.yexcr.2020.112180
- Kopp, F., and Mendell, J. T. (2018). Functional Classification and Experimental Dissection of Long Noncoding RNAs. *Cell* 172 (3), 393–407. doi:10.1016/j.cell.2018.01.011
- Leithner, K., Wohlkoe, C., Stacher, E., Lindenmann, J., Hofmann, N. A., Gallé, B., et al. (2014). Hypoxia Increases Membrane Metallo-Endopeptidase Expression in a Novel Lung Cancer *Ex Vivo* Model - Role of Tumor Stroma Cells. *BMC Cancer* 14, 40. doi:10.1186/1471-2407-14-40
- Li, N., and Zhan, X. (2019). Identification of Clinical Trait-Related lncRNA and mRNA Biomarkers with Weighted Gene Co-expression Network Analysis as Useful Tool for Personalized Medicine in Ovarian Cancer. *EPMA J.* 10 (3), 273–290. doi:10.1007/s13167-019-00175-0
- Li, X., Li, Y., Yu, X., and Jin, F. (2020). Identification and Validation of Stemness-Related lncRNA Prognostic Signature for Breast Cancer. *J. Transl. Med.* 18 (1), 331. doi:10.1186/s12967-020-02497-4
- Liang, Y., Song, X., Li, Y., Chen, B., Zhao, W., Wang, L., et al. (2020). lncRNA BCRT1 Promotes Breast Cancer Progression by Targeting miR-1303/PTBP3 axis. *Mol. Cancer* 19 (1), 85. doi:10.1186/s12943-020-01206-5
- Liu, S. J., Dang, H. X., Lim, D. A., Feng, F. Y., and Maher, C. A. (2021). Long Noncoding RNAs in Cancer Metastasis. *Nat. Rev. Cancer* 21, 446–460. doi:10.1038/s41568-021-00353-1
- Loibl, S., Poortmans, P., Morrow, M., Denkert, C., and Curigliano, G. (2021a). Breast Cancer. *Lancet.* doi:10.1016/s0140-6736(20)32381-3
- Loibl, S., Poortmans, P., Morrow, M., Denkert, C., and Curigliano, G. (2021b). Breast Cancer. *The Lancet* 397 (10286), 1750–1769. doi:10.1016/s0140-6736(20)32381-3
- Lv, Y., Wei, W., Huang, Z., Chen, Z., Fang, Y., Pan, L., et al. (2018). Long Non-coding RNA Expression Profile Can Predict Early Recurrence in Hepatocellular Carcinoma after Curative Resection. *Hepatol. Res.* 48 (13), 1140–1148. doi:10.1111/hepr.13220
- Ma, W., Zhao, F., Yu, X., Guan, S., Suo, H., Tao, Z., et al. (2020). Immune-related lncRNAs as Predictors of Survival in Breast Cancer: a Prognostic Signature. *J. Transl. Med.* 18 (1), 442. doi:10.1186/s12967-020-02522-6
- Marin-Acevedo, J. A., Dholaria, B., Soyano, A. E., Knutson, K. L., Chumsri, S., and Lou, Y. (2018). Next Generation of Immune Checkpoint Therapy in Cancer: New Developments and Challenges. *J. Hematol. Oncol.* 11 (1), 39. doi:10.1186/s13045-018-0582-8
- Marusyk, A., Almendro, V., and Polyak, K. (2012). Intra-tumour Heterogeneity: a Looking Glass for Cancer? *Nat. Rev. Cancer* 12 (5), 323–334. doi:10.1038/nrc3261
- Mlecnik, B., Bindea, G., Kirilovsky, A., Angell, H. K., Obenaus, A. C., Tosolini, M., et al. (2016). The Tumor Microenvironment and Immunoscore Are Critical Determinants of Dissemination to Distant Metastasis. *Sci. Transl. Med.* 8 (327), 327ra326. doi:10.1126/scitranslmed.aad6352
- Niu, Y., Bao, L., Chen, Y., Wang, C., Luo, M., Zhang, B., et al. (2020). HIF2-Induced Long Noncoding RNA RAB11B-AS1 Promotes Hypoxia-Mediated Angiogenesis and Breast Cancer Metastasis. *Cancer Res.* 80 (5), 964–975. doi:10.1158/0008-5472.Can-19-1532
- Noman, M. Z., Desantis, G., Janji, B., Hasmim, M., Karray, S., Dessen, P., et al. (2014). PD-L1 Is a Novel Direct Target of HIF-1 α , and its Blockade under Hypoxia Enhanced MDSC-Mediated T Cell Activation. *J. Exp. Med.* 211 (5), 781–790. doi:10.1084/jem.20131916
- O'Brien, K. M., Mooney, T., Fitzpatrick, P., and Sharp, L. (2018). Screening Status, Tumour Subtype, and Breast Cancer Survival: a National Population-Based Analysis. *Breast Cancer Res. Treat.* 172 (1), 133–142. doi:10.1007/s10549-018-4877-9
- Pardoll, D. M. (2012). The Blockade of Immune Checkpoints in Cancer Immunotherapy. *Nat. Rev. Cancer* 12 (4), 252–264. doi:10.1038/nrc3239
- Pei, J., Li, Y., Su, T., Zhang, Q., He, X., Tao, D., et al. (2020). Identification and Validation of an Immunological Expression-Based Prognostic Signature in Breast Cancer. *Front. Genet.* 11, 912. doi:10.3389/fgene.2020.00912
- Qian, Y., Shi, L., and Luo, Z. (2020). Long Non-coding RNAs in Cancer: Implications for Diagnosis, Prognosis, and Therapy. *Front. Med.* 7, 612393. doi:10.3389/fmed.2020.612393
- Samanta, D., and Semenza, G. L. (2018). Metabolic Adaptation of Cancer and Immune Cells Mediated by Hypoxia-Inducible Factors. *Biochim. Biophys. Acta (Bba) - Rev. Cancer* 1870 (1), 15–22. doi:10.1016/j.bbcan.2018.07.002
- Savas, P., Salgado, R., Denkert, C., Sotiropoulos, C., Darcy, P. K., Smyth, M. J., et al. (2016). Clinical Relevance of Host Immunity in Breast Cancer: from TILs to the Clinic. *Nat. Rev. Clin. Oncol.* 13 (4), 228–241. doi:10.1038/nrclinonc.2015.215
- Subramanian, A., Tamayo, P., Mootha, V. K., Mukherjee, S., Ebert, B. L., Gillette, M. A., et al. (2005). Gene Set Enrichment Analysis: A Knowledge-Based Approach for Interpreting Genome-wide Expression Profiles. *Proc. Natl. Acad. Sci.* 102 (43), 15545–15550. doi:10.1073/pnas.0506580102
- Sui, S., An, X., Xu, C., Li, Z., Hua, Y., Huang, G., et al. (2020). An Immune Cell Infiltration-Based Immune Score Model Predicts Prognosis and Chemotherapy Effects in Breast Cancer. *Theranostics* 10 (26), 11938–11949. doi:10.7150/thno.49451

- Sun, X., Qian, Y., Wang, X., Cao, R., Zhang, J., Chen, W., et al. (2020a). lncRNA TRG-AS1 Stimulates Hepatocellular Carcinoma Progression by Sponging miR-4500 to Modulate BACH1. *Cancer Cel Int* 20, 367. doi:10.1186/s12935-020-01440-3
- Sun, Z., Jing, C., Xiao, C., and Li, T. (2020b). Long Non-coding RNA Profile Study Identifies an Immune-Related lncRNA Prognostic Signature for Kidney Renal Clear Cell Carcinoma. *Front. Oncol.* 10, 1430. doi:10.3389/fonc.2020.01430
- Sung, H., Ferlay, J., Siegel, R. L., Laversanne, M., Soerjomataram, I., Jemal, A., et al. (2021). Global Cancer Statistics 2020: GLOBOCAN Estimates of Incidence and Mortality Worldwide for 36 Cancers in 185 Countries. *CA A. Cancer J. Clin.* 71, 209–249. doi:10.3322/caac.21660
- Szklarczyk, D., Morris, J. H., Cook, H., Kuhn, M., Wyder, S., Simonovic, M., et al. (2017). The STRING Database in 2017: Quality-Controlled Protein-Protein Association Networks, Made Broadly Accessible. *Nucleic Acids Res.* 45 (D1), D362–d368. doi:10.1093/nar/gkw937
- Thompson, A. A. R., Elks, P. M., Marriott, H. M., Eamsamarn, S., Higgins, K. R., Lewis, A., et al. (2014). Hypoxia-inducible Factor 2 α Regulates Key Neutrophil Functions in Humans, Mice, and Zebrafish. *Blood* 123 (3), 366–376. doi:10.1182/blood-2013-05-500207
- Vaupel, P., Schlenger, K., Knoop, C., and Höckel, M. (1991). Oxygenation of Human Tumors: Evaluation of Tissue Oxygen Distribution in Breast Cancers by Computerized O₂ Tension Measurements. *Cancer Res.* 51 (12), 3316–3322.
- Vaupel, P., Höckel, M., and Mayer, A. (2007). Detection and Characterization of Tumor Hypoxia Using pO₂ Histography. *Antioxid. Redox Signaling* 9 (8), 1221–1236. doi:10.1089/ars.2007.1628
- Vaupel, P., Mayer, A., and Höckel, M. (2004). Tumor Hypoxia and Malignant Progression. *Methods Enzymol.* 381, 335–354. doi:10.1016/s0076-6879(04)81023-1
- Wang, G. L., Jiang, B. H., Rue, E. A., and Semenza, G. L. (1995). Hypoxia-inducible Factor 1 Is a basic-helix-loop-helix-PAS Heterodimer Regulated by Cellular O₂ Tension. *Proc. Natl. Acad. Sci.* 92 (12), 5510–5514. doi:10.1073/pnas.92.12.5510
- Wang, G., Zhang, Z.-j., Jian, W.-g., Liu, P.-h., Xue, W., Wang, T.-d., et al. (2019a). Novel Long Noncoding RNA OTUD6B-AS1 Indicates Poor Prognosis and Inhibits clear Cell Renal Cell Carcinoma Proliferation via the Wnt/ β -Catenin Signaling Pathway. *Mol. Cancer* 18 (1), 15. doi:10.1186/s12943-019-0942-1
- Wang, L., Zhao, H., Xu, Y., Li, J., Deng, C., Deng, Y., et al. (2019b). Systematic Identification of lncRNA-based Prognostic Biomarkers by Integrating lncRNA Expression and Copy Number Variation in Lung Adenocarcinoma. *Int. J. Cancer* 144 (7), 1723–1734. doi:10.1002/ijc.31865
- Wang, W., Cheng, X., and Zhu, J. (2021). Long Non-coding RNA OTUD6B-AS1 Overexpression Inhibits the Proliferation, Invasion and Migration of Colorectal Cancer Cells via Downregulation of microRNA-3171. *Oncol. Lett.* 21 (3), 193. doi:10.3892/ol.2021.12454
- Wang, Y., Roche, O., Yan, M. S., Finak, G., Evans, A. J., Metcalf, J. L., et al. (2009). Regulation of Endocytosis via the Oxygen-Sensing Pathway. *Nat. Med.* 15 (3), 319–324. doi:10.1038/nm.1922
- Wang, Y., Yang, T., Han, Y., Ren, Z., Zou, J., Liu, J., et al. (2020a). lncRNA OTUD6B-AS1 Exacerbates As2O₃-Induced Oxidative Damage in Bladder Cancer via miR-6734-5p-Mediated Functional Inhibition of IDH2. *Oxidative Med. Cell Longevity* 2020, 1–22. doi:10.1155/2020/3035624
- Wang, Z., Xia, F., Feng, T., Jiang, B., Wang, W., and Li, X. (2020b). OTUD6B-AS1 Inhibits Viability, Migration, and Invasion of Thyroid Carcinoma by Targeting miR-183-5p and miR-21. *Front. Endocrinol.* 11, 136. doi:10.3389/fendo.2020.00136
- Xia, X., and Kung, A. L. (2009). Preferential Binding of HIF-1 to Transcriptionally Active Loci Determines Cell-type Specific Response to Hypoxia. *Genome Biol.* 10 (10), R113. doi:10.1186/gb-2009-10-10-r113
- Xie, H., Shi, S., Chen, Q., and Chen, Z. (2019). lncRNA TRG-AS1 Promotes Glioblastoma Cell Proliferation by Competitively Binding with miR-877-5p to Regulate SUZ12 Expression. *Pathol. - Res. Pract.* 215 (8), 152476. doi:10.1016/j.prp.2019.152476
- Yang, F., Zhang, H., Mei, Y., and Wu, M. (2014). Reciprocal Regulation of HIF-1 α and lncRNA-P21 Modulates the Warburg Effect. *Mol. Cel* 53 (1), 88–100. doi:10.1016/j.molcel.2013.11.004
- Yeo, J. G., Wasser, M., Kumar, P., Pan, L., Poh, S. L., Ally, F., et al. (2020). The Extended Polydimensional Immunome Characterization (EPIC) Web-Based Reference and Discovery Tool for Cytometry Data. *Nat. Biotechnol.* 38 (6), 679–684. doi:10.1038/s41587-020-0532-1
- Yuan, M., Yu, C., Chen, X., and Wu, Y. (2021). Investigation on Potential Correlation between Small Nuclear Ribonucleoprotein Polypeptide A and Lung Cancer. *Front. Genet.* 11, 1842. doi:10.3389/fgene.2020.610704
- Zhao, Y., Liu, L., Zhao, J., Du, X., Yu, Q., Wu, J., et al. (2021). Construction and Verification of a Hypoxia-Related 4-lncRNA Model for Prediction of Breast Cancer. *Ijgm Vol.* 14, 4605–4617. doi:10.2147/ijgm.S322007

Conflict of Interest: The authors declare that the research was conducted in the absence of any commercial or financial relationships that could be construed as a potential conflict of interest.

Publisher's Note: All claims expressed in this article are solely those of the authors and do not necessarily represent those of their affiliated organizations, or those of the publisher, the editors, and the reviewers. Any product that may be evaluated in this article, or claim that may be made by its manufacturer, is not guaranteed or endorsed by the publisher.

Copyright © 2021 Gu, Zhang, Wang, Ding, Wang, Liu, Wang, Li, Yan and Sun. This is an open-access article distributed under the terms of the Creative Commons Attribution License (CC BY). The use, distribution or reproduction in other forums is permitted, provided the original author(s) and the copyright owner(s) are credited and that the original publication in this journal is cited, in accordance with accepted academic practice. No use, distribution or reproduction is permitted which does not comply with these terms.



Long Non-Coding RNAs in Lung Cancer: The Role in Tumor Microenvironment

Shuang Dai^{1†}, Ting Liu^{2†}, Yan-Yang Liu^{1†}, Yingying He³, Tao Liu⁴, Zihan Xu¹, Zhi-Wu Wang^{5*} and Feng Luo^{1*}

¹Department of Medical Oncology, Lung Cancer Center, West China Hospital, Sichuan University, Chengdu, China, ²Department of Biotherapy, Cancer Center, West China Hospital, Sichuan University, Chengdu, China, ³Oncology Department, People's Hospital of Deyang City, Deyang, China, ⁴Department of Oncology, The First Affiliated Hospital of Chengdu Medical College, Chengdu Medical College, Chengdu, China, ⁵Department of Chemoradiotherapy, Tangshan People's Hospital, Tangshan, China

OPEN ACCESS

Edited by:

Zong Sheng Guo,
Roswell Park Comprehensive Cancer
Center, United States

Reviewed by:

Mario Cioce,
Campus Bio-Medico University, Italy
Claudia De Vitis,
Sapienza University, Italy

*Correspondence:

Feng Luo
hxlufeng@163.com
Zhi-Wu Wang
tcm2000@163.com

[†]These authors have contributed
equally to this work

Specialty section:

This article was submitted to
Molecular and Cellular Oncology,
a section of the journal
Frontiers in Cell and Developmental
Biology

Received: 15 October 2021

Accepted: 08 December 2021

Published: 03 January 2022

Citation:

Dai S, Liu T, Liu Y-Y, He Y, Liu T, Xu Z,
Wang Z-W and Luo F (2022) Long
Non-Coding RNAs in Lung Cancer:
The Role in Tumor Microenvironment.
Front. Cell Dev. Biol. 9:795874.
doi: 10.3389/fcell.2021.795874

The development of various therapeutic interventions, particularly immune checkpoint inhibitor therapy, have effectively induced tumor remission for patients with advanced lung cancer. However, few cancer patients can obtain significant and long-lasting therapeutic effects for the limitation of immunological nonresponse and resistance. For this case, it's urgent to identify new biomarkers and develop therapeutic targets for future immunotherapy. Over the past decades, tumor microenvironment (TME)-related long non-coding RNAs (lncRNAs) have gradually become well known to us. A large number of existing studies have indicated that TME-related lncRNAs are one of the major factors to realize precise diagnosis and treatment of lung cancer. Herein, this paper discusses the roles of lncRNAs in TME, and the potential application of lncRNAs as biomarkers or therapeutic targets for immunotherapy in lung cancer.

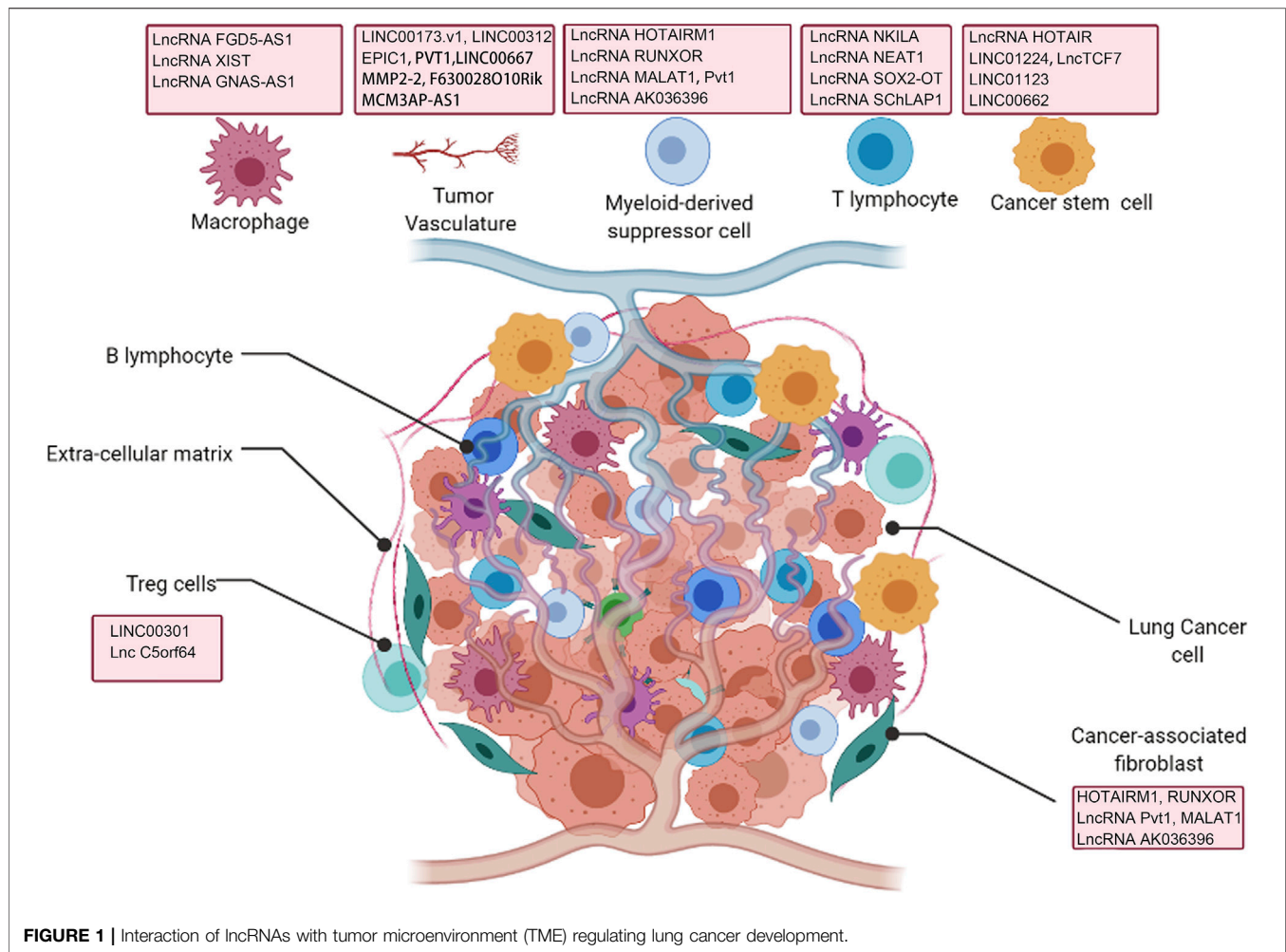
Keywords: lncRNA, non-small cell lung cancer, immunotherapy, tumor microenvironment, biomarker

INTRODUCTION

Lung cancer ranks the most important leading cause of cancer-related deaths globally (Bray et al., 2018; Nasim et al., 2019). Non-small cell lung cancer (NSCLC) accounts for more than 80% of all lung cancers (Bender, 2014). Despite the improvements of NSCLC treatment in traditional therapies, the overall cure and survival rates for NSCLC remain low, particularly in metastatic diseases (Siegel et al., 2020). Existing research suggests that combination treatment options (using immunotherapies or targeted therapies) may be the ultimate curative option. Hence, it is quite essential to investigate the precise molecular mechanism and biomarkers to promote the effectiveness of treatment, especially immune checkpoint inhibitors (ICIs).

ICIs reactivate dysfunctional and/or exhausted T cells by targeting immune checkpoints including cytotoxic T lymphocyte related protein 4 (CTLA-4), programmed cell death protein 1 (PD-1), or its ligand, PD-L1. To date, ICIs have altered treatment paradigm in multiple indications such as

Abbreviations: lncRNAs, Long Non-coding RNAs; LUAD, Lung adenocarcinoma; TME, Tumor microenvironment; ICIs, Immune checkpoint inhibitors; NSCLC, Non-small cell lung cancer; SQC, Lung squamous cell carcinoma; CTLA-4, cytotoxic T lymphocyte related protein 4; ORR, objective response rate; M1, Classically activated macrophages; M2, alternatively activated macrophage; MPS, monocyte macrophage system; EMT, Epithelial-to-mesenchymal transition; KCs, Kupffer cells; CTLs, Cytotoxic T lymphocyte cells; VEGF, Vascular endothelial growth factor; CSCs, Cancer stem cells; MDSCs, Myeloid-derived suppressor cells; Tregs, Regulatory T cells; VEGFA: vascular endothelial growth factor A.



melanoma, NSCLC, renal cell carcinoma (RCC) and so on (Pardoll, 2012; Hoos, 2016; Papaioannou et al., 2016; Munn and Jain, 2019; Xin Yu et al., 2019). However, the treatment response of ICIs remains unsatisfactory, and the objective response rate (ORR) for ICIs alone is only about 15–25%, and even lower in pancreatic carcinoma, triple negative breast cancer, and colorectal cancer with microsatellite stability (MSS) (Gao et al., 2019). Most patients still face the dilemmas of primary/acquired resistance of ICIs. A great number of studies have investigated the resistance mechanisms that limit the efficacy of ICIs such as disability of neoantigen presentation, activation of T cell, the impaired formation of T cell memory and the dysregulation of tumor microenvironment (TME) (Gajewski et al., 2013; Hegde et al., 2016; Jenkins et al., 2018; Yi et al., 2019; Schoenfeld and Hellmann, 2020). TME, comprised of the interaction between tumor cells, tumor-associated stromal cells as well as extracellular matrix, has been considered to be of great significance in activating the effect of ICIs. Notably, identifying abnormal TME and treatment-related biomarkers are not only the important means of antitumor therapy, but also of immune efficiency improvement (Gao et al., 2019).

LncRNAs, the most frequently expressed nonprotein-coding RNAs, have at least 200 nucleotides and are usually located in the cell nucleus, cytoplasm and exosomes where they interact with various molecules like DNA, RNA, proteins and so forth (Atianand and Fitzgerald, 2014). Multiple pathophysiological processes through the epigenetic, transcriptional and post-transcriptional regulation of gene are regulated by lncRNAs, of which lncRNAs include at least five categories including intergenic lncRNAs, intronic lncRNAs, antisense lncRNAs, sense lncRNAs and bidirectional lncRNAs (pseudogenes and retrotransposons) (Rinn and Chang, 2012). In TME, lncRNAs can directly or indirectly affect the growth of tumor cells, and play a nonnegligible role in the regulatory recircuit of the immune cells, promoting recruitment of immunosuppressive cells such as Tregs, M2-type macrophages and myeloid-derived suppressor cells (MDSCs), down-regulating the expression of adhesion molecules on endothelial cells, as well as up-regulating of immune checkpoints (PD-1/PD-L1 and CTLA4), which could contribute to tumor development and resistance to drugs or radiotherapy (Fu et al., 2021; Taheri et al., 2021). Specifically, lncRNAs are new emerging therapeutic targets and important prognostic biomarkers in multiple cancers including lung cancer

(Tokgun et al., 2020). Accumulating studies have identified that lncRNAs are essential mediators of intercellular communication between tumor and stromal cells in local and distant microenvironment of lung cancer.

In this review, we focus on describing how lncRNAs derived from tumor cells, immune cells or exosomes regulate the TME in lung cancer to promote tumor progression, emphasizing the role of these lncRNAs in tumor cells, lymphoid immune cells, macrophages, cancer-related fibroblasts, tumor vasculature and other components of TME (Figure 1).

LNCRNAS AFFECT LYMPHOID IMMUNE CELLS

Existing research has reported that lymphoid immune cells within tumors have two-sided (positive and negative) effects on tumorigenesis and tumor progression (Joyce and Pollard, 2009). lncRNAs as important regulator molecules influence the activity and sensitivity of tumor-infiltrating T cells. Duan et al. conducted lncRNA profiling to screen for differentially expressed lncRNAs related to CD8⁺ T cells and activated memory CD4⁺ T cells in NSCLC (Duan et al., 2020). A total of 90 DElncRNAs (differential expression lncRNA) showed different expression patterns in CD8⁺ T immune cells, and 48 DElncRNAs were associated with activated memory CD4⁺ T cells. The enrichment pathway analyses revealed that differentially expressed lncRNAs were mainly involved in cytokine–cytokine receptor interaction as well as viral protein interaction with cytokine–cytokine receptor, suggesting that T cell-specific lncRNAs mediated an immune response during NSCLC progression. This study provided a cursory but comprehensive indication of the vital role of lncRNAs in influencing the biological function of T lymphoid cells in lung cancer. Specifically, a study reported that a large proportion of CTLs/Th1 cells underwent apoptosis in NSCLC, a process that could be further facilitated by anti-CD3, while the proportion of Th2 cells/Treg cells were relatively low in TME, suggesting CTLs/Th1 cells were more sensitive to activation-induced cell death (AICD) than Tregs/Th2 cells. Further analysis indicted that STAT1-mediated transcription of NKILA caused AICD of CTLs/Th1 cells by suppressing NF- κ B which was upregulated in Tregs/Th2 cells compared with CTLs/Th1 cells (Huang et al., 2018). Tang et al. also observed that the proportion of Th2 was high in peripheral blood of NSCLC, and the proportion of CTLs/Th1 cell was lower than that in normal control. lncRNA NEAT1 was also reported to be upregulated in lung cancer tissues with high TILs. NEAT1 negatively regulated CD8⁺ T cells in lung cancer cells via increasing CXCL10, CCL5, and IFN- β expression, which directly induced cGAS/STING Signaling, to suppress immune response (Ma et al., 2020). In addition, signaling from SOX2-OT/miR-30d-5p/PDK1 contributed to apoptosis of CD8⁺ T cells, which in turn promoted immune escape of NSCLC (Chen et al., 2021). The direct interaction between SchLAP1 and AUF1 antagonized the binding between AUF1 and PD-L1 mRNA 3'-UTR, resulting in improving PD-L1 mRNA stability and expression, thereby attenuating CTLs function (Du et al.,

2021). Collectively, lncRNAs control lung cancer development and metastasis by affecting T cell function in TME, and targeting lncRNA may alter the activity of CTLs, thereby enhancing the effectiveness of immunotherapy.

LNCRNAS IN CANCER STEM CELLS

Cancer stem cells (CSCs) are regarded as a population of tumor cells characterized by abilities to self-renew or to differentiate into cancer non-stem progenies, and therefore often involved in the resistance to cancer therapies, tumorigenesis, epithelial-to-mesenchymal transition (EMT) and tumor metastases (Clarke and Fuller, 2006; Zhao, 2016). CD44, CD133, OCT-4, Bmi-1, ALDH1, ABCG2 and KLF4 are common CSC biomarkers that are specifically and highly expressed on the cell surface. For example, Prior researches elucidated the determinants about the resistance to cancer treatments including growth features associated with slow division and quiescence (Vidal et al., 2014; Ajani et al., 2015), ATP-binding cassette (ABC) transporters expression levels involved in elimination of drugs (Abdullah and Chow, 2013), and the presence of increased detoxification of endogenous and exogenous aldehyde substrates via the aid of aldehyde dehydrogenases (ALDHs) (Sládek, 2003; Ahmed Laskar and Younus, 2019). As a pivotal component of the TME, the maintenance of CSCs as well as the growth and progression of tumors are inseparable from the cancer microenvironment, together with various regulatory factors. To date, lncRNAs involved in both CSCs biological functions and cancer development have received considerable research attention (Schwerdtfeger et al., 2021). Here we have reviewed relevant literatures to summarize the functions.

In regulating tumorigenesis, lncRNA HOTAIR was reported to exert pro-cancer effects by inducing CSCs and EMT formation under the direct regulation of STAT3 under cigarette smoke exposure (Liu et al., 2015). The relationship between stemness and EMT programs has been reviewed in previous literature (Wilson et al., 2020). DUXAP10 was obviously upregulated in Cd-induced lung cancer cells. DUXAP10 knockdown induced the stemness markers including KLF4, KLF5 and Nanog downregulation, weakened the capacity of spheres formation and reduced the number of stem cells marked by CD133 via inhibiting the Hedgehog signaling pathway signal, which was involved in Cd carcinogenesis in lung cells (Lin et al., 2021). As for resistance to cancer therapies, Liu et al. revealed that lncRNA HOTAIR could cause cisplatin resistance via inducing stem cell-related biomarkers β -catenin and KLF4, especially directly regulating KLF4, to promote stemness (Liu et al., 2016). Similarly, LINC01224 is obviously upregulated in NSCLC cells and associated with NSCLC radioresistance. LINC01224 knockdown dramatically promotes the abilities of self-renew by regulating the expression of ZNF91 and therefore suppresses the irradiation sensitivity of NSCLC (Fu et al., 2021). In terms of EMT and metastasis, FOXF1-AS1 acted as a protective factor and interacted with PRC2 components EZH2 to hinder self-renewal of NSCLC CSCs and reduce the number of stem-like cells, thus leading to impaired EMT capacity of tumor cells (Miao et al.,

TABLE 1 | LncRNAs and their respective molecules or pathways involved in theTME.

LncRNA	Effects	Mechanism	References
FGD5-AS1	M2	Regulating FGD5-AS1/miR-944/MACC1 axis	Lv et al. (2021)
XIST	M2	Regulates M2 polarization	Sun and Xu (2019)
GNAS-AS1	M2	GNAS-AS1/miR-4319/NECAB3 axis	Li et al. (2020a)
SOX2-OT	M2	Targeting miR-627-3p/Smads signaling pathway	Zhou et al. (2021)
NKILA	CTLs/Th1	Enhancing AICD of CTLs/Th1 cells by suppressing NF- κ B	Huang et al. (2018)
NEAT1	CTLs	Suppressing cGAS/STING Signaling	Ma et al. (2020)
SOX2-OT	CTLs	SOX2-OT/miR-30d-5p/PDK1	Chen et al. (2021)
SChLAP1	CTLs	Regulating the AUF1/PDL1 axis	Du et al. (2021)
HOTAIR	CSCs	Inducing EMT and CSCs under the direct regulation of STAT3	Liu et al. (2015)
HOTAIR	CSCs	Inducing CSCs-related biomarkers β -catenin and Klf4	Liu et al. (2016)
FOXF1-AS1	CSCs	Interacting with EZH2 to inhibit the EMT ability of tumor cells	Miao et al. (2016)
TCF7	CSCs	Regulating TCF7/miR-200c/EpCAM	Wu and Wang (2017)
LINC00662	CSCs	Interacting with Lin28	Gong et al. (2018)
DUXAP10	CSCs	Inhibiting the Hedgehog signaling pathway signal	Lin et al. (2021)
MCF2L-AS1	CSCs	Regulating miR-873-5p	Li and Lin (2021)
LINC01224	CSCs	Interacting with ZNF91 to enhance irradiation resistance	Fu et al. (2021)
LINC01123	CSCs	Precipitating miR-449b-5p to activate NOTCH1 pathway signal	Zhang et al. (2020)
DANCR	CSCs	Activating DANCR/miR-216a signaling axis	Yu et al. (2020)
DHRS4-AS1	CSCs	Modulating DHRS4-AS1/miR-224-3p signaling	Yan et al. (2020)
MACC1-AS1	CSCs	MACC1-AS1/UPF1/LATS1/2 axis	Wang et al. (2020)
loc107985872	CSCs	Activating the notch1 signaling pathway	Guo et al. (2020)
SLNCR1	CSCs	Interacting with sPLA2	Xu et al. (2019)
LINC00887	CSCs	Stimulating multiple microRNAs (miRNAs)	Tian et al. (2019)
HAND2-AS1	CSCs	Interacting negatively with TGF- β 1	Miao et al. (2019)
TUSC-7	CSCs	sponging miR-146	Huang et al. (2019)
CASC11	CSCs	Interacting with TGF- β 1 to increase stemness of CSCs	Fu et al. (2019)
CCAT1	CSCs	Activating Wnt signalling	Xu et al. (2018)
DGCR5	CSCs	DGCR5/miR-330-5p/CD44 axis	Wang et al. (2018)
NEAT1	CSCs	Activating Wnt signalling	Jiang et al. (2018)
HOTAIRM1	MDSCs	Targeting HOXA1	Tian et al. (2018a)
RUNXOR	MDSCs	Regulating RUNX1 mRNA	Tian et al. (2018b)
LncRNA Pvt1	MDSCs	Attenuating Arg1 activity and ROS production	Zheng et al. (2019)
AK036396	MDSCs	Repressing Arg1 activity <i>in vitro</i> and CD244 expression	Tian et al. (2020)
MALAT1	MDSCs	Unknown	Zhou et al. (2018)
LINC00301	Tregs	Accumulating Tregs upon targeting TGF- β 1	Sun et al. (2020)
C5orf64	Tregs	Decreasing Tregs abundance	Pang et al. (2021)
NRK	CAFs	Unknown	Wei et al. (2021)
LINC00173.v1	Vasculature	Sponging miR-511-5p as a ceRNA	Chen et al. (2020)
EPIC1	Vasculature	Ang2 -Tie2 signaling pathway	Hou et al. (2021)
LINC00667	Vasculature	Inducing eukaryotic translation initiation factor 4A3 (EIF4A3)	Yang et al. (2020)
F630028O10Rik	Vasculature	Sponging miR-223-3p	Qin et al. (2020)
MCM3AP-AS1	Vasculature	Targeting miR-340-5p/KPNA4 axis	Li et al. (2020b)
PVT1	Vasculature	Targeting the miR-29c/VEGF signaling pathway	Mao et al. (2019)
LINC00312	Vasculature	Binding YBX1	Peng et al. (2018)
lnc-MMP2-2	Vasculature	Regulating MMP2 expression	Wu et al. (2018)

LncRNAs: Long Non-coding RNAs; CSCs: Cancer stem cells; MDSCs: Myeloid-derived suppressor cells; Tregs: Regulatory T cells; M2: alternatively activated macrophage.

2016). LncTCF7 overexpression increased NSCLC sphere formation and expression of specific markers (EpCAM, Sox2, Oct4 and Nanog). Further study of the molecular mechanism of TCF7 regulation of CSC revealed that TCF7 may exhibit oncogenic activity by regulating EpCAM via competitively binding miR-200c, which stimulated invasive activity and enhanced the self-renewal capacity of CSCs (Wu and Wang, 2017). The interaction with LINC00662 and its RNA binding protein Lin28 can elevate CSCs stemness and invasion ability of tumor cells, contributing to the poor prognosis of NSCLC (Gong et al., 2018). The expression of LINC01123 is up-regulated in LUAD. Mechanistically, LINC01123 could precipitate miR-449b-5p to release NOTCH1, thereby promoting downstream

NOTCH1 signaling and resulting in accelerating LUAD cell stemness and EMT (Zhang et al., 2020). More LncRNAs affecting CSC properties are summarized in **Table 1**. Taken together, all these data elucidate that dysregulation of lncRNAs affects CSCs traits and tumor invasion, and could be potential targets of tumor immunotherapy.

LNCRNAs CONTRIBUTE TO MACROPHAGE PLASTICITY

Macrophages, most of which derived from blood monocytes, are involved in EMT and are present in almost all tissues such as

hepatic Kupffer cells (KCs) or brain microglia (Varol et al., 2015). According to the different mechanisms of action, macrophages are roughly divided into classically activated macrophages known as “killer” macrophages (M1) activated by IFN- γ , TNF- α as well as lipopolysaccharide (LPS) and alternatively activated macrophages known as “repair” macrophage (M2) activated by IL-4, IL-10 or IL-13 (Li et al., 2019). Basic studies have indicated that in mouse models, high levels of MHC II molecules are expressed in tumor-associated macrophages (TAMs) with the hallmark of M1 during the early stages of tumor development. However, the advanced stage of tumor is mainly characterized by low-level MHC II molecules of M2, which indicates that an M1-to-M2 transformation is present in tumor progress (Mantovani et al., 2002; Wang et al., 2011). Obviously, the accumulation of macrophages is related to tumor angiogenesis, tumor invasion and immunosuppression (Condeelis and Pollard, 2006). lncRNAs expression has been implicated in many cellular and developmental processes like cell proliferation and apoptosis (Batista and Chang, 2013; Heward and Lindsay, 2014). Prior reports have suggested that lncRNAs are also involved in regulating macrophage polarization (Huang et al., 2016).

In recent years, it has been shown that lncRNAs originating from tumor cells are involved in the polarization of TAMs and result in tumor progression. Tumor cell-derived FGD5-AS1 *via* exosomes transportation promotes upregulation of M2 polarization markers (CD163, CD206, ARG1) and downregulation of M1 macrophage markers iNOS and IL-2 in NSCLC (Lv et al., 2021). Sun et al. summarized that the upregulated lncRNA XIST promoted macrophage conversion to M2 characterized by the deletion of specific makers like IL-10 and CD163, to affect tumor invasion and migration of lung cancer (Sun and Xu, 2019). GNAS-AS1 inhibits miR-4319 expression, and consequently activates N-terminal EF-hand calcium binding protein 3 (NECAB3) in THP-1-differentiated macrophages. Therefore, GNAS-AS1 increases the number of M2 macrophage and consequently promoting NSCLC cell growth and metastasis (Li Z. et al., 2020). Moreover, tumor-derived exosomal SOX2 overlapping transcript also play an important role in modulating the polarization of TAMs in NSCLC through regulating SOX2/miR-627-3p/Smads axis (Zhou et al., 2021). Taken together, lncRNAs directly or indirectly regulate the polarization of TAMs to affect lung cancer progression and metastasis, but the specific regulatory mechanism controlling the macrophages M2 polarization in lung cancer needs to be further studied.

LNCRNAS PROMOTE BY REGULATING IMMUNE SUPPRESSIVE CELLS

Studies have shown that the interactions between non-tumor cells exposed to the tumor microenvironment and tumor cells contribute to tumor progression and metastasis. In addition, T cells in tumors are often dysregulated and unable to generate specific responses to tumor cells in a timely manner. Immunosuppressive cells, including regulatory T cells (Tregs) usually expressing CD4, CD25 and FOXP3 markers (T cells that

are not immunosuppressive) and MDSC, can contribute directly or indirectly to immunosuppression, which are reviewed in detail below.

Myeloid-Derived Suppressor Cells

Myeloid-derived suppressor cells (MDSCs) express two specific markers, CD11b and Gr1, and represent a heterogeneous population of myeloid origin that are activated and proliferated by growth factors and cytokines released by tumor cells. Once MDSCs are activated, they accumulate in lymphoid organs and tumors and exert immunosuppression on T cells. Currently, the cellular mechanisms by which MDSCs have been shown to be involved in immunosuppressive activity are: 1) inhibition of CTL cells activation and proliferation in an MHC-restricted or unrestricted and antigen-specific manner (Nagaraj et al., 2007; Zou et al., 2021); 2) indirectly affects T cell activation via the induction of Treg proliferation and benefiting from TGF, IL-10 production (Serafini et al., 2008); 3) Stimulation of macrophage conversion to M2 by secreting IL-10 and down-regulation of IL-12 that promotes M1 generation (Sinha et al., 2007); 4) interaction with type II iNKT, which promotes tumor progression through IL-13 production, thereby inducing aggregation of MDSCs (Zou et al., 2021). Of note, MDSCs have immunosuppressive activity only when activated. The molecules that can activate MDSCs include two main categories: 1) tumor-derived soluble factor (TDSF), which inducing the proliferation of MDSCs through activating STAT3 to stimulate the proliferation of myeloid cells and inhibit the differentiation of mature myeloid cells, including VEGF, SCF, GM-CSF, G-CSF, IL-6, IL-10, IL-12, MMP9 and CCL2 (Talmadge, 2007; Marigo et al., 2008); 2) soluble factors released by activated T cells and tumor-derived stromal cells, such as IFN- γ , TLRs ligands, IL-4, IL-13 as well as TGF- β , are responsible for the activation of different transcription factors such as STAT6, STAT1 and NF κ B (Gabrilovich and Nagaraj, 2009). Recently, it has been shown that lncRNAs affect lung cancer progression by regulating the immunosuppressive function of MDSCs in TME. Tian et al. discovered that HOTAIRM1 is obviously downregulated in MDSCs and its expression reduces in peripheral blood of lung cancer. Overexpression of HOTAIRM1 can positively target HOXA1 and induce subsequent reduction of the immunosuppression function of MDSCs, as well as increase the number of Th1/CD8+ cytotoxic T lymphocyte cells (CTLs), thereby sustaining improving the antitumor immune response (Tian et al., 2018a). Moreover, they also observed that the expression of lncRNA RUNXOR is higher in the blood of lung cancer patients than the levels in healthy samples, while decreases after surgery. Further detection suggested that RUNXOR can promote the activation of MDSCs and decrease the proportion of Th1/CTL cells by regulating RUNX1 mRNA expression (Tian et al., 2018b). A study on lncRNA MALAT1 indicated that MALAT1 directly affected MDSCs differentiation in lung cancer (Zhou et al., 2018). Some studies are more detailed. Zheng et al. identified that the expression level of lncRNA Pvt1 was upregulated in G-MDSCs following induction of IL-6 and GM-CSF. In contrast, when Pvt1 was knocked down, Arg1 activity and ROS production were

significantly reduced and the ability of G-MDSCs to suppress T cells turned weak. In mice injected with Lewis lung carcinoma cells, they found that the number of CTLs/Th1 cells increased compared with the normal treatment group. The function of G-MDSCs was obviously upregulated under hypoxic conditions though targeting HIF-1 α , and inhibition of HIF-1 α by YC-1 apparently reduced Pvt1 expression in G-MDSCs (Zheng et al., 2019). Owing to the diverse phenotype of MDSCs, MDSCs tend to be classified into CD11b⁺Ly6G⁺Ly6C^{low} polymorphonuclear MDSCs (PMN-MDSCs) and CD11b⁺Ly6G⁺Ly6C^{hi} monocytic MDSCs (M-MDSCs) in mice (Youn et al., 2008). A latest study revealed that lncRNA AK036396 had a fairly high level of expression in PMN-MDSCs, whereas knockdown of AK036396 repressed Arg1 activity *in vitro* and CD244 expression leading to reduction of immunosuppressive effects of PMN-MDSCs (Sagiv et al., 2015). At the mechanistic level, the researchers found that lncRNA AK036396 could interact with Fcbl through abrogating its ubiquitination to enhance its stability in the cytoplasm of myeloid cells, to enhance the immunosuppression of PMN-MDSCs and attenuate Th1/CTL cells responses, and ultimately accelerating tumor progression (Tian et al., 2020). These studies have demonstrated that lncRNAs play a significant role in the aggregation and activation of MDSCs. However, the role and regulatory mechanism during tumor progression of these lncRNAs within MDSCs in lung cancer awaits further exploration.

Treg Cells

Regulatory T cells (Tregs), as a major subset of infiltrating CD4⁺ T cells in TME, specifically express the master transcription factor FOXP3 (Sakaguchi et al., 2020), and have been found to suppress anti-tumor immune responses in diverse ways, including: 1) targeting TGF- β , thus inhibits the anti-tumor effects promoted by CD4⁺ cells, CD8⁺ cells, and NK cells (Konkel and Chen, 2011; Sun et al., 2020); 2) disrupting metabolism by scavenging cytokines such as IL-2, or producing immunosuppressive adenosines by extracellular enzymes CD39 and CD73 (Spolski et al., 2018); 3) inhibiting the maturation and function of DC; 4) dissolved by granulase A or B and perforation induced CD8⁺ lymphocytes. Several studies involving humans and mice have shown that extrinsic tissue and tumors in different tissues contain the largest Tregs, and that the absence of Treg cells can significantly improve anti-tumor immunity. A few studies reported that lncRNA affects tumor progression by regulating the biological behaviors and function of Tregs. Sun et al. identified a novel lncRNA, LINC00301, that can promote the accumulation of Tregs and decrease CD8⁺ T cell in NSCLC upon targeting TGF- β 1 (Sun et al., 2020). Moreover, lncRNA C5orf64 expression is positively correlated with NSCLC survival, but negatively associated with Tregs levels (Pang et al., 2021).

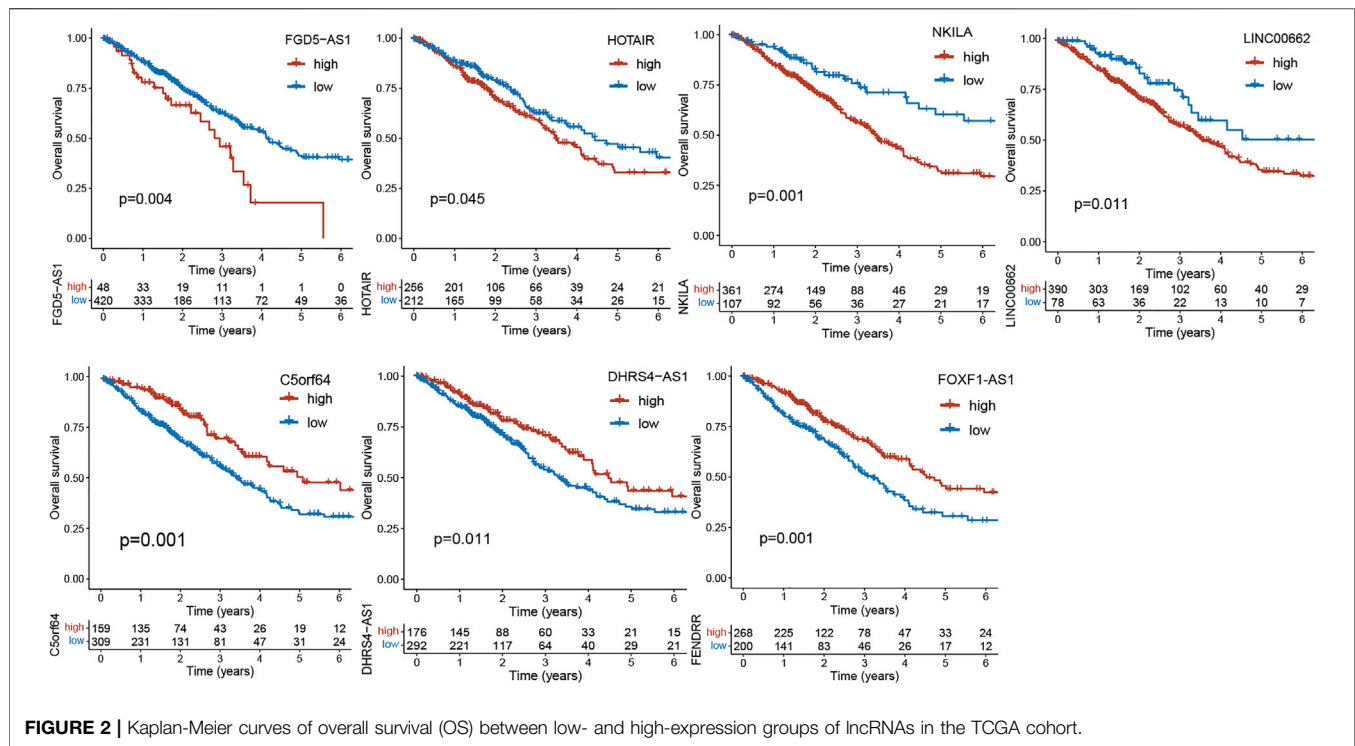
THE ROLE OF LNCRNA IN CANCER-ASSOCIATED FIBROBLASTS

Cancer-associated fibroblasts (CAFs), as one of major components in TME that derive from the differentiation of

quiescent fibroblasts by activation of various external factors like cytokines/chemokines, growth factors, hypoxia factors, lncRNAs and so on, participate in the entire cancer developmental process, from tumor initiation to progression, including carcinogenesis, proliferation, migration, EMT, drug resistance, metabolic reprogramming, angiogenesis and immunosuppression (Wu et al., 2017; Shoucair et al., 2020; Yang et al., 2021). Growing studies also reveal that lncRNAs also play a nonnegligible role in cancer cells and CAFs by shuttling via exosomes and directly within CAFs or cancer cells. But, the roles of lncRNAs in CAFs during lung cancer progression indeed remain unclear and are poorly studied. Teng et al. had attempted to identify differentially expressed lncRNAs between CAFs and normal fibroblasts in NSCLC using lncRNA profiling analysis with the intention of selecting important biomarkers working in TME. They found that upregulated lncRNAs were involved in important cancer-related regulatory pathways such as NOD-like receptor signaling (Teng et al., 2019). The roles and mechanisms of action of individual lncRNAs in CAFs of lung cancer are starting to be realized.

THE TUMOR VASCULATURE IS SUPPORTED BY LNCRNAs

In physiological environment, angiogenesis maintains a relatively dynamic homeostasis and is strictly controlled by pro-angiogenesis and anti-angiogenesis regulators (Ribatti et al., 2007). Hypoxia and acidosis in tumor bed are often attributed to a large consumption of oxygen and nutrients and an active metabolism under a disproportionate blood supply (Kerbel, 2008; Sun, 2012). In this case, it continues to induce the production of large amounts of pro-angiogenic factors in TME (Ronca et al., 2017). Meanwhile, various angiogenic factors such as Vascular endothelial growth factor (VEGF) (Ferrara et al., 2003), angiopoietin (ANGPT) (Fagiani and Christofori, 2013) and basic fibroblast growth factor (bFGF) (Zheng et al., 2018) also increase and have immunosuppressive functions. As a result, the balance of pro- and anti-angiogenesis is disturbed in cancer, leading to a shift to angiogenesis and immunosuppressive microenvironment (Ribatti et al., 2007). Some evidence has shown that lncRNAs act on tumor progression by regulation of VEGF in lung cancer. A report (Chen et al., 2020) showed that LINC00173.v1 is upregulated in lung squamous cell carcinoma (SQC) tissues and is negatively associated with SQC prognosis. Knockdown of LINC00173.v1 suppresses VEGFA expression, thus attenuating vascular endothelial cell proliferation and migration, as well as tumorigenesis of SQC cells. Mechanistic evidence has exhibited that LINC00173.v1 exerts these functions by sponging miR-511-5p as a ceRNA. Hou et al. (2021) reported that lncRNA EPIC1 is significantly upregulated in NSCLC tissues and cells. EPIC1 silence represses Ang2-Tie2 signaling pathway-related proteins, thereby inhibiting HUVECs (human umbilical vein endothelial cell) proliferation and channel forming abilities. lncRNA LINC00667 induces eukaryotic translation initiation factor 4A3 (EIF4A3) expression and secretion, and consequently activates the mRNA and protein levels of



VEGFA. Therefore, LINC00667 promotes angiogenesis of NSCLC cells and consequently results in NSCLC tumor growth and metastasis (Yang et al., 2020). Knockdown of lncRNA F630028O10Rik in lung cancer increases VEGFA and VEGFR2 expression by sponging miR-223-3p, which means that F630028O10Rik could inhibit tube formation in vascular endothelial cells, thus further influencing angiogenesis in lung cancer (Qin et al., 2020). Besides, lncRNAs, MCM3AP-AS1 (Li X. et al., 2020) and PVT1 (Mao et al., 2019) also play a key role in accelerating angiogenesis in lung cancer, respectively. These researches provide a rationale for using the anti-angiogenic effects of lncRNAs as a therapeutic option for lung cancer. Yet, the effect on tumor angiogenesis for lncRNAs still awaits further investigation.

LNCRNAs AS PROGNOSTIC BIOMARKERS

Diagnosis and therapies using lncRNAs are being developed. For example, the investigators have conducted clinical settings to identify lncRNA biomarkers from the plasma to facilitate detection of early lung cancer (NCT03830619). Studies have suggested that lncRNAs not only interact with the TME, but closely correlate with cancer prognosis. We extracted a number of gene expression profiles of lncRNAs in Lung adenocarcinoma from the TCGA database ($N = 468$). Based on the best cutoff value of gene expressions, we performed Kaplan-Meier survival analysis to validate the association between part of lncRNAs mentioned above and prognosis of lung cancer using the R package “Survminer”. As illustrated in **Figure 2**, the key lncRNAs exhibit good performance in prognostic prediction of

lung cancer ($p < 0.05$). For instance, FDG5-AS1, HOTAIR, NKILA and LINC00662 are regarded as risk factors for survival of lung cancer (Liu et al., 2015; Gong et al., 2018; Huang et al., 2018; Lv et al., 2021), while C5orf64, DHRS4-AS1 and FOXF1-AS1 are protective factors. These genes have important effects on lung cancer (Miao et al., 2016; Yan et al., 2020; Pang et al., 2021). As far as these lncRNAs are concerned, although there is no specific clinical application in lung cancer to date, they are still potential for the comprehensive treatment and diagnosis of lung cancer.

CONCLUSION AND FUTURE PERSPECTIVES

Lung cancer is a highly malignant tumor that poses a serious threat to human health and life. There is a lack of effective means to identify early-stage lung cancer, leading to high mortality and failure of comprehensive interventions. Meanwhile, with advances in immunotherapy, the role of TME in the lung cancer diagnosis and prognostic is becoming increasingly critical. Components of TME interacting with lncRNA have been shown to contribute to immunomodulation and cancer progress. Hence, we summarized recent advancement involving lncRNAs and their roles in the crosstalk between components of TME including infiltrated immune cells, CSCs, immune suppressive cells, macrophage, CAFs and part of the underlying molecular mechanisms. So far, only a small number of lncRNAs have been well elucidated in tumor-mesenchymal crosstalk, and in-depth studies are worthwhile to identify more lncRNAs and their specific biological functions and

mechanisms of involvement. A deeper understanding of the role played by lncRNAs in the tumor microenvironment may greatly facilitate further discovery of potential biomarkers and the development of novel targeted therapies for the treatment of lung cancer. To date, the pressing issue has been the in-depth and systematic elucidation of the regulatory determinant mechanism of lncRNAs.

In conclusion, the important regulatory roles of lncRNAs in the TME have been gradually described; however, the clinical applications of lncRNAs still need to be further explored. Along with further research, tumor-associated lncRNAs crosstalk will open a new era of anti-tumor therapy.

REFERENCES

- Abdullah, L. N., and Chow, E. K. H. (2013). Mechanisms of Chemoresistance in Cancer Stem Cells. *Clin. translational Med.* 2, 3. doi:10.1186/2001-1326-2-3
- Ahmed Laskar, A., and Younus, H. (2019). Aldehyde Toxicity and Metabolism: The Role of Aldehyde Dehydrogenases in Detoxification, Drug Resistance and Carcinogenesis. *Drug Metab. Rev.* 51, 42–64. doi:10.1080/03602532.2018.1555587
- Ajani, J. A., Song, S., Hochster, H. S., and Steinberg, I. B. (2015). Cancer Stem Cells: The Promise and the Potential. *Semin. Oncol.* 42 (1), S3–S17. doi:10.1053/j.seminoncol.2015.01.001
- Atianand, M. K., and Fitzgerald, K. A. (2014). Long Non-Coding RNAs and Control of Gene Expression in the Immune System. *Trends Molecular Medicine* 20, 623–631. doi:10.1016/j.molmed.2014.09.002
- Batista, P. J., and Chang, H. Y. (2013). Long Noncoding RNAs: Cellular Address Codes in Development and Disease. *Cell* 152, 1298–1307. doi:10.1016/j.cell.2013.02.012
- Bender, E. (2014). Epidemiology: The Dominant Malignancy. *Nature* 513, S2–S3. doi:10.1038/513S2a
- Bray, F., Ferlay, J., Soerjomataram, I., Siegel, R. L., Torre, L. A., and Jemal, A. (2018). Global Cancer Statistics 2018: GLOBOCAN Estimates of Incidence and Mortality Worldwide for 36 Cancers in 185 Countries. *CA: A Cancer J. Clinicians* 68, 394–424. doi:10.3322/caac.21492
- Chen, J., Liu, A., Wang, Z., Wang, B., Chai, X., Lu, W., et al. (2020). LINC00173.v1 Promotes Angiogenesis and Progression of Lung Squamous Cell Carcinoma by Sponging miR-511-5p to Regulate VEGFA Expression. *Mol. Cancer* 19, 98. doi:10.1186/s12943-020-01217-2
- Chen, Z., Chen, Z., Xu, S., and Zhang, Q. (2021). LncRNA SOX2-OT/miR-30d-5p/PDK1 Regulates PD-L1 Checkpoint through the mTOR Signaling Pathway to Promote Non-Small Cell Lung Cancer Progression and Immune Escape. *Front. Genet.* 12, 674856. doi:10.3389/fgenet.2021.674856
- Clarke, M. F., and Fuller, M. (2006). Stem Cells and Cancer: Two Faces of Eve. *Cell* 124, 1111–1115. doi:10.1016/j.cell.2006.03.011
- Condeelis, J., and Pollard, J. W. (2006). Macrophages: Obligate Partners for Tumor Cell Migration, Invasion, and Metastasis. *Cell* 124, 263–266. doi:10.1016/j.cell.2006.01.007
- Du, Z., Niu, S., Wang, J., Wu, J., Li, S., and Yi, X. (2021). SchLAP1 Contributes to Non-Small Cell Lung Cancer Cell Progression and Immune Evasion through Regulating the AUF1/PD-L1 Axis. *Autoimmunity* 54, 1–9. doi:10.1080/08916934.2021.1913582
- Duan, J., Pan, Y., Yang, X., Zhong, L., Jin, Y., Xu, J., et al. (2020). Screening of T Cell-Related Long Noncoding RNA-MicroRNA-mRNA Regulatory Networks in Non-Small-Cell Lung Cancer. *Biomed. Research International* 2020, 1–13. doi:10.1155/2020/5816763
- Fagiani, E., and Christofori, G. (2013). Angiopoietins in Angiogenesis. *Cancer Lett.* 328, 18–26. doi:10.1016/j.canlet.2012.08.018
- Ferrara, N., Gerber, H.-P., and LeCouter, J. (2003). The Biology of VEGF and its Receptors. *Nat. Med.* 9, 669–676. doi:10.1038/nm0603-669
- Fu, W., Zhao, J., Hu, W., Dai, L., Jiang, Z., Zhong, S., et al. (2021). LINC01224/ZNF91 Promote Stem Cell-Like Properties and Drive Radioresistance in Non-Small Cell Lung Cancer. *Cancer Manag. Res.* 13, 5671–5681. doi:10.2147/cmar.s313744
- Fu, Y., Zhang, P., Nan, H., Lu, Y., Zhao, J., Yang, M., et al. (2019). LncRNA CASC11 Promotes TGF- β 1, Increases Cancer Cell Stemness and Predicts Postoperative Survival in Small Cell Lung Cancer. *Gene* 704, 91–96. doi:10.1016/j.gene.2019.04.019
- Gabrilovich, D. I., and Nagaraj, S. (2009). Myeloid-derived Suppressor Cells as Regulators of the Immune System. *Nat. Rev. Immunol.* 9, 162–174. doi:10.1038/nri2506
- Gajewski, T. F., Woo, S.-R., Zha, Y., Spaepen, R., Zheng, Y., Corrales, L., et al. (2013). Cancer Immunotherapy Strategies Based on Overcoming Barriers within the Tumor Microenvironment. *Curr. Opin. Immunol.* 25, 268–276. doi:10.1016/j.coi.2013.02.009
- Gao, L., Yang, X., Yi, C., and Zhu, H. (2019). Adverse Events of Concurrent Immune Checkpoint Inhibitors and Antiangiogenic Agents: A Systematic Review. *Front. Pharmacol.* 10, 1173. doi:10.3389/fphar.2019.01173
- Gong, W., Su, Y., Liu, Y., Sun, P., and Wang, X. (2018). Long Non-Coding RNA Linc00662 Promotes Cell Invasion and Contributes to Cancer Stem Cell-Like Phenotypes in Lung Cancer Cells. *J. Biochem.* 164, 461–469. doi:10.1093/jb/mvy078
- Guo, H., Feng, Y., Yu, H., Xie, Y., Luo, F., and Wang, Y. (2020). A Novel lncRNA, Loc107985872, Promotes Lung Adenocarcinoma Progression via the Notch1 Signaling Pathway with Exposure to Traffic-Originated PM2.5 Organic Extract. *Environ. Pollut.* 266, 115307. doi:10.1016/j.envpol.2020.115307
- Hegde, P. S., Karanikas, V., and Evers, S. (2016). The Where, the When, and the How of Immune Monitoring for Cancer Immunotherapies in the Era of Checkpoint Inhibition. *Clin. Cancer Res.* 22, 1865–1874. doi:10.1158/1078-0432.ccr-15-1507
- Heward, J. A., and Lindsay, M. A. (2014). Long Non-Coding RNAs in the Regulation of the Immune Response. *Trends Immunology* 35, 408–419. doi:10.1016/j.it.2014.07.005
- Hoos, A. (2016). Development of Immuno-Oncology Drugs - from CTLA4 to PD1 to the Next Generations. *Nat. Rev. Drug Discov.* 15, 235–247. doi:10.1038/nrd.2015.35
- Hou, Y., Jia, H., Cao, Y., Zhang, S., Zhang, X., Wei, P., et al. (2021). LncRNA EPIC1 Promotes Tumor Angiogenesis via Activating the Ang2/Tie2 axis in Non-Small Cell Lung Cancer. *Life Sci.* 267, 118933. doi:10.1016/j.lfs.2020.118933
- Huang, D., Chen, J., Yang, L., Ouyang, Q., Li, J., Lao, L., et al. (2018). NKILA lncRNA Promotes Tumor Immune Evasion by Sensitizing T Cells to Activation-Induced Cell Death. *Nat. Immunol.* 19, 1112–1125. doi:10.1038/s41590-018-0207-y
- Huang, G., Wang, M., Li, X., Wu, J., Chen, S., Du, N., et al. (2019). TUSC7 Suppression of Notch Activation through Sponging MiR-146 Recapitulated the Asymmetric Cell Division in Lung Adenocarcinoma Stem Cells. *Life Sci.* 232, 116630. doi:10.1016/j.lfs.2019.116630
- Huang, Z., Luo, Q., Yao, F., Qing, C., Ye, J., Deng, Y., et al. (2016). Identification of Differentially Expressed Long Non-Coding RNAs in Polarized Macrophages. *Sci. Rep.* 6, 19705. doi:10.1038/srep19705
- Jenkins, R. W., Barbie, D. A., and Flaherty, K. T. (2018). Mechanisms of Resistance to Immune Checkpoint Inhibitors. *Br. J. Cancer* 118 (1), 9–16. doi:10.1038/bjc.2017.434
- Jiang, P., Xu, H., Xu, C., Chen, A., Chen, L., Zhou, M., et al. (2018). NEAT1 Contributes to the CSC-Like Traits of A549/CDDP Cells via Activating Wnt Signaling Pathway. *Chem. Biol. Interact.* 296, 154–161. doi:10.1016/j.cbi.2018.10.001

AUTHOR CONTRIBUTIONS

SD, TL and Y-Y L collated the data and wrote the manuscript. YH, TL, and ZX provided helpful discussion. Z-ZW and FL reviewed the manuscript. All authors reviewed the manuscript.

FUNDING

This study was supported by the Science and Technology Department of Sichuan Province (2018JY0389, 2019YFS0443).

- Joyce, J. A., and Pollard, J. W. (2009). Microenvironmental Regulation of Metastasis. *Nat. Rev. Cancer* 9, 239–252. doi:10.1038/nrc2618
- Kerbel, R. S. (2008). Tumor Angiogenesis. *N. Engl. J. Med.* 358, 2039–2049. doi:10.1056/NEJMra0706596
- Konkel, J. E., and Chen, W. (2011). Balancing Acts: The Role of TGF- β in the Mucosal Immune System. *Trends Mol. Med.* 17, 668–676. doi:10.1016/j.molmed.2011.07.002
- Li, S., and Lin, L. (2021). Long Noncoding RNA MCF2L-AS1 Promotes the Cancer Stem Cell-Like Traits in Non-Small Cell Lung Cancer Cells through Regulating miR-873-5p Level. *Environ. Toxicol.* 36, 1457–1465. doi:10.1002/tox.23142
- Li, X., Liu, R., Su, X., Pan, Y., Han, X., Shao, C., et al. (2019). Harnessing Tumor-Associated Macrophages as Aids for Cancer Immunotherapy. *Mol. Cancer* 18, 177. doi:10.1186/s12943-019-1102-3
- Li, X., Yu, M., and Yang, C. (2020b). YY1-Mediated Overexpression of Long Noncoding RNA MCM3AP-AS1 Accelerates Angiogenesis and Progression in Lung Cancer by Targeting miR-340-5p/KPNA4 Axis. *J. Cel Biochem* 121, 2258–2267. doi:10.1002/jcb.29448
- Li, Z., Feng, C., Guo, J., Hu, X., and Xie, D. (2020a). GNAS-AS1/miR-4319/NECB3 Axis Promotes Migration and Invasion of Non-Small Cell Lung Cancer Cells by Altering Macrophage Polarization. *Funct. Integr. Genomics* 20, 17–28. doi:10.1007/s10142-019-00696-x
- Lin, H.-P., Wang, Z., and Yang, C. (2021). LncRNA DUXAP10 Upregulation and the Hedgehog Pathway Activation Are Critically Involved in Chronic Cadmium Exposure-Induced Cancer Stem Cell-Like Property. *Toxicol. Sci. : official J. Soc. Toxicol.* 184, 33–45. doi:10.1093/toxsci/kfab099
- Liu, M.-Y., Li, X.-Q., Gao, T.-H., Cui, Y., Ma, N., Zhou, Y., et al. (2016). Elevated HOTAIR Expression Associated with Cisplatin Resistance in Non-Small Cell Lung Cancer Patients. *J. Thorac. Dis.* 8, 3314–3322. doi:10.21037/jtd.2016.11.75
- Liu, Y., Luo, F., Xu, Y., Wang, B., Zhao, Y., Xu, W., et al. (2015). Epithelial-Mesenchymal Transition and Cancer Stem Cells, Mediated by a Long Non-coding RNA, HOTAIR, Are Involved in Cell Malignant Transformation Induced by Cigarette Smoke Extract. *Toxicol. Appl. Pharmacol.* 282, 9–19. doi:10.1016/j.taap.2014.10.022
- Lv, J., Li, Q., Ma, R., Wang, Z., Yu, Y., Liu, H., et al. (2021). Long Noncoding RNA FGD5-AS1 Knockdown Decrease Viability, Migration, and Invasion of Non-Small Cell Lung Cancer (NSCLC) Cells by Regulating the MicroRNA-944/MACC1 Axis. *Technol. Cancer Res. Treat.* 20, 153303382199009. doi:10.1177/1533033821990090
- Ma, F., Lei, Y.-Y., Ding, M.-G., Luo, L.-H., Xie, Y.-C., and Liu, X.-L. (2020). LncRNA NEAT1 Interacted With DNMT1 to Regulate Malignant Phenotype of Cancer Cell and Cytotoxic T Cell Infiltration via Epigenetic Inhibition of P53, cGAS, and STING in Lung Cancer. *Front. Genet.* 11, 250. doi:10.3389/fgene.2020.00250
- Mantovani, A., Sozzani, S., Locati, M., Allavena, P., and Sica, A. (2002). Macrophage Polarization: Tumor-Associated Macrophages as a Paradigm for Polarized M2 Mononuclear Phagocytes. *Trends Immunology* 23, 549–555. doi:10.1016/s1471-4906(02)02302-5
- Mao, Z., Xu, B., He, L., and Zhang, G. (2019). PVT1 Promotes Angiogenesis by Regulating miR-29c/Vascular Endothelial Growth Factor (VEGF) Signaling Pathway in Non-Small-Cell Lung Cancer (NSCLC). *Med. Sci. Monit.* 25, 5418–5425. doi:10.12659/msm.917601
- Marigo, I., Dolcetti, L., Serafini, P., Zanovello, P., and Bronte, V. (2008). Tumor-induced Tolerance and Immune Suppression by Myeloid Derived Suppressor Cells. *Immunol. Rev.* 222, 162–179. doi:10.1111/j.1600-065X.2008.00602.x
- Miao, F., Chen, J., Shi, M., Song, Y., Chen, Z., and Pang, L. (2019). LncRNA HAND2-AS1 Inhibits Non-Small Cell Lung Cancer Migration, Invasion and Maintains Cell Stemness through the Interactions with TGF- β 1. *Biosci. Rep.* 39 (1), BSR20181525. doi:10.1042/bsr20181525
- Miao, L., Huang, Z., Zengli, Z., Li, H., Chen, Q., Yao, C., et al. (2016). Loss of Long Noncoding RNA FOXF1-AS1 Regulates Epithelial-Mesenchymal Transition, Stemness and Metastasis of Non-Small Cell Lung Cancer Cells. *Oncotarget* 7, 68339–68349. doi:10.18632/oncotarget.11630
- Munn, L. L., and Jain, R. K. (2019). Vascular Regulation of Antitumor Immunity. *Science* 365, 544–545. doi:10.1126/science.aaw7875
- Nagaraj, S., Gupta, K., Pisarev, V., Kinarsky, L., Sherman, S., Kang, L., et al. (2007). Altered Recognition of Antigen Is a Mechanism of CD8+ T Cell Tolerance in Cancer. *Nat. Med.* 13, 828–835. doi:10.1038/nm1609
- Nasim, F., Sabath, B. F., and Eapen, G. A. (2019). Lung Cancer. *Med. Clin. North America* 103, 463–473. doi:10.1016/j.mcna.2018.12.006
- Pang, Z., Chen, X., Wang, Y., Wang, Y., Yan, T., Wan, J., et al. (2021). Long Non-coding RNA C5orf64 Is a Potential Indicator for Tumor Microenvironment and Mutation Pattern Remodeling in Lung Adenocarcinoma. *Genomics* 113, 291–304. doi:10.1016/j.ygeno.2020.12.010
- Papaioannou, N. E., Beniata, O. V., Vitsos, P., Tsitsilonis, O., and Samara, P. (2016). Harnessing the Immune System to Improve Cancer Therapy. *Ann. Transl. Med.* 4, 261. doi:10.21037/atm.2016.04.01
- Pardoll, D. M. (2012). The Blockade of Immune Checkpoints in Cancer Immunotherapy. *Nat. Rev. Cancer* 12, 252–264. doi:10.1038/nrc3239
- Peng, Z., Wang, J., Shan, B., Li, B., Peng, W., Dong, Y., et al. (2018). The Long Noncoding RNA LINC00312 Induces Lung Adenocarcinoma Migration and Vasculogenic Mimicry through Directly Binding YBX1. *Mol. Cancer* 17, 167. doi:10.1186/s12943-018-0920-z
- Qin, L., Zhong, M., Adah, D., Qin, L., Chen, X., Ma, C., et al. (2020). A Novel Tumour Suppressor lncRNA F630028O10Rik Inhibits Lung Cancer Angiogenesis by Regulating miR-223-3p. *J. Cel Mol Med* 24, 3549–3559. doi:10.1111/jcmm.15044
- Ribatti, D., Nico, B., Crivellato, E., Roccaro, A. M., and Vacca, A. (2007). The History of the Angiogenic Switch Concept. *Leukemia* 21, 44–52. doi:10.1038/sj.leu.2404402
- Rinn, J. L., and Chang, H. Y. (2012). Genome Regulation by Long Noncoding RNAs. *Annu. Rev. Biochem.* 81, 145–166. doi:10.1146/annurev-biochem-051410-092902
- Ronca, R., Benkheil, M., Mitola, S., Struyf, S., and Liekens, S. (2017). Tumor Angiogenesis Revisited: Regulators and Clinical Implications. *Med. Res. Rev.* 37, 1231–1274. doi:10.1002/med.21452
- Sagiv, J. Y., Michaeli, J., Assi, S., Mishalian, I., Kisos, H., Levy, L., et al. (2015). Phenotypic Diversity and Plasticity in Circulating Neutrophil Subpopulations in Cancer. *Cel Rep.* 10, 562–573. doi:10.1016/j.celrep.2014.12.039
- Sakaguchi, S., Mikami, N., Wing, J. B., Tanaka, A., Ichiyama, K., and Ohkura, N. (2020). Regulatory T Cells and Human Disease. *Annu. Rev. Immunol.* 38, 541–566. doi:10.1146/annurev-immunol-042718-041717
- Schoenfeld, A. J., and Hellmann, M. D. (2020). Acquired Resistance to Immune Checkpoint Inhibitors. *Cancer cell* 37 (4), 443–455. doi:10.1016/j.ccell.2020.03.017
- Schwerdtfeger, M., Desiderio, V., Kobold, S., Regad, T., Zappavigna, S., and Caraglia, M. (2021). Long Non-Coding RNAs in Cancer Stem Cells. *Translational Oncol.* 14, 101134. doi:10.1016/j.tranon.2021.101134
- Serafini, P., Mgebroff, S., Noonan, K., and Borrello, I. (2008). Myeloid-Derived Suppressor Cells Promote Cross-Tolerance in B-Cell Lymphoma by Expanding Regulatory T Cells. *Cancer Res.* 68, 5439–5449. doi:10.1158/0008-5472.can-07-6621
- Shoucair, I., Weber Mello, F., Jabalee, J., Maleki, S., and Garnis, C. (2020). The Role of Cancer-Associated Fibroblasts and Extracellular Vesicles in Tumorigenesis. *Int. J. Mol. Sci.* 21, 6837. doi:10.3390/ijms21186837
- Siegel, R. L., Miller, K. D., and Jemal, A. (2020). Cancer Statistics, 2020. *CA A. Cancer J. Clin.* 70, 7–30. doi:10.3322/caac.21590
- Sinha, P., Clements, V. K., Bunt, S. K., Albelda, S. M., and Ostrand-Rosenberg, S. (2007). Cross-Talk between Myeloid-Derived Suppressor Cells and Macrophages Subverts Tumor Immunity toward a Type 2 Response. *J. Immunol.* 179, 977–983. doi:10.4049/jimmunol.179.2.977
- Sládek, N. E. (2003). Human Aldehyde Dehydrogenases: Potential Pathological, Pharmacological, and Toxicological Impact. *J. Biochem. Mol. Toxicol.* 17, 7–23. doi:10.1002/jbt.10057
- Spolski, R., Li, P., and Leonard, W. J. (2018). Biology and Regulation of IL-2: from Molecular Mechanisms to Human Therapy. *Nat. Rev. Immunol.* 18, 648–659. doi:10.1038/s41577-018-0046-y
- Sun, C.-C., Zhu, W., Li, S.-J., Hu, W., Zhang, J., Zhuo, Y., et al. (2020). FOXC1-Mediated LINC00301 Facilitates Tumor Progression and Triggers an Immune-Suppressing Microenvironment in Non-Small Cell Lung Cancer by Regulating the HIF1 α Pathway. *Genome Med.* 12, 77. doi:10.1186/s13073-020-00773-y
- Sun, W. (2012). Angiogenesis in Metastatic Colorectal Cancer and the Benefits of Targeted Therapy. *J. Hematol. Oncol.* 5, 63. doi:10.1186/1756-8722-5-63
- Sun, Y., and Xu, J. (2019). TCF-4 Regulated lncRNA-XIST Promotes M2 Polarization of Macrophages and Is Associated With Lung Cancer. *Onco Targets Ther.* 12, 8055–8062. doi:10.2147/ott.s210952

- Taheri, M., Shoorei, H., Tondro Anamag, F., Ghafouri-Fard, S., and Dinger, M. E. (2021). LncRNAs and miRNAs Participate in Determination of Sensitivity of Cancer Cells to Cisplatin. *Exp. Mol. Pathol.* 123, 104602. doi:10.1016/j.yexmp.2021.104602
- Talmadge, J. E. (2007). Pathways Mediating the Expansion and Immunosuppressive Activity of Myeloid-Derived Suppressor Cells and Their Relevance to Cancer Therapy. *Clin. Cancer Res.* 13, 5243–5248. doi:10.1158/1078-0432.ccr-07-0182
- Teng, C., Huang, G., Luo, Y., Pan, Y., Wang, H., Liao, X., et al. (2019). Differential Long Noncoding RNAs Expression in Cancer-Associated Fibroblasts of Non-small-cell Lung Cancer. *Pharmacogenomics* 20, 143–153. doi:10.2217/pgs-2018-0102
- Tian, X., Ma, J., Wang, T., Tian, J., Zhang, Y., Mao, L., et al. (2018a). Long Non-Coding RNA HOXA Transcript Antisense RNA Myeloid-Specific 1-HOXA1 Axis Downregulates the Immunosuppressive Activity of Myeloid-Derived Suppressor Cells in Lung Cancer. *Front. Immunol.* 9, 473. doi:10.3389/fimmu.2018.00473
- Tian, X., Ma, J., Wang, T., Tian, J., Zheng, Y., Peng, R., et al. (2018b). Long Non-Coding RNA RUNXOR Accelerates MDSC-Mediated Immunosuppression in Lung Cancer. *BMC cancer* 18, 660. doi:10.1186/s12885-018-4564-6
- Tian, X., Zheng, Y., Yin, K., Ma, J., Tian, J., Zhang, Y., et al. (2020). LncRNAAK036396Inhibits Maturation and Accelerates Immunosuppression of Polymorphonuclear Myeloid-Derived Suppressor Cells by Enhancing the Stability of Ficolin B. *Cancer Immunol. Res.* 8, 565–577. doi:10.1158/2326-6066.cir-19-0595
- Tian, Y., Yu, M., Sun, L., Liu, L., Huo, S., Shang, W., et al. (2019). Long Non-Coding RNA00887 Reduces the Invasion and Metastasis of Non-Small Cell Lung Cancer by Causing the Degradation of miRNAs. *Oncol. Rep.* 42, 1173–1182. doi:10.3892/or.2019.7228
- Tokgun, O., Tokgun, P. E., Inci, K., and Akca, H. (2020). lncRNAs as Potential Targets in Small Cell Lung Cancer: MYC -Dependent Regulation. *Anticancer Agents Med. Chem.* 20, 2074–2081. doi:10.2174/1871520620666200721130700
- Varol, C., Mildner, A., and Jung, S. (2015). Macrophages: Development and Tissue Specialization. *Annu. Rev. Immunol.* 33, 643–675. doi:10.1146/annurev-immunol-032414-112220
- Vidal, S. J., Rodriguez-Bravo, V., Galsky, M., Cordon-Cardo, C., and Domingo-Domenech, J. (2014). Targeting Cancer Stem Cells to Suppress Acquired Chemotherapy Resistance. *Oncogene* 33, 4451–4463. doi:10.1038/onc.2013.411
- Wang, B., Li, Q., Qin, L., Zhao, S., Wang, J., and Chen, X. (2011). Transition of Tumor-Associated Macrophages from MHC Class IIhi to MHC Class IIlow Mediates Tumor Progression in Mice. *BMC Immunol.* 12, 43. doi:10.1186/1471-2172-12-43
- Wang, R., Dong, H. X., Zeng, J., Pan, J., and Jin, X. Y. (2018). LncRNA DGCR5 Contributes to CSC-Like Properties via Modulating miR-330-5p/CD44 in NSCLC. *J. Cel Physiol* 233, 7447–7456. doi:10.1002/jcp.26590
- Wang, X., Yu, X., Wei, W., and Liu, Y. (2020). Long Noncoding RNA MACC1-AS1 Promotes the Stemness of Nonsmall Cell Lung Cancer Cells through Promoting UPFI -Mediated Destabilization of LAT51/2. *Environ. Toxicol.* 35, 998–1006. doi:10.1002/tox.22936
- Wei, T., Song, J., Liang, K., Li, L., Mo, X., Huang, Z., et al. (2021). Identification of a Novel Therapeutic Candidate, NRK, in Primary Cancer-Associated Fibroblasts of Lung Adenocarcinoma Microenvironment. *J. Cancer Res. Clin. Oncol.* 147, 1049–1064. doi:10.1007/s00432-020-03489-z
- Wilson, M. M., Weinberg, R. A., Lees, J. A., and Guen, V. J. (2020). Emerging Mechanisms by Which EMT Programs Control Stemness. *Trends Cancer* 6, 775–780. doi:10.1016/j.trecan.2020.03.011
- Wu, D.-M., Deng, S.-H., Liu, T., Han, R., Zhang, T., and Xu, Y. (2018). TGF- β -Mediated Exosomal Lnc-MMP2-2 Regulates Migration and Invasion of Lung Cancer Cells to the Vasculature by Promoting MMP2 Expression. *Cancer Med.* 7, 5118–5129. doi:10.1002/cam4.1758
- Wu, D., Zhuo, L., and Wang, X. (2017). Metabolic Reprogramming of Carcinoma-Associated Fibroblasts and its Impact on Metabolic Heterogeneity of Tumors. *Semin. Cel Develop. Biol.* 64, 125–131. doi:10.1016/j.semcdb.2016.11.003
- Wu, J., and Wang, D. (2017). Long Noncoding RNA TCF7 Promotes Invasiveness and Self-Renewal of Human Non-Small Cell Lung Cancer Cells. *Hum. Cel.* 30, 23–29. doi:10.1007/s13577-016-0147-5
- Xin Yu, J., Hubbard-Lucey, V. M., and Tang, J. (2019). Immuno-Oncology Drug Development Goes Global. *Nat. Rev. Drug Discov.* 18, 899–900. doi:10.1038/d41573-019-00167-9
- Xu, C., Xiao, G., Zhang, B., Wang, M., Wang, J., Liu, D., et al. (2018). CCAT1 Stimulation of the Symmetric Division of NSCLC Stem Cells through Activation of the Wnt Signalling cascade. *Gene Ther.* 25, 4–12. doi:10.1038/gt.2017.98
- Xu, W., Xu, Q., Kuang, D., Wang, Z., Lu, Q., Lin, Q., et al. (2019). Long Non-Coding RNA SLNCR1 Regulates Non-Small Cell Lung Cancer Migration, Invasion and Stemness through Interactions with Secretory Phospholipase A2. *Mol. Med. Rep.* 20, 2591–2596. doi:10.3892/mmr.2019.10518
- Yan, F., Zhao, W., Xu, X., Li, C., Li, X., Liu, S., et al. (2020). LncRNA DHRS4-AS1 Inhibits the Stemness of NSCLC Cells by Sponging miR-224-3p and Upregulating TP53 and TET1. *Front. Cel Dev. Biol.* 8, 585251. doi:10.3389/fcell.2020.585251
- Yang, H., Yang, W., Dai, W., Ma, Y., and Zhang, G. (2020). LINC00667 Promotes the Proliferation, Migration, and Pathological Angiogenesis in Non-Small Cell Lung Cancer through Stabilizing VEGFA by EIF4A3. *Cell Biol Int* 44, 1671–1680. doi:10.1002/cbin.11361
- Yang, J., Shi, X., Yang, M., Luo, J., Gao, Q., Wang, X., et al. (2021). Glycolysis Reprogramming in Cancer-Associated Fibroblasts Promotes the Growth of Oral Cancer through the lncRNA H19/miR-675-5p/PFKFB3 Signaling Pathway. *Int. J. Oral Sci.* 13, 12. doi:10.1038/s41368-021-00115-7
- Yi, M., Jiao, D., Qin, S., Chu, Q., Wu, K., and Li, A. (2019). Synergistic Effect of Immune Checkpoint Blockade and Anti-Angiogenesis in Cancer Treatment. *Mol. Cancer* 18, 60. doi:10.1186/s12943-019-0974-6
- Youn, J.-I., Nagaraj, S., Collazo, M., and Gabrilovich, D. I. (2008). Subsets of Myeloid-Derived Suppressor Cells in Tumor-Bearing Mice. *J. Immunol.* 181, 5791–5802. doi:10.4049/jimmunol.181.8.5791
- Yu, J. E., Ju, J. A., Musacchio, N., Mathias, T. J., and Vitolo, M. I. (2020). Long Noncoding RNA DANCER Activates Wnt/ β -Catenin Signaling through MiR-216a Inhibition in Non-Small Cell Lung Cancer. *Biomolecules* 10, 1646. doi:10.3390/biom10121646
- Zhang, M., Han, Y., Zheng, Y., Zhang, Y., Zhao, X., Gao, Z., et al. (2020). ZEB1-activated LINC01123 Accelerates the Malignancy in Lung Adenocarcinoma through NOTCH Signaling Pathway. *Cell Death Dis* 11, 981. doi:10.1038/s41419-020-03166-6
- Zhao, J. (2016). Cancer Stem Cells and Chemoresistance: The Smartest Survives the Raid. *Pharmacol. Ther.* 160, 145–158. doi:10.1016/j.pharmthera.2016.02.008
- Zheng, X., Liu, Q., Yi, M., Qin, S., and Wu, K. (2018). The Regulation of Cytokine Signaling by Retinal Determination Gene Network Pathway in Cancer. *Onco Targets Ther.* 11, 6479–6487. doi:10.2147/ott.s176113
- Zheng, Y., Tian, X., Wang, T., Xia, X., Cao, F., Tian, J., et al. (2019). Long Noncoding RNA Pvt1 Regulates the Immunosuppression Activity of Granulocytic Myeloid-Derived Suppressor Cells in Tumor-Bearing Mice. *Mol. Cancer* 18, 61. doi:10.1186/s12943-019-0978-2
- Zhou, D., Xia, Z., Xie, M., Gao, Y., Yu, Q., and He, B. (2021). Exosomal Long Non-Coding RNA SOX2 Overlapping Transcript Enhances the Resistance to EGFR-TKIs in Non-Small Cell Lung Cancer Cell Line H1975. *Hum. Cel.* 34, 1478–1489. doi:10.1007/s13577-021-00572-6
- Zhou, Q., Tang, X., Tian, X., Tian, J., Zhang, Y., Ma, J., et al. (2018). LncRNA MALAT1 Negatively Regulates MDSCs in Patients with Lung Cancer. *J. Cancer* 9, 2436–2442. doi:10.7150/jca.24796
- Zou, L., Yu, Q., Zhang, L., Yuan, X., Fang, F., and Xu, F. (2021). Identification of Inflammation Related lncRNAs and Gm33647 as a Potential Regulator in Septic Acute Lung Injury. *Life Sci.* 282, 119814. doi:10.1016/j.lfs.2021.119814

Conflict of Interest: The authors declare that the research was conducted in the absence of any commercial or financial relationships that could be construed as a potential conflict of interest.

Publisher's Note: All claims expressed in this article are solely those of the authors and do not necessarily represent those of their affiliated organizations, or those of the publisher, the editors and the reviewers. Any product that may be evaluated in this article, or claim that may be made by its manufacturer, is not guaranteed or endorsed by the publisher.

Copyright © 2022 Dai, Liu, Liu, He, Liu, Xu, Wang and Luo. This is an open-access article distributed under the terms of the Creative Commons Attribution License (CC BY). The use, distribution or reproduction in other forums is permitted, provided the original author(s) and the copyright owner(s) are credited and that the original publication in this journal is cited, in accordance with accepted academic practice. No use, distribution or reproduction is permitted which does not comply with these terms.



Oncogenic Roles of Small Nucleolar RNA Host Gene 7 (SNHG7) Long Noncoding RNA in Human Cancers and Potentials

Sajad Najafi¹, Soudeh Ghafouri-Fard², Bashdar Mahmud Hussien^{3,4}, Hazha Hadayat Jamal⁵, Mohammad Taheri^{6*} and Mohammad Hallajnejad^{7*}

¹Student Research Committee, Department of Medical Biotechnology, School of Advanced Technologies in Medicine, Shahid Beheshti University of Medical Sciences, Tehran, Iran, ²Department of Medical Genetics, School of Medicine, Shahid Beheshti University of Medical Sciences, Tehran, Iran, ³Department of Pharmacognosy, College of Pharmacy, Hawler Medical University, Erbil, Iraq, ⁴Center of Research and Strategic Studies, Lebanese French University, Erbil, Iraq, ⁵Department of Biology, College of Education, Salahaddin University-Erbil, Erbil, Iraq, ⁶Institute of Human Genetics, Jena University Hospital, Jena, Germany, ⁷Skull Base Research Center, Lohman Hakim Hospital, Shahid Beheshti University of Medical Sciences, Tehran, Iran

OPEN ACCESS

Edited by:

Shiv K. Gupta,
Mayo Clinic, United States

Reviewed by:

Atefe Abak,
Tabriz University of Medical
Sciences, Iran
Macrina Beatriz Silva Cázares,
Autonomous University of San Luis
Potosí, Mexico

*Correspondence:

Mohammad Taheri
mohammad_823@yahoo.com
Mohammad Hallajnejad
hallajnejad@gmail.com

Specialty section:

This article was submitted to
Molecular and Cellular Oncology,
a section of the journal
Frontiers in Cell and Developmental
Biology

Received: 04 November 2021

Accepted: 10 December 2021

Published: 17 January 2022

Citation:

Najafi S, Ghafouri-Fard S, Hussien BM, Jamal HH, Taheri M and Hallajnejad M (2022) Oncogenic Roles of Small Nucleolar RNA Host Gene 7 (SNHG7) Long Noncoding RNA in Human Cancers and Potentials. *Front. Cell Dev. Biol.* 9:809345. doi: 10.3389/fcell.2021.809345

Long noncoding RNAs (lncRNAs) are a class of noncoding transcripts characterized with more than 200 nucleotides of length. Unlike their names, some short open reading frames are recognized for them encoding small proteins. lncRNAs are found to play regulatory roles in essential cellular processes such as cell growth and apoptosis. Therefore, an increasing number of lncRNAs are identified with dysregulation in a wide variety of human cancers. SNHG7 is an lncRNA with upregulation in cancer cells and tissues. It is frequently reported with potency of promoting malignant cell behaviors *in vitro* and *in vivo*. Like oncogenic/tumor suppressor lncRNAs, SNHG7 is found to exert its tumorigenic functions through interaction with other biological substances. These include sponging target miRNAs (various numbers are identified), regulation of several signaling pathways, transcription factors, and effector proteins. Importantly, clinical studies demonstrate association between high SNHG7 expression and clinicopathological features in cancerous patients, worse prognosis, and enhanced chemoresistance. In this review, we summarize recent studies in three eras of cell, animal, and human experiments to bold the prognostic, diagnostic, and therapeutic potentials.

Keywords: SNHG7, non-coding RNA, lncRNA, cancer, biomarker

INTRODUCTION

Initially based on the central dogma of molecular biology lasting for decades, sequential flow of cell genetic information was defined through RNAs, which encoded proteins, and so messenger RNA (mRNA) were considered mediators of template DNA and downstream proteins (Crick, 1970). However, exceptions were gradually made, and RNAs that did not directly encode any protein or polypeptide were identified. Transfer RNAs (tRNA), ribosomal RNAs (rRNAs), and small nuclear and nucleolar RNAs (snRNAs and snoRNAs, respectively) were recognized as groups of non-protein-coding RNAs (ncRNAs) with functions in the translation of coding mRNAs and modification or processing of other RNAs (Hombach and Kretz, 2016). Nowadays, we know that a minority of large genomes in complex eukaryotic organisms encode protein or polypeptide

strands, and a majority [for instance, 98% in humans (Elgar and Vavouri, 2008)] does not encode for amino acids. This great proportion, formerly called “junk DNA,” however, is mainly [e.g., two thirds of the mammalian genomes (Mattick, 2001)] transcribed to thousands of RNA transcripts, including various types of known ncRNAs that are demonstrated to be involved in critical cellular processes through conducting regulatory functions (Najafi et al., 2022). By employment of high-throughput technologies, such as RNA-seq, identification of novel ncRNAs is accelerated, and new members are being introduced constantly (Taheri et al., 2021). Although the role of ncRNAs is not yet clear, however, their involvement in essential life processes have caused them to be the architects of complexity in eukaryotes (Mattick, 2001). The number of functional ncRNAs are growing, and several show regulatory roles on gene expression.

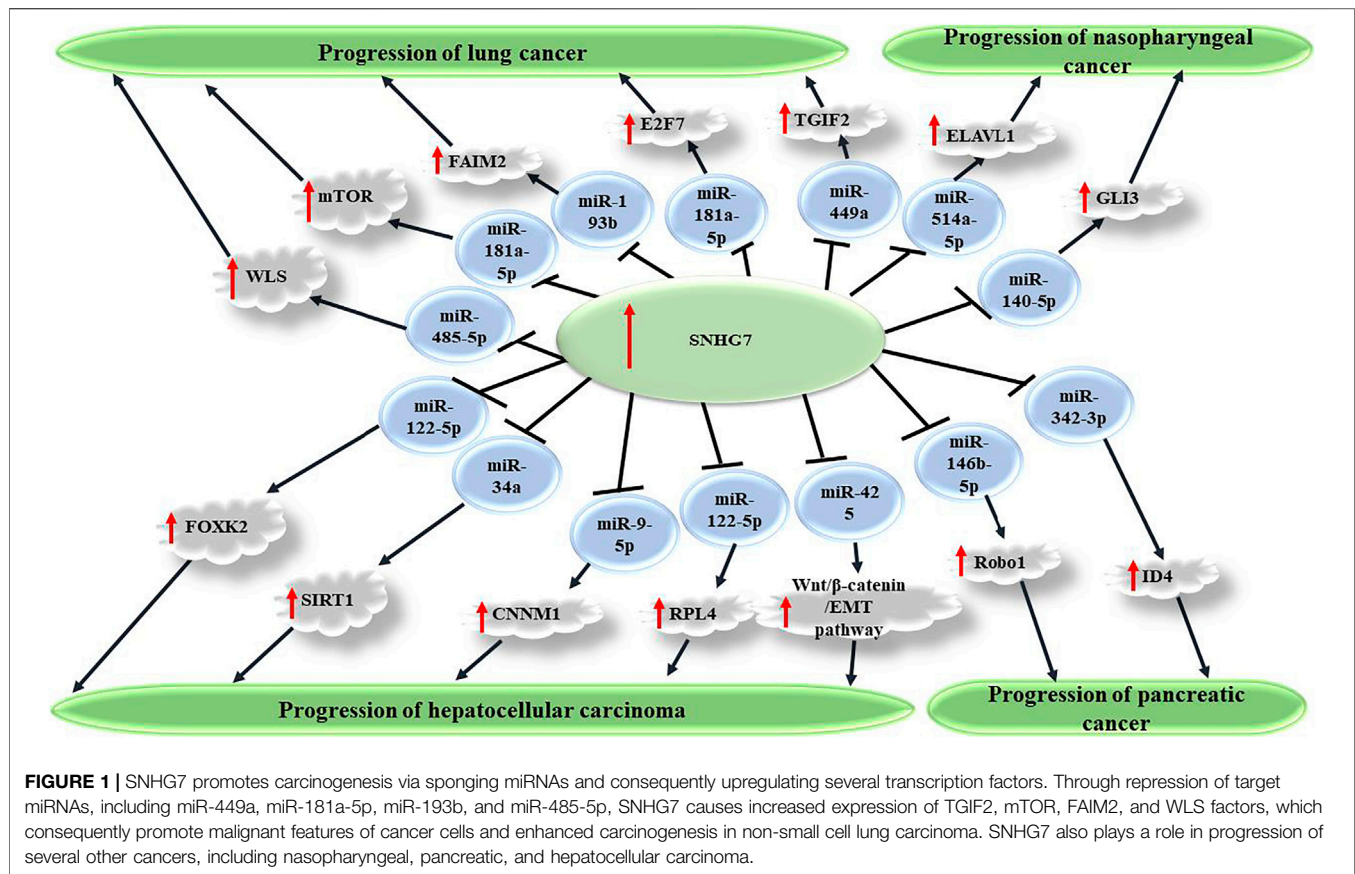
The size of the transcript is the main discriminating parameter used for classification of ncRNAs. Based on a size limit, ncRNAs are divided in two short and long classes. MicroRNAs (miRNAs), rRNAs, tRNAs, and snRNAs/snoRNAs are several described subclasses of short ncRNAs with a total length shorter than 200 nucleotides (Amin et al., 2019). Among them, miRNAs are studied more broadly compared with others, an increasing number identified in mammalian cells, and also a number are reported with altered expression in various human diseases.

Long noncoding RNAs (lncRNAs) are the second class of ncRNAs with characteristic length of >200 nucleotides. Thousands of lncRNA-related genes have been identified in the human genome and corresponding transcripts reported in large quantities by a large number ranging from 10,000 to 60,000 in human cells (Guttman et al., 2009; Iyer et al., 2015). They have been identified in a wide variety of eukaryotic species, and several show conserved sequences among different organisms suggesting evolution pressure (Ramírez-Colmenero et al., 2020). A number of exclusive properties have made lncRNAs different compared with regular mRNAs. These remarkable differences include characteristic biogenesis, localization, structure, and roles (Quinn and Chang, 2016). Unlike protein-coding RNAs, lncRNAs are mainly transcribed from regulatory and noncoding sequences such as promoters, enhancers, and introns. Furthermore, they could be generated from shared sequences with other transcripts (Al-Tobasei et al., 2016) although some researchers consider lncRNAs as noises or byproducts of transcription (Gao et al., 2020). Unlike their names, some short open reading frames are recognized for them that encode for small proteins (Hartford and Lal, 2020). According to the location of transcription, lncRNAs are classified into intronic and intergenic. Structurally, lncRNAs can be found in linear and circular forms, which are mainly referred to as the former structures; however, circular RNAs also have been found with regulatory functions and roles in pathogenesis of various human cancers (Rahmati et al., 2021; Sayad et al., 2021). lncRNAs show specific expression in cell-, tissue-, and developmental stage-specific manners (Sarropoulos et al., 2019). Their biogenesis is also forced to more strict regulation relative to protein-coding transcripts that, along with their conservation among species, suggests critical regulatory

functions for lncRNAs (Dahariya et al., 2019). Several strategies, including ribonuclease P cleavage, processing by ribonucleoproteins, and circularization via backsplicing, play a role in biogenesis of lncRNAs (Dahariya et al., 2019). Same as mRNAs, lncRNAs undergo post-transcriptional modifications on processing such as capping and polyadenylation at 5' and 3' ends, respectively, splicing and base modifications (Sarropoulos et al., 2019). They are mainly located at the nucleus exerting their epigenetic and gene expression regulatory functions via altering the histone modifications or transcription control through several mechanisms, including scaffold, signal, guide, and decoy (Zhang et al., 2019a; Dahariya et al., 2019). Through these ways, lncRNAs in interactions with DNA, proteins, and other RNAs, play a role in various biological phenomena, such as cell differentiation and reprogramming, organ development, immune responses, and cell cycle control (Statello et al., 2021).

Accordingly, a set of lncRNAs is found to be deregulated in various human disorders. An association between expression level of these transcripts and pathogenesis in major health conditions confirms critical roles of lncRNAs in essential health-affecting processes. Among an increasing number of pathogenic lncRNAs, a handful, such as XIST, MALAT1, HOTAIR, H19, ANRIL, and MEG3, are the best known and most often found transcripts. Playing a role particularly in cancer development and progression, differentially expressed lncRNAs in cancer tissues are functionally subdivided into two group of oncogenic and tumor suppressors.

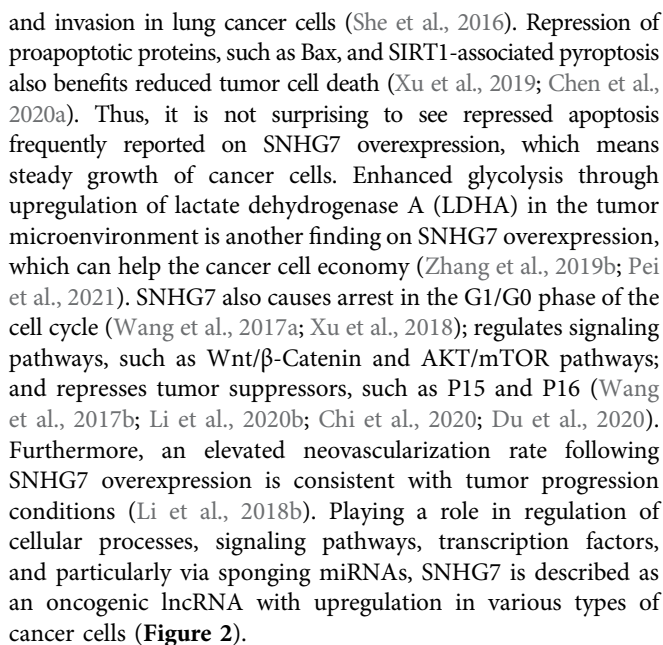
Small nucleolar RNA host gene 7 (SNHG7) is among the oncogenic lncRNAs with progressive effects in multiple human cancers although a single study suggests tumor suppressor function for SNHG7 in pituitary adenoma (Xue and Ge, 2020). Its corresponding gene, located on chromosome 9q34.3, encodes a 2157-base-pair-long transcript. SNHG7 was reported for the first time in 2013 by Chaudhry in X-ray-treated lymphoblastoid cells (Chaudhry, 2013). Rather than regulation of transcription factors, translation, or stability of mRNAs involved in several diseases such as cardiac fibrosis, hepatic fibrosis, and cardiac hypertrophy in addition to helping fracture repair (Chen et al., 2019a; Jing et al., 2019; Yu et al., 2019; Wang et al., 2020a), SNHG7 is found to be overregulated in cancer tissues compared with healthy tissues in a wide variety of human malignancies, including bladder, prostate, gastric, colorectal, and pancreatic cancers (Li et al., 2018a; Zhong et al., 2018a; Cheng et al., 2019a; Han et al., 2019; Zhang et al., 2020a). This upregulation also is demonstrated to accelerate cancer progression. It is shown that SNHG7 is negatively regulated by insulin-like growth factor 1 (IGF1) signaling at the post-transcriptional level through the MAPK pathway to control cell proliferation (Boone et al., 2020). In cell and animal studies, SNHG7 is shown with oncogenic roles in accordance with clinicopathological features and also diagnostic and prognostic values in cancerous patients. In this review, we have gathered recent findings on the oncogenic roles of this lncRNA in three levels of cell, animal, and human studies with a focus on clinical results predicting SNHG7 as a novel biomarker for different types of human cancers.



Cell Line Studies

Through study of SNHG7 knockdown or overexpression in cancer cell lines, it is demonstrated that expression of this oncogenic lncRNA promotes malignant features of the cells *in vitro*. This universal finding, although opposite effects have been described for SNHG7 at least in two distinct experiments (Pei et al., 2020; Huang et al., 2020), is reported for a broad spectrum of cancer cell types, such as breast, colorectal, bladder, gastric, liver, etc. Proliferation and colony formation experiments have unveiled increased cell and colony numbers in cancer cells in response to SNHG7 simulated excess expression compared with baseline conditions. Accordingly, reduced apoptosis consistent with elevated tumor cell growth hypothesizes the role of this lncRNA in cancer progression. Migratory and invasive potentials of cancer cells also show enhancement in Transwell and Matrigel assays, respectively. Conferring chemoresistance or desensitization has been concluded from cellular studies in which increased sensitivity of cancer cells to conventional chemotherapy agents and/or radiotherapy is seen on SNHG7 knockdown. For example, in two distinct experiments, enhanced sensitivity of breast cancer cells to Adriamycin and Trastuzumab is shown when SNHG7 is silenced or its target sponged miRNA (miR-34a or miR-186, respectively) is overexpressed (Li et al., 2020a; Zhang et al., 2020b). Knockdown studies employing RNA silencing confirm the overexpression experiment results by reversing the SNHG7 impacts on malignant cells behaviors. Via making a network, lncRNAs are

known to affect expression of a specific target miRNA. Dual luciferase reporter and RNA immunoprecipitation (RIP) assays confirm the association between SNHG7 and target miRNA consistent with bioinformatics predictions. These interactions seem to be conducted via complementary sequences as binding sites on miRNA for SNHG7. This regulatory effect is mainly repressive, and expression levels in quantitative real-time polymerase chain reaction (qRT-PCR) reveal a negative correlation between both. It is hypothesized that through downregulation of the target miRNA, SNHG7 as a competing endogenous RNA (ceRNA) or sponger exerts its regulatory impacts on downstream transcription factors playing a role in some signaling pathways (Figure 1). Activation of an oncogenic signaling pathway demonstrates why these lncRNAs are considered to have tumor promoting potentials. A handful of evidence on the acceleration of the cell cycle in response to SNHG7 overexpression or arrest in a phase under knockdown conditions suggests indirect enhancing influences of this lncRNA on cell proliferation and differentiation, which consequently, leads to cancer progression. For instance, She et al. (2018) find that SNHG7 upregulates the Fas apoptotic inhibitory molecule 2 (FAIM2) through sponging miR-193b in non-small cell lung cancer (NSCLC) cells. *In silico* investigations demonstrate binding sites for miR-193b on the SNHG7 sequence. FAIM2 is a membrane protein; shows antiapoptotic activity; is upregulated in several cancers; and is already known to promote tumor cell proliferation, migration,



Xenograft animal experiments with inoculation of cancer cells into nude mice try to simulate the cancer conditions in an animal

January 2022 | Volume 9 | Article 809345

TABLE 1 | Effects of SNHG7 on tumor growth and metastasis in animal studies.

Cancer type	Animal models	Function	References (s)
Pancreatic cancer	Nude mice	Δ SNHG7: ↓ tumor growth	Jian and Fan, (2021)
Breast cancer	Female BALB/C nude mice	Δ SNHG7: ↓ tumor growth	Cheng et al. (2019b)
	BALB/c nude mice	Δ SNHG7: ↓ tumor growth	Zhang et al. (2020b)
	BALB/c nude mice	Δ SNHG7: ↓ tumor growth	Li et al. (2020d)
	BALB/c athymic nude mice	Δ SNHG7: ↓ tumor growth, ↓EMT, and ↓Notch-1 pathway	Sun et al. (2019)
Colorectal cancer	Nude mice	Δ SNHG7: ↓ tumor growth	Li et al. (2018b)
Lung cancer (non-small cell lung cancer; NSCLC)	Nude mice	Δ SNHG7: ↓ tumor growth	Li et al. (2020b)
	Athymic nude mice	Δ SNHG7: ↓ tumor growth	Wang et al. (2020b)
	Nude mice	Δ SNHG7: ↓ tumor growth	She et al. (2018)
	BALB/c male nude mice	Δ SNHG7: ↓ tumor growth	Zhao et al. (2021)
Liver cancer (hepatocellular carcinoma; HCC)	BALB/c male nude mice	Δ SNHG7: ↓ tumor growth	Xie et al. (2020)
	BALB/c nude mice	Δ SNHG7: ↓ tumor growth, and ↓metastasis	Yang et al. (2019)
	BALB/c nude mice	Δ SNHG7: ↓ tumor growth	Yao et al. (2019)
	BALB/c mice	Δ SNHG7: ↓ tumor growth	Wang et al. (2017b)
Gastric cancer	Male nude mice	Δ SNHG7: ↓ tumor growth	Wang et al. (2020c)
Bladder cancer	Nude mice	Δ SNHG7: ↓ tumor growth	Yue et al. (2021)
Pituitary adenocarcinoma	BALB/c nude mice	Δ SNHG7: ↓ tumor growth	Jia et al. (2020)
Neuroblastoma	BALB/c nude mice	Δ SNHG7: ↓ tumor growth	Du et al. (2020)
Glioma	BALB/c nude mice	Δ SNHG7: ↓ tumor growth	Chen et al. (2021)
Thyroid	BALB/c nude mice	Δ SNHG7: ↓ tumor cell proliferation, and ↓ ¹³¹ I resistance	
Glioblastoma	BALB/c nude mice	Δ SNHG7: ↓ tumor growth, and ↓metastasis	Ren et al. (2018)
Ovarian cancer	BALB/c nude mice	Δ SNHG7: ↓ tumor growth	Bai et al. (2020)
Cervical cancer	BALB/c nude mice	Δ SNHG7: ↓ tumor growth	Zhao et al. (2020)
Prostate cancer	BALB/c nude mice	Δ SNHG7: ↓ tumor growth, and ↑cell cycle arrest	Qi et al. (2018)

and less lung metastasis of HCCLM3 cells in an SNHG7 knockdown mice group compared with the control group. Additionally, Yao et al. (2019) show that the expression of the metastasis-associated protein matrix metalloproteinase-9 (MMP-9) is increased in SNHG7-overexpressing HepG2 implanted cells, suggesting a mechanism for enhancing the effect of SNHG7 on tumor metastasis. Collectively, promoted tumor growth on SNHG7 overexpression and/or suppressed tumor proliferation on SNHG7 knockdown is reported in a body of studies. These results, along with cellular findings, confirm the oncogenic role of SNHG7, and the knockdown achievements may suggest therapeutic potentials for anticancer therapies.

Human Studies

Consistent with cellular findings, enormous expression assessments using qRT-PCR analysis demonstrate elevated SNHG7 expression in tissues retrieved from cancerous patients compared with healthy adjacent tissues. Increased SNHG7 tissue expression is frequently found to be associated with worse clinicopathological features, which are used in clinical classification and staging of human malignancies. Importantly, patients with more advanced clinicopathological characteristics are predicted to have worse prognosis and severe outcomes. These include larger tumor size, more advanced clinical stage, poor histologic grade, deeper tumor invasion, and lymph node metastasis in accordance with high SNHG7 expression in the

affected patients (Zeng et al., 2019; Pang et al., 2020; Zhu et al., 2021). This value is also shown in malignancies with broad and different features and in meta-analyses pooling data of tens of studies (Yu et al., 2021a; Yi et al., 2021; Yu et al., 2021b). For example, in acute myeloid leukemia (AML), an association between SNHG7 and SNHG12 lncRNAs and specific clinical/molecular features, including white blood cell (WBC) counts and mutations in *IDH1*, *RUNX1*, and *NPM1* genes, shows high value of SNHG7 in correlation with extensive features (Shi et al., 2020). These demonstrations suggest that elevated SNHG7 expression predicts poor clinicopathological characteristics. In other words, high SNHG7 expression can predict worse outcomes following poor clinicopathological determinants. In accordance with clinicopathological findings, SNHG7 also shows correlation with prognostic parameters. Survival analysis using a Kaplan–Meier curve indicates shorter survival time in overall survival (OS) and disease-free survival (DFS) for patients with high SNHG7 expression relative to those with low levels. This finding is reported for various human cancers, for which survival analysis is conducted (Table 2). For example, in three distinct studies that reported survival analyses in HCC patients, among a total of 150 patients, poorer OS time was reported separately for the patients with elevated tissue SNHG7 expression in comparison to those with low levels (Yang et al., 2019; Zhao et al., 2021; Yao et al., 2019). Additionally, recurrence is predicted to happen in shorter durations and higher rates among patients with high SNHG7 expression (Zhang et al., 2020c). Interestingly,

TABLE 2 | Clinical prognostic importance of SNHG7 in human cancers.

Cancer type	Clinical samples	Expression change in tumor tissues compared to normal tissues	Associated clinical features	Kaplan–Meier analysis	Multivariate cox regression	References (s)
Lung cancer	36 cancerous patient tissues and matched NATs	Upregulated	—	Patients with elevated expression levels of SNHG7 demonstrated decreased OS rate compared to those with lower levels	—	Li et al. (2020b)
	30 cancerous patient tissues and matched NATs	Upregulated	—	—	—	Wang et al. (2020b)
Esophageal cancer	40 cancerous patient tissues and matched NATs	Upregulated	—	—	—	Wang et al. (2021)
Liver (hepatocellular carcinoma; HCC)	30 cancerous patient tissues and matched NATs	Upregulated	Tumor size, TNM grade, and Distant metastasis	Log-rank test demonstrated that patients with high SNHG7 expression had poorer OS.	—	Zhao et al. (2021)
	25 cancerous patient tissues and matched NATs	Upregulated	—	—	—	Chen et al. (2020a)
	80 cancerous patient tissues and matched NATs	Upregulated	Tumor stages, tumor grade, and vascular invasion	Patients with high SNHG7 expression levels had poor OS.	—	Yang et al. (2019)
	40 cancerous patient tissues and matched NATs	Upregulated	TNM stage, and tumor metastasis	Elevated SNHG7 expression was markedly associated with poor OS in hepatic carcinoma patients	—	Yao et al. (2019)
	100 cancerous patient tissues and matched NATs	Upregulated	Tumor number, lymph node metastasis, and clinical stage	Patients with high SNHG7 expression demonstrated worse OS and PFS relative to those with low levels	SNHG7 expression acts as an independent prognostic factor in HCC patients	Shen et al. (2020)
Synchronous colorectal liver metastasis (SCLM)	96 SCLM patients	Upregulated	Differentiation of primary tumor, invasion depth of primary focus, lymph node metastases, number of liver metastases, and liver metastasis grade	Patients with high SNHG7 expression levels had poor OS.	SNHG7 expression acts as an independent prognostic factor for OS and occurrence in SCLM patients	Zhang et al. (2020c)
Pancreatic cancer	50 cancerous patient tissues and matched NATs	Upregulated	tumor size, TNM stage, lymph node metastasis, and distant metastasis	Patients with elevated expression levels of SNHG7 demonstrated decreased survival rate relative to those with lower levels	—	Jian and Fan, (2021)
	40 cancerous patient tissues and matched NATs	Upregulated	—	Patients with high SNHG7 expression levels had poor OS.	—	Cheng et al. (2019b)
Breast cancer	43 cancerous patient tissues	Upregulated	Tumor size, TNM stage, and Ki-67 index	Patients with high SNHG7 levels had lower DFS compared to those with lower levels	—	Li et al. (2020a)
	50 cancerous patient tissues and matched NATs	Upregulated	Pathological stage, and lymph node metastasis	—	—	Li et al. (2020d)
	837 cancerous patient tissues and matched NATs	Upregulated	—	High SNHG7 was associated with decreased survival in breast cancer patients	—	Zhang et al. (2019b)
	72 cancerous patient tissues and matched NATs	Upregulated	Clinical Stage, lymph node and distant metastasis	High SNHG7 was correlated with shorter survival time in breast cancer patients	—	Luo et al. (2018)

(Continued on following page)

TABLE 2 | (Continued) Clinical prognostic importance of SNHG7 in human cancers.

Cancer type	Clinical samples	Expression change in tumor tissues compared to normal tissues	Associated clinical features	Kaplan–Meier analysis	Multivariate cox regression	References (s)
Gastric cancer	30 cancerous patient tissues and 30 healthy tissues	Upregulated	—	—	—	Pei et al. (2021)
	36 cancerous patient tissues and matched NATs	Upregulated	—	—	—	Zhao and Liu, (2021)
	162 cancerous patient tissues and matched NATs	Upregulated	TNM stage, depth of invasion, lymph node and distant metastasis	Patients with high SNHG7 levels showed lower OS compared to those with high SNHG7 expression	SNHG7 acts as an independent factor for poor OS in patients with gastric cancer	Zhang et al. (2020a)
Bladder cancer	60 cancerous patient tissues and matched NATs	Upregulated	Clinical stage	Patients with high SNHG7 levels showed unfavorable prognosis	—	Wang et al. (2020c)
	92 cancerous patient tissues and matched NATs	Upregulated	Tumor range, lymph nodes, and pathological stage	Patients with high SNHG7 levels had poor OS compared to those with low levels	—	Chen et al. (2019b)
Pituitary adenocarcinoma	30 cancerous patient tissues and matched NATs	Upregulated	—	Patients with high SNHG7 levels showed unfavorable prognosis compared to those with low levels	—	Yue et al. (2021)
Glioma	30 cancerous patient tissues and matched NATs	Upregulated	—	—	—	Cheng et al. (2020)
	20 and 33 cancerous patient tissues and matched NATs	Upregulated	Tumor grade	—	—	(Du et al., 2020; Deng et al., 2021)
Glioblastoma	53 cancerous patient tissues and matched NATs	Upregulated	WHO Grade	--	--	Chen et al. (2020b)
	53 cancerous patient tissues and matched NATs	Upregulated	—	Patients with high SNHG7 levels had poor survival rates compared to those with low levels	—	Ren et al. (2018)
Neuroblastoma	45 cancerous patient tissues and matched NATs	Upregulated	Clinical stage	Patients with low SNHG7 levels demonstrated longer OS compared to those with high levels	—	Jia et al. (2020)
	92 cancerous patient tissues and matched NATs	Upregulated	Lymph node metastasis, INSS stage, and optic nerve invasion	Patients with high SNHG7 levels had poorer prognosis compared to those with high levels	—	Chi et al. (2019)
Thyroid cancer	56 normal samples and 578 tumor samples	Upregulated	Pathology stage	Patients with high SNHG7 levels shorter DFS times compared with those with low levels	—	Chen et al. (2019c)
Cervical cancer	45 cancerous patient tissues and matched NATs	Upregulated	Tumor Size, FIGO Stage, and lymph-Node Metastasis	Patients with high SNHG7 levels demonstrated poorer OS compared with those with low levels	—	Zhao et al. (2020)
	60 cancerous patient tissues and matched NATs	Upregulated	TNM stage, lymph node metastasis, and depth of tumor invasion	Patients with high SNHG7 levels demonstrated poorer OS compared with those with low levels	SNHG7 acts as an independent factor for poor OS in patients with gastric cancer	Zeng et al. (2019)

(Continued on following page)

TABLE 2 | (Continued) Clinical prognostic importance of SNHG7 in human cancers.

Cancer type	Clinical samples	Expression change in tumor tissues compared to normal tissues	Associated clinical features	Kaplan–Meier analysis	Multivariate cox regression	References (s)
Colorectal cancer	48 cancerous patient tissues and matched NATs	Upregulated	Clinical stage, lymph node and distant metastasis	High SNHG7 expression was correlated with poor survival	—	Shan et al. (2018)
	198 cancerous patient tissues and matched NATs	Upregulated	Invasion depth	High SNHG7 expression was correlated with poor OS.	SNHG7 expression is an independent prognostic risk factor for OS in CRC patients	Hu et al. (2019)
Prostate cancer	499 cancerous patient tissues and matched NATs	Upregulated	—	—	—	Han et al. (2019)
	42 cancerous patient tissues and matched NATs	Upregulated	Gleason score, and tumor stage	Patients with high SNHG7 expression had poor OS compared to those with low expression	—	Qi et al. (2018)
	127 cancerous patient tissues and matched NATs	Upregulated	TNM stage, Gleason score, bone, and pelvic lymph node metastasis	Patients with high SNHG7 expression had poor prognosis compared to those with low expression	SNHG7 acts as an independent factor for poor prognosis in patients with prostate cancer	Xia et al. (2020)
Osteosarcoma	30 cancerous patient tissues and matched NATs	Upregulated	Tumor size, high Enneking staging, and distant metastasis	Patients with high SNHG7 levels had shorter survival time compared with those with low levels	—	Deng et al. (2018)
Chromophobe renal cell carcinoma	Tissue expression of 59 patients retrieved from the TCGA database and 23 NATs	Upregulated	—	SNHG7 level was associated with OS	—	He et al. (2016)

OS: overall survival, DFS: disease-free survival, PFS: progression-free survival.

Cox regression analyses confirm the predictive value of SNHG7 as an independent prognostic factor among cancerous patients. This is particularly reported in several district experiments on human malignancies such as gastric cancer, cervical cancer, HCC, and liver metastasis following hepatectomy in CRC patients (Table 2) (Zeng et al., 2019; Zhang et al., 2020a; Zhang et al., 2020c; Shen et al., 2020). As for diagnostic values, an area under curve (AUC) of 0.84 in the receiver operating characteristic (ROC) curve is reported for SNHG7 in CRC patients (Hu et al., 2019). Importantly, SNHG7 is demonstrated as a potential therapeutic target as it is identified in several anticancer agents such as Cisplatin, Trastuzumab, and Folfirinox in the cancer cells (Chen et al., 2019d; Li et al., 2020a; Zhang et al., 2020b; Dai et al., 2020; Cheng et al., 2021; Pei et al., 2021). Also, metformin with anticancer properties is found to exert its effects in sensitization to Paclitaxel via regulation of SNHG7/miR-3127-5p-mediated autophagy in ovarian cancer cells (Yu et al., 2020). In another study, metformin is demonstrated to suppress growth of hypopharyngeal cancer cells through epigenetic silencing of SNHG7 (Wu et al., 2019). Taken together, human studies suggest SNHG7 lncRNA with promising diagnostic, prognostic, and therapeutic potentials in various types of cancer.

DISCUSSION

LncRNAs are a group of ncRNA transcripts defined with a length of >200 nucleotides. Although not elucidated, however, a number of regulatory functions are described for lncRNAs. They are involved in controlling several biological processes, such as cell cycle and proliferation. Accordingly, dysregulation of lncRNAs is identified in a number of human malignancies, suggesting diagnostic and therapeutic potentials. SNHG7 is an lncRNA that has been studied as an oncogenic transcript in a handful of cellular and animal experiments. It is upregulated in cancer cells and tissues retrieved from cancerous patients. SNHG7 is shown to be predominantly localized in the cytoplasm, where it serves as a ceRNA to sponge miRNAs and control expression of downstream targets (Hu et al., 2020). *In vitro* experiments frequently demonstrate a promoted malignant phenotype of cancer cells on SNHG7 overexpression, whereas its knockdown reverses tumor cell proliferation, migration, and invasion and enhances apoptosis. These regulatory effects are thought to be conducted through an axis of action affecting translation and stability of several transcription factors and signaling pathways mediated by sponging target miRNAs. Not a single one, but plenty of miRNAs are identified to be sponged by SNHG7 (see Table 3). Xenograft animal studies confirm the

TABLE 3 | An overview to the oncogenic influences of SNHG7 in cell studies of different types of cancer.

Cancer type	Targets/Regulators and signaling pathways	Assessed cell lines	Function	References(s)
Lung cancer	miR-485-5p/WLS axis	H1650, H1975, A549 and H1299	Δ SNHG7: ↓tumor cell proliferation, ↓migration, and ↓invasion	Li et al. (2020c)
	miR-181a-5p/AKT/mTOR axis	A549, and NCI-H1299	Δ SNHG7: ↓tumor cell proliferation, ↓migration, ↓invasion and ↑apoptosis	Li et al. (2020b)
	miR-193b/FAIM2 axis	Beas-2B, H125, 95D, and A549	↑↑ SNHG7: ↑↑FAIM2: ↑tumor cell proliferation, ↑migration, and ↑invasion	She et al. (2018)
	miR-181a-5p/E2F7 Axis	NCI-H520, SPC-A1, H-23, and BEAS-2B	Δ SNHG7: ↓tumor cell viability, ↓colony formation, ↓migration, ↓invasion and ↑apoptosis	Wang et al. (2020b)
	miR-449a/TGIF2 axis	BEAS-2B, A549, and H1299	Δ SNHG7: ↓tumor cell proliferation, ↓migration, ↓invasion, and ↓EMT	Pang et al. (2020)
	FAIM2	BEAS-2B, H125, 95D, and A594	Δ SNHG7: ↓tumor cell proliferation, ↓migration, ↓invasion and ↑apoptosis	She et al. (2016)
Esophageal cancer	miR-625/SNHG7 axis	TE1, EC109, TE13, and YES2	Δ SNHG7: ↓tumor cell proliferation, ↓migration, and ↓invasion	Wang et al. (2021)
	—	HEEC, Eca109, EC9706, TE-10, and TE-11	Δ SNHG7: ↓tumor cell proliferation, ↑cell cycle arrest, and ↑apoptosis	Xu et al. (2018)
Nasopharyngeal cancer	miR-514a-5p/ELAVL1 axis	NP69, CNE1, CNE2, C666-1 and HNE1	↑↑ SNHG7: ↑tumor cell proliferation, and ↑colony formation	Hu et al. (2020)
	miR-140-5p/GLI3 axis	CNE1, HONE1, C666-1, and CNE2	Δ SNHG7: ↓tumor cell proliferation, ↓colony formation, ↓drug resistance, and ↑apoptosis	Dai et al. (2020)
Liver cancer (hepatocellular carcinoma; HCC)	miR-122-5p/FOXK2 axis	SNU449, Hep3B, and THLE-2	Δ SNHG7: ↓tumor cell proliferation, ↓migration, ↓invasion, and ↓EMT	Zhao et al. (2021)
	miR-34a/SIRT1 axis	THLE-3, HEK-293, HepG2, and SK-hep-1	Δ SNHG7: ↑NLRP3-dependent pyroptosis	Chen et al. (2020a)
	miR-9-5p/CNNM1 axis	THLE-3, BEL-7404, HCCLM3, Hep3B and HepG2	Δ SNHG7: ↓tumor cell proliferation, ↓colony formation, and ↑apoptosis	Xie et al. (2020)
	miR-122-5p/RPL4 axis	Hhu7, Hep3B, HCCLM3, and MHCC97H	Δ SNHG7: ↓tumor cell proliferation, ↓migration, and ↓invasion	Yang et al. (2019)
	miR-425/Wnt/β-catenin/EMT pathway	HepG2, and HCC-LM3	Δ SNHG7: ↓tumor cell proliferation, ↓migration, and ↓invasion	Yao et al. (2019)
Pancreatic cancer	miR-146b-5p/Robo1 axis	PANC-1, SW 1990, BxPC-3 and AsPC-1	Δ SNHG7: ↓tumor cell proliferation, ↓migration, ↓invasion and ↑apoptosis	Jian and Fan, (2021)
	miR-342-3p/ID4 axis	HPDE6-C7, HEK293T, AsPC-1, BxPC-3, SW 1990, PANC-1, and PaCa-2	Δ SNHG7: ↓tumor cell proliferation, ↓migration, and ↓invasion	Cheng et al. (2019b)
	Notch1/Jagged1/Hes-1 Signaling Pathway	PANC-1, and AsPC-1	↑↑ SNHG7: ↑stemness, and ↓ apoptosis SNHG7 regulates Folfirinox resistance in pancreatic cancer cells	Cheng et al. (2021)
Breast cancer	miR-15a	MCF7, and T47D	Δ SNHG7: ↓tumor cell proliferation, and ↓invasion	Li et al. (2020d)
	miR-34a	MCF-7, and MDA-MB-231	Δ SNHG7: ↑chemosensitivity of cancer cells to Adriamycin	Li et al. (2020a)
	miR-186	SK-BR-3, and AU565	Δ SNHG7: ↓ tumor cell proliferation, ↓migration and ↓EMT, and ↑apoptosis in chemoresistant cancer cells Δ SNHG7: ↑Trastuzumab sensitivity	Zhang et al. (2020b)
	miR-34a-5p/LDHA (Glycolysis) axis	MCF10A, MDA-MMB-436, HS578T, SKBR3, MDA-MB-231, and MCF-7	Δ SNHG7: ↓ tumor cell proliferation, and ↓glycolysis	Zhang et al. (2019b)
	miR-381	MCF-10A, ZR-75-1, HCC-1973, MDA-MB-231, and MDA-MB-468	Δ SNHG7: ↓tumor cell proliferation, ↓colony formation, and ↓invasion	Gao and Zhou, (2019)
	miR-34a/Notch-1 pathway	MCF-10A, MCF-7, MDA-MB-231, MDA-MB-157, and MDA-MB-435	Δ SNHG7: ↓tumor cell proliferation, and ↓invasion	Sun et al. (2019)
	miR-186	MCF-10A, MCF-7, MDA-MB-231 and SKBR3	Δ SNHG7: ↓tumor cell proliferation, and ↓invasion	Luo et al. (2018)
Colorectal cancer	miR-23a-3p/CXCL12 axis	SW480, LoVo, RKO, and HCT116	Δ SNHG7: ↓tumor cell viability, ↓proliferation, and ↓migration	Liu et al. (2020)
	miR-193b/K-ras/ERK/cyclinD1 axis	—	Δ SNHG7: ↓tumor cell proliferation, and ↑apoptosis	Liu et al. (2019)
	miR-34a/GALNT7/PI3K/Akt/mTOR pathway	FHC, caco2, SW480, SW620, Hct116, and LoVo	Δ SNHG7: ↓tumor cell proliferation, ↓migration, ↓invasion, ↓vasculogenic mimicry, ↓cell cycle progression, and ↑apoptosis	Li et al. (2018b)
	miR-216b/GALNT1 axis	FHC, SW480, SW620, LOVO, and HCT-116	Δ SNHG7: ↓tumor cell proliferation, ↓migration, ↓invasion and ↑apoptosis	Shan et al. (2018)

(Continued on following page)

TABLE 3 | (Continued) An overview to the oncogenic influences of SNHG7 in cell studies of different types of cancer.

Cancer type	Targets/Regulators and signaling pathways	Assessed cell lines	Function	References(s)
Gastric cancer	miR-34a/LDHA (Glycolysis) axis	HGC27, and AGS	Δ SNHG7: ↓ tumor cell viability and ↑ chemosensitivity of cancer cells to cisplatin	Pei et al. (2021)
	miR-485-5p	HS746T, HGC-27, SNU-1, AGS, and GES-1	Δ SNHG7: ↓ tumor cell proliferation, ↓ migration, and ↓ invasion	Zhao and Liu, (2021)
	miR-34a/Snail/EMT axis	GES-1, MKN-45, SGC-7901, and N87	Δ SNHG7: ↓ tumor cell migration, and ↓ invasion	Zhang et al. (2020a)
	P15 and P16	GES-1, BGC823, MGC803, SGC7901, N87, and AGS	Δ SNHG7: ↓ tumor cell migration, ↓ colony formation, ↑ apoptosis, and ↑ cell cycle arrest	Wang et al. (2017b)
Bladder cancer	miR-2682-5p/ELK1/Src/FAK signaling pathway	T24, SW780, J82, UM-UC-3, 5637, and SE780	Δ SNHG7: ↓ tumor cell proliferation, ↓ migration, ↓ invasion, and ↑ apoptosis	Wang et al. (2020c)
	Bax, p21, and E-cadherin	SW780, T24, UMUC, and 5637	Δ SNHG7: ↓ tumor cell proliferation, ↓ invasion, ↑ apoptosis, and ↑ expression of Bax, p21 and E-cadherin proteins	Xu et al. (2019)
	Wnt/β-catenin pathway	SV-HUC-1, T24, 5637, 253 J, TCC, J82, and EJ	Δ SNHG7: ↓ tumor cell proliferation, ↓ colony formation, ↓ migration, and ↑ cell cycle arrest	Chen et al. (2019b)
	—	SV-HUC-1, T24, J82, and SW780	Δ SNHG7: ↓ tumor cell proliferation, ↓ invasion, ↓ EMT, and ↑ apoptosis	Zhong et al. (2018b)
Pituitary adenocarcinoma	miR-449a	GH1, RC-4B/C, GH3 and MMQ	Δ SNHG7: ↓ tumor cell proliferation, ↓ migration, and ↓ invasion	Yue et al. (2021)
Glioma	miR-342-3p/AKT2 axis	A172, U87, U251, and SHG44	↑↑ SNHG7: ↑ tumor cell proliferation, ↑ migration, and ↑ invasion	Cheng et al. (2020)
	miR-506-3p/CTNNB1 axis	NHA, U87, U251, SHG44, and A172	Δ SNHG7: ↓ tumor cell proliferation, ↓ colony formation, and ↑ apoptosis	Du et al. (2020)
	miR-138-5p/EZH2 axis	LN229, A172, U251, and U87	Δ SNHG7: ↓ tumor cell proliferation	Deng et al. (2021)
Glioblastoma (GBM)	miR-449b-5p/MYC axis	NHA, T98G, U87, U251, and LN229	Δ SNHG7: ↓ GBM cell viability, ↓ migration, and ↓ invasion	Chen et al. (2020b)
	miR-5095/Wnt/β-catenin pathway	HEB, A172, U87, T98G, and SHG44	Δ SNHG7: ↓ tumor cell proliferation, ↓ migration, ↓ invasion, and ↑ apoptosis	Ren et al. (2018)
Neuroblastoma	miR-323a-5p and miR-342-5p/CCND1 axis	SH-SY5Y, SK-N-SH, NB-1, SK-N-AS, and HUVEC	Δ SNHG7: ↓ tumor cell migration, ↓ invasion, and ↓ glycolysis	Jia et al. (2020)
	miR-653-5p/STAT2 axis	SK-N-AS, SK-N-SH, SH-SY5Y, IMR-32, and SK-N-BE Hombach and Kretz (2016) -C	Δ SNHG7: ↓ tumor cell proliferation, ↓ migration, ↓ invasion, ↓ EMT, ↑ cell cycle arrest, and ↑ apoptosis	Chi et al. (2019)
Ovarian cancer	EZH2/KLF2 axis	OC A2780, OCC1, H8710 and SK-OV3	Δ SNHG7: ↓ tumor cell proliferation, ↓ migration, ↓ invasion, and ↓ EMT	Bai et al. (2020)
Melanoma	six human UM cell lines	EZH2	Δ SNHG7: ↓ tumor cell proliferation, ↑ cell cycle arrest, and ↑ apoptosis	Huang et al. (2020)
Cervical cancer	DKK1/Wnt/β-catenin axis	H8, C-33A, CaSki, SiHa, and HeLa	Δ SNHG7: ↓ tumor cell proliferation, ↓ colony formation, and ↑ apoptosis	Chi et al. (2020)
	miR-485-5p/JUND axis	Ect1/E6E7, HEK-293T, HeLa, SIHA, C-33A and HT-3	Δ SNHG7: ↓ tumor cell proliferation, ↓ migration, ↓ invasion, and ↓ EMT	Zhao et al. (2020)
	—	HeLa, and C-33A	Δ SNHG7: ↓ tumor cell proliferation, and ↓ invasion	Zeng et al. (2019)
Thyroid cancer	miR-449a/ACSL1 axis	Nthy-ori-3-1, FTC133, TPC1, BCPAP, and 8505C	Δ SNHG7: ↓ tumor cell proliferation, ↓ migration, and ↑ apoptosis	Guo et al. (2020)
	—	CAL62, and SW579	Δ SNHG7: ↓ tumor cell proliferation, and ↓ cell cycle	Chen et al. (2019c)
	BDNF	K1, TPC-1, SW579, and Nthy-ori 3-1	Δ SNHG7: ↓ tumor cell proliferation, ↓ colony formation, and ↑ apoptosis	Wang et al. (2019)
	miR-9-5p/DPP4 axis	TPC-1, and B-CPAP	Δ SNHG7: ↓ tumor cell proliferation, and ↓ ¹³¹ I resistance	Chen et al. (2021)
Prostate cancer	miR-324-3p/WNT2B axis	RWPE, LNCaP, PC-3, and Du-145	Δ SNHG7: ↓ tumor cell proliferation, ↓ migration, ↓ invasion, and ↓ EMT	Han et al. (2019)
	miR-503/cyclin D1 axis	WPMY1, LNCaP, VCaP, 22RV1, DU145, and PC3	Δ SNHG7: ↓ tumor cell proliferation, and ↓ colony formation	Qi et al. (2018)
Osteosarcoma	p53/DNMT1 axis	U2OS, HOS, MG-63, and Saos-2	Δ SNHG7: ↓ tumor cell proliferation, ↑ cell cycle arrest, and ↑ apoptosis	Zhang et al. (2019c)
	miR-34a	hFOB1.19, MG63, SaOS2, HOS, and 143B	Δ SNHG7: ↓ tumor cell proliferation, ↓ migration, ↓ invasion, and ↓ EMT	Deng et al. (2018)
	miR-34a-5p/RAD9A axis	GSE70415 dataset	<i>in situ</i> evaluations showed that SNHG7 may enhance cell proliferation and metastasis	Wang et al. (2020d)

Δ: knockdown or silencing, ↓: decrease or repression, ↑: increase or induction, ↑↑: overexpression, EMT: epithelial-to-mesenchymal transition.

oncogenic role of SNHG7 as tumor growth and metastasis of grafted cancer cells are promoted, whereas SNHG7 knockdown represses them (see **Table 1**). For a reported association between upregulated SNHG7 expression and worse clinicopathological characteristics in cancerous patients, clinical studies support oncogenic features of SNHG7. Eventually, Kaplan–Meier survival and Cox univariate and multivariate analyses suggest SNHG7 as a potential prognostic and diagnostic biomarker for human malignancies. Importantly, knockdown experiences and also the contributing role of SNHG7 in chemoresistance suggest it as a potential therapeutic target, which can benefit the anticancer therapies.

Exosomal lncRNAs show high stability and concentrations and, thus, can be detected in body fluids (Tellez-Gabriel and Heymann, 2019). Regarding changes in expression levels of lncRNAs and their high diagnostic values, this makes them appropriate candidates for diagnosis and prediction of prognosis in human cancers (Qian et al., 2020). Several methodologies, including ultracentrifugation, are used to isolate exosomes and then detect the RNAs within. Although, due to low costs and higher accessibility, qRT-PCR is routinely used, high-throughput technologies such as next generation sequencing (NGS) and microarrays have facilitated detection of lncRNAs (Yamada et al., 2018). lncRNAs show acceptable values as diagnostic and prognostic biomarkers for several human cancers (Qian et al., 2020). In this review, we outline the cellular, animal, and clinical studies indicating that this lncRNA is almost universally upregulated in cancer tissues, promotes malignant

features of cancer cells, and has prognostic value in various malignancies; however, it seems that SNHG7 diagnostic accuracy in discrimination of human malignancies requires further investigation. Additionally, major limitations of detection methods, such as the impossibility of detecting the amplicon size, limit the number of lncRNAs that can be simultaneously detected, and nonspecific binding, which restricts the clinical application of commonly used qRT-PCR, requires more time to take the lncRNAs into the clinical setting (Jensen, 2012). Finally, there is no CRISPR-based genome editing or siRNA-based method approved or tested for suppression of SNHG7.

In conclusion, regarding a considerable number of studies that reveal oncogenic role of SNHG7 in human cancers and its prognostic value, SNHG7 is suggested as a potential cancer biomarker for human malignancies. Further investigations and more time are required for SNHG7 clinical applications in detection, prediction of prognosis, and treatment of human malignancies.

AUTHOR CONTRIBUTIONS

SG-F and SN wrote the draft and revised it. MT designed and supervised the study. BH, MH, and HJ collected the data and designed the figures and tables. All the authors read and approved the submitted version.

REFERENCES

- Al-Tobasei, R., Paneru, B., and Salem, M. (2016). Genome-wide Discovery of Long Non-coding RNAs in Rainbow trout. *PLoS One* 11 (2), e0148940. doi:10.1371/journal.pone.0148940
- Amin, N., McGrath, A., and Chen, Y.-P. P. (2019). Evaluation of Deep Learning in Non-coding RNA Classification. *Nat. Mach. Intell.* 1 (5), 246–256. doi:10.1038/s42256-019-0051-2
- Bai, Z., Wu, Y., Bai, S., Yan, Y., Kang, H., Ma, W., et al. (2020). Long Non-coding RNA SNHG7 Is Activated by SP1 and Exerts Oncogenic Properties by Interacting with EZH2 in Ovarian Cancer. *J. Cel Mol Med.* 24 (13), 7479–7489. PubMed PMID: 32420685. Epub 05/18. eng. doi:10.1111/jcmm.15373
- Boone, D. N., Warburton, A., Som, S., and Lee, A. V. (2020). SNHG7 Is a lncRNA Oncogene Controlled by Insulin-like Growth Factor Signaling through a Negative Feedback Loop to Tightly Regulate Proliferation. *Sci. Rep.* 10 (1), 8583. PubMed PMID: 32444795. Pubmed Central PMCID: PMC7244715. Epub 2020/05/24. eng. doi:10.1038/s41598-020-65109-7
- Chai, R., Xu, C., Lu, L., Liu, X., and Ma, Z. (2021). Quercetin Inhibits Proliferation of and Induces Apoptosis in Non-small-cell Lung Carcinoma via the lncRNA SNHG7/miR-34a-5p Pathway. *Immunopharmacology and immunotoxicology* 43 (6), 693–703. PubMed PMID: 34448661. Epub 2021/08/28. eng. doi:10.1080/08923973.2021.1966032
- Chaudhry, M. (2013). Expression Pattern of Small Nucleolar RNA Host Genes and Long Non-coding RNA in X-Rays-Treated Lymphoblastoid Cells. *Ijms* 14 (5), 9099–9110. PubMed PMID: 23698766. eng. doi:10.3390/ijms14059099
- Chen, K., Abuduwufer, A., Zhang, H., Luo, L., Suotesiyali, M., and Zou, Y. (2019). SNHG7 Mediates Cisplatin-Resistance in Non-small Cell Lung Cancer by Activating PI3K/AKT Pathway. *Eur. Rev. Med. Pharmacol. Sci.* 23 (16), 6935–6943. PubMed PMID: 31486493. Epub 2019/09/06. eng. doi:10.26355/eurrev_201908_18733
- Chen, L., Zhu, J., and Zhang, L. J. (2019). Long Non-coding RNA Small Nucleolar RNA Host Gene 7 Is Upregulated and Promotes Cell Proliferation in Thyroid Cancer. *Oncol. Lett.* 18 (5), 4726–4734. PubMed PMID: 31611982. Epub 08/27. eng. doi:10.3892/ol.2019.10782
- Chen, W., Yu, J., Xie, R., Zhou, T., Xiong, C., Zhang, S., et al. (2021). Roles of the SNHG7/microRNA-9-5p/DPP4 ceRNA Network in the Growth and T-R-Resistance of T-Hyroid C-Arcinoma C-ells through PI3K/Akt Activation. *Oncol. Rep.* 45 (4), 3. PubMed PMID: 33649840. Epub 03/02. eng. doi:10.3892/or.2021.7954
- Chen, Y., Yuan, S., Ning, T., Xu, H., and Guan, B. (2020). SNHG7 Facilitates Glioblastoma Progression by Functioning as a Molecular Sponge for MicroRNA-449b-5p and Thereby Increasing MYCN Expression. *Technology in Cancer Research & Treatment.*
- Chen, Y., Peng, Y., Xu, Z., Ge, B., Xiang, X., Zhang, T., et al. (2019). Knockdown of lncRNA SNHG7 Inhibited Cell Proliferation and Migration in Bladder Cancer through Activating Wnt/ β -Catenin Pathway. *Pathol. - Res. Pract.* 215 (2), 302–307. PubMed PMID: 30527358. Epub 2018/12/12. eng. doi:10.1016/j.prp.2018.11.015
- Chen, Z., Liu, Z., Shen, L., and Jiang, H. (2019). Long Non-coding RNA SNHG7 Promotes the Fracture Repair through Negative Modulation of miR-9. *Am. J. Transl. Res.* 11 (2), 974–982. PubMed PMID: 30899396. eng.
- Chen, Z., He, M., Chen, J., Li, C., and Zhang, Q. (2020). Long Non-coding RNA SNHG7 Inhibits NLRP3-dependent Pyroptosis by Targeting the miR-34a/SIRT1 axis in Liver Cancer. *Oncol. Lett.* 20 (1), 893–901. PubMed PMID: 32566017. Epub 05/18. eng. doi:10.3892/ol.2020.11635
- Cheng, D., Fan, J., Ma, Y., Zhou, Y., Qin, K., Shi, M., et al. (2019). lncRNA SNHG7 Promotes Pancreatic Cancer Proliferation through ID4 by Sponging miR-342-3p. *Cell Biosci.* 9 (1), 28–11. doi:10.1186/s13578-019-0290-2
- Cheng, D., Fan, J., Qin, K., Zhou, Y., Yang, J., Ma, Y., et al. (2021). lncRNA SNHG7 Regulates Mesenchymal Stem Cell through the Notch1/Jagged1/Hes-1 Signaling Pathway and Influences FOLFIRINOX Resistance in Pancreatic Cancer. *Front. Oncol.* 11 (3235). doi:10.3389/fonc.2021.719855
- Cheng, D., Fan, J., Ma, Y., Zhou, Y., Qin, K., Shi, M., et al. (2019). lncRNA SNHG7 Promotes Pancreatic Cancer Proliferation through ID4 by Sponging miR-342-3p. *Cel Biosci.* 9, 28. PubMed PMID: 30949340. Pubmed Central PMCID: PMC6431029. Epub 2019/04/06. eng. doi:10.1186/s13578-019-0290-2

- Cheng, G., Zheng, J., and Wang, L. (2020). LncRNA SNHG7 Promotes Glioma Cells Viability, Migration and Invasion by Regulating miR-342-3p/AKT2 axis. *Int. J. Neurosci.*, 1–13. PubMed PMID: 32628059. Epub 2020/07/07. eng. doi:10.1080/00207454.2020.1790556
- Chi, C., Li, M., Hou, W., Chen, Y., Zhang, Y., and Chen, J. (2020). Long Noncoding RNA SNHG7 Activates Wnt/ β -Catenin Signaling Pathway in Cervical Cancer Cells by Epigenetically Silencing DKK1. *Cancer Biother. Radiopharm.* 35 (5), 329–337. PubMed PMID: 32275170. Epub 2020/04/11. eng. doi:10.1089/cbr.2019.3004
- Chi, R., Chen, X., Liu, M., Zhang, H., Li, F., Fan, X., et al. (2019). Role of SNHG7-miR-653-5p-STAT2 Feedback Loop in Regulating Neuroblastoma Progression. *J. Cel Physiol.* 234 (8), 13403–13412. PubMed PMID: 30623419. Epub 2019/01/10. eng. doi:10.1002/jcp.28017
- Crick, F. (1970). Central Dogma of Molecular Biology. *Nature* 227 (5258), 561–563. doi:10.1038/227561a0
- Dahariya, S., Paddibhatla, I., Kumar, S., Raghuwanshi, S., Palapati, A., and Gutti, R. K. (2019). Long Non-coding RNA: Classification, Biogenesis and Functions in Blood Cells. *Mol. Immunol.* 112, 82–92. doi:10.1016/j.molimm.2019.04.011
- Dai, Y., Zhang, X., Xing, H., Zhang, Y., Cao, H., Sang, J., et al. (2020). Downregulated Long Non-coding RNA SNHG7 Restricts Proliferation and Boosts Apoptosis of Nasopharyngeal Carcinoma Cells by Elevating microRNA-140-5p to Suppress GLI3 Expression. *Cell Cycle* 19 (4), 448–463. PubMed PMID: 31944163. Epub 01/16. eng. doi:10.1080/15384101.2020.1712033
- Deng, Y., Cheng, L., Lv, Z., Zhu, H., and Meng, X. (2021). LncRNA SNHG7 Promotes Cell Proliferation in Glioma by Acting as a Competing Endogenous RNA and Sponging miR-138-5p to R-egulate EZH2 E-xpression. *Oncol. Lett.* 22 (1), 565. PubMed PMID: 34113393. Pubmed Central PMCID: PMC8185700. Epub 2021/06/12. eng. doi:10.3892/ol.2021.12826
- Deng, Y., Zhao, F., Zhang, Z., Sun, F., and Wang, M. (2018). Long Noncoding RNA SNHG7 Promotes the Tumor Growth and Epithelial-To-Mesenchymal Transition via Regulation of miR-34a Signals in Osteosarcoma. *Cancer Biother. Radiopharm.* 33 (9), 365–372. PubMed PMID: 29989838. Epub 2018/07/11. eng. doi:10.1089/cbr.2018.2503
- Du, L., Xu, Z., Wang, X., and Liu, F. (2020). Integrated Bioinformatics Analysis Identifies microRNA-376a-3p as a New microRNA Biomarker in Patient with Coronary Artery Disease. *Am. J. Transl Res.* 12 (2), 633–648.
- Elgar, G., and Vavouri, T. (2008). Tuning in to the Signals: Noncoding Sequence Conservation in Vertebrate Genomes. *Trends Genet.* 24 (7), 344–352. PubMed PMID: 18514361. Epub 2008/06/03. eng. doi:10.1016/j.tig.2008.04.005
- Gao, F., Cai, Y., Kapranov, P., and Xu, D. (2020). Reverse-genetics Studies of lncRNAs-What We Have Learnt and Paths Forward. *Genome Biol.* 21 (1), 93. doi:10.1186/s13059-020-01994-5
- Gao, Y. T., and Zhou, Y. C. (2019). Long Non-coding RNA (lncRNA) Small Nucleolar RNA Host Gene 7 (SNHG7) Promotes Breast Cancer Progression by Sponging miRNA-381. *Eur. Rev. Med. Pharmacol. Sci.* 23 (15), 6588–6595. PubMed PMID: 31378900. Epub 2019/08/06. eng. doi:10.26355/eurrev_201908_18545
- Guo, L., Lu, J., Gao, J., Li, M., Wang, H., and Zhan, X. (2020). The Function of SNHG7/miR-449a/ACSL1 axis in Thyroid Cancer. *J. Cel Biochem.* 121 (10), 4034–4042. PubMed PMID: 31961004. Epub 2020/01/22. eng. doi:10.1002/jcb.29569
- Guttman, M., Amit, I., Garber, M., French, C., Lin, M. F., Feldser, D., et al. (2009). Chromatin Signature Reveals over a Thousand Highly Conserved Large Non-coding RNAs in Mammals. *Nature* 458 (7235), 223–227. PubMed PMID: 19182780. Pubmed Central PMCID: PMC2754849. Epub 2009/02/03. eng. doi:10.1038/nature07672
- Han, Y., Hu, H., and Zhou, J. (2019). Knockdown of LncRNA SNHG7 Inhibited Epithelial-Mesenchymal Transition in Prostate Cancer Though miR-324-3p/WNT2B axis *In Vitro. Pathol. Res. Pract.* 215 (10), 152537. doi:10.1016/j.prp.2019.152537
- Hartford, C. C. R., and Lal, A. (2020). When Long Noncoding Becomes Protein Coding. *Mol. Cel Biol.* 40 (6), e00528–19. doi:10.1128/MCB.00528-19
- He, H., Xu, M., Kuang, Y., Han, X., Wang, M., and Yang, Q. (2016). Biomarker and Competing Endogenous RNA Potential of Tumor-specific Long Noncoding RNA in Chromophobe Renal Cell Carcinoma. *Ott* 9, 6399–6406. PubMed PMID: 27799788. eng. doi:10.2147/ott.s116392
- Hombach, S., and Kretz, M. (2016). Non-coding RNAs: Classification, Biology and Functioning. *Adv. Exp. Med. Biol.* 937, 3–17. PubMed PMID: 27573892. Epub 2016/08/31. eng. doi:10.1007/978-3-319-42059-2_1
- Hu, W., Li, H., and Wang, S. (2020). LncRNA SNHG7 Promotes the Proliferation of Nasopharyngeal Carcinoma by miR-514a-5p/ELAVL1 axis. *BMC cancer* 20 (1), 376. PubMed PMID: 32370736. eng. doi:10.1186/s12885-020-06775-8
- Hu, Y., Wang, L., Li, Z., Wan, Z., Shao, M., Wu, S., et al. (2019). Potential Prognostic and Diagnostic Values of CDC6, CDC45, ORC6 and SNHG7 in Colorectal Cancer. *Ott* 12, 11609–11621. PubMed PMID: 32021241. eng. doi:10.2147/ott.s231941
- Huang, W., Wu, X., Xue, Y., Zhou, Y., Xiang, H., Yang, W., et al. (2020). MicroRNA-3614 Regulates Inflammatory Response via Targeting TRAF6-Mediated MAPKs and NF-Kb Signaling in the Epicardial Adipose Tissue with Coronary Artery Disease. *Int. J. Cardiol.*
- Iyer, M. K., Niknafs, Y. S., Malik, R., Singhal, U., Sahu, A., Hosono, Y., et al. (2015). The Landscape of Long Noncoding RNAs in the Human Transcriptome. *Nat. Genet.* 47 (3), 199–208. doi:10.1038/ng.3192
- Jensen, E. C. (2012). Real-time Reverse Transcription Polymerase Chain Reaction to Measure mRNA: Use, Limitations, and Presentation of Results. *Anat. Rec.* 295 (1), 1–3. PubMed PMID: 22095866. Epub 2011/11/19. eng. doi:10.1002/ar.21487
- Jia, J., Zhang, D., Zhang, J., Yang, L., Zhao, G., Yang, H., et al. (2020). Long Non-coding RNA SNHG7 Promotes Neuroblastoma Progression through Sponging miR-323a-5p and miR-342-5p. *Biomed. Pharmacother.* 128, 110293. doi:10.1016/j.biopha.2020.110293
- Jian, Y., and Fan, Q. (2021). Long Non-coding RNA SNHG7 F-acilitates P-ancreatic C-ancer P-rogression by R-regulating the miR-146b-5p/Robo1 axis. *Exp. Ther. Med.* 21 (4), 398. PubMed PMID: 33680120. Epub 02/24. eng. doi:10.3892/etm.2021.9829
- Jing, L., Li, S., Wang, J., and Zhang, G. (2019). Long Non-coding RNA Small Nucleolar RNA Host Gene 7 Facilitates Cardiac Hypertrophy via Stabilization of SDA1 Domain Containing 1 mRNA. *J. Cel Biochem.* 120 (9), 15089–15097. PubMed PMID: 31026094. Epub 2019/04/27. eng. doi:10.1002/jcb.28770
- Li, L., Ye, D., Liu, L., Li, X., Liu, J., Su, S., et al. (2020). Long Noncoding RNA SNHG7 Accelerates Proliferation, Migration and Invasion of Non-small Cell Lung Cancer Cells by Suppressing miR-181a-5p through AKT/mTOR Signaling Pathway. *Cmar* 12, 8303–8312. PubMed PMID: 32982425. eng. doi:10.2147/cmar.s258487
- Li, W., Zheng, Y., Mao, B., Wang, F., Zhong, Y., and Cheng, D. (2020). SNHG17 Upregulates WLS Expression to Accelerate Lung Adenocarcinoma Progression by Sponging miR-485-5p. *Biochem. Biophysical Res. Commun.* 533 (4), 1435–1441. PubMed PMID: 33109341. Epub 2020/10/29. eng. doi:10.1016/j.bbrc.2020.09.130
- Li, Y., Guo, X., and Wei, Y. (2020). LncRNA SNHG7 Inhibits Proliferation and Invasion of Breast Cancer Cells by Regulating miR-15a Expression. *J. Buon* 25 (4), 1792–1798. PubMed PMID: 33099915. Epub 2020/10/26. eng.
- Li, Y., Zeng, C., Hu, J., Pan, Y., Shan, Y., Liu, B., et al. (2018). Long Non-coding RNA-SNHG7 Acts as a Target of miR-34a to Increase GALNT7 Level and Regulate PI3K/Akt/mTOR Pathway in Colorectal Cancer Progression. *J. Hematol. Oncol.* 11 (1), 89–17. doi:10.1186/s13045-018-0632-2
- Li, Y., Zeng, C., Hu, J., Pan, Y., Shan, Y., Liu, B., et al. (2018). Long Non-coding RNA-SNHG7 Acts as a Target of miR-34a to Increase GALNT7 Level and Regulate PI3K/Akt/mTOR Pathway in Colorectal Cancer Progression. *J. Hematol. Oncol.* 11 (1), 89. PubMed PMID: 29970122. eng. doi:10.1186/s13045-018-0632-2
- Li, Z.-h., Yu, N.-s., Deng, Q., Zhang, Y., Hu, Y.-y., Liu, G., et al. (2020). LncRNA SNHG7 Mediates the Chemoresistance and Stemness of Breast Cancer by Sponging miR-34a. *Front. Oncol.* 10, 592757. PubMed PMID: 33330080. eng. doi:10.3389/fonc.2020.592757
- Liu, K. L., Wu, J., Li, W. K., Li, N. S., Li, Q., and Lao, Y. Q. (2019). LncRNA SNHG7 Is an Oncogenic Biomarker Interacting with MicroRNA-193b in Colon Carcinogenesis. *Clin. Lab.* 65 (11). doi:10.7754/Clin.Lab.2019.190501PubMed PMID: 31721543. Epub 2019/11/14. eng
- Liu, Y., Li, Q., Tang, D., Li, M., Zhao, P., Yang, W., et al. (2020). SNHG17 Promotes the Proliferation and Migration of Colorectal Adenocarcinoma Cells by Modulating CXCL12-Mediated Angiogenesis. *Cancer Cel Int.* 20 (1), 566. PubMed PMID: 33292246. eng. doi:10.1186/s12935-020-01621-0

- Luo, X., Song, Y., Tang, L., Sun, D. H., and Ji, D. G. (2018). LncRNA SNHG7 Promotes Development of Breast Cancer by Regulating microRNA-186. *Eur. Rev. Med. Pharmacol. Sci.* 22 (22), 7788–7797. PubMed PMID: 30536320. Epub 2018/12/12. eng. doi:10.26355/eurrev_201811_16403
- Mattick, J. S. (2001). Non-coding RNAs: the Architects of Eukaryotic Complexity. *EMBO Rep.* 2 (11), 986–991. PubMed PMID: 11713189. eng. doi:10.1093/embo-reports/kve230
- Najafi, S., Tan, S. C., Raee, P., Rahmati, Y., Asemani, Y., Lee, E. H. C., et al. (2022). Gene Regulation by Antisense Transcription: A Focus on Neurological and Cancer Diseases. *Biomed. Pharmacother.* 145, 112265. doi:10.1016/j.biopha.2021.112265
- Pang, L., Cheng, Y., Zou, S., and Song, J. (2020). Long Noncoding RNA SNHG7 Contributes to Cell Proliferation, Migration, Invasion and Epithelial to Mesenchymal Transition in Non-small Cell Lung Cancer by Regulating miR-449a/TGIF2 axis. *Thorac. Cancer* 11 (2), 264–276. PubMed PMID: 31793741. Epub 12/03. eng. doi:10.1111/1759-7714.13245
- Pei, L.-J., Sun, P.-J., Ma, K., Guo, Y.-Y., Wang, L.-Y., and Liu, F.-D. (2021). LncRNA-SNHG7 Interferes with miR-34a to De-sensitize Gastric Cancer Cells to Cisplatin. *Cbm* 30, 127–137. doi:10.3233/cbm-201621
- Pei, Y.-f., He, Y., Hu, L.-z., Zhou, B., Xu, H.-y., and Liu, X.-q. (2020). The Crosstalk between LncRNA-SNHG7/miRNA-181/cbx7 Modulates Malignant Character in Lung Adenocarcinoma. *Am. J. Pathol.* 190 (6), 1343–1354. PubMed PMID: 32201260. Epub 2020/03/24. eng. doi:10.1016/j.ajpath.2020.02.011
- Qi, H., Wen, B., Wu, Q., Cheng, W., Lou, J., Wei, J., et al. (2018). Long Noncoding RNA SNHG7 Accelerates Prostate Cancer Proliferation and Cycle Progression through Cyclin D1 by Sponging miR-503. *Biomed. Pharmacother.* 102, 326–332. PubMed PMID: 29571017. Epub 2018/03/24. eng. doi:10.1016/j.biopha.2018.03.011
- Qian, Y., Shi, L., and Luo, Z. (2020). Long Non-coding RNAs in Cancer: Implications for Diagnosis, Prognosis, and Therapy. *Front. Med.* 30, 7. doi:10.3389/fmed.2020.612393
- Quinn, J. J., and Chang, H. Y. (2016). Unique Features of Long Non-coding RNA Biogenesis and Function. *Nat. Rev. Genet.* 17 (1), 47–62. doi:10.1038/nrg.2015.10
- Rahmati, Y., Asemani, Y., Aghamiri, S., Ezzatifar, F., and Najafi, S. (2021). CiRS-7/CDRIAs; an Oncogenic Circular RNA as a Potential Cancer Biomarker. *Pathol. - Res. Pract.* 227, 153639. doi:10.1016/j.prp.2021.153639
- Ramírez-Colmenero, A., Oktaba, K., and Fernandez-Valverde, S. L. (2020). Evolution of Genome-Organizing Long Non-coding RNAs in Metazoans. *Front. Genet.* 11 (1512).
- Ren, J., Yang, Y., Xue, J., Xi, Z., Hu, L., Pan, S.-J., et al. (2018). Long Noncoding RNA SNHG7 Promotes the Progression and Growth of Glioblastoma via Inhibition of miR-5095. *Biochem. Biophysical Res. Commun.* 496 (2), 712–718. PubMed PMID: 29360452. Epub 2018/01/24. eng. doi:10.1016/j.bbrc.2018.01.109
- Sarropoulos, I., Marin, R., Cardoso-Moreira, M., and Kaessmann, H. (2019). Developmental Dynamics of lncRNAs across Mammalian Organs and Species. *Nature* 571 (7766), 510–514. PubMed PMID: 31243368. Epub 06/26. eng. doi:10.1038/s41586-019-1341-x
- Sayad, A., Najafi, S., Kashi, A. H., Hosseini, S. J., Akrami, S. M., Taheri, M., et al. (2021). Circular RNAs in Renal Cell Carcinoma: Functions in Tumorigenesis and Diagnostic and Prognostic Potentials. *Pathol. - Res. Pract.*, 153720. doi:10.1016/j.prp.2021.153720
- Shan, Y., Ma, J., Pan, Y., Hu, J., Liu, B., and Jia, L. (2018). LncRNA SNHG7 Sponges miR-216b to Promote Proliferation and Liver Metastasis of Colorectal Cancer through Upregulating GALNT1. *Cell Death Dis.* 9 (7), 722. PubMed PMID: 29915311. eng. doi:10.1038/s41419-018-0759-7
- She, K., Yan, H., Huang, J., Zhou, H., and He, J. (2018). miR-193b Availability Is Antagonized by LncRNA-SNHG7 for FAIM2-Induced Tumour Progression in Non-small Cell Lung Cancer. *Cell Prolif* 51 (1), e12406. PubMed PMID: 29131440. Epub 11/12. eng. doi:10.1111/cpr.12406
- She, K., Huang, J., Zhou, H., Huang, T., Chen, G., and He, J. (2016). LncRNA-SNHG7 Promotes the Proliferation, Migration and Invasion and Inhibits Apoptosis of Lung Cancer Cells by Enhancing the FAIM2 Expression. *Oncol. Rep.* 36 (5), 2673–2680. doi:10.3892/or.2016.5105
- Shen, A., Ma, J., Hu, X., and Cui, X. (2020). High Expression of LncRNA-SNHG7 Is Associated with Poor Prognosis in Hepatocellular Carcinoma. *Oncol. Lett.* 19 (6), 3959–3963. PubMed PMID: 32382340. Pubmed Central PMCID: PMC7202315. Epub 2020/05/10. eng. doi:10.3892/ol.2020.11490
- Shi, J., Ding, W., and Lu, H. (2020). Identification of Long Non-coding RNA SNHG Family as Promising Prognostic Biomarkers in Acute Myeloid Leukemia. *Ott* 13, 8441–8450. PubMed PMID: 32922034. eng. doi:10.2147/ott.s265853
- Statello, L., Guo, C.-J., Chen, L.-L., and Huarte, M. (2021). Gene Regulation by Long Non-coding RNAs and its Biological Functions. *Nat. Rev. Mol. Cel Biol.* 22 (2), 96–118. doi:10.1038/s41580-020-00315-9
- Sun, X., Huang, T., Liu, Z., Sun, M., and Luo, S. (2019). LncRNA SNHG7 Contributes to Tumorigenesis and Progression in Breast Cancer by Interacting with miR-34a through EMT Initiation and the Notch-1 Pathway. *Eur. J. Pharmacol.* 856, 172407. doi:10.1016/j.ejphar.2019.172407
- Taheri, M., Najafi, S., Basiri, A., Hussen, B. M., Baniahmad, A., Jamali, E., et al. (2021). The Role and Clinical Potentials of Circular RNAs in Prostate Cancer. *Front. Oncol.* 11, 781414. PubMed PMID: 34804984. eng. doi:10.3389/fonc.2021.781414
- Tellez-Gabriel, M., and Heymann, D. (2019). Exosomal lncRNAs: the Newest Promising Liquid Biopsy. *Cancer Drug Resist.* 2 (4), 1002–1017. doi:10.20517/cdr.2019.69
- Wang, J., Zhang, S., Li, X., and Gong, M. (2020). LncRNA SNHG7 Promotes Cardiac Remodeling by Upregulating ROCK1 via Sponging miR-34-5p. *Aging* 12 (11), 10441–10456. PubMed PMID: 32507765. Pubmed Central PMCID: PMC7346013. Epub 2020/06/09. eng. doi:10.18632/aging.103269
- Wang, L., Zhang, L., and Wang, L. (2020). SNHG7 Contributes to the Progression of Non-small-cell Lung Cancer via the SNHG7/miR-181a-5p/E2F7 Axis. *Cmar* 12, 3211–3222. PubMed PMID: 32440218. eng. doi:10.2147/cmar.s240964
- Wang, M. W., Liu, J., Liu, Q., Xu, Q. H., Li, T. F., Jin, S., et al. (2017). LncRNA SNHG7 Promotes the Proliferation and Inhibits Apoptosis of Gastric Cancer Cells by Repressing the P15 and P16 Expression. *Eur. Rev. Med. Pharmacol. Sci.* 21 (20), 4613–4622. PubMed PMID: 29131253. Epub 2017/11/14. eng.
- Wang, W., Chen, S., Song, X., Gui, J., Li, Y., and Li, M. (20202020). ELK1/lncRNA-SNHG7/miR-2682-5p Feedback Loop Enhances Bladder Cancer Cell Growth. *Life Sci.* 262, 118386. doi:10.1016/j.lfs.2020.118386
- Wang, Y., Gao, Y., Guo, S., and Chen, Z. (2020). Integrated Analysis of lncRNA-Associated ceRNA Network Identified Potential Regulatory Interactions in Osteosarcoma. *Genet. Mol. Biol.* 43 (2), e20190090. doi:10.1590/1678-4685-GMB-2019-0090
- Wang, Y., Bao, D., Wan, L., Zhang, C., Hui, S., and Guo, H. (2021). Long Non-coding RNA Small Nucleolar RNA Host Gene 7 Facilitates the Proliferation, Migration, and Invasion of Esophageal Cancer Cells by Regulating microRNA-625. *J. Gastrointest. Oncol.* 12 (2), 423–432. PubMed PMID: 34012636. eng. doi:10.21037/jgo-21-147
- Wang, Y. H., Huo, B. L., Li, C., Ma, G., and Cao, W. (2019). Knockdown of Long Noncoding RNA SNHG7 Inhibits the Proliferation and Promotes Apoptosis of Thyroid Cancer Cells by Downregulating BDNF. *Eur. Rev. Med. Pharmacol. Sci.* 23 (11), 4815–4821. PubMed PMID: 31210313. Epub 2019/06/19. eng. doi:10.26355/eurrev_201906_18067
- Wang, Y., Wang, X., Li, Z., Chen, L., Zhou, L., Li, C., et al. (2017). Two Single Nucleotide Polymorphisms (Rs2431697 and Rs2910164) of miR-146a Are Associated with Risk of Coronary Artery Disease. *Ijeph* 14 (5), 514. doi:10.3390/ijeph14050514
- Wu, P., Tang, Y., Fang, X., Xie, C., Zeng, J., Wang, W., et al. (2019). Metformin Suppresses Hypopharyngeal Cancer Growth by Epigenetically Silencing Long Non-coding RNA SNHG7 in FaDu Cells. *Front. Pharmacol.* 10, 143. doi:10.3389/fphar.2019.00143
- Xia, Q., Li, J., Yang, Z., Zhang, D., Tian, J., and Gu, B. (2020). Long Non-coding RNA Small Nucleolar RNA Host Gene 7 Expression Level in Prostate Cancer Tissues Predicts the Prognosis of Patients with Prostate Cancer. *Medicine (Baltimore)* 99 (7), e18993. e. PubMed PMID: 32049793. eng. doi:10.1097/md.00000000000018993
- Xie, Y., Wang, Y., Gong, R., Lin, J., Li, X., Ma, J., et al. (2020). SNHG7 Facilitates Hepatocellular Carcinoma Occurrence by Sequestering miR-9-5p to Upregulate CNNM1 Expression. *Cancer Biother. Radiopharm.* 35 (10), 731–740. PubMed PMID: 32397799. Epub 2020/05/14. eng. doi:10.1089/cbr.2019.2996
- Xu, C., Zhou, J., Wang, Y., Wang, A., Su, L., Liu, S., et al. (2019). Inhibition of Malignant Human Bladder Cancer Phenotypes through the Down-Regulation of the Long Non-coding RNA SNHG7. *J. Cancer* 10 (2), 539–546. PubMed

- PMID: 30719150. Pubmed Central PMCID: PMC6360294. Epub 2019/02/06. eng. doi:10.7150/jca.25507
- Xu, L. J., Yu, X. J., Wei, B., Hui, H. X., Sun, Y., Dai, J., et al. (2018). LncRNA SNHG7 Promotes the Proliferation of Esophageal Cancer Cells and Inhibits its Apoptosis. *Eur. Rev. Med. Pharmacol. Sci.* 22 (9), 2653–2661. PubMed PMID: 29771415. Epub 2018/05/18. eng. doi:10.26355/eurrev_201805_14961
- Xue, Y. H., and Ge, Y. Q. (2020). Construction of LncRNA Regulatory Networks Reveal the Key lncRNAs Associated with Pituitary Adenomas Progression. *Math. Biosci. Eng.* 17 (3), 2138–2149. PubMed PMID: 32233527. Epub 2020/04/03. eng. doi:10.3934/mbe.2020113
- Yamada, A., Yu, P., Lin, W., Okugawa, Y., Boland, C. R., and Goel, A. (2018). A RNA-Sequencing Approach for the Identification of Novel Long Non-coding RNA Biomarkers in Colorectal Cancer. *Sci. Rep.* 8 (1), 575. PubMed PMID: 29330370. eng. doi:10.1038/s41598-017-18407-6
- Yang, X., Sun, L., Wang, L., Yao, B., Mo, H., and Yang, W. (2019). LncRNA SNHG7 Accelerates the Proliferation, Migration and Invasion of Hepatocellular Carcinoma Cells via Regulating miR-122-5p and RPL4. *Biomed. Pharmacother.* 118, 109386. doi:10.1016/j.biopha.2019.109386
- Yao, X., Liu, C., Liu, C., Xi, W., Sun, S., and Gao, Z. (2019). LncRNA SNHG7 Sponges miR-425 to Promote Proliferation, Migration, and Invasion of Hepatic Carcinoma Cells via Wnt/ β -catenin/EMT Signalling Pathway. *Cell Biochem Funct.* 37 (7), 525–533. PubMed PMID: 31478234. Epub 09/02. eng. doi:10.1002/cbf.3429
- Yi, P., Zhang, W., Yang, M., Lu, Q., and Wu, H. (2021). LncRNA SNHG7 Serves as a Potential Biomarker on the Prognosis of Human Solid Tumors: A Meta-Analysis. *Cpb* 22 (11), 1501–1510. PubMed PMID: 33397233. Epub 2021/01/06. eng. doi:10.2174/1389201022666210104121207
- Yu, F., Dong, P., Mao, Y., Zhao, B., Huang, Z., and Zheng, J. (2019). Loss of lncRNA-SNHG7 Promotes the Suppression of Hepatic Stellate Cell Activation via miR-378a-3p and DVL2. *Mol. Ther. - Nucleic Acids* 17, 235–244. PubMed PMID: 31272073. Epub 06/07. eng. doi:10.1016/j.omtn.2019.05.026
- Yu, K., Yuan, W., Huang, C., Xiao, L., Xiao, R., Zeng, P., et al. (2021). The Prognostic Value of Long Non-coding RNA SNHG7 in Human Cancer: A Meta-Analysis. *Curr. Pharm. Biotechnol.* 22, 1–13. doi:10.2174/1389201022666210810100607
- Yu, K., Yuan, W., Huang, C., Xiao, L., Xiao, R., Zeng, P., et al. (2021). The Prognostic Value of Long Non-coding RNA SNHG7 in Human Cancer: A Meta-Analysis. *Curr. Pharm. Biotechnol.* PubMed PMID: 34375186. Epub 2021/08/11. eng. doi:10.2174/1389201022666210810100607
- Yu, Z., Wang, Y., Wang, B., and Zhai, J. (2020). Metformin Affects Paclitaxel Sensitivity of Ovarian Cancer Cells through Autophagy Mediated by Long Noncoding RNASNHG7/miR-3127-5p Axis. *Cancer Biother. Radiopharm.* PubMed PMID: 32522016. Epub 2020/06/12. eng.
- Yue, X., Dong, C., Ye, Z., Zhu, L., Zhang, X., Wang, X., et al. (2021). LncRNA SNHG7 Sponges miR-449a to Promote Pituitary Adenomas Progression. *Metab. Brain Dis.* 36 (1), 123–132. PubMed PMID: 32880813. Epub 2020/09/04. eng. doi:10.1007/s11011-020-00611-5
- Zeng, J., Ma, Y. X., Liu, Z. H., and Zeng, Y. L. (2019). LncRNA SNHG7 Contributes to Cell Proliferation, Invasion and Prognosis of Cervical Cancer. *Eur. Rev. Med. Pharmacol. Sci.* 23 (21), 9277–9285. PubMed PMID: 31773679. Epub 2019/11/28. eng. doi:10.26355/eurrev_201911_19420
- Zhang, G. D., Gai, P. Z., Liao, G. Y., and Li, Y. (2019). LncRNA SNHG7 Participates in Osteosarcoma Progression by Down-Regulating P53 via Binding to DNMT1. *Eur. Rev. Med. Pharmacol. Sci.* 23 (9), 3602–3610. PubMed PMID: 31114984. Epub 2019/05/23. eng. doi:10.26355/eurrev_201905_17782
- Zhang, H., Zhang, X.-Y., Kang, X.-N., Jin, L.-J., and Wang, Z.-Y. (2020). LncRNA-SNHG7 Enhances Chemotherapy Resistance and Cell Viability of Breast Cancer Cells by Regulating miR-186. *Cmar* 12, 10163–10172. PubMed PMID: 33116871. eng. doi:10.2147/cmar.s270328
- Zhang, L., Fu, Y., and Guo, H. (2019). c-Myc-Induced Long Non-coding RNA Small Nucleolar RNA Host Gene 7 Regulates Glycolysis in Breast Cancer. *J. Breast Cancer* 22 (4), 533–547. PubMed PMID: 31897328. eng. doi:10.4048/jbc.2019.22.e54
- Zhang, P., Shi, L., Song, L., Long, Y., Yuan, K., Ding, W., et al. (2020). LncRNA CRNDE and LncRNA SNHG7 Are Promising Biomarkers for Prognosis in Synchronous Colorectal Liver Metastasis Following Hepatectomy. *Cmar* 12, 1681–1692. PubMed PMID: 32210611. eng. doi:10.2147/cmar.s233147
- Zhang, X., Wang, W., Zhu, W., Dong, J., Cheng, Y., Yin, Z., et al. (2019). Mechanisms and Functions of Long Non-coding RNAs at Multiple Regulatory Levels. *Ijms* 20 (22), 5573. PubMed PMID: 31717266. eng. doi:10.3390/ijms20225573
- Zhang, Y., Yuan, Y., Zhang, Y., Cheng, L., Zhou, X., and Chen, K. (2020). SNHG7 Accelerates Cell Migration and Invasion through Regulating miR-34a-Snail-EMT axis in Gastric Cancer. *Cell Cycle* 19 (1), 142–152. doi:10.1080/15384101.2019.1699753
- Zhao, D., Zhang, H., Long, J., and Li, M. (2020). LncRNA SNHG7 Functions as an Oncogene in Cervical Cancer by Sponging miR-485-5p to Modulate JUND Expression. *Ott* 13, 1677–1689. PubMed PMID: 32161467. eng. doi:10.2147/ott.s237802
- Zhao, Z., Gao, J., and Huang, S. (2021). LncRNA SNHG7 Promotes the HCC Progression through miR-122-5p/FOXK2 Axis. *Dig. Dis. Sci.* doi:10.1007/s10620-021-06918-2
- Zhao, Z., and Liu, X. (2021). LncRNA SNHG7 Regulates Gastric Cancer Progression by miR-485-5p. *J. Oncol.* 2021, 6147962. PubMed PMID: 34512753. eng. doi:10.1155/2021/6147962
- Zhong, X., Long, Z., Wu, S., Xiao, M., and Hu, W. (2018). LncRNA-SNHG7 Regulates Proliferation, Apoptosis and Invasion of Bladder Cancer Cells Assurance Guidelines. *J. BUON* 23 (3), 776–781.
- Zhong, X., Long, Z., Wu, S., Xiao, M., and Hu, W. (2018). LncRNA-SNHG7 Regulates Proliferation, Apoptosis and Invasion of Bladder Cancer Cells Assurance Guidelines. *J. Buon* 23 (3), 776–781. PubMed PMID: 30003751. Epub 2018/07/14. eng.
- Zhu, Y., Qian, X. H., Ji, G. Z., and Yang, L. H. (2021). Clinicopathological and Prognostic Value of Long Noncoding RNA SNHG7 in Cancer Patients: a Meta-Analysis. *Eur. Rev. Med. Pharmacol. Sci.* 25 (7), 2916–2926. PubMed PMID: 33877655. Epub 2021/04/21. eng. doi:10.26355/eurrev_202104_25545

Conflict of Interest: The authors declare that the research was conducted in the absence of any commercial or financial relationships that could be construed as a potential conflict of interest.

Publisher's Note: All claims expressed in this article are solely those of the authors and do not necessarily represent those of their affiliated organizations, or those of the publisher, the editors and the reviewers. Any product that may be evaluated in this article, or claim that may be made by its manufacturer, is not guaranteed or endorsed by the publisher.

Copyright © 2022 Najafi, Ghafouri-Fard, Hussien, Jamal, Taheri and Hallajnejad. This is an open-access article distributed under the terms of the Creative Commons Attribution License (CC BY). The use, distribution or reproduction in other forums is permitted, provided the original author(s) and the copyright owner(s) are credited and that the original publication in this journal is cited, in accordance with accepted academic practice. No use, distribution or reproduction is permitted which does not comply with these terms.



Identification of Circular RNA-Based Immunomodulatory Networks in Colorectal Cancer

Zongfeng Feng^{1,2,3†}, Leyan Li^{2,3,4†}, Yi Tu^{5†}, Xufeng Shu^{1,2,3†}, Yang Zhang^{1,2,3}, Qingwen Zeng^{1,2,3}, Lianghua Luo^{1,2,3}, Ahao Wu^{1,2}, Wenzheng Chen^{1,2,3}, Yi Cao^{1,2,3*} and Zhengrong Li^{1,2,3*}

OPEN ACCESS

Edited by:

Shiv K. Gupta,
Mayo Clinic, United States

Reviewed by:

Changming Lu,
University of Alabama at Birmingham,
United States
Paola Campomenosi,
University of Insubria, Italy

*Correspondence:

Zhengrong Li
lzl13@foxmail.com
Yi Cao
doctorcaoyi@126.com

[†]These authors share first authorship

Specialty section:

This article was submitted to
Molecular and Cellular Oncology,
a section of the journal
Frontiers in Oncology

Received: 19 September 2021

Accepted: 30 December 2021

Published: 27 January 2022

Citation:

Feng Z, Li L, Tu Y, Shu X, Zhang Y,
Zeng Q, Luo L, Wu A, Chen W, Cao Y
and Li Z (2022) Identification of Circular
RNA-Based Immunomodulatory
Networks in Colorectal Cancer.
Front. Oncol. 11:779706.
doi: 10.3389/fonc.2021.779706

¹ Department of General Surgery, First Affiliated Hospital of Nanchang University, Nanchang, China, ² Laboratory of Digestive Surgery, Nanchang University, Nanchang, China, ³ Medical Innovation Center, the First Affiliated Hospital of Nanchang University, Nanchang, China, ⁴ Queen Mary School, Medical Department of Nanchang University, Nanchang, China, ⁵ Department of Pathology, the First Affiliated Hospital of Nanchang University, Nanchang, China

Background: Circular RNAs (circRNAs) have been recently proposed as hub molecules in various diseases, especially in tumours. We found that circRNAs derived from ribonuclease P RNA component H1 (RPPH1) were highly expressed in colorectal cancer (CRC) samples from Gene Expression Omnibus (GEO) datasets.

Objective: We sought to identify new circRNAs derived from RPPH1 and investigate their regulation of the competing endogenous RNA (ceRNA) and RNA binding protein (RBP) networks of CRC immune infiltration.

Methods: The circRNA expression profiles miRNA and mRNA data were extracted from the GEO and The Cancer Genome Atlas (TCGA) datasets, respectively. The differentially expressed (DE) RNAs were identified using R software and online server tools, and the circRNA-miRNA-mRNA and circRNA-protein networks were constructed using Cytoscape. The relationship between targeted genes and immune infiltration was identified using the GEPIA2 and TIMER2 online server tools.

Results: A ceRNA network, including eight circRNAs, five miRNAs, and six mRNAs, was revealed. Moreover, a circRNA-protein network, including eight circRNAs and 49 proteins, was established. The targeted genes, ENOX1, NCAM1, SAMD4A, and ZC3H10, are closely related to CRC tumour-infiltrating macrophages.

Conclusions: We analysed the characteristics of circRNA from RPPH1 as competing for endogenous RNA binding miRNA or protein in CRC macrophage infiltration. The results point towards the development of a new diagnostic and therapeutic paradigm for CRC.

Keywords: circRNA, RPPH1, ceRNA network, RBP, M2 macrophages, Immunomodulatory

INTRODUCTION

Colorectal cancer (CRC) is the most common malignant tumour of the digestive tract. CRC cases diagnosed each year exceed 1.9 million globally and account for 935,000 cancer-related deaths annually (1). Patients with advanced CRC have few treatment options, poor prognosis, and high mortality rates. Chemotherapy, targeted therapy, and immunotherapy are the most commonly used methods to treat advanced CRC. However, patients are prone to drug resistance, which often leads to treatment failure (2). Therefore, it is vital to elucidate the pathogenesis of CRC to develop and utilise new drugs.

Circular RNAs (circRNAs) are circular transcripts that are more stable than their linear counterparts; they lack the termini by which certain RNases bind, conferring them resistance to degradation by pH and enzymatically catalysed hydrolysis. CircRNA can adsorb miRNAs (3) and proteins (4), and, intriguingly, some circRNAs even have translation functions (5). Emerging research has shown circRNAs' important role in various biological processes in tumour cells, especially in colon cancer. Peng et al. (6) suggested that circCUL2 mediates the miR-142-3p/ROCK2 axis to induce autophagy activation and regulate cisplatin sensitivity. Meanwhile, circPTK2 is well expressed in CRC tissue and cells and is associated with metastasis, making it a novel therapeutic target for metastatic colorectal cancer (7). Although studies have clarified the involvement of circRNAs in the biological processes in tumour cells, the role of circRNAs in immunoregulation remains unclear.

Macrophages take on two opposing roles: M1 macrophages are pro-inflammatory, whereas M2 macrophages are anti-inflammatory. M1 cells can swallow atypical or tumour cells and have a positive effect on the resilience of the immune system to tumour infiltration. Conversely, after induced polarisation to the M2 form, macrophages can help tumour cells to escape immune surveillance, promoting the proliferation and metastasis of tumour cells (8). Several studies have shown that M2 and tumour-associated macrophages (TAMs) are related to the poor prognosis of colon cancer patients and may promote tumour progression and metastasis (9, 10). Details of the polarisation process of macrophages and the mechanisms by which they aid tumour cells in immune system evasion remain undetermined.

Ribonuclease P NRA component H1 (RPPH1), a non-coding RNA (ncRNA) found on chromosome 14, plays a key role in several human tumours. Wu et al. (11) demonstrated that RPPH1 promotes non-small-cell lung cancer progression and resistance to standard cis-platinum drugs by targeting the WNT2B signalling axis miR-326. RPPH1 expression was also suggested to be associated with prognosis and further interfered with tumour suppressor factor p21 in gastric cancer (12). Moreover, Liang et al. (13) demonstrated that RPPH1 overexpression mediates macrophage M2 polarisation to promote colorectal cancer metastasis. CD44v6, the sixth variant exon of the CD44 gene, has been reported to contribute to CRC progression (14, 15). NCAM1, a surface biomarker of natural killer (NK) cells, is also known as CD56 (16). Gharagozloo (17) reported that patients with metastatic

colorectal cancer had significantly lower CD56+ NKT cell counts in the peripheral blood than did healthy individuals.

Here, we aimed to further investigate the role of RPPH1 in the molecular background of CRC by identifying circRNAs deriving from this gene and assessing the association between macrophages and targeted genes. In total, eight circRNAs derived from RPPH1 were identified; their expression in CRC cells was assessed, and bioinformatics tools were used to predict their interactions.

METHODS

Datasets of CRC

The circRNA expression profiles (GSE126094) (18) were downloaded from the Gene Expression Omnibus (GEO) database (<https://www.ncbi.nlm.nih.gov/geo/>). The miRNA and mRNA expression data for CRC were obtained from The Cancer Genome Atlas (TCGA) database (<https://portal.gdc.cancer.gov/>). The colon cancer mutation data were also downloaded from TCGA database.

Differentially Expressed circRNAs, miRNAs, and mRNAs

The differentially expressed (DE) circRNAs and DE mRNAs were screened in CRC patients and healthy individuals using the Bioconductor Limma package (version 3.48.1) (19). The thresholds of adjusted $p < 0.05$ and $|\log FC| > 1$ were used to identify DE circRNA from GSE126094 and DE mRNA from TCGA colorectal cancer datasets. The starBase v2.0 online web server (<http://starbase.sysu.edu.cn/>) (20) was used to analyse DE miRNA from TCGA colon cancer datasets.

Establishment of circRNA-miRNA-mRNA Network

CircRNA was visualised using the CSCD2.0 database (<http://gb.whu.edu.cn/CSCD2/#>). We first predicted the target-absorbed miRNAs of eight circRNAs using the circBank database (21); we then verified these prediction results and visualised the binding sites of miRNA adsorption using the circMIR1.0 software. We screened miRNAs with expression differences in the TCGA colon cancer datasets and found those that overlapped with the targeted miRNA. Next, the miRNA-forecasted mRNA and overlapping portions between the DE mRNAs were chosen to establish an miRNA-mRNA network related to CRC tumorigenesis. The MiRWalk (22) database, a comprehensive online target prediction tool, was used for the prediction of miRNA-targeted mRNA. To ensure more reliable results, a score of >0.95 for miRNA-mRNA pairs present in both the miRDB and miRTarbase miRNA-target prediction datasets were chosen for further study. Finally, we used Cytoscape software (version 3.6.0) (23) to visualise the competing endogenous RNA (ceRNA) network.

Construction of Protein–Protein Interaction Network and Identification of the Hub Genes

We constructed a protein–protein interaction (PPI) network *via* the STRING database (<https://string-db.org/>) (24) based on the DEmRNA in the ceRNA network. We set a score of >0.4 to filter the criterion in this PPI network. The intersections between the adjacent nodes determined to be ≥ 5 using R software were regarded as hub genes. Subsequently, we established a secondary circRNA–miRNA–mRNA subnetwork according to the identified hub genes.

Survival and Drug Sensitivity Analysis of the Hub Genes

To cross-validate the reliability of hub genes, the Xiantao search tool (<https://www.xiantao.love/>) was used to compare six hub genes by difference analysis and paired difference analysis derived from the TCGA database. The Prognoscan (<http://www.prognoscan.org/>) database was used to analyse the overall survival (OS) derived from the GEO database. The correspondence between hub genes and sensitivity to drugs was explored using the online search tool GSCALite (25).

Construction of circRNA–Protein Regulatory Network

We used the RBPmap tool (<http://rbpmap.technion.ac.il/>) to study the interaction between these circRNAs and RBPs (26). This tool takes custom RNA sequences as input and provides a list of RBP binding sites and assigns them probability values.

Relationship Between Targeted Genes and Immune Cells

We used the GEPIA2 server (<http://gepia2.cancer-pku.cn/>) to analyse the relationship between the expression of the four genes and the state of immune cell infiltration. Then, the XCELL, TIMER, CIBERSORT, CIBERSORT-ABS, QUANTISEQ, MCP-COUNTER, and EPIC algorithms were used to further evaluate the macrophage immune infiltration of CRC with TIMER2 (<http://timer.cistrome.org/>) (27).

Cell Culture and qRT-PCR Assays

Six CRC cell lines, namely, Caco-2, HCT-116, HT-29, SW-480, SW-620, and DLD-1, and normal intestinal mucosal epithelial cells (NCM-460) were cultured in Roswell Park Memorial Institute (RPMI) 1640 medium with 10% fetal bovine serum. Total RNA was extracted from CRC cell lines and reverse transcribed into cDNA with random primers, following the manufacturers' instructions. The amplified region of the primer design included the circRNA looped linker region. The main benefit of this approach is that it ensures the specificity of the primer. Glyceraldehyde 3-phosphate dehydrogenase (GAPDH) expression was used as an internal reference to normalise circRNAs and mRNA, and U6 expression was used as internal reference for miRNAs. **Table 1** and **Supplementary Table S1** described the circRNA, miRNA, and mRNA primers. Excel software was used for PCR data analysis,

TABLE 1 | Primers for circular RNA (circRNA) amplification.

Primer name	Sequence (5' to 3')
hsa_circ_0000511-F	TTTGCCGAGCTTGGAACA
hsa_circ_0000511-R	CGTTCTCTGGGAACACCTC
hsa_circ_0000512-F	AGTTCAATGGCTGAGGTGAGG
hsa_circ_0000512-R	TGTTCCAAGCTCCGGCAAAG
hsa_circ_0000514-F	GGTCAGACTGGGCAGGAGAT
hsa_circ_0000514-R	CCCGTTCTCTGGGAACCTAC
hsa_circ_0000515-F	GGTCAGACTGGGCAGGAGAT
hsa_circ_0000515-R	GAGTGACAGGACGCACTCAG
hsa_circ_0000517-F	GGGAGGTGAGTCCAGAG
hsa_circ_0000517-R	CAGGGAGAGCCCTGTTAGG
hsa_circ_0000518-F	GTGAGTCCCAGAGAACGGG
hsa_circ_0000518-R	GAGTGACAGGACGCACTCAG
hsa_circ_0000519-F	CTAACAGGGCTCTCCCTGAG
hsa_circ_0000519-R	CAGACCTTCCCAAGGGACAT
hsa_circ_0000520-F	GGGAAGGTCTGAGACTAGGG
hsa_circ_0000520-R	GGACATGGGAGTGGAGTGAC

and GraphPad was used for mapping. First, the quantification cycle (Cq) mean of the internal reference gene in the sample was calculated, and then, the Cq difference (ΔCq) between the target gene and internal reference gene was determined. Furthermore, the $2^{-\Delta\Delta Cq}$ formula was used to calculate the expression level. Finally, based on the expression level of NCM-460 cells, the relative expression level of the target genes in other colon cancer cell lines were calculated.

RESULTS

Differentially Expressed circRNAs, miRNAs, and mRNAs in Colon Cancer

The total number of 321 DEcircRNAs (179 upexpressed and 142 downexpressed) in GSE126094 was identified (**Figure 1A**). Eight co-upregulated circRNAs (hsa_circ_0000511, hsa_circ_0000512, hsa_circ_0000514, hsa_circ_0000515, hsa_circ_0000517, hsa_circ_0000518, hsa_circ_0000519, and hsa_circ_0000520) originating from the RPPH1 gene were identified (**Figure 1B**). **Figure 1C** shows eight circRNA-binding sites that potentially competitively bind to miRNA and RBPs. circMIR1.0 predicted the miRNAs bound by circRNAs and the corresponding binding regions (**Figure 2A**). Since eight circRNAs had the same nucleic acid sequences in multiple regions, their predicted miRNAs were mostly similar. Six downregulated miRNAs were identified in TCGA colon datasets containing 450 colon cancer and eight normal samples (hsa-miR-1296-5p, hsa-miR-296-5p, hsa-miR-326, hsa-miR-328-3p, hsa-miR-1306-5p, and hsa-miR-1976) (**Figures 2B–G**). A total of 7,877 DEmRNAs (5,590 upexpressed and 2,287 downexpressed) were authenticated from the TCGA colon cancer datasets.

CircRNA–miRNA–mRNA and PPI Networks

Cytoscape v3.6.0 was used to analyse and establish a circRNA–miRNA–mRNA network based on regulated and differentially expressed ceRNAs. The network included 8 circRNAs, 6 miRNAs, and 162 mRNAs (**Figure 3**). As described in

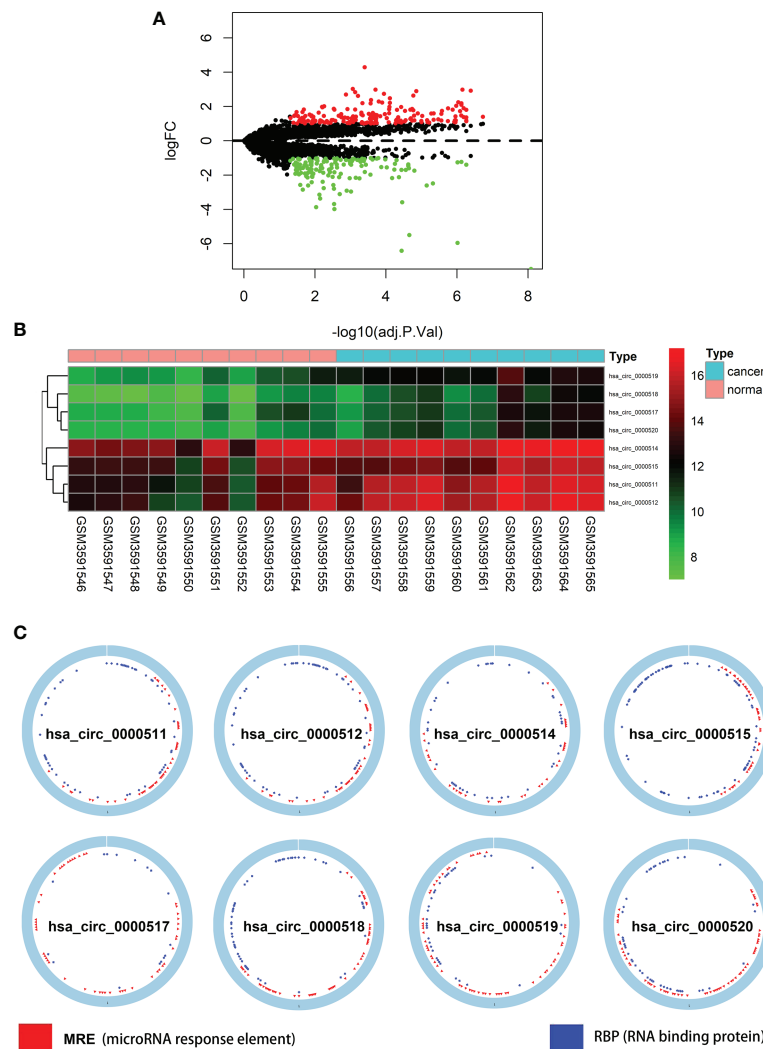


FIGURE 1 | Differentially expressed circular RNAs (circRNAs) from RPPH1 in colorectal cancer (CRC). **(A)** Volcano plots for differentially expressed circRNAs (DEcircRNAs) in CRC from the GSE126094 dataset. **(B)** Heatmap of the eight differentially expressed circRNAs from the RPPH1 gene. **(C)** Interaction patterns of the eight circRNAs based on CSD2.

Figure 4, to show the interaction of target genes in CRC, we constructed a PPI network based on the STRING database to include 151 differentially expressed genes predicted to be regulated by miRNAs.

Hub Gene and ceRNA Subnetwork

Genes from the PPI network in the STRING database, with adjacent differential gene interaction nodes ≥ 5 were regarded as hub genes potentially related to CRC: WNT5A, POLA1, SYP, NCAPG, NCAM1, and CD44 (**Figure 5A**). The ceRNA subnetwork, containing eight circRNAs, five miRNAs, and six mRNAs, as was established, is indicated in **Figure 5B** (hsa_circ_0000511\hsa-miR-296-5p\NCAM1, hsa_circ_0000511\hsa-miR-296-5p\CD44, hsa_circ_0000511\hsa-miR-1976\SYP, hsa_circ_0000512\hsa-miR-296-5p\NCAM1,

hsa_circ_0000512\hsa-miR-296-5p\CD44, hsa_circ_0000512\hsa-miR-1976\SYP, hsa_circ_0000514\hsa-miR-296-5p\NCAM1, hsa_circ_0000514\hsa-miR-296-5p\CD44, hsa_circ_0000514\hsa-miR-1976\SYP, hsa_circ_0000515\hsa-miR-296-5p\NCAM1, hsa_circ_0000515\hsa-miR-296-5p\CD44, hsa_circ_0000515\hsa-miR-1976\SYP, hsa_circ_0000515\hsa-miR-1306-5p\NCAPG, hsa_circ_0000515\hsa-miR-326\WNT5A, hsa_circ_0000515\hsa-miR-1296-5p\POLA1, hsa_circ_0000517\hsa-miR-1306-5p\NCAPG, hsa_circ_0000517\hsa-miR-326\WNT5A, hsa_circ_0000517\hsa-miR-1296-5p\POLA1, hsa_circ_0000518\hsa-miR-1306-5p\NCAPG, hsa_circ_0000518\hsa-miR-326\WNT5A, hsa_circ_0000518\hsa-miR-1296-5p\POLA1, hsa_circ_0000519\hsa-miR-1296-5p\POLA1, and hsa_circ_0000520\hsa-miR-1296-5p\POLA1).

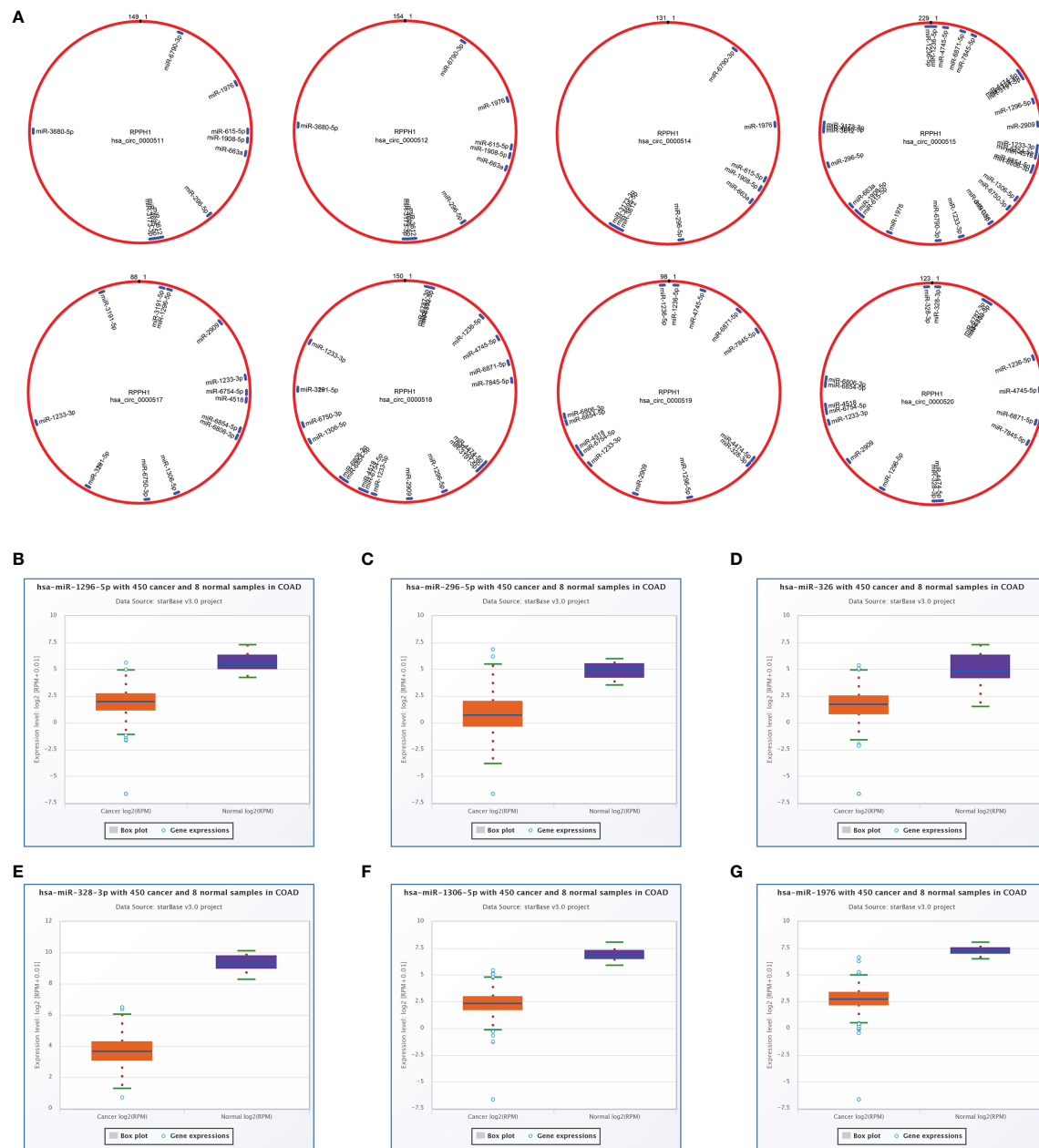
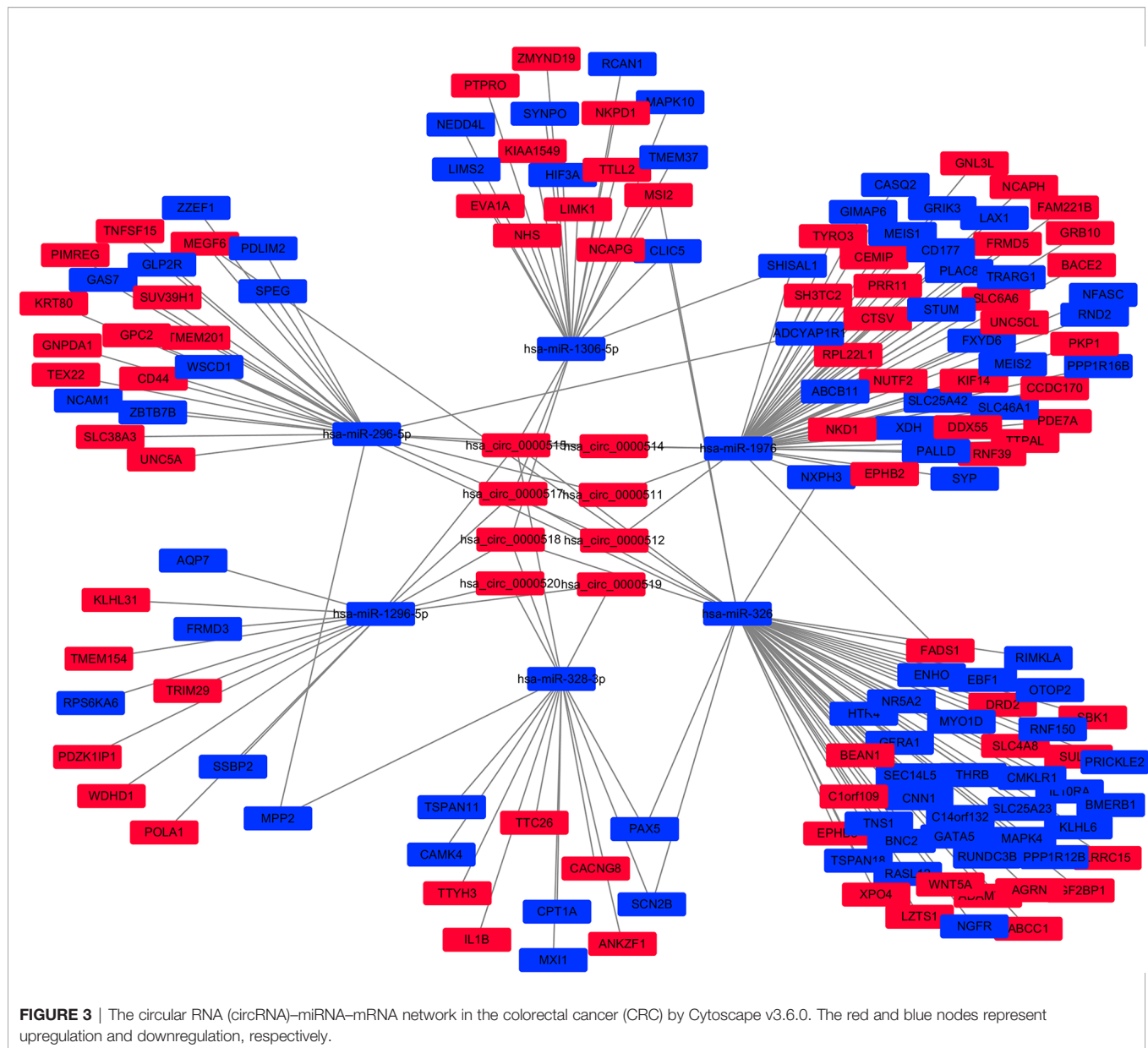


FIGURE 2 | Targeted sponge miRNA with eight circular RNAs (circRNAs). **(A)** The position and quantity of miRNA adsorption via circMIR1.0 software. **(B–G)** Six targeted sponge miRNAs with different expression levels in colorectal cancer (CRC) from starBase v2.0. **(B)** hsa-miR-1296-5p, **(C)** hsa-miR-296-5p, **(D)** hsa-miR-326, **(E)** hsa-miR-328-3p, **(F)** hsa-miR-1306-5p, **(G)** hsa-miR-1976.

Survival Analysis and Resistance of the Hub Genes

The Xiantao search tool was used to compare six hub genes by difference analysis and paired difference analysis derived from the TCGA database, and PrognScan was used to analyse the overall survival (OS) derived from the GEO database. As shown in **Figure 6A**, CD44 expression was significantly higher in CRC patients than in the control (healthy individuals). CD44-positive

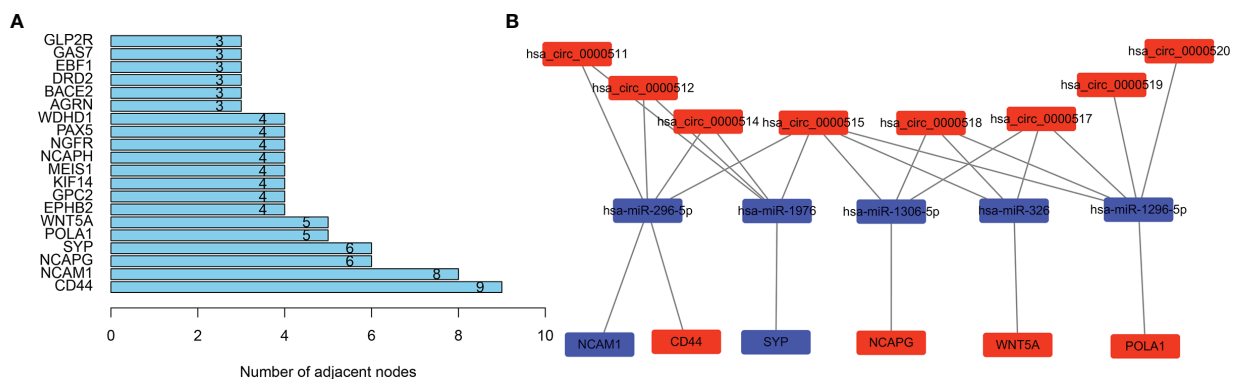
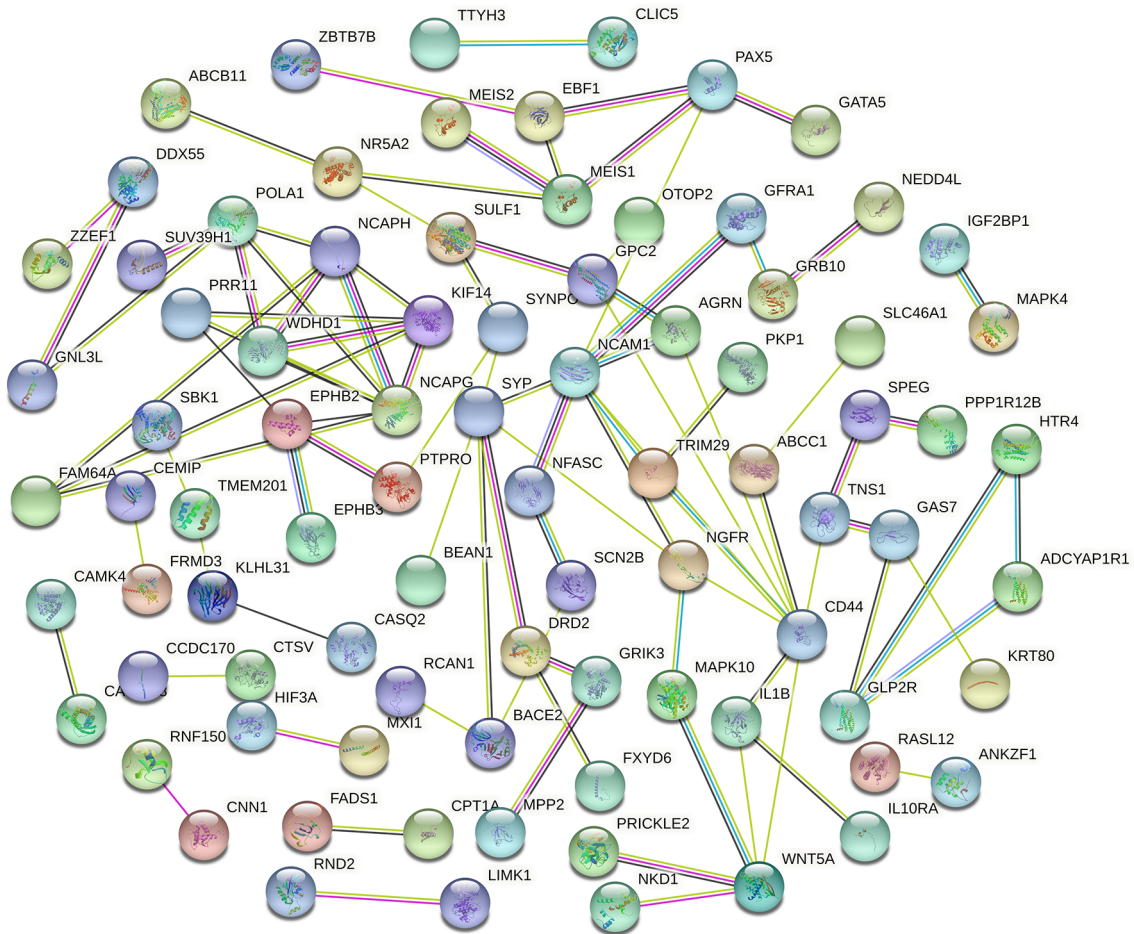
patients had a shorter survival than did CD-negative patients in the GSE12945 dataset. The hub genes POLA1, NCAPG, and WNT5A were well expressed in CRC patients and had similar prognosis results in the GSE17536 dataset (**Figures 6B, E, F**). In contrast, **Figures 6C, D** show that the hub genes NCAM1 and SYP were expressed at lower levels in colon cancer patients than in the control. From the GSE17536 dataset, patients with lower expression levels of POLA1, NCAPG, and WNT5A had better



survival than those with higher expression levels. In some instances, the expression levels of NCAM1 and SYP inhibited CRC progression. Subsequently, we performed a drug sensitivity (IC₅₀) evaluation of the expression levels of the targeted-network genes and found that a higher correlation represented a higher drug resistance. The expression levels of POLA1 and NCAPG were positively correlated with sensitivity to trametinib and the 17-AAG (HSP90 inhibitor). CD44 expression was positively correlated with sensitivity to the NPK76-II-72-1 (kinase inhibitor). Moreover, SYP expression was positively correlated with sensitivity to docetaxel (**Figure 7**). Therefore, drug sensitivity analysis could help toward the individualized and precise treatment of tumour patients, reducing the occurrence of tumour drug resistance.

Copy Number Variation and Mutation of Hub Genes

We analysed the copy number variation (CNV) and gene mutation of hub genes in TCGA colon cancer data. In CRC samples, the CNV mutation frequency of WNT5A reached 4%, mainly with CNV deletion. This was followed by NCAM1, while the CNV mutation frequency in CD44, SYP, and POLA1 was <1% (**Figure 8A**). **Figure 8B** shows the types of CNV mutations and chromosomal statuses of the hub genes. Among the 399 samples expressing the six hub genes, 49 (12.28%) were found to have gene mutations, most of which were missense mutations. NCAM1 accounted for 6%, NCAPG accounted for 5%, WNT5A and POLA1 both accounted for 3%, and CD44 accounted for 1% (**Figure 8C**).



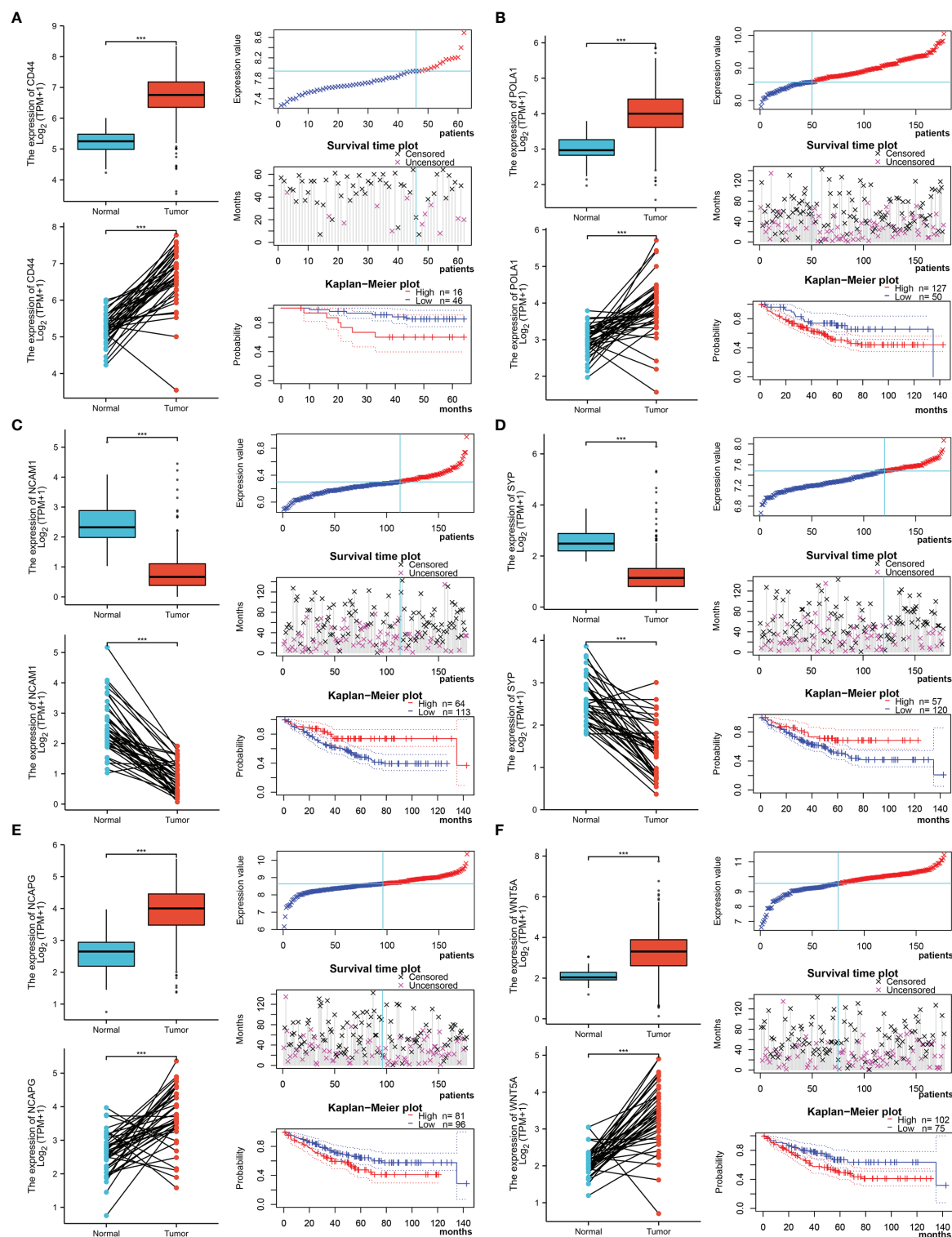


FIGURE 6 | Different expression and survival analysis of the hub genes by the Xiantao and PrognScan search tools. **(A)** For CD44, **(B)** for POLA1, **(C)** for NCAM1, **(D)** for SYP, **(E)** for NCAPG, and **(F)** for WNT5A. (***) $p \leq 0.001$.

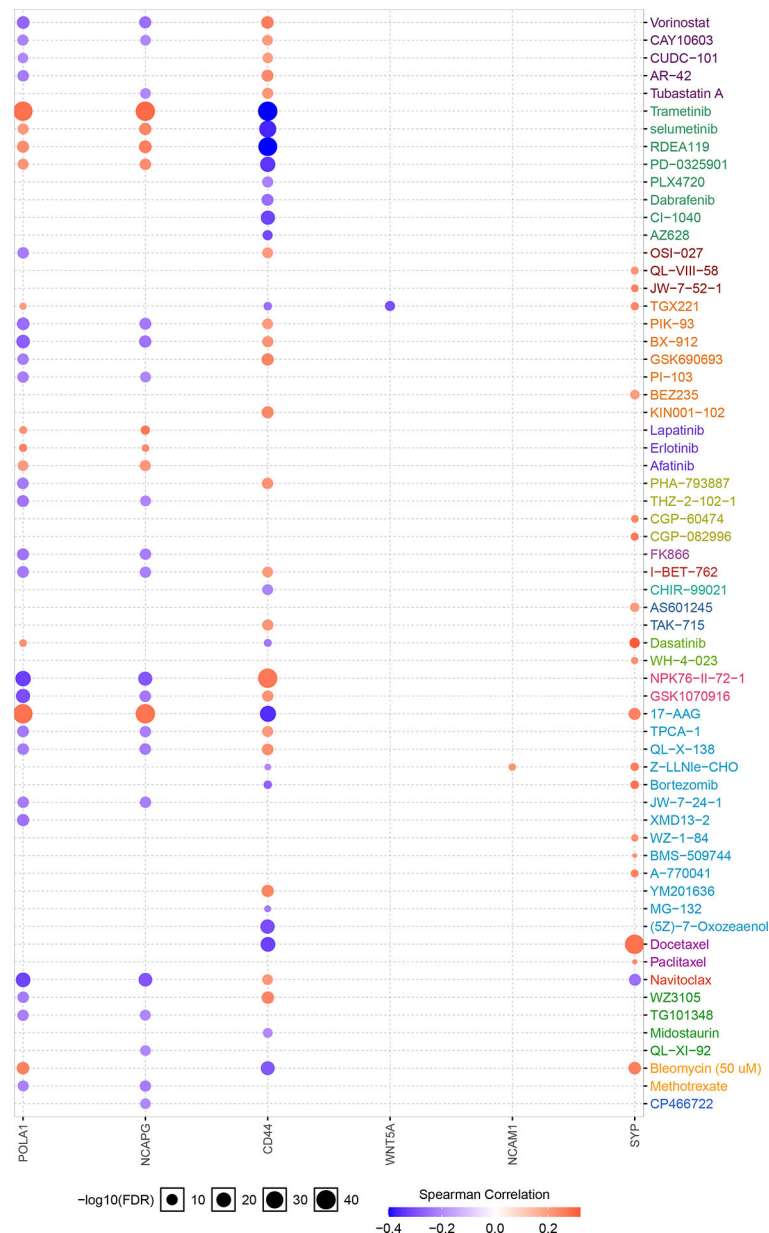


FIGURE 7 | Correlation between hub gene expression levels and small molecule/drug sensitivity via the online search tool GSCALite.

The CircRNA-Binding Protein Network

As depicted in **Figure 1C** for eight circRNAs, various protein-binding sites were detected, and many RBPs were predicted to bind to them. The RBPmap provided more information about the number of RBPs and their binding sites. We selected RBPs with $p < 0.05$, accompanied by high probability values (**Figure 9A**; **Supplementary Table S2**). Since these circRNAs all originate from the RPPH1 gene, their RNA-binding proteins are all the same, although some specific regions have different sequences and RBPs. Further analysis revealed that ZC3H10, SAMD4A, and ENOX1 are closely related to anti-tumour immunity against colon cancer. **Figure 9B** shows the number

of sites and positions where has_circ_0000515 binds to ZC3H10, SAMD4A, and ENOX1.

Relationship Between Immune-Related Genes and Macrophages

We explored the possible molecular mechanisms underlying the aetiology of CRC through immune cell infiltration. In particular, the relationship between four target genes, namely, NCAM1, ZC3H10, SAMD4A, and ENOX1, and macrophages was investigated.

First, we used GEPIA2 to analyse the association between the expression levels of the four genes and M1 macrophage (NOS2,

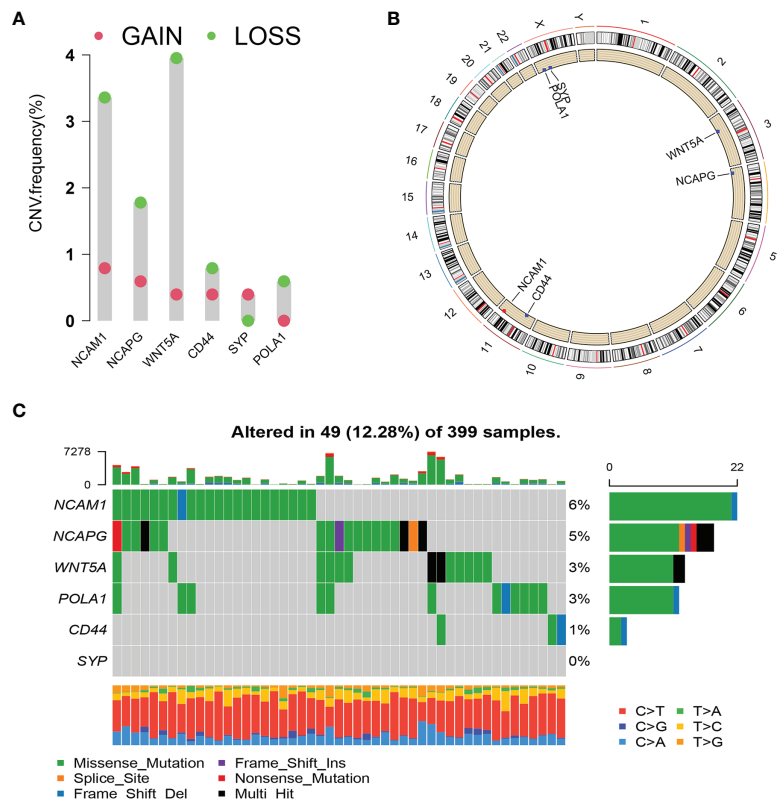


FIGURE 8 | Copy number variation (CNV) and mutation of hub genes. **(A)** CNV frequency of hub genes. **(B)** Circle diagram of CNV with hub genes. Red represents CNV gain; blue represents CNV loss. **(C)** Cascade of core gene mutations.

IRF5, and PTGS2), M2 macrophage (MS4A4A, VSIG4, MRC1, CD163, and MSR1), and TAM (CCL2, CD68, and IL10) markers. There was a positive correlation between ENOX1 expression and the M2 macrophage ($R = 0.7$, $p = 4.4E-42$), and TAM ($R = 0.73$, $p = 2.4E-46$), whereas the correlation with M1 macrophage marker genes ($R = 0.16$, $p = 0.0061$) was poor (**Figure 10A**). **Figure 10B** shows the correlation between NCAM1 and M2 macrophage ($R = 0.47$, $p = 1.1E-16$), TAM ($R = 0.53$, $p = 3.3E-21$), and M1 macrophage ($R = 0.21$, $p = 0.00046$). **Figure 10C** shows the correlation between SAMD4A and M2 macrophage ($R = 0.56$, $p = 3.8E-24$), TAM ($R = 0.58$, $p = 3.6E-26$), and M1 macrophage ($R = 0.30$, $p = 3.1E-07$). **Figure 10D** shows the correlation between ZC3H10 and M2 macrophage ($R = 0.55$, $p = 3.7E-23$), TAM ($R = 0.54$, $p = 4.3E-22$), and M1 macrophage ($R = 0.30$, $p = 3.1E-07$). These results strongly suggest that these genes are closely related to the polarisation of macrophages in colon cancer development. We observed similar results between ENOX1 expression and other different types of immune cells, such as CD4⁺ cells ($R = 0.70$, $p = 2.4E-42$) and NK cells ($R = 0.72$, $p = 3.5E-45$) (**Supplementary Figure S1**). Similar to ENOX1, the expression levels of NCAM1, SAMD4A, and ZC3H10 were positively correlated with the marker expression levels of immune cells (**Supplementary Figures S2-4**), indicating that the expression levels of these genes are closely related to tumour immunity.

We then used the XCELL, TIMER, CIBERSORT, CIBERSORT-ABS, QUANTISEQ, MCP-COUNTER, and EPIC algorithms to further evaluate the macrophage immune infiltration of CRC. All algorithms except XCELL found positive correlations between these four immune-related genes and M2 macrophages that were significantly higher than those with M1 macrophages (**Figure 11A**). Significant correlation was observed between the polarised M2 macrophages and ENOX1, NCAM1, SAMD4A, and ZC3H10 with respect to tumour purity (**Figures 11B-E**). The consistency of **Figures 10** and **11** further confirm the reliability of the relationship between these expression levels of these genes and polarisation of macrophages.

Expression Analysis of RPPH1 circRNAs, miRNA, and mRNA in CRC Cells

The expression levels of the circRNAs derived from RPPH1 in CRC cells were detected using quantitative reverse transcription PCR (qRT-PCR) assays (**Supplementary Table S3**). Hsa_circ_0000511 (**Figure 12A**), hsa_circ_0000514 (**Figure 12C**), and hsa_circ_0000519 (**Figure 12G**) were more expressed in all cancer cell lines than in the NCM-460 control cells. Compared with NCM-460, hsa_circ_0000512 had the highest expression levels in SW-620 cells and low expression in SW-480, CACO-2, and DLD-1, and was not detected in HT-29 cells (**Figure 12B**). Hsa_circ_0000515 was found to be expressed

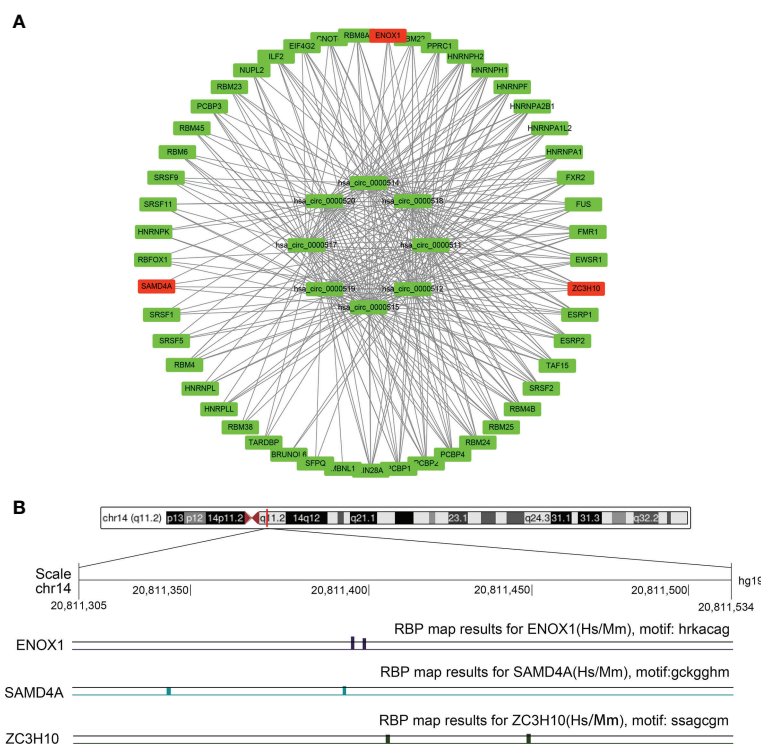


FIGURE 9 | The circRNA–protein network and binding site in the CRC. **(A)** Circular RNA (circRNA)–protein network in colorectal cancer (CRC) according to the RBPmap. The red nodes represent immune-related proteins, whereas the green nodes represent other proteins and eight circRNAs. **(B)** Chromosome positions and ENOX1, NCAM1, SAMD4A, and ZC3H10 binding sites of hsa_circ_0000515.

in SW-480, SW-620, and CACO-2 but was not detected in other CRC cell lines (**Figure 12D**). As shown in **Figure 12E**, the expression of hsa_circ_0000517 was the highest in SW-620 cells and the lowest in SW-480 cells and DLD-1 cells. The expression levels of hsa_circ_0000518 and hsa_circ_0000520 were higher in HCT-116, SW-620, and CACO-2 than in NCM-460

(**Figures 12F, H**). From the above results, the expression levels of circRNAs were low and even undetectable in CRC cell lines. In our results, circRNAs from the RPPH1 gene were the highest in SW-620 and CACO-2 and the lowest in NCM-460 and SW-480. MiR-296-5p was highly expressed in NCM-460 and CACO-2 compared with others. However, CD44, NCAM1, SYP, and

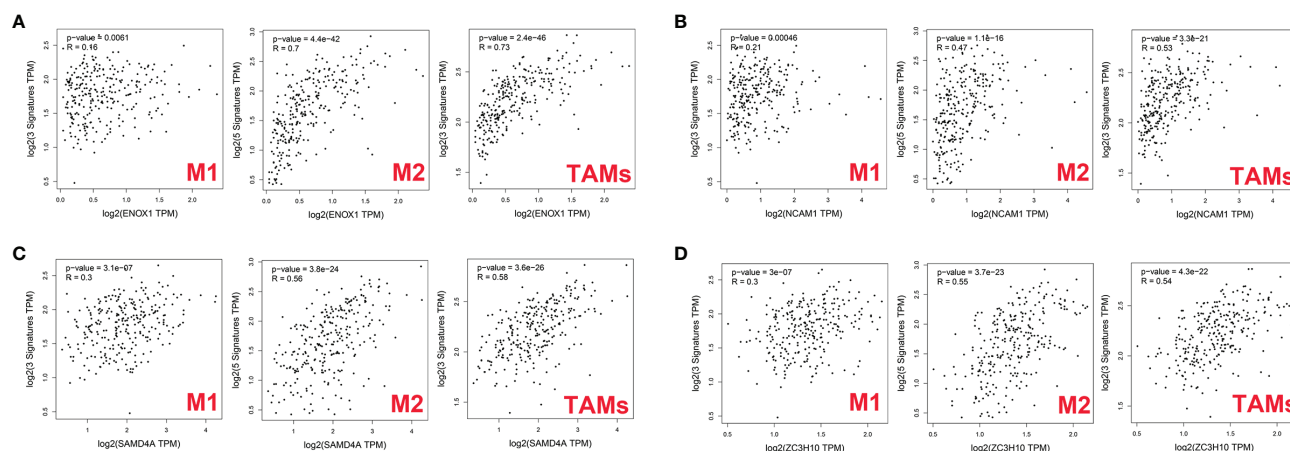


FIGURE 10 | Correlation between targeted gene expression levels and markers of macrophages as analysed via GEPIA2. **(A)** for ENOX1, **(B)** for NCAM1, **(C)** for SAMD4A, and **(D)** for ZC3H10.

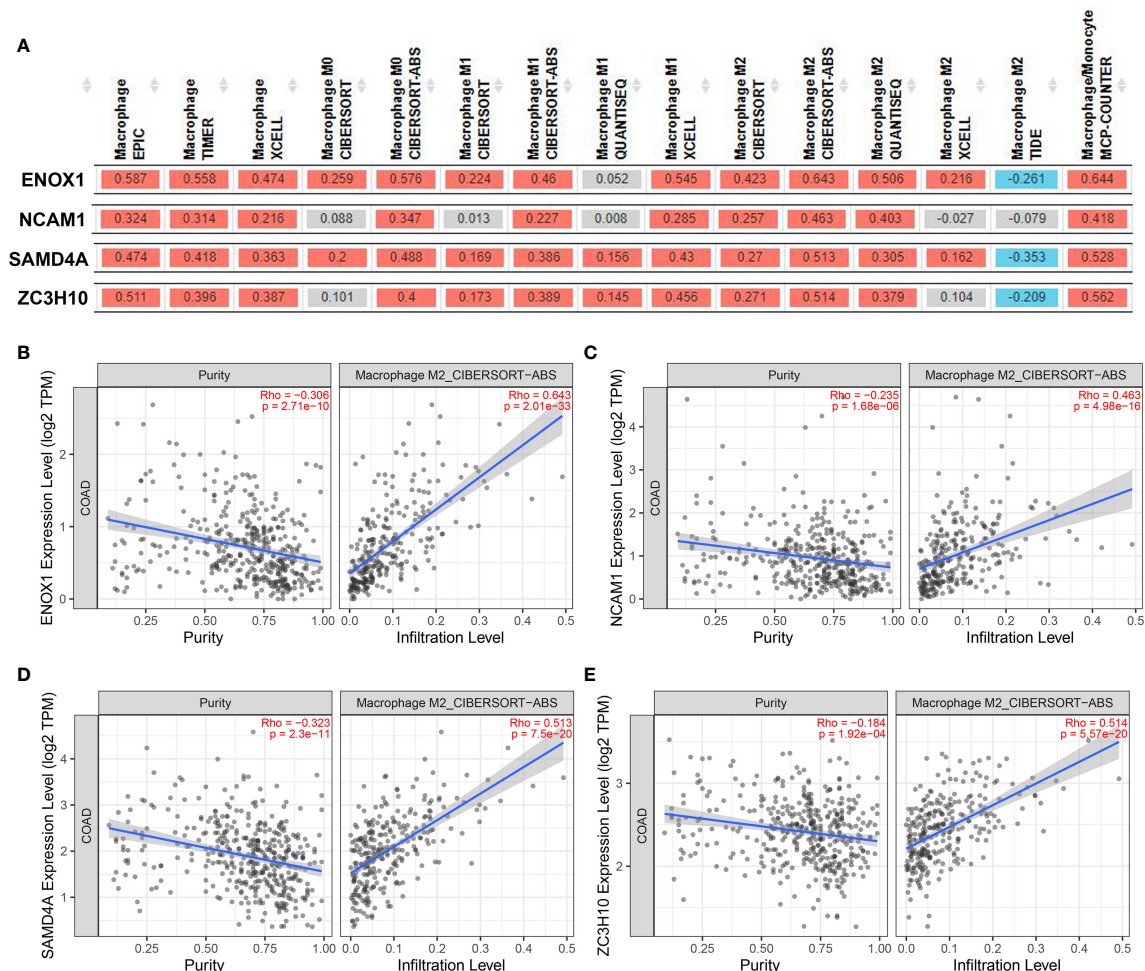


FIGURE 11 | Correlation between targeted gene expression levels and the infiltration level of macrophage cells. The XCELL, TIMER, CIBERSORT, CIBERSORT-ABS, QUANTISEQ, MCP-COUNTER, and EPIC algorithms were applied for immune infiltration estimations with ENOX1, NCAM1, SAMD4A, and ZC3H10. **(A)** Overview of the correlations between ENOX1, NCAM1, SAMD4A, and ZC3H10 and the macrophages. The CIBERSORT-ABS algorithm was used to estimate the correlations between ENOX1, NCAM1, SAMD4A, and ZC3H10 and the M2 macrophages after tumour purity adjusting in panels **(B–E)**. **(B)** ENOX1 and M2 macrophages, **(C)** NCAM1 and M2 macrophages, **(D)** SAMD4A and M2 macrophages, **(E)** ZC3H10 and M2 macrophages.

NCAPG showed higher expression levels than NCM-460 in the majority of colon cancer cell lines (**Supplementary Figure S6**).

DISCUSSION

CRC is a complex malignant tumour of the digestive tract caused by a wide variety of gene mutations and signal pathway disorders. Research has revealed the importance of circRNAs as a new type of transcriptional gene regulation molecule in the pathogenesis of various human diseases, including malignant tumours. circRNA is a closed circular nucleotide sequence that specifically binds a variety of miRNAs and proteins. In recent years, the role of circRNA in cancer tumorigenesis has gradually been uncovered but has remained largely unknown in CRC. To explore the important role of circRNA in CRC as the starting trigger point

for oncogene activation, we first screened DEcircRNA from GEO data and DEmiRNA and DemRNA from TCGA data. After predicting the interactions between circRNA, miRNA, and proteins, and their effects on the strength of biology and molecular mechanics, a circRNA-miRNA-mRNA and circRNA-protein regulatory network was described. Then, a PPI network model was constructed, and the following six genes were identified as central genes: WNT5A, POLA1, SYP, NCAPG, NCAM1, and CD44. We performed expression verification and survival analysis on these six core genes based on TCGA and GEO data, respectively, which further enhanced the reliability of the ceRNA network. We also constructed a circRNA-protein gene subnetwork based on related RNA-binding proteins and further analysed their binding relationships. By combining the regulated genes in ceRNA and circRNA binding protein genes, we comprehensively analysed their correlation with tumour immune regulation.

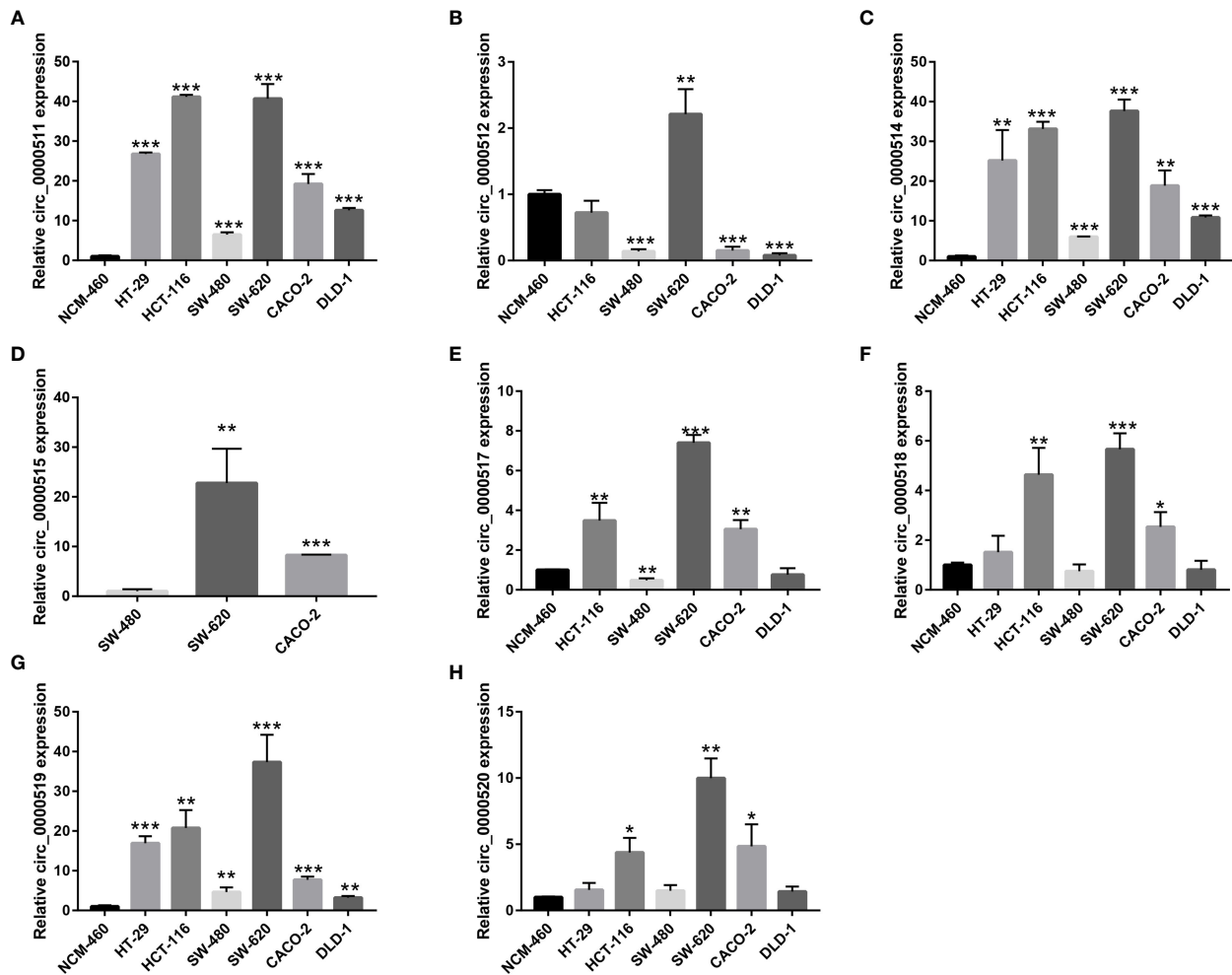


FIGURE 12 | Relative circular RNA (circRNA) expression in colorectal cancer (CRC) cells and NCM-460 normal cells by qRT-PCR. (A) For hsa_circ_0000511, (B) for hsa_circ_0000512, (C) for hsa_circ_0000514, (D) for hsa_circ_0000515, (E) for hsa_circ_0000517, (F) for hsa_circ_0000518, (G) for hsa_circ_0000519, and (H) for hsa_circ_0000520. (***) $p \leq 0.001$, (**) $p \leq 0.01$, (*) $p \leq 0.05$.

An increasing number of studies have shown that the abnormal expression of circRNA is related to the pathogenesis of CRC, indicating that circRNAs are potential therapeutic targets and biomarkers. Chen et al. (28) demonstrated that circGLIS2 was higher in CRC patients than in healthy individuals, and the overexpression of circGLIS2 sponged miR-671 to activate the nuclear factor kappa B (NF- κ B) signalling pathway. Yang et al. (7) highlighted that circPTK2, a novel circRNA, is elevated in CRC tissues, promotes the epithelial-mesenchymal transition of colorectal cancer cells, and serves as a potential target for late treatment and early diagnosis. However, our understanding of these RNA molecules is lacking, and further research is required to explore their relationship with CRC.

Eight circRNAs (hsa_circ_0000511, hsa_circ_0000512, hsa_circ_0000514, hsa_circ_0000515, hsa_circ_0000517, hsa_circ_0000518, hsa_circ_0000519, and hsa_circ_0000520)

originating from the RPPH1 gene were identified in the ceRNA network. Five of these eight circRNAs were reported to be involved in the development of malignant tumours. Has_circ_0000511 is overexpressed in cervical cancer and regulates the miR-296-5p/HMGA1 signalling pathway axis to inhibit HeLa and SiHa proliferation and invasion (29). Has_circ_0000515 can sponge miR-326 to promote cervical cancer progression by releasing ELK1 transcription and regulate the miR-296-5p/CXCL10 signalling pathway axis to induce the pathogenesis of breast cancer (30). Hsa_circ_0000517 was found to be significantly upregulated in hepatocellular carcinoma (HCC), and the expression of hsa_circ_0000517 was associated with HCC progression. Hsa_circ_0000517 acts as a miRNA sponge to regulate HCC growth and metastasis through hsa_circ_0000517/miR-326/IGF1R and the SMAD6 signalling pathway axis (31–33). Another circRNA, hsa_circ_0000518, was found to be

significantly elevated in breast cancer and can promote the progression, apoptosis, migration, and invasion of breast cancer cells by targeting miR-326/FGFR1 (34). Controversially, hsa_circ_0000520 has been reported in gastric, breast, and cervical cancers. Sun et al. (35) and Lv et al. (36) found that hsa_circ_0000520 was significantly downregulated in gastric cancer, and its overexpression may attenuate the PI3K-Akt signalling pathway, causing the reversal of resistance to Herceptin in gastric cancer cells.

Zang (37) and Zhou (38) simultaneously reported that hsa_circ_0000520 was highly expressed in breast cancer, which suggested the regulatory mechanism of hsa_circ_0000520/miR-1296. Zheng et al. (39) reported that silencing hsa_circ_0000520 blocks cell cycle progression and promotes apoptosis *via* the miR-1296/CDK2 signalling pathway axis. In contrast, Zhang et al. (40) reported that hsa_circ_0000520 overexpression decreased PAX5 expression by sponging miR-146b-3p and repressing cervical cancer cell proliferation. Our results also confirmed that these circRNAs are highly expressed in colon cancer tissues and cell lines. Nevertheless, whether they play a key role in the pathogenesis of colon cancer remains an open question requiring further exploration.

To elucidate the molecular mechanism of action of circRPPH1, circRNA-miRNA-mRNA and circRNA-protein networks were constructed. The six hub genes and four immune-related genes have been partially reported previously. The interaction between the proteins CD44 and MUC5AC conferred colon cancer cell resistance to 5-FU *via* the downregulation of p53 and p21 (41). Increasing numbers of studies have indicated that NK cells have achieved good efficacy in treating and killing tumours, especially in colon cancer, and have good prospects for transformation (42, 43). Ma (44) constructed an immune-related module that consists of SYP and 13 other genes, which may be innovative biomarkers for the prediction of colon cancer prognosis and response to immunological therapy. Opinion is divided over the importance of WNT5A—an essential protein of the non-canonical Wnt/ β -catenin signalling pathway—in colon cancer (45). Cecilia (46), Cheng (47), and Li (48) argued that WNT5A is a protective factor that delays disease progression in colon cancer patients. In contrast, Elvira (49) asserts that high WNT5A expression could induce colon cancer cell migration and invasion. POLA1 has been reported to influence the occurrence and development of tumours (50–52), and its expression can be suppressed by the novel compound ST1926 (53) and antitumor toxin CD437 (54). NCAPG has been reported as an oncogene in liver cancer (55), gastric cancer (56), breast cancer (57), and other tumours but has not yet been studied in CRC. **Figure 10** combined with **Figure 11** shows that the correlations between the ENOX1, ZC3H10, and SAMD4A genes and the M2 macrophages and TAMs were much better than those with the M1 macrophages. Existing studies generally believe that macrophage polarisation and TAMs are extremely important for tumour immune evasion and the establishment of an immune microenvironment. Hence, it could conceivably be hypothesised that these genes help colorectal cancer cells escape immune monitoring and clearance to a certain extent. At present, there is very little research on these

three genes related to immunity; this is a new research direction worth exploring. The NADH oxidase ENOX1 targets tumour vasculature and can be used in tumour treatment (58, 59). Coincidentally, Zhou et al. (60) also reported SAMD4A as a novel breast tumour angiogenesis suppressor in breast cancer. ZC3H10 regulates lipid metabolism and may also offer novel routes toward treatments for obesity (61).

CONCLUSION

In this study, we discovered novel circRNAs derived from the RPPH1 gene in CRC. The circRNAs work with other differentially expressed RNAs to constitute a pair of immunoregulatory circRNA-miRNA-mRNA and circRNA-protein networks that act upon CRC. We further explored the relationship between regulated genes and immune cell behaviours. Further research is required to elucidate the functional behaviour of these two molecular networks. We believe that the interaction networks of these eight circRNAs, five target genes, and four immune-related proteins offer a new paradigm for the understanding of CRC pathogenesis and could lead to entirely new approaches to treatment.

DATA AVAILABILITY STATEMENT

The original contributions presented in the study are included in the article/**Supplementary Material**, further inquiries can be directed to the corresponding author/s.

AUTHOR CONTRIBUTIONS

ZF, LLi, and XS drafted the manuscript. WC, QZ, and YZ participated in the data processing. LLu, AW, and YT participated in qRT-PCR assays. ZL and YC designed the study and revised the manuscript. All authors contributed to the article and approved the submitted version.

FUNDING

This work was supported by the National Natural Science Foundation of China (No. 81860428), the Leading Talents Program of Jiangxi (20213BCJL22050), the Youth Science Foundation of Jiangxi Province (No. 20202BABL216051), the Science and Technology Plan of Health Commission of Jiangxi Province (No. 20191026), the Spark Promotion Plan of Grassroots Health Appropriate Technology of the Health Commission of Jiangxi Province (No. 68120198012), the Project of Science and Technology Department of Jiangxi Province (No. 20203BBGL73187), and the Traditional Chinese Medicine Research Project of Jiangxi Province (No. 2019A185).

SUPPLEMENTARY MATERIAL

The Supplementary Material for this article can be found online at: <https://www.frontiersin.org/articles/10.3389/fonc.2021.779706/full#supplementary-material>

Supplementary Figure S1 | Correlation between ENOX1 expression and markers of immune cells as analysed through GEPIA2. (A) for B cell, (B) for CD4+ T cell, (C) for CD8+ T cell, (D) for dendritic cell, (E) for effector regulatory T (Treg) cell, (F) for eosinophils, (G) for exhausted T cell, (H) for mast cell, (I) for monocyte, (J) for neutrophils, (K) for natural killer (NK) cell, (L) for resting regulatory T (Treg) cell, (M) for T follicular helper (Tfh) cell, (N) for T helper type 1 (Th1) cell, (O) for Th2 cell, (P) for Th17 cell.

Supplementary Figure S2 | Correlation between NCAM1 expression and markers of immune cells as analysed through GEPIA2. (A) for B cell, (B) for CD4+ T cell, (C) for CD8+ T cell, (D) for dendritic cell, (E) for effector regulatory T (Treg) cell, (F) for eosinophils, (G) for exhausted T cell, (H) for mast cell, (I) for monocyte, (J) for neutrophils, (K) for natural killer (NK) cell, (L) for resting regulatory T (Treg) cell, (M) for T follicular helper (Tfh) cell, (N) for T helper type 1 (Th1) cell, (O) for Th2 cell, (P) for Th17 cell.

Supplementary Figure S3 | Correlation between SAMD4A expression and markers of immune cells as analysed through GEPIA2. (A) for B cell, (B) for CD4+ T cell, (C) for CD8+ T cell, (D) for dendritic cell, (E) for effector regulatory T (Treg) cell, (F) for eosinophils, (G) for exhausted T cell, (H) for mast cell, (I) for monocyte, (J) for neutrophils, (K) for natural killer (NK) cell, (L) for resting regulatory T (Treg) cell, (M) for T follicular helper (Tfh) cell, (N) for T helper type 1 (Th1) cell, (O) for Th2 cell, (P) for Th17 cell.

Supplementary Figure S4 | Correlation between ZC3H10 expression and markers of immune cells as analysed through GEPIA2. (A) for B cell, (B) for CD4+ T cell, (C) for CD8+ T cell, (D) for dendritic cell, (E) for effector regulatory T (Treg) cell, (F) for eosinophils, (G) for exhausted T cell, (H) for mast cell, (I) for monocyte, (J) for neutrophils, (K) for natural killer (NK) cell, (L) for resting regulatory T (Treg) cell, (M) for T follicular helper (Tfh) cell, (N) for T helper type 1 (Th1) cell, (O) for Th2 cell, and (P) for Th17 cell.

Supplementary Figure S5 | Melting curve of eight circular RNAs (circRNAs) and GAPDH in colorectal cancer (CRC). (A) for hsa_circ_0000511, (B) for hsa_circ_0000512, (C) for hsa_circ_0000514, (D) for hsa_circ_0000515, (E) for hsa_circ_0000517, (F) for hsa_circ_0000518, (G) for hsa_circ_0000519, (H) for hsa_circ_0000520, and (I) for GAPDH.

Supplementary Figure S6 | Relative miRNAs and mRNA expression in colorectal cancer (CRC) cells and NCM-460 normal cell. (A) for miRNA-296-5p, (B) for miRNA-1976, (C) for miRNA-1306-5p, (D) for miRNA-326, (E) for miRNA-1296-5p, (F) for NCAM1, (G) for CD44, (H) for SYP, (I) for NCAPG, (J) for WNT5A, and (K) for POLA1.

Supplementary Table S1 | Primers for miRNAs and mRNAs amplification in the competing endogenous RNA (ceRNA) network.

Supplementary Table S2 | The protein binding with eight circular RNAs (circRNAs) from the RBPmap tool.

Supplementary Table S3 | Expression levels of eight circular RNAs (circRNAs) in colorectal cancer (CRC) cells as detected by qRT-PCR assays.

REFERENCES

- Sung H, Ferlay J, Siegel RL, Laversanne M, Soerjomataram I, Jemal A, et al. Global Cancer Statistics 2020: GLOBOCAN Estimates of Incidence and Mortality Worldwide for 36 Cancers in 185 Countries. *CA Cancer J Clin* (2021) 71(3):209–49. doi: 10.3322/caac.21660
- Gao Q, Li XX, Xu YM, Zhang JZ, Rong SD, Qin YQ, et al. Ire1 α -Targeting Downregulates ABC Transporters and Overcomes Drug Resistance of Colon Cancer Cells. *Cancer Lett* (2020) 476:67–74. doi: 10.1016/j.canlet.2020.02.007
- Hansen TB, Jensen TI, Clausen BH, Bramsen JB, Finsen B, Damgaard CK, et al. Natural RNA Circles Function as Efficient microRNA Sponges. *Nature* (2013) 495(7441):384–8. doi: 10.1038/nature11993
- Okholm TLH, Sathe S, Park SS, Kamstrup AB, Rasmussen AM, Shankar A, et al. Transcriptome-Wide Profiles of Circular RNA and RNA-Binding Protein Interactions Reveal Effects on Circular RNA Biogenesis and Cancer Pathway Expression. *Genome Med* (2020) 12(1):112. doi: 10.1186/s13073-020-00812-8
- Lei M, Zheng G, Ning Q, Zheng J, Dong D. Translation and Functional Roles of Circular RNAs in Human Cancer. *Mol Cancer* (2020) 19(1):30. doi: 10.1186/s12943-020-1135-7
- Peng L, Sang H, Wei S, Li Y, Jin D, Zhu X, et al. Circul2 Regulates Gastric Cancer Malignant Transformation and Cisplatin Resistance by Modulating Autophagy Activation via miR-142-3p/ROCK2. *Mol Cancer* (2020) 19(1):156. doi: 10.1186/s12943-020-01270-x
- Yang H, Li X, Meng Q, Sun H, Wu S, Hu W, et al. CircPTK2 (Hsa_Circ_0005273) as a Novel Therapeutic Target for Metastatic Colorectal Cancer. *Mol Cancer* (2020) 19(1):13. doi: 10.1186/s12943-020-1139-3
- Zhou J, Tang Z, Gao S, Li C, Feng Y, Zhou X. Tumor-Associated Macrophages: Recent Insights and Therapies. *Front Oncol* (2020) 10:188. doi: 10.3389/fonc.2020.00188
- Lan J, Sun L, Xu F, Liu L, Hu F, Song D, et al. M2 Macrophage-Derived Exosomes Promote Cell Migration and Invasion in Colon Cancer. *Cancer Res* (2019) 79(1):146–58. doi: 10.1158/0008-5472.Can-18-0014
- Cheng Y, Zhu Y, Xu J, Yang M, Chen P, Xu W, et al. PKN2 in Colon Cancer Cells Inhibits M2 Phenotype Polarization of Tumor-Associated Macrophages via Regulating DUSP6-Erk1/2 Pathway. *Mol Cancer* (2018) 17(1):13. doi: 10.1186/s12943-017-0747-z
- Wu Y, Cheng K, Liang W, Wang X. lncRNA RPPH1 Promotes Non-Small Cell Lung Cancer Progression Through the miR-326/WNT2B Axis. *Oncol Lett* (2020) 20(4):105. doi: 10.3892/ol.2020.11966
- Yue K, Ma JL, Jiang T, Yue J, Sun SK, Shen JL, et al. lncRNA RPPH1 Predicts Poor Prognosis and Regulates Cell Proliferation and Migration by Repressing P21 Expression in Gastric Cancer. *Eur Rev Med Pharmacol Sci* (2020) 24(21):11072–80. doi: 10.26355/eurrev_202011_23593
- Liang ZX, Liu HS, Wang FW, Xiong L, Zhou C, Hu T, et al. lncRNA RPPH1 Promotes Colorectal Cancer Metastasis by Interacting With TUBB3 and by Promoting Exosomes-Mediated Macrophage M2 Polarization. *Cell Death Dis* (2019) 10(11):829. doi: 10.1038/s41419-019-2077-0
- Todaro M, Gaggiani M, Catalano V, Benfante A, Iovino F, Biffoni M, et al. CD44v6 Is a Marker of Constitutive and Reprogrammed Cancer Stem Cells Driving Colon Cancer Metastasis. *Cell Stem Cell* (2014) 14(3):342–56. doi: 10.1016/j.stem.2014.01.009
- Ma L, Dong L, Chang P. CD44v6 Engages in Colorectal Cancer Progression. *Cell Death Dis* (2019) 10(1):30. doi: 10.1038/s41419-018-1265-7
- Melsen JE, Lugthart G, Lankester AC, Schilham MW. Human Circulating and Tissue-Resident CD56(bright) Natural Killer Cell Populations. *Front Immunol* (2016) 7:262. doi: 10.3389/fimmu.2016.00262
- Gharagozloo M, Rezaei A, Kalantari H, Bahador A, Hassannejad N, Maracy M, et al. Decline in Peripheral Blood NKGD2+CD3+CD56+ NKT Cells in Metastatic Colorectal Cancer Patients. *Bratisl Lek Listy* (2018) 119(1):6–11. doi: 10.4149/bl_2018_002
- Chen Z, Ren R, Wan D, Wang Y, Xue X, Jiang M, et al. Hsa_circ_101555 Functions as a Competing Endogenous RNA of miR-597-5p to Promote Colorectal Cancer Progression. *Oncogene* (2019) 38(32):6017–34. doi: 10.1038/s41388-019-0857-8
- Ritchie ME, Phipson B, Wu D, Hu Y, Law CW, Shi W, et al. Limma Powers Differential Expression Analyses for RNA-Sequencing and Microarray Studies. *Nucleic Acids Res* (2015) 43(7):e47. doi: 10.1093/nar/gkv007
- Li JH, Liu S, Zhou H, Qu LH, Yang JH. Starbase V2.0: Decoding miRNA-ceRNA, miRNA-ncRNA and Protein-RNA Interaction Networks From Large-Scale CLIP-Seq Data. *Nucleic Acids Res* (2014) 42(Database issue):D92–7. doi: 10.1093/nar/gkt1248
- Liu M, Wang Q, Shen J, Yang BB, Ding X. Circbank: A Comprehensive Database for circRNA With Standard Nomenclature. *RNA Biol* (2019) 16(7):899–905. doi: 10.1080/15476286.2019.1600395

22. Sticht C, de la Torre C, Parveen A, Gretz N. Mirwalk: An Online Resource for Prediction of microRNA Binding Sites. *PLoS One* (2018) 13(10):e0206239. doi: 10.1371/journal.pone.0206239
23. Shannon P, Markiel A, Ozier O, Baliga NS, Wang JT, Ramage D, et al. Cytoscape: A Software Environment for Integrated Models of Biomolecular Interaction Networks. *Genome Res* (2003) 13(11):2498–504. doi: 10.1101/gr.1239303
24. Szklarczyk D, Gable AL, Lyon D, Junge A, Wyder S, Huerta-Cepas J, et al. STRING V11: Protein-Protein Association Networks With Increased Coverage, Supporting Functional Discovery in Genome-Wide Experimental Datasets. *Nucleic Acids Res* (2019) 47(D1):D607–13. doi: 10.1093/nar/gky1131
25. Liu CJ, Hu FF, Xia MX, Han L, Zhang Q, Guo AY. GSCALite: A Web Server for Gene Set Cancer Analysis. *Bioinformatics* (2018) 34(21):3771–2. doi: 10.1093/bioinformatics/bty411
26. Paz I, Kosti I, Ares M Jr, Cline M, Mandel-Gutfreund Y. RBPmap: A Web Server for Mapping Binding Sites of RNA-Binding Proteins. *Nucleic Acids Res* (2014) 42(Web Server issue):W361–367. doi: 10.1093/nar/gku406
27. Li T, Fu J, Zeng Z, Cohen D, Li J, Chen Q, et al. TIMER2.0 for Analysis of Tumor-Infiltrating Immune Cells. *Nucleic Acids Res* (2020) 48(W1):W509–14. doi: 10.1093/nar/gkaa407
28. Chen J, Yang X, Liu R, Wen C, Wang H, Huang L, et al. Circular RNA GLIS2 Promotes Colorectal Cancer Cell Motility via Activation of the NF- κ B Pathway. *Cell Death Dis* (2020) 11(9):788. doi: 10.1038/s41419-020-02989-7
29. Xie J, Chen Q, Zhou P, Fan W. Circular RNA Hsa_Circ_0000511 Improves Epithelial Mesenchymal Transition of Cervical Cancer by Regulating Hsa-Mir-296-5p/HMGA1. *J Immunol Res* (2021) 2021:9964538. doi: 10.1155/2021/9964538
30. Cai F, Fu W, Tang L, Tang J, Sun J, Fu G, et al. Hsa_circ_0000515 Is a Novel Circular RNA Implicated in the Development of Breast Cancer Through Its Regulation of the microRNA-296-5p/CXCL10 Axis. *FEBS J* (2021) 288(3):861–83. doi: 10.1111/febs.15373
31. He S, Guo Z, Kang Q, Wang X, Han X. Circular RNA Hsa_Circ_0000517 Modulates Hepatocellular Carcinoma Advancement via the miR-326/SMAD6 Axis. *Cancer Cell Int* (2020) 20:360. doi: 10.1186/s12935-020-01447-w
32. He S, Yang J, Jiang S, Li Y, Han X. Circular RNA Circ_0000517 Regulates Hepatocellular Carcinoma Development via miR-326/IGF1R Axis. *Cancer Cell Int* (2020) 20:404. doi: 10.1186/s12935-020-01496-1
33. Wang X, Wang X, Li W, Zhang Q, Chen J, Chen T. Up-Regulation of Hsa_Circ_0000517 Predicts Adverse Prognosis of Hepatocellular Carcinoma. *Front Oncol* (2019) 9:1105. doi: 10.3389/fonc.2019.01105
34. Jiang J, Lin H, Shi S, Hong Y, Bai X, Cao X. Hsa_circRNA_0000518 Facilitates Breast Cancer Development via Regulation of the miR-326/FGFR1 Axis. *Thorac Cancer* (2020) 11(11):3181–92. doi: 10.1111/1759-7714.13641
35. Sun H, Tang W, Rong D, Jin H, Fu K, Zhang W, et al. Hsa_circ_0000520, a Potential New Circular RNA Biomarker, Is Involved in Gastric Carcinoma. *Cancer Biomark* (2018) 21(2):299–306. doi: 10.3233/cbm-170379
36. Lv X, Li P, Wang J, Gao H, Hei Y, Zhang J, et al. Hsa_Circ_0000520 Influences Herceptin Resistance in Gastric Cancer Cells Through PI3K-Akt Signaling Pathway. *J Clin Lab Anal* (2020) 34(10):e23449. doi: 10.1002/jcla.23449
37. Zang H, Li Y, Zhang X, Huang G. Blocking Circ_0000520 Suppressed Breast Cancer Cell Growth, Migration and Invasion Partially via miR-1296/SP1 Axis Both *In Vitro* and *In Vivo*. *Cancer Manag Res* (2020) 12:7783–95. doi: 10.2147/cmar.S251666
38. Zhou Y, Ma G, Peng S, Tuo M, Li Y, Qin X, et al. Circ_0000520 Contributes to Triple-Negative Breast Cancer Progression Through Mediating the miR-1296/ZFX Axis. *Thorac Cancer* (2021) 12(18):2427–38. doi: 10.1111/1759-7714.14085
39. Zheng Q, Zhang J, Zhang T, Liu Y, Du X, Dai X, et al. Hsa_circ_0000520 Overexpression Increases CDK2 Expression via miR-1296 to Facilitate Cervical Cancer Cell Proliferation. *J Transl Med* (2021) 19(1):314. doi: 10.1186/s12967-021-02953-9
40. Zhang J, Cai R, Zhang Y, Wang X. Involvement of a Novel circularRNA, Hsa_Circ_0000520, Attenuates Tumorigenesis of Cervical Cancer Cell Through Competitively Binding With miR-146b-3p. *J Cell Mol Med* (2020) 24(15):8480–90. doi: 10.1111/jcmm.15414
41. Pothuraju R, Rachagani S, Krishn SR, Chaudhary S, Nimmakayala RK, Siddiqui JA, et al. Molecular Implications of MUC5AC-CD44 Axis in Colorectal Cancer Progression and Chemoresistance. *Mol Cancer* (2020) 19(1):37. doi: 10.1186/s12943-020-01156-y
42. Huang YW, Lin CW, Pan P, Shan T, Echeveste CE, Mo YY, et al. Black Raspberries Suppress Colorectal Cancer by Enhancing Smad4 Expression in Colonic Epithelium and Natural Killer Cells. *Front Immunol* (2020) 11:570683. doi: 10.3389/fimmu.2020.570683
43. Zhang Q, Bi J, Zheng X, Chen Y, Wang H, Wu W, et al. Blockade of the Checkpoint Receptor TIGIT Prevents NK Cell Exhaustion and Elicits Potent Anti-Tumor Immunity. *Nat Immunol* (2018) 19(7):723–32. doi: 10.1038/s41590-018-0132-0
44. Ma XB, Xu YY, Zhu MX, Wang L. Prognostic Signatures Based on Thirteen Immune-Related Genes in Colorectal Cancer. *Front Oncol* (2020) 10:591739. doi: 10.3389/fonc.2020.591739
45. Kikuchi A, Yamamoto H, Sato A, Matsumoto S. Wnt5a: Its Signalling, Functions and Implication in Diseases. *Acta Physiol (Oxf)* (2012) 204(1):17–33. doi: 10.1111/j.1748-1716.2011.02294.x
46. Lund CM, Dyhl-Polk A, Nielsen DL, Riis LB. Wnt5a Expression and Prognosis in Stage II-III Colon Cancer. *Transl Oncol* (2021) 14(1):100892. doi: 10.1016/j.tranon.2020.100892
47. Cheng R, Sun B, Liu Z, Zhao X, Qi L, Li Y, et al. Wnt5a Suppresses Colon Cancer by Inhibiting Cell Proliferation and Epithelial-Mesenchymal Transition. *J Cell Physiol* (2014) 229(12):1908–17. doi: 10.1002/jcp.24566
48. Li Q, Chen H. Silencing of Wnt5a During Colon Cancer Metastasis Involves Histone Modifications. *Epigenetics* (2012) 7(6):551–8. doi: 10.4161/epi.20050
49. Bakker ER, Das AM, Helvensteijn W, Franken PF, Swagemakers S, van der Valk MA, et al. Wnt5a Promotes Human Colon Cancer Cell Migration and Invasion But Does Not Augment Intestinal Tumorigenesis in Apc163N Mice. *Carcinogenesis* (2013) 34(11):2629–38. doi: 10.1093/carcin/bgt215
50. Rogers RF, Walton MI, Cherry DL, Collins I, Clarke PA, Garrett MD, et al. CHK1 Inhibition Is Synthetically Lethal With Loss of B-Family DNA Polymerase Function in Human Lung and Colorectal Cancer Cells. *Cancer Res* (2020) 80(8):1735–47. doi: 10.1158/0008-5472.Can-19-1372
51. Liu J, Liu S, Yang X. Construction of Gene Modules and Analysis of Prognostic Biomarkers for Cervical Cancer by Weighted Gene Co-Expression Network Analysis. *Front Oncol* (2021) 11:542063. doi: 10.3389/fonc.2021.542063
52. Cui L, Xue H, Wen Z, Lu Z, Liu Y, Zhang Y. Prognostic Roles of Metabolic Reprogramming-Associated Genes in Patients With Hepatocellular Carcinoma. *Aging (Albany NY)* (2020) 12(21):22199–219. doi: 10.18632/aging.104122
53. Abdel-Samad R, Aouad P, Gali-Muhtasib H, Sweidan Z, Hmadi R, Kadara H, et al. Mechanism of Action of the Atypical Retinoid ST1926 in Colorectal Cancer: DNA Damage and DNA Polymerase α . *Am J Cancer Res* (2018) 8(1):39–55.
54. Han T, Goralski M, Capota E, Padrick SB, Kim J, Xie Y, et al. The Antitumor Toxin CD437 Is a Direct Inhibitor of DNA Polymerase α . *Nat Chem Biol* (2016) 12(7):511–5. doi: 10.1038/nchembio.2082
55. Gong C, Ai J, Fan Y, Gao J, Liu W, Feng Q, et al. NCAPG Promotes the Proliferation of Hepatocellular Carcinoma Through PI3K/AKT Signaling. *Onco Targets Ther* (2019) 12:8537–52. doi: 10.2147/ott.S217916
56. Sun DP, Lin CC, Hung ST, Kuang YY, Hsueh YC, Fang CL, et al. Aberrant Expression of NCAPG Is Associated With Prognosis and Progression of Gastric Cancer. *Cancer Manag Res* (2020) 12:7837–46. doi: 10.2147/cmar.S248318
57. Jiang L, Ren L, Chen H, Pan J, Zhang Z, Kuang X, et al. NCAPG Confers Trastuzumab Resistance via Activating SRC/STAT3 Signaling Pathway in HER2-Positive Breast Cancer. *Cell Death Dis* (2020) 11(7):547. doi: 10.1038/s41419-020-02753-x
58. Geng L, Rachakonda G, Morr  DJ, Morr  DM, Crooks PA, Sonar VN, et al. Indolyl-Quinuclidinols Inhibit ENOX Activity and Endothelial Cell Morphogenesis While Enhancing Radiation-Mediated Control of Tumor Vasculature. *FASEB J* (2009) 23(9):2986–95. doi: 10.1096/fj.09-130005
59. Venkateswaran A, Friedman DB, Walsh AJ, Skala MC, Sasi S, Rachakonda G, et al. The Novel Antiangiogenic VJ115 Inhibits the NADH Oxidase ENOX1 and Cytoskeleton-Remodeling Proteins. *Invest New Drugs* (2013) 31(3):535–44. doi: 10.1007/s10637-012-9884-9
60. Zhou M, Wang B, Li H, Han J, Li A, Lu W. RNA-Binding Protein SAMD4A Inhibits Breast Tumor Angiogenesis by Modulating the Balance of Angiogenesis Program. *Cancer Sci* (2021) 112(9):3835–45. doi: 10.1111/cas.15053

61. Yi D, Nguyen HP, Dinh J, Viscarra JA, Xie Y, Lin F, et al. Dot1l Interacts With Zc3h10 to Activate Ucp1 and Other Thermogenic Genes. *Elife* (2020) 27(9): e59990. doi: 10.7554/eLife.59990

Conflict of Interest: The authors declare that the research was conducted in the absence of any commercial or financial relationships that could be construed as a potential conflict of interest.

Publisher's Note: All claims expressed in this article are solely those of the authors and do not necessarily represent those of their affiliated organizations, or those of

the publisher, the editors and the reviewers. Any product that may be evaluated in this article, or claim that may be made by its manufacturer, is not guaranteed or endorsed by the publisher.

Copyright © 2022 Feng, Li, Tu, Shu, Zhang, Zeng, Luo, Wu, Chen, Cao and Li. This is an open-access article distributed under the terms of the Creative Commons Attribution License (CC BY). The use, distribution or reproduction in other forums is permitted, provided the original author(s) and the copyright owner(s) are credited and that the original publication in this journal is cited, in accordance with accepted academic practice. No use, distribution or reproduction is permitted which does not comply with these terms.



A Novel Ferroptosis-Related lncRNA Prognostic Model and Immune Infiltration Features in Skin Cutaneous Melanoma

Shuya Sun^{1†}, Guanran Zhang^{2†} and Litao Zhang^{3*}

¹Graduate School, Tianjin Medical University, Tianjin, China, ²Key Laboratory for Experimental Teratology of Ministry of Education, Department of Histology and Embryology, School of Basic Medical Sciences, Shandong University, Jinan, China, ³Department of Dermatology, Tianjin Academy of Traditional Chinese Medicine Affiliated Hospital, Tianjin, China

OPEN ACCESS

Edited by:

Zong Sheng Guo,
Roswell Park Comprehensive Cancer
Center, United States

Reviewed by:

Hezhe Lu,
Institute of Zoology (CAS), China
Susana García-Silva,
Spanish National Cancer Research
Center (CNIO), Spain

*Correspondence:

Litao Zhang
zhanglitao@medmail.com.cn

[†]These authors have contributed
equally to this work and share first
authorship

Specialty section:

This article was submitted to
Molecular and Cellular Oncology,
a section of the journal
Frontiers in Cell and Developmental
Biology

Received: 06 October 2021

Accepted: 15 December 2021

Published: 03 February 2022

Citation:

Sun S, Zhang G and Zhang L (2022) A
Novel Ferroptosis-Related lncRNA
Prognostic Model and Immune
Infiltration Features in Skin
Cutaneous Melanoma.
Front. Cell Dev. Biol. 9:790047.
doi: 10.3389/fcell.2021.790047

Background: Skin cutaneous melanoma (SKCM) is an aggressive malignant skin tumor. Ferroptosis is an iron-dependent cell death that may mobilize tumor-infiltrating immunity against cancer. The potential mechanism of long non-coding RNAs (lncRNAs) in ferroptosis in SKCM is not clear. In this study, the prognostic and treatment value of ferroptosis-related lncRNAs was explored in SKCM, and a prognostic model was established.

Methods: We first explored the mutation state of ferroptosis-related genes in SKCM samples from The Cancer Genome Atlas database. Then, we utilized consensus clustering analysis to divide the samples into three clusters based on gene expression and evaluated their immune infiltration using gene-set enrichment analysis (GSEA) ESTIMATE and single-sample gene-set enrichment analysis (ssGSEA) algorithms. In addition, we applied univariate Cox analysis to screen prognostic lncRNAs and then validated their prognostic value by Kaplan–Meier (K-M) and transcripts per kilobase million (TPM) value analyses. Finally, we constructed an 18-ferroptosis-related lncRNA prognostic model by multivariate Cox analysis, and SKCM patients were allocated into different risk groups based on the median risk score. The prognostic value of the model was evaluated by K-M and time-dependent receiver operating characteristic (ROC) analyses. Additionally, the immunophenoscore (IPS) in different risk groups was detected.

Results: The top three mutated ferroptosis genes were TP53, ACSL5, and TF. The SKCM patients in the cluster C had the highest ferroptosis-related gene expression with the richest immune infiltration. Based on the 18 prognosis-related lncRNAs, we constructed a prognostic model of SKCM patients. Patients at low risk had a better prognosis and higher IPS.

Conclusion: Our findings revealed that ferroptosis-related lncRNAs were expected to become potential biomarkers and indicators of prognosis and immunotherapy treatment targets of SKCM.

Keywords: skin cutaneous melanoma, ferroptosis, immunotherapy, long non-coding RNA (lncRNA), prognosis

INTRODUCTION

Skin cutaneous melanoma (SKCM), one of the most aggressive malignant skin tumors (Mohammadpour et al., 2019), is a complex mainly affected by environmental and genetic factors (Tucker and Goldstein, 2003), causing nearly 55,500 deaths annually (Schadendorf et al., 2018). SKCM is generally diagnosed in the remote metastatic grade (Leonardi et al., 2018), and its response to therapy is weak. As a result, the 5-year overall survival (OS) is poor at 15% (Enninga et al., 2017).

Traditional treatments have been the mainstream against advanced or metastatic melanoma in recent decades, although their aims are mainly to relieve symptoms and reduce tumor burden, with little help for prolonging survival. Due to the loss of early diagnosis and effective intervention, the identification of potential biomarkers for prognosis prediction and valid therapeutic targets of SKCM is urgently needed (Namikawa and Yamazaki, 2019).

As a breakthrough approach for metastatic melanoma, immunotherapy is based on the activation of the anticancer endogenous immune system, whose representative immune checkpoints are cytotoxic T-lymphocyte-associated protein 4 (CTLA-4) and programmed cell death protein 1 (PD-1) (Marzagalli et al., 2019). However, patients who accept immunotherapy gradually develop intrinsic resistance or resistance to targeted therapy and immunotherapy (Winder and Virós, 2018).

Cancer cells seize more nutrients for multiplication, with an especially high iron demand, and hence are vulnerable to iron-dependent cell death, named ferroptosis (Hassannia et al., 2019; Liang et al., 2019). Ferroptosis, defined by Dixon et al. (2012), is an iron-dependent form of non-apoptotic cell death triggered by lipid-based reactive oxygen species (ROS) (Hirschhorn and Stockwell, 2019), which is related to the development of diseases, especially cancers. Ferroptosis, characterized by typical mitochondrial dysfunction, has been proven to be a hopeful choice for melanoma treatment *via* multifarious signaling pathways, such as the inhibition of selenoprotein glutathione peroxidase 4 (GPX4) (Hartman, 2020). Recent studies have verified that ferroptosis plays an important role in immune infiltration, and the tumor microenvironment (TME) is tightly associated with ferroptosis, suggesting that the combination of immunotherapy and ferroptosis inducers is a promising treatment (Wang M. et al., 2019). Notably, Tsoi et al. (2018) discovered that ferroptosis-inducing drugs could target innate and acquired resistance mechanisms to targeted therapies and immunotherapies in melanoma.

Nearly 98% of RNAs are non-protein coding RNAs (ncRNAs) (Qiu et al., 2013). Long non-coding RNAs (lncRNAs) are a type of ncRNA larger than 200 nucleotides in length (Rafiee et al., 2018). An increasing number of studies have revealed that lncRNAs play important roles in epigenetic regulation in physiological processes and disease development, especially in cancer progression. Their tumor specificity and stability make lncRNAs potential tumor biomarkers (Bhan et al., 2017). Recent studies have confirmed the roles of lncRNAs involved in ferroptosis in diverse types of cancers. Wang et al. (2019)

discovered that the highly expressed lncRNA LINC00336 acts as an oncogene inhibiting ferroptosis in lung cancer. Mao et al. (2018) demonstrated that lncRNA P53RRA plays a role as a tumor suppressor in promoting ferroptosis and apoptosis of breast cancer by regulating p53. However, there are few related studies on the potential mechanism of ferroptosis-related lncRNAs in SKCM, especially regarding their prognostic value.

In this study, we established an 18-ferroptosis-related lncRNA prognostic signature of SKCM, which is expected to provide a reference for the follow-up diagnosis and treatment of SKCM.

MATERIALS AND METHODS

Data Acquisition

RNA-seq data containing 471 SKCM tumor samples were extracted, and somatic mutation data was downloaded from The Cancer Genome Atlas (TCGA) database. Forty ferroptosis-related genes were acquired from WikiPathways (Martens et al., 2021), an open database of biological pathways (<https://www.wikipathways.org>). The study was free of the approval of the ethics committees for public access to the data acquisition. Subsequent data analyses were managed with the R (version 3.6.3) and R packages. A flowchart of the study is drawn in **Supplementary Figure S1**.

Mutation and Correlation Analysis

After the preparation of the mutation annotation format (MAF) of mutation data, the mutation state of ferroptosis-related genes was evaluated in SKCM samples using the “maftools” R package, which supplies numerous analyses and visualization modules for cancer genomic studies (Mayakonda et al., 2018). The mutation and expression of dependency in 40 ferroptosis-related genes were evaluated by Spearman’s correlation coefficient ($p < 0.05$ indicated statistical significance).

Consensus Clustering for Ferroptosis-Related Genes

SKCM patients were unsupervised and classified into different subgroups based on the expression of ferroptosis-related genes using the “ConsensusClusterPlus” R package (Wilkerson and Hayes, 2010). The clinical and pathological characteristics were visualized as heatmap plots *via* the “pheatmap” R package.

Gene Set Variation Analysis Enrichment Analysis

Gene set variation analysis (GSVA) enrichment analysis was performed to estimate the different Kyoto Encyclopedia of Genes and Genomes (KEGG) pathways between any two clusters using the “GSVA” R package, whose method is non-parametric and unsupervised to detect changes in pathway activation (Hänzelmann et al., 2013). The significant biological processes met the standard of adjusted p value < 0.05 .

Estimation of Immune Infiltration

Moreover, the “ESTIMATE” R package (Yoshihara et al., 2013) was used to calculate the infiltration level of stromal and immune cells in each sample of SKCM patients. The results of the ESTIMATE score, immune score, and stromal score in different clusters are presented in violin plots. The Kruskal–Wallis test was applied to explore the difference between each cluster, and $p < 0.05$ indicated statistical significance. After finishing all the steps above, a single-sample gene-set enrichment analysis (ssGSEA) algorithm was utilized to quantify the components of different types of immune cells in the TME of SKCM.

Identification and Verification of Prognosis-Related lncRNAs

Differential analyses between any two clusters were performed, as a standard of adjusted $p < 0.05$ was used to filter differentially expressed lncRNAs (DElncRNAs), followed by intersection to obtain the common DElncRNAs, which are further displayed in the Venn diagram. Finally, univariate Cox analysis was applied to screen lncRNAs with prognostic value. Hazard ratios (HRs) and 95% confidence intervals (CIs) were calculated. The results with $p < 0.05$ were selected for the subsequent analysis.

To test the predictive value of the prognostic lncRNAs obtained, unsupervised clustering was applied to the SKCM samples using the “ConsensusClusterPlus” R package once again. The clinicopathological characteristics in different subgroups are shown in heatmap plots, and Kaplan–Meier (K–M) curves were drawn to compare the survival outcomes between different clusters. In addition, the difference in transcripts per million (TPM) values of ferroptosis-related genes in each cluster was further explored.

Construction of Prognostic Model

Multivariate Cox analysis was performed to screen out a prognostic signature constructing 18 prognostic lncRNAs in SKCM patients. According to the median of the risk score, the SKCM patients were separated into a high-risk group and a low-risk group.

Survival Analysis

The K–M survival curves of OS as well as stratification analyses for clinicopathological characteristics (age, sex, tumor stage, T stage, N stage, M stage, TP53 expression, and TP53 mutation state) in the high-/low-risk group were generated *via* the “Survival” R package to test the model’s clinical application value. The time-dependent receiver operating characteristic (ROC) curve assessed the predictive value of the model, and the area under the curve (AUC) was calculated using the “pROC” package. p value < 0.05 indicated statistical significance. The 1-, 3-, 5-, 8-, and 10-year ROC curves of the model were painted. Additionally, the risk scores of SKCM patients in different survival states were also calculated to evaluate the model’s validity. The comparison between the two groups was performed *via* the Wilcoxon rank sum test, and $p < 0.05$ was considered statistically significant.

Patient Immunophenoscore

The Cancer Immunome Database (TCIA) database (<https://tcia.at/home>) is an open access website containing the intratumoral immune landscapes and cancer antigenomes from 20 solid cancers. The immunophenoscore (IPS) is a scoring scheme for the quantification of tumor immunogenicity *via* machine learning. Considering the gene expression of four cell types (effector cells, immunosuppressive cells, MHC molecules, and immunomodulators) that determine immunogenicity, the IPS was calculated as z scores of the gene expression above, with higher scores associated with increased immunogenicity (Charoentong et al., 2017). Four kinds of IPS scores of SKCM were obtained from TCIA database and then compared. The differences in all kinds of IPS between the two groups *via* the Wilcoxon rank sum test were calculated. p value < 0.05 was considered statistically significant.

Validation of Prognostic Model

To enhance the accuracy and persuasion of prognosis, the SKCM samples from TCGA database were randomly validated into training and validation sets twice to reverify the prognostic model. Once was divided from the middle, another time was at a ratio of 7:3. The chi-square test was used to verify the distribution difference between the training set and validation set, and $p < 0.05$ was considered statistically significant. Different risk groups were based on the median risk score. To assess the availability of the prognostic model, the K–M survival method was applied to evaluate the differences in survival outcomes between the high-risk group and the low-risk group ($p < 0.05$).

RESULTS

Mutation and Correlation Analysis

Melanoma is known as one of the most highly mutated malignancies (Davis et al., 2018). Having downloaded somatic mutation profiles of SKCM patients from TCGA database as well as 40 genes associated with ferroptosis from WikiPathways (<https://www.wikipathways.org/index.php/WikiPathways>;

Supplementary Table S1), we first analyzed and visualized the mutation state of ferroptosis-related genes in the SKCM samples. The waterfall plot showed that the high mutation frequency of ferroptosis genes correlated with each SKCM sample, of which the top three mutation ferroptosis genes were TP53 (14%), ACSL5 (6%), and TF (6%). Various colors with annotations at the bottom of **Figure 1A** present the proportion of mutation categories. Missense mutation was the maximum category, and C > T was the most common single-nucleotide variant (SNV) in SKCM. Moreover, the relationships of mutated ferroptosis genes showed co-occurrence, as the green color represents synergy, while red represents mutual exclusivity (**Figure 1B**). The 10 best relations were TP53 and PRNP, TP53 and MAP1LC3A, TP53 and NCOA4, TP53 and SLC7A11, ASCL5 and SLC40A11, ASCL5 and TF, ASCL5 and ASCL3, PRNP and SLC40A11, ACSL3 and SLC11A2, and ACSL3 and SLC3A2 ($p < 0.05$). The association between each ferroptosis-related gene was highly correlated, as shown in **Figure 1C**, where red represented a positive association

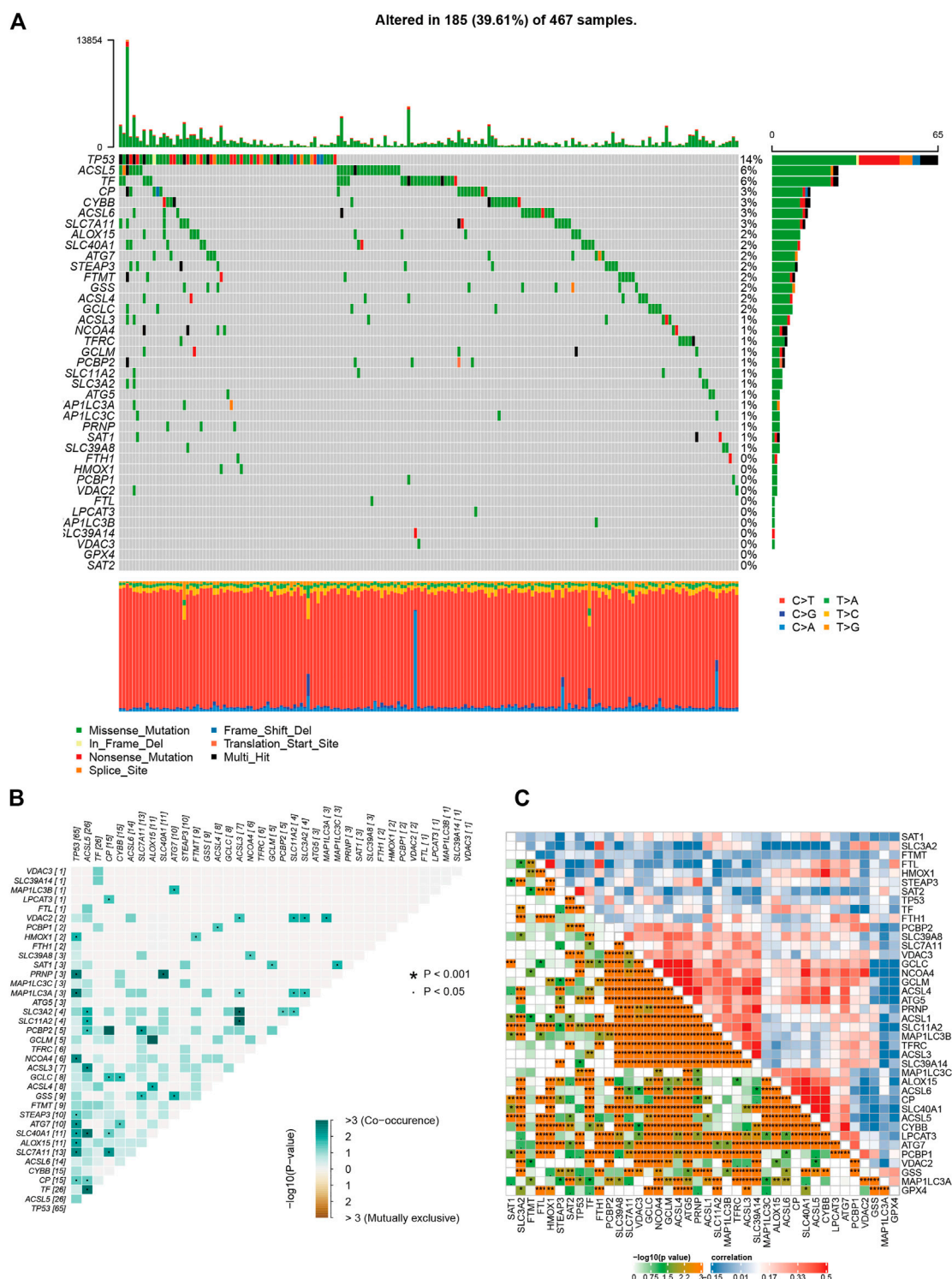


FIGURE 1 | The results of mutation and correlation analysis. **(A)** The waterfall plot showed the high frequency of mutations of 40 ferroptosis-related genes in SKCM as different colors representing different types of mutations. **(B)** The relationships of 40 mutation ferroptosis-related genes showed co-occurrence. **(C)** The correlations of gene expression of 40 ferroptosis-related genes.

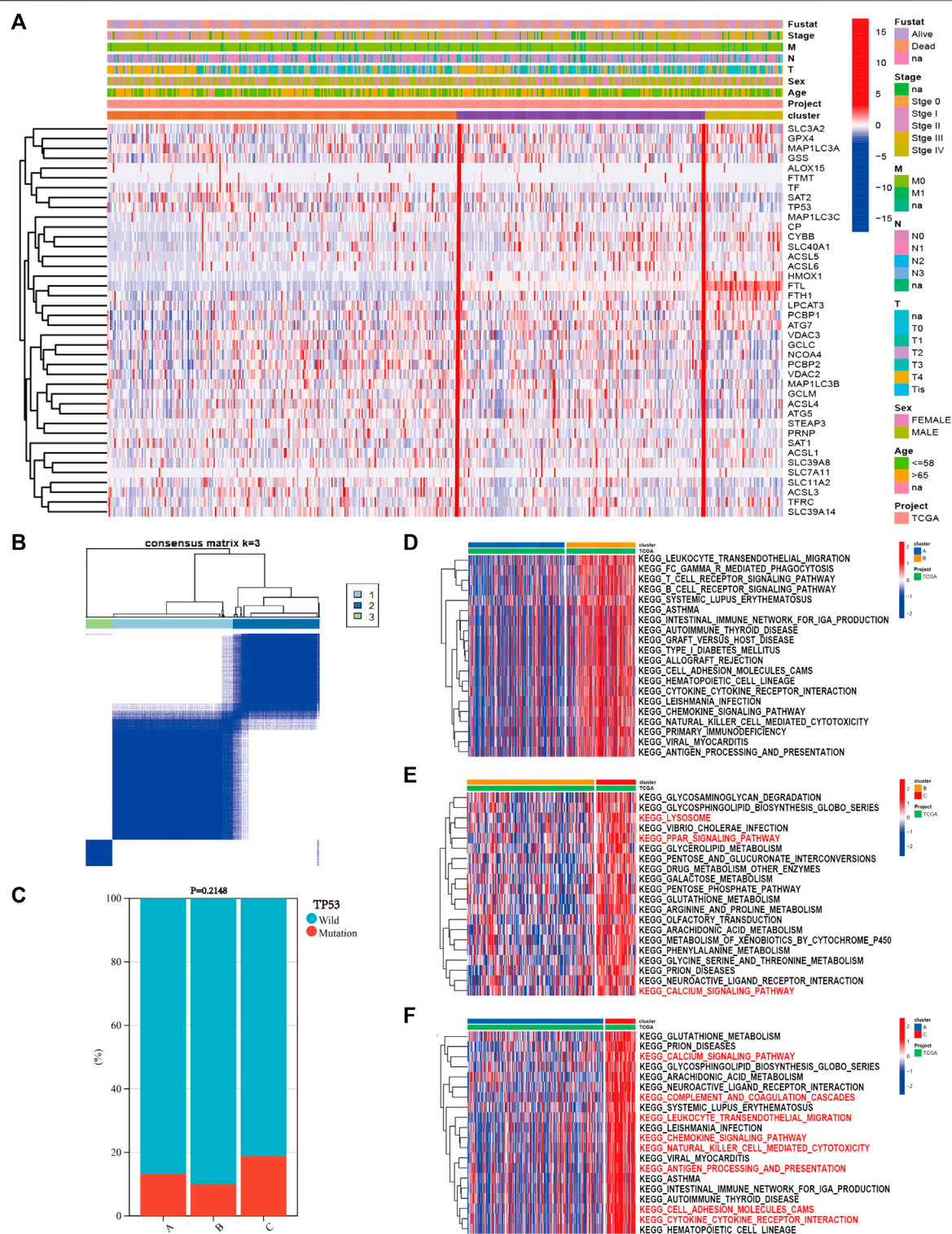
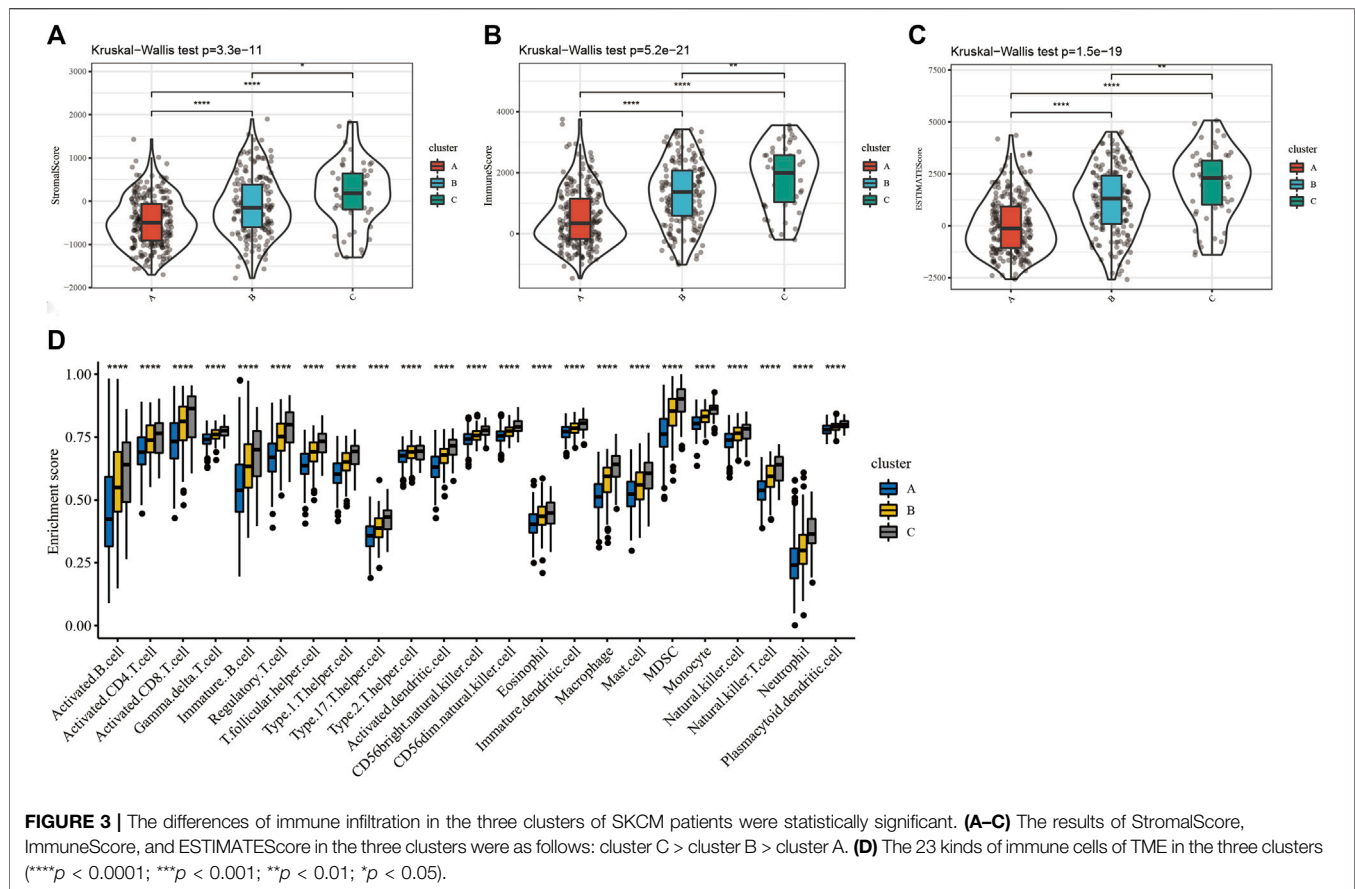


FIGURE 2 | The results of consensus clustering of ferroptosis-related genes with gene set variation analysis (GSVA) enrichment analysis. **(A)** The heatmap showed the detailed clinicopathological features of skin cutaneous melanoma (SKCM) patients in each cluster. **(B)** SKCM patients were divided into three clusters according to the consensus clustering ($k = 3$). **(C)** TP53 mutation state in each cluster. GSVA enrichment analysis revealed the top 20 significant biological pathways between every two clusters: **(D)** cluster A vs. cluster B, **(E)** cluster B vs. cluster C, and **(F)** cluster A vs. cluster C.



and blue a negative association. The deeper the orange color is, the closer the correlation. In summary, such a high rate of gene mutation in SKCM samples indicated the strong correlation of ferroptosis-related genes with SKCM.

Consensus Clustering of Ferroptosis-Related Genes With GSVA Enrichment Analysis and Immune Infiltration Estimation

Based on the expression of 40 ferroptosis-related genes, the SKCM patients were divided into three subgroups *via* the “ConsensusClusterPlus” R package. The clustering variable (k) was raised from two to nine, and $k = 3$ was chosen (Figure 2B). The cumulative distribution function (CDF), relative change in area under the CDF curve, and tracking plot are shown in Supplementary Figures S2–S4. The heatmap shows the detailed clinicopathological features of SKCM patients in each cluster, and cluster C showed the highest ferroptosis gene expression (Figure 2A). TP53 had the highest mutation frequency of SKCM samples in the previous study. As a result, the difference in the TP53 mutation state between the clusters was calculated. TP53 wild type had the highest proportion, and there was no difference between each cluster (Figure 2C, $p = 0.2148$). Then, we performed GSVA enrichment analysis between different

clusters to explore potential activated biological pathways (Supplementary Tables S2–S4). The top 20 significant pathways between every two clusters with the lowest adjusted p values were visualized in heatmaps, where red represents activated pathways and blue represents inhibited pathways. Cluster C possessed outstanding pathways in iron metabolism and immune activation, such as cytokine–cytokine receptor interactions and chemokine signaling pathways (Figure 2D–F).

Furthermore, the difference in the immune infiltration of SKCM samples was explored using ESTIMATE and the ssGSEA algorithm (Supplementary Tables S5 and S6). The average StromaScore (Figure 3A, $p = 3.3\text{e-}11$), ImmuneScore (Figure 3B, $p = 5.2\text{e-}21$), and ESTIMATEScore (Figure 3C, $p = 1.5\text{e-}19$) were consistently as follows: cluster C > cluster B > cluster A. Additionally, the infiltration level of 23 kinds of immune cells in cluster C was the highest (Figure 3D). In conclusion, the expression level of ferroptosis-related genes was positively correlated with the activation of immune infiltration in SKCM patients.

Screening and Validation of Prognostic lncRNAs

Based on the three clusters acquired from the previous steps, a differential analysis between any two of the clusters was conducted to screen out the significantly DElncRNAs as

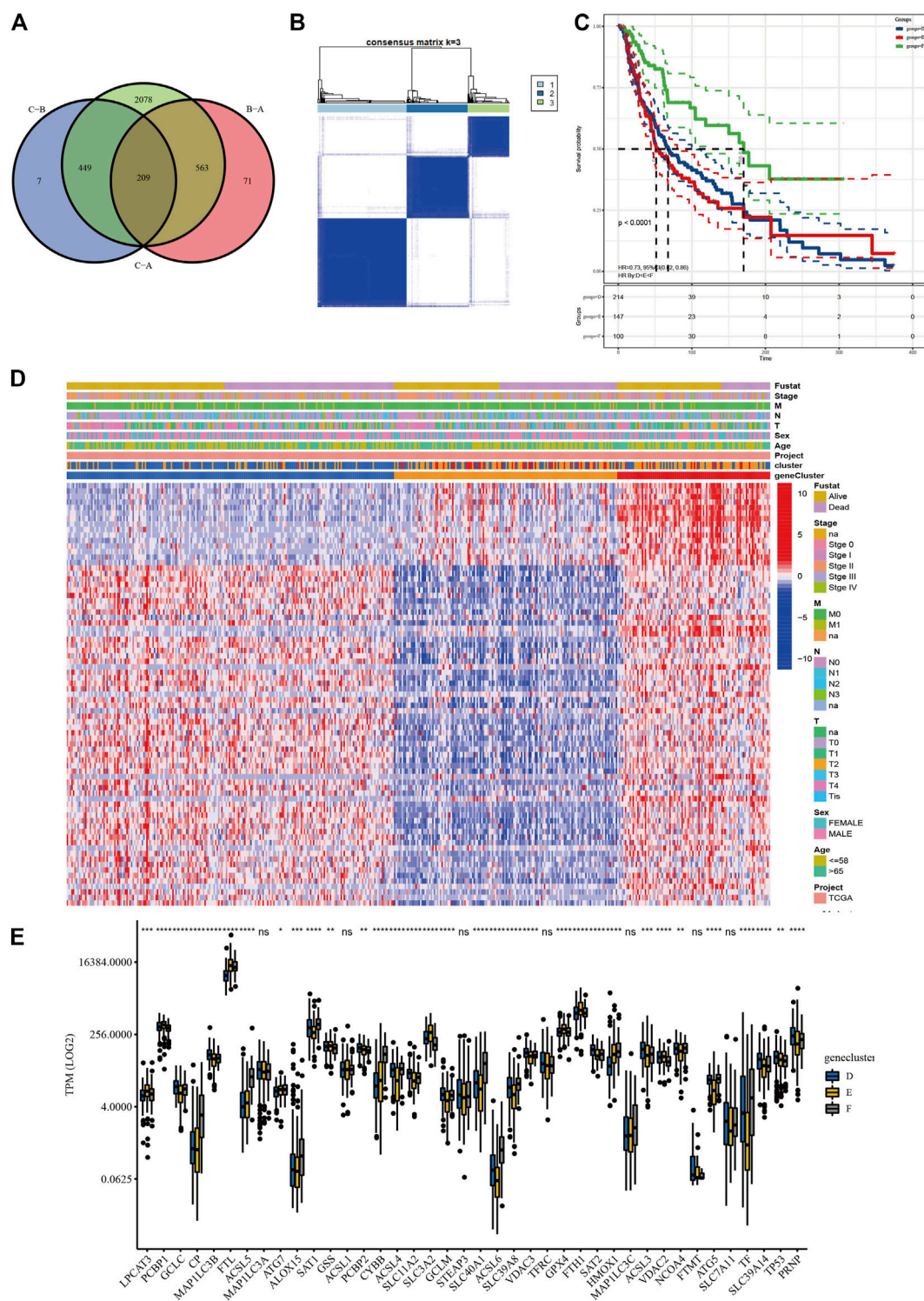


FIGURE 4 | Screening and validation of prognostic lncRNAs. **(A)** Venn diagram revealed the common differentially expressed lncRNAs (DElncRNAs). **(B)** Consensus clustering of SKCM patients based on the expression of 77 prognostic long non-coding RNAs (lncRNAs) ($k = 3$). **(C)** The overall survival (OS) analysis of SKCM patients in geneclusters D, E, and F, and genecluster F showed the most satisfied prognosis. **(D)** The heatmap of geneclusters D, E, and F with detailed clinicopathological information, where patients in genecluster F had better prognosis. **(E)** Significant differences in TPM values of ferroptosis-related genes among the three subgroups (**** $p < 0.0001$; *** $p < 0.001$; ** $p < 0.01$; * $p < 0.05$).

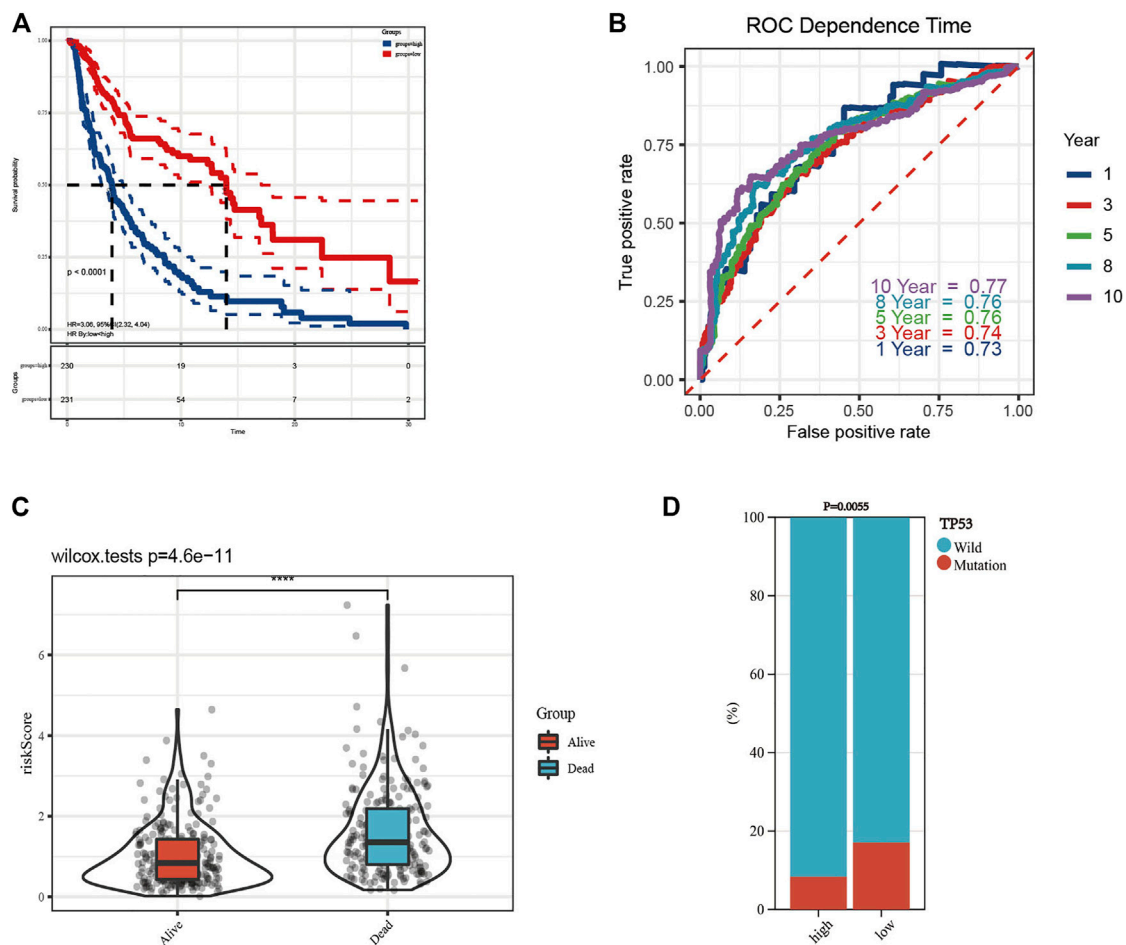


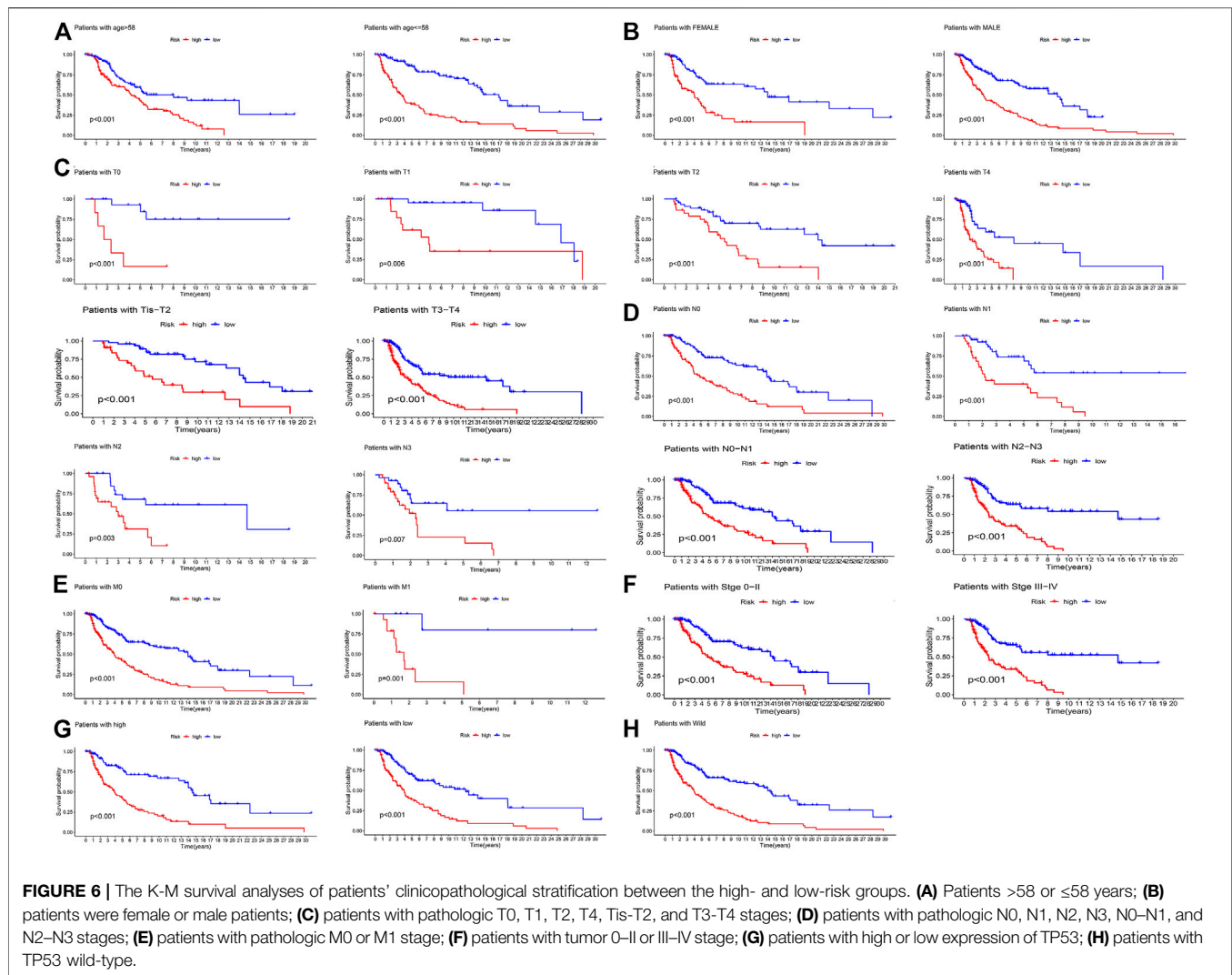
FIGURE 5 | Construction of prognostic model and survival analyses. **(A)** The Kaplan–Meier (K-M) overall survival curves in the high- and low-risk group. **(B)** The 1-, 3-, 5-, 8-, and 10-year receiver operating characteristic (ROC) curves of the prognostic model. **(C)** Risk scores of patients with different survival outcomes were of significant difference. **(D)** The difference of TP53 mutation state between the high- and low-risk groups was statistically significant.

the standard of adjusted p value < 0.05 . Subsequent intersections resulted in 209 DElncRNAs, as shown in the Venn diagram (Figure 4A). Finally, univariate Cox analysis was applied to obtain 77 lncRNAs with prognostic value ($p < 0.05$, Supplementary Table S7). To validate their prognostic efficiency, consensus clustering was performed on the SKCM samples based on the expression of 77 prognostic lncRNAs, which resulted in three subgroups named “geneclusters D, E, and F,” as shown in Figure 4B ($k = 3$). The CDF and relative change in area under the CDF curve are shown in Supplementary Figures S5 and S6. The heatmap presented the entire clinicopathological characteristics of SKCM patients in each genecluster (Figure 4D), where the genecluster F showed the highest expression of prognostic lncRNAs. In addition, the SKCM patients in genecluster F had the best survival outcomes compared with the other subgroups (Figure 4C, $p < 0.0001$). Additionally, the significant differences in TPM values of ferroptosis-related genes among the three geneclusters are displayed in

Figure 4E, which verified the effectiveness of prognostic lncRNA grouping. Interestingly, the ACSL family (ASCL4, ASCL5, and ASCL6), the SLC family (SLC39A8 and SLC40A1), NCOA4, TF, and HMOX1 were upregulated, while GPX4, GSS, PCBP1, the SLC family (SLC3A2 and SLC39A14), the VDAC family (VDAC2 and VDAC3), and TP53 were downregulated in the genecluster F ($p < 0.05$). The significantly different results of the above analyses were all between the clusters, which indicated that the 77 lncRNAs possessed prognostic value.

Construction of Prognostic Model and Survival Analyses

Using the 77 obtained prognostic lncRNAs, multivariate Cox analysis was utilized to construct a prognostic signature of SKCM composed of 18 prognostic lncRNAs (Supplementary Table S8). All SKCM patients were separated into a high-risk



group and a low-risk group according to the median risk score (**Supplementary Table S9**).

The K-M curve revealed that the patients in the high-risk group had a poorer prognosis than those in the low-risk group (**Figure 5A**, $p < 0.0001$). To evaluate the sensitivity and specificity of the prognostic signature, the ROC curves showed that the 1-, 3-, 5-, 8-, and 10-year AUCs were 0.73, 0.74, 0.76, 0.76, and 0.77, respectively (**Figure 5B**). In the above steps, survival outcomes in different risk groups of the prognosis model were explored. Therefore, the effectiveness of the risk signature was reversely tested by evaluating the difference in risk scores between patients with different survival outcomes, namely, alive or dead. As shown in **Figure 5C**, there was a significant difference in the risk scores of the different survival outcome groups ($p = 4.6e-11$). In addition, the difference in the mutation state of TP53 between the two groups was statistically significant (**Figure 5D**, $p = 0.0055$), and the wild type was still the mainstream. To further verify the prognostic efficiency of the model, stratified survival analyses for clinicopathological information between the high- and low-risk groups were analyzed. The significantly different OS

results of SKCM patients with different ages, sexes, tumor stages, T stages, N stages, M stages, TP53 expression, and wild-type TP53 levels between the high- and low-risk groups are shown in **Figure 6**, which demonstrates that the prognostic model was effective ($p < 0.05$).

IPS Estimation Between Different Risk Groups

Furthermore, the IPS data of SKCM was downloaded from the TCIA database. All four kinds of IPS showed significant differences between different risk groups, indicating that SKCM patients with low risk scores had better therapeutic effects (**Figure 7**, $p < 0.05$).

Validation of Prognostic Model

To verify the predictive ability of the prognostic model of SKCM patients, the SKCM patients were first randomly allocated from the TCGA dataset into a training set and validation set at 50% and 50% portion. The chi-square test was managed between the two

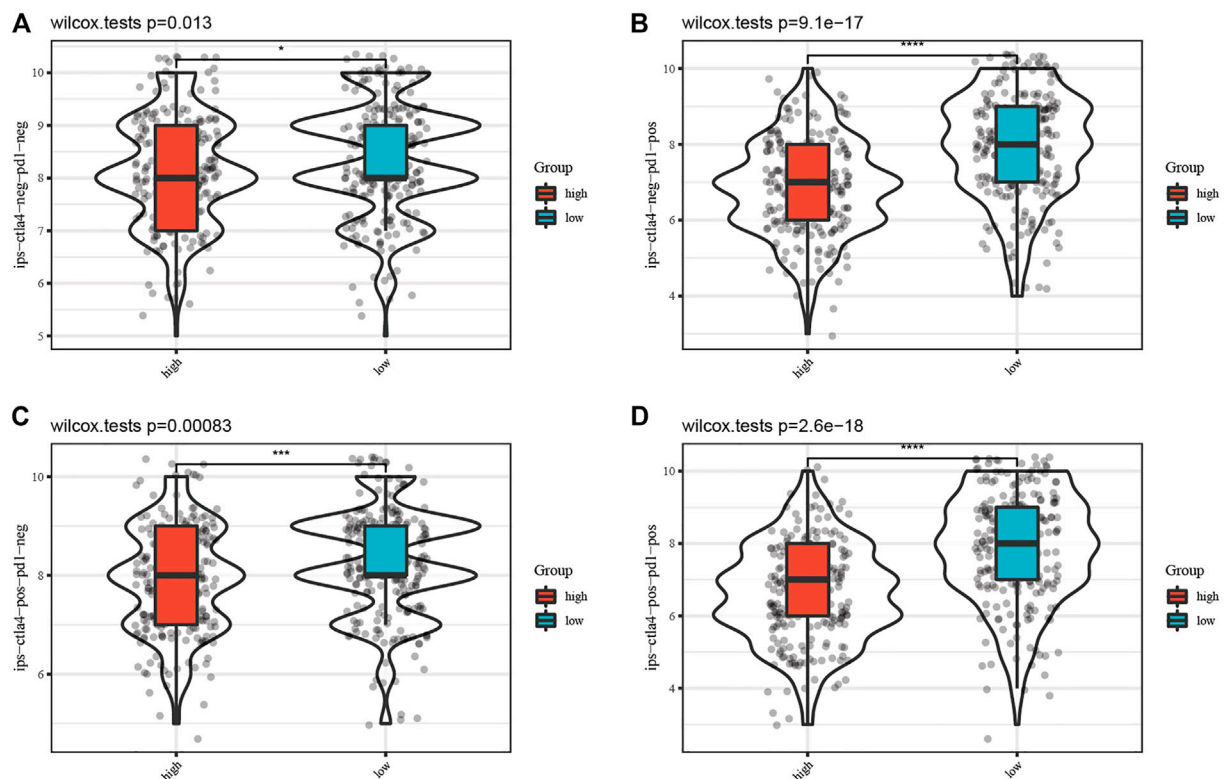


FIGURE 7 | Comparison of the IPS between the high-risk and low-risk groups. Each figure of (A–D) shows the significant difference of four kinds of immunophenoscore (IPS) between the high-risk group and low-risk group.

sets, and there was no allocation difference ($p > 0.05$, **Supplementary Table S10**). Each set was then divided into a high-risk group (training set was 112, validation set was 117, and total was 229) and a low-risk group (training set was 120, validation set was 111, and total was 231) using the median risk score (**Figure 8**). K-M survival analysis of OS showed that the low-risk group patients had significantly better outcomes than the high-risk group in the training set, whose result was consistent in the validation set ($p < 0.0001$).

For further validation, another random distribution was conducted, dividing patients into 70% and 30% proportions. The subsequent chi-square test was uneventful ($p > 0.05$, **Supplementary Table S11**), and the K-M curves in both the training set and validation set revealed that the patients in the low-risk group had significantly satisfied OS ($p < 0.0001$, **Supplementary Figure S7**). In conclusion, the prognostic model had favorable predictive value.

DISCUSSION

Melanoma is regarded as not only the most aggressive skin cancer with a steadily increasing worldwide incidence over the years but also the malignant tumor with the highest level of gene mutations of any cancer (Hayward et al., 2017). Metastatic cancer is equipped with a defense against immunological and cytotoxic

attacks. Therefore, conventional therapies, especially chemotherapy, are unsatisfactory (Gagliardi et al., 2019). The evolution of melanoma is attributed to the accumulation of pathogenic mutations especially triggered by ultraviolet-driven (UV) radiation (Hayward et al., 2017). Somatic mutations in melanoma disturb key cell signaling pathways related to proliferation and growth and have gradually become new therapeutic targets (Sarkar et al., 2015).

The combination of targeted therapy and immunotherapy in melanoma has progressed in recent decades, including BRAF inhibitors and BRAF/MEK combination therapy and CTLA-4 and PD-1 inhibitors, whose efficacy in advanced stages of melanoma has been demonstrated in randomized trials (Sun et al., 2020). However, accompanying cross-resistance and effects such as autoimmune disorders make novel therapeutic strategies urgently needed.

As distinguished from other programmed cell deaths (PCDs), such as apoptosis and necroptosis, ferroptosis is recognized as a new form of PCD (Yang et al., 2020). Activated by high levels of iron, ferroptosis is induced by cellular ROS production and lipid peroxide accumulation, which the mitogen-activated protein kinase (MAPK) family participates in (Ashrafizadeh et al., 2019). Ferroptosis is gradually recognized as a novel tumor-suppressive choice, where melanoma shows an especially sensitive response (Yang et al., 2020, Ashrafizadeh et al., 2019, Mou et al., 2019). In addition, Wang et al. (2019) detected that

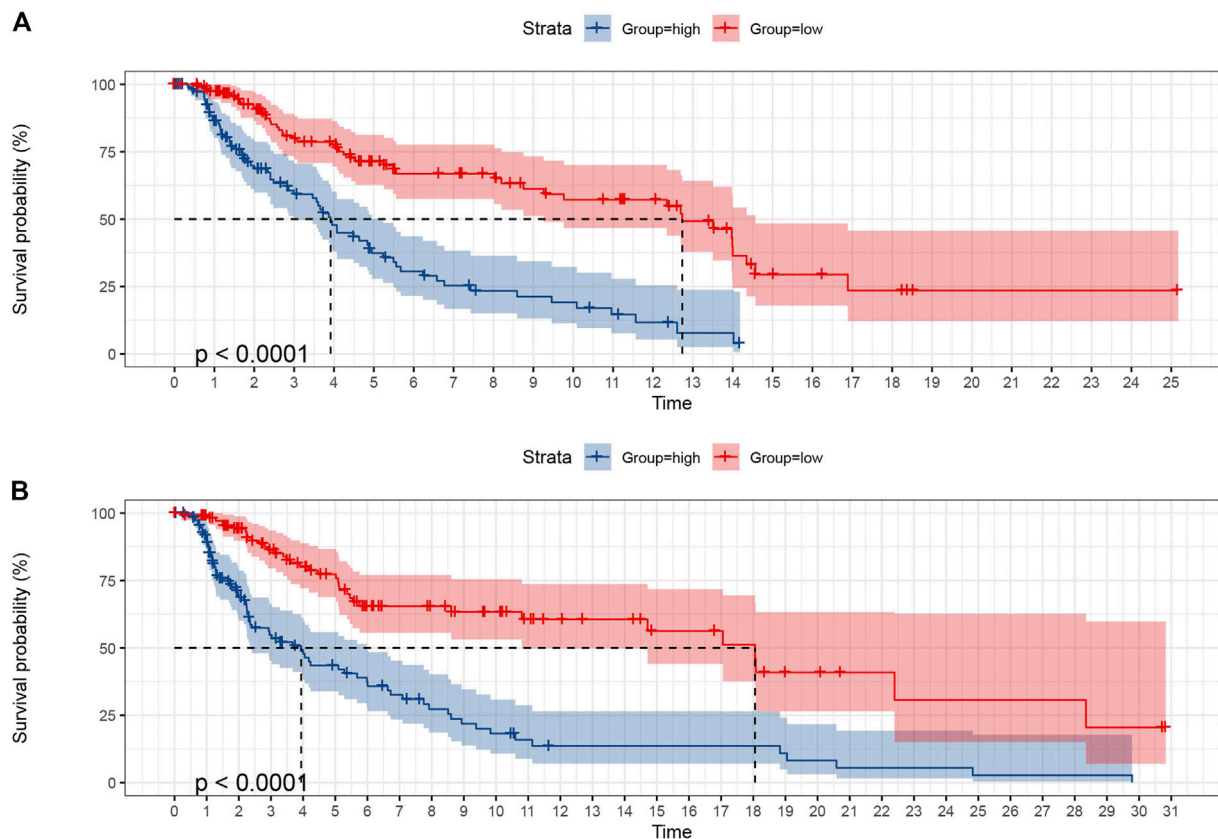


FIGURE 8 | The K-M curves of OS showed the favorable predictive value of the prognostic model in the training set **(A)** and validation set **(B)** as SKCM patients were randomly divided from the middle.

ferroptosis inhibited the growth of melanoma cells *via* a distinctive pathway that modulated DNA damage. Foxy migrating melanoma cells not only choose lymph as the first selection to avoid external pro-ferroptotic conditions but also alter the membrane defense to protect themselves against ferroptosis (Conrad and Novikova, 2020). The mutual promotion between immune activation and ferroptosis makes it possible to precisely treat cancer (Wang M. et al., 2019), while few studies have examined the prognostic value of ferroptosis-related genes in SKCM, especially the relationship between ferroptosis and immunity.

lncRNAs participate in the intricate regulation of ferroptosis and tumor immunity in various types of cancer cells (Tang et al., 2021), which has been discussed in many studies. For example, Meng et al. (2020) revealed that the lncRNA MT1DP could increase the sensitivity of non-small-cell lung cancer to ferroptosis by regulating the miR-365a3p/NRF2 axis. However, the roles of lncRNAs in ferroptosis in SKCM remain inconclusive.

In this study, we first analyzed the mutation state of ferroptosis-related genes in SKCM while TP53, ACSL5 and TF were the most frequently mutated genes. Missense mutation and C > T were the most common in SKCM. The C > T nucleotide transition has been reported to be mainly attributable to ultraviolet radiation (Hayward et al., 2017). The most

common somatic mutation in melanoma is the V600E substitution in BRAF. Triggered by ultraviolet radiation (UVR), BRAFV600E-expressing melanocytes develop canceration through targeting mutation of TP53, which is detected especially in advanced-stage melanomas (Viros et al., 2014; Shain et al., 2015).

The tumor suppressor protein p53 (TP53) plays a critical role in the cellular response to various stresses. Depending on the levels of stress, TP53 could bidirectionally regulate ferroptosis in a context-dependent manner (Liu et al., 2020). Somatic TP53 mutations are one of the most frequent alterations in human cancers (Huang et al., 2021) but are detected in less than 20% of SKCM patients (Hajkova et al., 2018), which confirms our results. Accordingly, mutated or depleted p53 in a variety of tumors destroys its original antitumor function (Kang et al., 2019). Moreover, ferroptosis regulation of TP53 in tumors no longer depends on stress level but rather on the mutation site of TP53 (Ou et al., 2016). In our study, there was no difference in TP53 mutation state between the three clusters grouped as the standard of the expression of ferroptosis genes but showed a significant difference in different risk groups. Interestingly, the proportion of TP53 mutation states in the low-risk group was higher than that in the high-risk group. Liu et al. (2020) developed a novel prognostic signature based on ferroptosis and immunity in

hepatocellular carcinoma, and the patients in the group with worse prognosis had more suppressors of ferroptosis and higher TP53 mutation frequencies. Hence, further studies on the effect of the TP53 mutation site on ferroptosis in SKCM patients are required.

ACSL5, belonging to the acyl-CoA synthetase long-chain (ACSL) family, is a nuclear-coded pro-apoptotic gene that participates in cancer suppressors; however, it shows a pro-oncogenic role in gastric cancer (Quan et al., 2021). TF encodes a glycoprotein that transports iron and removes allergens from serum.

Using ferroptosis-related gene expression, we divided SKCM patients into three clusters. Cluster C had the highest gene expression with the richest immune infiltration, which revealed that the expression of the clusters was significantly correlated with immune activation in the SKCM patients. Similarly, Jin et al. (2021) selected 11 ferroptosis regulators in uveal melanoma (UVM) samples from public databases and then used consensus clustering analysis to classify them into modules, of which one cluster showed a similar expression trend along with immune scores. In summary, ferroptosis-related genes may affect TME infiltration.

Furthermore, we identified 77 prognostic lncRNAs via univariate Cox regression analysis of the DElncRNAs selected from the clusters in SKCM patients. To test the prognostic abilities of the obtained lncRNAs, subsequent verified analyses were performed. Based on the expression of 77 prognostic lncRNAs, the SKCM patients were separated into three new clusters. Genecluster F had the most satisfactory overall survival rate, in which the ACSL family, SLC family, NCOA4, TF, and HMOX1 were upregulated, while GPX4 and TP53 were downregulated. In the review of ACSLs by Quan et al. (2021), the ACSL family contains five members, ACSL1 and ACSL3–6 in mammals, which regulate lipid metabolism and act as the key factors of ferroptosis. ACSL4 maintains a flexible role as a suppressor or an oncogene in different cancers, ACSL5 physiologically acts as a tumor suppressor in cancers, and ACSL6 is downregulated in diverse kinds of cancers, in addition to colorectal cancer. Yuan et al. (2016) provided novel evidence of the unique role of ASCL4, but not other ASCL family members, in lipid metabolism during ferroptosis. ACSL5 physiologically acts as a tumor suppressor in cancers but is upregulated in lung cancer (Wang et al., 2017). There is a lack of information on the effect of ASCL6 on cancer progression. ASCL6 encodes key membrane proteins predominantly found in brain tissue and erythrocytes (Soupeine et al., 2010) and has been proven to contribute to schizophrenia (Chen et al., 2011). NCOA4 (nuclear receptor coactivator 4) is a selective receptor for ferritinophagy in ferroptosis, whose overexpression promotes ferroptosis and vice versa (Hou et al., 2016). GPX4 is a ferroptosis inhibitor whose encoded gene was downregulated in the genecluster F. Wang W. et al. (2019) reported that interferon gamma (IFN γ) released from CD8⁺ T cells downregulates the expression of SLC3A2 and SLC7A11 and results in a drag on cystine uptake, which finally leads to tumor cell ferroptosis. In genecluster F,

SLC3A2 was significantly downregulated; however, SLC3A11 was specific.

Then, we utilized multivariate Cox analysis to establish the 18-lncRNA prognostic model. Because of the risk score, all SKCM patients were grouped into the high- or low-risk group. The K-M curves of the overall and clinicopathological stratification survival outcomes between different risk groups were satisfied. The 10-year AUC of the prognostic model was 0.77. Furthermore, we successfully verified it in the validation set twice. Moreover, low-risk patients showed a better response to immunotherapy, which is consistent with previous immune results.

After exploring published literature, the potential functions and clinical applications of AL606807.1, AC021078.1, AC004865.2, AC010245.2, AC018645.3, AC011511.5, AL021368.2, AC024909.1, AC100778.3, AC069222.1, AL592211.1, and KANS1 L-AS1 have not been reported until now. Bida et al. (2015) discovered a novel lncRNA and named it mitosis-associated long intergenic noncoding RNA 1 (MALINC1), which participates in cell cycle progression. High expression levels of MALINC1 are associated with poor survival outcomes in breast and lung cancer patients, while silencing MALINC1 makes cancer cells sensitive to paclitaxel, a chemotherapeutic drug. PPP1R26-AS1 was identified as an oncogenic lncRNA correlated with breast cancer, and its upregulation was associated with worse survival outcomes (Xu et al., 2017). It could play a role as a potential biomarker of neuroblastoma (Prajapati et al., 2019). AC026369.3 (Wan et al., 2021), LINC01871 (Chen Q. et al., 2020; He and Wang, 2020; Ma et al., 2020), USP30-AS1 (Chen P. et al., 2020; Xue et al., 2021), and AC093297.2 (Li et al., 2020) could become potential prognostic biomarkers for various malignant tumors in bioinformatics approaches.

Although our results indicated that ferroptosis-related lncRNAs might enhance immune activation, the role of lncRNAs in drug or immunotherapy resistance is seldom reported (Lazăr et al., 2020). Several lncRNAs, such as olfr29-ps1 (Shang et al., 2019), have also been identified as potential modulators of immunosuppression. However, a recent study identified a novel polycistronic lncRNA, namely, melanoma-overexpressed antigen (MELOE), which could potentially increase melanoma immunotherapy efficiency (Charpentier et al., 2016). More clinical studies are urgently needed to calculate the lncRNA level in the sensitive group vs. the resistance group of SKCM patients receiving immunotherapy.

There are some limitations in our study. First, the training set and the validation set were taken from the same database. Unfortunately, we failed to collect external clinical data from independent cohorts. Second, all analyses in our study are descriptive, and further functional experiments are needed to explore the molecular mechanisms of these lncRNAs. Third, we mainly focused on the prognostic value of lncRNAs but lacked other relevant interactions. Therefore, a comprehensive overview of interactions between lncRNAs and related upstream and downstream factors is necessary.

In this study, we conducted a novel prognostic 18-lncRNA signature for SKCM. Ferroptosis-related genes showed synergy

with immune activation. Gagliardi et al. (2020) think it is time to apply combined treatments containing ferroptosis with immune checkpoint blockers or BRAF/MEK inhibitors, which is also supported in our study. We hope that the prognostic signature may contribute to further immunotherapy.

DATA AVAILABILITY STATEMENT

The datasets presented in this study can be found in online repositories. The names of the repository/repositories and accession number(s) can be found in the article/**Supplementary Material**.

REFERENCES

- Ashrafizadeh, M., Mohammadinejad, R., Tavakol, S., Ahmadi, Z., Roomiani, S., and Katebi, M. (2019). Autophagy, Anoikis, Ferroptosis, Necroptosis, and Endoplasmic Reticulum Stress: Potential Applications in Melanoma Therapy. *J. Cell Physiol* 234 (11), 19471–19479. doi:10.1002/jcp.28740
- Bhan, A., Soleimani, M., and Mandal, S. S. (2017). Long Noncoding RNA and Cancer: A New Paradigm. *Cancer Res.* 77 (15), 3965–3981. doi:10.1158/0008-5472.CAN-16-2634
- Bida, O., Gidoni, M., Ideses, D., Efroni, S., and Ginsberg, D. (2015). A Novel Mitosis-Associated lncRNA, MA-linc1, Is Required for Cell Cycle Progression and Sensitizes Cancer Cells to Paclitaxel. *Oncotarget* 6 (29), 27880–27890. doi:10.18632/oncotarget.4944
- Charoentong, P., Finotello, F., Angelova, M., Mayer, C., Efremova, M., Rieder, D., et al. (2017). Pan-cancer Immunogenomic Analyses Reveal Genotype-Immunophenotype Relationships and Predictors of Response to Checkpoint Blockade. *Cell Rep.* 18 (1), 248–262. doi:10.1016/j.celrep.2016.12.019
- Charpentier, M., Croyal, M., Carboneille, D., Fortun, A., Florenceau, L., Rabu, C., et al. (2016). IRES-dependent Translation of the Long Non Coding RNA Meloe in Melanoma Cells Produces the Most Immunogenic MELOE Antigens. *Oncotarget* 7 (37), 59704–59713. doi:10.18632/oncotarget.10923
- Chen, J., Brunzell, D. H., Jackson, K., van der Vaart, A., Ma, J. Z., Payne, T. J., et al. (2011). ACSL6 Is Associated with the Number of Cigarettes Smoked and its Expression Is Altered by Chronic Nicotine Exposure. *PLoS One* 6 (12), e28790. doi:10.1371/journal.pone.0028790
- Chen, P., Gao, Y., Ouyang, S., Wei, L., Zhou, M., You, H., et al. (2020). A Prognostic Model Based on Immune-Related Long Non-coding RNAs for Patients with Cervical Cancer. *Front. Pharmacol.* 11, 585255. doi:10.3389/fphar.2020.585255
- Chen, Q., Hu, L., Huang, D., Chen, K., Qiu, X., and Qiu, B. (2020). Six-lncRNA Immune Prognostic Signature for Cervical Cancer. *Front. Genet.* 11, 533628. doi:10.3389/fgene.2020.533628
- Conrad, M., and Novikova, M. (2020). A Cozy Niche in an Iron World. *Sig Transduct Target. Ther.* 5 (1), 261. doi:10.1038/s41392-020-00368-4
- Davis, E. J., Johnson, D. B., Sosman, J. A., and Chandra, S. (2018). Melanoma: What Do All the Mutations Mean? *Cancer* 124 (17), 3490–3499. doi:10.1002/cncr.31345
- Dixon, S. J., Lemberg, K. M., Lamprecht, M. R., Skouta, R., Zaitsev, E. M., Gleason, C. E., et al. (2012). Ferroptosis: an Iron-dependent Form of Nonapoptotic Cell Death. *Cell* 149 (5), 1060–1072. doi:10.1016/j.cell.2012.03.042
- Enninga, E. A. L., Moser, J. C., Weaver, A. L., Markovic, S. N., Brewer, J. D., Leontovich, A. A., et al. (2017). Survival of Cutaneous Melanoma Based on Sex, Age, and Stage in the United States, 1992–2011. *Cancer Med.* 6 (10), 2203–2212. doi:10.1002/cam4.1152
- Gagliardi, M., Cotella, D., Santoro, C., Corà, D., Barlev, N. A., Piacentini, M., et al. (2019). Aldo-keto Reductases Protect Metastatic Melanoma from ER Stress-independent Ferroptosis. *Cell Death Dis* 10 (12), 902. doi:10.1038/s41419-019-2143-7
- Gagliardi, M., Saverio, V., Monzani, R., Ferrari, E., Piacentini, M., and Corazzari, M. (2020). Ferroptosis: a New Unexpected Chance to Treat Metastatic Melanoma? *Cell Cycle* 19 (19), 2411–2425. doi:10.1080/15384101.2020.1806426

AUTHOR CONTRIBUTIONS

SS and GZ wrote the manuscript and constructed the figures. LZ reviewed and modified the manuscript and approved the publication. All authors contributed to the article and approved the submitted version.

SUPPLEMENTARY MATERIAL

The Supplementary Material for this article can be found online at: <https://www.frontiersin.org/articles/10.3389/fcell.2021.790047/full#supplementary-material>

- Hajkova, N., Hojny, J., Nemejcova, K., Dundr, P., Ulrych, J., Jirsova, K., et al. (2018). Germline Mutation in the TP53 Gene in Uveal Melanoma. *Sci. Rep.* 8 (1), 7618. doi:10.1038/s41598-018-26040-0
- Hänzelmann, S., Castelo, R., and Guinney, J. (2013). GSEA: Gene Set Variation Analysis for Microarray and RNA-Seq Data. *BMC Bioinformatics* 14, 7. doi:10.1186/1471-2105-14-7
- Hartman, M. L. (2020). Non-Apoptotic Cell Death Signaling Pathways in Melanoma. *Ijms* 21 (8), 2980. doi:10.3390/ijms21082980
- Hassannia, B., Vandenabeele, P., and Vanden Berghe, T. (2019). Targeting Ferroptosis to Iron Out Cancer. *Cancer Cell* 35 (6), 830–849. doi:10.1016/j.ccell.2019.04.002
- Hayward, N. K., Wilmott, J. S., Waddell, N., Johansson, P. A., Field, M. A., Nones, K., et al. (2017). Whole-genome Landscapes of Major Melanoma Subtypes. *Nature* 545 (7653), 175–180. doi:10.1038/nature22071
- He, Y., and Wang, X. (2020). Identification of Molecular Features Correlating with Tumor Immunity in Gastric Cancer by Multi-Omics Data Analysis. *Ann. Transl. Med.* 8 (17), 1050. doi:10.21037/atm-20-922
- Hirschhorn, T., and Stockwell, B. R. (2019). The Development of the Concept of Ferroptosis. *Free Radic. Biol. Med.* 133, 130–143. doi:10.1016/j.freeradbiomed.2018.09.043
- Hou, W., Xie, Y., Song, X., Sun, X., Lotze, M. T., Zeh, H. J., 3rd, et al. (2016). Autophagy Promotes Ferroptosis by Degradation of Ferritin. *Autophagy* 12 (8), 1425–1428. doi:10.1080/15548627.2016.1187366
- Huang, C., Huang, R., Chen, H., Ni, Z., Huang, Q., Huang, Z., et al. (2021). Chromatin Accessibility Regulates Gene Expression and Correlates with Tumor-Infiltrating Immune Cells in Gastric Adenocarcinoma. *Front. Oncol.* 10, 609940. doi:10.3389/fonc.2020.609940
- Jin, Y., Wang, Z., He, D., Zhu, Y., Gong, L., Xiao, M., et al. (2021). Analysis of Ferroptosis-Mediated Modification Patterns and Tumor Immune Microenvironment Characterization in Uveal Melanoma. *Front. Cell Dev. Biol.* 9, 685120. doi:10.3389/fcell.2021.685120
- Kang, R., Kroemer, G., and Tang, D. (2019). The Tumor Suppressor Protein P53 and the Ferroptosis Network. *Free Radic. Biol. Med.* 133, 162–168. doi:10.1016/j.freeradbiomed.2018.05.074
- Lazăr, A. D., Dinescu, S., and Costache, M. (2020). The Non-coding Landscape of Cutaneous Malignant Melanoma: A Possible Route to Efficient Targeted Therapy. *Cancers* 12 (11), 3378. doi:10.3390/cancers12113378
- Leonardi, G., Falzone, L., Salemi, R., Zanghi, A., Spandidos, D., McCubrey, J., et al. (2018). Cutaneous Melanoma: From Pathogenesis to Therapy (Review). *Int. J. Oncol.* 52 (4), 1071–1080. doi:10.3892/ijo.2018.4287
- Li, Z., Li, Y., Wang, X., and Yang, Q. (2020). Identification of a Six-Immune-Related Long Non-coding RNA Signature for Predicting Survival and Immune Infiltrating Status in Breast Cancer. *Front. Genet.* 11, 680. doi:10.3389/fgene.2020.00680
- Liang, C., Zhang, X., Yang, M., and Dong, X. (2019). Recent Progress in Ferroptosis Inducers for Cancer Therapy. *Adv. Mater.* 31 (51), 1904197. doi:10.1002/adma.201904197
- Liu, Y., Zhang, X., Zhang, J., Tan, J., Li, J., and Song, Z. (2020). Development and Validation of a Combined Ferroptosis and Immune Prognostic Classifier for Hepatocellular Carcinoma. *Front. Cell Dev. Biol.* 8, 596679. doi:10.3389/fcell.2020.596679

- Ma, W., Zhao, F., Yu, X., Guan, S., Suo, H., Tao, Z., et al. (2020). Immune-related lncRNAs as Predictors of Survival in Breast Cancer: a Prognostic Signature. *J. Transl. Med.* 18 (1), 442. doi:10.1186/s12967-020-02522-6
- Mao, C., Wang, X., Liu, Y., Wang, M., Yan, B., Jiang, Y., et al. (2018). A G3BP1-Interacting lncRNA Promotes Ferroptosis and Apoptosis in Cancer via Nuclear Sequestration of P53. *Cancer Res.* 78 (13), 3454–3496. doi:10.1158/0008-5472.CAN-17-3454
- Martens, M., Ammar, A., Riutta, A., Waagmeester, A., Slenter, D. N., Hanspers, K., et al. (2021). WikiPathways: Connecting Communities. *Nucleic Acids Res.* 49 (D1), D613–D621. doi:10.1093/nar/gkaa1024
- Marzagalli, M., Ebelt, N. D., and Manuel, E. R. (2019). Unraveling the Crosstalk between Melanoma and Immune Cells in the Tumor Microenvironment. *Semin. Cancer Biol.* 59, 236–250. doi:10.1016/j.semcancer.2019.08.002
- Mayakonda, A., Lin, D.-C., Assenov, Y., Plass, C., and Koeffler, H. P. (2018). Maftools: Efficient and Comprehensive Analysis of Somatic Variants in Cancer. *Genome Res.* 28 (11), 1747–1756. doi:10.1101/gr.239244.118
- Meng, F., Zhou, Y., Dong, B., Dong, A., and Zhang, J. (2020). Long Non-coding RNA LINC01194 Promotes the Proliferation, Migration and Invasion of Lung Adenocarcinoma Cells by Targeting miR-641/SETD7 axis. *Cancer Cell Int* 20, 588. doi:10.1186/s12935-020-01680-3
- Mohammadpour, A., Derakhshan, M., Darabi, H., Hedayat, P., and Momeni, M. (2019). Melanoma: Where We Are and where We Go. *J. Cell Physiol* 234 (4), 3307–3320. doi:10.1002/jcp.27286
- Mou, Y., Wang, J., Wu, J., He, D., Zhang, C., Duan, C., et al. (2019). Ferroptosis, a New Form of Cell Death: Opportunities and Challenges in Cancer. *J. Hematol. Oncol.* 12 (1), 34. doi:10.1186/s13045-019-0720-y
- Namikawa, K., and Yamazaki, N. (2019). Targeted Therapy and Immunotherapy for Melanoma in Japan. *Curr. Treat. Options. Oncol.* 20 (1), 7. doi:10.1007/s11864-019-0607-8
- Ou, Y., Wang, S.-J., Li, D., Chu, B., and Gu, W. (2016). Activation of SAT1 Engages Polyamine Metabolism with P53-Mediated Ferroptotic Responses. *Proc. Natl. Acad. Sci. U.S.A.* 113, E6806–E6812. doi:10.1073/pnas.1607152113
- Prajapati, B., Fatma, M., Fatima, M., Khan, M. T., Sinha, S., and Seth, P. K. (2019). Identification of lncRNAs Associated with Neuroblastoma in Cross-Sectional Databases: Potential Biomarkers. *Front. Mol. Neurosci.* 12, 293. doi:10.3389/fnmol.2019.00293
- Qiu, M.-T., Hu, J.-W., Yin, R., and Xu, L. (2013). Long Noncoding RNA: an Emerging Paradigm of Cancer Research. *Tumor Biol.* 34 (2), 613–620. doi:10.1007/s13277-013-0658-6
- Quan, J., Bode, A. M., and Luo, X. (2021). ACSL Family: The Regulatory Mechanisms and Therapeutic Implications in Cancer. *Eur. J. Pharmacol.* 909, 174397. doi:10.1016/j.ejphar.2021.174397
- Rafiee, A., Riaz-Rad, F., Havaskary, M., and Nuri, F. (2018). Long Noncoding RNAs: Regulation, Function and Cancer. *Biotechnol. Genet. Eng. Rev.* 34 (2), 153–180. doi:10.1080/02648725.2018.1471566
- Sarkar, D., Leung, E. Y., Baguley, B. C., Finlay, G. J., and Askarian-Amiri, M. E. (2015). Epigenetic Regulation in Human Melanoma: Past and Future. *Epigenetics* 10 (2), 103–121. doi:10.1080/15592294.2014.1003746
- Schadendorf, D., van Akkooi, A. C. J., Berking, C., Griewank, K. G., Gutzmer, R., Hauschild, A., et al. (2018). Melanoma. *The Lancet* 392 (10151), 971–984. doi:10.1016/s0140-6736(18)31559-9
- Shain, A. H., Yeh, I., Kovalyshyn, I., Sriharan, A., Talevich, E., Gagnon, A., et al. (2015). The Genetic Evolution of Melanoma from Precursor Lesions. *N. Engl. J. Med.* 373 (20), 1926–1936. doi:10.1056/NEJMoa1502583
- Shang, W., Gao, Y., Tang, Z., Zhang, Y., and Yang, R. (2019). The Pseudogene Olfr29-Ps1 Promotes the Suppressive Function and Differentiation of Monocytic MDSCs. *Cancer Immunol. Res.* 7 (5), 813–827. doi:10.1158/2326-6066.CIR-18-0443
- Soupe, E., Dinh, N., Siliakus, M., and Kuypers, F. A. (2010). Activity of the Acyl-CoA Synthetase ACSL6 Isoforms: Role of the Fatty Acid Gate-Domains. *BMC Biochem.* 11, 18. doi:10.1186/1471-2091-11-18
- Sun, J., Carr, M. J., and Khushalani, N. I. (2020). Principles of Targeted Therapy for Melanoma. *Surg. Clin. North America* 100 (1), 175–188. doi:10.1016/j.suc.2019.09.013
- Tang, W., Zhu, S., Liang, X., Liu, C., and Song, L. (2021). The Crosstalk between Long Non-coding RNAs and Various Types of Death in Cancer Cells. *Technol. Cancer Res. Treat.* 20, 153303382110330. doi:10.1177/15330338211033044
- Tsoi, J., Robert, L., Paraiso, K., Galvan, C., Sheu, K. M., Lay, J., et al. (2018). Multi-stage Differentiation Defines Melanoma Subtypes with Differential Vulnerability to Drug-Induced Iron-dependent Oxidative Stress. *Cancer Cell* 33 (5), 890–904. doi:10.1016/j.ccell.2018.03.017
- Tucker, M. A., and Goldstein, A. M. (2003). Melanoma Etiology: where Are We? *Oncogene* 22 (20), 3042–3052. doi:10.1038/sj.onc.1206444
- Viros, A., Sanchez-Laorden, B., Pedersen, M., Furney, S. J., Rae, J., Hogan, K., et al. (2014). Ultraviolet Radiation Accelerates BRAF-Driven Melanomagenesis by Targeting TP53. *Nature* 511 (7510), 478–482. doi:10.1038/nature13298
- Wan, J., Guo, C., Fang, H., Xu, Z., Hu, Y., and Luo, Y. (2021). Autophagy-Related Long Non-coding RNA Is a Prognostic Indicator for Bladder Cancer. *Front. Oncol.* 11, 647236. doi:10.3389/fonc.2021.647236
- Wang, C.-Y., Shahi, P., Huang, J. T. W., Phan, N. N., Sun, Z., Lin, Y.-C., et al. (2017). Systematic Analysis of the Achaete-Scute Complex-like Gene Signature in Clinical Cancer Patients. *Mol. Clin. Oncol.* 6 (1), 7–18. doi:10.3892/mco.2016.1094
- Wang, M., Mao, C., Ouyang, L., Liu, Y., Lai, W., Liu, N., et al. (2019a). Long Noncoding RNA LINC00336 Inhibits Ferroptosis in Lung Cancer by Functioning as a Competing Endogenous RNA. *Cell Death Differ* 26 (11), 2329–2343. doi:10.1038/s41418-019-0304-y
- Wang, W., Green, M., Choi, J. E., Gijón, M., Kennedy, P. D., Johnson, J. K., et al. (2019b). CD8+ T Cells Regulate Tumour Ferroptosis during Cancer Immunotherapy. *Nature* 569 (7755), 270–274. doi:10.1038/s41586-019-1170-y
- Wang, Z., Jin, D., Ma, D., Ji, C., Wu, W., Xu, L., et al. (2019c). Ferroptosis Suppressed the Growth of Melanoma that May Be Related to DNA Damage. *Dermatol. Ther.* 32 (4), e12921. doi:10.1111/dth.12921
- Wilkerson, M. D., and Hayes, D. N. (2010). ConsensusClusterPlus: a Class Discovery Tool with Confidence Assessments and Item Tracking. *Bioinformatics* 26 (12), 1572–1573. doi:10.1093/bioinformatics/btq170
- Winder, M., and Virós, A. (2018). Mechanisms of Drug Resistance in Melanoma. *Handb. Exp. Pharmacol.* 249, 91–108. doi:10.1007/164_2017_17
- Xu, S., Kong, D., Chen, Q., Ping, Y., and Pang, D. (2017). Oncogenic Long Noncoding RNA Landscape in Breast Cancer. *Mol. Cancer* 16 (1), 129. doi:10.1186/s12943-017-0696-6
- Xue, L., Wu, P., Zhao, X., Jin, X., Wang, J., Shi, Y., et al. (2021). Using Immune-Related lncRNA Signature for Prognosis and Response to Immunotherapy in Cutaneous Melanoma. *Ijgm* 14, 6463–6475. doi:10.2147/IJGM.S335266
- Yang, Y., Luo, M., Zhang, K., Zhang, J., Gao, T., Connell, D. O., et al. (2020). Nedd4 Ubiquitylates VDAC2/3 to Suppress Erastin-Induced Ferroptosis in Melanoma. *Nat. Commun.* 11 (1), 433. doi:10.1038/s41467-020-14324-x
- Yoshihara, K., Shahmoradgoli, M., Martínez, E., Vegesna, R., Kim, H., Torres-García, W., et al. (2013). Inferring Tumour Purity and Stromal and Immune Cell Admixture from Expression Data. *Nat. Commun.* 4, 2612. doi:10.1038/ncomms3612
- Yuan, H., Li, X., Zhang, X., Kang, R., and Tang, D. (2016). Identification of ACSL4 as a Biomarker and Contributor of Ferroptosis. *Biochem. Biophysical Res. Commun.* 478 (3), 1338–1343. doi:10.1016/j.bbrc.2016.08.124

Conflict of Interest: The authors declare that the research was conducted in the absence of any commercial or financial relationships that could be construed as a potential conflict of interest.

Publisher's Note: All claims expressed in this article are solely those of the authors and do not necessarily represent those of their affiliated organizations, or those of the publisher, the editors, and the reviewers. Any product that may be evaluated in this article, or claim that may be made by its manufacturer, is not guaranteed or endorsed by the publisher.

Copyright © 2022 Sun, Zhang and Zhang. This is an open-access article distributed under the terms of the Creative Commons Attribution License (CC BY). The use, distribution or reproduction in other forums is permitted, provided the original author(s) and the copyright owner(s) are credited and that the original publication in this journal is cited, in accordance with accepted academic practice. No use, distribution or reproduction is permitted which does not comply with these terms.



Clinical Significance and Immune Landscape of a Pyroptosis-Derived LncRNA Signature for Glioblastoma

Zhe Xing^{1,2†}, Zaoqu Liu^{3†}, Xudong Fu^{1,2}, Shaolong Zhou^{1,2}, Long Liu⁴, Qin Dang⁵, Chunguang Guo⁶, Xiaoyong Ge³, Taoyuan Lu⁷, Youyang Zheng⁸, Lirui Dai^{1,2}, Xinwei Han^{3*} and Xinjun Wang^{1,2*}

¹Department of Neurosurgery, The Fifth Affiliated Hospital of Zhengzhou University, Zhengzhou, China, ²Henan International Joint Laboratory of Glioma Metabolism and Microenvironment Research, Zhengzhou, China, ³Department of Interventional Radiology, The First Affiliated Hospital of Zhengzhou University, Zhengzhou, China, ⁴Department of Hepatobiliary and Pancreatic Surgery, The First Affiliated Hospital of Zhengzhou University, Zhengzhou, China, ⁵Department of Colorectal Surgery, The First Affiliated Hospital of Zhengzhou University, Zhengzhou, China, ⁶Department of Endovascular Surgery, The First Affiliated Hospital of Zhengzhou University, Zhengzhou, China, ⁷Department of Cerebrovascular Disease, Zhengzhou University People's Hospital, Zhengzhou, China, ⁸Department of Cardiology, The First Affiliated Hospital of Zhengzhou University, Zhengzhou, China

OPEN ACCESS

Edited by:

Zong Sheng Guo,
Roswell Park Comprehensive Cancer
Center, United States

Reviewed by:

Yongzhang Luo,
Tsinghua University, China
Weihao Kong,
First Affiliated Hospital of Anhui
Medical University, China

*Correspondence:

Xinjun Wang
wangxj@zzu.edu.cn
Xinwei Han
fchxanxw@zzu.edu.cn

[†]These authors have contributed
equally to this work

Specialty section:

This article was submitted to
Molecular and Cellular Oncology,
a section of the journal
Frontiers in Cell and Developmental
Biology

Received: 30 October 2021

Accepted: 12 January 2022

Published: 10 February 2022

Citation:

Xing Z, Liu Z, Fu X, Zhou S, Liu L,
Dang Q, Guo C, Ge X, Lu T, Zheng Y,
Dai L, Han X and Wang X (2022)
Clinical Significance and Immune
Landscape of a Pyroptosis-Derived
LncRNA Signature for Glioblastoma.
Front. Cell Dev. Biol. 10:805291.
doi: 10.3389/fcell.2022.805291

Introduction: Pyroptosis was recently implicated in the initiation and progression of tumors, including glioblastoma (GBM). This study aimed to explore the clinical significance of pyroptosis-related lncRNAs (PRLs) in GBM.

Methods: Three independent cohorts were retrieved from the TCGA and CGGA databases. The consensus clustering and weighted gene coexpression network analysis (WGCNA) were applied to identify PRLs. The LASSO algorithm was employed to develop and validate a pyroptosis-related lncRNA signature (PRLS) in three independent cohorts. The molecular characteristics, clinical significances, tumor microenvironment, immune checkpoints profiles, and benefits of chemotherapy and immunotherapy regarding to PRLS were also explored.

Results: In the WGCNA framework, a key module that highly correlated with pyroptosis was extracted for identifying PRLs. Univariate Cox analysis further revealed the associations between PRLs and overall survival. Based on the expression profiles of PRLs, the PRLS was initially developed in TCGA cohort ($n = 143$) and then validated in two CGGA cohorts ($n = 374$). Multivariate Cox analysis demonstrated that our PRLS model was an independent risk factor. More importantly, this signature displayed a stable and accurate performance in predicting prognosis at 1, 3, and 5 years, with all AUCs above 0.7. The decision curve analysis also indicated that our signature had promising clinical application. In addition, patients with high PRLS score suggested a more abundant immune infiltration, higher expression of immune checkpoint genes, and better response to immunotherapy but worse to chemotherapy.

Conclusion: A novel pyroptosis-related lncRNA signature with a robust performance was constructed and validated in multiple cohorts. This signature provided new perspectives for clinical management and precise treatments of GBM.

Keywords: pyroptosis, long non-coding RNA, glioblastoma (GBM), prognostic signature, immune landscape, immunotherapy, chemotherapy

INTRODUCTION

Glioblastoma (GBM) is the most commonly occurring type of glioma, according to the 2016 World Health Organization (WHO) classification, and is also the most lethal primary brain tumor worldwide, which is closely related to significant morbidity and mortality in adults, with a 5-year overall survival (OS) rate of 5% (Roos et al., 2017; Wesseling and Capper, 2018; Oronsky et al., 2020; Majc et al., 2021). Despite the application of the optimum therapeutic options, including surgical resection, radiotherapy, chemotherapy as well as tumor-treating field treatment (TTF), the OS remains poor (Stupp et al., 2017; Delgado-Martin and Medina, 2020; Tan et al., 2020).

Pyroptosis, a novel fashion of programmed cell death, referred to as cellular inflammatory necrosis (Kovacs and Miao, 2017), is triggered by inflammasomes and mainly executed by the cleavage of gasdermin proteins, such as gasdermin D (GSDMD) and gasdermin E (GSDME), which can be cleaved by caspase-1 and caspase-3, respectively, to spark off pyroptosis (Shi et al., 2015; Ding et al., 2016). Pyroptosis participates in the development of multiple tumors, including glioma. Upregulation of transcription factor p53 inhibits tumor growth through prompting pyroptosis in non-small-cell lung cancer (Zhang et al., 2019). Galangin can exert antitumor effects by inducing apoptosis, pyroptosis, and protective autophagy in GBM cells (Kong et al., 2019). Therefore, the impacts of pyroptosis on glioma cannot be ignored.

Long noncoding RNAs (lncRNAs), a sort of noncoding RNA longer than 200 nucleotides, are involved in a wide range of biological processes, such as cell death, growth, differentiation, posttranscriptional regulation, chromatin modification, inflammatory pathology, epigenetic regulation, and subcellular transport (Rynkeviciene et al., 2018). Recently, an increasing number of studies have shown that lncRNAs play important roles in the pyroptosis progress, by acting directly or indirectly on the pyroptosis signaling, to exert effects on a variety of diseases, including tumors (Xie et al., 2019; He et al., 2020; Wan et al., 2020; Xu et al., 2020; Wang et al., 2021). However, the roles of pyroptosis-related lncRNAs (PRLs) in GBM have never been reported.

In the present study, we identified and validated a novel pyroptosis-related lncRNA signature (PRLS) in three independent datasets. The molecular characteristics, clinical significances, tumor microenvironment, immune checkpoints profiles, and benefits of chemotherapy and immunotherapy regarding PRLS were also explored. The PRLS demonstrated the outstanding performances in prognosis prediction, and more importantly, PRLS also has implications for the immunotherapy and chemotherapy of different risk groups. In summary, we believe that the PRLS contributes to furnishing extra evidence for risk stratification and treatment guidance for GBM patients.

METHODS AND MATERIALS

Patient data collection and acquisition of long noncoding RNAs

The RNA-sequencing (RNA-seq) data with relevant clinical information of GBM patients were downloaded using UCSC

Xena from the Cancer Genome Atlas (TCGA, <https://portal.gdc.cancer.gov/>). Two validation datasets were obtained from the Chinese Glioma Genome Atlas (CGGA, <http://www.cgga.org.cn>) database also including both the transcriptome data and the clinical characteristics. The clinical baseline data are summarized in the Supplementary Material: **Supplementary Table S1**.

A total of 51 pyroptosis-related genes (PRGs) were acquired from the REACTOME_PYROPTOSIS gene set in the Molecular Signatures Database (MSigDB) and prior published papers (Man and Kanneganti, 2015; Wang and Yin, 2017; Karki and Kanneganti, 2019; Xia et al., 2019), which are presented in **Supplementary Table S2**. Based on the annotation of the Genome Reference Consortium Human Build 38 (GRCh38), we extracted the expression matrix of 15,229 lncRNAs in the TCGA dataset (named TCGA) and 4,311 and 4,356 lncRNAs in the two CGGA datasets (named c325, c693), respectively.

Consensus clustering

Based on the expression profiles of the 51 PRGs, the consensus clustering was performed to decipher heterogeneous subtypes in the TCGA dataset. This process was implemented *via* the “ConsensusClusterPlus” R package with the parameters of 500 iterations, resample rate of 0.8. The clustering heatmaps, empirical cumulative distribution function (CDF), and proportion of ambiguous clustering (PAC) analysis were illustrated based on k-value (2–9). We further performed the principal component analysis (PCA) to compare the differences between different groups based on the clustering results.

Construction of weighted gene coexpression networks and identification of pyroptosis-related long noncoding RNAs in glioblastoma

Gene coexpression network analysis was specifically performed on tumor tissues using the “WGCNA” R package. First, we selected the top 5,000 genes with median absolute deviation (MAD), and the samples with outlier were removed using the hclust algorithm. The minimum number of module genes was set at 30. The cutreeDynamic function was employed for tree pruning of the gene hierarchical clustering dendrograms generating coexpression modules and correlated modules ($r > 0.75$) were merged. The disparity of the module Eigengenes (ME) was calculated using the module Eigengenes function. Correlation between Eigengenes values with the pyroptosis-related subtypes was evaluated by Pearson’s correlation coefficient. The module with the highest correlation coefficient was extracted for further investigation.

Development and validation of pyroptosis-related long noncoding RNAs

For the genes in the identified module, univariate Cox regression was performed to determine the associations between genes and OS in the TCGA cohort. Then the LASSO Cox regression algorithm was applied to identify the key lncRNAs and construct a prediction model. The lncRNAs with nonzero coefficients were defined as the key lncRNAs. Based on these key lncRNAs, the prognostic risk score was calculated for each patient predicated upon the formula shown below:

$$\text{Risk score} = \sum_{i=1}^n \text{Coef}_i \times \text{Expr}_i$$

where Coef_i was defined as the coefficient of lncRNAs 1) and Expr_i represented the expression level. Patients were classified into high- and low-risk groups according to the median value. The Kaplan–Meier (KM) survival analysis and log-rank test were conducted to estimate survival difference between two groups using the “survminer” R packages. Time-dependent receiver operating characteristic (ROC) curves were profiled to examine the predictive accuracy of this model using the “survivalROC” R package, and the area under the curve (AUC) values demonstrated distinction. The decision curve analysis (DCA) was performed to evaluate the intended clinical effectiveness of this model. Subsequently, this PRLS model was further validated in two CGGA cohorts (c325 and c693).

Gene set enrichment analysis

Gene set enrichment analysis (GSEA) was conducted to reveal the significantly enriched biological processes and potential molecular mechanisms regarding PRLS using the hallmark gene sets (h.all.v7.4. symbols). Hallmark summarizes and represents specific well-defined biological states or processes and demonstrates coherent expression (Liberzon et al., 2015). These gene sets were extensively utilized in cancer-related studies (Liu et al., 2021e; Liu et al., 2021f). The gene terms with |normalized enrichment score (NES)| >1 and false discovery rate (FDR) <0.01 were considered to be statistically significant.

Cell infiltration

Five algorithms, including ESTIMATE, CIBERSORT, xCell, ssGSEA, and MCPcounter, were applied to evaluate the immune infiltration patterns based on the transcriptome expression in the TCGA dataset. Correlations between the PRLS and the immune cell infiltration were further explored.

Evaluation of immune checkpoint profiles

The relationship of a total of 27 immune checkpoints with PRLS, including B7-CD28 family (PD-1, PD-L1, PD-L2, CTLA4, CD276, HHLA2, ICOS, ICOSLG, TMIGD2, and VTCN1), the TNF superfamily (BTLA, CD27, CD40, CD40LG, CD70, TNFRSF18, TNFRSF4, TNFRSF9, and TNFSF14), and several other molecules (ENTPD1, FGL1, HAVCR2, IDO1, LAG3, NCR3, NT5E, and SIGLEC15) (Liu et al., 2021c) were further explored.

Immunotherapy assessment

The Tumor Immune Dysfunction and Exclusion (TIDE) and T-cell inflammatory signature (TIS) methods were applied to predict the immunotherapeutic response to immune checkpoint blockade (ICB) for each patient. The TIDE algorithm is a kind of computational approach, with modules of two individual mechanisms of tumor immune evasion, including T-cell dysfunction and T-cell exclusion in tumors (Jiang et al., 2018). The TIS, proposed by Ayers et al. could predict the putative

efficacy of PD-1 inhibitors (Ayers et al., 2017). We then carried out the Subclass Mapping (SubMap) method, which employs the GSEA algorithm to evaluate the similarity of expression profiles between risk groups and patients with different responses to immunotherapy.

Estimation of the sensitivity of chemotherapeutic agents

We further applied the “pRRophetic” R package to estimate the chemotherapeutic response by predicting the half-maximal inhibitory concentration (IC50) of 138 agents between two groups (Liu et al., 2021b; Liu et al., 2021d). The “pRRophetic” R package utilized a ridge regression model to use expression data as predictors and output as drug sensitivity values (of the drug of interest) (Geeleher et al., 2014). Higher IC50 indicated higher drug sensitivity.

Statistics

All data processing, statistical analysis, and plotting were conducted in the R 4.0.5 software. Fisher’s exact test or Pearson’s Chi-squared test was applied to compare categorical variables. The Wilcoxon rank-sum test or t-test was utilized in continuous variables between the two groups. All *p*-values were two-sided, with *p*-value <0.05 deemed as statistically significant.

RESULTS

Identification of prognostic pyroptosis-related lncRNAs in glioblastoma patients

The workflow of our study is shown in **Supplementary Figure S1**. The GSEA was performed on 51 PRGs to assess whether pyroptosis was significantly associated with GBM in our study. The results demonstrated that the pyroptosis pathway of GBM is dysregulated compared with normal samples (**Figure 1A**). Subsequently, the clustering analysis classified the patients into different clusters, based on the expression levels of the PRGs. Eventually, *k*=2 was determined as the optimal clustering number according to the clustering heatmaps, PAC analysis, and CDF curves (**Figures 1C–E**). GBM patients in TCGA cohort were clustered into two clusters. The PCA results demonstrated the spatial distribution of gene profiles, and the two clusters were distributed into distinct directions indicating that pyroptosis genes can distinguish GBM patients (**Figure 1B**). The heatmap demonstrated higher expression levels of PRGs in cluster 1 versus cluster 2 (**Figure 1F**). As expected, most of the PRGs were overexpressed in cluster 1 (**Supplementary Figure S2**). In recognizing the lncRNAs associated with pyroptosis cluster, the “WGCNA” R package was employed to construct the weighted coexpression network. The soft power of $\beta=3$ (scale-free $R^2=0.95$) was chosen for the soft thresholding to acquire coexpressed gene modules (**Figure 2A**). Ultimately, we obtained a total of 15 modules for subsequent analysis, the heatmap graph of topological overlap matrix (TOM), and the

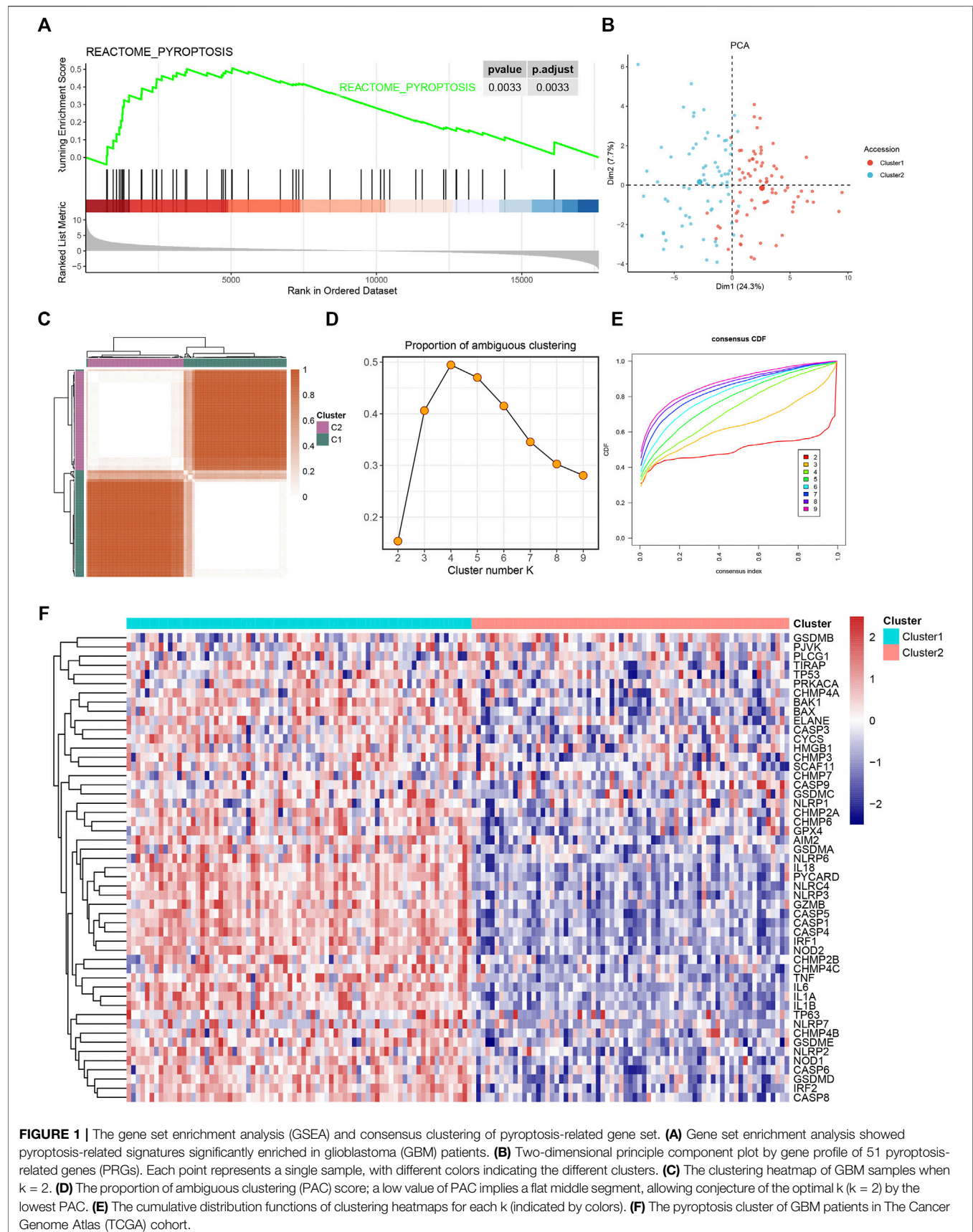


FIGURE 1 | The gene set enrichment analysis (GSEA) and consensus clustering of pyroptosis-related gene set. **(A)** Gene set enrichment analysis showed pyroptosis-related signatures significantly enriched in glioblastoma (GBM) patients. **(B)** Two-dimensional principle component plot by gene profile of 51 pyroptosis-related genes (PRGs). Each point represents a single sample, with different colors indicating the different clusters. **(C)** The clustering heatmap of GBM samples when $k = 2$. **(D)** The proportion of ambiguous clustering (PAC) score; a low value of PAC implies a flat middle segment, allowing conjecture of the optimal k ($k = 2$) by the lowest PAC. **(E)** The cumulative distribution functions of clustering heatmaps for each k (indicated by colors). **(F)** The pyroptosis cluster of GBM patients in The Cancer Genome Atlas (TCGA) cohort.

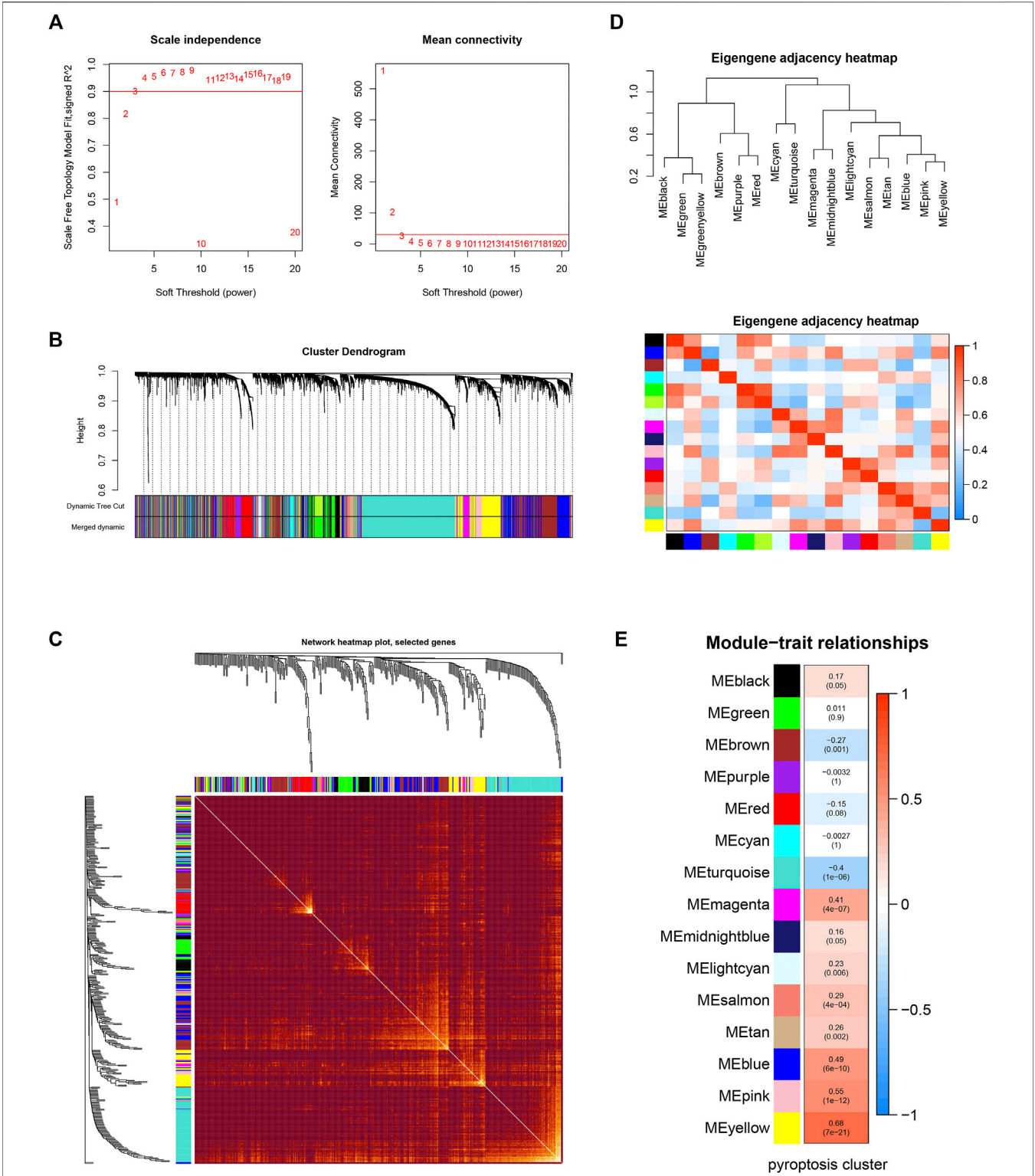
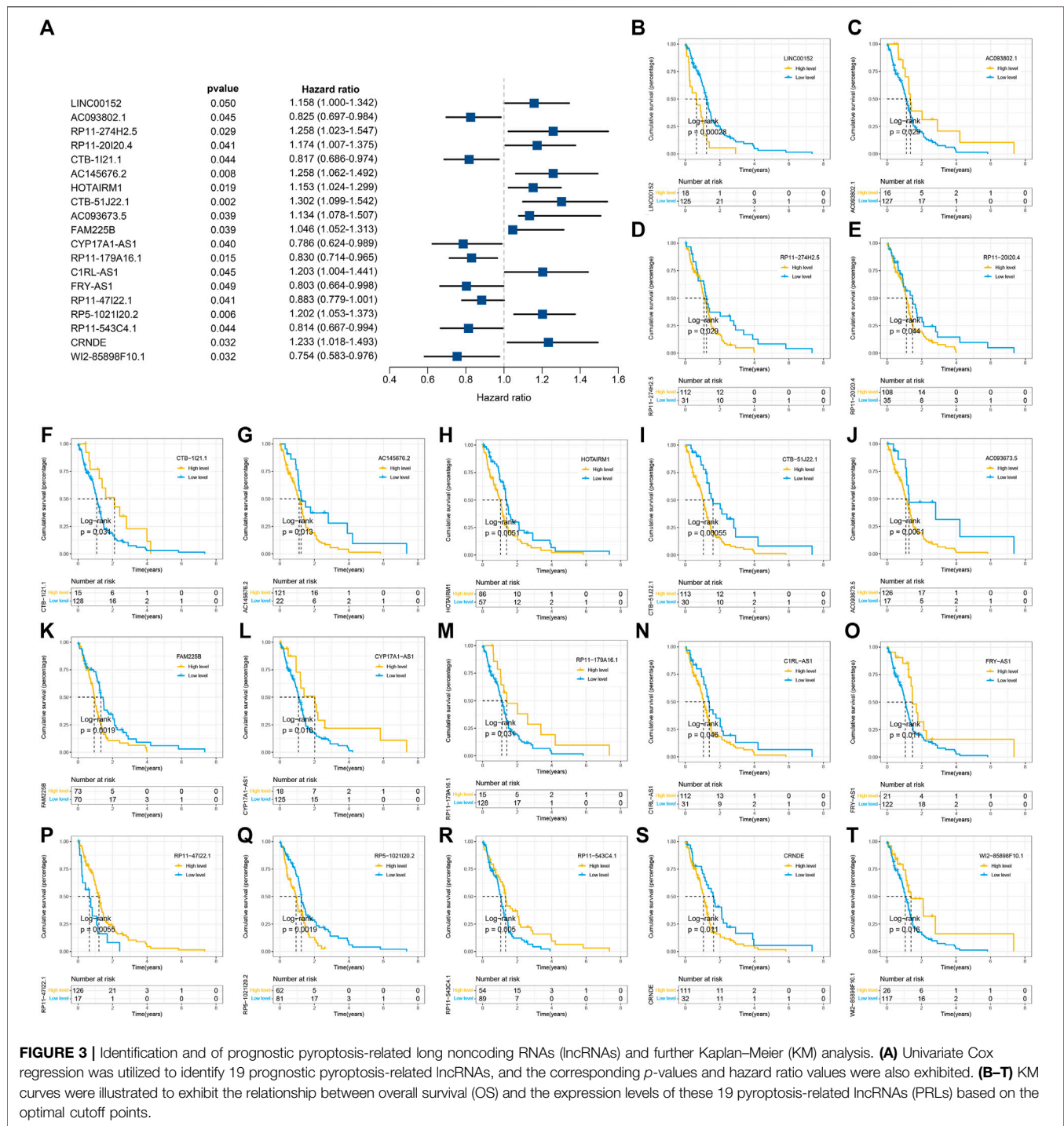


FIGURE 2 | Weighted gene coexpression network analysis. **(A)** Analysis of network topology for various soft-thresholding powers. The left panel shows the scale-free fit index (y-axis) as a function of the soft-thresholding power (x-axis). The right panel displays the mean connectivity (degree, y-axis) as a function of the soft-thresholding power (x-axis). **(B)** Clustering dendrogram of genes, with dissimilarity based on topological overlap, together with assigned module colors. **(C)** Visualizing the gene network using a heatmap plot. The heatmap depicts the Topological Overlap Matrix (TOM) among all genes in the analysis. Light color represents low overlap and the progressively darker red color represents a higher overlap. Blocks of darker colors along the diagonal are the modules. **(D)** Visualization of the eigengene network representing the relationships among the modules and the clinical trait weight. **(E)** Module-trait associations: Each row corresponds to a module eigengene and the column to the pyroptosis cluster. Each cell contains the corresponding correlation and *p*-value.



relationships among the modules are illustrated in **Figure 2**. The yellow module composed of 616 lncRNAs showed the highest gene significance with pyroptosis cluster and, hence, was selected for further analysis (**Figure 2E** and **Supplementary Figure S3**). Based on the selected module genes, we obtained 19 prognostic PRLs shared by three datasets. KM analysis was exploited to investigate the relationship between the expression levels of these

19 PRLs and OS. Consistent with the results of univariate Cox regression, 11 of the PRLs (LINC00152, RP11-274H2.5, RP11-20I20.4, AC145676.2, HOTAIRM1, CTB-51J22.1, AC093673.5, FAM225B, C1RL-AS1, RP5-102I20.2, and CRNDE) were risky factors, while the remaining 8 were protective factors, including AC093802.1, CTB-1I21.1, CYP17A1-AS1, RP11-179A16.1, FRY-AS1, RP11-47I22.1, RP11-543C4.1, and WI2-85898F10.1

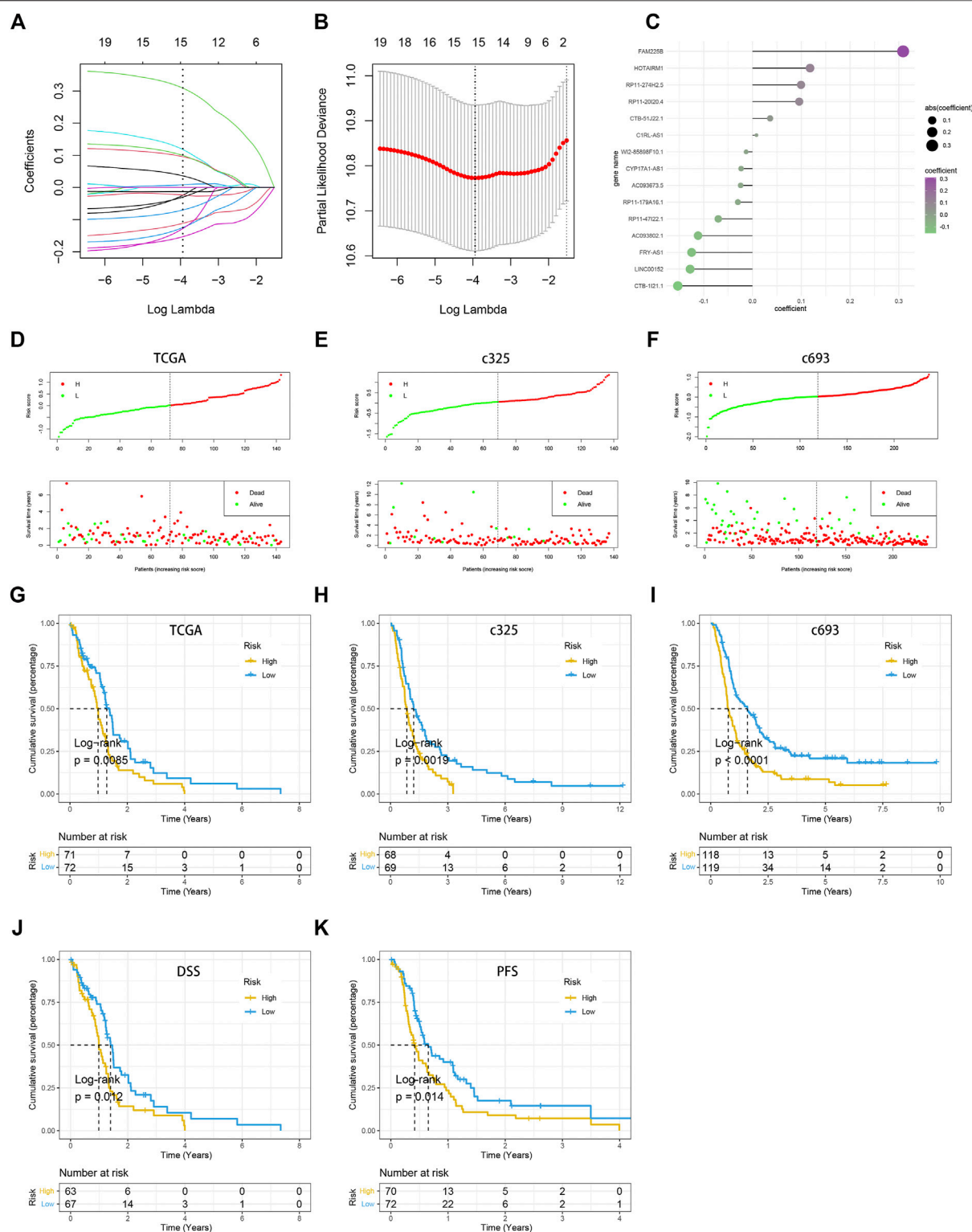
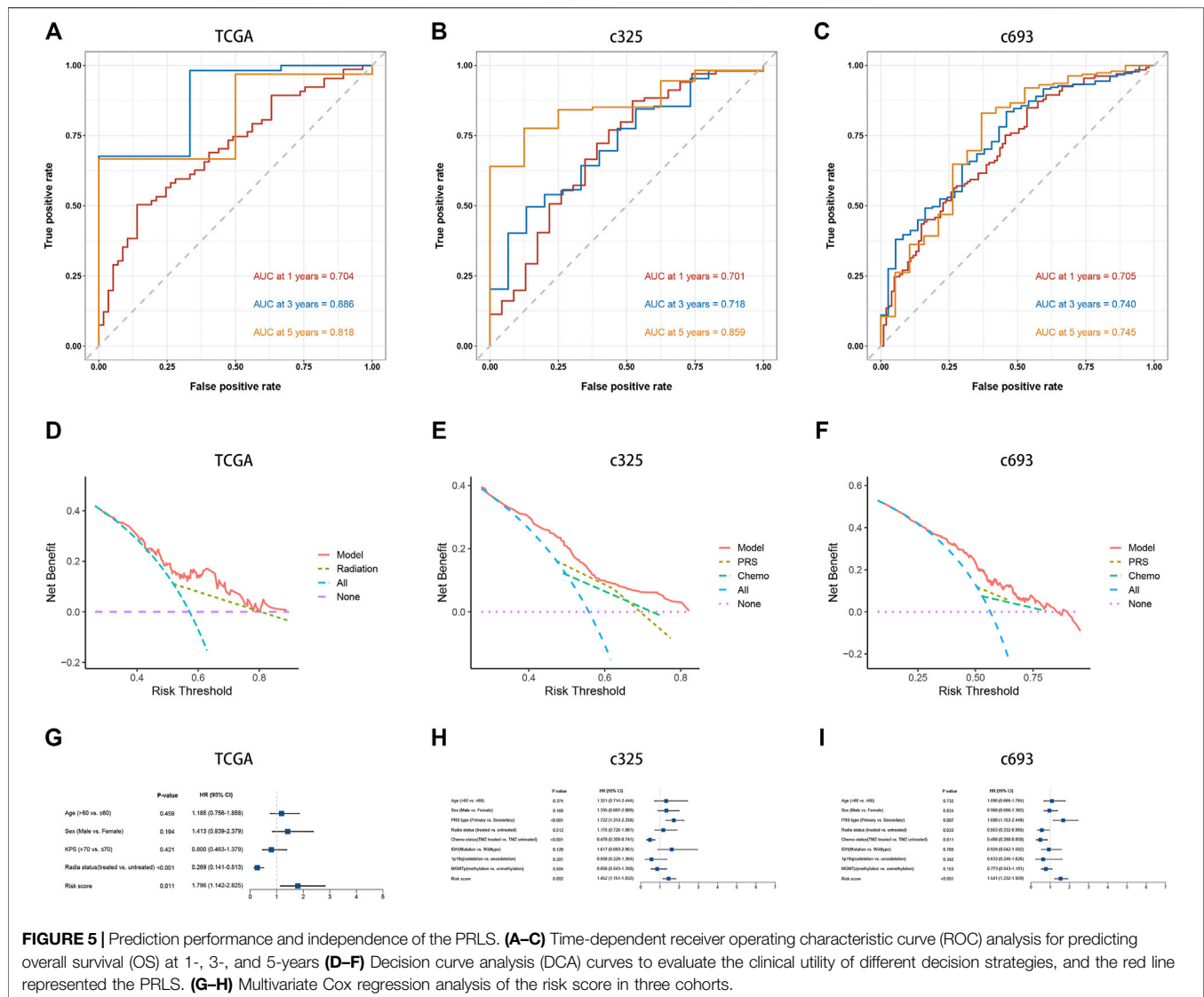


FIGURE 4 | Construction of the pyroptosis-related lncRNA signature (PRLS). **(A)** LASSO coefficient profiles of the candidate PRLs for PRLS construction. **(B)** Ten-time cross-validations to tune the parameter selection in the LASSO model. The two dotted vertical lines are drawn at the optimal values by minimum criteria (left) and 1-SE criteria (right). **(C)** LASSO coefficient profiles of the candidate genes for RAIS construction. **(D–F)** The scattergrams of the risk score (up) and survival status (down) of each patient in the TCGA, c325, c693 cohorts, respectively. In the upper parts of the scattergrams, the red and green dots represent high-risk (“H”) and low-risk groups (“L”), respectively, and in the lower part of the scattergrams, death and survival, respectively. **(G–I)** Kaplan–Meier overall survival (OS) analysis of the high-risk and low-risk groups based on the PRLS and median risk scores in the TCGA, c325, c693 cohorts, respectively. **(J)** Kaplan–Meier curve of disease-specific survival (DSS) in the TCGA cohort. **(K)** Kaplan–Meier curve of progression free survival (PFS) in the TCGA cohort.

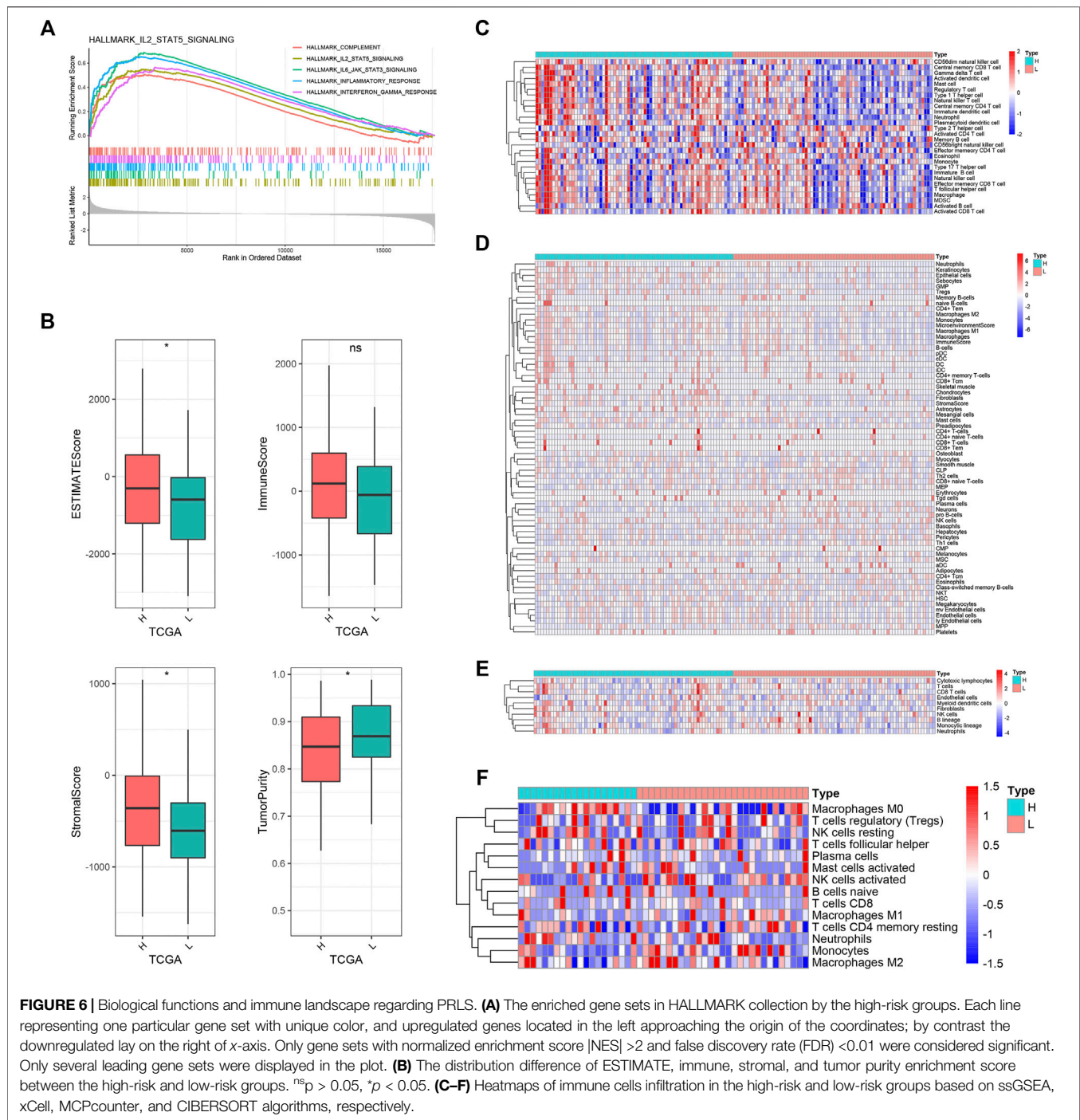


(Figure 3). Furthermore, the coexpression relationships between the 51 PRGs and the 19 lncRNAs were investigated (Supplementary Figure S4).

Construction and verification of the pyroptosis-related long noncoding RNAs

The LASSO Cox analysis was performed to generate a pyroptosis-related lncRNA signature of 15 PRLs (Figures 4A, B), including FAM225B, HOTAIRM1, RP11-274H2.5, RP11-20120.4, CTB-51J22.1, C1RL-AS1, W12-85898F10.1, CYP17A1-AS1, AC093673.5, RP11-179A16.1, RP11-47I22.1, AC093802.1, FRY-AS1, LINC00152, and CTB-11I21.1, of which regression coefficients are exhibited in Figure 4C. A risk score for each patient was calculated based on the expression and coefficients of PRLs, then the GBM patients were divided into two subgroups (low- and high-risk groups) using the median value in TCGA

cohort. The KM survival curves show that GBM patients in the high-risk group had significantly shorter OS compared with the low-risk group (Figure 4G). The scattergrams of the risk score and survival status revealed shorter OS time and more dismal events with increasing risk score (Figure 4D). The promising prediction ability of PRLs was corroborated by the ROC curves for 1-, 3-, and 5-year OS rates (AUC = 0.704, 0.886, and 0.818, respectively; Figures 5A, D). Decision curves showed the highest net benefit for the PRLs (“Model”) compared with default strategies (“All” and “None”) and clinical traits with prognostic significance (“Radiation” represented radiotherapy). Multivariate Cox regression analysis demonstrated that the PRLs was an independent prognostic factor even including available clinical variables (Figure 5G). Additionally, the disease-specific survival (DSS) and progression-free survival (PFS) regarding PRLs were further scrutinized. Patients in the high-risk group showed longer DSS as well as PFS (Figures 4J, K).



Assessment of the prognostic pyroptosis signature in external test cohorts

In two CGGA cohorts, c325 and c693, as we did in the TCGA database, the GBM patients were classified into high- and low-risk groups based on cutoff values of median risk scores as well (Figures 4H, I). The signature in both validation datasets showed favorable predictive performances for OS rates of 1-, 3-, and 5-years (AUC = 0.701, 0.718, and 0.859 in c325 and AUC = 0.705, 0.740,

and 0.745 in c693, respectively Figures 5B, C). The DCA also revealed the highest predictive value of clinical prognosis for the PRLS (“Model”) compared with the default strategies (“All” and “None”) and clinical variables with prognostic significance (“PRS” represented primary/secondary status; “Chemo” represented chemotherapy) (Figures 5E, F). In line with the TCGA training cohort, our PRLS model could independently predict the prognosis of GBM patients in two external test cohorts (Figures 5H, I).

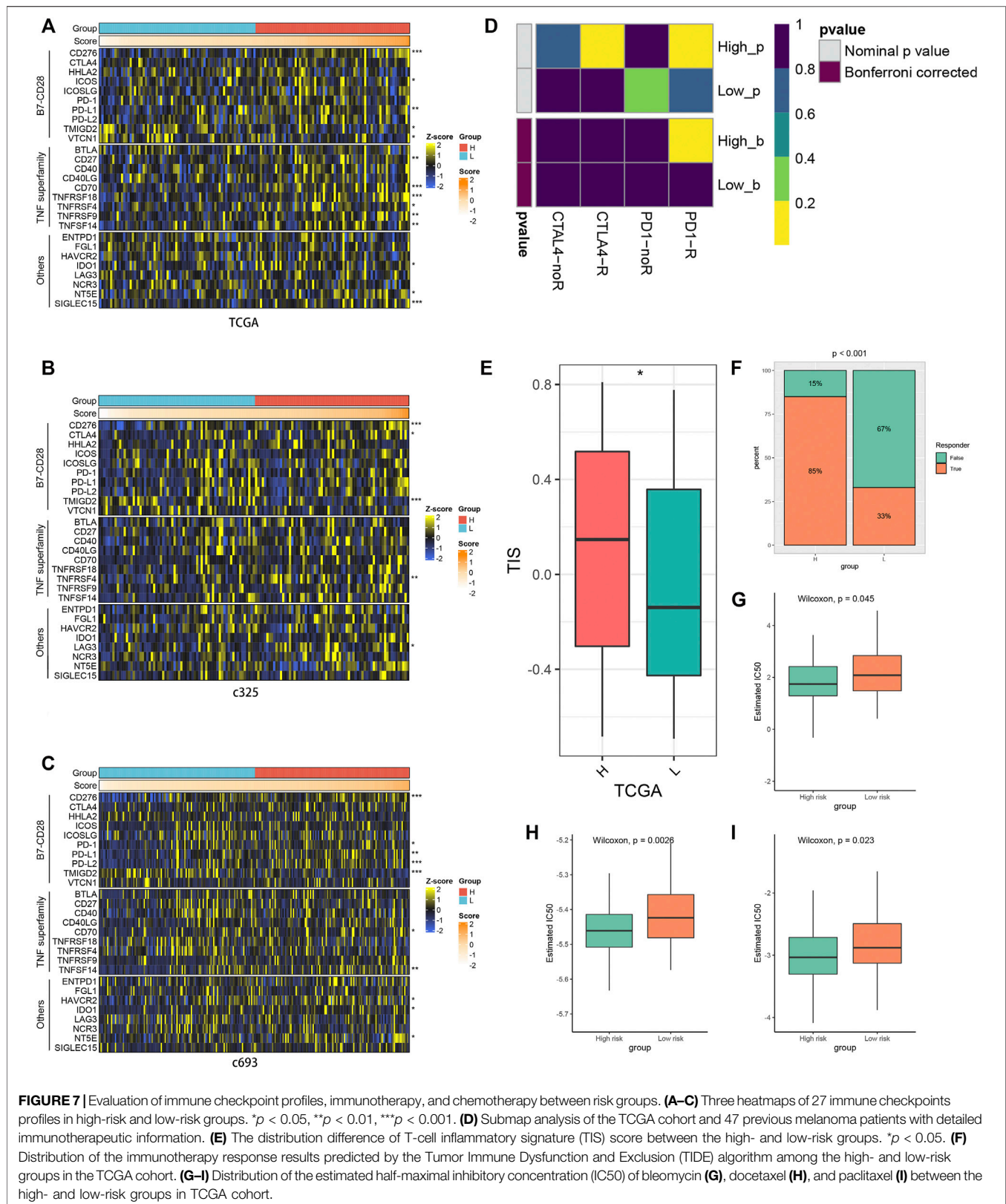


FIGURE 7 | Evaluation of immune checkpoint profiles, immunotherapy, and chemotherapy between risk groups. **(A–C)** Three heatmaps of 27 immune checkpoints profiles in high-risk and low-risk groups. $*p < 0.05$, $**p < 0.01$, $***p < 0.001$. **(D)** Submap analysis of the TCGA cohort and 47 previous melanoma patients with detailed immunotherapeutic information. **(E)** The distribution difference of T-cell inflammatory signature (TIS) score between the high- and low-risk groups. $*p < 0.05$. **(F)** Distribution of the immunotherapy response results predicted by the Tumor Immune Dysfunction and Exclusion (TIDE) algorithm among the high- and low-risk groups in the TCGA cohort. **(G–I)** Distribution of the estimated half-maximal inhibitory concentration (IC50) of bleomycin **(G)**, docetaxel **(H)**, and paclitaxel **(I)** between the high- and low-risk groups in TCGA cohort.

Immune landscape of pyroptosis-related long noncoding RNAs

The GSEA was carried out to explore the potential biological processes and mechanisms connected with different risk groups of GBM. The results manifested that the high-risk group enriched multiple immune-related hallmarks, including IL2_STAT5 signaling (NES = 2.24, FDR < 0.01), IL6_JAK_STAT3 signaling (NES = 2.46, FDR < 0.01), inflammatory response (NES = 2.66, FDR < 0.01), interferon_gamma response (NES = 2.31, FDR < 0.01), and complement (NES = 2.07, FDR < 0.01) (Figure 6A). Pathways closely related to the low-risk group showed limited significance with immunity, such as spermatogenesis (NES = -1.89, FDR < 0.01), pancreas_beta_cells (NES = -1.80, FDR < 0.01), KRAS_signaling (NES = -1.76, FDR < 0.01), E2F_targets (NES = -1.64, FDR < 0.01), and oxidative_phosphorylation (NES = -1.59, FDR < 0.01) (Supplementary Figure S5A).

Subsequently, we further investigated the immune landscape of PRLS. The ESTIMATE software was employed to deduce the proportion of stromal and immune fractions. The high-risk group showed the superior overall, stromal, and immune scores and lower tumor purity than the low-risk group in the TCGA dataset (Figure 6B). We then performed CIBERSORT, xCell, ssGSEA, and MCPcounter methods to further evaluate the proportion of immune cells. Overall, the infiltration of immune cells was more abundant in the high-risk group, and indicated more active immune status and immune response compared with the low-risk group (Figures 6C–F). The correlations between the PRLS and the immune cell infiltrations were further examined, some of which showed a higher level of immune infiltration in the high-risk group compared with the low-risk group, mainly comprising the T-cell family, such as central memory CD4 T cell, effector memory CD8 T cell, gamma delta T cell, type 1 T-helper cell, gamma delta T cell, natural killer T cell, neutrophil, CD56dim natural killer cell, plasmacytoid dendritic cell, etc. (Supplementary Figures S5B, C).

Evaluation of the immune checkpoint profiles and the efficacy of immunotherapy

The connections between immune checkpoints and the PRLS in three cohorts are presented in Figures 7A–C. Overall, most of them were significantly upregulated in the high-risk group, and it was noteworthy that CD276 and TMIGD2 showed this trend in all three cohorts, which suggested being potential therapeutic targets. The TIDE web tool and the TIS algorithm were applied to infer the responses to ICB. The results demonstrated that patients in the high-risk group showed more responders and higher TIS score, which indicated that they were more inclined to derive considerable clinical benefit from ICB treatment. The SubMap algorithm was performed to explore the response to immunotherapy based on 47 previous melanoma patients with immunotherapeutic information; as expected, the high-risk group showed better immunotherapy sensitivity (Figures 7D–F).

Other chemotherapeutic agents

Furthermore, we utilized the pRRophetic algorithm to predict the sensitivity to 138 drugs in the high- and low-risk groups. The results

revealed 70 drugs with a significant variation of treatment sensitivity between the high- and low-risk groups (Supplementary Figure S6). Most of the discrepant drugs displayed enhanced responses in the low-risk group, and the majority of which were gene-targeting drugs, such as BMS-536924, an orally available GF-1R/IR inhibitor in glioma, which inhibits viability and migration of glioma cells and suppresses glioma tumor growth (Zhou, 2015). There were also some chemotherapy drugs. Bleomycin, a water-soluble glycopeptide antibiotic, induces single- and double-stranded DNA breaks and can be enhanced by photochemical internalization (PCI) in glioma cells (Mathews et al., 2012) and showed higher sensitivity in the low-risk group as well. For two other chemotherapy drugs, docetaxel and paclitaxel, the differences of treatment between the two groups were in keeping with bleomycin (Figures 7G–I). These results provided new perspectives for adjuvant treatments in GBM.

DISCUSSION

A total of 517 GBM patients from TCGA and CGGA datasets were involved in our study to probe into the prognostic significance of pyroptosis-related lncRNAs. Nineteen PRLs were recognized to have prognostic value in all three public databases (TCGA, c325, and c693), and 15 of them were included to construct a PRLS for predicting the OS of GBM patients by using LASSO Cox analysis. Based on the median risk score as the cutoff value, GBM patients were divided into the high- and low-risk subgroups, and the former had worse clinical outcomes. ROC curves and DCA demonstrated good predictive power of our model. Multivariate Cox regression analysis showed that PRLS was an independent risk factor for OS. Furthermore, we utilized several current acknowledged algorithms to reveal the immune characteristics between subgroups. In general, the high-risk group showed higher immune infiltration fraction and activity. The immunotherapy and chemotherapy responses were further explored regarding the PRLS. Patients in the high-risk group showed higher sensitivity to immunotherapy but less to chemotherapy. Overall, the PRLS we developed showed excellent performance in assessing the immune landscape and the prognosis prediction and treatment of GBM patients; thus, the specific application in clinical practice in the future is worth expecting.

Pyroptosis is a hotspot that has been increasingly studied in recent years, and many research have demonstrated that it is involved in the body's inflammatory responses and closely related to the growth, development, and metastasis of various tumors (Xia et al., 2019; Fang et al., 2020; Ruan et al., 2020), but how it performs in an lncRNA-dependent manner during glioma progression remains unclear. Pyroptosis regulated a variety of biological processes in tumors mediated by lncRNAs. Downregulation of lncRNA-XIST suppressed the progression of non-small cell lung cancer (NSCLC) by triggering pyroptosis cell death mediated by miR-335/SOD2/ROS signal pathway (Liu et al., 2019). lncRNA ADAMTS9-AS2 activated pyroptosis cell death mediated by NLRP3 through sponging miR-223-3p to increase the sensitivity of cisplatin in gastric cancer (GC) to inhibit tumor development (Ren et al., 2020). Furthermore, lncRNA RP1-85F18.6 retrained the pyroptosis in colorectal cancer (CRC) by regulating the expression of ΔNp63

and promoted the proliferation and invasion of tumor cells. Having listed all the above, we believe that more attention should be paid to the roles of lncRNAs in the process of pyroptosis to determine potential prognostic markers and therapeutic targets of cancers.

We constructed a 15-PRL signature contributing to providing a novel tool of prognosis prediction, and some of them appeared in previous studies. FAM225B was found upregulated in recurrent GBMs (rGBMs), which was associated with the poor prognosis of rGBM patients (Li et al., 2020). High expression of HOTAIRM1 increased the evasion and migration of GBM cells (Xie et al., 2020). LINC00152 showed upregulated level in the mesenchymal subtype and isocitrate dehydrogenase1 wild type, and the expression of LINC00152 was increased with glioma grade (Wang et al., 2018). These genes mentioned above, which resulted in adverse outcomes with increased expression levels, also proved to be risk factors in the PRLS model. FRY-AS1 was demonstrated as a protective factor according to the research of Niu et al. (2020), which was consistent with the results of our study as well. Otherwise, some of the genes included in the PRLS have not been elucidated in glioma but in other tumors. A high expression level of C1RL-AS1 was shown to be associated with dismal prognosis of GC; similar results were presented in our study of GBM (Liu R. et al., 2021). There are also several genes that have never been reported in any tumor, which have significant prognostic value in our study, thus, needing further research.

Based on the PRLS, we aimed to interrogate and compare the characteristic differences in the immune microenvironment between tumor subgroups. GSEA demonstrated that the high-risk group is enriched in IL2-STAT5 signaling, IL6-JAK-STAT3 signaling, inflammatory response, interferon-gamma response, and complement in hallmark analysis, which suggested improved immunocompetence. The CIBERSORT, ssGSEA, xCell, and MCPcounter algorithms were applied to explore the immune cell infiltration in two groups, and some of them were found increased in the high-risk group, such as central memory CD4 T cell, central memory CD8 T cell, natural killer T cell, neutrophil, and so on. Moreover, we also detected enhanced levels of immune checkpoints in the high-risk group. Tumor immune microenvironment, mostly consisting of stromal immune cells, plays vital roles in the proliferation, migration, and invasion of tumors and may be a crucial determinant of response to immune checkpoint blockade therapy (Mohme et al., 2020; Liu R. et al., 2021; Zhang et al., 2021). Unsurprisingly, the high-risk group showed higher sensitivity to immunotherapy, which indicated our model points out new directions and shows optimistic clinical application prospects in distinguishing patients suitable for immunotherapy.

To further explore the underlying role of our model in clinical decision making, we extensively interrogated the sensitivity of various drugs, with emphasis on gene-targeted drugs and potential chemotherapeutic drugs regarding PRLS. BMS-536924, a GF-1R/IR inhibitor that suppresses the growth of glioma, showed better responses in the low-risk group. Similarly, several kinds of chemotherapy drugs like bleomycin, docetaxel, and paclitaxel also showed a better propensity for benefit in the low-risk group. This may provide more opportunities for patients to receive effective treatment early and curb tumor progression to prolong survival.

The present study has some limitations as well. First, the clinical information of public datasets was very insufficient; hence, the potential connections between risk groups and important clinical characteristics may be disregarded. Second, our work focused on all types of glioblastomas without taking molecular subtypes, spatial heterogeneity, and so forth, into account. Notably, patients with IDH mutation exhibited better outcome compared with patients with IDH wild type (Molinaro et al., 2020). More detailed comparisons of diverse subtypes of GBM demand substantial clinical and sequencing data to secure progressive results. Third, several genes we submitted have not been particularly studied yet, thus, corroborative experiments deserve future research. Last, machine learning algorithms were implemented to explore the efficiency of different groups to immunotherapy and chemotherapy; nevertheless, further clinical validation is needed.

In summary, we developed and verified a novel pyroptosis-related lncRNA signature with remarkable ability and stability for survival prediction in GBM. Patients in the high PRLS group displayed enhanced immune activity and better efficacy of immunotherapy, while those in the low PRLS group tended to benefit more from chemotherapy. These results amplified the perception of PRLs in GBM and facilitated precise treatment and clinical management.

DATA AVAILABILITY STATEMENT

The original contributions presented in the study are included in the article/**Supplementary Material**, further inquiries can be directed to the corresponding authors.

AUTHOR CONTRIBUTIONS

XW and XH designed this work. ZX and ZL integrated and analyzed the data, and wrote the manuscript. ZX, ZL, XF, SZ, LL, QD, CG, XG, TL, YZ, and LD edited and revised the manuscript. XW and XH read and approved the final manuscript. All authors read and approved the manuscript and agreed to be accountable for all aspects of the research in ensuring that the accuracy or integrity of any part of the work is appropriately investigated and resolved.

FUNDING

The study is supported by the National Natural Science Foundation of China (81972361) and the Natural Science Foundation of Henan Province (182300410379).

SUPPLEMENTARY MATERIAL

The Supplementary Material for this article can be found online at: <https://www.frontiersin.org/articles/10.3389/fcell.2022.805291/full#supplementary-material>

REFERENCES

- Ayers, M., Lunceford, J., Nebozhyn, M., Murphy, E., Loboda, A., Kaufman, D. R., et al. (2017). IFN- γ -related mRNA Profile Predicts Clinical Response to PD-1 Blockade. *J. Clin. Invest.* 127 (8), 2930–2940. doi:10.1172/JCI91190
- Delgado-Martin, B., and Medina, M. A. (2020). Advances in the Knowledge of the Molecular Biology of Glioblastoma and its Impact in Patient Diagnosis, Stratification, and Treatment. *Adv. Sci.* 7 (9), 1902971. doi:10.1002/adv.201902971
- Ding, J., Wang, K., Liu, W., She, Y., Sun, Q., Shi, J., et al. (2016). Erratum: Pore-Forming Activity and Structural Autoinhibition of the Gasdermin Family. *Nature* 540 (7631), 150. doi:10.1038/nature20106
- Fang, Y., Tian, S., Pan, Y., Li, W., Wang, Q., Tang, Y., et al. (2020). Pyroptosis: A New Frontier in Cancer. *Biomed. Pharmacother.* 121, 109595. doi:10.1016/j.bioph.2019.109595
- Geeleher, P., Cox, N., and Huang, R. S. (2014). pRRophetic: an R Package for Prediction of Clinical Chemotherapeutic Response from Tumor Gene Expression Levels. *PLoS One* 9 (9), e107468. doi:10.1371/journal.pone.0107468
- He, D., Zheng, J., Hu, J., Chen, J., and Wei, X. (2020). Long Non-coding RNAs and Pyroptosis. *Clinica Chim. Acta* 504, 201–208. doi:10.1016/j.cca.2019.11.035
- Jiang, P., Gu, S., Pan, D., Fu, J., Sahu, A., Hu, X., et al. (2018). Signatures of T Cell Dysfunction and Exclusion Predict Cancer Immunotherapy Response. *Nat. Med.* 24 (10), 1550–1558. doi:10.1038/s41591-018-0136-1
- Karki, R., and Kanneganti, T.-D. (2019). Diverging Inflammasome Signals in Tumorigenesis and Potential Targeting. *Nat. Rev. Cancer* 19 (4), 197–214. doi:10.1038/s41568-019-0123-y
- Kong, Y., Feng, Z., Chen, A., Qi, Q., Han, M., Wang, S., et al. (2019). The Natural Flavonoid Galangin Elicits Apoptosis, Pyroptosis, and Autophagy in Glioblastoma. *Front. Oncol.* 9, 942. doi:10.3389/fonc.2019.00942
- Kovacs, S. B., and Miao, E. A. (2017). Gasdermins: Effectors of Pyroptosis. *Trends Cell Biol.* 27 (9), 673–684. doi:10.1016/j.tcb.2017.05.005
- Li, J., Zhang, Q., Ge, P., Zeng, C., Lin, F., Wang, W., et al. (2020). FAM225B Is a Prognostic lncRNA for Patients with Recurrent Glioblastoma. *Dis. Markers* 2020, 1–7. doi:10.1155/2020/8888085
- Liberzon, A., Birger, C., Thorvaldsdóttir, H., Ghandi, M., Mesirov, J. P., and Tamayo, P. (2015). The Molecular Signatures Database Hallmark Gene Set Collection. *Cel Syst.* 1 (6), 417–425. doi:10.1016/j.cels.2015.12.004
- Liu, J., Yao, L., Zhang, M., Jiang, J., Yang, M., and Wang, Y. (2019). Downregulation of lncRNA-XIST Inhibited Development of Non-small Cell Lung Cancer by Activating miR-335/SOD2/ROS Signal Pathway Mediated Pyroptotic Cell Death. *Aging* 11 (18), 7830–7846. doi:10.18632/aging.102291
- Liu, R., Yang, F., Yin, J.-Y., Liu, Y.-Z., Zhang, W., and Zhou, H.-H. (2021a). Influence of Tumor Immune Infiltration on Immune Checkpoint Inhibitor Therapeutic Efficacy: A Computational Retrospective Study. *Front. Immunol.* 12, 685370. doi:10.3389/fimmu.2021.685370
- Liu, Z., Liu, L., Jiao, D., Guo, C., Wang, L., Li, Z., et al. (2021b). Association of RYR2 Mutation with Tumor Mutation Burden, Prognosis, and Antitumor Immunity in Patients with Esophageal Adenocarcinoma. *Front. Genet.* 12, 669694. doi:10.3389/fgenet.2021.669694
- Liu, Z., Lu, T., Li, J., Wang, L., Xu, K., Dang, Q., et al. (2021c). Clinical Significance and Inflammatory Landscape of a Novel Recurrence-Associated Immune Signature in Stage II/III Colorectal Cancer. *Front. Immunol.* 12, 702594. doi:10.3389/fimmu.2021.702594
- Liu, Z., Wang, L., Guo, C., Liu, L., Jiao, D., Sun, Z., et al. (2021d). TTN/OBSCN 'Double-Hit' Predicts Favourable Prognosis, 'immune-hot' Subtype and Potentially Better Immunotherapeutic Efficacy in Colorectal Cancer. *J. Cel Mol Med* 25 (7), 3239–3251. doi:10.1111/jcmm.16393
- Liu, Z., Wang, L., Liu, L., Lu, T., Jiao, D., Sun, Y., et al. (2021e). The Identification and Validation of Two Heterogeneous Subtypes and a Risk Signature Based on Ferroptosis in Hepatocellular Carcinoma. *Front. Oncol.* 11, 619242. doi:10.3389/fonc.2021.619242
- Liu, Z., Zhang, Y., Dang, Q., Wu, K., Jiao, D., Li, Z., et al. (2021f). Genomic Alteration Characterization in Colorectal Cancer Identifies a Prognostic and Metastasis Biomarker: FAM83A. *Front. Oncol.* 11, 632430. doi:10.3389/fonc.2021.632430
- Majc, B., Novak, M., Kopitar-Jerala, N., Jewett, A., and Breznik, B. (2021). Immunotherapy of Glioblastoma: Current Strategies and Challenges in Tumor Model Development. *Cells* 10 (2), 265. doi:10.3390/cells10020265
- Man, S. M., and Kanneganti, T.-D. (2015). Regulation of Inflammasome Activation. *Immunol. Rev.* 265 (1), 6–21. doi:10.1111/imr.12296
- Mathews, M. S., Blickenstaff, J. W., Shih, E.-C., Zamora, G., Vo, V., Sun, C.-H., et al. (2012). Photochemical Internalization of Bleomycin for Glioma Treatment. *J. Biomed. Opt.* 17 (5), 058001. doi:10.1117/1.JBO.17.5.058001
- Mohme, M., Maire, C. L., Schliffke, S., Joosse, S. A., Alawi, M., Matschke, J., et al. (2020). Molecular Profiling of an Osseous Metastasis in Glioblastoma during Checkpoint Inhibition: Potential Mechanisms of Immune Escape. *Acta Neuropathol. Commun.* 8 (1), 28. doi:10.1186/s40478-020-00906-9
- Molinari, A. M., Hervey-Jumper, S., Morshed, R. A., Young, J., Han, S. J., Chunduru, P., et al. (2020). Association of Maximal Extent of Resection of Contrast-Enhanced and Non-contrast-enhanced Tumor with Survival within Molecular Subgroups of Patients with Newly Diagnosed Glioblastoma. *JAMA Oncol.* 6 (4), 495–503. doi:10.1001/jamaoncol.2019.6143
- Niu, X., Sun, J., Meng, L., Fang, T., Zhang, T., Jiang, J., et al. (2020). A Five-lncRNAs Signature-Derived Risk Score Based on TCGA and CGGA for Glioblastoma: Potential Prospects for Treatment Evaluation and Prognostic Prediction. *Front. Oncol.* 10, 590352. doi:10.3389/fonc.2020.590352
- Oronsky, B., Reid, T. R., Oronsky, A., Sandhu, N., and Knox, S. J. (2020). A Review of Newly Diagnosed Glioblastoma. *Front. Oncol.* 10, 574012. doi:10.3389/fonc.2020.574012
- Ren, N., Jiang, T., Wang, C., Xie, S., Xing, Y., Piao, D., et al. (2020). lncRNA ADAMTS9-AS2 Inhibits Gastric Cancer (GC) Development and Sensitizes Chemoresistant GC Cells to Cisplatin by Regulating miR-223-3p/NLRP3 axis. *Aging* 12 (11), 11025–11041. doi:10.18632/aging.103314
- Roos, A., Ding, Z., Loftus, J. C., and Tran, N. L. (2017). Molecular and Microenvironmental Determinants of Glioma Stem-like Cell Survival and Invasion. *Front. Oncol.* 7, 120. doi:10.3389/fonc.2017.00120
- Ruan, J., Wang, S., and Wang, J. (2020). Mechanism and Regulation of Pyroptosis-Mediated in Cancer Cell Death. *Chemico-Biological Interactions* 323, 109052. doi:10.1016/j.cbi.2020.109052
- Rynkeviciene, R., Simiene, J., Strainiene, E., Stankevicius, V., Usinskiene, J., Miseikyte Kaubriene, E., et al. (2018). Non-Coding RNAs in Glioma. *Cancers* 11 (1), 17. doi:10.3390/cancers11010017
- Shi, J., Zhao, Y., Wang, K., Shi, X., Wang, Y., Huang, H., et al. (2015). Cleavage of GSDMD by Inflammatory Caspases Determines Pyroptotic Cell Death. *Nature* 526 (7575), 660–665. doi:10.1038/nature15514
- Stupp, R., Taillibert, S., Kanner, A., Read, W., Steinberg, D. M., Lhermitte, B., et al. (2017). Effect of Tumor-Treating Fields Plus Maintenance Temozolomide vs Maintenance Temozolomide Alone on Survival in Patients with Glioblastoma. *JAMA* 318 (23), 2306–2316. doi:10.1001/jama.2017.18718
- Tan, A. C., Ashley, D. M., López, G. Y., Malinzak, M., Friedman, H. S., and Khasraw, M. (2020). Management of Glioblastoma: State of the Art and Future Directions. *CA A. Cancer J. Clin.* 70 (4), 299–312. doi:10.3322/caac.21613
- Wan, P., Su, W., Zhang, Y., Li, Z., Deng, C., Li, J., et al. (2020). lncRNA H19 Initiates Microglial Pyroptosis and Neuronal Death in Retinal Ischemia/reperfusion Injury. *Cell Death Differ* 27 (1), 176–191. doi:10.1038/s41418-019-0351-4
- Wang, B., and Yin, Q. (2017). AIM2 Inflammasome Activation and Regulation: A Structural Perspective. *J. Struct. Biol.* 200 (3), 279–282. doi:10.1016/j.jsb.2017.08.001
- Wang, L.-Q., Zheng, Y.-Y., Zhou, H.-J., Zhang, X.-X., Wu, P., and Zhu, S.-M. (2021). lncRNA-Fendrr Protects against the Ubiquitination and Degradation of NLRC4 Protein through HERC2 to Regulate the Pyroptosis of Microglia. *Mol. Med.* 27 (1), 39. doi:10.1186/s10020-021-00299-y
- Wang, W., Wu, F., Zhao, Z., Wang, K.-Y., Huang, R.-Y., Wang, H.-Y., et al. (2018). Long Noncoding RNA LINC00152 Is a Potential Prognostic Biomarker in Patients with High-Grade Glioma. *CNS Neurosci. Ther.* 24 (10), 957–966. doi:10.1111/cns.12850
- Wesseling, P., and Capper, D. (2018). WHO 2016 Classification of Gliomas. *Neuropathol. Appl. Neurobiol.* 44 (2), 139–150. doi:10.1111/nan.12432
- Xia, X., Wang, X., Cheng, Z., Qin, W., Lei, L., Jiang, J., et al. (2019). The Role of Pyroptosis in Cancer: Pro-cancer or Pro-"host"? *Cell Death Dis* 10 (9), 650. doi:10.1038/s41419-019-1883-8

- Xie, C., Wu, W., Tang, A., Luo, N., and Tan, Y. (2019). lncRNA GAS5/miR-452-5p Reduces Oxidative Stress and Pyroptosis of High-Glucose-Stimulated Renal Tubular Cells. *DmsO* 12, 2609–2617. doi:10.2147/DMSO.S228654
- Xie, P., Li, X., Chen, R., Liu, Y., Liu, D., Liu, W., et al. (2020). Upregulation of HOTAIRM1 Increases Migration and Invasion by Glioblastoma Cells. *Aging* 13 (2), 2348–2364. doi:10.18632/aging.202263
- Xu, S., Wang, J., Jiang, J., Song, J., Zhu, W., Zhang, F., et al. (2020). TLR4 Promotes Microglial Pyroptosis via lncRNA-F630028O10Rik by Activating PI3K/AKT Pathway after Spinal Cord Injury. *Cel Death Dis* 11 (8), 693. doi:10.1038/s41419-020-02824-z
- Zhang, T., Li, Y., Zhu, R., Song, P., Wei, Y., Liang, T., et al. (2019). Transcription Factor P53 Suppresses Tumor Growth by Prompting Pyroptosis in Non-small-cell Lung Cancer. *Oxidative Med. Cell Longevity* 2019, 1–9. doi:10.1155/2019/8746895
- Zhang, Y., Liu, Z., Li, X., Liu, L., Wang, L., Han, X., et al. (2021). Comprehensive Molecular Analyses of a Six-Gene Signature for Predicting Late Recurrence of Hepatocellular Carcinoma. *Front. Oncol.* 11, 732447. doi:10.3389/fonc.2021.732447
- Zhou, Q. (2015). BMS-536924, an ATP-Competitive IGF-1R/IR Inhibitor, Decreases Viability and Migration of Temozolomide-Resistant Glioma Cells

In Vitro and Suppresses Tumor Growth *In Vivo*. *Ott* 8, 689–697. doi:10.2147/OTT.S80047

Conflict of Interest: The authors declare that the research was conducted in the absence of any commercial or financial relationships that could be construed as a potential conflict of interest.

Publisher's Note: All claims expressed in this article are solely those of the authors and do not necessarily represent those of their affiliated organizations, or those of the publisher, the editors, and the reviewers. Any product that may be evaluated in this article, or claim that may be made by its manufacturer, is not guaranteed nor endorsed by the publisher.

Copyright © 2022 Xing, Liu, Fu, Zhou, Liu, Dang, Guo, Ge, Lu, Zheng, Dai, Han and Wang. This is an open-access article distributed under the terms of the Creative Commons Attribution License (CC BY). The use, distribution or reproduction in other forums is permitted, provided the original author(s) and the copyright owner(s) are credited and that the original publication in this journal is cited, in accordance with accepted academic practice. No use, distribution or reproduction is permitted which does not comply with these terms.

GLOSSARY

AUC area under the curve

CDF cumulative distribution function

CGGA Chinese Glioma Genome Atlas

CRC colorectal cancer

DCA decision curve analysis

FDR false discovery rate

GBM glioblastoma

GC gastric cancer

GRCh38 Genome Reference Consortium Human Build 38

GSDMD gasdermin D

GSDME gasdermin E

GSEA Gene set enrichment analysis

IC50 half-maximal inhibitory concentration

ICB immune checkpoint blockade

KM Kaplan–Meier

lncRNA Long non-coding RNA

MAD median absolute deviation

ME module Eigengene

MSigDB Molecular Signatures Database

NES normalized enrichment score

NSCLC non-small cell lung cancer

OS overall survival

PAC proportion of ambiguous clustering

PCA principal component analysis

PCI photochemical internalization

PRG pyroptosis-related genes

PRL pyroptosis-related lncRNA

PRLS pyroptosis-related lncRNA signature

rGBM recurrent GBM

RNA-seq RNA-sequencing

ROC curve receiver operating characteristic curve

SubMap Subclass Mapping

TCGA the Cancer Genome Atlas

TIDE Tumor Immune Dysfunction and Exclusion

TIS T-cell inflammatory signature

TOM topological overlap matrix

WGCNA gene co-expression network analysis

WHO World Health Organization



DLX6-AS1: A Long Non-coding RNA With Oncogenic Features

Soudeh Ghafouri-Fard¹, Sajad Najafi², Bashdar Mahmud Hussien^{3,4}, Aryan R. Ganjo⁴, Mohammad Taheri^{5,6*} and Mohammad Samadian^{7*}

¹Department of Medical Genetics, School of Medicine, Shahid Beheshti University of Medical Sciences, Tehran, Iran,

²Department of Medical Biotechnology, School of Advanced Technologies in Medicine, Shahid Beheshti University of Medical Sciences, Tehran, Iran, ³Department of Pharmacognosy, College of Pharmacy, Hawler Medical University, Kurdistan Region, Erbil, Iraq, ⁴Center of Research and Strategic Studies, Lebanese French University, Erbil, Iraq, ⁵Urology and Nephrology Research Center, Shahid Beheshti University of Medical Sciences, Tehran, Iran, ⁶Institute of Human Genetics, Jena University Hospital, Jena, Germany,

⁷Skull Base Research Center, Loghman Hakim Hospital, Shahid Beheshti University of Medical Sciences, Tehran, Iran

OPEN ACCESS

Edited by:

Ri Cui,
Wenzhou Medical University, China

Reviewed by:

Hamed Shoorei,
Birjand University of Medical
Sciences, Iran
Huanlei Huang,
Guangdong Provincial People's
Hospital, China

*Correspondence:

Mohammad Taheri
Mohammad.taheri@uni-jena.de
Mohammad Samadian
mdsamadian@gmail.com

Specialty section:

This article was submitted to
Molecular and Cellular Oncology,
a section of the journal
Frontiers in Cell and Developmental
Biology

Received: 23 July 2021

Accepted: 04 February 2022

Published: 25 February 2022

Citation:

Ghafouri-Fard S, Najafi S, Hussien BM, Ganjo AR, Taheri M and Samadian M (2022) DLX6-AS1: A Long Non-coding RNA With Oncogenic Features. *Front. Cell Dev. Biol.* 10:746443. doi: 10.3389/fcell.2022.746443

Long non-coding RNAs (lncRNAs) are a heterogeneous group of ncRNAs with characteristic size of more than 200 nucleotides. An increasing number of lncRNAs have been found to be dysregulated in many human diseases particularly cancer. However, their role in carcinogenesis is not precisely understood. DLX6-AS1 is an lncRNAs which has been unveiled to be up-regulated in various number of cancers. In different cell studies, DLX6-AS1 has shown oncogenic role *via* promoting oncogenic phenotype of cancer cell lines. Increase in tumor cell proliferation, migration, invasion, and EMT while suppressing apoptosis in cancer cells are the effects of DLX6-AS1 in development and progression of cancer. In the majority of cell experiment, mediator miRNAs have been identified which are sponged and negatively regulated by DLX6-AS1, and they in turn regulate expression of a number of transcription factors, eventually affecting signaling pathways involved in carcinogenesis. These pathways form axes through which DLX6-AS1 promotes carcinogenicity of cancer cells. Xenograft animal studies, also have confirmed enhancing effect of DLX6-AS1 on tumor growth and metastasis. Clinical evaluations in cancerous patients have also shown increased expression of DLX6-AS1 in tumor tissues compared to healthy tissues. High DLX6-AS1 expression has shown positive association with advanced clinicopathological features in cancerous patients. Survival analyses have demonstrated correlation between high DLX6-AS1 expression and shorter survival. In cox regression analysis, DLX6-AS1 has been found as an independent prognostic factor for patients with various types of cancer.

Keywords: DLX6-AS1, non-coding RNA, lncRNA, cancer, miRNA 3

INTRODUCTION

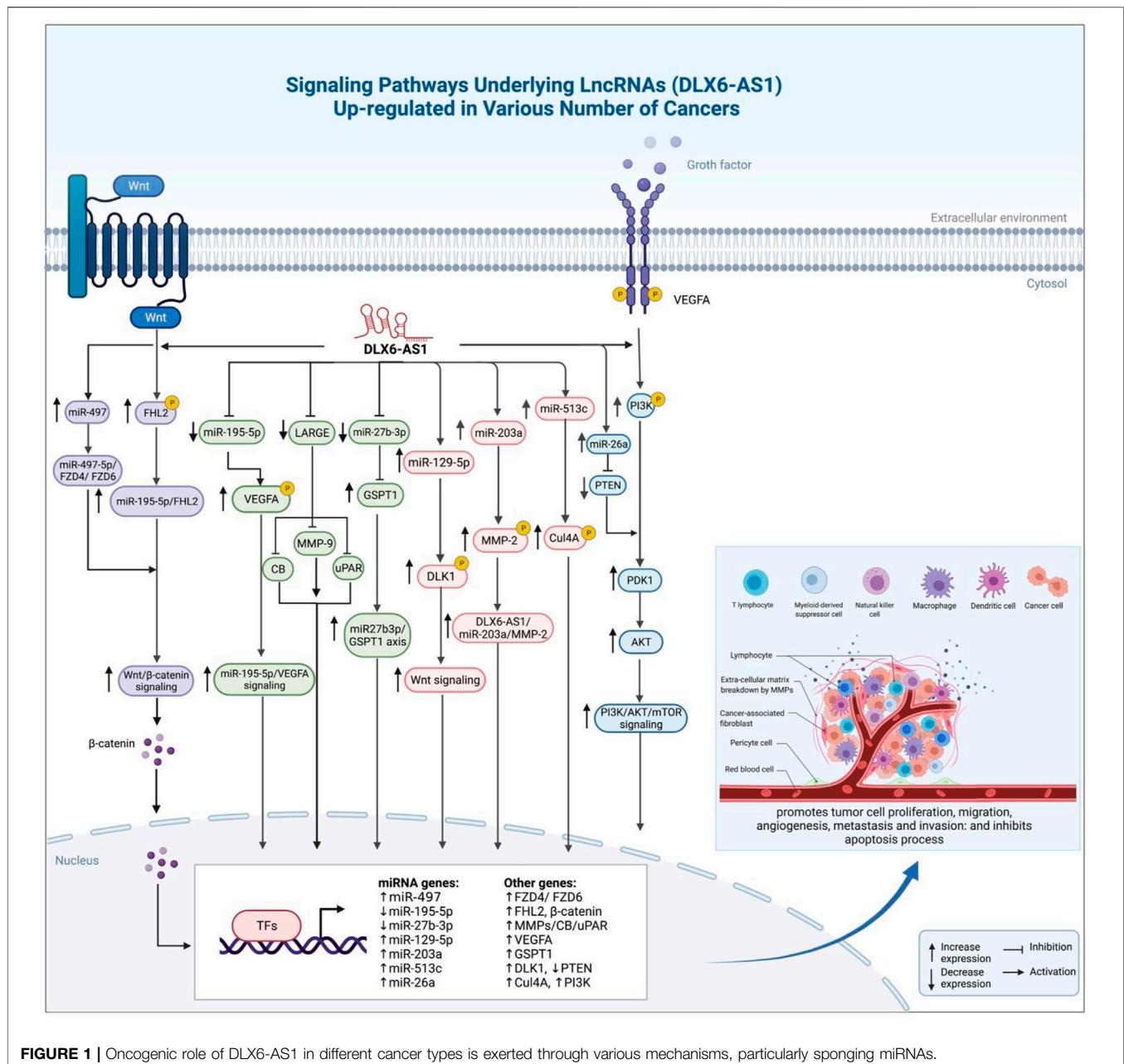
In complex organisms, genome sequencing analyses have unveiled that just a small fraction of genome (e.g., 1–2% for mammals) encodes for protein *via* coding RNAs or messenger RNAs (mRNAs) that are located in the middle of central dogma making connection between DNA and corresponding protein. These protein-coding regions are those which have been described as genes for more than half a century in biology literature. However, the majority of large genomes i.e., more than 80% is transcribed to non-coding RNAs (ncRNAs) for which no corresponding protein have

been found, but a huge number of regulatory functions are recognized. Unlike the primary expectations which termed ncRNAs as “junk” DNA without biological importance, today it is clarified that they are involved in gene regulation at transcriptional and post-transcriptional levels, and through which they play critical roles in a vast number of biological processes such as imprinting, methylation, and silencing *via* several interactions with DNA, RNA, and proteins (Mattick, 2001). Based on size and function of transcripts, ncRNAs are categorized in several classes including microRNAs (miRNAs), small interfering RNAs (siRNAs), PIWI-interacting RNAs and long ncRNAs (lncRNAs). Transcripts of more than 200 nucleotide length are classified as lncRNAs which were primarily reported by Okazaki *et al.* in an analysis of mouse transcriptome in 2002 (Okazaki *et al.*, 2002). RNA polymerase II is predominantly responsible for transcription of lncRNAs. They mainly endure capping, polyadenylation, splicing after transcription, and also trimethylation on histone 3 corresponding to lysine 4 (H3K4me3) (Losko *et al.*, 2016; Bertone *et al.*, 2004; Guttman *et al.*, 2009). Thousands of heterogeneous lncRNAs have been identified in multicellular organisms [60,000 encoding loci in human genome (Iyer *et al.*, 2015)] showing tissues specificity which is also conserved during evolution (Necsulea *et al.*, 2014) and acting as regulators of gene expression both in nucleus or cytoplasm (Fatica and Bozzoni, 2014) suggesting their involvement in specific biologic processes. Several databases have been created to store and provide access to an increasing number of lncRNAs. Examples of these databases are TRlnc for regulatory lncRNAs in humans (Li *et al.*, 2020a), lncRNASNP1 and 2 for single nucleotide polymorphisms (SNPs) of human and mouse lncRNAs (Gong *et al.*, 2014; Miao *et al.*, 2017), lncRNA2Target v2.0 for target genes of lncRNAs (Cheng *et al.*, 2018), CRISPRlnc for validated single guide RNAs (sgRNAs) used in clustered regularly interspaced short palindromic repeats (CRISPR)-associated protein number 9 (Cas9) gene editing technology for lncRNAs (Chen *et al.*, 2018) and clusLnc2Cancer for effective lncRNAs in human cancers (Ning *et al.*, 2015). They act in *cis* and *trans* modes by gathering and localizing transcription factors to a locus. Gene expression regulation at several levels including transcription, translation and splicing, epigenetic regulation in X-chromosome inactivation or dosage compensation, genomic imprinting, involvement in developmental and differential processes, neurogenesis, regulation of cell cycle, and cell transportation are among the fundamental roles which have been recognized for lncRNAs (Mattick, 2009; Wilusz *et al.*, 2009; Wu *et al.*, 2013; Dey *et al.*, 2014; Fatica and Bozzoni, 2014). Accordingly, an increasing number of lncRNAs have been associated with various types of human diseases. Dysregulation in expression levels or mutation of lncRNAs are found to play role in the pathogenesis of diseases like age-related diseases, cardiovascular diseases (Uchida and Dimmeler, 2015), kidney and liver diseases (Takahashi *et al.*, 2014; Ignarski *et al.*, 2019), ophthalmologic diseases (Wawrzyniak *et al.*, 2018), neurodegenerative and other diseases affecting central nervous system (CNS) (Pastori and Wahlestedt, 2012; Wan *et al.*, 2017), and particularly various types of cancer. Mediation of a number of cancer-associated

processes like cell cycle regulation, epigenetic regulation, and involvement in signaling pathways and hormone-related pathways indicate potential roles of lncRNAs act as contributors in the development and progression of cancer (Sahu *et al.*, 2015). MALAT1, HOTAIR, H19, HOTTIP, ANRIL, and NEAT1 are among the most famous lncRNAs which have been mostly studied in many types of cancer exhibiting dysregulation in cancer cells, tissues and body fluids of affected patients. In this review, we aim to have an overview of studies which have assessed tumorigenic effects of the lncRNA distal-less homeobox 6 antisense RNA 1 (DLX6-AS1) in three levels of cell, animal, and human studies. In humans, *DLX6-AS1* gene is located on chromosome 7q21.3, primarily identified by Feng *et al.* (2006) to promote *DLX5/6* function in *trans* mode. This lncRNA has been found to be up-regulated in a growing number of different types of cancerous tissues compared to normal tissues. Promoting carcinogenesis *via* increasing tumor cell proliferation, migration, and invasion through enhancing Epithelial–Mesenchymal Transition (EMT) along with suppression of apoptosis and chemosensitivity have been shown in cell studies of *DLX6-AS1* overexpression. Enhanced tumor growth and metastasis has confirmed tumorigenic potentials of *DLX6-AS1* in animal studies. Correlation between high *DLX6-AS1* expression and advanced clinicopathological features and also poor prognosis and survival in cancerous patients has suggested *DLX6-AS1* not only as a diagnostic and prognostic biomarker but also as a therapeutic target.

Functional Effects of DLX6-AS1 on Cell Proliferation, Apoptosis and Migration

Cancer cell lines have been used to evaluate function of *DLX6-AS1* in cell cycle progression, cell proliferation and apoptosis. Moreover, high throughput RNA sequencing and also confirmation *via* quantitative real-time polymerase chain reaction (qRT-PCR) analyses have facilitated identification of differentially expressed lncRNAs in cancer cell lines compared to controls. *In vitro* experiments have shown significant increase in expression levels of *DLX6-AS1* in cancer cell lines. In different cell experiment, it has been demonstrated that *DLX6-AS1* overexpression promotes tumor cell proliferation, migration, and invasion, while suppressing apoptosis. In cell counting, colony formation, and 5-Bromo-2-deoxyUridine (BrdU) assays, decreased proliferation of cancer cells is reported for *DLX6-AS1* knockdown. Wound healing, Matrigel and Transwell assays for assessment tumor cell migration and invasion show suppressed metastatic capability of cancerous cells under *DLX6-AS1* silencing. Flowcytometry also demonstrated cell cycle arrest in treated cancer cells. Furthermore, decreased cell viability and elevated apoptosis in 3-(4,5-dimethylthiazol-2-yl)-2,5-diphenyl-2H-tetrazolium bromide (MTT), flowcytometry, and apoptotic marker assays have unveiled increased apoptosis in *DLX6-AS1*-silenced cancer cells. In hepatocellular carcinoma (HCC), *DLX6-AS1* has been shown to be highly expressed in human HCC cell lines versus normal liver cells, while miR-513c as its downstream microRNA



exhibited down-regulation indicating DLX6-AS1 acts as sponge for this miRNA (Liu et al., 2020a). Cullin4A (*Cul4A*) was also known as target gene of miR-513c which showed increase in expression level following DLX6-AS1 up-regulation. In other words, DLX6-AS1 elevated *Cul4A* expression by binding to and sponging miR-513c. *Cul4A*, itself positively regulated activity of annexin A10 (*ANXA10*). DLX6-AS1 silencing using specific short hairpin RNA (shRNA) repressed cell viability, invasion, and migration of HCC cells. Also, *Cul4A* knockdown was shown to inhibit tumorigenic effects of HCC cells via inhibition of *ANXA10* degradation through ubiquitin-associated pathway. The results showed that DLX6-AS1 exerts its tumorigenic role via miR-513c/*Cul4A*/*ANXA10* axis. In a

distinct study (Zhang et al., 2017), DLX6-AS1 was shown to exert same tumorigenic roles in HCC cells via miR-203a/MMP-2 axis.

In other experiments, DLX6-AS1 has been shown to sponge many other miRNAs and affect transcription factors, genes or signaling pathways which eventually promotes malignant phenotypes. miRNAs which are mainly negatively regulated by up-stream DLX6-AS1 exhibit down-regulation in cancer tissues and cells, and their overexpression reverse the malignant phenotypes of DLX6-AS1 in cancer cell lines. Downstream factors demonstrate expression changes consistent with DLX6-AS1. Overexpression of these factors drives same influences with DLX6-AS1 overexpression. In a study in ovarian cancer (Kong and Zhang, 2020), miR-195-5p was shown to be down-regulated

TABLE 1 | an overview to the oncogenic influences of DLX6-AS1 in cell studies of different types of cancer.

Cancer type	Targets/Regulators and signaling pathways	Assessed cell lines	Function	References
HCC	miR-513c/Cul4A/ ANXA10 axis miR-203a/MMP-2 axis	Hep3B, HepG2, Huh7, PLC/PRF/5, and THLE-3 Hep3B, MHCC97L, HCCLM3, HepG2, Huh7, and LO2	Δ DLX6-AS1: \downarrow tumor cell viability, \downarrow invasion, and \downarrow migration Δ DLX6-AS1: \downarrow tumor cell proliferation, \downarrow invasion, and \downarrow migration	Liu et al. (2020a) Zhang et al. (2017)
Pancreas	miR-181b/ZEB2 axis miR-497-5p/FZD4/FZD6/ Wnt/ β -catenin axis	CAPAN-1, BxPC-3, SW 1990, PANC-1, and HPDE6-C7 Panc-1, AsPC-1, Bxpc-3, Capan-1, CFPAC-1, and MIA PaCa-2	Δ DLX6-AS1: \downarrow tumor cell proliferation, \downarrow migration, and \downarrow invasion $\uparrow\uparrow$ DLX6-AS1: \uparrow tumor cell proliferation, \uparrow migration, and \uparrow invasion, while Δ DLX6-AS1 reversed the tumorigenic effects	An et al. (2018) Yang et al. (2019a)
Prostate	miR-497-5p/SNCG axis DNMT1/LARGE axis	LNCap, DU145, PC-3, VCap, and WPMY1 CWR22rv1, LAPC-9, DU145, LNCaP, PC-3M, and PREC	Δ DLX6-AS1: \downarrow tumor cell proliferation, \uparrow apoptosis $\uparrow\uparrow$ DLX6-AS1: \uparrow tumor cell proliferation, \uparrow migration, and \uparrow invasion	Zhu et al. (2021) Zhao et al. (2020b)
Kidney (renal cell carcinoma; RCC) Liver	miR-26a/PTEN axis miR-424-5p/WEE1 axis CADM1/STAT3 axis	A498, ACHN, Caki-1, Caki-2, 786-O, G401, and HK-2 MHCC97L, HCCLM3, SK-HEP-1, Hep3B, Huh7, and HEK293T Hep3B, HepG2, SMMC-7721, HCCLM3, Huh7 and LO2	Δ DLX6-AS1: \downarrow tumor cell proliferation, and \downarrow colony formation Δ DLX6-AS1: \downarrow tumor cell proliferation, \downarrow migration, and \downarrow invasion Δ DLX6-AS1: \downarrow self-renewal, \downarrow amplification, and \downarrow proliferation in liver cancer stem cells	Zeng et al. (2017) Li et al. (2019a) Wu et al. (2019)
Neuroblastoma	miR-513c-5p/PLK4 axis miR-506-3p/STAT2 axis miR-497-5p/YAP1 axis miR-107/BDNF axis	SK-N-SH, SK-N-AS NB, and HUVEC SK-N-SH and LAN-6 SK-N-AS, SK-N-SH, SH-SY5Y, and SK-N-BE NB-1643, SK-N-SH, NB-1691, SK-N-AS, IMR-32, and SH-SY5Y	Δ DLX6-AS1: \downarrow tumor cell viability, \downarrow colony formation, \downarrow migration, \downarrow invasion, \uparrow apoptosis and \uparrow cell cycle arrest Δ DLX6-AS1: \downarrow tumor cell proliferation, \downarrow glycolysis and \uparrow cell cycle arrest at G1/S phase Δ DLX6-AS1: \downarrow tumor cell proliferation, \downarrow migration, \downarrow invasion, and \downarrow EMT Δ DLX6-AS1: \downarrow tumor cell proliferation, \downarrow migration, \downarrow invasion, and \uparrow apoptosis	Jia et al. (2020) Han et al. (2020) Li et al. (2020b) Li et al. (2019b)
Glioma	miR-197-5p/E2F1 axis	U251, T98G, U87MG, SHG44, and NHA	Δ DLX6-AS1: \downarrow tumor cell proliferation, and \downarrow invasion	Zhang et al. (2019b)
Osteosarcoma	miR-129-5p/DLK1 axis miR-641/HOXA9 axis	MG63 and U2OS Saos-2, MG-63, U2OS and hFOB	Δ DLX6-AS1: \downarrow number and size of tumor spheres, and \downarrow CSCs in osteosarcoma cell lines DLX6-AS1 triggers Wnt signaling Δ DLX6-AS1: \downarrow tumor cell proliferation, \downarrow migration, \downarrow invasion, and \uparrow apoptosis	Zhang et al. (2018) Zhang et al. (2019b)
Endometria	DLX6	HEC-1-B, HHUA, HEC-1-A, RL-952, and HEC-251	Δ DLX6-AS1: \downarrow tumor cell proliferation, \downarrow invasion, and \uparrow apoptosis DLX6-AS1 up-regulated DLX6 through inducing its promoter <i>via</i> p300/E2F1	Zhao and Xu, (2020)
Cervix	miR-16-5p/ARPP19 Axis miR-199a	SiHa, HeLa, C-33A, CaSki, and End1/E6E7 CaSki, ME-180, C-33A, SiHa, HeLa, and NC104	Δ DLX6-AS1: \downarrow tumor cell proliferation, \downarrow migration, \downarrow EMT and \uparrow apoptosis Δ DLX6-AS1: \downarrow tumor cell proliferation, \downarrow colony formation, \downarrow migration, and \uparrow apoptosis	Xie et al. (2020) Long et al. (2019)
Breast	miR-505-3p/RUNX2 axis	MDA-MB-231, MDA-MB-468, BT-474, MCF-7, T47D, and MCF-10A	Δ DLX6-AS1: \downarrow tumor cell proliferation, \downarrow migration, \downarrow invasion, and \uparrow apoptosis	Zhao et al. (2019)
Breast (triple-negative; TNBC)	miR-199b-5p/paxillin axis	CCD-1095Sk, MDA-MB-231, HCC 1806, HCC1599, and HS578 T	Δ DLX6-AS1: \downarrow tumor cell proliferation, \downarrow EMT, \uparrow apoptosis, and \downarrow chemoresistance to cisplatin	Du et al. (2020)
Ovaries	miR-195-5/FHL2 axis Notch	SKOV3, A2780, IOSE80, and 293 T IOSE80, HEY, SKOV3, and OVCAR-3	Δ DLX6-AS1: \downarrow tumor cell proliferation, \downarrow migration, \downarrow invasion, and \uparrow apoptosis Δ DLX6-AS1: \downarrow tumor cell proliferation, \downarrow migration, \downarrow invasion, and \uparrow apoptosis	Kong and Zhang, (2020) Zhao and Liu, (2019)
Bladder	miR-195-5p/VEGFA Wnt/ β -catenin	T24, RT4, 5637, J82, SW780, and SV-HUC-1 5637, J82, T24, and SV-HUC-1	Δ DLX6-AS1: \downarrow tumor cell proliferation, \downarrow migration, \downarrow invasion, and \uparrow apoptosis $\uparrow\uparrow$ DLX6-AS1: \uparrow tumor cell proliferation, \uparrow migration, \uparrow invasion, and \uparrow EMT. Knockdown reversed the malignancy phenotype of cells	Zhao et al. (2020a) Guo et al. (2019)

(Continued on following page)

TABLE 1 | (Continued) an overview to the oncogenic influences of DLX6-AS1 in cell studies of different types of cancer.

Cancer type	Targets/Regulators and signaling pathways	Assessed cell lines	Function	References
Colorectal	miR-223/HSP90B1 axis	T24, SW780, and SV-HUC-1	Δ DLX6-AS1: ↓ tumor cell proliferation, and ↓invasion	Fang et al. (2019)
	miR-26a/EZH2 Axis	DLD-1, HCT-116, HT-29, SW480, SW620, and NCM460	Δ DLX6-AS1: ↓ tumor cell proliferation, ↓migration, ↓invasion, and ↑cell cycle arrest	Kong et al. (2020)
	PI3K/AKT/mTOR pathway	HCT116, HT-29, SW480, and NCM460	↑↑ DLX6-AS1: ↑ tumor cell proliferation, ↑migration, ↑invasion, and ↓apoptosis. Δ DLX6-AS1 returned the malignant phenotype of cancer cells	Zhang et al. (2019a)
Larynx	miR-26a/TRPC3 axis	HEp-2 and Tu-177	Δ DLX6-AS1: ↓ tumor cell proliferation <i>via</i> decrease in mitochondrial radical oxygen species DLX6-AS1 regulates metabolism of cancer cells	Liu et al. (2020b)
	miR-376c	Hep2	Δ DLX6-AS1: ↓ tumor cell proliferation, ↓invasion, and ↑cell cycle arrest	Yang et al. (2019b)
Nasopharynx	miR-199a-5p/HIF-1α axis	S18, S26, CNE-1, CNE-2, HONE-1, 5-8F, and NP69	Δ DLX6-AS1: ↓ tumor cell proliferation, ↓migration, and ↓invasion	Yang et al. (2020)
Esophagus	--	EC109, KYSE30, and Het-1A	Δ DLX6-AS1: ↓ tumor cell proliferation, ↓migration, ↓invasion, and ↓EMT	Zhang et al. (2019c)
Stomach	miR-4290/PDK1 axis	HGC-27, SGC7901, MGC803, MKN45, and GES-1	Δ DLX6-AS1: ↓ tumor cell proliferation, ↑apoptosis, and caused glucose metabolism impairment	Qian et al. (2021)
	FUS/MAP4K1 axis	AGS, HGC-27, SGC-7901, BGC-823, and GES-1	Δ DLX6-AS1: ↓ tumor cell proliferation, ↓migration, and ↓EMT	Wu et al. (2020)
	miR-204-5p/OCT1 axis	MGC-803, HGC-27, MKN-7, MKN-28, MKN-45, AGS, SGC-7901, and GES-1	Δ DLX6-AS1: ↓ tumor cell proliferation, ↓migration, ↓invasion, and ↓EMT	Liang et al. (2020)
	--	HGC27, BGC823, SGC7901, AGS, and GES-1	Δ DLX6-AS1: ↓ tumor cell proliferation, ↓colony formation, ↓migration, ↓invasion, ↓EMT, and ↓cell cycle progression	Fu et al. (2019)
Lung (NSCLC)	miR-144/PRR11 axis	H1975 and A549	Δ DLX6-AS1: ↓ tumor cell proliferation, ↓migration, ↓invasion, and ↑apoptosis	Huang et al. (2019)
	miR27b3p/GSPT1 axis	CALU3, CALU6, A549, H1299, and HBE	Δ DLX6-AS1: ↓proliferation, ↓migration, and ↓invasion	Sun et al. (2019)
Ewing's sarcoma	miR-124-3p/CDK4 axis	SK-ES-1, A673, RD-ES, and mesenchymal stem cells (MSCs)	Δ DLX6-AS1: ↓ tumor cell proliferation, and ↑apoptosis	Lei et al. (2019)

Δ: knockdown or silencing, ↓: decrease or repression, ↑: increase or stimulation, ↑↑: overexpression, CSCs: cancer stem cells.

in cancer tissues and was identified as target of up-regulated DLX6-AS1. While DLX6-AS1 promoted cell proliferation, migration, and invasion in tumor cell lines, miR-195-5p overexpression reversed malignant phenotypes. Four and a half LIM domains protein 2 (FHL2) which is known to play role in development and progression of different types of cancer *via* activation of androgen receptor (AR or NR3C4), Wnt/β-catenin pathway or several genes was demonstrated as target of miR-195-5p. FHL2 overexpression exhibited same results on malignant phenotypes of cancer cells. In other words, DLX6-AS1 exerted its tumorigenic effects in ovarian cancer cells *via* miR-195-5p/FHL2 signaling axis. In bladder cancer, miR-195-5p as target of DLX6-AS1 was shown to down-regulate the vascular endothelial growth factor A (VEGFA) and consequently inhibit malignancy phenotype in cancer cells, while miR-195-5p inhibition returned the DLX6-AS1 tumorigenic effects (Zhao et al., 2020a).

Furthermore, DLX6-AS1 has been shown to up-regulated DLK1, a regulator of cell differentiation and prognostic factor for several cancers, through sponging miR-129-5p which in turn

triggers Wnt signaling, and eventually promotes stemness in osteosarcoma cell lines (Zhang et al., 2018). PI3K/AKT/mTOR signaling pathway is another critical tumorigenic pathway which is known to be activated by DLX6-AS1, promoting malignant phenotype of colorectal cancer cells (Zhang et al., 2019a).

Overall, it is demonstrated that DLX6-AS1 acts as an oncogenic lncRNA enhancing malignant phenotype of several cancer cells (Figure 1).

DLX6-AS1 is oncogenic lncRNA has been found to be up-regulated in a growing number of different types of cancerous tissues compared to normal tissues. Promoting carcinogenesis *via* increasing tumor cell proliferation, migration, and invasion through enhancing Epithelial–Mesenchymal Transition (EMT). miRNAs have been identified which are negatively regulated by DLX6-AS1, and they regulate expression of a number of transcription factors, eventually affecting signaling pathways involved in carcinogenesis.

Table 1 shows the findings of the studies conducted on DLX6-AS1 oncogenic role in various cancer cell lines.

TABLE 2 | Effects of DLX6-AS1 on tumor growth and metastasis in animal studies.

Cancer type	Animal models	Function	References
HCC	BALB/c nude mice BALB/c nude mice	Δ DLX6-AS1: \downarrow tumor growth Δ DLX6-AS1: \downarrow tumor growth	Liu et al. (2020a) Zhang et al. (2017)
Pancreas	BABL/c athymic nude mice BABL/c athymic nude mice	Δ DLX6-AS1: \downarrow tumor growth Δ DLX6-AS1: \downarrow tumor growth, and \downarrow metastasis	An et al. (2018) Yang et al. (2019a)
Prostate	BALB/c nude mice SCID mice	Δ DLX6-AS1: \downarrow tumor growth $\uparrow\uparrow$ DLX6-AS1: \uparrow tumor growth and \uparrow lymph node metastasis	Zhu et al. (2021) Zhao et al. (2020b)
Neuroblastoma	BALB/c nude mice BALB/c nude mice BALB/c nude mice BALB/c nude mice	Δ DLX6-AS1: \downarrow tumor growth Δ DLX6-AS1: \downarrow tumor growth Δ DLX6-AS1: \downarrow tumor growth Δ DLX6-AS1: \downarrow tumor growth	Jia et al. (2020) Han et al. (2020) Li et al. (2020b) Li et al. (2019b)
Glioma	Male nude mic	Δ DLX6-AS1: \downarrow tumor growth	Zhang et al. (2019b)
Endometria	32 healthy nude mice	Δ DLX6-AS1: \downarrow tumor growth	Zhao and Xu, (2020)
Cervix	BALB/c nude mice	Δ DLX6-AS1: \downarrow tumor growth	Xie et al. (2020)
Breast (TNBC)	BALB/c nude mice	Δ DLX6-AS1: \downarrow tumor growth, and \downarrow chemoresistance to cisplatin	Du et al. (2020)
Ovaries	BALB/c nude mice	Δ DLX6-AS1: \downarrow tumor growth	Kong and Zhang, (2020)
Bladder	BALB/c nude mice Male nude mice	Δ DLX6-AS1: \downarrow tumor growth Δ DLX6-AS1: \downarrow tumor growth	Zhao et al. (2020a) Guo et al. (2019)
Larynx	BALB/c nude mice	Δ DLX6-AS1: \downarrow tumor growth	Liu et al. (2020b)
Stomach	BALB/c nude mice	Δ DLX6-AS1: \downarrow tumor growth	Qian et al. (2021)
Osteosarcoma	BALB/c nude mice BALB/c nude mice	Δ DLX6-AS1: \downarrow tumor growth Δ DLX6-AS1: \downarrow tumor growth	Zhang et al. (2018) Zhang et al. (2019b)
Lung (NSCLC)	BALB/c nude mice BALB/c nude mice	Δ DLX6-AS1: \downarrow tumor growth Δ DLX6-AS1: \downarrow tumor growth	Huang et al. (2019) Sun et al. (2019)
Colorectal	Female nude mice	Δ DLX6-AS1: \downarrow tumor growth	Zhang et al. (2019a)
Liver	NOD-SCID mice	Δ DLX6-AS1: \downarrow tumorigenesis and \downarrow tumor growth	Wu et al. (2019)
Kidney (RCC)	BALB/c nude mice	Δ DLX6-AS1: \downarrow tumor growth	Zeng et al. (2017)

IMPACT OF DLX6-AS1 IN ENHANCEMENT OF TUMOR GROWTH

Experiments in animal models have confirmed oncogenic role of DLX6-AS1. It is expected that DLX6-AS1 overexpression or silencing increases or suppresses malignant features of cancer cells in xenograft models, respectively. To examine this claim, treated cells; either overexpressing or with silenced for DLX6-AS1; have been injected to the animals; mainly BALB/c nude mice, and then tumor size or volume, and metastasis in expected organ have been checked at certain intervals. Changes in chemosensitivity have also been assessed occasionally. Decreased tumor growth and metastasis, and also chemoresistance have been reported under DLX6-AS1 knockdown conditions in animal studies. Opposite findings have been reported when DLX6-AS1 was overexpressed in injected cancer cells to the nude mice. Taken together, these findings demonstrate oncogenic role of DLX6-AS1 in tumor progression and metastasis in animal studies are consistent with the results of cell studies (Table 2).

IMPACT OF DLX6-AS1 ON SURVIVAL OF PATIENTS WITH DIFFERENT TYPES OF CANCERS

Cancerous tissues resected from patients have shown significantly increased expression of DLX6-AS1 compared to matched normal adjacent tissues (NATs) and healthy people in microarray analysis and qRT-PCR. In non-small cell lung cancer (NSCLC), DLX6-AS1 high expression levels were found to be positively associated with advanced clinicopathological features including higher disease stage, tumor metastasis to lymph nodes and also weak differentiation of cancer cells in patients (Zhang et al., 2019c). Also, Guo et al. (2019) demonstrated high DLX6-AS1 expression in bladder cancer patients with advanced TNM stage, positive lymph node and distant metastases. Survival analysis *via* Kaplan-Meier curve has shown association between high DLX6-AS1 expression and shorter overall survival (OS), and/or disease-free survival (DFS) in several types of cancer like HCC (Liu et al., 2020a; Zhang et al., 2017), gastric cancer (Qian et al., 2021; Fu et al., 2019), glioma

TABLE 3 | Clinical prognostic importance of DLX6-AS1 in human cancers.

Cancer type	Clinical samples	Expression change in tumor tissues compared to normal tissues	Kaplan-Meier analysis	Multivariate cox regression	References
HCC	85 cancerous patients and matched NATs	Up	Patients with high DLX6-AS1 expression had poor OS compared to those with lower levels	--	Liu et al. (2020a)
	60 cancerous patients and matched NATs	Up	High DLX6-AS1 expression levels were correlated with poor OS in HCC patients compared to low levels	--	Zhang et al. (2017)
Larynx	43 cancerous patients and matched NATs	Up	Patients with high DLX6-AS1 expression had shorter OS compared to those with lower levels	--	Liu et al. (2020b)
Stomach	60 cancerous tissues and 28 NATs	Up	High DLX6-AS1 expression levels were associated with poor OS.	DLX6-AS1 expression is an independent predictor of poor prognosis	Qian et al. (2021)
	375 cancerous tissues and 32 NATs	Up	--	--	Liang et al. (2020)
	62 cancerous tissues and matched NATs	Up	High DLX6-AS1 expression levels correlated with shorter survival in gastric cancer patients compared to those with low levels	--	Fu et al. (2019)
Glioma	36 cancerous tissues and matched NATs	Up	Patients with high DLX6-AS1 expression levels exhibited shorter OS compared to those with low levels	--	Zhang et al. (2019b)
Osteosarcoma	80 cancerous tissues and matched NATs	Up	High DLX6-AS1 expression levels were correlated with shorter OS in osteosarcoma patients compared to low levels	DLX6-AS1 expression level is an independent prognostic factor	Zhang et al. (2018)
Breast	45 cancerous tissues and matched NATs	Up	High DLX6-AS1 expression levels were correlated with shorter OS in osteosarcoma patients compared to low levels	--	Zhao et al. (2019)
Pancreas	60 cancer tissues and matched NATs	Up	Patients with low DLX6-AS1 expression levels exhibited higher survival rate compared to those with high levels	--	Yang et al. (2019a)
	84 cancer tissues and matched NATs	Up	--	--	An et al. (2018)
Prostate	20 cancer tissues and matched NATs	Up	--	--	Zhu et al. (2021)
	32 cancerous patients and 28 patients with benign prostate hyperplasia	Up	--	--	Zhao et al. (2020b)
Neuroblastoma	20 cancer tissues and matched NATs	Up	--	--	Jia et al. (2020)
	31 cancer tissues and matched NATs	Up	--	--	Han et al. (2020)
	70 cancer tissues and matched NATs	Up	High DLX6-AS1 expression levels were significantly associated with shorter OS in neuroblastoma patients compared to those with low levels	--	Li et al. (2020b)
	88 cancer tissues and matched NATs	Up	High DLX6-AS1 expression levels were correlated with shorter OS in neuroblastoma patients compared to those with low levels	--	Li et al. (2019b)
Endometria	78 cancer tissues and matched NATs	Up	--	--	Zhao and Xu, (2020)
Breast (TNBC)	47 cancerous tissues and matched NATs	Up	--	--	Du et al. (2020)

(Continued on following page)

TABLE 3 | (Continued) Clinical prognostic importance of DLX6-AS1 in human cancers.

Cancer type	Clinical samples	Expression change in tumor tissues compared to normal tissues	Kaplan-Meier analysis	Multivariate cox regression	References
Ovaries	50 cancerous tissues and matched NATs	Up	--	--	Kong and Zhang, (2020) Zhao and Liu, (2019)
	128 cancerous tissues and matched NATs	Up	Patients with high DLX6-AS1 expression levels had shorter OS and DFS compared to those with low levels	DLX6-AS1 expression is an independent prognostic factor for survival in ovarian cancer patients	
Bladder	60 cancerous tissues and matched NATs	Up	--	--	Zhao et al. (2020a) Guo et al. (2019)
	54 cancerous tissues and matched NATs	Up	--	--	
Colorectal	76 cancerous tissues and matched NATs	Up	--	--	Kong et al. (2020) Zhang et al. (2019a)
	60 cancerous tissues and matched NATs	Up	--	--	
Larynx (LSCC)	23 cancerous tissues and matched NATs	Up	--	--	Yang et al. (2019b)
Osteosarcoma	40 cancerous tissues and matched NATs	Up	--	--	Zhang et al. (2019b)
Lung (NSCLC)	48 cancerous tissues and matched NATs	Up	--	--	Huang et al. (2019) Sun et al. (2019)
	51 cancerous tissues and matched NATs	Up	--	--	
Nasopharynx	72 cancerous tissues and matched NATs	Up	--	--	Yang et al. (2020)
Esophagus	73 cancerous tissues and matched NATs	Up	--	--	Zhang et al. (2019c)
Liver	30 cancerous tissues and matched NATs	Up	--	--	Li et al. (2019a)
Cervix	78 cancerous tissues and matched NATs	Up	--	--	Long et al. (2019)
Kidney (RCC)	15 cancerous tissues and matched NATs	Up	--	--	Zeng et al. (2017)
Ewing's sarcoma	20 cancerous tissues and matched NATs	Up	--	--	Lei et al. (2019)

(Zhang et al., 2019b), breast cancer (Zhao et al., 2019), and several others (Table 3). Competitive endogenous RNA (ceRNA) network analysis has demonstrated reliability of DLX6-AS1 along with three other lncRNAs and two more miRNAs in a signature as prognostic biomarkers in HCC patients (Long et al., 2019). Ding et al. (2021) showed serum exosomal levels of DLX6-AS1 can act as a prognostic biomarker in cervical cancer patients. Also, multivariate cox regression has shown that DLX6-AS1 is an independent prognostic factor for survival in a number of cancers such as gastric cancer (Qian et al., 2021), osteosarcoma (Zhang et al., 2018), and ovarian cancer (Zhao and Liu, 2019). Furthermore, a value of 0.795 for area under curve (AUC) in receiver operating characteristic (ROC) curve has shown

acceptable efficiency of DLX6-AS1 in diagnosis of glioma (Zhang et al., 2019b). Taken together, according to the clinical data, DLX6-AS1 is suggested as a potential prognostic biomarker for different types of human cancer and a putative factor to manage cancerous patients.

DISCUSSION

lncRNAs are a heterogeneous group of ncRNAs with characteristic size of more than 200 nucleotides. An increasing number of lncRNAs have been found to be dysregulated in many human diseases particularly cancer. However, their role in

carcinogenesis is not precisely understood. DLX6-AS1 is an lncRNAs which has been unveiled to be up-regulated in a various number of cancers. In different cell studies, DLX6-AS1 has shown oncogenic role *via* promoting oncogenic phenotype of cancer cell lines. Increase in tumor cell proliferation, migration, invasion, and EMT while suppressing apoptosis in cancer cells are the effects of DLX6-AS1 in the development and progression of cancer. Silencing experiments using specific shRNA against DLX6-AS1 have shown suppression of tumorigenic potential. Similar pattern of expression in different types of cancer originated from various tissues not only reveals its universal function in the tumorigenesis, but also emphasizes the suitability of therapeutic modalities against this lncRNA for a wide range of human malignancies.

In the majority of cell experiments, mediator miRNAs have been identified which are negatively regulated by DLX6-AS1, and they regulate expression of a number of transcription factors, eventually affecting signaling pathways involved in carcinogenesis. These pathways form axes through which DLX6-AS1 regulates transcription factors, and/or signaling pathways eventually promotes carcinogenicity of cancer cells. Identification of functional routes of DLX6-AS1 effects in the carcinogenesis is an important step toward design of targeted therapies in cancer. It is also important to mention that these therapies should not affect pathways with crucial roles in the physiological features of normal cells.

Xenograft animal studies also have confirmed enhancing effect of DLX6-AS1 on tumor growth and metastasis. Clinical evaluations in cancerous patients have shown increased expression of DLX6-AS1 in tumor tissues compared to healthy tissues. High DLX6-AS1 expression has shown positive

association with advanced clinicopathological features in cancerous patients. Survival analyses have demonstrated correlation between high DLX6-AS1 expression and shorter survival. In cox regression analysis, DLX6-AS1 has been suggested as an independent prognostic factor for patients with various types of cancer.

Animal and cell line studies have confirmed that therapeutic modalities targeting DLX6-AS1 can effectively reduce tumorigenic potential of malignant cells, induce their apoptosis and diminish tumor size and burden. However, the efficacy and safety of these methods have not been evaluated in the clinical settings.

Taken together, these findings demonstrate carcinogenic role of DLX6-AS1 in the development and progression of different human cancers suggesting diagnostic and prognostic potentials of DLX6-AS1 in human cancers. Known role of up-regulated DLX6-AS1 in cancer tissues and clinical samples also suggest therapeutic potentials in finding treatments for different types of cancer *via* targeting DLX6-AS1. Further studies are required to utilize diagnostic, prognostic, and therapeutic potentials of DLX6-AS1 in clinical settings. Moreover, measurement of DLX6-AS1 levels in biofluids is an important step towards identification of non-invasive routes for diagnostic purposes.

AUTHOR CONTRIBUTIONS

MT and SGF wrote the draft and revised it. SN and MS collected the data and designed the figures and tables. All the authors read and approved the submitted version.

REFERENCES

- An, Y., Chen, X.-m., Yang, Y., Mo, F., Jiang, Y., Sun, D.-L., et al. (2018). lncRNA DLX6-AS1 Promoted Cancer Cell Proliferation and Invasion by Attenuating the Endogenous Function of miR-181b in Pancreatic Cancer. *Cancer Cel Int* 18 (1), 143. doi:10.1186/s12935-018-0643-7
- Bertone, P., Stolc, V., Royce, T. E., Rozowsky, J. S., Urban, A. E., Zhu, X., et al. (2004). Global Identification of Human Transcribed Sequences with Genome Tiling Arrays. *Science* 306 (5705), 2242–2246. doi:10.1126/science.1103388
- Chen, W., Zhang, G., Li, J., Zhang, X., Huang, S., Xiang, S., et al. (2018). CRISPRlnc: a Manually Curated Database of Validated sgRNAs for lncRNAs. *Nucleic Acids Res.* 47 (D1), D63–D68. doi:10.1093/nar/gky904
- Cheng, L., Wang, P., Tian, R., Wang, S., Guo, Q., Luo, M., et al. (2018). lncRNA2Target v2.0: a Comprehensive Database for Target Genes of lncRNAs in Human and Mouse. *Nucleic Acids Res.* 47 (D1), D140–D144. doi:10.1093/nar/gky1051
- Dey, B. K., Mueller, A. C., and Dutta, A. (2014). Long Non-coding RNAs as Emerging Regulators of Differentiation, Development, and Disease. *Transcription* 5 (4), e944014. doi:10.4161/21541272.2014.944014
- Ding, X. Z., Zhang, S. Q., Deng, X. L., and Qiang, J. H. (2021). Serum Exosomal lncRNA DLX6-AS1 Is a Promising Biomarker for Prognosis Prediction of Cervical Cancer. *Technol. Cancer Res. Treat.* 20, 1533033821990060. doi:10.1177/1533033821990060
- Du, C., Wang, Y., Zhang, Y., Zhang, J., Zhang, L., and Li, J. (2020). lncRNA DLX6-AS1 Contributes to Epithelial-Mesenchymal Transition and Cisplatin Resistance in Triple-Negative Breast Cancer via Modulating Mir-199b-5p/Paxillin Axis. *Cel Transpl.* 29, 963689720929983. doi:10.1177/0963689720929983
- Fang, C., Xu, L., He, W., Dai, J., and Sun, F. (2019). Long Noncoding RNA DLX6-AS1 Promotes Cell Growth and Invasiveness in Bladder Cancer via Modulating the miR-223-Hsp90b1 axis. *Cell Cycle* 18 (23), 3288–3299. doi:10.1080/15384101.2019.1673633
- Fatica, A., and Bozzoni, I. (2014). Long Non-coding RNAs: New Players in Cell Differentiation and Development. *Nat. Rev. Genet.* 15 (1), 7–21. doi:10.1038/nrg3606
- Feng, J., Bi, C., Clark, B. S., Mady, R., Shah, P., and Kohtz, J. D. (2006). The Evt-2 Noncoding RNA Is Transcribed from the Dlx-5/6 Ultraconserved Region and Functions as a Dlx-2 Transcriptional Coactivator. *Genes Dev.* 20 (11), 1470–1484. doi:10.1101/gad.1416106
- Fu, X., Tian, Y., Kuang, W., Wen, S., and Guo, W. (2019). Long Non-coding RNA DLX6-AS1 Silencing Inhibits Malignant Phenotypes of Gastric Cancer Cells. *Exp. Ther. Med.* 17 (6), 4715–4722. doi:10.3892/etm.2019.7521
- Gong, J., Liu, W., Zhang, J., Miao, X., and Guo, A.-Y. (2014). lncRNASNP: a Database of SNPs in lncRNAs and Their Potential Functions in Human and Mouse. *Nucleic Acids Res.* 43 (D1), D181–D186. doi:10.1093/nar/gku1000
- Guo, J., Chen, Z., Jiang, H., Yu, Z., Peng, J., Xie, J., et al. (2019). The lncRNA DLX6-AS1 Promoted Cell Proliferation, Invasion, Migration and Epithelial-To-Mesenchymal Transition in Bladder Cancer via Modulating Wnt/ β -Catenin Signaling Pathway. *Cancer Cel Int* 19, 312. doi:10.1186/s12935-019-1010-z
- Guttman, M., Amit, I., Garber, M., French, C., Lin, M. F., Feldser, D., et al. (2009). Chromatin Signature Reveals over a Thousand Highly Conserved Large Non-coding RNAs in Mammals. *Nature* 458 (7235), 223–227. doi:10.1038/nature07672
- Han, J. Y., Guo, S., Wei, N., Xue, R., Li, W., Dong, G., et al. (2020). ciRS-7 Promotes the Proliferation and Migration of Papillary Thyroid Cancer by Negatively Regulating the miR-7/epidermal Growth Factor Receptor axis. *Biomed. Res. Int.* 2020, 9875636. doi:10.1155/2020/9875636

- Huang, Y., Ni, R., Wang, J., and Liu, Y. (2019). Knockdown of lncRNA DLX6-AS1 Inhibits Cell Proliferation, Migration and Invasion while Promotes Apoptosis by Downregulating PRR11 Expression and Upregulating miR-144 in Non-small Cell Lung Cancer. *Biomed. Pharmacother.* 109, 1851–1859. doi:10.1016/j.biopha.2018.09.151
- Ignarski, M., Islam, R., and Müller, R.-U. (2019). Long Non-coding RNAs in Kidney Disease. *Ijms* 20 (13), 3276. doi:10.3390/ijms20133276
- Iyer, M. K., Niknafs, Y. S., Malik, R., Singhal, U., Sahu, A., Hosono, Y., et al. (2015). The Landscape of Long Noncoding RNAs in the Human Transcriptome. *Nat. Genet.* 47 (3), 199–208. doi:10.1038/ng.3192
- Jia, P., Wei, E., Liu, H., Wu, T., and Wang, H. (2020). Silencing of Long Non-coding RNA DLX6-AS1 Weakens Neuroblastoma Progression by the miR-513c-5p/PLK4 axis. *IUBMB Life* 72 (12), 2627–2636. doi:10.1002/iub.2392
- Kong, L., and Zhang, C. (2020). lncRNA DLX6-AS1 Aggravates the Development of Ovarian Cancer via Modulating FHL2 by Sponging miR-195-5p. *Cancer Cell Int* 20, 370. doi:10.1186/s12935-020-01452-z
- Kong, W. Q., Liang, J. J., Du, J., Ye, Z. X., Gao, P., and Liang, Y. L. (2020). Long Noncoding RNA DLX6-AS1 Regulates the Growth and Aggressiveness of Colorectal Cancer Cells via Mediating miR-26a/EZH2 Axis. *Cancer Biother. Radiopharm.* 36 (9), 753–764. doi:10.1089/cbr.2020.3589
- Lei, X., Yang, S., Yang, Y., Zhang, J., Wang, Y., and Cao, M. (2019). Long Noncoding RNA DLX6-AS1 Targets miR-124-3p/CDK4 to Accelerate Ewing's Sarcoma. *Am. J. Transl. Res.* 11 (10), 6569–6576.
- Li, C., Wang, S., and Yang, C. (2020). RETRACTED: Long Non-coding RNA DLX6-AS1 Regulates Neuroblastoma Progression by Targeting YAP1 via miR-497-5p. *Life Sci.* 252, 117657. doi:10.1016/j.lfs.2020.117657
- Li, D., Tang, X., Li, M., and Zheng, Y. (2019). Long Noncoding RNA DLX6-AS1 Promotes Liver Cancer by Increasing the Expression of WEE1 via Targeting miR-424-5p. *J. Cel Biochem* 120 (8), 12290–12299. doi:10.1002/jcb.28493
- Li, X., Zhang, H., and Wu, X. (2019). Long Noncoding RNA DLX6-AS1 Accelerates the Glioma Carcinogenesis by Competing Endogenous Sponging miR-197-5p to Relieve E2F1. *Gene* 686, 1–7. doi:10.1016/j.gene.2018.10.065
- Li, Y., Li, X., Yang, Y., Li, M., Qian, F., Tang, Z., et al. (2020). TRlnc: a Comprehensive Database for Human Transcriptional Regulatory Information of lncRNAs. *Brief. Bioinformatics* 22 (2), 1929–1939. doi:10.1093/bib/bbaa011
- Liang, Y., Zhang, C.-D., Zhang, C., and Dai, D.-Q. (2020). DLX6-AS1/miR-204-5p/OCT1 Positive Feedback Loop Promotes Tumor Progression and Epithelial-Mesenchymal Transition in Gastric Cancer. *Gastric Cancer* 23 (2), 212–227. doi:10.1007/s10120-019-01002-1
- Liu, X., Peng, D., Cao, Y., Zhu, Y., Yin, J., Zhang, G., et al. (2020). Upregulated lncRNA DLX6-AS1 Underpins Hepatocellular Carcinoma Progression via the miR-513c/Cul4A/ANXA10 axis. *Cancer Gene Ther.* 28 (5), 486–501. doi:10.1038/s41417-020-00233-0
- Liu, Y., Liu, X., Zhang, X., Deng, J., Zhang, J., and Xing, H. (2020). lncRNA DLX6-AS1 Promotes Proliferation of Laryngeal Cancer Cells by Targeting the miR-26a/TRPC3 Pathway. *Cmar* Vol. 12, 2685–2695. doi:10.2147/cmar.s237181
- Long, J., Bai, Y., Yang, X., Lin, J., Yang, X., Wang, D., et al. (2019). Construction and Comprehensive Analysis of a ceRNA Network to Reveal Potential Prognostic Biomarkers for Hepatocellular Carcinoma. *Cancer Cell Int* 19, 90. doi:10.1186/s12935-019-0817-y
- Losko, M., Kotlinowski, J., and Jura, J. (2016). Long Noncoding RNAs in Metabolic Syndrome Related Disorders. *Mediators Inflamm.* 2016, 5365209. doi:10.1155/2016/5365209
- Mattick, J. S. (2001). Non-coding RNAs: the Architects of Eukaryotic Complexity. *EMBO Rep.* 2 (11), 986–991. doi:10.1093/embo-reports/kve230
- Mattick, J. S. (2009). The Genetic Signatures of Noncoding RNAs. *Plos Genet.* 5 (4), e1000459. doi:10.1371/journal.pgen.1000459
- Miao, Y.-R., Liu, W., Zhang, Q., and Guo, A.-Y. (2017). lncRNASNP2: an Updated Database of Functional SNPs and Mutations in Human and Mouse lncRNAs. *Nucleic Acids Res.* 46 (D1), D276–D280. doi:10.1093/nar/gkx1004
- Necsulea, A., Soumillon, M., Warnefors, M., Liechti, A., Daish, T., Zeller, U., et al. (2014). The Evolution of lncRNA Repertoires and Expression Patterns in Tetrapods. *Nature* 505 (7485), 635–640. doi:10.1038/nature12943
- Ning, S., Zhang, J., Wang, P., Zhi, H., Wang, J., Liu, Y., et al. (2015). lnc2Cancer: a Manually Curated Database of Experimentally Supported lncRNAs Associated with Various Human Cancers. *Nucleic Acids Res.* 44 (D1), D980–D985. doi:10.1093/nar/gkv1094
- Okazaki, Y., Furuno, M., Kasukawa, T., Adachi, J., Bono, H., Kondo, S., et al. (2002). Analysis of the Mouse Transcriptome Based on Functional Annotation of 60,770 Full-Length cDNAs. *Nature* 420 (6915), 563–573. doi:10.1038/nature01266
- Pastori, C., and Wahlestedt, C. (2012). Involvement of Long Noncoding RNAs in Diseases Affecting the central Nervous System. *RNA Biol.* 9 (6), 860–870. doi:10.4161/rna.20482
- Qian, Y., Song, W., Wu, X., Hou, G., Wang, H., Hang, X., et al. (2021). DLX6 Antisense RNA 1 Modulates Glucose Metabolism and Cell Growth in Gastric Cancer by Targeting microRNA-4290. *Dig. Dis. Sci.* 66 (2), 460–473. doi:10.1007/s10620-020-06223-4
- Sahu, A., Singhal, U., and Chinnaiyan, A. M. (2015). Long Noncoding RNAs in Cancer: From Function to Translation. *Trends Cancer* 1 (2), 93–109. doi:10.1016/j.trecan.2015.08.010
- Sun, W., Zhang, L., Yan, R., Yang, Y., and Meng, X. (2019). lncRNA DLX6-AS1 Promotes the Proliferation, Invasion, and Migration of Non-small Cell Lung Cancer Cells by Targeting the miR-27b-3p/GSPT1 axis. *Ott Vol.* 12, 3945–3954. doi:10.2147/ott.s196865
- Takahashi, K., Yan, I., Haga, H., and Patel, T. (2014). Long Noncoding RNA in Liver Diseases. *Hepatology* 60 (2), 744–753. doi:10.1002/hep.27043
- Uchida, S., and Dimmeler, S. (2015). Long Noncoding RNAs in Cardiovascular Diseases. *Circ. Res.* 116 (4), 737–750. doi:10.1161/circresaha.116.302521
- Wan, P., Su, W., and Zhuo, Y. (2017). The Role of Long Noncoding RNAs in Neurodegenerative Diseases. *Mol. Neurobiol.* 54 (3), 2012–2021. doi:10.1007/s12035-016-9793-6
- Wawrzyniak, O., Zarębska, Z., Rolle, K., and Gotz-Więckowska, A. (2018). Circular and Long Non-coding RNAs and Their Role in Ophthalmologic Diseases. *Acta Biochim. Pol.* 65 (4), 497–508. doi:10.18388/abp.2018_2639
- Wilusz, J. E., Sunwoo, H., and Spector, D. L. (2009). Long Noncoding RNAs: Functional Surprises from the RNA World. *Genes Dev.* 23 (13), 1494–1504. doi:10.1101/gad.1800909
- Wu, D. M., Zheng, Z. H., Zhang, Y. B., Fan, S. H., Zhang, Z. F., Wang, Y. J., et al. (2019). Down-regulated lncRNA DLX6-AS1 Inhibits Tumorigenesis through STAT3 Signaling Pathway by Suppressing CADM1 Promoter Methylation in Liver Cancer Stem Cells. *J. Exp. Clin. Cancer Res.* 38 (1), 237. doi:10.1186/s13046-019-1239-3
- Wu, P., Zuo, X., Deng, H., Liu, X., Liu, L., and Ji, A. (2013). Roles of Long Noncoding RNAs in Brain Development, Functional Diversification and Neurodegenerative Diseases. *Brain Res. Bull.* 97, 69–80. doi:10.1016/j.brainresbull.2013.06.001
- Wu, Q., Ma, J., Meng, W., and Hui, P. (2020). DLX6-AS1 Promotes Cell Proliferation, Migration and EMT of Gastric Cancer through FUS-Regulated MAP4K1. *Cancer Biol. Ther.* 21 (1), 17–25. doi:10.1080/15384047.2019.1647050
- Xie, F., Xie, G., and Sun, Q. (2020). Long Noncoding RNA DLX6-AS1 Promotes the Progression in Cervical Cancer by Targeting miR-16-5p/ARPP19 Axis. *Cancer Biother. Radiopharm.* 35 (2), 129–136. doi:10.1089/cbr.2019.2960
- Yang, B., Jia, L., Ren, H., Jin, C., Ren, Q., Zhang, H., et al. (2020). lncRNA DLX6-AS1 Increases the Expression of HIF-1 α and Promotes the Malignant Phenotypes of Nasopharyngeal Carcinoma Cells via Targeting MiR-199a-5p. *Mol. Genet. Genomic Med.* 8 (1), e1017. doi:10.1002/mgg3.1017
- Yang, J., Ye, Z., Mei, D., Gu, H., and Zhang, J. (2019). Long Noncoding RNA DLX6-AS1 Promotes Tumorigenesis by Modulating miR-497-5p/FZD4/FZD6/Wnt/ β -Catenin Pathway in Pancreatic Cancer. *Cmar* Vol. 11, 4209–4221. doi:10.2147/cmar.s194453
- Yang, Q., Sun, J., Ma, Y., Zhao, C., and Song, J. (2019). lncRNA DLX6-AS1 Promotes Laryngeal Squamous Cell Carcinoma Growth and Invasion through Regulating miR-376c. *Am. J. Transl. Res.* 11 (11), 7009–7017.
- Zeng, X., Hu, Z., Ke, X., Tang, H., Wu, B., Wei, X., et al. (2017). Long Noncoding RNA DLX6-AS1 Promotes Renal Cell Carcinoma Progression via miR-26a/PTEN axis. *Cell Cycle* 16 (22), 2212–2219. doi:10.1080/15384101.2017.1361072
- Zhang, J. J., Xu, W. R., Chen, B., Wang, Y. Y., Yang, N., Wang, L. J., et al. (2019). The Up-Regulated lncRNA DLX6-AS1 in Colorectal Cancer Promotes Cell Proliferation, Invasion and Migration via Modulating PI3K/AKT/mTOR Pathway. *Eur. Rev. Med. Pharmacol. Sci.* 23 (19), 8321–8331. doi:10.26355/eurrev_201910_19143
- Zhang, L., He, X., Jin, T., Gang, L., and Jin, Z. (2017). Long Non-coding RNA DLX6-AS1 Aggravates Hepatocellular Carcinoma Carcinogenesis by Modulating miR-203a/MMP-2 Pathway. *Biomed. Pharmacother.* 96, 884–891. doi:10.1016/j.biopha.2017.10.056

- Zhang, N., Meng, X., Mei, L., Zhao, C., and Chen, W. (2019). LncRNA DLX6-AS1 Promotes Tumor Proliferation and Metastasis in Osteosarcoma through Modulating miR-641/HOXA9 Signaling Pathway. *J. Cel Biochem* 120 (7), 11478–11489. doi:10.1002/jcb.28426
- Zhang, R. M., Tang, T., Yu, H. M., and Yao, X. D. (2018). LncRNA DLX6-AS1/miR-129-5p/DLK1 axis Aggravates Stemness of Osteosarcoma through Wnt Signaling. *Biochem. Biophys. Res. Commun.* 507 (1), 260–266. doi:10.1016/j.bbrc.2018.11.019
- Zhang, X., Guo, H., Bao, Y., Yu, H., Xie, D., and Wang, X. (2019). Exosomal Long Non-coding RNA DLX6-AS1 as a Potential Diagnostic Biomarker for Non-small Cell Lung Cancer. *Oncol. Lett.* 18 (5), 5197–5204. doi:10.3892/ol.2019.10892
- Zhao, H., and Xu, Q. (2020). Long Non-coding RNA DLX6-AS1 Mediates Proliferation, Invasion and Apoptosis of Endometrial Cancer Cells by Recruiting p300/E2F1 in DLX6 Promoter Region. *J. Cel. Mol. Med.* 24 (21), 12572–12584. doi:10.1111/jcmm.15810
- Zhao, J., and Liu, H. R. (2019). Down-regulation of Long Noncoding RNA DLX6-AS1 Defines Good Prognosis and Inhibits Proliferation and Metastasis in Human Epithelial Ovarian Cancer Cells via Notch Signaling Pathway. *Eur. Rev. Med. Pharmacol. Sci.* 23 (8), 3243–3252. doi:10.26355/eurev_201904_17684
- Zhao, P., Guan, H., Dai, Z., Ma, Y., Zhao, Y., and Liu, D. (2019). Long Noncoding RNA DLX6-AS1 Promotes Breast Cancer Progression via miR-505-3p/RUNX2 axis. *Eur. J. Pharmacol.* 865, 172778. doi:10.1016/j.ejphar.2019.172778
- Zhao, Y.-H., Wang, Z., Zhang, N., Cui, T., and Zhang, Y.-H. (2020). Effect of ciRS-7 Expression on clear Cell Renal Cell Carcinoma Progression. *Chin. Med. J.* 133 (17), 2084–2089. doi:10.1097/cm9.0000000000000867
- Zhao, Z., Liang, S., and Sun, F. (2020). LncRNA DLX6-AS1 Promotes Malignant Phenotype and Lymph Node Metastasis in Prostate Cancer by Inducing LARGE Methylation. *Front. Oncol.* 10, 1172. doi:10.3389/fonc.2020.01172
- Zhu, X., Ma, X., Zhao, S., and Cao, Z. (2021). DLX6-AS1 Accelerates Cell Proliferation through Regulating miR -497-5p/SNCG Pathway in Prostate Cancer. *Environ. Toxicol.* 36 (3), 308–319. doi:10.1002/tox.23036

Conflict of Interest: The authors declare that the research was conducted in the absence of any commercial or financial relationships that could be construed as a potential conflict of interest.

Publisher's Note: All claims expressed in this article are solely those of the authors and do not necessarily represent those of their affiliated organizations, or those of the publisher, the editors and the reviewers. Any product that may be evaluated in this article, or claim that may be made by its manufacturer, is not guaranteed or endorsed by the publisher.

Copyright © 2022 Ghafouri-Fard, Najafi, Hussien, Ganjo, Taheri and Samadian. This is an open-access article distributed under the terms of the Creative Commons Attribution License (CC BY). The use, distribution or reproduction in other forums is permitted, provided the original author(s) and the copyright owner(s) are credited and that the original publication in this journal is cited, in accordance with accepted academic practice. No use, distribution or reproduction is permitted which does not comply with these terms.



OPEN ACCESS

Edited by:

Shiv K. Gupta,
Mayo Clinic, United States

Reviewed by:

Ying Hu,
Harbin Institute of Technology, China
Jianjun Xie,
Shantou University, China
Lingwen Ding,
National University of Singapore,
Singapore
Zhizhou Shi,
Kunming University of Science and
Technology, China

*Correspondence:

Xiao-Qing Yuan
yuanxq7@mail.sysu.edu.cn
Yue Liu
13927651001@163.com
Dong Yin
yind3@mail.sysu.edu.cn

[†]These authors have contributed
equally to this work and share
first authorship

Specialty section:

This article was submitted to
Molecular and Cellular Oncology,
a section of the journal
Frontiers in Oncology

Received: 21 September 2021

Accepted: 31 January 2022

Published: 03 March 2022

Citation:

Peng L, Peng J-Y, Cai D-K, Qiu Y-T,
Lan Q-S, Luo J, Yang B, Xie H-T,
Du Z-P, Yuan X-Q, Liu Y and Yin D
(2022) Immune Infiltration and
Clinical Outcome of Super-
Enhancer-Associated lncRNAs in
Stomach Adenocarcinoma.
Front. Oncol. 12:780493.
doi: 10.3389/fonc.2022.780493

Immune Infiltration and Clinical Outcome of Super-Enhancer-Associated lncRNAs in Stomach Adenocarcinoma

Li Peng^{1,2†}, Jiang-Yun Peng^{1,2†}, Dian-Kui Cai^{1,3†}, Yun-Tan Qiu^{1,2}, Qiu-Sheng Lan^{1,4}, Jie Luo^{1,5}, Bing Yang^{1,2}, Hai-Tao Xie⁵, Ze-Peng Du⁶, Xiao-Qing Yuan^{1,7*}, Yue Liu^{8*} and Dong Yin^{1,2*}

¹ Guangdong Provincial Key Laboratory of Malignant Tumor Epigenetics and Gene Regulation, Guangdong-Hong Kong Joint Laboratory for RNA Medicine, Sun Yat-Sen Memorial Hospital, Sun Yat-Sen University, Guangzhou, China, ² Medical Research Center, Sun Yat-Sen Memorial Hospital, Sun Yat-Sen University, Guangzhou, China, ³ Department of Hepatobiliary Surgery, Sun Yat-sen Memorial Hospital, Sun Yat-sen University, Guangzhou, China, ⁴ Department of Gastrointestinal Surgery, Sun Yat-sen Memorial Hospital, Sun Yat-sen University, Guangzhou, China, ⁵ Department of Clinical Laboratory, The First Affiliated Hospital, Hengyang Medical School, University of South China, Hengyang, China, ⁶ Central Laboratory, Department of Pathology, Shantou Central Hospital, Shantou, China, ⁷ Breast Tumor Center, Sun Yat-sen Memorial Hospital, Sun Yat-sen University, Guangzhou, China, ⁸ Institute of Digestive Disease of Guangzhou Medical University, The Sixth Affiliated Hospital of Guangzhou Medical University, Qingyuan People's Hospital, Qingyuan, China

Super-enhancers (SEs) comprise large clusters of enhancers that highly enhance gene expression. Long non-coding RNAs (lncRNAs) tend to be dysregulated in cases of stomach adenocarcinoma (STAD) and are vital for balancing tumor immunity. However, whether SE-associated lncRNAs play a role in the immune infiltration of STAD remains unknown. In the present study, we identified SE-associated lncRNAs in the H3K27ac ChIP-seq datasets from 11 tumor tissues and two cell lines. We found that the significantly dysregulated SE-associated lncRNAs were strongly correlated with immune cell infiltration through the application of six algorithms (ImmuncellAI, CIBERSORT, EPIC, quantiSeq, TIMER, and xCELL), as well as immunomodulators and chemokines. We found that the expression of SE-associated lncRNA TM4SF1-AS1 was negatively correlated with the proportion of CD8+ T cells present in STAD. TM4SF1-AS1 suppresses T cell-mediated immune killing function and predicts immune response to anti-PD1 therapy. ChIP-seq, Hi-C and luciferase assay results verified that TM4SF1-AS1 was regulated by its super-enhancer. RNA-seq data showed that TM4SF1-AS1 is involved in immune and cancer-related processes or pathways. In conclusion, SE-associated lncRNAs are involved in the tumor immune microenvironment and act as indicators of clinical outcomes in STAD. This study highlights the importance of SE-associated lncRNAs in the immune regulation of STAD.

Keywords: super-enhancer (SE), long non-coding RNA (lncRNA), stomach adenocarcinoma (STAD), immune infiltration, clinical outcome, TM4SF1-AS1, T cell, PD1

INTRODUCTION

Stomach cancer is the fifth most common cause of cancer-related morbidity and fourth most common cause of mortality worldwide, accounting for over 1,000,000 new cases and approximately 769,000 deaths in 2020 (1). Infection with *Helicobacter pylori*, smoking, and diets high in nitrate and nitrite can lead to stomach cancer (2). With progress in diagnosis and treatment, the quality of life of patients with stomach cancer can be improved. Stomach adenocarcinoma (STAD), aka gastric adenocarcinoma, is the most common histological type of stomach cancer (approximately 95%) (3), and patients still have a poor prognosis (2, 4). Biomarkers such as PD1 and PDL1 are used increasingly often as immunotherapy for STAD, which benefits patients (2). Therefore, identifying credible biomarkers is important for the early identification of STAD and novel molecular targeting treatments.

Super-enhancers (SEs) comprise large clusters of activated enhancers in close proximity to one another that maintain cell-type-specific identity and fate (5). These enhancers are generally within 12.5 kb in genomic distance (6). Considerable progress regarding research on SE-associated protein-coding genes, such as HOXB8 (7), MEIS1 (8) and MYC (9) has been made recently. In addition, SEs reportedly drive the expression of long noncoding RNA (lncRNA) in various cancers, except stomach cancer. Importantly, Wen et al. reported a genome-wide reprogramming of enhancer and SE landscape in cases of STAD, which lead to dysregulated local and regional cancer gene expression (10). This finding indicates that SEs are vital for the occurrence and development of multiple cancers that involve STAD that regulate the expression of tumor-related genes. However, the roles of SE-associated long non-coding RNAs in STAD remain unclear.

MATERIALS AND METHODS

STAD Cell Lines

The STAD cell lines AGS and MKN45 were cultured in F12K and DMEM containing 10–15% fetal bovine serum at 37°C in a humidified atmosphere containing 5% CO₂.

Chromatin Immunoprecipitation Sequencing

The AGS cells were cross-linked with formaldehyde and sonicated using a Bioruptor (Diagenode, Belgium), and the precipitate was removed *via* centrifugation. Protein A/G magnetic beads (Pierce, USA) were incubated overnight with a histone-3-lysine-27 acetylation (H3K27ac) antibody (Abcam, USA) at 4°C. The DNA fragments were eluted and recycled for chromatin immunoprecipitation sequencing (ChIP-seq) on a BGISEQ-500 platform (BGI-Shenzhen, China).

ChIP-Seq Analysis

Raw ChIP-seq data of MKN45 cells and 11 STAD tumors were downloaded from the Gene Expression Omnibus database. The

downloaded raw data and our sequencing data were ordered *via* trimming, Bowtie2 read mapping, filtering, and MACS2 peak calling. Bam files were converted into bigwig files using bamCoverage. Hockey stick plots and positional information of super-enhancers were analyzed using the rank ordering of super enhancers algorithm (5). The Integrative Genomics Viewer was used to visualize the bigwig files of the ChIP-seq data.

Survival Analysis

The STAD dataset was downloaded from the Cancer Genome Atlas (TCGA; <https://cancergenome.nih.gov/>), which includes 375 tumor samples and 32 non-malignant stomach tissue samples. Patients with STAD who were included in the TCGA were divided into high and low expression groups according to the median. GraphPad software was used to draw all survival-related graphs. Statistical significance was set at $p < 0.05$.

Correlation of lncRNAs With the Tumor Immune Microenvironment and Immune Markers

Immune cell abundance was evaluated using six algorithms, namely ImmuCellAI (11), CIBERSORT (12), EPIC (13), quantiSeq (14), TIMER (15), and xCELL (16). The correlation of the lncRNA expression matrix with immune cell abundance was analyzed.

Immune markers including immunomodulators (immunoinhibitors and immunostimulators), MHC molecules, chemokines and chemokine receptor were downloaded from TISIDB (<http://cis.hku.hk/TISIDB/download.php>). The expression of these markers was from TCGA database. The correlation of the lncRNA expression matrix with immune markers level was also analyzed in STAD.

siRNA Transfection

The TM4SF1-AS1 small interference RNA (siRNA) sequences were designed and synthesized by GenePharma (Suzhou, China). The siRNA was diluted using sterile DEPC water and transfected into AGS and MKN45 cells using Lipofectamine RNAiMAX Transfection Reagent (Invitrogen, USA). The siRNA sequences of TM4SF1-AS1 are listed in **Table 1**.

RNA Isolation and qRT-PCR

RNA was isolated from cells using the TRIzol method. Cells in a 6-well plate were lysed with 1 mL Trizol in each well, and 200 µL chloroform was added, shaken, mixed, and centrifuged at 12,000 rpm at 4°C for 10 min after being incubated for 5 min. Next, 500 µL isopropanol was added, mixed, and centrifuged. After being washed twice with 75% alcohol, the RNA precipitate was dissolved in diethyl pyrocarbonate water. RNA was reverse transcribed to first-strand cDNA using Hifair III 1st Strand cDNA Synthesis SuperMix for qPCR (gDNA digester plus) (Yeasten, China).

TABLE 1 | siRNA sequences.

Gene name	siRNA sequences	
	Sense	Antisense
siTM4SF1-AS1#1	GGCAUUGACUGUGCAACUCCU	GGAGGAGUUGCACAGUCAAU
siTM4SF1-AS1#2	GCCCUUGUUGAGGCUUUGAAA	UCUUUCAAGCCUCAACCAGG
siTM4SF1-AS1#3	GGUGAAACUCUCCACUCCUTT	AGGAGUGGAGAGUUUCACCTT
siTM4SF1-AS1#4	GUUCAGACCAGUGAGAUUUTT	AAAUUCACUGGUCUGAACTT
siNC	UUCUCCGAACGUGUCACGUTT	ACGUGACACGUUCGGAGAATT

ChamQ Universal SYBR qPCR Master Mix (Vazyme, China) was used to perform qRT-PCR on a CFX96 Real-Time System (Bio-Rad, USA). Relative mRNA expression was calculated using the $2^{-\Delta\Delta CT}$ method and normalized to that of GAPDH. The primers are shown in **Table 2**.

CD8+ T Cell Separation From Human PBMCs

CD8+ T cells were separated from human PBMCs using the EasySep™ Human CD8+ T Cell Isolation Kit (STEMCELL Technologies, Canada). Samples were prepared at the indicated cell concentrations within the volume range. The isolation cocktail was added to the required tube, mixed, and incubated. Vortex RapidSpheres™, add it to the sample and mix them. The recommended medium was added to top up the sample to the indicated volume, then mixed by gently pipetting the sample up and down 2–3 times. The tube was placed into the magnet without a lid and incubated. The magnet was then picked up and the magnet and tube were inverted in one continuous motion, pouring the enriched cell suspension into a new tube.

T Cell Activation and *In Vitro* Killing Assays

First, stomach cancer cells were stained using the CellTrace CFSE Cell Proliferation Kit (Invitrogen, USA) for 20 min at 37°C. Activated CD8+ T cells (2×10^4) were generated by incubation with ImmunoCult™ Human CD3/CD28 T Cell Activator (STEMCELL Technologies, Canada) at 37°C and 5% CO₂ for up to 3 days, and were then added to cancer cells. Both activated CD8+ T cells and cancer cells were collected to be stained with propidium iodide (3.75 mM solution, 1:500 final dilution). These

cells were harvested and analyzed using flow cytometry after 12 h (Beckman CytoFLEX, USA).

Hi-C Analysis

Hi-C data of two STAD samples, T2000877 (GSM3333325) and T990275 (GSM3356360), were downloaded from the Gene Expression Omnibus database (GSE118391; <https://www.ncbi.nlm.nih.gov/geo/query/acc.cgi?acc=GSE118391>). The results of this analysis were visualized and graphed using WashU tool (<http://epigenomegateway.wustl.edu/browser/>).

Vector Construction

Each of the five enhancer regions (E1–E5) and their negative control (NC) were amplified using PCR or gene synthesis, then cloned into the pGL3-promoter vector. The primers used for PCR amplification of each enhancer are listed in **Table 2**.

Dual Luciferase Reporter Gene Assay

The vectors were transfected into STAD AGS and MKN45 cells, and pRL-TK plasmids were co-transfected as a normalization control. Luciferase assays were conducted using the Dual-Luciferase Reporter Assay System (Promega, USA).

RNA-Seq

Total RNA was extracted from cells using the TRIzol method as previously described, then qualified and quantified using a Nano Drop and Agilent 2100 bioanalyzer (ThermoFisher Scientific, USA). The mRNA library was constructed and sequenced on a BGISEQ500 system (BGI-Shenzhen, China).

Gene Set Enrichment Analysis (GSEA)

GSEA 4.1.0 software (<http://www.broadinstitute.org/gsea/index.jsp>) was downloaded and employed to analyze critical gene

TABLE 2 | Primer sequences.

Gene name	Primer sequences	
	Forward	Reverse
TM4SF1-AS1	CCCATGGATTGAGAAGGCTG	AAGCAGGAGTGGAGAGTTTCA
GAPDH	CTGGGCTACACTGAGCACC	AAGTGGTCGTTGAGGGCAATG
E1	TTACGCGTGCTAGCCCGGGCTCGAGGGGAAATTCCTCTCACTTCAAT	TGAGATGCAGATCGCAGATCTCTTCAACTAAAAGTGAAC
E2	TTACGCGTGCTAGCCCGGGCTCGAGAAATATGCATTACAAAACTTTCCA	TGAGATGCAGATCGCAGATCACCAGAAGGGCACACTT
E3	gene synthesis	
E4	TTACGCGTGCTAGCCCGGGCTCGAGACATGGCCTTTTGACCTTAT	TGAGATGCAGATCGCAGATTAGGGTCATGCTTATTTGGA
E5	gene synthesis	
NC	TTACGCGTGCTAGCCCGGGCTCGAGTATATAAGAATATTTTGATACC	TGAGATGCAGATCGCAGATACAGACATTTGTATATATTCAC

enrichment pathways between different groups based on FPKM values, which reflect relative gene expression.

Statistical Analysis

All data are presented as mean \pm SD. The Student's t-test or analysis of variance was performed using either SPSS or GraphPad 8.0.1 software. Values were considered statistically significant at $p < 0.05$ (*, $p < 0.05$; **, $p < 0.01$; ***, $p < 0.001$).

RESULTS

Identification of Super-Enhancer-Associated lncRNAs in STAD Samples and Cells

lncRNA plays a crucial role in biological processes and are regulated by SEs in several types of cancer. However, no studies on the relationship between lncRNAs and super-enhancers in STAD have been conducted to date. We first performed ChIP-seq with the H3K27ac antibody in AGS cell lines to identify SE-associated lncRNA in STAD, and downloaded raw data of 11 tissue samples and MKN45 cell lines from GEO database (GSE117953). We identified 1722, 1273, 1514, 2150, 2017, 1434, 1536, 1935, 983, 1978, and 2393 SE-associated lncRNAs in 11 STAD samples, respectively (T980401, T990275, and other 9 samples), and 1049 and 719 in two STAD cells, respectively (AGS and MKN45). Hockey stick plots of two representative tumor samples and both cells showed some SE-associated lncRNA (Figures 1A–D). Unsurprisingly, some common and vital lncRNAs that promote tumor progression are at the forefront of the H3K27ac signal, such as MALAT1, H19, and CCAT1 (Figures 1A–D). We also identified some novel SE-associated lncRNA in STAD (Figures 1A–D). According to the results of ChIP-seq, SE-associated lncRNAs in AGS and MKN45 cell lines intersected, and 386 common SE-associated lncRNAs were obtained (Figure 1E). The 386 SE-associated lncRNAs of the above two cell lines and the SE-associated lncRNAs obtained in the same way, which were present in over six STAD tissue samples, were intersected and 308 common SE-associated lncRNAs were obtained (Figure 1F). We analyzed 308 SE-associated lncRNAs in STAD samples and cells using ChIP-seq data against the H3K27ac antibody.

Expression Profile and Clinical Outcome of Super-Enhancer-Associated lncRNAs in STAD Patients

To further determine the expression profile and clinical value of SE-associated lncRNA, we first analyzed the expression changes of all lncRNAs in patients with STAD from TCGA database. The expression of 2961 lncRNAs in STAD patients were significantly upregulated or downregulated compared with that of normal samples (Figure 2A). The 2961 lncRNAs with altered expression in patients with intersected with the 308 SE-associated lncRNAs from the previous results, and 74 SE-associated and differentially expressed lncRNAs were obtained in total (Figure 2B). The heatmap revealed overall differential expression of these 74 SE-

associated lncRNAs in normal stomach and STAD samples (Figure 2C). We next utilized the least absolute shrinkage and selection operator (LASSO) algorithm to evaluate the prognosis role of 74 SE-associated lncRNAs in STAD patients. So that four SE-associated lncRNAs were included in this prognosis model according to the minimum criteria. We first observed the risk scores in alive and dead STAD patients, and found that the risk scores in dead STAD patients was indeed higher than those in alive patients (Figure 2D). We divided these SE-associated lncRNAs into two groups, high risk and low risk on basis of the RiskScore signature. High risk group was showed to be correlated with worse prognosis in STAD patients compared with low risk group (Figure 2E). The distribution of risk scores in STAD patients were showed (Figure 2F). Taken together, we elicited 74 differentially expressed SE-associated lncRNAs and assessed their correlation with the clinical importance of STAD patients.

The SE-Associated lncRNAs Are Correlated With Immune Cell Infiltration in STAD

Immune cells always affect the occurrence and development of tumors in the tumor microenvironment, and the relationship between immune cells and tumors can be used to develop specific drugs to inhibit tumor progression, such as PD1 and PDL1 inhibitors. We then examined whether SE-associated lncRNAs in STAD are related to the infiltration of immune cells. We used six algorithms to analyze the correlation between SE-associated lncRNAs and immune cells infiltration, namely ImmuCellAI, CIBERSORT, EPIC, quantiSeq, TIMER, and Xcell, respectively. It was found that all 74 differentially expressed SE-associated lncRNAs in STAD were significantly correlated with the immune cell infiltration using the ImmuCellAI (Figure 3A) and Xcell algorithms (Figure 3B). These immune cells included T and B cells, DC, neutrophils, and macrophage cells. In addition, most differentially expressed SE-associated lncRNAs in STAD were found to be significantly correlated with the immune cell infiltration by the other four algorithms, namely CIBERSORT (Supplementary Figure S1A), EPIC (Supplementary Figure S1B), quantiSeq (Supplementary Figure S1C), and TIMER (Supplementary Figure S1D). These data indicated that a correlation exists between differentially expressed SE-associated lncRNAs and immune cell infiltration in STAD.

SE-Associated lncRNAs Are Correlated With Immune Markers in STAD

In the tumor immune microenvironment, immune-related genes play a vital role in the regulation of tumor killing, including immunomodulators and chemokines. Therefore, we investigated whether SE-associated lncRNAs in STAD are related to immune makers. The list of immunomodulators and chemokines was downloaded from TISIDB database (<http://cis.hku.hk/TISIDB/download.php>). We first analyzed the correlation between SE-associated lncRNAs and immunomodulators in STAD and found that both immunoinhibitors and immunostimulators exhibited a significant correlation with SE-associated lncRNAs

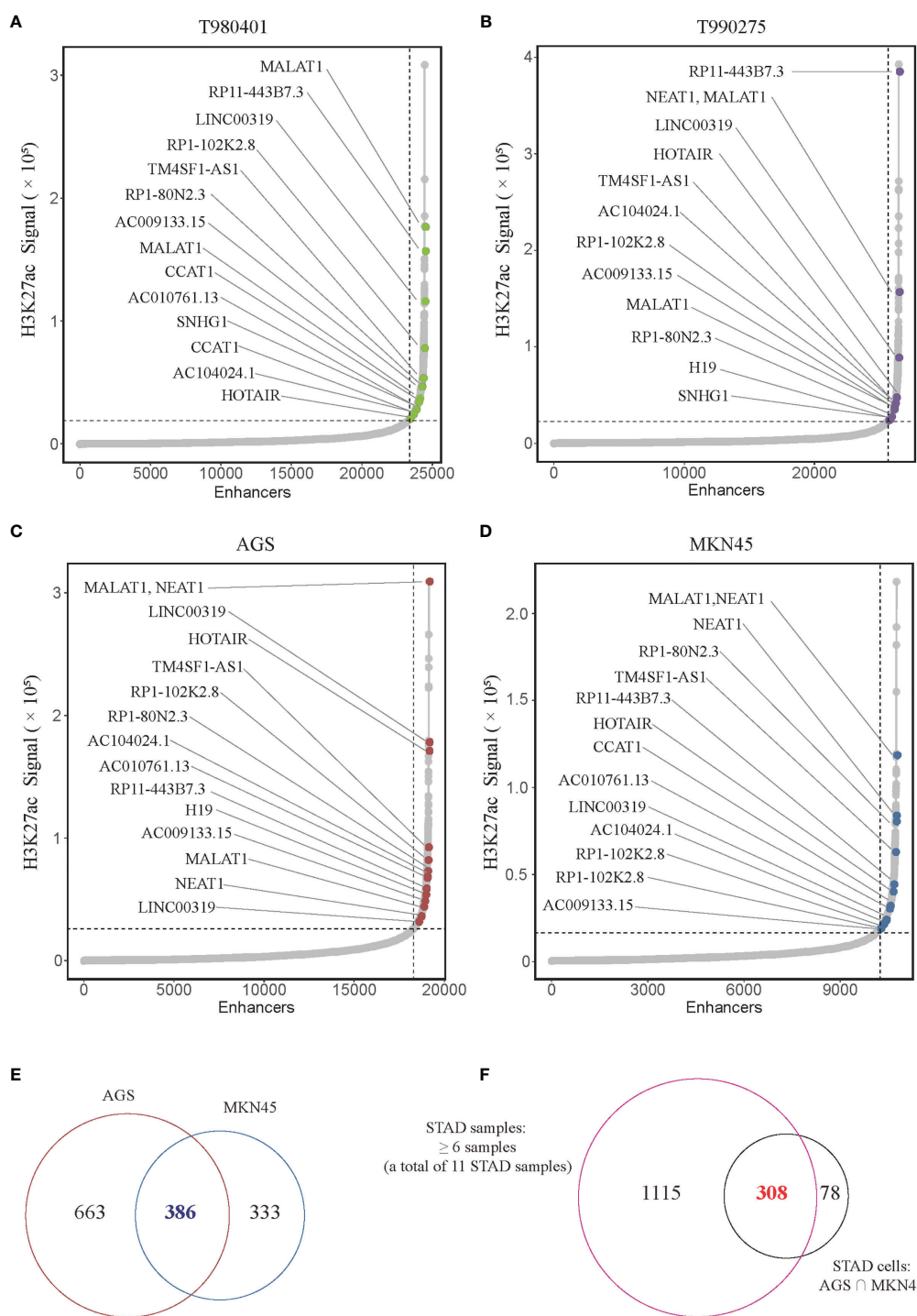


FIGURE 1 | Super-enhancer-associated lncRNAs present in STAD samples and cells. **(A–D)** Hockey stick plot of SE-associated lncRNAs in two tumor samples (T980401 and T990275) and two STAD cells (AGS and MKN45). Some representations of novel and known SE-associated lncRNAs are shown in color on the curve. **(E)** Venn diagram showing the intersection of SE-associated lncRNAs in two STAD cells (AGS and MKN45). **(F)** Venn diagram displaying the intersection of the SE-associated lncRNAs shared in two STAD cells and the SE-associated lncRNAs in at least 6 of 11 STAD samples. ChIP-seq with the H3K27ac antibody in AGS cell lines was from this study, and other H3K27ac ChIP-seq in 11 STAD tissue samples and MKN45 cell lines were downloaded from GEO database (GSE117953; <https://www.ncbi.nlm.nih.gov/geo/query/acc.cgi?acc=GSE117953>).

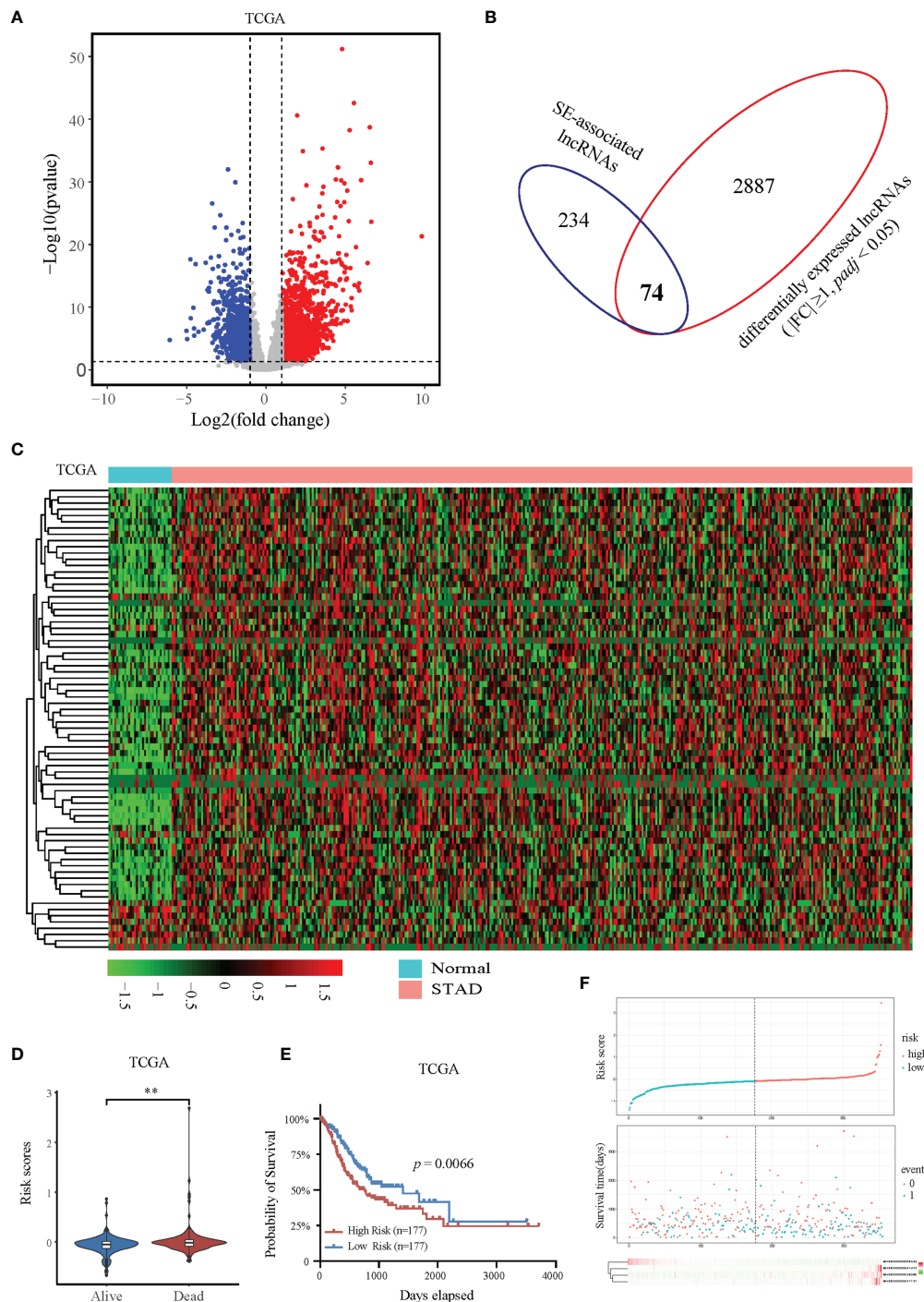


FIGURE 2 | Expression and prognostic analysis of super-enhancer-associated lncRNAs in patients with STAD. **(A)** Volcano plot showing the expression changes of SE-associated lncRNAs in STAD samples compared with normal stomach tissues. The red dots represent up-regulated lncRNAs ($FC \geq 1$, Q value < 0.05), and the blue dots represent down-regulated lncRNAs in STAD patients ($FC \leq -1$, Q value < 0.05). **(B)** Venn diagram representing the intersection of 2961 differentially expressed lncRNAs in patients with STAD and the 308 SE-associated lncRNAs identified above. **(C)** Expression profiling of 74 differentially expressed SE-associated lncRNAs in human STAD samples and normal stomach tissues. **(D)** The risk scores of alive or dead STAD patients predicted by expression of SE-associated lncRNAs from TCGA dataset. **(E)** The prognosis of SE-associated lncRNAs in STAD patients with high risk and low risk based on the RiskScore signature. **(F)** The distributions of the four lncRNAs in groups between high and low risk in STAD patients. The top was the risk score of STAD patients calculated according to the RiskScore signature and split into two groups on basis of medium score. The middle represented the survival status. The bottom heatmap showed the differential profile of four lncRNAs. The expression and clinical data of all lncRNAs were downloaded from TCGA database (<https://www.cancer.gov/>). **Indicates $p < 0.01$.

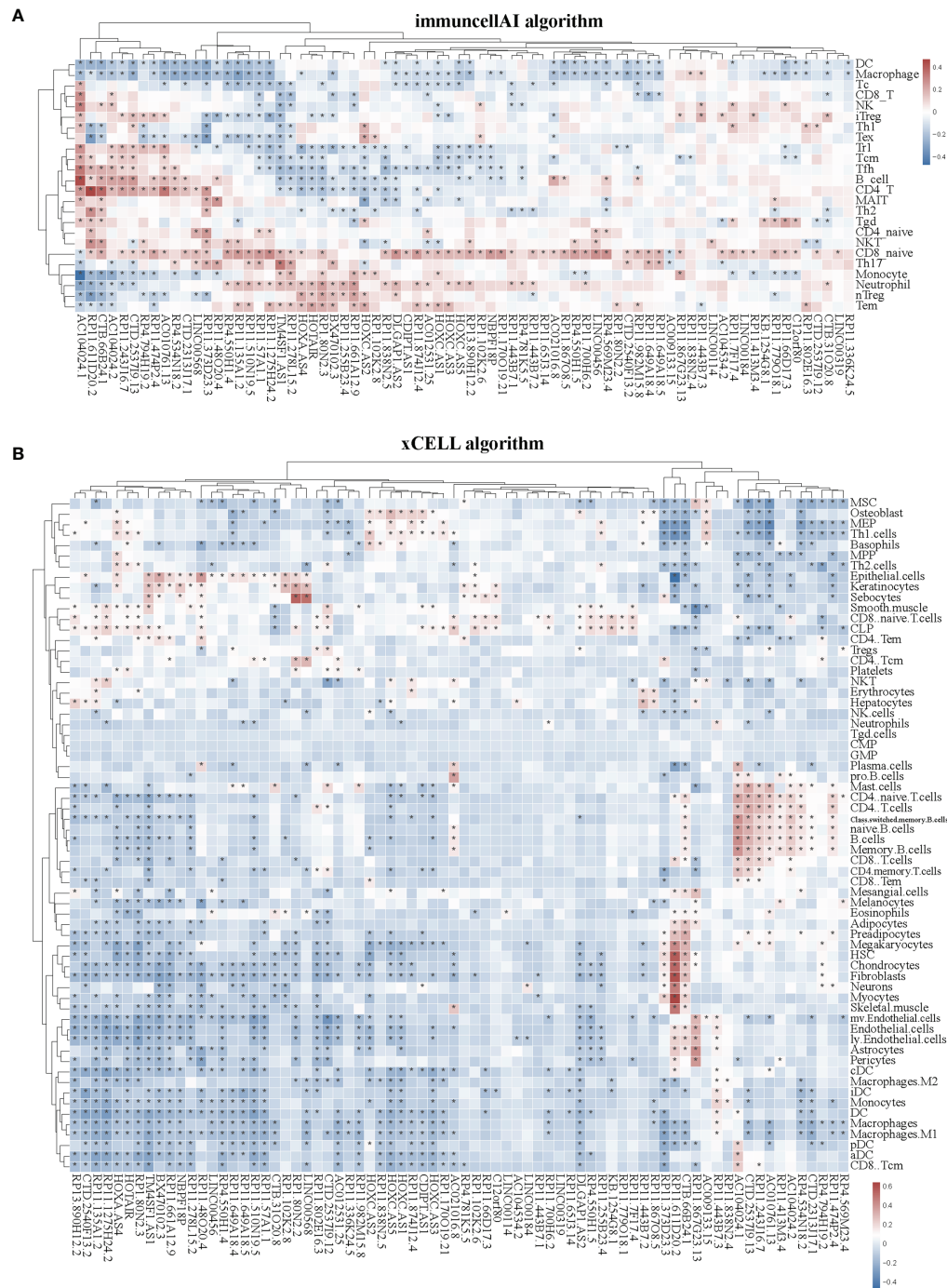


FIGURE 3 | Correlation between the expression of super-enhancer-associated lncRNA and immune cell infiltration in patients with STAD. **(A)** Cluster analysis of the correlation between 74 SE-associated lncRNAs expression and immune cells abundance calculated by using the ImmuCellAI algorithm. **(B)** Cluster analysis of the correlation between 74 SE-associated lncRNAs and immune cells abundance calculated with the Xcell algorithm. Red indicates positive correlation, while blue indicates negative correlation. The asterisk (*) signifies a significant correlation $p < 0.05$. The expression of 74 SE-associated lncRNAs were downloaded from TCGA database (<https://www.cancer.gov/>). Immune cell infiltration was calculated by using the ImmuCellAI (<http://bioinfo.life.hust.edu.cn/ImmuCellAI/#/>) and Xcell algorithm (<https://xcell.ucsf.edu/>) in STAD.

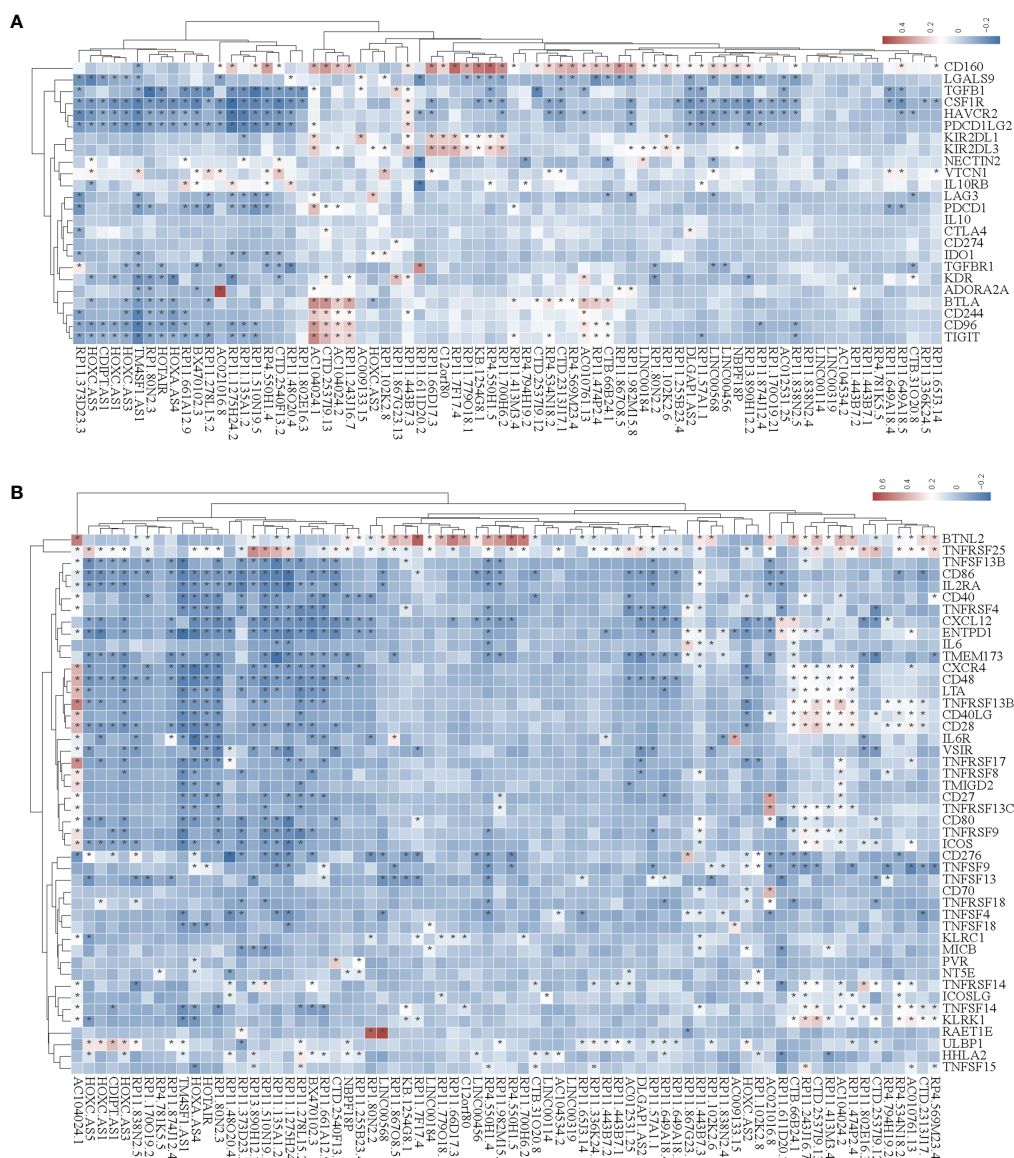


FIGURE 4 | The correlation between the expression of super-enhancer-associated lncRNA and immunomodulators in STAD. **(A)** Cluster analysis of the expression correlation between 74 SE-associated lncRNAs and immunoinhibitor-related markers. **(B)** Cluster analysis of the expression correlation between 74 SE-associated lncRNA strands and Immunostimulator-related markers. Red indicates positive correlation, while blue signifies negative correlation. The asterisk (*) indicates significant correlation ($p < 0.05$). The list of immunomodulators including immunoinhibitory and immunostimulator was downloaded from TISIDB database (<http://cis.hku.hk/TISIDB/download.php>). The expression of 74 SE-associated lncRNAs and immunomodulators were downloaded from TCGA database (<https://www.cancer.gov>).

(Figures 4A, B). In addition, SE-associated lncRNAs were significantly correlated with MHC molecules (Figure 5A).

We then analyzed the correlation between SE-associated lncRNAs and chemokines in STAD and found that chemokines and chemokine receptors were significantly related to SE-associated lncRNAs (Figures 5B, C). In summary, these data show that SE-associated lncRNAs in STAD are related to immunomodulators and chemokines, and they participate in tumor immune regulation of tumors.

TM4SF1-AS1 Is Involved in T Cell Mediated Immunity, and Predicts Immune Response to Anti-PD1 Therapy

We selected a CD8+ T cell-related lncRNA, TM4SF1-AS1, as a representation to investigate the role of SE-associated lncRNAs in tumor immune regulation of STAD. First, the expression of TM4SF1-AS1 in STAD samples was analyzed, and the expression of TM4SF1-AS1 was found to be significantly upregulated in STAD samples, which differed from normal stomach

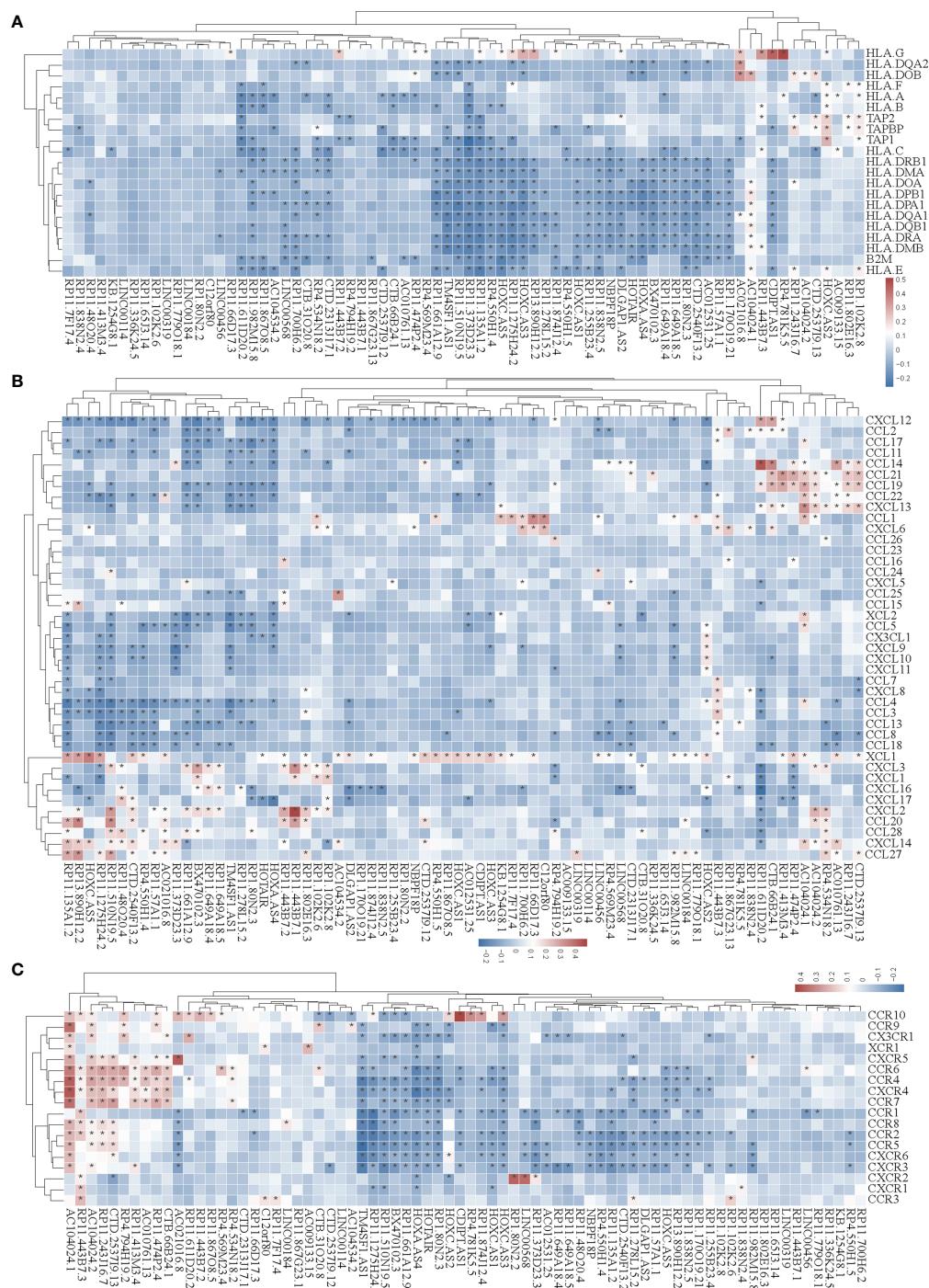


FIGURE 5 | Correlation analysis of the expression of super-enhancer-associated lncRNA and chemokines in STAD cells. **(A)** Results of cluster analysis of the expression correlation between 74 SE-associated lncRNAs and MHC molecules. **(B)** Cluster analysis results of the expression correlation between 74 SE-associated lncRNA and chemokines. **(C)** Results of the cluster analysis of the expression correlation between 74 SE-associated lncRNAs and chemokine receptors. Red signifies a positive correlation, while blue indicates negative correlation. The asterisk (*) is used to signify significant correlation ($p < 0.05$). The list of MHC molecules, chemokines and chemokine receptors was downloaded from TISIDB database (<http://cis.hku.hk/TISIDB/download.php>). The expression of 74 SE-associated lncRNAs, MHC molecules, chemokines and chemokine receptors were downloaded from TCGA database (<https://www.cancer.gov/>).

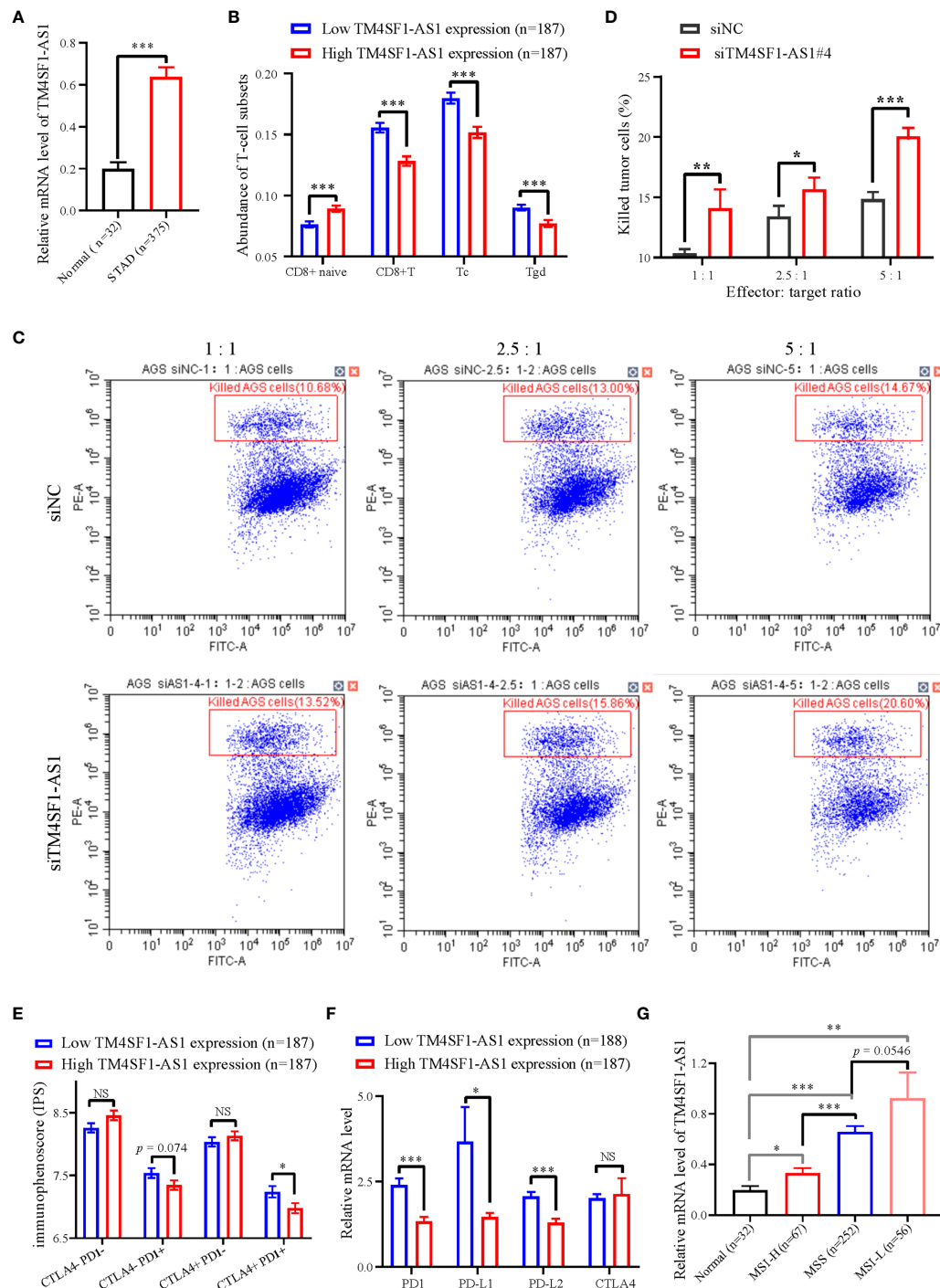


FIGURE 6 | The expression of TM4SF1-AS1 and its role in the tumor immune microenvironment in STAD. **(A)** Expression changes of TM4SF1-AS1 in human STAD samples compared with normal samples. **(B)** The abundance of CD8+ T cell between high and low expression of TM4SF1-AS1. **(B, C)** Flow cytometry showing the effect of TM4SF1-AS1 knockdown on the killing activities of activated T cells in AGS cells. **(C)** Immunophenoscore of CTLA4- PD1-, CTLA4- PD1+, CTLA4+ PD1- and CTLA4+ PD1+ patients in the groups with high and low TM4SF1-AS1 expression, respectively. **(D)** Expression of PD1, PD-L1, PD-L2 and CTLA4 in the high and low TM4SF1-AS1 expression groups. **(E)** Expression of TM4SF1-AS1 in groups among normal tissues, MSI-H, MSS and MSI-L. **(F)** Expression of PD1, PD-L1, PD-L2 and CTLA4 in the high and low TM4SF1-AS1 expression groups. **(G)** Expression of TM4SF1-AS1 in groups among normal tissues, MSI-H, MSS and MSI-L. The expression of TM4SF1-AS1, PD1, PD-L1, PD-L2 and CTLA4 were downloaded from TCGA database (<https://www.cancer.gov/>). Immunophenoscore information of CTLA4- PD1-, CTLA4- PD1+, CTLA4+ PD1- and CTLA4+ PD1+ patients were downloaded from TICA database (<https://tica.at/home>). NS stands for “no significance”, * refers to $p < 0.05$, ** indicates $p < 0.01$, and *** signifies $p < 0.001$.

samples (**Figure 6A**). We then observed the abundant differences in TM4SF1-AS1 expression in CD8⁺ T cells and classified subtypes as either high or low TM4SF1-AS1 expression. The abundance of CD8 naïve cells in the group with high TM4SF1-AS1 expression was found to be significantly lower than that of samples with low TM4SF1-AS1 expression. The abundance of CD8⁺ T, Tc, and Tgd cells was the opposite (**Figure 6B**).

We also performed an *in vitro* T cell killing assay to observe the killing effect of activated T cells on tumor cells with TM4SF1-AS1 interference. First, we found that the #3 and #4 siRNA against TM4SF1-AS1 had the best knockdown efficiency (**Supplementary Figures S2A, B**), and we selected siRNA#4 for further experimentation. Subsequently, the T cell killing assay showed that TM4SF1-AS1 interference significantly weakened the killing effect of activated CD8⁺ T cells on tumor cells in a T cell concentration-dependent manner (**Figures 6C, D**).

Furthermore, we analyzed immunophenoscore in CTLA⁺ PD1⁻, CTLA⁺ PD1⁺, CTLA⁻ PD1⁻ and CTLA⁺ PD1⁺ patients between the two groups with high and low TM4SF1-AS1 expression, respectively. Immunophenoscore information of CTLA⁺ PD1⁻, CTLA⁻ PD1⁺, CTLA⁺ PD1⁻ and CTLA⁺ PD1⁺ patients were downloaded from TICA database (<https://tica.at/home>). The immunophenoscore of CTLA⁺ PD1⁺ and CTLA⁺ PD1⁺ samples in the group with high TM4SF1-AS1 expression was significantly lower than that of samples with low TM4SF1-AS1 expression, while no significant difference was observed in CTLA⁻ PD1⁻ and CTLA⁺ PD1⁻ patients between the two groups (**Figure 6E**). We analyzed the expression of PD1, PD-L1, PD-L2, and CTLA4 in both groups. The expression of PD1, PD-L1, and PD-L2 was significantly higher in the group with high TM4SF1-AS1 expression (**Figure 6F**), and the expression of CTLA4 did not differ significantly between the high and low TM4SF1-AS1 expression groups (**Figure 6G**). In summary, these results indicate that TM4SF1-AS1 is involved in the T cell-mediated killing effect of tumor cells and monitors the immune response to anti-PD1 therapy.

TM4SF1-AS1 Is Driven by SEs in STAD

Since TM4SF1-AS1 was chosen as a representation of SE-associated lncRNAs in STAD, we further verified the regulation of the SE on TM4SF1-AS1. ChIP-seq data revealed one to two SE peaks in TM4SF1-AS1 in 11 STAD tumor samples and both AGS and MKN45 cell lines (**Figure 7A**). Subsequently, Hi-C data revealed that a spatial interaction exists between the SE regions and the TM4SF1-AS1 promoter (**Figure 7B**). We then cloned the five enhancer sequences and their negative control sequences into the PGL3-promotor vector for dual luciferase experiments. The fluorescence intensity of E2 and E3 was significantly higher than that of the NC group (**Figures 7C, D**). We confirmed that TM4SF1-AS1, a SE-associated lncRNA, is indeed regulated by its super-enhancer in STAD based on the above results.

TM4SF1-AS1 Is Involved in Immune Related Process

Finally, we performed RNA-seq on AGS and MKN45 cells after treating them with TM4SF1-AS1 interference to further

understand the tumor immune-related processes of TM4SF1-AS1 involved in STAD. First, we selected two siRNA targets, siTM4SF1-AS1#3 and siTM4SF1-AS1#4, for RNA-seq in two STAD cells. Next, we analyzed differentially expressed genes by comparing siTM4SF1-AS1 with siNC. We set the cut-off as $\log_2|FC| \geq 1$ and $Q < 0.05$, and identified both downregulated and upregulated genes following TM4SF1-AS1 knockdown in both AGS (**Figures 8A, B**) and MKN45 cells (**Figures 8C, D**). The shared differentially expressed genes in groups between siTM4SF1-AS1#3 and siTM4SF1-AS1#4 of AGS and MKN45 cell lines were 304 and 337, respectively (**Figures 8E, F**). Heatmap showed the expression change of shared differentially expressed genes in groups of siTM4SF1-AS1#3, siTM4SF1-AS1#4 in comparison with siNC group (**Figures 8G, H**). GSEA analysis revealed that TM4SF1-AS1 can regulate T cell-related biological processes in AGS (**Figures 8E, F**) and MKN45 cells (**Figures 8G, H**). KEGG pathway analysis revealed that TM4SF1-AS1 modulates several biological processes and pathways, including protein processing in endoplasmic reticulum (ER), cell cycle, microRNAs in cancer, cellular senescence, and virus infection in AGS (**Figures 8I, J**) and MKN45 cells (**Figures 8K, L**). These data further indicate that TM4SF1-AS1 is involved in tumor processes and immune regulation in STAD.

DISCUSSION

lncRNAs, which are transcribed by RNA polymerase II and independent transcriptional elements with lengths >200 bp, were thought to be unable to be translated into proteins (17). lncRNAs also play important roles in transcription, mRNA processing, post-transcriptional control, translation, and other biological processes (18, 19). Some lncRNAs are proven prospective markers of diagnosis, prognosis, and potential treatment targets in STAD, including EMT-associated lncRNA induced by TGFβ1 (ELIT-1) (20), LINC00346 (21), gastric cancer-associated lncRNA 1 (22) and gastric cancer metastasis-associated long noncoding RNA (23). lncRNAs play a crucial role in biological processes and have their own potential to act as biomarkers and therapeutic targets.

As mentioned before, lncRNAs can be epigenetically regulated by SEs to promote cancer malignancy. In ESCC, CCAT1 (24) and LINC01503 (25) are driven by SEs, which boost cancer progression. lncRNA UCA1 is activated by SE in cases of ovarian cancer, promoting tumor development (26). We previously found that SE-associated lncRNA HCCL5 was activated by ZEB1, which increased the malignancy of hepatocellular carcinoma (27). However, the biological function of SE-associated lncRNAs remains poorly characterized in tumors, especially in STAD. In the present study, we identified SE-associated lncRNAs in STAD for the first time to our knowledge and identified their potential oncogenic roles based on immune infiltration aspects and clinical outcomes.

The lncRNAs are reportedly involved in several biological processes containing the tumor immune microenvironment. Increased NKILA expression in T cells may aid cancer cells in

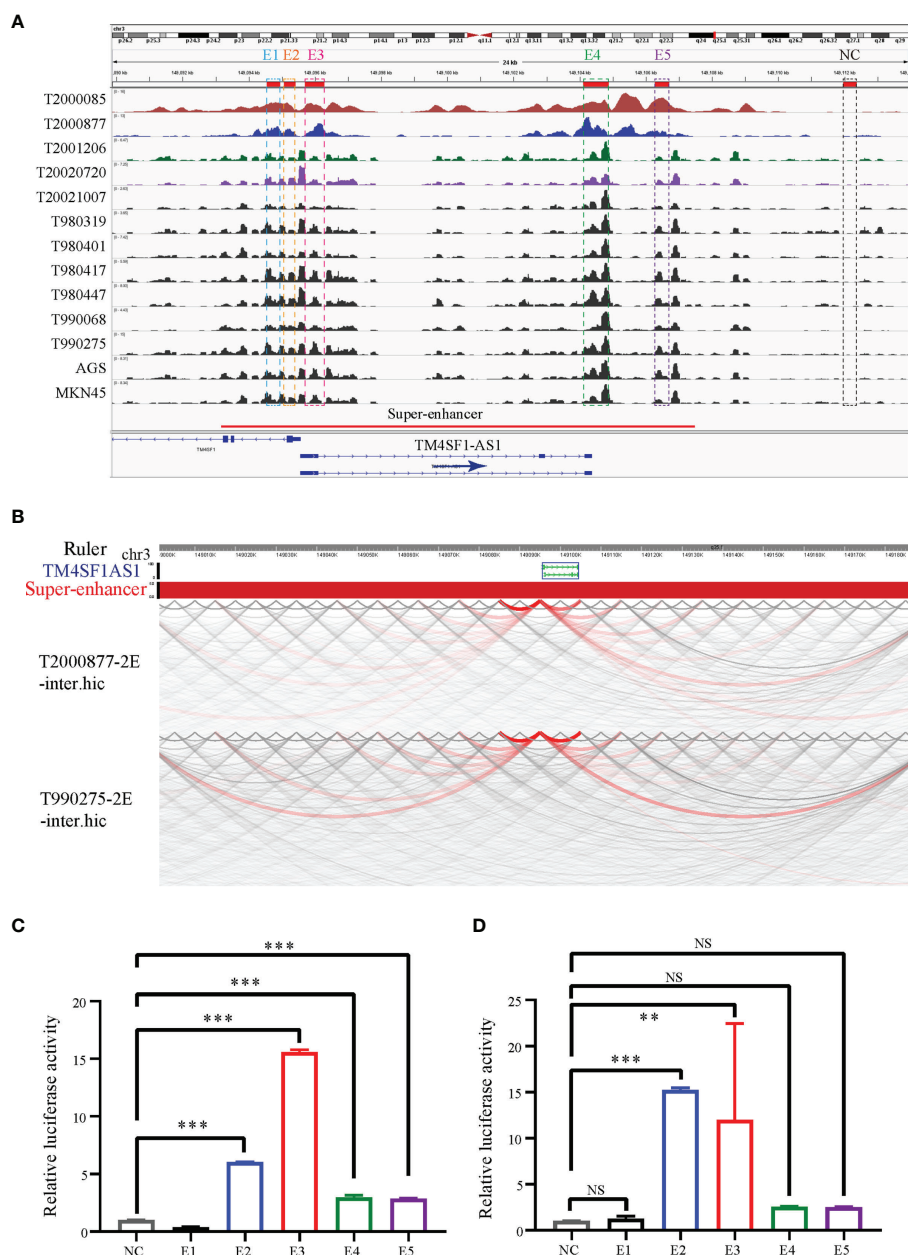


FIGURE 7 | TM4SF1-AS1 is driven by the super-enhancer in STAD. **(A)** ChIP-seq profiles of H3K27ac in 11 STAD samples and 2 STAD cells (AGS and MKN45). The super-enhancer region is divided into five enhancers, and their location information are showed. ChIP-seq with the H3K27ac antibody in AGS cell lines was from this study, and other H3K27ac ChIP-seq in 11 STAD tissue samples and MKN45 cell lines were downloaded from GEO database (GSE117953; <https://www.ncbi.nlm.nih.gov/geo/query/acc.cgi?acc=GSE117953>). **(B)** Hi-C data analysis of super-enhancer regions and promoter of TM4SF1-AS1 in two tumor samples (T980401 and T990275). Hi-C data in two tumor samples (T980401 and T990275) was downloaded from GEO database (GSE118391; <https://www.ncbi.nlm.nih.gov/geo/query/acc.cgi?acc=GSE118391>). **(C, D)** Dual luciferase experiments indicating the fluorescence intensity of all five enhancers compared with that of the NC group in **(C)** AGS **(D)** MKN45 cells. ns, no significance; ** $p < 0.01$, *** $p < 0.001$.

escaping immunological destruction *via* activation-induced cell death (28). Low SATB2-AS1 expression enhances tumor metastasis and increases immune cell density in CRC (29). The roles of SE-associated lncRNAs in the tumor immune microenvironment of STAD where T cell immunity is present

remains unknown. We first identified some SE-associated lncRNAs that were differentially expressed and correlated with immune cell infiltration in STAD in the present study.

Research on the tumor immune microenvironment has greatly promoted the development of tumor immunotherapy (30). T cells

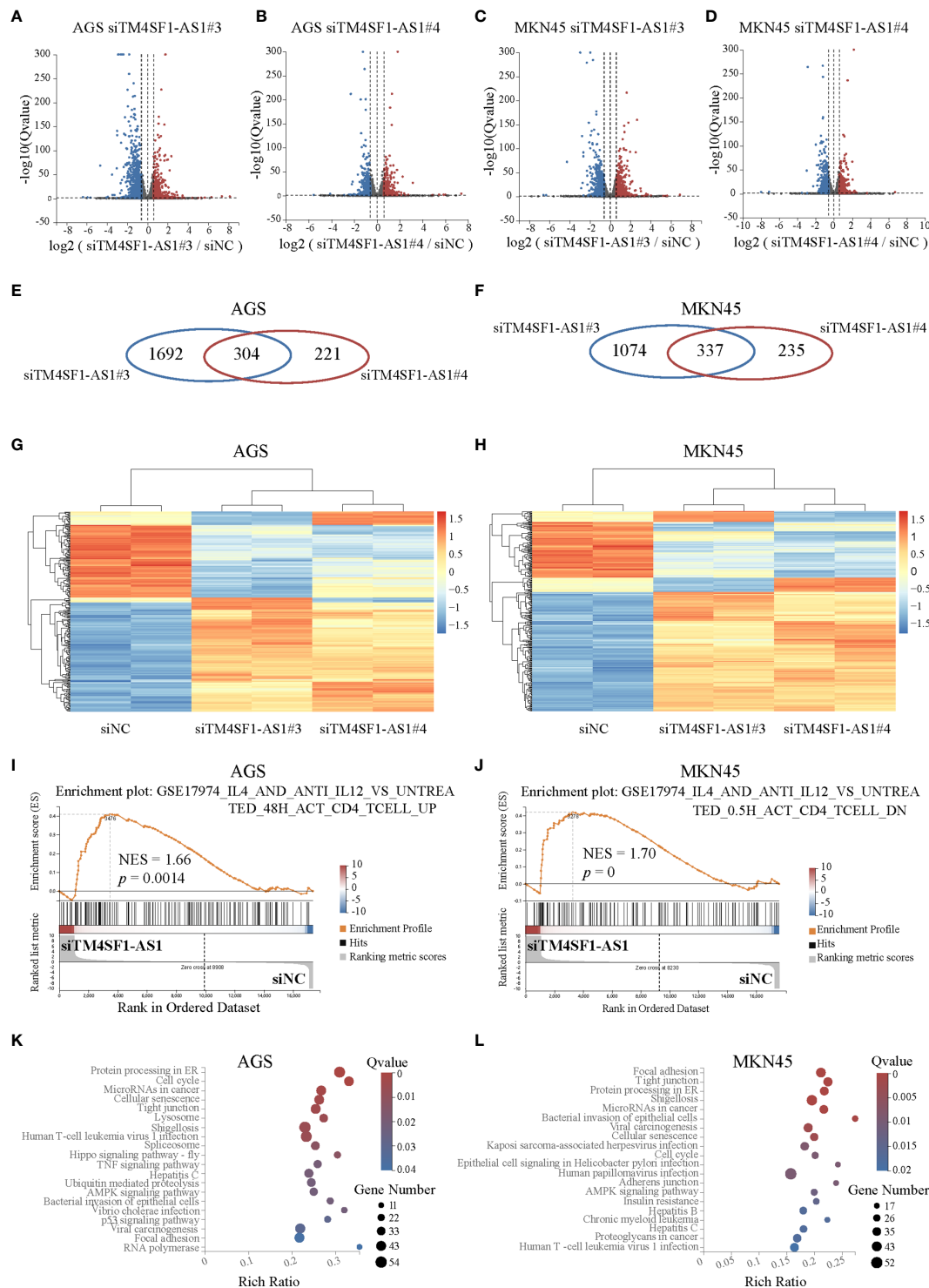


FIGURE 8 | Pathway analysis of TM4SF1-AS1 knockdown in two STAD cells. **(A–D)** Volcano map showing the up- and down-regulated genes after TM4SF1-AS1 knockdown in AGS and MKN45 cells with two siRNA targets (siTM4SF1-AS1#3 and siTM4SF1-AS1#4). The red dots indicate up-regulated genes, and blue dots signify down-regulated genes. **(E, F)** Venn diagram displaying the differentially expressed genes by the intersection of siTM4SF1-AS1#3 and siTM4SF1-AS1#3 in **(E)** AGS and **(F)** MKN45 cells. **(G, H)** Heatmap showing the up- and down-regulated genes after TM4SF1-AS1 knockdown in **(G)** AGS and **(H)** MKN45 cells with siTM4SF1-AS1#3 and siTM4SF1-AS1#4. The red dots indicate up-regulated genes, and blue dots signify down-regulated genes. **(I, J)** GSEA analysis was performed on **(I)** AGS and **(J)** MKN45 cells following TM4SF1-AS1 knockdown. **(K, L)** KEGG analysis was performed on the changed genes in **(K)** AGS and **(L)** MKN45 cells after TM4SF1-AS1 knockdown with siRNAs. RNA-seq data of TM4SF1-AS1 knockdown in AGS MKN45 cells was from this paper.

are the main cells involved in tumor immunotherapy and are responsible for defense against pathogen infection. It has been reported that TM4SF1-AS1 can exacerbate the progression of lung cancer (31), hepatocellular carcinoma (32) and gastric cancer (33). TM4SF1-AS1, a representative SE-associated lncRNA, was found to be involved in T cell immunity for the first time in the present study. Cancer cells evade the immune system's screening and attack in several ways. Previous studies have confirmed that PD-1 and CTLA-4 are crucial for deactivating T cells (34, 35). PD-1, which is located on the membrane surface, interacts with PD-L1 and PD-L2 to exhaust effector T cells and reduce the immune response (35). In contrast, CTLA-4 is expressed in activated CD4+ and CD8+ T cells and interacts with the B7 molecule to inhibit T cell activation (36). Cancer patients currently benefit tremendously from both anti-PD1 and anti-CTLA-4 immunotherapies. In addition, some lncRNAs such as GATA3-AS1 (37), MIR17HG (38), UCA1 (39) and SNHG15 (40) regulate PD-L1 expression in several cancers. In the present study, SE-associated lncRNA TM4SF1-AS1 exhibited an immune response to anti-PD1 therapy, and was associated with the expression of PD1, PDL1, and PDL2.

In conclusion, we identified SE-associated lncRNAs in STAD samples and cells and found that they were correlated with the immune microenvironment and clinical prognosis of patients with STAD. As a representation of SE-associated lncRNAs, TM4SF1-AS1 participated in T cell immunity and monitors the immune response to anti-PD1 therapy. Therefore, some specific SE-associated lncRNAs can be used as potential targets to design specific drugs to regulate the tumor immune system and thereby kill tumors.

DATA AVAILABILITY STATEMENT

The original contributions presented in the study are included in the article/**Supplementary Material**. Further inquiries can be directed to the corresponding authors.

REFERENCES

1. Sung H, Ferlay J, Siegel RL, Laversanne M, Soerjomataram I, Jemal A, et al. Global Cancer Statistics 2020: GLOBOCAN Estimates of Incidence and Mortality Worldwide for 36 Cancers in 185 Countries. *CA Cancer J Clin* (2021) 71:209–49. doi: 10.3322/caac.21660
2. Joshi SS, Badgwell BD. Current Treatment and Recent Progress in Gastric Cancer. *CA Cancer J Clin* (2021) 71:264–79. doi: 10.3322/caac.21657
3. Ajani JA, Lee J, Sano T, Janjigian YY, Fan D, Song S. Gastric Adenocarcinoma. *Nat Rev Dis Primers* (2017) 3:17036. doi: 10.1038/nrdp.2017.36
4. Nagaraja AK, Kikuchi O, Bass AJ. Genomics and Targeted Therapies in Gastroesophageal Adenocarcinoma. *Cancer Discovery* (2019) 9:1656–72. doi: 10.1158/2159-8290.cd-19-0487
5. Whyte WA, Orlando DA, Hnisz D, Abraham BJ, Lin CY, Kagey MH, et al. Master Transcription Factors and Mediator Establish Super-Enhancers at Key Cell Identity Genes. *Cell* (2013) 153:307–19. doi: 10.1016/j.cell.2013.03.035
6. Hnisz D, Abraham BJ, Lee TI, Lau A, Saint-André V, Sigova AA, et al. Super-Enhancers in the Control of Cell Identity and Disease. *Cell* (2013) 155:934–47. doi: 10.1016/j.cell.2013.09.053

AUTHOR CONTRIBUTIONS

Conception and design: LP. Administrative support: LP, YL, X-QY and DY. Provision of study materials: LP and Q-SL. Collection and assembly of data: LP, J-YP, and D-KC. Data analysis and interpretation: LP, J-YP, X-QY, and YB. Writing and review of the manuscript: LP, Y-TQ, J-YP, JL, H-TX, Z-PD, and X-QY. All authors contributed to the article and approved the submitted version.

FUNDING

This work was supported by the National Natural Science Foundation of China (grant no. 81972658 and 81802812 to LP), Guangdong Basic and Applied Basic Research Foundation (grant no. 2019A1515012114 and 2018A030313129 to LP), National Postdoctoral Program for Innovation Talents (grant no. BX20190395 to LP), China Postdoctoral Science Foundation (grant no. 2019M663254 to LP), the Fundamental Research Funds for the Central Universities (grant no. 20ykpy105 to LP). This study was also supported by grants from Guangdong Science and Technology Department (2020B1212060018, 2020B1212030004).

ACKNOWLEDGMENTS

The authors appreciate Bioinformatics Center of Sun Yat-Sen Memorial Hospital for providing computational resources. We are grateful for the invaluable suggestions of Jin-Gang Huang and Ya-Feng Zhu. We are also grateful for useful discussions with Jia-Hui Zhang in T cell related experiments.

SUPPLEMENTARY MATERIAL

The Supplementary Material for this article can be found online at: <https://www.frontiersin.org/articles/10.3389/fonc.2022.780493/full#supplementary-material>

7. Ying Y, Wang Y, Huang X, Sun Y, Zhang J, Li M, et al. Oncogenic HOXB8 Is Driven by MYC-Regulated Super-Enhancer and Potentiates Colorectal Cancer Invasiveness via BACH1. *Oncogene* (2020) 39:1004–17. doi: 10.1038/s41388-019-1013-1
8. Lin L, Huang M, Shi X, Mayakonda A, Hu K, Jiang YY, et al. Super-Enhancer-Associated MEIS1 Promotes Transcriptional Dysregulation in Ewing Sarcoma in Co-Operation With EWS-Flil1. *Nucleic Acids Res* (2019) 47:1255–67. doi: 10.1093/nar/gky1207
9. Scholz BA, Sumida N, de Lima CDM, Chachoua I, Martino M, Tzelepis I, et al. WNT Signaling and AHCTF1 Promote Oncogenic MYC Expression Through Super-Enhancer-Mediated Gene Gating. *Nat Genet* (2019) 51:1723–31. doi: 10.1038/s41588-019-0535-3
10. Ooi WF, Xing M, Xu C, Yao X, Ramlee MK, Lim MC, et al. Epigenomic Profiling of Primary Gastric Adenocarcinoma Reveals Super-Enhancer Heterogeneity. *Nat Commun* (2016) 7:12983. doi: 10.1038/ncomms12983
11. Miao YR, Zhang Q, Lei Q, Luo M, Xie GY, Wang H, et al. ImmuCellAI: A Unique Method for Comprehensive T-Cell Subsets Abundance Prediction and Its Application in Cancer Immunotherapy. *Adv Sci (Weinheim Baden-Wuerttemberg Germany)* (2020) 7:1902880. doi: 10.1002/adv.201902880

12. Newman AM, Liu CL, Green MR, Gentles AJ, Feng W, Xu Y, et al. Robust Enumeration of Cell Subsets From Tissue Expression Profiles. *Nat Methods* (2015) 12:453–7. doi: 10.1038/nmeth.3337
13. Marciniuk K, Trost B, Napper S. EpIC: A Rational Pipeline for Epitope Immunogenicity Characterization. *Bioinformatics* (2015) 31:2388–90. doi: 10.1093/bioinformatics/btv136
14. Finotello F, Mayer C, Plattner C, Laschober G, Rieder D, Hackl H, et al. Molecular and Pharmacological Modulators of the Tumor Immune Contexture Revealed by Deconvolution of RNA-Seq Data. *Genome Med* (2019) 11:34. doi: 10.1186/s13073-019-0638-6
15. Li T, Fan J, Wang B, Traugh N, Chen Q, Liu JS, et al. TIMER: A Web Server for Comprehensive Analysis of Tumor-Infiltrating Immune Cells. *Cancer Res* (2017) 77:e108–e10. doi: 10.1158/0008-5472.can-17-0307
16. Aran D, Hu Z, Butte AJ. Xcell: Digitally Portraying the Tissue Cellular Heterogeneity Landscape. *Genome Biol* (2017) 18:220. doi: 10.1186/s13059-017-1349-1
17. Yao RW, Wang Y, Chen LL. Cellular Functions of Long Noncoding RNAs. *Nat Cell Biol* (2019) 21:542–51. doi: 10.1038/s41556-019-0311-8
18. Goodall GJ, Wickramasinghe VO. RNA in Cancer. *Nat Rev Cancer* (2021) 21:22–36. doi: 10.1038/s41568-020-00306-0
19. Statello L, Guo CJ, Chen LL, Huarte M. Gene Regulation by Long Non-Coding RNAs and Its Biological Functions. *Nat Rev Mol Cell Biol* (2021) 22:96–118. doi: 10.1038/s41580-020-00315-9
20. Sakai S, Ohhata T, Kitagawa K, Uchida C, Aoshima T, Niida H, et al. Long Noncoding RNA ELIT-1 Acts as a Smad3 Cofactor to Facilitate Tgf β /Smad Signaling and Promote Epithelial-Mesenchymal Transition. *Cancer Res* (2019) 79:2821–38. doi: 10.1158/0008-5472.can-18-3210
21. Xu TP, Ma P, Wang WY, Shuai Y, Wang YF, Yu T, et al. KLF5 and MYC Modulated LINC00346 Contributes to Gastric Cancer Progression Through Acting as a Competing Endogenous RNA and Indicates Poor Outcome. *Cell Death Differ* (2019) 26:2179–93. doi: 10.1038/s41418-018-0236-y
22. Guo X, Lv X, Ru Y, Zhou F, Wang N, Xi H, et al. Circulating Exosomal Gastric Cancer-Associated Long Noncoding RNA1 as a Biomarker for Early Detection and Monitoring Progression of Gastric Cancer: A Multiphase Study. *JAMA Surg* (2020) 155:572–9. doi: 10.1001/jamasurg.2020.1133
23. Zhuo W, Liu Y, Li S, Guo D, Sun Q, Jin J, et al. Long Noncoding RNA GMAN, Up-Regulated in Gastric Cancer Tissues, Is Associated With Metastasis in Patients and Promotes Translation of Ephrin A1 by Competitively Binding GMAN-As. *Gastroenterology* (2019) 156:676–91.e11. doi: 10.1053/j.gastro.2018.10.054
24. Jiang Y, Jiang YY, Xie JJ, Mayakonda A, Hazawa M, Chen L, et al. Co-Activation of Super-Enhancer-Driven CCAT1 by TP63 and SOX2 Promotes Squamous Cancer Progression. *Nat Commun* (2018) 9:3619. doi: 10.1038/s41467-018-06081-9
25. Xie JJ, Jiang YY, Jiang Y, Li CQ, Lim MC, An O, et al. Super-Enhancer-Driven Long Non-Coding RNA LINC01503, Regulated by TP63, Is Over-Expressed and Oncogenic in Squamous Cell Carcinoma. *Gastroenterology* (2018) 154:2137–51.e1. doi: 10.1053/j.gastro.2018.02.018
26. Lin X, Spindler TJ, de Souza Fonseca MA, Corona RI, Seo JH, Dezem FS, et al. Super-Enhancer-Associated lncRNA UCA1 Interacts Directly With AMOT to Activate YAP Target Genes in Epithelial Ovarian Cancer. *iScience* (2019) 17:242–55. doi: 10.1016/j.isci.2019.06.025
27. Peng L, Jiang B, Yuan X, Qiu Y, Peng J, Huang Y, et al. Super-Enhancer-Associated Long Noncoding RNA HCCL5 Is Activated by ZEB1 and Promotes the Malignancy of Hepatocellular Carcinoma. *Cancer Res* (2019) 79:572–84. doi: 10.1158/0008-5472.can-18-0367
28. Huang D, Chen J, Yang L, Ouyang Q, Li J, Lao L, et al. NKILA lncRNA Promotes Tumor Immune Evasion by Sensitizing T Cells to Activation-Induced Cell Death. *Nat Immunol* (2018) 19:1112–25. doi: 10.1038/s41590-018-0207-y
29. Xu M, Xu X, Pan B, Chen X, Lin K, Zeng K, et al. lncRNA SATB2-AS1 Inhibits Tumor Metastasis and Affects the Tumor Immune Cell Microenvironment in Colorectal Cancer by Regulating SATB2. *Mol Cancer* (2019) 18:135. doi: 10.1186/s12943-019-1063-6
30. Binnewies M, Roberts EW, Kersten K, Chan V, Fearon DF, Merad M, et al. Understanding the Tumor Immune Microenvironment (TIME) for Effective Therapy. *Nat Med* (2018) 24:541–50. doi: 10.1038/s41591-018-0014-x
31. Zhou F, Wang J, Chi X, Zhou X, Wang Z. lncRNA TM4SF1-AS1 Activates the PI3K/AKT Signaling Pathway and Promotes the Migration and Invasion of Lung Cancer Cells. *Cancer Manage Res* (2020) 12:5527–36. doi: 10.2147/cmar.s254072
32. Zeng Z, Shi Z, Liu Y, Zhao J, Lu Q, Guo J, et al. HIF-1 α -Activated TM4SF1-AS1 Promotes the Proliferation, Migration, and Invasion of Hepatocellular Carcinoma Cells by Enhancing TM4SF1 Expression. *Biochem Biophys Res Commun* (2021) 566:80–6. doi: 10.1016/j.bbrc.2021.06.011
33. He C, Qi W, Wang Z. Effect and Mechanism of Downregulating the Long-Chain Noncoding RNA TM4SF1-AS1 on the Proliferation, Apoptosis and Invasion of Gastric Cancer Cells. *World J Surg Oncol* (2021) 19:226. doi: 10.1186/s12957-021-02334-y
34. Sharpe AH, Freeman GJ. The B7-CD28 Superfamily. *Nat Rev Immunol* (2002) 2:116–26. doi: 10.1038/nri727
35. Akin Telli T, Bregni G, Camera S, Deleporte A, Hendlitz A, Scalfani F. PD-1 and PD-L1 Inhibitors in Oesophago-Gastric Cancers. *Cancer Lett* (2020) 469:142–50. doi: 10.1016/j.canlet.2019.10.036
36. Phan GQ, Yang JC, Sherry RM, Hwu P, Topalian SL, Schwartzentruber DJ, et al. Cancer Regression and Autoimmunity Induced by Cytotoxic T Lymphocyte-Associated Antigen 4 Blockade in Patients With Metastatic Melanoma. *Proc Natl Acad Sci USA* (2003) 100:8372–7. doi: 10.1073/pnas.1533209100
37. Zhang M, Wang N, Song P, Fu Y, Ren Y, Li Z, et al. lncRNA GATA3-AS1 Facilitates Tumour Progression and Immune Escape in Triple-Negative Breast Cancer Through Destabilization of GATA3 But Stabilization of PD-L1. *Cell Proliferation* (2020) 53:e12855. doi: 10.1111/cpr.12855
38. Xu J, Meng Q, Li X, Yang H, Xu J, Gao N, et al. Long Noncoding RNA MIR17HG Promotes Colorectal Cancer Progression via miR-17-5p. *Cancer Res* (2019) 79:4882–95. doi: 10.1158/0008-5472.can-18-3880
39. Wang CJ, Zhu CC, Xu J, Wang M, Zhao WY, Liu Q, et al. The lncRNA UCA1 Promotes Proliferation, Migration, Immune Escape and Inhibits Apoptosis in Gastric Cancer by Sponging Anti-Tumor miRNAs. *Mol Cancer* (2019) 18:115. doi: 10.1186/s12943-019-1032-0
40. Dang S, Malik A, Chen J, Qu J, Yin K, Cui L, et al. lncRNA SNHG15 Contributes to Immuno-Escape of Gastric Cancer Through Targeting Mir141/PD-L1. *OncoTargets Ther* (2020) 13:8547–56. doi: 10.2147/ott.s251625

Conflict of Interest: The authors declare that the research was conducted in the absence of any commercial or financial relationships that could be construed as a potential conflict of interest.

Publisher's Note: All claims expressed in this article are solely those of the authors and do not necessarily represent those of their affiliated organizations, or those of the publisher, the editors and the reviewers. Any product that may be evaluated in this article, or claim that may be made by its manufacturer, is not guaranteed or endorsed by the publisher.

Copyright © 2022 Peng, Peng, Cai, Qiu, Lan, Luo, Yang, Xie, Du, Yuan, Liu and Yin. This is an open-access article distributed under the terms of the Creative Commons Attribution License (CC BY). The use, distribution or reproduction in other forums is permitted, provided the original author(s) and the copyright owner(s) are credited and that the original publication in this journal is cited, in accordance with accepted academic practice. No use, distribution or reproduction is permitted which does not comply with these terms.



MicroRNAs/LncRNAs Modulate MDSCs in Tumor Microenvironment

Xiaocui Liu^{1†}, Shang Zhao^{2†}, Hongshu Sui¹, Hui Liu¹, Minhua Yao¹, Yanping Su^{1*} and Peng Qu^{1,3*}

¹ Department of Histology and Embryology, Shandong First Medical University & Shandong Academy of Medical Sciences, Shandong, China, ² Department of Pathophysiology, Shandong First Medical University & Shandong Academy of Medical Sciences, Shandong, China, ³ National Institutes of Health (NIH), Bethesda, MD, United States

OPEN ACCESS

Edited by:

Shiv K. Gupta,
Mayo Clinic, United States

Reviewed by:

Erbao Bian,
Second Hospital of Anhui Medical
University, China
Kunal Shah,
Queen Mary University of London,
United Kingdom

*Correspondence:

Yanping Su
su-yanping@163.com
Peng Qu
pengquji2000@gmail.com

[†]These authors have contributed
equally to this work and share first
authorship

Specialty section:

This article was submitted to
Molecular and Cellular Oncology,
a section of the journal
Frontiers in Oncology

Received: 08 September 2021

Accepted: 14 February 2022

Published: 14 March 2022

Citation:

Liu X, Zhao S, Sui H, Liu H, Yao M,
Su Y and Qu P (2022) MicroRNAs/
LncRNAs Modulate MDSCs
in Tumor Microenvironment.
Front. Oncol. 12:772351.
doi: 10.3389/fonc.2022.772351

Myeloid-derived suppressor cells (MDSCs) are a heterogeneous group of immature cells derived from bone marrow that play critical immunosuppressive functions in the tumor microenvironment (TME), promoting cancer progression. According to base length, Non-coding RNAs (ncRNAs) are mainly divided into: microRNAs (miRNAs), lncRNAs, snRNAs and CircRNAs. Both miRNA and lncRNA are transcribed by RNA polymerase II, and they play an important role in gene expression under both physiological and pathological conditions. The increasing data have shown that miRNAs/lncRNAs regulate MDSCs within TME, becoming one of potential breakthrough points at the investigation and treatment of cancer. Therefore, we summarize how miRNAs/lncRNAs mediate the differentiation, expansion and immunosuppressive function of tumor MDSCs in TME. We will then focus on the regulatory mechanisms of exosomal MicroRNAs/LncRNAs on tumor MDSCs. Finally, we will discuss how the interaction of miRNAs/lncRNAs modulates tumor MDSCs.

Keywords: myeloid-derived suppressor cells, microRNAs, lncRNAs, networks, tumor microenvironment

INTRODUCTION

MDSCs are a heterogeneous population derived from bone marrow progenitor cells and immature myeloid cells (1). In normal physiology, immature myeloid cells are differentiated into monocytes, granulocytes, macrophages and dendritic cells, which exert immune activity (2). However, in cancers and other diseases (such as inflammation), MDSCs have the negative regulatory immune response to exacerbate disease status (2, 3). In the process of tumor progression, MDSCs cannot properly differentiated into monocytes and macrophages to play their immune roles, but abnormally proliferate and accumulate within TME (4). Tumor cells secrete many factors to

Abbreviations: MDSCs, Myeloid-derived suppressor cells; TME, Tumor microenvironment; TGF- β , The transforming growth factor- β ; IL-1 β , The cytokine interleukin-1 β ; IFN- γ , Interferon- γ ; VEGFA, vascular endothelial growth factor A; C/EBP, CCAAT/enhancer binding protein; CXCR2, C-X-C motif chemokine receptor 2; PTEN, Phosphatase and tensin homolog; SHIP-1, Src Homology 2-containing Inositol Phosphatase-1; YAP, Yes-associated protein; ASH2L, Absent small or homeotic-like; MLL1, Mixed lineage leukemia 1; CCL2, C-C motif chemokine ligand 2; MEF2C, Myocyte enhancer factor 2C; Rap1B, Ras-related protein Rap1B; MUC1, Transmembrane glycoprotein Mucin 1; IRF8, Interferon regulatory factor 8; NLRP3, NACHT; LRR; and PYD domains-containing protein 3; NFIA, Nuclear factor I A; AML1, Acute myeloid leukemia 1; IGF1, Insulin-like growth factor I; FOG2, Friend of Gata 2; PDCD4, Programmed cell death 4; SOCS3, Suppressor of cytokine signalling-3; PIAS3, Protein inhibitor of activated STAT3; SNAIL1, Snail family transcriptional repressor 1; Twist1, Twist-related protein 1; ZEB1, Zinc finger E-box binding homeobox 1; LAMB3, Laminin subunit beta-3; CHOP, C/EBP Homologous Protein.

inhibit the differentiation of immature myeloid cells and promote the proliferation and immunosuppressive roles of MDSCs (5). These mediators mainly include the TGF- β , Ligands for toll-like receptors, IL-1 β , IFN- γ , IL-6, FMS-like tyrosine kinase 3 ligand (FLT3L), Granulocyte colony-stimulating factor (G-CSF), Macrophage colony-stimulating factor (M-CSF), Granulocyte-macrophage colony stimulating factor (GM-CSF) and IL-4 (6). Most mediators activate the functional state of MDSCs by regulating signal converters and transcriptional activators (STATs and NF κ B) (7, 8). For example, IL-6 enhances both stimulatory and inhibitory roles of MDSCs *via* STAT3 signaling pathways in breast cancer (8, 9).

Tumor MDSCs are mainly divided into two main subtypes according to their phenotypes and origins, which are defined by cell surface markers of MDSCs in both tumor models and cancer patients (10, 11). The phenotypes of MDSCs in tumor-bearing mice are defined using Gr1 (Ly6G/Ly6C)/CD11b and further include two subtypes of MDSCs: Monocyte-MDSCs (M-MDSCs, CD11b+Ly6G–Ly6Chi) and Granulocyte-MDSCs (G-MDSCs, CD11b+Ly6G+Ly6Clo) (12, 13). The phenotypes of MDSCs are more diverse in cancer patients. MDSCs are cell populations expressing Lin-HLA-DR-CD33+ or CD11b-CD14-CD33+ in human body. The main subtypes are also divided into M-MDSCs (HLA-DR–/loCD11b+CD14– CD15–) and G-MDSCs (CD11b+ CD14– CD15+ or CD11b+CD14– CD66b+) (14). Third subtype known as early-MDSCs which has been found in human studies. They are defined as Lin-HLA-DR-CD33+, mainly consisting of colony-forming cells activity and other myeloid precursor cells (13, 15).

M-MDSCs account for about 80% of all tumor MDSCs, but their inhibitory roles are lower than those of G-MDSCs. M-MDSCs are modulated by producing NO and Arginases. In contrast, the roles of G-MDSCs are determined by ROS and H₂O₂ (16–19). The main function of G-MDSCs is to inhibit T cell function, while M-MDSCs mainly differentiate into TAMs in

cancer. It is well known that MDSCs have become the most important prognostic markers in cancer immunotherapy and contribute to immunosuppressive checkpoint resistance (20) (**Figure 1**).

MiRNAs are non-coding single-stranded small RNAs of approximately 22–24 nucleotides in length and are highly conserved evolutionarily, and are widely found in eukaryotic cells. They play vital regulatory roles in cells, especially in mRNA post-transcriptional regulation, and reduce mRNA expression levels by binding to the 3'UTR of mRNA and binding to the 5' UTR of mRNA to upregulate its transcription (10–12). MiRNAs are involved in regulating both a wide range of physiological activities such as cell cycle, differentiation, proliferation, maturation and immune response and pathological processes, such as inflammation and cancer (13). For example, our data have shown that miRNAs mediate the differentiation, expansion and function of tumor MDSCs (14).

LncRNAs are non-protein-coding RNAs of approximately 200 nucleotides in length (15). According to the position of lncRNAs in the genome relative to protein-coding genes, they can be divided into five categories: sense, antisense, bidirectional, intronic and intergenic (16, 17). LncRNAs are ever regarded byproducts of RNA polymerase II transcription as “noise” of genomic transcription without biological function (5, 17). However, the increasing evidences have revealed that lncRNAs mediate gene expression through chromatin modification, transcriptional regulation and post-transcriptional regulation in the nucleus and extranuclear, and are also involved in the occurrence and development of tumors (18–22) (**Figure 2**). LncRNAs have been found to mediate the carcinogenesis of colon cancer through a variety of molecular mechanisms, suggesting that lncRNAs can be used as biomarkers for early diagnosis and treatment of colon cancer (23). LncRNAs are overexpressed during the development, differentiation and activation of immune cells, such as monocytes, macrophages,

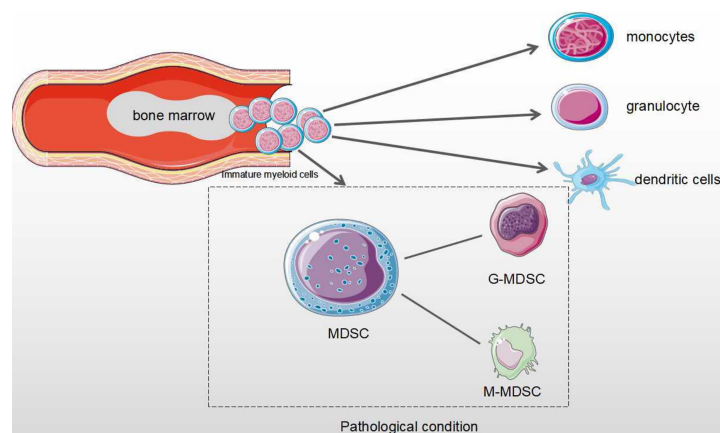


FIGURE 1 | The differentiation process of MDSCs in physiological and pathological conditions. Under normal physiological conditions, myeloid progenitor cells are differentiated into monocytes, granulocytes and dendritic cells that are involved in the regulation of immune response. Under pathological condition, myeloid progenitor cells are differentiated into MDSCs. MDSCs from Immature myeloid cells are divided as two subtypes: monocytic MDSCs (M-MDSCs) and Granulocytic MDSCs (G-MDSCs).

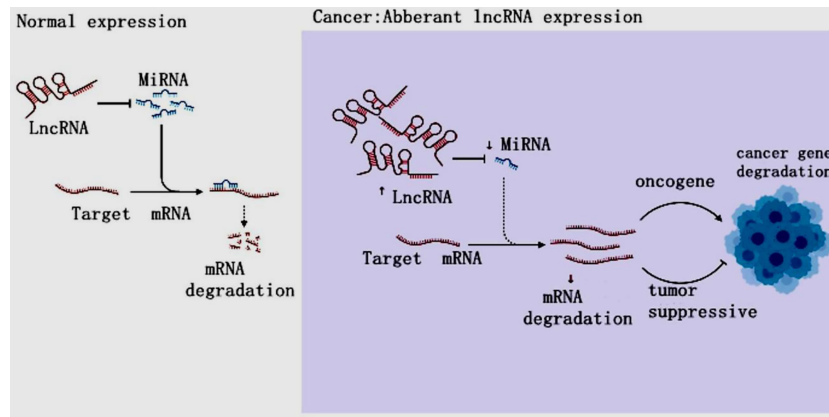


FIGURE 2 | The LncRNA Regulation in cancer. In cancer, lncRNAs inhibit targeted mRNAs through endogenous competition with miRNAs, resulting in mRNA downregulation and carcinogenesis, resulting in tumor gene disorder and cancer.

dendritic cells, neutrophils (24). Furthermore, the increasing data were conducted on the activity of lncRNAs on MDSCs in TME (16, 25–27). Both miRNA and lncRNAs, as Non-coding RNAs (ncRNAs) can modulate tumor MDSCs. Thus, here we discuss the regulatory mechanisms of miRNAs/lncRNAs on the biological status and immune activity of MDSCs in TME, and put forward our own opinions.

MIRNAS/LNCRNAS

ncRNAs are mainly divided by length into small (< 200 nucleotides) and long (> 200 nucleotides) RNAs according to base length. ncRNAs are: miRNAs, lncRNAs, snRNAs, circRNAs (28). ncRNAs act as regulatory molecules that regulate for a wide range of cellular processes, such as chromatin

remodeling, transcription and post-transcriptional modification (29). MiRNAs have been well investigated over the past decade, lncRNAs are actively studied for their diverse roles in gene expression regulation. Besides, lncRNAs themselves can interact with other ncRNAs, such as miRNAs (30). Both miRNA and lncRNA are transcribed by RNA polymerase II, and they play important roles in gene expression under both physiological and pathological conditions, as transcriptional and post-transcriptional regulators (28). Studies have shown that miRNAs and lncRNAs are involved in transcriptional regulation at different levels, miRNAs/lncRNAs directly determine gene expression by binding with mRNA, gene/transcript or histone modifiers (31). lncRNAs may play a functional role as miRNA sponges by base-pair blocking of miRNA binding to target mRNA-3'UTR (32) (**Figure 3**).

Recent studies have highlighted the diverse roles of MiRNAs/lncRNAs in cancer progression and metastasis. Increasing

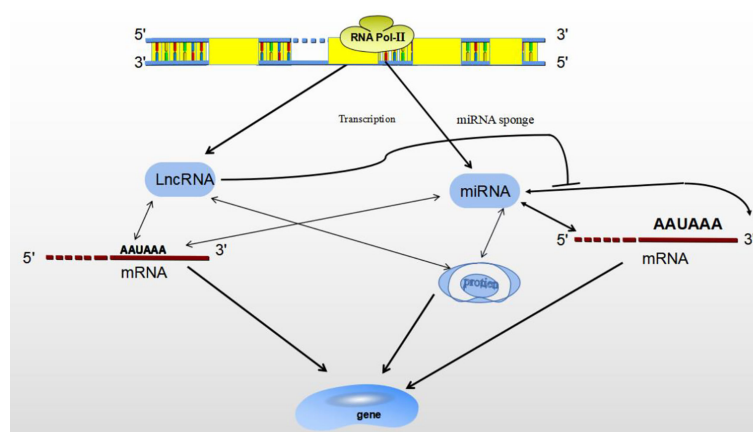


FIGURE 3 | The relationship between MiRNA and LncRNA. Both miRNA and lncRNA regulate gene expression through binding with mRNA, gene/transcript or histone modifiers. lncRNA may sponges miRNA by base-pair blocking of miRNA response elements binding to target mRNA-3'UTR.

numbers of miRNAs and lncRNAs are found to be dysregulated in cervical cancer, regulating metastasis through regulating metastasis-related genes and signaling pathways. Moreover, miRNAs can interact with lncRNAs respectively during this complex process (33, 34). In breast cancer, the lncRNA MALAT1 and miR-100 are indirectly interlinked through VEGFA. MALAT1 binds to miR-216b as a competing endogenous RNA to restore Pyridox(am)ine-5-phosphate Oxidase deficiency (PNPO) and promote cell proliferation, migration and invasion in breast cancer (33). Therefore, miRNAs/lncRNAs are involved in gene expression and transcriptional regulation. They also affect the development of cancer and regulate the expression of oncogenes and tumor suppressors in TME (28, 32, 35). Therefore, the regulation of miRNA/lncRNA is more conducive to the research of bioactive targets for cancer treatment.

POST-TRANSCRIPTIONAL REGULATION OF TUMOR MDSCS WITH MIRNAS/LNCRNA

Researchers have found that the interactions between miRNAs/lncRNAs and transcription factor modulated the biological status and immune activity of MDSCs in TME (36). Here, we describe the regulation of miRNA/lncRNA on MDSCs in the TME. The abnormal expression of miRNAs/lncRNAs in MDSCs and their regulatory mechanism on MDSCs have become potential breakthrough points.

Expansion of MDSCs

The expansion of tumor MDSCs is regulated through several pathways. Members of the CCAAT/enhancer binding protein (C/EBP) family, as key regulatory transcription factors, may

regulate many biological processes, including cell growth, differentiation, metabolism and death. In TME, C/EBP maintains the critical regulation of MDSCs (37, 38) (**Figure 4**). In Lewis lung carcinoma and B16 melanoma, the overexpression of miR-486 promotes the proliferation of MDSCs and inhibits the differentiation and apoptosis of MDSCs through targeting C/EBPA (39). During the tumor process, when the C-X-C motif chemokine receptor 2(CXCR2) is activated, the expression level of miR-449c targeting STAT6 mRNA in MDSCs is upgraded to promote the MDSC expansion (6). In 4T1-breast cancer cell, miRNA-494 which is upregulated by tumor-derived factor TGF- β 1, promotes the accumulation and activity of MDSCs through targeting Phosphatase and tensin homolog (PTEN) and activating Akt pathway (40). miR-155 and miR-21 promote the expansion of tumor MDSCs through targeting ship-1 and PTEN (41). Furthermore, miR-155 enhances tumor MDSC inhibitory activity through SocS1 repression (42–44). MiR-155 deficiency is also found to diminish the aggregation of functional MDSCs in the colon cancer, indicating that miRNA-155 could accelerate the accumulation of MDSCs (43–45). In lung tumor mouse model, miR-21 maintained MDSC accumulation in the TME by downregulating RUNX1 and upregulating Yes-associated protein (YAP), indicating that targeting miR-21 in MDSCs may be developed as an immunotherapeutic approach to combat lung cancer (46). In mixed leukemia, tumor-secreted factors GM-CSF/IL-6 upregulate high expression levels of miR-21a/21b/181b through STAT3/CEBP β pathway, further diminishing the expression of WD repeat-containing protein 5 (Wdr5), absent small or homeotic-like (ASH2L) and mixed lineage leukemia 1 (MLL1), which are involved in the expansion and differentiation of G-MDSC. Furthermore, knockdown of these miRNAs diminishes the expansion of GM-CSF/IL-6-induced G-MDSCs, suggesting that miR-21a/21b/181b stimulate accumulation of MDSCs in the TME (47) (**Table 1**).

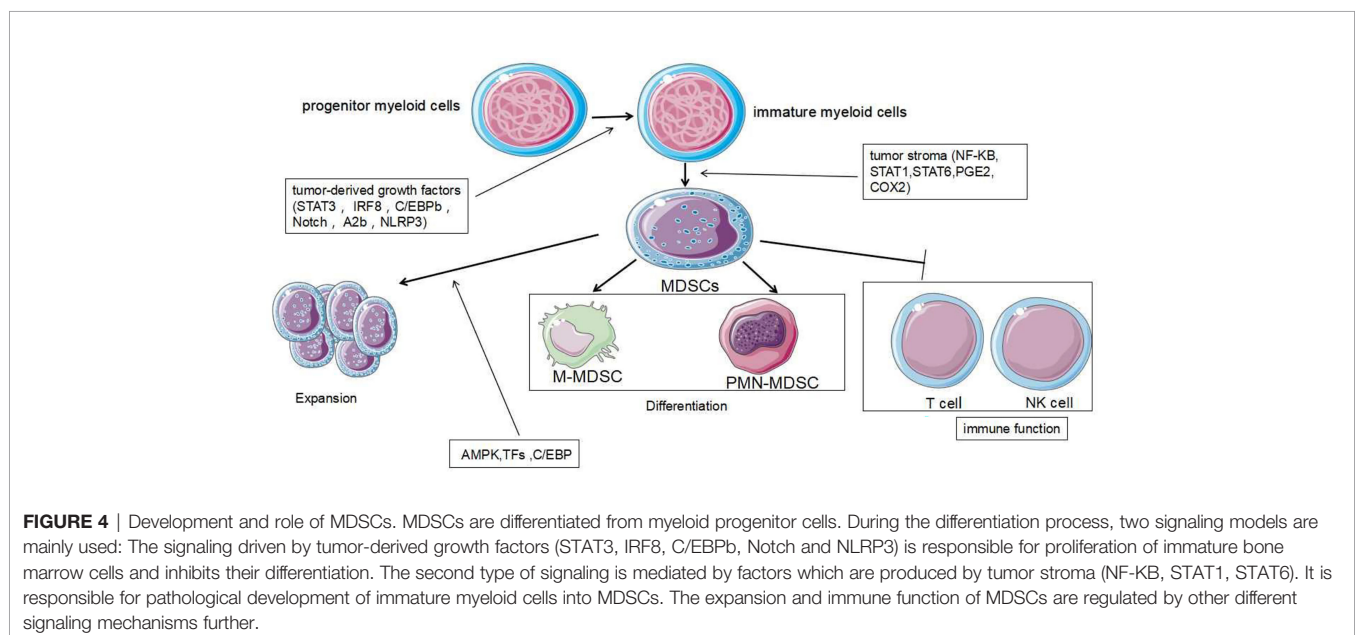


FIGURE 4 | Development and role of MDSCs. MDSCs are differentiated from myeloid progenitor cells. During the differentiation process, two signaling models are mainly used: The signaling driven by tumor-derived growth factors (STAT3, IRF8, C/EBPb, Notch and NLRP3) is responsible for proliferation of immature bone marrow cells and inhibits their differentiation. The second type of signaling is mediated by factors which are produced by tumor stroma (NF-KB, STAT1, STAT6). It is responsible for pathological development of immature myeloid cells into MDSCs. The expansion and immune function of MDSCs are regulated by other different signaling mechanisms further.

TABLE 1 | Regulation of MiRNAs on tumor MDSCs.

MiRNA	Targets/signal pathway	Function on MDSCs	Ref.
miR-449c	STAT6	To elevate the number	(6)
miR-142-3p	STAT3/CEBP β	To prevent the differentiation	(14, 36, 48)
miR-223	MEF2C	To block accumulation/differentiation	(39)
miR-486	C/EBP α	To stimulate proliferation	(40)
miR-494	PTEN/Akt	To promote the accumulation and activity	(49)
	TGF- β	To strengthen function	(41)
miR-155	PTEN	To increase the number	(41)
miR-21	AMKP	To exaggerate expansion	(47)
miR21a/21b/181b	AMPK	To maintain inhibitory roles	(50)
miR-34a	MUC1	To diminish the expansion	(51)
	TGF- β /IL10	To reduce the number	(52)
miR-10	STAT3/CEBPB	To stimulate expansion	(53, 54)
miR-708	RaP1B	To diminish the expansion and number	(55)
miR-424		To reduce numbers	(56)
miR-9	NFIA	To improve differentiation	(57)
miR-136		To promote differentiation	(58)
miR21/miR130b/miR155/miR28	IGF1/Jun	To enhance blockage activity	(59)
miR-200c		To enhancing inhibitory activity	(54)
miR-17-92	FOG2/PTEN	To diminish blockage roles	(60)
miR-195/miR-16	STAT	To block immunosuppressive function	(61)
miR-10a	PD-I	To improve the differentiation	(62)
miR-30a	Runx1	To enhance activity	(63)
miR-17	SOCS3	To prevent differentiation/activity	

Chemotherapy is one major method of cancer treatment. However, it also brings some side effects. Rong et al. found that chemotherapies (such as doxorubicin treatment) induced drug-resistance in breast cancers cells and stimulated proliferation and activation of MDSCs to inhibit T cell anti-tumor response. In doxorubicin-resistant breast cancer, Doxorubicin-induced miR-10 overexpression exaggerates the expansion and activation of MDSCs by activating the AMKP signaling pathway, leading to poor prognosis in breast cancer patients (52). Hox antisense intergenic RNA (HOTAIR) is one lncRNA which is regarded as oncogene to play crucial roles in the progression and metastasis of several cancers such as breast, colorectal and gastric cancers. Moreover, HOTAIR overexpression causes expansion and recruitment of MDSCs in cancer cells through the release of CCL2 (5) (**Table 2**).

MiRNAs/lncRNAs also negatively regulate the numbers and expansion of MDSCs in the TME. In our previous studies, negative roles of miRNAs on MDSCs have been described (14). In tumor-bearing mice, miR-223 reduces the accumulation of MDSCs and inhibits immature myeloid cells

differentiation into MDSCs by targeting Myocyte enhancer factor 2C (MEF2C) (36, 48). In ovarian cancer treatment, Lin et al. found that dexamethasone(DEX), a synthetic glucocorticoid (GC), stimulated miR-708 overexpression by targeting RaP1B, further diminishing the expansion and number of MDSCs in TME (53). Pyzer et al. demonstrated that miR34a overexpression led to the downregulation of c-myc expression by transmembrane glycoprotein Mucin 1 (MUC1) silencing, reducing the expansion of MDSCs in acute myeloid leukemia (AML) (50) (**Figure 5**).

Differentiation of MDSCs

Tumor-derived factors affect different stages of myeloid cell differentiation, leading to the generation of pathologically activated M-MDSCs and PMN-MDSCs. The differentiation process of MDSCs is mediated through two types of signaling panels. The first type of signaling, driven by tumor-derived growth factors (STAT3, IRF8, C/EBP β , Notch and NLRP3), is responsible for proliferation of immature bone marrow cells and inhibits their differentiation. The second type of signaling is

TABLE 2 | Regulation of LncRNAs on MDSCs.

LncRNAs	Target genes/signal pathway	Function on MDSCs	Ref.
HOTAIR	CCL2	To promote expansion and recruitment	(5)
RNCR3	miR-185 CHOP	To increases the inhibitory roles	(16)
Olfr29-ps1	IL-6	To accelerate roles	(16)
lnc-C/eBP β	C/EBP β /WDR5/IL-4il	To improve the differentiation	(47)
	C/EBP β subtypes LAP	To suppress immunosuppressive function	(46)
LNC-CHOP	CHOP and C/EBP β	To improve blockage the roles	(64)
lncRNAPVT1	hypoxia-inducible factor-1 α	To upgrade the inhibitory activity	(65)
AK036396	Ficolin B	To prevent the maturation	(66)
lncR MALAT1		To decrease the number	(67)

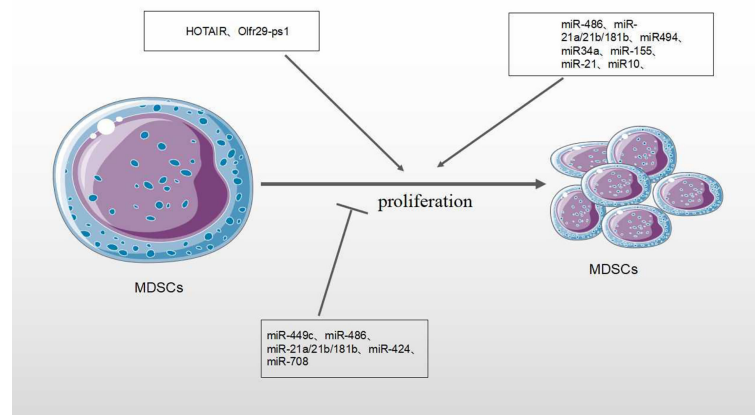


FIGURE 5 | Effect of MicroRNA/LncRNA on MDSC proliferation in the TME. MiRNAs/LncRNAs modulate the proliferation of MDSCs through different genes and signaling pathways. In each process, microRNA/LncRNA play positive: + or negative: - roles.

mediated by factors produced by tumor stroma (the NF- κ B Pathway, STAT1, STAT6). It is responsible for pathologically activating immature myeloid cells into MDSCs (68) (**Figure 4**). Accumulating evidence has demonstrated that tumor-related MDSCs are differentiated into mature myeloid cells, such as macrophages or neutrophils through the regulation of different miRNAs. The downregulation of miR-9 is found to improve the differentiation of tumor MDSCs *via* targeting Runx1, thereby hindering tumor growth (56). Shi et al. demonstrated that TNF- α -upregulated miR-136 enhanced the differentiation of MDSCs and inhibited tumor growth by targeting Nuclear factor I A (NFIA) (57).

MiRNAs/LncRNAs also negatively modulate the differentiation of MDSCs in the TME. The upregulation of miR-34a reduces immature myeloid cells differentiation into MDSCs *via* TGF- β and IL-10 (51). The productions of bone marrow are altered during tumor development, leading to the accumulation of immunosuppressive cells there. miR-142-3p is found to restrain the differentiation of MDSCs into mature cells by regulating STAT3 and C/EBP β signaling pathways (13, 14). MiR-17 family members (such as miR-17-5p, miR-20a and miR-106a) are overexpressed in human progenitor cells and inhibit AML1 (the leukemia-associated transcription factor acute myeloid leukemia 1; also known as runt-related transcription factor 1, or RUNX1), leading to downregulation of M-CSFR, which prevents differentiation and activity of tumor MDSCs (63). In human acute promyelocytic leukemia, the master transcription factor PU.1 is revealed to activate the transcription of miR-424 and repress NFI-A, an inhibitor of monocyte differentiation, thereby stimulating the differentiation of MDSCs into mature cells to reduce MDSC population (55) (**Table 1**).

Lnc-C/EBP β is an intermediate gene encoded on chromosome 4 that is highly conserved in mice, humans and other species. There are two subtypes of c/EBP β : liver-rich activating protein (LAP⁺, LAP) and liver-rich inhibitory

protein (LIP) (64). Expression of Lnc-C/EBP β in murine M-MDSCs is found to block the differentiation and inhibitory activity of MDSCs. This is through down-regulating the expression of IL-4, suggesting that it could be a potential target in tumor immunotherapy (46, 47). Metastasis-Associated Lung Adenocarcinoma Transcript 1 (MALAT1), a nuclear intergenic lncRNA, is highly conserved among species and involved in various diseases. Recently, lncRNA MALAT1 was found to stimulate the proliferation, invasion, and metastasis of many types of cancer cells such as cervical cancer, lung cancer, colorectal cancer and liver cancer (69). Knockout of MALAT1 genes in MDSCs lead to the increased number of MDSCs by the inhibition of MDSC differentiation (67). However, the regulatory mechanisms need to be investigated further (**Figure 6** and **Table 2**).

Immunosuppressive Function of MDSCs

In the TME, MDSCs inhibit the anti-tumor roles of many immune cells, such as Natural Killer (NK) cells, B cells and T cells. The inhibition of T cell function is most important for evaluating the activity of MDSCs (1) (**Figure 4**). MiRNAs/LncRNA upregulate the activity and immunosuppressive function of MDSCs through different signaling pathways and transcription factors within TME (39, 58). In B lymphoma mouse models, the expression of miR-30a in MDSCs promotes the immunosuppressive roles of MDSCs (56). In addition, miR-30a also targets SOCS3/STAT3 to enhance the inhibitory activity of MDSCs (55). In the most common type of non-Hodgkin lymphoma (NHL) — diffuse large B-cell lymphoma (DLBCL), four circulating miRNAs (miR-21, miR-130b, miR-155, and miR-28) are considered to be novel prognosis biomarkers of DLBCL and modulate RAS protein signaling transduction *via* Insulin-like growth factor I (IGF1) and Jun. These four miRNAs are associated with the induction of MDSCs and Th17 cells through cytokines TGF β 1, IL-6 and IL-17, resulting in the immune suppression of DLBCL (58). In gastric cancer, miR-

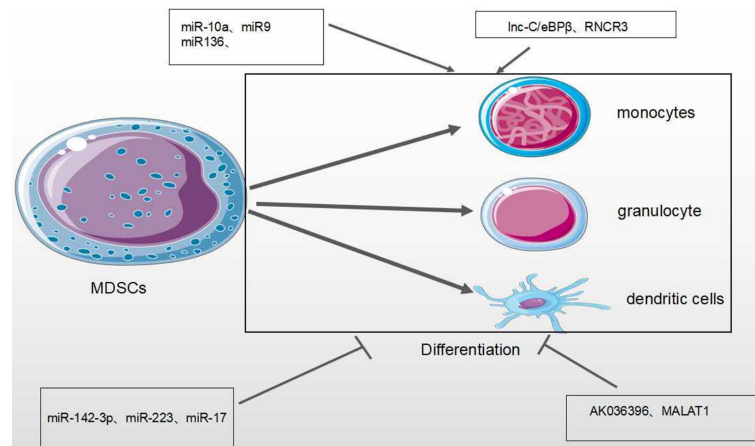


FIGURE 6 | Effect of MicroRNA/LncRNA on MDSC differentiation in the TME. MiRNAs/LncRNAs mediate the differentiation of MDSCs into monocyte, dendritic cells and neutrophils through different genes and signaling pathways. In each process, microRNA/LncRNA play positive: + or negative: - roles.

494 is positively associated with the expression of tumor-derived TGF- β which exaggerates the suppressive roles of MDSCs (49). In various tumor mouse models (such as lung cancer, breast cancer and colon cancer), it has been found that the tumor-derived factor GM-CSF induces miR-200c overexpression to activate Akt by negatively regulating the transcriptional regulator friend of Gata 2 (FOG2) and PTEN expression, further enhancing the immunosuppressive activity of MDSCs (59) (**Table 1**).

Olfactory Receptor 29 Pseudogene 1 (Olf29-ps1), as one lncRNA pseudogene, is conserved in vertebrates (70). Tumor-associated factors can increase the expression of Olf29-ps1 in MDSCs. In colon and rectal cancer, Olf29-ps1 stimulates proliferation and inhibitory activity of M-MDSC by the upregulation of pro-inflammatory factor IL-6 (16). Plasmacytoma Variant Translocation 1 (PVT1), an intergenic lncRNA, is conserved in humans and mice. In various cancers, tumor-associated factors induce the increased expression of PVT1 in MDSCs. Downregulation of Pvt1 expression in PMN-MDSCs can reduce suppressive activity of MDSCs through the reduced activity of both ROS and Arg-1. In addition, PVT1 also up-regulates the expression levels of hypoxia-inducible factor-1 α to enhance the immunosuppressive activity of G-MDSCs under hypoxia (65). Similarly, lnc-CHOP, as an intronic lncRNA, increases the activity of both ROS and Arg-1 through interacting with both CHOP and C/EBP β subtypes to promote C/EBP β activity and H3K4me3 enrichment, further enhancing the suppressive activity of MDSCs within the TME (64).

Tian et al. found that lncRNA AK036396 and its target Ficolin B were highly expressed in mouse PMN-MDSCs. The downregulation of lncRNA AK036396 improved differentiation and diminished the suppressive roles of PMN-MDSCs through reduced Ficolin B protein stability. In addition, human M-ficolin, as an ortholog of mouse Ficolin B, stimulates the suppressive activity of MDSCs in patients with lung cancer through the induction of arginase1 expression. These results indicate that lncRNA AK036396 could

accelerate inhibitory roles of PMN-MDSCs on T cell anti-tumor responses (66) (**Table 2**).

MiRNAs/LncRNAs also negatively modulate the immunosuppressive function of MDSCs in the TME. The STATs pathway is of vital regulatory function. In both lung carcinoma and 1D8 ovarian carcinoma, miR-17-92 cluster (miR-17-5p and miR-20a) could block the roles of MDSCs through targeting STATs (54). Tao et al. demonstrated that the restoration of miR-195 and miR-16 expression enhanced radiotherapy *via* T cell activation in TME by the inhibition of PD-L1 expression, after radiation with anti-PD-1 treatment on prostate cancer. The synergistic effect of immunotherapy and radiotherapy is associated with the proliferation of CD8 $^{+}$ T cells and inhibition of MDSCs and regulatory T cells (Treg), indicating that miR-195 and miR-16 may reduce the suppressive functions of MDSCs through PD-1 dependent pathways (60).

An intergenic lncRNA, HOXA Transcript Antisense RNA Myeloid-Specific1 (HOTAIRM1) has been shown to downregulate the suppressive functions of MDSCs in the TME, since HOTAIRM1 can induce the high expression of HOXA1 in MDSCs to reduce Arg-1 expression and ROS production. In addition, increased expression of HOXA1 has been shown to decrease the percentage of MDSCs, and enhance the immune response in a tumor mouse model (26).

Therefore, miRNAs/LncRNAs effectively regulate the differentiation, proliferation, and immunosuppressive functions of MDSCs (47, 71) (**Figure 7**).

MIRNAS/LNCRNAS FROM TUMOR-DERIVED EXOSOMES MEDIATE THE FUNCTION OF MDSCS IN TME

Exosomes are small extracellular vesicles with size 30-150nm in diameter that are secreted by most cells (72). Exosomes are rich

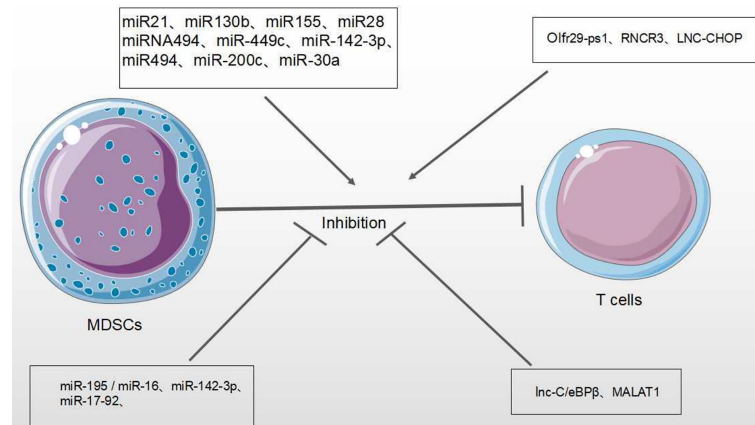


FIGURE 7 | Effect of miRNA/LncRNA on MDSC function in the TME. MiRNAs/LncRNAs modulate the immunosuppressive roles of MDSCs on T cell anti-tumor response. In each process, miRNAs/LncRNAs play positive → or negative ⊣ roles.

in genetic material and molecules: DNA, miRNA, lncRNAs, proteins and lipids, which are essential for cell-cell communication and physiological status. Moreover, exosomes are also involved in the regulation of tumor progression in the TME (11). Recently, it has been demonstrated that exosomes secreted by tumor cells play critical roles in cancer progression and invasion, including TME remodeling, tumor metastasis and tumor-associated immunosuppression (73).

MiRNAs in tumor-derived exosomes mediate the activity of MDSCs in TME through different expression patterns, transcription factors and signaling pathways (61, 74). In pancreatic cancer, the increased expression of miR-let-7i in TDEs affects the levels of myeloid inhibitory intracellular inflammatory cytokines (IL-6, IL-17, IL-1 β) and transcription factors, downregulating the anti-tumor immune response (74). In glioma, glioma-derived exosomes (GDEs) miR-29a and miR-92a increase the proliferation and suppressive roles of MDSCs through targeting high-mobility group box transcription factor 1 (Hbp1) and protein kinase cAMP-dependent type I regulatory subunit alpha (Prkar1a), respectively, further mediating the formation of suppressive TME (75). In LLC lung cancer model, miR-21a from LLC-Exosomes are revealed to increase both the autocrine production of IL-6 and phosphorylation levels of STAT3 by targeting Programmed cell death 4 (PDCD4), thereby preventing the activation of cytotoxic CD8⁺T cells and enhancing the proliferation and activity of MDSCs

(76). In addition, in hypoxia-induced GDEs miR-10a and miR-21 stimulate the expansion and activation of MDSCs by targeting RAR-related orphan receptor α (RORA) and PTEN (77). In breast cancer with high expression of interleukin-6, TDEs miR-9 and miR-181A activate the JAK/STAT to exaggerate the proliferation and inhibitory roles of MDSCs by targeting SOCS3 and PIAS3 (76). In gastric cancer, Ren et al. found that the TDE miR-107 prompted the proliferation and activation of MDSCs by targeting Dicer1 and PTEN (78) (Table 3).

lncRNAs are also secreted in exosomes as messengers of intercellular communication. Some lncRNAs are enriched in exosomes, while others are almost absent, suggesting that some lncRNAs are selectively trafficked into exosomes. Furthermore, RNA sequencing in exosomes derived from tumors revealed that most of the non-coding transcripts of exosomes were lncRNAs (79). Meanwhile, exosomal lncRNAs are often found in clinical cancer samples, indicating that lncRNA may be a potential biomarker for cancer diagnosis. In primary urothelial bladder cancer (UBC) cells, exosomal lncRNA HOTAIR is secreted by proteins (SNAIL1, TWIST1, ZEB1 and LAMB3), which regulate EMT, resulting in gene changes on epithelial cells. lncRNA ZFAS1 is found to increase in the serum exosomes of GC patients with gastric cancer (GC), suggesting that lncRNA ZFAS1 plays a positive role in the progression of gastric cancer (80). Exosomal lncRNA ZFAS1 also promotes the proliferation,

TABLE 3 | Tumor derived exosome miRNA on tumor MDSCs.

MiRNAs	Target genes/signal pathways	Function on MDSCs	Tumor	Ref.
miR-29a miR-92a	PDCD4/STAT3	To improve differentiation	Glioma	(75)
miR-10a/miR-21	Dicer1/PTEN	To enhance the expansion/activation	Glioma	(77)
miR-21a	SOCS3/PIAS3/JAK/STAT	To exaggerate the proliferation/immunosuppressive functions	LLC	(76)
miR-9/miR-181a	RORA/PTEN	To promote the proliferation and activity	Breast cancer	(76)
miR-107		To induce the proliferation/activation	Gastric cancer	(78)
miR-let-7i	IL-6/IL-17/IL-1 β	To restrain the roles	Pancreatic cancer	(74)

migration and invasion of tumor cells from esophageal carcinoma (ESCC), and inhibits the apoptosis of ESCC cells by up-regulating STAT3 and down-regulating MiR-124, leading to the carcinogenesis of ESCC. LncRNA ZFAS1 is believed to be a competitive endogenous RNA regulating MiR-124, thereby enhancing STAT3 expression (81). In bladder cancer (BCs), lncRNA-PTENP1 is found to be reduced in tissues and plasma exosomes. Cells which secrete exosomal PTENP1, deliver it to BC cells to inhibit the biological malignant behavior of BC cells by increasing apoptosis and decreasing invasion and migration (82). The regulatory mechanism of TDEs lncRNAs on MDSCs has not been clarified thoroughly. A few studies have shown that TDEs lncRNAs play the important regulatory role in TME and tumor cell interactions, accelerating tumor growth (24). TDEs lncRNAs are transported to the TME to modulate the roles of various cells, including macrophages, endothelial cells and fibroblasts (24). In liver cancer cells, lncRNA TUC339 induces M2 polarization by interacting with cytokine-cytokine receptors to exaggerate tumor metastasis (83). It is well known that lncRNA urothelial carcinoma-associated (UCA1) is an lncRNA associated with the occurrence and progression of various cancers, including colorectal cancer. Meanwhile, the mechanism of tumor-derived exosome lncRNA-UCA1 has also been studied. In colon cancer (CRC), UCA1 plays a key role in CRC tumor progression by packaging into exosome, and UCA1 sequesters mir-143 *via* a sponge mechanism (84) (Table 4). However, the mechanism by which exosome miRNA/lncRNA affects MDSC in TME remains to be studied.

LNCRNA/MIRNA INTERACTION REGULATE MDSCS IN TME

LncRNA not only directly participates in the regulation of gene expression, but also regulates the expression of miRNA (85). miRNA can regulate mRNA expression through the miRNA response elements (MREs) of mRNA 3' UTR. LncRNA can adsorb miRNA through MREs to competitively bind miRNA as one Competing endogenous RNA (ceRNA) and interfere with the binding of miRNA with downstream target genes, and then participate in various biological processes such as cell proliferation, differentiation, apoptosis and angiogenesis (86, 87). Luan et al. reported that lncRNA XLOC_006390z played a functional role as one ceRNA in cervical cancer. When XLOC_006390 is knocked out, the expression of Mir-331-3p target gene NRP2 and Mir-338-3p target gene PKM2 is

significantly downregulated, further promoting the occurrence and metastasis of cervical cancer (88). MiRNA can regulate lncRNA expression as well as target mRNA expression. LncRNA structure is similar to mRNA. LncRNAs indirectly inhibit the negative regulation of miRNAs on target genes by competing with miRNA to bind the 3'-UTR of target gene mRNA. Some of lncRNAs can form miRNA precursors through intracellular shearing, and then process and generate specific miRNAs to regulate the expression of target genes and exert functions. In addition, Individual lncRNAs function as endogenous miRNA sponges and inhibit miRNA expression, further performing biological roles. Therefore, integrated analysis of the regulatory relationship between miRNA-lncRNA-mrna can explain the occurrence and development of diseases comprehensively. These indicted that miRNA may regulate lncRNA expression through the similar mechanism by which mRNA is regulated (Figure 8).

Mir-155 was overexpressed in MEG01 leukemia cell line and the expression level of target lncRNA was significantly decreased. When Mir-155 was silenced, the expression of target lncRNA was significantly increased. These results indicated that miRNA could regulate the expression of lncRNA (89). lncRNAs can act as one ceRNA to sequester miRNAs, regulating the abundance and activity of miRNAs, resulting in the de-repression of genes targeted by corresponding miRNAs in cancer progression (34, 90). Recently, the regulation of lncRNA/miRNA in MDSCs has become increasingly important. Studies have speculated that lncRNA-miRNA may have synergistic effects on the roles of MDSCs. Mir-9 and or Runx1 overlapping RNA (RUNXOR) are two non-coding RNAs involved in the differentiation and activation of MDSCs. Tian et al. showed that miR-9 directly downregulated the expression of lncRNA Runx to stimulate the differentiation of MDSCs and reduce the suppressive ability of MDSCs (36). The retinal non-coding RNA3 (RNCR3), an intragenic lncRNA, which is conserved sequence in mammalian genomes, has been shown to be highly expressed in glioblastoma and prostate cancer (91). Furthermore, Shang et al. recognized that RNCR3 expression in MDSCs is upregulated by inflammatory and tumor associated factors. In the TME, the expression of RNCR3 was up-regulated in MDSC. RNCR3 may function as one ceRNA to upregulate the expression of Arg-1 and iNOS on MDSCs to enhance the roles of these MDSCs through sponge mir-185-5p which binds to CHOP to upregulate CHOP expression [104]. Therefore, those results suggest that RNCR3/miR-185-5p/Chop may strengthen suppressive roles of MDSCs in the TME.

TABLE 4 | Tumor derived exosome lncRNA on cancer.

LncRNAs	Target genes/signal pathways	Function on cancer	Tumor	Ref.
LncRNA HOTAIR	SNAI1/TWIST1/ZEB1/LAMB3	To changing epithelial cells	UBC	(80)
LncRNA ZFAS1		To promoting the cancer	Gastric cancer	(80)
LncRNA ZFAS1	STAT3/MiR-124	To promoting the proliferation, migration and invasion of tumor	Esophageal carcinoma	(81)
LncRNA-PTENP1	PTENP1	To inhibiting the biological malignant behavior of BC cells	Bladder cancer	(82)
LncRNA TUC339	M2 polarization	To exaggerating tumor metastasis	Liver cancer	(83)
LncRNA-UCA1	Mir-143	To promoting the cancer	Colon cancer	(84)

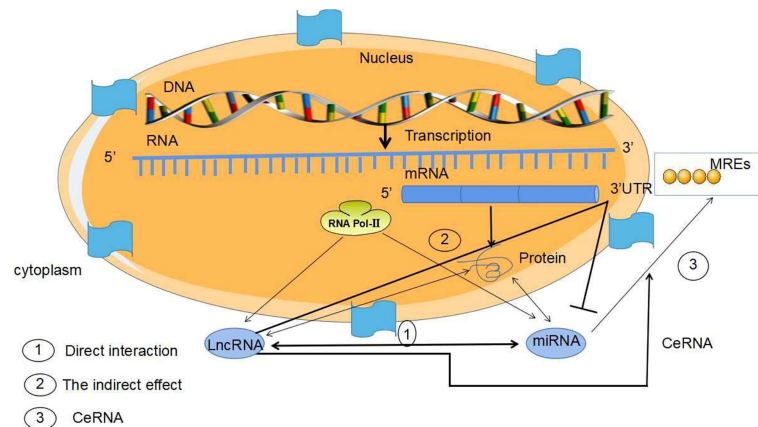


FIGURE 8 | Mechanism of MiRNA/LncRNA interaction. The interaction mechanism between miRNAs and LncRNAs is as follows: (1) The two directly interact with each other. (2) LncRNAs inhibit miRNAs by competitively binding the 3'-UTR of miRNA target mRNA. (3) LncRNAs, as ceRNA, inhibit the expression of miRNA by using the "miRNA sponge". MiRNAs may regulate LncRNA expression through the similar mechanism by which miRNAs regulate mRNA, since LncRNA structure is similar to that of mRNA.

CONCLUDING REMARKS AND PROSPECT

MDSCs, as immunosuppressive cells, seriously affect the progression, invasion and metastasis of tumors, and may be used as potential targets for tumor immunotherapy. The regulatory mechanism of tumor MDSCs has been widely investigated by us and other scientists (14, 92–95). Increasing evidence demonstrated that ncRNAs, especially miRNA and lncRNAs, played the key roles in the regulation of tumor MDSCs in the TME. Here we review that MiRNA/LncRNAs regulate the biological status and functional activity of tumor MDSCs through different regulatory mechanisms. Moreover, we discuss how both exosomal miRNAs/lncRNAs and the interaction of miRNAs/lncRNAs modulate tumor MDSCs. However, In the TME, the regulation of miRNAs/lncRNA on MDSCs is affected. It remains to be explored how those dysregulated miRNAs/lncRNA are combined in the TME to act on tumor MDSCs through tumor-related signaling pathway. In addition, the regulation of miRNA/lncRNAs on MDSCs provided opportunities and challenges for targeting MDSCs immunotherapy. Moreover, these functional data of miRNA/lncRNA on tumor MDSCs are gained from animal studies, there

are a few data from human patients with cancer. Thus, miRNAs/lncRNAs application for tumor MDSCs in clinical patients with cancer need be further clarified. In summary, the interaction of dysregulated miRNAs/lncRNA on tumor MDSCs with transcription factors, cofactors and chromatin modifiers may target specific signals to treat tumor MDSCs in the TME, providing novel strategies for cancer treatment.

AUTHOR CONTRIBUTIONS

XL and SZ wrote, reviewed, and revised manuscript, figures and tables. HS prepared the figures and tables. HL and MY reviewed and revised the manuscript. YS revised the manuscript. PQ wrote, reviewed, and revised manuscript, figures and tables. All authors contributed to the article and approved the submitted version.

FUNDING

This work was supported by the National Natural Science Foundation of China (Grant No. 81572868) and Science Foundation of Shandong (Grant No. ZR2018LC012).

REFERENCES

1. Law AMK, Valdes-Mora F, Gallego-Ortega D. Myeloid-Derived Suppressor Cells as a Therapeutic Target for Cancer. *Cells* (2020) 9(3):561. doi: 10.3390/cells9030561
2. Dysthe M, Parihar R. Myeloid-Derived Suppressor Cells in the Tumor Microenvironment. *Adv Exp Med Biol* (2020) 1224:117–40. doi: 10.1007/978-3-030-35723-8_8
3. Nakamura K, Smyth MJ. Myeloid Immunosuppression and Immune Checkpoints in the Tumor Microenvironment. *Cell Mol Immunol* (2020) 17(1):1–12. doi: 10.1038/s41423-019-0306-1
4. Fleming V, Hu X, Weber R, Nagibin V, Groth C, Altevogt P, et al. Targeting Myeloid-Derived Suppressor Cells to Bypass Tumor-Induced Immunosuppression. *Front Immunol* (2018) 9:398. doi: 10.3389/fimmu.2018.00398
5. Safarzadeh E, Asadzadeh Z, Safaei S, Hatefi A, Derakhshani A, Giovannelli F, et al. MicroRNAs and lncRNAs-A New Layer of Myeloid-Derived Suppressor Cells Regulation. *Front Immunol* (2020) 11:572323. doi: 10.3389/fimmu.2020.572323
6. Han X, Luan T, Sun Y, Yan W, Wang D, Zeng X, et al. MicroRNA 449c Mediates the Generation of Monocytic Myeloid-Derived Suppressor Cells by

- Targeting Stat6. *Molecules Cells* (2020) 43(9):793–803. doi: 10.14348/molcells.2020.2307
7. Dai H, Xu H, Wang S, Ma J. Connections Between Metabolism and Epigenetic Modification in MDSCs. *Int J Mol Sci* (2020) 21(19):7356. doi: 10.3390/ijms21197356
 8. Weber R, Riestler Z, Hüser L, Sticht C, Siebenmorgen A, Groth C, et al. IL-6 Regulates CCR5 Expression and Immunosuppressive Capacity of MDSC in Murine Melanoma. *J Immunother Cancer* (2020) 8(2):e000949. doi: 10.1136/jitc-2020-000949
 9. Groth C, Hu X, Weber R, Fleming V, Altevogt P, Utikal J, et al. Immunosuppression Mediated by Myeloid-Derived Suppressor Cells (MDSCs) During Tumour Progression. *Br J Cancer* (2019) 120(1):16–25. doi: 10.1038/s41416-018-0333-1
 10. Wang W, Hong G, Wang S, Gao W, Wang P. Tumor-Derived Exosomal miRNA-141 Promote Angiogenesis and Malignant Progression of Lung Cancer by Targeting Growth Arrest-Specific Homeobox Gene (GAX). *Bioengineered* (2021) 12(1):821–31. doi: 10.1080/21655979.2021.1886771
 11. Zheng W, Ye W, Wu Z, Huang X, Xu Y, Chen Q, et al. Identification of Potential Plasma Biomarkers in Early-Stage Nasopharyngeal Carcinoma-Derived Exosomes Based on RNA Sequencing. *Cancer Cell Int* (2021) 21(1):185. doi: 10.1186/s12935-021-01881-4
 12. Syeda ZA, Langden SSS, Munkhzul C, Lee M, Song SJ, et al. Regulatory Mechanism of MicroRNA Expression in Cancer. *Int J Mol Sci* (2020) 21(5):1723. doi: 10.3390/ijms21051723
 13. Daveri E, Vergani E, Shahaj E, Bergamaschi L, La Magra S, Dosi M, et al. microRNAs Shape Myeloid Cell-Mediated Resistance to Cancer Immunotherapy. *Front Immunol* (2020) 11:1214. doi: 10.3389/fimmu.2020.01214
 14. Su Y, Qiu Y, Qiu Z, Qu P. MicroRNA Networks Regulate the Differentiation, Expansion and Suppression Function of Myeloid-Derived Suppressor Cells in Tumor Microenvironment. *J Cancer* (2019) 10(18):4350–6. doi: 10.7150/jca.35205
 15. Lin Y-H. Crosstalk of lncRNA and Cellular Metabolism and Their Regulatory Mechanism in Cancer. *Int J Mol Sci* (2020) 21(8):2947. doi: 10.3390/ijms21082947
 16. Leija Montoya G, et al. Long Non-Coding RNAs: Regulators of the Activity of Myeloid-Derived Suppressor Cells. *Front Immunol* (2019) 10:1734. doi: 10.3389/fimmu.2019.01734
 17. Statello L, González Ramírez J, Sandoval Basilio J, Serafin Higuera I, Isiordia Espinoza M, González González R, et al. Gene Regulation by Long Non-Coding RNAs and its Biological Functions. *Nat Rev Mol Cell Biol* (2021) 22(2):96–118. doi: 10.1038/s41580-021-00330-4
 18. Wu P, Mo Y, Peng M, Tang T, Zhong Y, Deng X, et al. Emerging Role of Tumor-Related Functional Peptides Encoded by lncRNA and circRNA. *Mol Cancer* (2020) 19(1):22. doi: 10.1186/s12943-020-1147-3
 19. Mercer TR, Dinger ME, Mattick JS. Long Non-Coding RNAs: Insights Into Functions. *Nat Rev Genet* (2009) 10(3):155–9. doi: 10.1038/nrg2521
 20. Ferreira HJ, Esteller M. Non-Coding RNAs, Epigenetics, and Cancer: Tying it All Together. *Cancer Metastasis Rev* (2018) 37(1):55–73. doi: 10.1007/s10555-017-9715-8
 21. Hombach S, Kretz M. Non-Coding RNAs: Classification, Biology and Functioning. *Adv Exp Med Biol* (2016) 937:3–17. doi: 10.1007/978-3-319-42059-2_1
 22. de Goede OM, Nachun DC, Ferraro NM, Gloudemans MJ, Rao AS, Smail C, et al. Population-Scale Tissue Transcriptomics Maps Long non-Coding RNAs to Complex Disease. *Cell* (2021) 184(10):2633–48. doi: 10.1016/j.cell.2021.03.050
 23. Yang Y, Yan X, Li X, Ma Y, Goel A. Long Non-Coding RNAs in Colorectal Cancer: Novel Oncogenic Mechanisms and Promising Clinical Applications. *Cancer Lett* (2021) 504:67–80. doi: 10.1016/j.canlet.2021.01.009
 24. Pathania AS, Challagundla KB. Exosomal Long Non-Coding RNAs: Emerging Players in the Tumor Microenvironment. *Mol Ther Nucleic Acids* (2021) 23:1371–83. doi: 10.1016/j.omtn.2020.09.039
 25. Li J, Lu Z, Zhang Y, Xia L, Su Z. Emerging Roles of Non-Coding RNAs in the Metabolic Reprogramming of Tumor-Associated Macrophages. *Immunol Lett* (2021) 232:27–34. doi: 10.1016/j.imlet.2021.02.003
 26. Tian X, Ma J, Wang T, Tian J, Zhang Y, Mao L, et al. Long Non-Coding RNA HOXA Transcript Antisense RNA Myeloid-Specific 1-HOXA1 Axis Downregulates the Immunosuppressive Activity of Myeloid-Derived Suppressor Cells in Lung Cancer. *Front Immunol* (2018) 9:473. doi: 10.3389/fimmu.2018.00473
 27. Li Y, Jiang T, Zhou W, Li J, Li X, Wang Q, et al. Pan-Cancer Characterization of Immune-Related lncRNAs Identifies Potential Oncogenic Biomarkers. *Nat Commun* (2020) 11(1):1000. doi: 10.1038/s41467-020-14802-2
 28. Goodall GJ, Wickramasinghe VO. RNA in Cancer. *Nat Rev Cancer* (2021) 21(1):22–36. doi: 10.1038/s41568-020-00306-0
 29. Zhao Z, Sun W, Guo Z, Zhang J, Yu H, Liu B. Mechanisms of lncRNA/microRNA Interactions in Angiogenesis. *Life Sci* (2019) 254:116900. doi: 10.1016/j.lfs.2019.116900
 30. Paraskevopoulou MD, Hatzigeorgiou AG. Analyzing MiRNA-LncRNA Interactions. *Methods Mol Biol (Clifton NJ)* (2016) 1402:271–86. doi: 10.1007/978-1-4939-3378-5_21
 31. Panni S, Lovering RC, Porras P, Orchard S. Non-Coding RNA Regulatory Networks. *Biochim Biophys Acta Gene Regul Mech* (2020) 1863(6):194417. doi: 10.1016/j.bbagr.2019.194417
 32. Klinge CM. Non-Coding RNAs: Long Non-Coding RNAs and microRNAs in Endocrine-Related Cancers. *Endocr-Relat Cancer* (2018) 25(4):R259–82. doi: 10.1530/ERC-17-0548
 33. Crudele F, Bianchi N, Realì E, Galasso M, Agnoletto C, Volinia S. The Network of non-Coding RNAs and Their Molecular Targets in Breast Cancer. *Mol Cancer* (2020) 19(1):61. doi: 10.1186/s12943-020-01181-x
 34. Cheng T, Huang S. Roles of Non-Coding RNAs in Cervical Cancer Metastasis. *Front Oncol* (2021) 11:646192. doi: 10.3389/fonc.2021.646192
 35. Tomar D, Yadav AS, Kumar D, Bhadauriya G, Kundu GC. Non-Coding RNAs as Potential Therapeutic Targets in Breast Cancer. *Biochim Biophys Acta Gene Regul Mech* (2020) 1863(4):194378. doi: 10.1016/j.bbagr.2019.04.005
 36. Shabgah AG, Salmaninejad A, Thangavelu L, Alexander M, Yumashev AV, Goleij P, et al. The Role of non-Coding Genome in the Behavior of Infiltrated Myeloid-Derived Suppressor Cells in Tumor Microenvironment; a Perspective and State-of-the-Art in Cancer Targeted Therapy. *Prog Biophys Mol Biol* (2021) 161:17–26. doi: 10.1016/j.pbiomolbio.2020.11.006
 37. Salminen A, Kauppinen A, Kaarniranta K. AMPK Activation Inhibits the Functions of Myeloid-Derived Suppressor Cells (MDSC): Impact on Cancer and Aging. *J Mol Med (Berlin Germany)* (2019) 97(8):1049–64. doi: 10.1007/s00109-019-01795-9
 38. Wang W, Xia X, Mao L, Wang S. The CCAAT/Enhancer-Binding Protein Family: Its Roles in MDSC Expansion and Function. *Front Immunol* (2019) 10:1804. doi: 10.3389/fimmu.2019.01804
 39. Jiang J, et al. MiR-486 Promotes Proliferation and Suppresses Apoptosis in Myeloid Cells by Targeting Cebpa *In Vitro*. *Cancer Med* (2018) 7(9):4627–38. doi: 10.1002/cam4.1694
 40. Liu Y, Lai L, Chen Q, Song Y, Xu S, Ma F, et al. MicroRNA-494 Is Required for the Accumulation and Functions of Tumor-Expanded Myeloid-Derived Suppressor Cells via Targeting of PTEN. *J Immunol (Baltimore Md: 1950)* (2012) 188(11):5500–10. doi: 10.4049/jimmunol.1103505
 41. Li L, Zhang J, Diao W, Wang D, Wei Y, Zhang CY. MicroRNA-155 and MicroRNA-21 Promote the Expansion of Functional Myeloid-Derived Suppressor Cells. *J Immunol (Baltimore Md: 1950)* (2014) 192(3):1034–43. doi: 10.4049/jimmunol.1301309
 42. Huber V, Vallacchi V, Fleming V, Hu X, Cova A, Dugo M, et al. Tumor-Derived microRNAs Induce Myeloid Suppressor Cells and Predict Immunotherapy Resistance in Melanoma. *J Clin Invest* (2018) 128(12):5505–16. doi: 10.1172/JCI98060
 43. Wang J, Yu F, Jia X, Iwanowycz S, Wang Y, Huang S, et al. MicroRNA-155 Deficiency Enhances the Recruitment and Functions of Myeloid-Derived Suppressor Cells in Tumor Microenvironment and Promotes Solid Tumor Growth. *Int J Cancer* (2015) 136(6):E602–13. doi: 10.1002/ijc.29151
 44. Kim S, Song JH, Kim S, Qu P, Martin BK, Sehareen WS, et al. Loss of Oncogenic miR-155 in Tumor Cells Promotes Tumor Growth by Enhancing C/EBP- β -Mediated MDSC Infiltration. *Oncotarget* (2016) 7(10):11094–112. doi: 10.18632/oncotarget.7150
 45. Chen S, Wang L, Fan J, Ye C, Dominguez D, Zhang Y, et al. Host Mir155 Promotes Tumor Growth Through a Myeloid-Derived Suppressor Cell-Dependent Mechanism. *Cancer Res* (2015) 75(3):519–31. doi: 10.1158/0008-5472.CAN-14-2331
 46. Haverkamp JM, Smith AM, Weinlich R, Dillon CP, Qualls JE, Neale G, et al. Myeloid-Derived Suppressor Activity Is Mediated by Monocytic Lineages Maintained by Continuous Inhibition of Extrinsic and Intrinsic Death Pathways. *Immunity* (2014) 41(6):947–59. doi: 10.1016/j.immuni.2014.10.020

47. Gao Y, Shang W, Zhang D, Zhang S, Zhang X, Zhang Y, et al. Modulates Differentiation of MDSCs Through Downregulating IL41l With C/Ebp β LIP and WDR5. *Front Immunol* (2019) 10:1661. doi: 10.3389/fimmu.2019.01661
48. Liu Q, Zhang M, Jiang X, Zhang Z, Dai L, Min S, et al. miR-223 Suppresses Differentiation of Tumor-Induced CD11b⁺ Gr1⁺ Myeloid-Derived Suppressor Cells From Bone Marrow Cells. *Int J Cancer* (2011) 129(11):2662–73. doi: 10.1002/ijc.25921
49. Moaaz M, Lotfy H, Elsherbini B, Motawea MA, Fadali G. TGF- β Enhances the Anti-Inflammatory Effect of Tumor- Infiltrating CD33+11b+HLA-DR Myeloid-Derived Suppressor Cells in Gastric Cancer: A Possible Relation to MicroRNA-494. *Asian Pac J Cancer Prev* (2020) 21(11):3393–403. doi: 10.31557/APJCP.2020.21.11.3393
50. Pyzer AR, Stroopinsky D, Rajabi H, Washington A, Tagde A, Coll M, et al. MUC1-Mediated Induction of Myeloid-Derived Suppressor Cells in Patients With Acute Myeloid Leukemia. *Blood* (2017) 129(13):1791–801. doi: 10.1182/blood-2016-07-730614
51. Wang X, Chang X, Zhuo G, Sun M, Yin K. Twist and miR-34a Are Involved in the Generation of Tumor-Educated Myeloid-Derived Suppressor Cells. *Int J Mol Sci* (2013) 14(10):20459–77. doi: 10.3390/ijms141020459
52. Rong Y, Yuan CH, Qu Z, Zhou H, Guan Q, Yang N, et al. Doxorubicin Resistant Cancer Cells Activate Myeloid-Derived Suppressor Cells by Releasing PGE2. *Sci Rep* (2016) 6:23824. doi: 10.1038/srep23824
53. Lin K-T, Sun SP, Wu JI, Wang LH. Low-Dose Glucocorticoids Suppresses Ovarian Tumor Growth and Metastasis in an Immunocompetent Syngeneic Mouse Model. *PLoS One* (2017) 12(6):e0178937. doi: 10.1371/journal.pone.0178937
54. Zhang M, Liu Q, Mi S, Liang X, Zhang Z, Su X, et al. Both miR-17-5p and miR-20a Alleviate Suppressive Potential of Myeloid-Derived Suppressor Cells by Modulating STAT3 Expression. *J Immunol (Baltimore Md: 1950)* (2011) 186(8):4716–24. doi: 10.4049/jimmunol.1002989
55. Zhang C, Wang S, Liu Y, Yang C. Epigenetics in Myeloid Derived Suppressor Cells: A Sheathed Sword Towards Cancer. *Oncotarget* (2016) 7(35):57452–63. doi: 10.18632/oncotarget.10767
56. Tian J, Rui K, Tang X, Ma J, Wang Y, Tian X, et al. MicroRNA-9 Regulates the Differentiation and Function of Myeloid-Derived Suppressor Cells via Targeting Runx1. *J Immunol (Baltimore Md: 1950)* (2015) 195(3):1301–11. doi: 10.4049/jimmunol.1500209
57. Mei S, Liu Y, Wu X, He Q, Min S, Li L, et al. TNF- α -Mediated microRNA-136 Inhibits Differentiation of Myeloid Cells by Targeting NFIA. *J Leukocyte Biol* (2016) 99(2):301–10. doi: 10.1189/jlb.1A0115-032RR
58. Sun R, Zheng Z, Wang L, Cheng S, Shi Q, Qu B, et al. A Novel Prognostic Model Based on Four Circulating miRNA in Diffuse Large B-Cell Lymphoma: Implications for the Roles of MDSC and Th17 Cells in Lymphoma Progression. *Mol Oncol* (2021) 15(1):246–61. doi: 10.1002/1878-0261.12834
59. Mei S, Xin J, Liu Y, Zhang Y, Liang X, Su X, et al. MicroRNA-200c Promotes Suppressive Potential of Myeloid-Derived Suppressor Cells by Modulating PTEN and FOG2 Expression. *PLoS One* (2015) 10(8):e0135867. doi: 10.1371/journal.pone.0135867
60. Tao Z, Xu S, Ruan H, Wang T, Song W, Qian L, et al. MiR-195/-16 Family Enhances Radiotherapy via T Cell Activation in the Tumor Microenvironment by Blocking the PD-L1 Immune Checkpoint. *Cell Physiol Biochem: Int J Exp Cell Physiol Biochem Pharmacol* (2018) 48(2):801–14. doi: 10.1159/000491909
61. Wang W, Han Y, Jo HA, Lee J, Song YS. Non-Coding RNAs Shuttled via Exosomes Reshape the Hypoxic Tumor Microenvironment. *J Hematol Oncol* (2020) 13(1):67. doi: 10.1186/s13045-020-00893-3
62. Xu Z, Ji J, Xu J, Li D, Shi G, Liu F, et al. MiR-30a Increases MDSC Differentiation and Immunosuppressive Function by Targeting SOCS3 in Mice With B-Cell Lymphoma. *FEBS J* (2017) 284(15):2410–24. doi: 10.1111/febs.14133
63. Chen S, Zhang Y, Kuzel TM, Zhang B. Regulating Tumor Myeloid-Derived Suppressor Cells by MicroRNAs. *Cancer Cell Microenviron* (2015) 2(1):e637. doi: 10.14800/ccm.637
64. Gao Y, Wang T, Li Y, Zhang Y, Yang R. Promotes Immunosuppressive Function of Myeloid-Derived Suppressor Cells in Tumor and Inflammatory Environments. *J Immunol (Baltimore Md: 1950)* (2018) 200(8):2603–14. doi: 10.4049/jimmunol.1701721
65. Zheng Y, Tian X, Wang T, Xia X, Cao F, Tian J, et al. Long Noncoding RNA Pvt1 Regulates the Immunosuppression Activity of Granulocytic Myeloid-Derived Suppressor Cells in Tumor-Bearing Mice. *Mol Cancer* (2019) 18(1):61. doi: 10.1186/s12943-019-0978-2
66. Tian X, Zheng Y, Yin K, Ma J, Tian J, Zhang Y, et al. LncRNA Inhibits Maturation and Accelerates Immunosuppression of Polymorphonuclear Myeloid-Derived Suppressor Cells by Enhancing the Stability of Ficolin B. *Cancer Immunol Res* (2020) 8(4):565–77. doi: 10.1158/2326-6066.CIR-19-0595
67. Zhou Q, Tang X, Tian X, Tian J, Zhang Y, Ma J, et al. LncRNA MALAT1 Negatively Regulates MDSCs in Patients With Lung Cancer. *J Cancer* (2018) 9(14):2436–42. doi: 10.7150/jca.24796
68. Gabrilovich DI. Myeloid-Derived Suppressor Cells. *Cancer Immunol Res* (2017) 5(1):3–8. doi: 10.1158/2326-6066.CIR-16-0297
69. Wang Z, Wang X, Zhang T, Su L, Liu B, Zhu Z, et al. LncRNA MALAT1 Promotes Gastric Cancer Progression via Inhibiting Autophagic Flux and Inducing Fibroblast Activation. *Cell Death Dis* (2021) 12(4):368. doi: 10.1038/s41419-021-03645-4
70. Shang W, Gao Y, Tang Z, Zhang Y, Yang R. The Pseudogene Promotes the Suppressive Function and Differentiation of Monocytic MDSCs. *Cancer Immunol Res* (2019) 7(5):813–27. doi: 10.1158/2326-6066.CIR-18-0443
71. Wencong, et al. The Pseudogene Olfr29-Ps1 Promotes the Suppressive Function and Differentiation of Monocytic MDSCs. *Cancer Immunol Res* (2019) 7(5):813–27. doi: 10.1158/2326-6066.CIR-18-0443
72. Tang Z, Li D, Hou S, Zhu X. The Cancer Exosomes: Clinical Implications, Applications and Challenges. *Int J Cancer* (2020) 146(11):2946–59. doi: 10.1002/ijc.32762
73. Li X, Liu Y, Zheng S, Zhang T, Wu J, Sun Y, et al. Role of Exosomes in the Immune Microenvironment of Ovarian Cancer. *Oncol Lett* (2021) 21(5):377. doi: 10.3892/ol.2021.12638
74. Tan S, Xia L, Yi P, Han Y, Tang L, Pan Q, et al. Exosomal miRNAs in Tumor Microenvironment. *J Exp Clin Cancer Res: CR* (2020) 39(1):67. doi: 10.1186/s13046-020-01570-6
75. Elewally MI, Elsergany AR. Emerging Role of Exosomes and Exosomal microRNA in Cancer: Pathophysiology and Clinical Potential. *J Cancer Res Clin Oncol* (2021) 147(3):637–48. doi: 10.1007/s00432-021-03534-5
76. Zhang X, Li F, Tang Y, Ren Q, Xiao B, Wan Y, et al. miR-21a in Exosomes From Lewis Lung Carcinoma Cells Accelerates Tumor Growth Through Targeting PDCD4 to Enhance Expansion of Myeloid-Derived Suppressor Cells. *Oncogene* (2020) 39(40):6354–69. doi: 10.1038/s41388-020-01406-9
77. Guo X, Qiu W, Liu Q, Qian M, Wang S, Zhang Z, et al. Immunosuppressive Effects of Hypoxia-Induced Glioma Exosomes Through Myeloid-Derived Suppressor Cells via the miR-10a/Rora and miR-21/Pten Pathways. *Oncogene* (2018) 37(31):4239–59. doi: 10.1038/s41388-018-0261-9
78. Ren W, Zhang X, Li W, Feng Q, Feng H, Tong Y, et al. Exosomal miRNA-107 Induces Myeloid-Derived Suppressor Cell Expansion in Gastric Cancer. *Cancer Manage Res* (2019) 11:4023–40. doi: 10.2147/CMAR.S198886
79. Xie Y, Dang W, Zhang S, Yue W, Yang L, Zhai X, et al. The Role of Exosomal Noncoding RNAs in Cancer. *Mol Cancer* (2019) 18(1):37. doi: 10.1186/s12943-019-0984-4
80. Pan L, Liang W, Fu M, Huang ZH, Li X, Zhang W, et al. Exosomes-Mediated Transfer of Long Noncoding RNA ZFAS1 Promotes Gastric Cancer Progression. *J Cancer Res Clin Oncol* (2017) 143(6):991–1004. doi: 10.1007/s00432-017-2361-2
81. Li Z, Qin X, Bian W, Li Y, Shan B, Yao Z, et al. Exosomal lncRNA ZFAS1 Regulates Esophageal Squamous Cell Carcinoma Cell Proliferation, Invasion, Migration and Apoptosis via microRNA-124/STAT3 Axis. *J Exp Clin Cancer Res: CR* (2019) 38(1):477. doi: 10.1186/s13046-019-1473-8
82. Zheng R, Du M, Wang X, Xu W, Liang J, Wang W, et al. Exosome-Transmitted Long non-Coding RNA PTENP1 Suppresses Bladder Cancer Progression. *Mol Cancer* (2018) 17(1):143. doi: 10.1186/s12943-018-0880-3
83. Han S, Qi Y, Luo Y, Chen X, Liang H. Exosomal Long Non-Coding RNA: Interaction Between Cancer Cells and Non-Cancer Cells. *Front Oncol* (2020) 10:617837. doi: 10.3389/fonc.2020.617837
84. Luan Y, Li X, Luan Y, Zhao R, Li Y, Liu L, et al. Circulating lncRNA UCA1 Promotes Malignancy of Colorectal Cancer via the miR-143/MYO6 Axis. *Mol Ther Nucleic Acids* (2020) 19:790–803. doi: 10.1016/j.omtn.2019.12.009
85. Salmena L, Poliseno L, Tay Y, Kats L, Pandolfi PP. A ceRNA Hypothesis: The Rosetta Stone of a Hidden RNA Language? *Cell* (2011) 146(3):353–8. doi: 10.1016/j.cell.2011.07.014

86. Botla SK, Savant S, Jandaghi P, Bauer AS, Mücke O, Moskalev EA, et al. Early Epigenetic Downregulation of microRNA-192 Expression Promotes Pancreatic Cancer Progression. *Cancer Res* (2016) 76(14):4149–59. doi: 10.1158/0008-5472.CAN-15-0390
87. Ouyang H, Gore J, Deitz S, Korc M. microRNA-10b Enhances Pancreatic Cancer Cell Invasion by Suppressing TIP30 Expression and Promoting EGF and TGF- β Actions. *Oncogene* (2014) 33(38):4664–74. doi: 10.1038/onc.2013.405
88. Luan X, Wang Y. LncRNA XLOC_006390 Facilitates Cervical Cancer Tumorigenesis and Metastasis as a ceRNA Against miR-331-3p and miR-338-3p. *J Gynecol Oncol* (2018) 29(6):e95. doi: 10.3802/jgo.2018.29.e95
89. Calin GA, Liu CG, Ferracin M, Hyslop T, Spizzo R, Sevignani C, et al. Ultraconserved Regions Encoding ncRNAs are Altered in Human Leukemias and Carcinomas. *Cancer Cell* (2007) 12(3):215–29. doi: 10.1016/j.ccr.2007.07.027
90. Zuo L, Su H, Zhang Q, Wu WY, Zeng Y, Li XM, et al. Comprehensive Analysis of lncRNAs N 6 -Methyladenosine Modification in Colorectal Cancer. *Aging (Albany NY)* (2021) 12(3):4182–98. doi: 10.18632/aging.202383
91. Mercer TR, Qureshi IA, Gokhan S, Dinger ME, Li G, Mattick JS, et al. Long Noncoding RNAs in Neuronal-Glial Fate Specification and Oligodendrocyte Lineage Maturation. *BMC Neurosci* (2010) 11:14. doi: 10.1186/1471-2202-11-14
92. Qu P, Boelte KC, Lin PC. Negative Regulation of Myeloid-Derived Suppressor Cells in Cancer. *Immunol Investigat* (2012) 41(6-7):562–80. doi: 10.3109/08820139.2012.685538
93. Ben-Meir K, Twaik N, Baniyash M. Plasticity of Myeloid-Derived Suppressor Cells in Cancer. *Curr Opin Immunol* (2018) 51:76–82. doi: 10.1016/j.coi.2018.03.009
94. Ben-Meir K, Twaik N, Baniyash M. Plasticity and Biological Diversity of Myeloid Derived Suppressor Cells. *Curr Opin Immunol* (2018) 51:154–61. doi: 10.1016/j.coi.2018.03.015
95. Bronte V, Brandau S, Chen SH, Colombo MP, Frey AB, Greten TF, et al. Recommendations for Myeloid-Derived Suppressor Cell Nomenclature and Characterization Standards. *Nat Commun* (2016) 7:12150. doi: 10.1038/ncomms12150

Conflict of Interest: The authors declare that the research was conducted in the absence of any commercial or financial relationships that could be construed as a potential conflict of interest.

Publisher's Note: All claims expressed in this article are solely those of the authors and do not necessarily represent those of their affiliated organizations, or those of the publisher, the editors and the reviewers. Any product that may be evaluated in this article, or claim that may be made by its manufacturer, is not guaranteed or endorsed by the publisher.

Copyright © 2022 Liu, Zhao, Sui, Liu, Yao, Su and Qu. This is an open-access article distributed under the terms of the Creative Commons Attribution License (CC BY). The use, distribution or reproduction in other forums is permitted, provided the original author(s) and the copyright owner(s) are credited and that the original publication in this journal is cited, in accordance with accepted academic practice. No use, distribution or reproduction is permitted which does not comply with these terms.



Comprehensive Analysis of the Prognostic Signature of Mutation-Derived Genome Instability-Related lncRNAs for Patients With Endometrial Cancer

Jinhui Liu^{1†}, Guoliang Cui^{2†}, Jun Ye^{3†}, Yutong Wang^{3†}, Can Wang⁴ and Jianling Bai^{5*}

¹Department of Gynecology, The First Affiliated Hospital of Nanjing Medical University, Nanjing, China, ²Department of Gastroenterology, The Second Affiliated Hospital of Nanjing University of Chinese Medicine, Nanjing, China, ³The First Clinical Medical College of Nanjing Medical University, Nanjing, China, ⁴The First Clinical Medical College, Nanjing University of Chinese Medicine, Nanjing, China, ⁵Department of Biostatistics, School of Public Health, Nanjing Medical University, Nanjing, China

OPEN ACCESS

Edited by:

Shiv K. Gupta,
Mayo Clinic, United States

Reviewed by:

Xiao Yang,
Peking University People's Hospital,
China
Meng Zhou,
Wenzhou Medical University, China
Yuxiong Yi,
Wuhan University, China

*Correspondence:

Jianling Bai
baijianling@njmu.edu.cn

[†]These authors have contributed
equally to this work

Specialty section:

This article was submitted to
Molecular and Cellular Oncology,
a section of the journal
Frontiers in Cell and Developmental
Biology

Received: 16 August 2021

Accepted: 21 February 2022

Published: 01 April 2022

Citation:

Liu J, Cui G, Ye J, Wang Y, Wang C
and Bai J (2022) Comprehensive
Analysis of the Prognostic Signature of
Mutation-Derived Genome Instability-
Related lncRNAs for Patients With
Endometrial Cancer.
Front. Cell Dev. Biol. 10:753957.
doi: 10.3389/fcell.2022.753957

Background: Emerging evidence shows that genome instability-related long non-coding RNAs (lncRNAs) contribute to tumor-cell proliferation, differentiation, and metastasis. However, the biological functions and molecular mechanisms of genome instability-related lncRNAs in endometrial cancer (EC) are underexplored.

Methods: EC RNA sequencing and corresponding clinical data obtained from The Cancer Genome Atlas (TCGA) database were used to screen prognostic lncRNAs associated with genomic instability via univariate and multivariate Cox regression analysis. The genomic instability-related lncRNA signature (GILncSig) was developed to assess the prognostic risk of high- and low-risk groups. The prediction performance was analyzed using receiver operating characteristic (ROC) curves. The immune status and mutational loading of different risk groups were compared. The Genomics of Drug Sensitivity in Cancer (GDSC) and the CellMiner database were used to elucidate the relationship between the correlation of prognostic lncRNAs and drug sensitivity. Finally, we used quantitative real-time PCR (qRT-PCR) to detect the expression levels of genomic instability-related lncRNAs in clinical samples.

Results: GILncSig was built using five lncRNAs (AC007389.3, PIK3CD-AS2, LINC01224, AC129507.4, and GLIS3-AS1) associated with genomic instability, and their expression levels were verified using qRT-PCR. Further analysis revealed that risk score was negatively correlated with prognosis, and the ROC curve demonstrated the higher accuracy of GILncSig. Patients with a lower risk score had higher immune cell infiltration, a higher immune score, lower tumor purity, higher immunophenoscores (IPSS), lower mismatch repair protein expression, higher microsatellite instability (MSI), and a higher tumor mutation burden (TMB). Furthermore, the level of expression of prognostic lncRNAs was significantly related to the sensitivity of cancer cells to anti-tumor drugs.

Conclusion: A novel signature composed of five prognostic lncRNAs associated with genome instability can be used to predict prognosis, influence immune status, and chemotherapeutic drug sensitivity in EC.

Keywords: endometrial cancer, genome instability, long non-coding RNAs, risk score, prognosis predicting, immune status

INTRODUCTION

According to the most recent cancer statistics, endometrial cancer (EC) is the most commonly diagnosed gynecologic cancer in the United States, with estimated 65,620 new cases and 12,590 deaths (Siegel et al., 2020). However, no significant improvement in the 5-year relative survival of these patients has been achieved. The Surveillance, Epidemiology, and End Results (SEER) database contained 83.05% of data in 2018 and 82.36% in 1988 (Doll et al., 2018). EC is broadly classified into two types based on distinct pathological and clinical outcomes. Changes in multiple pathways, most notably the PTEN/PI3K/AKT/mTOR pathway, are implicated in type I EC. Moreover, the RAS/RAF/mitogen-activated extracellular signal-regulated kinase 1 (MEK)/extracellular signal-related kinase (ERK) and WNT/ β -catenin signaling pathway are frequently aberrantly activated (Dong et al., 2013; Morice et al., 2016). Meanwhile, obesity and high circulating estrogen levels are strongly linked to type I EC. Other risk factors for type I EC include tamoxifen use after breast cancer, physical inactivity, hyperinsulinemia, reproductive history, and oral contraceptives (Bergman et al., 2000; Parslov et al., 2000; Kaaks et al., 2002). Type II EC has lower morbidity but a higher mortality rate than type I EC. However, this classification of EC has flaws due to the overlapping morphological and immunohistochemical characteristics of type I and II EC (Soslow, 2013).

Long non-coding RNAs (lncRNAs) are a type of transcripts, typically longer than 200 nucleotides (nt), and have no protein-coding capacity but can regulate gene expression (Evans et al., 2016). The abnormal expression of lncRNAs influences cell proliferation, tumor metastasis, and progression by interacting with specific signaling proteins, mRNAs, and micro-RNAs, allowing the formation of sophisticated networks that can contribute to phenotypic diversity in tumor cells (Dong et al., 2019). Several abnormally expressed lncRNAs have been discovered in different cancers, but their function is unknown. Tong et al. found that the lncRNA NORAD holds great promise as a prognostic biomarker in EC because it plays an important role in EC progression as a tumor suppressor (Han et al., 2020).

Genomic instability, characterized by an increased tendency for genomic changes ranging from base pair mutations to chromosomal aberrations, contributes to somatic heterogeneity and genetic diversity, as well as the progression of genetically related diseases, including cancer (Andor et al., 2017). Genomic instability is widely regarded as one of the hallmarks of cancer as it accelerates tumor progression and decreases patient survival (Negrini et al., 2010). Many studies on the classification of endometrial carcinoma have been conducted to judge the prognosis and guide treatment, and the findings revealed that

the majority of endometrial carcinoma were microsatellite instable hypermutated (MSI-H) (Kandoth et al., 2013). Hypermethylation of the MMR gene promoter in MSI-H type EC resulted in the accumulation of DNA replication errors in tumor proliferation, characterized by insertion and deletion of microsatellite sequences, as well as a significantly higher genomic mutation frequency than in microsatellite-stable tumors (Zhao et al., 2014). Therefore, the degree of EC genomic instability has important diagnostic, treatment, and prognosis implications (Khanduja et al., 2016). Furthermore, because effective EC biomarkers for assessing prognosis and determining appropriate treatment are still limited, it is critical to identify novel available markers (Salvesen et al., 2012). Mounting evidence demonstrates that lncRNA is strongly linked to genomic instability (Liu, 2016). Recently, Zhaohua et al. showed that nuclear lncRNA BGL3 directly plays a role in the regulation of the DNA damage response pathway by preventing the BRCA1/BARD1 complex from accumulating on the DNA double-strand breaks (Hu et al., 2020). So far, however, few studies have been reported on this phenomenon in EC.

In this study, we attempted to integrate the expression profiles and somatic mutation profiles of patients with EC to construct a genome instability-associated lncRNAs based on risk score for prognosis prediction, immune status determination, and therapeutic scheme selection.

MATERIALS AND METHODS

Data Acquisition and Preprocessing

The Cancer Genome Atlas (TCGA), a public database interacting with 33 cancer types, was used to obtain data on the expression profile, somatic mutation, and clinical information of endometrial carcinoma patients. The project was TCGA-UCEC, and the transcriptome data files were labeled “FPKM.” lncRNA and mRNA were extracted from the transcriptional profiling data, separately. We obtained complete lncRNA expression profiles, mRNA expression profiles, clinical features, and somatic mutation profiles for 511 samples.

Differential lncRNA Expression and Co-Expression Analysis

The computational framework was designed to identify the lncRNAs associated with genomic instability, and then, the number of mutations was counted in each sample (Bao et al., 2020). Subsequently, we arranged subjects in descending order based on the number of somatic mutations. The patients were divided into high ($\geq 25\%$ mutation number) and low mutation

TABLE 1 | Clinical features of included patients.

Covariates	Type	Total	Train	Test	p value
Age	≤60	199(38.94%)	93(36.33%)	106(41.57%)	0.26
	>60	312(61.06%)	163(63.67%)	149(58.43%)	
Histological_type	Endometrial	384(75.15%)	191(74.61%)	193(75.69%)	0.86
	Mixed and serous	127(24.85%)	65(25.39%)	62(24.31%)	
Grade	G1 & G2	91(17.81%)	50(19.53%)	41(16.08%)	0.37
	G3 & G4	420(82.19%)	206(80.47%)	214(83.92%)	
Stage	Stage I & Stage II	370(72.41%)	185(72.27%)	185(72.55%)	1.00
	Stage III Stage IV	141(27.59%)	71(27.73%)	70(27.45%)	

number (<25% mutation number) groups, respectively, and designated as the genomic unstable (GU) groups and the genomic stable (GS) groups according to the mutation number. The “limma” package in R software was used to identify differentially expressed lncRNAs (DELs) between the high and low mutation number groups with a $|\log FC| > 1$ threshold and a false discovery rate adjusted p -value < 0.05 . The co-expression network of the DELs and genes was established with a coefficient $|R^2| > 0.3$ and $p < 0.001$. Next, 511 EC samples were randomly divided into training (256 patients) and testing sets (255 patients) using the R software package “caret.” **Table 1** shows the clinical and pathological characteristics of the tumor samples between two sets ($p > 0.05$, Chi-square test). The preprocessing processes were as follows: (1) RNA sequencing annotation with reference file; (2) eliminating missing values; and (3) normalizing expression values by R software (3.4.0) and correcting background using the robust multichip averaging algorithm.

Functional Enrichment Analysis

Gene Ontology (GO) and Kyoto Encyclopedia of Genes and Genomes (KEGG) enrichment analyses were conducted *via* the Annotation, Visualization, and Integrated Discovery (DAVID) 6.8 (<https://david.ncifcrf.gov>) (Yu et al., 2012). $p < 0.05$ was regarded as significantly enriched.

Construction of Prognosis Predictive-Model and Nomogram

All patients were randomly assigned to the training and validation cohorts on a 1:1 ratio. The expression profile of DELs was then combined with prognosis data. Employing the survival package, the prognosis prediction model was developed with the formula of “ $Riskscore = \sum coef * Exp(genes)$ ”. Patients with risk scores higher than the median were assigned to the high-risk group, whereas others were assigned to the low-risk group. The Kaplan–Meier survival curve was used to compare the prognosis difference of high- and low-risk groups (Liu et al., 2020a). The receiver operating characteristic (ROC) curve was used to assess the predictive potential of our prognosis model. Dimensionality was reduced using principal component analysis (PCA) (Liu et al., 2019). Risk scores and clinical characteristics of patients were combined to establish a nomogram for improved predictive ability, which was then tested using calibration plots. Genomic instability-related lncRNA signature (GILncSig)

prognosis was assessed using univariate and multivariate Cox regression analyses, as well as stratified analyses. We compared the areas under the ROC curves (AUCs) to evaluate GILncSig performance.

Immune Microenvironment, Checkpoint Analysis, and Gene Set Enrichment Analysis

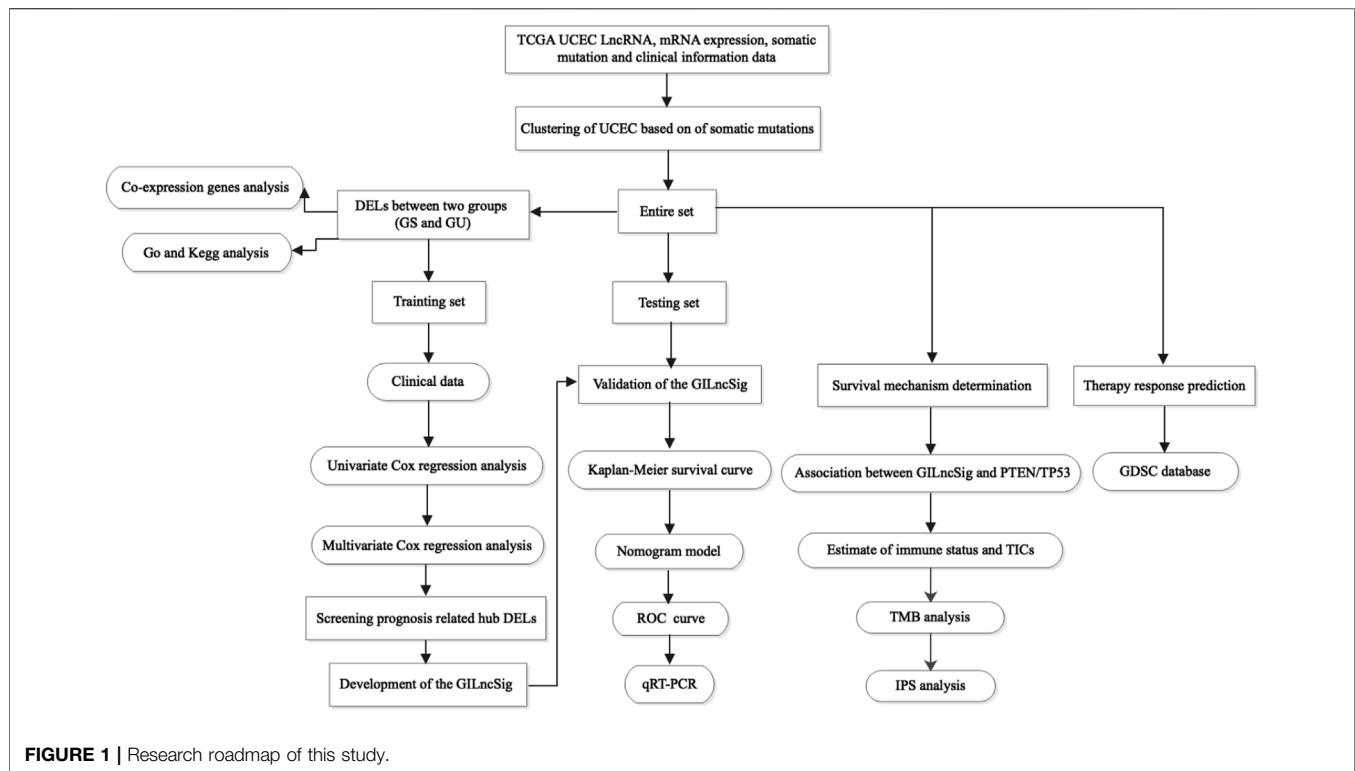
The immune cell landscape in the tumor microenvironment was quantified by ssGSEA algorithms (Zhu et al., 2016). When compared to traditional quantification algorithms, ssGSEA had a higher degree of freedom in calculating multiple immune cell scores based on the expression profile. The expression of immune checkpoint genes was also examined in the high- and low-risk groups to investigate the underlying effect on immunotherapy. GSEA (<http://software.broadinstitute.org/gsea/index.jsp>) was used to identify biological processes with a high gene rank. The EC samples in the TCGA set were divided into high-risk and low-risk groups based on the riskscore model. The underlying biological functions of the two groups were identified by comparing the enrichment of biological processes. The collection of annotated gene sets in the Molecular Signatures Database (MSigDB, <http://software.broadinstitute.org/gsea/msigdb/index.jsp>) served as the reference gene set in GSEA software. The Nom. $p < 0.05$ was chosen as the cutoff criterion (Song et al., 2017). The c2.cp.kegg.v7.4.symbols.gmt was chosen as the reference file.

Immunophenoscore Analysis

The immunophenoscores (IPs) of patients with EC were obtained from The Cancer Immunome Atlas (<https://tcia.at/home>). The IPS analysis was performed randomly using machine learning to determine the immunogenicity of four categories of genes: effector cells, suppressive cells, major histocompatibility complex molecules, and immune modulators or checkpoints. The IPS was calculated using weighted averaged Z-scores from the above categories with a range of 0–10, and the scores were increased with higher immunogenicity (Charoentong et al., 2017).

ESTIMATE Algorithm

Estimation of Stromal and Immune cells in Malignant Tumours using Expression data (ESTIMATE) is an algorithm for determining the levels of stromal and immune cell infiltration in tumors (Yoshihara et al., 2013). ESTIMATE algorithm was



used to evaluate the immune cell content (immune score), stromal cell infiltration (stromal score), strom-immune synthesis score (ESTIMATE score), and tumor purity for each EC sample.

TMB Calculation and Clinical Data Analysis

The tumor mutation burden (TMB) level was calculated by dividing the total number of mutations by the size of the coding region of the target region. The EC samples were divided into high-TMB and low-TMB groups based on the median TMB level. The TMB level from the TCGA database was combined with the corresponding survival data from each sample, and the differences in OS between different TMB level groups and different TMB levels combined with different risk groups were compared using Kaplan–Meier analysis. The Wilcoxon rank sum test was used to investigate the correlation of TMB with the risk score.

Somatic Mutation, Tumor Stemness, and Drug Sensitivity Analysis

The mutation data of endometrial carcinoma patients were obtained from the TCGA (Data Category = copy number variation; “maf” file). Fall plots were used to visualize the top 10 mutation genes *via* the maftools packages in R software (Mayakonda et al., 2018). As previously reported, the stem-like indices for each endometrial carcinoma sample were calculated using one-class logistic regression (Yi et al., 2020). Then, in the high-risk and low-risk groups of GILncSig, we estimated the half-maximal inhibitory concentration (IC50) of selected drugs from a

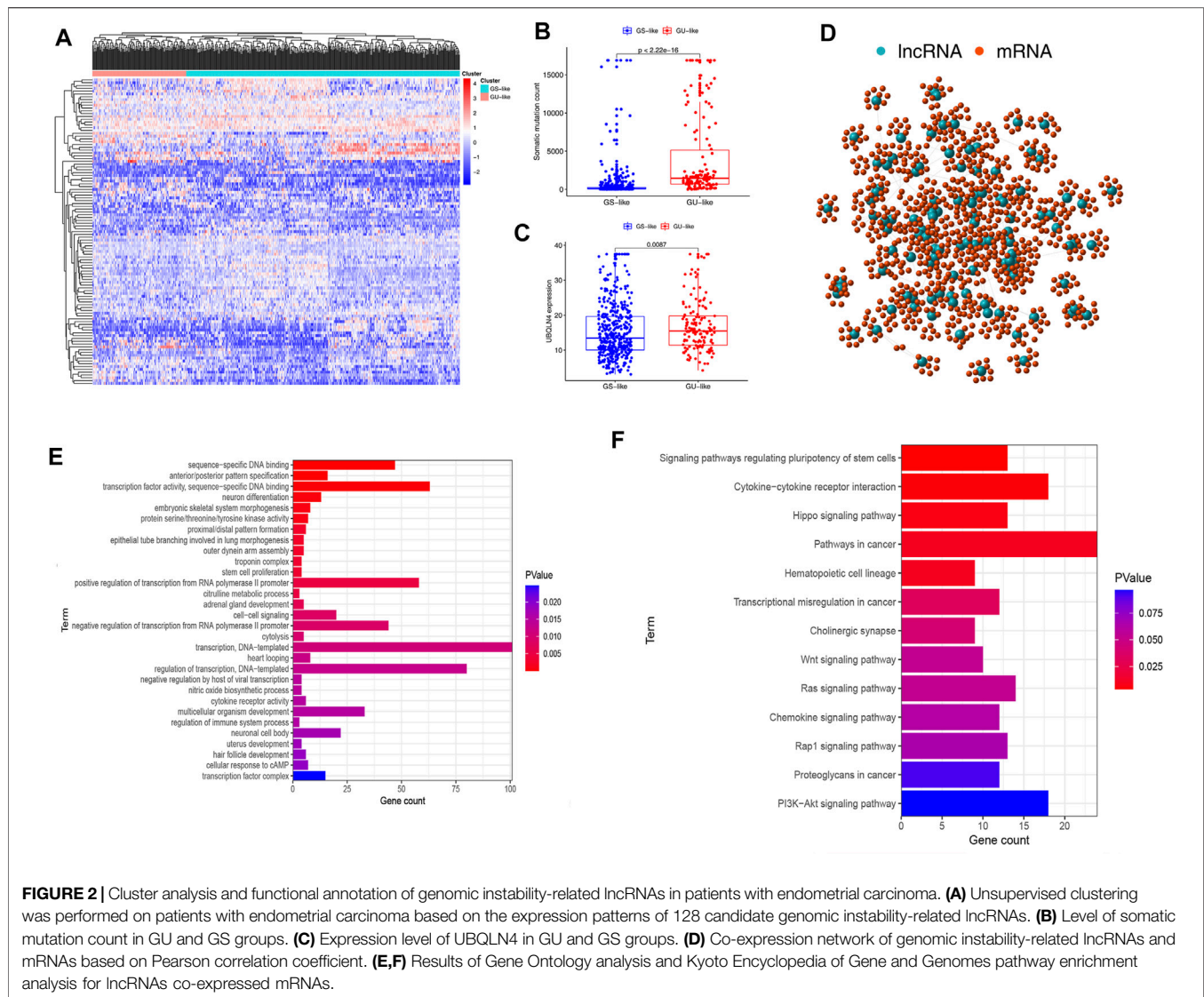
public database called Genomics of Drug Sensitivity in Cancer (GDSC; <https://www.cancerrxgene.org>) using the “pRRophetic” packages (Song et al., 2020). The NCI-60 database, which was assessed *via* the CellMiner interface (<https://discover.nci.nih.gov/cellminer>), is currently the most widely used for cancer drug testing (Dong et al., 2020). Pearson correlation analysis was performed to explore the underlying drug sensitivity difference between the high- and low-risk groups.

Quantitative Real-Time PCR

A total of 15 paired EC tissues and normal tissues were obtained from patients at the First Affiliated Hospital of Nanjing Medical University. The Ethics Committee of the First Affiliated Hospital of Nanjing Medical University (Nanjing, China) approved this study. All patients signed informed consent forms. Total RNA was isolated from samples using TRIZOL reagent (Thermo Fisher Scientific, USA), then reverse-transcribed into cDNA using a Revert Aid First Strand cDNA Synthesis kit (Thermo Fisher Scientific, USA), and analyzed by quantitative real-time PCR (qRT-PCR) with an SYBR-Green PCR kit (Takara, Tokyo, Japan). GAPDH was used to normalize the relative expression of the lncRNA. The sequences are listed in **Supplementary Table S1**.

Statistical Analysis

All the analyses were performed using the R software (version 4.1.0). All statistical tests were two-sided, with a *p*-value of less than 0.05 considered statistically significant. The Student *t*-test was used to compare the normally distributed variables in two groups, and the Wilcox test was used to compare non-normally distributed continuous variables.



RESULTS

Sample Clustering and Enrichment Analysis

Figure 1 depicts the research procedure for this study. According to the cumulative somatic mutations, we assigned the top 25% highest mutation and the bottom 25% lowest mutation to the GU ($n = 133$) and GS groups ($n = 131$). There were 109 DELs between the two groups, with 31 lncRNAs upregulated and 78 lncRNAs downregulated in the GU group (adj. p -value < 0.05 , $|\log FC| > 1$) (**Supplementary Table S2**). **Supplementary Figure S1** shows a heatmap of 20 most significantly upregulated lncRNAs and 20 most significantly downregulated lncRNAs. Unsupervised hierarchical clustering analysis was used to classify all TCGA samples into GU (higher cumulative somatic mutations) and GS (lower cumulative somatic mutations) groups based on the set of 109 DELs (**Figure 2A**). As one of the members of the ubiquitin-like and ubiquitin-associated (UBL-UBA) protein family, UBQLN4 plays an important role in sustaining genomic

stability by affecting nucleotide excision repair. Recent studies have revealed that the mutation of UBQLN4 could reflect genomic instability in cancers, thus affecting prognosis and the chemotherapy response (Jachimowicz et al., 2019). Therefore, UBQLN4 was selected to reflect the genomic instability. Similarly, the GU-like group had a higher level of somatic mutation count and UBQLN4 expression (**Figures 2B,C**). Meanwhile, a co-expression network of these lncRNAs and mRNA was constructed (**Figure 2D**). GO analysis revealed that the lncRNAs were significantly enriched in “sequence-specific DNA binding,” “anterior/posterior pattern specification,” “transcription factor activity, sequence-specific DNA binding,” “neuron differentiation,” and “regulation of immune system process” (**Figure 2E**). KEGG analysis demonstrated that the lncRNAs were significantly enriched in “signaling pathways regulating pluripotency of stem cells,” “cytokine-cytokine receptor interaction,” “hippo signaling pathway,” “pathways in cancer,” and “hematopoietic cell lineage” (**Figure 2F**). As of now,

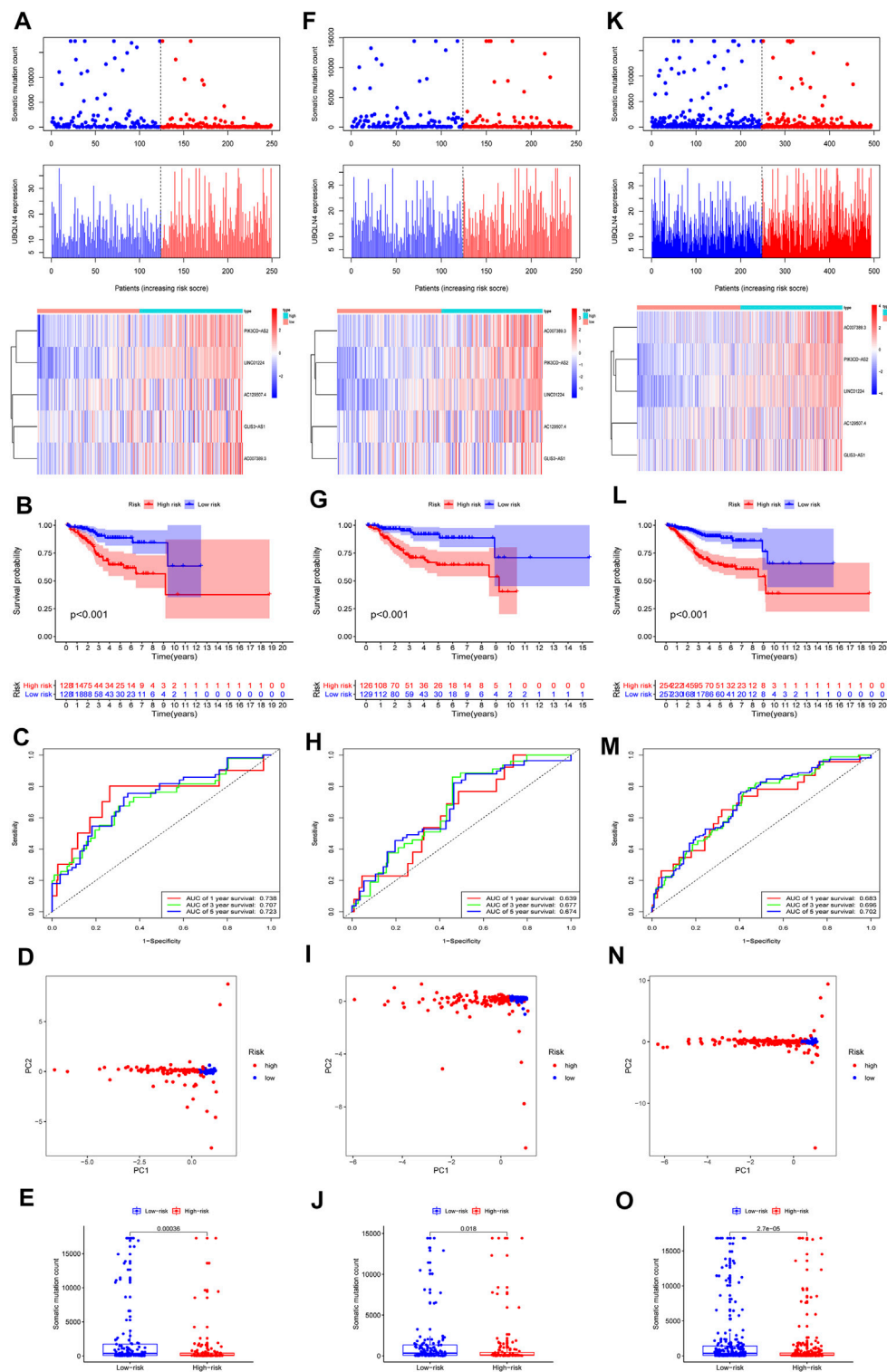


FIGURE 3 | Construction of the GILncSig prediction model of genomic instability-related lncRNA. In training set, (A) distribution of somatic mutation, the expression level of UBQLN4 and five lncRNAs expression patterns as the risk score increased. (B) Prognostic prediction in the high-risk group and low-risk group by Kaplan-Meier. (C) Time-dependent ROC curves were used to verify the survival prediction model. (D) PCA analysis revealed the difference between the high- and low-risk groups. (E) Level of somatic mutation count in the high- and low-risk groups. GILncSig evaluation in the testing set. (F) Distribution of somatic mutation and expression level of UBQLN4 as well as expression patterns of five lncRNAs as the risk score increased. (G) Prognostic prediction in the high- group and low-risk groups by Kaplan-Meier. (H) Time-dependent ROC curves were used to verify the survival prediction model. (I) PCA analysis revealed the difference between the high- and low-risk groups. (Continued)

FIGURE 3 | low-risk groups. **(J)** Level of somatic mutation count in the high- and low-risk groups. GILncSig evaluation in the TCGA set. **(K)** Distribution of somatic mutation and expression levels of UBQLN4 as well as expression patterns of five lncRNAs as the risk score increased. **(L)** Prognostic prediction in the high- and low-risk groups by Kaplan–Meier. **(M)** Time-dependent ROC curves were used to verify the survival prediction model. **(N)** PCA analysis revealed the difference between the high- and low-risk groups. **(O)** Level of somatic mutation count in the high-risk and low-risk groups. Red color represents the high-risk group, and blue color represents the low risk-group.

109 lncRNAs have been identified as genome instability-related lncRNAs.

Constructing the OS Prediction Model

We randomly divided 511 EC samples into a training group ($n = 256$) and a test group ($n = 255$) to investigate the prognostic value of 109 candidate lncRNAs associated with genomic instability. The Chi-square test and the Wilcoxon rank sum test were used to demonstrate that no significant differences in clinicopathological covariates existed between the training and the testing groups (Table 1). We used univariate and multivariate Cox proportional hazards regression to select five of 14 candidate lncRNAs as prognostic lncRNAs (Supplementary Tables S3, S4). Finally, in the training cohort, the lncRNAs AC007389.3, PIK3CD-AS2, LINC01224, AC129507.4, and GLIS3-AS1 were included in our prognosis model with the formula of “Risk score = $AC129507.4 * 0.0336 + GLIS3-AS1 * 0.0183 + PIK3CD-AS2 * 0.1192 + LINC01224 * 0.1728 + AC007389.3 * 0.2166$ ”. Then, on the basis of the median value of the risk score, we calculated the risk score for each EC sample in the training set and divided it into the low-risk group ($n = 128$) and high-risk group ($n = 128$). The patients with EC were ranked in ascending order based on the risk score and observed the changes in the trend of GILncSig, the number of somatic mutations, and the level of expression of UBQLN4 (Figure 3A). The heatmap compared clinicopathological features between two groups based on the expression of five lncRNAs associated with genomic instability. The analysis revealed significant differences in terms of stage, grade, histological, type, and age (Supplementary Figure S2, $p < 0.01$). In the Kaplan–Meier analysis, we found that overall survival (OS) was higher in the low-risk group than that in the high-risk group (Figure 3B). According to the ROC curve, our GILncSig model exhibited good sensitivity and specificity in predicting the OS of patients with EC (5 years, AUC = 0.723; 3 years, AUC = 0.707; 1 year, AUC = 0.738) (Figure 3C). The PCA revealed that samples from the two groups were distributed in opposite directions (Figure 3D). Meanwhile, it was discovered that the number of somatic mutations was lower in the high-risk group than that in the low-risk group (Figure 3E).

Validating the Prognostic Prediction Model in the Testing Set

Using the same risk scoring formula as in the training set, a total of 255 samples in the testing set were divided into the low-risk group ($n = 129$) and high-risk group ($n = 126$), and the predictive power was demonstrated in the testing set. The changes in the GILncSig trend, number of somatic mutations, and UBQLN4 expression level in the training set were similar to those in the testing set (Figure 3F). Moreover, the testing set exhibited

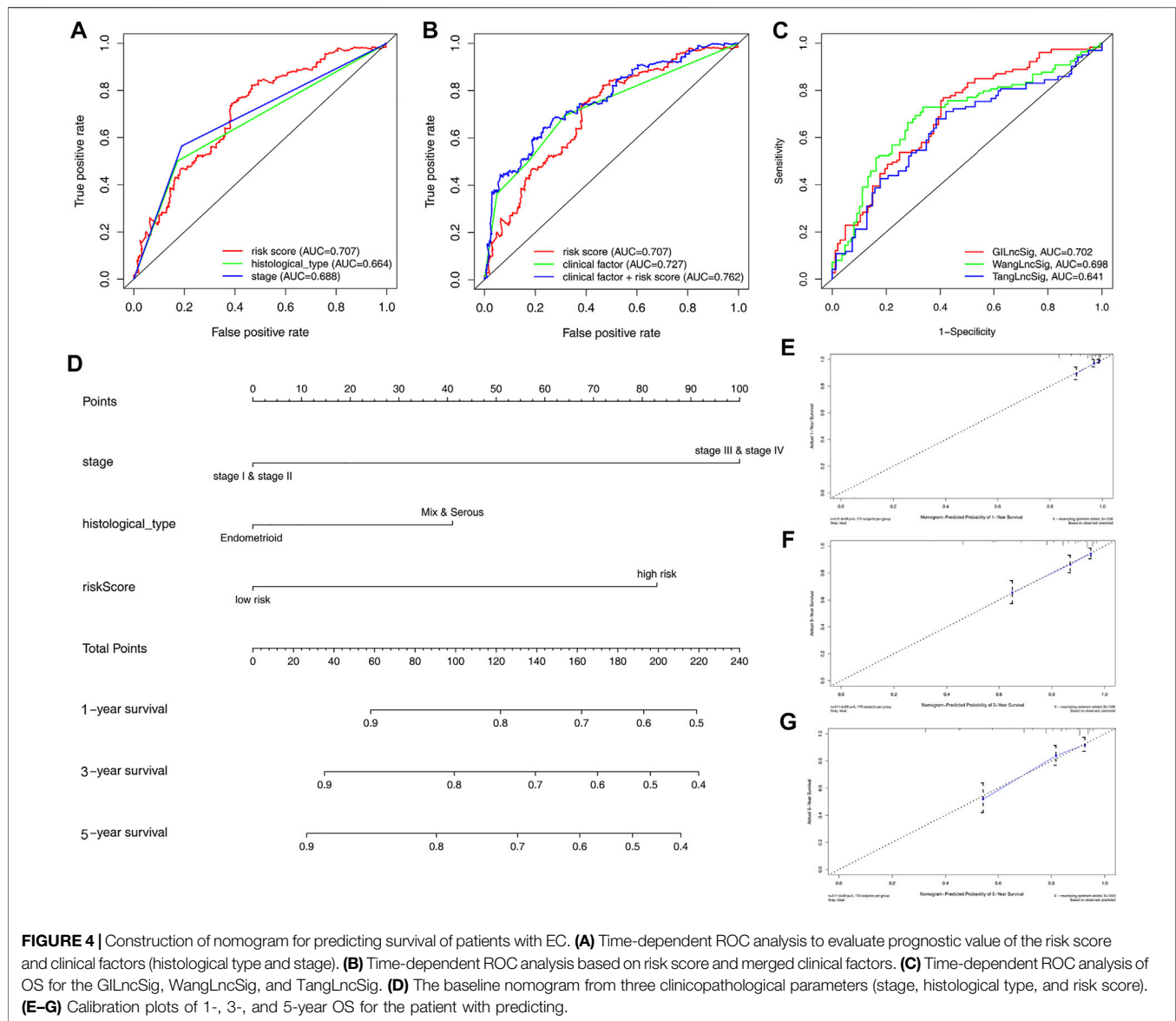
prognostic patterns similar to the testing set (Figure 3G). The ROC curve demonstrated that the model had good sensitivity and specificity in predicting patient OS in the testing set (5 years, AUC = 0.674; 3 years, AUC = 0.677; 1 year, AUC = 0.639) (Figure 3H). PCA analysis displayed a different distribution pattern for the low-risk and high-risk groups according to the expression of five lncRNAs in the testing set (Figure 3I). The number of somatic mutations in the high-risk group was lower than in the low-risk group (Figure 3J).

Validating the Prognostic Prediction Model in the TCGA Set

The 511 samples in the TCGA set were stratified into low-risk ($n = 257$) and high-risk groups ($n = 254$) based on the cutoffs in the training set to further validate the prediction model. The distribution patterns of GILncSig, somatic mutation number, and UBQLN4 expression level were consistent with the above results for training and testing sets (Figure 3K). In addition, the high-risk group had a much lower OS than the low-risk group (Figure 3L). The ROC curve revealed that the GILncSig in the TCGA set had good sensitivity and specificity in predicting patient OS in the testing set (5 years, AUC = 0.702; 3 years, AUC = 0.696; 1 year, AUC = 0.683) (Figure 3M). In the TCGA set, PCA analysis displayed a distinct distribution pattern for the low-risk and high-risk groups (Figure 3N). The number of somatic mutations in the high-risk group was lower than in the low-risk group (Figure 3O). Furthermore, GSEA was used to examine the transcript message of genomic instability-related lncRNAs in the high-risk and low-risk subgroups. Representative KEGG pathways in the high-risk subgroup model were “base excision repair,” “cell cycle,” “DNA replication,” “mismatch repair,” (MMR) and “nucleotide excision repair.” Representative KEGG pathways in the low-risk subgroup model were “asthma,” “autoimmune thyroid disease,” “cytokine-cytokine receptor interaction,” “graft-versus-host disease,” and “intestinal immune network for IgA production” (Supplementary Figure S3).

ROC Analysis of Clinical Factors and the Risk Score

ROC curve analysis revealed that the AUC of risk score was 0.707 and the clinical factor was 0.727 in this model, both significantly higher than histological type (AUC = 0.664) and stage (AUC = 0.688). Intriguingly, the AUC of clinical factor plus risk score (AUC = 0.762) was the highest in this ROC curve (Figures 4A,B). The ROC curve demonstrated a better predictive potential of GILncSig; however, combining clinical factors and GILncSig yielded the best predicting effect on OS in patients with EC. To demonstrate further the predictive performance of the ROC



curve for lncRNA in this model, we compared two recently published articles on the signatures of lncRNAs (Tang et al., 2019; Wang et al., 2020a). Using the same TCGA patient cohort, it was revealed that the AUC of OS for the GILncSig in this model is 0.702, significantly higher than other models such as WangLncSig (AUC = 0.698) and TangLncSig (AUC = 0.641) (Figure 4C). As such, a nomogram incorporating risk score and clinical factors were developed to provide clinicians with a quantitative method for predicting OS in patients with EC (Figure 4D). The calibration curve of 1-, 3-, and 5-year survival showed that the nomogram was nearly an ideal model (Figures 4E–G). The prognostic factors of patients with EC are shown in Supplementary Figure S4; it was revealed that age, grades 3 and 4, histological type, and stage were the most important factor affecting the prognosis of patients with EC, whereas initial stage (grades 1 and 2) did not affect prognosis between the high-risk and low-risk groups. These findings suggest

that, compared to nomograms based on lncRNA signatures, those based on GILncSig may better predict outcome and clinical features for patients with EC, thereby aiding clinical management.

Assessing the Independent Prognostic Significance of Risk Score and Clinical Stratification Analysis

We performed univariate and multivariate Cox regression analyses on three datasets (training, testing, and TCGA) for variables, including age, histological type, stage, grade, and risk score to see if it is an independent prognostic factor from the clinicopathological features. After adjusting for other clinical factors, including age, gender, and tumor stage, clinical stratification analyses of the prognostic performance of GILncSig in the TCGA dataset revealed that patients in the low-risk group had better survival outcomes than those in the

TABLE 2 | Univariate and multivariable Cox regression analysis of the GILncSig and overall survival in different patient sets.

Variable	Univariable model			Multivariable model		
	HR	95% CI	p-value	HR	95% CI	p-value
Training set (<i>n</i> = 256)						
Risk score	1.216	1.133–1.305	5.54E-08	1.176	1.087–1.272	4.97E-05
Age	1.337	0.7116–2.513	0.368			
Grade	2.965	1.062–8.282	0.038	1.566	0.514–4.771	0.430
Stage	3.154	1.765–5.636	0.000	2.220	1.170–4.212	0.015
Histological_type	2.216	1.228–3.999	0.008	1.439	0.774–2.676	0.250
Testing set (<i>n</i> = 255)						
Risk score	1.000	1.000–1.000	0.006	1.000	1.000–1.000	0.031
Age	2.447	1.204–4.973	0.013	1.713	0.810–3.619	0.159
Grade	4.170	1.007–17.266	0.049	1.684	0.379–7.475	0.493
Stage	5.806	3.036–11.104	1.06E-07	3.906	1.946–7.840	0.000
Histological_type	4.247	2.320–7.774	2.75E-06	2.477	1.253–4.894	0.009
TCGA set (<i>n</i> = 511)						
Risk score	1.000	1.000–1.000	0.003	1.000	1.000–1.000	0.020
Age	1.778	1.112–2.843	0.016	1.582	0.967–2.589	0.068
Grade	3.363	1.467–7.770	0.004	1.532	0.632–3.713	0.345
Stage	4.116	2.670–6.275	4.82E-11	3.252	2.055–5.1483	4.82E-07
Histological_type	3.044	2.003–4.624	1.84E-07	1.875	1.179–2.9	0.008

high-risk group across all clinically stratified subgroups ($p < 0.05$, log-rank test; **Table 2**). These results suggested that the prognostic significance of GILncSig in patients with EC is independent of other clinicopathological variables.

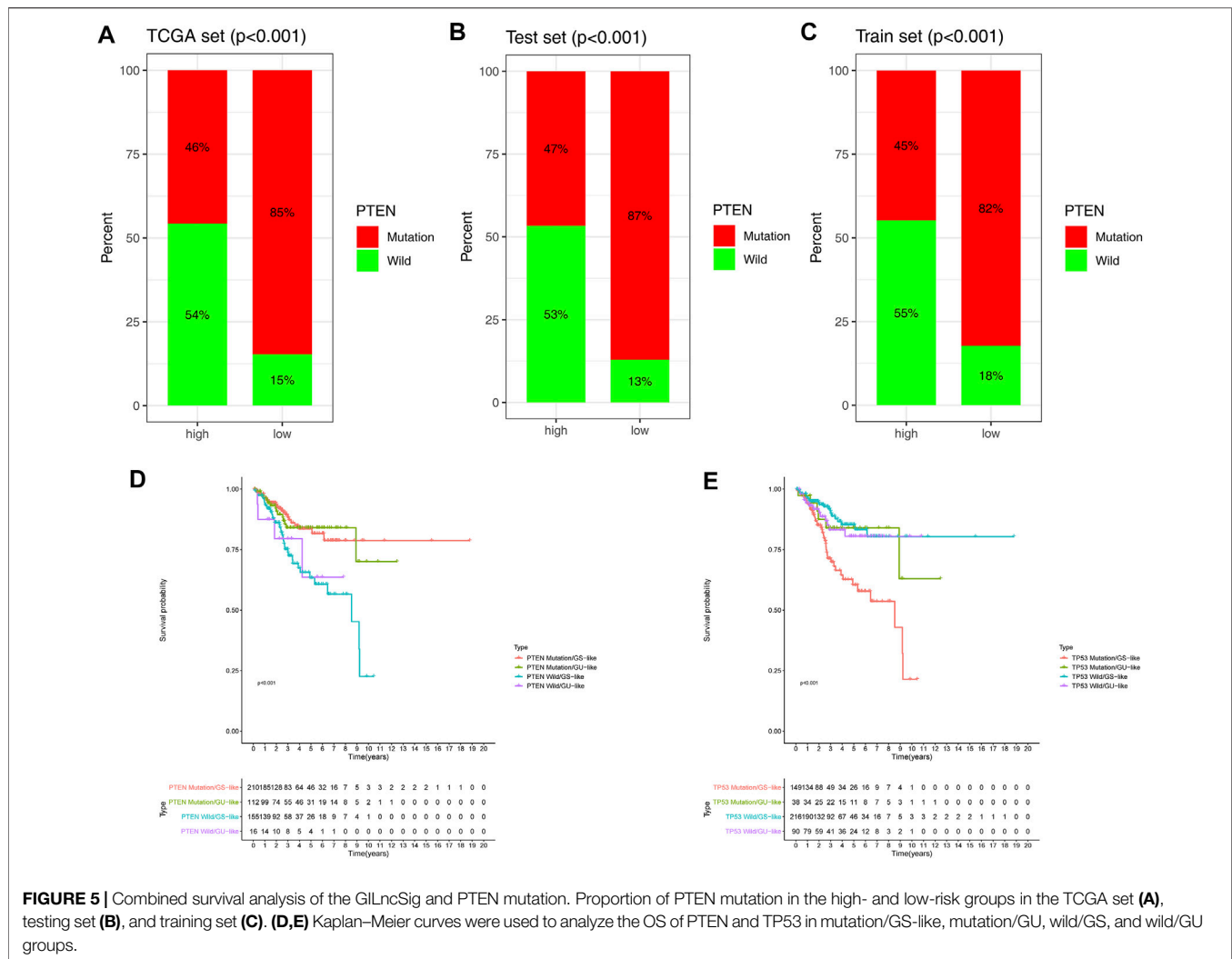
Prediction Performance Between the GILncSig and PTEN

Previous research has demonstrated that the phosphate and tension homolog deleted on chromosome 10 (PTEN) gene plays a critical role in EC progression (Wang et al., 2021). To learn more about the relationship between the GILncSig and PTEN mutations, we examined the proportion of patients with PTEN mutations in three groups. The analysis showed that PTEN mutations in the low-risk group were significantly higher than those in the high-risk group in the TCGA, testing, and training sets (**Figures 5A–C**). However, it is unclear whether higher PTEN mutation was a better predictor of survival outcomes than GILncSig. Compelling evidence shows that the TP53 mutation is an important prognostic factor in EC (Hollis et al., 2020), as such, we compared the predictive performance of GILncSig and the TP53 mutation simultaneously. PTEN/TP53-sequence wild type (PTEN/TP53 wild) and PTEN/TP53-sequence mutation type (PTEN/TP53 mutation) EC patients were divided into GU and GS groups. PTEN wild EC patients in the GS groups (defined as PTEN wild/GS-like) had a worse prognosis than PTEN mutation EC patients in GS groups (defined as PTEN wild/GS-like) ($p < 0.001$) and PTEN mutation EC patients in GU groups (defined as PTEN mutation/GU-like) ($p < 0.001$). Whereas, TP53 mutation in the GS groups (defined as TP53 mutation/GS-like) had worse OS than TP53 wild in the GS groups (defined as TP53 wild/GS-like) ($p < 0.001$) and in the GU groups (defined as TP53 wild/GU-like) ($p < 0.05$). Meanwhile, there was no difference in survival between the other groups (**Figures 5D–E**). These findings demonstrate that GILncSig holds great promise as an effective tool in predicting OS as PTEN mutation and TP53 mutation.

Analysis of the Mutation Profiles of Two Risk Groups

To assess the immune status in the high-risk and low-risk groups, we compared the ESTIMATE scores (including immune scores and stromal scores) with tumor purity. The ESTIMATE algorithm results revealed that the ESTIMATE score, immune score, and stromal score of the high-risk group were lower than those of the low-risk group. Tumor purity, on the other hand, was higher in the high-risk group (**Figure 6A**). Human leukocyte antigen (HLA)-related genes had significant effects on immune regulation, and HLA-related gene expression was significantly lower in the high-risk group compared to the low-risk group (**Figure 6B**). Previous evidence shows that lncRNAs mediate the function of tumor-infiltrating immune cells (TICs) (Athie et al., 2020); therefore, we looked at the relationship between five prognostic lncRNAs and TICs (**Supplementary Figure S5**). Immune cells significantly impact the tumor immune microenvironment; as such, we compared tumor immune-related cells across the risk groups. The results showed that the abundances of aDCs were significantly decreased in the low-risk group, whereas the abundances of CD8⁺ T cells, DCs, iDCs, mast cells, neutrophils, pDCs, T helper cells, Tfh, Th1 cells, Th2 cells, TIL, and Treg cells were significantly decreased in the high-risk group (**Figure 6C**). The correlation of risk score and tumor immune-related cells, as well as the most relevant tumor immune cells, are illustrated in **Figures 6D,E**. Comparisons of 13 immune-related functions confirmed the difference of APC costimulation, CCR, checkpoint, cytolytic activity, HLA, inflammation-promoting, T cell co-inhibition, T cell costimulation, type I IFN response, type II IFN response in the high-risk and low-risk groups (**Figure 6F**).

Immune checkpoint proteins were involved in immune response and interacted with immune cells in various ways. Among many immune checkpoint proteins, CD27, CD40,

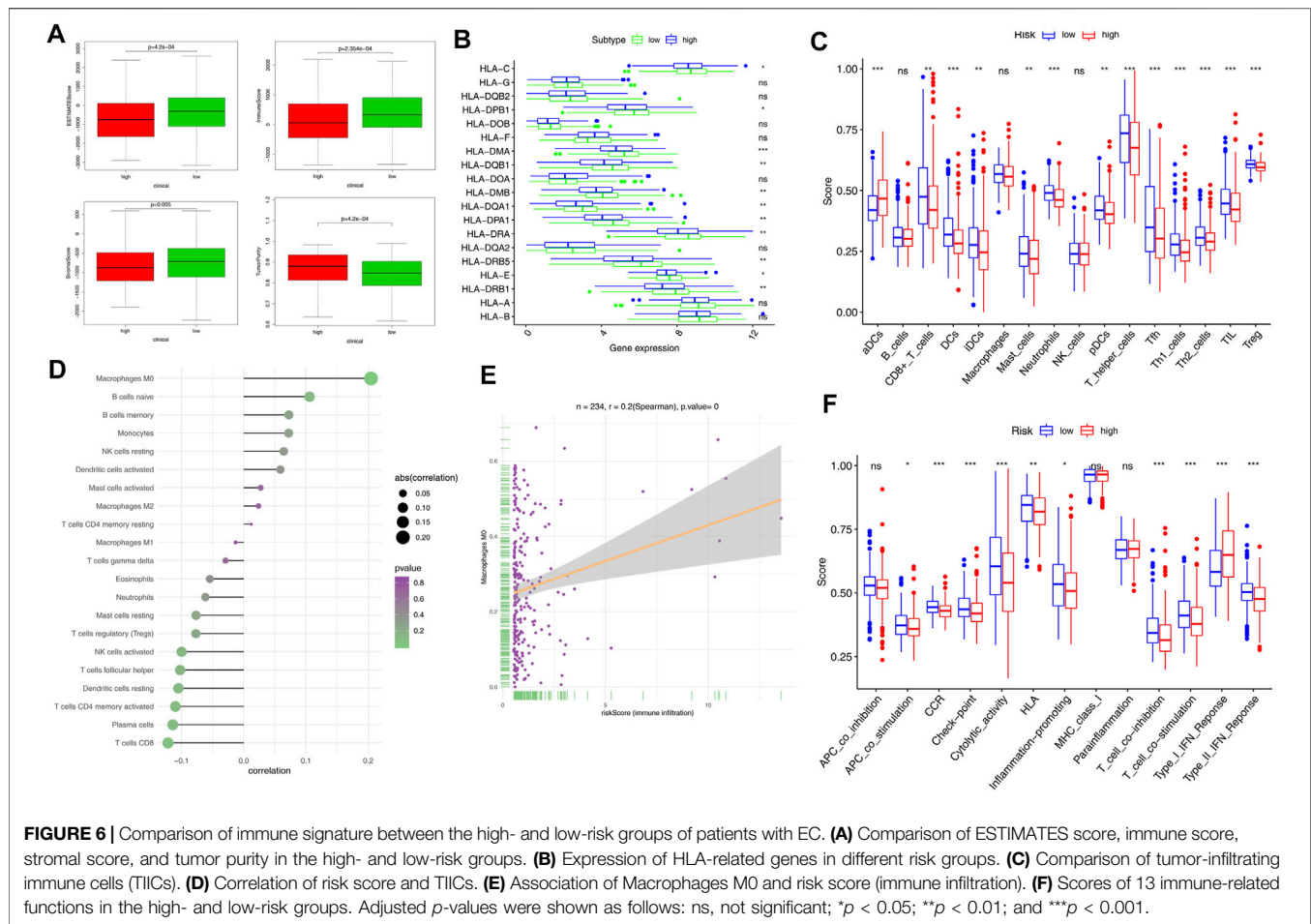


CD70, CD270, B7-H3, B7-H4, IDO1, PD-1, PD-L1, PD-L2, TIM-3, TIGIT, CTLA4, CD86, ICOS, and LAG3 have been extensively studied and are thought to be important immunomodulators. First, we looked at the correlations between immune checkpoint proteins and risk score (Figure 7A); the top six immune checkpoint proteins that were most negatively associated with the risk score are shown in Figure 7B. The scores of IPS, IPS-CTLA4, IPS-PD1-PD-L1-PD-L2, and IPS-PD1-PD-L1-PD-L2-CTLA4 in the high-risk and low-risk groups were calculated to evaluate immune signature and predict the potential role of immune checkpoint inhibitors (Figure 7C). Moreover, we found that the risk score was negatively correlated with MSI ($p = 0.00063$, Figure 7D). In addition, the expression levels of MLH1, MSH2, MSH6, and PMS2 were significantly higher in the high-risk group compared to the low-risk group (Figure 7E).

Genome-Wide Mutation Profiling in EC Between Two Risk Groups

To investigate the prognostic value of TMB, we calculated the TMB value of EC samples in the TCGA database and divided

them into high-TMB and low-TMB groups based on the median TMB value. The survival rate of the two groups was analyzed using the K-M curves and the results showed the best prognosis in patients with EC with high-TMB (Figure 8A). When the risk score and TMB analyses were combined, it was revealed that patients with EC with low-TMB and high-risk scores had the worst prognosis, whereas patients with EC with high-TMB and low-risk scores had the best prognosis (Figure 8B). Furthermore, we analyzed genome-wide mutations in EC high- and low-risk groups and found that missense mutations were the most common among different types of mutations, single-nucleotide polymorphisms were more common than deletions or insertions, and C > T transitions accounted for the highest proportion in both groups. Horizontal histogram demonstrated that the top 10 mutated genes in the two groups differed, but PTEN was among the top two (Supplementary Figure S6). In the high-risk group, 10 genes were mutated at a rate of more than 21%: TP53 (56%), PTEN (45%), PIK3CA (44%), ARID1A (33%), TTN (30%), PIK3R1 (23%), CHD4 (22%), CSMD3 (21%), KMT2D (21%), and PPP2R1A (21%). In the low-risk group, 10 genes were mutated at a rate of more than 29%: PTEN (84%), ARID1A



(57%), PIK3CA (54%), TTN (47%), PIK3R1 (39%), CTCF (36%), CTNNB1 (33%), KMT2D (32%), ZFH3 (31%), and MUC16 (29%) (**Figures 8C,D**). Moreover, we found that the risk score was negatively correlated with TMB ($p = 0.01426$, **Figure 8E**). TMB appeared to be higher in patients with EC in the low-risk group than in those in the high-risk group (**Figure 8F**). We also discovered that the low-risk group had more samples with PTEN, ARID1A, CTNNB1, CTCF, TTN, PIK3R1, KMT2D, and PIK3CA mutations than the high-risk group (**Figure 8G**). The mRNA stemness indices in the high-risk group were higher than those in the low-risk group, and there was no difference in the EREG-mRNA stemness indices between the two groups (**Figures 8H,I**).

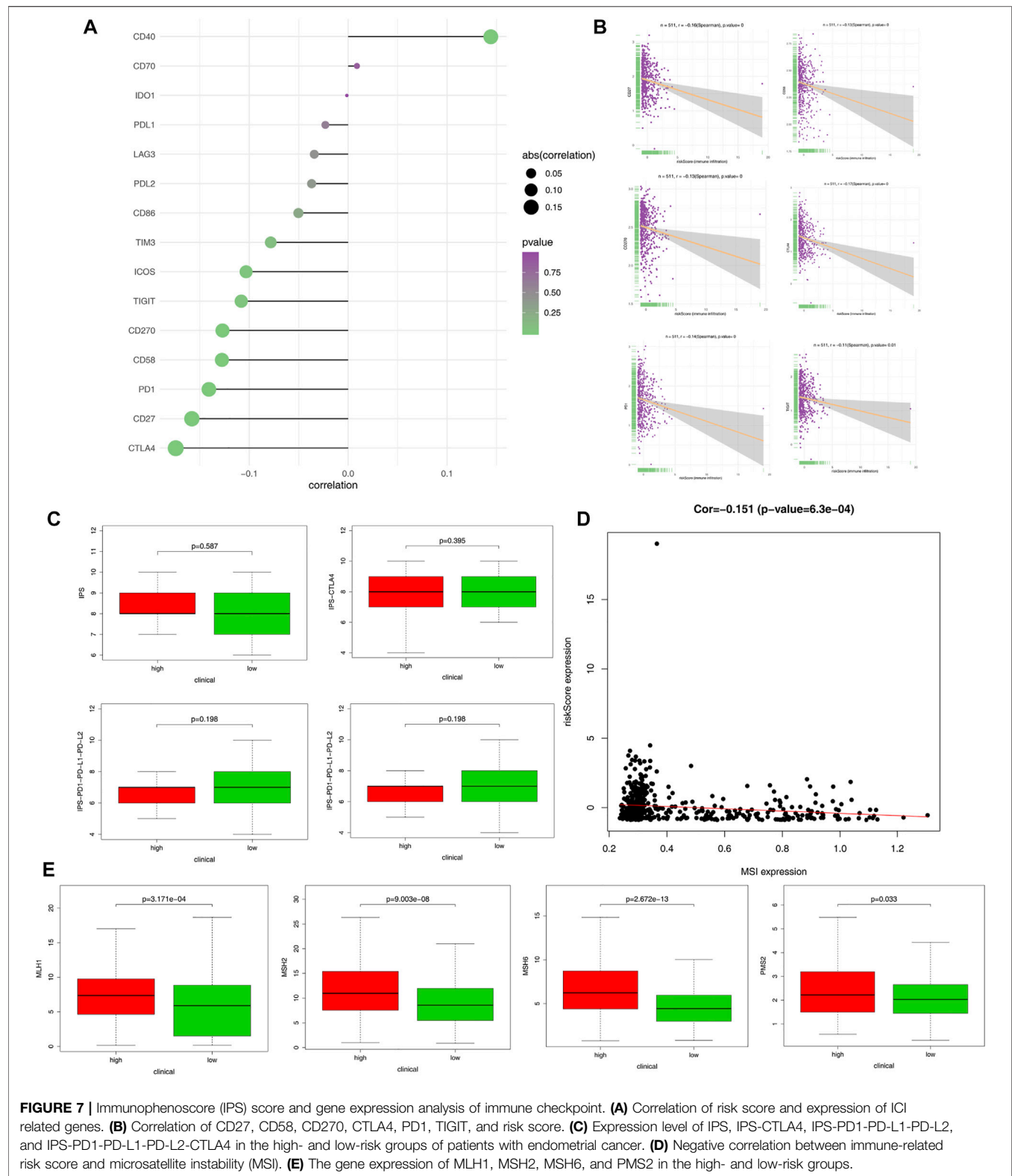
Prognostic lncRNAs Expression and Cancer Cell Sensitivity to Chemotherapy

The IC50 of each EC sample was calculated and compared using a common chemical drug prediction model. We screened 20 chemotherapeutic drugs with lower IC50 (including Bicaluramide, AKT.inhibitor.VIII, X17.AGG, RDEA119, Bryostatin.1, FTL277, AZD6244, XMD8.85, PD.0325901, Roscovitine, SB.216763, CHIR.99021, AZD6482, PF.562271, PD.0332991, Embelin, Bexarotene, Nutlin.3a, BMS.708163,

Lapatinib, FH535, AZ628, BMS.754807, BMS.536924, LFM.A13) in comparison to the high-risk group ($p < 0.05$) (**Supplementary Figure S7**). Furthermore, we investigated the correlation of expression of the lncRNAs related to genetic instability in NCI-60 cell lines and the relationship between expression and drug sensitivity. The analysis demonstrated that increased LINC01224 expression was associated with decreased drug sensitivity of cancer cells to ARRY-162, Trametinib, Cobimetinib, Selumetinib, Dabrafenib, and Vemurafenib, whereas increased PIK3CD-AS2 expression was associated with increased drug resistance of cancer cells to 6-Mercaptopurine, Copanlisib, Dasatinib, and Pipamperone. Furthermore, as GLIS3-AS1 expression increased, cancer cell drug sensitivity to Vorinostat and 6-Thioguanine decreased (**Figure 9**). The results showed that lncRNAs associated with genome instability were potentially related to chemotherapy drug sensitivity ($p < 0.05$).

Validating Genome Expression Levels of Instability-Related lncRNAs in EC Samples

To validate the expression levels of genome instability-related lncRNAs, we used qRT-PCR to detect the expression levels of five genome instability-related lncRNAs in 15 EC



samples and 15 normal tissues. The findings revealed that PIK3CD-AS2 was significantly downregulated, whereas AC129507.4 was highly expressed (**Supplementary Figures**

S8A,B). However, there was no difference in the expression of GLIS3.AS1, LINC01224, and AC007389.3 between EC and normal samples (**Supplementary Figures S8C-E**).

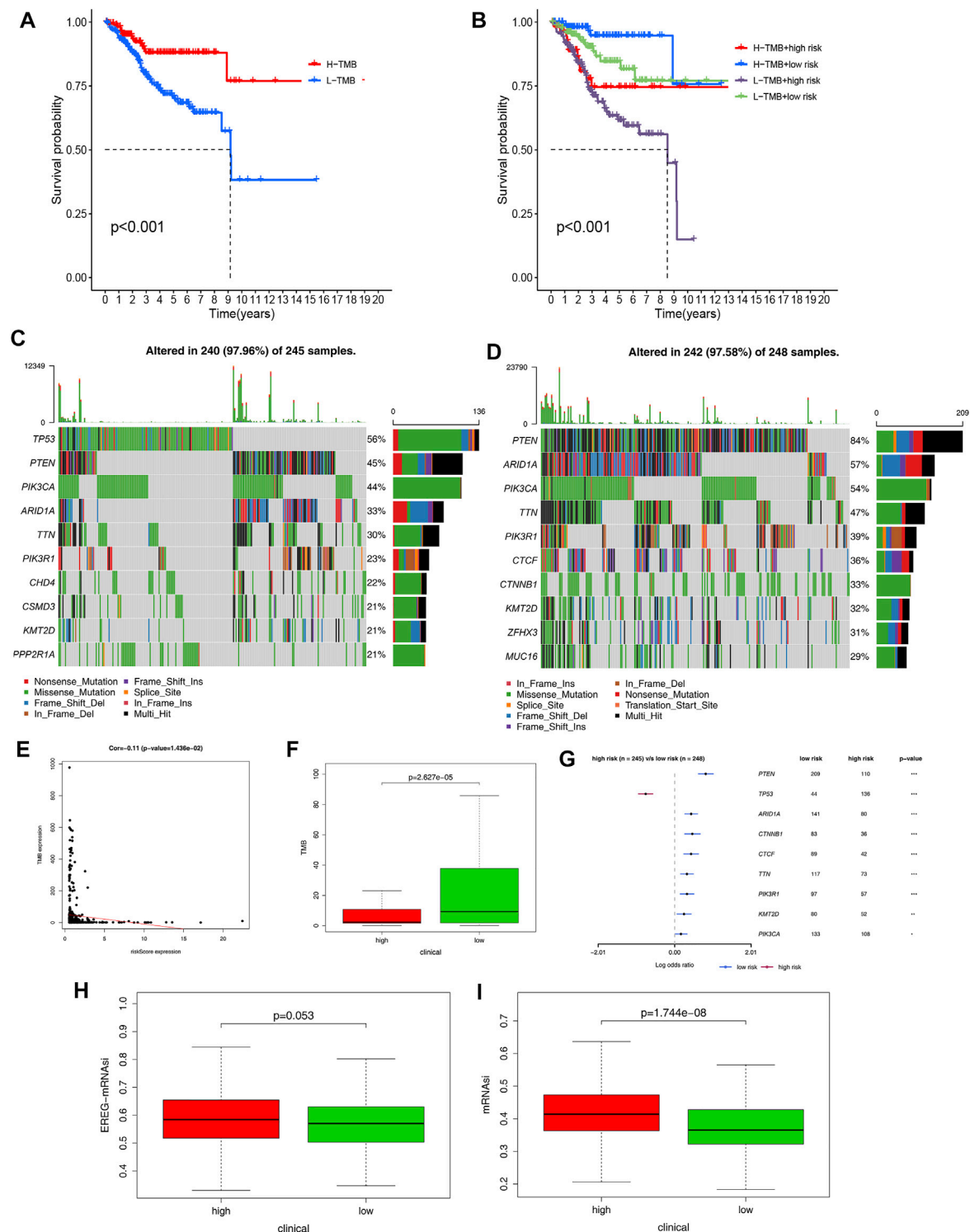
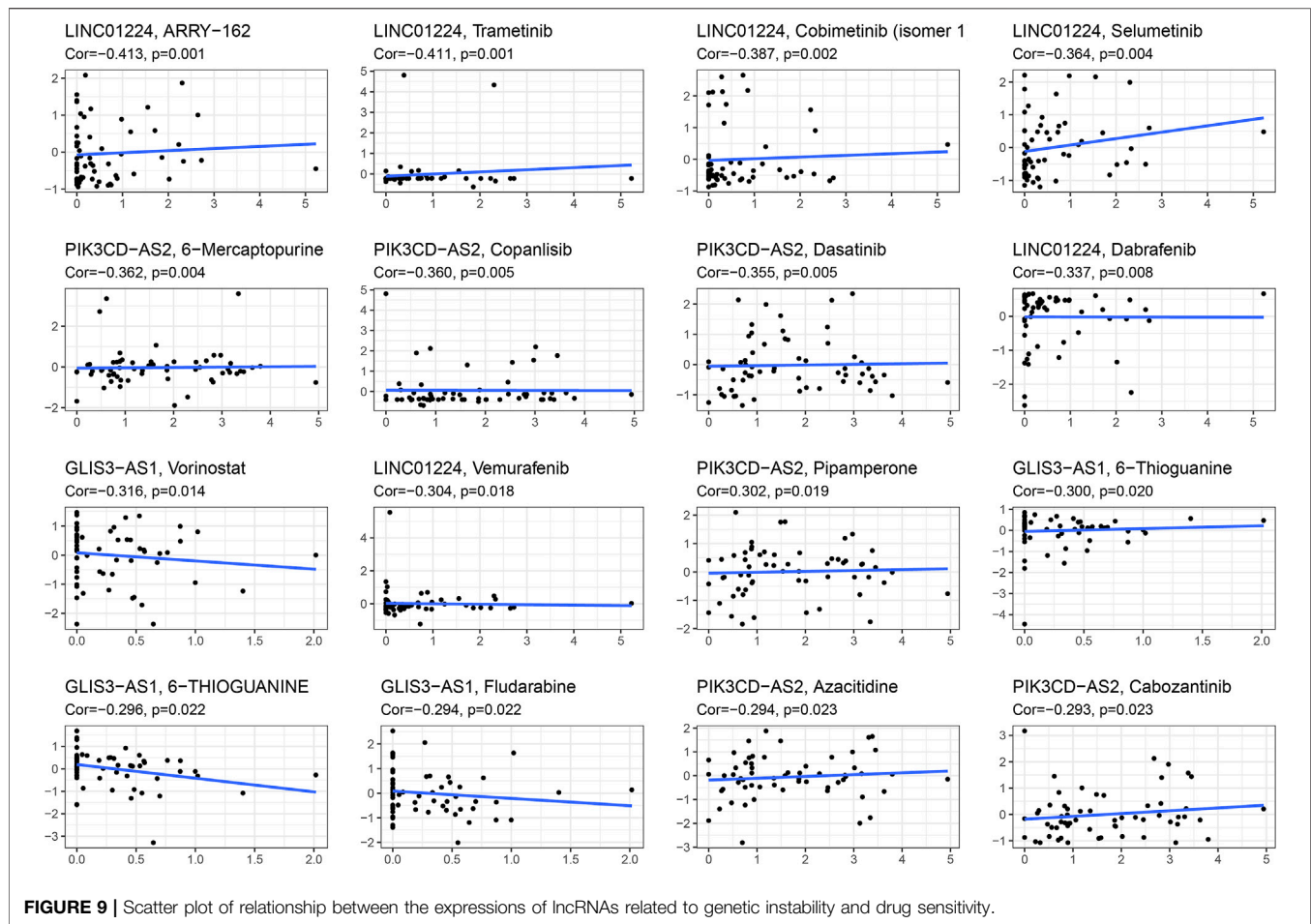


FIGURE 8 | TMB level and Somatic mutation analysis. **(A)** Survival analysis between patients with high- and low-TMB EC. **(B)** Two-factor survival analyses of risk score and TMB levels. **(C,D)** Landscape of mutation profiles was shown in the waterfall plot, in which the type of mutation is shown in the comment bar (bottom) and genes are ordered by their mutation frequency. **(E)** Relationship between tumor mutation burden (TMB) and immune-related risk score. **(F)** Differences of tumor mutation burden in the high-risk and low-risk groups. **(G)** Differences of mutated genes between the high- and low-risk groups. **(H,I)** mRNA stemness indices between the high- and low-risk groups.



DISCUSSION

Globally, EC is among the most common female genital cancers and the prevalence of EC continues to increase every year. The lack of significant improvement in the 5-year survival rate for patients with EC suggests that the disease remains a serious threat to female health (Bray et al., 2018; Feng et al., 2019). Therefore, there is an urgent need for better surveillance and treatment programs for EC. The current study was aimed at identifying the GILncSig and its prognostic value in EC.

To investigate the value of lncRNA-related genomic instability on the prognosis of patients with EC, the patients were grouped based on mutation frequency and filter the target genes. First, a total of 109 lncRNAs with different expression levels in the quarter highest and quarter lowest mutation frequency samples were identified. The lncRNAs were then screened to be associated with genomic instability in patients with EC. In addition, it was also investigated whether the genomic instability-associated lncRNAs could predict clinical outcomes. Results of the present study showed that patients in the high-risk group had the worse outcomes and lower somatic mutation, which was validated by the testing set as well as the TCGA set.

Results of the ROC curve analysis show that the clinical factor combined with risk score exhibited the most significant effect in

the model as compared with other models. The construction and validation of GILncSig revealed that GILncSig effectively predicted the prognosis and gene instability of patients with EC. Further, among the numerous lncRNAs, lncRNAs AC007389.3, PIK3CD-AS2, LINC01224, AC129507.4, and GLIS3-AS1 were included in the prognosis model employed in the current study. It has been reported that LINC01224 is highly expressed in epithelial ovarian cancer and can promote the development of the cancer through miR-485-5p-mediated PAK4 (Gong et al., 2020). Therefore, interference with the expression of LINC01224 can inhibit the proliferation of colon cancer cells and induce cell cycle arrest in G0-G1 phase (Xing et al., 2020). The PIK3CD-AS2 lncRNAs also promotes tumor cell proliferation and inhibit apoptosis, and this is thus associated with poor prognosis of lung adenocarcinoma (Zheng et al., 2020). On the other hand, GLIS3-AS1 lncRNAs may be a biomarker for pancreatic duct adenocarcinoma (Permuth et al., 2017).

In addition, it was evident that the largest difference in mutations between these two groups of lncRNAs (PIK3CD-AS2 and GLIS3-AS1) was PTEN mutation, which was more common in the low-risk samples than in the high-risk samples. A previous study conducted by Erkanli et al. reported that the mutation or deletion rate of PTEN protein in I type EC was between 34% and 55%, and even >80% (Erkanli et al., 2006).

Moreover, the analysis of PTEN gene mutation in patients with EC and precancerous lesions revealed that 83% of the patients had PTEN mutation and 55% of precancerous lesions also had genetic mutation, whereas normal endometrial tissue samples did not have PTEN mutation (Mutter et al., 2000). The results of the present study indicated that low-risk patients with more PTEN mutation have worse prognosis outcome than high-risk patients with fewer PTEN mutations. Therefore, the enrichment of co-expressed genes was associated with carcinogenesis, and genome stability as well as immune and genomic instability-related lncRNAs were found to predict the prognosis and be an indicator of genomic instability of patients with the cancer.

Currently, with the increase in understanding of the tumor microenvironment, the importance of and the role that immune cells play has been extensively elucidated. A previous study on head and neck cancer (HNC) has confirmed that some immune cells, such as M0 macrophages and NK cells, have longer dormancy time in tumor tissues than in the adjacent normal tissues, whereas other cells, such as B cell naïve, are shorter and thus are significantly relevant in the HNC survival (Xie et al., 2018; Liu et al., 2020b). Unlike other tumor-associated macrophages, it has been reported that M0 macrophages play a specific role in survival of patients with HNC.

In pancreatic ductal adenocarcinoma, Cansu et al., through tumor proliferation and apoptosis assay of their study, showed that M0 macrophages harbor anti-tumorigenic activities that M1 and M2 did not share (Helm et al., 2014; Tekin et al., 2020). In addition, investigation carried out by Peipei et al. demonstrated that NK cells are regulated by lncRNA GAS5 through upregulation of the expression of miR-544 to perform its role as liver cancer killer (Fang et al., 2019). Elsewhere, Mohsen et al. reported that the number of memory B cells, which can express granzyme B (GZMB), was smaller in metastatic as compared with non-metastatic lymph nodes, and this hence emphasized the importance of GZMB + b cells in patients with breast invasive ductal carcinoma (Arabpour et al., 2019; Chesneau et al., 2020). Cytokine negatively regulates IFN γ signaling through CSF1R expression, thus modulating the functions of tumor infiltration (Wang et al., 2020b).

Immune-microenvironment of the tumor has been considered to be crucial in the progression of the tumor and response to therapies. The present study showed that patients in the low-risk group were more prone to mutations as compared with those in the high-risk group. Further analysis confirmed that the risk score was positively correlated with tumor immune-related cells and negatively associated with TMB and MSI. In addition, it has been found that the immune checkpoint inhibitors prevent tumors from activating immune checkpoint protein receptors on the surface of immune cells. This prevented tumors from evasive immune responses and cause of the immune system to produce an anti-tumor response (Intlekofer and Thompson, 2013). In addition, some studies have shown a breakthrough in the treatment of advanced EC with a combination of PD-L1 inhibitor Pembrolizumab and Lenvatinib (Pakish and Jazaeri, 2017; Makker et al., 2019; Makker et al., 2020).

Results of the present study found that 25% of patients with EC were associated with defects of DNA MMR, which is characterized by an error in nucleotide repeats during DNA

replication, also referred to as microsatellite instability (MSI) (Le et al., 2015). MMR defects led to a higher rate of somatic cell mutation, which increased the tumor antigen load and the number of tumor-infiltrating lymphocytes of these tumors with MMR defects, corresponding to the increased expression of PD-1 as well as PD-L1 (du Rusquec et al., 2019; Howitt et al., 2015). Therefore, the high incidence of MSI in EC has promoted application of immunosuppressive agents as a new therapeutic intervention. The validation results hence indicated that the GILncSig not only predicts the prognosis and genomic instability but also is an indicator of immune infiltration of patients with EC.

The relationship between the effectiveness of chemo-drug and genomic instability-related lncRNAs on different risk groups was predicted by GDSC database. Results of the present study showed that LINC01224 was negatively associated with reduced sensitivity of cancer cells to drug such as ARRY-162, Trametinib, Cobimetinib, Selumetinib, Dabrafenib, and Vemurafenib. Further, ARRY-162 and Trametinib, as well as Cobimetinib and Selumetinib are the reversible inhibitor of MEK1 and MEK2 (Lugowska et al., 2015). In addition, it was evident that Trametinib inhibits BRAF V600 mutation-positive melanoma cell growth both *in vitro* and *in vivo* through activating MEK1/2 to regulate ERK pathway, which had been approved by Food and Drug Administration (FDA) to treat BRAF V600E or V600K mutation-positive melanoma and non-small cell lung cancer (Geraud et al., 2020; Roskoski, 2020). Meanwhile, Dabrafenib and Vemurafenib are also effective drugs for the treatment of melanoma (Chapman et al., 2011; Hauschild et al., 2012).

The increased expression of PIK3CD-AS2 was associated with increased drug resistance of cancer cells to 6-Mercaptopurine, Copanlisib, Dasatinib, and Pipamperone. Furthermore, drug sensitivity of cancer cells to Vorinostat and 6-Thioguanine was downregulated as the expression of GLIS3-AS1 was increased. It was also suggested that 6-mercaptopurine can be used as a maintenance therapy for acute lymphoblastic leukemia (Bell et al., 2004; Escherich et al., 2011). Results of the present study found that Copanlisib is a generic I type PI3K inhibitor with significant activity against PI3K α and PI3K δ subtypes, both of which play important roles in B-cell malignancies (Decaudin et al., 1999; Swerdlow et al., 2016).

Follicular lymphoma (FL) is a common form of indolent non-Hodgkin's lymphoma, and the FDA has accelerated approval of copanlisib for the treatment of relapsed or refractory FL in adults who have received at least two systemic treatments (Magagnoli et al., 2020). Therefore, the reported correlation between the genomic instability-related lncRNAs and chemotherapy drugs suggested that GILncSig exhibited high therapeutic potential in patients with EC. The results of the present study also demonstrated that genomic instability-related lncRNAs can be used as therapeutic targets to overcome drug resistance or adjuvant drug sensitivity.

However, the current study has some limitations. First, patients in the representative samples were predominantly Western people, and thus, so whether the research results need to be verified if they hold true for Asians and other people in the world. Second, the conclusions of the present study may exhibit deviation because some clinical indicators records were incomplete. Furthermore, the

preliminary findings still require to be further validated on a larger cohort and with biological experiments.

CONCLUSION

In conclusion, the present study identified and validated the GILncSig. Further, the prognostic prediction, somatic mutation, and chemotherapeutic drug sensitivity were performed to explore the roles of GILncSig in patients with EC. Therefore, the current study provided a critical approach of investigating the prognostic role of genome instability-related lncRNA, particularly in the areas of immune response, tumor microenvironment, and drug resistance, which is essential for the development of personalized cancer therapies.

DATA AVAILABILITY STATEMENT

The datasets presented in this study can be found in online repositories. The names of the repository/repositories and accession number(s) can be found in the article/Supplementary Material.

ETHICS STATEMENT

Written informed consent was obtained from the individual(s) for the publication of any potentially identifiable images or data included in this article.

AUTHOR CONTRIBUTIONS

JB and JL conceived the study and participated in the study design, performance, and manuscript writing. GC, JY,

and YW conducted the bioinformatics analysis. CW revised the manuscript. All authors read and approved the final manuscript.

ACKNOWLEDGMENTS

We would like to thank the researchers and study participants for their contributions.

SUPPLEMENTARY MATERIAL

The Supplementary Material for this article can be found online at: <https://www.frontiersin.org/articles/10.3389/fcell.2022.753957/full#supplementary-material>

Supplementary Figure 1 | Heatmap of 20 most significantly upregulated lncRNAs and 20 most significantly downregulated lncRNAs between GS and GU group.

Supplementary Figure 2 | Relationship between the expressions of five genetic instability-related lncRNAs and clinicopathological features.

Supplementary Figure 3 | Functional enrichment of transcript message of genomic instability-related lncRNAs in the high- and low-risk groups.

Supplementary Figure 4 | Stratified analyses of clinicopathological factors in EC between the high-risk and low-risk groups: (A,B) age, (C,D) grade, and (E,F) histological type.

Supplementary Figure 5 | Correlation between the expression of five prognostic lncRNAs and tumor-infiltrating immune cells (TICs).

Supplementary Figure 6 | Distribution of variants based on variant classification, type, and SNV class. Bottom part (from left to right) indicates mutation load for each sample and the top 10 mutated genes in patients with endometrial cancer (A,B).

Supplementary Figure 7 | Prediction of response to common chemo-drugs between the high-risk and low-risk groups based on GDSC database. IC₅₀, half-maximal inhibitory concentration.

Supplementary Figure 8 | Expression level of PIK3CD-AS2, AC129507.4, GLIS3.AS1, LINC01224, and AC007389.3 in clinical samples.

REFERENCES

- Andor, N., Maley, C. C., and Ji, H. P. (2017). Genomic Instability in Cancer: Teetering on the Limit of Tolerance. *Cancer Res.* 77 (9), 2179–2185. doi:10.1158/0008-5472.can-16-1553
- Arabpour, M., Rasolmali, R., Talei, A.-R., Mehdipour, F., and Ghaderi, A. (2019). Granzyme B Production by Activated B Cells Derived from Breast Cancer-Draining Lymph Nodes. *Mol. Immunol.* 114, 172–178. doi:10.1016/j.molimm.2019.07.019
- Athie, A., Marchese, F. P., González, J., Lozano, T., Raimondi, I., Juvvuna, P. K., et al. (2020). Analysis of Copy Number Alterations Reveals the lncRNA ALAL-1 as a Regulator of Lung Cancer Immune Evasion. *J. Cell Biol.* 219 (9). doi:10.1083/jcb.201908078
- Bao, S., Zhao, H., Yuan, J., Fan, D., Zhang, Z., Su, J., et al. (2020). Computational Identification of Mutator-Derived lncRNA Signatures of Genome Instability for Improving the Clinical Outcome of Cancers: a Case Study in Breast Cancer. *Brief. Bioinformatics* 21 (5), 1742–1755. doi:10.1093/bib/bbz118
- Bell, B. A., Brockway, G. N., Shuster, J. J., Erdmann, G., Sterikoff, S., Bostrom, B., et al. (2004). A Comparison of Red Blood Cell Thiopurine Metabolites in Children with Acute Lymphoblastic Leukemia Who Received Oral Mercaptopurine Twice Daily or once Daily: a Pediatric Oncology Group Study (Now the Children's Oncology Group). *Pediatr. Blood Cancer* 43 (2), 105–109. doi:10.1002/pbc.20089
- Bergman, L., Beelen, M. L., Gallee, M. P., Hollema, H., Benraadt, J., and van Leeuwen, F. E. (2000). Risk and Prognosis of Endometrial Cancer after Tamoxifen for Breast Cancer. *The Lancet* 356 (9233), 881–887. doi:10.1016/S0140-6736(00)02677-5
- Bray, F., Ferlay, J., Soerjomataram, I., Siegel, R. L., Torre, L. A., and Jemal, A. (2018). Global Cancer Statistics 2018: GLOBOCAN Estimates of Incidence and Mortality Worldwide for 36 Cancers in 185 Countries. *CA: a Cancer J. clinicians* 68 (6), 394–424. doi:10.3322/caac.21492
- Chapman, P. B., Hauschild, A., Robert, C., Haanen, J. B., Ascierto, P., Larkin, J., et al. (2011). Improved Survival with Vemurafenib in Melanoma with BRAF V600E Mutation. *N. Engl. J. Med.* 364 (26), 2507–2516. doi:10.1056/nejmoa1103782
- Charoentong, P., Finotello, F., Angelova, M., Mayer, C., Efremova, M., Rieder, D., et al. (2017). Pan-cancer Immunogenomic Analyses Reveal Genotype-Immunophenotype Relationships and Predictors of Response to Checkpoint Blockade. *Cell Rep.* 18 (1), 248–262. doi:10.1016/j.celrep.2016.12.019
- Chesneau, M., Mai, H. L., Danger, R., Le Bot, S., Nguyen, T. V., Bernard, J., et al. (2020). Efficient Expansion of Human Granzyme B-Expressing B Cells with Potent Regulatory Properties. *J. Immunol.* 205 (9), 2391–2401. doi:10.4049/jimmunol.2000335
- Decaudin, D., Lepage, E., Brousse, N., Brice, P., Harousseau, J.-L., Belhadj, K., et al. (1999). Low-Grade Stage III-IV Follicular Lymphoma: Multivariate Analysis of Prognostic Factors in 484 Patients-A Study of the Groupe d'Etude des Lymphomes de l'Adulte. *Jco* 17 (8), 2499. doi:10.1200/jco.1999.17.8.2499

- Doll, K. M., Rademaker, A., and Sosa, J. A. (2018). Practical Guide to Surgical Data Sets: Surveillance, Epidemiology, and End Results (SEER) Database. *JAMA Surg.* 153 (6), 588–589. doi:10.1001/jamasurg.2018.0501
- Dong, P., Kaneuchi, M., Konno, Y., Watari, H., Sudo, S., and Sakuragi, N. (2013). Emerging Therapeutic Biomarkers in Endometrial Cancer. *Biomed. Res. Int.* 2013, 130362. doi:10.1155/2013/130362
- Dong, P., Xiong, Y., Yue, J., J B Hanley, S., Todo, Y., and Watari, H. (2019). Exploring lncRNA-Mediated Regulatory Networks in Endometrial Cancer Cells and the Tumor Microenvironment: Advances and Challenges. *Cancers (Basel)* 11 (2). doi:10.3390/cancers11020234
- Dong, Q., Li, F., Xu, Y., Xiao, J., Xu, Y., Shang, D., et al. (2020). RNAactDrug: a Comprehensive Database of RNAs Associated with Drug Sensitivity from Multi-Omics Data. *Brief. Bioinformatics* 21 (6), 2167–2174. doi:10.1093/bib/bbz142
- du Rusquec, P., de Calbiac, O., Robert, M., Campone, M., and Frenel, J. S. (2019). Clinical Utility of Pembrolizumab in the Management of Advanced Solid Tumors: an Evidence-Based Review on the Emerging New Data. *Cmar* 11, 4297–4312. doi:10.2147/cmar.s151023
- Erkanli, S., Kayaselcuk, F., Kuscü, E., Bagis, T., Bolat, F., Haberal, A., et al. (2006). Expression of Survivin, PTEN and P27 in normal, Hyperplastic, and Carcinomatous Endometrium. *Int. J. Gynecol. Cancer* 16 (3), 1412–1418. doi:10.1111/j.1525-1438.2006.00541.x
- Escherich, G., Richards, S., Richards, S., Stork, L. C., and Vora, A. J. (2011). Meta-analysis of Randomised Trials Comparing Thiopurines in Childhood Acute Lymphoblastic Leukaemia. *Leukemia* 25 (6), 953–959. doi:10.1038/leu.2011.37
- Evans, J. R., Feng, F. Y., and Chinnaiyan, A. M. (2016). The Bright Side of Dark Matter: lncRNAs in Cancer. *J. Clin. Invest.* 126 (8), 2775–2782. doi:10.1172/jci84421
- Fang, P., Xiang, L., Chen, W., Li, S., Huang, S., Li, J., et al. (2019). lncRNA GAS5 Enhanced the Killing Effect of NK Cell on Liver Cancer through Regulating miR-544/RUNX3. *Innate Immun.* 25 (2), 99–109. doi:10.1177/1753425919827632
- Feng, R.-M., Zong, Y.-N., Cao, S.-M., and Xu, R.-H. (2019). Current Cancer Situation in China: Good or Bad News from the 2018 Global Cancer Statistics? *Cancer Commun.* 39 (1), 22. doi:10.1186/s40880-019-0368-6
- Geraud, A., Mezquita, L., Auclin, E., Combarel, D., Delahousse, J., Gougis, P., et al. (2020). Chronic Plasma Exposure to Kinase Inhibitors in Patients with Oncogene-Addicted Non-small Cell Lung Cancer. *Cancers (Basel)* 12 (12). doi:10.3390/cancers12123758
- Gong, D., Feng, P.-C., Ke, X.-F., Kuang, H.-L., Pan, L.-L., Ye, Q., et al. (2020). Silencing Long Non-coding RNA LINC01224 Inhibits Hepatocellular Carcinoma Progression via MicroRNA-330-5p-Induced Inhibition of CHEK1. *Mol. Ther. - Nucleic Acids* 19, 482–497. doi:10.1016/j.omtn.2019.10.007
- Han, T., Wu, Y., Hu, X., Chen, Y., Jia, W., He, Q., et al. (2020). NORAD Orchestrates Endometrial Cancer Progression by Sequestering FUBP1 Nuclear Localization to Promote Cell Apoptosis. *Cell Death Dis* 11 (6), 473. doi:10.1038/s41419-020-2674-y
- Hauschild, A., Grob, J.-J., Demidov, L. V., Jouary, T., Gutzmer, R., Millward, M., et al. (2012). Dabrafenib in BRAF-Mutated Metastatic Melanoma: a Multicentre, Open-Label, Phase 3 Randomised Controlled Trial. *The Lancet* 380 (9839), 358–365. doi:10.1016/s0140-6736(12)60868-x
- Helm, O., Held-Feindt, J., Grage-Griebenow, E., Reiling, N., Ungefroren, H., Vogel, I., et al. (2014). Tumor-associated Macrophages Exhibit Pro- and Anti-inflammatory Properties by Which They Impact on Pancreatic Tumorigenesis. *Int. J. Cancer* 135 (4), 843–861. doi:10.1002/ijc.28736
- Hollis, R. L., Thomson, J. P., Stanley, B., Churchman, M., Meynert, A. M., Rye, T., et al. (2020). Molecular Stratification of Endometrioid Ovarian Carcinoma Predicts Clinical Outcome. *Nat. Commun.* 11 (1), 4995. doi:10.1038/s41467-020-18819-5
- Howitt, B. E., Shukla, S. A., Sholl, L. M., Ritterhouse, L. L., Watkins, J. C., Rodig, S., et al. (2015). Association of Polymerase E-Mutated and Microsatellite-Unstable Endometrial Cancers with Neoantigen Load, Number of Tumor-Infiltrating Lymphocytes, and Expression of PD-1 and PD-L1. *JAMA Oncol.* 1 (9), 1319–1323. doi:10.1001/jamaoncol.2015.2151
- Hu, Z., Mi, S., Zhao, T., Peng, C., Peng, Y., Chen, L., et al. (2020). BGL3 lncRNA Mediates Retention of the BRCA1/BARD1 Complex at DNA Damage Sites. *EMBO J.* 39 (12), e104133. doi:10.15252/embj.2019104133
- Intlekofer, A. M., and Thompson, C. B. (2013). At the Bench: Preclinical Rationale for CTLA-4 and PD-1 Blockade as Cancer Immunotherapy. *J. Leukoc. Biol.* 94 (1), 25–39. doi:10.1189/jlb.1212621
- Jachimowicz, R. D., Beleggia, F., Isensee, J., Velpula, B. B., Goergens, J., Bustos, M. A., et al. (2019). UBQLN4 Represses Homologous Recombination and Is Overexpressed in Aggressive Tumors. *Cell* 176 (3), 505–519. doi:10.1016/j.cell.2018.11.024
- Kaaks, R., Lukanova, A., and Kurzer, M. S. (2002). Obesity, Endogenous Hormones, and Endometrial Cancer Risk: a Synthetic Review. *Cancer Epidemiol. Biomarkers Prev.* 11 (12), 1531–1543. Available at <http://cebp.aacrjournals.org/content/11/12/1531>.
- Kandath, C., Kandath, C., Schultz, N., Cherniack, A. D., Akbani, R., Liu, Y., et al. (2013). Integrated Genomic Characterization of Endometrial Carcinoma. *Nature* 497 (7447), 67–73. doi:10.1038/nature12113
- Khanduja, J. S., Calvo, I. A., Joh, R. L., Hill, I. T., and Motamedi, M. (2016). Nuclear Noncoding RNAs and Genome Stability. *Mol. Cel.* 63 (1), 7–20. doi:10.1016/j.molcel.2016.06.011
- Le, D. T., Uram, J. N., Wang, H., Bartlett, B. R., Kemberling, H., Eyring, A. D., et al. (2015). PD-1 Blockade in Tumors with Mismatch-Repair Deficiency. *N. Engl. J. Med.* 372 (26), 2509–2520. doi:10.1056/nejmoa1500596
- Liu, H. (2016). Linking lncRNA to Genomic Stability. *Sci. China Life Sci.* 59 (3), 328–329. doi:10.1007/s11427-016-5009-6
- Liu, J., Tan, Z., He, J., Jin, T., Han, Y., Hu, L., et al. (2020). Identification of Three Molecular Subtypes Based on Immune Infiltration in Ovarian Cancer and its Prognostic Value. *Biosci. Rep.* 40 (10). doi:10.1042/BSR20201431
- Liu, J., Xu, W., Li, S., Sun, R., and Cheng, W. (2020). Multi-omics Analysis of Tumor Mutational burden Combined with Prognostic Assessment in Epithelial Ovarian Cancer Based on TCGA Database. *Int. J. Med. Sci.* 17 (18), 3200–3213. doi:10.7150/ijms.50491
- Liu, J., Zhou, S., Li, S., Jiang, Y., Wan, Y., Ma, X., et al. (2019). Eleven Genes Associated with Progression and Prognosis of Endometrial Cancer (EC) Identified by Comprehensive Bioinformatics Analysis. *Cancer Cell Int* 19, 136. doi:10.1186/s12935-019-0859-1
- Lugowska, I., Kosela-Paterczyk, H., Kozak, K., and Rutkowski, P. (2015). Trametinib: a MEK Inhibitor for Management of Metastatic Melanoma. *Onco Targets Ther.* 8, 2251–2259. doi:10.2147/OTT.S72951
- Magagnoli, M., Carlo-Stella, C., and Santoro, A. (2020). Copanlisib for the Treatment of Adults with Relapsed Follicular Lymphoma. *Expert Rev. Clin. Pharmacol.* 13 (8), 813–823. doi:10.1080/17512433.2020.1787829
- Makker, V., Rasco, D., Vogelzang, N. J., Brose, M. S., Cohn, A. L., Mier, J., et al. (2019). Lenvatinib Plus Pembrolizumab in Patients with Advanced Endometrial Cancer: an Interim Analysis of a Multicentre, Open-Label, Single-Arm, Phase 2 Trial. *Lancet Oncol.* 20 (5), 711–718. doi:10.1016/s1470-2045(19)30020-8
- Makker, V., Taylor, M. H., Aghajanian, C., Oaknin, A., Mier, J., Cohn, A. L., et al. (2020). Lenvatinib Plus Pembrolizumab in Patients with Advanced Endometrial Cancer. *Jco* 38 (26), 2981–2992. doi:10.1200/jco.19.02627
- Mayakonda, A., Lin, D.-C., Assenov, Y., Plass, C., and Koeffler, H. P. (2018). Maftools: Efficient and Comprehensive Analysis of Somatic Variants in Cancer. *Genome Res.* 28 (11), 1747–1756. doi:10.1101/gr.239244.118
- Morice, P., Leary, A., Creutzberg, C., Abu-Rustum, N., and Darai, E. (2016). Endometrial Cancer. *The Lancet* 387 (10023), 1094–1108. doi:10.1016/s0140-6736(15)00130-0
- Mutter, G. L., Lin, M. C., Fitzgerald, J. T., Kum, J. B., Baak, J. P., Lees, J. A., et al. (2000). Altered PTEN Expression as a Diagnostic Marker for the Earliest Endometrial Precancers. *J. Natl. Cancer Inst.* 92 (11), 924–930. doi:10.1093/jnci/92.11.924
- Negrini, S., Gorgoulis, V. G., and Halazonetis, T. D. (2010). Genomic Instability - an Evolving Hallmark of Cancer. *Nat. Rev. Mol. Cell Biol* 11 (3), 220–228. doi:10.1038/nrm2858
- Pakish, J. B., and Jazaeri, A. A. (2017). Immunotherapy in Gynecologic Cancers: Are We There yet? *Curr. Treat. Options. Oncol.* 18 (10), 59. doi:10.1007/s11864-017-0504-y
- Parslov, M., Lidegaard, O., Klintorp, S., Pedersen, B., Jønsson, L., Eriksen, P. S., et al. (2000). Risk Factors Among Young Women with Endometrial Cancer: a Danish Case-Control Study. *Am. J. Obstet. Gynecol.* 182 (1 Pt 1), 23–29. doi:10.1016/s0002-9378(00)70486-8
- Permuth, J. B., Chen, D.-T., Yoder, S. J., Li, J., Smith, A. T., Choi, J. W., et al. (2017). Linc-ing Circulating Long Non-coding RNAs to the Diagnosis and Malignant

- Prediction of Intraductal Papillary Mucinous Neoplasms of the Pancreas. *Sci. Rep.* 7 (1), 10484. doi:10.1038/s41598-017-09754-5
- Roskoski, R., Jr. (2020). Properties of FDA-Approved Small Molecule Protein Kinase Inhibitors: A 2020 Update. *Pharmacol. Res.* 152, 104609. doi:10.1016/j.phrs.2019.104609
- Salvesen, H. B., Haldorsen, I. S., and Trovik, J. (2012). Markers for Individualised Therapy in Endometrial Carcinoma. *Lancet Oncol.* 13 (8), e353–e361. doi:10.1016/s1470-2045(12)70213-9
- Siegel, R. L., Miller, K. D., and Jemal, A. (2020). Cancer Statistics, 2020. *CA A. Cancer J. Clin.* 70 (1), 7–30. doi:10.3322/caac.21590
- Song, C., Guo, Z., Yu, D., Wang, Y., Wang, Q., Dong, Z., et al. (2020). A Prognostic Nomogram Combining Immune-Related Gene Signature and Clinical Factors Predicts Survival in Patients with Lung Adenocarcinoma. *Front. Oncol.* 10, 1300. doi:10.3389/fonc.2020.01300
- Song, P., Jiang, B., Liu, Z., Ding, J., Liu, S., and Guan, W. (2017). A Three-lncRNA Expression Signature Associated with the Prognosis of Gastric Cancer Patients. *Cancer Med.* 6 (6), 1154–1164. doi:10.1002/cam4.1047
- Soslow, R. A. (2013). High-grade Endometrial Carcinomas - Strategies for Typing. *Histopathology* 62 (1), 89–110. doi:10.1111/his.12029
- Swerdlow, S. H., Campo, E., Pileri, S. A., Harris, N. L., Stein, H., Siebert, R., et al. (2016). The 2016 Revision of the World Health Organization Classification of Lymphoid Neoplasms. *Blood* 127 (20), 2375–2390. doi:10.1182/blood-2016-01-643569
- Tang, H., Wu, Z., Zhang, Y., Xia, T., Liu, D., Cai, J., et al. (2019). Identification and Function Analysis of a Five-Long Noncoding RNA Prognostic Signature for Endometrial Cancer Patients. *DNA Cel. Biol.* 38 (12), 1480–1498. doi:10.1089/dna.2019.4944
- Tekin, C., Abersson, H. L., Bijlsma, M. F., and Spek, C. A. (2020). Early Macrophage Infiltrates Impair Pancreatic Cancer Cell Growth by TNF- α Secretion. *BMC cancer* 20 (1), 1183. doi:10.1186/s12885-020-07697-1
- Wang, L., Piskorz, A., Bosse, T., Jimenez-Linan, M., Rous, B., Gilks, C. B., et al. (2021). Immunohistochemistry and Next-Generation Sequencing Are Complementary Tests in Identifying PTEN Abnormality in Endometrial Carcinoma Biopsies. *Int. J. Gynecol. Pathol.* 41, 12–19. doi:10.1097/pgp.0000000000000763
- Wang, L., Simons, D. L., Lu, X., Tu, T. Y., Avalos, C., Chang, A. Y., et al. (2020). Breast Cancer Induces Systemic Immune Changes on Cytokine Signaling in Peripheral Blood Monocytes and Lymphocytes. *EBioMedicine* 52, 102631. doi:10.1016/j.ebiom.2020.102631
- Wang, Y., Liu, Y., Guan, Y., Li, H., Liu, Y., Zhang, M., et al. (2020). Integrated Analysis of Immune-Related Genes in Endometrial Carcinoma. *Cancer Cell Int* 20, 477. doi:10.1186/s12935-020-01572-6
- Xie, Y., Zhang, Y., Du, L., Jiang, X., Yan, S., Duan, W., et al. (2018). Circulating Long Noncoding RNA Act as Potential Novel Biomarkers for Diagnosis and Prognosis of Non-small Cell Lung Cancer. *Mol. Oncol.* 12 (5), 648–658. doi:10.1002/1878-0261.12188
- Xing, S., Zhang, Y., and Zhang, J. (2020). LINC01224 Exhibits Cancer-Promoting Activity in Epithelial Ovarian Cancer through microRNA-485-5p-Mediated PAK4 Upregulation. *Ott* 13, 5643–5655. doi:10.2147/ott.s254662
- Yi, L., Huang, P., Zou, X., Guo, L., Gu, Y., Wen, C., et al. (2020). Integrative Stemness Characteristics Associated with Prognosis and the Immune Microenvironment in Esophageal Cancer. *Pharmacol. Res.* 161, 105144. doi:10.1016/j.phrs.2020.105144
- Yoshihara, K., Shahmoradgoli, M., Martínez, E., Vegesna, R., Kim, H., Torres-Garcia, W., et al. (2013). Inferring Tumour Purity and Stromal and Immune Cell Admixture from Expression Data. *Nat. Commun.* 4, 2612. doi:10.1038/ncomms3612
- Yu, G., Wang, L.-G., Han, Y., and He, Q.-Y. (2012). clusterProfiler: an R Package for Comparing Biological Themes Among Gene Clusters. *OMICS: A J. Integr. Biol.* 16 (5), 284–287. doi:10.1089/omi.2011.0118
- Zhao, H., Thienpont, B., Yesilyurt, B. T., Moisse, M., Reumers, J., Coenegrachts, L., et al. (2014). Mismatch Repair Deficiency Endows Tumors with a Unique Mutation Signature and Sensitivity to DNA Double-Strand Breaks. *eLife* 3, e02725. doi:10.7554/eLife.02725
- Zheng, X., Zhang, J., Fang, T., Wang, X., Wang, S., Ma, Z., et al. (2020). The Long Non-coding RNA PIK3CD-AS2 Promotes Lung Adenocarcinoma Progression via YBX1-Mediated Suppression of P53 Pathway. *Oncogenesis* 9 (3), 34. doi:10.1038/s41389-020-0217-0
- Zhu, X., Tian, X., Yu, C., Shen, C., Yan, T., Hong, J., et al. (2016). A Long Non-coding RNA Signature to Improve Prognosis Prediction of Gastric Cancer. *Mol. Cancer* 15 (1), 60. doi:10.1186/s12943-016-0544-0

Conflict of Interest: The authors declare that the research was conducted in the absence of any commercial or financial relationships that could be construed as a potential conflict of interest.

Publisher's Note: All claims expressed in this article are solely those of the authors and do not necessarily represent those of their affiliated organizations or those of the publisher, the editors, and the reviewers. Any product that may be evaluated in this article, or claim that may be made by its manufacturer, is not guaranteed or endorsed by the publisher.

Copyright © 2022 Liu, Cui, Ye, Wang, Wang and Bai. This is an open-access article distributed under the terms of the Creative Commons Attribution License (CC BY). The use, distribution or reproduction in other forums is permitted, provided the original author(s) and the copyright owner(s) are credited and that the original publication in this journal is cited, in accordance with accepted academic practice. No use, distribution or reproduction is permitted which does not comply with these terms.



miR-874: An Important Regulator in Human Diseases

Qiudan Zhang^{1,2}, Chenming Zhong², Qianqian Yan², Ling-hui Zeng¹, Wei Gao^{1*} and Shiwei Duan^{1,2*}

¹School of Medicine, Zhejiang University City College, Hangzhou, China, ²Medical Genetics Center, School of Medicine, Ningbo University, Ningbo, China

OPEN ACCESS

Edited by:

Zong Sheng Guo,
Roswell Park Comprehensive Cancer
Center, United States

Reviewed by:

Mario Cioce,
Campus Bio-Medico University, Italy
Apollonia Tullo,
National Research Council, Italy

*Correspondence:

Wei Gao
weig@zucc.edu.cn
Shiwei Duan
duansw@zucc.edu.cn

Specialty section:

This article was submitted to
Molecular and Cellular Oncology,
a section of the journal
Frontiers in Cell and Developmental
Biology

Received: 28 September 2021

Accepted: 23 March 2022

Published: 06 April 2022

Citation:

Zhang Q, Zhong C, Yan Q, Zeng L-h,
Gao W and Duan S (2022) miR-874: An
Important Regulator in Human Diseases.
Front. Cell Dev. Biol. 10:784968.
doi: 10.3389/fcell.2022.784968

miR-874 is located at 5q31.2, which is frequently deleted in cancer. miR-874 is downregulated in 22 types of cancers and aberrantly expressed in 18 types of non-cancer diseases. The dysfunction of miR-874 is not only closely related to the diagnosis and prognosis of tumor patients but also plays an important role in the efficacy of tumor chemotherapy drugs. miR-874 participates in the ceRNA network of long non-coding RNAs or circular RNAs, which is closely related to the occurrence and development of cancer and other non-cancer diseases. In addition, miR-874 is also involved in the regulation of multiple signaling pathways, including the Wnt/ β -catenin signaling pathway, Hippo signaling pathway, PI3K/AKT signaling pathway, JAK/STAT signaling pathway, and Hedgehog signaling pathway. This review summarizes the molecular functions of miR-874 in the biological processes of tumor cell survival, apoptosis, differentiation, and tumorigenesis, and reveal the value of miR-874 as a cancer biomarker in tumor diagnosis and prognosis. Future work is necessary to explore the potential clinical application of miR-874 in chemotherapy resistance.

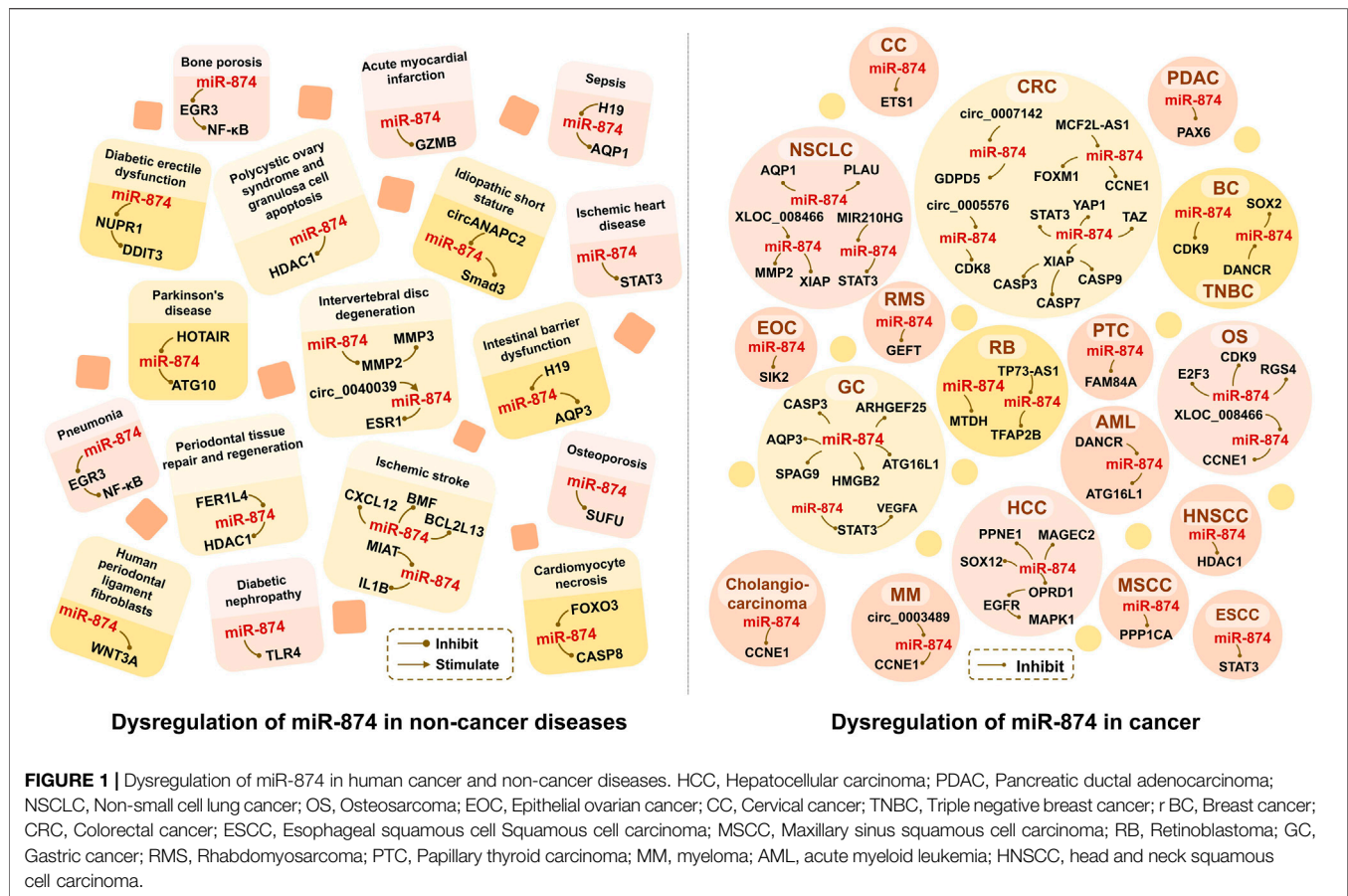
Keywords: miR-874, cancer, tumor suppressor, non-cancer, diagnosis, prognosis, ceRNA, pathway

BACKGROUND

MicroRNA (miRNA) is a short RNA of 19–25 nucleotides in length that can regulate the post-transcriptional silencing of target genes. A single miRNA can target hundreds of mRNAs, thereby affecting the signal transduction of multiple pathways (Lu and Rothenberg, 2018). miRNA expression profiling shows that abnormal miRNA expression is related to the occurrence and progression of tumors and the response to anticancer drugs (Iorio and Croce, 2017). In addition, almost all developmental, physiological, and disease-related processes seem to be linked to miRNAs (Sun and Lai, 2013).

microRNA-874 (miR-874) is a new anti-cancer miRNA (Zhang et al., 2018b). It was originally obtained by sequencing a small RNA library (Song et al., 2016) and was first characterized in normal human cervical tissue samples (Xia et al., 2018). miR-874 is located on chromosome 5q31.2 that is often deleted in cancer (Zhang et al., 2018b). There are many target genes of miR-874 (Figure 1). By inhibiting the expression of these target genes, miR-874 is widely involved in cell proliferation, apoptosis, invasion, migration, cell cycle, epithelial-mesenchymal transition (EMT), and other cellular processes.

Since there is no comprehensive introduction of miR-874, this work summarizes the abnormal expression of miR-874 in cancer and non-cancerous diseases, and outlines the molecular mechanisms between it and protein-coding genes and non-coding RNAs.



THE ABERRANT EXPRESSION OF MIR-874 IN HUMAN DISEASES

As shown in **Table 1**, miR-874 is downregulated in at least 22 human malignancies, such as colorectal cancer (CRC) (Huang et al., 2020a; Yu et al., 2020; Que et al., 2017; Zhao and Dong, 2016; Han et al., 2016; Wang et al., 2021; Zhang et al., 2021c), gastric cancer (GC) (Huang et al., 2018; Sun et al., 2020; Yuan et al., 2020; Liu et al., 2017; Zhang et al., 2015; Jiang et al., 2014), hepatocellular carcinoma (HCC) (Zhang et al., 2018b; Jiang et al., 2017; Leong et al., 2017; Song et al., 2016), esophageal squamous cell carcinoma (ESCC) (Yuan et al., 2018), pancreatic ductal adenocarcinoma (PDAC) (Diao et al., 2018), non-small cell lung cancer (NSCLC) (Bu et al., 2020; Yang et al., 2017; Ahmad et al., 2015; Kesanakurti et al., 2013; Wang et al., 2020b), osteosarcoma (OS) (Tang et al., 2018; Liu et al., 2020; Dong et al., 2016; Ghosh et al., 2017), epithelial ovarian cancer (EOC) (Xia et al., 2018) cervical cancer (CC) (Liao et al., 2018; Liu et al., 2021a), retinoblastoma (RB) (Zhang et al., 2018a; Wang et al., 2020a), prostate cancer (PCa) (Pashaei et al., 2017) maxillary sinus squamous cell carcinoma (MSCC) (Nohata et al., 2011), breast cancer (BC) (Li et al., 2020; Zhang et al., 2017; Wang et al., 2014), triple-negative breast cancer (TNBC) (Wu et al., 2020), rhabdomyosarcoma (RMS) (Shang et al., 2019), papillary thyroid carcinoma (PTC) (Ding et al., 2021),

endometrial cancer (Witek et al., 2021), cholangiocarcinoma (Pan et al., 2021), glioma (Li et al., 2021a), myeloma (MM) (Tian et al., 2021), head and neck squamous cell carcinoma (HNSCC) (Nohata et al., 2013) and acute myeloid leukemia (AML) (Zhang et al., 2021a).

HNSCC is the sixth most common cancer in the world (Nohata et al., 2013). The expression of miR-874-3p is reduced in HNSCC, and miR-874-3p can be upregulated after 5-Aza-dC treatment, indicating that the downregulation of miR-874-3p in HNSCC may be due to the methylation of its upstream CpG island (Nohata et al., 2013). Histone deacetylase 1 (HDAC1) belongs to the HDAC family. HDAC removes acetyl groups from histones and other nuclear proteins that induce chromatin condensation and transcriptional inhibition. HDAC plays an important role in the abnormal epigenetic changes associated with human cancer (Witt et al., 2009). In HNSCC, miR-874-3p can directly target HDAC1, significantly inhibit cell proliferation, and induce cell cycle arrest and apoptosis (Nohata et al., 2013).

Also, miR-874 plays an important role in non-cancer diseases. Low expression of miR-874 is associated with the risk of ischemic stroke (IS) (Jiang et al., 2019; Xie et al., 2020; Zhang et al., 2021b), ischemic heart disease (IHD) (Chen et al., 2019), cardiomyocyte necrosis (Wang et al., 2013), diabetic erectile dysfunction (DMED) (Huo et al., 2020), diabetic nephropathy (DN) (Yao et al., 2018), sepsis (Fang et al.,

TABLE 1 | The role of miR-874 in various cancers.

Cancer Type	The expression of miR-874	Effect <i>in vivo</i>	Effect <i>in vitro</i>	Regulatory mechanism	References
CRC	downregulation	tumor growth↓	proliferation↓, apoptosis↑	circ_0007142/miR-874-3p/GDPD5	Wang et al. (2021)
	downregulation	tumor growth↓	proliferation↓, migration↓, invasion↓	lncRNA MCF2L-AS1/miRNA-874-3p/FOXO1	Zhang et al. (2021c)
	downregulation	tumor growth↓	proliferation↓, migration ↓, invasion↓, EMT↓	lncRNA MCF2L-AS1/miRNA-874-3p/CCNE1	Huang et al. (2020a)
	downregulation	tumor growth↓	proliferation↓, apoptosis↑	circ_0005576/miRNA-874-3p/CDK8/Wnt/β-catenin	Yu et al. (2020)
	downregulation	tumor growth↓	chemosensitivity↓	miR-874-3p/YAP1, TAZ/Hippo signaling	Que et al. (2017)
	downregulation	tumor growth↓	cell growth↓, apoptosis↑	miR-874-3p/STAT3	Zhao and Dong, (2016)
	downregulation	tumor growth↓	proliferation↓, colony formation↓, apoptosis↑, chemosensitivity↓	miR-874-3p/XIAP/CASP3, CASP7, CASP9/5-FU	Han et al. (2016)
GC	downregulation	prognosis↑	autophagy↓, chemosensitivity↓	miR-874-3p/ATG16L1	Huang et al. (2018)
	downregulation	tumor growth↓	proliferation↓, apoptosis↑	miR-874-3p/SPAG9	Sun et al. (2020)
	downregulation	tumor growth↓	proliferation↓, migration↓, invasion↓, EMT↓	IIA (TSN)/miR-874-3p/HMGB2/Wnt/β-catenin	Yuan et al. (2020)
	downregulation	tumor growth ↓	migration ↓, invasion↓, proliferation↓, angiogenesis↓	miR-874/ARHGEF25	Huang et al. (2018)
	downregulation	tumor growth↓	tube formation↓, proliferation↓, migration↓, invasion↓	miR-874-3p/STAT3/VEGFA	Zhang et al. (2015)
HCC	downregulation	tumor growth↓	proliferation↓, colony formation↓, migration↓, invasion↓	miR-874-3p/CASP3, AQP3	Jiang et al. (2014)
	downregulation	tumor growth↓	proliferation↓, migration↓, invasion↓, EMT↓	miR-874/OPRD1/EGFR/MAPK1 cagga	Zhang et al. (2018b)
	downregulation	tumor growth↓	migration↓, invasion↓, EMT↓	miR-874-3p/SOX12	Jiang et al. (2017)
	downregulation	tumour growth↓	cell growth ↓, colony formation↓, apoptosis↑	miR-874-3p/PPNE1	Leong et al. (2017)
	downregulation	tumor growth ↓	proliferation↓, invasion↓	miR-874-3p/MAGEC2	Song et al. (2016)
ESCC	downregulation	tumor growth↓	proliferation↓, migration↓, invasion↓	miR-874-3p/STAT3	Yuan et al. (2018)
PDAC NSCLC	downregulation	tumor growth↓	proliferation↓, migration↓, invasion↓	miR-874-3p/PAX6	Diao et al. (2018)
	downregulation	tumor growth↓	proliferation↓, migration↓, invasion↓, EMT↓	miR-874-3p/AQP1	Wang et al. (2020b)
		xenograft growth↓	proliferation↓, migration↓, invasion↓	MIR210HG/miRNA-874-3p/STAT3	Bu et al. (2020)
	downregulation	tumor growth↓	proliferation ↓, invasion↓, apoptosis↑	lncRNA XLOC_008466/miR-874-3p/MMP2, XIAP	Yang et al. (2017)
	downregulation	invasion↓		CDF/miR-874/MMP2 25901198	Ahmad et al. (2015)
OS	downregulation	tumor growth ↓	invasion↓, de-differentiation↑, migration↓	miR-874-3p/MMP2, PLAU	Kesanakurti et al. (2013)
	downregulation	tumor growth↓	proliferation↓, migration↓, invasion↓	miR-874-3p/CDK9	Tang et al. (2018)
	downregulation	tumor growth↓	proliferation↓, migration↓, invasion↓	miR-874-3p/RGS4	Liu et al. (2020)
	downregulation	tumor growth ↓	proliferation↓, apoptosis↑, migration↓, invasion↓	miR-874-3p/E2F3	Dong et al. (2016)
	downregulation	tumor growth↓	invasion↓, migration↓	lncRNA XLOC_008466/miR-874-3p/CCNE1	Ghosh et al. (2017)
EOC	downregulation	tumor growth↓	colony formation↓, apoptosis↑, paclitaxel sensitivity↑, migration↓, invasion↓, chemoresistance↓	miR-874-3p, miR-874-5p/SIK2	Xia et al. (2018)
CC	downregulation	tumor growth↓	proliferation↓, migration↓, invasion↓	miR-874/ETS1	Liu et al. (2021a)
PCa	downregulation	tumor growth↓	proliferation↓, apoptosis↑, migration↓, invasion↓		Liao et al. (2018)
TNBC	downregulation	tumor growth↓	proliferation↓, migration↓, invasion↓, EMT↓	lncRNA DANCR/miRNA-874-3p/SOX2	Pashaei et al. (2017)
BC	downregulation	tumor growth↓			Wu et al. (2020)
					Zhang et al. (2017)

(Continued on following page)

TABLE 1 | (Continued) The role of miR-874 in various cancers.

Cancer Type	The expression of miR-874	Effect <i>in vivo</i>	Effect <i>in vitro</i>	Regulatory mechanism	References
	downregulation	tumor growth↓	proliferation↓, apoptosis↑, cell cycle↓	miR-874/CDK9	Wang et al. (2014)
HNSCC	downregulation	tumor growth↓	proliferation↓, cell cycle↓, apoptosis↑	miR-874-3p/HDAC1	Nohata et al. (2013)
MSCC	downregulation	tumor growth↓	proliferation↓, invasion↓	miR-874-3p/PPP1CA	Nohata et al. (2011)
RB	downregulation	tumor growth↓	proliferation↓, migration↓, invasion↓, apoptosis↑	miR-874-3p/MTDH	Zhang et al. (2018a)
	downregulation	tumor growth↓	proliferation↓, migration↓, invasion↓, EMT↓	lncRNA TP73-AS1/miRNA-874-3p/TFAP2B/Wnt/β-catenin	Wang et al. (2020a)
RMS	downregulation	tumor growth↓	migration↓, invasion↓, apoptosis↑	miR-874-3p/GEFT	Shang et al. (2019)
Glioma	downregulation	tumor growth↓	proliferation↓, migration ↓, invasion↓		Li et al. (2021a)
Cholangiocarcinoma	downregulation	tumor growth↓	migration↓, invasion↓, EMT↓	miR-874-3p/CCNE1/NF-κB signaling pathway	Pan et al. (2021)
MM	downregulation	tumor growth↓	viability↓, proliferation↓, autophagy↓, apoptosis↑	circ_0003489/miR-874-3p/HDAC1	Tian et al. (2021)
PTC	downregulation	tumor growth↓	proliferation↓, migration↓, invasion↓, apoptosis↑, EMT↓	miR-874-3p/FAM84A/Wnt/β-catenin	Ding et al. (2021)
Endometrial cancer	downregulation	tumor growth↓	cell cycle↓		Witek et al. (2021)
AML	downregulation	tumor growth↓	autophagy↑	lncRNA DANCER/miR-874-3p/ATG16L1	Zhang et al. (2021a)

HCC, Hepatocellular carcinoma; PDAC, Pancreatic ductal adenocarcinoma; NSCLC, Non-small cell lung cancer; OS, Osteosarcoma; EOC, Epithelial ovarian cancer; CC, Cervical cancer; PCa, Prostate cancer; TNBC, Triple negative breast cancer; BC, Breast cancer; CRC, Colorectal cancer; ESCC, Esophageal squamous cell carcinoma; MSCC, Maxillary sinus squamous cell carcinoma; RB, Retinoblastoma; GC, Gastric cancer; RMS, Rhabdomyosarcoma; PTC, Papillary thyroid carcinoma; MM, myeloma; AML, acute myeloid leukemia; HNSCC, head and neck squamous cell carcinoma; CDF, Novel difluorobenzylidene analogue of curcumin; TSN, Tanshinone IIA; EMT, epithelial-mesenchymal transition.

2018), osteoporosis (Lin et al., 2018), Parkinson's disease (PD) (Zhao et al., 2020), acute myocardial infarction (AMI) (Yan et al., 2017), intestinal barrier dysfunction (Su et al., 2016), periodontal tissue repair and regeneration (Huang et al., 2020b), idiopathic short stature (ISS) (Liu et al., 2021b), intervertebral disc degeneration (IDD) (Song et al., 2021a), pneumonia (Yang et al., 2021), and human periodontal ligament fibroblasts (Song et al., 2021b) (Table 2).

Highly expressed miR-874-3p is associated with the risk of bone porous (Kushwaha et al., 2016) and polycystic ovary syndrome (PCOS) (Wei et al., 2021), IDD (Li et al., 2021b). miR-874-3p in maternal osteoblasts increased 4–6 times during the child's weaning period. Increasing the expression of miR-874-3p could enhance bone formation and restore the mother's bone quality after pregnancy and lactation (Kushwaha et al., 2016). In granulosa cells, testosterone promotes p53 acetylation and expression by upregulating the expression of miR-874-3p and induces granulosa cell apoptosis (Wei et al., 2021), thereby promoting the occurrence and development of PCOS (Wei et al., 2021) (Table 2).

However, the results of the association between miR-874-3p expression and IDD are divergent. The expression level of miR-874-3p in the NP tissues of IDD patients was significantly reduced, thereby upregulating the expression of MMP2 and MMP3, eventually leading to the occurrence of IDD (Song et al., 2021a). In nucleus pulposus cells (NPCs), circ_0040039

can increase the stability of miR-874-3p and upregulate the miR-874-3p/ESR1 pathway to aggravate IDD (Li et al., 2021b). The different effects of miR-874-3p in IDD may be related to the tested sample types. It is worth noting that the sample size of IDD-related studies is small, and there is a lack of follow-up experiments to further explore the *in vivo* function of miR-874-3p. In the future, more samples and *in vivo* experiments are needed to confirm the mechanism of miR-874-3p in IDD.

THE EFFECT OF MIR-874 ON PROGNOSIS AND CHEMORESISTANCE

In patients of HCC, OS, or RMS, decreased expression of miR-874 is associated with tumor size, vascular infiltration, lymph node metastasis, tumor-node-metastasis (TNM) staging, clinical staging, and tumor differentiation (Dong et al., 2016; Zhang et al., 2018b; Shang et al., 2019). Subsequent cell function experiments revealed the tumor suppressor effects of miR-874, including inhibition of proliferation, invasion, metastasis, and promotion of apoptosis (Diao et al., 2018) (Table 3).

As shown in Table 3, compared with cancer patients with high miR-874 expression, patients with low miR-874 expression have a significantly worse prognosis. These cancers include GC (Huang et al., 2018), CRC (Han et al., 2016), HCC (Zhang et al., 2018b), ESCC (Yuan et al., 2018),

TABLE 2 | The role of miR-874 in human non-cancer diseases.

Non-cancer Type	The expression of miR-874	Effect <i>in vivo</i>	Effect <i>in vitro</i>	Regulatory mechanism	References
Ischemic stroke	downregulation	cerebral I/R injury↓	proliferation↑, apoptosis↓	miR-874-3p/BMF, BCL2L13	Jiang et al. (2019)
	downregulation		apoptosis↑	MIAT/miR-874-3p/IL1B	Zhang et al. (2021b)
	downregulation	angiogenesis↑, inflammatory factor release↓	apoptosis↓	miR-874-3p/CXCL12/Wnt/β-catenin	Xie et al. (2020)
Ischemic heart disease	downregulation	cardiac function↓	apoptosis↑	miR-874-3p/STAT3	Chen et al. (2019)
Cardiomyocyte necrosis	downregulation		apoptosis↑, necrosis↑	FOXO3/miR-874/CASP8	Wang et al. (2013)
Diabetic nephropathy	downregulation	inflammatory cytokines expression↓	proliferation↑, apoptosis↓	miR-874-3p/TLR4	Yao et al. (2018)
Diabetic erectile dysfunction	downregulation	erectile dysfunction↓	apoptosis↓	miR-874-3p/NUPR1/DDIT3	Huo et al. (2020)
Sepsis	downregulation	sepsis↓		lncRNA H19/miR-874/AQP1	Fang et al. (2018)
Periodontal tissue repair and regeneration				lncRNA FER1L4/miR-874-3p/VEGFA	Huang et al. (2020b)
Osteoporosis	downregulation		proliferation↑, apoptosis↓, osteoblasts in S phase↑, ALP activity↑, calcium nodules↑	miR-874-3p/SUFU/Hedgehog pathway	Lin et al. (2018)
Parkinson's disease	downregulation		MPP + -induced neuronal injury↓	lncRNA HOTAIR/miR-874-5p/ATG10	Zhao et al. (2020)
Bone porosis	upregulation	osteoblast differentiation↑, mineralization↑		miR-874-3p/HDAC1/RUNX2	Kushwaha et al. (2016)
Acute myocardial infarction	downregulation		apoptosis↑	miR-874-3p/GZMB	Yan et al. (2017)
Intestinal barrier dysfunction	downregulation			lncRNA H19/miR-874-3p/AQP3	Su et al. (2016)
Intervertebral disc degeneration	downregulation			miR-874-3p/MMP2/MMP3	Song et al. (2021a)
	upregulation		proliferation↓, apoptosis↑	circ_0040039/miR-874-3p/ESR1	Li et al. (2021b)
Polycystic ovary syndrome and granulosa cell apoptosis	upregulation		apoptosis↑	miR-874-3p/HDAC1/p53 axis	Wei et al. (2021)
Idiopathic short stature	downregulation		proliferation↓, cell cycle↓	circANAPC2/miR-874-3p/Smad3	Liu et al. (2021b)
Human periodontal ligament fibroblasts	downregulation		differentiation↑	miR-874-3p/WNT3A, WNT/β-catenin	Song et al. (2021b)
Pneumonia	downregulation		apoptosis↓	miR-874-3p/EGR3/NF-κB	Yang et al. (2021)

I/R, *ischaemia/reperfusion*; ALP, *Alkaline phosphatase*.

NSCLC (Li et al., 2020), CC (Liao et al., 2018), BC (Zhang et al., 2017), RB (Wang et al., 2020a), and glioma (45).

In GC, CRC, NSCLC, and EOC, miR-874 can reduce the drug resistance of cancer cells (Huang et al., 2018; Han et al., 2016; Que et al., 2017; Bu et al., 2020; Xia et al., 2018). Among them, the upregulation of miR-874 expression in CRC cells can increase the sensitivity to 5-FU (Han et al., 2016; Que et al., 2017). The overexpression of miR-874 significantly enhanced the sensitivity of GC cells to DDP, VCR, and 5-FU (Huang et al., 2018). The MIR210HG/miR-874/STAT3 axis plays a carcinogenic regulatory role in the radiosensitivity and drug resistance of NSCLC (Bu et al., 2020). miR-874-3p and miR-874-5p can enhance the chemical sensitivity of EOC cells (Xia et al., 2018).

Cancer cells use autophagy to provide energy and develop resistance to anti-cancer drugs; therefore, inhibiting

autophagy may promote cancer cell death and help overcome drug resistance (Levy et al., 2017). Autophagy involved in miR-874-3p is an important mechanism for regulating chemotherapy resistance in AML (Zhang et al., 2021a). In AML, the DANCER/miR-874-3p/ATG16L1 axis can promote autophagy, thereby enhancing the resistance of human AML cells to Ara-C (Zhang et al., 2021a). In addition, knocking out circ_0003489 can upregulate miR-874-3p and inhibit HDAC1, thereby prompting MM cells to switch from autophagy to apoptosis, and reducing the growth of MM cells (Tian et al., 2021).

The above findings indicate that miR-874 can be developed as a new diagnostic and prognostic biomarker for patients with the above cancer types and suggest a potential value of miR-874 in cancer drug resistance.

TABLE 3 | The contribution of miR-874 to the treatment, clinicopathological characteristics, and prognosis in cancer.

Cancer Type	Sample size	Expression pattern of miR-874	Radiosensitivity/Chemoresistance	Clinicopathological characteristics/Prognostic value	References
GC	50 paired tissues	downregulation	DDP, VCR, 5-FU	prognostic factor of OS	Huang et al. (2018)
CRC	32 paired tissues	downregulation	5-FU	prognostic factor of OS correlated with lymph node metastasis and TNM stage	Han et al. (2016)
	20 paired tissues	downregulation	5-FU		Que et al. (2017)
HCC	120 paired tissues	downregulation		prognostic factor of OS and RFS correlated with tumour size, vascular invasion, TNM stage, tumour differentiation and inferior patient outcomes	Zhang et al. (2018b)
ESCC	121 paired tissues	downregulation		independent prognostic factor of OS	Yuan et al. (2018)
NSCLC	32 paired tissues	downregulation	Radiosensitivity, chemoresistance		Bu et al. (2020)
	49 paired tissues	downregulation		prognostic factor of OS	Li et al. (2020)
PDAC	29 paired tissues	downregulation		correlated with TNM stage, tumor size, and lymph node metastasis	Diao et al. (2018)
OS	40 paired tissues	downregulation		correlated with TNM stage, tumor size, and lymph node metastasis	Dong et al. (2016)
EOC	20 paired tissues	downregulation	chemoresistance		Xia et al. (2018)
CC	49 paired tissues	downregulation		prognostic factor of OS correlated with tumour differentiation and lymph node metastasis	Liao et al. (2018)
BC	26 paired tissues	downregulation		correlated with pathological differentiation and tumor size	Wang et al. (2014)
	47 paired tissues	downregulation		prognostic factor of OS correlated with pathological differentiation, TNM staging and lymph node metastasis	Zhang et al. (2017)
RB	26 paired tissues	downregulation		correlated with tumor stage	Zhang et al. (2018a)
	50 paired tissues	downregulation		prognostic factor of OS correlated with different clinicopathological stage	Wang et al. (2020a)
RMS	10 paired tissues	downregulation		correlated with the advanced clinical stage, lymph node metastasis, and distant metastasis of RMS	Shang et al. (2019)
AML	HL60, U937, and KG1a	downregulation	Ara-C		Zhang et al. (2021a)
MM	MM1.R	downregulation	BTZ		Tian et al. (2021)
Glioma	105 paired tissues	downregulation		independent prognostic factor for OS correlated with tumor size, KPS score, and TNM stage	Li et al. (2021a)

GC, Gastric cancer; CRC, Colorectal cancer; HCC, Hepatocellular carcinoma; ESCC, Esophageal squamous cell Squamous cell carcinoma; NSCLC, Non-small cell lung cancer; PDAC, Pancreatic ductal adenocarcinoma; OS, Osteosarcoma; EOC, Epithelial ovarian cancer; CC, Cervical cancer; r BC, Breast cancer; RB, Retinoblastoma; RMS, Rhabdomyosarcoma; MM, myeloma; AML, acute myeloid leukemia; TNM, Tumor node metastasis; OS, Overall survival rate; RFS, Recurrence free survival.

THE CERNA NETWORK CENTERED ON MIR-874

Non-coding RNA can regulate gene expression, thereby affecting cell proliferation, survival, and migration, and is related to genome stability and malignant transformation of inflammatory cells (Zhang et al., 2021a). There are interactions between non-coding RNAs. For example, lncRNAs and circRNAs can be used as ceRNAs to sponge miRNAs (Zhang et al., 2021a). The ceRNA network centered on miR-874 is involved with at least 10 lncRNAs or 12 circRNAs. The dysfunction of miR-874 is closely related to the occurrence and development of tumors and other diseases (Figure 2).

In TNBC, lncRNA DANCER acts as a ceRNA for miR-874-3p, thereby regulating the derepression of SOX2 and promoting the EMT in TNBC (Wu et al., 2020). In CRC,

the MCF2LAS1/miR-874-3p/FOXO1 axis (Liao et al., 2018) and MCF2LAS1/miR-874-3p/CCNE1 axis (Huang et al., 2020a) can promote cancer cell apoptosis, inhibit cancer cell proliferation, invasion, migration and EMT process. Also, the circ_0005576/miR-874/CDK8 axis can promote the malignant progression of CRC (Yu et al., 2020). In CRC cells, circ_0007142 can regulate the level of GSDME by sponging miR-874-3p (12). Knock-down of circ_0007142 can induce ferroptosis through the circ_0007142/miR-874-3p/GSDME axis, thereby increasing the effectiveness of chemotherapy or radiotherapy and inhibiting the malignant progression of CRC (Wang et al., 2021). In RB, the expression of lncRNA TP73-AS1 is upregulated, and the downregulated TP73-AS1/miR-874-3p/TFAP2B axis can inhibit the Wnt/ β -catenin signaling pathway, thereby inhibiting tumor progression (Wang et al., 2020a). In NSCLC, the

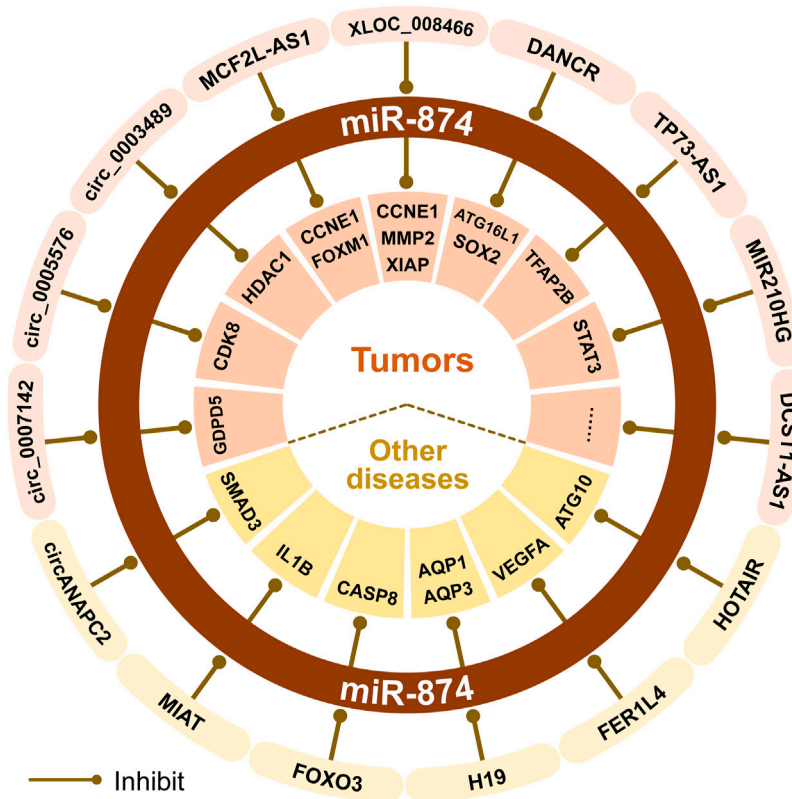


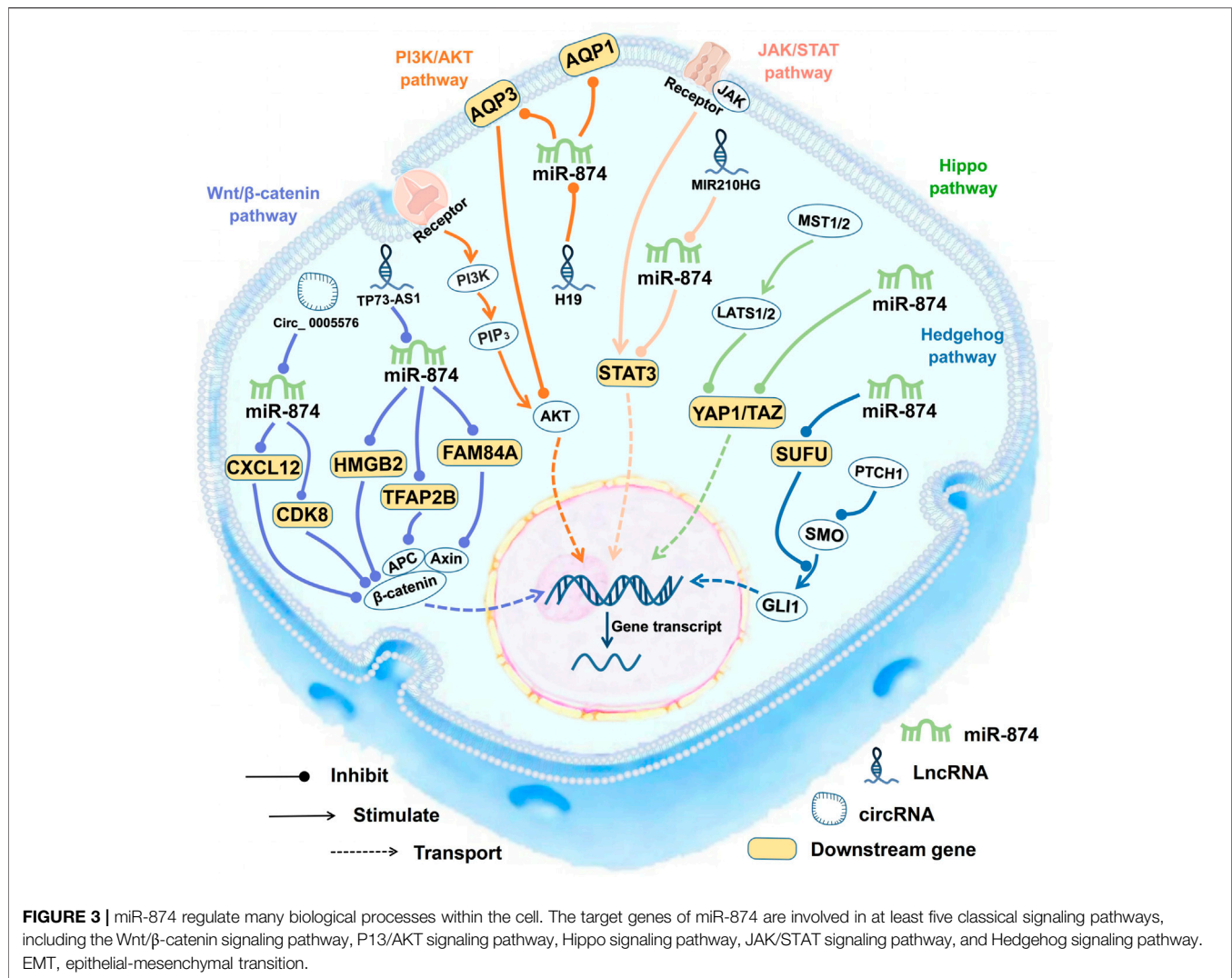
FIGURE 2 | The ceRNA mechanisms of miR-874 in cancer and other non-cancer diseases.

miR210HG/miR-874-3p/STAT3 axis plays a role in the progression of NSCLC cells (Bu et al., 2020). Besides, XLOC_008466, as the ceRNA of miR-874-3p, can increase the expression of MMP2 and XIAP and affect NSCLC cell proliferation, apoptosis, and invasion (Yang et al., 2017; Bu et al., 2020). In OS, the downregulated lncRNA XLOC_008466/miR-874-3p/CCNE1 axis can also inhibit tumor growth (Ghosh et al., 2017). The expression of lncRNA DCST1-AS1 increases in cervical cancer tissues and cells, and inhibition of DCST1-AS1 can increase the expression of miR-874-3p, thereby inhibiting the proliferation, migration and invasion of cervical cancer cells (Liu et al., 2021a). In PTC, miR-874-3p can inhibit FAM84A and exert carcinogenic effects through the Wnt/ β -catenin signal transduction (Ding et al., 2021). LncRNA DANCER is a promising tumor-related lncRNA that can enhance cancer cell proliferation, stemness, invasion, and metastasis (Zhang et al., 2021a). In AML, DANCER regulates autophagy by promoting the miR-874-3p/ATG16L1 axis, thereby reducing Ara-C resistance in human AML cells (Zhang et al., 2021a). BTZ is a first-class proteasome inhibitor approved by the FDA for the treatment of newly diagnosed and relapsed MM patients. In MM, the circ_0003489/miR-874-3p/HDAC1 axis plays a crucial role in controlling the balance of autophagy and apoptosis in MM cells. Downregulation of circ_0003489 can increase the inhibition of miR-874-3p on

HDAC1, and improve the efficacy of BTZ in the treatment of MM (Tian et al., 2021).

Besides, we found that the ceRNA network of miR-874 also plays an important role in non-cancer diseases. The H19/miR-874/AQP1 axis can help restore inflammatory response to lipopolysaccharide (LPS) and inflammation associated with sepsis-induced myocardial dysfunction (Fang et al., 2018). Also, the H19/miR-874/AQP3 axis plays an important role in maintaining the intestinal barrier function (Su et al., 2016). During the continuous osteogenic differentiation of periodontal ligament stromal cells (PDLSCs), the FER1L4/miR-874-3p/VEGFA axis can positively regulate the osteogenic differentiation of PDLSCs (Huang et al., 2020b). In PD, the HOTAIR/miR-874-5p/ATG10 axis can promote MPP⁺-induced neuronal damage (Zhao et al., 2020). miR-874-3p can reduce the levels of TNF- α , IL-1, IL-6, and IL-8, increase the level of IL-10, reduce neuronal apoptosis, and significantly inhibit brain inflammation in the IS model mice. LncRNA MIAT can sponge miR-874-3p to increase the risk of IS (Zhang et al., 2021b). In addition, circANAPC2 is upregulated in ISS patients, and it can inhibit the proliferation, hypertrophy, and endochondral ossification of chondrocytes through the circANAPC2/miR-874-3p/SMAD3 axis *in vitro* (Liu et al., 2021b).

It is worth noting that circRNA-mediated regulation of miRNA expression consists of two modes (Piwecka et al., 2017). One is the classical sponge mechanism, in which



circRNA inhibits or does not affect miRNA expression. The other is a stabilization mechanism in which circRNAs increase the expression of miRNAs. In IDD, circ_0040039 can stabilize miR-874-3p and inhibit the expression level of ESR1, thereby promoting the apoptosis of the NPCs and inhibiting the growth of NPCs (Li et al., 2021b).

THE MIR-874 RELATED SIGNALING PATHWAYS

The target genes of miR-874 are involved in at least five classical signaling pathways, including the Wnt/β-catenin pathway [TFAP2B (Wang et al., 2020a), CDK8 (Yu et al., 2020), HMGB2 (Yuan et al., 2020), CXCL12 (Xie et al., 2020), and FAM84A (Ding et al., 2021)], the Hippo pathway [YAP1 and TAZ (Que et al., 2017)], the PI3K/AKT pathway [AQP3 (Li et al., 2020)], the JAK/STAT pathway [STAT3 (Zhang et al., 2015; Li et al., 2020; Zhao and Dong, 2016; Bu et al., 2020; Yuan et al., 2018; Shang et al., 2019)] and the Hedgehog signaling pathway [SUFU (Lin et al., 2018)] (Figure 3).

The Wnt/β-Catenin Signaling Pathway

The close relationship between miR-874 and Wnt/β-catenin signaling pathway is of great significance not only for tumor diseases but also for IS (Figure 3). Wnt/β-catenin signaling pathway plays a key role in regulating cell growth, cell development, and normal stem cell differentiation. Constitutive activation of the Wnt/β-catenin signaling pathway has been found in many human cancers (Yao et al., 2011). In RB tissues and cells, the TP73-AS1/miR-874-3p/TFAP2B axis can activate the Wnt/β-catenin signaling pathway and enhance the expression of downstream tumor-related factors TCF4, BCL2, CCND1, and MYC (Wang et al., 2020a).

Abnormal activation of the Wnt/β-catenin signaling pathway occurs in almost all CRC (Wang et al., 2020a). In CRC, the circ_0005576/miR-874-3p/CDK8 axis can cause the abnormal activation of the Wnt/β-catenin signaling pathway and the proliferation of CRC cells (Yu et al., 2020). In GC cell lines the downregulation of the miR-874-3p/HMGB2 axis can upregulate the expression of β-catenin, CCND1, and MYC, which shows that the abnormal activation Wnt/β-catenin

signaling pathway may be regulated by the miR-874-3p/HMGB2 axis in GC (Yuan et al., 2020).

The expression of serum CXCL12 in patients with IS was higher than that in healthy controls. CXCL12 can act as a ligand for CXC motif chemokine receptor 4 (CXCR4) and is a downstream target gene of miR-874-3p (Xie et al., 2020). In mice with IS, the Wnt/ β -catenin signaling pathway is inhibited, and downregulation of CXCL12 can activate the Wnt/ β -catenin signaling pathway, thereby promoting angiogenesis and inhibiting the brain tissue apoptosis in mice with IS (Xie et al., 2020). This suggests that the miR-874-3p/CXCL12 axis can activate the Wnt/ β -catenin signaling pathway, which provides a new hint for the treatment of IS (Xie et al., 2020).

In PTC, FAM84A can activate EMT and the Wnt/ β -catenin signaling pathway, thereby inducing tumorigenesis of thyroid cancer (Ding et al., 2021). miR-874-3p can target the 3'UTR of FAM84A, thereby reducing the expression of FAM84A. Attenuation of miR-874-3p/FAM84A/Wnt/ β -catenin axis can inhibit PTC tumor progression (Ding et al., 2021).

In addition, miR-874-3p/WNT/ β -catenin axis can inhibit the osteogenic differentiation of hPDLF. During osteogenic differentiation of hPDLF, the downregulation of miR-874-3p corresponds to the increase in WNT3A expression, while overexpression of miR-874-3p can inhibit WNT3A expression, thereby upregulating the expression of the β -catenin protein (Song et al., 2021b).

The Hippo Signaling Pathway

The Hippo signaling pathway can regulate cell growth, differentiation, aging, contact inhibition, and other biological processes, and plays an important role in maintaining cell growth and maintaining the stability of apoptosis balance (Que et al., 2017). YAP1 and TAZ are downstream transcriptional effectors of the Hippo signaling pathway, which can promote cell growth, invasion, and migration (Que et al., 2017). In CRC cells, the ectopic expression of miR-874-3p can inhibit the expression of YAP1 and TAZ, and by downregulating the expression of BCL2 and BCL2L1, increasing the activity of CASP9 and CASP3, thereby promoting 5-FU-induced apoptosis (Que et al., 2017). Downregulation of miR-874-3p can inactivate the Hippo signaling pathway, thereby increasing the resistance of cells to 5-FU chemotherapy (Que et al., 2017) (Figure 3).

The PI3K/AKT Signaling Pathway

The PI3K/AKT signaling pathway is downstream of many growth factor receptors. It promotes the proliferation and malignant transformation of tumor cells and inhibits tumor cell apoptosis through the phosphorylation of PI3K and AKT proteins (Lu et al., 2019). Downregulation of miR-874 in NSCLC tissues and cell lines can increase the expression of its target gene AQP3, promote p-PI3K and p-AKT phosphorylation, and activate the PI3K/AKT signaling pathway (Wang et al., 2020b). The above implies that miR-874 deactivates the PI3K/AKT signaling pathway by targeting AQP3 and exerts its tumor suppressor effect (Wang et al., 2020b) (Figure 3).

The JAK/STAT Signaling Pathway

The JAK/STAT signaling pathway includes a family of receptor-associated cytoplasmic tyrosine kinases (JAKs) that phosphorylate tyrosine residues in STAT homologs (Wang et al., 2019). The JAK/STAT signaling pathway plays an inhibitory role in various physiological processes, such as cell development and differentiation (Wang et al., 2019).

miR-874-3p can inhibit the JAK/STAT signaling pathway by inhibiting STAT3 (Figure 3). As an anti-apoptotic factor, STAT3 plays an important role in the regulation of gene expression and mitochondrial electron transport during cellular stress (Wang et al., 2019). miR-874-3p can inhibit STAT3 in several cancers, including GC (Zhang et al., 2015), CRC (Zhao and Dong, 2016), NSCLC (Bu et al., 2020), and ESCC (Yuan et al., 2018). In gastric cancer, constitutive STAT3 activation promotes VEGF-A expression and stimulates tumor angiogenesis. miR-874 can bind to the 3'-UTR of STAT3 and downregulate STAT3 expression, thereby inhibiting angiogenesis (Zhang et al., 2015). In CRC, miR-874 inhibits STAT3 expression by targeting its mRNA 3'UTR, thereby inhibiting cell growth and inducing apoptosis (Zhao and Dong, 2016). In NSCLC cells, miR210HG can downregulate the expression of miR-874, thereby promoting the expression of STAT3 (Bu et al., 2020). In ESCC, the overexpression of miR-874 can inhibit tumor development by targeting STAT3. Besides, in IHD, inhibiting miR-874-3p can activate the JAK2/STAT3 signaling pathway, thereby inhibiting the expression of BAX, upregulating BCL2, reducing cardiomyocyte apoptosis, and ultimately reducing the risk of ischemia/reperfusion (I/R) damage in mice (Chen et al., 2019).

The Hedgehog Signaling Pathway

The Hedgehog signaling pathway is conservative and it is involved in the proliferation and differentiation of a variety of cells (Lin et al., 2018). SUFU is a negative regulator of the Hedgehog signaling pathway in vertebrates. SUFU can inhibit the GLI transcription factor and induce skeletal dysplasia, osteoarthritis, or chondroma (Lin et al., 2018). By inhibiting SUFU and activating the Hedgehog signaling pathway, miR-874 can promote osteoblast proliferation, increase alkaline phosphatase activity and calcium nodules, and inhibit osteoblast apoptosis (Lin et al., 2018).

SUMMARY

miR-874 is downregulated in many cancers and non-cancer diseases, suggesting that it plays a key role in the physiological and pathological processes of human disease. miR-874 plays an important role in the progression of malignant tumors by regulating a complex ceRNA network. The ceRNA network centered on miR-874 includes at least 10 ncRNAs and 12 protein-coding genes. miR-874 has also been shown to participate in at least 4 important signaling pathways, including the Hippo signaling pathway, Wnt/ β -catenin signaling pathway, JAK/STAT signaling pathway, and Hedgehog signaling pathway.

It is worth noting that in the relevant research of IDD, the expression of miR-874-3p is inconsistent. This may be related to the cell state and type, and these differences need to be further verified in large-scale experiments. In IDD, circ_0040039 can enhance miR-874-3p through a stabilization mechanism. In the future, further exploration of miR-874-related stabilization mechanisms will help to understand the ceRNA network of miR-874 and the clinical effectiveness of targeting miR-874.

The abnormal expression of miR-874 is closely related to the clinicopathological characteristics of 15 cancers. Therefore, miR-874 can be used as a potential biomarker for the early prediction of cancer. In addition, in AML and MM, miR-874 participates in the regulation of autophagy-related functions and affects drug resistance of cells, which provides new ideas for overcoming drug resistance. However, the current research of miR-874 is focused on the exploration of the mechanism of its upstream and downstream genes. The potential clinical application of miR-874 in cancer prognosis and chemotherapy resistance is still lacking.

In existing studies, miR-874 is downregulated in all cancers studied and is related to the clinicopathological characteristics of cancer. Therefore, miR-874 is promising as a potential biomarker

for the early prediction of cancer. In addition, in recent years, more and more non-cancer diseases have also recognized the evidence related to miR-874, but the specific regulatory mechanism of miR-874 in non-cancer diseases remains to be revealed. Future work is necessary to explore the mechanism of miR-874-related ceRNA network in cancer and non-cancer disease.

AUTHOR CONTRIBUTIONS

SD, WG and QZ contributed to the conception, design and final approval of the submitted version. QZ, QY and CZ collected and analyzed literature. QZ, CZ, L-hZ, WG, and SD contributed to manuscript writing. All the authors conceived and gave the approval of the final manuscript.

FUNDING

The research was supported by the grant of Zhejiang Provincial Health Department Project (No. 2020KY680).

REFERENCES

- Ahmad, A., Sayed, A., Ginnebaugh, K. R., Sharma, V., Suri, A., and Saraph, A. (2015). Molecular Docking and Inhibition of Matrix Metalloproteinase-2 by Novel Difluorinatedbenzylidene Curcumin Analog. *Am. J. Transl Res.* 7 (2), 298–308.
- Bu, L., Zhang, L., Tian, M., Zheng, Z., Tang, H., and Yang, Q. (2020). LncRNA MIR210HG Facilitates Non-small Cell Lung Cancer Progression through Directly Regulation of miR-874/STAT3 Axis. *Dose Response* 18 (3), 1559325820918052. doi:10.1177/1559325820918052
- Chen, P. J., Shang, A. Q., Yang, J. P., and Wang, W. W. (2019). microRNA-874 Inhibition Targeting STAT3 Protects the Heart from Ischemia-Reperfusion Injury by Attenuating Cardiomyocyte Apoptosis in a Mouse Model. *J. Cel Physiol* 234 (5), 6182–6193. doi:10.1002/jcp.27398
- Diao, J., Su, X., Cao, L., Yang, Y., and Liu, Y. (2018). MicroRNA874 Inhibits Proliferation and Invasion of Pancreatic Ductal Adenocarcinoma Cells by Directly Targeting Paired Box 6. *Mol. Med. Rep.* 18 (1), 1188–1196. doi:10.3892/mmr.2018.9069
- Ding, Y., Wu, L., Zhuang, X., Cai, J., Tong, H., Si, Y., et al. (2021). The Direct miR-874-3p-Target FAM84A Promotes Tumor Development in Papillary Thyroid Cancer. *Mol. Oncol.* 15 (5), 1597–1614. doi:10.1002/1878-0261.12941
- Dong, D., Gong, Y., Zhang, D., Bao, H., and Gu, G. (2016). miR-874 Suppresses the Proliferation and Metastasis of Osteosarcoma by Targeting E2F3. *Tumour Biol.* 37 (5), 6447–6455. doi:10.1007/s13277-015-4527-3
- Fang, Y., Hu, J., Wang, Z., Zong, H., Zhang, L., Zhang, R., et al. (2018). LncRNA H19 Functions as an Aquaporin 1 Competitive Endogenous RNA to Regulate microRNA-874 Expression in LPS Sepsis. *Biomed. Pharmacother.* 105, 1183–1191. doi:10.1016/j.biopha.2018.06.007
- Ghosh, T., Varshney, A., Kumar, P., Kaur, M., Kumar, V., Shekhar, R., et al. (2017). MicroRNA-874-mediated Inhibition of the Major G1/S Phase Cyclin, CCNE1, Is Lost in Osteosarcomas. *J. Biol. Chem.* 292 (52), 21264–21281. doi:10.1074/jbc.M117.808287
- Han, J., Liu, Z., Wang, N., and Pan, W. (2016). MicroRNA-874 Inhibits Growth, Induces Apoptosis and Reverses Chemoresistance in Colorectal Cancer by Targeting X-Linked Inhibitor of Apoptosis Protein. *Oncol. Rep.* 36 (1), 542–550. doi:10.3892/or.2016.4810
- Huang, F. K., Zheng, C. Y., Huang, L. K., Lin, C. Q., Zhou, J. F., and Wang, J. X. (2020a). Long Non-coding RNA MCF2L-AS1 Promotes the Aggressiveness of Colorectal Cancer by Sponging miR-874-3p and Thereby Up-Regulating CCNE1. *J. Gene Med.* 36, e3285. doi:10.1002/jgm.3285
- Huang, H., Tang, J., Zhang, L., Bu, Y., and Zhang, X. (2018). miR-874 Regulates Multiple-Drug Resistance in Gastric Cancer by Targeting ATG16L1. *Int. J. Oncol.* 53 (6), 2769–2779. doi:10.3892/ijo.2018.4593
- Huang, Y., Han, Y., Guo, R., Liu, H., Li, X., Jia, L., et al. (2020b). Long Non-coding RNA FER1L4 Promotes Osteogenic Differentiation of Human Periodontal Ligament Stromal Cells via miR-874-3p and Vascular Endothelial Growth Factor A. *Stem Cel Res Ther* 11 (1), 5. doi:10.1186/s13287-019-1519-z
- Huo, W., Li, H., Zhang, Y., and Li, H. (2020). Epigenetic Silencing of microRNA-874-3p Implicates in Erectile Dysfunction in Diabetic Rats by Activating the Nupr1/Chop-Mediated Pathway. *FASEB J.* 34 (1), 1695–1709. doi:10.1096/fj.201902086R
- Iorio, M. V., and Croce, C. M. (2017). MicroRNA Dysregulation in Cancer: Diagnostics, Monitoring and Therapeutics. A Comprehensive Review. *EMBO Mol. Med.* 9 (6), 852. doi:10.15252/emmm.201707779
- Jiang, B., Li, Z., Zhang, W., Wang, H., Zhi, X., Feng, J., et al. (2014). miR-874 Inhibits Cell Proliferation, Migration and Invasion through Targeting Aquaporin-3 in Gastric Cancer. *J. Gastroenterol.* 49 (6), 1011–1025. doi:10.1007/s00535-013-0851-9
- Jiang, D., Sun, X., Wang, S., and Man, H. (2019). Upregulation of miR-874-3p Decreases Cerebral Ischemia/reperfusion Injury by Directly Targeting BMF and BCL2L13. *Biomed. Pharmacother.* 117, 108941. doi:10.1016/j.biopha.2019.108941
- Jiang, T., Guan, L. Y., Ye, Y. S., Liu, H. Y., and Li, R. (2017). MiR-874 Inhibits Metastasis and Epithelial-Mesenchymal Transition in Hepatocellular Carcinoma by Targeting SOX12. *Am. J. Cancer Res.* 7 (6), 1310–1321.
- Kesanakurti, D., Maddirela, D. R., Chittivelu, S., Rao, J. S., and Chetty, C. (2013). Suppression of Tumor Cell Invasiveness and *In Vivo* Tumor Growth by microRNA-874 in Non-small Cell Lung Cancer. *Biochem. Biophys. Res. Commun.* 434 (3), 627–633. doi:10.1016/j.bbrc.2013.03.132
- Kushwaha, P., Khedgikar, V., Sharma, D., Yuen, T., Gautam, J., Ahmad, N., et al. (2016). MicroRNA 874-3p Exerts Skeletal Anabolic Effects Epigenetically during Weaning by Suppressing Hdac1 Expression. *J. Biol. Chem.* 291 (8), 3959–3966. doi:10.1074/jbc.M115.687152
- Leong, K. W., Cheng, C. W., Wong, C. M., Ng, I. O., Kwong, Y. L., and Tse, E. (2017). miR-874-3p Is Down-Regulated in Hepatocellular Carcinoma and Negatively Regulates PIN1 Expression. *Oncotarget* 8 (7), 11343–11355. doi:10.18632/oncotarget.14526

- Levy, J. M. M., Towers, C. G., and Thorburn, A. (2017). Targeting Autophagy in Cancer. *Nat. Rev. Cancer* 17 (9), 528–542. doi:10.1038/nrc.2017.53
- Li, Y., Chen, X., Xue, W., Liang, J., and Wang, L. (2021a). MiR-874 Inhibits Cell Proliferation, Migration, and Invasion of Glioma Cells and Correlates with Prognosis of Glioma Patients. *Neuromolecular Med.* 23 (2), 247–255. doi:10.1007/s12017-020-08608-0
- Li, Y. L., Wang, X. M., Qiao, G. D., Zhang, S., Wang, J., Cong, Y. Z., et al. (2020). Up-regulated Lnc-Lung Cancer Associated Transcript 1 Enhances Cell Migration and Invasion in Breast Cancer Progression. *Biochem. Biophys. Res. Commun.* 521 (2), 271–278. doi:10.1016/j.bbrc.2019.08.040
- Li, Y., Wang, X., Xu, H., Li, G., Huo, Z., Du, L., et al. (2021b). Circ_0040039 May Aggravate Intervertebral Disk Degeneration by Regulating the MiR-874-3p-ESR1 Pathway. *Front. Genet.* 12, 656759. doi:10.3389/fgene.2021.656759
- Liao, H., Pan, Y., Pan, Y., Shen, J., Qi, Q., Zhong, L., et al. (2018). MicroRNA874 Is Downregulated in Cervical Cancer and Inhibits Cancer Progression by Directly Targeting ETS1. *Oncol. Rep.* 40 (4), 2389–2398. doi:10.3892/or.2018.6624
- Lin, J. C., Liu, Z. G., Yu, B., and Zhang, X. R. (2018). MicroRNA-874 Targeting SUFU Involves in Osteoblast Proliferation and Differentiation in Osteoporosis Rats through the Hedgehog Signaling Pathway. *Biochem. Biophys. Res. Commun.* 506 (1), 194–203. doi:10.1016/j.bbrc.2018.09.187
- Liu, B., Li, F., Zhao, H. P., Chen, J. B., Li, Y. P., and Yu, H. H. (2017). miR-874 Inhibits Metastasis-Relevant Traits via Targeting SH2B Adaptor Protein 1 (SH2B1) in Gastric Cancer. *Int. J. Clin. Exp. Pathol.* 10 (8), 8577–8584.
- Liu, J., Zhang, J., Hu, Y., Zou, H., Zhang, X., and Hu, X. (2021a). Inhibition of lncRNA DCST1-AS1 Suppresses Proliferation, Migration and Invasion of Cervical Cancer Cells by Increasing miR-874-3p Expression. *J. Gene Med.* 23 (1), e3281. doi:10.1002/jgm.3281
- Liu, W. G., Zhuo, L., Lu, Y., Wang, L., Ji, Y. X., and Guo, Q. (2020). miR-874-3p Inhibits Cell Migration through Targeting RGS4 in Osteosarcoma. *J. Gene Med.* 22 (9), e3213. doi:10.1002/jgm.3213
- Liu, X., Du, Z., Yi, X., Sheng, T., Yuan, J., and Jia, J. (2021b). Circular RNA circANAPC2 Mediates the Impairment of Endochondral Ossification by miR-874-3p/SMAD3 Signalling Pathway in Idiopathic Short Stature. *J. Cel Mol Med* 25 (7), 3408–3426. doi:10.1111/jcmm.16419
- Lu, T. X., and Rothenberg, M. E. (2018). MicroRNA. *J. Allergy Clin. Immunol.* 141 (4), 1202–1207. doi:10.1016/j.jaci.2017.08.034
- Lu, Y., Li, L., Wu, G., Zhuo, H., Liu, G., and Cai, J. (2019). Effect of PI3K/Akt Signaling Pathway on PRAS40Thr246 Phosphorylation in Gastric Cancer Cells. *Iran J. Public Health* 48 (12), 2196–2204.
- Nohata, N., Hanazawa, T., Kikkawa, N., Sakurai, D., Fujimura, L., Chiyomaru, T., et al. (2011). Tumour Suppressive microRNA-874 Regulates Novel Cancer Networks in Maxillary Sinus Squamous Cell Carcinoma. *Br. J. Cancer* 105 (6), 833–841. doi:10.1038/bjc.2011.311
- Nohata, N., Hanazawa, T., Kinoshita, T., Inamine, A., Kikkawa, N., Itesako, T., et al. (2013). Tumour-suppressive microRNA-874 Contributes to Cell Proliferation through Targeting of Histone Deacetylase 1 in Head and Neck Squamous Cell Carcinoma. *Br. J. Cancer* 108 (8), 1648–1658. doi:10.1038/bjc.2013.122
- Pan, X., Wang, G., and Wang, B. (2021). Ectopic Expression of microRNA-874 Represses Epithelial Mesenchymal Transition through the NF-kappaB Pathway via CCNE1 in Cholangiocarcinoma. *Cell Signal* 82, 109927. doi:10.1016/j.cellsig.2021.109927
- Pashaei, E., Pashaei, E., Ahmady, M., Ozen, M., and Aydin, N. (2017). Meta-analysis of miRNA Expression Profiles for Prostate Cancer Recurrence Following Radical Prostatectomy. *PLoS One* 12 (6), e0179543. doi:10.1371/journal.pone.0179543
- Piwecka, M., Glazar, P., Hernandez-Miranda, L. R., Memczak, S., Wolf, S. A., Rybak-Wolf, A., et al. (2017). Loss of a Mammalian Circular RNA Locus Causes miRNA Deregulation and Affects Brain Function. *Science* 357 (6357). doi:10.1126/science.aam8526
- Que, K., Tong, Y., Que, G., Li, L., Lin, H., Huang, S., et al. (2017). Downregulation of miR-874-3p Promotes Chemotherapeutic Resistance in Colorectal Cancer via Inactivation of the Hippo Signaling Pathway. *Oncol. Rep.* 38 (6), 3376–3386. doi:10.3892/or.2017.6041
- Shang, H., Liu, Y., Li, Z., Liu, Q., Cui, W., Zhang, L., et al. (2019). MicroRNA-874 Functions as a Tumor Suppressor in Rhabdomyosarcoma by Directly Targeting GEFT. *Am. J. Cancer Res.* 9 (4), 668–681.
- Song, Q., Zhang, F., Wang, K., Chen, Z., Li, Q., Liu, Z., et al. (2021a). MiR-874-3p Plays a Protective Role in Intervertebral Disc Degeneration by Suppressing MMP2 and MMP3. *Eur. J. Pharmacol.* 895, 173891. doi:10.1016/j.ejphar.2021.173891
- Song, S., Yan, Z., and Wu, W. (2021b). MiR-874-3p Inhibits Osteogenic Differentiation of Human Periodontal Ligament Fibroblasts through Regulating Wnt/beta-Catenin Pathway. *J. Dent Sci.* 16 (4), 1146–1153. doi:10.1016/j.jds.2021.02.006
- Song, X., Song, W., Wang, Y., Wang, J., Li, Y., Qian, X., et al. (2016). MicroRNA-874 Functions as a Tumor Suppressor by Targeting Cancer/Testis Antigen HCA587/MAGE-C2. *J. Cancer* 7 (6), 656–663. doi:10.7150/jca.13674
- Su, Z., Zhi, X., Zhang, Q., Yang, L., Xu, H., and Xu, Z. (2016). LncRNA H19 Functions as a Competing Endogenous RNA to Regulate AQP3 Expression by Sponging miR-874 in the Intestinal Barrier. *FEBS Lett.* 590 (9), 1354–1364. doi:10.1002/1873-3468.12171
- Sun, K., and Lai, E. C. (2013). Adult-specific Functions of Animal microRNAs. *Nat. Rev. Genet.* 14 (8), 535–548. doi:10.1038/nrg3471
- Sun, Q. H., Yin, Z. X., Li, Z., Tian, S. B., Wang, H. C., Zhang, F. X., et al. (2020). miR-874 Inhibits Gastric Cancer Cell Proliferation by Targeting SPAG9. *BMC Cancer* 20 (1), 522. doi:10.1186/s12885-020-06994-z
- Tang, W., Wang, W., Zhao, Y., and Zhao, Z. (2018). MicroRNA-874 Inhibits Cell Proliferation and Invasion by Targeting Cyclin-dependent Kinase 9 in Osteosarcoma. *Oncol. Lett.* 15 (5), 7649–7654. doi:10.3892/ol.2018.8294
- Tian, F. Q., Chen, Z. R., Zhu, W., Tang, M. Q., Li, J. H., Zhang, X. C., et al. (2021). Inhibition of Hsa_circ_0003489 Shifts Balance from Autophagy to Apoptosis and Sensitizes Multiple Myeloma Cells to Bortezomib via miR-874-3p/HDAC1 axis. *J. Gene Med.* 23 (9), e3329. doi:10.1002/jgm.3329
- Wang, K., Liu, F., Zhou, L. Y., Ding, S. L., Long, B., Liu, C. Y., et al. (2013). miR-874 Regulates Myocardial Necrosis by Targeting Caspase-8. *Cell Death Dis* 4, e709. doi:10.1038/cddis.2013.233
- Wang, L., Gao, W., Hu, F., Xu, Z., and Wang, F. (2014). MicroRNA-874 Inhibits Cell Proliferation and Induces Apoptosis in Human Breast Cancer by Targeting CDK9. *FEBS Lett.* 588 (24), 4527–4535. doi:10.1016/j.febslet.2014.09.035
- Wang, L., Wang, C., Wu, T., and Sun, F. (2020a). Long Non-coding RNA TP73-AS1 Promotes TFAP2B-Mediated Proliferation, Metastasis and Invasion in Retinoblastoma via Decoying of miRNA-874-3p. *J. Cel Commun Signal* 14 (2), 193–205. doi:10.1007/s12079-020-00550-x
- Wang, S., Wu, Y., Yang, S., Liu, X., Lu, Y., Liu, F., et al. (2020b). miR-874 Directly Targets AQP3 to Inhibit Cell Proliferation, Mobility and EMT in Non-small Cell Lung Cancer. *Thorac. Cancer* 11 (6), 1550–1558. doi:10.1111/1759-7714.13428
- Wang, W., Li, J., Ding, Z., Li, Y., Wang, J., Chen, S., et al. (2019). Tanshinone I Inhibits the Growth and Metastasis of Osteosarcoma via Suppressing JAK/STAT3 Signalling Pathway. *J. Cel Mol Med* 23 (9), 6454–6465. doi:10.1111/jcmm.14539
- Wang, Y., Chen, H., and Wei, X. (2021). Circ_0007142 Downregulates miR-874-3p-Mediated GPD5 on Colorectal Cancer Cells. *Eur. J. Clin. Invest.* 51 (7), e13541. doi:10.1111/eci.13541
- Wei, Y., Wang, Z., Wei, L., Li, S., Qiu, X., and Liu, C. (2021). MicroRNA-874-3p Promotes Testosterone-Induced Granulosa Cell Apoptosis by Suppressing HDAC1-Mediated P53 Deacetylation. *Exp. Ther. Med.* 21 (4), 359. doi:10.3892/etm.2021.9790
- Witek, L., Janikowski, T., Gabriel, I., Bodzek, P., and Olejek, A. (2021). Analysis of microRNA Regulating Cell Cycle-Related Tumor Suppressor Genes in Endometrial Cancer Patients. *Hum. Cel* 34 (2), 564–569. doi:10.1007/s13577-020-00451-6
- Witt, O., Deubzer, H. E., Milde, T., and Oehme, I. (2009). HDAC Family: What Are the Cancer Relevant Targets? *Cancer Lett.* 277 (1), 8–21. doi:10.1016/j.canlet.2008.08.016
- Wu, G., Zhou, H., Li, D., Zhi, Y., Liu, Y., Li, J., et al. (2020). LncRNA DANCER Upregulation Induced by TUFT1 Promotes Malignant Progression in Triple Negative Breast Cancer via miR-874-3p-SOX2 axis. *Exp. Cel Res* 396 (2), 112331. doi:10.1016/j.yexcr.2020.112331
- Xia, B., Lin, M., Dong, W., Chen, H., Li, B., Zhang, X., et al. (2018). Upregulation of miR-874-3p and miR-874-5p Inhibits Epithelial Ovarian Cancer Malignancy via SIK2. *J. Biochem. Mol. Toxicol.* 32 (8), e22168. doi:10.1002/jbt.22168
- Xie, K., Cai, Y., Yang, P., Du, F., and Wu, K. (2020). Upregulating microRNA-874-3p Inhibits CXCL12 Expression to Promote Angiogenesis and Suppress Inflammatory Response in Ischemic Stroke. *Am. J. Physiol. Cel Physiol* 319 (3), C579–C588. doi:10.1152/ajpcell.00001.2020

- Yan, Y., Song, X., Li, Z., Zhang, J., Ren, J., Wu, J., et al. (2017). Elevated Levels of Granzyme B Correlated with miR-874-3p Downregulation in Patients with Acute Myocardial Infarction. *Biomark Med.* 11 (9), 761–767. doi:10.2217/bmm-2017-0144
- Yang, H., Dong, Y., Zhou, Y., and Li, H. (2021). Overexpression of miR-874-3p Alleviates LPS-Induced Apoptosis and Inflammation in Alveolar Epithelial Cell by Targeting EGR3/NF-kappaB. *Acta Biochim. Pol.* 68 (2), 231–238. doi:10.18388/abp.2020_5523
- Yang, R., Li, P., Zhang, G., Lu, C., Wang, H., and Zhao, G. (2017). Long Non-coding RNA XLOC_008466 Functions as an Oncogene in Human Non-small Cell Lung Cancer by Targeting miR-874. *Cell Physiol Biochem* 42 (1), 126–136. doi:10.1159/000477121
- Yao, H., Ashihara, E., and Maekawa, T. (2011). Targeting the Wnt/beta-Catenin Signaling Pathway in Human Cancers. *Expert Opin. Ther. Targets* 15 (7), 873–887. doi:10.1517/14728222.2011.577418
- Yao, T., Zha, D., Gao, P., Shui, H., and Wu, X. (2018). MiR-874 Alleviates Renal Injury and Inflammatory Response in Diabetic Nephropathy through Targeting Toll-like Receptor-4. *J. Cel Physiol* 234 (1), 871–879. doi:10.1002/jcp.26908
- Yu, C., Li, S., and Hu, X. (2020). Circ_0005576 Promotes Malignant Progression through miR-874/CDK8 Axis in Colorectal Cancer. *Onco Targets Ther.* 13, 7793–7805. doi:10.2147/OTT.S249494
- Yuan, F., Zhao, Z. T., Jia, B., Wang, Y. P., and Lei, W. (2020). TSN Inhibits Cell Proliferation, Migration, Invasion, and EMT through Regulating miR-874/HMGB2/beta-Catenin Pathway in Gastric Cancer. *Neoplasia* 67 (5), 1012–1021. doi:10.4149/neo_2020_190919N931
- Yuan, R. B., Zhang, S. H., He, Y., Zhang, X. Y., and Zhang, Y. B. (2018). MiR-874-3p Is an Independent Prognostic Factor and Functions as an Anti-oncomir in Esophageal Squamous Cell Carcinoma via Targeting STAT3. *Eur. Rev. Med. Pharmacol. Sci.* 22 (21), 7265–7273. doi:10.26355/eurrev_201811_16261
- Zhang, H., Liu, L., Chen, L., Liu, H., Ren, S., and Tao, Y. (2021a). Long Noncoding RNA DANCER Confers Cytarabine Resistance in Acute Myeloid Leukemia by Activating Autophagy via the miR-874-3p/ATG16L1 axis. *Mol. Oncol.* 15 (4), 1203–1216. doi:10.1002/1878-0261.12661
- Zhang, L., Yan, D. L., Yang, F., Wang, D. D., Chen, X., Wu, J. Z., et al. (2017). DNA Methylation Mediated Silencing of microRNA-874 Is a Promising Diagnosis and Prognostic Marker in Breast Cancer. *Oncotarget* 8 (28), 45496–45505. doi:10.18632/oncotarget.17569
- Zhang, S., Zhang, Y., Wang, N., Wang, Y., Nie, H., Zhang, Y., et al. (2021b). Long Non-coding RNA MIAT Impairs Neurological Function in Ischemic Stroke via Up-Regulating microRNA-874-3p-Targeted IL1B. *Brain Res. Bull.* 175, 81–89. doi:10.1016/j.brainresbull.2021.07.005
- Zhang, X., Tang, J., Zhi, X., Xie, K., Wang, W., Li, Z., et al. (2015). miR-874 Functions as a Tumor Suppressor by Inhibiting Angiogenesis through STAT3/VEGF-A Pathway in Gastric Cancer. *Oncotarget* 6 (3), 1605–1617. doi:10.18632/oncotarget.2748
- Zhang, Y., Wang, X., and Zhao, Y. (2018a). MicroRNA874 Prohibits the Proliferation and Invasion of Retinoblastoma Cells by Directly Targeting Metadherin. *Mol. Med. Rep.* 18 (3), 3099–3105. doi:10.3892/mmr.2018.9295
- Zhang, Y., Wei, Y., Li, X., Liang, X., Wang, L., Song, J., et al. (2018b). microRNA-874 Suppresses Tumor Proliferation and Metastasis in Hepatocellular Carcinoma by Targeting the DOR/EGFR/ERK Pathway. *Cel Death Dis* 9 (2), 130. doi:10.1038/s41419-017-0131-3
- Zhang, Z., Yang, W., Li, N., Chen, X., Ma, F., Yang, J., et al. (2021c). LncRNA MCF2L-AS1 Aggravates Proliferation, Invasion and Glycolysis of Colorectal Cancer Cells via the Crosstalk with miR-874-3p/FOXO1 Signaling axis. *Carcinogenesis* 42 (2), 263–271. doi:10.1093/carcin/bgaa093
- Zhao, B., and Dong, A. S. (2016). MiR-874 Inhibits Cell Growth and Induces Apoptosis by Targeting STAT3 in Human Colorectal Cancer Cells. *Eur. Rev. Med. Pharmacol. Sci.* 20 (2), 269–277.
- Zhao, J., Li, H., and Chang, N. (2020). LncRNA HOTAIR Promotes MPP+-Induced Neuronal Injury in Parkinson's Disease by Regulating the miR-874-5p/ATG10 axis. *EXCLI J.* 19, 1141–1153. doi:10.17179/excli2020-2286

Conflict of Interest: The authors declare that the research was conducted in the absence of any commercial or financial relationships that could be construed as a potential conflict of interest.

Publisher's Note: All claims expressed in this article are solely those of the authors and do not necessarily represent those of their affiliated organizations, or those of the publisher, the editors and the reviewers. Any product that may be evaluated in this article, or claim that may be made by its manufacturer, is not guaranteed or endorsed by the publisher.

Copyright © 2022 Zhang, Zhong, Yan, Zeng, Gao and Duan. This is an open-access article distributed under the terms of the Creative Commons Attribution License (CC BY). The use, distribution or reproduction in other forums is permitted, provided the original author(s) and the copyright owner(s) are credited and that the original publication in this journal is cited, in accordance with accepted academic practice. No use, distribution or reproduction is permitted which does not comply with these terms.



Construction of an Immune-Related lncRNA Signature That Predicts Prognosis and Immune Microenvironment in Osteosarcoma Patients

OPEN ACCESS

Edited by:

Zong Sheng Guo,
Roswell Park Comprehensive Cancer
Center, United States

Reviewed by:

Juan Ren,
The First Affiliated Hospital of Xi'an
Jiaotong University, China
Gemma Di Pompo,
Rizzoli Orthopedic Institute
(IRCCS), Italy

*Correspondence:

Hongbo You
hbyou360@hotmail.com
Hao Cheng
chenghao@tjh.tjmu.edu.cn

Specialty section:

This article was submitted to
Molecular and Cellular Oncology,
a section of the journal
Frontiers in Oncology

Received: 01 September 2021

Accepted: 23 March 2022

Published: 14 April 2022

Citation:

He Y, Zhou H, Xu H, You H and
Cheng H (2022) Construction of
an Immune-Related lncRNA
Signature That Predicts Prognosis
and Immune Microenvironment in
Osteosarcoma Patients.
Front. Oncol. 12:769202.
doi: 10.3389/fonc.2022.769202

Yi He¹, Haiting Zhou², Haoran Xu¹, Hongbo You^{1*} and Hao Cheng^{1*}

¹ Department of Orthopedics, Tongji Hospital, Tongji Medical College, Huazhong University of Science and Technology, Wuhan, China, ² Department of Oncology, Tongji Hospital, Tongji Medical College, Huazhong University of Science and Technology, Wuhan, China

Osteosarcoma is one of the most common bone tumors in teenagers. We hope to provide a reliable method to predict the prognosis of osteosarcoma and find potential targets for early diagnosis and precise treatment. To address this issue, we performed a detailed bioinformatics analysis based on the Cancer Genome Atlas (TCGA). A total of 85 osteosarcoma patients with gene expression data and clinicopathological features were included in this study, which was considered the entire set. They were randomly divided into a train set and a test set. We identified six lncRNAs (ELFN1-AS1, LINC00837, OLMALINC, AL669970.3, AC005332.4 and AC023157.3), and constructed a signature that exhibited good predictive ability of patient survival and metastasis. What's more, we found that risk score calculated by the signature was positively correlated to tumor purity, CD4⁺ naive T cells, and negatively correlated to CD8⁺ T cells. Furthermore, we investigated each lncRNA in the signature and found that these six lncRNAs were associated with tumorigenesis and immune cells in the tumor microenvironment. In conclusion, we constructed and validated a signature, which had good performance in the prediction of survival, metastasis and immune microenvironment. Our study indicated possible mechanisms of these lncRNAs in the development of osteosarcoma, which may provide new insights into the precise treatment of osteosarcoma.

Keywords: immune, long non-coding RNA, osteosarcoma, TCGA, signature

INTRODUCTION

Osteosarcoma is one of the most common bone tumors, most commonly occurring in young children and adolescents (1). This tumor is most likely to happen in the metaphyses of the distal femur, proximal tibia, and proximal humerus (2–4). Osteosarcoma is prone to pulmonary metastases, and 20% of patients are found to have pulmonary metastases at the time of initial diagnosis (5). Medical advances have significantly reduced the mortality rate of osteosarcoma patients. However, the lack of specific markers makes early screening for osteosarcoma still difficult. Treatment of osteosarcoma is mainly based on local excision and chemotherapy, but chemotherapy for osteosarcoma is prone to drug resistance and has great toxic side effects (6–8). As a result, overall survival is still not satisfactory. It is urgent to figure out the mechanism of tumorigenesis, metastasis and drug resistance in osteosarcoma, and to discover potential target for earlier diagnosis and gene therapy.

The immune system is an important part of the human body. It can help us fight against pathogen infections and participate in the monitoring and prevention of cancer, playing an essential role in maintaining the integrity of the body. However, some tumor cells can evade the surveillance by immune system, or suppress the immune response, making cancer progression. Meanwhile, more and more evidence has shown that the imbalance of immune state in tumor microenvironment plays a decisive role in tumor development (9). Therefore, the role of immune-related factors in tumor development deserves to be studied.

lncRNAs are highly heterogeneous RNA characterized by their length of more than 200 nucleotides and do not encode proteins. With advances in gene chip technology, lncRNAs are being rapidly identified. Numerous studies have found that lncRNAs are involved in various physiological processes, including cellular differentiation, immune response, and tumor progression (10, 11). lncRNAs appear to play an important role in tumor progression, exhibiting tumor-inhabiting and tumor-promoting functions (12). lncRNA-ATB was reported to function as a tumor promoter in papillary thyroid cancer (13). LOC285194 was reported to function as a tumor suppressor in non-small cell lung cancer and osteosarcoma (14, 15). As a result, lncRNAs are expected to be new biomarkers and therapeutic targets for cancer (16).

There was little research studied on the immune-related lncRNAs in osteosarcoma. In this study, we screened immune-related lncRNAs in osteosarcoma and made a bioinformatics analysis for them on the basis of TCGA data. The flowchart of our study is as follows (Figure 1).

MATERIALS AND METHODS

Sample Datasets

The RNAseq (level 3) data and corresponding clinical data of osteosarcoma were come from the TCGA database (<https://portal.gdc.cancer.gov/>), and all data was normalized by TMM

method. We used the Ensembl Genome Browser website to annotate the mRNAs and lncRNAs in the expression matrix and subsequently extracted the mRNA and lncRNA expression matrix separately. To make the analysis accurate, we removed the samples with incomplete clinical information and overall survival time lower than 30 days (17). In total, 85 cases were contained for the following study. All TCGA data is available to the public, so there is no further approval needed from the Ethics Committee.

Immune-related lncRNA Acquisition

We acquired immune-related genes from the Molecular Signature Database v 7.1 (MSigDB) (<http://www.broad.mit.edu/gsea/msigdb/>) (17, 18). IMMUNE_RESPONSE.gmt and IMMUNE_SYSTEM_PROCESS.gmt were chosen as the annotated gene sets. We removed overlapped genes and ultimately obtained 331 immune-related genes. The expression information of these 331 immune-related genes was extracted from the mRNA expression matrix. Then Pearson correlation analysis was performed to calculate the correlation coefficient of each lncRNA with immune-related mRNAs. lncRNAs with coefficient > 0.6 and P value < 0.001 were defined as immune-related lncRNAs. Finally, the expression matrix of these immune-related lncRNAs was extracted.

Signature Construction

These 85 cases were separated into a train set and a test set randomly by “caret” package of R software (v 3.6.2). Meanwhile, all 85 cases were taken as the entire set. The train set was used to construct the prognostic signature. The test set and the entire set were used to verify the accuracy of the signature.

In the train set, we performed univariate Cox regression analysis to identify prognostic-related lncRNAs with $p < 0.01$. Then Least absolute shrinkage and selection operator (LASSO) regression was performed to remove lncRNAs that could lead to phenomenon of overfitting. Finally, the lncRNAs was further screened by using multivariate Cox regression analysis. The coefficient, HR value and P value for each lncRNA were calculated. The risk score of each sample was calculated by the signature:

$$\text{Risk score} = \beta(\text{gene1}) * \text{expr}(\text{gene1}) + \beta(\text{gene2}) * \text{expr}(\text{gene2}) + \dots + \beta(\text{genen}) * \text{expr}(\text{genen})$$

β is the coefficient of lncRNA, and $\text{expr}(\text{genen})$ stands for the expression value of lncRNA.

Signature Application and Validation

Firstly, we did the analysis in the train set. We used the formula above to calculate the risk score of each patient and divided patients into high or low risk groups according to the risk score by using “survminer” package. We ranked the patients by the risk score and plotted the dot-plot for the survival status of each patient. We mapped the lncRNA expression heatmap to observe the expression of lncRNAs in the high and low risk groups. We applied Kaplan-Meier method to explore the survival differences between high-risk group and low-risk group. Finally, receiver operating characteristic (ROC) curve of 5-years was applied for identifying the diagnostic value of the risk scoring signature.

Abbreviations: lncRNA, Long non-coding RNA; TCGA, The Cancer Genome Atlas; ROC, Operating characteristic curve; PCA, Principal component analysis; GSEA, Gene set enrichment analysis; AUC, Area under curve; LASSO, Least absolute shrinkage and selection operator; K-M, Kaplan–Meier.

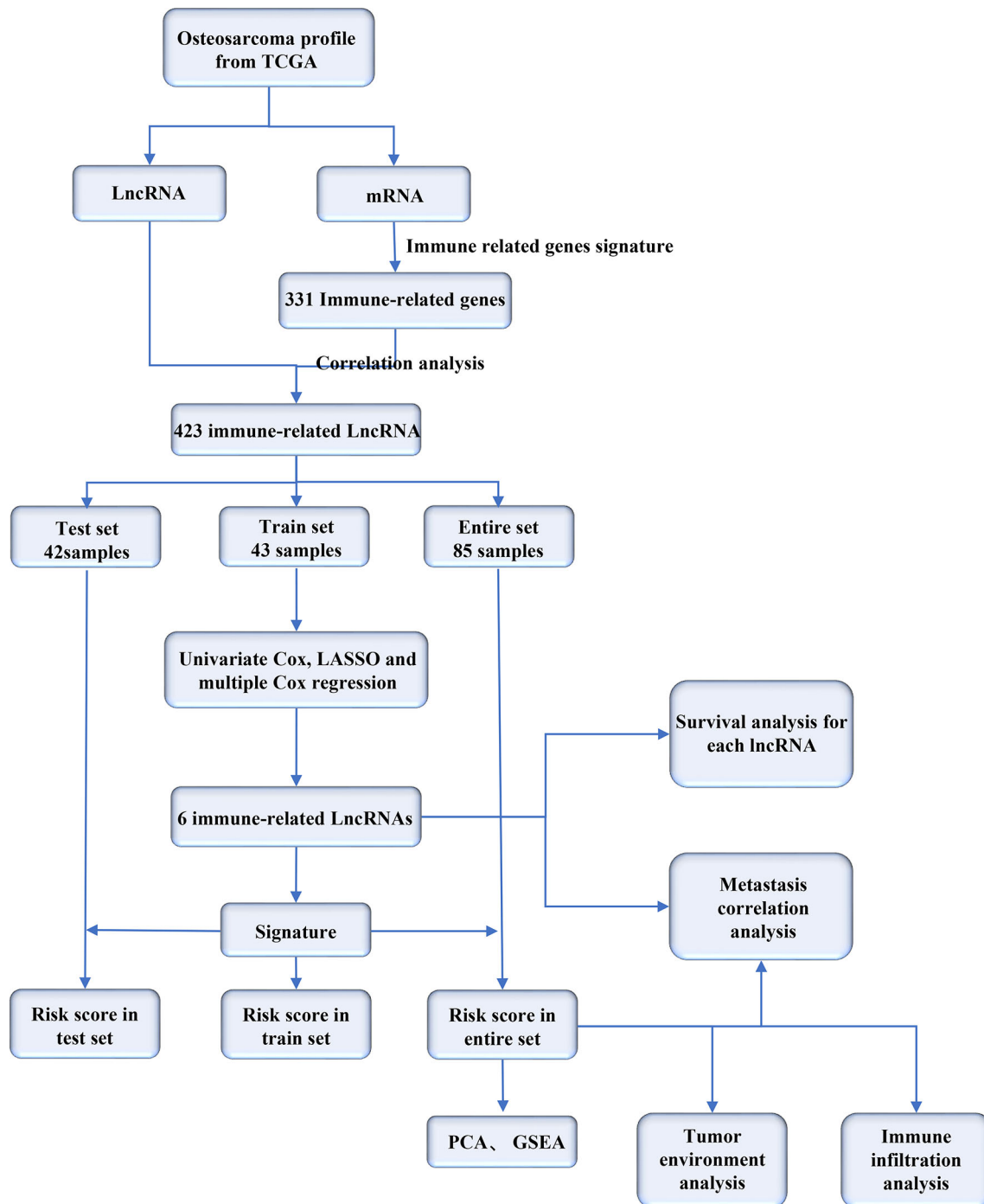


FIGURE 1 | Flowchart of our study.

Subsequently, the same analysis was performed in the test set and the entire set to verify the accuracy of the signature.

Comprehensive Analysis in the Entire Set

The entire set was used for the subsequent analysis. Firstly, principal component analysis (PCA) was used to test whether the

signature can better distinguish the risk status. Secondly, survival analysis for each lncRNA in the signature was performed to estimate the effect of individual lncRNA on survival. Thirdly, metastasis correlation analysis was carried out to investigate the potential correlation between risk score and metastasis. Fourthly, Gene set enrichment analysis (GSEA; <https://www.gsea-msigdb>).

org/gsea/index.jsp) (17) was performed based on two gene sets (IMMUNE_RESPONSE.gmt and IMMUNE_SYSTEM_PROCESS.gmt) to analyze immune response enrichment in the two groups. Fifthly, ESTIMATE algorithm (19) was used to assess the proportion of immune and stromal components, and to infer the tumor purity of the samples. We subsequently analyzed the relationship between tumor purity and risk scores. Finally, CIBERSORT method (20) was used to analyze the infiltration of 22 immune cells between high and low risk groups. The correlation between the infiltrating proportion of immune cells and risk scores and the lncRNAs were also analyzed.

All analyses were performed on the R software (version 3.6.2, <https://www.r-project.org/>). And $P < 0.05$ was considered statistically significant.

RESULTS

Construction of Signature

By comparing mRNA expression data with two gene sets from MSigDB, we matched 331 immune-related genes. We calculated the expression correlation between lncRNAs and immune-related genes to obtain the immune-related lncRNAs. Subsequently, 423 immune-related lncRNAs was identified. Eight of them were screened out by univariate Cox regression analysis (Table 1). The result of the LASSO regression analysis showed that the partial likelihood deviation was smallest when $-3 < \lambda < -2$ (Figure 2A), at which point AL137002.1 was excluded (Figure 2B). Finally, six lncRNAs were screened from the remaining seven lncRNAs by using multivariate Cox regression analysis, and their coefficients, HR values and p-values were calculated respectively (Table 2). The signature was constructed with the coefficients of lncRNAs as below.

$$\begin{aligned} \text{Risk score} = & (0.4707 * ELFN1 - AS1) + (0.1634 * LINC00837) + \\ & (0.4341 * AL669970.3) + (0.2696 * OLMALINC) + \\ & (-1.1261 * AC005332.4) + (-2.2230 * AC023157.3). \end{aligned}$$

Among these lncRNAs, five immune-related lncRNAs were independent prognostic factors. One immune-related lncRNAs acted as a complement to others.

Validation of the Signature

We calculated the risk score of each sample by the signature and divided patients into the low-risk and the high-risk groups by the median value of risk score. We ranked patient by the risk score (Figure 3A) and plotted the dot-plot for the survival status of each patient (Figure 3B). The results showed that the higher risk score patients had, the shorter survival time patients might have. According to the heatmap, the expression levels of ELFN1-AS1, LINC00837, OLMALINC and AL669970.3 were higher in the high-risk group, while AC005332.4 and AC023157.3 were higher in the low-risk group (Figure 3C). The survival curve shows that the patients in the high-risk group had a lower survival time

(Figure 3D). The area under curve (AUC) of 5 years in the train set was 0.937 (Figure 3E).

The same signature was used in the test set and the entire set. And we got similar results in the two sets as we expected. Patients in the low-risk group have better overall survival. The results in the test set (Figures 4A, C, E, G) and the entire set (Figures 4B, D, F, H) were presented in the figure below. The area under curve (AUC) of 5 years in the test set was 0.797, and 0.879 in the entire set (Figures 4I, J).

In order to test whether the signature can better distinguish the risk status, PCA analysis was carried out using the signature and genome-wide expression. When using the signature, the risk status of the patients was separated well (Figure 5A). While it did not display a clear separation when using the whole genome expression (Figure 5B).

Survival Analysis for lncRNAs in the Signature

In order to estimate the effect of expression of individual lncRNAs in the signature, we performed survival analysis for each lncRNA in the signature. Patients with higher expression of AC005332.4 and AC023157.3 indicated better overall survival than those with lower expression (Figures 6A, B). However, the results for other lncRNAs were not statistically significant (Figures 6C–F).

Metastasis Correlation Analysis

The prognosis of osteosarcoma is strongly related to the presence of metastasis, so it is important to verify whether the signature is predictive of metastasis. We carried out metastasis correlation analysis to investigate the potential correlation between risk score and metastasis in the entire set. The result showed that the risk score was correlated to metastatic status ($P=0.0049$) (Figure 7A). And one of the lncRNA, AC023157.3, was down-regulated in metastatic patients ($P<0.05$) (Figure 7B).

Analysis of Tumor Environment and Immune Infiltration

Further analysis by GSEA showed that immune response pathways were enriched in the low-risk groups (Figures 8A, B). The immune score calculated by ESTIMATE algorithm suggested that immune component was significantly higher in the low-risk group ($P<0.01$) (Figure 9A). The stromal

TABLE 1 | Eight lncRNAs obtained after univariable Cox regression analysis.

lncRNA	HR	HR.95L	HR.95H	P value
AL137002.1	1.9475	1.1789	3.2173	0.0093
ELFN1-AS1	1.3253	1.1129	1.5783	0.0016
LINC00837	1.1374	1.0336	1.2516	0.0084
AC010654.1	0.0796	0.0139	0.4565	0.0045
AL669970.3	1.6130	1.1893	2.1877	0.0021
OLMALINC	1.3049	1.0831	1.5721	0.0051
AC005332.4	0.2580	0.0965	0.6900	0.0070
AC023157.3	0.2577	0.1002	0.6630	0.0049

HR: Hazard ratio.

HR.95L: Lower 95% confidence interval of hazard ratio.

HR.95H: Higher 95% confidence interval of hazard ratio.

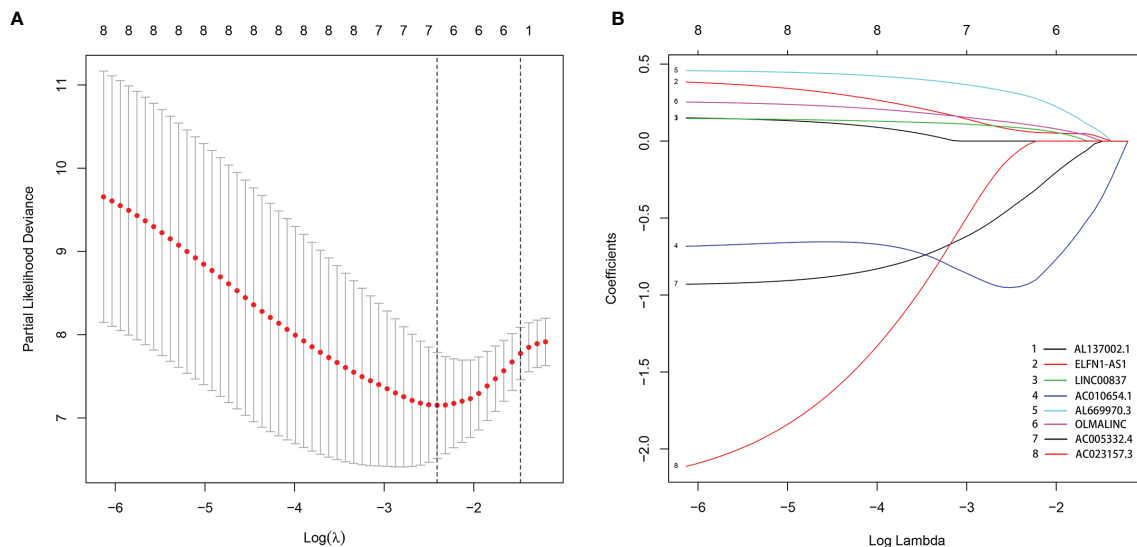


FIGURE 2 | The LASSO regression analysis. When $-3 < \lambda < -2$, the partial likelihood deviation was smallest (A), at which point AL137002.1 was excluded (B).

score was also higher in the low-risk group, but it did not achieve statistical significance ($P > 0.05$) (Figure 9B). The ESTIMATE score was higher in the low-risk group, suggesting the lower tumor purity in low-risk group (Figure 9C). We also found that the risk score was negatively correlated with immune score, stromal score and ESTIMATE score by correlation analysis (Figures 9D–F). We calculated the proportion of 22 immune cell in each sample using the CIBERSORT algorithm. The results showed the main components of the immune environment were T lymphocytes and macrophages (Figure 10A). We then group the samples according to the risk scores, and found that the high-risk group was enriched with CD4⁺ naive T cells ($P = 0.043$), while the low-risk group was enriched with CD8⁺ T cells ($p = 0.041$) and CD4⁺ activated memory T cells ($p = 0.033$) (Figure 10B). In addition, we also analyzed the correlation between risk scores and 22 immune cells, and found risk scores was negatively correlated to CD8⁺ T cells and positively correlated to CD4⁺ naive T cells (Figures 10C, D). We then also analyzed the relationship between each gene in the signature and the proportion of immune cells. ELFN1-AS1 was negatively related

to plasma cells (Figure 11A). LINC00837 was positively related to resting dendritic cells (Figure 11B). AL669970.3 was positively related to activated CD4⁺ memory T cells (Figure 11C). AC023157.3 was positively related to monocytes and M2 macrophages, and negatively related to memory B cells and M0 macrophages (Figures 11D–G). OLMALINC was positively related to activated mast cells, CD4⁺ naive T cells and negatively related to memory B cells (Figures 10H–J). AC005332.4 did not show association with immune cells.

DISCUSSION

Although the application of new treatment has increased overall survival in osteosarcoma, the prognosis for patients, especially the metastatic and recurrent patients, remains poor due to the lack of specific biomarkers and therapeutic target for early diagnosis and precise treatment. Therefore, it is urgent to find specific biomarkers and therapeutic target for osteosarcoma. Studies have emphasized that the immune response in the microenvironment plays a crucial role in the development of a variety of cancers, and lncRNAs are an important regulator of the immune response (21, 22). Many studies have also reported that lncRNAs were involved in the proliferation, metastasis and drug resistance of osteosarcoma (14, 23–26). There are also emerging evidence indicating that immune-related lncRNAs are valuable in predicting prognosis and also maybe targets for specific treatment (27, 28).

Based on a TCGA dataset, we included 85 samples with complete clinical information in our study. Then we identified a potential prognostic six-lncRNAs signature. This signature included ELFN1-AS1, LINC00837, OLMALINC, AL669970.3, AC005332.4 and AC023157.3. It was of great value in predicting

TABLE 2 | Six lncRNAs obtained after multivariable Cox regression analysis.

lncRNA	Coef	HR	HR.95L	HR.95H	P value
ELFN1-AS1	0.4704	1.6006	1.1239	2.2794	0.0091
LINC00837	0.1634	1.1775	1.0381	1.3357	0.0110
AL669970.3	0.4341	1.5436	1.0049	2.3708	0.0474
OLMALINC	0.2696	1.3094	1.0390	1.6502	0.0223
AC005332.4	-1.1261	0.3243	0.0771	1.3640	0.1244
AC023157.3	-2.2230	0.1083	0.0215	0.5447	0.0070

Coef: Coefficient.

HR: Hazard ratio.

HR.95L: Lower 95% confidence interval of hazard ratio.

HR.95H: Higher 95% confidence interval of hazard ratio.

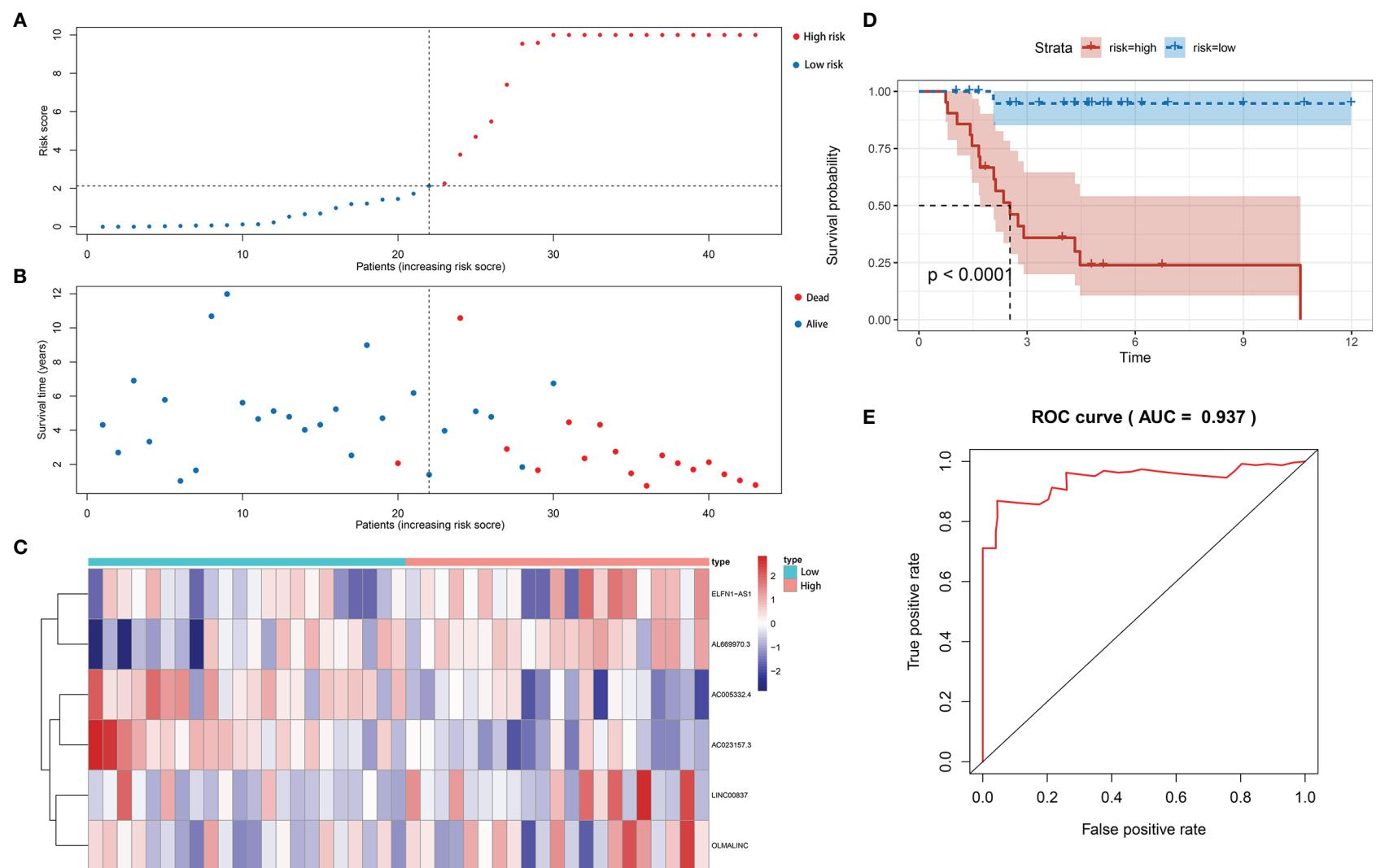


FIGURE 3 | Construction of immune-related lncRNA signature for osteosarcoma. **(A)** The risk curve of each patient reordered by risk score in train set. **(B)** The scatter plot of all patient's survival state in train set. **(C)** The heatmap showed the expression levels of six lncRNAs between the low-risk group and high-risk group in train set. **(D)** Patients in the high-risk group indicated worse overall survival than those in the low-risk group in train set. **(E)** AUC for risk score of 5-year survival according to the ROC curves in train set.

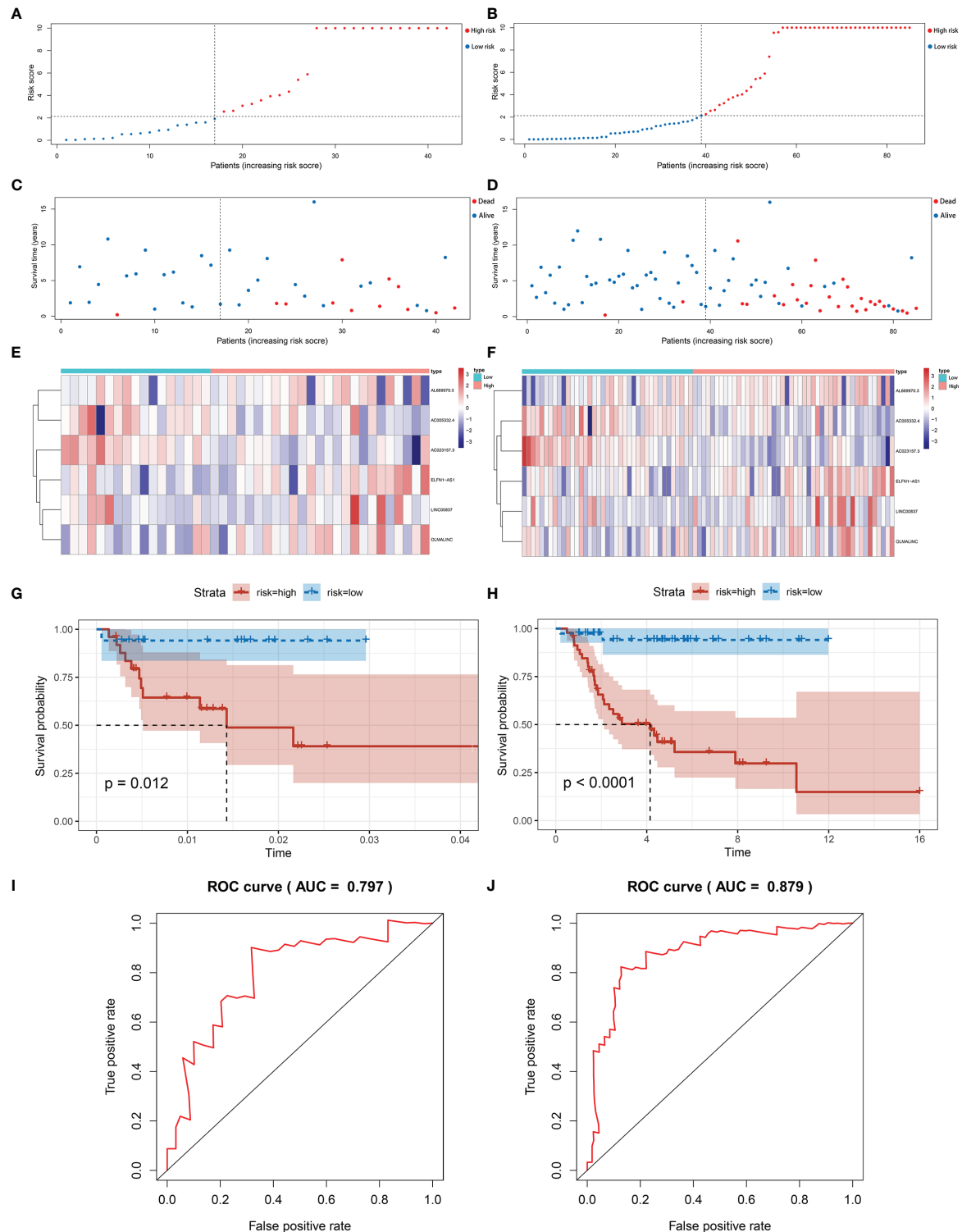


FIGURE 4 | Validation of immune-related lncRNA signature for osteosarcoma. **(A, B)** The risk curve of each patient reordered by risk score in test set and entire set. **(C, D)** The scatter plot of all patient's survival state in test set and entire set. **(E, F)** Patients in the high-risk group indicated worse overall survival than those in the low-risk group in test set and entire set. **(G, H)** The heatmap showed the expression levels of six lncRNAs between the low-risk group and high-risk group in test set and entire set. **(I, J)** AUC for risk score of 5-year survival according to the ROC curves in test set and entire set.

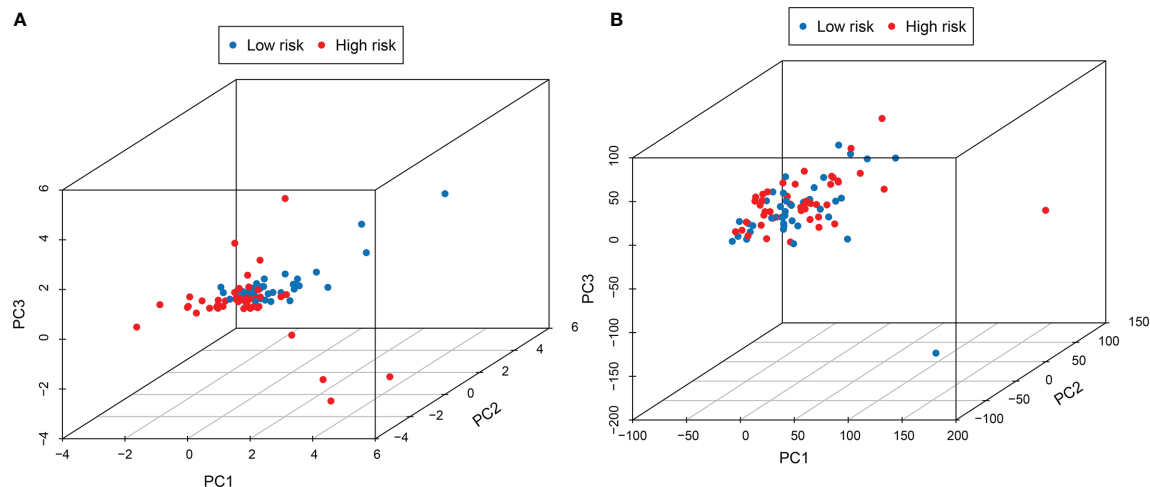


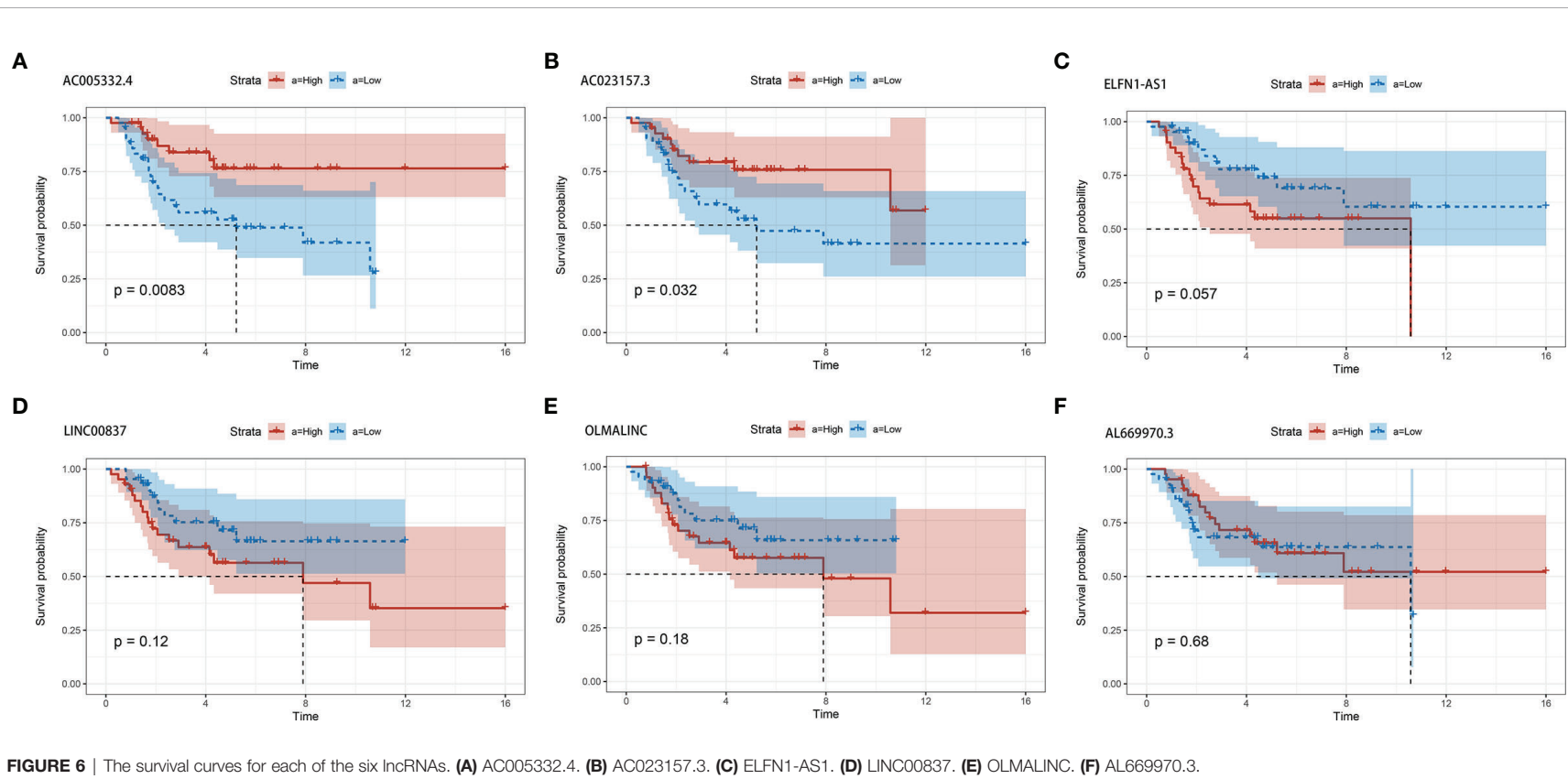
FIGURE 5 | PCA analysis showed that the use of this signature **(A)** could better distinguish the risk status of patients than the use of the whole genome **(B)**.

the prognosis of patients in all set as we hope. The 5-years AUC of ROC was 0.879 in the entire set. The prognosis of almost all tumors is highly correlated with metastasis, especially osteosarcoma. We found that the risk score based on the signature was highly correlated with metastasis, suggesting that signature is also a better predictor of osteosarcoma metastasis. It might be one of the reasons that this signature is such a good predictor of patient outcomes. Principal component analysis showed that the patient's risk status can be well differentiated when using this signature. Moreover, we found that AC005332.4 and AC023157.3 were mainly expressed in the low-risk groups, and they may improve the overall survival of patient. While ELFN1-AS1, LINC00837, OLMALINC and AL669970.3 were mainly expressed in the high-risk groups, and may reduce the overall survival.

Previous research has identified ELFN1-AS1 was overexpressed in tumors and indicated that it might play an essential role in carcinogenesis (29). Importantly, Down-regulation of ELFN1-AS1 could inhibit the proliferation and migration of tumor cells in esophageal cancer and colorectal cancer. ELFN1-AS1 promoted tumor cell proliferation and metastasis by acting as a sponge of miR-183-3p to upregulate GFPT1 in esophageal cancer (30). ELFN1-AS1 could promote proliferation, metastasis and exert anti-apoptosis effect by up-regulating TRIM44 by sponging miR-4644 in colorectal cancer (31). However, till now the specific function of the lncRNA remains unknown in osteosarcoma. In our study, we found that ELFN1-AS1 was negatively related to plasma cells. Plasma cells have been shown to be positively associated with patient prognosis in colon cancer, non-small cell lung cancer and triple-negative breast cancer (32–34). We speculate that ELFN1-AS1 may influence the development of osteosarcoma by affecting the proliferation and function of plasma cells, and the exact mechanism remains to be further investigated. OLMALINC was reported to overexpress in the white matter of the human brain, which played a role in maintaining the maturation of oligodendrocytes (35). In our

study, we found that OLMALINC was positively related to activated mast cells and CD4⁺ naive T cells, and negatively related to memory B cells. Mast cells have been observed to increase in tumor and peritumor tissues (36). However, Mast cells have different roles in different types of tumors. Mast cells were associated with promoting tumorigenesis in bladder cancer, colorectal cancer, lung cancer and hepatocellular cancer (37–40). Mast cells have antitumor activities in breast cancer, diffuse large B-cell lymphoma and ovarian cancer (41–43). Naive T cells were reported to express functional CXCL8 and promote tumorigenesis (44). Blocking naive CD4⁺ T cell recruitment into tumors reversed immunosuppression in breast cancer, which may be an attractive strategy for antitumor treatment (45). Memory B cells were associated with a good prognosis in gastric cancer and non-small cell lung cancer (46, 47). These studies were consistent with our results. OLMALINC may affect osteosarcoma development by inhibiting memory B cell proliferation and function, recruiting mast cells, and naive CD4⁺ T cells.

While, there was little research studied on the role of LINC00837, AL669970.3, AC005332.4 and AC023157.3. In our study, we found that LINC00837 was positively related to resting dendritic cells. Dendritic cells are the most important antigen-presenting cells in the immune system, playing a key role in regulating immunity. However, resting dendritic cells can induce immune tolerance through T cell deletion and induction of regulatory T cells (48). AL669970.3 was positively related to activated T CD4⁺ memory cells. But this is contrary to our common perception that activated T CD4⁺ memory cells can positively modulate immune function and inhibit tumor growth (49). It warrants further investigation. AC023157.3 was positively related to monocytes and M2 macrophages, while negatively related to memory B cells and M0 macrophages. Using a three-dimensional vascularized microfluidic model, Boussommier-Calleja et al. demonstrated that monocytes were able to directly reduce cancer cell extravasation, but that such an effect was lost when monocytes



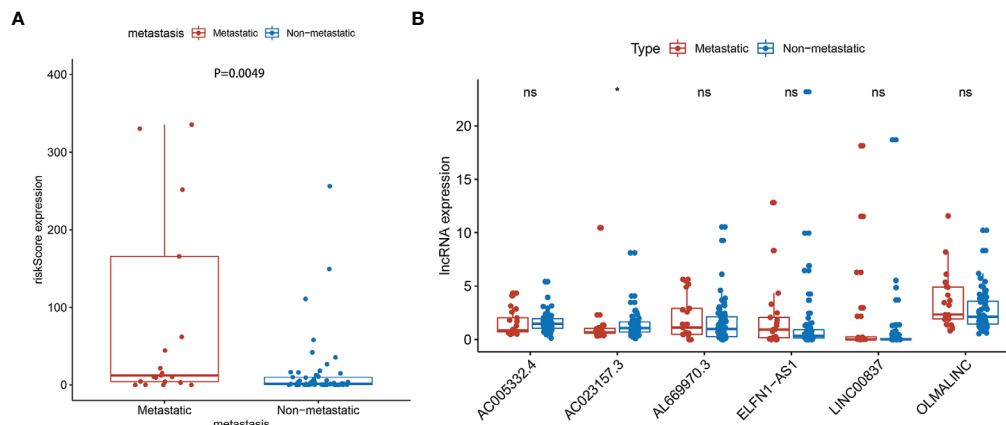


FIGURE 7 | Metastasis correlation analysis in the entire sets. **(A)** The risk score was correlated with metastatic ($P=0.0049$) (Some outliers are not shown in the figure). **(B)** AC023157.3 was highly correlated with metastasis ($P<0.05$). *: $P<0.05$, ns: $P>0.05$.

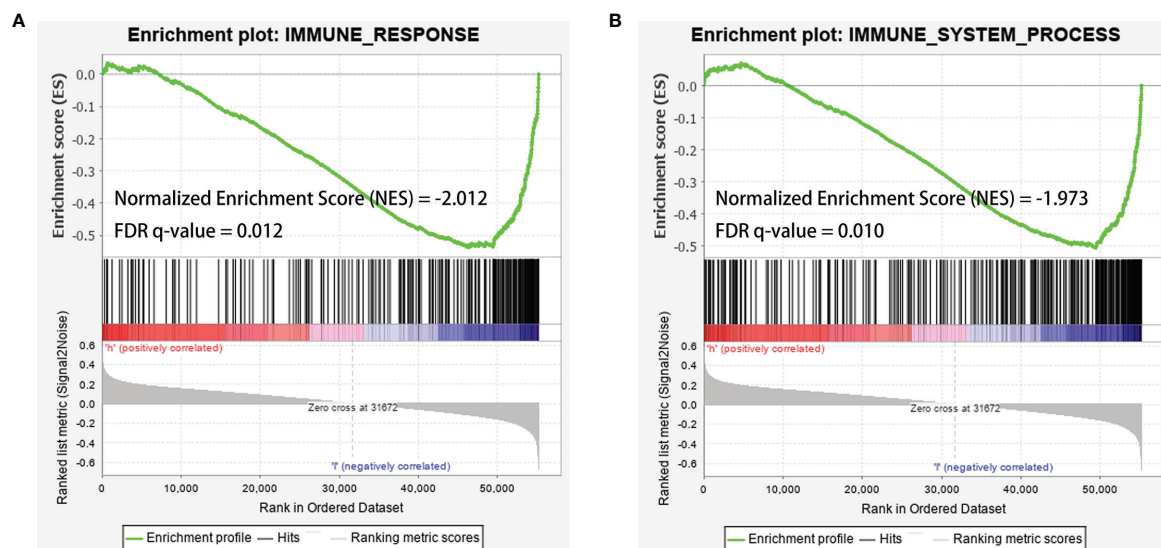


FIGURE 8 | GSEA analysis showed that immune-related responses were enriched in the low-risk groups. **(A)** GSEA analysis based on IMMUNE_RESPONSE gene set. **(B)** GSEA analysis based on IMMUNE_SYSTEM_PROCESS gene set. The green line was the running enrichment score (ES) for the gene set as the analysis walks down the ranked list. A positive value of ES indicates that the gene set was enriched in the high risk group, and a negative value of ES indicates that the gene set was enriched in the low risk group. The ranking metric score indicated a gene's correlation with a phenotype. A positive value refers to high risk and a negative value refers to low risk. NES, normalized enrichment score; FDR, false discovery rates.

were converted to macrophages (50). Many studies have suggested that M2 polarized tumor-associated-macrophages (TAM) are associated with tumor growth, invasion, and metastasis (51, 52). However, Anne Gomez-Brouchet et al. found that the presence of CD163-positive M2-polarized macrophages was critical to inhibit OS progression (53). This suggests that M2-polarized macrophages may be influenced by other factors to exert distinctly different pro- or anti-tumor effects. Zhang et al. indicated that the level of polarization of M0 to M1 or M2 macrophages may be an important factor (54). It was also reported that the balance

between M1 and M2 macrophage would affect the PD-1/PDL-1, which is an important immune regulatory system (55). In addition, we found that among these six RNAs, AC023157.3 was highly expressed in patients without metastasis. We speculate that AC023157.3 may inhibit tumor growth and metastasis by promoting the proliferation and function of monocytes and by regulating the level of polarization of M0 to M1 or M2 macrophages. The specific mechanism deserves further investigation. Combined with the above findings, we found that all the six RNAs in the signature had some relationship with tumorigenesis or the immune

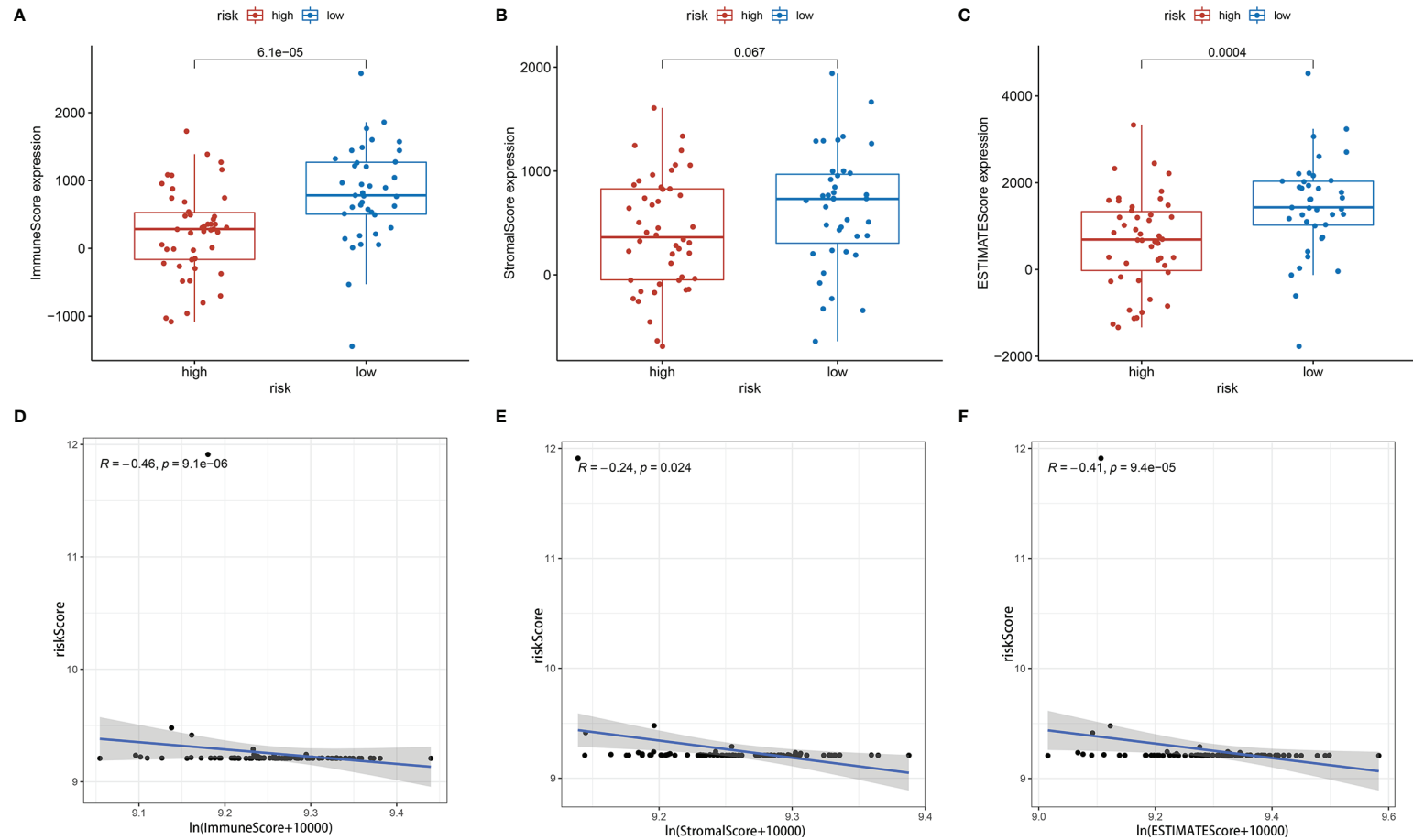


FIGURE 9 | Tumor microenvironment analysis showed risk score was negatively correlated with tumor purity. **(A)** Immune score between high-risk group and low-risk group. **(B)** Stromal score between high-risk group and low-risk group. **(C)** ESTIMATE score between high-risk group and low-risk group. **(D–F)** Immune score, stromal score and ESTIMATE score were negatively correlated with risk score.

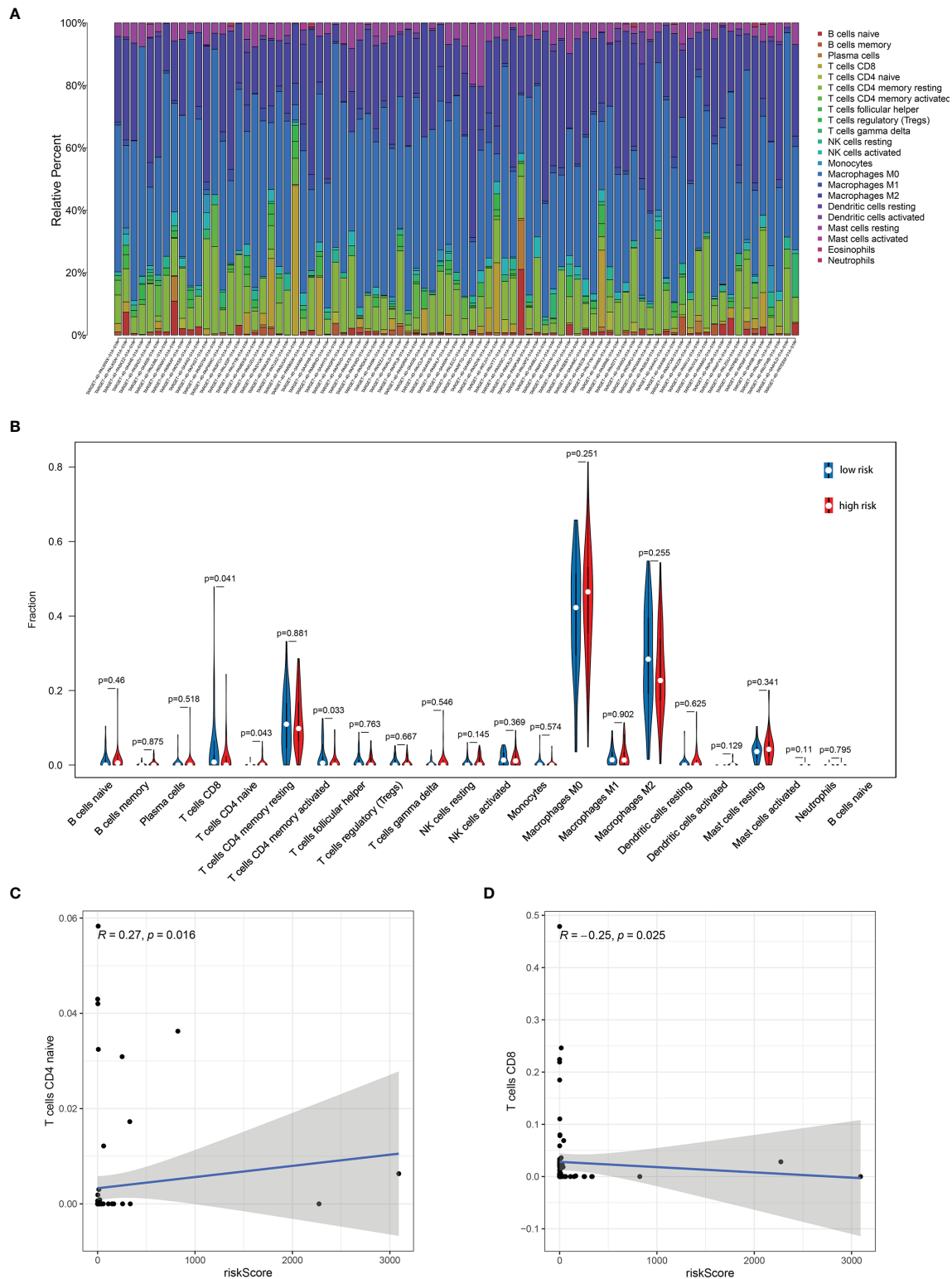


FIGURE 10 | Immune infiltration analysis showed the relationship between risk score and immune cells. **(A)** The main components of the immune environment were T-lymphocytes and macrophages in osteosarcoma. **(B)** The composition of immune cells between high-risk group and low-risk group. **(C, D)** Risk score was negatively correlated to CD8⁺ T cells and positively correlated to CD4⁺ naive T cells.

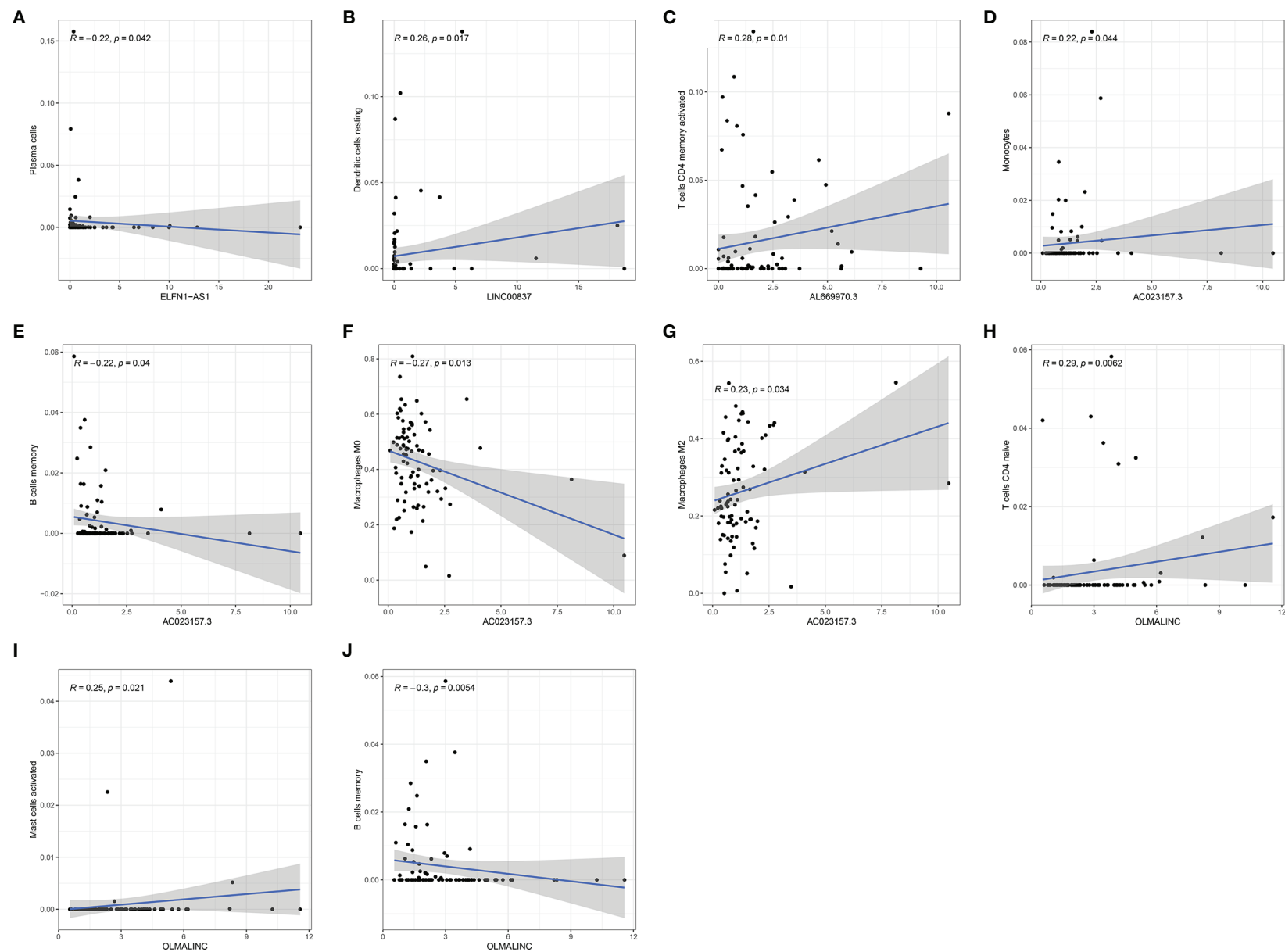


FIGURE 11 | The relationship of each gene in the signature to the immune cells. **(A)** ELFN1-AS1. **(B)** LINC00837. **(C)** AL669970.3. **(D–G)** AC023157.3. **(H–J)** OLMALINC.

system, which could provide a theoretical basis for immunotherapy of osteosarcoma.

We analyzed the enrichment of immune-related pathways in high- and low-risk groups by GSEA analysis, and found that the immune-related pathways were mainly enriched in the low-risk group, suggesting that the development of osteosarcoma may be highly associated with a lack of immune response. ESTIMATE analysis showed that the low-risk group contained more immune cells with a higher immune score and ESTIMATE score, indicating the lower tumor purity. The risk score was also negatively correlated with immune score, stromal score and ESTIMATE score. The results indicated that risk scores were positively correlated with tumor purity. There were studies reported that a lower tumor purity and more immune cell components mean a poor prognosis (19, 54). However, it was different in osteosarcoma that patients with increased microenvironmental immune cell infiltration had a better prognosis (54), which was consistent with our results. It was reported that the main components of the immune environment in osteosarcoma are T-lymphocytes and macrophages (55). CIBERSORT analysis in our study showed similar results. There were more mature lymphocytes, including CD8⁺ T cells ($p=0.041$) and CD4⁺ activated memory T cells, enriched in the low-risk group. Meanwhile, CD4⁺ naive T cells were enriched in the high-risk group. The risk scores were also negatively correlated to CD8⁺ T cells, while positively correlated to CD4⁺ naive T cells. These results suggested immature immune function in the high-risk group might be an important factor for the development of osteosarcoma. Therefore, targeting the immune system and changing the composition and proportion of immune cells in the tumor microenvironment is a promising treatment option for osteosarcoma.

However, our study has limitations. First, the sample sizes of osteosarcoma are small. More data is needed to verify the accuracy of the signature. Second, because the microarray data

for osteosarcoma are relatively scarce and the platforms used are relatively old, which are not sensitive enough for lncRNA, we did not find other external cohorts with survival information to validate the signature. Third, we need further experiments, such as immunohistochemical analysis, PCR, or western blot, to support these findings. Despite these limitations, we constructed a six lncRNAs signature with a good prognostic value in osteosarcoma. These lncRNAs may play essential roles in the progression of osteosarcoma. They deserve further study.

CONCLUSION

In conclusion, we identified an immune-related lncRNAs for osteosarcoma, which possess good performance in the prediction of survival, metastasis and immune microenvironment. Our study not only has great significance in predicting the prognosis but also has potential to guide future immunotherapy in osteosarcoma.

DATA AVAILABILITY STATEMENT

Publicly available datasets were analyzed in this study. This data can be found here: <https://portal.gdc.cancer.gov/>.

AUTHOR CONTRIBUTIONS

HC and YH performed the conception and design of this manuscript. HZ provided useful suggestions in methodology. HZ and HX performed data analysis and prepared the figures. YH drafted the manuscript. HC and HY revised the manuscript. All authors read and approved the final manuscript.

REFERENCES

- Luetke A, Meyers PA, Lewis I, Juergens H. Osteosarcoma Treatment - Where Do We Stand? A State of the Art Review. *Cancer Treat Rev* (2014) 40(4):523–32. doi: 10.1016/j.ctrv.2013.11.006
- Ritter J, Bielack SS. Osteosarcoma. *Ann Oncol* (2010) 21 Suppl 7:vii320–5. doi: 10.1093/annonc/mdq276
- Ottaviani G, Jaffe N. The Epidemiology of Osteosarcoma. *Cancer Treat Res* (2009) 152:3–13. doi: 10.1007/978-1-4419-0284-9_1
- Rickel K, Fang F, Tao J. Molecular Genetics of Osteosarcoma. *Bone* (2017) 102:69–79. doi: 10.1016/j.bone.2016.10.017
- Evola FR, Costarella L, Pavone V, Caff G, Cannavo L, Sessa A, et al. Biomarkers of Osteosarcoma, Chondrosarcoma, and Ewing Sarcoma. *Front Pharmacol* (2017) 8:150. doi: 10.3389/fphar.2017.00150
- Chen R, Wang G, Zheng Y, Hua Y, Cai Z. Drug Resistance-Related microRNAs in Osteosarcoma: Translating Basic Evidence Into Therapeutic Strategies. *J Cell Mol Med* (2019) 23(4):2280–92. doi: 10.1111/jcmm.14064
- Chindamo G, Sapino S, Peira E, Chirio D, Gonzalez MC, Gallarate M. Bone Diseases: Current Approach and Future Perspectives in Drug Delivery Systems for Bone Targeted Therapeutics. *Nanomaterial (Basel)* (2020) 10(5):875. doi: 10.3390/nano10050875
- Izadpanah S, Shabani P, Aghebati-Maleki A, Baghbanzadeh A, Fotouhi A, Bisadi A, et al. Prospects for the Involvement of Cancer Stem Cells in the Pathogenesis of Osteosarcoma. *J Cell Physiol* (2020) 235(5):4167–82. doi: 10.1002/jcp.29344
- Yu WD, Wang H, He QF, Xu Y, Wang XC. Long Noncoding RNAs in Cancer-Immunity Cycle. *J Cell Physiol* (2018) 233(9):6518–23. doi: 10.1002/jcp.26568
- Huarte M. The Emerging Role of lncRNAs in Cancer. *Nat Med* (2015) 21(11):1253–61. doi: 10.1038/nm.3981
- Chen Y, Li C, Pan Y, Han S, Feng B, Gao Y, et al. The Emerging Role and Promise of Long Noncoding RNAs in Lung Cancer Treatment. *Cell Physiol Biochem* (2016) 38(6):2194–206. doi: 10.1159/000445575
- Bhan A, Soleimani M, Mandal SS. Long Noncoding RNA and Cancer: A New Paradigm. *Cancer Res* (2017) 77(15):3965–81. doi: 10.1158/0008-5472.Can-16-2634
- Fu XM, Guo W, Li N, Liu HZ, Liu J, Qiu SQ, et al. The Expression and Function of Long Noncoding RNA lncRNA-ATB in Papillary Thyroid Cancer. *Eur Rev Med Pharmacol Sci* (2017) 21(14):3239–46.
- Pasic I, Shlien A, Durbin AD, Stavropoulos DJ, Baskin B, Ray PN, et al. Recurrent Focal Copy-Number Changes and Loss of Heterozygosity Implicate Two Noncoding RNAs and One Tumor Suppressor Gene at Chromosome 3q13.31 in Osteosarcoma. *Cancer Res* (2010) 70(1):160–71. doi: 10.1158/0008-5472.Can-09-1902
- Zhou H, Chen A, Shen J, Zhang X, Hou M, Li J, et al. Long Non-Coding RNA LOC285194 Functions as a Tumor Suppressor by Targeting P53 in Non-Small

- Cell Lung Cancer. *Oncol Rep* (2019) 41(1):15–26. doi: 10.3892/or.2018.6839
16. Renganathan A, Felley-Bosco E. Long Noncoding RNAs in Cancer and Therapeutic Potential. *Adv Exp Med Biol* (2017) 1008:199–222. doi: 10.1007/978-981-10-5203-3_7
 17. Subramanian A, Tamayo P, Mootha VK, Mukherjee S, Ebert BL, Gillette MA, et al. Gene Set Enrichment Analysis: A Knowledge-Based Approach for Interpreting Genome-Wide Expression Profiles. *Proc Natl Acad Sci USA* (2005) 102(43):15545–50. doi: 10.1073/pnas.0506580102
 18. Liberzon A, Birger C, Thorvaldsdóttir H, Ghandi M, Mesirov JP, Tamayo P. The Molecular Signatures Database (MSigDB) Hallmark Gene Set Collection. *Cell Syst* (2015) 1(6):417–25. doi: 10.1016/j.cels.2015.12.004
 19. Yoshihara K, Shahmoradgol M, Martínez E, Vegesna R, Kim H, Torres-García W, et al. Inferring Tumour Purity and Stromal and Immune Cell Admixture From Expression Data. *Nat Commun* (2013) 4:2612. doi: 10.1038/ncomms3612
 20. Chen B, Khodadoust MS, Liu CL, Newman AM, Alizadeh AA. Profiling Tumor Infiltrating Immune Cells With CIBERSORT. *Methods Mol Biol* (2018) 1711:243–59. doi: 10.1007/978-1-4939-7493-1_12
 21. Rooney MS, Shukla SA, Wu CJ, Getz G, Hacohen N. Molecular and Genetic Properties of Tumors Associated With Local Immune Cytolytic Activity. *Cell* (2015) 160(1–2):48–61. doi: 10.1016/j.cell.2014.12.033
 22. Wang L, Felts SJ, Van Keulen VP, Scheid AD, Block MS, Markovic SN, et al. Integrative Genome-Wide Analysis of Long Noncoding RNAs in Diverse Immune Cell Types of Melanoma Patients. *Cancer Res* (2018) 78(15):4411–23. doi: 10.1158/0008-5472.Can-18-0529
 23. Li M, Chen H, Zhao Y, Gao S, Cheng C. H19 Functions as a ceRNA in Promoting Metastasis Through Decreasing miR-200s Activity in Osteosarcoma. *DNA Cell Biol* (2016) 35(5):235–40. doi: 10.1089/dna.2015.3171
 24. Sun J, Wang X, Fu C, Wang X, Zou J, Hua H, et al. Long Noncoding RNA FGFR3-AS1 Promotes Osteosarcoma Growth Through Regulating Its Natural Antisense Transcript Fgfr3. *Mol Biol Rep* (2016) 43(5):427–36. doi: 10.1007/s11033-016-3975-1
 25. Zhang CL, Zhu KP, Shen GQ, Zhu ZS. A Long non-Coding RNA Contributes to Doxorubicin Resistance of Osteosarcoma. *Tumour Biol* (2016) 37(2):2737–48. doi: 10.1007/s13277-015-4130-7
 26. Shen P, Cheng Y. Long Noncoding RNA IncARSR Confers Resistance to Adriamycin and Promotes Osteosarcoma Progression. *Cell Death Dis* (2020) 11(5):362. doi: 10.1038/s41419-020-2573-2
 27. Li X, Meng Y. Survival Analysis of Immune-Related lncRNA in Low-Grade Glioma. *BMC Cancer* (2019) 19(1):813. doi: 10.1186/s12885-019-6032-3
 28. Khadirnaikar S, Kumar P, Pandi SN, Malik R, Dhanasekaran SM, Shukla SK. Immune Associated lncRNAs Identify Novel Prognostic Subtypes of Renal Clear Cell Carcinoma. *Mol Carcinog* (2019) 58(4):544–53. doi: 10.1002/mc.22949
 29. Polev DE, Karnaukhova IK, Krukovskaya LL, Kozlov AP. ELFN1-AS1: A Novel Primate Gene With Possible microRNA Function Expressed Predominantly in Human Tumors. *BioMed Res Int* (2014) 2014:398097. doi: 10.1155/2014/398097
 30. Zhang C, Lian H, Xie L, Yin N, Cui Y. lncRNA ELFN1-AS1 Promotes Esophageal Cancer Progression by Up-Regulating GFPT1 via Sponging miR-183-3p. *Biol Chem* (2020) 401(9):1053–61. doi: 10.1515/hsz-2019-0430
 31. Lei R, Feng L, Hong D. ELFN1-AS1 Accelerates the Proliferation and Migration of Colorectal Cancer via Regulation of miR-4644/TRIM44 Axis. *Cancer Biomark* (2020) 27(4):433–43. doi: 10.3233/cbm-190559
 32. Berntsson J, Nodin B, Eberhard J, Mücke P, Jirström K. Prognostic Impact of Tumor-Infiltrating B Cells and Plasma Cells in Colorectal Cancer. *Int J Cancer* (2016) 139(5):1129–39. doi: 10.1002/ijc.30138
 33. Yeong J, Lim JCT, Lee B, Li H, Chia N, Ong CCH, et al. High Densities of Tumor-Associated Plasma Cells Predict Improved Prognosis in Triple Negative Breast Cancer. *Front Immunol* (2018) 9:1209. doi: 10.3389/fimmu.2018.01209
 34. Gholiha AR, Hollander P, Hedstrom G, Sundstrom C, Molin D, Smedby KE, et al. High Tumour Plasma Cell Infiltration Reflects an Important Microenvironmental Component in Classic Hodgkin Lymphoma Linked to Presence of B-Symptoms. *Br J Haematol* (2019) 184(2):192–201. doi: 10.1111/bjh.15703
 35. Mills JD, Kavanagh T, Kim WS, Chen BJ, Waters PD, Halliday GM, et al. High Expression of Long Intervening Non-Coding RNA OLMALINC in the Human Cortical White Matter Is Associated With Regulation of Oligodendrocyte Maturation. *Mol Brain* (2015) 8:2. doi: 10.1186/s13041-014-0091-9
 36. Marone G, Varricchi G, Loffredo S, Granata F. Mast Cells and Basophils in Inflammatory and Tumor Angiogenesis and Lymphangiogenesis. *Eur J Pharmacol* (2016) 778:146–51. doi: 10.1016/j.ejphar.2015.03.088
 37. Takanami I, Takeuchi K, Naruke M. Mast Cell Density Is Associated With Angiogenesis and Poor Prognosis in Pulmonary Adenocarcinoma. *Cancer* (2000) 88(12):2686–92. doi: 10.1002/1097-0142(20000615)88:12<2686::AID-CNCR6>3.0.CO;2-6
 38. Ammendola M, Sacco R, Sammarco G, Donato G, Montemurro S, Ruggieri E, et al. Correlation Between Serum Tryptase, Mast Cells Positive to Tryptase and Microvascular Density in Colo-Rectal Cancer Patients: Possible Biological-Clinical Significance. *PLoS One* (2014) 9(6):e99512. doi: 10.1371/journal.pone.0099512
 39. Rao Q, Chen Y, Yeh CR, Ding J, Li L, Chang C, et al. Recruited Mast Cells in the Tumor Microenvironment Enhance Bladder Cancer Metastasis via Modulation of ErbB/CCL2/CCR2 EMT/MMP9 Signals. *Oncotarget* (2016) 7(7):7842–55. doi: 10.18632/oncotarget.5467
 40. Tu JF, Pan HY, Ying XH, Lou J, Ji JS, Zou H. Mast Cells Comprise the Major of Interleukin 17-Producing Cells and Predict a Poor Prognosis in Hepatocellular Carcinoma. *Med (Baltimore)* (2016) 95(13):e3220. doi: 10.1097/md.0000000000003220
 41. Chan JK, Magistris A, Loizzi V, Lin F, Rutgers J, Osann K, et al. Mast Cell Density, Angiogenesis, Blood Clotting, and Prognosis in Women With Advanced Ovarian Cancer. *Gynecol Oncol* (2005) 99(1):20–5. doi: 10.1016/j.ygyno.2005.05.042
 42. Hedström G, Berglund M, Molin D, Fischer M, Nilsson G, Thunberg U, et al. Mast Cell Infiltration Is a Favourable Prognostic Factor in Diffuse Large B-Cell Lymphoma. *Br J Haematol* (2007) 138(1):68–71. doi: 10.1111/j.1365-2141.2007.06612.x
 43. Rajput AB, Turbin DA, Cheang MC, Voduc DK, Leung S, Gelmon KA, et al. Stromal Mast Cells in Invasive Breast Cancer are a Marker of Favourable Prognosis: A Study of 4,444 Cases. *Breast Cancer Res Treat* (2008) 107(2):249–57. doi: 10.1007/s10549-007-9546-3
 44. Crespo J, Wu K, Li W, Kryczek I, Maj T, Vatan L, et al. Human Naive T Cells Express Functional CXCL8 and Promote Tumorigenesis. *J Immunol* (2018) 201(2):814–20. doi: 10.4049/jimmunol.1700755
 45. Su S, Liao J, Liu J, Huang D, He C, Chen F, et al. Blocking the Recruitment of Naive CD4(+) T Cells Reverses Immunosuppression in Breast Cancer. *Cell Res* (2017) 27(4):461–82. doi: 10.1038/cr.2017.34
 46. Centuori SM, Gomes CJ, Kim SS, Putnam CW, Larsen BT, Garland LL, et al. Double-Negative (CD27(-)IgD(-)) B Cells Are Expanded in NSCLC and Inversely Correlate With Affinity-Matured B Cell Populations. *J Transl Med* (2018) 16(1):30. doi: 10.1186/s12967-018-1404-z
 47. Ni Z, Xing D, Zhang T, Ding N, Xiang D, Zhao Z, et al. Tumor-Infiltrating B Cell Is Associated With the Control of Progression of Gastric Cancer. *Immunol Res* (2021) 69(1):43–52. doi: 10.1007/s12026-020-09167-z
 48. Adema GJ. Dendritic Cells From Bench to Bedside and Back. *Immunol Lett* (2009) 122(2):128–30. doi: 10.1016/j.imlet.2008.11.017
 49. Broderick L, Yokota SJ, Reineke J, Mathiowitz E, Stewart CC, Barcos M, et al. Human CD4+ Effector Memory T Cells Pervsist in the Microenvironment of Lung Cancer Xenografts are Activated by Local Delivery of IL-12 to Proliferate, Produce IFN-Gamma, and Eradicate Tumor Cells. *J Immunol* (2005) 174(2):898–906. doi: 10.4049/jimmunol.174.2.898
 50. Boussemnier-Calleja A, Atiyas Y, Haase K, Headley M, Lewis C, Kamm RD. The Effects of Monocytes on Tumor Cell Extravasation in a 3D Vascularized Microfluidic Model. *Biomaterials* (2019) 198:180–93. doi: 10.1016/j.biomaterials.2018.03.005
 51. Yamaguchi T, Fushida S, Yamamoto Y, Tsukada T, Kinoshita J, Oyama K, et al. Tumor-Associated Macrophages of the M2 Phenotype Contribute to Progression in Gastric Cancer With Peritoneal Dissemination. *Gastric Cancer* (2016) 19(4):1052–65. doi: 10.1007/s10120-015-0579-8
 52. Yao RR, Li JH, Zhang R, Chen RX, Wang YH. M2-Polarized Tumor-Associated Macrophages Facilitated Migration and Epithelial-Mesenchymal Transition of HCC Cells via the TLR4/STAT3 Signaling Pathway. *World J Surg Oncol* (2018) 16(1):9. doi: 10.1186/s12957-018-1312-y
 53. Gomez-Brouchet A, Illac C, Gilhodes J, Bouvier C, Aubert S, Guinebretiere JM, et al. CD163-Positive Tumor-Associated Macrophages and CD8-Positive Cytotoxic Lymphocytes are Powerful Diagnostic Markers for the Therapeutic Stratification of Osteosarcoma Patients: An Immunohistochemical Analysis of

- the Biopsies From the French OS2006 Phase 3 Trial. *Oncoimmunology* (2017) 6(9):e1331193. doi: 10.1080/2162402x.2017.1331193
54. Zhang C, Zheng JH, Lin ZH, Lv HY, Ye ZM, Chen YP, et al. Profiles of Immune Cell Infiltration and Immune-Related Genes in the Tumor Microenvironment of Osteosarcoma. *Aging (Albany NY)* (2020) 12(4):3486–501. doi: 10.18632/aging.102824
55. Heymann MF, Lézot F, Heymann D. The Contribution of Immune Infiltrates and the Local Microenvironment in the Pathogenesis of Osteosarcoma. *Cell Immunol* (2019) 343:103711. doi: 10.1016/j.cellimm.2017.10.011

Conflict of Interest: The authors declare that the research was conducted in the absence of any commercial or financial relationships that could be construed as a potential conflict of interest.

Publisher's Note: All claims expressed in this article are solely those of the authors and do not necessarily represent those of their affiliated organizations, or those of the publisher, the editors and the reviewers. Any product that may be evaluated in this article, or claim that may be made by its manufacturer, is not guaranteed or endorsed by the publisher.

Copyright © 2022 He, Zhou, Xu, You and Cheng. This is an open-access article distributed under the terms of the Creative Commons Attribution License (CC BY). The use, distribution or reproduction in other forums is permitted, provided the original author(s) and the copyright owner(s) are credited and that the original publication in this journal is cited, in accordance with accepted academic practice. No use, distribution or reproduction is permitted which does not comply with these terms.



The Emerging Roles of Circ-ABCB10 in Cancer

Zhenjun Huang¹, Renfeng Shan¹, Wu Wen¹, Jianfeng Li¹, Xiaohong Zeng^{2*} and Renhua Wan^{1*}

¹Department of General Surgery, The First Affiliated Hospital of Nanchang University, Nanchang University, Nanchang, China,

²Imaging Department, The First Affiliated Hospital of Nanchang University, Nanchang University, Nanchang, China

OPEN ACCESS

Edited by:

Zong Sheng Guo,
Roswell Park Comprehensive Cancer
Center, United States

Reviewed by:

Thasni Karedath,
Qatar Biomedical Research Institute,
Qatar

Demitrios Vynios,
University of Patras, Greece
Carlo V. Bruschi,
University of Salzburg, Austria

*Correspondence:

Xiaohong Zeng
Zeng775112840@qq.com
Renhua Wan
Wanzww726696@sina.com

Specialty section:

This article was submitted to
Molecular and Cellular Oncology,
a section of the journal
Frontiers in Cell and Developmental
Biology

Received: 25 September 2021

Accepted: 30 March 2022

Published: 13 May 2022

Citation:

Huang Z, Shan R, Wen W, Li J, Zeng X
and Wan R (2022) The Emerging Roles
of Circ-ABCB10 in Cancer.
Front. Cell Dev. Biol. 10:782938.
doi: 10.3389/fcell.2022.782938

Circular RNAs (circRNAs) are non-coding RNAs (ncRNAs) without 5' caps and 3' tails, which are formed from precursor mRNAs (pre-mRNAs) that are inversely back-spliced by exons. CircRNAs are characterized by a covalently closed circular structure and are abundantly expressed in eukaryotic cells. With the development of RNA-sequencing, it was discovered that circRNAs play important roles in the regulation of numerous human genes and are related to the occurrence, development, and prognosis of diseases. Studies in various cancers have revealed that circRNAs have both positive and negative effects on the occurrence and development of tumors. Circ-ABCB10, a circular RNA originating from exons of ABCB10 located on chromosome 1q42, has been proven to play an important role in different types of cancers. Here, we report the primary findings of recent research studies by many contributors about the roles of circ-ABCB10 in cancer and clearly formulate its influence and functions in different aspects of cancer biology, which gives us a broad picture of circ-ABCB10. Thus, this study aimed to generalize the roles of circ-ABCB10 in the diagnosis and treatment of different types of tumors and its related miRNA genes. In this way, we wish to provide a sufficient understanding and assess the future development direction of the research on circ-ABCB10.

Keywords: circRNA, circ-ABCB10, cancer, microRNA, tumor biology

INTRODUCTION

Circular RNAs (circRNAs) are a class of endogenous single-stranded closed circular RNAs formed by reverse splicing and covalent binding without a 5' cap and 3' poly (a) tail (Sanger et al., 1976; Chen, 2016; Pamudurti et al., 2017; Kristensen et al., 2018; Qu et al., 2018). CircRNAs were first discovered in RNA viruses in 1976 (Sanger et al., 1976) and were initially considered "splicing noise" in organisms but have become a research hotspot in the meantime (Kristensen et al., 2018). With the rapid development of RNA-sequencing technology, many circRNAs have been discovered. To date, more than 30,000 cyclic RNAs with unique structures have been identified and have attracted increasing attention. Most circRNAs are evolutionarily conserved across species (Pamudurti et al., 2017). CircRNAs can originate from introns, exons, or from both introns and exons (Su et al., 2019; Yu and Kuo, 2019). Because circRNAs have a specific closed-ring structure, they are more resistant to exonucleases than linear RNAs (Salzman et al., 2013; Shang et al., 2019). In addition, most circRNAs are usually found in the cytoplasm and are derived from protein-coding genes. These genes contain one or more exons toward the 5' cap of the gene, with long introns on both sides (Dong et al., 2017a; Nicolet et al., 2018). The long introns containing the wing region will become circRNAs, which usually contain specific sequences (Qu et al., 2015). They can induce the formation of circRNAs by mutually complementing with circRNA promoters and are usually expressed in a cell type- or tissue-specific manner (Patop and

Kadener, 2018; Shi et al., 2020). Moreover, it was found that circRNAs are abnormally expressed in colorectal cancer (CRC) and osteoarthritis (Bachmayr-Heyda et al., 2015; Yang et al., 2020a). Thus, circRNAs are widely expressed in various human cell types and will perhaps become a new direction in research on disease biomarkers for aging (Bahn et al., 2015) and therapy (Hou and Zhang, 2017; Tang et al., 2017). According to gene structures and their specific molecular cycling mechanisms, circRNAs are divided into four types: exonic circRNAs (ecRNAs) (Salzman et al., 2012), circular intronic RNAs (ciRNAs) (Zhang et al., 2013), exon-intron circRNAs (eiRNAs) (Li et al., 2015), and intergenic circRNAs (Tang and Hann, 2020). Generally speaking, ecRNAs are mainly found in the cytoplasm (Memczak et al., 2013) and regulate the expression of genes. ciRNAs and eiRNAs tend to be localized in the nucleus and play a significant role in regulating parental genes.

Studies have shown that circRNAs produced *via* back-splicing feature different biogenesis than typical splicing of linear RNA. First, acting as miRNA sponges, circRNAs are more likely to bind to other miRNAs and are known as “super sponges” (Hansen et al., 2013). According to previous reports, circRNAs can inhibit miRNAs from binding to their target genes (Thomas and Sætrum, 2014). Second, by binding to proteins and RNA-binding proteins (RBPs), circRNAs can affect their function and interaction with other proteins (Zang et al., 2020). Studies demonstrate that RBPs can also regulate the formation of circRNAs by forming RNA-protein complexes (RPCs) (Conn et al., 2015). Third, circRNAs retained in the nucleus can regulate alternative splicing, transcription, or translation (Li et al., 2018a; Guarnierio et al., 2019). For example, Circ-ubr5 might undergo a specific RNA-RNA interaction by binding to the splicing regulator QKI (Qin et al., 2018). CircITGA7 could increase the transcriptional expression of integrin alpha 7 (ITGA7) by inhibiting RAS-responsive element-binding protein 1 (RREB1) (Li et al., 2018a).

Moreover, circRNAs can function as autophagy regulators, affecting tumorigenesis. For example, Circ_104075 was found to act as an autophagy regulator in glioma cells (Chi et al., 2019). In general, the abnormal expression of circRNAs is associated with the occurrence and progression of human cancer by affecting the growth, migration, invasion, proliferation, and other pathological processes of cells (Conn et al., 2015; Khan et al., 2016; Dong et al., 2019). In addition, circRNAs are also associated with clinicopathological characteristics, such as lymph node metastasis, differentiation, or distant metastasis. All of these findings provide the basis for potential biomarkers and therapeutic targets in the diagnosis and treatment of human cancers. In addition, circRNAs can act as a protein sponge to adsorb one or more proteins through binding sites, thus acting as a protein scaffold to directly mediate protein-protein interactions and regulate gene expression. Recent studies have found that the abnormal expression of Circ-ABCB10, also known as hsa_circ_000871, may be involved in the occurrence and development of many different tumors, such as esophageal squamous carcinoma cells, glioma, non-small cell lung cancer, oral squamous cell carcinoma, lung cancer, epithelial ovarian cancer, breast cancer, thyroid cancer, and hepatocellular

carcinoma (Cortés-López and Miura, 2016; Wang et al., 2017). Thus, it is significant to summarize the function of Circ-ABCB10 in the occurrence and progression of human cancers.

THE FEATURES AND BIOLOGICAL FUNCTIONS OF CIRC-ABCB10

Circ-ABCB10 originates from exons 2 and 3 of the ABCB10 gene, located on chromosome 1 (Duan et al., 2020). The antisense strand of Circ-ABCB10 undergoes back-splicing of the 5' and 3' ends to form circular RNA (**Figure 1**) With specific expression in different developmental stages and tissues, Circ-ABCB10 was first reported to promote breast cancer proliferation and migration by sponging miR-1271 (Chen et al., 2019). It was also found that Circ-ABCB10 is highly expressed in human brain regions such as the forebrain, cerebellum, occipital lobe, frontal cortex, and parietal lobe (Memczak et al., 2013). Different from linear RNAs, circRNAs are single-chain circular RNAs without 5' to 3' polarity or a polyadenylated tail. This blocked structure makes circ-ABCB10 more resistant to RNA degradation. Due to these unique characteristics, circ-ABCB10 is related to several characteristics of cancers (Jayson et al., 2014). Some studies have demonstrated that circ-ABCB10 could stimulate tumor growth (Liang et al., 2017; Zhao et al., 2021) and insulin resistance (IR) (Lux and Bullinger, 2018; Ouyang et al., 2018). Furthermore, the high expression of circ-ABCB10 was closely related to the pathological grade and tumor lymph node metastasis stage (Luo et al., 2018). Thus, circ-ABCB10 may be a promising diagnostic and prognostic biomarker and a target for novel treatment strategies in the future.

CIRC-ABCB10 FUNCTIONS AS A MIRNA SPONGE

Like lncRNAs, the main role of circRNAs in molecular regulation is to act as a “sponge” to absorb functional miRNA to decrease their abundance in the cytoplasm and thereby regulate gene expression (Dong et al., 2017b; Li et al., 2017). Among the target miRNAs that can be regulated by circRNAs, it was demonstrated that miR-1252 can provide potential biomarkers and therapeutic targets in non-small cell lung cancer (Tian et al., 2019) and epithelial ovarian cancer (Chen et al., 2019). Similarly, it was also found that circ-ABCB10 can sponge miR-1271, which may have a complementary sequence, possibly regulating cell proliferation and migration of breast cancer and epithelial ovarian cancer cells (Liang et al., 2017; Lin et al., 2021; Zhao et al., 2021). Furthermore, since conserved miR-1271 target sites on circ-ABCB10 are complementary to miR-1271, these sites could be a lodging site for transport (Lin et al., 2021). In addition, circ-ABCB10 was reported to sponge miR-145-5p, affecting the miR-620/FABP5 axis, miR-1252 FOXR2, and miR-670-3p in oral squamous cell carcinoma, glioma, non-small cell lung cancer, and esophageal squamous cell carcinoma, respectively (Tian et al., 2019; Chen et al., 2020; Sun et al., 2020; Zhang et al., 2020). Furthermore, circ-ABCB10 was also found to promote glycolysis and colony

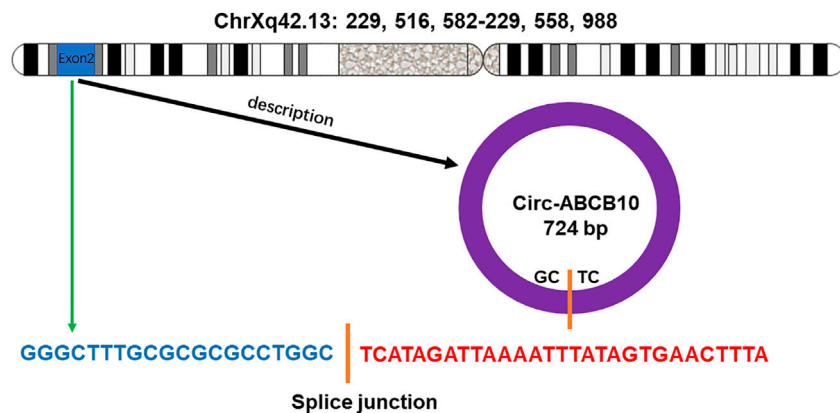


FIGURE 1 | Gene encoding circ-ABCB10 is located on the chromosome Xq42.13. The antisense strand of circ-ABCB10 undergoes back-splicing of the 5' and 3' ends to form circular RNA. The green arrow indicates the "head-to-tail" splicing site of circ-ABCB10.

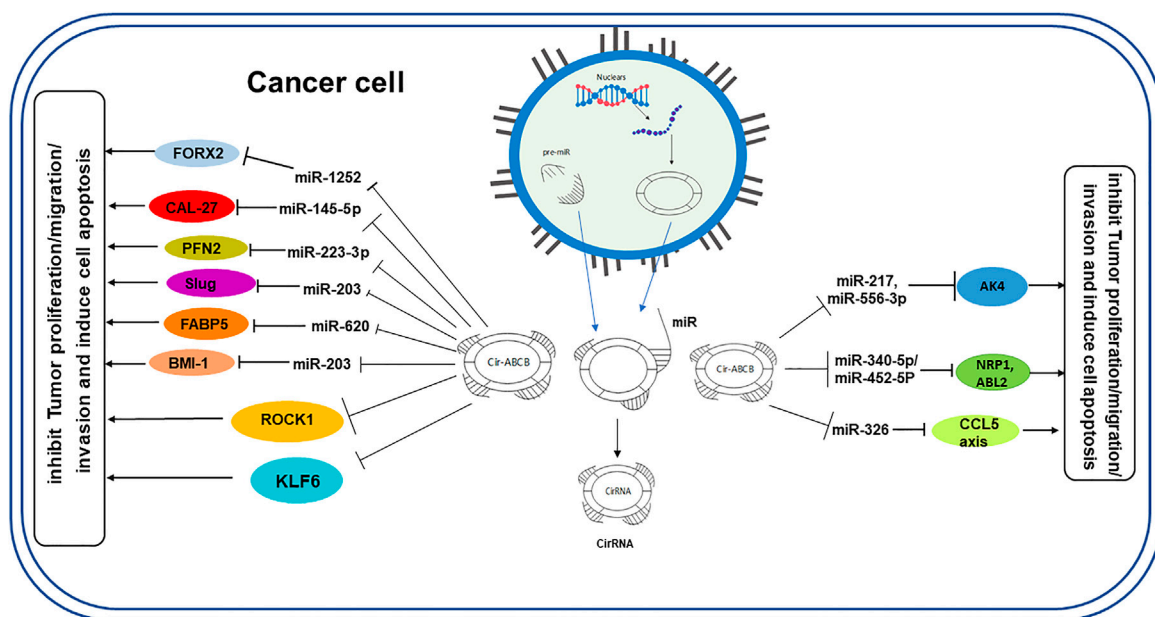


FIGURE 2 | Overview of circ-ABCB10 function as a miRNA sponge in the proliferation and metastasis of various cancer cell types. Circ-ABCB10 is released from the nucleus, acting as a sponge of miRNAs that regulate target genes to promote or inhibit tumor growth.

formation by sponging miR-229-3p (Zhao et al., 2020). In addition, Circ-ABCB10 can promote angiogenesis *via* the microRNA-29b-3p/vascular endothelial growth factor A-axis (Tang et al., 2020) (Figure 2).

THE ROLES OF CIRC-ABCB10 IN CANCER PROGRESSION

With the progress of circRNA research, relevant studies demonstrated that Circ-ABCB10 is abnormally expressed in various cancers, such as esophageal squamous cell carcinoma

(Zhang et al., 2020) and esophageal cancer (Wang et al., 2020). The upregulation of circ-ABCB10 was found to promote cell proliferation in various tumors, including esophageal squamous cell carcinoma (Zhang et al., 2020), esophageal cancer (Wang et al., 2020), glioma (Sun et al., 2020), non-small cell lung cancer (Tian et al., 2019), and oral squamous cell carcinoma (Chen et al., 2020). However, the overexpression of circ-ABCB10 was also found to inhibit the migration and invasion of lung cancer cells (Hu et al., 2020; Wu et al., 2020), hepatocellular carcinoma cells (Yang et al., 2020b), and rectal cancer cells (Xian et al., 2020). Generally speaking, these studies indicate that the expression of Circ-ABCB10 is dynamically regulated in

TABLE 1 | Expression and functions of circ-ABCB10 in different cancers.

Cancer type	Level	Biological function	Related miRNA genes	Target axis	References
Esophageal squamous cell carcinoma (ESCC)	Up	Promote proliferation, migration, and invasion	miR-670-3p	Circ-ABCB10—miR-670-3p	Zhang et al. (2020)
Esophageal cancer (EC)	Up	Promote proliferation, migration, and invasion	miR-203 and slug	Circ-ABCB10—miR-203—slug	Wang et al. (2020)
Glioma (GL)	Up	Promote migration, invasion, and cell cycle progression and inhibits apoptosis	miR-620/FABP5	Circ-ABCB10—miR620/FABP5	Sun et al. (2020)
Non-small-cell lung cancer (NSCLC)	Up	Promote proliferation and migration	miR-1252 and FOXR2	Circ-ABCB10—miR-1252—FOXR2	Tian et al. (2019)
			miR-584-5p, E2F5	Circ-ABCB10—miR-584-5p—E2F5	
Oral squamous cell carcinoma (OSCC)	Up	Promote cell growth and migration	miR-145-5p	Circ-ABCB10—miR-145-5p	Chen et al. (2020)
Epithelial ovarian cancer (EOC)	Up	Promote proliferation, migration, and invasion and reduce apoptosis	miR-1271, Capn4/Wnt/ β -catenin miR-1252, miR-203	Circ-ABCB10—miR-1271—Capn4/Wnt/ β -catenin Circ-ABCB10—miR-1252/ miR-203	Chen et al. (2019); Lin et al. (2021)
Breast cancer (BC)	Up	Promote proliferation, migration, and invasion Enhance glycolysis and colony formation Mediate PTX resistance, apoptosis, invasion, and autophagy	miR-223-3p/PFN2 miR-1271	Circ-ABCB10—miR-223-3p—PFN2 Circ-ABCB10—miR-1271	Liang et al. (2017); Zhao et al. (2020)
Clear cell renal cell carcinoma (ccRCC)	Up	Promote proliferation and progression. Inhibit apoptosis	miR-331-3p/miR-1228-5p	Circ-ABCB10—miR-331-3p/ miR-1228-5p	Huang et al. (2019)
Nasopharyngeal carcinoma (NPC)	Up	Promote growth and metastasis	Rock1	Circ-ABCB10—Rock1	Duan et al. (2020)
Osteosarcoma	Up	Promote proliferation and invasion inhibit apoptosis	miR-203, Bmi-1	Circ-ABCB10—miR-203—Bmi-1	Zhou et al. (2018)
Lung cancer (LC)	Down	Inhibit proliferation and migration	miR-556-3p/AK4	Circ-ABCB10—miR-556-3p—AK4	Hu et al. (2020); Wu et al. (2020)
Hepatocellular carcinoma (HCC)	Up Down	Promote the proliferation and migration Enhance apoptosis Inhibit proliferation Suppress invasion and migration	miR-217 miR-340-5p/miR-452-5P, NRP1, ABL2	Circ-ABCB10—miR-217 Circ-ABCB10—miR-340-5p/ miR-452-5P—NRP1/ABL2	Yang et al. (2020b)
Rectal cancer (RC)	Down	Inhibit ferroptosis and apoptosis	miR-326/CCL5	CircA-BCB10—miR-326—CCL5	Xian et al. (2020)
Cervical cancer (cc)	Down	Inhibits proliferation, invasion, and EMT and promotes apoptosis	miR-128-3p/ZEB1 axis	Circ-ABCB10—miR-128-3p/ ZEB1 axis	Feng et al. (2021)

tumor progression. The details of its diverse roles are summarized in **Table 1**.

1) In Proliferation and Invasion

It has been reported that circ-ABCB10 participates in tumor proliferation and migration by sponging several miRNAs *via* various transmitting pathways. It has been found that circ-ABCB10 can sponge miR-1252 and miR-584-5p in non-small cell lung cancer cells and accordingly stimulate the expression of the downstream targeted genes FOXR2 and E2F5 (He et al., 2018). It is worth saying that in the previous study, miR-584-5p exerts a promoting effect on gastric cancer. Thus, we can speculate that circ-ABCB10 may sponge different miRNAs to regulate the same tumor growth. At the same time, circ-ABCB10 can sponge miR-620 and upregulate the expression of the FABP5 axis to promote tumor growth and proliferation in glioma (Sun et al., 2020). In addition, circ-ABCB10 can sponge miR-203 and

promote the proliferation of EC cells (Wang et al., 2020). MiR-203 can suppress slug/E-cadherin signals to inhibit cell invasion (Gao et al., 2017a). In addition, circ-ABCB10 can also promote the function of Bmi-1 by sponging miR-203 and enhance the tumor growth in osteosarcoma (Zhou et al., 2018). It indicates that there may be a correlation between circ-ABCB10 and miR-203 in the proliferation of tumor. Furthermore, the overexpression of circ-ABCB10 can stimulate tumor proliferation and invasion by sponging miR-1271, which is also a pivotal miRNA in most regulation processes of circRNAs in breast cancer (Wang et al., 2018) and promote the proliferation and progression of clear cell renal cell carcinoma by activating the target gene—miR-331-3p/miR-1228-5p (Huang et al., 2019). The interesting thing is that in rectal cancer, the number of circ-ABCB10 is decreasing but has an effect of inhibiting ferroptosis and apoptosis by regulating miR-326/CCL5 (Xian et al., 2020). This illustrates that the level of circ-ABCB10 can also have an influence on the proliferation and

invasion of tumor. However, in hepatocellular carcinoma, *in vivo* experiments indicate that circ-ABCB10 may be an anti-oncogenic factor (Gao et al., 2017a). With the upregulation of circ-ABCB10, the downstream targeted genes of the signaling axis, namely, NRP1 and ABL2 are upregulated. In this case, it can easily be supposed that circ-ABCB10 can regulate the expression of multiple downstream genes, which has a synergistic effect on tumor growth. Coincidentally, circ-ABCB10 can also regulate the proliferation and EMT of cervical cancer by inhibiting the miR-128-3p/ZEB1 axis (Feng et al., 2021). In general, circ-ABCB10 can act as an oncogene by promoting tumor proliferation and migration in glioma, non-small cell lung cancer, esophageal cancer, breast cancer, and renal cancer (Tang et al., 2017; Deng et al., 2018; Wang et al., 2018; Wang et al., 2020; Zhao et al., 2020) and can also be an anti-oncogene by inhibiting the growth in hepatocellular carcinoma and cervical cancer (Gao et al., 2017a; Feng et al., 2021). It was also shown that circ-ABCB10 plays an obvious role in the proliferation and migration of tumors, with different effects on different cancers.

2) In Metastasis

Metastasis is an important step in cancer progression, and circ-ABCB10 can influence cancer metastasis in different ways (Gao et al., 2017b; Liang et al., 2017; Tang et al., 2017; Zhao et al., 2021). In oral squamous cell carcinoma, circ-ABCB10 was found to be upregulated and related to metastasis and tumor clinical staging of oral squamous cell carcinoma (OSCC) patients, aggravating the progression of OSCC by sponging miR-145-5p (Chen et al., 2020). In breast cancer, circ-ABCB10 acts as a miR-223-3p sponge and regulates the expression of the miR-223-3p targeted gene PFN2 to induce cell migration (Zhao et al., 2021). In addition, it can also promote invasion by sponging miR-1271 and reducing IR sensitivity (Tang et al., 2017). Similarly, the expression of ROCK1 is upregulated and is correlated with circ-ABCB10 expression in NPC cells (Liang et al., 2017). ROCK1 was upregulated following the overexpression of circ-ABCB10 in NPC (Liang et al., 2017). It is demonstrated that circ-ABCB10 has a positive role in cancer metastasis. Similar to proliferation and invasion, circ-ABCB10 also has an adverse effect on tumor metastasis. It is also seen in hepatocellular carcinoma that circ-ABCB10 can suppress the migration and metastasis by inhibiting the miR-340-5p/miR-452-5p—NRP1/ABL2 axis (Yang et al., 2020b). Thus, circ-ABCB10 plays a key role in tumor metastasis in different cancers.

3) In Angiogenesis

Angiogenesis, the creation of new blood vessels, plays a significant role in bone regeneration and osteoblast differentiation and provides essential nutrients and oxygen during bone formation (Hu et al., 2013; Kusumbe et al., 2014). Recently, it was found that circRNAs may be involved in the progression of angiogenesis during the occurrence and development of disease (Zheng et al., 2016; Zhong et al., 2016; Gao et al., 2017b; Deng et al., 2018; He et al., 2018). For example, there is evidence that circ-IARS in pancreatic cancer cells can influence human umbilical vein endothelial cell

(HUVEC) monolayers to promote tumor metastasis (Li et al., 2018b). This fact indicates that circ-ABCB10 may also influence the angiogenesis of HUVECs. Vascular endothelial growth factor (VEGF) is another significant cytokine that promotes angiogenesis (Siveen et al., 2017). Kim et al. found that human amnion-derived mesenchymal stem cells (hAMSCs) can promote angiogenesis (Kim et al., 2012), and further research confirmed that hAMSCs can significantly increase the expression of VEGF and circ-ABCB10 (Tang et al., 2020). This implies that circ-ABCB10 may promote cell growth through related pathways. A series of experiments demonstrated that circ-ABCB10 can enhance the angiogenesis of HUVECs by sponging miR-29b-3p and VEGFA (Tang et al., 2020). It was also demonstrated that conditioned medium from hAMSCs (hAMSC-CM) can indirectly promote circ-ABCB10 transcription but not the release of hAMSC-CM by exosomes (Tang et al., 2020). However, there are still numerous questions related to the mechanisms through which circ-ABCB10 may promote angiogenesis.

CONCLUSION

In recent years, it has been found that circRNAs originate from the cyclization of pre-mRNAs and have many unique features not found in other RNAs. Because of their unique stable structure and tissue-specific expression, circRNAs have potential applications as novel biomarkers for assessing tumor progression (Jin et al., 2016; Zhang et al., 2017; Jakobi and Dieterich, 2019) and for the diagnosis and treatment of tumors (Lux and Bullinger, 2018; Ouyang et al., 2018). Increasing numbers of studies have found that circRNAs are abnormally expressed during tumorigenesis. In this article, we discussed and reviewed the role of circ-ABCB10 in different cancers and comprehensively summarized a list of related signaling pathways in various tumors. Circ-ABCB10 was found to promote the proliferation, migration, and metastasis of diverse cancers, such as esophageal squamous cell carcinoma, lung cancer, epithelial ovarian cancer, breast cancer, and hepatocellular carcinoma. Moreover, some studies demonstrated that circ-ABCB10 may also contribute to angiogenesis (Tang et al., 2020). From this perspective, circ-ABCB10 might be a potential biomarker for the diagnosis and prognosis of human cancers. However, the knowledge on the roles of circ-ABCB10 in cancer is still limited, and there are still many unresolved problems. For example, there is a lack of knowledge related to the relevant set of miRNA genes for each cancer. In addition, it is also necessary to identify the main sponging targets of circ-ABCB10. Understanding these processes may lead to completely new tumor therapies.

AUTHOR CONTRIBUTIONS

RS and WW collected the related manuscript. ZH drafted and revised the manuscript. XZ designed the review. JL participated in the design of the review and helped draft and revise the manuscript. All authors read and approved the final manuscript.

REFERENCES

- Bachmayr-Heyda, A., Reiner, A. T., Auer, K., Sukhbaatar, N., Aust, S., Bachleitner-Hofmann, T., et al. (2015). Correlation of Circular RNA Abundance with Proliferation - Exemplified with Colorectal and Ovarian Cancer, Idiopathic Lung Fibrosis and normal Human Tissues. *Sci. Rep.* 5, 8057. doi:10.1038/srep08057
- Bahn, J. H., Zhang, Q., Li, F., Chan, T.-M., Lin, X., Kim, Y., et al. (2015). The Landscape of microRNA, Piwi-Interacting RNA, and Circular RNA in Human Saliva. *Clin. Chem.* 61 (1), 221–230. doi:10.1373/clinchem.2014.230433
- Chen, F., Li, X. H., Liu, C., Zhang, Y., and Wang, R. J. (2020). Circ-ABCB10 Accelerates the Malignant Progression of Oral Squamous Cell Carcinoma by Absorbing miRNA-145-5p. *Eur. Rev. Med. Pharmacol. Sci.* 24 (2), 681–690. doi:10.26355/eurrev_202001_20045
- Chen, L.-L. (2016). The Biogenesis and Emerging Roles of Circular RNAs. *Nat. Rev. Mol. Cell Biol.* 17 (4), 205–211. doi:10.1038/nrm.2015.32
- Chen, Y., Ye, X., Xia, X., and Lin, X. (2019). Circular RNA ABCB10 Correlates with Advanced Clinicopathological Features and Unfavorable Survival, and Promotes Cell Proliferation while Reduces Cell Apoptosis in Epithelial Ovarian Cancer. *Cbm* 26 (2), 151–161. doi:10.3233/cbm-190064
- Chi, G., Xu, D., Zhang, B., and Yang, F. (2019). Matrine Induces Apoptosis and Autophagy of Glioma Cell Line U251 by Regulation of circRNA-104075/BCL-9. *Chemico-Biological Interactions* 308, 198–205. doi:10.1016/j.cbi.2019.05.030
- Conn, S. J., Pillman, K. A., Toubia, J., Conn, V. M., Salamanidis, M., Phillips, C. A., et al. (2015). The RNA Binding Protein Quaking Regulates Formation of circRNAs. *Cell* 160 (6), 1125–1134. doi:10.1016/j.cell.2015.02.014
- Cortés-López, M., and Miura, P. (2016). Emerging Functions of Circular RNAs. *Yale J. Biol. Med.* 89 (4), 527–537.
- Deng, N., Li, L., Gao, J., Zhou, J., Wang, Y., Wang, C., et al. (2018). Hsa_circ_0009910 Promotes Carcinogenesis by Promoting the Expression of miR-449a Target IL6R in Osteosarcoma. *Biochem. Biophysical Res. Commun.* 495 (1), 189–196. doi:10.1016/j.bbrc.2017.11.028
- Dong, R., Ma, X.-K., Chen, L.-L., and Yang, L. (2017). Increased Complexity of circRNA Expression during Species Evolution. *RNA Biol.* 14 (8), 1064–1074. doi:10.1080/15476286.2016.1269999
- Dong, W., Dai, Z.-h., Liu, F.-c., Guo, X.-g., Ge, C.-m., Ding, J., et al. (2019). The RNA-Binding Protein RBM3 Promotes Cell Proliferation in Hepatocellular Carcinoma by Regulating Circular RNA SCD-circRNA 2 Production. *EBioMedicine* 45, 155–167. doi:10.1016/j.ebiom.2019.06.030
- Dong, Y., He, D., Peng, Z., Peng, W., Shi, W., Wang, J., et al. (2017). Circular RNAs in Cancer: an Emerging Key Player. *J. Hematol. Oncol.* 10 (1), 2. doi:10.1186/s13045-016-0370-2
- Duan, Z. N., Dong, C. G., and Liu, J. H. (2020). Circ-ABCB10 Promotes Growth and Metastasis of Nasopharyngeal Carcinoma by Upregulating ROCK1. *Eur. Rev. Med. Pharmacol. Sci.* 24 (23), 12208–12215. doi:10.26355/eurrev_202012_24011
- Feng, W., Guo, R., Zhang, D., and Zhang, R. (2021). Circ-ABCB10 Knockdown Inhibits the Malignant Progression of Cervical Cancer through microRNA-128-3p/ZEB1 axis. *Biol. Proced. Online* 23 (1), 17. doi:10.1186/s12575-021-00154-8
- Gao, P., Wang, S., Jing, F., Zhan, J., and Wang, Y. (2017). microRNA-203 Suppresses Invasion of Gastric Cancer Cells by Targeting ERK1/2/Slug/E-Cadherin Signaling. *Cbm* 19 (1), 11–20. doi:10.3233/cbm-160167
- Gao, Y.-L., Zhang, M.-Y., Xu, B., Han, L.-J., Lan, S.-F., Chen, J., et al. (2017). Circular RNA Expression Profiles Reveal that Hsa_circ_0018289 Is Up-Regulated in Cervical Cancer and Promotes the Tumorigenesis. *Oncotarget* 8 (49), 86625–86633. doi:10.18632/oncotarget.21257
- Guarnerio, J., Zhang, Y., Cheloni, G., Panella, R., Mae Katon, J., Simpson, M., et al. (2019). Intragenic Antagonistic Roles of Protein and circRNA in Tumorigenesis. *Cell Res* 29 (8), 628–640. doi:10.1038/s41422-019-0192-1
- Hansen, T. B., Jensen, T. I., Clausen, B. H., Bramsen, J. B., Finsen, B., Damgaard, C. K., et al. (2013). Natural RNA Circles Function as Efficient microRNA Sponges. *Nature* 495 (7441), 384–388. doi:10.1038/nature11993
- He, Q., Zhao, L., Liu, Y., Liu, X., Zheng, J., Yu, H., et al. (2018). circ-SHKBP1 Regulates the Angiogenesis of U87 Glioma-Exposed Endothelial Cells through miR-544a/FOXP1 and miR-379/FOXP2 Pathways. *Mol. Ther. - Nucleic Acids* 10, 331–348. doi:10.1016/j.omtn.2017.12.014
- Hou, L.-D., and Zhang, J. (2017). Circular RNAs: An Emerging Type of RNA in Cancer. *Int. J. Immunopathol Pharmacol.* 30 (1), 1–6. doi:10.1177/0394632016686985
- Hu, N., Jiang, D., Huang, E., Liu, X., Li, R., Liang, X., et al. (2013). BMP9-regulated Angiogenic Signaling Plays an Important Role in the Osteogenic Differentiation of Mesenchymal Progenitor Cells. *J. Cell Sci* 126 (Pt 2), 532–541. doi:10.1242/jcs.114231
- Hu, T. Y., Zhu, Q. X., Duan, Q. Y., Jin, X. Y., and Wu, R. (2020). CircABCB10 Promotes the Proliferation and Migration of Lung Cancer Cells through Down-Regulating microRNA-217 Expression. *Eur. Rev. Med. Pharmacol. Sci.* 24 (11), 6157–6165. doi:10.26355/eurrev_202006_21511
- Huang, Y., Zhang, Y., Jia, L., Liu, C., and Xu, F. (2019). Circular RNA ABCB10 Promotes Tumor Progression and Correlates with Pejorative Prognosis in clear Cell Renal Cell Carcinoma. *Int. J. Biol. Markers* 34 (2), 176–183. doi:10.1177/1724600819842279
- Jakobi, T., and Dieterich, C. (2019). Computational Approaches for Circular RNA Analysis. *Wiley Interdiscip. Rev. RNA* 10 (3), e1528. doi:10.1002/wrna.1528
- Jayson, G. C., Kohn, E. C., Kitchener, H. C., and Ledermann, J. A. (2014). Ovarian Cancer. *The Lancet* 384 (9951), 1376–1388. doi:10.1016/s0140-6736(13)62146-7
- Jin, X., Feng, C.-y., Xiang, Z., Chen, Y.-p., and Li, Y.-m. (2016). CircRNA Expression Pattern and circRNA-miRNA-mRNA Network in the Pathogenesis of Nonalcoholic Steatohepatitis. *Oncotarget* 7 (41), 66455–66467. doi:10.18632/oncotarget.12186
- Khan, M. A. F., Reckman, Y. J., Aufiero, S., van den Hoogenhof, M. M. G., van der Made, I., Beqqali, A., et al. (2016). RBM20 Regulates Circular RNA Production from the Titin Gene. *Circ. Res.* 119 (9), 996–1003. doi:10.1161/circresaha.116.309568
- Kim, S.-W., Zhang, H.-Z., Kim, C. E., An, H. S., Kim, J.-M., and Kim, M. H. (2012). Amniotic Mesenchymal Stem Cells Have Robust Angiogenic Properties and Are Effective in Treating Hindlimb Ischaemia. *Cardiovasc. Res.* 93 (3), 525–534. doi:10.1093/cvr/cvr328
- Kristensen, L. S., Hansen, T. B., Venø, M. T., and Kjems, J. (2018). Circular RNAs in Cancer: Opportunities and Challenges in the Field. *Oncogene* 37 (5), 555–565. doi:10.1038/onc.2017.361
- Kusumbe, A. P., Ramasamy, S. K., and Adams, R. H. (2014). Coupling of Angiogenesis and Osteogenesis by a Specific Vessel Subtype in Bone. *Nature* 507 (7492), 323–328. doi:10.1038/nature13145
- Li, J., Li, Z., Jiang, P., Peng, M., Zhang, X., Chen, K., et al. (2018). Circular RNA IARS (Circ-IARS) Secreted by Pancreatic Cancer Cells and Located within Exosomes Regulates Endothelial Monolayer Permeability to Promote Tumor Metastasis. *J. Exp. Clin. Cancer Res.* 37 (1), 177. doi:10.1186/s13046-018-0822-3
- Li, X., Wang, J., Zhang, C., Lin, C., Zhang, J., Zhang, W., et al. (2018). Circular RNA circITGA7 Inhibits Colorectal Cancer Growth and Metastasis by Modulating the Ras Pathway and Upregulating Transcription of its Host geneITGA7. *J. Pathol.* 246 (2), 166–179. doi:10.1002/path.5125
- Li, Y., Dong, Y., Huang, Z., Kuang, Q., Wu, Y., Li, Y., et al. (2017). Computational Identifying and Characterizing Circular RNAs and Their Associated Genes in Hepatocellular Carcinoma. *PLoS One* 12 (3), e0174436. doi:10.1371/journal.pone.0174436
- Li, Z., Huang, C., Bao, C., Chen, L., Lin, M., Wang, X., et al. (2015). Exon-intron Circular RNAs Regulate Transcription in the Nucleus. *Nat. Struct. Mol. Biol.* 22 (3), 256–264. doi:10.1038/nsmb.2959
- Liang, H. F., Zhang, X. Z., Liu, B. G., Jia, G. T., and Li, W. L. (2017). Circular RNA Circ-ABCB10 Promotes Breast Cancer Proliferation and Progression through Sponging miR-1271. *Am. J. Cancer Res.* 7 (7), 1566–1576.
- Lin, X., Chen, Y., Ye, X., and Xia, X. (2021). Circular RNA ABCB10 Promotes Cell Proliferation and Invasion, but Inhibits Apoptosis via Regulating the microRNA-1271-mediated Capn4/Wnt/β-catenin S-signaling P-athway in E-pithelial O-varian C-ancer. *Mol. Med. Rep.* 23 (5), 26. doi:10.3892/mmr.2021.12026
- Luo, L., Gao, Y., and Sun, X. (2018). Circ-ITCH Correlates with Small Tumor Size, Decreased FIGO Stage and Prolonged Overall Survival, and it Inhibits Cells Proliferation while Promotes Cells Apoptosis in Epithelial Ovarian Cancer. *Cbm* 23 (4), 505–513. doi:10.3233/cbm-181609
- Lux, S., and Bullinger, L. (2018). Circular RNAs in Cancer. *Adv. Exp. Med. Biol.* 1087, 215–230. doi:10.1007/978-981-13-1426-1_17
- Memczak, S., Jens, M., Elefsinioti, A., Torti, F., Krueger, J., Rybak, A., et al. (2013). Circular RNAs Are a Large Class of Animal RNAs with Regulatory Potency. *Nature* 495 (7441), 333–338. doi:10.1038/nature11928
- Nicolet, B. P., Engels, S., Agliarolo, F., van den Akker, E., von Lindern, M., and Wolkers, M. C. (2018). Circular RNA Expression in Human Hematopoietic Cells Is Widespread and Cell-type Specific. *Nucleic Acids Res.* 46 (16), 8168–8180. doi:10.1093/nar/gky721
- Ouyang, S. B., Wang, J., Zhao, S. Y., Zhang, X. H., and Liao, L. (2018). CircRNA_0109291 Regulates Cell Growth and Migration in Oral Squamous

- Cell Carcinoma and its Clinical Significance. *Iran J. Basic Med. Sci.* 21 (11), 1186–1191. doi:10.22038/IJBMS.2018.30347.7313
- Pamudurti, N. R., Bartok, O., Jens, M., Ashwal-Fluss, R., Stottmeister, C., Ruhe, L., et al. (2017). Translation of CircRNAs. *Mol. Cell* 66 (1), 9–21. doi:10.1016/j.molcel.2017.02.021
- Patop, I. L., and Kadener, S. (2018). circRNAs in Cancer. *Curr. Opin. Genet. Develop.* 48, 121–127. doi:10.1016/j.gde.2017.11.007
- Qin, M., Wei, G., and Sun, X. (2018). Circ-UBR5: An Exonic Circular RNA and Novel Small Nuclear RNA Involved in RNA Splicing. *Biochem. Biophysical Res. Commun.* 503 (2), 1027–1034. doi:10.1016/j.bbrc.2018.06.112
- Qu, S., Liu, Z., Yang, X., Zhou, J., Yu, H., Zhang, R., et al. (2018). The Emerging Functions and Roles of Circular RNAs in Cancer. *Cancer Lett.* 414, 301–309. doi:10.1016/j.canlet.2017.11.022
- Qu, S., Yang, X., Li, X., Wang, J., Gao, Y., Shang, R., et al. (2015). Circular RNA: A New Star of Noncoding RNAs. *Cancer Lett.* 365 (2), 141–148. doi:10.1016/j.canlet.2015.06.003
- Salzman, J., Chen, R. E., Olsen, M. N., Wang, P. L., and Brown, P. O. (2013). Cell-type Specific Features of Circular RNA Expression. *Plos Genet.* 9 (9), e1003777. doi:10.1371/journal.pgen.1003777
- Salzman, J., Gawad, C., Wang, P. L., Lacayo, N., and Brown, P. O. (2012). Circular RNAs Are the Predominant Transcript Isoform from Hundreds of Human Genes in Diverse Cell Types. *PLoS One* 7 (2), e30733. doi:10.1371/journal.pone.0030733
- Sanger, H. L., Klotz, G., Riesner, D., Gross, H. J., and Kleinschmidt, A. K. (1976). Viroids Are Single-Stranded Covalently Closed Circular RNA Molecules Existing as Highly Base-Paired Rod-like Structures. *Proc. Natl. Acad. Sci. U.S.A.* 73 (11), 3852–3856. doi:10.1073/pnas.73.11.3852
- Shang, Q., Yang, Z., Jia, R., and Ge, S. (2019). The Novel Roles of circRNAs in Human Cancer. *Mol. Cancer* 18 (1), 6. doi:10.1186/s12943-018-0934-6
- Shi, X., Wang, B., Feng, X., Xu, Y., Lu, K., and Sun, M. (2020). circRNAs and Exosomes: A Mysterious Frontier for Human Cancer. *Mol. Ther. - Nucleic Acids* 19, 384–392. doi:10.1016/j.omtn.2019.11.023
- Siveen, K. S., Prabhu, K., Krishnakutty, R., Kuttikrishnan, S., Tsakou, M., Alali, F. Q., et al. (2017). Vascular Endothelial Growth Factor (VEGF) Signaling in Tumor Vascularization: Potential and Challenges. *Curr. Vasc. Pharmacol.* 15 (4), 339–351. doi:10.2174/1570161115666170105124038
- Su, M., Xiao, Y., Ma, J., Tang, Y., Tian, B., Zhang, Y., et al. (2019). Circular RNAs in Cancer: Emerging Functions in Hallmarks, Stemness, Resistance and Roles as Potential Biomarkers. *Mol. Cancer* 18 (1), 90. doi:10.1186/s12943-019-1002-6
- Sun, W. Y., Lu, Y. F., Cai, X. L., Li, Z. Z., Lv, J., Xiang, Y. A., et al. (2020). Circ-ABCB10 Acts as an Oncogene in Glioma Cells via Regulation of the miR-620/FABP5 axis. *Eur. Rev. Med. Pharmacol. Sci.* 24 (12), 6848–6857. doi:10.26355/eurev_202006_21674
- Tang, Q., and Hann, S. S. (2020). Biological Roles and Mechanisms of Circular RNA in Human Cancers. *Ott Vol.* 13, 2067–2092. doi:10.2147/ott.s233672
- Tang, W., Ji, M., He, G., Yang, L., Niu, Z., Jian, M., et al. (2017). Silencing CDR1as Inhibits Colorectal Cancer Progression through Regulating microRNA-7. *Ott Vol.* 10, 2045–2056. doi:10.2147/ott.s131597
- Tang, Z., Tan, J., Yuan, X., Zhou, Q., Yuan, Z., Chen, N., et al. (2020). Circular RNA-ABCB10 Promotes Angiogenesis Induced by Conditioned Medium from Human Amnion-Derived Mesenchymal Stem Cells via the microRNA-29b-3p/vascular Endothelial Growth Factor A axis. *Exp. Ther. Med.* 20 (3), 2021–2030. doi:10.3892/etm.2020.8939
- Thomas, L. F., and Sæthrom, P. (2014). Circular RNAs Are Depleted of Polymorphisms at microRNA Binding Sites. *Bioinformatics* 30 (16), 2243–2246. doi:10.1093/bioinformatics/btu257
- Tian, X., Zhang, L., Jiao, Y., Chen, J., Shan, Y., and Yang, W. (2019). CircABCB10 Promotes Non-small Cell Lung Cancer Cell Proliferation and Migration by Regulating the miR-1252/FOXO2 axis. *J. Cell Biochem.* 120 (3), 3765–3772. doi:10.1002/jcb.27657
- Wang, M., Gao, W., Lu, D., and Teng, L. (2018). MiR-1271 Inhibits Cell Growth in Prostate Cancer by Targeting ERG. *Pathol. Oncol. Res.* 24 (2), 385–391. doi:10.1007/s12253-017-0254-y
- Wang, T., Wang, J., Ren, W., Chen, S., Cheng, Y.-F., and Zhang, X.-M. (2020). CircRNA-0008717 Promotes Cell Proliferation, Migration, and Invasion by Regulating miR-203/Slug in Esophageal Cancer Cells. *Ann. Transl. Med.* 8 (16), 999. doi:10.21037/atm-20-5205
- Wang, Y., Mo, Y., Gong, Z., Yang, X., Yang, M., Zhang, S., et al. (2017). Circular RNAs in Human Cancer. *Mol. Cancer* 16 (1), 25. doi:10.1186/s12943-017-0598-7
- Wu, Z., Gong, Q., Yu, Y., Zhu, J., and Li, W. (2020). Knockdown of Circ-ABCB10 Promotes Sensitivity of Lung Cancer Cells to Cisplatin via miR-556-3p/AK4 axis. *BMC Pulm. Med.* 20 (1), 10. doi:10.1186/s12890-019-1035-z
- Xian, Z. Y., Hu, B., Wang, T., Cai, J. L., Zeng, J. Y., Zou, Q., et al. (2020). CircABCB10 Silencing Inhibits the Cell Ferroptosis and Apoptosis by Regulating the miR-326/CCL5 axis in Rectal Cancer. *Neoplasma* 67 (5), 1063–1073. doi:10.4149/neo_2020_191024N1084
- Yang, W., Ju, H. Y., and Tian, X. F. (2020). Circular RNA-ABCB10 Suppresses Hepatocellular Carcinoma Progression through Upregulating NRP1/ABL2 via Sponging miR-340-5p/miR-452-5p. *Eur. Rev. Med. Pharmacol. Sci.* 24 (5), 2347–2357. doi:10.26355/eurev_202003_20501
- Yang, Y., Yujiao, W., Fang, W., Linhui, Y., Ziqi, G., Zhichen, W., et al. (2020). The Roles of miRNA, lncRNA and circRNA in the Development of Osteoporosis. *Biol. Res.* 53 (1), 40. doi:10.1186/s40659-020-00309-z
- Yu, C.-Y., and Kuo, H.-C. (2019). The Emerging Roles and Functions of Circular RNAs and Their Generation. *J. Biomed. Sci.* 26 (1), 29. doi:10.1186/s12929-019-0523-z
- Zang, J., Lu, D., and Xu, A. (2020). The Interaction of circRNAs and RNA Binding Proteins: An Important Part of circRNA Maintenance and Function. *J. Neurosci. Res.* 98 (1), 87–97. doi:10.1002/jnr.24356
- Zhang, S., Zhu, D., Li, H., Li, H., Feng, C., and Zhang, W. (2017). Characterization of circRNA-Associated-ceRNA Networks in a Senescence-Accelerated Mouse Prone 8 Brain. *Mol. Ther.* 25 (9), 2053–2061. doi:10.1016/j.ymthe.2017.06.009
- Zhang, W. Q., Liu, K. Q., Pei, Y. X., Tan, J., Ma, J. B., and Zhao, J. (2020). Circ-ABCB10 Promotes Proliferation and Invasion of Esophageal Squamous Cell Carcinoma Cells by Modulating microRNA-670-3p. *Eur. Rev. Med. Pharmacol. Sci.* 24 (11), 6088–6096. doi:10.26355/eurev_202006_21504
- Zhang, Y., Zhang, X.-O., Chen, T., Xiang, J.-F., Yin, Q.-F., Xing, Y.-H., et al. (2013). Circular Intronic Long Noncoding RNAs. *Mol. Cell* 51 (6), 792–806. doi:10.1016/j.molcel.2013.08.017
- Zhao, Y., Zhong, R., Deng, C., and Zhenlin, Z. (2020). Circle RNA circABCB10 Modulates PFN2 to Promote Breast Cancer Progression, as Well as Aggravate Radioresistance through Facilitating Glycolytic Metabolism via miR-223-3p. *Cancer Biother. Radiopharm.* 36 (6), 477–490. doi:10.1089/cbr.2019.3389
- Zhao, Y., Zhong, R., Deng, C., and Zhou, Z. (2021). Circle RNA circABCB10 Modulates PFN2 to Promote Breast Cancer Progression, as Well as Aggravate Radioresistance through Facilitating Glycolytic Metabolism via miR-223-3p. *Cancer Biother. Radiopharm.* 36 (6), 477–490. doi:10.1089/cbr.2019.3389
- Zheng, Q., Bao, C., Guo, W., Li, S., Chen, J., Chen, B., et al. (2016). Circular RNA Profiling Reveals an Abundant circHIPK3 that Regulates Cell Growth by Sponging Multiple miRNAs. *Nat. Commun.* 7, 11215. doi:10.1038/ncomms11215
- Zhong, Z., Lv, M., and Chen, J. (2016). Screening Differential Circular RNA Expression Profiles Reveals the Regulatory Role of circTCF25-miR-103a-3p/miR-107-CDK6 Pathway in Bladder Carcinoma. *Sci. Rep.* 6, 30919. doi:10.1038/srep30919
- Zhou, X., Natino, D., Qin, Z., Wang, D., Tian, Z., Cai, X., et al. (2018). Identification and Functional Characterization of circRNA-0008717 as an Oncogene in Osteosarcoma through Sponging miR-203. *Oncotarget* 9 (32), 22288–22300. doi:10.18632/oncotarget.23466

Conflict of Interest: The authors declare that the research was conducted in the absence of any commercial or financial relationships that could be construed as a potential conflict of interest.

Publisher's Note: All claims expressed in this article are solely those of the authors and do not necessarily represent those of their affiliated organizations, or those of the publisher, the editors, and the reviewers. Any product that may be evaluated in this article, or claim that may be made by its manufacturer, is not guaranteed or endorsed by the publisher.

Copyright © 2022 Huang, Shan, Wen, Li, Zeng and Wan. This is an open-access article distributed under the terms of the Creative Commons Attribution License (CC BY). The use, distribution or reproduction in other forums is permitted, provided the original author(s) and the copyright owner(s) are credited and that the original publication in this journal is cited, in accordance with accepted academic practice. No use, distribution or reproduction is permitted which does not comply with these terms.

Advantages of publishing in Frontiers



OPEN ACCESS

Articles are free to read
for greatest visibility
and readership



FAST PUBLICATION

Around 90 days
from submission
to decision



HIGH QUALITY PEER-REVIEW

Rigorous, collaborative,
and constructive
peer-review



TRANSPARENT PEER-REVIEW

Editors and reviewers
acknowledged by name
on published articles

Frontiers

Avenue du Tribunal-Fédéral 34
1005 Lausanne | Switzerland

Visit us: www.frontiersin.org

Contact us: frontiersin.org/about/contact



REPRODUCIBILITY OF RESEARCH

Support open data
and methods to enhance
research reproducibility



DIGITAL PUBLISHING

Articles designed
for optimal readership
across devices



FOLLOW US

@frontiersin



IMPACT METRICS

Advanced article metrics
track visibility across
digital media



EXTENSIVE PROMOTION

Marketing
and promotion
of impactful research



LOOP RESEARCH NETWORK

Our network
increases your
article's readership